frontiers | Research Topics

Insights in integrative physiology: 2021

Edited by
James Todd Pearson, Jacqueline Kathleen Phillips and Geoffrey A. Head

Published in
Frontiers in Physiology

FRONTIERS EBOOK COPYRIGHT STATEMENT

The copyright in the text of individual articles in this ebook is the property of their respective authors or their respective institutions or funders. The copyright in graphics and images within each article may be subject to copyright of other parties. In both cases this is subject to a license granted to Frontiers.

The compilation of articles constituting this ebook is the property of Frontiers.

Each article within this ebook, and the ebook itself, are published under the most recent version of the Creative Commons CC-BY licence. The version current at the date of publication of this ebook is CC-BY 4.0. If the CC-BY licence is updated, the licence granted by Frontiers is automatically updated to the new version.

When exercising any right under the CC-BY licence, Frontiers must be attributed as the original publisher of the article or ebook, as applicable.

Authors have the responsibility of ensuring that any graphics or other materials which are the property of others may be included in the CC-BY licence, but this should be checked before relying on the CC-BY licence to reproduce those materials. Any copyright notices relating to those materials must be complied with.

Copyright and source acknowledgement notices may not be removed and must be displayed in any copy, derivative work or partial copy which includes the elements in question.

All copyright, and all rights therein, are protected by national and international copyright laws. The above represents a summary only. For further information please read Frontiers' Conditions for Website Use and Copyright Statement, and the applicable CC-BY licence.

ISSN 1664-8714
ISBN 978-2-83252-135-9
DOI 10.3389/978-2-83252-135-9

About Frontiers

Frontiers is more than just an open access publisher of scholarly articles: it is a pioneering approach to the world of academia, radically improving the way scholarly research is managed. The grand vision of Frontiers is a world where all people have an equal opportunity to seek, share and generate knowledge. Frontiers provides immediate and permanent online open access to all its publications, but this alone is not enough to realize our grand goals.

Frontiers journal series

The Frontiers journal series is a multi-tier and interdisciplinary set of open-access, online journals, promising a paradigm shift from the current review, selection and dissemination processes in academic publishing. All Frontiers journals are driven by researchers for researchers; therefore, they constitute a service to the scholarly community. At the same time, the *Frontiers journal series* operates on a revolutionary invention, the tiered publishing system, initially addressing specific communities of scholars, and gradually climbing up to broader public understanding, thus serving the interests of the lay society, too.

Dedication to quality

Each Frontiers article is a landmark of the highest quality, thanks to genuinely collaborative interactions between authors and review editors, who include some of the world's best academicians. Research must be certified by peers before entering a stream of knowledge that may eventually reach the public - and shape society; therefore, Frontiers only applies the most rigorous and unbiased reviews. Frontiers revolutionizes research publishing by freely delivering the most outstanding research, evaluated with no bias from both the academic and social point of view. By applying the most advanced information technologies, Frontiers is catapulting scholarly publishing into a new generation.

What are Frontiers Research Topics?

Frontiers Research Topics are very popular trademarks of the *Frontiers journals series*: they are collections of at least ten articles, all centered on a particular subject. With their unique mix of varied contributions from Original Research to Review Articles, Frontiers Research Topics unify the most influential researchers, the latest key findings and historical advances in a hot research area.

Find out more on how to host your own Frontiers Research Topic or contribute to one as an author by contacting the Frontiers editorial office: frontiersin.org/about/contact

Insights in integrative physiology: 2021

Topic editors

James Todd Pearson — National Cerebral and Cardiovascular Center, Japan
Jacqueline Kathleen Phillips — Macquarie University, Australia
Geoffrey A. Head — Baker Heart and Diabetes Institute, Australia

Citation

Pearson, J. T., Phillips, J. K., Head, G. A., eds. (2023). *Insights in integrative physiology: 2021*. Lausanne: Frontiers Media SA. doi: 10.3389/978-2-83252-135-9

The authors declare that the research was conducted in the absence of any commercial or financial relationships that could be construed as a potential conflict of interest.

Table of contents

06 Editorial: Insights in integrative physiology: 2021
James T. Pearson, Jacqueline K. Phillips and Geoffrey A. Head

10 The Bezold-Jarisch Reflex and The Inflammatory Response Modulation in Unanesthetized Endotoxemic Rats
Fernanda Brognara, Jaci Airton Castania, Aline Barbosa Ribeiro, Nilton Nascimento Santos-Júnior and Helio Cesar Salgado

18 Vasopressin and Breathing: Review of Evidence for Respiratory Effects of the Antidiuretic Hormone
Michał Proczka, Jacek Przybylski, Agnieszka Cudnoch-Jędrzejewska, Ewa Szczepańska-Sadowska and Tymoteusz Żera

34 Altering Early Life Gut Microbiota Has Long-Term Effect on Immune System and Hypertension in Spontaneously Hypertensive Rats
Francois M. Abboud, Michael Z. Cicha, Aaron Ericsson, Mark W. Chapleau and Madhu V. Singh

43 Sensory Afferent Renal Nerve Activated $G\alpha i_2$ Subunit Proteins Mediate the Natriuretic, Sympathoinhibitory and Normotensive Responses to Peripheral Sodium Challenges
Jesse D. Moreira, Kayla M. Nist, Casey Y. Carmichael, Jill T. Kuwabara and Richard D. Wainford

59 A 30-Year Journey Through Integrative Physiology Research and Education, Courtesy of Angiotensin II
Kathleen S. Curtis

62 Stimulation of Angiotensin Converting Enzyme 2: A Novel Treatment Strategy for Diabetic Nephropathy
Haru Nomura, Sanjaya Kuruppu and Niwanthi W. Rajapakse

69 New Insights Into Energy Substrate Utilization and Metabolic Remodeling in Cardiac Physiological Adaption
Xiaomeng Shi and Hongyu Qiu

85 Optimal Parameters of Laser Therapy to Improve Critical Calvarial Defects
Matheus AFM Santos, Daniela N. Silva, Karla Rovaris, Frederico B. Sousa, Eugenia LA Dantas, Lucas A. Loureiro, Thiago M. C. Pereira, Silvana S. Meyrelles, Rossiene M. Bertollo and Elisardo C. Vasquez

95 Unraveling Brain Microcircuits, Dendritic Spines, and Synaptic Processing Using Multiple Complementary Approaches
Alberto A. Rasia-Filho

103 The Role of Peroxisome Proliferator-Activated Receptor Gamma and Atherosclerosis: Post-translational Modification and Selective Modulators
Liqin Yin, Lihui Wang, Zunhan Shi, Xiaohui Ji and Longhua Liu

114 New Insights Into the Role of Inflammation in the Brain in Heart Failure
Emilio Badoer

121 The Influence of Modifiable Factors on Breast and Prostate Cancer Risk and Disease Progression
Keely Tan and Matthew J. Naylor

129 The Paraventricular Nucleus of the Hypothalamus in Control of Blood Pressure and Blood Pressure Variability
Bojana Savić, David Murphy and Nina Japundžić-Žigon

143 A Novel Organ-Specific Approach to Selectively Target Sensory Afferents Innervating the Aortic Arch
Khalid Elsaafien, Scott W. Harden, Dominique N. Johnson, Aecha K. Kimball, Wanhui Sheng, Justin A. Smith, Karen A. Scott, Charles J. Frazier, Annette D. de Kloet and Eric G. Krause

156 Arterial Baroreflex Inhibits Muscle Metaboreflex Induced Increases in Effective Arterial Elastance: Implications for Ventricular-Vascular Coupling
Joseph Mannozzi, Jong-Kyung Kim, Javier A. Sala-Mercado, Mohamed-Hussein Al-Hassan, Beruk Lessanework, Alberto Alvarez, Louis Massoud, Tauheed Bhatti, Kamel Aoun and Donal S. O'Leary

171 Human Face Perception Using Electroencephalography and Magnetoencephalography
Kensaku Miki, Yasuyuki Takeshima, Shoko Watanabe and Ryusuke Kakigi

182 Benefits of Curcumin in the Vasculature: A Therapeutic Candidate for Vascular Remodeling in Arterial Hypertension and Pulmonary Arterial Hypertension?
Ke-Xue Li, Zi-Chao Wang, Jeremiah Ong'Achwa Machuki, Meng-Zhen Li, Yu-Jie Wu, Ming-Kai Niu, Kang-Ying Yu, Qing-Bo Lu and Hai-Jian Sun

206 Regional Differences in Sympathetic Nerve Activity Are Generated by Multiple Arterial Baroreflex Loops Arranged in Parallel
Kenju Miki, Shizuka Ikegame and Misa Yoshimoto

214 Gut Microbial Community and Host Thermoregulation in Small Mammals
Xue-Ying Zhang and De-Hua Wang

224 Protein Restriction in the Peri-Pubertal Period Induces Autonomic Dysfunction and Cardiac and Vascular Structural Changes in Adult Rats
Anna Rebeka Oliveira Ferreira, Maiara Vanusa Guedes Ribeiro, Maria Natalia Chimirri Peres, Silvano Piovan, Géssica Dutra Gonçalves, Lucas Paulo Jacinto Saavedra, Juliana Nunes de Lima Martins, Marcos Divino Ferreira Junior, Keilah Valeria Naves Cavalcante, Gabriel kian Guimarães Lopes, Mariane Carneiro, Douglas Lopes Almeida, Rodrigo Mello Gomes, Jurandir Fernando Comar, James Andrew Armitage, Paulo Cezar de Freitas Mathias and Kesia Palma-Rigo

238 Acute Cannabigerol Administration Lowers Blood Pressure in Mice
Victoria L. Vernail, Sarah S. Bingaman, Yuval Silberman, Wesley M. Raup-Konsavage, Kent E. Vrana and Amy C. Arnold

245 Cardiometabolic Effects of Postnatal High-Fat Diet Consumption in Offspring Exposed to Maternal Protein Restriction *In Utero*
Aiany Cibelle Simões-Alves, Ana Paula Fonseca Cabral Arcoverde-Mello, Jéssica de Oliveira Campos, Almir Gonçalves Wanderley, Carol Virginia Gois Leandro, João Henrique da Costa-Silva and Viviane de Oliveira Nogueira Souza

256 Osmoregulation and the Hypothalamic Supraoptic Nucleus: From Genes to Functions
André Souza Mecawi, Wamberto Antonio Varanda and Melina Pires da Silva

276 Conditional Regulation of Blood Pressure in Response to Emotional Stimuli by the Central Nucleus of the Amygdala in Rats
Ko Yamanaka and Hidefumi Waki

287 New Perspectives on Sex Steroid and Mineralocorticoid Receptor Signaling in Cardiac Ischemic Injury
Laura A. Bienvenu, James R. Bell, Kate L. Weeks, Lea M. D. Delbridge and Morag J. Young

296 Integrative physiological study of adaptations induced by aerobic physical training in hypertensive hearts
Suenimeire Vieira, Bruno A. Aguilar, Ana Catarine Veiga, Stella V. Philbois, Ana Caroline S. Freitas, Karine P. Rodrigues, Jens Tank and Hugo C. D. Souza

frontiers | Frontiers in Physiology

TYPE Editorial
PUBLISHED 27 March 2023
DOI 10.3389/fphys.2023.1186581

Check for updates

OPEN ACCESS

EDITED AND REVIEWED BY
John D. Imig,
University of Arkansas for Medical Sciences, United States

*CORRESPONDENCE
Jacqueline K. Phillips,
jacqueline.phillips@mq.edu.au

SPECIALTY SECTION
This article was submitted to Integrative Physiology, a section of the journal Frontiers in Physiology

RECEIVED 15 March 2023
ACCEPTED 20 March 2023
PUBLISHED 27 March 2023

CITATION
Pearson JT, Phillips JK and Head GA (2023), Editorial: Insights in integrative physiology: 2021.
Front. Physiol. 14:1186581.
doi: 10.3389/fphys.2023.1186581

COPYRIGHT
© 2023 Pearson, Phillips and Head. This is an open-access article distributed under the terms of the Creative Commons Attribution License (CC BY). The use, distribution or reproduction in other forums is permitted, provided the original author(s) and the copyright owner(s) are credited and that the original publication in this journal is cited, in accordance with accepted academic practice. No use, distribution or reproduction is permitted which does not comply with these terms.

Editorial: Insights in integrative physiology: 2021

James T. Pearson[1,2], Jacqueline K. Phillips[3]* and Geoffrey A. Head[4]

[1]National Cerebral and Cardiovascular Center, Suita, Japan, [2]Department of Physiology, Monash Biomedicine Discovery Institute, Monash University, Clayton, VIC, Australia, [3]Macquarie Medical School, Macquarie University, Sydney, NSW, Australia, [4]Baker Heart and Diabetes Institute, Melbourne, VIC, Australia

KEYWORDS

metabolic, endocrine, immune, cardiovascular, respiratory, renal, reflex, neural

Editorial on the Research Topic
Insights in integrative physiology: 2021

The past decade has seen significant advancements in the field of Integrative Physiology. This series, Insights in Integrative Physiology 2021, published in Frontiers in Physiology, aims to highlight these developments, providing a comprehensive overview of what has been achieved and future challenges, in order to inform, inspire and provide direction and guidance to researchers in the field. The series is unified by the exploration of interconnected metabolic, endocrine, immune, cardiovascular, respiratory, renal, and neural systems that work together to maintain homeostasis. Each paper offers a distinct perspective on this topic. And while the papers are organised thematically in this editorial, it should be apparent to readers that it is challenging to examine each system independently of the others.

As a perfect start to the Research Topic, the commentary provided by Curtis provides a perspective on the importance of integrative physiology education, seen through the lens of angiotensin II research over the last 30 years. The author argues that the field of physiology has shifted towards the cellular, molecular and genetic, resulting in inadequate understanding of whole body integrative physiological function. The author contends that while students have extensive knowledge of the molecular biology of angiotensin signalling, they do not know about the outcome of that signalling, which is crucial for understanding the interrelated and complementary neural, cardiovascular, renal, and endocrine elements. The take home message is that integrative physiology should be given more attention to ensure its significance and appreciation are reinforced in both education and research.

The paper by Simões-Alves et al. reviews the cardiometabolic effects resulting from postnatal hyperlipidic diets in protein-restricted subjects, and the epigenetic repercussions occasioned by a phenomenon termed nutritional transition. The authors describe a trend over the last decade whereby maternal protein undernutrition during pregnancy and lactation followed by a high-fat diet has been linked to the development of cardiometabolic diseases in the offspring. Nutritional transition is associated with growth restriction, increased blood pressure, dyslipidaemia, and insulin resistance, as well as sympathetic overactivity, hypertension, and disruptions in respiratory control. They examine the epigenetic mechanisms proposed to be involved in these cardiometabolic effects including changes in DNA methylation and increased transcription of genes involved in the regulation of blood pressure and insulin sensitivity. The paper highlights how our

understanding of complex epigenetic mechanisms may help understand cardiovascular disease risk with intergenerational and transgenerational implications.

Original research in this Research Topic also examines the consequences of protein restriction during sensitive windows of postnatal growth and how this can also predispose to cardiovascular disease. Oliveira Ferreira et al. demonstrate that the peri-pubertal period in male rats is a sensitive period that is vulnerable to the programming of autonomic dysfunction and cardiovascular remodelling in adulthood. Moreover, this research team revealed that a brief exposure to the low protein diet and subsequent catch-up growth evoked elevated peripheral sympathetic activity (hypertension with increased arterial pressure low frequency power spectral density) and altered redox state in both the brainstem and the heart that led to the onset of cardiac remodelling.

The topic also attracted a number of in-depth reviews covering other aspects of metabolism. Shi and Qiu reviewed some of the newer reports on myocardial energy substrate metabolism, cardiac metabolic remodelling during exercise and cardiac development. Tan and Naylor reviewed how new knowledge of metabolic, protein and transcriptional pathways that occur in breast and prostate cancer can be influenced by modifiable lifestyle factors to change cancer cell physiology to reduce risk and benefit prognosis.

Blood pressure regulation and sodium-water homeostasis are modulated by the mineralocorticoid receptor (MR) through endogenous aldosterone and corticosteroids. For this reason, MR antagonists have received considerable attention as valuable first line therapies for hypertension and heart failure. However, beyond the vasculature, chronic activation of MR in cardiomyocytes is shown by Bienvenu et al. to adversely alter extracellular matrix composition and myocardial inflammatory state, redox balance, intracellular ion composition and apoptosis, leading to increased vulnerability of the heart to ischaemia. This mini-review presents compelling evidence for sex-specific differences in MR signaling involving estrogen receptor interactions that need to be further explored if we are to reduce the greater heart failure burden that exists in women.

Another key process that regulates sodium-water homeostasis is osmoregulation and vital to the regulation of osmolarity is the neuroendocrine supraoptic nucleus (SON) of the hypothalamus. Mecawi et al. provide an overview of the current understanding of the mechanisms that regulate plasma osmolarity within the SON, including osmosensing, transcriptomic plasticity of during long term hyperosmolality and the somatodendritic release of neuropeptides in response to osmotic challenge.

Touching on several themes within the Research Topic Badoer reviews the important contributions of circulating cytokines and locally-induced inflammation in the brain and overactivation of the sympathoadrenal and central renin angiotensin (RAS) systems in the promotion and potentiation of autonomic dysfunction in heart failure. The work highlights likely reasons why anti-inflammatory therapies have often been ineffective in preventing central inflammation in heart failure and the challenges associated with identifying targets within the brain and effective methods of delivery of therapeutic compounds across the blood-brain barrier.

A relatively new area of research is the influence of the gut microbiome on the immune and the cardiovascular systems. Abboud et al. examined the effect of altering post-natal gut microbiota in the spontaneously hypertensive rat (SHR) on the development of the immune system and the development of hypertension. The method used was cross fostering which changed two major bacteria taxa to those of the normotensive strain, also a pro inflammatory immune cell population was reduced in the spleen and aorta as was the blood pressure of cross-fostered SHR. However, the changes in the microbiome of the normotensive control rats that were cross fostered by SHR, did not change blood pressure in these animals. The mechanism likely involves the changes to the gut biome since it is known that faecal transplants from normotensive rats also lowers blood pressure in SHR (Toral et al., 2019).

Linking the immune and neural systems, Bognara et al. examine the relationship between a centrally mediated autonomic reflex and inflammation. The Bezold-Jarisch reflex is a well characterised response to stimulation of afferents in the cardiopulmonary region that evokes bradycardia, hypotension, and apnoea. Typically, a selective serotonergic 5-HT3 receptor agonist, phenylbiguanide can be used experimentally to activate the reflex. In order to determine whether evoking this reflex could modulate the immune system, the authors measured cytokines in spleen, heart, blood and hypothalamus during lipopolysaccharide induced inflammation. Interestingly, the reflex reduced plasma levels of tumour necrosis factor and interleukin 6 levels in spleen compared to controls but no changes in other cytokines in other tissues were observed. While the precise mechanism is not known, the study confirms the novel interaction between the nervous system and inflammation, helping us to understand this important relationship.

Exploring vascular pathology, Li et al. review the potential of curcumin, a compound found in turmeric, as a therapeutic agent for hypertension and vascular remodelling. They highlight its ability to inhibit protein tyrosine kinase activity, suppress protein kinase C activity, and block protein kinase and mitogen-activated protein kinase (MAPK) pathways. Curcumin has also been shown to block platelet-derived growth factor (PDGF) and the epidermal growth factor receptor (EGFR), both of which are linked to signaling cascades associated with the proliferation and migration of vascular smooth muscle cells. However, the authors also acknowledge challenges in the use of curcumin as a therapeutic agent, such as poor bioavailability, inconsistencies between animal and human studies, potential side effects, and a lack of evidence for drug interactions. Their review highlights the need to bridge the gap between molecular mechanisms and physiological outcomes in order to unlock the full translational potential of research.

The work by Vieira et al. examines the impact of aerobic physical training on hypertensive hearts, and specifically how training impacts cardiac autonomic control, morphology, and functionality. Using the SHR as a model, the authors show that untrained animals had greater sympathetic contribution to basal heart rate and increased morphological parameters when compared to untrained normotensive rats (WKY), as well as lower coronary bed reactivity and reduced left ventricular contractility in response to increased flow or beta-adrenergic agonist administration. Twelve weeks of swim training resulted in an improved in all but the cardiac morphological parameters. The authors conclude that aerobic physical training could reduce arterial pressure in patients with hypertension through integrative systemic adaptations.

In the brief research report of Vernail et al., the authors utilise gold standard arterial pressure radiotelemetry in mice to investigate for the first time how the non-psychoactive cannabinoid compound cannabigerol (CBG) affects blood pressure following acute administration. These first experiments reaffirm that CBG is indeed a potent inhibitor of sympathetic activity to the peripheral vasculature and heart through its high affinity for inhibitory presynaptic α2-adrenergic receptors, inhibiting noradrenaline release and thus lowering blood pressure and heart rate. The cardiovascular actions of CBG warrant further investigation considering the increasing interest in the use of CBG as a treatment for various neurological conditions and cancer.

Vasopressin, also known as antidiuretic hormone, is typically associated with its role in regulating urine concentration. However, it also has a key role in maintaining homeostasis across many of the systems included in this Research Topic. Proczka et al. present a novel perspective on vasopressin, suggesting that it may play a role in modulating ventilation through both direct actions as a circulating hormone and by acting as a central neurotransmitter *via* vasopressin V1a receptors within respiratory centres of the brainstem. As many factors including hypovolemia, hypotension, glycaemic state, exercise, and angiotensin II all are stimulants of vasopressin release, the evidence for respiratory modulation is carefully assessed and future perspectives to test this hypothesis of a role in fine-tuning respiratory homeostasis are provided.

The kidneys are the final mediator of responses to sodium challenge, but this is regulated by integrated cardiovascular, sympathoinhibitory and natriuretic responses. Having previously demonstrated that Gαi2 subunit proteins in the CNS are necessary to preserve sodium balance, and that these proteins are upregulated in the hypothalamic paraventricular nucleus (PVN) when there is a high intake of salt, Moreira et al., aimed to determine the role of $G\alpha i_2$ proteins in response to central *versus* peripheral sodium challenge and the role of known sodium sensing mechanisms on central $G\alpha i_2$ protein-mediated responses and expression. Using oligodeoxynucleotide (ODN) administration to downregulate brain $G\alpha i_2$, they show that these proteins are essential in mediating the integrated responses to peripheral, but not central, alterations in sodium homeostasis. Their studies further suggest a novel interaction between salt sensitive renal afferent nerves and the upregulation and activation of PVN Gαi2 protein gated pathways which are required to maintain a salt resistant phenotype.

Diabetic nephropathy is a leading cause of chronic kidney disease, with activation of the renin angiotensin aldosterone system playing a leading role as a driver of renal inflammation and fibrosis. However, ACE2, an enzyme that converts angiotensin II into angiotensin 1–7, has renoprotective properties that counteract these effects. In their comprehensive review, Nomura et al. propose that activating this pathway may mitigate kidney inflammation and fibrosis and improve kidney function in diabetic nephropathy. Although several compounds that stimulate ACE2 have been identified, none have progressed to clinical use, presenting a promising opportunity for novel drug development to treat this increasingly prevalent clinical condition.

Several papers in the topic look in depth at centrally mediated physiological reflexes that regulate the cardiovascular system. The PVN for example possesses dual neuroendocrine and autonomic functions and Savić et al. present an overview of its role as a major integrative centre for the regulation of blood pressure and blood pressure variability.

In another review article, Miki et al. consider context-specific changes in response to behaviour and external stress in sympathetic nerve activity (SNA) and the shifts in arterial baroreflex loops that accompany these differences. The arterial baroreflex loop is a CNS control system that regulates the blood supply in parallel to individual organs. The review highlights three examples under which the system is challenged (freezing, REM sleep, and treadmill exercise). They show that regionally specific and co-ordinated changes in SNA, heart rate and arterial pressure under these different conditions and resultant behaviours is the result of changes in baroreflex curves, permitting optimised circulatory regulation. From a translational perspective, the authors conclude while these shifts may also occur in the disease state, they are dysfunctional, perturbing their interaction with other regulatory systems and thereby compounding the disease presentation.

The muscle metaboreflex is a centrally mediated physiological response to prolonged exercise, in which the accumulation of excess metabolites in active skeletal muscle activates metabosensitive skeletal muscle afferents. Due to subsequent enhanced sympathetic outflow to the heart and peripheral vasculature, this enables the dynamic matching of changes in left ventricular elastance with peripheral arterial elastance during physical activity. In heart failure, there is a break down in this ventricular-vascular coupling leading to enhanced systemic vasoconstriction and under perfusion of skeletal muscle. Mannozzi et al. hypothesise that under normal conditions, the arterial baroreflex functions to restrain the muscle metaboreflex induced increase in effective arterial elastance in order to maintain muscle perfusion, but that in heart failure, this restraint is attenuated by impaired arterial baroreflex function. The authors elegantly demonstrate this is indeed the case in chronically instrumented canines.

Staying within the theme of supplying energy to active skeletal muscles through the circulatory system, Yamanaka and Waki present an original study focussed on the amygdala, which is an important integrative site for the processing of behavioural, emotional and cardiovascular responses to aversive and non-aversive stressors. The central nucleus is one of the important subnuclei that is a major area involved with the cardiovascular component of the reaction to stress but its role in dynamically changing stimuli has not been investigated. In a major study in rats, the authors examined this topic by recording the blood pressure and heart rate of head restrained rats given dynamically changing appetitive and aversive classical conditioning tasks (Pavlovian procedures). Through a complex series of unpredictive changing events from neutral, aversive to appetitive stimuli, the authors found that the central nucleus is important for adaptively and rapidly regulation of blood pressure in response to emotional conditioned stimuli.

We return now to the gut microbiome, but this time how microbial metabolites and by-products impact the nervous system to modulate thermal sensation, neural conductance, and thermogenesis. In the review by Zhang and Wang, the authors detail recent discoveries that have led to our understanding of how the gut microbiota contributes to the host's ability to thermoregulate in cold climates. Symbiotic gut microbiota is sensitive to the temperature of

the air and can promote non-shivering thermogenesis by the production of bacterial metabolites and such as short-chain fatty acids and secondary bile acids. It is a fascinating example of coevolution of host-microorganism symbionts which help small animals survive in harsh and variable environment.

The final paper we present is the opinion article of Rasia-Filho. They provide a comprehensive overview of evolving techniques used to explore the intricate and diverse characteristics of postsynaptic dendritic spines in regional and cell-specific contexts. High-resolution imaging and single-cell genomics approaches have provided new insights into brain microcircuits and neural plasticity. The author argues that a multilevel analysis combining single-cell transcriptome data, epigenome databases, and detailed neuroanatomy is needed to understand the function of dendritic spines in information processing and connectivity within regional networks. This could include using large-scale nanoscopy and biochemical analysis of protein distributions across dendrites.

In the fast-growing field of Integrative Physiology, major advancements have been made in the last few years, leading to exceptional achievements as we move into the third decade of the 21st Century. This special edition Research Topic, consisting of 26 outstanding submissions, has provided a thorough overview of the current state of the art of the field, highlighting not only the progress made but also the future challenges. The significance of integrative physiology in comprehending intricate homeostatic mechanisms, both in healthy and pathological conditions cannot be overstated and the Research Topic identifies the importance of exploring the underlying mechanisms of proposed therapeutic interventions, be they related to lifestyle, diet, pharmacological or interventional approaches. Furthermore, we must integrate not only at the systems level but also delve into the cellular, molecular, and genetic. This approach is crucial in attaining a thorough understanding of complex physiological processes and implementing effective therapeutics for improved health outcomes.

Author contributions

JTP, JKP, and GH were all contributing editors to the series. All participated in the drafting of the editorial and its revision, read, and approved the submitted version.

Acknowledgments

We thank all the authors and reviewers who participated in this Research Topic.

Conflict of interest

The authors declare that the research was conducted in the absence of any commercial or financial relationships that could be construed as a potential conflict of interest.

Publisher's note

All claims expressed in this article are solely those of the authors and do not necessarily represent those of their affiliated organizations, or those of the publisher, the editors and the reviewers. Any product that may be evaluated in this article, or claim that may be made by its manufacturer, is not guaranteed or endorsed by the publisher.

Reference

Toral, M., Robles-Vera, I., De La Visitación, N., Romero, M., Sánchez, M., Gómez-Guzmán, M., et al. (2019). Role of the immune system in vascular function and blood pressure control induced by faecal microbiota transplantation in rats. *Acta Physiol. (Oxf)* 227, e13285. doi:10.1111/apha.13285

frontiers in Physiology

BRIEF RESEARCH REPORT
published: 20 September 2021
doi: 10.3389/fphys.2021.745285

The Bezold-Jarisch Reflex and The Inflammatory Response Modulation in Unanesthetized Endotoxemic Rats

*Fernanda Brognara[1], Jaci Airton Castania[1], Aline Barbosa Ribeiro[1], Nilton Nascimento Santos-Júnior[2] and Helio Cesar Salgado[1]**

[1]Department of Physiology, Ribeirão Preto Medical School, University of São Paulo, Ribeirão Preto, Brazil, [2]Minas Gerais State University, Passos, Brazil

Evidence indicates that the activation of the parasympathetic branch of the autonomic nervous system may be effective in treating inflammatory diseases. Previously, we have described that baroreflex activation displays anti-inflammatory properties. Analogous to the baroreflex, the Bezold-Jarisch reflex also promotes parasympathetic activation with simultaneous inhibition of the sympathetic system. Thus, the present study aimed to evaluate whether the activation of the Bezold-Jarisch reflex would also have the ability to reduce inflammation in unanesthetized rats. We used lipopolysaccharide (LPS) injection (5 mg/kg, i.p.) to induce systemic inflammation in male Wistar Hannover rats and phenylbiguanide (PBG) administration (5 μg/kg, i.v.) to activate the Bezold-Jarisch reflex. Spleen, heart, hypothalamus, and blood samples were collected to determine the levels of cytokines. Compared to baseline, PBG reduced the arterial pressure (115 ± 2 vs. 88 ± 5 mmHg) and heart rate (380 ± 7 vs. 114 ± 26 bpm), immediately after its administration, confirming the activation of the parasympathetic system and inhibition of the sympathetic system. From the immunological point of view, the activation of the Bezold-Jarisch reflex decreased the plasma levels of TNF (LPS: 775 ± 209 vs. PBG + LPS: 248 ± 30 pg/ml) and IL-6 levels in the spleen (LPS: 39 ± 6 vs. PBG + LPS: 24 ± 4 pg/mg of tissue). However, it did not change the other cytokines in the plasma or the other tissues evaluated. These findings confirm that the activation of the Bezold-Jarisch reflex can modulate inflammation and support the understanding that the cardiovascular reflexes regulate the immune system.

Keywords: Bezold-Jarisch reflex, parasympathetic activation, sympathetic inhibition, phenylbiguanide, inflammation, rats

OPEN ACCESS

Edited by:
Geoffrey A. Head, Baker Heart and Diabetes Institute, Australia

Reviewed by:
Toru Kawada, National Cerebral and Cardiovascular Center, Japan
Leonardo Cardoso, Universidade Federal de Ouro Preto, Brazil

****Correspondence:***
Helio Cesar Salgado
hcsalgado@fmrp.usp.br

Specialty section:
This article was submitted to Integrative Physiology, a section of the journal Frontiers in Physiology

Received: *21 July 2021*
Accepted: *23 August 2021*
Published: *20 September 2021*

Citation:
Brognara F, Castania JA, Ribeiro AB, Santos-Júnior NN and Salgado HC (2021) The Bezold-Jarisch Reflex and The Inflammatory Response Modulation in Unanesthetized Endotoxemic Rats. Front. Physiol. 12:745285. doi: 10.3389/fphys.2021.745285

INTRODUCTION

Several studies highlighted the role of the parasympathetic system in controlling the inflammation in numerous inflammatory diseases (Pavlov et al., 2020). More recently, the baroreflex was identified as a modulator of the inflammatory response (Bassi et al., 2015; Brognara et al., 2018), in addition to its typical function of regulating arterial pressure (Krieger et al., 1982; Chapleau et al., 1988). When activated, the baroreflex results in a neural response that comprises parasympathetic activation and sympathetic activity inhibition contributing to arterial pressure homeostasis (Krieger et al., 1982; Chapleau et al., 1988). Thus, the anti-inflammatory role

played by baroreflex activation is probably associated with its influence on both branches – sympathetic and parasympathetic – of the autonomic nervous system.

The Bezold-Jarisch reflex is a cardiopulmonary reflex in which the parasympathetic innervation of the cardiopulmonary region is crucial to regulate heart rate, systemic vasomotor tone, and respiration, and when activated, promotes bradycardia, hypotension, and apnea (Aviado and Guevara Aviado, 2001). In experimental studies, the Bezold-Jarisch reflex is activated by some pharmacological agents, including a selective serotonergic 5-HT3 receptor agonist, the phenylbiguanide (PBG; Daly and Kirkman, 1988; Bell et al., 1993; Salo et al., 2007; Bezerra et al., 2011; Silva et al., 2016). Analogous to the baroreflex, the Bezold-Jarisch reflex also promotes parasympathetic activation with concomitant inhibition of the sympathetic nervous system. In addition, the baroreflex and the Bezold-Jarisch reflex share a common central pathway in the brainstem (Verberne and Guyenet, 1992; Verberne et al., 1999; Kashihara, 2009).

Considering that baroreflex activation has anti-inflammatory properties, it is reasonable to expect that the Bezold-Jarisch reflex would also have a similar ability since both reflexes share the same central pathway and analogous efferent autonomic response. Therefore, this study aimed to evaluate if the activation of the Bezold-Jarisch reflex can modulate the systemic inflammatory response in unanesthetized endotoxemic rats.

MATERIALS AND METHODS

Experimental Animals

Male Wistar Hannover rats (250–300 g) from the Main Animal Facility of the University of São Paulo (Campus of Ribeirão Preto; Ribeirão Preto, SP, Brazil) were used to perform the study. The animals were kept under a constant light-dark cycle (12 h) and controlled temperature (23°C) with free access to water and food. The experimental protocol of the present study was evaluated and approved by the Committee of Ethics in Animal Research from the Ribeirão Preto Medical School – University of São Paulo (protocol #161/2016).

Surgical Procedures

A cocktail of ketamine and xylazine (50 mg/kg and 10 mg/kg, i.p.) was used to anesthetize the animals to perform the surgical procedures of catheterization. The left femoral artery and vein were catheterized with polyethylene tubing (PE-50 soldered to a PE-10 polyethylene tube; Intramedic, Clay Adams, Parsippany, NJ, United States) for arterial pressure recording and PBG or saline (vehicle) administration, respectively. Furthermore, a catheter (PE-50 polyethylene tube; Intramedic, Clay Adams, Parsippany, NJ, United States) was inserted into the abdominal cavity for the administration of (lipopolysaccharide) LPS from *Escherichia coli* 0111:B4 (Sigma-Aldrich, St. Louis, MO, United States) or saline (vehicle). The catheters were pulled up through a subcutaneous track to the animal's neck and exteriorized at the nape, and surgical incisions were sutured. Analgesic (tramadol hydrochloride: 2 mg/kg, s.c.) was administered to avoid pain.

Experimental Protocol

Forty-eight hours after the surgical procedures, the rats were assigned into four groups:

1. **Sal + Sal:** saline administration (i.v.) followed by saline injection (i.p.).
2. **PBG + Sal:** phenylbiguanide administration (i.v.) followed by saline injection (i.p.).
3. **Sal + LPS:** saline administration (i.v.) followed by LPS injection (i.p.).
4. **PBG + LPS:** phenylbiguanide administration (i.v.) followed by LPS injection (i.p.).

With the animal unanesthetized, the arterial catheter was connected to a polyethylene tube, filled with saline solution, hanging loosely over the cage. This extension was connected to the pressure transducer attached to the recording system. The venous and peritoneal catheters were connected to other polyethylene tubes in order to allow for drug administration. Although the animals were still connected to extensor tubes, the length of extensions allowed the animals to move freely throughout the recording period. Thus, the experiment was conducted with the animals moving freely in their cages, but carefully supervised by the investigator. Silence was maintained in the room to minimize environmental stress. The experimental protocol consisted of 30 min of basal recordings of pulsatile arterial pressure, followed by the administration of PBG (5 μg/kg, i.v.; Bezerra et al., 2011) – to promote the activation of the Bezold-Jarisch reflex – or saline (as control). Five minutes later, the LPS (5 mg/kg, i.p.; Brognara et al., 2018) was administered – to induce systemic inflammation – or saline (as control) was injected. The arterial pressure was recorded until completing 90 min after LPS or saline injection. Next, the arterial pressure recording was suspended, and a blood sample was collected through the catheter from the femoral artery with heparin. Then, the rats were killed by decapitation for quick collection of samples from the spleen, the heart, and the whole hypothalamus, which were immediately frozen in liquid nitrogen. Blood samples were kept on ice until centrifugation at 3500 rpm for 15 min at 4°C. The plasma was then collected, and all biological material was stored at −80°C.

Arterial Pressure Recording and Analysis

The pulsatile arterial pressure was recorded using a pressure transducer (MLT844; ADInstruments, Bella Vista, Australia), an amplifier (ML224; ADInstruments, Bella Vista, Australia), and an analog-to-digital interface (PowerLab, ADInstruments, Bella Vista, Australia). The mean arterial pressure and heart rate analysis were carried out using computer software (LabChart 7.0, ADInstruments, Bella Vista, Australia). The analysis from the prompt response to saline or PBG administration was carried out within the first 5 s after

its injection. For the other moments, a period of 10 min was used.

Cytokine Measurements

On the day of the assay, the tissue samples were homogenized in 0.5 ml of PBS using a homogenizer (Polytron-PT-3100, Evisa, Kinematica, Luzern, Switzerland) and then centrifuged at 1000 rpm for 10 min at 4°C. The plasma and tissue supernatant samples were used to measure the cytokine [tumor necrosis factor-alpha (TNF-α), interleukin (IL)-6, IL-1β, and IL-10] levels by the immunoenzymatic method (ELISA) using Duo set kits from R&D Systems (Minneapolis, MN, United States) according to the manufacturer's instructions.

Statistical Analysis

The analysis of the hemodynamic data was carried out using two-way ANOVA for repeated measures, followed by the Tukey *post-hoc* test. The analysis of inflammatory mediators was carried out using one-way ANOVA, followed by the same *post-hoc* test. Differences were considered statistically significant if $p < 0.05$. Statistical analysis was performed using the SigmaPlot 12.0 software (Systat Software, San Jose, CA, United States), and the results are presented as mean ± standard error of the mean.

RESULTS

Hemodynamic Response to Phenylbiguanide

Right after saline administration (first 5 s), no change was seen in the arterial pressure (112 ± 1 vs. 112 ± 2 mmHg; $p = 0.847$) or heart rate (389 ± 8 vs. 392 ± 9 bpm; $p = 0.887$; **Figures 1A**,**B**). However, the prompt response observed after PBG administration was characterized by a reduction in arterial pressure (115 ± 2 vs. 88 ± 5 mmHg; $p < 0.001$; **Figure 1A**) and an abrupt bradycardia (380 ± 7 vs. 114 ± 26 bpm; $p < 0.001$; **Figure 1B**).

Time Course of Arterial Pressure and Heart Rate

Comparing all the groups at each moment, no changes in arterial pressure were observed over time at any time evaluated (all $p > 0.05$; **Figures 2A**,**B**). That is to say, the injection of LPS or PBG did not promote alterations in arterial pressure over 90 min. Nevertheless, comparing all the moments within the same group, there is an increase in arterial pressure in the PBG + LPS group at 90 min compared to 30 min (108 ± 4 vs. 118 ± 4 mmHg; $p = 0.008$; **Figure 2B**). Saline or PBG administration did not change the heart rate over time (**Figure 2C**). However, all groups that received LPS had an increase in the heart rate starting 60 min after LPS injection which was maintained until the end of the protocol at 90 min (**Figure 2D**). In addition, PBG administration did not prevent the tachycardia induced by LPS over time (**Figure 2D**).

Bezold-Jarisch Reflex Activation and Cytokine Level

The administration of saline associated, or not, with PBG did not modify the plasma cytokine levels (**Figures 3A**–**D**). Instead, the administration of LPS increased all the cytokines evaluated in plasma 90 min after its injection (all $p < 0.05$; **Figures 3A**–**D**). The activation of the Bezold-Jarisch reflex decreased, by more than 60%, the release of TNF-α in plasma 90 min after LPS compared to Sal + LPS (Sal + LPS: 775 ± 209 vs. PBG + LPS: 248 ± 30 pg/ml; $p = 0.044$; **Figure 3A**). However, it did not prevent the increase of the other cytokines induced by LPS (**Figures 3B**–**D**). The analysis of tissue cytokines showed that LPS administration augmented most of the cytokines analyzed in the spleen (**Figures 3E**–**H**), heart (**Figures 3I**–**L**), and

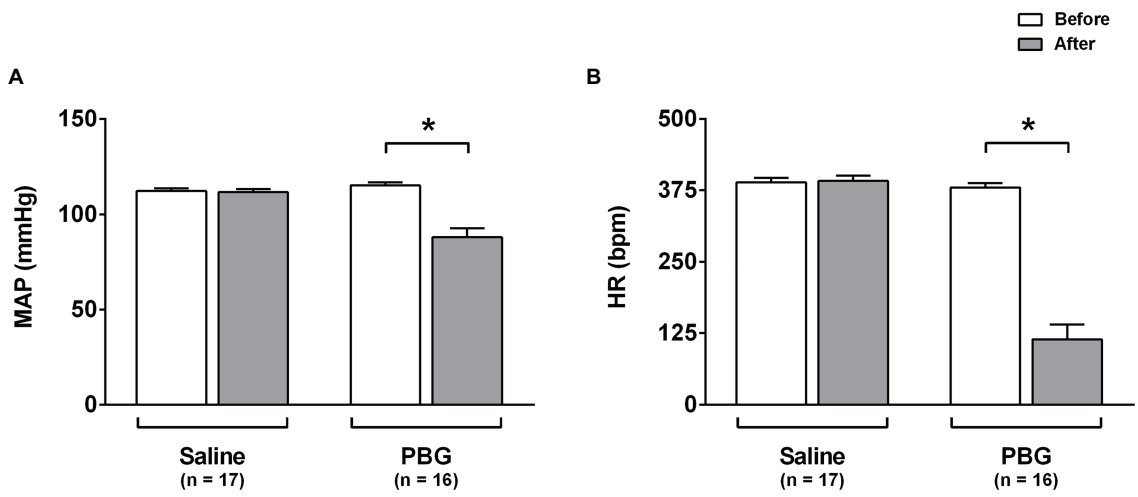

FIGURE 1 | Hemodynamic response to phenylbiguanide. Bar graphs show the mean arterial pressure [MAP **(A)**] and heart rate [HR **(B)**] at baseline (white bars) and after administration (gray bars) of phenylbiguanide (PBG) or saline. LPS, lipopolysaccharide; PBG, phenylbiguanide; and Sal, saline. *$p < 0.05$. Two-way ANOVA for repeated measures with Tukey's *post-hoc* test.

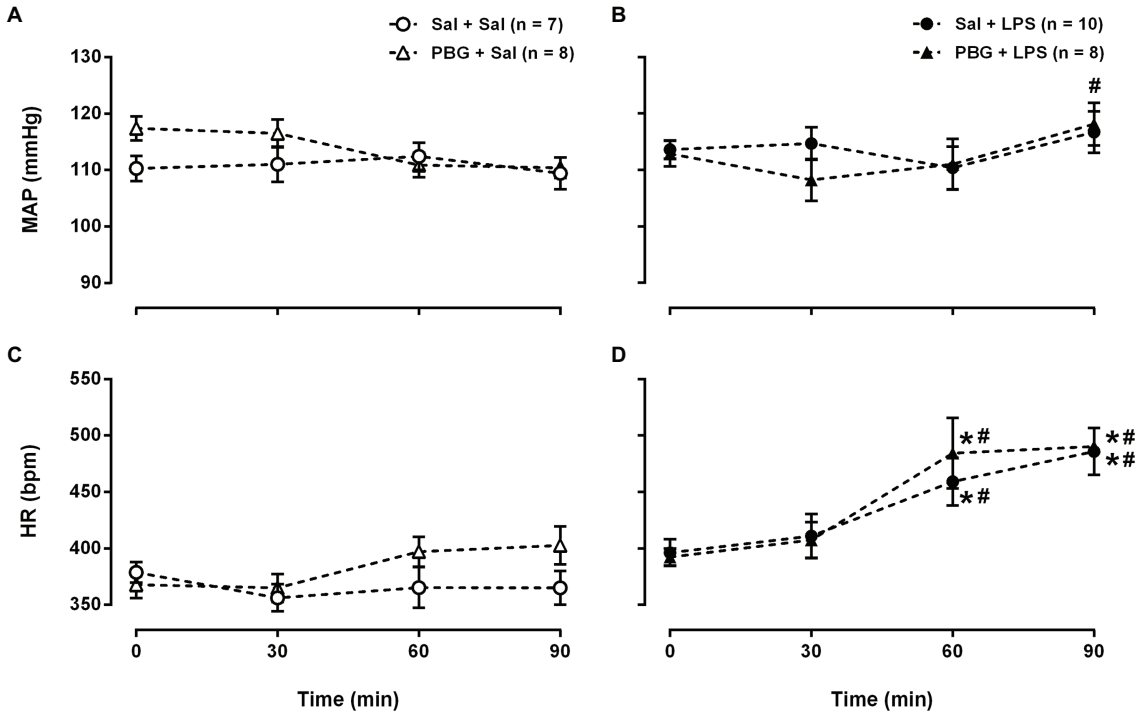

FIGURE 2 | Time course of hemodynamic response to phenylbiguanide and LPS. Mean arterial pressure [MAP **(A)** and **(B)**] and heart rate [HR **(C)** and **(D)**] at baseline (time zero), 30, 60, and 90 min after the administration of LPS or saline from the different groups. LPS, lipopolysaccharide; PBG, phenylbiguanide; and Sal, saline. $^{*}p < 0.05$ vs. 0 min; $^{\#}p < 0.05$ vs. 30 min. Two-way ANOVA for repeated measures with Tukey's *post-hoc* test.

hypothalamus (**Figures 3N–P**). In the spleen, the activation of the Bezold-Jarisch reflex reduced the IL-6 release induced by LPS (Sal + LPS: 39 ± 6 vs. PBG + LPS: 24 ± 4 pg/mg of tissue; $p = 0.037$; **Figure 3F**) but did not decrease the levels of the other cytokines induced by LPS (**Figures 3E,G,H**). In the heart and hypothalamus, the administration of PBG, associated with LPS, did not reduce the release of any cytokine evaluated in the present study (**Figures 3I–P**). Undetected levels of TNF-α were observed in the hypothalamus (**Figure 3M**).

DISCUSSION

Classically, the activation of the Bezold-Jarisch reflex promotes hypotension and bradycardia (Aviado and Guevara Aviado, 2001). The reflex vasodilation of the Bezold-Jarisch reflex is, in fact, because of the inhibition of the sympathetic vasoconstrictor tone (Bell et al., 1993; Verberne et al., 2003). This sympathetic inhibition due to the activation of the Bezold-Jarisch reflex was demonstrated in the lumbar (Verberne and Guyenet, 1992; Sartor and Verberne, 2006), splanchnic (Sartor and Verberne, 2006), splenic (Weaver et al., 1984), and renal nerves (Weaver et al., 1984; Bell et al., 1993). On the other hand, the bradycardia in the Bezold-Jarisch reflex is predominantly due to parasympathetic activation (Daly and Kirkman, 1988; Verberne and Guyenet, 1992). Of note, the hypotension and bradycardia promoted by the activation of the Bezold-Jarisch reflex, evoked by PBG administration, were observed in both anesthetized (Salo et al., 2007; Futuro Neto et al., 2011) and unanesthetized (Chianca and Machado, 1996; Bezerra et al., 2011; Silva et al., 2016) rats. Both responses were observed in the present study indicating that the administration of PBG promoted conspicuous parasympathetic activation and sympathetic inhibition, validating the activation of the Bezold-Jarisch reflex in the chosen model.

The tachycardia observed after LPS administration in the present study aligns with the literature (Altavilla et al., 2002; Brognara et al., 2019). Regarding the arterial pressure response, some studies reported that, over time, LPS reduced the arterial pressure (Mehanna et al., 2007; Sallam et al., 2018). On the other hand, other reports described an increase (Lee et al., 2005; Brognara et al., 2019), or even no changes in the arterial pressure (Brognara et al., 2018) due to LPS administration in unanesthetized rats. Thus, the effects of LPS in the arterial pressure are quite variable in rats, and definitely involve many factors, such as gender, strain, quality and dose of the LPS, and level of anesthesia, among others. The increase in the peripheral vascular resistance over time after LPS administration, due to a rise in sympathetic nerve activity observed in anesthetized rats (Tohyama et al., 2018) and the augmented sympathetic modulation of the vessels demonstrated by the power of the low frequency band of the systolic arterial pressure in unanesthetized rats (Brognara et al., 2019), has also been proposed as a mechanism to explain the LPS impact on arterial pressure.

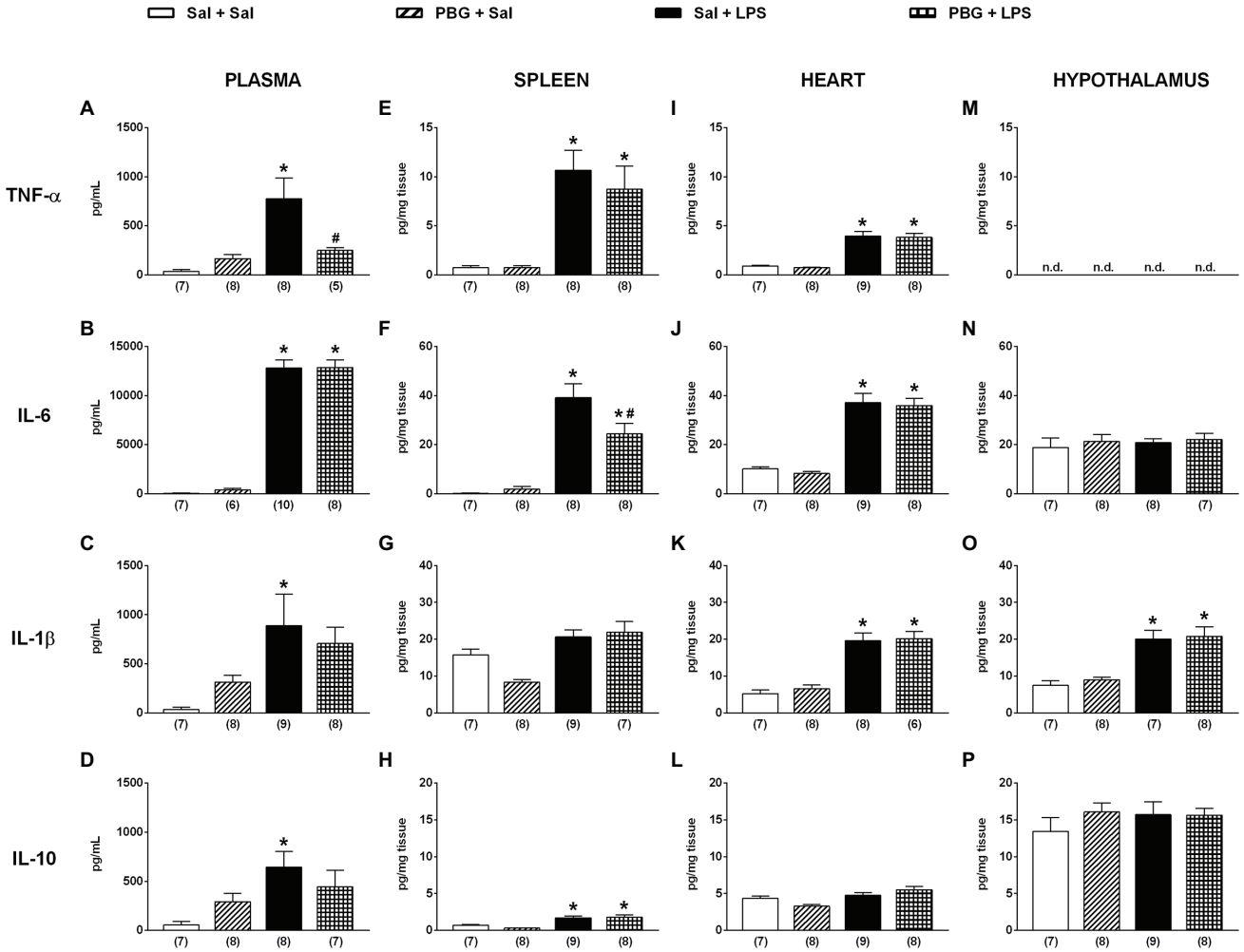

FIGURE 3 | Bezold-Jarisch reflex activation decreased the release of TNF-α induced by LPS in plasma and IL-6 in the spleen. Bar graphs show the levels of TNF-α, IL-6, IL-1β, and IL-10 in plasma **(A-D)**, spleen **(E-H)**, heart **(I-L)**, and hypothalamus **(M-P)** 90 min after the administration of LPS or saline in the different groups. IL-6, interleukin 6; IL-1β, interleukin 1β; IL-10, interleukin 10; LPS, lipopolysaccharide; n.d, not detected; PBG, phenylbiguanide; Sal, saline; and TNF-α, tumor necrosis factor-alpha. $^{*}p < 0.05$ vs. Sal + Sal group; $^{\#}p < 0.05$ vs. Sal + LPS group. One-way ANOVA with Tukey's *post-hoc* test. The number in parentheses represents the number of samples of each group.

The central activation pathways for the Bezold-Jarisch reflex consist of the same paths as the baroreflex (Verberne and Guyenet, 1992; Verberne et al., 1999; Kashihara, 2009). Considering that previous reports from our laboratory demonstrated that the stimulation of the baroreflex promoted anti-inflammatory effects in rats (Bassi et al., 2015; Brognara et al., 2018), it was expected that the activation of the Bezold-Jarisch reflex would also produce the same result. Our findings showed that the activation of the Bezold-Jarisch reflex reduced the cytokine release induced by systemic inflammation in unanesthetized rats. However, the anti-inflammatory effects of the activation of the Bezold-Jarisch reflex were not the same as those shown for the baroreflex activation. Brognara et al. (2018) demonstrated that baroreflex activation reduced TNF, IL-6, IL1β, and IL-10 in the hypothalamus of endotoxemic rats without changing the levels of the same cytokines in plasma, spleen, or heart. In the current study, the Bezold-Jarisch reflex did not decrease the inflammation in the hypothalamus or the heart but reduced the levels of TNF-α in the plasma and IL-6 in the spleen. These data indicate that as: (1) although limited to some cytokines and territories, the Bezold-Jarisch reflex exhibited systemic anti-inflammatory modulation and (2) that parasympathetic activation and sympathetic inhibition promoted by the Bezold-Jarisch reflex have different anti-inflammatory properties than those resulting from baroreflex stimulation.

It is noteworthy that the study by Brognara et al. (2018) was also conducted on unanesthetized rats which were subjected to the induction of systemic inflammation through the administration of LPS, as in the present study. However, an essential factor may justify the differences observed in the anti-inflammatory effects promoted by each reflex: The method chosen to activate the parasympathetic and inhibit the sympathetic nervous system. In the experiments from Brognara et al. (2018),

the baroreflex was activated through electrical stimulation of the aortic depressor nerve; in other words, a neurostimulation approach was used. In the current study, a pharmacological method was chosen to trigger the Bezold-Jarisch reflex. Thus, although the efferent autonomic response was practically the same for both reflexes, resulting in parasympathetic activation and concomitant sympathetic inhibition, the different afferent approaches used to activate these reflexes appeared to interfere with the effector inflammatory response.

In the present study, the anti-inflammatory effect of the Bezold-Jarisch reflex was limited for TNF-α in plasma and IL-6 in the spleen. Nevertheless, although limited to some cytokines, these data deserve special attention since this reduction by more than 60% in circulating TNF-α could produce a crucial biological role, as TNF-α alone can induce a local and systemic inflammatory profile (Tracey et al., 1986, 1987). Likewise, the cytokine reduction in the spleen is consistent with "cholinergic anti-inflammatory pathway" activation (Tracey, 2002). It is possible that efferent parasympathetic pathway – stimulated by the Bezold-Jarisch reflex – has activated, *via* the vagus nerve and the splenic nerves, which in turn resulted in the recruitment of acetylcholine-producing T cells in the spleen and downregulated the inflammation by the alpha-7 nicotinic acetylcholine receptor on macrophages, as previously proposed in the literature on the "cholinergic anti-inflammatory pathway" (Wang et al., 2003; Tracey, 2010; Rosas-Ballina et al., 2011; Dantzer, 2018). Thus, this reduction of TNF in plasma and IL-6 in the spleen suggests that the activation of the Bezold-Jarisch reflex can have an even more significant biological function than previously believed, involving an anti-inflammatory role. However, further studies are needed to identify whether these anti-inflammatory effects promoted by the activation of the Bezold-Jarisch reflex are predominantly due to parasympathetic activation or sympathetic inhibition.

Of note, the influence of the Bezold-Jarisch reflex on the other cytokines in plasma (IL-6, IL-1β, and IL-10) and the spleen (TNF-α, IL-1β, and IL-10) may have a different time course, occurring later, or even earlier. That is to say, the anti-inflammatory effect produced by the parasympathetic activation and sympathetic inhibition due to the activation of the Bezold-Jarisch reflex would require more, or less, than 90 min after LPS to be effective. In that regard, the literature has suggested that the anti-inflammatory effects promoted by vagus nerve stimulation are related to how long after vagal activation the injury is induced, suggesting that this anti-inflammatory pathway needs a complex neuroimmune interaction that may not occur immediately (Inoue et al., 2016). Therefore, we comprehend that the data presented here are preliminary and need further studies to deeply understand the role of the Bezold-Jarisch reflex in controlling inflammation. The conceivable studies would involve the evaluation of the cytokine levels in plasma and tissues at different times during the development of the systemic inflammatory response in unanesthetized rats; a longer period for the activation of the Bezold-Jarisch reflex before inducing the systemic inflammation; tests of different doses of LPS and PBG; and also subdiaphragmatic vagotomy to exclude a non-neuronal effect.

Recently, it was demonstrated that the magnitude of the bradycardic response promoted by the activation of the Bezold-Jarisch reflex is increased 3 and 24 h after LPS administration in rats (Amorim et al., 2019). The authors suggest that during systemic inflammation, the increase in the cardiac component of the Bezold-Jarisch reflex could be beneficial to modulate the inflammatory response. Although Amorim et al. (2019) evaluated the Bezold-Jarisch reflex after LPS administration and, in the present study, the activation of this reflex was conducted before the induction of the immune challenge, the current data confirm the influence of the activation of the Bezold-Jarisch reflex on the modulation of the systemic inflammation in rats, in agreement with the literature speculated previously.

In recent years, serotonin has been associated with several functions of the immune system in addition to its role in regulating other physiological mechanisms (Herr et al., 2017). Immune cells express serotonin receptors, including the 5-HT3 receptor (Khan and Poisson, 1999), modulating the inflammatory response. Serotonin reduced cytokine production in human monocytes (Arzt et al., 1991; Cloëz-Tayarani et al., 2003), in primary rat aortic smooth muscle cells (Yu et al., 2008), and also *in vivo* (Nau et al., 2013). Moreover, central serotonin administration decreased plasma and spleen cytokine release induced by LPS in rats (Mota et al., 2019). Serotonin also has a pro-inflammatory effect stimulating the release of cytokine (Ito et al., 2000). This dual role of serotonin may be related to the serotonin receptor subtype class that is activated (Dürk et al., 2005). Selective activation of serotonin 5-HT2A receptors prevented the IL-6 release during a systemic inflammatory response (Nau et al., 2013). On the other hand, the inhibition of 5-HT3 receptors abolished the release of LPS-induced cytokine, suggesting that this serotonin receptor subtype activation participates in the release of pro-inflammatory cytokines, possessing not an anti-inflammatory but a pro-inflammatory function (Fiebich et al., 2004). Thus, since a selective serotonergic 5-HT3 receptor agonist was used to activate the Bezold-Jarisch reflex, it is reasonable to suggest that the anti-inflammatory effects observed in the present study are due to the Bezold-Jarisch reflex activation and not to the direct effect of serotonin receptor stimulation in the immune cells.

In conclusion, this is the first study confirming that the activation of the Bezold-Jarisch reflex induced by PBG administration possesses specific anti-inflammatory effects in rats. In other words, PBG administration to unanesthetized endotoxemic rats elicits the activation of the Bezold-Jarisch reflex and can modulate the release of TNF-α in plasma and IL-6 in the spleen. This novel mechanism of neuromodulation will undoubtedly present new noteworthy questions concerning the investigation of the neural control of inflammation. Further studies should be conducted under different inflammatory conditions to deeply understand the role of cardiovascular reflexes in the inflammatory response, including the mechanisms involved in the activation of the Bezold-Jarisch reflex and the reduction in production and release of cytokines.

DATA AVAILABILITY STATEMENT

The raw data supporting the conclusions of this article will be made available by the authors, without undue reservation.

ETHICS STATEMENT

The animal study was reviewed and approved by the Committee of Ethics in Animal Research from the Ribeirão Preto Medical School – University of São Paulo (protocol # 161/2016).

AUTHOR CONTRIBUTIONS

FB and HS: conception or design of the work. FB, JC, AR, and NS-J: acquisition or analysis or interpretation of data for the work. FB, JC, AR, NS-J, and HS: drafting the work or revising it critically for important intellectual content. All authors approved the final version of the manuscript and agreed to be accountable for all aspects of the work in ensuring that questions related to the accuracy or integrity of any part of the work are appropriately investigated and resolved.

FUNDING

This work was supported by the São Paulo Research Foundation (FAPESP; process #2013/20549–7; #2017/05163–6; #2018/20939–3; #2018/10455–9; and #2020/06043–7), Foundation for the Support of Teaching, Research and Service (FAEPA; process #580/21 and #581/21), and the Academic Excellence Program (PROEX) from the Coordination for the Improvement of Higher Education Personnel (CAPES; process #88887.505419/2020–00).

ACKNOWLEDGMENTS

The São Paulo Research Foundation (FAPESP), the Coordination for the Improvement of Higher Education Personnel (CAPES), the Foundation for the Support of Teaching, Research and Service (FAEPA), and the University of São Paulo (USP) are gratefully acknowledged.

REFERENCES

Altavilla, D., Squadrito, G., Minutoli, L., Deodato, B., Bova, A., Sardella, A., et al. (2002). Inhibition of nuclear factor-kappaB activation by IRFI 042, protects against endotoxin-induced shock. *Cardiovasc. Res.* 54, 684–693. doi: 10.1016/S0008-6363(02)00276-6

Amorim, M. R., de Deus, J. L., Cazuza, R. A., Mota, C. M. D., da Silva, L. E. V., Borges, G. S., et al. (2019). Neuroinflammation in the NTS is associated with changes in cardiovascular reflexes during systemic inflammation. *J. Neuroinflammation* 16:125. doi: 10.1186/s12974-019-1512-6

Arzt, E., Costas, M., Finkielman, S., and Nahmod, V. E. (1991). Serotonin inhibition of tumor necrosis factor-alpha synthesis by human monocytes. *Life Sci.* 48, 2557–2562. doi: 10.1016/0024-3205(91)90612-F

Aviado, D. M., and Guevara Aviado, D. (2001). The Bezold-Jarisch reflex. A historical perspective of cardiopulmonary reflexes. *Ann. N. Y. Acad. Sci.* 940, 48–58. doi: 10.1111/j.1749-6632.2001.tb03666.x

Bassi, G. S., Brognara, F., Castania, J. A., Talbot, J., Cunha, T. M., Cunha, F. Q., et al. (2015). Baroreflex activation in conscious rats modulates the joint inflammatory response via sympathetic function. *Brain Behav. Immun.* 49, 140–147. doi: 10.1016/j.bbi.2015.05.002

Bell, L. B., O'Hagan, K. P., and Clifford, P. S. (1993). Cardiac but not pulmonary receptors mediate depressor response to IV phenyl biguanide in conscious rabbits. *Am. J. Phys.* 264, R1050–R1057. doi: 10.1152/ajpregu.1993.264.6.R1050

Bezerra, VM, Xavier, CH, Menezes, RCAde, Fontes, MAP, Cardoso, LM, Fernandes, LG, et al. (2011). Bezold–Jarisch reflex in sino-aortic denervated malnourished rats. *Auton. Neurosci. Basic Clin.* 162, 48–53. doi:10.1016/j.autneu.2011.03.006.

Brognara, F., Castania, J. A., Dias, D. P. M., Kanashiro, A., and Salgado, H. C. (2019). Time course of hemodynamic responses to different doses of lipopolysaccharide in Unanesthetized male rats. *Front. Physiol.* 10:771. doi: 10.3389/fphys.2019.00771

Brognara, F., Castania, J. A., Dias, D. P. M., Lopes, A. H., Fazan, R. Jr., Kanashiro, A., et al. (2018). Baroreflex stimulation attenuates central but not peripheral inflammation in conscious endotoxemic rats. *Brain Res.* 1682, 54–60. doi: 10.1016/j.brainres.2018.01.003

Chapleau, M. W., Hajduczok, G., and Abboud, F. M. (1988). Mechanisms of resetting of arterial baroreceptors: an overview. *Am. J. Med. Sci.* 295, 327–334.

Chianca, D. A., and Machado, B. H. (1996). Microinjection of NMDA antagonist into the NTS of conscious rats blocks the Bezold-Jarisch reflex. *Brain Res.* 718, 185–188. doi: 10.1016/0006-8993(96)00010-8

Cloëz-Tayarani, I., Petit-Bertron, A., Venters, H. D., and Cavaillon, J. (2003). Differential effect of serotonin on cytokine production in lipopolysaccharide-stimulated human peripheral blood mononuclear cells: involvement of 5-hydroxytryptamine2A receptors. *Int. Immunol.* 15, 233–240. doi: 10.1093/intimm/dxg027

Daly, M. D., and Kirkman, E. (1988). Cardiovascular responses to stimulation of pulmonary C fibres in the cat: their modulation by changes in respiration. *J. Physiol.* 402, 43–63. doi: 10.1113/jphysiol.1988.sp017193

Dantzer, R. (2018). Neuroimmune interactions: From the brain to the immune system and vice versa. *Physiol. Rev.* 98, 477–504. doi: 10.1152/physrev.00039.2016

Dürk, T., Panther, E., Müller, T., Sorichter, S., Ferrari, D., Pizzirani, C., et al. (2005). 5-Hydroxytryptamine modulates cytokine and chemokine production in LPS-primed human monocytes via stimulation of different 5-HTR subtypes. *Int. Immunol.* 17, 599–606. doi: 10.1093/intimm/dxh242

Fiebich, B., Akundi, R., Lieb, K., Candelario-Jalil, E., Gmeiner, D., Haus, U., et al. (2004). Antiinflammatory effects of 5-HT3 receptor antagonists in lipopolysaccharide-stimulated primary human monocytes. *Scand. J. Rheumatol.* 33, 28–32. doi: 10.1080/03009740410006998

Futuro Neto, H. A., Macedo, S. M., Silva, N. F., Cabral, A. M., and Pires, J. G. P. (2011). Central 5-HT 2A receptors modulate the vagal bradycardia in response to activation of the von Bezold-Jarisch reflex in anesthetized rats. *Braz. J. Med. Biol. Res.* 44, 224–228. doi: 10.1590/S0100-879X2011007500016

Herr, N., Bode, C., and Duerschmied, D. (2017). The effects of serotonin in immune cells. *Front. Cardiovasc. Med.* 4:48. doi: 10.3389/fcvm.2017.00048

Inoue, T., Abe, C., Sung, S. J., Moscalu, S., Jankowski, J., Huang, L., et al. (2016). Vagus nerve stimulation mediates protection from kidney ischemia-reperfusion injury through α7nAChR^{+} splenocytes. *J. Clin. Invest.* 126, 1939–1952. doi: 10.1172/JCI83658

Ito, T., Ikeda, U., Shimpo, M., Yamamoto, K., and Shimada, K. (2000). Serotonin increases Interleukin-6 synthesis in human vascular smooth muscle cells. *Circulation* 102, 2522–2527. doi: 10.1161/01.CIR.102.20.2522

Kashihara, K. (2009). Roles of arterial baroreceptor reflex during bezold-jarisch reflex. *Curr. Cardiol. Rev.* 5, 263–267. doi: 10.2174/157340309789317805

Khan, N.-A., and Poisson, J.-P. (1999). 5-HT3 receptor-channels coupled with Na+ influx in human T cells: role in T cell activation. *J. Neuroimmunol.* 99, 53–60. doi: 10.1016/S0165-5728(99)00101-0

Krieger, E. M., Salgado, H. C., and Michelini, L. C. (1982). Resetting of the baroreceptors. *Int. Rev. Physiol.* 26, 119–146.

Lee, C.-C., Lin, N.-T., Hsu, Y. H., and Chen, H. I. (2005). Inducible nitric oxide synthase inhibition potentiates multiple organ dysfunction induced

by endotoxin in conscious rats. *J. Cardiovasc. Pharmacol.* 45, 396–403. doi: 10.1097/01.fjc.0000157438.72483.ae

Mehanna, A., Vitorino, D. C., Panis, C., Blanco, E. E. A., Pinge-Filho, P., and Martins-Pinge, M. C. (2007). Cardiovascular and pulmonary effects of NOS inhibition in endotoxemic conscious rats subjected to swimming training. *Life Sci.* 81, 1301–1308. doi: 10.1016/j.lfs.2007.09.006

Mota, C., Borges, G., Amorim, M., Carolino, R., Batalhão, M., Anselmo-Franci, J., et al. (2019). Central serotonin prevents hypotension and hypothermia and reduces plasma and spleen cytokine levels during systemic inflammation. *Brain Behav. Immun.* 80, 255–265. doi: 10.1016/j.bbi.2019.03.017

Nau, F. J., Yu, B., Martin, D., and Nichols, C. D. (2013). Serotonin 5-HT2A receptor activation blocks TNF-α mediated inflammation In vivo. *PLoS One* 8:e75426. doi: 10.1371/journal.pone.0075426

Pavlov, V. A., Chavan, S. S., and Tracey, K. J. (2020). Bioelectronic medicine: From preclinical studies on the inflammatory reflex to new approaches in disease diagnosis and treatment. *Cold Spring Harb. Perspect. Med.* 10:a034140. doi: 10.1101/cshperspect.a034140

Rosas-Ballina, M., Olofsson, P. S., Ochani, M., Valdés-Ferrer, S. I., Levine, Y. A., Reardon, C., et al. (2011). Acetylcholine-synthesizing T cells relay neural signals in a vagus nerve circuit. *Science* 334, 98–101. doi: 10.1126/science.1209985

Sallam, M. Y., El-Gowilly, S. M., El-Gowelli, H. M., El-Lakany, M. A., and El-Mas, M. M. (2018). Additive counteraction by α7 and α4β2-nAChRs of the hypotension and cardiac sympathovagal imbalance evoked by endotoxemia in male rats. *Eur. J. Pharmacol.* 834, 36–44. doi: 10.1016/j.ejphar.2018.07.008

Salo, L. M., Woods, R. L., Anderson, C. R., and McAllen, R. M. (2007). Nonuniformity in the von Bezold-Jarisch reflex. *Am. J. Physiol. Regul. Integr. Comp. Physiol.* 293, R714–R720. doi: 10.1152/ajpregu.00099.2007

Sartor, D. M., and Verberne, A. J. M. (2006). The sympathoinhibitory effects of systemic cholecystokinin are dependent on neurons in the caudal ventrolateral medulla in the rat. *Am. J. Physiol. Regul. Integr. Comp. Physiol.* 291, R1390–R1398. doi: 10.1152/ajpregu.00314.2006

Silva, F. C., Paiva, F. A., Müller-Ribeiro, F. C., Caldeira, H. M. A., Fontes, M. A. P., de Menezes, R. C. A., et al. (2016). Chronic treatment with Ivabradine does not affect cardiovascular autonomic control in rats. *Front. Physiol.* 7:305. doi: 10.3389/fphys.2016.00305

Tohyama, T., Saku, K., Kawada, T., Kishi, T., Yoshida, K., Nishikawa, T., et al. (2018). Impact of lipopolysaccharide-induced acute inflammation on baroreflex-controlled sympathetic arterial pressure regulation. *PLoS One* 13:e0190830. doi: 10.1371/journal.pone.0190830

Tracey, K. J. (2002). The inflammatory reflex. *Nature* 420, 853–859. doi: 10.1038/nature01321

Tracey, K. J. (2010). Understanding immunity requires more than immunology. *Nat. Immunol.* 11, 561–564. doi: 10.1038/ni0710-561

Tracey, K. J., Beutler, B., Lowry, S. F., Merryweather, J., Wolpe, S., Milsark, I. W., et al. (1986). Shock and tissue injury induced by recombinant human cachectin. *Science* 234, 470–474. doi: 10.1126/science.3764421

Tracey, K., Fong, Y., Hesse, D., Manogue, K., Lee, A., Kuo, G., et al. (1987). Anti-cachectin/TNF monoclonal antibodies prevent septic shock during lethal bacteraemia. *Nature* 330, 662–664. doi: 10.1038/330662a0

Verberne, A. J., and Guyenet, P. G. (1992). Medullary pathway of the Bezold-Jarisch reflex in the rat. *Am. J. Phys.* 263, R1195–R1202. doi: 10.1152/ajpregu.1992.263.6.R1195

Verberne, A. J. M., Saita, M., and Sartor, D. M. (2003). Chemical stimulation of vagal afferent neurons and sympathetic vasomotor tone. *Brain Res. Rev.* 41, 288–305. doi: 10.1016/S0165-0173(02)00269-2

Verberne, A. J., Stornetta, R. L., and Guyenet, P. G. (1999). Properties of C1 and other ventrolateral medullary neurones with hypothalamic projections in the rat. *J. Physiol.* 517, 477–494. doi: 10.1111/j.1469-7793.1999.0477t.x

Wang, H., Yu, M., Ochani, M., Amella, C. A., Tanovic, M., Susarla, S., et al. (2003). Nicotinic acetylcholine receptor alpha7 subunit is an essential regulator of inflammation. *Nature* 421, 384–388. doi: 10.1038/nature01339

Weaver, L. C., Fry, H. K., and Meckler, R. L. (1984). Differential renal and splenic nerve responses to vagal and spinal afferent inputs. *Am. J. Phys.* 246:R78. doi: 10.1152/ajpregu.1984.246.1.R78

Yu, B., Becnel, J., Zerfaoui, M., Rohatgi, R., Boulares, A. H., and Nichols, C. D. (2008). Serotonin 5-Hydroxytryptamine2A receptor activation suppresses tumor necrosis factor-α-induced inflammation with extraordinary potency. *J. Pharmacol. Exp. Ther.* 327, 316–323. doi: 10.1124/jpet.108.143461

Conflict of Interest: The authors declare that the research was conducted in the absence of any commercial or financial relationships that could be construed as a potential conflict of interest.

Publisher's Note: All claims expressed in this article are solely those of the authors and do not necessarily represent those of their affiliated organizations, or those of the publisher, the editors and the reviewers. Any product that may be evaluated in this article, or claim that may be made by its manufacturer, is not guaranteed or endorsed by the publisher.

Copyright © 2021 Brognara, Castania, Ribeiro, Santos-Júnior and Salgado. This is an open-access article distributed under the terms of the Creative Commons Attribution License (CC BY). The use, distribution or reproduction in other forums is permitted, provided the original author(s) and the copyright owner(s) are credited and that the original publication in this journal is cited, in accordance with accepted academic practice. No use, distribution or reproduction is permitted which does not comply with these terms.

frontiers in Physiology

REVIEW
published: 26 October 2021
doi: 10.3389/fphys.2021.744177

Vasopressin and Breathing: Review of Evidence for Respiratory Effects of the Antidiuretic Hormone

*Michał Proczka[1], Jacek Przybylski[2], Agnieszka Cudnoch-Jędrzejewska[3], Ewa Szczepańska-Sadowska[3] and Tymoteusz Żera[3]**

[1]Department of Experimental and Clinical Physiology, Doctoral School, Medical University of Warsaw, Warsaw, Poland, [2]Department of Biophysics, Physiology, and Pathophysiology, Laboratory of Centre for Preclinical Research, Medical University of Warsaw, Warsaw, Poland, [3]Department of Experimental and Clinical Physiology, Laboratory of Centre for Preclinical Research, Medical University of Warsaw, Warsaw, Poland

Vasopressin (AVP) is a key neurohormone involved in the regulation of body functions. Due to its urine-concentrating effect in the kidneys, it is often referred to as antidiuretic hormone. Besides its antidiuretic renal effects, AVP is a potent neurohormone involved in the regulation of arterial blood pressure, sympathetic activity, baroreflex sensitivity, glucose homeostasis, release of glucocorticoids and catecholamines, stress response, anxiety, memory, and behavior. Vasopressin is synthesized in the paraventricular (PVN) and supraoptic nuclei (SON) of the hypothalamus and released into the circulation from the posterior lobe of the pituitary gland together with a C-terminal fragment of pro-vasopressin, known as copeptin. Additionally, vasopressinergic neurons project from the hypothalamus to the brainstem nuclei. Increased release of AVP into the circulation and elevated levels of its surrogate marker copeptin are found in pulmonary diseases, arterial hypertension, heart failure, obstructive sleep apnoea, severe infections, COVID-19 due to SARS-CoV-2 infection, and brain injuries. All these conditions are usually accompanied by respiratory disturbances. The main stimuli that trigger AVP release include hyperosmolality, hypovolemia, hypotension, hypoxia, hypoglycemia, strenuous exercise, and angiotensin II (Ang II) and the same stimuli are known to affect pulmonary ventilation. In this light, we hypothesize that increased AVP release and changes in ventilation are not coincidental, but that the neurohormone contributes to the regulation of the respiratory system by fine-tuning of breathing in order to restore homeostasis. We discuss evidence in support of this presumption. Specifically, vasopressinergic neurons innervate the brainstem nuclei involved in the control of respiration. Moreover, vasopressin V1a receptors (V1aRs) are expressed on neurons in the respiratory centers of the brainstem, in the circumventricular organs (CVOs) that lack a blood-brain barrier, and on the chemosensitive type I cells in the carotid bodies. Finally, peripheral and central administrations of AVP or antagonists of V1aRs increase/decrease phrenic nerve activity and pulmonary ventilation in a site-specific manner. Altogether, the findings discussed in this review strongly argue for the hypothesis that vasopressin affects ventilation both as a blood-borne neurohormone and as a neurotransmitter within the central nervous system.

Keywords: antidiuretic hormone, respiration, cardiovascular system, carotid body, sympathetic nervous system, circumventricular organs, brainstem, paraventricular nucleus of the hypothalamus

OPEN ACCESS

Edited by:
James Todd Pearson, National Cerebral and Cardiovascular Center, Japan

Reviewed by:
Rohit Ramchandra, The University of Auckland, New Zealand
Débora Simões A. Colombari, São Paulo State University, Brazil
Steven Allen Crone, Cincinnati Children's Hospital Medical Center, United States

****Correspondence:***
Tymoteusz Żera
tzera@wum.edu.pl

Specialty section:
This article was submitted to Integrative Physiology, a section of the journal Frontiers in Physiology

Received: *19 July 2021*
Accepted: *27 September 2021*
Published: *26 October 2021*

Citation:
Proczka M, Przybylski J, Cudnoch-Jędrzejewska A, Szczepańska-Sadowska E and Żera T (2021) Vasopressin and Breathing: Review of Evidence for Respiratory Effects of the Antidiuretic Hormone. Front. Physiol. 12:744177. doi: 10.3389/fphys.2021.744177

INTRODUCTION

Vasopressin (AVP), also known as antidiuretic hormone, is a neurohormone critically involved in maintaining body homeostasis. It is synthesized in discrete nuclei of the hypothalamus and transported to the posterior lobe of the pituitary gland, from where it is released into the circulation in response to increase of extracellular fluid osmolality. In the bloodstream, AVP is paramount for maintaining water balance thanks to its renal action resulting in water reabsorption and urine concentration. The other stimuli for AVP release include hypovolemia, hypotension, hypoxia, hypoglycemia, strenuous exercise, and angiotensin II (Ang II; Szczepanska-Sadowska et al., 2017). The same stimuli also promote increases in pulmonary ventilation and are often associated with life-threatening conditions (Doerschug et al., 2010; Frier, 2014; Thompson et al., 2016; Convertino et al., 2019; Lüning et al., 2019).

In addition to its effects in the kidney, AVP exerts numerous extra-renal effects, including circulatory, nervous, endocrine, metabolic, and behavioral ones, which are discussed in detail in recent reviews (Szczepanska-Sadowska et al., 2017; Japundžić-Žigon et al., 2020). Together, these AVP-mediated responses counteract disturbances of the body homeostasis and help in adjusting body function to internal and environmental stressors. Along with the control of circulatory and nervous system, the precise regulation of the respiratory system is also critical for the homeostatic adjustments. It is important to realize that changes in pulmonary ventilation fulfil their adaptive role only when they are matched with parallel changes in cardiac output and body metabolism. In this review, we summarize the most important studies analyzing regulation of AVP release and discuss the effects of this neuropeptide on the respiration under physiological and pathophysiological conditions, acting both as a blood-borne neurohormone and as a neurotransmitter within the central nervous system.

PHYSIOLOGY OF VASOPRESSIN

Vasopressin: Synthesis, Receptors, and Release

Vasopressin is synthesized in the form of pre-pro-AVP, which is processed into AVP, neurophysin II and C-terminal fragment of pre-pro-AVP known as copeptin. The neurohormone is produced predominantly in the paraventricular (PVN) and supraoptic nuclei (SON) of the hypothalamus in two histologically and functionally distinct pools of neurons – magnocellular cells projecting to the posterior pituitary and parvocellular cells projecting to the median eminence and extrahypothalamic brain structures, especially to the limbic system (Buijs, 1978; Dumais and Veenema, 2016) and the brainstem (Buijs, 1978; Kc and Dick, 2010; Kc et al., 2010). Vasopressin is released into the circulation together with copeptin from the axonal terminals of the magnocellular neurons located in the posterior lobe of the pituitary gland (neurohypophysis; Schrier et al., 1979; Szczepanska-Sadowska et al., 2017; Bichet, 2019). Vasopressin is also released from the nerve terminals of the PVN parvocellular cells in the median eminence into the hypothalamic-pituitary circulation, through which AVP reaches anterior lobe of the pituitary gland and promotes ACTH release (Gonzalez-Luque et al., 1970; Lee et al., 2015). Besides hypothalamic synthesis in the PVN and the SON, AVP, or AVP mRNA is locally expressed in peripheral organs, such as the adrenal medulla and the heart (Nussey et al., 1987; Hupf et al., 1999; Takeda et al., 2002). Measurements of plasma concentrations of AVP are highly variable due to binding of the neurohormone to platelets and its short biological half-life (Nickel et al., 2012; Bankir et al., 2017). Copeptin, co-released with AVP in equimolar quantities, is very stable and may serve as a biomarker of AVP release (Morgenthaler et al., 2006; Bankir et al., 2017).

Vasopressin acts *via* three subtypes of receptors, which belong to the G-protein coupled receptors: V1aR, V1bR, and V2R. Vasopressin released into the circulation exerts its cardiovascular effects mainly through V1aRs, which mediate vasoconstriction and increase in vascular resistance in most of the vascular beds (Szczepanska-Sadowska et al., 2017; Japundžić-Žigon et al., 2020), and complex effects in the coronary circulation and cardiac hemodynamics (Pelletier et al., 2014). Binding of AVP to V1aRs expressed on thrombocytes stimulates procoagulant activity of platelets (Launay et al., 1987; Horstman et al., 1995; Colucci et al., 2014).

Vasopressin also exerts numerous endocrine effects mediated by V1aRs and V1bRs that include regulation of insulin and glucagon release from the pancreatic islets, release of catecholamines in the adrenal medulla and glucocorticoids in the adrenal cortex, and stimulation of corticotropin release from the pituitary gland (Nussey et al., 1987; Aguilera and Rabadan-Diehl, 2000; Takeda et al., 2002; Szczepanska-Sadowska et al., 2017; Mohan et al., 2019). In addition, AVP released into the circulation promotes gluconeogenesis and glycogenolysis in the liver and lipid metabolism in the fat tissue (Nakamura et al., 2017).

Vasopressin plays a critical role in the regulation of water-electrolyte balance *via* its V2Rs in the kidney, which depends on upregulation of the aquaporin 2 with resultant water trafficking in the apical membrane of the principal cells of the collecting duct (Wade et al., 1981; Schrier, 2008; Bankir et al., 2017).

Besides the systemic effects of AVP in the bloodstream, the neurohormone serves as a peptidergic neurotransmitter with both synaptic and "volume" mode of neurotransmission (Landgraf and Neumann, 2004). Vasopressin is released in the central nervous system from the nerve terminals of vasopressinergic neurons, whose cell bodies are located in the parvocellular division of the PVN. Up to 40% of the parvocellular cells of the PVN synthesize AVP and project to the brainstem and the spinal cord, where they terminate on sympathetic neurons (Pyner, 2009; Nunn et al., 2011). Vasopressinergic neurons exert either V1aR-dependent sympthoexcitatory effects accompanied by a rise in arterial blood pressure, or sympathoinhibition with activation of the parasympathetic system and sensitization of the arterial baroreflex (Szczepanska-Sadowska et al., 2017; Japundžić-Žigon et al., 2020).

In addition to the central cardiovascular effects, both V1aRs and V1bRs participate in the regulation of mood, anxiety, aggression, pain, cognitive processes and memory, and adaptation to stress (Aguilera and Rabadan-Diehl, 2000; Szczepanska-Sadowska et al., 2017). Emerging evidence indicates that V1bRs may serve as autoreceptors on the vasopressinergic neurons in the hypothalamus (Corbani et al., 2018). Recently, it has been shown that V1bRs may be involved in SARS-CoV-2 infection by participating in the endocytosis of the virus' particles (Yeung et al., 2021). The tissue distribution of AVP receptors, their diverse biological functions, as well as agonists and antagonists are discussed in detail elsewhere (Koshimizu et al., 2012; Szczepanska-Sadowska et al., 2017). The respiratory actions of AVP are discussed in detail in the following sections.

Vasopressin Release and Respiration: Coincidence or Relationship?

The evidence discussed below indicates that stimuli that activate vasopressinergic neurons and increase AVP levels also affect respiratory activity (**Figure 1**). This raises a question whether release of AVP and changes in respiration in response to these stimuli are coincidental, or if there is a functional relationship between AVP and the regulation of the respiratory system. Next, we discuss studies showing increased release of AVP and its surrogate marker copeptin under medical conditions accompanied by respiratory disturbances. Then, we analyze the evidence for AVP involvement in the regulation of respiratory system.

Regulation of Vasopressin Release

Activation of the vasopressinergic neurons and release of AVP into the circulation occurs in response to osmotic and non-osmotic stimuli. The magno- and parvocellular vasopressinergic cells of the hypothalamus are distinctly activated by various stimuli, with magnocellular cells being mostly activated by increase in sodium ion concentration and osmolality, hypovolemia, hypotonia, and hypoxia, while the parvocellular cells are more sensitive to various stressors, such as pain, injury, and psychological stress (Aguilera et al., 2008; Ueta et al., 2011; Bankir et al., 2017; Szczepanska-Sadowska et al., 2017). Next, we discuss main stimuli for AVP release and how they affect the respiratory system.

Osmotic - Dependent AVP Release

Vasopressin is released into the circulation in response to increase in plasma osmolality and sodium ion concentration in directly proportional manner (Verney, 1947; Quillen and Cowley, 1983; Thornton et al., 1986; Baylis, 1987; Verbalis, 2007). In young healthy men, plasma AVP concentration starts to increase at plasma osmolality of 285 mOsm/kg, and continues to rise till values of osmolality exceed 310 mOsm/kg (Baylis and Robertson, 1980; Baylis, 1987). The changes in osmolality are detected in the organum vasculosum of the lamina terminalis (OVLT), in the subfornical organ (SFO), and in the magnocellular neurons of the PVN and the SON (Anderson et al., 2000, 2001; Verbalis, 2007; Bankir et al., 2017; Szczepanska-Sadowska et al., 2017). The changes of extracellular fluid osmolality are mostly affected by changes in sodium ion concentration; however, other osmotically active substances (e.g., mannitol) that affect cell volume also trigger AVP release (Verbalis, 2007). On the other hand, osmotically active solutes freely passing through the cell membrane (e.g., urea), have much weaker effect on cell volume and AVP release (Verbalis, 2007). In addition, changes in activity of AVP neurons and subsequent release of AVP in the posterior pituitary lobe are regulated by availability of water and sensation of thirst and may precede actual changes in the extracellular fluid osmolality (Bankir et al., 2017).

Several studies indicate that plasma osmolality and concentration of sodium ions may contribute to the control of respiration. Specifically, hyperosmolality was shown to inhibit respiration and to reduce increase in pulmonary ventilation evoked by thermoregulatory panting or adjustments to acid-base balance disturbances in animals (Baker and Dawson, 1985; Kasserra et al., 1991; Kasserra and Jones, 1993) and humans (Senay, 1969; Moen et al., 2014). However, it should be noted that experiments in the *in situ* preparations revealed direct excitatory effects of hyperosmolality on the carotid sinus nerve and the phrenic nerve activity (Trzebski et al., 1978; Kasserra et al., 1991; O'Connor and Jennings, 2001; da Silva et al., 2019).

In contrast to hyperosmolality, acute hypoosmolality has been shown to stimulate breathing in conscious dogs (Anderson et al., 1990) and transiently in rats (O'Connor and Jennings, 2001). In women and men, hypoosmolality induced by ingestion of water also increases ventilation, although, this may be in part compensatory response to metabolic acidosis induced by ingestion of tap water (Moen et al., 2014).

Earlier experiments *in vivo* on cats have shown that perfusion of the carotid bodies with hypoosmotic solutions increases activity of the carotid sinus nerve (Gallego and Belmonte, 1979) that is associated with increase in breathing. This stimulatory effect of hypoosmolality, at least in part, may be attributed to activation of calcium currents and depolarization of chemoreceptors in the carotid body directly induced by hypoosmotic stimulus, as shown in a rat (Molnár et al., 2003). Another potential mechanism may depend on vasoconstriction of vessels supplying the carotid body, leading to decrease in the carotid body blood flow and activation of the chemosensitive glomus cells (Brognara et al., 2021). It has been shown that hypoosmolality causes constriction of the vascular smooth muscles in various vascular beds (Lang et al., 1995; Aoki et al., 2014), and this mechanism was postulated to be involved in the activation of carotid bodies and increased activity of the carotid sinus nerve (Gallego and Belmonte, 1979).

Non-osmotic - Dependent AVP Release

Vasopressinergic neurons can be activated and AVP secreted into the circulation in response to numerous non-osmotic stimuli. The most critical ones are hypovolemia and hypotension, physical exercise, hypoglycemia, hypoxia, and Ang II. Of note, these stimuli also affect the pulmonary ventilation and/or activate the carotid body and arterial chemoreflex.

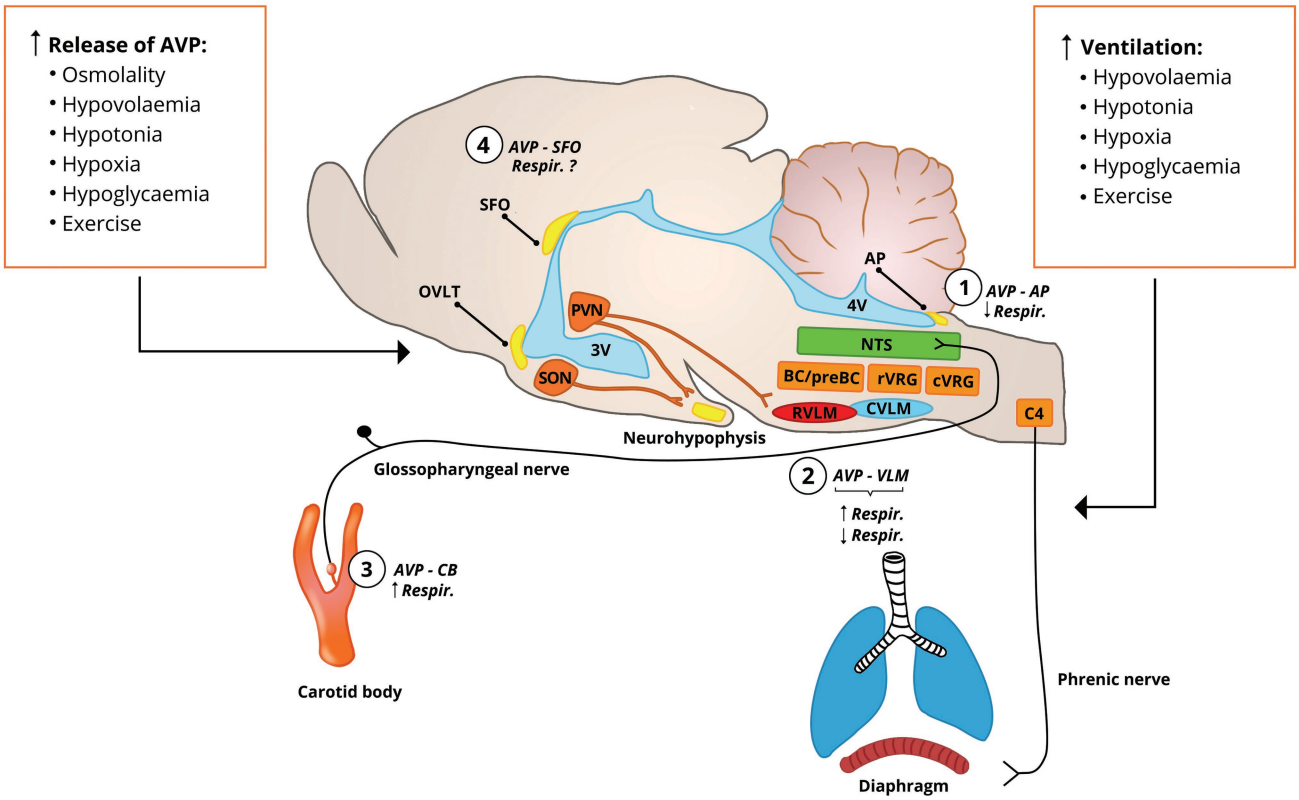

FIGURE 1 | Stimuli that cause AVP release into the bloodstream and activation of the vasopresinergic PVN neurons also increase the pulmonary ventilation. AVP in the bloodstream accesses the circumventricular organs (SFO, AP, and OVLT) that lack the blood-brain barrier and the carotid body at the carotid bifurcation. Vasopressinergic PVN neurons project to cardiovascular (RVLM) and respiratory (preBC/BC, rVRG, and C4 phrenic nucleus) centers, suggesting their involvement in the respiratory control (Kc et al., 2002a, 2010). (1) AVP at the AP inhibits phrenic nerve activity (Yang et al., 2006); (2) vasopressinergic projections to the rVRG tonically stimulate respiratory activity (Kc et al., 2010) and AVP applied into the rVRG or pre-Bötzinger complex stimulates activity of diaphragm (Kc et al., 2002a, 2010), which is accompanied by increase in arterial blood pressure; this is in contrast to findings indicating that AVP administered into the rVRG inhibits phrenic nerve activity with and without changes in arterial blood pressure (Chuang et al., 2003, 2005; Cheng et al., 2004); (3) AVP locally administered into the carotid bifurcation slightly increases ventilation (Żera et al., 2018); and (4) vasopressin receptors are expressed in the SFO (Ostrowski et al., 1994), and electric stimulation of SFO increases respiratory activity (Ferguson et al., 1989), but the respiratory effects of AVP acting at SFO have not been determined. AP, area postrema; AVP, vasopressin; BC, Bötzinger complex; C4, phrenic nuclei; CVLM, caudal ventrolateral medulla; cVRG, caudal ventral respiratory group; NTS, nucleus of the solitary tract; OVLT, organum vasculosum of the lamina terminalis; preBC, pre-Bötzinger complex; PVN, paraventricular nucleus of the hypothalamus; RVLM, rostral ventrolateral medulla; rVRG, rostral ventral respiratory group; SFO, subfornical organ; SON, supraoptic nucleus; and VLM, ventral lateral medulla.

Hypovolemia and Hypotension

Vasopressinergic neurons are tonically inhibited by sensory input from cardiopulmonary low-pressure mechanoreceptors and high-pressure arterial baroreceptors located in the cardiac atria and large systemic veins and the walls of the aortic arch and the carotid sinus, respectively (Schrier et al., 1979; Baylis, 1987; Norsk, 1989). Decrease in the central blood volume and arterial blood pressure leads to unloading of these two groups of cardiovascular mechanoreceptors, which in turn results in activation of the hypothalamic vasopressinergic neurons (Baylis, 1987; Szczepanska-Sadowska et al., 2017). Consequently, hypovolemia, hypotension, or hemorrhage lead to massive release of AVP and its surrogate marker copeptin into the circulation (Arnauld et al., 1977; Fyhrquist et al., 1981; Wehberg et al., 1991; Scott et al., 1994; Muller et al., 2007; Johnson et al., 2014; Bankir et al., 2017). It has been shown that in humans the arterial baroreceptors of the carotid sinus play a critical role in AVP release induced by decrease in arterial blood pressure (Norsk, 1989).

Hypovolemia and hypotension, caused by hemorrhage or pharmacologically induced vasodilation, lead to the increase in pulmonary ventilation (D'Silva et al., 1966; Ohtake and Jennings, 1992; Matsuoka et al., 1994; Walker and Jennings, 1998). Progressive reduction of the central blood volume raises ventilation in men (Convertino et al., 2009) and even small decreases in arterial pressure exert stimulatory effects on breathing in dogs (Ohtake and Jennings, 1992). Of note, under conditions of reduced cardiac output, this increase in pulmonary ventilation may serve as a pulmonary pump that by increasing the amplitude of changes in intrathoracic and intraabdominal pressures promotes venous return to the right cardiac ventricle and limits the decrease in stroke volume (Skytioti et al., 2018). The changes in respiratory activity are dependent on the intra-sinus pressure sensed by the arterial baroreceptors

(Brunner et al., 1982). As the carotid baroreceptors are unloaded, the pulmonary ventilation increases, and vice versa, stimulation of the baroreceptors inhibits ventilation (Brunner et al., 1982). This inhibitory effect of the baroreflex on the respiratory system is particularly prominent during expiration in the *in situ* preparation in rat (Baekey et al., 2010) and is dependent on the respiratory drive in anesthetized rats (McMullan et al., 2009).

Physical Exercise

Physical activity is an acute stressor for the body homeostasis that robustly triggers release of AVP into the circulation proportionally to the intensity of exercise (Wade and Claybaugh, 1980; Popovic et al., 2019). Although exercise-induced hyperosmolality may be involved in the release of AVP (Takamata et al., 2000), during high-intensity physical activity the increase in plasma AVP (or its surrogate marker copeptin) may be present despite hyponatremia or lack of changes in plasma osmolality (Wade and Claybaugh, 1980; Inder et al., 1998; Hew-Butler et al., 2011), which indicates a non-osmotic release of AVP during intense physical exercise. Furthermore, it appears that prominent release of AVP in response to strenous exercise may lead to exercise-induced hyponatremia (Hew-Butler et al., 2017).

Physical activity is also the main physiological stimulus for the increase in pulmonary ventilation. In humans, both the high intensity dynamic exercise and the isometric muscle contractions may cause hyperventilation, especially at the end of exercise or during recovery phase, respectively (Imms and Mehta, 1989; Johnson et al., 1992). Thus, it is attractive to conjecture that AVP released during physical exercise may fine-tune respiratory responses and prevent excessive pulmonary ventilation, however, this requires further investigations.

Hypoglycemia

Insulin-induced hypoglycemia causes AVP release into the circulation both in animals (Plotsky et al., 1985; Berkenbosch et al., 1989; Caraty et al., 1990) and in human subjects (Baylis et al., 1981; Chiodera et al., 1992). The increased release of AVP in response to hypoglycemia appears to be independent of insulin (Chiodera et al., 1992).

The hypoglycemia-induced AVP release counteracts low plasma concentrations of glucose by gluconeogenic and glycogenolytic effects of AVP in the liver and on the AVP-induced activation of the hypothalamic-pituitary-adrenal cortex axis resulting in glucocorticoid release (Nakamura et al., 2017; Szczepanska-Sadowska et al., 2017). Both experimental studies in animals and clinical observations in humans suggest that carotid bodies may be involved in mediating the counter-regulatory response to decreased blood glucose (Koyama et al., 2000; Wehrwein et al., 2015; Kakall et al., 2019). Both in men and rats, hypoglycemia also induces pronounced hyperventilation, which depends on the release of humoral factors, such as adrenaline acting at the carotid bodies (Bin-Jaliah et al., 2004; Ward et al., 2007; Thompson et al., 2016).

Hypoxia

Hypoxia is a key trigger for the peripheral chemoreflex elicited from the carotid bodies, which results in increase of the pulmonary ventilation, sympathoexcitation, and arousal (Marshall, 1994; Kumar and Prabhakar, 2012; Zera et al., 2019).

Hypoxia is also an important chemical stimulus for AVP release (Iovino et al., 2013; Szczepanska-Sadowska et al., 2017). It increases neurohypophyseal blood flow and increases plasma concentration of AVP both in animals (Wang et al., 1984; Wilson et al., 1987; Hanley et al., 1988; Raff, 2011), and humans (Koller et al., 1991). The effect of hypoxia on AVP release depends on the sensory input from the carotid bodies (Levy, 1966; Wilson et al., 1987; Iovino et al., 2013). The rise of plasma AVP counteracts the hypoxia-induced vasodilation and helps in maintaining the peripheral vascular resistance (Walker, 1986; Louwerse and Marshall, 1993), the action that complements the hypoxia-evoked sympathoexcitation.

Angiotensin II

Angiotensin II is a potent hormone that causes vasoconstriction and activates the sympathetic nervous system, promotes renal reabsorption of sodium ions directly by acting on the renal tubules and indirectly through the aldosterone pathway (Sztechman et al., 2018). It is also the key hormonal factor causing AVP release (Fyhrquist et al., 1979; Flôr et al., 2018; Szczepanska-Sadowska et al., 2018). This allows for integration of water-electrolyte balance and regulation of osmolality and volume of extracellular fluid (Szczepańska-Sadowska, 1996).

Besides its cardiovascular, renal and sympathetic effects, Ang II also increases ventilation in dogs (Potter and McCloskey, 1979) and rats (Melo et al., 2020), however acute studies in humans show insignificant effect of Ang II on pulmonary ventilation (Bristow et al., 1971; Solaiman et al., 2014). In animals, the stimulatory effect of Ang II on the respiratory system may be reciprocally inhibited by AVP in a V1aR-dependent manner (Anderson et al., 1990; Walker and Jennings, 1994, 1995), which may involve inhibition of the renin release (Bunag et al., 1967).

VASOPRESSIN/COPEPTIN RELEASE UNDER PATHOLOGICAL CONDITIONS

Next, we briefly summarize clinical observations indicating that AVP is released in excess under conditions of pulmonary dysfunction and medical conditions associated with abnormal breathing patterns. This raises a possibility that AVP is not only a biomarker of respiratory disturbances and hypoxia, but that it may also contribute to the regulation of the respiratory system.

Respiratory Disorders

Increased plasma concentration of copeptin, which reflects the increase in AVP release, is observed in several respiratory disturbances (Szczepanska-Sadowska et al., 2017). It is present in chronic obstructive pulmonary disease (COPD), in which copeptin level is predictive for the recurrence of exacerbation and all-cause mortality (Muller et al., 2007; Zhao et al., 2014). Increased plasma copeptin level is also present in patients with lower respiratory tract infection, especially in

patients with community acquired pneumonia, in whom it has a predictive value for all-cause mortality, clinical instability, and deterioration (Muller et al., 2007; Kruger et al., 2010; Kolditz et al., 2012). High copeptin concentration is also present in acute respiratory distress syndrome, acute lung injury, and cardiopulmonary oedema, where elevated copeptin has a better predictive value for short-term mortality than NT-proBNP, a marker of cardiac ventricles' overload (Lin et al., 2012). Finally, some studies also indicate the potential role of copeptin in the diagnosis and risk stratification of patients with pulmonary hypertension (Nickel et al., 2013) and pulmonary embolisms (Hellenkamp et al., 2018). Recently, it has been shown that elevated concentrations of copeptin are associated with worse outcome in COVID-19 patients with SARS-CoV-2 infection (Gregoriano et al., 2021) and may discriminate between patients with COVID-19 and patients with community-acquired pneumonia (Kuluöztürk et al., 2021).

Non-respiratory Disorders

Besides disturbances of the respiratory system, elevated plasma concentrations of AVP or copeptin are found in several non-respiratory disorders that are often accompanied by abnormal respiratory patterns and increased ventilation. Specifically, elevated copeptin concentration is predictive of worse outcome in patients with traumatic brain injury (Yang et al., 2014; Zhang et al., 2014; Choi et al., 2017), a condition associated with increased expression of V1aRs in the brain (Szmydynger-Chodobska et al., 2004) and abnormal respiratory patterns (Racca et al., 2020). They are also seen in children with febrile and epileptic seizures (Evers et al., 2020). Furthermore, increased plasma concentration of copeptin has been found in patients with acute and chronic heart failure (Maisel et al., 2011; Düngen et al., 2018; Schill et al., 2021), a condition usually accompanied by abnormal respiratory patterns, such as Cheyne-Stokes breathing and sleep apnoea (Cowie et al., 2021). Increase copeptin levels are also found in patients admitted to intensive care unit or emergency department with acute severe dyspnoea due to non-respiratory causes and accompanied by hypoxia and increased respiratory rate (Ara-Somohano et al., 2017).

THE RESPIRATORY EFFECTS OF VASOPRESSIN

Vasopressin affects the respiratory system both as a neurohormone and as a neurotransmitter. Available evidence indicates that its respiratory effects are mainly mediated by V1aRs. Vasopressin present in the bloodstream may affect the respiratory system by interacting with V1aRs expressed in the lungs (Tahara et al., 1998), the circumventricular organs (CVOs; Raggenbass et al., 1989; Ostrowski et al., 1994; Tribollet et al., 1999; Hindmarch et al., 2011), and in the carotid bodies (Żera et al., 2018). In addition to circulating AVP, vasopressinergic neurons projecting to the brainstem respiratory centers affect respiratory activity *via* V1aRs (Kc et al., 2002a, 2010; Chuang et al., 2005; Kc and Dick, 2010). It appears that the effects of AVP on the respiratory function is site-specific and may result in opposing effects, as discussed below.

Vasopressin Receptors in the Respiratory System, Chemoreceptors and Respiratory Centers of the Brain

Lungs and Pulmonary Circulation

It has been shown that V1aRs are predominantly expressed in the lung (Hirasawa et al., 1994; Tahara et al., 1998) and in the pulmonary arteries (Enomoto et al., 2014). Contrary to arteries in the systemic circulation, AVP does not cause vasoconstriction of the pulmonary arteries, but rather it causes vasodilation, especially under conditions of hypoxic vasoconstriction of pulmonary vessels in animals (Walker et al., 1989; Wallace et al., 1989; Enomoto et al., 2014; Sugawara et al., 2019) and humans (Jeon et al., 2006; Currigan et al., 2014). Thus, AVP does not increase pulmonary vascular resistance and the right ventricle's afterload, but it only selectively increases the vascular resistance in systemic circulation (Walker et al., 1989; Jeon et al., 2006).

Retrograde transneuronal labeling indicates that the airway-related vagal preganglionic neurons receive innervation from vasopressinergic neurons of the PVN (Kc et al., 2006, 2010). Furthermore, AVP acting on V1aRs depolarizes and increases firing rate of these preganglionic neurons (Yan et al., 2017), which is suggestive of the broncho-constrictive and secretory effect of AVP. Nonetheless, available evidence points to limited effects of AVP on bronchoconstriction in laboratory animals (Bhoola et al., 1962; Zheng et al., 2017) and humans (Knox et al., 1989).

Arterial Chemoreceptors

Recently, we showed presence of immunostaining for both C-terminal and N-terminal fragments of the V1aR in the chemosensitive glomus cells of the carotid bodies collected from the normotensive Sprague-Dawley rats (Żera et al., 2018). Furthermore, expression of G protein q/11 and phosphokinase C, key intracellular components of the V1aR signaling, has been detected in the chemosensitive glomus cells with the single-cell transcriptomics in mouse (Zhou et al., 2016). These findings indicate that circulating AVP may affect the glomus cells expressing V1aRs and presumably modulate the activity of the carotid body.

Circumventricular Organs

Circumventricular organs (CVOs) include the organum vasculosum laminae terminalis (OVLT) and the SFO that are located close to the third cerebral ventricle, and the area postrema (AP), which is situated in the dorsal surface of the medulla oblongata. They express numerous receptors, lack the blood-brain barrier and are accessible for hormones and mediators circulating in the bloodstream (Ufnal and Skrzypecki, 2014). All CVOs express receptors for AVP, predominantly V1aRs (Raggenbass et al., 1989; Jurzak and Schmid, 1998; McKinley et al., 1999; Tribollet et al., 1999; Kc and Dick, 2010; Hindmarch et al., 2011). Upon binding to V1aRs in the CVOs

of the third ventricle, AVP exerts sympathoexcitatory and pressor effects (Ufnal and Skrzypecki, 2014; Szczepanska-Sadowska et al., 2017; Japundžić-Žigon et al., 2020). In contrast, stimulation of V1aRs in the AP sensitizes the arterial baroreflex and results in hypotension (Hasser and Bishop, 1990; Japundžić-Žigon et al., 2020), which indicates opposite effects of AVP depending on the place of its action. A limited number of studies indicates that administration of AVP into the cerebral ventricles or directly into the AP decreases respiratory rate and phrenic nerve activity (Zerbe and Feuerstein, 1985; Yang et al., 2006).

Respiratory Centers of the Brain

In rats, V1aRs are expressed on the sympathetic neurons of the rostral ventrolateral medulla (RVLM) and the respiratory neurons located in the rostral ventral respiratory column (rVRC; Kc and Dick, 2010) and pre-Bötzinger complex (Kc et al., 2002a). Retrograde labeling studies show that in addition to these nuclei, the phrenic nuclei receive vasopressinergic innervation from the PVN (Kc et al., 2002a,b). The expression of V1aRs in these brainstem structures is augmented by exposure of the animals to hypoxia (Kc and Dick, 2010; Kc et al., 2010). Furthermore, a significant subpopulation of the vasopressinergic PVN neurons are activated by hypercapnia (Kc et al., 2002b). Importantly, binding of AVP to V1 receptors was found in neurons across the nucleus of the solitary tract (NTS), including its caudal part (Raggenbass et al., 1989) that receives sensory input from the arterial chemoreceptors (Lipski et al., 1976, 1977; Finley and Katz, 1992; Zera et al., 2019).

Respiratory Effects of Vasopressin Acting as a Hormone

Circulating AVP may affect the neural control of the respiratory system either by binding to its receptors in the CVOs or receptors located in other peripheral tissues, especially the arterial chemoreceptors (**Figure 1**). Overall, prevailing evidence indicates that AVP as a hormone present in the bloodstream supresses ventilation. We hypothesize that under conditions of hypoxia, oligo/hypovolemia, hypotonia, hypoglycemia, exercise, activation of renin-angiotensin system, the increase in AVP plasma concentration may help in limiting excessive increase in ventilation and prevent development of hypocapnia. Thus, it is likely that inhibition of ventilation by AVP may provide a fine-tuning mechanism that maintains respiratory activity at the most efficient level.

Vasopressin Circulating in the Bloodstream

Intravenous infusions of AVP transiently decrease pulmonary ventilation and phrenic nerve activity in conscious dogs (Ohtake and Jennings, 1993), anesthetized and awake rats (Louwerse and Marshall, 1993; Walker and Jennings, 1998; Żera et al., 2018; Brackley and Toney, 2021) and fetal lambs (Bessho et al., 1997). Recently published pilot study in patients with autosomal dominant polycystic kidney disease showed that upon initiation of treatment with tolvaptan, a selective V2R antagonist, plasma copeptin level increased 6-fold and this was associated with a modest but significant increase in arterial carbon-dioxide and plasma acidity (Heida et al., 2021), suggestive of ventilatory inhibition by increased AVP levels in the bloodstream and enhanced stimulation of V1 receptors, which were not blocked by tolvaptan.

The inhibitory effects of AVP on the respiratory activity depend on V1aRs, as blockade of these receptors with selective antagonists completely prevents changes in pulmonary ventilation induced by systemic administration of AVP in anesthetized rats (Louwerse and Marshall, 1993; Żera et al., 2018; Brackley and Toney, 2021). Furthermore, administration of V1aR antagonists may result in the increase in pulmonary ventilation in awake dogs (Walker and Jennings, 1994). However, it should be noted that insignificant effect of V1aR blockade on pulmonary ventilation was seen in conscious rats (Walker and Jennings, 1998). Furthermore, intravenous administration of V1aR peptidergic antagonist, that does not cross the blood-brain barrier, has insignificant effects on hypoxia-induced increase in the pulmonary ventilation in conscious dogs (Overgaard et al., 1996), suggesting lack of involvement of V1aRs located in the peripheral organs or CVOs in the increase in ventilation evoked by activation of the arterial chemoreflex in this species. However, systemic administration of V1aR antagonist unmasks stimulatory effects of Ang II on the respiration in dogs (Walker and Jennings, 1995). Interestingly, oxytocin, which is structurally related to AVP and acts as a weak agonist of the V1aRs (Szczepanska-Sadowska et al., 2017), is capable of reversing the opioid-induced respiratory depression and this effect is fully unmasked by blockade of V1aRs (Brackley and Toney, 2021).

One of the plausible explanations of the inhibitory action of systemic administration of AVP on ventilation is a baroreflex-mediated inhibition of the medullary respiratory neurons (Richter and Seller, 1975; Brunner et al., 1982; Baekey et al., 2010; McMullan and Pilowsky, 2010) due to the AVP-mediated rise in arterial blood pressure. However, as mentioned above the arterial baroreflex-mediated inhibition of the pulmonary ventilation in the conscious rat is vaguely pronounced (Walker and Jennings, 1996). Thus, another mechanism is presumably at play.

Vasopressin and the Circumventricular Organs

Based on the experimental work, Jennings (1994) suggested that angiotensin II and AVP present in the bloodstream may affect ventilation *via* interaction with the CVOs. Thus, one of such mechanisms may involve stimulation of the V1aRs in the CVOs, specifically in the AP. In addition to the AP neurons responding to both AVP and the rise in blood pressure, indicating their pressure-sensitivity, there are at least two pools of neurons in the AP that respond to circulating AVP independently from the changes in arterial blood pressure, indicating their AVP-sensitivity. One pool increases and another one decreases the firing rate in response to intravenous AVP (Smith et al., 1994). Both types of responses are dependent on vasopressin V1 receptors, as their inhibition abolishes AVP-induced changes in the discharge frequency (Smith et al., 1994). Furthermore, in the medial regions of the NTS there are neurons that respond with increased or decreased firing

in response to AVP microinjections into the AP (Cai et al., 1994), indicating that the circulating neurohormone may affect activity of the NTS involved in the baro- and chemoreflexes *via* the neuronal pathway including the AP. In fact, application of AVP into the AP significantly reduces the phrenic nerve activity in mechanically ventilated, urethane anesthetized rats, and the inhibitory effect is prevented by local administration of V1aR antagonist into the AP or by pharmacological inhibition of the NTS (Yang et al., 2006). This is further supported by observations that AVP administered into the cerebral ventricles, thus allowing for interaction of the neurohormone with the CVOs, decreases respiratory rate in the anesthetized rat (Zerbe and Feuerstein, 1985). However, it should be noted that intracerebroventricular infusion of AVP in conscious macaque monkey had no effect on ventilatory parameters (Lee et al., 1985). This is contrary to the studies with electrical and pharmacological stimulation of the AP neurons in rabbits, which results in increased phrenic nerve activity (Srinivasan et al., 1993; Bongianni et al., 1994). It should be noted that electrical stimulation of the AP may trigger both excitation or inhibition of the NTS neurons in rodents (Chrobok et al., 2021). Similarly, electric stimulation of the SFO increases ventilation in rats (Ferguson et al., 1989). Although, the V1aRs are expressed in the SFO (Ostrowski et al., 1994), thus far it has not been determined how their stimulation affects the respiratory system. Available evidence and anatomical proximity to the respiratory neurons of the brainstem point to the AP as a putative CVO involved in mediating the respiratory effects of circulating AVP. However, given the limited number of studies that evaluated respiratory responses to AVP directly administered into the CVO, the role of CVOs in neural control of respiration by AVP awaits further corroboration from experiments specifically targeting AVP and the AP and/or the SFO, especially under conditions associated with activation of vasopressinergic system and in awake animals.

Vasopressin and the Carotid Bodies

Circulating AVP may also affect control of the respiratory system by binding to its receptors within the carotid body. We showed that in normotensive rats, AVP administered locally into the carotid body *via* the internal carotid artery causes a modest increase in the pulmonary ventilation without significant changes in the blood pressure (Żera et al., 2018). Further studies are needed to determine whether these effects are directly dependent on activation of the chemosensitive glomus cells that express V1aRs (Żera et al., 2018) or rather on AVP-mediated decrease in the carotid body blood flow that may sensitize the chemoreceptors (Przybylski, 1981; Brognara et al., 2021).

Respiratory Effects of Vasopressin Acting as a Neurotransmitter in the Central Nervous System

The paraventricular nucleus of the hypothalamus is the main source of the vasopressinergic innervation of the brainstem and provides projections to the discrete nuclei of the brainstem and the spinal cord (Coote, 1995; Pyner, 2009; Coote and Spyer, 2018). Available evidence indicates that these vasopressinergic pathways may participate in the regulation of breathing.

Vasopressin and the Paraventricular Nucleus

Retrograde labeling and functional studies show neural pathways between the PVN and the NTS, the RVLM, and the presympathetic neurons of the spinal cord (Yang and Coote, 1998; Yang et al., 2002; Ferguson et al., 2008; Affleck et al., 2012). The PVN is involved in the peripheral chemoreflex, as the inhibition or disinhibition of the PVN neurons result in the respective attenuation or augmentation of the peripheral chemoreflex-evoked sympathetic and respiratory responses (Reddy et al., 2005). Furthermore, retrograde labeling studies combined with immunostaining for V1aRs show that the PVN vasopressinergic fibers terminate on neurons in the RVLM, the rVRC, the pre-Bötzinger complex, the NTS, and the phrenic nuclei (Kc et al., 2002a, 2010; Jackson et al., 2005; **Figure 1**). In a series of experiments, Kc et al. (2002b) showed that hypercapnia activates vasopressinergic neurons in the PVN and hypoxia upregulates V1aRs in the RVLM, the ventral respiratory group and in the phrenic nuclei in the spinal cord (Kc et al., 2010). They also showed that in anesthetized mechanically ventilated and vagotomized rats, disinhibition of the PVN leads to increase in respiratory activity, as estimated by means of electromyography of the diaphragm and genioglossal muscle and that this increase can be prevented by a pre-treatment of the RVLM and the rVRC with selective V1aR antagonist (Kc et al., 2010). Along with the upregulation of V1aRs, the respiratory responses were augmented by chronic intermittent hypoxia (Kc et al., 2010). The increases in respiratory activity evoked by disinhibition of the PVN were accompanied by pressor response and dependent on V1aRs (Kc and Dick, 2010, Kc et al., 2010). Together, these studies indicate that activation of the vasopressinergic PVN projections to the RVLM/rVRC increases the respiratory activity *via* V1aRs.

Vasopressin and the Ventral Lateral Medulla

In addition, microinjections of AVP into the pre-Bötzinger complex or RVLM/rVRC also increased the diaphragm's muscle activity in a V1aR-dependent manner (Kc et al., 2002a, 2010). The increases in respiratory activity evoked by local application of AVP was accompanied by pressor response (Kc et al., 2002a). Furthermore, microinjection of the V1aR antagonist into the RVLM/rVRC resulted in a decrease in respiratory activity in rats exposed to chronic intermittent hypoxia (Kc et al., 2010), suggestive of tonic vasopressinergic input to the respiratory neurons. Together, these studies indicate that AVP and V1aRs in the RVLM and rVRC are involved in stimulation of the respiratory activity.

Contrary effects were reported in a series of experiments, in which AVP was microinjected into various sites of the ventrolateral medulla (VLM) caudal from the RVLM determined as a pressor region of the VLM in urethane anesthetized and vagotomized rats that were paralyzed and mechanically ventilated.

In these experiments, microinjections of AVP applied into the VLM and the rostral ventral respiratory group (rVRG) caudal from the RVLM resulted in apnoea with subsequent inhibition of the phrenic nerve discharges (Chuang et al., 2003, 2005). Although, the inhibitory effect of AVP on the respiratory activity was consistent, the pressor response was dependent on the site of injection. Applications of AVP into the lateral part of the VLM decreased the phrenic nerve activity and concomitantly elevated arterial blood pressure, whereas AVP application into the medial part of the VLM attenuated only the phrenic nerve activity, without significant effect on the arterial blood pressure (Chuang et al., 2003, 2005; Cheng et al., 2004). Microinjections of AVP into the VLM and the rVRG were also shown to inhibit activity of the hypoglossal nerve (Chuang et al., 2005). Of note, these inhibitory effects of AVP on phrenic nerve activity were diminished by hypercapnia (Chuang et al., 2003; Cheng et al., 2004) and were completely abolished by pre-treatment with a selective V1aR antagonist (Chuang et al., 2003, 2005; Cheng et al., 2004). Administration of the V1aR antagonist under resting conditions had insignificant effect on blood pressure and phrenic nerve activity in these experiments (Chuang et al., 2003, 2005; Cheng et al., 2004), suggesting lack of significant impact of vasopressinergic efferents innervating these structures on ventilation at rest. Together, these findings suggest inhibitory action of AVP on the respiratory neurons of the rVRG located caudally from the RVLM.

These two series of reports provide apparently conflicting results that may be caused by the several differences in the experimental paradigms, including use of neuromuscular blockade and atropine. In addition, mechanical ventilation with continuous positive end-expiratory pressure potently increases plasma concentration of AVP (Annat et al., 1983; Venus et al., 1985) and this activation of AVP release depends on the hydration status of the ventilated animal (Venus et al., 1985). Thus, various levels of baseline activity of vasopressinergic system could have been present across the above studies. It should be also noted that acute experiments under anesthesia investigating the autonomic responses related to the function of the brainstem and the hypothalamus may yield conflicting results to physiological responses observed in conscious animals (Kannan et al., 1989). Nonetheless, it seems that in the more rostral part of the VLM/rVRC AVP promotes respiratory activity, whereas in the more caudal area, it inhibits respiration.

Vasopressin and the Nucleus of the Solitary Tract

The carotid body-evoked hyperglycemic response has been recognized as a contributing factor in the pathophysiology of metabolic syndrome (Conde et al., 2017) and blockade of V1aRs in the NTS was shown to attenuate increase in the plasma concentration of glucose induced by activation of the peripheral chemoreflex (Montero et al., 2006). Moreover, inhibition of the V1aRs in the NTS substantially reduces pressor and tachycardic effects of electrical stimulation of the PVN (Pittman and Franklin, 1985). Thus, it is probable that AVP in the NTS also modulates respiratory reflexes, especially those originating from the peripheral chemoreceptors. This assumption is further substantiated by evidence indicating that almost half of the NTS neurons respond with excitation to local application of AVP in the coronal sections of the rat's brainstem (Raggenbass et al., 1989). Furthermore, in anesthetized cat, iontophoretic applications of AVP into the NTS revealed excitatory effects of the neuropeptide on the inspiratory neurons of the NTS (Henry and Sessle, 1989). However, microinjections of AVP into a discrete region of the NTS rostral to the calamus scriptorius also produced inhibition of the phrenic nerve activity in rats (Yang et al., 2006). Further investigations are required to elucidate the significance of AVP action in the NTS for regulation of respiration.

The role of endogenous AVP and vasopressinergic neurons in the regulation of the respiratory system is also indirectly supported by spectral analysis of the blood pressure variability, the heart rate variability, and selective pharmacological inhibition of AVP receptors in the central nervous system in awake rats, which suggests that vasopressin and V1aR/V1bRs are involved in enhancing ventilation and respiratory-induced blood pressure oscillations (Japundzic-Zigon, 2001; Milutinović et al., 2006). Furthermore, experiments in the Brattleboro rats lacking AVP indicate that although under resting conditions their breathing is normal, under challenging conditions of septic shock their respiratory adaptation, i.e., increase in respiration, is absent (Brackett et al., 1983), which suggests the important role of the neuropeptide in respiratory adaptation to disturbed homeostasis. This is further supported by known respiratory problems, including sleep apnoea, decreased ventilation and spells in patients with Wolfram syndrome characterized by diabetes insipidus and a lack of AVP (Thompson et al., 1989; Licis et al., 2019).

FUTURE PERSPECTIVES

Evidence pointing to the involvement of AVP in the regulation of respiration mainly emerges from experimental studies in anesthetized animals, in which either local or systemic injections of the neuropeptide or its selective antagonists were performed. Given the complexity of AVP-induced responses including water-electrolyte, cardiovascular, metabolic and behavioral ones, novel approaches are needed to decipher the integrative role of AVP in the regulation of breathing in conscious and intact animals under physiological conditions and in disturbed homeostasis.

Targeted control and modification of the vasopressinergic neurons with optogenetics and chemogenetics have been proposed for determining the role of AVP in the regulation of physiological functions and behavior (Murphy et al., 2012; Yoshimura and Ueta, 2019). These novel techniques open prospects for dissecting vasopressinergic pathways and functional role of AVP in the regulation of the respiratory system. Recently, chemogenetic activation of endogenous AVP has been applied in figuring out the anorexigenic effects of AVP (Yoshimura et al., 2017; Sanada et al., 2021). Targeted optogenetic stimulation/inhibition of vasopressinergic neurons in the hypothalamus and extra-hypothalamic regions or

vasopressinergic efferents innervating specific brain structures have been used in various experimental models (Ishii et al., 2016; Smith et al., 2016; Hume et al., 2019; Yoshimura and Ueta, 2019; Tabarean, 2021)., Moreover, successful optogenetic stimulation or inhibition of the SFO or the OVLT neurons revealed novel information on the regulation of thirst and drinking, vasopressinergic neurons and control of blood pressure (Oka et al., 2015; Zimmerman et al., 2016; Pool et al., 2020; Frazier et al., 2021). The optogenetic approach has been also proposed (Abdala et al., 2015) and successfully applied in delineating respiratory networks of the brainstem (Alsahafi et al., 2015; Basting et al., 2015; Koizumi et al., 2016; Cregg et al., 2017; Malheiros-Lima et al., 2018; Fortuna et al., 2019; Ikeda et al., 2019; Souza et al., 2020). These new technologies may help in dissecting the role of AVP in regulation of breathing by precise chemogenetic or optogenetic activation of vasopressinergic neurons projecting to the brainstem, optogenetic inhibition or stimulation of specific pools of respiratory neurons within the brainstem and CVOs, especially ones with V1aR phenotype, and targeted modulation of vasopressinergic fibers supplying them. Such experimental manipulations carried out in awake animals in physiological state and under conditions of hypo/hyperosmolality, hypovolemia, hypotension, hypoglycemia, hypoxia, exercise, or activation of renin-angiotensin system will bring to light the integrative role of AVP acting both as a neurohormone and a neurotransmitter in adjusting the respiratory system to disturbed homeostasis.

CONCLUSION

Vasopressin is one of the key hormones involved in maintaining body homeostasis and plays critical role in adjusting various body systems to changing internal and external environments. A great attention has been dedicated the role of AVP in maintaining renal water-electrolyte balance and regulation of the circulatory system. Recently, the central effects of AVP related to cognition, mood, memory, and pain have been recognized. Available evidence indicates that AVP also plays a complex role in the regulation of the respiratory system. As a neurohormone present in the circulation, AVP influences the respiratory activity *via* the circumventricular organs, especially the AP, and the arterial chemoreceptors, specifically those located in the carotid bodies. In the area postrema, AVP inhibits the phrenic nerve activity, whereas in the carotid bodies it appears to promote ventilation. Acting as a neurotransmitter in the brainstem, AVP exerts both stimulatory and inhibitory effects on the phrenic nerve activity in a site-specific manner; however, this awaits further investigations in conscious animals. The respiratory effects of AVP appear to be predominantly mediated by the vasopressin V1a receptors. Strong evidence indicates that vasopressin may be an important neuropeptide involved in maintaining respiratory homeostasis.

AUTHOR CONTRIBUTIONS

MP designed the study, prepared the figure, and drafted the initial version of the manuscript. JP designed the study and revised the manuscript. AC-J and ES-S revised the manuscript. TŻ conceived the idea of the review, designed the study, prepared the figure, and revised and edited the final version of the manuscript. All authors contributed to the article and approved the submitted version.

FUNDING

The study was funded by Diamond Grant from the Polish Ministry of Education and Science, grant number DI2018 020648, awarded to MP. The study was carried out with the use of CePT infrastructure financed by the European Union – the European Regional Development Fund within the Operational Programme "Innovative economy" for 2007–2013.

ACKNOWLEDGMENTS

We thank Aleksandra Pelc for help with graphical preparation of the figure.

REFERENCES

Abdala, A. P., Paton, J. F. R., and Smith, J. C. (2015). Defining inhibitory neurone function in respiratory circuits: opportunities with optogenetics? *J. Physiol.* 593, 3033–3046. doi: 10.1113/jphysiol.2014.280610

Affleck, V. S., Coote, J. H., and Pyner, S. (2012). The projection and synaptic organisation of NTS afferent connections with presympathetic neurons, GABA and nNOS neurons in the paraventricular nucleus of the hypothalamus. *Neuroscience* 219, 48–61. doi: 10.1016/j.neuroscience.2012.05.070

Aguilera, G., and Rabadan-Diehl, C. (2000). Vasopressinergic regulation of the hypothalamic-pituitary-adrenal axis: implications for stress adaptation. *Regul. Pept.* 96, 23–29. doi: 10.1016/s0167-0115(00)00196-8

Aguilera, G., Subburaju, S., Young, S., and Chen, J. (2008). The parvocellular vasopressinergic system and responsiveness of the hypothalamic pituitary adrenal axis during chronic stress. *Prog. Brain Res.* 170, 29–39. doi: 10.1016/S0079-6123(08)00403-2

Alsahafi, Z., Dickson, C. T., and Pagliardini, S. (2015). Optogenetic excitation of preBötzinger complex neurons potently drives inspiratory activity in vivo. *J. Physiol.* 593, 3673–3692. doi: 10.1113/JP270471

Anderson, J. W., Sarda, I. R., and Jennings, D. B. (1990). Acute changes in osmolality and renin and respiratory control of arterial PCO2 and [H+]. *Respir. Physiol.* 80, 1–16. doi: 10.1016/0034-5687(90)90002-G

Anderson, J. W., Smith, P. M., and Ferguson, A. V. (2001). Subfornical organ neurons projecting to paraventricular nucleus: whole-cell properties. *Brain Res.* 921, 78–85. doi: 10.1016/S0006-8993(01)03093-1

Anderson, J. W., Washburn, D. L., and Ferguson, A. V. (2000). Intrinsic osmosensitivity of subfornical organ neurons. *Neuroscience* 100, 539–547. doi: 10.1016/S0306-4522(00)00313-4

Annat, G., Viale, J. P., Bui Xuan, B., Hadj Aissa, O., Benzoni, D., Vincent, M., et al. (1983). Effect of PEEP ventilation on renal function, plasma renin, aldosterone, neurophysins and urinary ADH, and prostaglandins. *Anesthesiology* 58, 136–141. doi: 10.1097/00000542-198302000-00006

Aoki, R., Yokoyama, U., Ichikawa, Y., Taguri, M., Kumagaya, S., Ishiwata, R., et al. (2014). Decreased serum osmolality promotes ductus arteriosus constriction. *Cardiovasc. Res.* 104, 326–336. doi: 10.1093/cvr/cvu199

Ara-Somohano, C., Bonadona, A., Carpentier, F., Pavese, P., Vesin, A., Hamidfar-Roy, R., et al. (2017). Evaluation of eight biomarkers to predict short-term mortality in patients with acute severe dyspnea. *Minerva Anestesiol.* 83, 824–835. doi: 10.23736/S0375-9393.17.10882-5

Arnauld, E., Czernichow, P., Fumoux, F., and Vincent, J. D. (1977). The effects of hypotension and hypovolaemia on the liberation of vasopressin during haemorrhage in the unanaesthetized monkey (Macaca mulatta). *Pflugers Arch.* 371, 193–200. doi: 10.1007/BF00586258

Baekey, D. M., Molkov, Y. I., Paton, J. F. R., Rybak, I. A., and Dick, T. E. (2010). Effect of baroreceptor stimulation on the respiratory pattern: insights into respiratory-sympathetic interactions. *Respir. Physiol. Neurobiol.* 174, 135–145. doi: 10.1016/j.resp.2010.09.006

Baker, M. A., and Dawson, D. D. (1985). Inhibition of thermal panting by intracarotid infusion of hypertonic saline in dogs. *Am. J. Physiol.* 249, R787–R791. doi: 10.1152/ajpregu.1985.249.6.R787

Bankir, L., Bichet, D. G., and Morgenthaler, N. G. (2017). Vasopressin: physiology, assessment and osmosensation. *J. Intern. Med.* 282, 284–297. doi: 10.1111/joim.12645

Basting, T. M., Burke, P. G. R., Kanbar, R., Viar, K. E., Stornetta, D. S., Stornetta, R. L., et al. (2015). Hypoxia silences retrotrapezoid nucleus respiratory chemoreceptors via alkalosis. *J. Neurosci.* 35, 527–543. doi: 10.1523/JNEUROSCI.2923-14.2015

Baylis, P. H. (1987). Osmoregulation and control of vasopressin secretion in healthy humans. *Am. J. Physiol.* 253, R671–R678. doi: 10.1152/ajpregu.1987.253.5.R671

Baylis, P. H., and Robertson, G. L. (1980). Plasma vasopressin response to hypertonic saline infusion to assess posterior pituitary function. *J. R. Soc. Med.* 73, 255–260. doi: 10.1177/014107688007300408

Baylis, P. H., Zerbe, R. L., and Robertson, G. L. (1981). Arginine vasopressin response to insulin-induced hypoglycemia in man. *J. Clin. Endocrinol. Metab.* 53, 935–940. doi: 10.1210/jcem-53-5-935

Berkenbosch, F., De Goeij, D. C., and Tilders, F. J. (1989). Hypoglycemia enhances turnover of corticotropin-releasing factor and of vasopressin in the zona externa of the rat median eminence. *Endocrinology* 125, 28–34. doi: 10.1210/endo-125-1-28

Bessho, T., Murata, Y., Ninomiya, Y., Ibara, S., Yamamoto, T., Miyake, Y., et al. (1997). Effect of arginine vasopressin on breathing movements of chronically instrumented fetal lambs. *Acta Obstet. Gynecol. Scand.* 76, 107–111. doi: 10.3109/00016349709050063

Bhoola, K. D., Collier, H. O., Schachter, M., and Shorley, P. G. (1962). Actions of some peptides on bronchial muscle. *Br. J. Pharmacol. Chemother.* 19, 190–197. doi: 10.1111/j.1476-5381.1962.tb01439.x

Bichet, D. G. (2019). Regulation of thirst and vasopressin release. *Annu. Rev. Physiol.* 81, 359–373. doi: 10.1146/annurev-physiol-020518-114556

Bin-Jaliah, I., Maskell, P. D., and Kumar, P. (2004). Indirect sensing of insulin-induced hypoglycaemia by the carotid body in the rat. *J. Physiol.* 556, 255–266. doi: 10.1113/jphysiol.2003.058321

Bongianni, F., Mutolo, D., Srinivasan, M., Staderini, G., Baccari, M. C., Calamai, F., et al. (1994). Gastric relaxation in response to chemical stimulation of the area postrema in the rabbit. *Brain Res.* 646, 307–311. doi: 10.1016/0006-8993(94)90095-7

Brackett, D. J., Schaefer, C. F., and Wilson, M. F. (1983). The role of vasopressin in the maintenance of cardiovascular function during early endotoxin shock. *Adv. Shock Res.* 9, 147–156.

Brackley, A. D., and Toney, G. M. (2021). Oxytocin receptor activation rescues opioid-induced respiratory depression by systemic fentanyl in the rat. *J. Pharmacol. Exp. Ther.* 378, 96–107. doi: 10.1124/jpet.121.000535

Bristow, J. D., Brown, E. B. J., Cunningham, D. J., Goode, R. C., Howson, M. G., and Sleight, P. (1971). The effects of hypercapnia, hypoxia and ventilation on the baroreflex regulation of the pulse interval. *J. Physiol.* 216, 281–302. doi: 10.1113/jphysiol.1971.sp009525

Brognara, F., Felippe, I. S. A., Salgado, H. C., and Paton, J. F. R. (2021). Autonomic innervation of the carotid body as a determinant of its sensitivity: implications for cardiovascular physiology and pathology. *Cardiovasc. Res.* 117, 1015–1032. doi: 10.1093/cvr/cvaa250

Brunner, M. J., Sussman, M. S., Greene, A. S., Kallman, C. H., and Shoukas, A. A. (1982). Carotid sinus baroreceptor reflex control of respiration. *Circ. Res.* 51, 624–636. doi: 10.1161/01.RES.51.5.624

Buijs, R. M. (1978). Intra- and extrahypothalamic vasopressin and oxytocin pathways in the rat. Pathways to the limbic system, medulla oblongata and spinal cord. *Cell Tissue Res.* 192, 423–435. doi: 10.1007/BF00212323

Bunag, R. D., Page, I. H., and McCubbin, J. W. (1967). Inhibition of renin release by vasopressin and angiotensin*. *Cardiovasc. Res.* 1, 67–73. doi: 10.1093/cvr/1.1.67

Cai, Y., Hay, M., and Bishop, V. S. (1994). Stimulation of area postrema by vasopressin and angiotensin II modulates neuronal activity in the nucleus tractus solitarius. *Brain Res.* 647, 242–248. doi: 10.1016/0006-8993(94)91323-4

Caraty, A., Grino, M., Locatelli, A., Guillaume, V., Boudouresque, F., Conte-Devolx, B., et al. (1990). Insulin-induced hypoglycemia stimulates corticotropin-releasing factor and arginine vasopressin secretion into hypophysial portal blood of conscious, unrestrained rams. *J. Clin. Invest.* 85, 1716–1721. doi: 10.1172/JCI114626

Cheng, M.-T., Chuang, C.-W., Lin, J.-T., and Hwang, J.-C. (2004). Cardiopulmonary response to vasopressin-induced activation on V1A receptors in the lateral ventrolateral medulla in the rat. *Chin. J. Phys.* 47, 31–42.

Chiodera, P., Volpi, R., Capretti, L., Speroni, G., Marcato, A., Rossi, G., et al. (1992). Hypoglycemia-induced arginine vasopressin and oxytocin release is mediated by glucoreceptors located inside the blood-brain barrier. *Neuroendocrinology* 55, 655–659. doi: 10.1159/000126185

Choi, K.-S., Cho, Y., Jang, B.-H., Kim, W., Ahn, C., Lim, T. H., et al. (2017). Prognostic role of copeptin after traumatic brain injury: a systematic review and meta-analysis of observational studies. *Am. J. Emerg. Med.* 35, 1444–1450. doi: 10.1016/j.ajem.2017.04.038

Chrobok, L., Wojcik, M., Klich, J. D., Pradel, K., Lewandowski, M. H., and Piggins, H. D. (2021). Phasic neuronal firing in the rodent nucleus of the solitary tract ex vivo. *Front. Physiol.* 12:638695. doi: 10.3389/fphys.2021.638695

Chuang, C.-W., Cheng, M.-T., Lin, J.-T., Hsien, H.-Y., Hung, H.-Y., and Hwang, J.-C. (2003). Arginine vasopressin produces inhibition upon respiration without pressor effect in the rat. *Chin. J. Phys.* 46, 71–81.

Chuang, C.-W., Cheng, M.-T., Yang, S.-J., and Hwang, J.-C. (2005). Activation of ventrolateral medulla neurons by arginine vasopressin via V1A receptors produces inhibition on respiratory-related hypoglossal nerve discharge in the rat. *Chin. J. Phys.* 48, 144–154.

Colucci, G., Stutz, M., Rochat, S., Conte, T., Pavicic, M., Reusser, M., et al. (2014). The effect of desmopressin on platelet function: a selective enhancement of procoagulant COAT platelets in patients with primary platelet function defects. *Blood* 123, 1905–1916. doi: 10.1182/blood-2013-04-497123

Conde, S. V., Ribeiro, M. J., Melo, B. F., Guarino, M. P., and Sacramento, J. F. (2017). Insulin resistance: a new consequence of altered carotid body chemoreflex? *J. Physiol.* 595, 31–41. doi: 10.1113/JP271684

Convertino, V. A., Lye, K. R., Koons, N. J., and Joyner, M. J. (2019). Physiological comparison of hemorrhagic shock and VO(2)max: a conceptual framework for defining the limitation of oxygen delivery. *Exp. Biol. Med.* 244, 690–701. doi: 10.1177/1535370219846425

Convertino, V. A., Rickards, C. A., Lurie, K. G., and Ryan, K. L. (2009). Hyperventilation in response to progressive reduction in central blood volume to near syncope. *Aviat. Space Environ. Med.* 80, 1012–1017. doi: 10.3357/ASEM.2598.2009

Coote, J. H. (1995). Cardiovascular function of the paraventricular nucleus of the hypothalamus. *Biol. Signals* 4, 142–149. doi: 10.1159/000109434

Coote, J. H., and Spyer, K. M. (2018). Central control of autonomic function. *Brain Neurosci. Adv.* 2:2398212818812012. doi: 10.1177/2398212818812012

Corbani, M., Marir, R., Trueba, M., Chafai, M., Vincent, A., Borie, A. M., et al. (2018). Neuroanatomical distribution and function of the vasopressin V(1B) receptor in the rat brain deciphered using specific fluorescent ligands. *Gen. Comp. Endocrinol.* 258, 15–32. doi: 10.1016/j.ygcen.2017.10.011

Cowie, M. R., Linz, D., Redline, S., Somers, V. K., and Simonds, A. K. (2021). Sleep disordered breathing and cardiovascular disease: JACC state-of-the-art review. *J. Am. Coll. Cardiol.* 78, 608–624. doi: 10.1016/j.jacc.2021.05.048

Cregg, J. M., Chu, K. A., Dick, T. E., Landmesser, L. T., and Silver, J. (2017). Phasic inhibition as a mechanism for generation of rapid respiratory rhythms. *Proc. Natl. Acad. Sci. U. S. A.* 114, 12815–12820. doi: 10.1073/pnas.1711536114

Currigan, D. A., Hughes, R. J. A., Wright, C. E., Angus, J. A., and Soeding, P. F. (2014). Vasoconstrictor responses to vasopressor agents in human pulmonary and radial arteries: an in vitro study. *Anesthesiology* 121, 930–936. doi: 10.1097/ALN.0000000000000430

da Silva, E. F., Bassi, M., Menani, J. V., Colombari, D. S. A., Zoccal, D. B., Pedrino, G. R., et al. (2019). Carotid bodies contribute to sympathoexcitation induced by acute salt overload. *Exp. Physiol.* 104, 15–27. doi: 10.1113/EP087110

Doerschug, K. C., Delsing, A. S., Schmidt, G. A., and Ashare, A. (2010). Renin-angiotensin system activation correlates with microvascular dysfunction in a prospective cohort study of clinical sepsis. *Crit. Care* 14:R24. doi: 10.1186/cc8887

D'Silva, J. L., Gill, D., and Mendel, D. (1966). The effects of acute haemorrhage on respiration in the cat. *J. Physiol.* 187, 369–377. doi: 10.1113/jphysiol.1966.sp008096

Dumais, K. M., and Veenema, A. H. (2016). Vasopressin and oxytocin receptor systems in the brain: sex differences and sex-specific regulation of social behavior. *Front. Neuroendocrinol.* 40, 1–23. doi: 10.1016/j.yfrne.2015.04.003

Düngen, H.-D., Tscholl, V., Obradovic, D., Radenovic, S., Matic, D., Musial Bright, L., et al. (2018). Prognostic performance of serial in-hospital measurements of copeptin and multiple novel biomarkers among patients with worsening heart failure: results from the MOLITOR study. *ESC Hear. Fail.* 5, 288–296. doi: 10.1002/ehf2.12231

Enomoto, M., Pan, J., Shifrin, Y., and Belik, J. (2014). Age dependency of vasopressin pulmonary vasodilatory effect in rats. *Pediatr. Res.* 75, 315–321. doi: 10.1038/pr.2013.221

Evers, K. S., Hügli, M., Fouzas, S., Kasser, S., Pohl, C., Stoecklin, B., et al. (2020). Serum neurofilament levels in children with febrile seizures and in controls. *Front. Neurosci.* 14:579958. doi: 10.3389/fnins.2020.579958

Ferguson, A. V., Beckmann, L. M., and Fisher, J. T. (1989). Effects of subfornical organ stimulation on respiration in the anesthetized rat. *Can. J. Physiol. Pharmacol.* 67, 1097–1101. doi: 10.1139/y89-173

Ferguson, A. V., Latchford, K. J., and Samson, W. K. (2008). The paraventricular nucleus of the hypothalamus—a potential target for integrative treatment of autonomic dysfunction. *Expert Opin. Ther. Targets* 12, 717–727. doi: 10.1517/14728222.12.6.717

Finley, J. C., and Katz, D. M. (1992). The central organization of carotid body afferent projections to the brainstem of the rat. *Brain Res.* 572, 108–116. doi: 10.1016/0006-8993(92)90458-L

Flôr, A. F. L., de Brito Alves, J. L., França-Silva, M. S., Balarini, C. M., Elias, L. L. K., Ruginsk, S. G., et al. (2018). Glial cells are involved in ANG-II-induced vasopressin release and sodium intake in awake rats. *Front. Physiol.* 9:430. doi: 10.3389/fphys.2018.00430

Fortuna, M. G., Kügler, S., and Hülsmann, S. (2019). Probing the function of glycinergic neurons in the mouse respiratory network using optogenetics. *Respir. Physiol. Neurobiol.* 265, 141–152. doi: 10.1016/j.resp.2018.10.008

Frazier, C. J., Harden, S. W., Alleyne, A. R., Mohammed, M., Sheng, W., Smith, J. A., et al. (2021). An angiotensin-responsive connection from the lamina terminalis to the paraventricular nucleus of the hypothalamus evokes vasopressin secretion to increase blood pressure in mice. *J. Neurosci.* 41, 1429–1442. doi: 10.1523/JNEUROSCI.1600-20.2020

Frier, B. M. (2014). Hypoglycaemia in diabetes mellitus: epidemiology and clinical implications. *Nat. Rev. Endocrinol.* 10, 711–722. doi: 10.1038/nrendo.2014.170

Fyhrquist, F., Eriksson, L., and Wallenius, M. (1979). Plasma vasopressin in conscious goats after cerebroventricular infusions of angiotensins, sodium chloride, and fructose. *Endocrinology* 104, 1091–1095. doi: 10.1210/endo-104-4-1091

Fyhrquist, F., Tikkanen, I., and Linkola, J. (1981). Plasma vasopressin concentration and renin in the rat: effect of hydration and hemorrhage. *Acta Physiol. Scand.* 113, 507–510. doi: 10.1111/j.1748-1716.1981.tb06929.x

Gallego, R., and Belmonte, C. (1979). The effects of blood osmolality changes on cat carotid body chemoreceptors in vivo. *Pflugers Arch.* 380, 53–58. doi: 10.1007/BF00582612

Gonzalez-Luque, A., L'age, M., Dhariwal, A. P., and Yates, F. E. (1970). Stimulation of corticotropin release by corticotropin-releasing factor (CRF) or by vasopressin following intrapituitary infusions in unanesthetized dogs: inhibition of the responses by dexamethasone. *Endocrinology* 86, 1134–1142. doi: 10.1210/endo-86-5-1134

Gregoriano, C., Molitor, A., Haag, E., Kutz, A., Koch, D., Haubitz, S., et al. (2021). Activation of vasopressin system during COVID-19 is associated with adverse clinical outcomes: an observational study. *J. Endocr. Soc.* 5:bvab045. doi: 10.1210/jendso/bvab045

Hanley, D. F., Wilson, D. A., Feldman, M. A., and Traystman, R. J. (1988). Peripheral chemoreceptor control of neurohypophysial blood flow. *Am. J. Physiol.* 254, H742–H750. doi: 10.1152/ajpheart.1988.254.4.H742

Hasser, E. M., and Bishop, V. S. (1990). Reflex effect of vasopressin after blockade of V1 receptors in the area postrema. *Circ. Res.* 67, 265–271. doi: 10.1161/01.RES.67.2.265

Heida, J. E., Gansevoort, R. T., and Meijer, E. (2021). Acid-base homeostasis during vasopressin V2 receptor antagonist treatment in autosomal dominant polycystic kidney disease patients. *Kidney Int. Rep.* 6, 839–841. doi: 10.1016/j.ekir.2020.12.021

Hellenkamp, K., Pruszczyk, P., Jiménez, D., Wyzgał, A., Barrios, D., Ciurzyński, M., et al. (2018). Prognostic impact of copeptin in pulmonary embolism: a multicentre validation study. *Eur. Respir. J.* 51:1702037. doi: 10.1183/13993003.02037-2017

Henry, J. L., and Sessle, B. J. (1989). Vasopressin and oxytocin express excitatory effects on respiratory and respiration-related neurones in the nuclei of the tractus solitarius in the cat. *Brain Res.* 491, 150–155. doi: 10.1016/0006-8993(89)90097-8

Hew-Butler, T., Hoffman, M. D., Stuempfle, K. J., Rogers, I. R., Morgenthaler, N. G., and Verbalis, J. G. (2011). Changes in copeptin and bioactive vasopressin in runners with and without hyponatremia. *Clin. J. Sport Med.* 21, 211–217. doi: 10.1097/JSM.0b013e31821a62c2

Hew-Butler, T., Loi, V., Pani, A., and Rosner, M. H. (2017). Exercise-associated hyponatremia: 2017 update. *Front. Med.* 4:21. doi: 10.3389/fmed.2017.00021

Hindmarch, C. C. T., Fry, M., Smith, P. M., Yao, S. T., Hazell, G. G. J., Lolait, S. J., et al. (2011). The transcriptome of the medullary area postrema: the thirsty rat, the hungry rat and the hypertensive rat. *Exp. Physiol.* 96, 495–504. doi: 10.1113/expphysiol.2010.056515

Hirasawa, A., Hashimoto, K., and Tsujimoto, G. (1994). Distribution and developmental change of vasopressin V1A and V2 receptor mRNA in rats. *Eur. J. Pharmacol.* 267, 71–75. doi: 10.1016/0922-4106(94)90226-7

Horstman, L. L., Valle-Riestra, B. J., Jy, W., Wang, F., Mao, W., and Ahn, Y. S. (1995). Desmopressin (DDAVP) acts on platelets to generate platelet microparticles and enhanced procoagulant activity. *Thromb. Res.* 79, 163–174. doi: 10.1016/0049-3848(95)00102-W

Hume, C., Allchorne, A., Grinevich, V., Leng, G., and Ludwig, M. (2019). Effects of optogenetic stimulation of vasopressinergic retinal afferents on suprachiasmatic neurones. *J. Neuroendocrinol.* 31:e12806. doi: 10.1111/jne.12806

Hupf, H., Grimm, D., Riegger, G. A., and Schunkert, H. (1999). Evidence for a vasopressin system in the rat heart. *Circ. Res.* 84, 365–370. doi: 10.1161/01.RES.84.3.365

Ikeda, K., Igarashi, H., Yawo, H., Kobayashi, K., Arata, S., Kawakami, K., et al. (2019). Optogenetic analysis of respiratory neuronal networks in the ventral medulla of neonatal rats producing channelrhodopsin in Phox2b-positive cells. *Pflugers Arch.* 471, 1419–1439. doi: 10.1007/s00424-019-02317-9

Imms, F. J., and Mehta, D. (1989). Respiratory responses to sustained isometric muscle contractions in man: the effect of muscle mass. *J. Physiol.* 419, 1–14. doi: 10.1113/jphysiol.1989.sp017857

Inder, W. J., Hellemans, J., Swanney, M. P., Prickett, T. C., and Donald, R. A. (1998). Prolonged exercise increases peripheral plasma ACTH, CRH, and AVP in male athletes. *J. Appl. Physiol.* 85, 835–841. doi: 10.1152/jappl.1998.85.3.835

Iovino, M., Guastamacchia, E., Giagulli, V. A., Fiore, G., Licchelli, B., Iovino, E., et al. (2013). Role of central and peripheral chemoreceptors in vasopressin secretion control. *Endocr Metab Immune Disord Drug Targets* 13, 250–255. doi: 10.2174/18715303113136660042

Ishii, M., Hashimoto, H., Ohkubo, J.-I., Ohbuchi, T., Saito, T., Maruyama, T., et al. (2016). Transgenic approach to express the channelrhodopsin 2 gene in arginine vasopressin neurons of rats. *Neurosci. Lett.* 630, 194–198. doi: 10.1016/j.neulet.2016.08.001

Jackson, K., Silva, H. M. V., Zhang, W., Michelini, L. C., and Stern, J. E. (2005). Exercise training differentially affects intrinsic excitability of autonomic and neuroendocrine neurons in the hypothalamic paraventricular nucleus. *J. Neurophysiol.* 94, 3211–3220. doi: 10.1152/jn.00277.2005

Japundzic-Zigon, N. (2001). Effects of nonpeptide V1a and V2 antagonists on blood pressure fast oscillations in conscious rats. *Clin. Exp. Hypertens.* 23, 277–292. doi: 10.1081/CEH-100102667

Japundžić-Žigon, N., Lozić, M., Šarenac, O., and Murphy, D. (2020). Vasopressin & oxytocin in control of the cardiovascular system: an updated review. *Curr. Neuropharmacol.* 18, 14–33. doi: 10.2174/1570159X17666190717150501

Jennings, D. B. (1994). The physicochemistry of [H+] and respiratory control: roles of PCO2, strong ions, and their hormonal regulators. *Can. J. Physiol. Pharmacol.* 72, 1499–1512. doi: 10.1139/y94-216

Jeon, Y., Ryu, J. H., Lim, Y. J., Kim, C. S., Bahk, J.-H., Yoon, S. Z., et al. (2006). Comparative hemodynamic effects of vasopressin and norepinephrine after milrinone-induced hypotension in off-pump coronary artery bypass surgical patients. *Eur. J. Cardiothorac. Surg.* 29, 952–956. doi: 10.1016/j.ejcts.2006.02.032

Johnson, B. D., Saupe, K. W., and Dempsey, J. A. (1992). Mechanical constraints on exercise hyperpnea in endurance athletes. *J. Appl. Physiol.* 73, 874–886. doi: 10.1152/jappl.1992.73.3.874

Johnson, B. D., van Helmond, N., Curry, T. B., van Buskirk, C. M., Convertino, V. A., and Joyner, M. J. (2014). Reductions in central venous pressure by lower body negative pressure or blood loss elicit similar hemodynamic responses. *J. Appl. Physiol.* 117, 131–141. doi: 10.1152/japplphysiol.00070.2014

Jurzak, M., and Schmid, H. A. (1998). Vasopressin and sensory circumventricular organs. *Prog. Brain Res.* 119, 221–245. doi: 10.1016/s0079-6123(08)61572-1

Kakall, Z. M., Cohen, E. M., Farnham, M. M. J., Kim, S. J., Nedoboy, P. E., and Pilowsky, P. M. (2019). Integration of hindbrain and carotid body mechanisms that control the autonomic response to cardiorespiratory and glucoprivic insults. *Respir. Physiol. Neurobiol.* 265, 83–91. doi: 10.1016/j.resp.2018.08.008

Kannan, H., Hayashida, Y., and Yamashita, H. (1989). Increase in sympathetic outflow by paraventricular nucleus stimulation in awake rats. *Am. J. Physiol.* 256, R1325–R1330. doi: 10.1152/ajpregu.1989.256.6.R1325

Kasserra, C. E., and Jones, D. R. (1993). Hyperosmolality alters the ventilatory response to acute hypercapnia and hypoxia. *Respir. Physiol.* 94, 189–203. doi: 10.1016/0034-5687(93)90047-E

Kasserra, C. E., Jones, D. R., and Hughes, M. R. (1991). Acid-base disturbance and ventilatory response to changes in plasma osmolality in Pekin ducks. *Respir. Physiol.* 85, 383–393. doi: 10.1016/0034-5687(91)90076-U

Kc, P., Balan, K. V., Tjoe, S. S., Martin, R. J., Lamanna, J. C., Haxhiu, M. A., et al. (2010). Increased vasopressin transmission from the paraventricular nucleus to the rostral medulla augments cardiorespiratory outflow in chronic intermittent hypoxia-conditioned rats. *J. Physiol.* 588, 725–740. doi: 10.1113/jphysiol.2009.184580

Kc, P., and Dick, T. E. (2010). Modulation of cardiorespiratory function mediated by the paraventricular nucleus. *Respir. Physiol. Neurobiol.* 174, 55–64. doi: 10.1016/j.resp.2010.08.001

Kc, P., Haxhiu, M. A., Tolentino-Silva, F. P., Wu, M., Trouth, C. O., and Mack, S. O. (2002a). Paraventricular vasopressin-containing neurons project to brain stem and spinal cord respiratory-related sites. *Respir. Physiol. Neurobiol.* 133, 75–88. doi: 10.1016/s1569-9048(02)00131-3

Kc, P., Haxhiu, M. A., Trouth, C. O., Balan, K. V., Anderson, W. A., and Mack, S. O. (2002b). CO(2)-induced c-Fos expression in hypothalamic vasopressin containing neurons. *Respir. Physiol.* 129, 289–296. doi: 10.1016/s0034-5687(01)00321-8

Kc, P., Karibi-Ikiriko, A., Rust, C. F., Jayam-Trouth, A., and Haxhiu, M. A. (2006). Phenotypic traits of the hypothalamic PVN cells innervating airway-related vagal preganglionic neurons. *Respir. Physiol. Neurobiol.* 154, 319–330. doi: 10.1016/j.resp.2006.01.006

Knox, A. J., Britton, J. R., and Tattersfield, A. E. (1989). Effect of vasopressin on bronchial reactivity to histamine. *Clin. Sci.* 77, 467–471. doi: 10.1042/cs0770467

Koizumi, H., Mosher, B., Tariq, M. F., Zhang, R., Koshiya, N., and Smith, J. C. (2016). Voltage-dependent rhythmogenic property of respiratory pre-bötzinger complex glutamatergic, Dbx1-derived, and somatostatin-expressing neuron populations revealed by graded optogenetic inhibition. *eNeuro* 3:ENEURO.0081–16.2016. doi: 10.1523/ENEURO.0081-16.2016

Kolditz, M., Halank, M., Schulte-Hubbert, B., Bergmann, S., Albrecht, S., and Hoffken, G. (2012). Copeptin predicts clinical deterioration and persistent instability in community-acquired pneumonia. *Respir. Med.* 106, 1320–1328. doi: 10.1016/j.rmed.2012.06.008

Koller, E. A., Bührer, A., Felder, L., Schopen, M., and Vallotton, M. B. (1991). Altitude diuresis: endocrine and renal responses to acute hypoxia of acclimatized and non-acclimatized subjects. *Eur. J. Appl. Physiol. Occup. Physiol.* 62, 228–234. doi: 10.1007/BF00643747

Koshimizu, T., Nakamura, K., Egashira, N., Hiroyama, M., Nonoguchi, H., and Tanoue, A. (2012). Vasopressin V1a and V1b receptors: from molecules to physiological systems. *Physiol. Rev.* 92, 1813–1864. doi: 10.1152/physrev.00035.2011

Koyama, Y., Coker, R. H., Stone, E. E., Lacy, D. B., Jabbour, K., Williams, P. E., et al. (2000). Evidence that carotid bodies play an important role in glucoregulation in vivo. *Diabetes* 49, 1434–1442. doi: 10.2337/diabetes.49.9.1434

Kruger, S., Ewig, S., Giersdorf, S., Hartmann, O., Suttorp, N., and Welte, T. (2010). Cardiovascular and inflammatory biomarkers to predict short- and long-term survival in community-acquired pneumonia: results from the German competence network, CAPNETZ. *Am. J. Respir. Crit. Care Med.* 182, 1426–1434. doi: 10.1164/rccm.201003-0415OC

Kuluöztürk, M., İn, E., Telo, S., Karabulut, E., and Geçkil, A. A. (2021). Efficacy of copeptin in distinguishing COVID-19 pneumonia from community-acquired pneumonia. *J. Med. Virol.* 93, 3113–3121. doi: 10.1002/jmv.26870

Kumar, P., and Prabhakar, N. R. (2012). Peripheral chemoreceptors: function and plasticity of the carotid body. *Compr. Physiol.* 2, 141–219. doi: 10.1002/cphy.c100069

Landgraf, R., and Neumann, I. D. (2004). Vasopressin and oxytocin release within the brain: a dynamic concept of multiple and variable modes of neuropeptide communication. *Front. Neuroendocrinol.* 25, 150–176. doi: 10.1016/j.yfrne.2004.05.001

Lang, F., Busch, G. L., Zempel, G., Ditlevsen, J., Hoch, M., Emerich, U., et al. (1995). Ca2+ entry and vasoconstriction during osmotic swelling of vascular smooth muscle cells. *Pflugers Arch.* 431, 253–258. doi: 10.1007/BF00410198

Launay, J. M., Vittet, D., Vidaud, M., Rondot, A., Mathieu, M. N., Lalau-Keraly, C., et al. (1987). V1a-vasopressin specific receptors on human platelets: potentiation by ADP and epinephrine and evidence for homologous down-regulation. *Thromb. Res.* 45, 323–331. doi: 10.1016/0049-3848(87)90221-0

Lee, T. F., Mora, F., and Myers, R. D. (1985). Effect of intracerebroventricular vasopressin on body temperature and endotoxin fever of macaque monkey. *Am. J. Physiol.* 248, R674–R678. doi: 10.1152/ajpregu.1985.248.6.R674

Lee, A. K., Tse, F. W., and Tse, A. (2015). Arginine vasopressin potentiates the stimulatory action of CRH on pituitary corticotropes via a protein kinase C-dependent reduction of the background TREK-1 current. *Endocrinology* 156, 3661–3672. doi: 10.1210/en.2015-1293

Levy, M. N. (1966). Effect of carotid chemoreceptor stimulation on plasma antidiuretic hormone titer. *Am. J. Physiol.* 210, 157–161. doi: 10.1152/ajplegacy.1966.210.1.157

Licis, A., Davis, G., Eisenstein, S. A., Lugar, H. M., and Hershey, T. (2019). Sleep disturbances in Wolfram syndrome. *Orphanet J. Rare Dis.* 14:188. doi: 10.1186/s13023-019-1160-z

Lin, Q., Fu, F., Chen, H., and Zhu, B. (2012). Copeptin in the assessment of acute lung injury and cardiogenic pulmonary edema. *Respir. Med.* 106, 1268–1277. doi: 10.1016/j.rmed.2012.05.010

Lipski, J., McAllen, R. M., and Spyer, K. M. (1977). The carotid chemoreceptor input to the respiratory neurones of the nucleus of tractus solitarus. *J. Physiol.* 269, 797–810. doi: 10.1113/jphysiol.1977.sp011930

Lipski, J., McAllen, R. M., and Trzebski, A. (1976). Carotid baroreceptor and chemoreceptor inputs onto single medullary neurones. *Brain Res.* 107, 132–136. doi: 10.1016/0006-8993(76)90101-3

Louwerse, A. M., and Marshall, J. M. (1993). The role of vasopressin in the regional vascular responses evoked in the spontaneously breathing rat by systemic hypoxia. *J. Physiol.* 470, 463–472. doi: 10.1113/jphysiol.1993.sp019869

Lüning, H., Mangelus, C., Carlström, E., Nilson, F., and Börjesson, M. (2019). Incidence and characteristics of severe exercise-associated collapse at the world's largest half-marathon. *PLoS One* 14:e0217465. doi: 10.1371/journal.pone.0217465

Maisel, A., Xue, Y., Shah, K., Mueller, C., Nowak, R., Peacock, W. F., et al. (2011). Increased 90-day mortality in patients with acute heart failure with elevated copeptin: secondary results from the biomarkers in acute heart failure (BACH) study. *Circ. Heart Fail.* 4, 613–620. doi: 10.1161/CIRCHEARTFAILURE.110.960096

Malheiros-Lima, M. R., Totola, L. T., Lana, M. V. G., Strauss, B. E., Takakura, A. C., and Moreira, T. S. (2018). Breathing responses produced by optogenetic stimulation of adrenergic C1 neurons are dependent on the connection

with preBötzinger complex in rats. *Pflugers Arch.* 470, 1659–1672. doi: 10.1007/s00424-018-2186-0

Marshall, J. M. (1994). Peripheral chemoreceptors and cardiovascular regulation. *Physiol. Rev.* 74, 543–594. doi: 10.1152/physrev.1994.74.3.543

Matsuoka, T., Saiki, C., and Mortola, J. P. (1994). Metabolic and ventilatory responses to anemic hypoxia in conscious rats. *J. Appl. Physiol.* 77, 1067–1072. doi: 10.1152/jappl.1994.77.3.1067

McKinley, M. J., Gerstberger, R., Mathai, M. L., Oldfield, B. J., and Schmid, H. (1999). The lamina terminalis and its role in fluid and electrolyte homeostasis. *J. Clin. Neurosci.* 6, 289–301. doi: 10.1054/jocn.1998.0056

McMullan, S., Dick, T. E., Farnham, M. M. J., and Pilowsky, P. M. (2009). Effects of baroreceptor activation on respiratory variability in rat. *Respir. Physiol. Neurobiol.* 166, 80–86. doi: 10.1016/j.resp.2009.02.006

McMullan, S., and Pilowsky, P. M. (2010). The effects of baroreceptor stimulation on central respiratory drive: a review. *Respir. Physiol. Neurobiol.* 174, 37–42. doi: 10.1016/j.resp.2010.07.009

Melo, M. R., Gasparini, S., Silva, E. F., Karlen-Amarante, M., Speretta, G. F., Lauar, M. R., et al. (2020). Renovascular hypertension elevates pulmonary ventilation in rats by carotid body-dependent mechanisms. *Am. J. Phys. Regul. Integr. Comp. Phys.* 318, R730–R742. doi: 10.1152/ajpregu.00134.2019

Milutinović, S., Murphy, D., and Japundzić-Zigon, N. (2006). The role of central vasopressin receptors in the modulation of autonomic cardiovascular controls: a spectral analysis study. *Am. J. Phys. Regul. Integr. Comp. Phys.* 291, R1579–R1591. doi: 10.1152/ajpregu.00764.2005

Moen, V., Brudin, L., Rundgren, M., and Irestedt, L. (2014). Osmolality and respiratory regulation in humans: respiratory compensation for hyperchloremic metabolic acidosis is absent after infusion of hypertonic saline in healthy volunteers. *Anesth. Analg.* 119, 956–964. doi: 10.1213/ANE.0000000000000404

Mohan, S., Moffett, R. C., Thomas, K. G., Irwin, N., and Flatt, P. R. (2019). Vasopressin receptors in islets enhance glucose tolerance, pancreatic beta-cell secretory function, proliferation and survival. *Biochimie* 158, 191–198. doi: 10.1016/j.biochi.2019.01.008

Molnár, Z., Petheo, G. L., Fülöp, C., and Spät, A. (2003). Effects of osmotic changes on the chemoreceptor cell of rat carotid body. *J. Physiol.* 546, 471–481. doi: 10.1113/jphysiol.2002.024125

Montero, S. A., Yarkov, A., Lemus, M., de Alvarez-Buylla, E. R., and Alvarez-Buylla, R. (2006). Carotid chemoreceptor reflex modulation by arginine-vasopressin microinjected into the nucleus tractus solitarius in rats. *Arch. Med. Res.* 37, 709–716. doi: 10.1016/j.arcmed.2006.03.001

Morgenthaler, N. G., Struck, J., Alonso, C., and Bergmann, A. (2006). Assay for the measurement of copeptin, a stable peptide derived from the precursor of vasopressin. *Clin. Chem.* 52, 112–119. doi: 10.1373/clinchem.2005.060038

Muller, B., Morgenthaler, N., Stolz, D., Schuetz, P., Muller, C., Bingisser, R., et al. (2007). Circulating levels of copeptin, a novel biomarker, in lower respiratory tract infections. *Eur. J. Clin. Investig.* 37, 145–152. doi: 10.1111/j.1365-2362.2007.01762.x

Murphy, D., Konopacka, A., Hindmarch, C., Paton, J. F. R., Sweedler, J. V., Gillette, M. U., et al. (2012). The hypothalamic-neurohypophyseal system: from genome to physiology. *J. Neuroendocrinol.* 24, 539–553. doi: 10.1111/j.1365-2826.2011.02241.x

Nakamura, K., Velho, G., and Bouby, N. (2017). Vasopressin and metabolic disorders: translation from experimental models to clinical use. *J. Intern. Med.* 282, 298–309. doi: 10.1111/joim.12649

Nickel, C. H., Bingisser, R., and Morgenthaler, N. G. (2012). The role of copeptin as a diagnostic and prognostic biomarker for risk stratification in the emergency department. *BMC Med.* 10:7. doi: 10.1186/1741-7015-10-7

Nickel, N., Lichtinghagen, R., Golpon, H., Olsson, K. M., Brand, K., Welte, T., et al. (2013). Circulating levels of copeptin predict outcome in patients with pulmonary arterial hypertension. *Respir. Res.* 14:130. doi: 10.1186/1465-9921-14-130

Norsk, P. (1989). Influence of low- and high-pressure baroreflexes on vasopressin release in humans. *Acta Endocrinol.* 121, 3–27. doi: 10.1530/acta.0.1210003-a

Nunn, N., Womack, M., Dart, C., and Barrett-Jolley, R. (2011). Function and pharmacology of spinally-projecting sympathetic pre-autonomic neurones in the paraventricular nucleus of the hypothalamus. *Curr. Neuropharmacol.* 9, 262–277. doi: 10.2174/157015911795596531

Nussey, S. S., Prysor-Jones, R. A., Taylor, A., Ang, V. T., and Jenkins, J. S. (1987). Arginine vasopressin and oxytocin in the bovine adrenal gland. *J. Endocrinol.* 115, 141–149. doi: 10.1677/joe.0.1150141

O'Connor, M. D., and Jennings, D. B. (2001). Respiratory and metabolic effects of decreased osmolality in conscious rats. *Can. J. Physiol. Pharmacol.* 79, 768–778. doi: 10.1139/y01-056

Ohtake, P. J., and Jennings, D. B. (1992). Ventilation is stimulated by small reductions in arterial pressure in the awake dog. *J. Appl. Physiol.* 73, 1549–1557. doi: 10.1152/jappl.1992.73.4.1549

Ohtake, P. J., and Jennings, D. B. (1993). Angiotensin II stimulates respiration in awake dogs and antagonizes baroreceptor inhibition. *Respir. Physiol.* 91, 335–351. doi: 10.1016/0034-5687(93)90110-V

Oka, Y., Ye, M., and Zuker, C. S. (2015). Thirst driving and suppressing signals encoded by distinct neural populations in the brain. *Nature* 520, 349–352. doi: 10.1038/nature14108

Ostrowski, N. L., Lolait, S. J., and Young, W. S. (1994). Cellular localization of vasopressin V1a receptor messenger ribonucleic acid in adult male rat brain, pineal, and brain vasculature. *Endocrinology* 135, 1511–1528. doi: 10.1210/endo.135.4.7925112

Overgaard, C. B., Walker, J. K., and Jennings, D. B. (1996). Respiration during acute hypoxia: angiotensin- and vasopressin-receptor blocks. *J. Appl. Physiol.* 80, 810–817. doi: 10.1152/jappl.1996.80.3.810

Pelletier, J.-S., Dicken, B., Bigam, D., and Cheung, P.-Y. (2014). Cardiac effects of vasopressin. *J. Cardiovasc. Pharmacol.* 64, 100–107. doi: 10.1097/FJC.0000000000000092

Pittman, Q. J., and Franklin, L. G. (1985). Vasopressin antagonist in nucleus tractus solitarius/vagal area reduces pressor and tachycardia responses to paraventricular nucleus stimulation in rats. *Neurosci. Lett.* 56, 155–160. doi: 10.1016/0304-3940(85)90122-3

Plotsky, P. M., Bruhn, T. O., and Vale, W. (1985). Hypophysiotropic regulation of adrenocorticotropin secretion in response to insulin-induced hypoglycemia. *Endocrinology* 117, 323–329. doi: 10.1210/endo-117-1-323

Pool, A.-H., Wang, T., Stafford, D. A., Chance, R. K., Lee, S., Ngai, J., et al. (2020). The cellular basis of distinct thirst modalities. *Nature* 588, 112–117. doi: 10.1038/s41586-020-2821-8

Popovic, M., Timper, K., Seelig, E., Nordmann, T., Erlanger, T. E., Donath, M. Y., et al. (2019). Exercise upregulates copeptin levels which is not regulated by interleukin-1. *PLoS One* 14:e0217800. doi: 10.1371/journal.pone.0217800

Potter, E. K., and McCloskey, D. I. (1979). Respiratory stimulation by angiotensin II. *Respir. Physiol.* 36, 367–373. doi: 10.1016/0034-5687(79)90048-3

Przybylski, J. (1981). Do arterial chemoreceptors play a role in the pathogenesis of hypertension? *Med. Hypotheses* 7, 127–131. doi: 10.1016/0306-9877(81)90109-2

Pyner, S. (2009). Neurochemistry of the paraventricular nucleus of the hypothalamus: implications for cardiovascular regulation. *J. Chem. Neuroanat.* 38, 197–208. doi: 10.1016/j.jchemneu.2009.03.005

Quillen, E. W. J., and Cowley, A. W. J. (1983). Influence of volume changes on osmolality-vasopressin relationships in conscious dogs. *Am. J. Physiol.* 244, H73–H79. doi: 10.1152/ajpheart.1983.244.1.H73

Racca, F., Vianello, A., Mongini, T., Ruggeri, P., Versaci, A., Vita, G. L., et al. (2020). Practical approach to respiratory emergencies in neurological diseases. *Neurol. Sci.* 41, 497–508. doi: 10.1007/s10072-019-04163-0

Raff, H. (2011). Endocrine Adaptation to Hypoxia. *Compr. Physiol.* 1259-1275. doi: 10.1002/cphy.cp040254

Raggenbass, M., Tribollet, E., Dubois-Dauphin, M., and Dreifuss, J. J. (1989). Vasopressin receptors of the vasopressor (V1) type in the nucleus of the solitary tract of the rat mediate direct neuronal excitation. *J. Neurosci.* 9, 3929–3936. doi: 10.1523/JNEUROSCI.09-11-03929.1989

Reddy, M. K., Patel, K. P., and Schultz, H. D. (2005). Differential role of the paraventricular nucleus of the hypothalamus in modulating the sympathoexcitatory component of peripheral and central chemoreflexes. *Am. J. Phys. Regul. Integr. Comp. Phys.* 289, R789–R797. doi: 10.1152/ajpregu.00222.2005

Richter, D. W., and Seller, H. (1975). Baroreceptor effects on medullary respiratory neurones of the cat. *Brain Res.* 86, 168–171. doi: 10.1016/0006-8993(75)90651-4

Sanada, K., Yoshimura, M., Ikeda, N., Baba, K., Nishimura, H., Nishimura, K., et al. (2021). Chemogenetic activation of endogenous arginine vasopressin exerts anorexigenic effects via central nesfatin-1/NucB2 pathway. *J. Physiol. Sci.* 71:18. doi: 10.1186/s12576-021-00802-4

Schill, F., Timpka, S., Nilsson, P. M., Melander, O., and Enhörning, S. (2021). Copeptin as a predictive marker of incident heart failure. *ESC Hear. Fail.* 8, 3180–3188. doi: 10.1002/ehf2.13439

Schrier, R. W. (2008). Vasopressin and aquaporin 2 in clinical disorders of water homeostasis. *Semin. Nephrol.* 28, 289–296. doi: 10.1016/j.semnephrol.2008.03.009

Schrier, R. W., Berl, T., and Anderson, R. J. (1979). Osmotic and nonosmotic control of vasopressin release. *Am. J. Physiol.* 236, F321–F332. doi: 10.1152/ajprenal.1979.236.4.F321

Scott, C. S., Sharp-Kehl, J., Redekopp, C. A., and Ledsome, J. R. (1994). Regulation of plasma vasopressin by plasma osmolality and carotid sinus pressure in anesthetized rabbits. *Am. J. Physiol.* 266, R796–R801. doi: 10.1152/ajpregu.1994.266.3.R796

Senay, L. C. J. (1969). Increased blood osmolarity and its effect on respiration of dehydrating men. *Pflugers Arch.* 309, 165–175. doi: 10.1007/BF00586966

Skytioti, M., Søvik, S., and Elstad, M. (2018). Respiratory pump maintains cardiac stroke volume during hypovolemia in young, healthy volunteers. *J. Appl. Physiol.* 124, 1319–1325. doi: 10.1152/japplphysiol.01009.2017

Smith, P. M., Lowes, V. L., and Ferguson, A. V. (1994). Circulating vasopressin influences area postrema neurons. *Neuroscience* 59, 185–194. doi: 10.1016/0306-4522(94)90109-0

Smith, A. S., Williams Avram, S. K., Cymerblit-Sabba, A., Song, J., and Young, W. S. (2016). Targeted activation of the hippocampal CA2 area strongly enhances social memory. *Mol. Psychiatry* 21, 1137–1144. doi: 10.1038/mp.2015.189

Solaiman, A. Z., Feehan, R. P., Chabitnoy, A. M., Leuenberger, U. A., and Monahan, K. D. (2014). Ventilatory responses to chemoreflex stimulation are not enhanced by angiotensin II in healthy humans. *Auton. Neurosci.* 183, 72–79. doi: 10.1016/j.autneu.2014.01.010

Souza, G. M. P. R., Stornetta, R. L., Stornetta, D. S., Abbott, S. B. G., and Guyenet, P. G. (2020). Differential contribution of the retrotrapezoid nucleus and C1 neurons to active expiration and arousal in rats. *J. Neurosci.* 40, 8683–8697. doi: 10.1523/JNEUROSCI.1006-20.2020

Srinivasan, M., Bongianni, F., Fontana, G. A., and Pantaleo, T. (1993). Respiratory responses to electrical and chemical stimulation of the area postrema in the rabbit. *J. Physiol.* 463, 409–420. doi: 10.1113/jphysiol.1993.sp019601

Sugawara, Y., Mizuno, Y., Oku, S., and Goto, T. (2019). Effects of vasopressin during a pulmonary hypertensive crisis induced by acute hypoxia in a rat model of pulmonary hypertension. *Br. J. Anaesth.* 122, 437–447. doi: 10.1016/j.bja.2019.01.014

Szczepańska-Sadowska, E. (1996). Interaction of vasopressin and angiotensin II in central control of blood pressure and thirst. *Regul. Pept.* 66, 65–71. doi: 10.1016/0167-0115(96)00053-5

Szczepanska-Sadowska, E., Czarzasta, K., and Cudnoch-Jedrzejewska, A. (2018). Dysregulation of the renin-angiotensin system and the vasopressinergic system interactions in cardiovascular disorders. *Curr. Hypertens. Rep.* 20:19. doi: 10.1007/s11906-018-0823-9

Szczepanska-Sadowska, E., Zera, T., Sosnowski, P., Cudnoch-Jedrzejewska, A., Puszko, A., and Misicka, A. (2017). Vasopressin and related peptides; potential value in diagnosis, prognosis and treatment of clinical disorders. *Curr. Drug Metab.* 18, 306–345. doi: 10.2174/1389200218666170119145900

Szmydynger-Chodobska, J., Chung, I., Kozniewska, E., Tran, B., Harrington, F. J., Duncan, J. A., et al. (2004). Increased expression of vasopressin v1a receptors after traumatic brain injury. *J. Neurotrauma* 21, 1090–1102. doi: 10.1089/0897715041651033

Sztechman, D., Czarzasta, K., Cudnoch-Jedrzejewska, A., Szczepanska-Sadowska, E., and Zera, T. (2018). Aldosterone and mineralocorticoid receptors in regulation of the cardiovascular system and pathological remodelling of the heart and arteries. *J. Physiol. Pharmacol.* 69, 829-845. doi: 10.26402/jpp.2018.6.01

Tabarean, I. V. (2021). Activation of preoptic arginine vasopressin neurons induces hyperthermia in male mice. *Endocrinology* 162:bqaa217. doi: 10.1210/endocr/bqaa217

Tahara, A., Tomura, Y., Wada, K., Kusayama, T., Tsukada, J., Ishii, N., et al. (1998). Characterization of vasopressin receptor in rat lung. *Neuropeptides* 32, 281–286. doi: 10.1016/S0143-4179(98)90049-X

Takamata, A., Nose, H., Kinoshita, T., Hirose, M., Itoh, T., and Morimoto, T. (2000). Effect of acute hypoxia on vasopressin release and intravascular fluid during dynamic exercise in humans. *Am. J. Phys. Regul. Integr. Comp. Phys.* 279, R161–R168. doi: 10.1152/ajpregu.2000.279.1.R161

Takeda, M., Dubey, R., Phillips, J. K., Matsumoto, S., and Lipski, J. (2002). Effects of vasopressin on isolated rat adrenal chromaffin cells. *Regul. Pept.* 106, 55–65. doi: 10.1016/S0167-0115(02)00036-8

Thompson, C. J., Charlton, J., Walford, S., Baird, J., Hearnshaw, J., McCulloch, A., et al. (1989). Vasopressin secretion in the DIDMOAD (Wolfram) syndrome. *Q. J. Med.* 71, 333–345.

Thompson, E. L., Ray, C. J., Holmes, A. P., Pye, R. L., Wyatt, C. N., Coney, A. M., et al. (2016). Adrenaline release evokes hyperpnoea and an increase in ventilatory CO_2 sensitivity during hypoglycaemia: a role for the carotid body. *J. Physiol.* 594, 4439–4452. doi: 10.1113/JP272191

Thornton, S. N., Leng, G., Bicknell, R. J., Chapman, C., and Purdew, T. (1986). Vasopressin, but not oxytocin, is released in response to water deprivation in conscious goats. *J. Endocrinol.* 110, 335–340. doi: 10.1677/joe.0.1100335

Tribollet, E., Raufaste, D., Maffrand, J., and Serradeil-Le Gal, C. (1999). Binding of the non-peptide vasopressin V1a receptor antagonist SR-49059 in the rat brain: an in vitro and in vivo autoradiographic study. *Neuroendocrinology* 69, 113–120. doi: 10.1159/000054409

Trzebski, A., Chruścielewski, L., and Majcherczyk, S. (1978). Effect of osmotic stimuli on the carotid baroreceptor and chemoreceptor discharges in cats. *Acta Phys. Pol. A* 29, 373–377.

Ueta, Y., Dayanithi, G., and Fujihara, H. (2011). Hypothalamic vasopressin response to stress and various physiological stimuli: visualization in transgenic animal models. *Horm. Behav.* 59, 221–226. doi: 10.1016/j.yhbeh.2010.12.007

Ufnal, M., and Skrzypecki, J. (2014). Blood borne hormones in a cross-talk between peripheral and brain mechanisms regulating blood pressure, the role of circumventricular organs. *Neuropeptides* 48, 65–73. doi: 10.1016/j.npep.2014.01.003

Venus, B., Mathru, M., Smith, R. A., Pham, C. G., Shirakawa, Y., and Sugiura, A. (1985). Renal function during application of positive end-expiratory pressure in swine: effects of hydration. *Anesthesiology* 62, 765–769. doi: 10.1097/00000542-198506000-00011

Verbalis, J. G. (2007). How does the brain sense osmolality? *J. Am. Soc. Nephrol.* 18, 3056–3059. doi: 10.1681/ASN.2007070825

Verney, E. B. (1947). The antidiuretic hormone and the factors which determine its release. *Proc. R. Soc. Lond. Ser. B Biol. Sci.* 135, 25–106.

Wade, C. E., and Claybaugh, J. R. (1980). Plasma renin activity, vasopressin concentration, and urinary excretory responses to exercise in men. *J. Appl. Physiol.* 49, 930–936. doi: 10.1152/jappl.1980.49.6.930

Wade, J. B., Stetson, D. L., and Lewis, S. A. (1981). ADH action: evidence for a membrane shuttle mechanism. *Ann. N. Y. Acad. Sci.* 372, 106–117. doi: 10.1111/j.1749-6632.1981.tb15464.x

Walker, B. R. (1986). Role of vasopressin in the cardiovascular response to hypoxia in the conscious rat. *Am. J. Physiol.* 251, H1316–H1323. doi: 10.1152/ajpheart.1986.251.6.H1316

Walker, B. R., Haynes, J. J., Wang, H. L., and Voelkel, N. F. (1989). Vasopressin-induced pulmonary vasodilation in rats. *Am. J. Physiol.* 257, H415–H422. doi: 10.1152/ajpheart.1989.257.2.H415

Walker, J. K., and Jennings, D. B. (1994). Angiotensin mediates stimulation of ventilation after vasopressin V1 receptor blockade. *J. Appl. Physiol.* 76, 2517–2526. doi: 10.1152/jappl.1994.76.6.2517

Walker, J. K., and Jennings, D. B. (1995). During acute hypercapnia vasopressin inhibits an angiotensin drive to ventilation in conscious dogs. *J. Appl. Physiol.* 79, 786–794. doi: 10.1152/jappl.1995.79.3.786

Walker, J. K., and Jennings, D. B. (1996). Ventilatory effects of angiotensin and vasopressin in conscious rats. *Can. J. Physiol. Pharmacol.* 74, 1258–1264. doi: 10.1139/y96-140

Walker, J. K., and Jennings, D. B. (1998). Respiratory effects of pressor and depressor agents in conscious rats. *Can. J. Physiol. Pharmacol.* 76, 707–714. doi: 10.1139/y98-081

Wallace, A. W., Tunin, C. M., and Shoukas, A. A. (1989). Effects of vasopressin on pulmonary and systemic vascular mechanics. *Am. J. Physiol.* 257, H1228–H1234. doi: 10.1152/ajpheart.1989.257.4.H1228

Wang, B. C., Sundet, W. D., and Goetz, K. L. (1984). Vasopressin in plasma and cerebrospinal fluid of dogs during hypoxia or acidosis. *Am. J. Physiol.* 247, E449–E455. doi: 10.1152/ajpendo.1984.247.4.E449

Ward, D. S., Voter, W. A., and Karan, S. (2007). The effects of hypo- and hyperglycaemia on the hypoxic ventilatory response in humans. *J. Physiol.* 582, 859–869. doi: 10.1113/jphysiol.2007.130112

Wehberg, K. E., Gala, G. J., and Brunner, M. J. (1991). Comparison of carotid baroreflex control of plasma AVP concentration in conscious and anesthetized dogs. *Am. J. Physiol.* 261, R950–R956. doi: 10.1152/ajpregu.1991.261.4.R950

Wehrwein, E. A., Limberg, J. K., Taylor, J. L., Dube, S., Basu, A., Basu, R., et al. (2015). Effect of bilateral carotid body resection on the counterregulatory response to hypoglycaemia in humans. *Exp. Physiol.* 100, 69–78. doi: 10.1113/expphysiol.2014.083154

Wilson, D. A., Hanley, D. F., Feldman, M. A., and Traystman, R. J. (1987). Influence of chemoreceptors on neurohypophyseal blood flow during hypoxic hypoxia. *Circ. Res.* 61, 194–101.

Yan, X., Chen, X., Guo, Y., He, D., Chen, Y., Xia, C., et al. (2017). Arginine vasopressin alters both spontaneous and phase-locked synaptic inputs to airway vagal preganglionic neuron via activation of V(1a) receptor: insights into stress-related airway vagal excitation. *Front. Cell. Neurosci.* 11:12. doi: 10.3389/fncel.2017.00012

Yang, Z., and Coote, J. H. (1998). Influence of the hypothalamic paraventricular nucleus on cardiovascular neurones in the rostral ventrolateral medulla of the rat. *J. Physiol.* 513, 521–530. doi: 10.1111/j.1469-7793.1998.521bb.x

Yang, S.-J., Lee, K.-Z., Wu, C.-H., Lu, K.-T., and Hwang, J.-C. (2006). Vasopressin produces inhibition on phrenic nerve activity and apnea through V(1A) receptors in the area postrema in rats. *Chin. J. Phys.* 49, 313–325.

Yang, Z., Wheatley, M., and Coote, J. H. (2002). Neuropeptides, amines and amino acids as mediators of the sympathetic effects of paraventricular nucleus activation in the rat. *Exp. Physiol.* 87, 663–674. doi: 10.1113/eph8702439

Yang, D.-B., Yu, W.-H., Dong, X.-Q., Du, Q., Shen, Y.-F., Zhang, Z.-Y., et al. (2014). Plasma copeptin level predicts acute traumatic coagulopathy and progressive hemorrhagic injury after traumatic brain injury. *Peptides* 58, 26–29. doi: 10.1016/j.peptides.2014.05.015

Yeung, M. L., Teng, J. L. L., Jia, L., Zhang, C., Huang, C., Cai, J.-P., et al. (2021). Soluble ACE2-mediated cell entry of SARS-CoV-2 via interaction with proteins related to the renin-angiotensin system. *Cell* 184, 2212. e12–2228.e12. doi: 10.1016/j.cell.2021.02.053

Yoshimura, M., Nishimura, K., Nishimura, H., Sonoda, S., Ueno, H., Motojima, Y., et al. (2017). Activation of endogenous arginine vasopressin neurons inhibit food intake: by using a novel transgenic rat line with DREADDs system. *Sci. Rep.* 7:15728. doi: 10.1038/s41598-017-16049-2

Yoshimura, M., and Ueta, Y. (2019). Advanced genetic and viral methods for labelling and manipulation of oxytocin and vasopressin neurones in rats. *Cell Tissue Res.* 375, 311–327. doi: 10.1007/s00441-018-2932-9

Zera, T., Moraes, D. J. A., da Silva, M. P., Fisher, J. P., and Paton, J. F. R. (2019). The logic of carotid body connectivity to the brain. *Physiology* 34, 264–282. doi: 10.1152/physiol.00057.2018

Żera, T., Przybylski, J., Grygorowicz, T., Kasarełło, K., Podobińska, M., Mirowska-Guzel, D., et al. (2018). Vasopressin V1a receptors are present in the carotid body and contribute to the control of breathing in male Sprague-Dawley rats. *Peptides* 102, 68–74. doi: 10.1016/j.peptides.2018.03.004

Zerbe, R. L., and Feuerstein, G. (1985). Cardiovascular effects of centrally administered vasopressin in conscious and anesthetized rats. *Neuropeptides* 6, 471–483. doi: 10.1016/0143-4179(85)90146-5

Zhang, Z.-Y., Zhang, L.-X., Dong, X.-Q., Yu, W.-H., Du, Q., Yang, D.-B., et al. (2014). Comparison of the performances of copeptin and multiple biomarkers in long-term prognosis of severe traumatic brain injury. *Peptides* 60, 13–17. doi: 10.1016/j.peptides.2014.07.016

Zhao, Y., Jiang, Y., Zhou, L., and Wu, X. (2014). The value of assessment tests in patients with acute exacerbation of chronic obstructive pulmonary disease. *Am. J. Med. Sci.* 347, 393–399. doi: 10.1097/MAJ.0b013e31829a63b1

Zheng, F., Copotoiu, R., Tacquard, C., Demoulin, B., Malinovsky, J. M., Levy, B., et al. (2017). Epinephrine but not vasopressin attenuates the airway response to anaphylactic shock in rats. *Exp. Lung Res.* 43, 158–166. doi: 10.1080/01902148.2017.1323981

Zhou, T., Chien, M.-S., Kaleem, S., and Matsunami, H. (2016). Single cell transcriptome analysis of mouse carotid body glomus cells. *J. Physiol.* 594, 4225–4251. doi: 10.1113/JP271936

Zimmerman, C. A., Lin, Y.-C., Leib, D. E., Guo, L., Huey, E. L., Daly, G. E., et al. (2016). Thirst neurons anticipate the homeostatic consequences of eating and drinking. *Nature* 537, 680–684. doi: 10.1038/nature18950

Conflict of Interest: The authors declare that the research was conducted in the absence of any commercial or financial relationships that could be construed as a potential conflict of interest.

Publisher's Note: All claims expressed in this article are solely those of the authors and do not necessarily represent those of their affiliated organizations, or those of the publisher, the editors and the reviewers. Any product that may be evaluated in this article, or claim that may be made by its manufacturer, is not guaranteed or endorsed by the publisher.

Copyright © 2021 Proczka, Przybylski, Cudnoch-Jędrzejewska, Szczepańska-Sadowska and Żera. This is an open-access article distributed under the terms of the Creative Commons Attribution License (CC BY). The use, distribution or reproduction in other forums is permitted, provided the original author(s) and the copyright owner(s) are credited and that the original publication in this journal is cited, in accordance with accepted academic practice. No use, distribution or reproduction is permitted which does not comply with these terms.

frontiers in Physiology

ORIGINAL RESEARCH
published: 29 October 2021
doi: 10.3389/fphys.2021.752924

Altering Early Life Gut Microbiota Has Long-Term Effect on Immune System and Hypertension in Spontaneously Hypertensive Rats

*Francois M. Abboud[1,2,3], Michael Z. Cicha[1,4], Aaron Ericsson[5], Mark W. Chapleau[1,2,3] and Madhu V. Singh[1,4]**

[1] Abboud Cardiovascular Research Center, Carver College of Medicine, University of Iowa, Iowa City, IA, United States, [2] Department of Internal Medicine, Carver College of Medicine, University of Iowa, Iowa City, IA, United States, [3] Department of Molecular Physiology and Biophysics, Carver College of Medicine, University of Iowa, Iowa City, IA, United States, [4] Department of Internal Medicine, Division of Endocrinology and Metabolism, Carver College of Medicine, University of Iowa, Iowa City, IA, United States, [5] Metagenomics Center, University of Missouri, Columbia, MO, United States

Hypertension is regulated by immunological components. Spontaneously hypertensive rats (SHR) display a large population of proinflammatory CD161 + immune cells. We investigated the effect of early post-natal gut microbiota on the development of the immune system and resulting hypertension in the SHR. We first examined the microbial populations in the fecal samples of SHR and normotensive control WKY using 16S rDNA sequencing. We found that in the newborn SHR (1-week old) the gut microbiota was qualitatively and quantitatively different from the newborns of normotensive WKY. The representation of the predominant bacterial phylum Proteobacteria was significantly less in 1-week old SHR pups than in WKY (94.5% Proteobacteria in WKY vs. 65.2% in SHR neonates). Even within the phylum Proteobacteria, the colonizing genera in WKY and SHR differed dramatically. Whereas WKY microbiota was predominantly comprised of *Escherichia-Shigella*, SHR microbiota was represented by other taxa of *Enterobacteriaceae* and *Pasteurellaceae*. In contrast, the representation of phylum Firmicutes in the neonatal SHR gut was greater than WKY. Cross-fostering newborn SHR pups by lactating WKY dams caused a dramatic shift in 1-week old cross-fostered SHR gut microbiota. The two major bacterial taxa of phylum Proteobacteria, *Enterobacteriaceae and Pasteurellaceae* as well as *Lactobacillus intestinalis, Proteus, Romboustia* and *Rothia* were depleted after cross-fostering and were replaced by the predominant genera of WKY (*Escherichia-Shigella*). A proinflammatory IL-17F producing CD161 + immune cell population in the spleen and aorta of cross-fostered SHR was also reduced (30.7% in self-fostered SHR vs. 12.6% in cross-fostered SHR at 30 weeks of age) as was the systolic blood pressure in adult cross-fostered SHR at 10 weeks of age. Thus, altered composition of gut microbiota of SHR toward WKY at early neonatal age had a long-lasting effect on immune system by reducing proinflammatory immune cells and lowering systolic blood pressure.

Keywords: microbiome, immune system, gut microbiome, hypertension, SHR (spontaneously hypertensive rat), T helper (T) 17 cells, RORgamma t

OPEN ACCESS

Edited by:
Geoffrey A. Head, Baker Heart and Diabetes Institute, Australia

Reviewed by:
You-Lin Tain, Kaohsiung Chang Gung Memorial Hospital, Taiwan
Francine Marques, Monash University, Australia

***Correspondence:**
Madhu V. Singh
madhu-singh@uiowa.edu

Specialty section:
This article was submitted to Integrative Physiology, a section of the journal Frontiers in Physiology

Received: *03 August 2021*
Accepted: *08 October 2021*
Published: *29 October 2021*

Citation:
Abboud FM, Cicha MZ, Ericsson A, Chapleau MW and Singh MV (2021) Altering Early Life Gut Microbiota Has Long-Term Effect on Immune System and Hypertension in Spontaneously Hypertensive Rats. Front. Physiol. 12:752924. doi: 10.3389/fphys.2021.752924

INTRODUCTION

Gut microbes exert profound effects on health and disease by assisting in development of the gut, maintaining gut barrier function, providing energy and protecting against pathogenic invasion. The early neonatal gut microbiome primes the development of the host immune system (Hooper et al., 2012; Gensollen et al., 2016; Li et al., 2017) with potentially long-lasting health consequences in a manner dependent on the genetic background of the host (Macpherson et al., 2017). The composition of the early gut microbiome is dependent on host genetic factors and the environment (Turnbaugh et al., 2009; Benson et al., 2010) and can be altered by changing the environment at an early post-natal age (Daft et al., 2015).

Hypertension is associated with neurogenic, environmental, and immunologic factors. The spontaneously hypertensive rat (SHR) is a widely studied model of genetic hypertension that is linked to both immune disorder (Singh et al., 2017) and "unhealthy" gut microbiome (dysbiosis) (Yang et al., 2015). Treatment of SHR with antibiotics or fecal transplant from normotensive rats reduces blood pressure suggesting a role of resident gut microbiota in SHR hypertension (Galla et al., 2018). These results indicate a potential interaction of the immune system and gut microbiome in SHR hypertension. Effects of gut microbiome on adult blood pressure in other models have been reported. Use of angiotensin II (Ang II) was correlated with change in gut microbiome (Yang et al., 2015), oral administration of minocycline antibiotic reduced blood pressure presumably by altering the gut microbiome and fecal transplants from normotensive rats to stroke-prone SHR (SHRSP) reduced blood pressure (Adnan et al., 2017). However, these models have inherent limitations; considering the quick effect of Ang II on hypertension, it is not clear whether in Ang II-induced hypertension the change in gut microbiota was a consequence of Ang II administration. Minocycline antibiotic crosses the blood-brain barrier (Shi et al., 2010; Hu et al., 2013) and can have direct neurogenic effects in hypertension, whereas SHRSP is a distinct strain of rat that genetically diverged considerably from SHR (Nabika et al., 2012). Moreover, late age colonization of the gut by introduced microbiota does not fully restore the immune system in germ free mice (El Aidy et al., 2013). Therefore, it appears that gut microbiome may affect hypertension at different stages through different mechanisms.

We and others have used animal models to show the roles of pro-inflammatory immune cells in development of hypertension. We have shown that the SHR displays an abnormally high preponderance of CD161 + immune cells at birth that increases with age (Singh et al., 2017). These cells also express high levels of RORγt transcription factor-dependent proinflammatory prohypertensive cytokines IL-17A and IL-17F that contribute to hypertension (Singh et al., 2017). IL-17A and -17F are members of the IL-17 family of proinflammatory cytokines that are produced by T helper 17 (Th17) cells, γδT cells, and other cells that express RORγt transcription factor (Ivanov et al., 2006). Th17 cells play a prominent role in several autoimmune diseases and their abundance is regulated by specific gut microbiota (Ivanov et al., 2008; Eberl, 2017).

In the SHR, significantly lower blood pressure levels were observed in adulthood, when the neonatal pups were cross-fostered by normotensive Wistar-Kyoto (WKY) or Sprague-Dawley dams (Cierpial and McCarty, 1987). Although, the outcome of cross-fostering on SHR hypertension has been attributed to altered maternal behavior, we hypothesized that cross-fostering alters the gut microbiota of the neonatal SHR resulting in a favorable immune-response and lesser hypertension in adulthood. Indeed, it is known that the development of the immune system can be affected by gut microbiota as early as in the fetal stage (Cierpial et al., 1988; Mishra et al., 2021). Here, we investigated whether altering the neonatal gut microbiota of the SHR pups by cross fostering with normotensive dams favorably alters their immune response and their hypertension in adulthood.

MATERIALS AND METHODS

Animal Breeding and Cross-Fostering

All animal protocols were approved by the Institutional Animal Care and Use Committee of the University of Iowa. WKY and SHR rats were obtained from Charles River Laboratories and were bred in-house. All rats were maintained on a standard rat chow diet (Cat # 7013, Envigo, United States). Cages of pregnant dams (1 dam per cage) were monitored daily, and the day of the pups' birth was considered day-1. Pups were weaned at 3 weeks of age. Pups of WKY and SHR strains were cross-fostered within 48 h of birth by presenting the entire litter (8 to 10 pups each litter) to the cages of the fostering dams of the other strain. Only male pups were used in the experiments.

Fecal Samples and DNA Extraction

Fecal or colonic samples were obtained from 1 week old, 5 weeks old and 12 weeks old (equivalent to early adulthood in humans) male rats. All fecal samples were obtained in the mornings. For 1 week old pups, colonic samples were obtained by decapitation of pups under anesthesia (isoflurane) and exposure of the body cavity and gentle extrusion of fecal matter using sterile blunt forceps. For older rats, fecal samples, free from urine, were obtained by placing the rats in sterilized cages and pellets were collected on first appearance. All samples were handled using sterile forceps and stored in sterile screw-cap tubes by quick freezing in liquid nitrogen, followed by transfer to −80°C until further analyses. DNA was extracted using PowerFecal kits (Qiagen) according to the manufacturer's instructions, with the exception that samples were homogenized in the provided bead tubes using a TissueLyser II (Qiagen, Venlo, Netherlands) for 3 min at 30 beats/sec. DNA yields were quantified by fluorometry (Qubit 2.0, Invitrogen, Carlsbad, CA, United States) using quant-iT BR dsDNA reagent kits (Invitrogen) and normalized to a uniform concentration and volume.

16S rRNA Gene Sequencing

16S rRNA amplicon libraries were generated and sequenced at the MU Genomics Technologies Core facility. Bacterial 16S rRNA amplicons were constructed via amplification of the V4 region

of the 16S rRNA gene with universal primers (U515F/806R) previously developed against the V4 region, flanked by Illumina standard adapter sequences (Caporaso et al., 2011; Walters et al., 2011). Oligonucleotide sequences are available at proBase (Loy et al., 2007). Dual-indexed forward and reverse primers were used in all reactions. PCR was performed in 50 μL reactions containing 100 ng metagenomic DNA, primers (0.2 μM each), dNTPs (200 μM each), and Phusion high-fidelity DNA polymerase (1U, Thermo Fisher). Amplification parameters were $98°C(^{3\ min}) + [98°C(^{15\ sec}) + 50°C(^{30\ sec}) + 72°C(^{30\ sec})] \times 25$ cycles $+ 72°C(^{7\ min})$. Amplicon pools (5 μL/reaction) were combined, thoroughly mixed, and then purified by addition of Axygen Axyprep Mag PCR clean-up beads (Corning, United States) to an equal volume of 50 μL of amplicons and incubated for 15 min at room temperature. Products were then washed multiple times with 80% ethanol and the dried pellet was resuspended in 32.5 μL EB buffer (Qiagen), incubated for 2 min at room temperature, and then placed on the magnetic stand for 5 min. The final amplicon pool was evaluated using the Advanced Analytical Fragment Analyzer automated electrophoresis system, quantified using quant-iT HS dsDNA reagent kits, and diluted according to Illumina's standard protocol for sequencing on the MiSeq instrument as 2 × 250 bp paired-end reads.

Microbiome Analysis

DNA sequences were assembled and annotated at the MU Informatics Research Core facility. Primers were designed to match the 5′ ends of the forward and reverse reads. Cutadapt (Martin, 2011) (version 2.6[1]) was used to remove the primer from the 5′ end of the forward read. If found, the reverse complement of the primer to the reverse read was then removed from the forward read as were all bases downstream. Thus, a forward read could be trimmed at both ends if the insert was shorter than the amplicon length. The same approach was used on the reverse read, but with the primers in the opposite roles. Read pairs were rejected if one read or the other did not match a 5′ primer, and an error-rate of 0.1 was allowed. Two passes were made over each read to ensure removal of the second primer. A minimal overlap of three bp with the 3′ end of the primer sequence was required for removal.

The QIIME2 (Bolyen et al., 2019) DADA2 (Callahan et al., 2016) plugin (version 1.10.0) was used to denoise, de-replicate, and count ASVs (amplicon sequence variants), incorporating the following parameters: (1) forward and reverse reads were truncated to 150 bases, (2) forward and reverse reads with number of expected errors higher than 2.0 were discarded, and (3) Chimeras were detected using the "consensus" method and removed. R version 3.5.1 and Biom version 2.1.7 were used in QIIME2. Taxonomies were assigned to final sequences using the Silva.v132 (Pruesse et al., 2007) database, using the classify-sklearn procedure. Rarefaction of data was performed using https://docs.qiime2.org/2021.8/plugins/available/diversity/core-metrics-phylogenetic/. In summary, data were rarefied to one less than the lowest read count greater than 10,000 reads. Alpha (Shannon diversity index) and beta-diversity (Bray-Curtis similarities) were calculated and principal coordinate analysis plots were generated using Past3 software.

[1]https://github.com/marcelm/cutadapt

Tissue Processing for Flow Cytometry

Rats were euthanized under anesthesia and single cell suspensions from spleens were obtained by disaggregating spleen tissue between frosted glass microscopy slides. Erythrocytes were lysed by suspending splenocytes pellets in a hypotonic solution (155 mM NH4Cl, 12 mM NaHCO3, 0.1 mM EDTA), nucleated cells were washed twice with phosphate buffered saline (PBS). Flow cytometry was performed as described earlier (Singh et al., 2017). Briefly, washed splenocytes were suspended in Fc blocking buffer (2% v/v fetal bovine serum and 1% v/v normal mouse serum in PBS). An aliquot of 10^6 cells was taken from each sample and mixed with FITC-CD161, PerCP-CD8a, APC-CD4, PE-CD3, and PE-Cy5-CD45RA antibodies (1 μl each antibody, all antibodies from BD Biosciences). After incubation with antibodies on ice for 30 min, cells were washed twice with PBS and resuspended in 400 μl PBS and flow cytometry was performed on a Beckton-Dickinson Aria flow cytometer. Thoracic aorta were minced with a razor blade and digested in 0.05% w/v Collagenase Type I and 0.05% w/v Collagenase Type II in HBSS. Cells were dissociated by trituration and filtered through a nylon membrane followed by two washes with ice cold PBS. Cells were then processed as described above for the spleen cells.

Tail Cuff Pressure Measurements

Tail cuff pressure measurements were done as previously described (Singh et al., 2019). Briefly, a week prior to recordings, rats were acclimatized in the holders without tail cuff pressure measurements for at least three sessions. Systolic blood pressure (SBP) was recorded every week by tail cuff plethysmography on a VisiTech 2000 system (VisiTech, Denver, CO, United States). Weekly SBPs reported were averages of 20 recordings per animal per session each week. Statistical analyses of SBPs were performed with a two-way ANOVA (Prism Software, version 7.0a; GraphPad Software, La Jolla, CA, United States) on SBP data starting from 6 weeks of age, when the increase in pressure in SHR became evident. Investigators were blinded for blood pressure and microbiome analyses.

Statistical Tests

Statistical tests were performed using GraphPad Prism. Results are presented as mean ± SEM. For comparisons between WKY and SHR or between self-fostered and cross-fostered groups, one-way ANOVA with Sidak's *post hoc* test was applied for comparisons between multiple groups. For blood pressure, a two-way ANOVA was used. P values < 0.05 were considered statistically significant.

RESULTS

We examined the gut microbiome using 16S rDNA sequencing from the fecal samples of neonatal (1 week), of weanlings (5 weeks), and of adult (12 weeks) male SHR and WKY rats. Two

major comparisons were made. One was between neonatal rats and older (weanlings and adults) rats. The other was between the two strains, SHR and WKY.

In the neonates of both strains, the number of microbial species (Amplicon Sequence Variants, ASV) and their complexity (Shannon index) were significantly less than in the weanlings and adult counterparts (**Figures 1A,B**). No major difference between the microbiome of the older rats of the two strains were seen (**Figures 1B,C**). In the neonates, the phylum Proteobacteria was more dominant in WKY than in SHR (**Figure 1D**) and consisted primarily of *Escherichia-Shigella* (93.2%), whereas in neonatal SHR there was a total lack of *Escherichia-Shigella*, and instead the Proteobacteria of *Enterobacteriaceae* and *Pasteurellaceae* prevailed at 35.0 and 27.9%, respectively (**Figure 1D**). In contrast, the phylum Firmicutes was more prevalent in SHR (30.7%) than in WKY (4.6%) with *Lactobacillus* constituting 21.0% in SHR and essentially lacking in WKY (0.86%, **Figure 1D**).

In the weanlings and adults of both strains the phylum Proteobacteria was notably absent, but the Firmicutes was significantly and equally represented as was the phylum Bacteroidota (**Figure 1D**). Thus, the major difference between the strains was in their neonatal state. The Proteobacteria *Escherichia-Shigella* was absent in neonatal SHR, yet dominant in WKY and the Firmicutes *Lactobacillus* present in SHR was absent in WKY. The Firmicutes to Bacteroidota ratio (F/B ratio) in 5-weeks old WKY and SHR were 1.06 and 1.23, respectively (**Figure 1D**). The F/B ratio in 12-weeks old WKY and SHR were also similar (WKY 1.56 and SHR 1.48).

We then cross-fostered newborn SHR and WKY pups with WKY and SHR dams, respectively. Cross-fostering of SHR dramatically shifted their Proteobacteria to resemble the distribution seen in self-fostered WKY. *Escherichia-Shigella*, which is essentially absent in the self-fostered neonatal SHR, increased to 73.9% by cross-fostering (**Figure 2A**) replacing *Enterobacteriaceae* and *Pasteurellaceae* taxa that are prominent in neonatal SHR and dropped to undetectable levels with cross-fostering (**Figure 2A**).

Equally significant changes were observed in cross-fostered WKY with a reduction in the Proteobacteria *Escherichia-Shigella* from the level of 93.2% seen in self-fostered WKY to 52.1% in the cross-fostered, and the new appearance of the Firmicutes *Lactobacillus* in the cross-fostered WKY to 22.0%, a level comparable to the self-fostered SHR (21.0%). The significant differences of the major taxa, which constitute approximately 98% of total taxa between 1-week old self-fostered WKY and self-fostered SHR, were abolished in cross-fostered WKY and cross-fostered SHR (**Figure 2B**). Comparison of these groups showed elimination of *Haemophilus*, *Lactobacillus intestinalis* (*L. intestinalis*), *Romboustia*, and *Rothia* in cross-fostered SHR (**Figure 2B**). In addition, *Enterobacteriaceae* and *Pasteurellaceae* taxa were also eliminated in cross-fostered SHR. In contrast, cross-fostered SHR showed increased *Escherichia-Shigella*.

The systolic blood pressure measured by tail cuff method increased progressively more in self-fostered SHR than in cross-fostered SHR, and was significantly lower in cross-fostered adult SHR (**Figure 3A**) similar to the previous report (Cierpial and McCarty, 1987). The systolic blood pressure of self-fostered and cross fostered WKY did not increase with age and did not differ between the groups (**Figure 3B**).

We have previously reported in SHR a post-natal progressive increase in proinflammatory immune cells that express a CD161 surface marker with age. These cells produce IL-17F that influences the blood pressure in SHR (Singh et al., 2017). In this study, the splenic population of CD161 + cells in cross-fostered SHR did not increase with age when compared to the self-fostered SHR (**Figure 4A**). Similarly, CD4 + CD161 + cells, known to overexpress RORγt transcription factor and increase IL-17F cytokine upon induction, were also decreased (**Figure 4B**). Moreover, of pathological significance, infiltration of CD161 + cells in aortic tissue of cross-fostered SHR was also decreased (**Figure 4C**) and was similar to that observed in cross-fostered WKY (**Figures 4C,D**).

DISCUSSION

In this report, using SHR as a genetic model of hypertension, we have shown that altering gut microbiome of the neonatal SHR results in long term immune alteration and attenuated hypertension. Our 16S rDNA sequence data suggest that neonatal SHR gut microbiome is dramatically different from that of neonatal WKY much before the onset of hypertension. However, remarkable changes occurred as these rats from either strain aged. First, the number of bacterial taxa increase after weaning and second, the differences between the microbiome of the two strains diminishes. Indeed, similar results of low complexity of gut microbiome in infancy and increased microbial diversity with shift to solid food from mother's milk have been reported in humans in longitudinal as well as population studies (Koenig et al., 2011; Yatsunenko et al., 2012; Arrieta et al., 2014). In addition, in the neonatal gut the taxa representing the order *Enterobacteriales* are predominant (Arrieta et al., 2014; Tsukuda et al., 2021), an observation that is consistent in our data of neonatal WKY. In the neonatal WKY the *Enterobacteriaceae* family was predominantly represented by *Escherichia-Shigella*, whereas this taxon was almost completely absent in neonatal SHR. Instead, other taxa of *Enterobacteriaceae* family were detected in the neonatal SHR. This is a remarkable deviation in SHR gut microbiome from normotensive WKY.

Age-related increase in the taxa of gut bacteria is usually accompanied with the increase in Firmicutes. We observed increased Firmicutes in both WKY and SHR with age. However, the Firmicutes population in neonatal gut was much greater in SHR than in neonatal WKY. A higher Firmicutes to Bacteroidetes ratio (F/B ratio) is considered to be a hallmark of hypertension (Yang et al., 2015; Zhang et al., 2021). Indeed, in our study, the neonatal SHR had much greater F/B ratio than neonatal WKY, primarily because early neonatal gut is devoid of Bacteroidota taxa. Nevertheless, this difference was increased in cross-fostered SHR suggesting that F/B ratio alone is not a reliable predictor of a disease state (Magne et al., 2020).

We observed major differences in several bacterial genera between the two strains. First, the neonatal WKY had

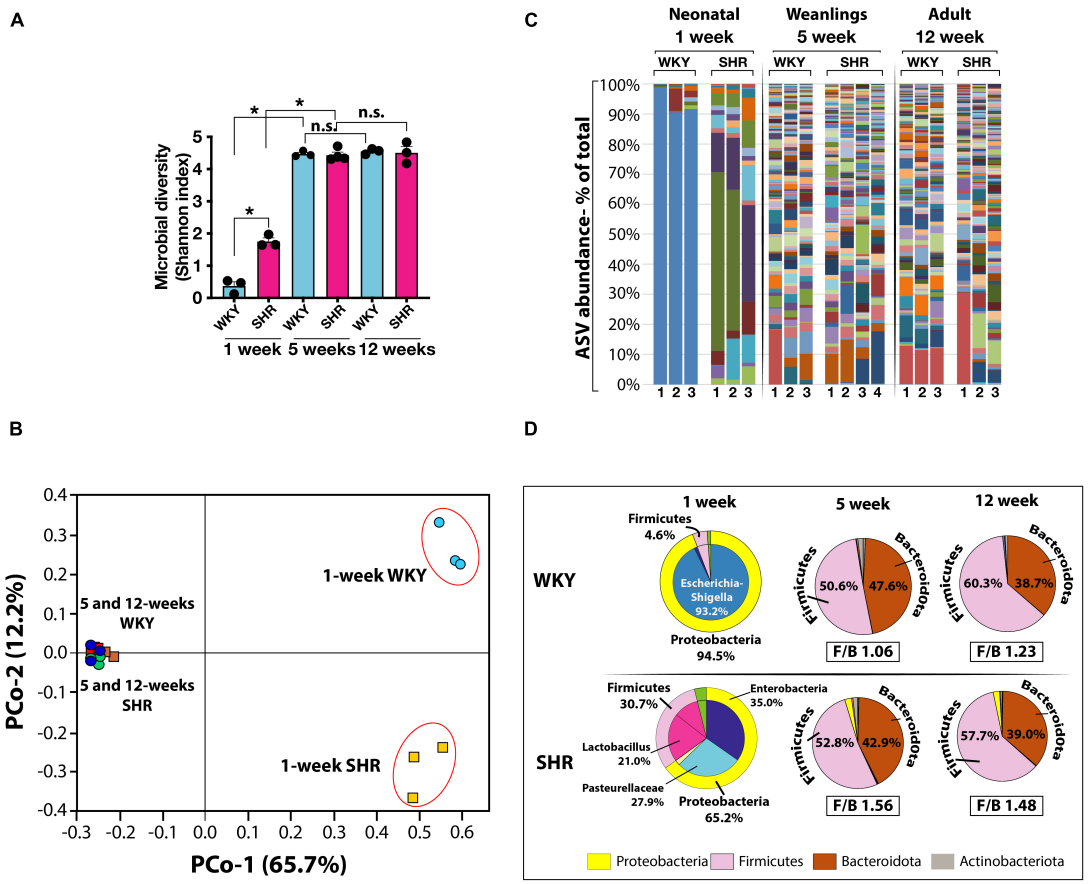

FIGURE 1 | (A) Microbial diversity (Shannon Index) and complexity are significantly greater in weanling (5-weeks old) and adult (12-weeks old) WKY (blue bars) and SHR (red bars) compared to neonatal (1-week old) rats. (n = 3 each group except n = 4 in 5-weeks old SHR). Asterisks indicate significant difference (*P < 0.0001). **(B)** Principal component (PCo) analysis of clustering of microbiotas is also very different in neonatal 1-week old than older rats (PCo1, x-axis) and between 1-week old WKY and SHR (PCo2, y-axis). **(C)** Graphical display of major ASV (Amplicon Sequence Variants) in WKY and SHR from 1-week (n = 3 each), 5-weeks (WKY n = 3, SHR n = 4) and 12-weeks old (n = 3 each) rats. Different taxa are displayed in different colors and the height of each colored bar represents the population size (percent of total population). Each lane represents one sample from a mouse. **(D)** Pie charts display the major phyla and constituent ASV at different ages in WKY and SHR (n = 3 in each group except n = 4 in 5-weeks old SHR). Corresponding Firmicutes to Bacteroidota ratio (F/B ratio) are shown for 5- and 12- weeks old rats. F/B ratios for 1-week old rats were not calculated due to extremely low content of Bacteroidota taxa.

predominant presence *of Escherichia-Shigella* whereas these bacteria were absent in SHR. In contrast, neonatal SHR had predominantly *Haemophilus*, *Lactobacillus intestinalis, Romboustia, Rothia and other taxa of Enterobacteriaceae, Pasteurellaceae*, and *Lactobacilli.* More importantly, cross-fostering of SHR by normotensive WKY dams significantly increased *Escherichia-Shigella* in 1-week old SHR, reduced *Lactobacillus* and almost completely depleted taxa of *Enterobacteriaceae*, *Pasteurellaceae*, *Romboustia*, and *Rothia*. These changes were associated with attenuated hypertension and decreased CD4 + CD161 + cells that produce high levels of IL-17F cytokine on induction (Singh et al., 2017) in adulthood.

We found a decrease in proinflammatory CD161 + cells in spleen as well as in aorta of the cross-fostered SHR. The decrease in systolic blood pressure of cross-fostered SHR at adulthood associates with the decrease in this cell population suggesting that the gut microbiome influences genetic hypertension through immunological development. Development and maturation of the mammalian immune system predominantly depends on the early neonatal interactions with the gut colonizing microbiota (Gensollen et al., 2016). We have previously demonstrated that the population of proinflammatory immune cells (CD161 + RORγt +) in SHR express IL-17F to influence the vasculature to influence blood pressure in SHR (Singh et al., 2017). Proliferation and abundance of IL-17 producing Th17 cells has been shown to be dependent on the presence of segmented filamentous bacteria (SFB, *Candidatus arthromitus*) in the gut (Ivanov et al., 2009; Ericsson et al., 2014). In our study, there was undetectable SFB in the neonatal (1 week old) pups of either SHR or WKY strain, which did not change after cross-fostering. However, SFB abundance was high in both WKY and SHR after weaning (5-weeks old), which declined in WKY more than in SHR at 12-weeks of age. It is likely that one or more of the bacteria present in neonatal SHR that were eliminated in cross-fostered SHR could contribute to the increase in the CD161 + immune cells leading to hypertension.

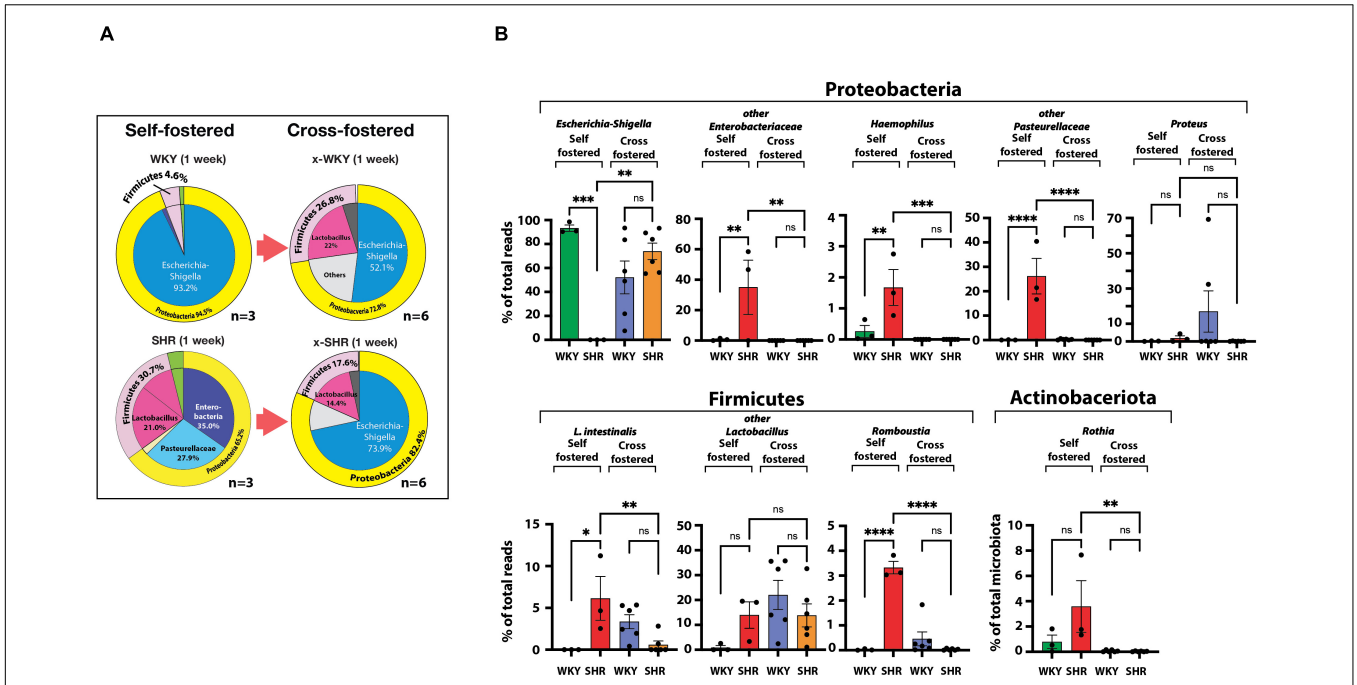

FIGURE 2 | (A) Differences in neonatal major phyla between self-fostered (n = 3 each) and cross-fostered x-WKY and x-SHR (n = 6 each). **(B)** Changes in major ASV of the gut microbiota between 1-week old self-fostered WKY and SHR (n = 3 each) and between 1-week old cross-fostered x-WKY and x-SHR (n = 6 each). Asterisks denote statistically significant difference (*P < 0.05, **P < 0.01, ***P < 0.001, ****P ≤ 0.0001, one-way ANOVA with Sidak's *post hoc* multiple comparison test), n.s. denotes not statistically significant.

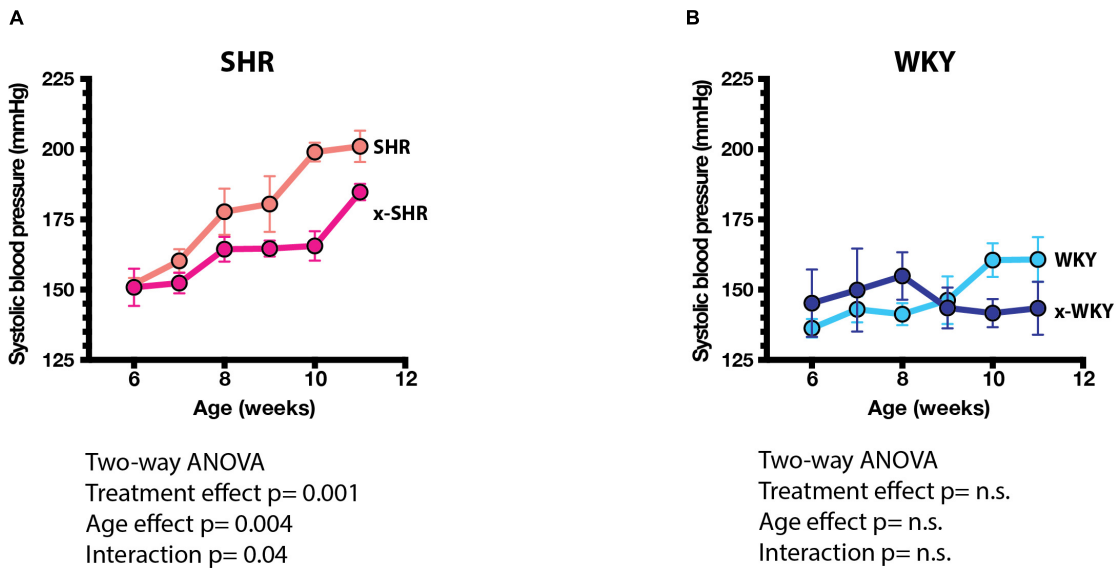

FIGURE 3 | (A) Systolic blood pressures (SBP) of self-fostered SHR vs. cross-fostered SHR, and **(B)** self-fostered vs. cross-fostered WKY at different ages. SBP was significantly lower in cross-fostered than self-fostered SHR. Results were analyzed by two-way ANOVA as shown.

Mechanistically, gut microbe-host interaction is of key importance in establishing healthy gut barrier function, host-tolerance to commensal bacteria, and retrieval of metabolic products from the gut microbes. In addition to direct interaction between microbes and host mucosal cells, several nutritionally important metabolites produced by these commensal bacteria influence the health of the host (El Aidy et al., 2013; Mishra et al., 2021; Tsukuda et al., 2021). Gut bacteria produce short chain fatty acids (Correa-Oliveira et al., 2016; Natarajan et al., 2016; Li et al., 2018; Bartolomaeus et al., 2019) (SCFA) and

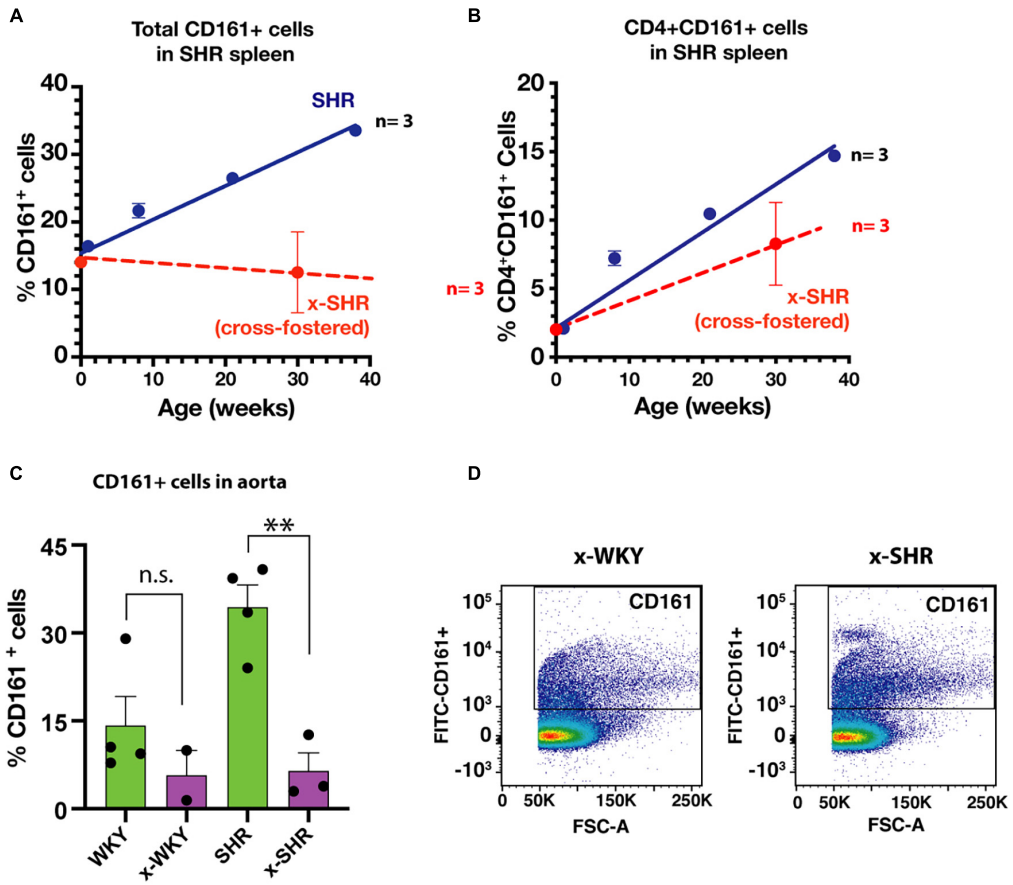

FIGURE 4 | (A) Cross-fostering of SHR prevents the age dependent increase in CD161 + cells and **(B)** CD4 + CD161 + cells observed in self-fostered SHR as previously reported (Singh et al., 2017) (Blue line). **(C)** Comparison of infiltration of proinflammatory CD161 + immune cells in aortic tissue in self-fostered cross-fostered WKY and SHR. **(D)** Representative dot plot of CD161 + cells in thoracic aorta of cross-fostered WKY (x-WKY) and cross-fostered SHR (x-SHR). Asterisks denote statistically significant (**$P < 0.0075$), whereas n.s. denotes statistically not significant results by one-way ANOVA and Sidak's *post hoc* test.

trimethylamine-3-oxide (Jaworska et al., 2017) (TMAO) that are utilized as nutrients as well as serving as ligands for specific receptors (Macia et al., 2015) on host cells to profoundly affect the immune response and hypertension. We also observed that a number of previously reported SCFA-producing bacteria of SHR (Yang et al., 2015) were not detected in our study. However, SHR gut microbiome contains a high number of SCFA producing *Lactobacillus* (Koopman et al., 2019). Our study does not address the underlying mechanism of metabolites or direct microbe-host cell interaction, but it does identify *Haemophilus, L. intestinalis, Proteus, Romboustia*, and *Rothia* as potential bacteria that might be contributing to SHR hypertension.

The blood pressure in WKY that were cross-fostered by hypertensive SHR dams was not increased. Our results are consistent with previous cross-fostering studies (Cierpial et al., 1988). These findings are also consistent with a genetic propensity for hypertension in the SHR compared to WKY (Yamamoto et al., 2013). Despite the changes in the microbiome of WKY that were cross-fostered by SHR, these changes, in the absence of the genetic predisposition, were not sufficient to cause hypertension. In summary, we conclude that a remarkable difference between the gut microbiome of neonatal SHR and WKY exists; this difference diminishes into adulthood and yet has a lasting effect on the immune response and the development of hypertension. More importantly, cross-fostering of SHR with WKY changes the neonatal gut microbiome of SHR to reflect that of the WKY and has measurable long term favorable outcomes in reducing the inflammation and the level of hypertension in adult SHR. Although fecal microbiota transplant (FMT) in adult SHR reduces the inflammatory response and hypertension (Toral et al., 2019), our results show an additional different role of the early neonatal gut microbiota in development of hypertension in adulthood by modulating the long-term immune response.

DATA AVAILABILITY STATEMENT

The datasets presented in this study can be found in online repositories. The names of the repository/repositories and accession number(s) can be found below: NCBI (accession: PRJNA763085).

ETHICS STATEMENT

The animal study was reviewed and approved by IACUC, University of Iowa.

AUTHOR CONTRIBUTIONS

FA contributed to conception of the study and writing the manuscript. MCi recorded blood pressure and assisted in all other experiments. AE performed the sequencing and statistical analysis. MCh contributed to the design of the study and revised and edited the manuscript. MS contributed to the conception and design of the study, performed experiments, wrote the first draft of the manuscript, analyzed data, and prepared the final draft. All authors contributed to manuscript revision, read, and approved the submitted version.

FUNDING

This study was funded by the American Heart Association (16IRG27260323) and Fraternal Order of the Eagles of Iowa to MS and by NHLBI PPG HL-14388 to FA.

REFERENCES

Adnan, S., Nelson, J. W., Ajami, N. J., Venna, V. R., Petrosino, J. F., Bryan, R. M. Jr., et al. (2017). Alterations in the gut microbiota can elicit hypertension in rats. *Physiol Genomics* 49, 96–104. doi: 10.1152/physiolgenomics.00081.2016

Arrieta, M. C., Stiemsma, L. T., Amenyogbe, N., Brown, E. M., and Finlay, B. (2014). The intestinal microbiome in early life: health and disease. *Frontiers in immunology* 5:427. doi: 10.3389/fimmu.2014.00427

Bartolomaeus, H., Balogh, A., Yakoub, M., Homann, S., Marko, L., Hoges, S., et al. (2019). Short-Chain Fatty Acid Propionate Protects From Hypertensive Cardiovascular Damage. *Circulation* 139, 1407–1421. doi: 10.1161/CIRCULATIONAHA.118.036652

Benson, A. K., Kelly, S. A., Legge, R., Ma, F., Low, S. J., Kim, J., et al. (2010). Individuality in gut microbiota composition is a complex polygenic trait shaped by multiple environmental and host genetic factors. *Proc Natl Acad Sci U S A* 107, 18933–18938. doi: 10.1073/pnas.1007028107

Bolyen, E., Rideout, J. R., Dillon, M. R., Bokulich, N. A., Abnet, C. C., Al-Ghalith, G. A., et al. (2019). Reproducible, interactive, scalable and extensible microbiome data science using QIIME 2. *Nat Biotechnol* 37, 852–857. doi: 10.1038/s41587-019-0209-9

Callahan, B. J., McMurdie, P. J., Rosen, M. J., Han, A. W., Johnson, A. J., and Holmes, S. P. (2016). DADA2: High-resolution sample inference from Illumina amplicon data. *Nature methods* 13, 581–583. doi: 10.1038/nmeth.3869

Caporaso, J. G., Lauber, C. L., Walters, W. A., Berg-Lyons, D., Lozupone, C. A., Turnbaugh, P. J., et al. (2011). Global patterns of 16S rRNA diversity at a depth of millions of sequences per sample. *Proc Natl Acad Sci USA* 108(Suppl. 1), 4516–4522. doi: 10.1073/pnas.1000080107

Cierpial, M. A., and McCarty, R. (1987). Hypertension in SHR rats: contribution of maternal environment. *Am J Physiol* 253, H980–H984. doi: 10.1152/ajpheart.1987.253.4.H980

Cierpial, M. A., Konarska, M., and McCarty, R. (1988). Maternal effects on the development of spontaneous hypertension. *Health psychol.* 7, 125–135. doi: 10.1037/0278-6133.7.2.125

Correa-Oliveira, R., Fachi, J. L., Vieira, A., Sato, F. T., and Vinolo, M. A. (2016). Regulation of immune cell function by short-chain fatty acids. *Clin Transl Immunology* 5, e73. doi: 10.1038/cti.2016.17

Daft, J. G., Ptacek, T., Kumar, R., Morrow, C., and Lorenz, R. G. (2015). Cross-fostering immediately after birth induces a permanent microbiota shift that is shaped by the nursing mother. *Microbiome* 3, 17. doi: 10.1186/s40168-015-0080-y

Eberl, G. (2017). RORγt, a multitask nuclear receptor at mucosal surfaces. *Mucosal immunology* 10, 27–34. doi: 10.1038/mi.2016.86

El Aidy, S., Hooiveld, G., Tremaroli, V., Backhed, F., and Kleerebezem, M. (2013). The gut microbiota and mucosal homeostasis: colonized at birth or at adulthood, does it matter? *Gut Microbes* 4, 118–124. doi: 10.4161/gmic.23362

Ericsson, A. C., Hagan, C. E., Davis, D. J., and Franklin, C. L. (2014). Segmented filamentous bacteria: commensal microbes with potential effects on research. *Comp Med* 64, 90–98. doi: <doi>

Galla, S., Chakraborty, S., Cheng, X., Yeo, J., Mell, B., Zhang, H., et al. (2018). Disparate effects of antibiotics on hypertension. *Physiol Genomics* 50, 837–845. doi: 10.1152/physiolgenomics.00073.2018

Gensollen, T., Iyer, S. S., Kasper, D. L., and Blumberg, R. S. (2016). How colonization by microbiota in early life shapes the immune system. *Science* 352, 539–544. doi: 10.1126/science.aad9378

Hooper, L. V., Littman, D. R., and Macpherson, A. J. (2012). Interactions between the microbiota and the immune system. *Science* 336, 1268–1273. doi: 10.1126/science.1223490

Hu, P., Thinschmidt, J. S., Yan, Y., Hazra, S., Bhatwadekar, A., Caballero, S., et al. (2013). CNS inflammation and bone marrow neuropathy in type 1 diabetes. *Am J Pathol* 183, 1608–1620. doi: 10.1016/j.ajpath.2013.07.009

Ivanov, I. I., Atarashi, K., Manel, N., Brodie, E. L., Shima, T., Karaoz, U., et al. (2009). Induction of intestinal Th17 cells by segmented filamentous bacteria. *Cell* 139, 485–498. doi: 10.1016/j.cell.2009.09.033

Ivanov, I. I., de Frutos, R., Manel, N., Yoshinaga, K., Rifkin, D. B., Sartor, B. R., et al. (2008). Specific Microbiota Direct the Differentiation of IL-17-Producing T-Helper Cells in the Mucosa of the Small Intestine. *Cell host & microbe* 4, 337–349. doi: 10.1016/j.chom.2008.09.009

Ivanov, I. I., McKenzie, B. S., Zhou, L., Tadokoro, C. E., Lepelley, A., Lafaille, J. J., et al. (2006). The orphan nuclear receptor RORgammat directs the differentiation program of proinflammatory IL-17+ T helper cells. *Cell* 126, 1121–1133. doi: 10.1016/j.cell.2006.07.035

Jaworska, K., Huc, T., Samborowska, E., Dobrowolski, L., Bielinska, K., Gawlak, M., et al. (2017). Hypertension in rats is associated with an increased permeability of the colon to TMA, a gut bacteria metabolite. *PLoS One* 12:e0189310. doi: 10.1371/journal.pone.0189310

Koenig, J. E., Spor, A., Scalfone, N., Fricker, A. D., Stombaugh, J., Knight, R., et al. (2011). Succession of microbial consortia in the developing infant gut microbiome. *Proc Natl Acad Sci U S A* 108(Suppl. 1), 4578–4585. doi: 10.1073/pnas.1000081107

Koopman, N., Molinaro, A., Nieuwdorp, M., and Holleboom, A. G. (2019). Review article: can bugs be drugs? The potential of probiotics and prebiotics as treatment for non-alcoholic fatty liver disease. *Aliment Pharmacol Ther* 50, 628–639. doi: 10.1111/apt.15416

Li, J., Zhao, F., Wang, Y., Chen, J., Tao, J., Tian, G., et al. (2017). Gut microbiota dysbiosis contributes to the development of hypertension. *Microbiome* 5, 14. doi: 10.1186/s40168-016-0222-x

Li, M., van Esch, B., Wagenaar, G. T. M., Garssen, J., Folkerts, G., and Henricks, P. A. J. (2018). Pro- and anti-inflammatory effects of short chain fatty acids on immune and endothelial cells. *European journal of pharmacology* 831, 52–59. doi: 10.1016/j.ejphar.2018.05.003

Loy, A., Maixner, F., Wagner, M., and Horn, M. (2007). probeBase–an online resource for rRNA-targeted oligonucleotide probes: new features 2007. *Nucleic Acids Res* 35, D800–D804. doi: 10.1093/nar/gkl856

Macia, L., Tan, J., Vieira, A. T., Leach, K., Stanley, D., Luong, S., et al. (2015). Metabolite-sensing receptors GPR43 and GPR109A facilitate dietary fibre-induced gut homeostasis through regulation of the inflammasome. *Nat Commun* 6, 6734. doi: 10.1038/ncomms7734

Macpherson, A. J., de Aguero, M. G., and Ganal-Vonarburg, S. C. (2017). How nutrition and the maternal microbiota shape the neonatal immune system. *Nat Rev Immunol* 17, 508–517. doi: 10.1038/nri.2017.58

Magne, F., Gotteland, M., Gauthier, L., Zazueta, A., Pesoa, S., Navarrete, P., et al. (2020). The Firmicutes/Bacteroidetes Ratio: A Relevant Marker of Gut Dysbiosis in Obese Patients? *Nutrients* 12, 1474. doi: 10.3390/nu12051474

Martin, M. (2011). Cutadapt removes adapter sequences from high-throughput sequencing reads. *EMBnetjournal* 17, 10–12. doi: 10.14806/ej.17.1.200

Mishra, A., Lai, G. C., Yao, L. J., Aung, T. T., Shental, N., Rotter-Maskowitz, A., et al. (2021). Microbial exposure during early human development primes fetal immune cells. *Cell* 184, 3394–409e20. *pgch doi: 10.1016/j.cell.2021.04.039

Nabika, T., Ohara, H., Kato, N., and Isomura, M. (2012). The stroke-prone spontaneously hypertensive rat: still a useful model for post-GWAS genetic studies? *Hypertens Res* 35, 477–484. doi: 10.1038/hr.2012.30

Natarajan, N., Hori, D., Flavahan, S., Steppan, J., Flavahan, N. A., Berkowitz, D. E., et al. (2016). Microbial short chain fatty acid metabolites lower blood pressure via endothelial G protein-coupled receptor 41. *Physiol Genomics* 48, 826–834. doi: 10.1152/physiolgenomics.00089.2016

Pruesse, E., Quast, C., Knittel, K., Fuchs, B. M., Ludwig, W., Peplies, J., et al. (2007). SILVA: a comprehensive online resource for quality checked and aligned ribosomal RNA sequence data compatible with ARB. *Nucleic Acids Res* 35, 7188–7196. doi: 10.1093/nar/gkm864

Shi, P., Diez-Freire, C., Jun, J. Y., Qi, Y., Katovich, M. J., Li, Q., et al. (2010). Brain microglial cytokines in neurogenic hypertension. *Hypertension* 56, 297–303. doi: 10.1161/HYPERTENSIONAHA.110.150409

Singh, M. V., Cicha, M. Z., Kumar, S., Meyerholz, D. K., Irani, K., Chapleau, M. W., et al. (2017). Abnormal CD161+ immune cells and retinoic acid receptor-related orphan receptor γt-mediate enhanced IL-17F expression in the setting of genetic hypertension. *The Journal of allergy and clinical immunology* 140, 809–821.e3. doi: 10.1016/j.jaci.2016.11.039

Singh, M. V., Cicha, M. Z., Nunez, S., Meyerholz, D. K., Chapleau, M. W., and Abboud, F. M. (2019). Angiotensin II-induced hypertension and cardiac hypertrophy are differentially mediated by TLR3- and TLR4-dependent pathways. *Am J Physiol Heart Circ Physiol* 316, H1027–H1038. doi: 10.1152/ajpheart.00697.2018

Toral, M., Robles-Vera, I., de la Visitacion, N., Romero, M., Sanchez, M., Gomez-Guzman, M., et al. (2019). Role of the immune system in vascular function and blood pressure control induced by faecal microbiota transplantation in rats. *Acta Physiol.* 227, e13285. doi: 10.1111/apha.13285

Tsukuda, N., Yahagi, K., Hara, T., Watanabe, Y., Matsumoto, H., Mori, H., et al. (2021). Key bacterial taxa and metabolic pathways affecting gut short-chain fatty acid profiles in early life. *ISME J* 15, 2574–2590. doi: 10.1038/s41396-021-00937-7

Turnbaugh, P. J., Hamady, M., Yatsunenko, T., Cantarel, B. L., Duncan, A., Ley, R. E., et al. (2009). A core gut microbiome in obese and lean twins. *Nature* 457, 480–484. doi: 10.1038/nature07540

Walters, W. A., Caporaso, J. G., Lauber, C. L., Berg-Lyons, D., Fierer, N., and Knight, R. (2011). PrimerProspector: de novo design and taxonomic analysis of barcoded polymerase chain reaction primers. *Bioinformatics* 27, 1159–1161. doi: 10.1093/bioinformatics/btr087

Yamamoto, H., Okuzaki, D., Yamanishi, K., Xu, Y., Watanabe, Y., Yoshida, M., et al. (2013). Genetic analysis of genes causing hypertension and stroke in spontaneously hypertensive rats. *Int J Mol Med* 31, 1057–1065. doi: 10.3892/ijmm.2013.1304

Yang, T., Santisteban, M. M., Rodriguez, V., Li, E., Ahmari, N., Carvajal, J. M., et al. (2015). Gut dysbiosis is linked to hypertension. *Hypertension* 65, 1331–1340. doi: 10.1161/HYPERTENSIONAHA.115.05315

Yatsunenko, T., Rey, F. E., Manary, M. J., Trehan, I., Dominguez-Bello, M. G., Contreras, M., et al. (2012). Human gut microbiome viewed across age and geography. *Nature* 486, 222–227. doi: 10.1038/nature11053

Zhang, G. X., Jin, L., Jin, H., and Zheng, G. S. (2021). Influence of Dietary Components and Traditional Chinese Medicine on Hypertension: A Potential Role for Gut Microbiota. *Evid Based Complement Alternat Med* 2021, 5563073. doi: 10.1155/2021/5563073

Conflict of Interest: The authors declare that the research was conducted in the absence of any commercial or financial relationships that could be construed as a potential conflict of interest.

Publisher's Note: All claims expressed in this article are solely those of the authors and do not necessarily represent those of their affiliated organizations, or those of the publisher, the editors and the reviewers. Any product that may be evaluated in this article, or claim that may be made by its manufacturer, is not guaranteed or endorsed by the publisher.

Copyright © 2021 Abboud, Cicha, Ericsson, Chapleau and Singh. This is an open-access article distributed under the terms of the Creative Commons Attribution License (CC BY). The use, distribution or reproduction in other forums is permitted, provided the original author(s) and the copyright owner(s) are credited and that the original publication in this journal is cited, in accordance with accepted academic practice. No use, distribution or reproduction is permitted which does not comply with these terms.

frontiers in Physiology

ORIGINAL RESEARCH
published: 30 November 2021
doi: 10.3389/fphys.2021.771167

Sensory Afferent Renal Nerve Activated $G\alpha i_2$ Subunit Proteins Mediate the Natriuretic, Sympathoinhibitory and Normotensive Responses to Peripheral Sodium Challenges

Jesse D. Moreira[1,2†], Kayla M. Nist[1,3†], Casey Y. Carmichael[1,4], Jill T. Kuwabara[1,4] and Richard D. Wainford[1,4]*

[1] Whitaker Cardiovascular Institute, School of Medicine, Boston University, Boston, MA, United States, [2] Department of Medicine, School of Medicine, Boston University, Boston, MA, United States, [3] Department of Anatomy & Neurobiology, School of Medicine, Boston University, Boston, MA, United States, [4] Department of Pharmacology and Experimental Therapeutics, School of Medicine, Boston University, Boston, MA, United States

OPEN ACCESS

Edited by:
Geoffrey A. Head,
Baker Heart and Diabetes Institute, Australia

Reviewed by:
De-Pei Li,
University of Missouri, United States
Khalid Elsaafien,
University of Florida, United States

***Correspondence:**
Richard D. Wainford
rwainf@bu.edu

† These authors have contributed equally to this work

Specialty section:
This article was submitted to Integrative Physiology, a section of the journal Frontiers in Physiology

Received: 06 September 2021
Accepted: 09 November 2021
Published: 30 November 2021

Citation:
Moreira JD, Nist KM, Carmichael CY, Kuwabara JT and Wainford RD (2021) Sensory Afferent Renal Nerve Activated $G\alpha i_2$ Subunit Proteins Mediate the Natriuretic, Sympathoinhibitory and Normotensive Responses to Peripheral Sodium Challenges. Front. Physiol. 12:771167. doi: 10.3389/fphys.2021.771167

We have previously reported that brain $G\alpha i_2$ subunit proteins are required to maintain sodium homeostasis and are endogenously upregulated in the hypothalamic paraventricular nucleus (PVN) in response to increased dietary salt intake to maintain a salt resistant phenotype in rats. However, the origin of the signal that drives the endogenous activation and up-regulation of PVN $G\alpha i_2$ subunit protein signal transduction pathways is unknown. By central oligodeoxynucleotide (ODN) administration we show that the pressor responses to central acute administration and central infusion of sodium chloride occur independently of brain $G\alpha i_2$ protein pathways. In response to an acute volume expansion, we demonstrate, via the use of selective afferent renal denervation (ADNX) and anteroventral third ventricle (AV3V) lesions, that the sensory afferent renal nerves, but not the sodium sensitive AV3V region, are mechanistically involved in $G\alpha i_2$ protein mediated natriuresis to an acute volume expansion [peak natriuresis (μeq/min) sham AV3V: 43 ± 4 vs. AV3V 45 ± 4 vs. AV3V + $G\alpha i_2$ ODN 25 ± 4, $p < 0.05$; sham ADNX: 43 ± 4 vs. ADNX 23 ± 6, AV3V + $G\alpha i_2$ ODN 25 ± 3, $p < 0.05$]. Furthermore, in response to chronically elevated dietary sodium intake, endogenous up-regulation of PVN specific $G\alpha i_2$ proteins does not involve the AV3V region and is mediated by the sensory afferent renal nerves to counter the development of the salt sensitivity of blood pressure (MAP [mmHg] 4% NaCl; Sham ADNX 124 ± 4 vs. ADNX 145 ± 4, $p < 0.05$; Sham AV3V 125 ± 4 vs. AV3V 121 ± 5). Additionally, the development of the salt sensitivity of blood pressure following central ODN-mediated $G\alpha i_2$ protein down-regulation occurs independently of the actions of the brain angiotensin II type 1 receptor. Collectively, our data suggest that in response to alterations in whole body sodium the peripheral sensory afferent renal nerves, but not

the central AV3V sodium sensitive region, evoke the up-regulation and activation of PVN $G\alpha i_2$ protein gated pathways to maintain a salt resistant phenotype. As such, both the sensory afferent renal nerves and PVN $G\alpha i_2$ protein gated pathways, represent potential targets for the treatment of the salt sensitivity of blood pressure.

Keywords: central $G\alpha i_2$ proteins, afferent renal sympathetic nerves, sodium homeostasis, blood pressure, natriuresis

INTRODUCTION

Hypertension, or high blood pressure, is the leading risk factor for multiple cardiovascular diseases including stroke, myocardial infarction and chronic kidney disease. Hypertension is estimated to impact 1 in 2 United States adults (Reboussin et al., 2018) and to directly contribute to 10.4 million deaths worldwide per year (Unger et al., 2020). Multiple studies support that excess dietary salt intake increases blood pressure and the risk of premature cardiovascular morbidity and mortality (Appel et al., 2011; Campbell et al., 2011; He et al., 2013; Cook et al., 2014). Despite the mounting evidence of the adverse cardiovascular impact of excess dietary salt approximately 90% of United States adults exceed of the American Heart Association recommended daily intake of <2,300 mmol of sodium for most adults (Lloyd-Jones et al., 2010). The salt sensitivity of blood pressure, an exaggerated blood pressure response to salt intake, is estimated to be present in 50% of hypertensive patients and 25% of normotensive individuals (Kotchen et al., 2013) and increases both hypertension risk and the risk of adverse cardiovascular outcomes (Franco and Oparil, 2006).

It is well established that dietary salt intake can modulate sympathetic nervous system activity and blood pressure through actions in several sites located in the forebrain (Stocker et al., 2013). The circumventricular organs (CVO), particularly the AV3V region which contains the sodium sensitive subfornical organ (SFO) and organum vasculosum of the lamina terminalis (OVLT), play a central role in the actions of salt on sympathetic outflow and blood pressure regulation (Larsen and Mikkelsen, 1995; Stocker et al., 2013; Simmonds et al., 2014). In addition to these central sodium sensing sites, there is increasing evidence that the renal sensory afferent nerves, that project from the renal pelvis to the central nervous system, influence central sympathetic outflow, renal sodium handling and blood pressure in response to perturbations in sodium homeostasis (Kopp, 2015; Frame et al., 2016, 2019).

Despite our understanding that the activation of multiple G-protein coupled receptors (GPCR's) can evoke sympathoinhibition and natriuresis (e.g., $GABA_B$, α_2-adrenoceptor) there is limited understanding of the downstream signal transduction pathways activated by GPCR's *in vivo* in response to alterations in sodium homeostasis. Our laboratory has demonstrated a critical role of central $G\alpha i_2$ subunit [guanine nucleotide-binding protein G(i) subunit alpha-2] proteins, which are inhibitory intracellular signaling proteins coupled to GPCRs, in mediating the sympathoinhibitory and normotensive responses to acute peripheral challenges to sodium homeostasis (volume expansion, sodium chloride infusion or sodium chloride bolus administration) in normotensive male Sprague Dawley rats (Kapusta et al., 2012; Wainford et al., 2013; Carmichael et al., 2016, 2020). Significantly, we have reported that dietary sodium-evoked endogenous up-regulation of PVN specific $G\alpha i_2$ subunit proteins represents a conserved mechanism that is required to maintain salt resistance and sympathoinhibition during high dietary salt intake in salt resistant rat phenotypes (Sprague Dawley, Brown Norway and the Dahl Salt Resistant rat) (Kapusta et al., 2013; Wainford et al., 2015; Moreira et al., 2019; Carmichael et al., 2020). In contrast, the Dahl Salt Sensitive rat fails to up-regulate PVN $G\alpha i_2$ proteins during high salt intake and exhibits the attenuated salt sensitivity of blood pressure when the levels of PVN $G\alpha i_2$ proteins are increased (Wainford et al., 2015). Suggesting that $G\alpha i_2$ proteins play a role in blood pressure regulation in human subjects, single nucleotide polymorphisms in the GNAI2 gene associate with hypertension risk and the salt sensitivity of blood pressure in the Genetic Epidemiology of Salt Sensitivity dataset (Zhang et al., 2018).

It remains unknown whether the integrated normotensive and sympathoinhibitory responses to challenges to sodium homeostasis, that are mediated by central $G\alpha i_2$ subunit protein signal transduction pathways, occur in response to changes in sodium detected centrally or peripherally. The current studies were designed to investigate the potential role(s) of central $G\alpha i_2$ proteins in the cardiovascular, sympathoinhibitory and natriuretic responses to central versus peripheral sodium challenges and the influence of established sodium sensing mechanisms on central $G\alpha i_2$ proteins. These studies were conducted in normotensive 3-month-old male Sprague Dawley rats, pre-treated centrally with either a control scrambled (SCR) or targeted $G\alpha i_2$ oligodeoxynucleotide (ODN), prior to undergoing an acute or chronic central versus peripheral sodium loading paradigm.

MATERIALS AND METHODS

Ethical Approval

All animal protocols were approved by the Institutional Animal Care and Use Committee (IACUC) in accordance with the guidelines of Boston University School of Medicine and the National Institutes of Health *Guide for the Care and Use of Laboratory Animals.* As detailed in our surgical procedures, all steps possible were taken to minimize pain and suffering. Additionally, all animal studies detailed in this manuscript fully comply with the ethical principles of Frontiers in Physiology.

Animals

Three-month-old male Sprague Dawley rats, weighing 275–299 g, were purchased from Envigo (Indianapolis, IN, United States) for use in these studies. Prior to surgical intervention animals were pair-housed and were then housed individually post-surgery. Animals were housed in the Laboratory Animal Science Center at Boston University under a 12 h:12 h light:dark cycle under temperature (20–26°C) and humidity (30–70%) controlled conditions. Animals were provided tap water and standard irradiated rodent normal salt (NS) diet *ad libitum* [Envigo Teklad, WI, Teklad Global Diet #2918: 18% protein, 5% crude fat, 5% fiber, 0.6% K^+ content, with a total NaCl content of 0.6% (174 mEquiv Na^+ kg)]. For elevated dietary sodium intake studies, animals were fed an experimental high salt (HS) diet *ad libitum* [Envigo Teklad Diets, WI, TD.03095: 19% protein, 5% crude fat, 3% fiber, 0.8% K^+ content, with a total NaCl content of 4% [678 m Equiv Na^+ kg)]. All rats were randomly assigned to experimental groups.

SURGICAL PROCEDURES

Intracerebroventricular (i.c.v.) Cannula Implantation

To enable acute oligodeoxynucleotide (ODN)-mediated down-regulation of central $G\alpha i_2$ proteins animals were anesthetized [ketamine, 30 mg kg intraperitoneally (I.P.) in combination with xylazine, 3 mg kg I.P.] and stereotaxically implanted with a stainless steel cannula (Plastics One Inc., Roanoke, VA, United States) into the right lateral cerebral ventricle (0.3 mm posterior to bregma, 1.3 mm lateral to the midline, and 4.5 mm below the skull surface) (Wainford and Kapusta, 2009, 2010, 2012; Kapusta et al., 2012; Wainford et al., 2013; Carmichael et al., 2016). In all studies i.c.v. cannula implantation occurred at least 5–7 days prior to experimentation.

Intracerebroventricular (i.c.v.) Oligodeoxynucleotide Infusion

Down-regulation of brain $G\alpha i_2$ protein expression levels in rats was achieved by continuous i.c.v. infusion of a phosphodiesterase oligodeoxynucleotide (ODN) probe that selectively targets $G\alpha i_2$ proteins (5′-CTT GTC GAT CAT CTT AGA-3′) (The Midland Certified Reagent Company Inc., TX, United States). Control studies involved i.c.v. infusion of a scrambled (SCR) ODN (5′-GGG CGA AGT AGG TCT TGG-3′). An NCBI Basic Local Alignment Search Tool search of the *Rattus norvegicus* RefSeq protein database was conducted to confirm the specificity of the $G\alpha i_2$ ODN for the rat $G\alpha i_2$ protein sequence and that the SCR ODN does not match any known rat protein sequence. Multiple publications from our laboratory have confirmed effective (approx. 85%) ODN-mediated down-regulation of $G\alpha i_2$ protein expression and no effect of a control SCR ODN on Gα-subunit protein expression in the acute setting as assessed by Western blotting (Kapusta et al., 2012; Wainford and Kapusta, 2012; Wainford et al., 2013). For chronic ODN infusion, animals were anesthetized (ketamine, 30 mg/kg I.P. in combination with xylazine, 3 mg/kg I.P.) and stereotaxically implanted with a stainless steel cannula into the right lateral cerebral ventricle, which was connected via silastic tubing to a miniosmotic pump (model 2004; Durect Corporation, Cupertino, CA, United States). ODNs were dissolved in isotonic saline and infused i.c.v. at 25 μg/6 μl/day (Kapusta et al., 2013; Moreira et al., 2019; Carmichael et al., 2020).

Acute Femoral Vein, Femoral Artery and Bladder Cannulation

On the day of the acute study rats were anesthetized with sodium methohexital (20 mg kg I.P., supplemented with 10 mg kg I.V. as required). Rats were instrumented with PE-50 catheters in the left femoral vein and left femoral artery and a PE-240 catheter in the bladder to allow I.V. administration of isotonic saline and experimental sodium challenges, measurement of mean arterial pressure (MAP) and heart rate (HR), and assessment of renal excretory function, respectively (Walsh et al., 2016; Frame et al., 2019; Carmichael et al., 2020; Puleo et al., 2020). Rats were placed in a Plexiglas rat holder and an I.V. infusion of isotonic saline (20 μl min) was maintained during a 2 h surgical recovery period allowing rats to return to full consciousness and renal and cardiovascular function to stabilize prior to study. Mean arterial pressure (MAP) and heart rate (HR) were recorded continuously via the femoral artery cannula using computer-driven BIOPAC data acquisition software (MP150 and AcqKnowledge 3.8.2; BIOPAC Systems Inc., Goleta, CA, United States) connected to an external pressure transducer (P23XL; Viggo Spectramed Inc., Oxnard, CA, United States).

Radiotelemetry Probe Implantation

Rats were anesthetized with ketamine combined with xylazine (30 mg kg I.P. ketamine, 3 mg kg I.P. xylazine). A radiotelemetry probe (PA-C40, DSI, New Brighton, MN, United States) was implanted into the abdominal aorta via the left femoral artery (Brouwers et al., 2015; Foss et al., 2015; Wainford et al., 2015). All animals underwent surgical recovery for 5–7 days prior to subsequent osmotic minipump implantation.

Selective Afferent Renal Nerve Ablation

Selective afferent renal nerve ablation (ADNX) was performed via direct application of 33 mM capsaicin to the renal nerves (Foss et al., 2015; Frame et al., 2019). As previously described, under sodium pentobarbital anesthesia (20 mg kg I.P.), each kidney was exposed via a dorsal flank incision and the renal artery and vein were gently separated from the surrounding fascia. Capsaicin (33 mM in isotonic saline containing 5% ethanol and 5% Tween-20) was applied to the isolated renal artery and vein avoiding contact with the surrounding tissue to prevent off-target capsaicin exposure. Any excess capsaicin was dried before suturing the flank muscle and skin. In the sham group, each kidney was exposed and the renal artery and vein were visualized before suturing. A sub-group of ADNX rats underwent an i.c.v. cannula implantation procedure (as described above) 5–7 days post-ADNX surgery to allow an acute i.c.v. $G\alpha i_2$ ODN pre-treatment. The efficacy of selective ADNX was confirmed at the

end of the study via (1) ELISA analysis of norepinephrine (NE) content in kidney tissue as per the manufacturer's instructions (IB89537, IBL America, Minneapolis, MN, United States), and (2) ELISA analysis of renal pelvic calcitonin gene related peptide (CGRP) content as per manufacturer's instructions (no. 589001, Cayman Chemical Co., Ann Arbor, MI, United States) (Foss et al., 2015; Frame et al., 2019).

AV3V Lesion

Rats were anesthetized with ketamine combined with xylazine (30 mg kg I.P. ketamine and 3 mg kg I.P. xylazine). An anodal electrolytic lesion (2.5 mA for 25 s) was stereotaxically delivered to the AV3V [stereotaxic coordinates: 0.3 mm posterior to bregma, on midline, 7.5 mm ventral to the midsagittal sinus (Simmonds et al., 2014)] using an insulated 23-g nichrome wire exposed only at the tip. In a separate sham group, the nichrome wire was inserted 4 mm into the brain for 25 s but no lesion was delivered. Immediately following AV3V or sham surgery all rats underwent an i.c.v. cannula implantation procedure (as described above) to allow the pharmacological verification of an AV3V lesion and in certain study groups acute i.c.v. $G\alpha i_2$ ODN pre-treatment. Rats were placed in their home cages and monitored during surgical recovery. The AV3V lesion was verified in all groups by observation of postlesion adipsia assessed as fluid intake less than 5 mL during the first 24 h post-lesion (Callahan et al., 1988) and the absence of a pressor response to i.c.v. angiotensin II (Ang II; 200 ng) (Moreira et al., 2009; Vieira et al., 2013) assessed post-volume expansion study or blood pressure measurement study. Adipsic rats were given 5% sucrose water *ad libitum* to encourage drinking and gradually weaned to normal water over 5-days prior to assignment to an experimental study group.

EXPERIMENTAL PROTOCOLS

Acute Intracerebroventricular (i.c.v.) Oligodeoxynucleotide Pre-treatment

Twenty-four hours prior to the day of the study, down-regulation of brain $G\alpha i_2$ protein expression levels in rats was achieved by i.c.v. injection (25 μg per 5 μL delivered over 60 s) of a phosphodiesterase ODN probe dissolved in isotonic saline that selectively targets $G\alpha i_2$ proteins (5′-CTT GTC GAT CAT CTT AGA-3′). Control studies involved i.c.v. injection of a SCR ODN (5′-GGG CGA AGT AGG TCT TGG-3′) (The Midland Certified Reagent Company, Midland, TX, United States).

Acute i.c.v. 1 M NaCl Studies

These studies were conducted in groups of conscious animals pretreated centrally with either a control SCR or targeted $G\alpha i_2$ ODN 24-h prior to study. On the day of study all animals underwent an acute femoral vein and femoral artery cannulation and a 2-h stabilization period, in which rats were infused IV with isotonic saline (20 μl/min) and returned to full consciousness. Following a 2-h recovery and measurement of baseline mean arterial pressure (MAP) over a 30-min period an i.c.v. infusion of 1 M NaCl or 0.9% saline (5 μl over 60 s) (Kinsman et al., 2017a,b) was administered in a randomized order 1 h apart. MAP was recorded continuously via the femoral artery cannula using computer-driven BIOPAC data acquisition software (MP150 and AcqKnowledge 3.8.2; BIOPAC Systems Inc., Goleta, CA, United States) connected to an external pressure transducer (P23XL; Viggo Spectramed Inc., Oxnard, CA, United States) to allow the calculation of the peak ΔMAP (N = 6/group). Post-blood pressure recording, animals were euthanized and brains collected and stored at −80°C for analysis of PVN $G\alpha i_2$ protein levels.

Volume Expansion Studies

Volume expansion studies were conducted on groups of conscious animals maintained on a normal salt diet that had previously undergone ADNX or AV3V surgery and an i.c.v. cannula implantation and subgroups of ADNX and AV3V animals that received an acute i.c.v. $G\alpha i_2$ ODN pre-treatment. After surgical instrumentation and a 2-h stabilization period in which rats were infused IV with isotonic saline (20 μl/min) and returned to full consciousness cardiovascular and renal excretory parameters were measured, and urine was collected during a 20-min control period. The infusate was then increased so that rats received an isotonic saline load equivalent to 5% of body weight (BW) over a 30-min period. Continuous 10-min urine samples were collected during the VE period. The isotonic saline infusate was then returned to a rate of 20 μl/min, after which urine samples were collected during a 90-min recovery period (Wainford and Kapusta, 2010; Kapusta et al., 2012; Carmichael et al., 2016) (N = 6 per treatment group). Cardiovascular parameters were continuously recorded during the 120-min experimental protocol. Following completion of the study all animals that received a sham or AV3V lesion received an i.c.v. bolus of Ang II (200 ng/5 μl delivered in 30 s) (Gao et al., 2020) and the peak pressor response over 20 min was recorded. In subgroups of AV3V animals post-fixed brains were sectioned at 20 μm, stained with H&E, and visualized on bright field on a Keyence BZ9000 Microscope for verification of lesion. In all ADNX animals post protocol completion kidneys were collected and stored at −80°C prior to analysis of renal NE content and renal pelvic CGRP levels.

14-Day i.c.v. 0.8 M NaCl Infusion Studies

Rats that previously underwent radiotelemetry probe implantation were implanted with osmotic minipumps connected to an i.c.v. cannula to deliver a central infusion of a control SCR or targeted $G\alpha i_2$ ODN (25 μg/6 μl/day). Following a 5-day surgical recovery blood pressure was recorded by radiotelemetry in conscious animals [Dataquest A.R.T. 4.2 software (DSI)] via scheduled sampling for 10 s every 10-min for a 5-day control period (Brouwers et al., 2015; Foss et al., 2015; Wainford et al., 2015). Rats were then randomly assigned to either continue to receive an ODN infusion in 0.9% NaCl or osmotic minipumps were replaced with 0.8 M NaCl (Bunag and Miyajima, 1984; Miyajima and Bunag, 1984) in combination with ODN infusion at 25 μg/day (N = 6 per treatment group) and blood pressure was recorded for a further 14-days. Following

protocol completion animals were sacrificed by conscious decapitation and plasma was collected for analysis of plasma NE and brains were collected and stored at −80°C for analysis of PVN $G\alpha i_2$ protein levels.

21-Day Dietary Sodium Intake Studies

Following ADNX or sham surgery all animals were immediately assigned to receive either 21 days of a normal salt or a high salt diet, *ad libitum*. Following AV3V lesion or sham surgery, and observation of postlesion adipsia during the first 24 h post-lesion, animals were assigned to receive either 21 days of high salt or normal salt diet, *ad libitum* starting 10-days post-lesion. Metabolic balance studies (including assessment of food intake) were conducted on day 20 of salt intake and then animals underwent acute blood pressure measurement on day 21. After surgical instrumentation and a 2-h stabilization period in which rats were infused i.v. with isotonic saline (20 μl/min) and returned to full consciousness, baseline MAP was recorded continuously over a 30-min period in conscious rats (N = 6/treatment group/diet). Following completion of the study, all animals that received a sham or AV3V lesion received an i.c.v. bolus of Ang II (200 ng/5 μl delivered in 30 s) (Gao et al., 2020) and the peak pressor response over 20 min was recorded. At the end of protocol, whole brains and both kidneys were collected and stored at −80°C for assessment of PVN $G\alpha i_2$ protein levels and efficacy of ADNX, respectively, as well as assessment of renal norepinephrine content. As previously reported by our laboratory we observed no differences in food intake between the 0.6 and 4% NaCl diet formulations with animals consuming approximately 20 g of food per day.

Central Losartan Studies

Groups of animals, instrumented with an i.c.v. cannula attached to an osmotic minipumps received either an i.c.v. $G\alpha i_2$ ODN infusion, an i.c.v. losartan (5 μg/hour) (Zimmerman et al., 2004; Wei et al., 2009; Walch et al., 2013) infusion or a $G\alpha i_2$ ODN infusion in combination with losartan. Immediately post cannula implantation animals were randomly assigned to a 21-day normal or high dietary salt intake study. On day 20 all animals underwent a metabolic balance study. On day 21 animals underwent surgical instrumentation and a 2-h stabilization period in which rats were infused i.v. with isotonic saline (20 μl/min) and returned to full consciousness and mean arterial blood pressure was recorded continuously over a 30-min period in conscious rats (N = 6/treatment group/diet). After measurement of baseline mean arterial pressure and acute Ang II administration (i.c.v. bolus 200 ng/5 μl delivered in 30 s) (Gao et al., 2020), animals received an acute i.c.v. injection of guanabenz (5 μg/5 μl) and peak changes in heart rate (HR) and MAP were recorded as previously described (N = 6/treatment group/diet) (Wainford and Kapusta, 2012; Kapusta et al., 2013).

Metabolic Balance Studies

Metabolic balance studies were conducted in all groups of rats included in **Figures 5**, **6**. Rats, previously habituated to the metabolic cage for 48 h, were housed in individual metabolic cages (model 18cv, Fenco, MA, United States) with external food containers and water bottles. Metabolic cages were equipped with a double-fine mesh screen that allowed separation of food and feces contamination from urine that was collected in vials containing a layer of mineral oil to prevent evaporation. Rats were randomly assigned to receive a normal or high sodium intake diet and provided access to their respective rodent chow and allowed tap water *ad libitum* via external trays and bottles, respectively. On the day of study, measurements were made for body weight, food and water intake, and urine output during a 24-h period enabling calculation of daily sodium and water balance (Kapusta et al., 2012, 2013; Wainford et al., 2015). Daily sodium balance was determined by calculating the difference between sodium intake (dietary sodium intake) and sodium output (urinary sodium excretion) to enable calculation of whole body sodium retention.

Measurement of Brain Gα-Subunit Protein Levels

Following completion of certain experimental protocols, whole brains were removed and frozen at −80°C. Hypothalamic paraventricular nucleus (PVN) samples were extracted from frozen brains cut on a cryostat using a brain punch tool (Stoelting, IL, United States) as previously described (Kapusta et al., 2012, 2013). Tissue lysates were prepared from individual brain punch samples (i.e., samples were not pooled from multiple animals) and protein levels were quantified using a BCA assay as per manufacturers' instruction (Thermo Scientific, IL, United States). Individual non-pooled tissue lysates were loaded at a concentration of 20 μg total protein and were resolved on a 10% SDS-PAGE gel and transferred to nitrocellulose membrane (GE Healthcare, NJ, United States). $G\alpha i_2$ levels were determined as previously published by our laboratory (Kapusta et al., 2012, 2013) using a commercially available primary antibody purchased from Santa Cruz Biotechnologies (Santa Cruz, CA, United States), directed against $G\alpha i_2$ (1:200, sc-13534, RRID:AB_627644) and protein levels were normalized to GAPDH (anti-GAPDH 1:1000, ab-9483, Abcam, MA, RRID:AB 307273). In all cases, blots were exposed to a horseradish peroxidase-conjugated secondary antibody (Invitrogen, Thermo Fisher, catalog no. 62-6520, Waltham, MA, United States; RRID:AB_2533947). Chemiluminescent immunoreactive bands were detected by Amersham™ ECL™ Prime western blotting detection reagent (GE Healthcare, RPN2232) and data was imaged and semi-quantified using Bio-Rad Quantity One image analysis software (Kapusta et al., 2012; Wainford et al., 2015; Moreira et al., 2019).

ANALYTICAL TECHNIQUES

Analysis of Urine

Urine volume was determined gravimetrically assuming 1 g = 1 ml. Urinary and plasma sodium concentrations were measured by flame photometry (model 943, Instrumentation Laboratories, MA, United States) (Kapusta et al., 2013; Wainford et al., 2013, 2015).

Analysis of Plasma

Plasma norepinephrine (NE) levels were determined as previously described (Kapusta et al., 2013; Wainford et al., 2013, 2015). In brief, following plasma collection samples were frozen and stored at −80°C for later analysis. Plasma NE levels were quantified using an ELISA kit (Immuno-Biological Laboratories, Inc., Minneapolis, MN, United States; cat#IB89552) as per manufacturers' instructions (Wainford et al., 2015; Frame et al., 2019; Moreira et al., 2019).

Analysis of Renal Norepinephrine Content

Kidneys were harvested from rats following completion of the experimental protocol, flash frozen and stored at −80°C. NE content of kidney was determined with an ELISA (Immuno-Biological Laboratories, Inc., Minneapolis, MN, United States; cat#IB89537) as per manufacturers' instructions.

Analysis of Renal Pelvic Calcitonin Gene Related Peptide Content

Kidneys were harvested from rats following completion of the experimental protocol, and the renal pelvis was extracted, flash frozen and stored at −80°C. Renal pelvic GCRP content was determined with an ELISA (no. 589001, Cayman Chemical Co., Ann Arbor, MI, United States) as per manufacturers' instructions (Foss et al., 2015; Frame et al., 2019).

STATISTICAL ANALYSIS

All data are expressed as mean ± SEM. Peak change in MAP and HR, plasma NE content, 24-h sodium and water balance and Gαi$_2$ protein levels were compared with respective group control values by a student's *t*-test. Differences occurring between treatment groups were assessed by a two-way ANOVA with a subsequent Sidak's multiple comparisons test. The magnitude of change in cardiovascular and renal excretion parameters at different time points after acute volume expansion were compared with respective group control values by a one-way repeated-measures (RM) ANOVA with a subsequent Dunnett's multiple comparisons test. Differences occurring between treatment groups were assessed by a two-way RM (mixed-model) ANOVA (treatment × time) with a subsequent Sidak's multiple comparisons test. All statistical analyses were performed using Graphpad (GraphPad Prism v.8 for Mac OS X, GraphPad Software, San Diego, CA, United States). In each case, statistical significance was defined as $p < 0.05$.

RESULTS

Acute i.c.v. 1 M NaCl Evokes a Brain Gαi$_2$ Protein-Independent Response

In all animals i.c.v. saline administration, either pre- or post i.c.v. 1 M NaCl did not alter blood pressure in conscious rats (baseline MAP [mmHg]; SCR ODN 124 ± 4, Gαi$_2$ ODN 126 ± 5). In contrast i.c.v. 1 M NaCl evoked a significant acute pressor response in both SCR and Gαi$_2$ ODN pre-treated conscious male rats, the magnitude of which was not altered by ODN-mediated down-regulation of central Gαi$_2$ proteins (peak ΔMAP [mmHg]; SCR ODN + 10.6 ± 2.3 vs. Gαi$_2$ ODN + 11.3 ± 2.2, **Figures 1A–C**). The efficacy of central Gαi$_2$ ODN pre-treatment was confirmed by the observation of a significant reduction (approximately 80%) in the expression of PVN Gαi$_2$ proteins (**Figures 1D,E**).

Brain Gαi$_2$ Protein-Dependent Responses to an Acute i.v. Volume Expansion Occur Independent of the AV3V Region

An acute 5% BW volume expansion did not alter MAP or HR at any time point in sham AV3V lesioned conscious rats (**Figures 2A,B**). In sham AV3V rats, replicating our prior published data in male Sprague Dawley rats an acute 5% BW volume expansion evoked profound natriuresis and diuresis (**Figure 2A**). In conscious animals that underwent an AV3V lesion the response to an acute 5% volume expansion was indistinguishable from that observed in sham AV3V lesioned animals. In contrast, in conscious animals that underwent an AV3V lesion in combination with a 24-h Gαi$_2$ ODN pre-treatment we observed profoundly attenuated natriuretic and diuretic responses to a 5% BW volume expansion [peak V (μL/min) sham: 368 ± 32 vs. AV3V 374 ± 18 vs. AV3V + Gαi$_2$ ODN 193 ± 18, $p < 0.05$; peak UNaV (μeq/min) sham: 43 ± 4 vs. AV3V 45 ± 4 vs. AV3V + Gαi$_2$ ODN 25 ± 4, $p < 0.05$] with no change in cardiovascular parameters throughout the protocol (**Figures 2A,B**).

To confirm the efficacy of AV3V lesions all rats underwent confirmation of post-lesion adipsia (**Figure 2C**). Following completion of the acute volume expansion protocol all animals received an acute i.c.v. bolus injection of Ang II (200 ng). In sham animals we observed a pressor response to Ang II which was absent in all AV3V lesioned rats (**Figure 2D**). AV3V lesions were also confirmed histologically (**Figure 2E**).

Brain Gαi$_2$ Protein-Dependent Responses to an Acute i.v. Volume Expansion Involve the Afferent Renal Nerves

Replicating our prior published data in conscious male Sprague Dawley rats an acute 5% BW volume expansion did not alter MAP or HR, but evoked a profound diuretic and natriuretic response in sham ADNX rats (**Figures 3A,B**). In animals that underwent ADNX surgery we observed a profound volume expansion-evoked diuretic response of the same magnitude as seen in sham ADNX animals with no change in HR. In contrast, a 5% BW volume expansion in conscious ADNX animals evoked a significant increase in MAP and profoundly attenuated the natriuretic response [peak MAP (mmHg) sham: 125 ± 3 vs. ADNX 135 ± 2, $p < 0.05$; peak UNaV (μeq/min) sham: 43 ± 4 vs. ADNX 23 ± 6, $p < 0.05$] (**Figures 3A,B**). In conscious

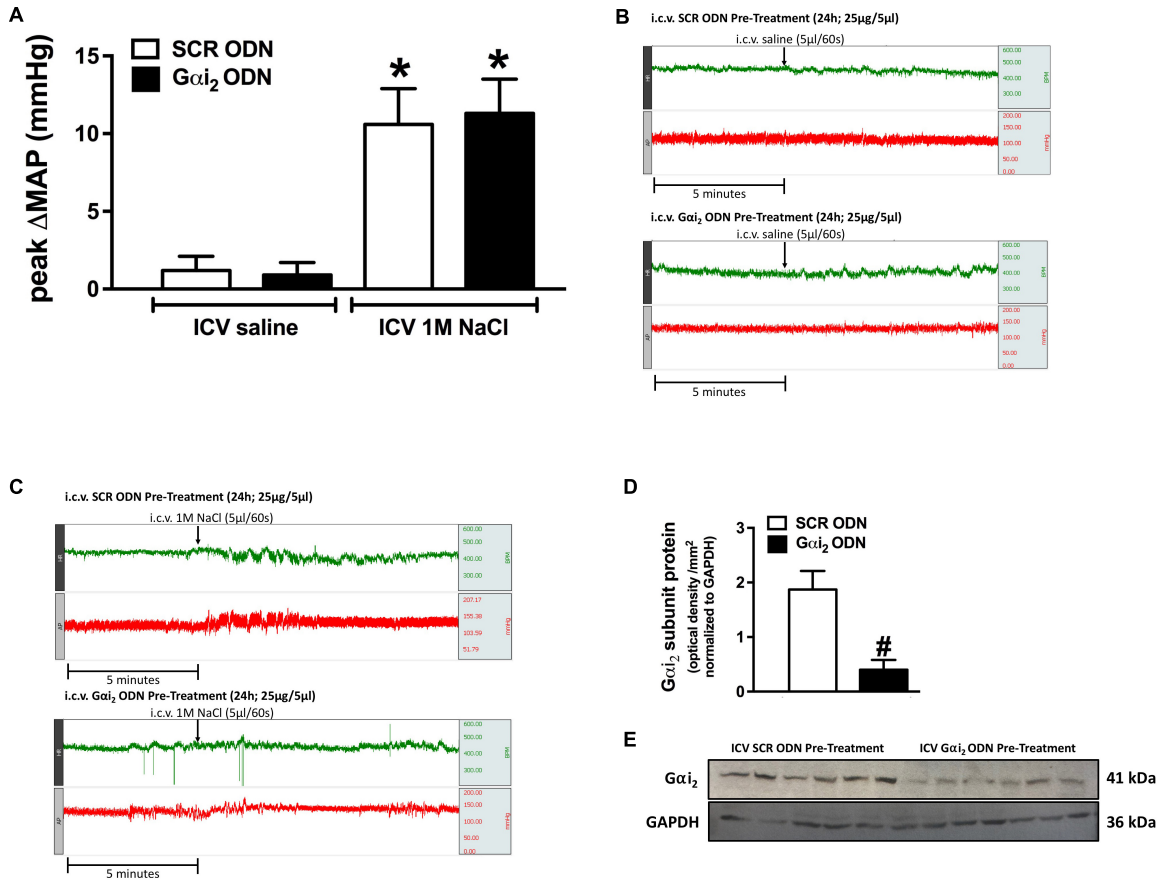

FIGURE 1 | Effect of central Gαi$_2$ protein down-regulation on the pressor response to acute central administration of 1 M NaCl. **(A)** Peak change in mean arterial pressure (MAP) in response to the acute i.c.v. administration of 1 M NaCl or 0.9% saline (5 µl over 60 s) in a randomized order 1 h apart in animals pre-treated i.c.v. with an acute SCR or Gαi$_2$ ODN injection (25 µg/5 µl) 24-h prior to the day of study, **(B)** representative raw traces of heart rate and blood pressure in conscious male Sprague Dawley rats receiving an acute i.c.v. bolus of 0.9% saline 24-h post an i.c.v. SCR or Gαi$_2$ ODN pre-treatment (25 µg/5 µl), **(C)** representative raw traces of heart rate and blood pressure in conscious male Sprague Dawley rats receiving an acute i.c.v. bolus of 1 M NaCl 24-h post an i.c.v. SCR or Gαi$_2$ ODN pre-treatment (25 µg/5 µl), **(D)** Gαi$_2$-subunit protein expression normalized to GAPDH in the paraventricular nucleus (PVN) of male Sprague Dawley rats that received an i.c.v. SCR or Gαi$_2$ ODN pre-treatment (25 µg/5 µl) 24-h prior to the day of study for which the blood pressure responses to i.c.v. 1 M NaCl and 0.9% NaCl are depicted in **(A)**. **(E)** Representative immunoblots of non-pooled PVN samples, loaded equally at a concentration of 20 µg total protein per lane, illustrating hypothalamic Gαi$_2$-subunit protein levels in Sprague Dawley rats pre-treated centrally with a SCR or Gαi$_2$ ODN. Data are presented as mean ± SEM, N = 6/group, $^*p < 0.05$ vs. respective i.c.v. saline group value; $^\#p < 0.05$ vs. SCR ODN group value.

animals that underwent ADNX in combination with a 24-h Gαi$_2$ ODN pre-treatment, the physiological blood pressure and natriuretic responses to an acute 5% volume expansion were indistinguishable from those observed in ADNX animals with the addition of a profoundly attenuated diuretic response.

To confirm the efficacy of ADNX all rats underwent analysis of renal NE and renal pelvic CGRP. The surgical procedure of ADNX did not alter renal NE levels vs. sham animals and reduced renal pelvic CGRP content to undetectable levels (**Figures 3C,D**).

Chronic i.c.v. 0.8 M NaCl Evokes a Brain Gαi$_2$ Protein-Independent Response

A 14-day i.c.v. saline infusion, in combination with either a SCR or Gαi$_2$ ODN did not alter blood pressure or plasma NE levels (**Figures 4A,B**). In contrast, i.c.v. 0.8 M NaCl infusion evoked a significant rapid and persistent significant elevation in MAP in both SCR and Gαi$_2$ ODN co-infused conscious rats that was accompanied by an increase in plasma NE levels, the magnitude of which was not altered by ODN-mediated down-regulation of central Gαi$_2$ proteins (**Figures 4A,B**). The efficacy of chronic central Gαi$_2$ ODN pre-treatment was confirmed by the observation of a significant reduction (approximately 85%) in the expression of PVN Gαi$_2$ proteins (**Figure 4C**).

Brain Gαi$_2$ Protein-Dependent Responses to Dietary Salt Intake Involve the Afferent Renal Nerves

In conscious sham AV3V, sham ADNX and AV3V lesioned rats, in which the afferent renal nerves are intact, a 21-day high salt intake did not alter MAP or sodium balance and evoked

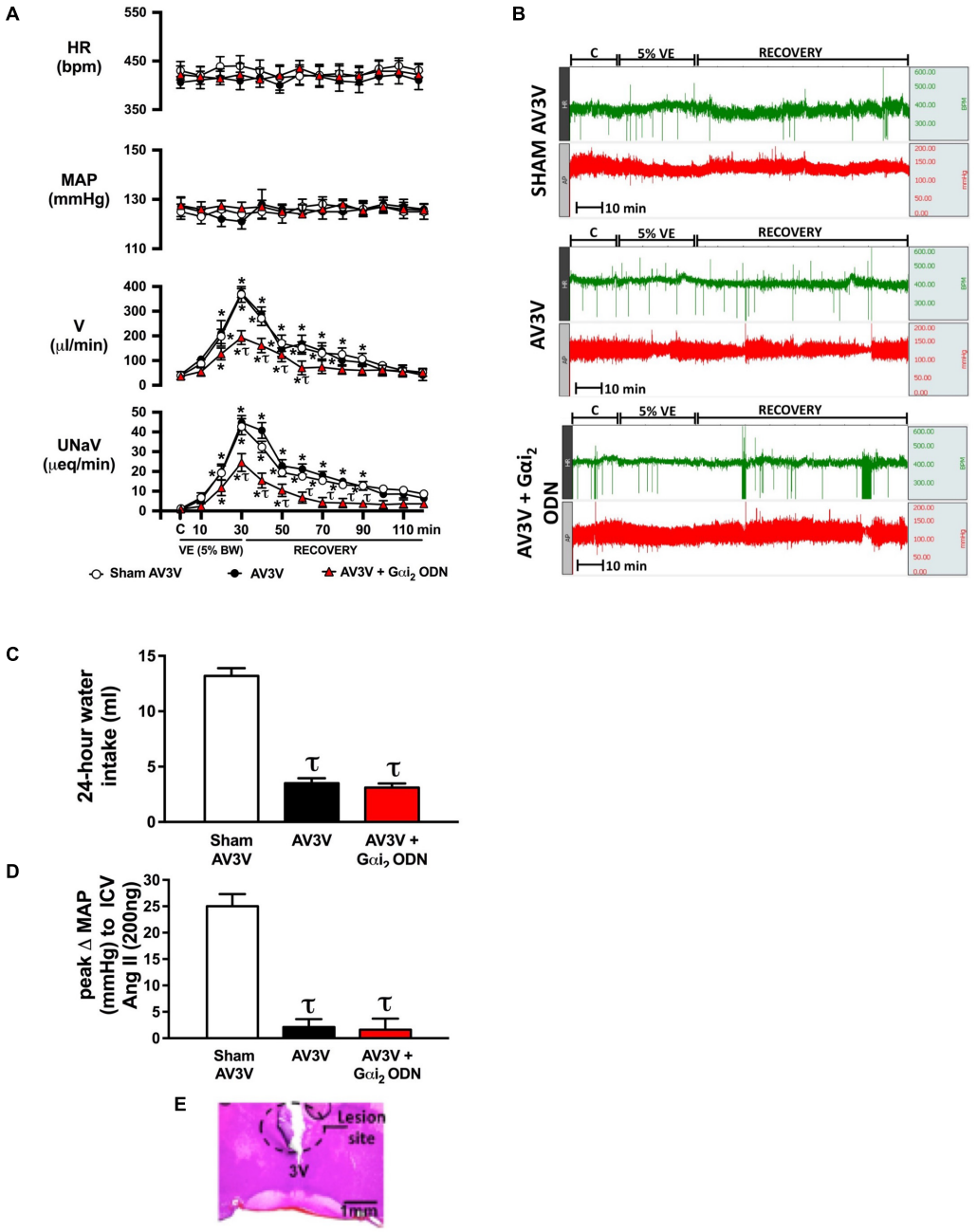

FIGURE 2 | Effect of AV3V lesion alone, and in combination with central Gαi$_2$ protein down-regulation, on the cardiovascular and renal excretory responses to an acute volume expansion. **(A)** Cardiovascular and renal responses to a 30-min 5% body weight isotonic saline volume expansion (VE) followed by a 90-min recovery period in conscious male Sprague Dawley rats receiving a sham AV3V lesion, an AV3V lesion or an AV3V lesion and an i.c.v. Gαi$_2$ ODN pre-treatment (25 μg/5 μl) 24-h prior to the day of study, **(B)** representative raw traces of heart rate and blood pressure in conscious male Sprague Dawley rats receiving a sham AV3V lesion, an AV3V lesion or an AV3V lesion and an i.c.v. Gαi$_2$ ODN pre-treatment (25 μg/5 μl) 24-h prior to the day of study, **(C)** water intake in the 24-h post-AV3V lesion, **(D)** peak change in mean arterial pressure (MAP) to i.c.v. injection of Ang II (200 ng) in sham AV3V, AV3V, and AV3V + Gαi$_2$ ODN pre-treated conscious male Sprague Dawley rats, and **(E)** representative image of an AV3V lesion. Data are presented as mean ± SEM, *N* = 6/group. HR, heart rate (bpm); MAP, mean arterial pressure (mmHg); V, urinary flow rate (μL/min); UNaV, urinary sodium excretion (μeq/min). $^{*}p < 0.05$ vs. respective group baseline control value (denoted C); $^{\tau}p < 0.05$ vs. respective sham AV3V group value.

global and renal sympathoinhibition that was accompanied by the up-regulation of PVN Gαi$_2$ protein levels (**Figure 5** and **Table 1**). In contrast, we observed the development of sodium retention, sympathoexcitation and the salt sensitivity of blood pressure in conscious ADNX animals (**Figure 5** and **Table 1**). Critically, in ADNX rats, which developed

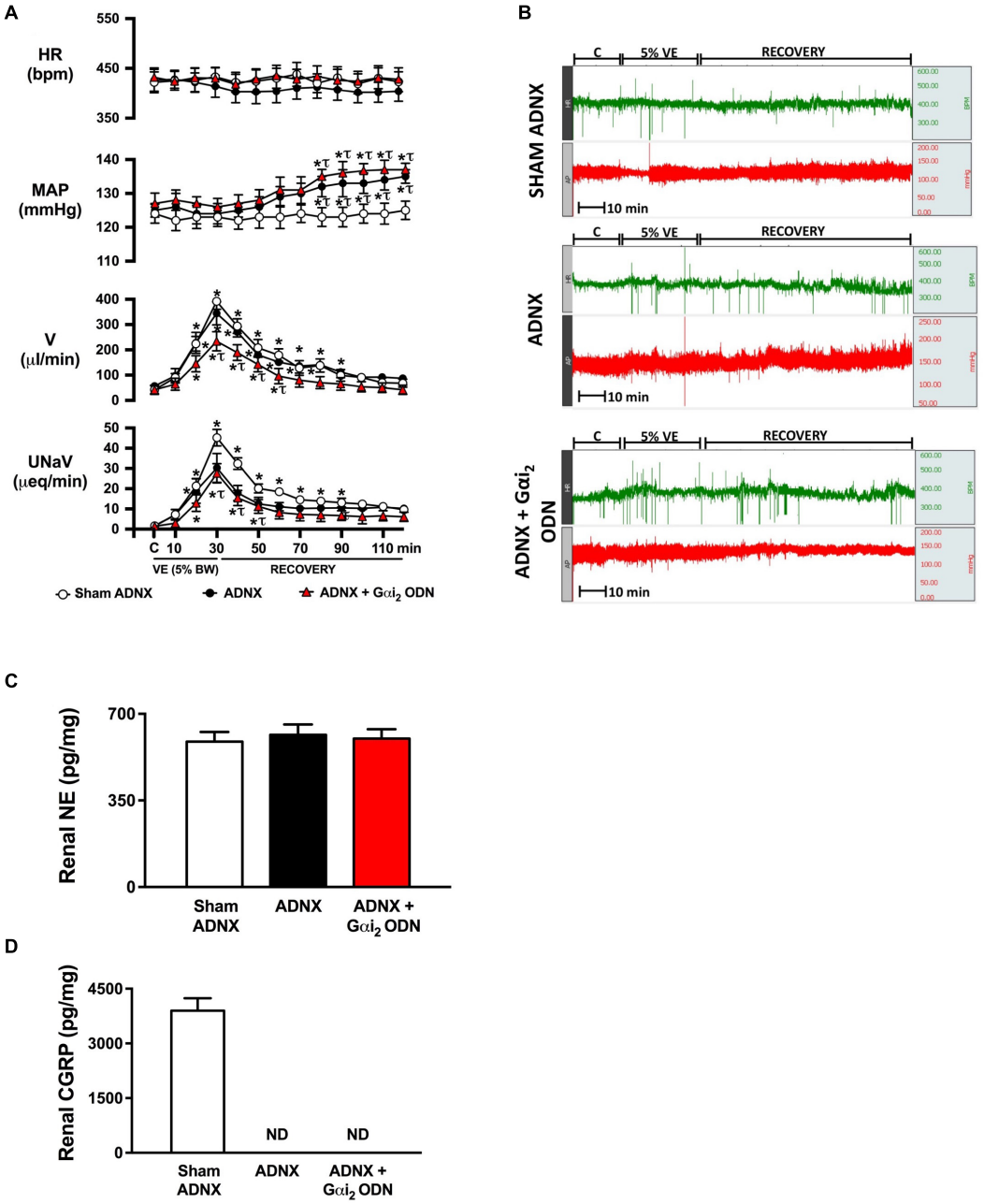

FIGURE 3 | Effect of afferent renal denervation (ADNX) alone, and in combination with central Gαi$_2$ protein down-regulation, on the cardiovascular and renal excretory responses to an acute volume expansion. **(A)** Cardiovascular and renal responses to a 30-min 5% body weight isotonic saline volume expansion (VE) followed by a 90-min recovery period in conscious male Sprague Dawley rats receiving a sham ADNX, ADNX, or ADNX and an i.c.v. Gαi$_2$ ODN pre-treatment (25 μg/5 μl) 24-h prior to the day of study, **(B)** representative raw traces of heart rate and blood pressure in conscious male Sprague Dawley rats receiving a sham ADNX, ADNX, or ADNX and an i.c.v. Gαi$_2$ ODN pre-treatment (25 μg/5 μl) 24-h prior to the day of study, **(C)** renal norepinephrine content (pg/mg), and **(D)** renal pelvic CGRP content (pg/mg). Data are presented as mean ± SEM, *N* = 6/group. HR, heart rate (bpm); MAP, mean arterial pressure (mmHg); V, urinary flow rate (μL/min); UNaV, urinary sodium excretion (μeq/min). ND, not detectable. $^{*}p < 0.05$ vs. respective group baseline control value (denoted C). $^{\tau}p < 0.05$ vs. respective sham ADNX group value.

the salt sensitivity of blood pressure, we did not observe dietary sodium-evoked up-regulation of PVN Gαi$_2$ proteins (**Figure 5**). The efficacy of AV3V lesions was confirmed by the observation of post-lesion adipsia and the absence of a pressor response to an acute i.c.v. bolus injection of Ang II (200 ng) (**Table 1**). Confirming the efficacy of ADNX on day 21 days post-ADNX renal pelvic CGRP levels were less than 90% of sham animals (**Table 1**).

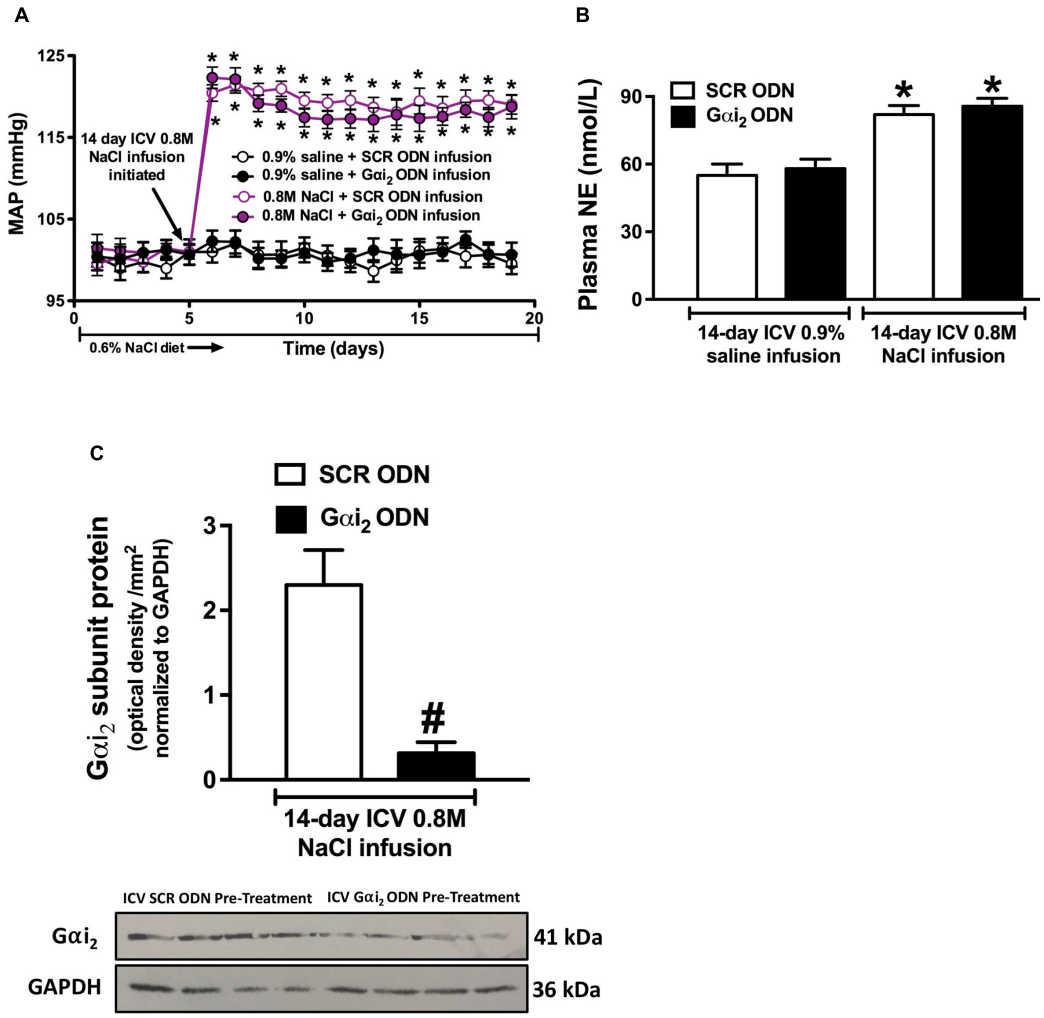

FIGURE 4 | Effect of central Gαi$_2$ protein down-regulation on the blood pressure and sympathetic response to central infusion of 0.8 M NaCl. **(A)** Blood pressure response to i.c.v. infusion of 0.8 M NaCl or 0.9% saline in conscious male Sprague Dawley receiving an i.c.v. co-infusion of a SCR or Gαi$_2$ ODN injection (25 μg/6 μl/day), **(B)** renal norepinephrine content (pg/mg), and **(C)** Gαi$_2$-subunit protein expression of non-pooled PVN samples, loaded equally at a concentration of 20 μg total protein per lane, normalized to GAPDH in the paraventricular nucleus (PVN) of male Sprague Dawley rats that received an i.c.v., SCR or Gαi$_2$ ODN infusion (25 μg/6 μl/day) in combination with 0.8 M NaCl for which the blood pressure response is depicted in **(A)**. Data are presented as mean ± SEM, N = 6/group, $^{*}p < 0.05$ vs. respective i.c.v. saline group value; $^{\#}p < 0.05$ vs. SCR ODN group value.

Central Gαi$_2$ Oligodeoxynucleotide-Mediated Salt Sensitivity of Blood Pressure Occurs Independently of Brain Angiotensin II Type 1 Receptor (AT1R) Signaling

Replicating our prior data (**Figure 5**) a central Gαi$_2$ ODN infusion evoked the development of the salt sensitivity of blood pressure following 7-days HS intake that was accompanied by fluid and sodium retention (**Figure 6A** and **Table 2**). Central losartan infusion did not impact blood pressure in animals maintained on a normal or high salt intake. Further, central losartan co-infusion had no effect on the magnitude of the salt sensitivity of blood pressure, fluid retention or sodium retention in animals receiving an i.c.v. Gαi$_2$ ODN infusion (MAP [mmHg]; Gαi$_2$ ODN HS 150 ± 4 vs. Losartan + Gαi$_2$ ODN HS 147 ± 5, **Figure 6A** and **Table 2**). In these animals the efficacy of AT1R antagonism was confirmed by the absence of a pressor and dipsogenic response to i.c.v. Ang II administration (**Figures 6B,C**). The efficacy of central Gαi$_2$ protein down-regulation was confirmed pharmacologically (Kapusta et al., 2012; Wainford and Kapusta, 2012) by the observation of a bradycardic response to i.c.v. guanabenz in the absence of a hypotensive response (**Table 2**).

DISCUSSION

These studies were designed to determine the potential role(s) of central Gαi$_2$ proteins in the integrated cardiovascular,

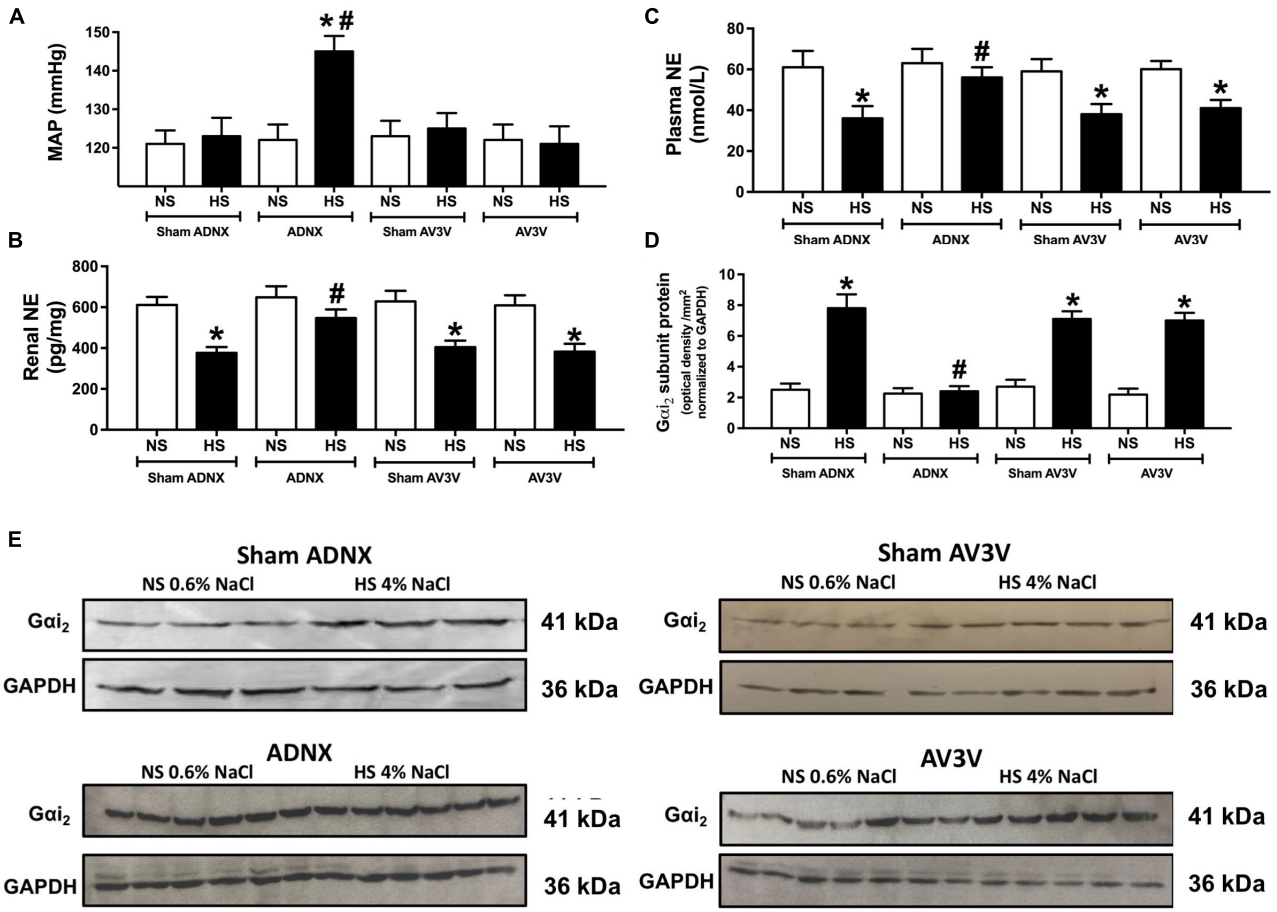

FIGURE 5 | Effect of an AV3V lesion or ADNX on PVN Gαi$_2$ protein expression and the salt sensitivity of blood pressure. **(A)** MAP (mmHg), **(B)** renal norepinephrine (NE) content (pg/mg) **(C)** plasma NE content (nmol/L), **(D)** Gαi$_2$-subunit protein expression of non-pooled PVN samples normalized to GAPDH in the paraventricular nucleus (PVN) of male Sprague Dawley rats that underwent an AV3V lesion or ADNX, and **(E)** representative immunoblots of non-pooled PVN samples, loaded equally at a concentration of 20 μg total protein per lane in male Sprague Dawley rats that underwent an AV3V lesion or ADNX that were maintained on a normal or high salt-intake for 21-days. Data are presented as mean ± SEM, *N* = 6/group. $^{*}p < 0.05$ vs. respective normal salt-intake group value. $^{\#}p < 0.05$ vs. sham ADNX high salt-intake group value.

TABLE 1 | 24-h sodium balance (meq), Renal pelvic CGRP content (pg/mg), 24-h water intake (ml) post lesion and peak ΔMAP (mmHg) post-i.c.v. Ang II (200 ng) in male Sprague Dawley rats that underwent a sham surgery, ADNX surgery or AV3V lesion prior to 21-days normal or high salt sodium diet.

	Sham ADNX		ADNX		Sham AV3V		AV3V	
Parameter	**0.6% NaCl**	**4% NaCl**	**0.6% NaCl**	**4% NaCl**	**0.6% NaCl**	**4% NaCl**	**0.6% NaCl**	**4% NaCl**
24 h Na^+ balance (meq)	0.33 ± 0.1	0.40 ± 0.38	0.41 ± 0.2	2.89 ± 0.4$^{*\#}$	0.38 ± 0.2	0.34 ± 0.2	0.29 ± 0.1	0.31 ± 0.1
Renal pelvic CGRP (pg/mg)	4103 ± 308	3962 ± 344	362 ± 58$^{\#}$	389 ± 46$^{\#}$	–	–	–	–
24 h water intake (ml) post lesion	–	–	–	–	12.4 ± 1.4	13.2 ± 1.6	4.5 ± 1$^{\#}$	3.9 ± 0.8$^{\#}$
Peak ΔMAP (mmHg) to i.c.v. Ang II 200 ng	–	–	–	–	22 ± 2.3	24 ± 1.4	1.5 ± 1.2$^{\#}$	0.9 ± 1.4$^{\#}$

The values are the means ± SEM (N = 6 per group). $^{*}p < 0.05$ compared with respective normal sodium intake group value. $^{\#}p < 0.05$ compared with respective sham group value.

sympathoinhibitory and natriuretic responses to central versus peripheral sodium challenges and the role(s) of established sodium sensing mechanisms on central Gαi$_2$ protein-mediated responses and expression. Our studies demonstrate that the acute and chronic central administration of NaCl evokes a pressor response that is independent from brain Gαi$_2$ subunit protein signal transduction pathways. Second, we demonstrate that the sensory afferent renal nerves are required to facilitate dietary sodium-evoked PVN Gαi$_2$ protein up-regulation, natriuresis and normotension following chronic high dietary sodium intake. Thirdly, we provide evidence that the salt sensitivity of blood pressure that develops following the down-regulation of central

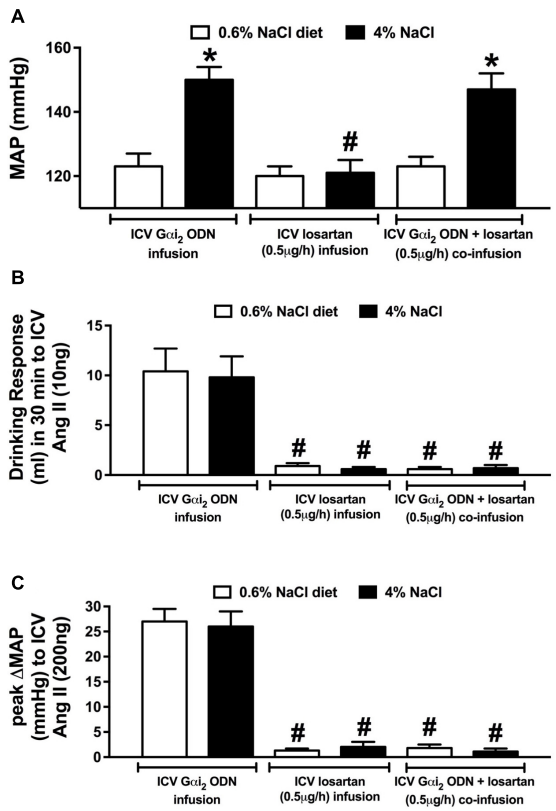

FIGURE 6 | Effect of brain AT1R antagonism on the salt sensitivity of blood pressure in central Gαi$_2$ ODN infused rats. **(A)** MAP (mmHg), **(B)** drinking response (ml) in 30 min to i.c.v. Ang II (10 ng), and **(C)** peak change in mean arterial pressure (MAP) to i.c.v. injection of Ang II (200 ng) in conscious male Sprague Dawley rats receiving a central Gαi$_2$ ODN infusion (25 μg/6 μl/day), a central losartan infusion (0.5 μg/h) or a central Gαi$_2$ ODN:losartan co-infusion (25 μg/6 μl/day) for 21-days that were maintained on a normal or high salt-intake. Data are presented as mean ± SEM, N = 6/group. $^{*}p < 0.05$ vs. respective normal salt-intake group value. $^{\#}p < 0.05$ vs. respective i.c.v. Gαi$_2$ ODN infusion group value.

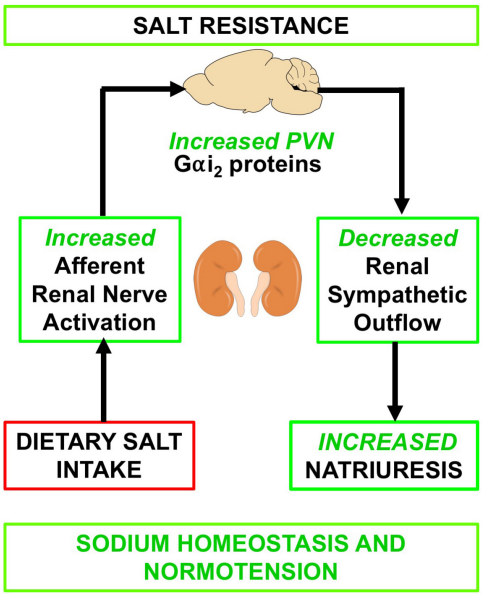

FIGURE 7 | Schematic of proposed mechanism by which the sensory afferent renal nerves influence PVN Gαi$_2$ subunit proteins in response to dietary salt intake.

Gαi$_2$ proteins does not involve a brain AT1R signal transduction mechanism. Collectively our data suggest that central Gαi$_2$ proteins are essential in mediating the integrated cardiovascular and renal responses to peripheral, but not central, alterations in sodium homeostasis. Further, the maintenance of salt resistance, which involves PVN specific up-regulation of PVN Gαi$_2$ proteins is driven by the sensory afferent renal nerves.

Central NaCl Evokes a Brain Gαi$_2$ Protein-Independent Pressor Response

Several central sites, including the SFO and OVLT, (Larsen and Mikkelsen, 1995; Stocker et al., 2013; Simmonds et al., 2014) play an important role in mediating the actions of NaCl on blood pressure, in part through these areas' connections with the hypothalamic PVN, an integrative neural control center that modulates blood pressure and sympathetic outflow (Stocker et al., 2013; Fujita and Fujita, 2016). Our prior studies have shown a key role of central, and PVN specific, Gαi$_2$ proteins in influencing the cardiovascular, renal and sympathetic nervous system responses to acute challenges to sodium homeostasis and chronic elevations in dietary sodium intake (**Figure 7**; Kapusta et al., 2012, 2013; Wainford et al., 2013; Moreira et al., 2019; Carmichael et al., 2020). However, the impact of central Gαi$_2$ proteins on the blood pressure responses to direct increases in central NaCl remain unknown. In these studies, we utilized two different central NaCl challenges: an acute i.c.v. 1 M NaCl bolus (Kinsman et al., 2017a,b) and a chronic 14-day 0.8 M i.c.v. NaCl infusion (Bunag and Miyajima, 1984; Miyajima and Bunag, 1984). In response to both an acute i.c.v. 1 M NaCl bolus injection and a 0.8 M NaCl i.c.v. infusion we observed a significant increase in blood pressure that was not impacted by Gαi$_2$ protein down-regulation. The down-regulation of Gαi$_2$ proteins by acute ODN pre-treatment and continuous ODN infusion was confirmed by immunoblotting of the PVN as previously reported by our laboratory (Kapusta et al., 2012, 2013; Wainford et al., 2013; Moreira et al., 2019; Carmichael et al., 2020). These results suggest that central administration of NaCl, which evokes a pressor response, does so via mechanisms independent of brain Gαi$_2$ protein-gated pathways.

Acute Volume Expansion Evokes an Afferent Renal Nerve and Gαi$_2$ Protein-Independent Natriuretic Response

An acute isotonic volume expansion is a well-established sympathoinhibitory challenge that evokes profound diuresis and natriuresis, partly via suppression of renal sympathetic outflow, to maintain fluid and electrolyte balance and normotension.

TABLE 2 | 24-h water balance (ml), 24-h sodium balance (meq), peak ΔHR (bpm) post-i.c.v. guanabenz (5 μg) and peak ΔMAP (mmHg) post-i.c.v. guanabenz (5 μg) in male Sprague Dawley rats receiving either an i.c.v. infusion of a $G\alpha i_2$ ODN (25 μg/6 μl/day), an i.c.v. infusion of losartan (12 μg/6 μl/day – 0.5 μg/hour), or an i.c.v. co-infusion of a $G\alpha i_2$ ODN (25 μg/day) and losartan (12 μg/day) measured on day 7 of a normal or high salt sodium diet.

	i.c.v. $G\alpha i_2$ ODN infusion		**i.c.v. losartan infusion**		**i.c.v. losartan and $G\alpha i_2$ ODN co-infusion**	
Parameter	**0.6% NaCl**	**4% NaCl**	**0.6% NaCl**	**4% NaCl**	**0.6% NaCl**	**4% NaCl**
24 h H_20 balance (ml)	12.4 ± 1.1	19.9 ± 2.8*	10.8 ± 1.4	12.7 ± 2.1	12.8 ± 1.5	22.4 ± 3.9*#
24 h Na^+ balance (meq)	0.36 ± 0.18	2.62 ± 0.28*	0.45 ± 0.21	0.39 ± 0.19	0.42 ± 0.18	2.34 ± 0.22*#
Peak ΔHR (bpm) to i.c.v. guanabenz	−85 ± 8	−92 ± 6	−73 ± 8	−86 ± 9	−81 ± 7	−77 ± 7
Peak ΔMAP (mmHg) to i.c.v. guanabenz	−2.1 ± 1.4#	1.3 ± 1.2#	−22.4 ± 2.6	−20 ± 3.1	−1.6 ± 1.4#	−2.0 ± 1.8#

*The values are the means ± SEM (N = 6 per group). *$p < 0.05$ compared with respective normal sodium intake group value. #$p < 0.05$ compared with respective i.c.v. losartan infused group value.*

We have previously demonstrated that brain, and PVN specific, $G\alpha i_2$ subunit protein gated-signal transduction pathways mediate the full natriuretic and diuretic responses to an i.v. volume expansion (Kapusta et al., 2012; Carmichael et al., 2020). These studies were designed to investigate the association between central $G\alpha i_2$ proteins and the sodium/osmo-sensitive AV3V region as well as the sensory afferent renal nerves during an acute volume expansion. Our data, which show that validated AV3V lesions (lesion validated physiologically, pharmacologically, and histologically), had no impact on the cardiovascular and renal responses to an acute volume expansion or the ability of $G\alpha i_2$ down-regulation to attenuate volume expansion evoked natriuretic and diuretic responses. This suggests that the AV3V sodium sensitive region has no role in the acute $G\alpha i_2$ protein-mediated physiological responses to an acute volume expansion.

In contrast, our data show that validated ADNX (ADNX validated by absence of renal pelvic CGRP and the presence of unchanged renal NE levels) attenuates volume expansion-evoked natriuresis and results in an increase in blood pressure – data that replicates our prior findings (Frame et al., 2019). In animals in which $G\alpha i_2$ proteins are downregulated, ADNX is shown not to impact $G\alpha i_2$ ODN-mediated reductions in diuresis or natriuresis and evokes increased blood pressure in response to a volume expansion. Collectively these data suggest that the renal sensory afferent nerves and not the central sodium sensing AV3V region mediate the integrated physiological responses to an acute volume expansion – potentially by mediating a sympathoinhibitory reno-renal reflex to mediate suppression of renal sympathetic nerve traffic and subsequent natriuresis (Kopp et al., 1987; Kopp, 2015; Frame et al., 2019). Further our data suggests potential cross talk between the renal sensory afferent nerves and central $G\alpha i_2$ subunit protein-gated pathways to mediate the natriuretic, but not diuretic or blood pressure, response to perturbations in whole body sodium homeostasis evoked by an acute volume expansion. In these animals which underwent an acute volume expansion, we did not validate $G\alpha i_2$ protein down-regulation by immunoblotting – however, given that in all animals which received a $G\alpha i_2$ ODN we observed the same pattern and magnitude of attenuated natriuresis and diuresis as we have previously published, (Kapusta et al., 2012; Carmichael et al., 2020) we are confident in the efficacy of our approach.

The Sensory Afferent Renal Nerves Are Required for Dietary Sodium-Evoked Up-Regulation of Paraventricular Nucleus $G\alpha i_2$ Proteins to Counter the Development of Salt Sensitive Hypertension

We have previously reported that endogenous up-regulation of PVN $G\alpha i_2$ proteins in response to dietary salt intake is required to for salt resistance in both the Sprague Dawley and Dahl Salt Resistant rat phenotypes (Kapusta et al., 2013; Wainford et al., 2015; Moreira et al., 2019; Carmichael et al., 2020). Our prior studies have demonstrated that the dietary sodium evoked up-regulation of $G\alpha i_2$ proteins, which is conserved across Sprague Dawley and Dahl Salt resistant rats, is specific to the PVN of the hypothalamus with no change observed in the posterior hypothalamus, the supraoptic nucleus or ventrolateral medulla and is specific to $G\alpha i_2$ proteins with no change in the protein expression of $G\alpha i_1$, $G\alpha i_3$ or $G\alpha o$ proteins in any brain region studied (Kapusta et al., 2013; Wainford et al., 2015; Carmichael et al., 2020). In these studies, we initially replicated our finding that an i.c.v. $G\alpha i_2$ ODN infusion downregulates the protein expression of central $G\alpha i_2$ proteins and evokes the development of the salt sensitivity of blood pressure. At present, the stimulus that evokes the up-regulation of PVN $G\alpha i_2$ proteins in response to dietary salt to remains unknown.

To address this question, we examined blood pressure, PVN $G\alpha i_2$ protein expression, sodium retention and indices of sympathetic tone during normal or high salt intake in animals that underwent an AV3V lesion or ADNX prior to high salt intake. In these studies, animals that underwent a sham or AV3V lesion (verified by adipsia post lesion and absence of pressor response to i.c.v. AngII) exhibited high dietary salt-evoked up-regulation of PVN $G\alpha i_2$ proteins, sympathoinhibition, sodium balance and normotension. In contrast to rats that underwent a sham ADNX procedure, which upregulated PVN $G\alpha i_2$ proteins and remained normotensive, ADNX (verified by reduced renal pelvic CGRP levels) prevented dietary sodium-evoked increase in PVN $G\alpha i_2$ proteins and evoked increased sympathetic outflow and the salt sensitivity of blood pressure. Evidence supporting this is a significant increase in blood pressure during high salt intake, renal sodium retention and increased renal and global

sympathetic tone. The magnitude of hypertension observed after ADNX and 21-days high salt-intake was approximately 20 mmHg and is in accord with that observed in our prior studies following central $G\alpha i_2$ protein down-regulation and 21-day high salt intake in Sprague Dawley and Dahl Salt Resistant rats (Kapusta et al., 2013; Wainford et al., 2015). It should be noted that our prior study, Frame et al. (2019) and current work contrast with a prior study, Foss et al. (2015) that suggested the afferent renal nerves have no impact on blood pressure in the Sprague Dawley rat during stepped increases in dietary sodium intake. However, in the prior Foss et al. (2015) study, which concluded 7-weeks post ADNX (1) afferent renal nerve-independent adaptive mechanisms could have been activated to facilitate sodium homeostasis and normotension over the 7-week study period, (2) it is likely physical afferent renal nerve re-innervation occurred but was not functionally assessed, (3) a different experimental paradigm is explored (i.e., stepped increase in dietary sodium vs. ADNX immediately prior to challenge with a high salt intake). Our studies in this, and our prior study Frame et al. (2019) are designed to address the potential confounding effects of non-afferent renal nerve-mediated compensatory mechanisms and functional afferent renal nerve reinnervation. To avoid these potential confounders ADNX was performed immediately prior to the start of high salt intake.

Collectively our current data, which replicate our prior study in Sprague Dawley rats and the Dahl Salt resistant rat in which ADNX immediately prior to high salt intake evoked the salt sensitivity of blood pressure (Frame et al., 2019), suggest that the sympathoinhibitory afferent renal nerve reno-renal reflex is a protective mechanism against the initial increase in blood pressure observed following high salt intake – an observation supported by prior studies following generalized sensory afferent denervation via dorsal rhizotomy or subcutaneous capsaicin treatment in SD rats (Wang et al., 1998, 2001; Kopp et al., 2003). Given that the renal afferent nerves have projections to the PVN our studies suggest that brain $G\alpha i_2$ protein-gated normotensive sympathoinhibitory pathways are upregulated by chronic elevated dietary sodium intake at the level of the kidney via the sensory renal afferent nerves. Based on our prior studies which reported no change in plasma sodium coupled with an increase in urine output to a level that would activate the mechanosensitive afferent renal nerves, (Frame et al., 2019) we speculate it is a mechanosensitive stimulus that evokes up-regulation of PVN $G\alpha i_2$ proteins. Future studies, utilizing retrograde tracing and neuronal phenotyping, will address the potential phenotypes of PVN neurons that express $G\alpha i_2$ proteins that are influenced by activation of the sensory afferent renal nerves.

Central $G\alpha i_2$ Oligodeoxynucleotide-Mediated Salt Sensitivity of Blood Pressure Occurs Independently of Brain Angiotensin II Type 1 Receptor Signal Transduction

It is well established that activation of the brain AT1R evokes neurogenic hypertension. There is mounting evidence for several shared physiological responses across central AngII-mediated hypertension and our observation of $G\alpha i_2$ protein-dependent salt sensitive hypertension including neuroinflammation and increased sympathetic outflow (Shi et al., 2010; Wainford et al., 2013; Moreira et al., 2019; Carmichael et al., 2020; Mohammed et al., 2020). To investigate the potential interactions between centrally acting AngII and $G\alpha i_2$ subunit protein-gated pathways, we utilized pharmacological antagonism of the AT1R. Evidenced by the fact that verified pharmacological antagonism of the AT1R with losartan did not impact the magnitude of hypertension in $G\alpha i_2$ ODN infused rats on a high salt diet, our data suggest central AT1R activity does not play a role in the development of the salt sensitivity of blood pressure following the down-regulation of brain $G\alpha i_2$ proteins. Collectively, these data support the hypothesis that the salt sensitivity of blood pressure that develops following down-regulation of central $G\alpha i_2$ proteins does not involve a brain AT1R signal transduction mechanism.

CONCLUSION

These studies shed light on the interactions of brain $G\alpha i_2$-gated pathways and the sodium/osmosensitive CVOs and sensory afferent renal nerves, sites that influence renal sodium retention and blood pressure. Our data strongly suggest that the central $G\alpha i_2$ gated pathways that regulate blood pressure are activated in part by the sensory afferent renal nerves but are not responsive to central alterations in sodium levels. It appears that central $G\alpha i_2$-gated pathways, which are sympathoinhibitory in nature, are distinct from central salt-activated excitatory pathways that increase blood pressure independently of $G\alpha i_2$ protein signal transduction. Additionally, our data suggest that brain $G\alpha i_2$ protein-gated pathways represent a separate integrated blood pressure regulatory mechanism that is responsive to alterations in whole body sodium homeostasis that functions independently of the brain AT1R. These findings provide new mechanistic insight into the integrated physiological mechanisms that maintain sodium homeostasis and normotension. Given the association of a SNPs in the GNAI2 gene correlating with the salt sensitivity of blood pressure in a sub-set of subjects in the Genetic Epidemiology of Salt Sensitivity dataset, (Zhang et al., 2018) these data suggest pharmacological targeting of the central $G\alpha i_2$ signal transduction system may improve blood pressure control, particularly in a subset of salt sensitive subjects.

DATA AVAILABILITY STATEMENT

The raw data supporting the conclusions of this article will be made available by the authors, without undue reservation.

ETHICS STATEMENT

The animal study was reviewed and approved by Boston University Institutional Animal Care and Use Committee.

AUTHOR CONTRIBUTIONS

JK, CC, JM, and RW performed the experiments. RW prepared the figures. KN, JM, and RW drafted the manuscript. All authors approved final version of manuscript.

FUNDING

This study was supported by National Heart, Lung, and Blood Institute (NHLBI) R01HL141406 and R01HL139867, and National Institute on Aging (NIA) R01AG062515 to RW.

SUPPLEMENTARY MATERIAL

The Supplementary Material for this article can be found online at: https://www.frontiersin.org/articles/10.3389/fphys.2021.771167/full#supplementary-material

REFERENCES

Appel, L. J., Frohlich, E. D., Hall, J. E., Pearson, T. A., Sacco, R. L., Seals, D. R., et al. (2011). The importance of population-wide sodium reduction as a means to prevent cardiovascular disease and stroke: a call to action from the American Heart Association. *Circulation* 123, 1138–1143. doi: 10.1161/CIR.0b013e31820d0793

Brouwers, S., Smolders, I., Wainford, R. D., and Dupont, A. G. (2015). Hypotensive and sympathoinhibitory responses to selective central AT2 receptor stimulation in spontaneously hypertensive rats. *Clin. Sci.* 129, 81–92. doi: 10.1042/cs20140776

Bunag, R. D., and Miyajima, E. (1984). Baroreflex impairment precedes hypertension during chronic cerebroventricular infusion of hypertonic sodium chloride in rats. *J. Clin. Invest.* 74, 2065–2073. doi: 10.1172/JCI111630

Callahan, M. F., Cunningham, J. T., Kirby, R. F., Johnson, A. K., and Gruber, K. A. (1988). Role of the anteroventral third ventricle (AV3V) region of the rat brain in the pressor response to gamma 2-melanocyte-stimulating hormone (gamma 2-MSH). *Brain Res.* 444, 177–180. doi: 10.1016/0006-8993(88)90925-0

Campbell, N., Correa-Rotter, R., Neal, B., and Cappuccio, F. P. (2011). New evidence relating to the health impact of reducing salt intake. *Nutr. Metab. Cardiovasc. Dis.* 21, 617–619. doi: 10.1016/j.numecd.2011.08.001

Carmichael, C. Y., Carmichael, A. C., Kuwabara, J. T., Cunningham, J. T., and Wainford, R. D. (2016). Impaired sodium-evoked paraventricular nucleus neuronal activation and blood pressure regulation in conscious Sprague-Dawley rats lacking central Galphai2 proteins. *Acta Physiol.* 216, 314–329. doi: 10.1111/apha.12610

Carmichael, C. Y., Kuwabara, J. T., Pascale, C. L., Moreira, J. D., Mahne, S. E., Kapusta, D. R., et al. (2020). Hypothalamic paraventricular nucleus Galphai2 (guanine nucleotide-binding protein alpha inhibiting activity polypeptide 2) protein-mediated neural control of the kidney and the salt sensitivity of blood pressure. *Hypertension* 75, 1002–1011. doi: 10.1161/HYPERTENSIONAHA.119.13777

Cook, N. R., Appel, L. J., and Whelton, P. K. (2014). Lower levels of sodium intake and reduced cardiovascular risk. *Circulation* 129, 981–989. doi: 10.1161/circulationaha.113.006032

Foss, J. D., Wainford, R. D., Engeland, W. C., Fink, G. D., and Osborn, J. W. (2015). A novel method of selective ablation of afferent renal nerves by periaxonal application of capsaicin. *Am. J. Physiol. Regul. Integr. Comp. Physiol.* 308, R112–R122. doi: 10.1152/ajpregu.00427.2014

Frame, A. A., Carmichael, C. Y., Kuwabara, J. T., Cunningham, J. T., and Wainford, R. D. (2019). Role of the afferent renal nerves in sodium homeostasis and blood pressure regulation in rats. *Exp. Physiol.* 104, 1306–1323. doi: 10.1113/ep087700

Frame, A. A., Carmichael, C. Y., and Wainford, R. D. (2016). Renal afferents. *Curr. Hypertens. Rep.* 18:69.

Franco, V., and Oparil, S. (2006). Salt sensitivity, a determinant of blood pressure, cardiovascular disease and survival. *J. Am. College Nutr.* 25, 247S–255S.

Fujita, M., and Fujita, T. (2016). The role of CNS in the effects of salt on blood pressure. *Curr. Hypertens. Rep.* 18:10.

Gao, J., Denys, I., Shahien, A., Sutphen, J., and Kapusta, D. R. (2020). Downregulation of brain Galpha12 attenuates angiotensin II-dependent hypertension. *Am. J. Hypertens.* 33, 198–204. doi: 10.1093/ajh/hpz176

He, F. J., Li, J., and MacGregor, G. A. (2013). Effect of longer term modest salt reduction on blood pressure: cochrane systematic review and meta-analysis of randomised trials. *BMJ* 346:f1325. doi: 10.1136/bmj.f1325

Kapusta, D. R., Pascale, C. L., Kuwabara, J. T., and Wainford, R. D. (2013). Central nervous system Galphai2-subunit proteins maintain salt resistance via a renal nerve-dependent sympathoinhibitory pathway. *Hypertension* 61, 368–375. doi: 10.1161/HYPERTENSIONAHA.111.00014

Kapusta, D. R., Pascale, C. L., and Wainford, R. D. (2012). Brain heterotrimeric Galphai(2)-subunit protein-gated pathways mediate central sympathoinhibition to maintain fluid and electrolyte homeostasis during stress. *FASEB J.* 26, 2776–2787. doi: 10.1096/fj.11-196550

Kinsman, B. J., Browning, K. N., and Stocker, S. D. (2017a). NaCl and osmolarity produce different responses in organum vasculosum of the lamina terminalis neurons, sympathetic nerve activity and blood pressure. *J. Physiol.* 595, 6187–6201. doi: 10.1113/JP274537

Kinsman, B. J., Simmonds, S. S., Browning, K. N., and Stocker, S. D. (2017b). Organum vasculosum of the lamina terminalis detects NaCl to elevate sympathetic nerve activity and blood pressure. *Hypertension* 69, 163–170. doi: 10.1161/hypertensionaha.116.08372

Kopp, U. C. (2015). Role of renal sensory nerves in physiological and pathophysiological conditions. *Am. J. Physiol. Regul. Integr. Comp. Physiol.* 308, R79–R95.

Kopp, U. C., Cicha, M. Z., and Smith, L. A. (2003). Dietary sodium loading increases arterial pressure in afferent renal-denervated rats. *Hypertension* 42, 968–973. doi: 10.1161/01.HYP.0000097549.70134.D8

Kopp, U. C., Smith, L. A., and DiBona, G. F. (1987). Impaired renorenal reflexes in spontaneously hypertensive rats. *Hypertension* 9, 69–75.

Kotchen, T. A., Cowley, A. W. Jr., and Frohlich, E. D. (2013). Salt in health and disease–a delicate balance. *N. Engl. J. Med.* 368, 2531–2532. doi: 10.1056/nejmc1305326

Larsen, P. J., and Mikkelsen, J. D. (1995). Functional identification of central afferent projections conveying information of acute "stress" to the hypothalamic paraventricular nucleus. *J. Neurosci.* 15, 2609–2627. doi: 10.1523/JNEUROSCI.15-04-02609.1995

Lloyd-Jones, D. M., Hong, Y., Labarthe, D., Mozaffarian, D., Appel, L. J., Van Horn, L., et al. (2010). Defining and setting national goals for cardiovascular health promotion and disease reduction: the American Heart Association's strategic Impact Goal through 2020 and beyond. *Circulation* 121, 586–613.

Miyajima, E., and Bunag, R. D. (1984). Chronic cerebroventricular infusion of hypertonic sodium chloride in rats reduces hypothalamic sympatho-inhibition and elevates blood pressure. *Circ. Res.* 54, 566–575.

Mohammed, M., Berdasco, C., and Lazartigues, E. (2020). Brain angiotensin converting enzyme-2 in central cardiovascular regulation. *Clin. Sci.* 134, 2535–2547. doi: 10.1042/cs20200483

Moreira, J. D., Chaudhary, P., Frame, A. A., Puleo, F., Nist, K. M., Abkin, E. A., et al. (2019). Inhibition of microglial activation in rats attenuates paraventricular nucleus inflammation in Gαi2 protein-dependent, salt-sensitive hypertension. *Exp. Physiol.* 104, 1892–1910. doi: 10.1113/EP087924

Moreira, T. S., Takakura, A. C., Colombari, E., and Menani, J. V. (2009). Antihypertensive effects of central ablations in spontaneously hypertensive rats. *Am. J. Physiol. Regul. Integr. Comp. Physiol.* 296, R1797–R1806.

Puleo, F., Kim, K., Frame, A. A., Walsh, K. R., Ferdaus, M. Z., Moreira, J. D., et al. (2020). Sympathetic regulation of the NCC (sodium chloride cotransporter) in dahl salt-sensitive hypertension. *Hypertension* 76, 1461–1469. doi: 10.1161/HYPERTENSIONAHA.120.15928

Reboussin, D. M., Allen, N. B., Griswold, M. E., Guallar, E., Hong, Y., Lackland, D. T., et al. (2018). Systematic review for the 2017 ACC/AHA/AAPA/ABC/ACPM/AGS/APhA/ASH/ASPC/NMA/PCNA guideline for the prevention, detection, evaluation, and management of high blood pressure in adults: a report of the American College of Cardiology/American Heart Association Task Force on Clinical Practice Guidelines. *Hypertension* 71, 2176–2198.

Shi, P., Diez-Freire, C., Jun, J. Y., Qi, Y., Katovich, M. J., Li, Q., et al. (2010). Brain microglial cytokines in neurogenic hypertension. *Hypertension* 56, 297–303. doi: 10.1161/hypertensionaha.110.150409

Simmonds, S. S., Lay, J., and Stocker, S. D. (2014). Dietary salt intake exaggerates sympathetic reflexes and increases blood pressure variability in normotensive rats. *Hypertension* 64, 583–589. doi: 10.1161/HYPERTENSIONAHA.114.03250

Stocker, S. D., Monahan, K. D., and Browning, K. N. (2013). Neurogenic and sympathoexcitatory actions of NaCl in hypertension. *Curr. Hypertens. Rep.* 15, 538–546.

Unger, T., Borghi, C., Charchar, F., Khan, N. A., Poulter, N. R., Prabhakaran, D., et al. (2020). 2020 international society of hypertension global hypertension practice guidelines. *Hypertension* 75, 1334–1357. doi: 10.1161/hypertensionaha.120.15026

Vieira, A. A., Colombari, E., De Luca, L. A. Jr., Colombari, D. S., De Paula, P. M., and Menani, J. V. (2013). Cardiovascular responses to injections of angiotensin II or carbachol into the rostral ventrolateral medulla in rats with AV3V lesions. *Neurosci. Lett.* 556, 32–36. doi: 10.1016/j.neulet.2013.09.045

Wainford, R. D., Carmichael, C. Y., Pascale, C. L., and Kuwabara, J. T. (2015). Galphai2-protein-mediated signal transduction: central nervous system molecular mechanism countering the development of sodium-dependent hypertension. *Hypertension* 65, 178–186. doi: 10.1161/HYPERTENSIONAHA.114.04463

Wainford, R. D., and Kapusta, D. R. (2009). Chronic high-NaCl intake prolongs the cardiorenal responses to central N/OFQ and produces regional changes in the endogenous brain NOP receptor system. *Am. J. Physiol. Regul. Integr. Comp. Physiol.* 296, R280–R288. doi: 10.1152/ajpregu.00096.2008

Wainford, R. D., and Kapusta, D. R. (2010). Hypothalamic paraventricular nucleus G alpha q subunit protein pathways mediate vasopressin dysregulation and fluid retention in salt-sensitive rats. *Endocrinology* 151, 5403–5414. doi: 10.1210/en.2010-0345

Wainford, R. D., and Kapusta, D. R. (2012). Functional selectivity of central Galpha-subunit proteins in mediating the cardiovascular and renal excretory responses evoked by central alpha(2) -adrenoceptor activation in vivo. *Br. J. Pharmacol.* 166, 210–220. doi: 10.1111/j.1476-5381.2011.01662.x

Wainford, R. D., Pascale, C. L., and Kuwabara, J. T. (2013). Brain Galphai2-subunit protein-gated pathways are required to mediate the centrally evoked sympathoinhibitory mechanisms activated to maintain sodium homeostasis. *J. Hypertens.* 31, 747–757. doi: 10.1097/HJH.0b013e32835ebd54

Walch, J. D., Carreno, F. R., and Cunningham, J. T. (2013). Intracerebroventricular losartan infusion modulates angiotensin II type 1 receptor expression in the subfornical organ and drinking behaviour in bile-duct-ligated rats. *Exp. Physiol.* 98, 922–933. doi: 10.1113/expphysiol.2012.068593

Walsh, K. R., Kuwabara, J. T., Shim, J. W., and Wainford, R. D. (2016). Norepinephrine-evoked salt-sensitive hypertension requires impaired renal sodium chloride cotransporter activity in Sprague-Dawley rats. *Am. J. Physiol. Regul. Integr. Comp. Physiol.* 310, R115–R124. doi: 10.1152/ajpregu.00514.2014

Wang, D. H., Li, J., and Qiu, J. (1998). Salt-sensitive hypertension induced by sensory denervation: introduction of a new model. *Hypertension* 32, 649–653. doi: 10.1161/01.hyp.32.4.649

Wang, D. H., Wu, W., and Lookingland, K. J. (2001). Degeneration of capsaicin-sensitive sensory nerves leads to increased salt sensitivity through enhancement of sympathoexcitatory response. *Hypertension* 37(2 Pt 2), 440–443. doi: 10.1161/01.hyp.37.2.440

Wei, S. G., Yu, Y., Zhang, Z. H., and Felder, R. B. (2009). Angiotensin II upregulates hypothalamic AT1 receptor expression in rats via the mitogen-activated protein kinase pathway. *Am. J. Physiol. Heart Circ. Physiol.* 296, H1425–H1433. doi: 10.1152/ajpheart.00942.2008

Zhang, X., Frame, A. A., Williams, J. S., and Wainford, R. D. (2018). GNAI2 polymorphic variance associates with salt sensitivity of blood pressure in the Genetic Epidemiology Network of Salt Sensitivity study. *Physiol. Genomics* 50, 724–725. doi: 10.1152/physiolgenomics.00141.2017

Zimmerman, M. C., Lazartigues, E., Sharma, R. V., and Davisson, R. L. (2004). Hypertension caused by angiotensin II infusion involves increased superoxide production in the central nervous system. *Circ. Res.* 95, 210–216. doi: 10.1161/01.RES.0000135483.12297.e4

Conflict of Interest: The authors declare that the research was conducted in the absence of any commercial or financial relationships that could be construed as a potential conflict of interest.

Publisher's Note: All claims expressed in this article are solely those of the authors and do not necessarily represent those of their affiliated organizations, or those of the publisher, the editors and the reviewers. Any product that may be evaluated in this article, or claim that may be made by its manufacturer, is not guaranteed or endorsed by the publisher.

Copyright © 2021 Moreira, Nist, Carmichael, Kuwabara and Wainford. This is an open-access article distributed under the terms of the Creative Commons Attribution License (CC BY). The use, distribution or reproduction in other forums is permitted, provided the original author(s) and the copyright owner(s) are credited and that the original publication in this journal is cited, in accordance with accepted academic practice. No use, distribution or reproduction is permitted which does not comply with these terms.

frontiers in Physiology

PERSPECTIVE
published: 13 December 2021
doi: 10.3389/fphys.2021.785878

A 30-Year Journey Through Integrative Physiology Research and Education, Courtesy of Angiotensin II

*Kathleen S. Curtis**

Center for Health Sciences, Oklahoma State University, Tulsa, OK, United States

Keywords: angiotensin II, estrogen, body fluid balance, graduate training, medical education

SUMMARY

This brief article is a personal perspective on the importance of integrative physiology education and research, using angiotensin II as an example of how integrative physiology occurs and why it matters. It also offers suggestions and strategies to ensure that integrative physiology remains vibrant and appreciated.

Picture it: University of Pittsburgh, circa 1994. Graduate students in a lab are discussing findings from recent experiments, leading to the idea that maintaining body fluid balance requires second-by-second monitoring of the post-ingestive consequences of water intake on body fluid status, and the real-time adjustment of ongoing intake in the face of those consequences. It was a behavioral neuroscience lab, after all, and the research questions fell under the umbrella of how the brain coordinated physiological and behavioral processes to ensure survival in the face of internal and external challenges. A student from a nearby lab that employed patch-clamp recording to investigate ionic conductances and their role in long-term potentiation in hippocampal neurons entered the lab. The spirited discussion continued until, recognizing the befuddled look on the face of the newcomer, the senior graduate student said "I'm sorry. We get carried away with this big-picture stuff." The newcomer laughed a bit uncertainly and replied "Hey, to me the **cell** is the big picture."

This was nearly 30 years ago, when the technological revolutions that allow researchers to investigate the molecular bases of cellular function and drill down further and further into the regulation of the genome itself were in their infancy. Even then, however, there was the perception that those who studied integrative physiology were the red-headed stepchildren of the scientific world, while those who used complex techniques to investigate (intra)cellular processes attained almost mythical status, striding the globe like colossuses. I'm sure it is obvious that I was in the former group. What may be less obvious is that attitudes haven't changed that much in the intervening years. To be clear, I am absolutely not arguing that cellular/molecular/genetic approaches to investigate mechanisms underlying physiological function are not of value or that they have not advanced our knowledge of physiology. But I ***would*** argue that both research and education have moved so far in the direction of cellular/molecular/genetic biology that comprehension of basic physiology, in general, and integrative physiology, in particular, have suffered. This is bad enough for physiology research, but medical education also has shifted to a more cellular/molecular/genetic focus which can readily be seen by leafing through physiology textbooks. Indeed, many United States medical schools no longer require a physiology course for admission, but consider it an elective, along with cell and molecular biology [see Association of American Medical Colleges (AAMC), 2021]. The long-term impact that derives from inadequate understanding of integrative physiological functioning among healthcare providers remains to be seen.

Having been trained in behavioral neuroscience by advisors with an appreciation for and encyclopedic knowledge of the physiological underpinnings of body fluid balance, integrative physiology was an integral part of my graduate training and research. I still clearly recall the specific

OPEN ACCESS

Edited by:
Jacqueline Kathleen Phillips, Macquarie University, Australia

Reviewed by:
John S. Clemmer, University of Mississippi Medical Center, United States
Minolfa C. Prieto, Tulane University, United States

***Correspondence:**
Kathleen S. Curtis
kath.curtis@okstate.edu

Specialty section:
This article was submitted to Integrative Physiology, a section of the journal Frontiers in Physiology

Received: *29 September 2021*
Accepted: *23 November 2021*
Published: *13 December 2021*

Citation:
Curtis KS (2021) A 30-Year Journey Through Integrative Physiology Research and Education, Courtesy of Angiotensin II. Front. Physiol. 12:785878. doi: 10.3389/fphys.2021.785878

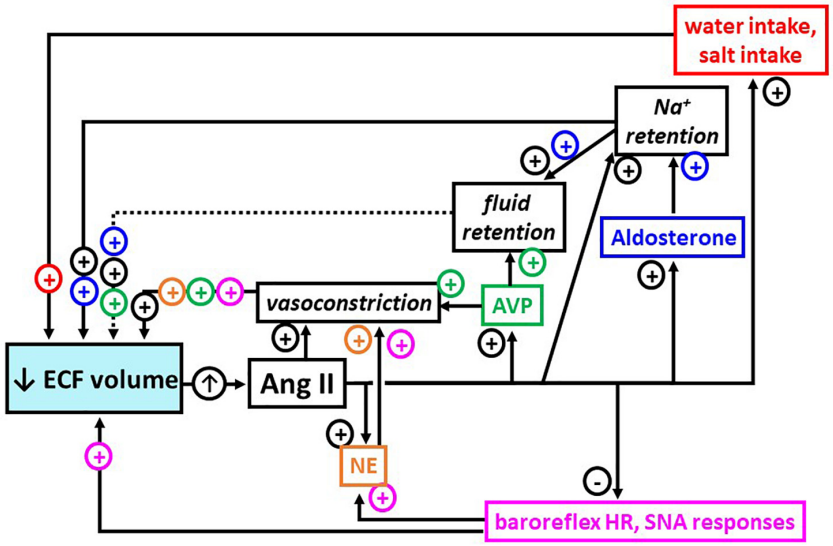

FIGURE 1 | Multi-system, integrated responses after release of angiotensin II (Ang II; up arrow) stimulated by loss of extracellular fluid (ECF) volume (blue box, down arrow). Arrows indicate effects stimulated (+) or inhibited (−) by Ang II and their positive impact on fluid volume, directly or *via* increased blood pressure; dashed arrow indicates minor role in ECF volume control. Together, these responses are integrated to maintain blood flow to organs and tissues in the face of ECF volume loss. As indicated by black font, boxes, and + signs, Ang II has direct actions that contribute to restoring ECF volume. In addition, as indicated by pink, gold, green, blue, and red font, boxes and + or − signs, Ang II has actions on a number of other effectors that indirectly serve to restore ECF volume (pink = baroreflex heart rate (HR), sympathetic nerve activity (SNA) responses; gold = norepinephrine (NE); green = arginine vasopressin (AVP); blue = aldosterone; red = water intake, salt intake).

paper that put it into perspective for me: Robinson and Evered, 1987. These investigators held blood pressure constant to assess the effects of angiotensin manipulations on water intake, recognizing that manipulations of the renin-angiotensin system frequently employed in studies of drinking behavior also affect variables such as blood pressure and renal sodium handling. Such unintended consequences could, in turn, alter drinking, thereby dictating the need for more cautious interpretation of the data—and for more thoughtful experimental design (see also, Evered, 1992). It was a "light bulb moment" for me. "Of course!" I thought. "We're investigating a system that, by definition, integrates interrelated complementary neural, cardiovascular, renal, and endocrine elements to elicit physiological and behavioral responses intended to compensate for body fluid challenges." In fact, I attempted to map it all out, an effort that required more sophisticated artistic skills than I possessed at the time. In retrospect, my response seems overly simplistic; it was (or should have been) patently obvious, rather than the light bulb moment I perceived it to be. Nonetheless, it was a perspective that informed my graduate research and that I strive to incorporate into my own research about the central effects of estrogen on body fluid balance.

But as time has passed, I find that students come into the classroom and into the lab with an impressive amount of knowledge about the molecular biology of angiotensin signaling but far less knowledge of the outcome of that signaling. Admittedly, the sophisticated techniques now available allow us to dig ever deeper into intracellular pathways such as those involved in angiotensin signaling. Indeed, there are numerous comprehensive reviews of angiotensin receptor activation (e.g., Forrester et al., 2018) that focus on intracellular signaling molecules associated with angiotensin receptors in physiological systems ranging from renal to immune. However, the majority of these papers appear to rely on the reader to fill in the blanks about the significance of this signaling. For those of us trained as integrative physiologists, filling in the blanks of the multi-system effects of angiotensin II may be easier. We understand the neural, cardiovascular, renal, and endocrine impacts of angiotensin receptor activation. But for students and trainees who haven't had the benefit of this perspective in their education or in their research training, the blanks may remain in this reduced perspective. As a result, their big picture is, quite simply, smaller.

This is not to say that a reductionist approach is intrinsically wrong or bad. Complex systems must be reduced if research is to be tractable. However, when the point of view is reduced along with the approach, we may be amassing more and more information about the cellular, molecular, and genetic mechanisms that underlie individual physiological functions, while losing our understanding of the role of each function, let alone how the functions are integrated to promote the survival of the whole animal. In other words, absent the perspective provided by integrative physiology, the bigger picture trends increasingly toward being the cell.

How do we address this? As educators we can emphasize integrative physiology and promote integrative thinking in our entry level and advanced physiology courses (see, e.g., Curtis et al., 2020). In addition, we can write or contribute to textbooks to do the same, while incorporating the concept of integrated functioning into our undergraduate, graduate, and medical curricula as a whole. As researchers, we must educate ourselves and our trainees about integrative physiology and about how interactions among physiological systems can influence our

findings. There are undoubtedly papers that provided light bulb moments for all of us, papers that profoundly influenced not only our research, but also our thinking about the field in which we work. I make sure to discuss the Robinson and Evered paper with trainees, particularly new trainees and most especially with undergraduate students. But we also must keep in mind interactions among physiological systems while interpreting our data and ensure that our students do too, so that we do not overinterpret or overgeneralize from those findings. To help my students and trainees appreciate the importance of this, I also provide a diagram I devised (**Figure 1**) illustrating the complex interrelatedness of the effects of angiotensin II. I should note, however, that while drawing software made it possible for me to generate this diagram, I still don't possess the skills to create an illustration summarizing *all* the changes that occur after loss of extracellular fluid volume; thus, the focus remains on angiotensin.

Grasping the concept of integrated, complementary responses that underpin the role of angiotensin II in body fluid regulation is critical for my laboratory's studies of estrogen effects on body fluid regulation. These studies must take into account that estrogen has both peripheral and central actions that may influence any of the angiotensin effects shown in **Figure 1**. As only a few examples, estrogen actions may be exerted by directly affecting end organs (e.g., Suzuki and Kondo, 2012) or by altering biosynthesis and/or release of the hormones of body fluid regulation (e.g., Hartley et al., 2004). Moreover, estrogen may alter angiotensin synthesis (e.g., Gallagher et al., 1999) and/or sensitivity by up- or down-regulating receptors for angiotensin II (e.g., Kisley et al., 1999; Krause et al., 2006).

I use my own research as an example of the need for students to have an appreciation of integrative physiological systems in order to design and interpret their studies—and the complexity of our studies further illustrates the necessity for integrated physiology research and education. Perhaps more to the point, however, increased understanding of this aspect of integrative physiology will inform other areas, building upon knowledge gained to better understand the bigger picture in the lab. Ultimately, the goal is to incorporate that knowledge into the classroom so that, in the end, it can be translated into improved health and healthcare.

DATA AVAILABILITY STATEMENT

The original contributions presented in the study are included in the article/supplementary material, further inquiries can be directed to the corresponding author/s.

AUTHOR CONTRIBUTIONS

KC wrote the manuscript, developed the figure, and approved the manuscript submission.

FUNDING

Over the years, my research has been supported by grants from the National Institutes of Health (DC006360 and GM110593), the Oklahoma Center for the Advancement of Science and Technology (HR09-123, HR12-196, and HR18-089), and the Oklahoma State University (President's Faculty Fellows program, intramural funding).

REFERENCES

Curtis, K. S., Benjamin, B., Curtis, J. T., Finn, W., and Rouch, A. J. (2020). Selected omissions and capstone presentations: a new approach to student centered integrative physiology education. *Adv. Physiol. Educ.* 44, 448–452. doi: 10.1152/advan.00080.2020

Evered, M. D. (1992). Investigating the role of angiotensin II in thirst: interactions between arterial pressure and the control of drinking. *Can. J. Phys. Pharm.* 70, 92–105. doi: 10.1139/y92-105

Forrester, S. J., Booz, G. W., Sigmund, C. D., Coffman, T., Kawai, T., Rizzo, V., et al. (2018). Angiotensin II signal transduction: an update on mechanisms of physiology and pathophysiology. *Phys. Revs.* 98, 1627–1738. doi: 10.1152/physrev.00038.2017

Gallagher, P. E., Li, P., Lenhart, J. R., Chappell, M. C., and Brosnihan, K. B. (1999). Estrogen regulation of angiotensin-converting enzyme mRNA. *Hypertension* 33, 323–328. doi: 10.1161/01.hyp.33.1.323

Hartley, D. E., Dickson, S. L., and Forsling, M. L. (2004). Plasma vasopressin concentrations and Fos protein expression in the supraoptic nucleus following osmotic stimulation or hypovolemia in the ovariectomized rat: effect of estradiol replacement. *J. Neuroendocrinol.* 16, 191–197. doi: 10.1111/j.0953-8194.2004.01150.x

Kisley, L. R., Sakai, R. R., and Fluharty, S. J. (1999). Estrogen decreases hypothalamic angiotensin II AT1 receptor binding and mRNA in the female rat. *Brain Res.* 844, 34–42. doi: 10.1016/s0006-8993(99)01815-6

Krause, E. G., Curtis, K. S., Stincic, T. L., Markle, J. P., and Contreras, R. J. (2006). Ooestrogen and weight loss decrease isoproterenol-induced Fos immunoreactivity and angiotensin type 1 mRNA in the subfornical organ of female rats. *J. Physiol.* 573, 251–262. doi: 10.1113/jphysiol.2006.106740

Association of American Medical Colleges (AAMC) (2021). Medical School Admission Requirements™ (MSAR®) Report for Applicants and Advisors: Admission Policies and Information 2022. Available online at: https://students-residents.aamc.org/medical-school-admission-requirements/medical-school-admission-requirements-reports-applicants-and-advisors (accessed November 12, 2021).

Robinson, M. M., and Evered, M. D. (1987). Pressor action of intravenous angiotensin II reduces drinking response in rats. *Am. J. Physiol. Regul. Intergrat. Comp. Physiol.* 252:R7540R759. doi: 10.1152/ajpregu.1987.252.4.R754

Suzuki, H., and Kondo, K. (2012). Chronic kidney disease in postmenopausal women. *Hypertens. Res.* 35, 142–147.

Conflict of Interest: The author declares that the research was conducted in the absence of any commercial or financial relationships that could be construed as a potential conflict of interest.

Publisher's Note: All claims expressed in this article are solely those of the authors and do not necessarily represent those of their affiliated organizations, or those of the publisher, the editors and the reviewers. Any product that may be evaluated in this article, or claim that may be made by its manufacturer, is not guaranteed or endorsed by the publisher.

Copyright © 2021 Curtis. This is an open-access article distributed under the terms of the Creative Commons Attribution License (CC BY). The use, distribution or reproduction in other forums is permitted, provided the original author(s) and the copyright owner(s) are credited and that the original publication in this journal is cited, in accordance with accepted academic practice. No use, distribution or reproduction is permitted which does not comply with these terms.

frontiers in Physiology

MINI REVIEW
published: 11 January 2022
doi: 10.3389/fphys.2021.813012

Stimulation of Angiotensin Converting Enzyme 2: A Novel Treatment Strategy for Diabetic Nephropathy

*Haru Nomura[1], Sanjaya Kuruppu[2] and Niwanthi W. Rajapakse[1]**

[1] School of Biomedical Sciences, University of Queensland, Brisbane, QLD, Australia, [2] Biomedicine Discovery Institute, Monash University, Melbourne, VIC, Australia

Despite current therapies for diabetic nephropathy, many patients continue to progress to end-stage renal disease requiring renal replacement therapy. While the precise mechanisms underlying diabetic nephropathy remain to be determined, it is well established that chronic activation of the renin angiotensin aldosterone system (RAAS) plays a substantial role in the pathogenesis of diabetic nephropathy. Angiotensin converting enzyme 2 (ACE2), the enzyme responsible for activating the reno-protective arm of the RAAS converts angiotensin (Ang) II into Ang 1-7 which exerts reno-protective effects. Chronic RAAS activation leads to kidney inflammation and fibrosis, and ultimately lead to end-stage kidney disease. Currently, angiotensin converting enzyme inhibitors and Ang II receptor blockers are approved for renal fibrosis and inflammation. Targeting the reno-protective arm of the RAAS should therefore, provide further treatment options for kidney fibrosis and inflammation. In this review, we examine how targeting the reno-protective arm of the RAAS can ameliorate kidney inflammation and fibrosis and rescue kidney function in diabetic nephropathy. We argue tissue ACE2 stimulation provides a unique and promising therapeutic approach for diabetic nephropathy.

Keywords: diabetes, diabetic nephropathy, renin angiotensin aldosterone system (RAAS), angiotensin converting enzyme 2, angiotensin converting enzyme 2 stimulators

OPEN ACCESS

Edited by:
Geoffrey A. Head, Baker Heart and Diabetes Institute, Australia

Reviewed by:
Robert Widdop, Monash University, Australia

****Correspondence:***
Niwanthi W. Rajapakse
n.rajapakse@uq.edu.au

Specialty section:
This article was submitted to Integrative Physiology, a section of the journal Frontiers in Physiology

Received: *11 November 2021*
Accepted: *20 December 2021*
Published: *11 January 2022*

Citation:
Nomura H, Kuruppu S and Rajapakse NW (2022) Stimulation of Angiotensin Converting Enzyme 2: A Novel Treatment Strategy for Diabetic Nephropathy. Front. Physiol. 12:813012. doi: 10.3389/fphys.2021.813012

INTRODUCTION

The prevalence of diabetes mellitus continues to increase in both Australia and worldwide and it remains the number one cause of chronic kidney disease (Whiting et al., 2011; International Diabetes Federation, 2019; ANZDATA Registry, 2020). Despite the current treatments for diabetic nephropathy, patients progress to end-stage renal disease requiring renal replacement therapy (ANZDATA Registry, 2020). In addition to renin angiotensin aldosterone system (RAAS) blockade or SGLT2 inhibition, more therapies that reduce nephron loss and thus, halt the progression of diabetic nephropathy is required (McGrath and Edi, 2019; Perkovic et al., 2019). Chronic activation of the RAAS is a key driver of diabetic nephropathy, and as such, new approaches targeting the reno-protective arm of the RAAS can provide the basis for developing new treatments. Here, we review the evidence which indicate that targeting kidney tubular and glomerular angiotensin converting enzyme 2 (ACE2) can provide unique therapeutic options for diabetic nephropathy.

CHRONIC ACTIVATION OF THE RENIN ANGIOTENSIN ALDOSTERONE SYSTEM AS A MAIN DRIVER OF DIABETIC NEPHROPATHY

Chronic RAAS activation and consequent increase in oxidative stress, renal inflammation, and fibrosis are major contributors to the progression of diabetic nephropathy (Mezzano et al., 2003; Lakshmanan et al., 2011; Liu et al., 2011; Tojo et al., 2016; Wysocki et al., 2017; Zhao et al., 2018; Malek et al., 2019; Tang et al., 2019; Wang et al., 2019; Warren et al., 2019; Lu et al., 2020; Yang et al., 2020; de Alcantara Santos et al., 2021). Increased levels of the RAAS components have been detected in experimental diabetic nephropathy as well as in renal biopsies of patients with diabetic kidney disease (Mezzano et al., 2003; Lakshmanan et al., 2011; Liu et al., 2011). While ACE inhibitors and Ang II receptor blockers remain as the first line treatment for diabetic nephropathy, there is a need to develop new treatment approaches which can rescue kidney function, particularly kidney fibrosis (McGrath and Edi, 2019). In this context, enhancing the activity of the counter-regulatory arm of the RAAS can further reduce the effects of Ang II thereby, having anti-inflammatory and anti-fibrotic effects.

It is well established that fibrosis and inflammation in the kidney tubules play a substantial role in driving diabetic nephropathy (Lin et al., 2018). Significant increase in mRNA and protein levels of tumour growth factor-β1 (TGF-β1), plasminogen activator inhibitor-1 (PAI-1) and fibronectin was observed in the renal cortex of *db/db* mice (Zhou et al., 2014). Furthermore, augmented mRNA and protein levels of pro-inflammatory marker tumour necrosis factor-α (TNF-α) was observed in the renal cortex of *db/db* mice compared to control mice (Zhou et al., 2014). This was associated with increased urinary albumin excretion (Zhou et al., 2014). Administration of Ang 1-7 ameliorates diabetic kidney disease in a wide variety of experimental diabetic models, indicating that activation of the counter-regulatory arm of the RAAS is highly beneficial in diabetic nephropathy (Giani et al., 2012; Mori et al., 2014; Zhang et al., 2015; Cassis et al., 2019).

COUNTER-REGULATORY ARM OF THE RENIN ANGIOTENSIN ALDOSTERONE SYSTEM ASSOCIATED WITH ANGIOTENSIN CONVERTING ENZYME 2/ANG 1-7/MAS RECEPTOR

A new component of the RAAS was discovered over a decade ago, known as ACE2 (Donoghue et al., 2000). It is a zinc-dependent monocarboxypeptidase with 60% sequence similarity to ACE. ACE2 is mainly found in the heart, kidneys, testes and intestine (Tipnis et al., 2000). ACE2 plays a major role in the breakdown of Ang II and therefore, it is recognised as a negative regulator of the classical RAAS (Patel et al., 2014). While ACE2 is localised to the cell membrane, it can shed to produce a soluble form of the enzyme which is often detected in the urine of diabetic patients (Liang et al., 2015; Gutta et al., 2018). This is mediated by a disintegrin and metalloproteinase-17 (ADAM17). Hyperglycemia and Ang II enhances the activity of ADAM17 which can underpin increased levels of soluble ACE2 in the setting of diabetes (Salem et al., 2014; Xiao et al., 2014). Indeed, knockout of ADAM17 in the renal proximal tubules of streptozotocin (STZ)-induced diabetic mice showed reduced circulating ACE2 when compared with diabetic wild type control mice (Palau et al., 2021).

Cleavage of Ang II by ACE2 results in the formation of Ang 1-7 which then binds to the Mas receptor expressed in the kidney. Binding of Ang 1-7 to the Mas receptor exerts vasodilatory, anti-fibrotic and anti-inflammatory effects, thereby counteracting the pathological effects mediated by excess levels of Ang II (Donoghue et al., 2000). Ang 1-7 may also have the ability to modulate blood glucose levels as ACE2 knockout in wild type mice presented with significantly higher fasting glucose than the control wild type mice (Bindom and Lazartigues, 2009). ACE2 can also cleave Ang I to form Ang 1-7 *via* an intermediate peptide, Ang 1-9 (Donoghue et al., 2000). However, the catalytic efficiency of ACE2 with Ang II is 400-fold greater than that for Ang I (Vickers et al., 2002). Furthermore, assessment of kidney biopsies from living human transplant donors showed that ACE2 was the predominant enzyme responsible in the formation of Ang 1-7 (Domenig et al., 2016). Thus, in humans, the primary pathway for Ang 1-7 production is *via* the direct cleavage of Ang II. Ang 1-7 is also formed by direct cleavage of Ang I by neprilysin (NEP) or indirectly by cleaving Ang 1-9 (Domenig et al., 2016). It was reported in the kidney of normal mice that NEP is the major enzyme responsible in producing Ang 1-7 from Ang 1-9, rather than ACE2 (Domenig et al., 2016). NEP-mediated Ang 1-7 production was prominent in the renal cortical region, which was reduced in the presence of a NEP inhibitor, DL-Thiorphan (Domenig et al., 2016). Although Ang 1-7 formation by NEP is not the major route in humans, it is important to consider this pathway because dual inhibition of NEP and AT_1R (LCZ696: sacubitril/valsartan) is considered as an alternative treatment approach in addition to RAAS inhibition for various cardiovascular diseases including heart failure (McMurray et al., 2014).

Reno-Protective Effects of the Counter-Regulatory Arm of the Renin Angiotensin Aldosterone System

Modulating the activity and/or expression of ACE2 is a promising therapeutic approach for diabetic nephropathy due to the ability of ACE2 to both degrade Ang II and generate Ang 1-7 (Oudit et al., 2010; Shiota et al., 2010; Liu et al., 2011). Administration of recombinant human ACE2 (rhACE2) in diabetic Akita mice for 4 weeks significantly reduced renal fibrosis, glomerular hypertrophy, and glomerular basement membrane thickness (Oudit et al., 2010). Adenovirus-mediated ACE2 overexpression in STZ-induced diabetic rats resulted in significant downregulation in pro-fibrotic TGF-β1 and collagen IV expression (Liu et al., 2011). This coincided with significant reductions in albuminuria, glomerulosclerosis and oxidative

stress (Liu et al., 2011). These reno-protective effects of ACE2 overexpression were similar to that seen with ACE inhibitor treatment (benazepril) (Liu et al., 2011). Similarly, podocyte-specific overexpression of ACE2 in STZ-induced diabetic mice resulted in reduced levels of mesangial expansion and glomerular hypertrophy, further supporting the reno-protective effects of ACE2 (Nadarajah et al., 2012).

On the other hand, ACE2-knockout in STZ-induced diabetic mice demonstrated accelerated glomerulosclerosis, tubular injury, interstitial fibrosis, podocyte apoptosis and increased serum creatinine levels (Shiota et al., 2010). Pharmacological inhibition of ACE2 using MLN-4760 in *db/db* mice and in STZ-induced diabetic mice resulted in increased fibronectin and collagen deposition in the glomerulus and tubulointerstitial area, in addition to mesangial matrix expansion (Ye et al., 2006; Soler et al., 2007). Collectively, results from these studies indicate that decreased levels of ACE2 lead to kidney injury in diabetes.

ANGIOTENSIN CONVERTING ENZYME 2 DISTRIBUTION IN THE KIDNEY VASCULATURE

In renal biopsies from healthy human subjects, ACE2 was found in the smooth muscle cells of interlobular arteries (Lely et al., 2004). Additionally, ACE2 expression was evident in the endothelium of interlobular arteries and in small to medium-sized veins in the kidney of these subjects (Lely et al., 2004). Within the glomerulus of these subjects, ACE2 expression was observed in the glomerular visceral and parietal epithelial cells (Lely et al., 2004). ACE2 expression was absent in mesangial cells and glomerular endothelial cells in human subjects (Hamming et al., 2004; Lely et al., 2004). In the mouse renal vasculature, ACE2 was only expressed in the vascular smooth muscle cells of the renal arterioles and its expression was absent in the endothelial cells (Soler et al., 2009). ACE2 was also found in arcuate arteries and interlobular arteries in mice (Soler et al., 2009). In rats, ACE2 expression was evident in both vascular smooth muscle cells and endothelial cells of large arteries and afferent arterioles, and in the vasa recta (Li et al., 2005; Kamilic et al., 2010). Within the glomeruli of both mice and rats, ACE2 expression was absent in the endothelial cells, which is consistent with that seen in humans (Ye et al., 2006; Kamilic et al., 2010). In mice, ACE2 was found to be expressed on the podocyte foot processes, body and slit diaphragm of the podocyte, and mesangial cells to a lesser extent (Ye et al., 2006). ACE2 expression was observed in the glomerular visceral and parietal epithelial cells while no expression was detected in the mesangial cells of the rat glomeruli (Kamilic et al., 2010).

ANGIOTENSIN CONVERTING ENZYME 2 DISTRIBUTION IN THE KIDNEY TUBULES

In both human and rodent kidneys, ACE2 is highly abundant in the apical membrane of the proximal tubule (Hamming et al., 2004; Lely et al., 2004; Ye et al., 2004, 2006). Single-cell RNA sequencing analysis of 15 normal human kidney samples revealed high abundance of ACE2 in the proximal convoluted and straight tubules, further supporting the localization of ACE2 in the proximal tubules (Pan et al., 2020). High expression of ACE2 in this section of the nephron likely negates the harmful effects arising from the high concentration of Ang II evident in the lumen of the proximal tubules in humans (Li et al., 2005). In rats, ACE2 protein and mRNA expressions were evident throughout the nephron except in the medullary thick ascending limb (Li et al., 2005). More specifically, ACE2 expression was found in the proximal tubules (convoluted and straight), Loop of Henle (outer medullary thin limb and cortical thick ascending limb), distal tubules, and collecting ducts (Li et al., 2005). In line with the expression of ACE2, significant generation of Ang 1-7 was observed in the proximal straight tubules of normal rats (Li et al., 2005). Intracellular expression of ACE2 was also observed in proximal tubules, distal tubules and collecting ducts in normal rat and human kidneys (Hamming et al., 2004; Lely et al., 2004; Li et al., 2005; Joyner et al., 2007).

CHANGES IN THE CLASSICAL AND RENO-PROTECTIVE ARM OF THE RENIN ANGIOTENSIN ALDOSTERONE SYSTEM IN DIABETIC NEPHROPATHY

Changes in ACE2 expression and activity that occur in diabetic nephropathy have been investigated intensively in both pre-clinical models and in patients with diabetic nephropathy (Wysocki et al., 2006; Reich et al., 2008). In hypertensive mRen2.Lewis rats with STZ-induced early-onset diabetes, the levels of circulating ACE2 in serum was increased in early stages of diabetes (Yamaleyeva et al., 2012). Increased ACE2 activity and protein levels were also observed in the renal cortical region of both *db/db* mice and STZ-induced diabetic mice at early stages of the disease, while observing no change in its mRNA levels (Wysocki et al., 2006). On the other hand, downregulation in ACE mRNA levels, protein expression and activity were observed in *db/db* mice and in STZ-induced diabetic mice (Ye et al., 2004; Wysocki et al., 2006). These opposing changes in ACE and ACE2 expression and/or activity may be a possible mechanism to compensate for the chronic activation of the RAAS and accumulation of Ang II in the kidney (Wysocki et al., 2006).

While increased activity and expression of ACE2 were reported in early stages of diabetes, downregulation in ACE2 expression has been observed in both pre-clinical studies and in patients with advanced stages of diabetic nephropathy (Tikellis et al., 2003; Reich et al., 2008). Reduced ACE2 expression has been reported in renal tubules and glomeruli of rodent diabetic animals (Tikellis et al., 2003). Consistent with these pre-clinical studies, ACE2 mRNA expression was significantly reduced in proximal tubules and in the glomerular compartment of renal biopsies obtained from patients with diabetic nephropathy (Reich et al., 2008). Moreover, in these patients, expression of ACE mRNA was significantly greater in both proximal tubules and

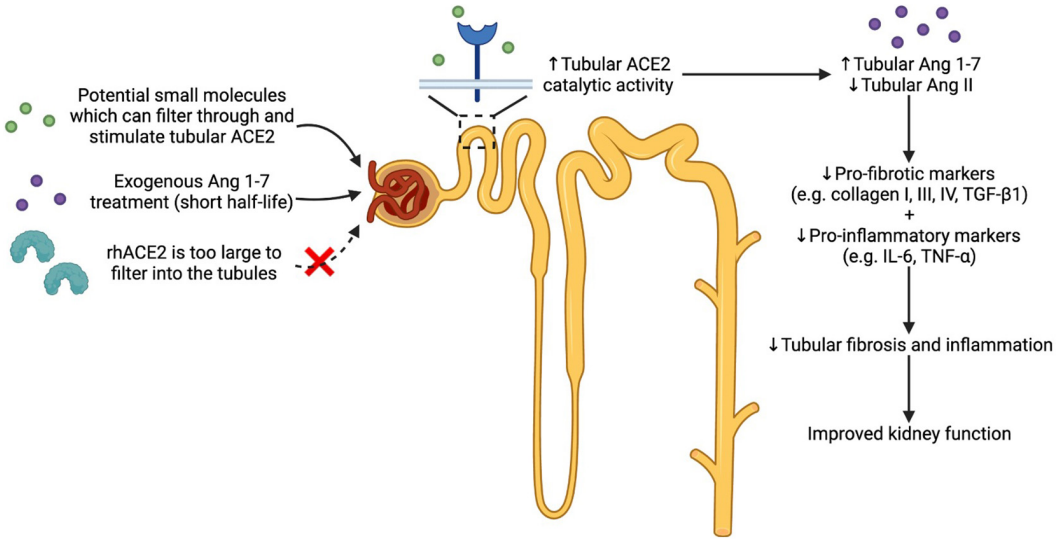

FIGURE 1 | Effects of theoretical use of small molecules which activate the reno-protective arm of the RAAS (ACE2/Ang 1-7/Mas receptor axis). Activating the ACE2/Ang 1-7/Mas receptor axis is one approach in treating diabetic nephropathy where chronic activation of the classical RAAS is observed. ACE2 stimulation using potential small molecules which can filter into the renal tubules can increase the catalytic activity of tubular ACE2. This in turn can enhance the production of Ang 1-7 and degradation of Ang II, thereby reducing renal inflammation and fibrosis, leading to improved kidney function. Ang 1-7-based therapy is another approach in activating the reno-protective arm of the RAAS. However, the short half-life of Ang 1-7 is a major drawback, making it challenging to translate Ang 1-7-based therapy to the clinic. Additionally, large proteins such as rhACE2 cannot reach the renal tubular cells due to the limited capillary permeability. Abbreviations: RAAS: renin angiotensin aldosterone system; ACE2: angiotensin converting enzyme 2; Ang: angiotensin; rhACE2: recombinant human angiotensin converting enzyme 2; TGF-β1: tumour growth factor-β1; IL-6: interleukin-6; TNF-α: tumour necrosis factor-α.

glomeruli when compared to healthy control subjects (Konoshita et al., 2006; Reich et al., 2008). These findings suggest that the increase in ACE2 activity and expression observed in early stages of diabetes gradually decreases with disease progression (Tikellis et al., 2003; Reich et al., 2008).

TECHNIQUES TO MEASURE ANGIOTENSIN CONVERTING ENZYME 2 ACTIVITY

Since ACE2 activity changes with disease progression in diabetes, it is critical to develop robust techniques to measure its activity in biological samples and tissues. Fluorometric ACE2 activity assay kits are commercially available but the accuracy of these tests in measuring tissue and plasma ACE2 activity remains to be validated. There are recent developments in novel assays to measure ACE2 activity in biological fluids using hydrolysis of an intramolecularly quenched fluorogenic ACE2 substrate (Xiao and Burns, 2017). Such assays can be the basis for development of more robust and accurate commercially available kits in future which can be widely used in experimental and clinical settings. Mass spectrometry-based methods are also available for measurement of ACE2 activity in the experimental setting (Elased et al., 2006). Of note, RAAS fingerprint using liquid chromatography-mass spectrometry (LC-MS)/MS technique is a gold standard technique to measure components of the RAAS and should be employed in quantifying ACE2 activity in diabetes (van Rooyen et al., 2016).

APPROACHES TO INCREASE THE EFFECTS OF ANGIOTENSIN CONVERTING ENZYME 2 IN DIABETIC NEPHROPATHY

Recombinant Human Angiotensin Converting Enzyme 2 Administration

One approach to enhance the reno-protective effects of ACE2 is by exogenous administration of rhACE2. Administration of rhACE2 has progressed into phase I clinical trials (Haschke et al., 2013). In healthy human subjects, single dose of rhACE2 administration (100, 200, 400, 800, and 1200 μg/kg) significantly reduced plasma Ang II levels (Haschke et al., 2013). Corresponding increase in plasma Ang 1-7 levels were also observed following administration of rhACE2 at doses of 100 and 200 μg/kg (Haschke et al., 2013). However, there was no difference in plasma Ang 1-7 levels in subjects receiving doses higher than 400 μg/kg of rhACE2 (Haschke et al., 2013). Similar effects were observed in normal healthy subjects receiving daily consecutive administration of rhACE2 (400 μg/kg for 3 or 6 days) (Haschke et al., 2013). It is important to note that rhACE2 has not been tested in patients with diabetic nephropathy.

In diabetic Akita mice administered rhACE2 for 4 weeks, plasma and renal cortical levels of Ang II were significantly lower than that of control diabetic mice (Oudit et al., 2010). In line with this finding, Ang 1-7 levels in the renal cortex was significantly greater than in control diabetic mice (Oudit et al., 2010). In these mice, urinary albumin excretion rate was significantly reduced

compared to control diabetic Akita mice (Oudit et al., 2010). Administration of rhACE2 (0.1, 1 or 5 mg/kg/day) to healthy control mice for 3 consecutive days tended to reduce plasma Ang II levels and increase plasma Ang 1-7 levels, however, no significant effects on ACE2 activity in the renal cortex was observed (Wysocki et al., 2010). This lack of effect at the tissue level may be explained by the limited capillary permeability of a healthy glomerulus which limits the filtration of large proteins such as rhACE2 and thus, fail to reach renal tubular cells (Haschke et al., 2013; Wysocki et al., 2017). Therefore, rhACE2 as a therapy may only be effective in advanced diabetic nephropathy where patients experience overt proteinuria due to significantly injured glomerular filtration barrier, allowing rhACE2 to filter into the tubules (Wysocki et al., 2017). In the setting of advanced diabetic nephropathy, where local ACE2 levels are reduced and chronic activation of the RAAS is observed, it is crucial to target endogenous renal ACE2 to achieve optimum therapeutic benefit (Wysocki et al., 2010, 2017).

Ang 1-7-Based Therapy

Ang 1-7 have demonstrated reno-protective effects in the setting of diabetic nephropathy (Mori et al., 2014). Chronic Ang 1-7 administration in experimental diabetes demonstrated improved pathophysiology of diabetic nephropathy (Mori et al., 2014). However, Ang 1-7 has a short half-life of 0.5 h and to overcome this, stable versions of Ang 1-7 have been developed such as AVE 0991 and cyclised Ang 1-7 (Wiemer et al., 2002; Kluskens et al., 2009). Cyclic Ang 1-7 exerts reno protection in BTBR *ob/ob* diabetic mice and also improves blood glucose levels in experimental diabetes (Cassis et al., 2019; Kuipers et al., 2019). However, to date, none of the stabilised versions of Ang 1-7 have progressed into the clinic, highlighting the challenges in translating Ang 1-7-based therapies to the clinic (Touyz and Montezano, 2018). Alternatively, targeting endogenous tissue ACE2 is a unique approach to increase Ang 1-7 levels. Stimulation of renal tubular ACE2 provides a unique approach to target tubular fibrosis and inflammation.

Angiotensin Converting Enzyme 2 Stimulators Provide a Unique Approach to Target Tubular and Glomerular Angiotensin Converting Enzyme 2

Previous studies have reported the identification of two molecules, xanthenone and diminazene aceturate (DIZE), as ACE2 stimulators (Hernández Prada José et al., 2008; Kulemina and Ostrov, 2011). It was initially reported that xanthenone can decrease blood pressure, improve cardiac function, and reverse cardiac and renal fibrosis in spontaneously hypertensive rats (Hernández Prada José et al., 2008). However, it was later reported that these protective effects of xanthenone was independent of ACE2 stimulation (Haber Philipp et al., 2014). Similarly, DIZE was initially reported to reduce hypertension, and cardiac and renal fibrosis *in vivo*. However, its pharmacological effects were also found to be independent of ACE2 stimulation (Haber Philipp et al., 2014). Furthermore, a high concentration of DIZE (100 μM) inhibited the activity of ACE2 (Haber Philipp et al., 2014).

Hence to date, there is no ACE2 stimulator that has progressed into the clinic, indicating that there is an unmet need for clinically useful ACE2 stimulators. An effective small molecule ACE2 stimulator will promote protective effects by activating the ACE2/Ang 1-7/Mas receptor axis of the RAAS, thereby shifting the balance from Ang II to Ang 1-7 (Reich et al., 2008). The strength of stimulating the catalytic activity of tubular ACE2 is the ability to both produce tissue Ang 1-7 and degrade excess Ang II, thereby reducing tubular fibrosis and inflammation in the setting of diabetes (**Figure 1**). It is important to note that Ang 1-7-based therapies cannot alter Ang II levels. Moreover, rhACE2 treatment is unable to cross the glomerular filtration barrier to reach kidney tubular cells, limiting its use for tubular injury in diabetic nephropathy.

CONCLUSION

The prevalence of diabetic nephropathy and the consequent progression to end-stage renal disease is increasing worldwide. Current therapies and management strategies mainly aim to delay disease progression but are unable to halt or restore kidney function. Chronic activation of the RAAS plays a central role in inducing renal inflammation and fibrosis, ultimately leading to decline in kidney function. Compounds which increase ACE2 catalytic activity provides a unique approach to target tubular and glomerular ACE2, opening up new treatment approaches for diabetic nephropathy. There is the need to develop new ACE2 stimulators with clinical translational potential.

AUTHOR CONTRIBUTIONS

HN, SK, and NR equally and directly contributed to the manuscript. All authors contributed to the article and approved the submitted version.

REFERENCES

ANZDATA Registry (2020). *43rd Anuual Report, Chapter 1: Incidence of Renal Replacement Therapy for End Stage Kidney Disease*. Adelaide, SA: ANZDATA Registry.

Bindom, S. M., and Lazartigues, E. (2009). The sweeter side of ACE2: physiological evidence for a role in diabetes. *Mol. Cell. Endocrinol.* 302, 193–202. doi: 10.1016/j.mce.2008.09.020

Cassis, P., Locatelli, M., Corna, D., Villa, S., Rottoli, D., Cerullo, D., et al. (2019). Addition of cyclic angiotensin-(1-7) to angiotensin-converting enzyme inhibitor therapy has a positive add-on effect in experimental diabetic nephropathy. *Kidney Int.* 96, 906–917. doi: 10.1016/j.kint.2019.04.024

de Alcantara Santos, R., Guzzoni, V., Silva, K. A. S., Aragão, D. S., De Paula Vieira, R., Bertoncello, N., et al. (2021). Resistance exercise shifts the balance of renin-angiotensin system toward ACE2/Ang 1-7 axis and reduces inflammation in the kidney of diabetic rats. *Life Sci.* 287:120058. doi: 10.1016/j.lfs.2021.120058

Domenig, O., Manzel, A., Grobe, N., Königshausen, E., Kaltenecker, C. C., Kovarik, J. J., et al. (2016). Neprilysin is a mediator of alternative renin-angiotensin-system activation in the murine and human kidney. *Sci. Rep.* 6:33678. doi: 10.1038/srep33678

Donoghue, M., Hsieh, F., Baronas, E., Godbout, K., Gosselin, M., Stagliano, N., et al. (2000). A novel angiotensin-converting enzyme–related carboxypeptidase (ACE2) converts angiotensin I to angiotensin 1-9. *Circ. Res.* 87, e1–e9. doi: 10.1161/01.res.87.5.e1

Elased, K. M., Cunha, T. S., Gurley, S. B., Coffman, T. M., and Morris, M. (2006). New mass spectrometric assay for angiotensin-converting enzyme 2 activity. *Hypertension* 47, 1010–1017. doi: 10.1161/01.HYP.0000215588.38536.30

Giani, J. F., Burghi, V., Veiras, L. C., Tomat, A., Muñoz, M. C., Cao, G., et al. (2012). Angiotensin-(1–7) attenuates diabetic nephropathy in Zucker diabetic fatty rats. *Am. J. Physiol. Renal Physiol.* 302, F1606–F1615. doi: 10.1152/ajprenal.00063.2012

Gutta, S., Grobe, N., Kumbaji, M., Osman, H., Saklayen, M., Li, G., et al. (2018). Increased urinary angiotensin converting enzyme 2 and neprilysin in patients with type 2 diabetes. *Am. J. physiol. Renal physiol.* 315, F263–F274. doi: 10.1152/ajprenal.00565.2017

Haber Philipp, K., Ye, M., Wysocki, J., Maier, C., Haque Syed, K., and Batlle, D. (2014). Angiotensin-converting enzyme 2–independent action of presumed angiotensin-converting enzyme 2 activators. *Hypertension* 63, 774–782. doi: 10.1161/HYPERTENSIONAHA.113.02856

Hamming, I., Timens, W., Bulthuis, M. L. C., Lely, A. T., Navis, G. J., and Van Goor, H. (2004). Tissue distribution of ACE2 protein, the functional receptor for SARS coronavirus. A first step in understanding SARS pathogenesis. *J. Pathol.* 203, 631–637. doi: 10.1002/path.1570

Haschke, M., Schuster, M., Poglitsch, M., Loibner, H., Salzberg, M., Bruggisser, M., et al. (2013). Pharmacokinetics and pharmacodynamics of recombinant human angiotensin-converting enzyme 2 in healthy human subjects. *Clin. Pharmacokinet.* 52, 783–792. doi: 10.1007/s40262-013-0072-7

Hernández Prada José, A., Ferreira Anderson, J., Katovich Michael, J., Shenoy, V., Qi, Y., Santos Robson, A. S., et al. (2008). Structure-based identification of small-molecule angiotensin-converting enzyme 2 activators as novel antihypertensive agents. *Hypertension* 51, 1312–1317. doi: 10.1161/HYPERTENSIONAHA.107.108944

International Diabetes Federation (2019). *IDF Diabetes Atlas*, 9th Edn. Brussels: International Diabetes Federation.

Joyner, J., Neves, L. A. A., Granger, J. P., Alexander, B. T., Merrill, D. C., Chappell, M. C., et al. (2007). Temporal-spatial expression of ANG-(1-7) and angiotensin-converting enzyme 2 in the kidney of normal and hypertensive pregnant rats. American journal of physiology-regulatory. *Integr. Comp. Physiol.* 293, R169–R177. doi: 10.1152/ajpregu.00387.2006

Kamilic, J., Hamming, I., Kreutz, R., Bolbrinker, J., Siems, W.-E., Nassar, I., et al. (2010). Renal ACE2 expression and activity is unaltered during established hypertension in adult SHRSP and TGR(mREN2)27. *Hypertens. Res.* 33, 123–128. doi: 10.1038/hr.2009.191

Kluskens, L. D., Nelemans, S. A., Rink, R., De Vries, L., Meter-Arkema, A., Wang, Y., et al. (2009). Angiotensin-(1-7) with thioether bridge: an angiotensin-converting enzyme-resistant, potent angiotensin-(1-7) analog. *J. Pharmacol. Exp. Ther.* 328, 849–854. doi: 10.1124/jpet.108.146431

Konoshita, T., Wakahara, S., Mizuno, S., Motomura, M., Aoyama, C., Makino, Y., et al. (2006). Tissue gene expression of renin-angiotensin system in human type 2 diabetic nephropathy. *Diabetes Care* 29, 848–852. doi: 10.2337/diacare.29.04.06.dc05-1873

Kuipers, A., Moll, G. N., Wagner, E., and Franklin, R. (2019). Efficacy of lanthionine-stabilized angiotensin-(1-7) in type I and type II diabetes mouse models. *Peptides* 112, 78–84. doi: 10.1016/j.peptides.2018.10.015

Kulemina, L. V., and Ostrov, D. A. (2011). Prediction of off-target effects on angiotensin-converting enzyme 2. *J. Biomol. Screen.* 16, 878–885. doi: 10.1177/1087057111413919

Lakshmanan, A. P., Watanabe, K., Thandavarayan, R. A., Sari, F. R., Harima, M., Giridharan, V. V., et al. (2011). Telmisartan attenuates oxidative stress and renal fibrosis in streptozotocin induced diabetic mice with the alteration of angiotensin-(1–7) mas receptor expression associated with its PPAR-γ agonist action. *Free Radic. Res.* 45, 575–584. doi: 10.3109/10715762.2011.560149

Lely, A. T., Hamming, I., Van Goor, H., and Navis, G. J. (2004). Renal ACE2 expression in human kidney disease. *J. Pathol.* 204, 587–593. doi: 10.1002/path.1670

Li, N., Zimpelmann, J., Cheng, K., Wilkins, J. A., and Burns, K. D. (2005). The role of angiotensin converting enzyme 2 in the generation of angiotensin 1–7 by rat proximal tubules. *Am. J. Physiol. Renal Physiol.* 288, F353–F362.

Liang, Y., Deng, H., Bi, S., Cui, Z., A, L., Zheng, D., et al. (2015). Urinary angiotensin converting enzyme 2 increases in patients with type 2 diabetic mellitus. *Kidney Blood Pressure Res.* 40, 101–110. doi: 10.1159/000368486

Lin, Y. C., Chang, Y. H., Yang, S. Y., Wu, K. D., and Chu, T. S. (2018). Update of pathophysiology and management of diabetic kidney disease. *J. Formos. Med. Assoc.* 117, 662–675.

Liu, C. X., Hu, Q., Wang, Y., Zhang, W., Ma, Z. Y., Feng, J. B., et al. (2011). Angiotensin-converting enzyme (ACE) 2 overexpression ameliorates glomerular injury in a rat model of diabetic nephropathy: a comparison with ACE inhibition. *Mol. Med.* 17, 59–69. doi: 10.2119/molmed.2010.00111

Lu, C. C., Hu, Z. B., Wang, R., Hong, Z. H., Lu, J., Chen, P. P., et al. (2020). Gut microbiota dysbiosis-induced activation of the intrarenal renin-angiotensin system is involved in kidney injuries in rat diabetic nephropathy. *Acta Pharmacol. Sin.* 41, 1111–1118. doi: 10.1038/s41401-019-0326-5

Malek, V., Sharma, N., Sankrityayan, H., and Gaikwad, A. B. (2019). Concurrent neprilysin inhibition and renin-angiotensin system modulations prevented diabetic nephropathy. *Life Sci.* 221, 159–167. doi: 10.1016/j.lfs.2019.02.027

McGrath, K., and Edi, R. (2019). Diabetic kidney disease: diagnosis, treatment, and prevention. *Am. Fam. Physician* 99, 751–759.

McMurray, J. J. V., Packer, M., Desai, A. S., Gong, J., Lefkowitz, M. P., Rizkala, A. R., et al. (2014). Angiotensin–neprilysin inhibition versus enalapril in heart failure. *N. Engl. J. Med.* 371, 993–1004.

Mezzano, S., Droguett, A., Burgos, M. E., Ardiles, L. G., Flores, C. A., Aros, C. A., et al. (2003). Renin-angiotensin system activation and interstitial inflammation in human diabetic nephropathy. *Kidney Int.* 64, S64–S70. doi: 10.1046/j.1523-1755.64.s86.12.x

Mori, J., Patel, V. B., Ramprasath, T., Alrob, O. A., Desaulniers, J., Scholey, J. W., et al. (2014). Angiotensin 1–7 mediates renoprotection against diabetic nephropathy by reducing oxidative stress, inflammation, and lipotoxicity. *Am. J. Physiol. Renal Physiol.* 306, F812–F821. doi: 10.1152/ajprenal.00655.2013

Nadarajah, R., Milagres, R., Dilauro, M., Gutsol, A., Xiao, F., Zimpelmann, J., et al. (2012). Podocyte-specific overexpression of human angiotensin-converting enzyme 2 attenuates diabetic nephropathy in mice. *Kidney Int.* 82, 292–303. doi: 10.1038/ki.2012.83

Oudit, G. Y., Liu, G. C., Zhong, J., Basu, R., Chow, F. L., Zhou, J., et al. (2010). Human recombinant ACE2 reduces the progression of diabetic nephropathy. *Diabetes* 59, 529–538. doi: 10.2337/db09-1218

Palau, V., Nugraha, B., Benito, D., Pascual, J., Emmert, M. Y., Hoerstrup, S. P., et al. (2021). Both specific endothelial and proximal tubular adam17 deletion protect against diabetic nephropathy. *Int. J. Mol. Sci.* 22:5520. doi: 10.3390/ijms22115520

Pan, X.-W., Xu, D., Zhang, H., Zhou, W., Wang, L.-H., and Cui, X.-G. (2020). Identification of a potential mechanism of acute kidney injury during the COVID-19 outbreak: a study based on single-cell transcriptome analysis. *Intensive Care Med.* 46, 1114–1116. doi: 10.1007/s00134-020-06026-1

Patel, V. B., Clarke, N., Wang, Z., Fan, D., Parajuli, N., Basu, R., et al. (2014). Angiotensin II induced proteolytic cleavage of myocardial ACE2 is mediated by TACE/ADAM-17: a positive feedback mechanism in the RAS. *J. Mol. Cell. Cardiol.* 66, 167–176. doi: 10.1016/j.yjmcc.2013.11.017

Perkovic, V., Jardine, M. J., Neal, B., Bompoint, S., Heerspink, H. J. L., Charytan, D. M., et al. (2019). Canagliflozin and renal outcomes in type 2 diabetes and nephropathy. *N. Engl. J. Med.* 380, 2295–2306.

Reich, H. N., Oudit, G. Y., Penninger, J. M., Scholey, J. W., and Herzenberg, A. M. (2008). Decreased glomerular and tubular expression of ACE2 in patients with type 2 diabetes and kidney disease. *Kidney Int.* 74, 1610–1616. doi: 10.1038/ki.2008.497

Salem, E. S. B., Grobe, N., and Elased, K. M. (2014). Insulin treatment attenuates renal ADAM17 and ACE2 shedding in diabetic Akita mice. *Am. J. Physiol. Renal Physiol.* 306, F629–F639. doi: 10.1152/ajprenal.00516.2013

Shiota, A., Yamamoto, K., Ohishi, M., Tatara, Y., Ohnishi, M., Maekawa, Y., et al. (2010). Loss of ACE2 accelerates time-dependent glomerular and tubulointerstitial damage in streptozotocin-induced diabetic mice. *Hypertens. Res.* 33, 298–307. doi: 10.1038/hr.2009.231

Soler, M. J., Wysocki, J., Ye, M., Lloveras, J., Kanwar, Y., and Batlle, D. (2007). ACE2 inhibition worsens glomerular injury in association with increased ACE expression in streptozotocin-induced diabetic mice. *Kidney Int.* 72, 614–623. doi: 10.1038/sj.ki.5002373

Soler, M. J., Ye, M., Wysocki, J., William, J., Lloveras, J., and Batlle, D. (2009). Localization of ACE2 in the renal vasculature: amplification by angiotensin II type 1 receptor blockade using telmisartan. *Am. J. Physiol. Renal Physiol.* 296, F398–F405. doi: 10.1152/ajprenal.90488.2008

Tang, J., Wysocki, J., Ye, M., Vallés, P. G., Rein, J., Shirazi, M., et al. (2019). Urinary renin in patients and mice with diabetic kidney disease. *Hypertension* 74, 83–94. doi: 10.1161/HYPERTENSIONAHA.119.12873

Tikellis, C., Johnston Colin, I., Forbes Josephine, M., Burns Wendy, C., Burrell Louise, M., Risvanis, J., et al. (2003). Characterization of renal angiotensin-converting enzyme 2 in diabetic nephropathy. *Hypertension* 41, 392–397. doi: 10.1161/01.HYP.0000060689.38912.CB

Tipnis, S., Hooper, N., Hyde, R., Karran, E. H., Christie, G., and Turner, A. J. (2000). A human homolog of angiotensin-converting enzyme. Cloning and functional expression as a captopril-insensitive carboxypeptidase. *J. Biol. Chem.* 275, 33238–33243. doi: 10.1074/jbc.M002615200

Tojo, A., Kinugasa, S., Fujita, T., and Wilcox, C. S. (2016). A local renal renin-angiotensin system activation via renal uptake of prorenin and angiotensinogen in diabetic rats. *Diabetes Metab. Syndr. Obes.* 9, 1–10. doi: 10.2147/DMSO.S91245

Touyz, R. M., and Montezano, A. C. (2018). Angiotensin-(1–7) and Vascular Function. *Hypertension* 71, 68–69.

van Rooyen, J. M., Poglitsch, M., Huisman, H. W., Mels, C., Kruger, R., Malan, L., et al. (2016). Quantification of systemic renin-angiotensin system peptides of hypertensive black and white African men established from the RAS-Fingerprint®. *J. Renin Angiotensin Aldosterone Syst.* 17:1470320316669880. doi: 10.1177/1470320316669880

Vickers, C., Hales, P., Kaushik, V., Dick, L., Gavin, J., Tang, J., et al. (2002). Hydrolysis of biological peptides by human angiotensin-converting enzyme-related carboxypeptidase. *J. Biol. Chem.* 277, 14838–14843. doi: 10.1074/jbc.M200581200

Wang, Y., Fang, Q., Jin, Y., Liu, Z., Zou, C., Yu, W., et al. (2019). Blockade of myeloid differentiation 2 attenuates diabetic nephropathy by reducing activation of the renin-angiotensin system in mouse kidneys. *Br. J. Pharmacol.* 176, 2642–2657. doi: 10.1111/bph.14687

Warren, A. M., Knudsen, S. T., and Cooper, M. E. (2019). Diabetic nephropathy: an insight into molecular mechanisms and emerging therapies. *Expert Opin. Ther. Targets* 23, 579–591. doi: 10.1080/14728222.2019.1624721

Whiting, D. R., Guariguata, L., Weil, C., and Shaw, J. (2011). IDF diabetes atlas: global estimates of the prevalence of diabetes for 2011 and 2030. *Diabetes Res. Clin. Pract.* 94, 311–321. doi: 10.1016/j.diabres.2011.10.029

Wiemer, G., Dobrucki Lawrence, W., Louka Febee, R., Malinski, T., and Heitsch, H. (2002). AVE 0991, a nonpeptide mimic of the effects of angiotensin-(1–7) on the endothelium. *Hypertension* 40, 847–852. doi: 10.1161/01.hyp.0000037979.53963.8f

Wysocki, J., Ye, M., Khattab, A. M., Fogo, A., Martin, A., David, N. V., et al. (2017). Angiotensin-converting enzyme 2 amplification limited to the circulation does not protect mice from development of diabetic nephropathy. *Kidney Int.* 91, 1336–1346. doi: 10.1016/j.kint.2016.09.032

Wysocki, J., Ye, M., Rodriguez, E., González-Pacheco Francisco, R., Barrios, C., Evora, K., et al. (2010). Targeting the degradation of angiotensin II with recombinant angiotensin-converting enzyme 2. *Hypertension* 55, 90–98. doi: 10.1161/HYPERTENSIONAHA.109.138420

Wysocki, J., Ye, M., Soler, M. J., Gurley, S. B., Xiao, H. D., Bernstein, K. E., et al. (2006). ACE and ACE2 activity in diabetic mice. *Diabetes* 55, 2132–2139. doi: 10.2337/db06-0033

Xiao, F., and Burns, K. D. (2017). Measurement of angiotensin converting enzyme 2 activity in biological fluid (ACE2). *Methods Mol. Biol.* 1527, 101–115. doi: 10.1007/978-1-4939-6625-7_8

Xiao, F., Zimpelmann, J., Agaybi, S., Gurley, S. B., Puente, L., and Burns, K. D. (2014). Characterization of angiotensin-converting enzyme 2 ectodomain shedding from mouse proximal tubular cells. *PLoS One* 9:e85958. doi: 10.1371/journal.pone.0085958

Yamaleyeva, L. M., Gilliam-Davis, S., Almeida, I., Brosnihan, K. B., Lindsey, S. H., and Chappell, M. C. (2012). Differential regulation of circulating and renal ACE2 and ACE in hypertensive mRen2.Lewis rats with early-onset diabetes. *Am. J. Physiol. Renal Physiol.* 302, F1374–F1384. doi: 10.1152/ajprenal.00656.2011

Yang, Y., He, X., Cheng, R., Chen, Q., Shan, C., Chen, L., et al. (2020). Diabetes-induced upregulation of kallistatin levels exacerbates diabetic nephropathy via RAS activation. *FASEB J.* 34, 8428–8441. doi: 10.1096/fj.201903149R

Ye, M., Wysocki, J., Naaz, P., Salabat Mohammad, R., Lapointe Michael, S., and Batlle, D. (2004). Increased ACE 2 and decreased ACE protein in renal tubules from diabetic mice. *Hypertension* 43, 1120–1125. doi: 10.1161/01.HYP.0000126192.27644.76

Ye, M., Wysocki, J., William, J., Soler, M. J., Cokic, I., and Batlle, D. (2006). Glomerular localization and expression of angiotensin-converting enzyme 2 and angiotensin-converting enzyme: implications for albuminuria in diabetes. *J. Am. Soc. Nephrol.* 17, 3067–3075. doi: 10.1681/ASN.2006050423

Zhang, K., Meng, X., Li, D., Yang, J., Kong, J., Hao, P., et al. (2015). Angiotensin(1-7) attenuates the progression of streptozotocin-induced diabetic renal injury better than angiotensin receptor blockade. *Kidney Int.* 87, 359–369. doi: 10.1038/ki.2014.274

Zhao, S., Ghosh, A., Lo, C.-S., Chenier, I., Scholey, J. W., Filep, J. G., et al. (2018). Nrf2 deficiency upregulates intrarenal angiotensin-converting enzyme-2 and angiotensin 1-7 receptor expression and attenuates hypertension and nephropathy in diabetic mice. *Endocrinology* 159, 836–852. doi: 10.1210/en.2017-00752

Zhou, G., Cheung, A. K., Liu, X., and Huang, Y. (2014). Valsartan slows the progression of diabetic nephropathy in db/db mice via a reduction in podocyte injury, and renal oxidative stress and inflammation. *Clin. Sci.* 126, 707–720. doi: 10.1042/CS20130223

Conflict of Interest: The authors declare that the research was conducted in the absence of any commercial or financial relationships that could be construed as a potential conflict of interest.

Publisher's Note: All claims expressed in this article are solely those of the authors and do not necessarily represent those of their affiliated organizations, or those of the publisher, the editors and the reviewers. Any product that may be evaluated in this article, or claim that may be made by its manufacturer, is not guaranteed or endorsed by the publisher.

Copyright © 2022 Nomura, Kuruppu and Rajapakse. This is an open-access article distributed under the terms of the Creative Commons Attribution License (CC BY). The use, distribution or reproduction in other forums is permitted, provided the original author(s) and the copyright owner(s) are credited and that the original publication in this journal is cited, in accordance with accepted academic practice. No use, distribution or reproduction is permitted which does not comply with these terms.

frontiers in Physiology

REVIEW
published: 25 February 2022
doi: 10.3389/fphys.2022.831829

New Insights Into Energy Substrate Utilization and Metabolic Remodeling in Cardiac Physiological Adaption

*Xiaomeng Shi and Hongyu Qiu**

Center for Molecular and Translational Medicine, Institute of Biomedical Sciences, Georgia State University, Atlanta, GA, United States

Cardiac function highly relies on sufficient energy supply. Perturbations in myocardial energy metabolism play a causative role in cardiac pathogenesis. Accumulating evidence has suggested that modifications of cardiac metabolism are also an essential part of the adaptive responses to various physiological conditions in the heart to meet specific energy needs. The review highlighted some new studies on basic myocardial energy substrate metabolism and updated recent findings regarding cardiac metabolic remodeling and their associated mechanisms under physiological conditions, including exercise and cardiac development. Studying basic metabolic profiles in the heart in these conditions can contribute to understanding the significance of metabolic regulation in the heart during physiological adaption and gaining further insights into the maladaptive metabolic changes associated with cardiac pathogenesis, thus opening up new avenues to exploring novel therapeutic strategies in cardiac diseases.

Keywords: metabolism, substrate utilization, heart, physiology, cardiac disease

OPEN ACCESS

Edited by:
Geoffrey A. Head, Baker Heart and Diabetes Institute, Australia

Reviewed by:
Helen E. Collins, University of Louisville, United States
Michinari Nakamura, Rutgers University–Newark, United States

***Correspondence:**
Hongyu Qiu
Hqiu@gsu.edu

Specialty section:
This article was submitted to Integrative Physiology, a section of the journal Frontiers in Physiology

Received: *08 December 2021*
Accepted: *10 February 2022*
Published: *25 February 2022*

Citation:
Shi X and Qiu H (2022) New Insights Into Energy Substrate Utilization and Metabolic Remodeling in Cardiac Physiological Adaption. Front. Physiol. 13:831829. doi: 10.3389/fphys.2022.831829

INTRODUCTION

The heart demands high energy production and turnover to maintain its proper functioning. Cardiomyocytes navigate their metabolic activities to meet specific energy demands with each contraction cycle. Multifaceted interactions and coordinations between metabolic pathways and networks underlie the integrated metabolic homeostasis of the heart regarding ATP production, biosynthesis, signaling regulation, and control of redox state. Perturbations in myocardial energy metabolism have been considered causative for cardiac pathogenesis, eventually progressing to ventricular dysfunction, arrhythmias, and heart failure, contributing to poor prognosis and high cardiovascular mortality rates. Therefore, it is of great significance to elucidate the critical role of metabolic regulation in the heart.

Metabolic remodeling, in general concept, refers to the reconstruction of the metabolic landscape or metabolomics profiling that results in a shift toward a greater reliance on alternative fuel metabolism (van Bilsen et al., 2008), which is involved in the regulation of essential cellular functions such as the process of substrate utilization, the tricarboxylic acid (TCA) cycle, oxidative phosphorylation, and high-energy phosphate metabolism. Although numerous studies have focused on the abnormal metabolic remodeling in heart diseases, such as myocardial infarction (MI), diabetic cardiomyopathy (DCM), and heart failure (HF) (Chong et al., 2017; Chen et al., 2019; Zuurbier et al., 2020), the mechanisms and characteristics of cardiac metabolic remodeling in modulating either beneficial or detrimental cardiac functional processes remain largely unknown.

On the other hand, accumulating evidence has suggested that cardiac metabolic remodeling is an essential adaptation to various physiological conditions of the heart to meet the specific energy requirements, such as during exercise and cardiac development. Under these physiological conditions, the heart can efficiently switch energy substrate utilization to provide sufficient ATP supply to the constantly varying demand of cardiac myocytes through a complex network of signaling pathways. Gaining more knowledge in this specific field will enable us to achieve a deeper understanding of the fundamental biology and metabolism in cardiac function and explore novel therapeutic strategies to slow down or reverse pathological remodeling, thus integratively promoting overall cardiac health.

In the review, we summarized continuing research progress on myocardial energy substrate utilization and also discussed a portion of recent findings regarding cardiac metabolic remodeling and the associated mechanisms under different physiological conditions, including exercise and cardiac development. Reviewing and discussing the current progress on cardiac metabolism in these conditions can contribute to better understanding the significance of metabolic regulations in the heart during physiological adaption and receiving fresh perspectives on the maladaptive metabolic changes underlying cardiac pathogenesis.

NEW PROGRESS OF METABOLIC SUBSTRATE UTILIZATION IN THE HEART

Virtually, the selection, partition, and coordination of different substrates for energy production in the myocardium ultimately depend on the complex cardiac dynamics over time. Lately, Murashige et al. (2020) conducted a comprehensive and quantitative mapping of cardiac fuel use via measuring dynamic uptake and release of metabolites in the human heart by liquid chromatography-mass spectrometry. It was found that the heart consumed all species of free fatty acids (FFAs) and acquired the most carbons from FFAs, taking up over 70% of total carbons extracted from the circulation. The heart acquired another 15% of total carbons from ketone extraction. Acetate, which accounted for the highest percentage of short-chain FAs produced by gut bacteria, was avidly extracted by the heart, accounting for 2% of myocardial carbon uptake. Meanwhile, the heart secreted most of the essential amino acids, particularly those with greater nitrogen content. Among them, glutamine and alanine were the two most abundant amino acids secreted, with the release of the former nearly equal to glutamate uptake. In addition, histidine was identified to be the most highly secreted essential amino acid, and considering that myoglobin, a heme protein abundantly present in cardiac tissues, contained a greater histidine content than other cardiac proteins, they could be serving as a potential carbon reservoir (Murashige et al., 2020). In comparison, the failing hearts of patients with a left ventricular ejection fraction (LVEF) below 40% exhibited an almost threefold increase in ketone consumption, a twofold increase in lactate consumption, and a doubled rate of proteolysis together with suppressed FFA use, but there was no evidence of increased secretion of acylcarnitines found, which contradicted with the previous findings that associated increased plasma long-chain acylcarnitines with heart failure (Ahmad et al., 2016). Myocardial consumption of three fuels, including acetate, 3-hydroxybutyrate (3-OHB), and glutamate, was directly proportional to their circulating concentrations, which suggested that the utilization of these substrates were predominantly driven by their availability instead of relying on substantial regulations like glucose and FFAs. Furthermore, the fractional uptake of these three fuels exhibited a strong correlation with each other, which suggested that tissue perfusion was another key determinant for their fuel utilization efficiency. Unexpectedly, lactate uptake by the heart was also not proportional to its blood concentrations, which directly contradicted the previous evidence stating that myocardial lactate extraction was directly proportional to its circulating concentrations (Gertz et al., 1988). As it is known, cardiac metabolism is a vital research topic and has been extensively characterized in various models of heart diseases in the past. Thus, this review mainly highlighted some of the new progress about myocardial metabolism, focused on the newly developed methodologies and the recent discovery of metabolic substrate utilization, to improve our understanding of this appreciated topic.

Glucose and Fatty Acids

Unlike most tissues, the heart mainly utilizes long-chain fatty acids, accounting for 60–70% of its fuel metabolism. Distinctively, glucose oxidation is less favored in the heart because the heart has very little glycogen available. It gets depleted very quickly under hypoxic conditions, plus little gluconeogenesis occurs in the heart. Metabolic remodeling involving glucose and lipid metabolism has been intensely characterized in the heart with preexisting dysfunctions, such as heart failure, myocardial infarction, and diabetic cardiomyopathy. In mature animal models of heart failure that is most commonly elicited by either pressure-overload or ischemia, the energy-deficient heart switches from fatty acid oxidation to more oxygen-efficient glucose oxidation accompanied by markedly upregulated cardiac glucose uptake (Nabben et al., 2018). Such metabolic shift is not always detrimental as higher oxygen efficiency could ameliorate ischemia in the hypoxic myocardium, but not in pressure-overloaded heart. Conversely, the diabetic heart has to depend more on fatty acid oxidation to compensate for crippled glucose oxidation and its unfavorable interactions with the defective insulin signaling, which in turn results in excessive accumulation of toxic lipid intermediates, potentially resulting in cardiac lipotoxicity that further impairs cardiac contractile functions (Chong et al., 2017). Aside from these well-characterized metabolic features in the stressed hearts, there has also been progress on the redox interplay of metabolic regulation in cardiac glucose and fatty acid metabolism. Cardiac-specific overexpression of NADPH oxidase 4 (Nox4) has recently been found to modulate substantial reprogramming of glucose and fatty acid metabolism in the heart of Nox4 transgenic (TG) mice compared to the wild type (WT) group (Nabeebaccus et al., 2017). Specifically, unstressed Nox4 TG

hearts exhibited significantly decreased glucose oxidation rates and lowered glycolysis, subsequently increasing the accumulation of proximal glycolytic metabolites and upregulating fatty acid oxidation rate. Similar changes were observed in hypertrophied Nox4 TG hearts compared to the hypertrophied WT controls. Nox4 overexpression significantly promoted glucose diversion into the hexosamine biosynthetic pathway (HBP), producing the substrate, uridine diphosphate-*N*-acetylglucosamine (UDP-GlcNAc), for the posttranslational *O*-linked glycosylation (*O*-GlcNAcylation), via increasing activating transcription factor 4 and its direct transcriptional target, fructose-6-phosphate aminotransferase 1. While Nox4 TG and WT mice exhibited similar cardiac energetics and function at baseline, the former showed a significantly preserved energetic state when challenged with acute isoproterenol compared with WT control. Together, these results suggested that Nox4-redirected glucose utilization and subsequently increased fatty acid oxidation might be a beneficial response of the myocardium adapting to stress.

Previously, most studies investigating cardiac fatty acid and glucose metabolism were performed in an *ex vivo* model of perfused, isolated hearts. In recent years, the rapid development and application of isotopic labeling and metabolomics have greatly encouraged and facilitated the assessment of fuel availability and fate in the heart *in vivo*. For example, Schnelle et al. (2020) assessed the metabolic fate of glucose in the hearts of mice that underwent 2 weeks of transverse aortic constriction (TAC) and aortocaval fistula (shunt) surgery, respectively, via *in vivo* [U-^{13}C] glucose labeling combined with isotopomer analysis with nuclear magnetic resonance spectroscopy (NMR spectroscopy). Male adult mice received 30-min continuous intravenous infusion of [U-^{13}C] glucose before their hearts were excised for the *ex vivo* analysis. In pressure overloaded TAC hearts that exhibited significant concentric hypertrophy and reduced EF, ^{13}C was significantly enriched in lactate, succinate, glutamate, glutamine, and aspartate in the heart compared with the sham group but were overall less pronounced in the plasma. There were no significant changes of ^{13}C enrichment between volume overloaded shunt-treated hearts that showed prominent eccentric hypertrophy with unchanged LVEF and the sham group. However, increased plasma ^{13}C enrichment of succinate was detected in the shunt group while the abundance of aspartate was too low in the plasma to trace its ^{13}C enrichment. These findings indicated that their experimental approach primarily captured the cardiac-driven metabolic flux of glucose instead of systemic effects. The enrichment of [1,2,3-^{13}C] lactate metabolized from [1,2,3-^{13}C] pyruvate following glycolysis was significantly increased in TAC hearts together with markedly upregulated expressions of glucose transporter 1 (GLUT1), hexokinase-1, and lactate dehydrogenase A (LDHA) compared with the sham group. Both the enrichment of [4,5-^{13}C] glutamate as a readout for the activity of pyruvate dehydrogenase (PDH) and [2,3-^{13}C] glutamate indicative of anaplerotic reactions in the TCA cycle was significantly increased in TAC hearts compared with sham together with increased gene expression of PDH E1 component subunit α (PDHαE1), which suggested augmented pyruvate flux directly into the TCA cycle and greater anaplerosis. Such changes were not observed in the shunt group. However, the gene expression of pyruvate dehydrogenase kinase 4 (PDK4) was markedly decreased compared with the sham group. In addition, other than in shunt, TAC hearts exhibited a significant increase in the enrichment of [4,5-^{13}C] glutamine and the total levels of glutamine measured by NMR as well as the protein levels of glutamine synthetase and glutaminase compared with sham. The *in vivo* ^{13}C-labeling strategy employed in this study held unique advantages of directly tracing the metabolic pathway activities over conventional studies in which pathway analysis relied heavily on detecting changes in gene, mRNA, and protein expression levels that indirectly reflected pathway activities. The results gained also corroborated with the previously observed general pattern of increased glucose metabolism in pressure overload-induced heart failure.

In addition, Fulghum et al. (2022) recently examined the impact of cardiac-specific alterations of phosphofructokinase-1 (PFK1) activity on ancillary biosynthetic pathways of glucose metabolism in the myocardium of adult male mice by tracing the metabolic fate of dietary $^{13}C_6$-glucose administered through a standardized $^{13}C_6$-containing liquid diet. By overexpressing cardiac phosphatase-deficient or kinase-deficient 6-phosphofructo-2-kinase/fructose-2,6-bisphosphatase (PFK-2/FBPase-2/PFKFB), the Glyco^{Lo} and Glyco^{Hi} hearts were excised and subjected to NMR and ion exchange chromatography-mass spectrometry (IC-MS) to qualify metabolite abundance and ^{13}C enrichment. In this study, Glyco^{Lo} mice hearts with low PFK-1 activity exhibited increased glycogen synthetic metabolites such as glucose-6-phosphate (G6P) and fructose-6-phosphate, and glucose-1-phosphate together with increased ^{13}C-labeled glycogen (Fulghum et al., 2022). However, cardiac PFK-1 activity did not significantly affect the HBP pathway but mildly enhanced the levels of metabolic intermediates involved in pyrimidine biosynthetic pathways. Moreover, both unlabeled and ^{13}C-labeled 5-aminoimidazole-4-carboxamide-1-β-D-ribofuranoside (AICAR) and phosphoribosyl pyrophosphate were markedly increased in the Glyco^{Lo} hearts. Further investigation revealed that the metabolic routing of glucose-derived ^{13}C carbons to AICAR induced by low PFK-1 activity was associated with chaperones-containing large multimeric complexes and metabolic enzymes, such as phosphoribosylaminoimidazole carboxylase. This study focused on the relatively slower biosynthetic pathways of glucose metabolism compared with the majority of *in vivo* ^{13}C labeling approaches previously reported (Josan et al., 2013; Schnelle et al., 2020), in which ^{13}C glucose was administered by infusion or injections and thus was limited to only tracing the fast turnover pathways such as glycolysis due to their transient nature. Besides, these methods could not only induce stress responses because of involved procedures such as anesthesia or physical restraint but also could produce unknown artifacts that could cause potential discrepancies, which could be eliminated by oral administration.

Ketone Bodies

A recent study demonstrated that ketone bodies could serve as a primary fuel source for cardiac energy production instead of a "thrifty-fuel" as high 3-OHB concentrations in aerobically perfused hearts extracted from 12-week-old male

mice could markedly boost ketone oxidation and efficiently produce ATP without suppressing physiological glucose and palmitate metabolism rates (Ho et al., 2021). This finding collaborated with the lately recognized theory that ketones are the "preferred" fuel for the heart and the brain, despite the presence of adequate glucose. Their study did not observe improved cardiac efficiency upon increased ketone oxidation in healthy normal mice models. On the contrary, the diminished capacity of the failing heart to utilize fatty acids and glucose drives the metabolic machinery to shift to the alternative ketone oxidation pathway, raising circulating ketone bodies and promoting D-β-hydroxybutyrate dehydrogenase (BDH1) activities that catalyze ketone bodies back to acetyl coenzyme A (acetyl-CoA) (Aubert et al., 2016). Permanently elevated plasma ketone levels by knocking out the 3-oxoacid CoA-transferase 1 gene that encodes the ketolytic succinyl-CoA:3-ketoacid-CoA transferase 1 could ameliorate inflammatory infiltrates in failing hearts of male mice at 8–10 weeks of age subjected to TAC (Byrne et al., 2020). Therefore, while ketone bodies seem to be just a super fuel for a healthy heart, they have been further explored as a therapeutic strategy, such as acute intravenous infusion of 3-OHB to provide an additional fuel source to maintain energy stability in the failing myocardium (Lopaschuk et al., 2020). Uchihashi et al. (2017) produced a cardiac-specific Bdh1 overexpression TG mouse model to study ketone body metabolism in pressure overloaded hearts. Increased ketone body oxidation was observed in the hearts of both Bdh1 transgenic male mice at 10–12 weeks of age and sex-and age-matched mice who were subjected to TAC-induced pressure overload. *In vitro*, adenovirus-mediated Bdh1 overexpression was found to markedly mitigate 3-OHB-induced intracellular reactive oxygen species (ROS) production and cardiomyocyte apoptosis while enhancing the mRNA expressions of antioxidant enzymes such as metallothionein 2, catalase, and superoxide dismutases in H9c2 cells that were exposed to 5-mmol/L 3-OHB. Besides, the magnitude of 3-OHB-induced increase in histone hyperacetylation was greater in Bdh1 TG mice than WT control treated with the same infusion. The novel Bdh1 TG model provided further evidence of intervening myocardial ketone body metabolism as a potential therapeutic strategy for treating heart failure.

Lactate

The myocardium has been considered a net lactate consumer that uptakes lactate directly proportional to its circulating concentrations over the past few decades (Gertz et al., 1988; Gibb and Hill, 2018). During high-intensity exercises, serum lactate is massively elevated under fully aerobic conditions, which outweighs glucose oxidation and starts to dominate the fuel supply for the heart via the cell–cell lactate shuttle that carries lactate from the skeleton muscles to the myocardium (Brooks, 2021). During uncompensated MI, circulating lactate levels also surges due to poor systemic perfusion, which has been clinically correlated as an independent prognostic marker for acute MI patients (Frydland et al., 2019). Aside from being a crucial cardiac fuel and major gluconeogenic precursor, transient lactate accumulation from anaerobic glycolysis also acts as a ' physicochemical buffer' that could blunt acute aggravation of the ischemic injury at early reperfusion in myocardial ischemia/reperfusion injury (Qiao et al., 2013).

Amino Acids

Amino acids play an obligatory role in maintaining the metabolic milieu of the heart, thus gaining more and more attention for exerting a marked influence on cardiac pathophysiology. Amino acids, such as glutamine and glutamate, can replenish a small amount of ATP in the stressed heart via non-oxidative metabolism, thus free from contributing to acidification and free radical formation (Drake et al., 2012). Glutamine is the most abundant amino acid in the body, and the majority of it is degraded into glutamate by glutaminase (glutaminolysis), which is consumed by the heart more than any other amino acid. Thus, glutamine and glutamate are considered preferential fuels for cardiac metabolism and have been highlighted as anaplerotic precursors of TCA intermediates. Watanabe et al. (2021) conducted an isotope tracing study to assess metabolic remodeling regarding the intracellular levels of glutamine, glutamate, and α-ketoglutarate in rat neonatal cardiomyocytes subjected to H_2O_2-induced oxidative stress. H_2O_2-treated cardiomyocytes exhibited enhanced glutaminolysis and a subsequent increase in ATP production through glutamine anaplerotic reactions to compensate for compromised substrate oxidation under immense oxidative stress, thus conferring cardioprotective effects in the stressed heart.

In recent years, there has also been some rapid progress on branched-chain amino acids (BCAAs) metabolism involved in cardiac metabolic remodeling, and it is receiving more attention nowadays than ever before. BCAAs, referring to leucine, isoleucine, and valine, serves as a major nitrogen donor for glutamine synthesis in muscles where BCAA catabolism primarily occurs due to robust BCAA transaminase (BCAT) activity that converts BCAAs and α-KG to α-ketoacids (BCKA) and glutamate. Defective BCAA catabolism and subsequent tissue accumulation of toxic byproducts such as medium- and long-chain acylcarnitines (AC), valine catabolite, 3-hydroxyisobutyrate (3HIB) as well as BCAA themselves have been extensively reported to impair fasting glucose and stimulate mammalian target of rapamycin complex 1(mTORC1) overactivation-induced insulin resistance (IR) (Yoon, 2016; Bloomgarden, 2018).

Sun et al. (2016) studied a knockout mouse model with deficient expression of protein phosphatase 2C in mitochondria (PP2Cm) and resultant inhibition on branched-chain alpha-keto acid dehydrogenase (BCKD) activity. Intramyocardial BCKA levels were significantly elevated in the heart of PP2Cm-KO mice after fasting, reaching the BCKA levels shown in failing WT mouse and human hearts recruited in this study. This increase became much greater in PP2Cm-KO hearts from fed mice, suggesting a potential influence of diet on cardiac BCAA accumulation. Functionally, 3-month-old PP2Cm-KO mice exhibited a modest decrease in systolic cardiac function, which was further reduced in 18-month-old PP2Cm-KO mice compared with age-matched WT. Since there were no major cardiac remodeling events in young PP2Cm-KO hearts, such a finding suggested that abnormal BCAA catabolism alone could

induce systolic dysfunction over time without any external pathological stimuli. Moreover, PP2Cm-KO mice subjected to 8-week pressure overload started to exhibit signs of heart failure, highlighting an increased susceptibility to heart failure under pathological stress.

Dietary BCAAs have been repeatedly observed to have a damaging effect on the stressed heart (Wang et al., 2016; Li et al., 2020; Jiang et al., 2021). However, there is still a lack of sufficient knowledge about how dietary BCAA impacts cardiac metabolic dynamics and its interaction with cardiac function. Latimer et al. (2021) interrogated whether the timing of BCAA consumption could impact cardiometabolic outcomes in healthy and pressure-overloaded hearts as both temporal and spatial substrate abundance and partitioning could determine the metabolic fate of the substrates. For starters, mice at 20 weeks of age fed with a 4 h-long late high BCAA diet (LHB) at Zeitgeber time (ZT) 16 of the dark (active) phase exhibited a significant drop in cardiac output but a rapid and dramatic increase in both biventricular weight and cardiomyocyte size compared with those on a late low BCAA diet (LLB), whereas no hypertrophic responses were observed in mice fed with an early high BCAA diet (EHB) at ZT12. Upon further probing, cardiac protein synthesis was found to be dramatically elevated in LHB mice compared with LLB mice over BCAA selectively promoted activation of the mTOR signaling at the end of the active period. However, although mice subjected to a 4-week LHB diet exhibited hypertrophic responses at ZT24 compared with EHB mice, there were no significant cardiac changes at ZT16 between LHB mice and EHB mice, revealing a transient and highly dynamic nature of BCAA-induced cardiac growth. Additionally, cardiac-specific BMAL1 knockout (CBK) mice that displayed a dysfunctional circadian clock were recruited and fed with a high BCAA diet either at ZT12 or ZT16 for 4 weeks using the long-term EHB and LHB feeding regimens. There were no significant differences in cardiac mass, cardiomyocyte size, or mTOR activity between EHB and LHB fed CBK mice, suggesting that circadian misalignment could abolish time-of-day dependent cardiac responsiveness of dietary BCAAs. Moreover, CBK mice fed with a normal BCAA diet in an *ad libitum* manner exhibited significant cardiac hypertrophic responses compared with littermate control, whereas oscillatory fluctuations in mTORC1 activities observed in control littermates were completely abolished in CBK mice, indicating that clock-defective mice chronically developed increased sensitivity to a BCAA diet. Given that BCAA-induced hypertrophic growth in the healthy mouse hearts did not establish an accumulative effect, mice were subjected to TAC surgery to induce cardiac pressure overload and were fed with either the LHB diet or EHB diet. LHB mice exhibited significant hypertrophy and fibrosis and declined function compared with EHB mice, implying that repetitive BCAA consumption at the end of the active phase could build up a damaging effect on the pressure-overloaded heart. Overall, this study was the first to probe how circadian rhythms converged with BCAA metabolism to modulate cardiac remodeling, which recapitulated the importance of the often-neglected temporal regulation of cardiac metabolites in both the normal and stressed heart.

As a prevalent yet understudied BCAA intermediate, the metabolic fate of BCKA has been surrounded with inquisitive eyes and was recently traced to be primarily reanimated back to valine and subsequent catabolite, 3-hydroxyisobutyrate in a BCAT-dependent manner in the heart of recruited male rats (Walejko et al., 2021). Furthermore, accumulation of reaminated BCAA together with persistently increased BCKA supply in BCKA-perfused hearts of obese mice could activate total protein synthesis by promoting phosphorylation of eukaryotic translation initiation factor 4E-binding protein 1, thus revealing a potential pathophysiological mechanism of cardiac BCKA reamination in obesity-induced cardiac metabolic remodeling.

Despite these exciting discoveries, it is notable that BCAAs accounted for less than 5% of total carbon combustion in the heart; thus, defective BCAA catabolism observed in heart failure is likely to be mediated by alternative mechanisms beyond the control of energy production.

Comprehensive Regulation and Dynamic Adaptation of Nutrient Utilization in the Heart

In addition to the above experiment studies using animal models primarily focused on characterizing each substrate utilization and the underlying molecular mechanisms in the heart individually, offering only a partial insight into the whole picture of dynamic adaptation of nutrient utilization in the heart, many recent studies focus on the comprehensive regulation among different metabolic substrates and the dynamic adaptation of nutrient utilization in the heart.

Newhardt et al. (2019) tested the impact of constitutively enhanced cardiac glycolysis on cardiac metabolism and mitochondrial function in response to nutrient availability using a transgenic mouse model (Glyco^{Hi} mice) that expressed sustained glycolysis through the increased activity of phosphofructokinase-2 (PFK-2). Both transgenic mice and their WT littermates were fed with either a standard low-fat chow diet (LFD) or challenged with a 7-day high-fat diet (HFD). As a result, both the genotype and the diet manipulation significantly affected global cardiac metabolism due to increased depletion of early glycolytic intermediates by upregulated glycolysis. Subsequent global proteomic analysis revealed an increased abundance of proteins involved in both glucose and lipid metabolism in HFD-treated Glyco^{Hi} hearts, whereas HFD-treated WT mice had consistently greater abundance in lipid metabolism proteins but declined abundance in proteins involved in glucose metabolism, suggesting that Glyco^{Hi} mouse hearts were able to sustain elevated expression of glycolytic proteins against short-term HFD challenge. There was also a striking increase of BCAAs in HFD-treated Glyco^{Hi} mice, accompanied by a diet-independent decrease in BCKD E1α subunit. Such an increase in BCAAs was considered a unique effect as other amino acids had a decreased abundance in Glyco^{Hi} hearts compared to WT. This study depicted both genotype and diet-dependent impact of sustained glycolysis on global cardiac metabolism, in which PFK-2 induced increase in the content of BCAAs and PDK4 was identified as novel compensatory mechanisms of the heart to manage nutrient

stress. This study also provides clues to potential outcomes of metabolic remodeling that could occur if glucose metabolism takes up a larger proportion of cardiac energy metabolism in a healthy heart.

Fillmore et al. (2018) subjected 12-weeks old mice to HFD and LFD, respectively, for 10 weeks to directly examine the relationship between cardiac BCAA oxidation and IR. In this study, the isolated, perfused hearts from mice with HFD-induced IR exhibited significantly reduced BCAA oxidation rate, markedly impaired glucose oxidation and the ability of insulin to promote glucose oxidation compared with the LFD group. The results clarified that inhibited BCAA oxidation negatively impacted cardiac insulin signaling potentially through increasing BCAA accumulation rather than inhibiting fatty acid and glucose oxidation. Uddin et al. (2021) recruited a cardiac-specific mitochondrial BCAT (BCATm) knockout mice model to investigate whether it was BCAAs or BCKAs or both of them that was incriminated in the mediation of IR. 8-week-old BCATm$^{-/-}$ male mice exhibited decreased BCAA oxidation, increased individual BCAAs, and decreased BCKAs in the heart, with circulating BCAA levels remaining unchanged compared with their control counterparts. These results indicated that increased accumulation of BCAAs instead of BCKAs should be held responsible for triggering the mTOR-mediated hypertrophic responses in the heart, and BCKAs could exert an inhibitory effect on insulin-promoted cardiac glucose oxidation potentially through downregulating AKT and PDH activities.

Additionally, Li et al. (2017) demonstrated the novel metabolic and physiological functions of BCAA catabolism in the heart by investigating cardiac metabolic flux in PP2Cm-KO mice 2–3 months of age. PP2CmKO mice exhibited elevated circulating and cardiac BCAA levels as expected compared with WT littermates accompanied by a significant inhibition on glycogen synthesis from exogenous glucose, which was further attributed to suppressed glucose uptake following selectively reduced mitochondrial pyruvate flux. Further investigation revealed that chronic BCAAs accumulation at high concentrations could substantially inhibit PDH activity by suppressing *O*-GlcNAcylation. Although there were no evident pathological changes at baseline, KO mice subjected to myocardial IR insults exhibited worsened I/R injury compared with WT littermates when administered with a high level of BCAA supplements. Such negative changes could be rescued by either 3,6-dichlorobenzo[b]thiophene-2-carboxylic acid (BT2) treatment or GLUT1 overexpression in double transgenic PP2CmKO/GLUT1TG mice. Li's study revealed a novel regulatory role of BCAA in cardiac glucose metabolism and an increased vulnerability of the PP2CmKO heart to IR injury following defective BCAA catabolism.

Reciprocally, cardiac glucose metabolism was found to negatively regulate BCAA breakdown through the actions of the above-described transcriptional regulator, Kruppel like factor 15 (KLF15) (Shao et al., 2018). RNA microarray and gene ontology enrichment analysis on transgenic mouse hearts (Glut1-TG) at the age of 10–12 weeks with cardiac-specific GLUT1 overexpression revealed that downregulated genes within the BCAA degradation pathway were significantly enriched, especially KLF15, along with dramatically decreased expression of key BCAA catabolic enzymes, particularly BCAT2, BCKDH, and PP2Cm. Applied metabolomics detected a higher level of glycolytic metabolites, a selective increase in BCAAs, and reduced downstream BCAA catabolites following enhanced glucose uptake in Glut1-TG hearts, which suggested that glucose could negatively modulate BCAA breakdown. Further investigation on KLF15 regulation of BCAA metabolism identified downregulated binding of the cAMP response element-binding protein to the KLF15 promoter region in cultured cardiomyocytes exposed to high glucose or overexpressing Glut1, indicating that glucose served as a negative regulator of KLF15, through which BCAA degradation was held back. This study then returned to play with pathological cardiac hypertrophy, suggesting a potential association between glucose reliance and BCAA degradation in pathological cardiac hypertrophy. This study further uncovered that the glucose-KLF15-BCAA degradation pathway enabled cardiac hypertrophic growth under pathological stimuli through the actions of its end-effector mTOR, whose sustained activation required glucose to down-regulate BCAA degradation. The above two studies combined revealed a negative reciprocal regulatory axis between BCAA and glucose metabolism in the normal heart, as well as how metabolic rewiring in the context of cardiac ischemia and pressure overload stealthily induced pathological cardiac remodeling.

Altogether, these studies have advanced our understanding of how fatty acid and glucose metabolism regulates BCAA and contributes to the normal physiology of the heart as well as how alterations in BCAA catabolism impact the well-characterized derangements in glucose and lipid metabolism intensifies maladaptive metabolic remodeling in the stressed heart. This emerging new paradigm implicating defective metabolic regulation in the pathogenesis of major adverse cardiac events could provide essential knowledge for developing efficacious therapeutic strategies such as pharmacologically inhibiting BCKD activity with BT2 treatment to restore BCAA catabolic flux in pressure-overload induced heart failure and myocardial IR injury (Li et al., 2017; Chen et al., 2019).

However, the fundamental structure supporting cardiac metabolic plasticity and flexibility is, no doubt, the mitochondria. Whether it is lipids, polysaccharides, or proteins, they are all degraded into acetyl-CoA and then enter the TCA cycle coupled with oxidative phosphorylation apparatus inside the mitochondria to generate ATP. Therefore, the mitochondria serve as a converging hub for energy substrate crossovers and play a central role in metabolic homeostasis. Dysfunctional mitochondria are directly responsible for remodeled metabolic patterns and disruption of energy homeostasis in the heart, which underlie the pathological outcomes of many heart diseases. For example, deficient mitochondrial pyruvate carrier 1, which transports pyruvate from glycolysis into the mitochondria, could lead to ventricular hypertrophy, heart failure, and premature death in mice hearts upon a series of metabolic remodeling, predominantly glucose overreliance and diminished TCA activity (Zhang et al., 2020). Meanwhile, although this paper primarily focused on major metabolic substrates in the heart, it is no doubt that all the metabolic intermediates fulfilled a crucial and

unique role in cardiac metabolism that requires further profiling and identification. All the discussed studies are summarized in **Table 1**.

METABOLIC ADAPTION IN THE HEART UNDER PHYSIOLOGICAL CONDITIONS

Although metabolic remodeling predominantly occurs in the cardiac pathological condition in response to mechanical stress, myocardial metabolism can also adapt to the energy demand under the different physiological conditions. While the cardiac metabolism remodeling in pathological conditions has been well-reviewed (Wang et al., 2014; Chen et al., 2019; Geraets et al., 2019; Tran and Wang, 2019), much fewer studies have been on the metabolic adaption in the heart under physiological conditions despite the importance of the topic. Thus, we summarized the recent discovery in physiologic cardiac metabolic modification, focusing on exercise and cardiac development.

Exercise-Induced Metabolic Remodeling in the Heart

Exercises have been reported to induce cardiomyocyte hypertrophy, promote physiological cardiac growth, and improve cardiovascular health. The metabolic responses ensuing different types of exercises vary, shaping the heart muscle broadly into either eccentric or concentric hypertrophy with individual heterogeneity (Weeks and McMullen, 2011). Endurance training, usually referred to as aerobic exercises, such as swimming, walking, or jogging on a treadmill, tends to elicit eccentric hypertrophy along with chamber dilation due to greater growth in myocyte length than width, whereas resistance training or anaerobic exercises such as free weights tends to induce concentric hypertrophy without chamber dilation resulted from a greater increase in myocyte width over length (Fernandes et al., 2011). Heart-pumping aerobic exercises, or in other terms, cardiovascular exercises, could progressively challenge the cardiorespiratory system and improve their function and performance, thus benefiting many aspects of health, especially heart health.

So far, how exercise-induced adaptations in cardiac metabolism promote cardiac remodeling has not yet been fully investigated. First of all, metabolic flexibility of the mitochondria as an efficient adaptation to energy resources plays a pivotal role in balancing periodic shifts between primary fuel utilization such as glucose and FA oxidation as well as employing alternative fuels upon dynamic energy demand and supply in the heart. How endurance exercises promote cardiac mitochondrial structural and functional quality has been extensively reported in cardiac disease models, particularly in diabetic and failing hearts (Campos et al., 2017; Wang et al., 2020). For example, in diabetic mouse hearts, treadmill exercise could markedly improve cardiac function by mitigating oxidative stress from accumulated ROS inside the mitochondria while boosting its oxidative capacity by increasing oxidative enzyme activities. Not only that, endurance training by treadmill could switch myocardial metabolism from the defective fatty acid oxidation that undermines cardiac efficiency to glucose oxidation through restoring the cardiac expression of peroxisome proliferator-activated receptor-γ coactivator (PGC-1α).

In non-stressed hearts of 8-week-old male mice, endurance exercise was reported to induce mitochondrial biogenesis through the actions of nitric oxide, a key mediator of cardiovascular responses to exercises (Vettor et al., 2014). Compared with the hearts of sedentary WT mice, swim-trained WT mouse hearts exhibited markedly increased endothelial nitric oxide synthase (eNOS) mRNA, protein, and activity accompanied by increased mitochondrial DNA (mtDNA) content and higher mRNA levels of PGC-1α, nuclear respiratory factor 1, and mitochondrial transcription factor A, which are master regulators of mitochondrial biogenesis. However, swim training failed to induce mitochondrial biogenesis nor subsequent increase in cardiomyocyte glucose uptake in eNOS knockout ($eNOS^{-/-}$) mice compared to sedentary ($eNOS^{-/-}$) mice. In contrast, trained WT mice exhibited significantly increased cardiac GLUT1 expression and upregulated insulin sensitivity that markedly promoted cardiac glucose uptake, all of which remained unchanged in trained $eNOS^{-/-}$ mice. These findings revealed novel eNOS-dependent mitochondrial biogenesis induced by endurance exercise, which substantially orchestrated metabolic adaptations of the heart to exercise through promoting basal and insulin-stimulated cardiac glucose uptake.

Besides, Sun et al. (2019) demonstrated exercise-induced insulin-independent glucose transport in treadmill-trained male mice at 8–12 weeks old through the action of slightly but significantly increased Thr208 phosphorylation of sucrose non-fermenting AMPK-related kinase (SNARK), a crucial regulator of glucose uptake previously characterized in skeletal muscle. Explicitly, SNARK overexpression could markedly increase basal instead of insulin-stimulated glycogen content in WT SNARK-transfected HL1 cardiomyocytes compared with empty vector (EV) cells, whereas exercise-stimulated basal glucose transport was completely blunted in both SNARK (shRNA)-infected HL1 cells and the heart of trained SNARK heterozygotic knockout mice compared with control cells and WT littermates, respectively, while insulin-stimulated glucose transport remained essentially unchanged. Taken together, the above studies demonstrated that exercise-induced basal and insulin-dependent glucose transport and uptake serve as a crucial chapter for exercise-promoted metabolic remodeling in the heart, providing a valid therapeutic perspective in improving the capability of cardiomyocytes to take up and utilize glucose. Following its uptake, glucose enters the glycolytic pathway upon being phosphorylated by hexokinase to G6P. Glycolysis is tightly controlled by the coordinated actions of glycolytic enzymes, which without doubt pose an imperative impact on downstream glucose oxidation in the heart.

Gibb et al. (2017) also characterized regular exercise-induced metabolic periodicity on glucose metabolism through glycolytic activity modulation. Trained male and female mice were discovered to exhibit 15% higher circulating insulin-like growth factor I (IGF-1) than sedentary mice. Next, the bifunctional 6-phosphofructo-2-kinase/fructose-2,6-biphosphatase 2 (PFKFB2)

TABLE 1 | Summarization of recent studies on myocardial substrate utilization involved in cardiac pathophysiology.

Major metabolic substrates studied in the heart	Research focus and highlights
Fatty acid and glucose	Characterization of myocardial glucose metabolism in heart failure (Chong et al., 2017; Nabben et al., 2018).
	Deep metabolic network tracing *in vivo*; stable isotope tracing; ^{13}C metabolic flux analysis of glucose metabolism (Schnelle et al., 2020).
Ketone	Ketone utilization as a preferred fuel in the heart of healthy normal mice (Ho et al., 2021).
	Cardiac protection of OXCT1 knockout in TAC-induced heart failure (Byrne et al., 2020).
	BHB treatment in the failing myocardium as an additional fuel source (Lopaschuk et al., 2020).
	Cardioprotection of Bdh1 overexpression in TAC-induced heart failure (Uchihashi et al., 2017).
Lactate	Lactate dominates myocardial fuel supply during exercises (Brooks, 2021).
Glutamate and glutamine	Isotope tracing study on cardioprotection from myocardial oxidative stress and major fuel deficit through anaplerotic reactions (Watanabe et al., 2021).
BCAAs	Cardiac BCAA accumulation impairs insulin signaling (Fillmore et al., 2018).
	Further identification of differential roles of BCAAs and BCKAs in the heart using BCATm knockout model (Uddin et al., 2021).
	Molecular mechanisms of BCAA catabolism in PP2Cm deficient heart (Sun et al., 2016).
	Negative regulation of defective cardiac BCAA catabolism on glucose metabolism in PP2Cm deficient heart (Li et al., 2017).
	Identification of glucose-KLF15-BCAA degradation pathway in cardiac BCAA catabolism (Shao et al., 2018).
	Temporal regulation of BCAA metabolism in the heart (Latimer et al., 2021).
	The metabolic fate of BCKA (Walejko et al., 2021).

PFK-1, phosphofructokinase-1; Nox4, NADPH oxidase 4; OXCT1, 3-oxoacid CoA-transferase 1; BHB, beta-hydroxybutyrate; Bdh1, 3-hydroxybutyrate dehydrogenase 1; MI, myocardial infarction; BCAA, branched-chain amino acid; BCKAs, branched-chain α-keto acids; BCATm, mitochondrial branched-chain aminotransferase; PP2Cm, protein phosphatase 2Cm; KLF15, Kruppel Like Factor 15.

that catalyzes F2,6BP synthesis and breakdown in the heart was examined for its phosphorylation level at S483. Compared to sedentary mice, significantly increased PFKFB2 phosphorylation at S483 by Akt in response to insulin and IGF-1 was detected in the exercise-adapted heart of trained mice, potentially contributing to upregulated glycolytic activities in the exercise-adapted heart. In contrast, during early recovery or right after a bout of exercise, PFK-2 phosphorylation was acutely diminished, accompanied by evident glycogen buildup and a sharp fall in circulating glucose, suggesting substantially reduced glucose utilization which eventually returned to an elevated level during full recovery. Furthermore, cardiac-specific kinase-deficient ($Glyco^{Lo}$) and phosphatase-deficient ($Glyco^{Hi}$) TG mice were developed to constitutively manipulate myocardial PFK-1 activity, which resulted in mild cardiac hypertrophy in both $Glyco^{Lo}$ and $Glyco^{Hi}$ mice accompanied by irreversible mitochondrial inflexibility. Only $Glyco^{Lo}$ hearts exhibited seemingly beneficial cardiac remodeling patterns similar to but not exceeding that of exercise-adapted WT mice and without evident upstream AKT activation. Additionally, Newhardt et al. (2019) studied the separate and combined influence of metabolic genotypes and diet types on cardiac metabolism in $Glyco^{Hi}$ hearts that expressed sustained glycolysis through increased PFK-2 activity. Both $Glyco^{Hi}$ mice and their WT littermates at 30–36 weeks of age were fed with either a standard LFD or challenged with a 7-day HFD. As a result, both the genotype and the diet manipulation significantly affected global cardiac metabolism. Pathway analysis uncovered a marked increase of PDK4 in HFD-treated WT hearts, and such increase was even more pronounced in HFD-treated $Glyco^{Hi}$ mouse hearts reflected through PDH activity. Besides, fasted $Glyco^{Hi}$ mouse hearts exhibited significantly higher PDK4 levels than fasted WT hearts, and fed $Glyco^{Hi}$ mouse hearts also had greater PDK4 levels than fed WT mouse hearts, suggesting that enhanced glycolysis could elicit an increase in PDK4 to dial down glucose oxidation. The above two studies together provided unique evidence for the pervasive effects of sustained glycolysis on cardiac metabolic remodeling at the mechanistic level in response to exercises and nutrient availability, respectively, which further contributed to an improved understanding of dynamic interactions between diet, exercises, and genotypes, the three major components necessary to determine individual cardiac health.

More than that, myocardial expression of CCAAT enhancer binding protein beta (Cebpb), whose reduction has previously been reported to serve as a central signal controlling exercise-induced physiological hypertrophy (Boström et al., 2010), was observed to remain unchanged between exercise-adapted and sedentary $Glyco^{Lo}$ mice. Meanwhile, myocardial expression of Cited4, whose cardiac overexpression has been shown to induce physiological hypertrophy with normal systolic function that mimics the effects of endurance exercises (Bezzerides et al., 2016), was found to bear no statistically significant difference between the two groups. On the contrary, WT mice subjected to treadmill training exhibited significantly downregulated myocardial Cebpb expression and upregulated Cbp/P300 interacting transactivator with Glu/Asp rich carboxy-terminal

domain 4 (Cited4) expression, which was consistent with the previously reported findings compared with sedentary mice. Besides, Glyco^{Lo} hearts exhibited intrinsically lower myocardial Cebpb expression and higher Cited4 expression at baseline than their WT counterparts. These results together suggest that constitutively low glycolysis alone was enough for maximal cardiac growth through modulating the Cebpb/Cited4 transcriptional program, whereas Glyco^{Hi} hearts developed a more dilated phenotype and did not engage in gene programs that induce physiological cardiac growth. Additionally, both Glyco^{Lo} and Glyco^{Hi} hearts exhibited substantially altered myocardial gene expressions involved in various cellular processes and signaling compared with WT hearts. In particular, among an array of differentially regulated genes by glycolysis, low glycolytic rates in Glyco^{Lo} hearts exerted a strong influence on genes involved in redox reactions, lipid metabolism, and cell responses to cAMP, whereas high levels of glycolysis in Glyco^{Hi} hearts had a major impact on genes involved in cellular responses to cAMP and hormone stimuli, angiogenesis and differentiation, as well as transcriptional activities. Collectively, this study serves as a paradigmatic example in demonstrating how exercise-induced dynamic changes in cardiac metabolites modulate cardiac remodeling within and beyond the realm of fuel metabolism.

Davogustto et al. (2021) investigated the impact of mTORC1 in the development of cardiac hypertrophy of the adult mice subjected to voluntary exercise training, whose sustained activation was unraveled to modulate cardiac glucose metabolism preceding a subsequent hypertrophic response. In the said study, a transgenic mouse model with inducible, cardiac-specific sustained mTORC1 activation through tuberous sclerosis complex 2 deletion (mTORC1^{iSA}) developed a concentric LV hypertrophy accompanied with increased systolic function at 28-week old compared to littermate controls, which resembled adaptive cardiac hypertrophy. Retrogradely perfused mTORC1^{iSA} heart at 12-week old exhibited markedly decreased glucose uptake and oxidation while the downstream product of hexokinase 2, G6P, was significantly increased, suggesting a considerably decreased glucose influx to the glycolytic pathway. Further investigation discovered a persistent decrease in protein expression and enzymatic activity of glucose 6-phosphate isomerase (GPI) from as early as 12-week old all the way to 28-week old. WT mice subjected to 6-day wheel running showed increased mTOR phosphorylation at Ser 2448 accompanied by decreased GPI protein expression but increased enzymatic activities compared with sedentary WT mice, whereas oral administration of rapamycin for the last 8 weeks of the project prevented the increase in GPI activity at 12-week old and hypertrophic alterations seen at 28-week old in both mTORC ^{iSA} mice and trained WT mice. WT mice subjected to a 6-week wheel running protocol developed significantly increased cardiac hypertrophic changes together with increased GPI activity, which were again prevented with the rapamycin diet, suggesting a consistent rapamycin inhibition on mTORC1-induced glucose changes during both short-term and long-term voluntary exercises. The mTORC1 signaling has been considered as a metabolic rheostat that integrates inputs from nutrient sensing with cell growth (Valvezan and Manning, 2019). Sustained mTORC1 activation has been reported to play an adaptive role in both physiological and pathological hypertrophic hearts, whose inhibition has frequently been described to confer cardioprotection in the stressed heart (Daneshgar et al., 2021). The non-pathological cardiac metabolic changes and subsequent hypertrophic responses observed in this study revealed a continuum hypertrophic outcome rather than the generally accepted dichotomous pattern between physiological and pathologic cardiac remodeling under the mediation of mTORC1. Meanwhile, such a study recapitulated the stealth metabolic remodeling processes that preceded, triggered, and sustained structural and functional remodeling of the heart to a measurable extent.

Following the fast-acting glucose that quickly gets depleted during exercise, fatty acid oxidation takes the place of glucose oxidation to keep up with the increased energy demand in the heart accompanied by increased lipolytic activities in adipose tissue. Thus, alterations in fatty acid metabolism could naturally serve as a sensitive indicator that predicts exercise-driven cardiac metabolic shift. Foryst-Ludwig et al. (2015) provided novel evidence that palmitoleic acid (C16:1n7), a common fatty acid constituent of white adipose tissue (WAT) triglycerides (TG), played an indispensable role in prolonged physical exercise-induced non-proliferative left ventricle hypertrophy LVH. Since adipose triglyceride lipase (Atgl) catalyzes the initial step in adipose TG lipolysis, adipose tissue-specific Atgl knockout (atATGL-KO) female mice at 5-week-old age with accordingly curtailed WAT lipolysis were subjected to chronic treadmill running together with their WT littermates. As expected, trained WT mice exhibited decreased cardiac glucose uptake and considerably increased cardiac fatty acid uptake along with significantly increased LV mass compared to sedentary WT mice. Reciprocally, genetic deletion of Atgl expression in trained atATGL-KO mice completely abrogated exercise-induced cardiac fatty acid uptake, resulting in an attenuated cardiac hypertrophic response, which revealed that FAs potentially served as prohypertrophic mediators. Intriguingly, C16:1n7 was singled out from a mixture of fatty acids for exerting prohypertrophic effects in cultured HL-1 cells was significantly increased in trained WT mice, but not atATGL-KO mice. Furthermore, short-term treatment of HL-1 cells with C16:1n7 greatly augmented Akt phosphorylation, and dietary C16:1n7 enrichment successfully salvaged the impaired LVH induced by exercise in trained atATGL-KO mice, bringing it to a comparable level with their WT littermates under sedentary conditions. Serum FA analysis on highly trained endurance human athletes revealed a markedly significant linear correlation between C16:1n7 level and diastolic interventricular septum thickness, suggesting a therapeutic potential using lipid-derived supplements to prevent adverse cardiovascular events. The findings from the above study combined provided a fresh perspective that peripheral substrate metabolism such as FA mobilization from adipose tissues did not just provide energy supply upon substrate partitioning in the heart but also took part in the exercise-induced metabolic and physiological remodeling processes of the heart. This study also

reminded us that we should not only concentrate on the heart itself when investigating alterations in cardiac metabolism but extend further into the mutual interplay between cardiac and systemic metabolism. The main findings from these new studies have been summarized in **Figure 1**.

Metabolic Remodeling in Heart Development

Another type of physiological metabolic remodeling in the heart occurs during normal cardiac development. Difference from the adult heart, the fetal heart mainly utilizes glucose and lactate as predominant sources to generate ATP due to carbohydrate-enriched nutrient supply. Immediately after birth, the neonatal heart quickly switches to fatty acid oxidation upon mitochondrial reorganization, at least partially driven by dramatically increased oxygen availability and increased workload while maintaining its glycolytic capacity (Lemay et al., 2021). The unique metabolic transitions in the heart during cardiac maturation have been intensively studied but are still not fully elucidated. Studying fetal metabolic adaptations in the heart contributes to a better understanding of the pathogenic mechanisms in adult heart diseases, such as ischemia, hypertrophy, and heart failure. In heart failure, impaired mitochondria oxidative capacity drives a stereotypic metabolic shift from primary fatty acid oxidation to glucose oxidation accompanied by reactivation of several fetal genes whose presence is believed to attune the failing myocardium to non-physiological hypoxia and preserve cardiac function till a breakpoint (van der Pol et al., 2020).

Hypoxia-inducible factor (HIF)-1 has been a primary focus during the fetal metabolic transition whose deficiency has been reported to markedly attenuate cardiomyogenesis of embryonic stem cells in mice (Kudová et al., 2016). Highly expressed HIF provides embryonic cardiomyocytes sufficient resistance to the hypoxic intrauterine environment and meanwhile promotes cardiac anaerobic glycolysis through upregulating a suite of glycolytic genes (Cerychova and Pavlinkova, 2018). In contrast, HIF expression drastically declines after birth allowing a fatty-acid dominant to quickly occur, which powers a subsequent adaptive hypertrophic response that profoundly drives cardiomyocytes to gradually lose their proliferative capacity and achieve terminal maturation. Breckenridge et al. (2013) reported that HIFα-signaling dependent cardiac transcription factor the heart and neural crest-derived transcript-1 (Hand1) that was highly expressed in the developing heart underwent a sharp fall right after birth, whereas its prolonged perinatal expression in Hand 1 TG mouse hearts was found to yield glycogen stores to depletion and meantime inhibit lipid uptake and incorporation into metabolic handling of fatty acid species compared with littermate controls potentially attributable to Hand1 overexpression-prevented increase in expression of genes involved in lipid metabolism (Breckenridge et al., 2013). This study identified a novel regulatory mechanism of the HIF1a/Hand1 signaling pathway in controlling cardiac fetal-neonatal energy switch, and experimentally upregulated Hand1 expression in adult hearts subjected to IR injury was observed to dramatically decrease cardiomyocyte death, suggesting its therapeutic potential in ischemia protection of the adult heart.

In addition, Walejko et al. (2018) adopted a multi-omics approach to integrating data from metabolomics, lipidomics, and transcriptomics in order to comprehensively profile fetal-neonatal metabolic transition in ovine heart tissues. The metabolomics analysis revealed a clear distinction of metabolite compositions between the term fetal heart and the neonatal heart. Metabolites, such as lactate, succinate, and alanine, were detected in greater abundance in fetal heart tissues, while AMP, glutamate, choline, and 1,2-propanediol were highly elevated in the neonatal heart. Lipid profiling of cardiac tissue disclosed a marked separation in lipids between fetal and neonatal hearts. Eight lipid classes showed greater abundance in neonatal cardiac tissues, of which TG accounted for the majority, whereas 7 lipid classes were found to be more elevated in fetal cardiac tissues, such as sphingomyelin, suggesting significantly altered lipid profile between fetal and neonatal cardiac tissues. Transcriptomic profiling revealed 893 significantly elevated genes in the neonatal heart and 940 significantly elevated genes in the fetal heart compared with each other. The differential expression of these genes was identified to regulate downstream pathways involved in BCAA degradation, fatty acid degradation, and the metabolic fate of β-alanine, butanoate, and tryptophan. Meanwhile, genes associated with cardiomyopathy were also shown to be strongly expressed in the fetal heart, which corresponded to hypertrophic remodeling of the term fetal heart during terminal maturation. Further integrated analysis of the above omics together unraveled multiple clusters of cardiac metabolic pathways of lipids, amino acids, and glucose, respectively, which were consistent with the altered expression of genes controlling the corresponding metabolic activities. This multi-omics approach adequately captured the dynamic metabolic alterations during heart maturation, in which highly expressed transcripts for genes involved in BCAA degradation pathways in the fetal heart offered additional insight into a potential mechanism by which increased BCAA catabolism could promote cardiac protein synthesis and growth in the term fetal heart.

A transcriptome analysis conducted by Iruretagoyena et al. (2014) profiled metabolic genes in the developing heart using human fetal cardiac tissues prospectively collected between 10 and 18 weeks of gestational age, which were divided into three groups as 10–12 (H1), 13–15 (H2), and 16–18 (H3) weeks. Their study detected significantly increased gene expressions involved in either fatty acid metabolism or structural remodeling in H3 hearts compared with H1 hearts, while glycolytic genes remained highly but not differentially expressed in all three groups. Their results were highly consistent with previous animal studies on fetal heart maturation that fatty acid metabolism started to dominate as the fetus developed while glucose oxidation was consistently maintained at a high level to provide basal energy production in the fetal heart.

So far, various animal species have been recruited to study fetal heart growth, such as the murine and ovine fetal hearts described above. However, considering distinct interspecies differences in embryo development and limited

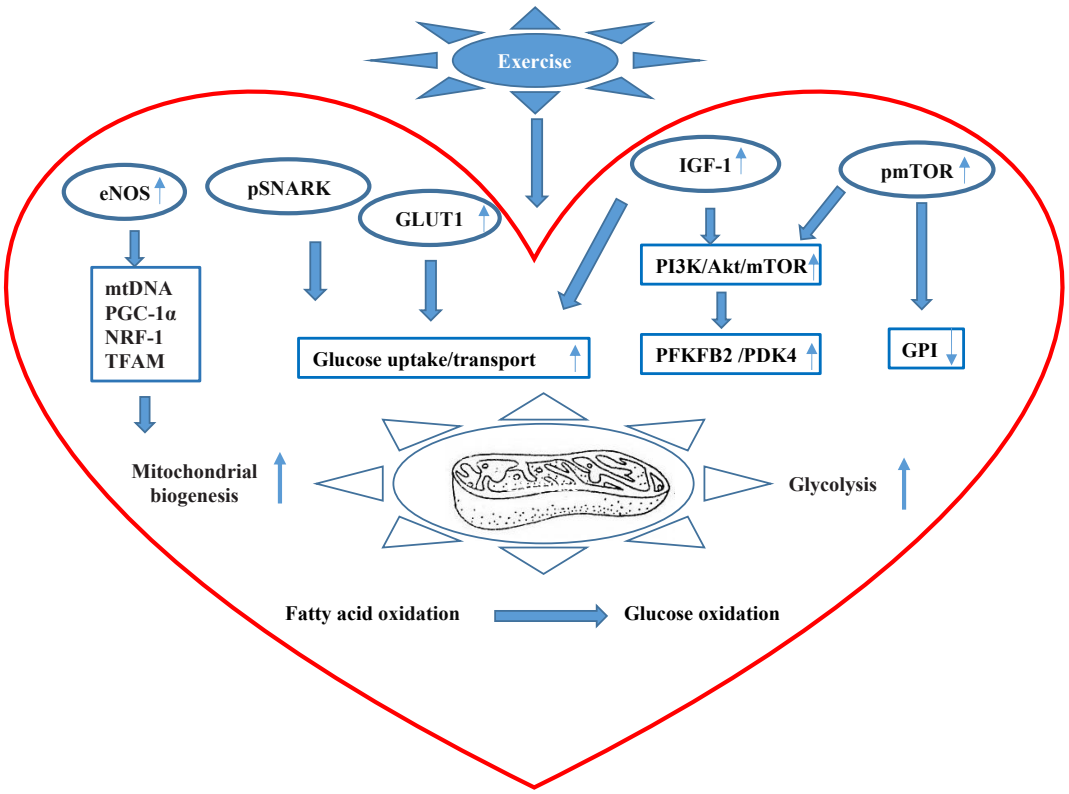

FIGURE 1 | The scheme of major mechanisms of exercise-promoted metabolic remodeling in the heart summarized in this review. Exercise can improve cardiac mitochondrial biogenesis through the eNOS signaling pathway that promotes mitochondrial DNA (mtDNA) content, peroxisome proliferator-activated receptor γ coactivator 1α (PGC-1α), nuclear respiratory factor 1 (NRF-1), and mitochondrial transcription factor A (TFAM). Exercise can also upregulate the phosphorylation level of sucrose non-fermenting AMPK-related kinase (SNARK), enhancing glucose uptake and utilization. Besides, exercise stimulates circulating insulin-like growth factor (IGF-1) and insulin that increase overall glucose transport and uptake and also upregulates serine phosphorylation of 6-phosphofructo-2-kinase/fructose-2,6-biphosphatase 2 (PFKFB2) that boost glycolysis in the heart. In addition, exercise augments the activation of the mammalian target of rapamycin (mTOR) and reduces the activity of glucose 6-phosphate isomerase (GPI). Systemically, exercise can stimulate peripheral fatty acid mobilization from adipose tissue, and increased palmitoleic acid (C16:1n7) stimulates Akt phosphorylation that mediates metabolic remodeling in the heart.

samples of human fetal heart, *in vitro* human embryonic stem cell-derived cardiomyocytes (hESC-CMs) with an immature metabolic phenotype have been extensively used to study human fetal cardiomyocyte metabolic maturation and potentially provide alternative cell-based approaches to cardiac regeneration and repair (Liu et al., 2018; Romagnuolo et al., 2019). Nakano et al. (2017) investigated specifically how changes in glucose metabolism manipulated hESC-CMs maturation by culturing them in media containing various concentrations of glucose. Their study observed that hESC-CMs cultured in low glucose media exhibited more robust differentiation and a consistent increase in cardiomyocyte size compared with those cultured in high glucose. Moreover, glucose deprivation was found to boost mitochondrial respiration in hESC-CMs, promoting its functional maturation, whereas high glucose conditions dose-dependently blocked mitochondrial pyruvate utilization in hESC-CMs and greatly held back cardiac maturation through a metabolic pathway parallel to glycolysis, the pentose phosphate pathway (PPP) whose oxidative branch generates precursors for nucleotide biosynthesis. Further, uridine rescue was observed to substantially restore the reduced proliferative capacity of hESC-CMs cultured in low glucose, while nucleotides deprivation, on the contrary, markedly induced hESC-CMs maturation following glucose deprivation, suggesting that the inhibitory effects of glucose on hESC-CMs maturation depended on nucleotide synthesis through the PPP pathway. Subsequent *in vivo* study revealed drastically downregulated fetal cardiac glucose uptake albeit relatively stable uterine glucose supply during late gestation or the early postnatal period. Additionally, fetal and neonatal hearts from diabetic pregnancy of Akita heterozygous mice showed elevated mitotic activity and increased biventricular wall thickness in company with decreased cardiomyocyte size compared with control littermates, suggesting that hyperglycemia could impede fetal cardiac maturation and potentially contribute to cardiomyopathy in infants of diabetic mothers (Nakano et al., 2017). This study provides novel evidence on glucose metabolism from the PPP pathway instead of the glycolytic pathway mediated the balance between proliferation and differentiation of fetal cardiomyocytes through nucleotide biosynthesis.

Hu et al. (2018) studied hESC-CMs cultured in media with different compositions, specifically glucose-containing media, glucose media with the addition of fatty acids, and glucose-free fatty acids only media, to investigate potential signaling pathways underpinning the metabolic and functional maturation of hESC-CMs. Glucose cultured hESC-CMs exhibited significantly higher hexokinase activities and lactate levels than those cultured in media with fatty acids alone, which indicated a glycolytic dominant metabolic regulation mimicking embryonic and postnatal cardiac metabolic patterns. Contrarily, hESC-CMs cultured in media with fatty acids alone displayed greatly enhanced mitochondrial oxidative capacity and ATP production compared with those cultured in media containing either glucose or glucose and fatty acids, featuring adult-like cardiac metabolic characteristics. Further exploration revealed aberrant activation of HIF1α with higher nuclear localization and subsequently increased LDHA expression in glucose cultured hESC-CMs compared with those cultured in fatty acid medium lacking sugar source. Conversely, inhibition of the HIF1α/LDHA axis was discovered to promote metabolic maturation of hESC-CMs through attenuated glycolysis and enhanced oxidative respiration to generate more ATP. The above studies on *in vitro* hESC-CMs metabolic maturation well corroborated with *in vivo* discoveries regarding fetal cardiac metabolic changes during terminal maturation, leading to a more comprehensive understanding of fetal cardiac metabolic remodeling.

Emanuelli et al. (2021) very recently characterized the metabolic profile of human cardiomyocytes induced from pluripotent stem cell-derived cardiomyocytes (hiPSC-CM) during their maturation from 6 to 12 weeks in culture. hiPSC-CMs exhibited ongoing structural maturation but no significant change in the glycolytic reserve, glucose uptake, or main glycolytic enzymes over 6 weeks of prolonged culture. The expression of PDHαE1 was increased twofold together with an evident isoform switch between pyruvate dehydrogenase kinase-1 (PDK1) and PDK4 at week 12, whereas ^{13}C isotope labeling revealed that glucose flux branching into the PPP pathway was significantly lowered at week 12. Besides, although there was no significant difference in overall protein *O*-GlcNAcylation, both UDP-GlcNAc abundance and glutamine-fructose-6-phosphate aminotransferase 2 expression were significantly reduced at week 12, suggesting reduced flux to the HBP pathway. These findings indicated that the metabolic flux that passed through the glycolytic pathway was preferentially directed toward the entry of the TCA cycle. hiPSC-CM at week 12 also exhibited a more mature mitochondrial network and a tendency to shift to a more oxidative metabolic profile over time as fatty acid oxidation increasingly contributed to total oxygen consumption rate at the cost of glucose oxidation.

Overall speaking, the fetal metabolic transition is achieved through coordinated control and regulation of substrate partitioning under the combinatorial effects of the metabolic and signaling network, especially the repeatedly highlighted HIF1α signaling both *in vivo* and *in vitro*. In addition, studying the progression of fetal cardiac remodeling conferred substantial value on deciphering the pathological metabolic alterations in the ischemic and failing hearts, thus encouraging the development of minimally invasive and regenerative therapeutics for a series of heart diseases. The main findings from these new studies have been summarized in **Figure 2**.

CONCLUSION AND FUTURE PERSPECTIVES

This review primarily focused on presenting the current knowledge of myocardial substrate metabolism and the latest progress regarding cardiac metabolic remodeling under physiological conditions such as during exercise and cardiac development. Especially, many novel signaling pathways have been linked to the metabolic remodeling in the heart under physiological conditions of endurance exercises and cardiac development, which remarkably increases our knowledge of the heart's potential in response to the states with diverse energy requirements under the physiological condition. We also dabbled into the correlation of metabolic patterns between physiological and pathological cardiac metabolism, which all together strived to gain a deeper understanding of the impact of metabolic remodeling in the heart under physiological conditions. Despite the significant impacts of these advances in this field, many aspects remain unknown and require future investigations:

New Insights in Substrate Utilization and Associated Signaling in Metabolic Remodeling

It is no doubt that every substrate matters, and each substrate serves not only as a fuel source but also as an indispensable part of the metabolic signaling pathways that together induce structural and functional remodeling in the heart. The current studies bring new insights into the substrate utilization of the heart in physiological conditions. First, although glucose and fatty acid metabolism remain a research hotspot, cardiac lactate and ketone metabolism have gained growing attention, especially the ketone body, whose increase serves as a general feature of maladaptive metabolism in the aging heart and the failing heart. As a result, a large body of research has been devoted to investigating their pervasive cardioprotective effects by applying a ketogenic diet or administering exogenous ketogenic agents to induce therapeutic ketosis. Secondly, many emerging roles of BCAA metabolism in the heart have been brought to light, such as the relationship between cardiac BCAA oxidation and insulin resistance; transcriptional regulation of BACC catabolism by upstream regulators such as KFL15, BCAT2, BCKDH, and PP2Cm; third, most importantly, as previous studies primarily focused on characterizing each substrate utilization and the underlying molecular mechanisms in the heart individually, many recent studies focus on the interaction among different metabolic substrates and the dynamic adaptation of nutrient utilization in the heart, by using a combination of the various animal models, such as the newly discovered metabolic interplay and reciprocal regulation between glucose and BCAA metabolism.

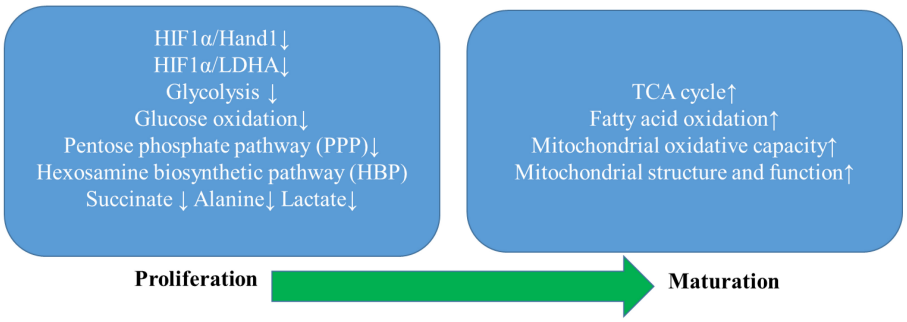

FIGURE 2 | Summarization of progress of metabolic remodeling in the developing heart. The developing heart undergoes a unique metabolic switch from the primary utilization of glucose through the glycolytic pathway and auxiliary biosynthetic pathways, including the pentose phosphate pathway (PPP) and the hexosamine biosynthesis pathway (HBP) to fatty acid oxidation as the mitochondrial structure and function mature to substantially improve mitochondrial oxidative capacity. Intermediate metabolites that are specifically increased during proliferation, such as lactate, alanine, succinate, and triglycerides, are markedly decreased during maturation. At the transcriptional level, maturation of cardiomyocytes relies on a sharp decrease in the expression of the hypoxia-inducible factor 1 subunit a (HIF1a), HIF1a-dependent cardiac transcription factor heart, and neural crest-derived transcript-1 (Hand1), and lactate dehydrogenase A (LDHA). Thus, inhibition of the HIF1α/Hand1 and HIF1α/LDHA signaling plays a crucial role in the time-dependent metabolic shift toward increased metabolic flux to the TCA cycle as the predominant metabolic pathway of oxidative metabolism.

These studies highlighted the comprehensive regulations in cardiac metabolism.

Despite the exciting findings from the recent studies, it remains largely unknown regarding the complex regulatory mechanisms governing cardiac energy substrate metabolism under physiological conditions, not to mention numerous unidentified metabolic remodeling processes under pathological stimuli. For example, although physiological and pathological myocardial hypertrophy has long been considered as two separate entities and sustained, mTORC1 activation was heavily incriminated in producing divergent hypertrophic outcomes in them, the recently reported intermediate non-pathological-hypertrophic phenotype in the presence of persistent mTORC1 activation indicative of a continuum of influence of this key regulator on cardiac growth. Additionally, glycolytic activities were observed to exhibit a periodic pattern in exercise-adapted hearts, and genetically downregulated cardiac glycolysis could maximize physiological myocardial hypertrophy. The more newly discovered metabolic pathways aside from the most characterized IGF-1 and mTOR signalings involved in exercise-promoted cardioprotection, such as the eNOS and the SNARK signaling, greatly contributed to identifying novel promising molecular targets. Furthermore, the differential role of BCAAs and BCKAs on mediating cardiac IR has been recently clarified, and recruiting BCAA oxidation as a promising treatment target to improve insulin sensitivity in heart diseases associated with IR has become a new focus. So far, only a few genes and transcriptional factors involved in BCAA metabolism were identified and analyzed as shown above, which says that very little is known about the underpinning pathways and molecular regulation of BCAA metabolism in response to various physiological and pathological stimuli as well as its potential interactions with other metabolic processes in the heart, which require further investigations in the future. It is beyond doubt that cardiac research on metabolism is heading toward the path of multidisciplinary analysis and quantification with a plethora of powerful and promising molecular methods that can more accurately and comprehensively characterize cardiac metabolism.

New Approaches for Measuring Cardiac Metabolism

The conventional *ex vivo* and *in vitro* models and experimentation exerted more uncertainty in interpreting the gained results to the *in vivo* system. On top of these traditional techniques, the application of novel strategies to enable deep metabolic network tracing or studies employing advanced analytical technologies and informatics to unravel the dynamic and complex metabolic nature of cardiomyocytes. Systemic delivery of metabolic substrates, such as C16:1n7, could exert a localized effect on exercise-induced cardiac growth, which served as a fresh reminder that metabolic remodeling under any circumstance is an outcome of both local and systemic metabolic responses. The advancement of metabolomics and isotope tracing as well as their individual and combined applications in studying heart metabolism *ex vivo* and *in vivo* has provided novel and alternative approaches for characterizing cardiac metabolism. So far, it remains challenging to investigate cardiac metabolic changes in response to exercise training due to its dynamic nature of systemic involvement, thus causing larger magnitudes of more complex discrepancies. Therefore, the application of metabolomics, isotope tracing, and other future technological innovations will substantially provide more accuracy and reduce the difficulties in delineating numerous exercise-promoted cardiac metabolic signatures. In addition, alternative experimental approaches such as *in vitro* hESC-CMs and hiPSC-CMs testing revealed more knowledge of the metabolic changes during fetal cardiomyocyte proliferation and maturation. Studying metabolic remodeling in the developing heart also brought promising therapeutic targets as fetal metabolic gene reprogramming has been repeatedly recognized in the adult heart under pathological conditions.

Therapeutic Potential

Recent studies also provide evidence for developing new therapeutic strategies. For example, most recent studies have indicated that dietary BCAAs could be used as a potentially efficacious intervention for heart failure in some reports. However, in others, they have been shown to increase the susceptibility of the heart to pathological stimuli. The conflict on this topic remains unsolved as the specific experimental models and diet protocols employed in each study varied, and the hemostasis of BCAA metabolism in the heart is always the result of multifactorial regulation, such as the often understudied temporal regulations. There are a significant number of targets for potential therapeutic interventions waiting to be discovered within the metabolic realm, in which pharmacological targeting of energy metabolic signaling and pathways has just emerged. Therefore, our quest has just begun to uncover the entire blueprint of cardiac metabolism.

AUTHOR CONTRIBUTIONS

XS performed the literature searching and drafted the manuscript. HQ revised the manuscript. Both authors contributed to the article and approved the submitted version.

FUNDING

This work was partially supported by NIH grants HL115195-01 (HQ), HL137962 (HQ), and HL142291 (HQ).

REFERENCES

Ahmad, T., Kelly, J. P., Mcgarrah, R. W., Hellkamp, A. S., Fiuzat, M., Testani, J. M., et al. (2016). Prognostic Implications of Long-Chain Acylcarnitines in Heart Failure and Reversibility With Mechanical Circulatory Support. *J. Am. Coll. Cardiol.* 67, 291–299. doi: 10.1016/j.jacc.2015.10.079

Aubert, G., Martin, O. J., Horton, J. L., Lai, L., Vega, R. B., Leone, T. C., et al. (2016). The Failing Heart Relies on Ketone Bodies as a Fuel. *Circulation* 133, 698–705. doi: 10.1161/circulationaha.115.017355

Bezzerides, V. J., Platt, C., Lerchenmüller, C., Paruchuri, K., Oh, N. L., Xiao, C., et al. (2016). CITED4 induces physiologic hypertrophy and promotes functional recovery after ischemic injury. *JCI Insight* 1:e85904. doi: 10.1172/jci.insight.85904

Bloomgarden, Z. (2018). Diabetes and branched-chain amino acids: what is the link?. *J. Diabetes* 10, 350–352.

Boström, P., Mann, N., Wu, J., Quintero, P. A., Plovie, E. R., Panáková, D., et al. (2010). C/EBPβ controls exercise-induced cardiac growth and protects against pathological cardiac remodeling. *Cell* 143, 1072–1083. doi: 10.1016/j.cell.2010.11.036

Breckenridge, R. A., Piotrowska, I., Ng, K. E., Ragan, T. J., West, J. A., Kotecha, S., et al. (2013). Hypoxic regulation of hand1 controls the fetal-neonatal switch in cardiac metabolism. *PLoS Biol.* 11:e1001666. doi: 10.1371/journal.pbio.1001666

Brooks, G. A. (2021). Role of the Heart in Lactate Shuttling. *Front. Nutr.* 8:663560. doi: 10.3389/fnut.2021.663560

Byrne, N. J., Soni, S., Takahara, S., Ferdaoussi, M., Al Batran, R., Darwesh, A. M., et al. (2020). Chronically Elevating Circulating Ketones Can Reduce Cardiac Inflammation and Blunt the Development of Heart Failure. *Circ. Heart Fail.* 13:e006573. doi: 10.1161/CIRCHEARTFAILURE.119.006573

Campos, J. C., Queliconi, B. B., Bozi, L. H. M., Bechara, L. R. G., Dourado, P. M. M., Andres, A. M., et al. (2017). Exercise reestablishes autophagic flux and mitochondrial quality control in heart failure. *Autophagy* 13, 1304–1317. doi: 10.1080/15548627.2017.1325062

Cerychova, R., and Pavlinkova, G. (2018). HIF-1, Metabolism, and Diabetes in the Embryonic and Adult Heart. *Front. Endocrinol.* 9:460. doi: 10.3389/fendo.2018.00460

Chen, L., Song, J., and Hu, S. (2019). Metabolic remodeling of substrate utilization during heart failure progression. *Heart Fail. Rev.* 24, 143–154. doi: 10.1007/s10741-018-9713-0

Chong, C. R., Clarke, K., and Levelt, E. (2017). Metabolic Remodeling in Diabetic Cardiomyopathy. *Cardiovasc. Res.* 113, 422–430. doi: 10.1093/cvr/cvx018

Daneshgar, N., Rabinovitch, P. S., and Dai, D. F. (2021). TOR Signaling Pathway in Cardiac Aging and Heart Failure. *Biomolecules* 11:168. doi: 10.3390/biom11020168

Davogustto, G. E., Salazar, R. L., Vasquez, H. G., Karlstaedt, A., Dillon, W. P., Guthrie, P. H., et al. (2021). Metabolic remodeling precedes mTORC1-mediated cardiac hypertrophy. *J. Mol. Cell Cardiol.* 158, 115–127. doi: 10.1016/j.yjmcc.2021.05.016

Drake, K. J., Sidorov, V. Y., Mcguinness, O. P., Wasserman, D. H., and Wikswo, J. P. (2012). Amino acids as metabolic substrates during cardiac ischemia. *Exp. Biol. Med.* 237, 1369–1378. doi: 10.1258/ebm.2012.012025

Emanuelli, G., Zoccarato, A., Reumiller, C. M., Papadopoulos, A., Chong, M., Rebs, S., et al. (2021). A roadmap for the characterization of energy metabolism in human cardiomyocytes derived from induced pluripotent stem cells. *J. Mol. Cell Cardiol.* 164, 136–147. doi: 10.1016/j.yjmcc.2021.12.001

Fernandes, T., Soci, U. P., and Oliveira, E. M. (2011). Eccentric and concentric cardiac hypertrophy induced by exercise training: microRNAs and molecular determinants. *Braz. J. Med. Biol. Res.* 44, 836–847. doi: 10.1590/s0100-879x2011007500112

Fillmore, N., Wagg, C. S., Zhang, L., Fukushima, A., and Lopaschuk, G. D. (2018). Cardiac branched-chain amino acid oxidation is reduced during insulin resistance in the heart. *Am. J. Physiol. Endocrinol. Metab.* 315, E1046–E1052. doi: 10.1152/ajpendo.00097.2018

Foryst-Ludwig, A., Kreissl, M. C., Benz, V., Brix, S., Smeir, E., Ban, Z., et al. (2015). Adipose Tissue Lipolysis Promotes Exercise-induced Cardiac Hypertrophy Involving the Lipokine C16:1n7-Palmitoleate. *J. Biol. Chem.* 290, 23603–23615. doi: 10.1074/jbc.M115.645341

Frydland, M., Møller, J. E., Wiberg, S., Lindholm, M. G., Hansen, R., Henriques, J. P. S., et al. (2019). Lactate is a Prognostic Factor in Patients Admitted With Suspected ST-Elevation Myocardial Infarction. *Shock* 51, 321–327. doi: 10.1097/SHK.0000000000001191

Fulghum, K. L., Audam, T. N., Lorkiewicz, P. K., Zheng, Y., Merchant, M., Cummins, T. D., et al. (2022). In vivo deep network tracing reveals phosphofructokinase-mediated coordination of biosynthetic pathway activity in the myocardium. *J. Mol. Cell Cardiol.* 162, 32–42. doi: 10.1016/j.yjmcc.2021.08.013

Geraets, I. M. E., Glatz, J. F. C., Luiken, J., and Nabben, M. (2019). Pivotal role of membrane substrate transporters on the metabolic alterations in the pressure-overloaded heart. *Cardiovasc. Res.* 115, 1000–1012. doi: 10.1093/cvr/cvz060

Gertz, E. W., Wisneski, J. A., Stanley, W. C., and Neese, R. A. (1988). Myocardial substrate utilization during exercise in humans. Dual carbon-labeled carbohydrate isotope experiments. *J. Clin. Invest.* 82, 2017–2025. doi: 10.1172/JCI113822

Gibb, A. A., Epstein, P. N., Uchida, S., Zheng, Y., Mcnally, L. A., Obal, D., et al. (2017). Exercise-Induced Changes in Glucose Metabolism Promote Physiological Cardiac Growth. *Circulation* 136, 2144–2157. doi: 10.1161/CIRCULATIONAHA.117.028274

Gibb, A. A., and Hill, B. G. (2018). Metabolic Coordination of Physiological and Pathological Cardiac Remodeling. *Circ. Res.* 123, 107–128. doi: 10.1161/CIRCRESAHA.118.312017

Ho, K. L., Karwi, Q. G., Wagg, C., Zhang, L., Vo, K., Altamimi, T., et al. (2021). Ketones can become the major fuel source for the heart but do not increase cardiac efficiency. *Cardiovasc. Res.* 117, 1178–1187. doi: 10.1093/cvr/cva a143

Hu, D., Linders, A., Yamak, A., Correia, C., Kijlstra, J. D., Garakani, A., et al. (2018). Metabolic Maturation of Human Pluripotent Stem Cell-Derived Cardiomyocytes by Inhibition of HIF1α and LDHA. *Circ. Res.* 123, 1066–1079. doi: 10.1161/CIRCRESAHA.118.313249

Iruretagoyena, J. I., Davis, W., Bird, C., Olsen, J., Radue, R., Teo Broman, A., et al. (2014). Metabolic gene profile in early human fetal heart development. *Mol. Hum. Reprod.* 20, 690–700. doi: 10.1093/molehr/gau026

Jiang, Y. J., Sun, S. J., Cao, W. X., Lan, X. T., Ni, M., Fu, H., et al. (2021). Excessive ROS production and enhanced autophagy contribute to myocardial injury induced by branched-chain amino acids: roles for the AMPK-ULK1 signaling pathway and α7nAChR. *Biochim. Biophys. Acta Mol. Basis Dis.* 1867:165980. doi: 10.1016/j.bbadis.2020.165980

Josan, S., Park, J. M., Hurd, R., Yen, Y. F., Pfefferbaum, A., Spielman, D., et al. (2013). In vivo investigation of cardiac metabolism in the rat using MRS of hyperpolarized [1-13C] and [2-13C]pyruvate. *NMR Biomed.* 26, 1680–1687. doi: 10.1002/nbm.3003

Kudová, J., Procházková, J., Vašièek, O., Pereèko, T., Sedláèková, M., Pešl, M., et al. (2016). HIF-1alpha Deficiency Attenuates the Cardiomyogenesis of Mouse Embryonic Stem Cells. *PLoS One* 11:e0158358. doi: 10.1371/journal.pone. 0158358

Latimer, M. N., Sonkar, R., Mia, S., Frayne, I. R., Carter, K. J., Johnson, C. A., et al. (2021). Branched chain amino acids selectively promote cardiac growth at the end of the awake period. *J. Mol. Cell Cardiol.* 157, 31–44. doi: 10.1016/j.yjmcc. 2021.04.005

Lemay, S. E., Awada, C., Shimauchi, T., Wu, W. H., Bonnet, S., Provencher, S., et al. (2021). Fetal Gene Reactivation in Pulmonary Arterial Hypertension: GOOD, BAD, or BOTH?. *Cells* 10:1473. doi: 10.3390/cells1006 1473

Li, T., Zhang, Z., Kolwicz, S. C. Jr., Abell, L., Roe, N. D., Kim, M., et al. (2017). Defective Branched-Chain Amino Acid Catabolism Disrupts Glucose Metabolism and Sensitizes the Heart to Ischemia-Reperfusion Injury. *Cell Metab.* 25, 374–385. doi: 10.1016/j.cmet.2016.11.005

Li, Y., Xiong, Z., Yan, W., Gao, E., Cheng, H., Wu, G., et al. (2020). Branched chain amino acids exacerbate myocardial ischemia/reperfusion vulnerability via enhancing GCN2/ATF6/PPAR-α pathway-dependent fatty acid oxidation. *Theranostics* 10, 5623–5640. doi: 10.7150/thno.44836

Liu, Y. W., Chen, B., Yang, X., Fugate, J. A., Kalucki, F. A., Futakuchi-Tsuchida, A., et al. (2018). Human embryonic stem cell-derived cardiomyocytes restore function in infarcted hearts of non-human primates. *Nat. Biotechnol.* 36, 597–605.

Lopaschuk, G. D., Karwi, Q. G., Ho, K. L., Pherwani, S., and Ketema, E. B. (2020). Ketone metabolism in the failing heart. *Biochim. Biophys. Acta Mol. Cell Biol. Lipids* 1865:158813.

Murashige, D., Jang, C., Neinast, M., Edwards, J. J., Cowan, A., Hyman, M. C., et al. (2020). Comprehensive quantification of fuel use by the failing and nonfailing human heart. *Science* 370, 364–368. doi: 10.1126/science.abc8861

Nabben, M., Luiken, J., and Glatz, J. F. C. (2018). Metabolic remodelling in heart failure revisited. *Nat. Rev. Cardiol.* 15:780. doi: 10.1038/s41569-018-0116-7

Nabeebaccus, A. A., Zoccarato, A., Hafstad, A. D., Santos, C. X., Aasum, E., Brewer, A. C., et al. (2017). Nox4 reprograms cardiac substrate metabolism via protein O-GlcNAcylation to enhance stress adaptation. *JCI Insight* 2:e96184. doi: 10.1172/jci.insight.96184

Nakano, H., Minami, I., Braas, D., Pappoe, H., Wu, X., Sagadevan, A., et al. (2017). Glucose inhibits cardiac muscle maturation through nucleotide biosynthesis. *Elife* 6:e29330. doi: 10.7554/eLife.29330

Newhardt, M. F., Batushansky, A., Matsuzaki, S., Young, Z. T., West, M., Chin, N. C., et al. (2019). Enhancing cardiac glycolysis causes an increase in PDK4 content in response to short-term high-fat diet. *J. Biol. Chem.* 294, 16831–16845. doi: 10.1074/jbc.RA119.010371

Qiao, X., Xu, J., Yang, Q. J., Du, Y., Lei, S., Liu, Z. H., et al. (2013). Transient acidosis during early reperfusion attenuates myocardium ischemia reperfusion injury via PI3k-Akt-eNOS signaling pathway. *Oxid. Med. Cell Longev.* 2013:126083. doi: 10.1155/2013/126083

Romagnuolo, R., Masoudpour, H., Porta-Sánchez, A., Qiang, B., Barry, J., Laskary, A., et al. (2019). Human Embryonic Stem Cell-Derived Cardiomyocytes Regenerate the Infarcted Pig Heart but Induce Ventricular Tachyarrhythmias. *Stem Cell Rep.* 12, 967–981. doi: 10.1016/j.stemcr.2019. 04.005

Schnelle, M., Chong, M., Zoccarato, A., Elkenani, M., Sawyer, G. J., Hasenfuss, G., et al. (2020). In vivo [U-(13)C]glucose labeling to assess heart metabolism in murine models of pressure and volume overload. *Am. J. Physiol. Heart Circ. Physiol.* 319, H422–H431. doi: 10.1152/ajpheart.00219. 2020

Shao, D., Villet, O., Zhang, Z., Choi, S. W., Yan, J., Ritterhoff, J., et al. (2018). Glucose promotes cell growth by suppressing branched-chain amino acid degradation. *Nat. Commun.* 9:2935. doi: 10.1038/s41467-018-05 362-7

Sun, H., Olson, K. C., Gao, C., Prosdocimo, D. A., Zhou, M., Wang, Z., et al. (2016). Catabolic Defect of Branched-Chain Amino Acids Promotes Heart Failure. *Circulation* 133, 2038–2049. doi: 10.1161/CIRCULATIONAHA.115.02 0226

Sun, X. L., Lessard, S. J., An, D., Koh, H. J., Esumi, H., Hirshman, M. F., et al. (2019). Sucrose nonfermenting AMPK-related kinase (SNARK) regulates exercise-stimulated and ischemia-stimulated glucose transport in the heart. *J. Cell Biochem.* 120, 685–696. doi: 10.1002/jcb.27425

Tran, D. H., and Wang, Z. V. (2019). Glucose Metabolism in Cardiac Hypertrophy and Heart Failure. *J. Am. Heart Assoc.* 8:e012673. doi: 10.1161/JAHA.119. 012673

Uchihashi, M., Hoshino, A., Okawa, Y., Ariyoshi, M., Kaimoto, S., Tateishi, S., et al. (2017). Cardiac-Specific Bdh1 Overexpression Ameliorates Oxidative Stress and Cardiac Remodeling in pressure Overload-Induced Heart Failure. *Circ. Heart Fail.* 10:e004417. doi: 10.1161/CIRCHEARTFAILURE.117.00 4417

Uddin, G. M., Karwi, Q. G., Pherwani, S., Gopal, K., Wagg, C. S., Biswas, D., et al. (2021). Deletion of BCATm increases insulin-stimulated glucose oxidation in the heart. *Metabolism* 124:154871. doi: 10.1016/j.metabol.2021.15 4871

Valvezan, A. J., and Manning, B. D. (2019). Molecular logic of mTORC1 signalling as a metabolic rheostat. *Nat. Metab.* 1, 321–333. doi: 10.1038/s42255-019-0038-7

van Bilsen, M., Van Nieuwenhoven, F. A., and Van Der Vusse, G. J. (2008). Metabolic remodelling of the failing heart: beneficial or detrimental?. *Cardiovasc. Res.* 81, 420–428. doi: 10.1093/cvr/cv n282

van der Pol, A., Hoes, M. F., De Boer, R. A., and Van Der Meer, P. (2020). Cardiac foetal reprogramming: a tool to exploit novel treatment targets for the failing heart. *J. Intern. Med.* 288, 491–506. doi: 10.1111/joim.13094

Vettor, R., Valerio, A., Ragni, M., Trevellin, E., Granzotto, M., Olivieri, M., et al. (2014). Exercise training boosts eNOS-dependent mitochondrial biogenesis in mouse heart: role in adaptation of glucose metabolism. *Am. J. Physiol. Endocrinol. Metab.* 306, E519–E528. doi: 10.1152/ajpendo.00617.2013

Walejko, J. M., Christopher, B. A., Crown, S. B., Zhang, G. F., Pickar-Oliver, A., and Yoneshiro, T. (2021). Branched-chain α-ketoacids are preferentially reaminated and activate protein synthesis in the heart. *Nat. Commun.* 12:1680. doi: 10.1038/s41467-021-21962-2

Walejko, J. M., Koelmel, J. P., Garrett, T. J., Edison, A. S., and Keller-Wood, M. (2018). Multiomics approach reveals metabolic changes in the heart at birth. *Am. J. Physiol. Endocrinol. Metab.* 315, E1212–E1223. doi: 10.1152/ajpendo. 00297.2018

Wang, S. Y., Zhu, S., Wu, J., Zhang, M., Xu, Y., Xu, W., et al. (2020). Exercise enhances cardiac function by improving mitochondrial dysfunction and maintaining energy homoeostasis in the development of diabetic cardiomyopathy. *J. Mol. Med.* 98, 245–261. doi: 10.1007/s00109-019-01861-2

Wang, W., Zhang, F., Xia, Y., Zhao, S., Yan, W., Wang, H., et al. (2016). Defective branched chain amino acid catabolism contributes to cardiac dysfunction and remodeling following myocardial infarction. *Am. J. Physiol. Heart Circ. Physiol.* 311, H1160–H1169. doi: 10.1152/ajpheart.00114.2016

Wang, Z. V., Li, D. L., and Hill, J. A. (2014). Heart failure and loss of metabolic control. *J. Cardiovasc. Pharmacol.* 63, 302–313. doi: 10.1097/FJC. 0000000000000054

Watanabe, K., Nagao, M., Toh, R., Irino, Y., Shinohara, M., Iino, T., et al. (2021). Critical role of glutamine metabolism in cardiomyocytes under oxidative stress. *Biochem. Biophys. Res. Commun.* 534, 687–693. doi: 10.1016/j.bbrc.2020.11.018

Weeks, K. L., and McMullen, J. R. (2011). The athlete's heart vs. the failing heart: can signaling explain the two distinct outcomes?. *Physiology* 26, 97–105. doi: 10.1152/physiol.00043.2010

Yoon, M. S. (2016). The Emerging Role of Branched-Chain Amino Acids in Insulin Resistance and Metabolism. *Nutrients* 8:405. doi: 10.3390/nu8070405

Zhang, Y., Taufalele, P. V., Cochran, J. D., Robillard-Frayne, I., Marx, J. M., Soto, J., et al. (2020). Mitochondrial pyruvate carriers are required for myocardial stress adaptation. *Nat. Metab.* 2, 1248–1264. doi: 10.1038/s42255-020-00288-1

Zuurbier, C. J., Bertrand, L., Beauloye, C. R., Andreadou, I., Ruiz-Meana, M., Jespersen, N. R., et al. (2020). Cardiac metabolism as a driver and therapeutic target of myocardial infarction. *J. Cell Mol. Med.* 24, 5937–5954. doi: 10.1111/jcmm.15180

Conflict of Interest: The authors declare that the research was conducted in the absence of any commercial or financial relationships that could be construed as a potential conflict of interest.

Publisher's Note: All claims expressed in this article are solely those of the authors and do not necessarily represent those of their affiliated organizations, or those of the publisher, the editors and the reviewers. Any product that may be evaluated in this article, or claim that may be made by its manufacturer, is not guaranteed or endorsed by the publisher.

Copyright © 2022 Shi and Qiu. This is an open-access article distributed under the terms of the Creative Commons Attribution License (CC BY). The use, distribution or reproduction in other forums is permitted, provided the original author(s) and the copyright owner(s) are credited and that the original publication in this journal is cited, in accordance with accepted academic practice. No use, distribution or reproduction is permitted which does not comply with these terms.

frontiers in Physiology

ORIGINAL RESEARCH
published: 25 February 2022
doi: 10.3389/fphys.2022.841146

Optimal Parameters of Laser Therapy to Improve Critical Calvarial Defects

*Matheus AFM Santos[1], Daniela N. Silva[1], Karla Rovaris[2], Frederico B. Sousa[3], Eugenia LA Dantas[4], Lucas A. Loureiro[5], Thiago M. C. Pereira[5], Silvana S. Meyrelles[1], Rossiene M. Bertollo[1] and Elisardo C. Vasquez[5]**

[1] Dentistry Graduate Program, Federal University of Espirito Santo, UFES, Vitoria, Brazil, [2] Department of Pathology & Clinical Dentistry, Federal University of Piaui, Teresina, Brazil, [3] Department of Morphology, Federal University of Paraiba, UFPB, Joao Pessoa, Brazil, [4] Dentistry Graduate Program, UFPB, Joao Pessoa, Brazil, [5] Pharmaceutical Sciences Graduate Program, Vila Velha University, Vila Velha, Brazil

Body bones play diverse pivotal roles, including the protection of vital organs. For instance, the integrative functions of the brain controlling diverse peripheral actions can be affected by a traumatic injury on the calvaria and the reparative process of a large defect is a challenge in the integrative physiology. Therefore, the development of biomaterials and approaches to improve such defects still requires substantial advances. In this regard, the most attractive approaches have been covering the cavity with inorganic bovine bone (IBB) and, more recently, also using low-level laser therapy (LT), but this issue has opened many questions. Here, it was determined the number of LT sessions required to speed up and to intensify the recovery process of two 5-mm-diameter defects promoted in the calvaria of each subgroup of six adult Wistar rats. The quantitative data showed that 30 days post-surgery, the recovery process by using blood clot-filling was not significantly influenced by the number of LT sessions. However, in the IBB-filled defects, the number of LT sessions markedly contributed to the improvement of the reparative process. Compared to the Control group (non-irradiated), the percentage of mineralization (formation of new bone into the cavities) gradually increased 25, 49, and 52% with, respectively, 4, 7, and 11 sessions of LT. In summary, combining the use of IBB with seven sessions of LT seems to be an optimal approach to greatly improve the recovery of calvarial defects. This translational research opens new avenues targeting better conditions of life for those suffering from large bone traumas and in the present field could contribute to preserve the integrative functions of the brain.

Keywords: calvarial defect, IBB, blood clot, laser therapy, brain function

OPEN ACCESS

Edited by:
Geoffrey A. Head, Baker Heart and Diabetes Institute, Australia

Reviewed by:
Roberta Okamoto, Universidade Estadual Paulista "Júlio de Mesquita Filho", Brazil
Gustavo Vicentis de Oliveira Fernandes, University of Michigan, United States

****Correspondence:***
Elisardo C. Vasquez
evasquez@terra.com.br

Specialty section:
This article was submitted to Integrative Physiology, a section of the journal Frontiers in Physiology

Received: *22 December 2021*
Accepted: *21 January 2022*
Published: *25 February 2022*

Citation:
Santos MA, Silva DN, Rovaris K, Sousa FB, Dantas EL, Loureiro LA, Pereira TMC, Meyrelles SS, Bertollo RM and Vasquez EC (2022) Optimal Parameters of Laser Therapy to Improve Critical Calvarial Defects. Front. Physiol. 13:841146. doi: 10.3389/fphys.2022.841146

INTRODUCTION

Body bones play a pivotal role, protecting the vital organs, articulating body movements, producing blood cells, and contributing to calcium homeostasis. A characteristic of this tissue is that when injured it heals without scarring and, despite exhibiting cellular machinery and all components to initiate a necessary regenerative process, there are some circumstances when this does not occur (Tarride et al., 2016; Wijbenga et al., 2016; Wang et al., 2018). For instance, large bone defects, such as trauma, tumor resection, and skeletal abnormalities can compromise integrative brain

areas (Dimitriou et al., 2012; Wang et al., 2018), an issue with which we acquired experience and have contributed to a better understanding of the integrative brain function in health and disease (Vasquez et al., 1992, 1997, 1998; Sert Kuniyoshi et al., 2011; Viña et al., 2021).

Regarding advances in the filling of large bone defects, inorganic bovine bone (IBB), which promotes deposition and mineralization of the bone matrix, is an attractive research field in translational research (Aludden et al., 2018; Kasuya et al., 2018). Moreover, this osteoconductive material with particles of varying size preserves the space within the tissue and acts as a scaffold for deposition and mineralization of the bone matrix (Kasuya et al., 2018). It has been recommended mainly because its unlimited availability simplifies the surgical procedure (Aludden et al., 2018). But, to date and despite the scientific and biotechnological advances, there are many open questions, including its potential to interact with bone defects critical enough to preclude spontaneous and complete bone healing, including critical-sized defects.

More recently, experimental and clinical studies have focused on infrared wavelength, which seems to be more effective than the red wavelength and has also been a promisor complement for the process of critical defects (Brassolatti et al., 2018). However, irradiation of large bone defects with laser devices still needs more investigation to clear some important questions, such as the number of sessions required to achieve improvements in new therapies (Vajgel et al., 2014; Santinoni et al., 2017; Brassolatti et al., 2018). The use of low level laser therapy (LT) is considered a promising approach to improve the osteoconductive and reparative potential when combined with the biomaterial IBB (Barbosa et al., 2013; Marques et al., 2015; Acar et al., 2016; Bosco et al., 2016; de Oliveira et al., 2018). At the same time, the low-level laser therapy (LT) figures as an innovative invasive treatment of bone lesions that stimulates osteogenesis and accelerates tissue healing (Bai et al., 2021). Although the mechanisms regarding regenerative bone tissue are unclear, recent findings indicate that the light absorbed by the plasma membrane triggers a variety of biochemical reactions that activate transcription factors and modulate cell migration, mitosis, and tissue repair (Kunimatsu et al., 2018).

Considering that low-level laser therapy may improve the osteoconductive and reparative potential of the biomaterial IBB (de Oliveira et al., 2018), this study was designed to evaluate how many sessions of LT are required to improve the effects of IBB filling of large bone injuries in the head.

MATERIALS AND METHODS

Ethical Aspects and Sample

This animal study was previously approved by the Ethics Committee on Animals Use of the Federal University of Espírito Santo (CEUA-UFES #010/2014). The procedures complied with those established by the European Community guidelines for animal experimentation. A total of 42 male Wistar rats *(Rattus norvegicus albinus)* with body weight between 250 and 300 g, were kept in individual cages at 22 ± 2°C, 50 ± 10% relative humidity, 12 h light/dark cycles, with free access to water and standard chow.

Study Design

The animals were randomly assigned to seven groups of six animals each according to the number of laser therapy and evaluation sessions 0 (non-irradiated; Control group), 4, 7, or 11 and with the evaluation periods of 15- or 30-days post-surgery: 0LT15d and 0LT30d; 4LT15d and 4LT30d; 7LT15d and 7LT30d; 11LT30d. This last group could only be evaluated at 30 days since the last session occurred on the 21st day.

Surgical Procedure

After aseptic preparation, animals were anesthetized by intraperitoneal injection of 50 mg/kg ketamine (Instituto BioChimico Industria Farmaceutica, Rio de Janeiro, Brazil) and 5 mg/kg xylazine (Syntec do Brazil, Santana do Parnaiba, Brazil). After trichotomy of the dorsal cranium of each animal and antisepsis of the skin and surrounding hair with 2% chlorhexidine digluconate, a longitudinal incision of approximately 2.5 cm was made along the sagittal suture to expose the calvaria bone cortex. Two circular critical sized defects, approximately 2 mm from each other, were prepared on the right and left sides of the parietal bone without damaging the surrounding sutures (sagittal, coronal, and lambdoid) (**Figure 1**). Craniotomy was performed with a 5-mm external diameter trephine bur (W&F Cirurgicos, Barueri, Brazil) mounted in a 20:1 low-speed hand piece at 1,500 rpm (Kavo, Joinville, Brazil) and under abundant irrigation with sterile 0.9% saline solution. Both external and internal cortical were cut without injury to the dura mater since a plastic device was coupled to the bur to limit the cutting depth (**Figure 1**). In all groups, the right cavity spontaneously filled a blood clot, while the left cavity was filled with 14.7 μL of IBB (Bio-Oss®0.25 – 1 mm granules, Geistlich Pharma, Wolhusen, Switzerland) (Hallman and Thor, 2008).

The periosteum and scalp were sutured in a single plane with interrupted stitches made with 3.0 silk thread (Johnson & Johnson, São Paulo, Brazil) and the rat skin was marked with a dermographic pen to facilitate the application of the laser. Next, animals were kept in the prone position in their respective cages and under supervision for anesthesia recovery. A single dose of antibiotics (Enrofloxacin 2.5% 10 mg/kg, Vencofarma, Londrina, Brazil) was administered subcutaneously. To control postoperative pain over the next 3 d, 30 drops of analgesic (Tylenol, 200 mg/mL, Janssen-Cilag Farmaceutica, São Jose dos Campos, Brazil) were diluted in each 200 mL of drinking water.

Laser Therapy

The transcutaneous LT protocol began immediately after the surgery and followed 4, 7, or 11 sessions at 48 h intervals (de Oliveira et al., 2014). The animals were sedated in an inhalation chamber by using a cotton pad soaked with 2.5 mL of anesthetic (Isoflurane®, Instituto BioChimico Industria Farmaceutica, Rio de Janeiro, Brazil). A gallium-aluminum-arsenide (GaAlAs) diode laser (Laser Duo, MMOptics, São Carlos, Brazil) was applied at a continuous infrared wavelength of 808 nm, power output of 100 mW, ø ∼ 3 mm^2, 60 s, and energy density of

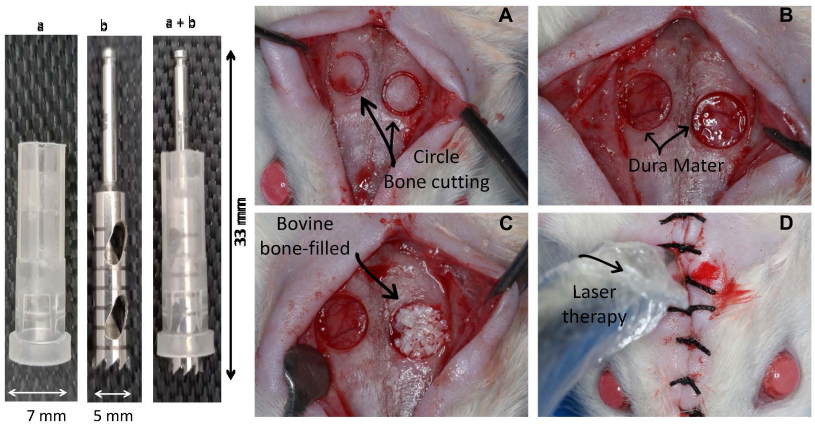

FIGURE 1 | Device and approach used to induce bone damage in the head of Wistar rats. In the left side is shown the device used to remove a circular 5-mm-diameter and 2-mm-deep bone area on the top of a rat. The device was constructed by using a 7-mm-diameter protective plastic tube ("a") covering a metallic diamond bur ("b") and the mounted device ("a" + "b"). In the right side is illustrated the sequential steps of the surgical approach. **(A)** Shows the area delimited by the cutting device; **(B)** illustration of the integrity of the dura mater after removing the bone; **(C)** right side cavity filled with inorganic bovine bone (IBB); **(D)** radiation of the cavities with a low-level laser device.

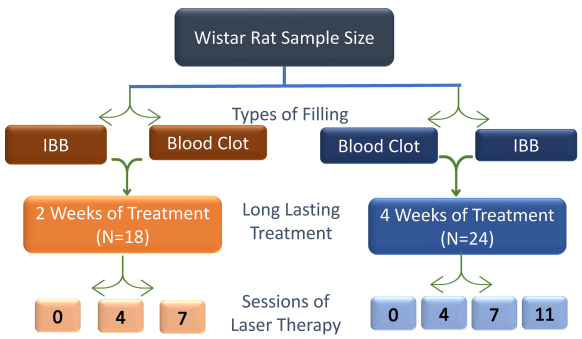

FIGURE 2 | Schematic design used to achieve the aim of this study, the effectiveness, and the number of sessions of low-level LT required to improve the recovery of bone injury. Sessions were scheduled to occur at intervals of 48 h.

200 J/cm^2 per session (Cunha et al., 2014; de Almeida et al., 2014; Moreira et al., 2018). Irradiation was conducted with the laser tip in contact with the skin at each cavity (right and left) (**Figure 1D**). After the postoperative periods of 15 and 30 days, the animals were euthanized by the same operator with a lethal dose of ketamine (150 to 225 mg/kg) and xylazine (15 to 30 mg/kg). Samples of the calvarial grafted areas were collected and immediately fixed in 10% neutral buffered formalin (Histopot-Serosep, County Limerick, Ireland).

Histological and Histomorphometric Analyses

Calvarial samples were decalcified in a 10% formic acid with daily changes for five consecutive days, sectioned in the sagittal direction (at the greatest CSD diameter) and then subjected to a series of baths for histological processing. Serial sections with a 6-μm thickness were obtained and stained with standard hematoxylin and eosin (H&E). A photomicrograph of one section representing the central area of each CSD was obtained with a microscope coupled to a digital camera (Leica DM50 + ICC50 HD, Leica Reichert & Jung Products, Wetzlar, Germany) with 10 × magnification. For the histomorphometric analysis, the total area and the areas of newly formed bone were marked by a previously trained and blinded evaluator with the aid of imaging software (Image J, National Institute of Mental Health, Bethesda, MD, United States). The findings were calculated as percentages of mineralized tissue to the total area.

Microtomographic Analysis

Calvarial bone blocks were scanned at the Laboratory of Microscopy and Biological Image of the Federal University of Paraiba with a computed microtomography machine (SkyScan 1172, Bruker, Kontich, Belgium) set with the following parameters: 80 kVp, 120 μA, 0.5 Al filter, 14 μm voxel size, 0.3° rotation step, 3 frames, and a 180° rotation. The cross-section slices were reconstructed by using beam-hardening artifact correction of 20% (NRecon, Bruker) and volume realignment (DataViewer, Bruker). After the delimitation of the entire CSD area (5-mm-diameter circular-shaped structure and the total calvarial thickness), the following bone parameters were quantified: bone volume (BV), trabecular number (Tb.N), and thickness (Tb. Th) (CT Analyzer, Bruker).

Statistical Analysis

D'Agostino-Pearson, Shapiro-Wilk, and Kolmogorov-Smirnov tests were applied to assess the normal distribution of the data, which was confirmed by the agreement of at least two tests. Then, groups were statistically compared using one- or two-way analysis of variance (ANOVA) and Tukey's *post hoc* multiple comparisons at a significance level of $p < 0.05$ (Prism 8.0, GraphPad Software, San Diego, CA, United States).

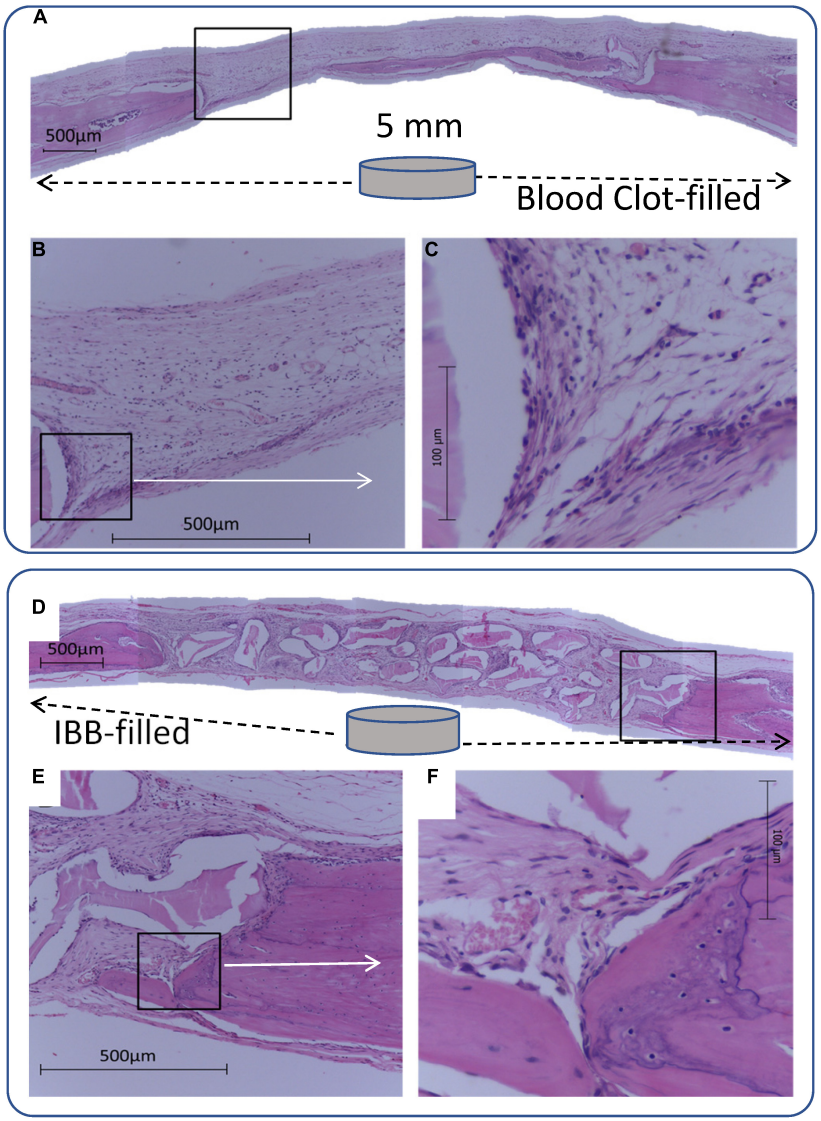

FIGURE 3 | Panoramic view of a 5-mm-diameter defect produced in a rat. Cavity defects were filled with blood clot **(A–C)** or inorganic bovine bone **(D–F)**, associated with 7 sessions of laser irradiation can be compared. Images were magnified (C and F) to highlight the recovery process, suggesting an improvement when the filling of the cavity is through IBB, as indicated by intense osteoblastic and fibroblastic activity at the margins with deposition of bone matrix and collagen fibers.

RESULTS

Histology of Clot-Filled Cavities

In the 0LT subgroups, it was observed in typical images that regardless of the subgroup, bone tissue regeneration was not complete at the observation periods. After 30 days, less fibrous tissue was observed. A small amount of mineralized bone matrix at the margins and in some CSD central spots, a large amount of connective tissue with collagen fibers parallel to the periosteum and limited osteoblastic activity were observed.

As illustrated by typical images in **Figure 3**, differently from the Control group, all experimental groups showed similar characteristics such as greater deposition and mineralization of bone matrix both at the margins and in the CSD central area, mineralized areas joined together by bridges of bone tissue toward the central area with a greater tendency for complete closure, more intense osteoblastic activity, and a lesser amount of connective tissue at the two evaluation periods.

Histology of IBB-Filled Cavities

Regardless of the group, the biomaterial graft induced bone formation throughout the cavities and with a thickness similar to the surrounding bone tissue.

In the 0LT15d (Control group) filled with IBB, there was connective tissue with parallel collagen fibers with the presence of osteoblasts and new blood vessels. Osteoclasts around the biomaterial particles were found in some areas and a few mineralized spots were observed at the CSD margins. After

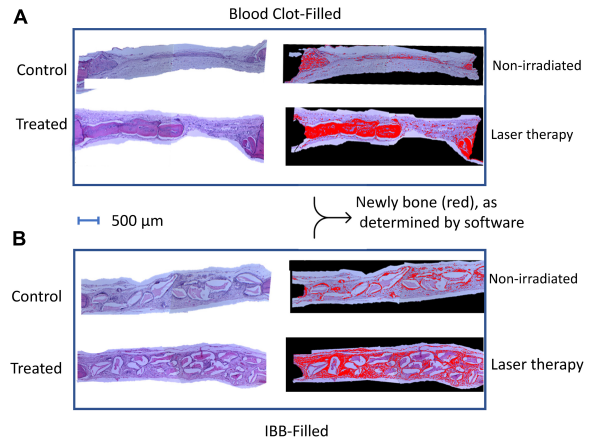

FIGURE 4 | Photomicrographs of representative images of hematoxylin-eosin (HE) sections of both subgroups, the blood clot **(A)**, and the IBB filled cavities **(B)**. Images were delimited with the aid of imaging software to compare the areas of newly formed bone (in red color).

30 days, more pronounced matrix mineralization around and between IBB particles was observed in addition to moderate mineralization in the central CSD area.

Figure 3 (bottom panel) illustrates panoramic views of the effect of IBB filling in a 7LT15d animal. All groups presented similar findings such as the great amount of well-organized connective tissue with parallel collagen fibers, intense osteoblastic activity, and numerous blood vessels. At the 15-days evaluation, a moderate increase of mineralized areas at the margins and sparse islands of mineralization at the margins and between the particles were found (**Figures 3E,F**). After 30 days, a greater amount of mineralized matrix was observed at the margins and toward the CSD center. Moreover, mineralized matrix was observed between and within some porosities of biomaterial particles.

Figure 4 shows typical images from a rat of seven sessions of LT on the clot-filled cavity and compared with a non-irradiated Control rat (top panel). In the bottom panel is shown a typical image of a 7LT15d rat with IBB-filled and compared with a 0 non-irradiated animal (0LT15d). Images were delimited with the aid of imaging software to compare the areas of newly formed bone (in red color).

The percentage of mineralized areas which was facilitated by clot, a natural regenerative material, or by IBB in the cavities and analyzed at 15 days post-surgery is summarized in the violin graphs of **Figure 5**.

In the group of rats with cavities filled by a blood clot, the percentage of mineralized area in the reparative process of bone tissue in a period of 2 weeks averaged 30 ± 4% in the Control group (0LT15d) and was significantly augmented in the 4LT15d group (47 ± 5%) and even higher in the 7LT15d group ($p < 0.05$) reaching a mean of 58 ± 5%. When the period of time is extended to 4 weeks, we did not observe a so great improvement, probably due to the fact that the blood clot, by itself, had a great reparative effect, as indicated by the high percentage of mineralization (59 ± 6%) observed in the Control group (0LT30d). Note that the violin graph of this group was of the lest variability, indicating that all animals of this group were very similar (low variability). The 4LT30d group exhibited similar values (62 ± 5%) when compared to the Control values but significantly improved effect as compared with the group of 4LT15d. The group of seven sessions into the 30 days (7LT30d) showed an additional improvement to 66 ± 4%, but even increasing the number of sessions to 11 in the sub-group 11LT30d, the values returned to a level (60 ± 3%) similar to the Control group.

In the subgroups in which IBB was used as biomaterial to fill the cavities, the bone mineralization was 22 ± 3% in the Control group (0LT15d) and was similarly augmented in the 4LT15d (37 ± 3%; $p < 0.05$) and 42 ± 3% in the 7LT15d group. Still, in this group of IBB-filled material with the analysis done 30 days post-surgery, the Control non-irradiated group (0LT30d) showed an area 36 ± 3% of mineralization and it was statistically improved in the 4LT30d group (45 ± 3%) and higher when the number of sessions increased (7LT30d and 11LT30d groups), reaching similar averages of 52 ± 3% and 53 ± 3%, respectively ($p < 0.05$).

To avoid the confounder factor of differences in the referential values observed in each of the four Control groups, we decided to provide an additional analysis of the data, which is presented in **Figure 6**. In the additional analysis we show the average values of bone mineralization caused by the type of cavity filling and the required number of LT sessions. These values were compared to the reference levels of the Control groups, which were expressed as 100%. In this way, IBB-filled provided much better reparative effects than those observed in the blood clot-filled ones. The data also show that 4 sessions is sufficient to increase generation of new bone and that there is no benefit going longer than 7 sessions (**Figure 6**).

Microtomographic Analysis

The results described above are corroborated by the qualitative and quantitative analysis provided by three-dimensional microtomography (**Figure 7**). As seen in the typical images (top panel), the defect area of the Control animal (blood clot- or IBB-filled) lacks new bone, when examined 2 weeks later (A) and shows some improvement when examined at 4 weeks later ("a"). In contrast, the LT irradiation of cavities filled with blood and bone showed gradual improvements (B and C) and with a remarkable regenerative process (neoformation of bone tissue) when the cavities were filled with IBB and concurrent LT ("a").

Column graphs at the bottom of **Figure 7** show descriptive statistics of 3 parameters measured by three-dimensional microtomography. An amount of 4.0 ± 0.2 mm^3 of new bone was found in the cavities filled with IBB, indicating that this biomaterial combined with concurrent LT results in approximately twofold that amount formed in cavities filled with blood clot (1.872 ± 0.2 mm^3, $p < 0.05$). A similar volume was observed in the Control group (1.9 ± 0.2 mm^3, $p > 0.05$). The data about trabecular thickness did not show significant differences among groups, indicating that the increased volume was not due to augmented thickness of the trabeculae. In fact, the next analysis showed an increase of approximately threefold in the trabecular number in the group IBB-filled (0.160 ± 0.02 mm^{-1}), compared with the blood clot-filled group

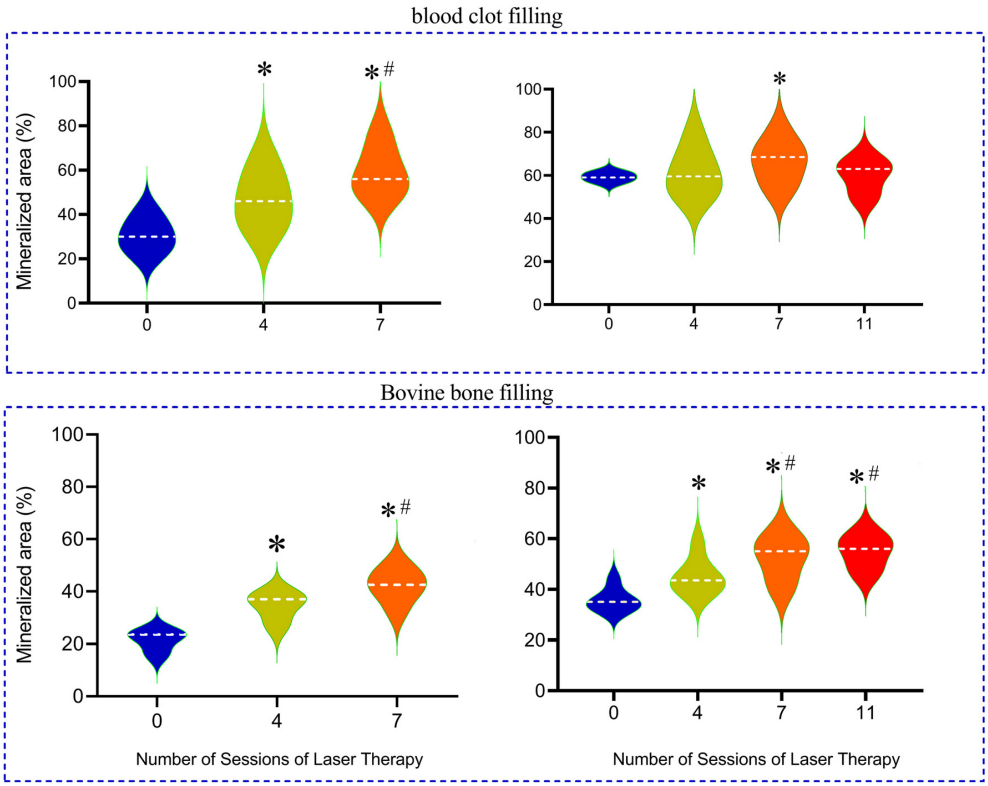

FIGURE 5 | Percentage of mineralized bone produced in the cavities that were filled with inorganic bovine bone (IBB) in comparison with blood clot-filled groups, mainly when associated with 4 to 11 sessions of LT and when compared with the non-irradiated group (0). The horizontal dashed line into the violin repress represents the mean values for each group. *$p < 0.05$ compared with the mean values of the Control group; #$p < 0.05$ compared with the 4 sessions group.

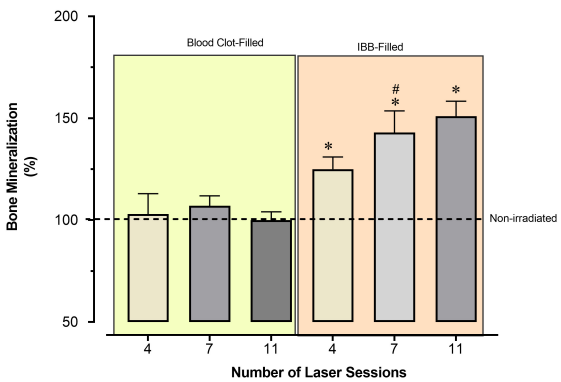

FIGURE 6 | Average percentage of bone mineralization caused by the type of cavity filling and the required number of sessions of LT, compared to the reference values observed in the Control group, expressed as 100% (horizontal dashed line). Values indicate the mean and the mean standard error. *$p < 0.05$ vs. Control group; #$p < 0.05$ vs. the previous time-point of the same group. Statistical analysis: two-way ANOVA for $N = 6$ rats per group.

(0.0387 ± 0.01 mm^{-1}, $p < 0.05$), which was remarkably close to that observed in the Control group (0.04 ± 0.01 mm^{-1}). Therefore, one of the possible mechanisms by which LT speeds up and improves the recovery process of critical bone defects seems to include the augmented trabecular number and volume of new bone.

DISCUSSION

The present study was motivated by the challenge to contribute to the knowledge about the reparative process of large calvarial defects, and then, to create novel approaches to obtain a fast, non-invasive, not painful, not expensive, and an efficient approach to repair critical bone defects. The quantitative data generated can be expressed as summarized here. IBB-filled large defects provided a faster and better recovery of bone function than the blood clot-filled alternative. The formation of new bone into the cavities gradually increased when the bone injury was filled with IBB, and it was greatly improved when the grafting was combined with sessions of LT. The new bone formed into the cavity increased approximately 25%, 50%, and 55%, respectively, with 4, 7, and 11 sessions of LT and compared to referential Control values obtained in IBB-filled but not irradiated with low-level laser, i.e., combining the use of IBB with seven sessions of LT seems to be an optimal approach to greatly improve the recovery of calvarial defects. It would be important to verify if the optimal effects of seven sessions of LT on bone mineralization are also observed in cavities filled with other biomaterials such as the

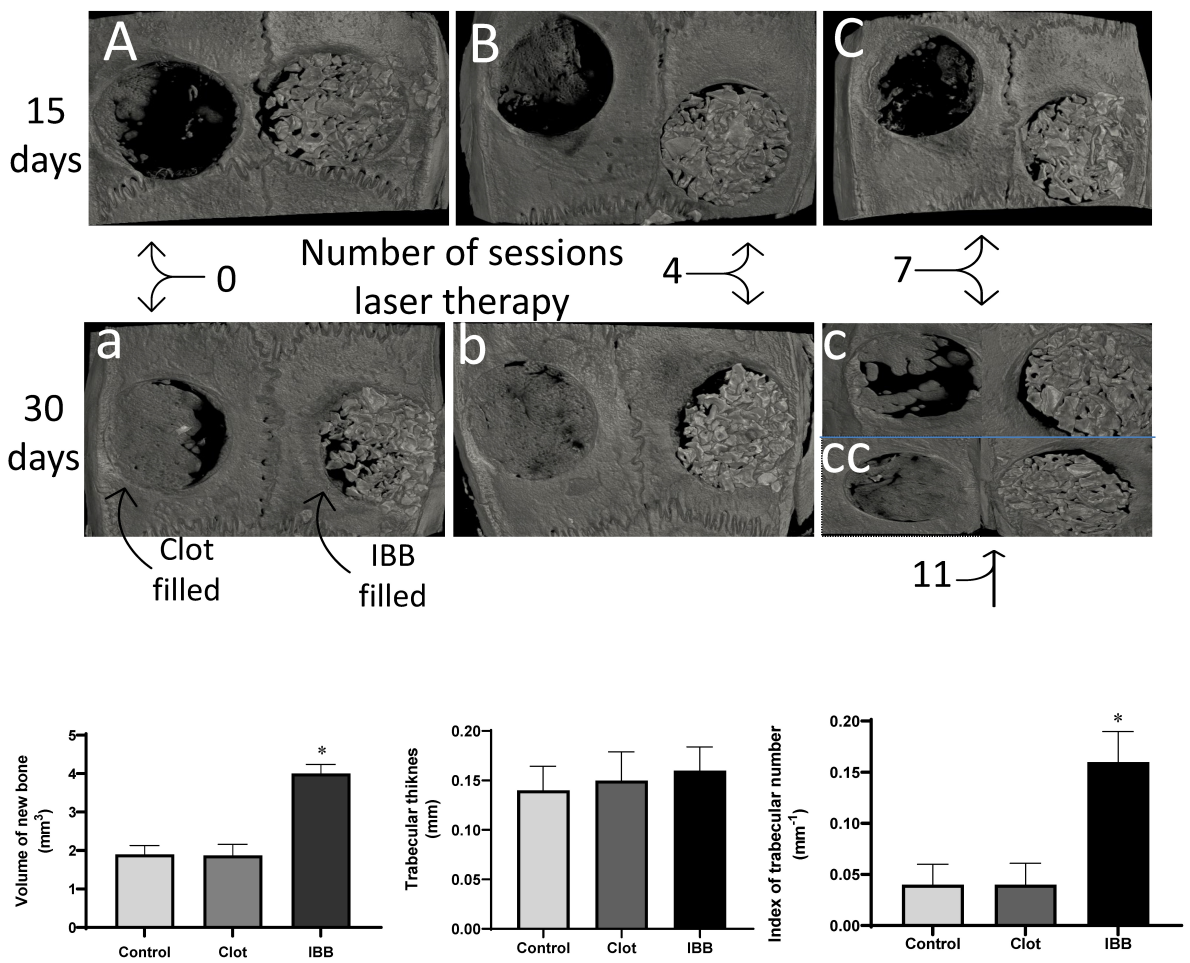

FIGURE 7 | Typical 3D microtomographic images, comparing blood clot-filled (left) with IBB-filed (right) cavities and comparing the analysis at 15 days (A, B, and C) with 30 days (a, b, c, and cc). Figure illustrates the effects of the number of sessions of LT, which in the group of 30 days was extended to a group of 11 sessions (cc). At the bottom are shown the qualitative data obtained by the microtomographic analysis. Values are mean ± Standard error of the mean. *$p < 0.05$ vs, Control and clot-filled groups. Statistical analysis: two-way ANOVA for $N = 6$ rats per group.

bioactive glass particles which have been used in *in vitro* studies from other investigators (Alves et al., 2017).

To avoid possible bias and inappropriate analysis and consequent conclusion, our protocols followed rigorous procedures as follows. The development of a device (**Figure 1**) allowed us to produce exactly the same diameter and depth of the cavities in all animals. Moreover, the effectiveness of each kind of filling was possible to be precisely evaluated in the animals of the three main groups (non-irradiated Control and irradiated and examined at 15 vs. 30 days). In addition, all animals received the same grafting material from the same manufacture (Bio-Oss®; Geistlich Pharma, Wolhusen, Switzerland). Despite the cavity requiring a very small amount of grafted material, we are confident that in each cavity of each animal, the volume of the biomaterial was exactly the same in all of them (14.7 μL), which was reliable due to the use of a device that was used in all animals. Therefore, we believe that important sources of bias commonly occurred in this type of study were prevented, and this is the reason of our interpretation that the differences in the results are due to the therapeutic characteristics of the biomaterial, accompanied by the irradiation with low-level LT.

The preparation of two critical sized defects with both experimental and control sites or blood clot-filled and IBB in the same rat calvaria (paired split design) was provided as a goal to reduce possible bias caused by the variability between different animals (Vajgel et al., 2014). Despite the lack of consensual opinion, it is assumed that a 5-mm-diameter defect seems to avoid complete closure with newly formed bone in a short period of time (de Almeida et al., 2014; Vajgel et al., 2014; Brassolatti et al., 2018).

In this study, the histological analysis of the cavities filled with a blood clot showed that bone formation was not complete after

30 d post-surgery. Regarding the fact that this is a controversial issue (Hawkins and Abrahamse, 2005; Cunha et al., 2014; Brassolatti et al., 2018; Noba et al., 2018), in the present study, we tried to use consensual dosimetric parameters (wavelength, application time, and energy density per session) that have been reported by previous prestigious investigators (Cunha et al., 2014; de Almeida et al., 2014; Moreira et al., 2018.) Considering the premise that a beneficial effect of LT on bone tissue formation in 5-mm-diameter critical sized defects has been already evidenced and that the number of LT sessions used to be directly related to the final amount of stimulation delivered to the tissue and could interfer in the final result of the process (Brassolatti et al., 2018). The present investigation specifically focused on the number of LT sessions required to significantly improve the recovery process.

The histomorphometry analysis has been considered the "gold standard" for the evaluation of bone healing and quantification of cell activity in terms of percentage of newly formed bone (Pinheiro et al., 2012; Acar et al., 2015). Furthermore, using this technique one can measure *ex vivo* bone volume and represent a viable alternative to qualitative and quantitative analyses in the research field of repairment of hard tissues (Schmidt et al., 2003; Schambach et al., 2010). The microtomographic analysis was able to accurately identify newly formed bone in critical sized defects at both 15- and 30-days evaluations. The use of high-resolution images and statistical procedures of normalization of reference values (Control group), it was possible to measure trabecular structures of the calvarial defects, and to detect differences in the volume of newly formed bone and in the trabecular number between, when comparing the IBB group with a bone clot or the Control groups. These findings are not a surprise because they are in agreement with the results obtained with the analysis using HE staining shown in **Figure 6**. Although we did not find significant differences in the average values of trabecular thickness among groups, the lack of difference does not seem to be due to technical aspects interfering in the analysis of microtomographic parameters (Schambach et al., 2010) because we acted with maximal rigor and the procedures were performed by skilled researchers in all steps (Chatterjee et al., 2017). Moreover, some authors suggest that microtomography presents limited sensitivity to identify differences in bone tissue after only 2- and 4-weeks post-surgery since the matrix is not completely mineralized at that time (Schambach et al., 2010; Ramalingam et al., 2016; de Oliveira et al., 2018).

The histomorphometric analysis of clot-filled cavities indicates that a greater number of LT sessions accelerated bone tissue formation during the initial stages of the bone repair process, which is stabilized later. Thus, LT seems more effective at the initial phase of intense cell proliferation following deposition and mineralization of bone matrix (Ozawa et al., 1998; Matsumoto et al., 2009; Marques et al., 2015). However, our results agree with previous studies showing that LT increases the formation of bone tissue in both clot- and IBB-filled cavities (Rasouli Ghahroudi et al., 2014).

Considering that the cavities were grafted with IBB and analyzed after 15 days, we did not expect that a higher number of LT sessions would benefit a better outcome, and in fact, we did not observe important differences in bone formation between 4LT15d and 7LT15d sub-groups. In contrast, after 30 days we found significant differences when comparing the percentage of mineralization in 7LT30d and 11LT30d sub-groups and, in comparison, with Control groups (non-irradiated). The fact that the 4LT30d sub-group was not significantly different from 0LT30d sub-group could indicate that a minimum number of LT sessions is needed to increase bone tissue formation. Conversely, the absence of a significant difference between 7LT30d and 11LT30d sub-groups suggests that the amount of mineralized tissue tends to stabilize after 7 LT sessions.

Our findings indicated that beneficial effect of LT in IBB-filled cavities evaluated 15 and 30 days post-surgery. However, one could argue that this could be a misinterpretation because in the group of 30 days one of the Control groups had levels of mineralization completely different from the other sub-groups. To avoid this confounding factor, we decided to normalize and to use the most accepted solution when one deals with comparison of groups exhibiting marked and unexpected differences in the basal or control values. Surprisingly (see **Figure 6**), we found remarkably interesting results that led us to propose changes in our initial hypothesis. What we found was that the differences between the experimental sub-groups (number of sessions) and the non-irradiated Control group are not influenced by the number of sessions with LT in blood clot-filled cavities. In contrast, in IBB-filled cavities groups it was observed that the percentage of mineralization is clearly associated with the increase of LT sessions, and that the magnitude of the response does not recommend using more than seven sessions of LT is an exciting result.

Other authors have been pioneers in the demonstration of the beneficial effects of combining IBB, which has similarity to human bone, with low-level LT (Cunha et al., 2014). The present data provides a contribution to this research field, by focusing on the number of LT sessions required to speed and amplify the effects of this combination. Despite our exciting results using IBB, other bioactive materials such as bioactive glass particles (Alves et al., 2014) could also be tested. We are confident about our results because we were challenged to perform a three-dimension microtomographic analysis, which has been an important approach in this research field (Alves et al., 2014). That procedure showed that the combination seven sessions of LT with IBB resulted in a significant increase in the volume of new bone formation (∼twofold) and an increase in the trabecular number (∼threefold). However, other avenues have been opened with this translational research and need to be pursued before moving up to clinical trials.

One exciting contribution to the mechanisms involved with the osteogenic and mineralization of cellular and extracellular matrix in the recovery of calvaria bone defects was recently provided by Alves et al. (2014). Through *in vitro* manipulation of newborn osteogenic cells those authors revealed some conditions favoring immunolabeling proteins as important contributors to the osteoblastic activities and differentiation and formation of mineralized matrix (Alves et al., 2014). Based on this scenario,

we conclude that our findings show that IBB-filled cavities irradiated during seven sessions of LT could favor the regenerative process of great-sized defects and challenge other investigators to join us in the search for rational solutions in the fighting against critical calvaria defects.

CONCLUSION

The present study is related with approaches to achieve rapid and effective repair of critical bone defects by using grafting inorganic material and low-level LT. Our data demonstrated that critical calvaria defects filled with IBB produces have much better reparative results than those filled with blood clot, and that the combination of these techniques with low-level LT accelerates and increases the bone healing. We determine the number of sessions of laser therapy required to obtain minimal and maximal effects in the regenerative process of bone critical defects. The data revealed that a maximum benefit is obtained using IBB combined with seven sessions of low-level LT. Therefore, the present results greatly contribute to the expected promotion of better conditions for those suffering from bone trauma- and other cause-related critical injuries. The present study and conclusions may provide new insights and motivate clinical trials in this research field.

DATA AVAILABILITY STATEMENT

The raw data supporting the conclusions of this article will be made available by the authors, without undue reservation.

ETHICS STATEMENT

The animal study was reviewed and approved by Ethics Committee in the Use of Animals, Federal University of Espirito Santo, Brazil.

AUTHOR CONTRIBUTIONS

MS, DS, RB, SM, and EV made substantial contributions to the concept and design of the study and interpretation of the data. MS conducted the experiments and provided acquisition and analysis. KR, FS, and ED performed the microtomographic analysis. LL and EV processed the spreadsheet data, constructed the graphs, and provided statistical analysis. TP contributed with the concept, analysis, and production of **Figure 6** and collaboration in the illustration of microtomographic images of a new graph suggested by the reviewers. EV coordinated the critical revision of the manuscript and provided the final version. All authors contributed to the article and approved the submitted version.

FUNDING

The payment of the production fee was shared by Frontiers in Physiology, PRONEX, which is a scientific union composed by the National Council for the Development of Science and Technology (CNPq), Ministry of Health (MS), and State Foundation for Science and Innovation (FAPES), Edital 24/2018 and TO 569/2018, and by voluntary contribution of the co-authors EV and MS.

REFERENCES

Acar, A. H., Yolcu, U., Altındiç, S., Gül, M., Alan, H., and Malkoç, S. (2016). Bone regeneration by low-level laser therapy and low-intensity pulsed ultrasound therapy in the rabbit calvarium. *Arch. Oral Biol.* 61, 60–65. doi: 10.1016/j.archoralbio.2015.10.011

Acar, A. H., Yolcu, U., Gül, M., Keleç, A., Erdem, N. F., and Altundag Kahraman, S. (2015). Micro-computed tomography and histomorphometric analysis of the effects of platelet-rich fibrin on bone regeneration in the rabbit calvarium. *Arch. Oral Biol.* 60, 606–614. doi: 10.1016/j.archoralbio.2014.09.017

Aludden, H., Dahlin, A., Starch-Jensen, T., Dahlin, C., and Mordenfeld, A. (2018). Histomorphometric analyses of area fraction of different ratios of Bio-Oss® and bone prior to grafting procedures - An in vitro study to demonstrate a baseline. *Clin. Oral Implants Res.* 29, 185–191. doi: 10.1111/clr.13079

Alves, L. B., Souza, S., Taba, M. Jr., Novaes, A. B. Jr., Oliveira, P. T., and Palioto, D. B. (2017). Bioactive glass particles in two-dimensional and three-dimensional osteogenic cell cultures. *Brazilian Dent. J.* 28, 307–316. doi: 10.1590/0103-6440201600953

Alves, R. D., Eijken, M., van de Peppel, J., and van Leeuwen, J. P. (2014). Calcifying vascular smooth muscle cells and osteoblasts: independent cell types exhibiting extracellular matrix and biomineralization-related mimicries. *BMC Genet.* 15:965. doi: 10.1186/1471-2164-15-965

Bai, J., Li, L., Kou, N., Bai, Y., Zhang, Y., Lu, Y., et al. (2021). Low level laser therapy promotes bone regeneration by coupling angiogenesis and osteogenesis. *Stem Cell Res. Ther.* 12:432. doi: 10.1186/s13287-021-02493-5

Barbosa, D., de Souza, R. A., Xavier, M., da Silva, F. F., Arisawa, E. A., and Villaverde, A. G. (2013). Effects of low-level laser therapy (LLLT) on bone repair in rats: optical densitometry analysis. *Lasers Med. Sci.* 28, 651–656. doi: 10.1007/s10103-012-1125-0

Bosco, A. F., Faleiros, P. L., Carmona, L. R., Garcia, V. G., Theodoro, L. H., and de Araujo, N. (2016). Effects of low-level laser therapy on bone healing of critical-size defects treated with bovine bone graft. *J. Photochem. Photobiol. B Biol.* 163, 303–310. doi: 10.1016/j.jphotobiol.2016.08.040

Brassolatti, P., de Andrade, A., Bossini, P. S., Orth, D. L., Duarte, F. O., and Dos Anjos Souza, A. B. (2018). Photobiomodulation on critical bone defects of rat calvaria: a systematic review. *Lasers Med. Sci.* 33, 1841–1848. doi: 10.1007/s10103-018-2653-z

Chatterjee, M., Faot, F., Correa, C., Duyck, J., Naert, I., and Vandamme, K. (2017). A robust methodology for the quantitative assessment of the rat jawbone microstructure. *Int. J. Oral Sci.* 9, 87–94. doi: 10.1038/ijos.2017.11

Cunha, M. J., Esper, L. A., Sbrana, M. C., de Oliveira, P. G., do Valle, A. L., and de Almeida, A. L. (2014). Effect of low-level laser on bone defects treated with bovine or autogenous bone grafts: in vivo study in rat calvaria. *BioMed. Res. Int.* 2014:104230. doi: 10.1155/2014/104230

de Almeida, A. L., Medeiros, I. L., Cunha, M. J., Sbrana, M. C., de Oliveira, P. G., and Esper, L. A. (2014). The effect of low-level laser on bone healing in critical size defects treated with or without autogenous bone graft: an experimental study in rat calvaria. *Clin. Oral Implants Res.* 25, 1131–1136. doi: 10.1111/clr.12239

de Oliveira, A. M., Castro-Silva, I. I., Fernandes, G. V. D. O., Melo, B. R., Alves, A. T. N. N., Silva Júnior, A., et al. (2014). Effectiveness and acceleration of bone repair in critical-sized rat calvarial defects using low-level laser therapy. *Lasers Surg. Med.* 46, 61–67. doi: 10.1002/lsm.22198

de Oliveira, G., Aroni, M., Medeiros, M. C., Marcantonio, E. Jr., and Marcantonio, R. (2018). Effect of low-level laser therapy on the healing of sites grafted with coagulum, deproteinized bovine bone, and biphasic ceramic made of hydroxyapatite and β-tricalcium phosphate. In vivo study in rats. *Lasers Surg. Med. [Online ahead of print]* 10.1002/lsm.22787. doi: 10.1002/lsm.22787

Dimitriou, R., Mataliotakis, G. I., Calori, G. M., and Giannoudis, P. V. (2012). The role of barrier membranes for guided bone regeneration and restoration of large bone defects: current experimental and clinical evidence. *BMC Med.* 10:81. doi: 10.1186/1741-7015-10-81

Hallman, M., and Thor, A. (2008). Bone substitutes and growth factors as an alternative/complement to autogenous bone for grafting in implant dentistry. *Periodontology* 2000, 172–192. doi: 10.1111/j.1600-0757.2008.00251.x

Hawkins, D., and Abrahamse, H. (2005). Biological effects of helium-neon laser irradiation on normal and wounded human skin fibroblasts. *Photomed. Laser Surg.* 23, 251–259. doi: 10.1089/pho.2005.23.251

Kasuya, S., Kato-Kogoe, N., Omori, M., Yamamoto, K., Taguchi, S., and Fujita, H. (2018). New bone formation process using bio-oss and collagen membrane for rat calvarial bone defect: histological observation. *Implant Dent.* 27, 158–164. doi: 10.1097/ID.0000000000000738

Kunimatsu, R., Gunji, H., Tsuka, Y., Yoshimi, Y., Awada, T., and Sumi, K. (2018). Effects of high-frequency near-infrared diode laser irradiation on the proliferation and migration of mouse calvarial osteoblasts. *Lasers Med. Sci.* 33, 959–966. doi: 10.1007/s10103-017-2426-0

Marques, L., Holgado, L. A., Francischone, L. A., Ximenez, J. P., Okamoto, R., and Kinoshita, A. (2015). New LLLT protocol to speed up the bone healing process-histometric and immunohistochemical analysis in rat calvarial bone defect. *Lasers Med. Sci.* 30, 1225–1230. doi: 10.1007/s10103-014-1580-x

Matsumoto, M. A., Ferino, R. V., Monteleone, G. F., and Ribeiro, D. A. (2009). Low-level laser therapy modulates cyclo-oxygenase-2 expression during bone repair in rats. *Lasers Med. Sci.* 24, 195–201. doi: 10.1007/s10103-008-0544-4

Moreira, G. S., Machado Alves, P. H., Esper, L. A., Sbrana, M. C., da Silva Dalben, G., and Neppelenbroek, K. H. (2018). Effect of low-level laser on the healing of bone defects filled with autogenous bone or bioactive glass: in vivo study. *Int. J. Oral Maxillofac Implants* 33, 169–174. doi: 10.11607/jomi.5900

Noba, C., Mello-Moura, A., Gimenez, T., Tedesco, T. K., and Moura-Netto, C. (2018). Laser for bone healing after oral surgery: systematic review. *Lasers Med. Sci.* 33, 667–674. doi: 10.1007/s10103-017-2400-x

Ozawa, Y., Shimizu, N., Kariya, G., and Abiko, Y. (1998). Low-energy laser irradiation stimulates bone nodule formation at early stages of cell culture in rat calvarial cells. *Bone* 22, 347–354. doi: 10.1016/s8756-3282(97)00294-9

Pinheiro, A. L., Soares, L. G., Barbosa, A. F., Ramalho, L. M., and dos Santos, J. N. (2012). Does LED phototherapy influence the repair of bone defects grafted with MTA, bone morphogenetic proteins, and guided bone regeneration? A description of the repair process on rodents. *Lasers Med. Sci.* 27, 1013–1024. doi: 10.1007/s10103-011-1033-8

Ramalingam, S., Al-Rasheed, A., ArRejaie, A., Nooh, N., Al-Kindi, M., and Al-Hezaimi, K. (2016). Guided bone regeneration in standardized calvarial defects using beta-tricalcium phosphate and collagen membrane: a real-time in vivo micro-computed tomographic experiment in rats. *Odontology* 104, 199–210. doi: 10.1007/s10266-015-0211-8

Rasouli Ghahroudi, A. A., Rokn, A. R., Kalhori, K. A., Khorsand, A., Pournabi, A., Pinheiro, A. L., et al. (2014). Effect of low-level laser therapy irradiation and Bio-Oss graft material on the osteogenesis process in rabbit calvarium defects: a double blind experimental study. *Lasers Med. Sci.* 29, 925–932. doi: 10.1007/s10103-013-1403-5

Santinoni, C. D., Oliveira, H. F., Batista, V. E., Lemos, C. A., and Verri, F. R. (2017). Influence of low-level laser therapy on the healing of human bone maxillofacial defects: a systematic review. *J. Photochem. Photobiol. B, Biol.* 169, 83–89. doi: 10.1016/j.jphotobiol.2017.03.004

Schambach, S. J., Bag, S., Schilling, L., Groden, C., and Brockmann, M. A. (2010). Application of micro-CT in small animal imaging. *Methods (San Diego, Calif.)* 50, 2–13. doi: 10.1016/j.ymeth.2009.08.007

Schmidt, C., Priemel, M., Kohler, T., Weusten, A., Müller, R., and Amling, M. (2003). Precision and accuracy of peripheral quantitative computed tomography (pQCT) in the mouse skeleton compared with histology and microcomputed tomography (microCT). *J. Bone Miner Res.* 18, 1486–1496. doi: 10.1359/jbmr.2003.18.8.1486

Sert Kuniyoshi, F. H., Singh, P., Gami, A. S., Garcia-Touchard, A., van der Walt, C., Pusalavidyasagar, S., et al. (2011). Patients with obstructive sleep apnea exhibit impaired endothelial function after myocardial infarction. *Chest* 33140, 62–67. doi: 10.1378/chest.10-1722

Tarride, J. E., Burke, N., Leslie, W. D., Morin, S. N., Adachi, J. D., and Papaioannou, A. (2016). Loss of health related quality of life following low-trauma fractures in the elderly. *BMC Geriatr.* 16:84. doi: 10.1186/s12877-016-0259-5

Vajgel, A., Mardas, N., Farias, B. C., Petrie, A., Cimões, R., and Donos, N. (2014). A systematic review on the critical size defect model. *Clin. Oral Implants Res.* 25, 879–893. doi: 10.1111/clr.12194

Vasquez, E. C., Johnson, R. F., Beltz, T. G., Haskell, R. E., Davidson, B. L., and Johnson, A. K. (1998). Replication-deficient adenovirus vector transfer of gfp reporter gene into supraoptic nucleus and subfornical organ neurons. *Expl. Neurol.* 154, 353–365. doi: 10.1006/exnr.1998.6917

Vasquez, E. C., Lewis, S. J., Varner, K. J., and Brody, M. J. (1992). Chronic lesion of rostral ventrolateral medulla in spontaneously hypertensive rats. *Hypertension* 1979 19(Suppl. 2), II154–II158. doi: 10.1161/01.hyp.19.2_suppl.ii154

Vasquez, E. C., Meyrelles, S. S., Mauad, H., and Cabral, A. M. (1997). Neural reflex regulation of arterial pressure in pathophysiological conditions: interplay among the baroreflex, the cardiopulmonary reflexes and the chemoreflex. *Brazilian J. Med. Biol. Res.* 30, 521–532. doi: 10.1590/s0100-879x1997000400014

Viña, D., Seoane, N., Vasquez, E. C., and Campos-Toimil, M. (2021). cAMP Compartmentalization in cerebrovascular endothelial cells: new therapeutic opportunities in Alzheimer's disease. *Cells* 10:1951. doi: 10.3390/cells10081951

Wang, Y. H., Wu, J. Y., Kong, S. C., Chiang, M. H., Ho, M. L., and Yeh, M. L. (2018). Low power laser irradiation and human adipose-derived stem cell treatments promote bone regeneration in criticalsized calvarial defects in rats. *PLoS One* 13:e0195337. doi: 10.1371/journal.pone.0195337

Wijbenga, J. G., Schepers, R. H., Werker, P. M., Witjes, M. J., and Dijkstra, P. U. (2016). A systematic review of functional outcome and quality of life following reconstruction of maxillofacial defects using vascularized free fibula flaps and dental rehabilitation reveals poor data quality. *J. Plast, Reconstr. Aesthet. Surg: JPRAS* 69, 1024–1036. doi: 10.1016/j.bjps.2016.05.003

Conflict of Interest: The authors declare that the research was conducted in the absence of any commercial or financial relationships that could be construed as a potential conflict of interest.

Publisher's Note: All claims expressed in this article are solely those of the authors and do not necessarily represent those of their affiliated organizations, or those of the publisher, the editors and the reviewers. Any product that may be evaluated in this article, or claim that may be made by its manufacturer, is not guaranteed or endorsed by the publisher.

Copyright © 2022 Santos, Silva, Rovaris, Sousa, Dantas, Loureiro, Pereira, Meyrelles, Bertollo and Vasquez. This is an open-access article distributed under the terms of the Creative Commons Attribution License (CC BY). The use, distribution or reproduction in other forums is permitted, provided the original author(s) and the copyright owner(s) are credited and that the original publication in this journal is cited, in accordance with accepted academic practice. No use, distribution or reproduction is permitted which does not comply with these terms.

frontiers in Physiology

OPINION
published: 28 February 2022
doi: 10.3389/fphys.2022.831568

Unraveling Brain Microcircuits, Dendritic Spines, and Synaptic Processing Using Multiple Complementary Approaches

Alberto A. Rasia-Filho [1,2*]

[1] *Department of Basic Sciences/Physiology, Graduate Program in Biosciences, Universidade Federal de Ciências da Saúde de Porto Alegre, Porto Alegre, Brazil,* [2] *Graduate Program in Neuroscience, Universidade Federal do Rio Grande do Sul, Porto Alegre, Brazil*

Keywords: brain cytology, neural networks, neural plasticity, neuronal morphology, higher-order processing, synaptic plasticity

OPEN ACCESS

Edited by:
James Todd Pearson, National Cerebral and Cardiovascular Center, Japan

Reviewed by:
Pirta Elina Hotulainen, Minerva Foundation Institute for Medical Research, Finland
Mathias De Roo, Université de Genève, Switzerland

***Correspondence:**
Alberto A. Rasia-Filho
aarf@ufcspa.edu.br; rasiafilho@yahoo.com

Specialty section:
This article was submitted to Integrative Physiology, a section of the journal Frontiers in Physiology

Received: *08 December 2021*
Accepted: *26 January 2022*
Published: *28 February 2022*

Citation:
Rasia-Filho AA (2022) Unraveling Brain Microcircuits, Dendritic Spines, and Synaptic Processing Using Multiple Complementary Approaches. Front. Physiol. 13:831568. doi: 10.3389/fphys.2022.831568

INTRODUCTION

Innovative experimental approaches and technological advancements have provided an unprecedented level of detail for the nervous system. New findings advanced our knowledge about the complexity of genetic profiles, neuroanatomical and connectional parcellation of cortical areas, and cytoarchitectonic and synaptic organization in humans compared to other species (DeFelipe, 2011; Vogt, 2015; Bruner et al., 2017; Hodge et al., 2019; Assem et al., 2020; Benavides-Piccione et al., 2020; Eze et al., 2021; Girskis et al., 2021; Viscardi et al., 2021). We can now observe neuronal features on a nanoscale level and envisage possible links for cells and circuits when identifying genes, constitutive proteins, subpopulations of neurons, networks with high-speed actions, higher-ordered mental states, and a multitude of disparate behaviors (Fuzik et al., 2016; Turcotte et al., 2019; Hodge et al., 2020; Close et al., 2021; Demas et al., 2021; Helm et al., 2021). Therefore, we need to integrate different fields of knowledge about dendritic spines into a coherent vision of where this field of research is going using new techniques (**Figure 1**).

Dendritic spines are specialized postsynaptic compartments (Yuste, 2010; Stewart et al., 2014; Helm et al., 2021) for monosynaptic or, in some cases, multisynaptic inputs (Brusco et al., 2014; Dall'Oglio et al., 2015). Spines are significant in that their morphology appears to change with various inputs and brain disorders (Chidambaram et al., 2019; Baczyńska et al., 2021). Understanding their role in synaptic connectivity is a fruitful approach to elucidating relationships among connectivity of different cellular structures in the brain. However, the study of spines represents a huge challenge when considering neural networks that show region- and cell type-specific characteristics and differences within and among species [Lavenex et al., 2009; Cembrowski and Spruston, 2019; Hodge et al., 2019; Winnubst et al., 2019; Yang et al., 2019; BRAIN Initiative Cell Census Network (BICCN), 2021]. Complementary approaches to the structure-function relationship of the components of an inherently intricate system as the brain are needed. For example, *in vitro* and *in vivo* studies demonstrate the high level of structural and functional complexity of the cerebral cortex (Scheperjans et al., 2008; Rigotti et al., 2013; Vogt, 2015; Glasser et al., 2016; Real et al., 2018; Leopold et al., 2019; Assem et al., 2020; Finkelstein et al., 2021; Foster et al., 2021). In both allocortex and neocortex, morphological heterogeneity within classical

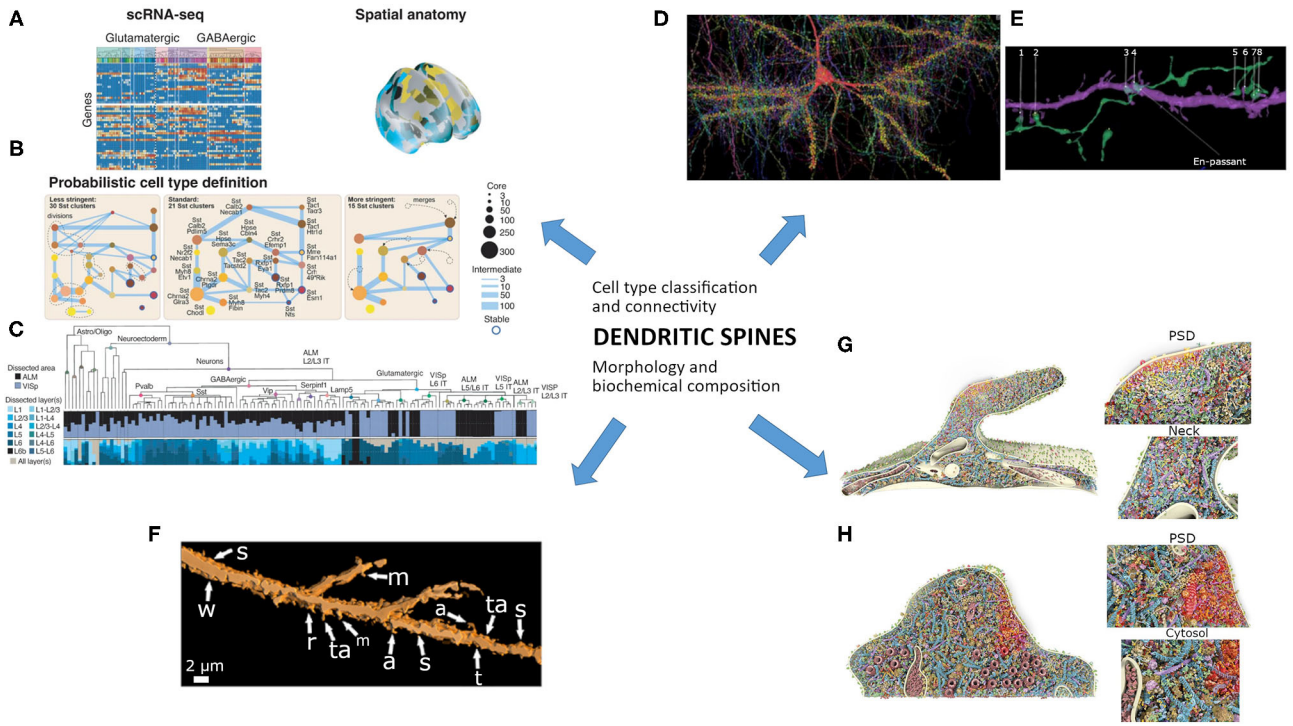

FIGURE 1 | The study of dendritic spines needs to integrate different current fields of knowledge into a coherent vision. Cell type classification and connectivity would be associated with morphology and nanoscale biochemical composition. **(A–C)** The probabilistic definition of a neuronal type needs that: **(A)** "A transcriptome-based cell-type taxonomy is constructed from scRNA-seq data, related epigenomic datasets and neuroanatomy. **(B)** Cell types are initially defined based on transcriptomic signatures in a probabilistic manner with multiresolution clustering and statistical analysis to identify robustness and variability. **(C)** Reproducible gene expression patterns identify hierarchies of putative cell types that are subject to further analyses and validation." **(A–C)** are reproduced and adapted from Yuste et al. (2020) "A community-based transcriptomics classification and nomenclature of neocortical cell types" (a–c images from Figure 5 were reused without changes), Nat. Neurosci. 23, 1456–1468, doi: 10.1038/s41593-020-0685-8; used under CC BY 4.0 license and copyright. **(D,E)** Image of a petascale reconstruction of human parietal cortex for the study of cells and connectivity. **(D)** "The axonal innervation to a "pyramidal cell (red) is rendered along with all incoming synapses (yellow discs) and presynaptic axons." **(E)** "Excitatory axon forming 8 synapses onto a spiny dendrite of an excitatory cell. One of these connections is *en passant*, the rest required directed growth of the axon to contact this same dendrite." Note the axo-spinous contacts (numbered 1, 2, 5–8), which would be further studied by focused ion beam/scanning electron microscopy. **(D,E)** are reproduced and slightly adapted from Shapson-Coe et al. (2021) "A connectomic study of a petascale fragment of human cerebral cortex" (removed letters and changed number size from the original Figure 6), bioRxiv 2021.05.29.446289; doi: 10.1101/2021.05.29.446289; used under aCC-BY-NC-ND 4.0 International license and copyright. **(F)** Morphological features of 3D-reconstructed dendritic spines of a Golgi-impregnated neuron from the human cortical amygdala. Spine shapes include: stubby (s), wide (w), thin (t), mushroom-like (m), ramified (r), transitional (ta), atypical (a) or multiform. Reused and slightly adapted from Vásquez et al. (2018) "Neuronal types of the human cortical amygdaloid nucleus" (Figure 6e), J. Comp. Neurol. 526, 2776–2801. doi: 10.1002/cne.24527; under license # 5223180562839 from Copyright Clearance Center's RightsLink® originally published by John Wiley & Sons, Inc. **(G,H)** 3D model of dendritic spines using large-scale nanoscopy and biochemistry analysis. Multiple constitutive proteins are colored and "shown to scale, with the copy numbers and locations measured in this study and configurations according to literature. For clarity, the highly abundant monomeric actin is not shown. **(G)** View into a mushroom spine. Magnifications into the postsynaptic density (PSD, highlighted with red glow) and neck are depicted. **(H)** View into a stubby spine. Again, a magnification of the PSD is shown and a zoom into the cytosolic region of the spine." Reused and slight adaptation from Helm et al. (2021) manuscript) after Helm et al. (2021) "A large-scale nanoscopy and biochemistry analysis of postsynaptic dendritic spines" (removed letters in Figure 7), Nat. Neurosci. 24, 1151–1162. doi: 10.1038/s41593-021-00874-w under license # 5223201496130 from Copyright Clearance Center's RightsLink®, originally published by Springer Nature.

cell types can be the rule as occur for the spiny pyramidal neurons (Morishima and Kawaguchi, 2006; Ramaswamy and Markram, 2015; Cembrowski and Spruston, 2019; Benavides-Piccione et al., 2020; Rasia-Filho et al., 2021). Indeed, discrete and continuous variations may coexist and underlie cell-type diversity, forming a "combination of specification through evolutionarily driven and developmentally regulated genetic mechanisms, and refinement of cellular identities through intercellular interactions within the network in which the cells are embedded" [BRAIN Initiative Cell Census Network (BICCN), 2021]. Henceforth, the probabilistic definition of each neuronal type will require single-cell transcriptomic data associated to morphology (**Figure 1A**; Hodge et al., 2019; Yuste et al., 2020). Dendritic spines may be further studied in specific subpopulations of neurons and circuits to address their functional roles in information processing (**Figure 1B**).

BRAIN NETWORKS, CELLULAR CONNECTIVITY, AND THE RELEVANCE OF DENDRITIC SPINES

Recent approaches advanced the study of brain cells, microcircuits, and connections. The connectomic study of a fragment of the human temporal cortex (1 mm^3, >5,000 slices cut at ∼30 nm), imaged using a high-speed multi-beam scanning electron microscopy (EM) and three-dimensional (3D) reconstruction, exhibited 57,216 cells and ∼133 million synapses in a 1.4-petabyte volume (Shapson-Coe et al., 2021). Dense digital reconstruction of a 0.3 mm^3 cortical circuit containing ∼31,000 neurons, ∼37 million excitatory and inhibitory synapses, and 55 morphological cell types served to identify hub neurons that could modulate cortical dynamics (Gal et al., 2021). Additional highly multiplexed, high-resolution brain-wide cell-type mapping, and high-throughput spatially resolved transcriptomics approaches can link cell types with connectivity mapping and functional data (Close et al., 2021) for advanced molecular neuroanatomical maps (Ortiz et al., 2021). Some techniques may link functional data with different spatial scales. For example, patch-clamp electrophysiology and single-cell semi-quantitative PCR would identify neuronal subtypes (Fuzik et al., 2016). On the other hand, high-resolution magnetic resonance imaging (MRI) would locate different nuclei in the brain (Saygin et al., 2017 for human amygdala) and help to identify likely borders for each area of interest (e.g., to separate the medial and cortical amygdaloid nuclei, Dall'Oglio et al., 2013; Vásquez et al., 2018). These data are relevant for understanding the complex expression of emotion in different species (Quirk et al., 1995; Zebarjadi et al., 2021; including mice affiliative touch in prosocial interaction, Wu et al., 2021) and what feelings are to humans (Zeki, 2007; Gendron and Barrett, 2009; de Boer et al., 2012; Diano et al., 2017; LeDoux and Brown, 2017; Fogazzi et al., 2020; Šimić et al., 2021).

To process manifold stimuli from external and internal milieux engenders specialization and functional integration of neural areas, cells, and networks (e.g., Rasia-Filho, 2006; Rasia-Filho et al., 2018; Freiwald, 2020; Barnett et al., 2021). Dendritic spine function comprises an important part of this complex scenario (Ramón y Cajal, 1909–1911; Bourne and Harris, 2009; von Bohlen und Halbach, 2009; Yuste, 2010; Spruston et al., 2013; Dall'Oglio et al., 2015; Helm et al., 2021). That is, spines increase the connectivity between neurons and the packing density of synapses without increasing the brain's overall volume (Bourne and Harris, 2009). This feature adds and maximizes the connectivity repertoire governing the shape of dendritic arbors (Wen et al., 2009). Dendritic spines modulate the excitatory synaptic transmission in the brain. The majority of input contacts on dendritic spines are from glutamatergic axon terminals (Yuste, 2013; but see also GABAergic and dopaminergic innervation in Brusco et al., 2014; Kubota et al., 2016; Iino et al., 2020; Kasai et al., 2021). Spines are morphologically diverse, ranging in a *continuum* of number, shape, and size classified according to their head and neck features (**Figure 1C**). These include: stubby/wide, thin, mushroom, ramified, "atypical" or multiform spines, including "intermediate" shapes, "double" spines, and thorny excrescences, among others (Fiala and Harris, 1999; Arellano et al., 2007; Bourne and Harris, 2007, 2009; Stewart et al., 2014; Fuentealba-Villarroel et al., 2021; see also Ruszczycki et al., 2012; Pchitskaya and Bezprozvanny, 2020). Spine shape involves local actin organization, second messengers, and organelles (e.g., endoplasmic reticulum and ribosomes, Yuste, 2010; Sala and Segal, 2014; Miermans et al., 2017; Okabe, 2020; for mitochondria see Li et al., 2004). This can lead to biochemical compartmentalization and affect the electrical signaling of synapses (Chen and Sabatini, 2012; Tønnesen and Nägerl, 2016; Obashi et al., 2021). The balance between spine number, structure, and function may represent synaptic processing for learning and memory (Bourne and Harris, 2007, 2009) with stimulus-specific features (Knafo et al., 2005) in selective synaptic ensembles (Hayashi-Takagi et al., 2015). Optogenetic manipulation allowed the identification and erasure of specific synaptic memory traces in potentiated spines of the mouse motor cortex (Hayashi-Takagi et al., 2015). This was a remarkable achievement since the functional mapping of single-spine synaptic inputs to the same dendrite can be highly heterogeneous, as revealed by high-resolution two-photon imaging of auditory-evoked NMDA-dependent calcium transients in mouse cortical neurons *in vivo* (Chen et al., 2011).

Dendritic spine dynamics in different neural circuits result from various phenomena. These include phylogenetic, ontogenetic, and epigenetic events (García-López et al., 2010; DeFelipe, 2011; Reza-Zaldivar et al., 2020). Activity-dependent and activity-independent actions promote stabilization, differentiation, and remodeling with enlargement or shrinkage and pruning of spines (Oray et al., 2006; Zancan et al., 2018; Runge et al., 2020; Kasai et al., 2021). Spines can be found relatively isolated or in clusters in the same dendritic segments, as evidenced after 3D image reconstruction of Golgi-impregnated neurons in humans from our laboratory (Reberger et al., 2018; Rasia-Filho et al., 2021) and other approaches using transmission EM (Arellano et al., 2007; Bourne and Harris, 2009; Brusco et al., 2014; Stewart et al., 2014), rapid structured illumination microscopy and enhanced resolution confocal microscopy (for spinules, Zaccard et al., 2020), high-resolution transmission, focused ion beam (FIB) scanning and EM tomography (Rollenhagen et al., 2020), and/or FIB/scanning EM in humans and other animals (Cano-Astorga et al., 2021). Clustered spines can show spike-timing-dependent cooperativity and plasticity (Tazerart et al., 2020). Therefore, synaptic integration made by each spine type can impact cellular activity differently depending upon its location and spatiotemporal processing along proximal to distal dendritic domains (Spruston et al., 2013). In addition, its passive and/or active biophysical properties associated with those of parent dendrites may play a role (Sala and Segal, 2014; Gidon et al., 2020; Obashi et al., 2021). Dendritic spines modulate both stable and/or transitory connections (Oray et al., 2006) and synaptic plasticity using various molecules in variable biochemical pathways for short-term to long-term cellular effects (Sala and Segal, 2014; Chidambaram et al., 2019).

There are many frontiers to explore the structure and integrated function of dendritic spines for synaptic plasticity. The impact of heterogeneous glial cells and the role of the extracellular matrix in tetrapartite synapses need to be addressed (Chelini et al., 2018; Mederos et al., 2018; Tønnesen et al., 2018; Nguyen et al., 2020; Klimczak et al., 2021). The elucidation of the evolutionary reason for the divergence in gene expression patterns in the cerebral cortex, and the features that determine neuronal diversity and specialization in humans are important (Hodge et al., 2019, 2020; Kalmbach et al., 2021). Regarding the latter, some features of human cortical pyramidal neurons include: (1) larger dendritic length and branch complexity than macaque and mice (Mohan et al., 2015; Benavides-Piccione et al., 2020); (2) a class of calcium-mediated graded dendritic action potentials that would classify linearly non-separable inputs (Gidon et al., 2020); and (3) membrane properties that significantly enhance synaptic charge-transfer from dendrites to soma and spike propagation along the axon (Eyal et al., 2016). This indicates that extrapolations on some neuronal features from other species to the human brain have to be done carefully. Human dendritic spines are systematically larger and longer and exist at higher densities than in the mouse cortex (Benavides-Piccione et al., 2020), likely increasing our capacity of synaptic processing and plasticity (DeFelipe, 2011). Human spines, also, show a high diversity of size and shapes (Dall'Oglio et al., 2015; Vásquez et al., 2018; Rasia-Filho et al., 2021). The functional implication of long "silent" spines (Yuste, 2013) and those of convoluted shapes, observed from subcortical to cortical human neurons (Dall'Oglio et al., 2015; Fuentealba-Villarroel et al., 2021), need additional studies. Multiform spines likely indicate the existence of multisynaptic sites for signaling compartmentalization and further computational possibilities within functional microdomains (Chen and Sabatini, 2012; Dall'Oglio et al., 2015; Reberger et al., 2018).

The postsynaptic density (PSD) is a dense area behind the postsynaptic membrane, as seen by EM. It consists of many proteins, including receptors, ion channels, and adhesion proteins, shared with the membrane, cytoskeletal proteins, and scaffolding proteins, all arranged in a hierarchical fashion (Cohen, 2013). Like dendritic spines, PSDs can display morphological alterations with various physiological and behavioral inputs. PSD area can relate to spine head diameter (Arellano et al., 2007) depending on an NMDA receptor-mediated long-term potentiation plasticity (Borczyk et al., 2019). Stubby and mushroom spines show similar average protein copy number and topology for PSD composition identified after summing EM, stimulated emission depletion microscopy, mass spectrometry, fluorescence microscopy, and 3D reconstruction procedures in cultured hippocampal neurons of rats (Helm et al., 2021; **Figure 1D**). However, proteins related to synaptic strength, spine dynamics, ion channels, endocytosis cofactors, cytoskeletal structure, signaling and trafficking, secretory proteins, and ribosomes are more evident in mushroom spines (Helm et al., 2021). These findings open the possibility to test different spines also in neuropathological conditions (Forrest et al., 2018; Chidambaram et al., 2019; Runge et al., 2020; Baczyńska et al., 2021; Montero-Crespo et al., 2021). From this perspective, dendritic spines are sexually dimorphic and/or affected by gonadal steroids (Woolley and McEwen, 1993; Rasia-Filho et al., 2012; Luine and Frankfurt, 2020), sexual experience and motherhood (Rasia-Filho et al., 2004; Zancan et al., 2018). These phenomena are relevant to sexual differentiation in healthy brain connectivity and as a biological variable in neuropsychiatric research (Joel and McCarthy, 2017; Rubinow and Schmidt, 2019; Arnold, 2020; Hidalgo-Lopez et al., 2021).

Lastly, the human cerebral cortex shows a highly polygenic architecture (Grasby et al., 2020) and ∼16 billion neurons (Herculano-Houzel et al., 2014). One cortical pyramidal neuron can form ∼30,000 synapses, 90% of them being excitatory (DeFelipe, 2011). From ∼100 trillion spines in the human cortex (Kasai et al., 2021), ∼99.5% of all spines lie in pyramidal neurons (Kubota et al., 2016; see also Foggetti et al., 2019) for the organization of the ongoing synaptic transmission from multiple neurochemical circuits (Palomero-Gallagher and Zilles, 2019). This complexity is exemplified by the huge spine density and shape variation in a human CA1 pyramidal neuron related to circuits for memory modulation and self-identity (see Figure 9 in Rasia-Filho et al., 2021). On a spine-by-spine basis (Oray et al., 2006), there can be a high degree of synaptic processing arising from spatiotemporal and functional heterogeneity among individual synapses on the same dendrite, between different neurons, and across and between brain regions (Grant and Fransén, 2020). Synaptic diversity and strength are finely adjusted to code information (Grant and Fransén, 2020), enabling coincidence detection (Chabrol et al., 2015) and merging multimodal inputs from parallel pathways (Soltesz and Losonczy, 2018). The integrated synaptic processing and complex plasticity linked to the role of an increasing number of specialized neurons and glia cells within circuits may ultimately lead to the emergence of multiple sensorimotor, cognitive, emotional, abstract, creative and conscious elaborations, visceral reactions, and behavioral displays (for a parallel discussion see Timo-Iaria and Valle, 1995; DeFelipe, 2011; Jezek et al., 2011; Hodge et al., 2019; Freiwald, 2020; Grant and Fransén, 2020; Rasia-Filho et al., 2021).

CONCLUSION

Dendritic spines are key elements for innovative research in integrative physiology. Various approaches can expand our knowledge on spines studying them at both network-scale and synapse-scale in the brain. For example, we still do not know the implications of dendritic spines in different subpopulations of neurons for the cytoarchitectonics, rich networks connections, and complex information processing in the insular cortex. This is an interesting cortical area that is strongly activated when "you see the person you are in love with, try to listen to your own heartbeat, suffer from a headache, or crave for a chocolate cookie" (Gogolla, 2017; see also Benarroch, 2019). As mentioned by Mancuso et al. (2014): "Anatomical changes occur on a full range of scales from the trafficking of individual proteins, to alterations in synaptic morphology both individually and on a systems level, to reductions in long-distance connectivity and brain volume."

Dendritic spines relate to all these processes in the brain and with a notable integrative complexity in humans. Unraveling the dynamic role of dendritic spines for synaptic processing is a task that needs multiple complementary approaches. The level of complexity for this endeavor resides in the fact we are looking for representative data that is likely on the astonishing scale of 10^{15} ongoing connections in the human brain.

AUTHOR CONTRIBUTIONS

The author confirms being the sole contributor of this work and has approved it for publication.

FUNDING

Grants from the Brazilian Agencies CAPES and CNPq (Brazilian Ministry of Science Technology and Innovation RRID), Grant/Award Numbers: 314352/2020-1, SCR_002876.

ACKNOWLEDGMENTS

I thank Prof. Rochelle S. Cohen for her valuable suggestions on this manuscript and Mr. Josué Renner for his help with figure preparation.

REFERENCES

Arellano, J. I., Benavides-Piccione, R., DeFelipe, J., and Yuste, R. (2007). Ultrastructure of dendritic spines: correlation between synaptic and spine morphologies. *Front. Neurosci.* 1:131–143. doi: 10.3389/neuro.01.1.1.010.2007

Arnold, A. P. (2020). Sexual differentiation of brain and other tissues: five questions for the next 50 years. *Horm. Behav.* 120, 104691. doi: 10.1016/j.yhbeh.2020.104691

Assem, M., Glasser, M. F., Van Essen, D. C., and Duncan, J. (2020). A domain-general cognitive core defined in multimodally parcellated human cortex. *Cereb. Cortex* 30, 4361–4380. doi: 10.1093/cercor/bhaa023

Baczyńska, E., Pels, K. K., Basu, S., Włodarczyk, J., and Ruszczycki, B. (2021). Quantification of dendritic spines remodeling under physiological stimuli and in pathological conditions. *Int. J. Mol. Sci.* 22, 4053. doi: 10.3390/ijms22084053

Barnett, S. C., Parr-Brownliebde, L. C., Perry, B. A. L., Young, C. K., Wicky, H. E., Hughes, S. M., et al. (2021). Anterior thalamic nuclei neurons sustain memory. *Curr. Res. Neurobiol.* 2, 100022. doi: 10.1016/j.crneur.2021.100022

Benarroch, E. E. (2019). Insular cortex: functional complexity and clinical correlations. *Neurology* 93, 932–938. doi: 10.1212/WNL.0000000000008525

Benavides-Piccione, R., Regalado-Reyes, M., Fernaud-Espinosa, I., Kastanauskaite, A., Tapia-González, S., León-Espinosa, G., et al. (2020). Differential structure of hippocampal CA1 pyramidal neurons in the human and mouse. *Cereb. Cortex* 30, 730–752. doi: 10.1093/cercor/bhz122

Borczyk, M., Sliwińska, M. A., Caly, A., and Bernas, T., Radwanska, K. (2019). Neuronal plasticity affects correlation between the size of dendritic spine and its postsynaptic density. *Sci. Rep.* 9, 1693. doi: 10.1038/s41598-018-38412-7

Bourne, J., and Harris, K. M. (2007). Do thin spines learn to be mushroom spines that remember? *Curr. Opin. Neurobiol.* 17, 381–386. doi: 10.1016/j.conb.2007.04.009

Bourne, J. N., and Harris, K. M. (2009). "Ultrastructural analysis of spine plasticity," in *Encyclopedia of Neuroscience*, ed L. R. Squire (New York, NY: Elsevier), 11–17. doi: 10.1016/B978-008045046-9.01771-X

BRAIN Initiative Cell Census Network (BICCN). (2021). A multimodal cell census and atlas of the mammalian primary motor cortex. *Nature* 598, 86–102. doi: 10.1038/s41586-021-03950-0

Bruner, E., Preuss, T. M., Chen, X., and Rilling, J. K. (2017). Evidence for expansion of the precuneus in human evolution. *Brain Struct. Funct.* 222, 1053–1060. doi: 10.1007/s00429-015-1172-y

Brusco, J., Merlo, S., Ikeda, É. T., Petralia, R. S., Kachar, B., Rasia-Filho, A. A., et al. (2014). Inhibitory and multisynaptic spines, and hemispherical synaptic specialization in the posterodorsal medial amygdala of male and female rats. *J. Comp. Neurol.* 522, 2075–2088. doi: 10.1002/cne.23518

Cano-Astorga, N., DeFelipe, J., and Alonso-Nanclares, L. (2021). Three-dimensional synaptic organization of layer III of the human temporal neocortex. *Cereb. Cortex* 31, 4742–4764. doi: 10.1093/cercor/bhab120

Cembrowski, M. S., and Spruston, N. (2019). Heterogeneity within classical cell types is the rule: lessons from hippocampal pyramidal neurons. *Nat. Rev. Neurosci.* 20, 193–204. doi: 10.1038/s41583-019-0125-5

Chabrol, F. P., Arenz, A., Wiechert, M. T., Margrie, T. W., and DiGregorio, D. A. (2015). Synaptic diversity enables temporal coding of coincident multisensory inputs in single neurons. *Nat. Neurosci.* 18, 718–727. doi: 10.1038/nn.3974

Chelini, G., Pantazopoulos, H., Durning, P., and Berretta, S. (2018). The tetrapartite synapse: a key concept in the pathophysiology of schizophrenia. *Eur. Psychiatry* 50, 60–69. doi: 10.1016/j.eurpsy.2018.02.003

Chen, X., Leischner, U., Rochefort, N. L., Nelken, I., and Konnerth, A. (2011). Functional mapping of single spines in cortical neurons *in vivo*. *Nature* 475, 501–505. doi: 10.1038/nature10193

Chen, Y., and Sabatini, B. L. (2012). Signaling in dendritic spines and spine microdomains. *Curr. Opin. Neurobiol.* 22, 389–396. doi: 10.1016/j.conb.2012.03.003

Chidambaram, S. B., Rathipriya, A. G., Bolla, S. R., Bhat, A., Ray, B., Mahalakshmi, A. M., et al. (2019). Dendritic spines: revisiting the physiological role. *Prog. Neuropsychopharmacol. Biol. Psychiatry* 92, 161–193. doi: 10.1016/j.pnpbp.2019.01.005

Close, J. L., Long, B. R., and Zeng, H. (2021). Spatially resolved transcriptomics in neuroscience. *Nat. Methods* 18, 23–25. doi: 10.1038/s41592-020-01040-z

Cohen, R. S. (2013). "The postsynaptic density," in *Neuroscience in the 21st Century*, ed D. W. Pfaff (New York, NY: Springer), 403–437. doi: 10.1007/978-1-4614-1997-6_17

Dall'Oglio, A., Dutra, A. C., Moreira, J. E., and Rasia-Filho, A. A. (2015). The human medial amygdala: structure, diversity, and complexity of dendritic spines. *J. Anat.* 227, 440–459. doi: 10.1111/joa.12358

Dall'Oglio, A., Xavier, L. L., Hilbig, A., Ferme, D., Moreira, J. E., Achaval, M., et al. (2013). Cellular components of the human medial amygdaloid nucleus. *J. Comp. Neurol.* 521, 589–611. doi: 10.1002/cne.23192

de Boer, A., Van Buel, E. M., and Ter Horst, G. J. (2012). Love is more than just a kiss: a neurobiological perspective on love and affection. *Neuroscience* 201, 114–124. doi: 10.1016/j.neuroscience.2011.11.017

DeFelipe, J. (2011). The evolution of the brain, the human nature of cortical circuits, and intellectual creativity. *Front. Neuroanat.* 5, 29. doi: 10.3389/fnana.2011.00029

Demas, J., Manley, J., Tejera, F., Barber, K., Kim, H., Traub, F. M., et al. (2021). High-speed, cortex-wide volumetric recording of neuroactivity at cellular resolution using light beads microscopy. *Nat. Methods* 18, 1103–1111. doi: 10.1038/s41592-021-01239-8

Diano, M., Tamietto, M., Celeghin, A., Weiskrantz, L., Tatu, M. K., Bagnis, A., et al. (2017). Dynamic changes in amygdala psychophysiological connectivity reveal distinct neural networks for facial expressions of basic emotions. *Sci. Rep.* 7, 1–13. doi: 10.1038/srep45260

Eyal, G., Verhoog, M. B., Testa-Silva, G., Deitcher, Y., Lodder, J. C., Benavides-Piccione, R., et al. (2016). Unique membrane properties and enhanced signal processing in human neocortical neurons. *eLife* 5:e16553. doi: 10.7554/eLife.16553

Eze, U. C., Bhaduri, A., Haeussler, M., Nowakowski, T. J., and Kriegstein, A. R. (2021). Single-cell atlas of early human brain development highlights heterogeneity of human neuroepithelial cells and early

radial glia. *Nat. Neurosci.* 24, 584–594. doi: 10.1038/s41593-020-00794-1

Fiala, J. C., and Harris, K. M. (1999). "Dendrite structure," in *Dendrites*, eds G. Stuart, N. Spruston, and M. Häusser (New York, NY: Oxford University Press), 1–34.

Finkelstein, A., Fontolan, L., Economo, M. N., Li, N., Romani, S., et al. (2021). Attractor dynamics gate cortical information flow during decision-making. *Nat. Neurosci.* 24, 843–850. doi: 10.1038/s41593-021-00840-6

Fogazzi, D. V., Neary, J. P., Sonza, A., Reppold, C. T., Kaiser, V., Scassola, C. M., et al. (2020). The prefrontal cortex conscious and unconscious response to social/emotional facial expressions involve sex, hemispheric laterality, and selective activation of the central cardiac modulation. *Behav. Brain Res.* 393, 112773. doi: 10.1016/j.bbr.2020.112773

Foggetti, A., Baccini, G., Arnold, P., Schiffelholz, T., and Wulff, P. (2019). Spiny and non-spiny parvalbumin-positive hippocampal interneurons show different plastic properties. *Cell Rep.* 27, 3725–3732.e5. doi: 10.1016/j.celrep.2019.05.098

Forrest, M. P., Parnell, E., and Penzes, P. (2018). Dendritic structural plasticity and neuropsychiatric disease. *Nat. Rev. Neurosci.* 19, 215–234. doi: 10.1038/nrn.2018.16

Foster, N. N., Barry, J., Korobkova, L., Garcia, L., Gao, L., Becerra, M., et al. (2021). The mouse cortico–basal ganglia–thalamic network. *Nature* 598, 188–194. doi: 10.1038/s41586-021-03993-3

Freiwald, W. A. (2020). Social interaction networks in the primate brain. *Curr. Opin. Neurobiol.* 65, 49–58. doi: 10.1016/j.conb.2020.08.012

Fuentealba-Villarroel, F. J., Renner, J., Hilbig, A., Bruton, O. J., and Rasia-Filho, A. A. (2021). Spindle-shaped neurons in the human posteromedial (precuneus) cortex. *Front. Synaptic Neurosci.* 13, 769228. doi: 10.3389/fnsyn.2021.769228

Fuzik, J., Zeisel, A., Máté, Z., Calvigioni, D., Yanagawa, Y., Szabó, G., et al. (2016). Integration of electrophysiological recordings with single-cell RNA-seq data identifies neuronal subtypes. *Nat. Biotech.* 34, 175–183. doi: 10.1038/nbt.3443

Gal, E., Amsalem, O., Schindel, A., London, M., Schürmann, F., Markram, H., et al. (2021). The role of hub neurons in modulating cortical dynamics. *Front. Neural Circuits* 15, 718270. doi: 10.3389/fncir.2021.718270

García-López, P., García-Marín, V., and Freire, M. (2010). Dendritic spines and development: towards a unifying model of spinogenesis - a present day review of Cajal's histological slides and drawings. *Neural Plast.* 2010, 769207. doi: 10.1155/2010/769207

Gendron, M., and Barrett, L. F. (2009). Reconstructing the past: A century of ideas about emotion in psychology. *Emotion Rev.* 1, 316–339. doi: 10.1177/1754073909338877

Gidon, A., Zolnik, T. A., Fidzinski, P., Bolduan, F., Papoutsi, A., Poirazi, P., et al. (2020). Dendritic action potentials and computation in human layer 2/3 cortical neurons. *Science* 367, 83–87. doi: 10.1126/science.aax6239

Girskis, K. M., Stergachis, A. B., DeGennaro, E. M., Doan, R. N., Qian, X., Johnson, M. B., et al. (2021). Rewiring of human neurodevelopmental gene regulatory programs by human accelerated regions. *Neuron* 109, 239–3251.e7. doi: 10.1016/j.neuron.2021.08.005

Glasser, M. F., Coalson, T. S., Robinson, E. C., Hacker, C. D., Harwell, J., Yacoub, E., et al. (2016). A multi-modal parcellation of human cerebral cortex. *Nature* 536, 171–178. doi: 10.1038/nature18933

Gogolla, N. (2017). The insular cortex. *Curr. Biol.* 27, R580–586. doi: 10.1016/j.cub.2017.05.010

Grant, S. G., and Fransén, E. (2020). The synapse diversity dilemma: molecular heterogeneity confounds studies of synapse function. *Front. Synaptic Neurosci.* 12:590403. doi: 10.3389/fnsyn.2020.590403

Grasby, K. L., Jahanshad, N., Painter, J. N., Colodro-Conde, L., Bralten, J., Hibar, D. P., et al. (2020). The genetic architecture of the human cerebral cortex. *Science* 367, eaay6690. doi: 10.1126/science.aay6690

Hayashi-Takagi, A., Yagishita, S., Nakamura, M., Shirai, F., Wu, Y. I., Loshbaugh, A. L., et al. (2015). Labeling and optical erasure of synaptic memory traces in the motor cortex. *Nature* 525, 333–338. doi: 10.1038/nature15257

Helm, M. S., Dankovich, T. M., Mandad, S., Rammner, B., Jähne, S., Salimi, V., et al. (2021). A large-scale nanoscopy and biochemistry analysis of postsynaptic dendritic spines. *Nat. Neurosci.* 24, 1151–1162. doi: 10.1038/s41593-021-00874-w

Herculano-Houzel, S., Manger, P. R., and Kaas, J. H. (2014). Brain scaling in mammalian evolution as a consequence of concerted and mosaic changes in numbers of neurons and average neuronal cell size. *Front. Neuroanat.* 8:77. doi: 10.3389/fnana.2014.00077

Hidalgo-Lopez, E., Zeidman, P., Harris, T., Razi, A., and Pletzer, B. (2021). Spectral dynamic causal modeling in healthy women reveals brain connectivity changes along the menstrual cycle. *Commun Biol.* 4:954. doi: 10.1038/s42003-021-02447-w

Hodge, R. D., Bakken, T. E., Miller, J. A., Smith, K. A., Barkan, E. R., Graybuck, L. T., et al. (2019). Conserved cell types with divergent features in human versus mouse cortex. *Nature* 573, 61–68. doi: 10.1038/s41586-019-1506-7

Hodge, R. D., Miller, J. A., Novotny, M., Kalmbach, B. E., Ting, J. T., Bakken, T. E., et al. (2020). Transcriptomic evidence that von Economo neurons are regionally specialized extratelencephalic-projecting excitatory neurons. *Nat. Commun.* 11, 1172. doi: 10.1038/s41467-020-14952-3

Iino, Y., Sawada, T., Yamaguchi, K., Tajiri, M., Ishii, S., Kasai, H., et al. (2020). Dopamine D2 receptors in discrimination learning and spine enlargement. *Nature* 579, 555–560. doi: 10.1038/s41586-020-2115-1

Jezek, K., Henriksen, E. J., Treves, A., Moser, E. I., and Moser, M.-B. (2011). Theta-paced flickering between place-cell maps in the hippocampus. *Nature* 478, 246–249. doi: 10.1038/nature10439

Joel, D., and McCarthy, M. M. (2017). Incorporating sex as a biological variable in neuropsychiatric research: where are we now and where should we be? *Neuropsychopharmacology* 42, 379–385. doi: 10.1038/npp.2016.79

Kalmbach, B. E., Hodge, R. D., Jorstad, N. L., Owen, S., de Frates, R., Yanny, A. M., et al. (2021). Signature morpho-electric, transcriptomic, and dendritic properties of human layer 5 neocortical pyramidal neurons. *Neuron* 109, 2914–2927.e5. doi: 10.1016/j.neuron.2021.08.030

Kasai, H., Ziv, N. E., Okazaki, H., Yagishita, S., and Toyoizumi, T. (2021). Spine dynamics in the brain, mental disorders and artificial neural networks. *Nat. Rev. Neurosci.* 22, 407–422. doi: 10.1038/s41583-021-00467-3

Klimczak, P., Rizzo, A., Castillo-Gómez, E., Perez-Rando, M., Gramuntell, Y., Beltran, M., et al. (2021). Parvalbumin interneurons and perineuronal nets in the hippocampus and retrosplenial cortex of adult male mice after early social isolation stress and perinatal NMDA receptor antagonist treatment. *Front. Synaptic Neurosci.* 13:733989. doi: 10.3389/fnsyn.2021.733989

Knafo, S., Libersat, F., and Barkai, E. (2005). Olfactory learning-induced morphological modifications in single dendritic spines of young rats. *Eur. J. Neurosci.* 21, 2217–2226. doi: 10.1111/j.1460-9568.2005.04041.x

Kubota, Y., Karube, F., Nomura, M., and Kawaguchi, Y. (2016). The diversity of cortical inhibitory synapses. *Front. Neural Circuits* 10:27. doi: 10.3389/fncir.2016.00027

Lavenex, P., Lavenex, P. B., Bennett, J. L., and Amaral, D. G. (2009). Postmortem changes in the neuroanatomical characteristics of the primate brain: hippocampal formation. *J. Comp. Neurol.* 512, 27–51. doi: 10.1002/cne.21906

LeDoux, J. E., and Brown, R. (2017). Emotions as higher-order states of consciousness. *Proc. Natl. Acad. Sci. USA* 114, E2016–E2025. doi: 10.1073/pnas.1619316114

Leopold, D. A., Strick, P. L., Bassett, D. S., Bruno, R. M., Cuntz, H., Harris, K. M., et al. (2019). "Functional architecture of the cerebral cortex," in *The Neocortex*, ed W. Singer (Cambridge: MA: MIT Press), 141–164.

Li, Z., Okamoto, K., Hayashi, Y., and Sheng, M. (2004). The importance of dendritic mitochondria in the morphogenesis and plasticity of spines and synapses. *Cell* 119, 873–887. doi: 10.1016/j.cell.2004.11.003

Luine, V., and Frankfurt, M. (2020). Estrogenic regulation of memory: the first 50 years. *Horm. Behav.* 121:104711. doi: 10.1016/j.yhbeh.2020.104711

Mancuso, J. J., Cheng, J.,Yin, Z.,Gilliam, J. C., Xia, X., Li, X., et al. (2014). Integration of multi scale dendritic spine structure and function data into systems biology models. *Front. Neuroanat.* 8:130. doi: 10.3389/fnana.2014.00130

Mederos, S., González-Arias, C., and Perea,. G. (2018). Astrocyte–neuron networks: a multilane highway of signaling for homeostatic brain function. *Front. Synaptic Neurosci.* 10:45. doi: 10.3389/fnsyn.2018.00045

Miermans, C. A., Kusters, R. P., Hoogenraad, C. C., and Storm, C. (2017). Biophysical model of the role of actin remodeling on dendritic spine morphology. *PLoS ONE* 12, e0170113. doi: 10.1371/journal.pone.0170113

Mohan, H., Verhoog, M. B., Doreswamy, K. K., Eyal, G., Aardse, R., Lodder, B. N., et al. (2015). Dendritic and axonal architecture of individual pyramidal

neurons across layers of adult human neocortex. *Cereb. Cortex* 25, 4839–4853. doi: 10.1093/cercor/bhv188

Montero-Crespo, M., Domínguez-Álvaro, M., Alonso-Nanclares, L., DeFelipe, J., and Blazquez-Llorca, L. (2021). Three-dimensional analysis of synaptic organization in the hippocampal CA1 field in Alzheimer's disease. *Brain* 144, 553–573. doi: 10.1093/brain/awaa406

Morishima, M., and Kawaguchi, Y. (2006). Recurrent connection patterns of corticostriatal pyramidal cells in frontal cortex. *J. Neurosci.* 26, 4394–4405. doi: 10.1523/JNEUROSCI.0252-06.2006

Nguyen, P. T., Dorman, L. C., Pan, S., Vainchtein, I. D., Han, R. T., Nakao-Inoue, H., et al. (2020). Microglial remodeling of the extracellular matrix promotes synapse plasticity. *Cell* 182, 388–403.e15. doi: 10.1016/j.cell.2020.05.050

Obashi, K., Taraska, J. W., and Okabe, S. (2021). The role of molecular diffusion within dendritic spines in synaptic function. *J. Gen. Physiol*. 153, e202012814. doi: 10.1085/jgp.202012814

Okabe, S. (2020). Regulation of actin dynamics in dendritic spines: nanostructure, molecular mobility, and signaling mechanisms. *Mol. Cell. Neurosci.* 109, 103564. doi: 10.1016/j.mcn.2020.103564

Oray, S., Majewska, A., and Sur, M. (2006). Effects of synaptic activity on dendritic spine motility of developing cortical layer V pyramidal neurons. *Cereb. Cortex* 16, 730–741. doi: 10.1093/cercor/bhj019

Ortiz, C., Carlén, M., and Meletis, K. (2021). Spatial transcriptomics: molecular maps of the mammalian brain. *Ann. Rev. Neurosci.* 44, 547–562. doi: 10.1146/annurev-neuro-100520-082639

Palomero-Gallagher, N., and Zilles, K. (2019). Cortical layers: cyto-, myelo-, receptor- and synaptic architecture in human cortical areas. *NeuroImage* 197, 716-741. doi: 10.1016/j.neuroimage.2017.08.035

Pchitskaya, E., and Bezprozvanny, I. (2020). Dendritic spines shape analysis - classification or clusterization? *Perspective. Front. Synaptic Neurosci.* 12, 31. doi: 10.3389/fnsyn.2020.00031

Quirk, G. J., Repa, J. C., and LeDoux, J. E. (1995). Fear conditioning enhances short-latency auditory responses of lateral amygdala neurons: parallel recordings in the freely behaving rat. *Neuron* 15, 1029–1039. doi: 10.1016/0896-6273(95)90092-6

Ramaswamy, S., and Markram, H. (2015). Anatomy and physiology of the thick-tufted layer 5 pyramidal neuron. *Front. Cell. Neurosci.* 9:233. doi: 10.3389/fncel.2015.00233

Ramón y Cajal (1909–1911). *Histologie du système nerveux de l'homme et des vertébrés*, Paris: Maloine. doi: 10.5962/bhl.title.48637

Rasia-Filho, A. A. (2006). Is there anything "autonomous" in the nervous system? *Adv. Physiol. Educ.* 30, 9–12. doi: 10.1152/advan.00022.2005

Rasia-Filho, A. A., Andrejew, R., and Belló-Klein, A. (2018). "Integrating concepts of resilience from cellular functioning to human behavior," in *Amygdala: Mechanisms, Structure and Role in Disease*, ed. A. Manu (Hauppauge: Nova Science Publishers), 1–30.

Rasia-Filho, A. A., Dalpian, F., Menezes, I. C., Brusco, J., and Moreira, J. E., Cohen, R. S. (2012). Dendritic spines of the medial amygdala: plasticity, density, shape, and subcellular modulation by sex steroids. *Histol. Histopathol.* 8, 985–1011. doi: 10.14670/HH-27.985

Rasia-Filho, A. A., Fabian, C., Rigoti, K. M., and Achaval, M. (2004). Influence of sex, estrous cycle and motherhood on dendritic spine density in the rat medial amygdala revealed by the Golgi method. *Neuroscience* 126, 839–847. doi: 10.1016/j.neuroscience.2004.04.009

Rasia-Filho, A. A., Guerra, K. T. K., Vásquez, C. E., Dall'Oglio, A., Reberger, R., Jung, C. R., et al. (2021). The subcortical-allocortical-neocortical *continuum* for the emergence and morphological heterogeneity of pyramidal neurons in the human brain. *Front. Synaptic Neurosci.* 13:616607. doi: 10.3389/fnsyn.2021.616607

Real, R., Peter, M., Trabalza, A., Khan, S., Smith, M. A., Dopp, J., et al. (2018). *In vivo* modeling of human neuron dynamics and Down syndrome. *Science* 362, eaau1810. doi: 10.1126/science.aau1810

Reberger, R., DallOglio, A., Jung, C. R., and Rasia-Filho, A. A. (2018). Structure and diversity of human dendritic spines evidenced by a new three-dimensional reconstruction procedure for Golgi staining and light microscopy. *J. Neurosci. Methods* 293, 27–36. doi: 10.1016/j.jneumeth.2017.09.001

Reza-Zaldivar, E. E., Hernández-Sápiens, M. A., Minjarez, B., Gómez-Pinedo, U., Sánchez-González, V. J., Márquez-Aguirre, A. L., et al. (2020). Dendritic spine and synaptic plasticity in Alzheimer's disease: a focus on microRNA. *Front. Cell Dev. Biol.* 8:255. doi: 10.3389/fcell.2020.00255

Rigotti, M., Barak, O., Warden, M., Wang, X.-J., Daw, N. D., Miller, E. K., et al. (2013). The importance of mixed selectivity in complex cognitive tasks. *Nature* 497, 585–590. doi: 10.1038/nature12160

Rollenhagen, A., Walkenfort, B., Yakoubi, R., Klauke, S. A., Schmuhl-Giesen, S. F., Heinen-Weiler, J., et al. (2020). Synaptic organization of the human temporal lobe neocortex as revealed by high-resolution transmission, focused ion beam scanning, and electron microscopic tomography. *Int. J. Mol. Sci.* 21, 5558. doi: 10.3390/ijms21155558

Rubinow, D. R., and Schmidt, P. J. (2019). Sex differences and the neurobiology of affective disorders. *Neuropsychopharmacol* 44, 111–128. doi: 10.1038/s41386-018-0148-z

Runge, K., Cardoso, C., and de Chevigny, A. (2020). Dendritic spine plasticity: function and mechanisms. *Front. Synaptic Neurosci.* 12, 36. doi: 10.3389/fnsyn.2020.00036

Ruszczycki, B., Szepesi, Z., Wilczynski, G. M., Bijata, M., Kalita, K., Kaczmarek, L., et al. (2012). Sampling issues in quantitative analysis of dendritic spines morphology. *BMC Bioinformatics* 13, 213. doi: 10.1186/1471-2105-13-213

Sala, C., and Segal, M. (2014). Dendritic spines: the locus of structural and functional plasticity. *Physiol. Rev.* 94, 141–188. doi: 10.1152/physrev.00012.2013

Saygin, Z. M., Kliemann, D., Iglesias, J. E., van der Kouwe, A. J. W., Boyd, E., Reuter, M., et al. (2017). High-resolution magnetic resonance imaging reveals nuclei of the human amygdala: manual segmentation to automatic atlas. *Neuroimage* 155, 370–382. doi: 10.1016/j.neuroimage.2017.04.046

Scheperjans, F., Eickhoff, S. B., Hömke, L., Mohlberg, H., Hermann, K., Amunts, K., et al. (2008). Probabilistic maps, morphometry, and variability of cytoarchitectonic areas in the human superior parietal cortex. *Cereb. Cortex* 18, 2141–2157. doi: 10.1093/cercor/bhm241

Shapson-Coe, A., Januszewski, M., Berger, D. R., Pope, A., Wu, Y., Blakely, T., et al. (2021). A connectomic study of a petascale fragment of human cerebral cortex. *bioRxiv*. 2021.05.29.446289. doi: 10.1101/2021.05.29.446289

Šimić, G., Tkalčić, M., Vukić, V., Mulc, D., Španić, E., Šagud, M. et al. (2021). Understanding emotions: Origins and roles of the amygdala. *Biomolecules* 11, 823. doi: 10.3390/biom11060823

Soltesz, I., and Losonczy, A. (2018). CA1 pyramidal cell diversity enabling parallel information processing in the hippocampus. *Nat. Neurosci.* 21, 484–493. doi: 10.1038/s41593-018-0118-0

Spruston, N., Häusser, M., and Stuart, G. (2013). "Information processing in dendrites and spines," in *Fundamental Neuroscience*, eds L. R. Squire, D. Berg, F. E. Bloom, S. du Lac, A. Ghosh, and N. C. Spitzer, (Waltham: Academic Press), 231–260. doi: 10.1016/B978-0-12-385870-2.00011-1

Stewart, M. G., Popov, V. I., Kraev, I. V., Medvedev, N., and Davies, H. A. (2014). "Structure and complexity of the synapse and dendritic spine," in *The Synapse*, eds V. Pickel and M. Segal (New York, NY: Academic Press), 1–20. doi: 10.1016/B978-0-12-418675-0.00001-8

Tazerart, S., Mitchell, D. E., Miranda-Rottmann, S., and Araya, R. (2020). A spike-timing-dependent plasticity rule for dendritic spines. *Nat. Commun.* 11:4276. doi: 10.1038/s41467-020-17861-7

Timo-Iaria, C., and Valle, A. C. (1995). The functional role of the conscious process. *Ciência e Cultura J. Braz. Assoc. Adv. Sci.* 47, 221–234.

Tønnesen, J., Inavalli, V. V. G. K., and Nägerl, U. V. (2018). Super-Resolution Imaging of the extracellular space in living brain tissue. *Cell* 172, 1108–1121.e15. doi: 10.1016/j.cell.2018.02.007

Tønnesen, J., and Nägerl, V. (2016). Dendritic spines as tunable regulators of synaptic signals. *Front. Psychol.* 7, 101. doi: 10.3389/fpsyt.2016.00101

Turcotte, R., Liang, Y., Tanimoto, M., Zhang, Q., Li, Z., Koyama, M., et al. (2019). Dynamic super-resolution structured illumination imaging in the living brain. *Proc. Natl. Acad. Sci. USA* 116, 9586–9591. doi: 10.1073/pnas.1819965116

Vásquez, C. E., Reberger, R., Dall'Oglio, A., Calcagnotto, M. E., and Rasia-Filho, A. A. (2018). Neuronal types of the human cortical amygdaloid nucleus. *J. Comp. Neurol.* 526, 2776–2801. doi: 10.1002/cne.24527

Viscardi, L. H., Imparato, D. O., Bortolini, M. C., and Dalmolin, R. J. S. (2021). Ionotropic receptors as a driving force behind human synapse establishment. *Mol. Biol. Evol.* 38, 735–744. doi: 10.1093/molbev/msaa252

Vogt, B. A. (2015). "Mapping cingulate subregions," in *Brain Mapping: An Encyclopedic Reference*, ed A. W. Toga, (Oxford: Academic Press), 325–339. doi: 10.1016/B978-0-12-397025-1.00230-X

von Bohlen und Halbach, O. (2009). Structure and function of dendritic spines within the hippocampus. *Ann. Anat.* 191, 518–531. doi: 10.1016/j.aanat.2009.08.006

Wen, Q., Stepanyants, A., Elston, G. N., Grosberg, A. Y., and Chklovskii, D. B. (2009). Maximization of the connectivity repertoire as a statistical principle governing the shapes of dendritic arbors. *Proc. Natl. Acad. Sci. USA* 106, 12536–12541. doi: 10.1073/pnas.0901530106

Winnubst, J., Bas, E., Ferreira, T. A., Wu, Z., Economo, M. N., Edson, P., et al. (2019)... Reconstruction of 1,000 projection neurons reveals new cell types and organization of long-range connectivity in the mouse brain. *Cell* 179, 268–281.e13. doi: 10.1016/j.cell.2019.07.042

Woolley, C. S., and McEwen, B. S. (1993). Roles of estradiol and progesterone in regulation of hippocampal dendritic spine density during the estrous cycle in the rat. *J. Comp. Neurol.* 336, 293–306. doi: 10.1002/cne.903360210

Wu, Y. E., Dang, J., Kingsbury, L., Zhang, M., Sun, F., Hu, R. K., et al. (2021). Neural control of affiliative touch in prosocial interaction. *Nature* 599, 262–267. doi: 10.1038/s41586-021-03962-w

Yang, L., Yang, Y., Yuan, J., Sun, Y., Dai, J., and Su, B. (2019). Transcriptomic landscape of von Economo neurons in human anterior cingulate cortex revealed by microdissected-cell RNA sequencing. *Cereb. Cortex* 29, 838–851. doi: 10.1093/cercor/bhy286

Yuste, R. (2010). *Dendritic Spines.* Cambridge: MIT Press. doi: 10.7551/mitpress/9780262013505.001.0001

Yuste, R. (2013). Electrical compartmentalization in dendritic spines. *Annu. Rev. Neurosci.* 36, 429–449. doi: 10.1146/annurev-neuro-062111-150455

Yuste, R., Hawrylycz, M., Aalling, N., Aguilar-Valles, A., Arendt, D., Armañanzas, R., et al. (2020). A community-based transcriptomics classification and nomenclature of neocortical cell types. *Nat. Neurosci.* 23, 1456–1468. doi: 10.1038/s41593-020-0685-8

Zaccard, C. R., Shapiro, L., Martin-de-Saavedra, M. D., Pratt, C., Myczek, K., Song, A., et al. (2020). Rapid 3D enhanced resolution microscopy reveals diversity in dendritic spinule dynamics, regulation, and function. *Neuron* 107, 522–537. doi: 10.1016/j.neuron.2020.04.025

Zancan, M., da Cunha, R. S. R., Schroeder, F., Xavier, L. L., and Rasia-Filho, A. A. (2018). Remodeling of the number and structure of dendritic spines in the medial amygdala: from prepubertal sexual dimorphism to puberty and effect of sexual experience in male rats. *Eur. J Neurosci.* 48, 1851–1865. doi: 10.1111/ejn.14052

Zebarjadi, N., Adler, E., Kluge, A., Jääskeläinen, I. P., Sams, M., and Levy, J. (2021). Rhythmic neural patterns during empathy to vicarious pain: beyond the affective-cognitive empathy dichotomy. *Front. Hum. Neurosci.* 15:708107. doi: 10.3389/fnhum.2021.708107

Zeki, S. (2007). The neurobiology of love. *FEBS Lett.* 581, 2575–2579. doi: 10.1016/j.febslet.2007.03.094

Conflict of Interest: The author declares that the research was conducted in the absence of any commercial or financial relationships that could be construed as a potential conflict of interest.

Publisher's Note: All claims expressed in this article are solely those of the authors and do not necessarily represent those of their affiliated organizations, or those of the publisher, the editors and the reviewers. Any product that may be evaluated in this article, or claim that may be made by its manufacturer, is not guaranteed or endorsed by the publisher.

Copyright © 2022 Rasia-Filho. This is an open-access article distributed under the terms of the Creative Commons Attribution License (CC BY). The use, distribution or reproduction in other forums is permitted, provided the original author(s) and the copyright owner(s) are credited and that the original publication in this journal is cited, in accordance with accepted academic practice. No use, distribution or reproduction is permitted which does not comply with these terms.

frontiers in Physiology

REVIEW
published: 02 March 2022
doi: 10.3389/fphys.2022.826811

The Role of Peroxisome Proliferator-Activated Receptor Gamma and Atherosclerosis: Post-translational Modification and Selective Modulators

Liqin Yin[1†], *Lihui Wang*[2†], *Zunhan Shi*[1†], *Xiaohui Ji*[1] *and Longhua Liu*[1*]

[1] School of Kinesiology, Shanghai University of Sport, Shanghai, China, [2] Department of Medical Imaging, Shanghai East Hospital (East Hospital Affiliated to Tongji University), Tongji University, Shanghai, China

Atherosclerosis is the hallmark of cardiovascular disease (CVD) which is a leading cause of death in type 2 diabetes patients, and glycemic control is not beneficial in reducing the potential risk of CVD. Clinically, it was shown that Thiazolidinediones (TZDs), a class of peroxisome proliferator-activated receptor gamma (PPARγ) agonists, are insulin sensitizers with reducing risk of CVD, while the potential adverse effects, such as weight gain, fluid retention, bone loss, and cardiovascular risk, restricts its use in diabetic treatment. PPARγ, a ligand-activated nuclear receptor, has shown to play a crucial role in anti-atherosclerosis by promoting cholesterol efflux, repressing monocytes infiltrating into the vascular intima under endothelial layer, their transformation into macrophages, and inhibiting vascular smooth muscle cells proliferation as well as migration. The selective activation of subsets of PPARγ targets, such as through PPARγ post-translational modification, is thought to improve the safety profile of PPARγ agonists. Here, this review focuses on the significance of PPARγ activity regulation (selective activation and post-translational modification) in the occurrence, development and treatment of atherosclerosis, and further clarifies the value of PPARγ as a safe therapeutic target for anti-atherosclerosis especially in diabetic treatment.

Keywords: PPARγ, atherosclerosis, post-translational modifications, selective modulators, cardiovascular disease

OPEN ACCESS

Edited by:
Geoffrey A. Head,
Baker Heart and Diabetes Institute, Australia

Reviewed by:
Makoto Makishima,
Nihon University, Japan
Karin Jandeleit-Dahm,
Monash University, Australia

***Correspondence:**
Longhua Liu
liulonghua@sus.edu.cn

[†] These authors have contributed equally to this work

Specialty section:
This article was submitted to Integrative Physiology, a section of the journal Frontiers in Physiology

Received: *01 December 2021*
Accepted: *11 February 2022*
Published: *02 March 2022*

Citation:
Yin L, Wang L, Shi Z, Ji X and Liu L (2022) The Role of Peroxisome Proliferator-Activated Receptor Gamma and Atherosclerosis: Post-translational Modification and Selective Modulators. Front. Physiol. 13:826811. doi: 10.3389/fphys.2022.826811

INTRODUCTION

Atherosclerosis is the hallmark of CVD which is a leading cause of death in type 2 diabetes patients, and glycemic control is not beneficial in reducing the potential risk of CVD (Libby et al., 2016; Vallee et al., 2019; Machado-Oliveira et al., 2020). Atherosclerosis is a disease caused by the combination of high oxidative stress, inflammation (Finn et al., 2012), immune response, lipid deposition, and genetic traits (Falk, 2006; Yu et al., 2013; Johnson, 2017). Atherosclerosis is initiated by a large number of abnormally metabolized lipids including apolipoprotein B-containing lipoproteins (apoB LPs) continuously enter into the vascular intima to trigger an inflammatory response dominated by macrophages in the vascular wall (Chistiakov et al., 2015; Tabas, 2017), promote the migration and proliferation of vascular smooth muscle cells (VSMCs) (Durham et al., 2018), cause

the vascular wall thickening and the lumen narrowing, and finally develop atherosclerosis (Wang et al., 2015; Bennett et al., 2016).

PPARγ is a ligand-activated nuclear receptor, that regulates glucose and lipid metabolism, endothelial function, and inflammation (Lehrke and Lazar, 2005; Janani and Ranjitha Kumari, 2015). Due to the different selected promoters and alternative shear modes, the PPARγ gene can transcriptionally generate two PPARγ transcript variants, and translate into two isoforms, PPARγ1 and PPARγ2, with PPARγ2 has 30 more amino acid residues at the N-end (Fajas et al., 1997). PPARγ1 is expressed nearly in all cells, while PPARγ2 is mainly expressed in adipocytes and vascular endothelial cells. Nevertheless, PPARγ2 is a more potent transcription activator (Lehrke and Lazar, 2005; Janani and Ranjitha Kumari, 2015). PPARγ plays a crucial role in anti-atherosclerosis by promoting cholesterol efflux (Ozasa et al., 2011; Tsuboi et al., 2020), inhibiting monocytes infiltrating into the vascular intima under endothelial layer (Namgaladze et al., 2013), and inhibiting their transformation into macrophages (Zhang and Chawla, 2004; Charo, 2007; Oppi et al., 2020), inhibiting VSMCs proliferation and migration (Zhang et al., 2011; Durham et al., 2018). PPARγ has emerged as one of the most promising therapeutic targets for cardiovascular complications, and its synthetic ligands (Lim et al., 2015), such as Thiazolidinediones (TZDs) have also been shown to have anti-atherosclerosis function (Viles-Gonzalez et al., 2004; Nakaya et al., 2009). Although their advantages are recognized, the profiles of numerous adverse effects hinder the continued use of these drugs.

To develop a safer and better treatment of cardiovascular complications targeting PPARγ, novel strategies that preserve the "good" potent insulin sensitization, while reducing or eliminating "bad"-related side effects should be used. These novel strategies may include downstream effectors of PPARγ-mediated insulin sensitization, targeting specific post-translational modification (PTMs) (Wang and Tafuri, 2003; Brunmeir and Xu, 2018) of PPARγ, and selective PPARγ modulators (SPPARMs) (Higgins and Depaoli, 2010; Dunn et al., 2011). PTMs such as phosphorylation (Yin et al., 2006; Choi et al., 2011; Montanari et al., 2020), acetylation (Qiang et al., 2012; Kraakman et al., 2018; Liu L. et al., 2020), ubiquitination (Garin-Shkolnik et al., 2014), and sumoylation (Pascual et al., 2005) are all involved in regulating PPARγ activity. These PTMs of PPARγ could regulate its transcription of downstream genes via changing protein conformation, regulating protein interactions, or altering the affinity between receptors and ligands (van Beekum et al., 2009; Brunmeir and Xu, 2018). PPARγ activation requires ligand recognition and binding to receptor regulatory receptor mediated gene transcription (Lehrke and Lazar, 2005; Janani and Ranjitha Kumari, 2015). The binding site and binding region of the ligand with PPARγ determine the conformation of PPARγ and the subsequent changes in cofactor recruitment (Higgins and Depaoli, 2010; Montanari et al., 2020). The selective PPARγ modulators (SPPARMs) is thought to improve the safety profile of PPARγ agonists avoiding TZDs' adverse reactions.

In this review, we focus on the significance of PPARγ activity regulation (PTMs and SPPARMs) in the occurrence, development and treatment of atherosclerotic diseases, and further clarifies the value of PPARγ as a therapeutic target for anti-atherosclerosis.

PEROXISOME PROLIFERATOR-ACTIVATED RECEPTOR GAMMA AND ATHEROSCLEROSIS

PPARγ has a typical structure of nuclear hormone receptors, including the N-terminal A/B domain, DNA binding domain (DBD) and ligand binding domain (LBD) (Lehrke and Lazar, 2005; Chandra et al., 2008; Janani and Ranjitha Kumari, 2015). Both forms of PPARγ1 and PPARγ2 have a similar structural, except for PPARγ2 containing an N-terminal extension of 28 amino acids (Chandra et al., 2008). PPARγ usually form a heterodimer with Retinoid X Receptor α (RXRα Chandra et al., 2008) and binds to PPRE. When the ligand is not bound, PPARγ/RXRα mainly binds to some co-repressors, such as Nuclear Receptor Corepressor (NCoR) or Silencing Mediator of Retinoic Acid and Thyroid Hormone Receptor (SMRT). When the ligand binds to LBD, it will change the conformation of PPARγ, and the co-repressors will be replaced by some co-activators, e.g., cAMP responsive element binding protein (CREBP), PPARγ coactivator-1 (PGC-1), Steroid Receptor Coactivator (SRC), and CBP/P300 (Lehrke and Lazar, 2005; Chandra et al., 2008). The recruited cofactors vary in their transcriptional regulatory target genes, and their transcriptional levels and biological functions will change accordingly.

PPARγ not only participates in fat formation, lipid and glucose metabolism, but also plays an important role on vascular biology and inflammation, and the development of atherosclerosis (Kvandová et al., 2016; Hernandez-Quiles et al., 2021). PPARγ has anti-atherosclerotic effects through the following aspects (**Figure 1**): (1) PPARγ regulates the expression of cell adhesion molecules, such as inducible nitric oxide synthase (Chen et al., 2001), intracellular cell adhesion molecule-1(ICAM-1), vascular cell adhesion molecule-1(VCAM-1) (Babaev et al., 2005), and inhibit endothelial cells activation and attenuation of monocyte chemoattractant protein 1 (MCP-1), matrix metalloproteinase 9 (MMP9), and metallopeptidase inhibitor 1 (TIMP-1) which induced monocyte migration across endothelial cells (Verrier et al., 2004; Calabrò et al., 2005); (2) PPARγ activates the PPARγ/liver X receptor α (LXR-α) pathway to stimulate the expression of cholesterol efflux-related genes– ATP binding cassette transporter A1 (ABCA1) (Akiyama et al., 2002) and Acy1 Coenzyme A: Cholesterol Acyltransferases (ABCG1) (Sueyoshi et al., 2010; Srivastava, 2011), accelerates the efflux of cholesterol from macrophages (Liu D. et al., 2020; Oppi et al., 2020), therefore inhibits the formation of foam cells (Li et al., 2004; Zhang et al., 2021); (3) PPARγ inhibits the expression of pro-inflammatory factors, such as TNF-α (Zhang et al., 2014), IL-6, IL-18 (Chen et al., 2008), and induces the macrophages differentiation into an anti-inflammatory M2 phenotype (Oppi et al., 2020). And the expression of M2 markers, such as MR, AMAC1, and IL-10 levels correlate positively with the expression of PPARγ (Bouhlel et al., 2007). Therefore, PPARγ can improve the inflammatory response of cardiovascular cells, inhibit

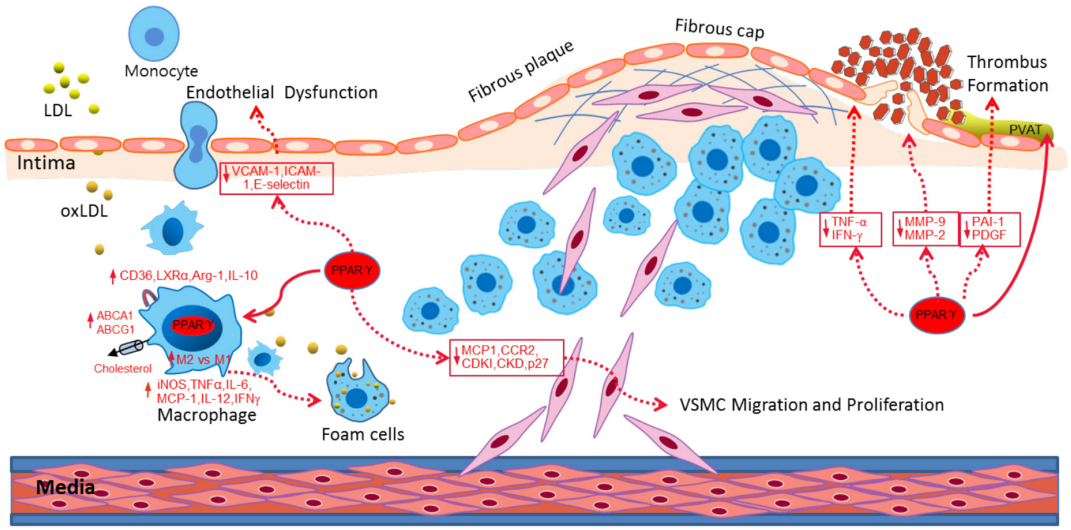

FIGURE 1 | PPARγ attenuated atherosclerosis through different aspects, including alleviating endothelial dysfunction, promoting cholesterol efflux, inducing M1-M2 transition, inhibiting VSMC migration and proliferation and stabilizing the fibrous cap and plaque.

plaque formation, and maintain plaques stability. (4) PPARγ inhibits VSMCs proliferation and migration by suppressing TLR4-mediated inflammation (Gu et al., 2019) and ultimately attenuates intimal hyperplasia after carotid injury (Meredith et al., 2009; Osman and Segar, 2016). Meanwhile, PPARγ prevents the degradation of cyclin-dependent kinase inhibitors (CDKIs) and p27 induced by growth factors, and inhibits the formation of cyclin-dependent kinase complex (Cyclin-CDK), thereby inhibits proliferation, migration, and apoptosis (Law et al., 2000; Fu et al., 2001). (5) PPARγ inhibits the expression of MMP-9 and MMP-2 that can decompose collagen and fibers in macrophages (Luo et al., 2007; Reinhold et al., 2020), reduces the fragility of the fiber cap and enhances the stability of the plaque. Therefore, the functional regulation of PPARγ is of very important for the prevention and treatment of atherosclerosis.

POST-TRANSLATIONAL MODIFICATIONS OF PEROXISOME PROLIFERATOR-ACTIVATED RECEPTOR GAMMA AND ATHEROSCLEROSIS

The PPARγ transcriptional activity regulates in diverse ways, including protein expression levels, ligands, and transcriptional cofactors. PTMs of proteins can alter protein conformation, regulate protein interactions, and alter the affinity between receptors and ligands, thus regulating the transcription of downstream genes (Brunmeir and Xu, 2018).

Phosphorylation

The phosphorylation regulation of PPARγ is one of the main ways to regulate its activity (Montanari et al., 2020). With different stimuli, PPARγ could be phosphorylated at different sites and resulting diverse biological effects (Choi et al., 2011). Cyclin-dependent kinase (CDK) (Choi et al., 2010, 2011; Laghezza et al., 2018) and mitogen-activated protein kinase (MAPK) (Yin et al., 2006; Yang et al., 2013; Ge et al., 2018) are involving in the phosphorylation of PPARγ, and the main sites include Ser273 (245 in isoform 1) (Dias et al., 2020; Hall et al., 2020) and Ser112 (Ser82 in isoform 1) (**Figure 2A**; Ge et al., 2018). CDK5-mediated phosphorylation of PPARγ S273 results in a decrease in its transcriptional activity and adipogenesis. One of TZDs' major side effects is due to its activation of PPARγ in adipose tissue, and high-fat diet increased CDK5-mediated of PPARγ phosphorylation, which was negatively associated with TZDs' insulin sensitization in humans. Meanwhile PPARγ phosphorylation can up-regulate lipid uptake of CD36 and SR-A1 related proteins, inhibit cholesterol efflux ABCA1 and ABCG1 related proteins, induce the expression of TNF-α, IL-1β and other inflammatory factors, and promote the formation of foam cells to accelerate the process of atherosclerosis (Choi et al., 2010, 2011; Banks et al., 2015). PPARγ phosphorylation by CDK5 may contribute to its dissociation with PGC1α and TIF2 coactivators but interaction with SMRT and NCoR corepressors (Dias et al., 2020). NCoR can regulate the phosphorylation of PPARγ on Ser 273 by stabilizing CDK5 (Li et al., 2011). Mice with fat cell NCoR knockout ($NCoR^{-/-}$) improves glucose tolerance and insulin sensitivity and reduces macrophage infiltration and inflammation (Ribeiro Filho et al., 2019). As from CDK5 studies, compounds can be designed to alter specific PTMs of PPARγ to partly prevent disturbed fat metabolism while retaining anti-diabetic potency. CDK9/CDK7-mediated phosphorylation of S112 can increase the transcriptional activity of PPARγ and promote adipocyte differentiation (Iankova et al., 2006; Li et al., 2017; Ge et al., 2018).

MAPK can phosphorylate PPARγ in the AF1 region (PPARγ2 Ser112, PPARγ1 Ser82), inhibiting the ligand binding and changing the recruitment of co-factors, and then change the transcriptional activity (Yin et al., 2006; Yang et al., 2013; Ge et al., 2018). MAPK-mediated phosphorylation of

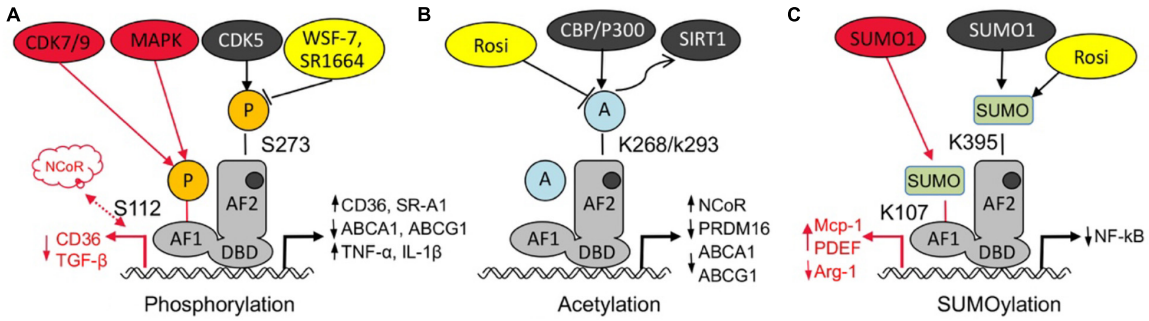

FIGURE 2 | Post-translational modification of PPARγ regulates atherosclerosis. **(A)** Both phosphorylation of PPARγ at S112 by CDK7/9 or MAPK and phosphorylation of PPARγ at S273 accelerates foam cell formation and atherosclerosis through different signaling pathway, some PPARγ agonist (WSF-7, SR1664) can block cdk5 mediated Ser273 phosphorylation. **(B)** Acetylation of PPARγ at K268/K293 increases atherosclerosis through upregulating ABCA1, ABCG1, and NcoR but inhibiting PRDM16,while deacetylation of PPARγ at K268 and K293 alleviates atherosclerosis, while PPARγ agonist rosiglitazone (Rosi) could deacetylate PPARγ at K268/K293. **(C)** Sumoylation of PPARγ at K107 promotes VSMCs proliferation and migration, but sumoylation of PPARγ at K395, such as by Rosi, has anti-inflammation effect.

PPARγ, which promotes the formation of foam cells by macrophages exposed to ox-LDL (Yin et al., 2006). Growth factors can phosphorylate PPARγ by the MAPK signaling pathway and reduce the transcriptional activity of PPARγ (Yin et al., 2006), such as epidermal growth factor (EGF) and platelet-derived growth factor (PDGF) (Osman and Segar, 2016). In addition, Choi et al. (2015) recently described the phosphorylation of Y78, is also important for the cytokine and chemokine gene expression's regulation. PPARγ phosphorylation can alter its transcriptional activity, and the blockage of PPARγ phosphorylation is related to improve insulin sensitization (Choi et al., 2014). However, PPARγ phosphorylation mediated by different enzymes, conformational changes at different sites can cause the recruitment response of different cofactors, its role in atherosclerosis and its mechanism need to be further studied, and also provide ideas for the drug design of PPAR ligand.

Acetylation

Acetylation of PPARγ is a ligand- independent activation of PPARγ. Qiang et al. (2012) showed that five lysine residues (K98, K107, K218, K268, and K293) could be acetylated, of which two K268/K293 could be deacetylated by TZD rosiglitazone (Rosi) via activation of the NAD (Nicotinamide adenine dinucleotide)-dependent deacetylase sirtuin-1 (SIRT1) deacetylase (**Figure 2B**; Kraakman et al., 2018). PPARγ is acetylated by p300 or CBP (Kim et al., 2006), and it may play an important role in lipid synthesis (Tian et al., 2014). Acetylation of PPARγ at K268/K293 increases atherosclerosis through upregulating ABCA1, ABCG1, and NcoR but inhibiting PRDM16, while deacetylation of PPARγ at K268 and K293 alleviates atherosclerosis.

PPARγ deacetylation on K268 and K293 induces brown remodeling of white adipose tissue and reduces the adverse effects of TZDs while maintaining insulin sensitization (Qiang et al., 2012; Liu L. et al., 2020). Deacetylation of PPARγ can selective regulation the target genes, it could inhibit aP2, Cd36, upregulation genes ucp1 and adipsin on lipid oxidative genes cpt1a (Kraakman et al., 2018). PPARγ deacetylation improves endothelial function with diabetes treatment. The aortic arch lesion size was reduced in 2KR (K268 and K293) $LDLr^{-/-}$ mice, the expression of iNOS, Nox2, and IL-6 in endothelial cells were decreased, while the side effects of TZD, including fluid retention and bone loss were reduced (Liu L. et al., 2020). Deacetylation of PPARγ inhibits the cholesterol efflux PPARγ/LXRα/ABCA1 pathway (Cao et al., 2014; Yang et al., 2015), increased production of proinflammatory M1 macrophages and promotes the development of inflammatory response (Chen et al., 2008, 2010), leading to the onset and development of atherosclerosis. From a mechanistic perspective, deacetylated PPARγ preferentially interacts with PRDM16 and disrupts the binding of the transcriptional corepressor NCoR (Qiang et al., 2012). Therefore, manipulating PPARγ acetylation is a promising therapeutic strategy to anti-atherosclerosis.

Sumoylation

PPARγ sumoylation with SUMO1 modification of K107 (K77 in PPARγ1) (**Figure 2C**), and ubiquitin carrier protein 9 (Ubc9) and PIAS1 (protein inhibitor of activated STAT1) are involved as PPARγ specific E2 binding enzymes and E3 ligases, respectively (Lim et al., 2009). Sumoylation of PPARγ K107 inhibits its transcriptional activity, and is enhanced by the K107 mutation (K107R). PPARγ sumoylation at K107 position strongly inhibited VSMCs proliferation and migration (Katafuchi et al., 2018), and reduced neointimal formation after balloon injury (Lim et al., 2009). Desumoylation at K107 in PPARγ may inhibit serum-stimulated VSMCs proliferation (Lim et al., 2009; Osman and Segar, 2016), might play an important role against atherosclerosis. Moreover, K107R improves insulin sensitivity without body weight gain or adiposity (Wadosky and Willis, 2012; Pourcet et al., 2013). However, some studies have shown that K107 sumoylation plays an important role in the anti-inflammatory response triggered by apoptotic cells, possibly by stabilizing the co-inhibitor NCoR on the target gene (Jennewein et al., 2008; Lu et al., 2013). The sumoylation modification of PPARγ1 inhibits the M2 polarization of macrophages by inhibiting the transcription of Arg-1 (Haschemi et al., 2011). Pascual et al. (2005) shows that the PPAR agonist TZD can

exert anti-diabetic and anti-atherosclerotic effects through the NF-kB inflammatory pathway, the first response is associated with TZD-mediated SUMO1 modification of K365 (K395 in PPARγ2) followed by targeted regulation of the PPAR co-cofactor NCoR. The exact biological role of the two modifications in anti-inflammatory responses, especially the potential functional overlap, remains to be determined. Nevertheless, targeting PPARγ sumoylation may provide a novel mechanism for anti-atherosclerosis.

Ubiquitination

Ubiquitination modification cannot only regulate the proteasome-mediated degradation of target proteins, but also serve as a "scaffold" to recruit other proteins to form signal complexes. PPARγ undergoes conformational changes after binding to the ligand. On the one hand, Makorin RING finger protein 1 (MKRN1) (Kim et al., 2014) and Seven *in absentia* homolog 2 (SIAH2) (Kilroy et al., 2012) services as PPARγ E3 ligases, targeting PPARγ for proteasomal degradation. Ubiquitination of PPARγ on K184 and K185 inhibits its activity in mature 3T3-L1 adipocytes (Kilroy et al., 2012; Kim et al., 2014). On the other hand, it can also recruit the binding of ubiquitination-related enzymes and induce proteasome-dependent degradation, thereby negatively regulating the transcriptional activity of PPARγ. Rosiglitazone reduces the inflammatory response in diabetic plaques, less ubiquitin, proteasome 20S, TNF-α, and NF-κB, ubiquitin-proteasome activity with diabetic plaque NF-κB-mediated inflammatory response is involved (Marfella et al., 2006). This study strengthens the earlier findings on PPARγ regulation through modulation of its stability. Currently, the use of ubiquitination modifications for the regulation of PPARγ transcriptional activity is still controversial (Watanabe et al., 2015). It has been reported that the ubiquitin-proteasome pathway can mediate the protein renewal of PPARγ (Li et al., 2016), a process that is required for the efficient transcription of its downstream genes, while the ubiquitin activase inhibitor E1 inhibitor, and the proteasome inhibitor MG-132 can cause a decrease in PPARγ transcriptional activity.

SELECTIVE PPARγ MODULATORS AND ATHEROSCLEROSIS

PPARγ ligands are generally lipid-derived compounds with natural and synthetic properties, and different ligands have different affinity-binding receptors and activate the receptors. Synthetic ligands TZDs reduce atherosclerosis in certain mouse models (Martens et al., 2002). However, severe side effects associated with TZD use, such as weight gain, fluid retention, bone loss, cardiovascular disk, etc., restricts the use of TZDs (Zinn et al., 2008). In order to maximize the PPAR-mediated insulin sensitization and to minimize the occurrence of related adverse reactions, the concept of "selective PPAR regulator (selective PPARγ modulators, SPPARMs)" was proposed and developed (Higgins and Depaoli, 2010; Camejo, 2016). In contrast to rosiglitazone, SPPRAMs has similar or different PPAR receptor binding sites, or has different affinity or specificity of recruitment receptor cofactors, or a range of target genes where PPAR are biased and selective for regulating transcription. The currently found SPPRAMs that associated with atherosclerosis mainly consists of three types: partial PPARγ agonist, dual PPAR α/γ agonist, and non-agonist PPARγ ligand.

Partial Peroxisome Proliferator-Activated Receptor Gamma Agonist

In fact, partial PPARγ agonist is different from the classic TZDs, with rosiglitazone as the "full agonist." It is generally believed that 20–60% of rosiglitazone efficacy is a partial activator (**Table 1**), such as GQ-177 (Silva et al., 2016), S 26948 (Carmona et al., 2007), WSF-7 (Zhang et al., 2020) lobeglitazone (Lim et al., 2015), and INT131 (Xie et al., 2017). LDLr$^{-/-}$ mice treated with GQ-177 can significant decrease the VLDL, LDL fractions and increase mean HDL, Glut4 levels, increased the expression of apoA1, CD36, ABCA1, SR-B1, and ABCG5 in hepatic, contrary to rosiglitazone, GQ-177 did not affect fat accumulation and bone mineral density (Silva et al., 2016). It was shown that TZDs facilitated the transport of BM-derived circulating progenitor cells to adipose tissue and their differentiation into multilocular adipose cells (Crossno et al., 2006). Meanwhile, Hu et al. (2021) found RANKL from bone marrow adipose lineage cells promoted osteoclast formation and bone loss. S26948 improves lipid parameters (LDLs, VLDL) and reduces atherosclerotic lesions in ob/ob male C57BL/6 mice (Carmona et al., 2007). WSF-7 upregulated PPARγ-responsive genes, such as adiponectin and Glut4, inhibits PPARγ phosphorylation at Ser273 by obesity and enhances insulin sensitivity in 3T3-L1 Adipocytes (Zhang et al., 2020). Lobeglitazone inhibits the VSMCs proliferation and migration, reduces the vascular cells adhesion, NF-kB p65 translocation, and improves circulating factors related to atherosclerosis, then reduced neointimal formation significantly in balloon injury rat carotid arteries in ApoE$^{-/-}$ mice (Lim et al., 2015; Song et al., 2021). In the presence of pro-inflammatory stimulation, Lobeglitazone effectively inhibited expression of pro-inflammatory gene expression in macrophages and adipocytes (Sohn et al., 2018). The latest study has found that macrophages targeted PPARγ activator Lobeglitazone could rapidly stabilize a coronary artery-sized inflammatory plaque (Song et al., 2021). Both non-clinical and clinical studies have demonstrated that INT131 have the potential to separate insulin-sensitizing actions and undesirable side effects in Patients With Type 2 Diabetes (DePaoli et al., 2014), and it also has the potential to decrease free fatty acids, increase HDL-C (Dunn et al., 2011). However, there is still no relevant study on the effect of INT131 on atherosclerosis.

Full agonist-TZDs forms a key hydrogen bond with the side chain of Y473 on helix 12, mainly interacts with residues from arm I in the ligand binding pocket, to enhance the binding affinity of coactivators/weaken corepressors, inducing transcriptional activation (Brust et al., 2018). Unlike full agonist TZDs, some partial agonists have different binding mode, such as GQ-177 interacts through hydrophobic contacts with residues from arm II (Barros et al., 2010), lobeglitazone makes additional

TABLE 1 | Selective PPARγ modulators associated with atherosclerosis.

Class	Compound	Target gene	Function	Mechanisms	References
Partial PPARγ agonist	GQ-177	apoA1, ABCA1, SR-B1 ABCG5, ABCG8, and HDL-c	Inhibits the progression of atherosclerotic lesions. not affect fat accumulation, bone mineral density.	Hydrophobic contacts with residues from arm II.	Silva et al., 2016
	S 26948	LDLs, VLDL, LPL, aP2↓, UCP1	Promotes cholesterol transfer and reduce lesions surface.	No-recruit DRIP205 or PCG-1α.	Carmona et al., 2007
	WSF-7	Adiponectin and Glut4↑	Enhances insulin sensitivity, Reduce the fat accumulation.	Inhibits PPARγ Ser273 phosphorylation.	Zhang et al., 2020
	Lobeglitazone	hsCRP, MCP-1, ABCA1, leptin↓	Inhibits VSMC proliferation, Powerful anti-inflammatory effect.	Additional hydrophobic contacts with the Ω-pocket.	Lim et al., 2015
Dual PPAR α/γ agonist	GQ-11	Mcp-1,VLDL-C↓HDL-C, Apoa1↑, ABCA1, Sr-b1, IL-10↑	Ameliorated insulin sensitivity, promotes cholesterol transfer, no body weight gain.	Hydrogen bond with the PPARγ residue Ser289 at helix 3.	Silva, 2018
	P633H	ACO, aP2,	Not reported with atherosclerosis.	Not reported.	Chen et al., 2009
	C333H	TG, T-CHO, FFA	Reduces blood lipid and glucose concentration	Not reported.	Xu et al., 2006
	LT175	Glut4, Adipoq, Fabp4,NCoR1, CD36↓	Modulating lipid and glucose metabolism, avoiding weight gain	Impaired the recruitment of CBP coactivator	Gilardi et al., 2014
	Compound 3q	VCAM-1, MCP-1, CD36, P-selectin↑	Increases atherogenesis.	Not reported.	Calkin et al., 2007
	Tesaglitazar	SAA, NFκB, ICAM-1, MCP-1↓	Reduce LDL-C, less peripheral edema and body weight gain; heart failure and myocardial ischemia	Acetylation/deactivation of cardiac PGC-1α	Zadelaar et al., 2006
Non-agonist PPARγ	SR1664	Not affect aP2, Glut4, Lpl,CD36	Anti-diabetic, without promoting fluid retention or altering bone formation	Directly block Cdk5 dependent phosphorylation of PPARγ Ser273, do not stabilize helix 12	Choi et al., 2011
	UHC1	TNF-α, LPS, IL-1β, IL-6, MCP-1, IL-10↑	Inhibits the inflammatory responses in adipocytes and macrophages.	Directly block cdk5 mediated PPARγ K395 phosphorylation	Choi et al., 2014
	MSDC		Insulin sensitization, regulate the lipid metabolism	Target Mitochondrial pyruvate carrier2 (MPC2).	Colca et al., 2018

hydrophobic contacts with the Ω-pocket. There are also some partial agonists having similar binding sites to TZDs, but the recruiting cofactors were different. For example, INT131 activates PPARγ, but does not recruit the cofactor MED1 (key factor in regulating adipogenesis) (Lee et al., 2012; Xie et al., 2017), S26948 is unable to recruit DRIP205 or PCG-1α (Key genes in regulating gluconeogenesis), so that it selectively reduces blood glucose without the obvious adverse effects of adipogenesis (Carmona et al., 2007; Sohn et al., 2009). Compared to rosiglitazone, Lobeglitazone strongly blocks the phosphorylation of PPARγ at Ser245, but the pharmacological effects of this translational modification change need further studied (Jang et al., 2018). Although the exact mechanism beyond these effects remains to be determined, partial agonist might represent a new class of therapeutic molecules for the treatment of atherosclerosis.

Dual Peroxisome Proliferator-Activated Receptor α/γ Agonist

Dual PPARα/γ agonist has been focusing on the activation of both PPARα and PPARγ, which may provide a wider range of metabolic benefits. Studies have shown that most of the Dual PPARα/γ agonist play an active role in anti-atherosclerosis, such as GQ-11 (Silva, 2018), P633H (Chen et al., 2009), C333H (Xu et al., 2006), LT175 (Gilardi et al., 2014), and Tesaglitazar (Zadelaar et al., 2006; Chira et al., 2007; **Table 1**). GQ-11 improved insulin sensitivity and enhanced Glut4 expression in the adipose tissue, meanwhile the levels of MCP-1were reduced and the levels of IL-10 were increased. Furthermore, it also upregulation of Apoa1 and ABCA1 gene expression, then reduced triglycerides and VLDL cholesterol and increased HDL cholesterol in $LDLr^{-/-}$ mice (Silva et al., 2018). P633H can be accompanied by the upregulation of ACO and aP2 expression in db/db and KK-A^{y} mice, and is targeted to regulate PPARα in the liver and PPARγ in adipose tissue, respectively (Chen et al., 2009). C333H efficiently reduced blood lipid and glucose concentration in db/db mice (Xu et al., 2006). LT175 activates PPARγ in adipocytes, increases the expression of PPARγ target gene Glut4 and Adipoq in 3T3-L1 adipocytes and in a mouse model. Moreover, LT175 can also activate PPARα in the liver, trigger triglyceride and fatty acid catabolism, and achieve to eliminate the side effects of some conventional PPAR agonists (Gilardi et al., 2014). However, such effects are not clear in human situation. Tesaglitazar reduces atherosclerosis, reduces macrophage inflammation, number of adhesion monocytes and nuclear factor activity of the vessel wall (Zadelaar et al., 2006). However, some Dual PPARα/γ agonist such as compound 3q may accelerate atherosclerosis, it may related to the

increase expression of the vascular endothelial activation and inflammation markers, such as P-selectin, MCP-1, VCAM-1, and CD36, that are also associated with plaque complexity (Calkin et al., 2007). Dual agonists such as Tesaglitazar also showed better insulin sensitization effects as well as the prevention of atherosclerosis progression in clinical studies, but due to adverse side effects, including heart failure and myocardial ischemia, it has been discontinued in phase III clinical trials (Yamaguchi et al., 2014).

The PPARγ agonists shown to increase adipogenesis and body weight, whereas PPARα agonists counteract these effects by decreasing food intake and fat deposits. However, both its PPAR binding mode and its downstream targeting will change accordingly. LT175 impaired the recruitment of CBP coactivator, Tesaglitazar is accounted for by inhibition of both expression and acetylation/deactivation of cardiac PGC1α both in healthy C57BL/6 and diabetic db/db mice. Consistent with other partial agonists, GQ-11 only hydrogen bond with the PPARγ residue Ser289 at helix 3, which could reflect in weak PPARγ agonistic activities, and also interacts and weakly activates PPARα (Silva, 2018). Most of the dual PPARα/γ agonists, although they can improve insulin resistance as the full agonists, and do not have similar weight gain, negative bone effects, but it will appear adverse effects on the urothelial, renal, and cardiovascular system (Kaul et al., 2019; Chen et al., 2021). For the adverse side effects of PPARγ agonists in fluid retention, most studies have shown that this effect was due to increased reabsorption of sodium and water by the renal tubules, but the role of specific renal unit segments and sodium carriers was unclear. PPARγ-induced EGF receptors and non-genomic trans-activation of downstream extracellular signal-modulating kinases (ERKs) may augment sodium reabsorption in the proximal tubule (Beltowski et al., 2013). TZDs-like compounds significantly inhibited PPARγ phosphorylation in Ser112 while telmisartan did not (Kolli et al., 2014). Thus, telmisartan did not have a significant effect on osteoclast differentiation and osteogenesis. Dual PPARα/γ Tesaglitazar activation inhibits SIRT1-PGC1α axis and causes cardiac dysfunction. It was showed that this cardiac dysfunction was associated with reduced PGC1α expression. These effects are related to competition between PPARα and PPARγ to regulate Ppargc1a gene expression and to reduce cardiac SIRT1 expression (Kalliora et al., 2019). PGC1α is a regulator of mitochondrial function in thermogenic tissues, such as brown fat. Lehman et al. (2000) also found cardiac-specific overexpression of PGC1α in mice lead to uncontrolled mitochondrial proliferation in cardiomyocytes, resulting in loss of sarcomere structure and dilated cardiomyopathy. Inhibiting PGC1α on dual PPARα/γ activation is potentially as a key event that mediates the cardiotoxic effect, which would provide a guide for design of future PPAR agonists.

Non-agonist Peroxisome Proliferator-Activated Receptor Gamma Ligand

Non-agonist (Antagonists) PPARγ ligand, also known as PPAR modulators, exhibit high affinity but do not activate PPARγ. The Antagonists consists of two main categories, and one is known as PPARγ phosphorylation inhibitors, such as SR1664 (Cariou et al., 2012; Dias et al., 2020) and UHC1 (Choi et al., 2014). Taken SR1664 as an example, it has basically no transcriptional activation effect on PPARγ, but has a high affinity with PPARγ and belongs to a phosphorylation inhibitor, blocking the CDK5-mediated phosphorylation of PPARγ in Ser273 (Laghezza et al., 2018; Dias et al., 2020). SR1664 did not stimulate lipid accumulation or adipogenesis gene expression (such as aP2, Glut4, Lpl, CD36) in differentiating fat cells. UHC1 blocking CKD5-mediated PPARγ phosphorylation at position K395 in LBD, reducing macrophages inflammatory factor LPS-induced nitric oxide (NO) production both *in vitro* and in HFD-fed mice (Choi et al., 2014; Ribeiro Filho et al., 2019). Comparison with conventional full agonists, these antagonists do not stabilize helix 12 and display negligible changes in activation, but make unfavorable interactions with F282 on helix 3 (Asteian et al., 2015). Another class of PPAR modulators is relatively special, with structurally TZDs analogs, but with little effect on PPARγ, represent the compound as MSDC. It have been showed a potential therapeutic avenue for treating non-alcoholic steatohepatitis, improve the insulin resistance effect, regulate the lipid metabolism (Colca et al., 2018). However, the current study of atherosclerosis has not been reported. Its target of action was reported as a line Mitochondrial pyruvate carrier 2 (MPC2), which is the mitochondrial target of thiazolidinediones (mTOT) (Vigueira et al., 2017). Although not directly stimulated to PPARγ, but still has the potency of insulin sensitization.

CONCLUSION AND PERSPECTIVE

PPARγ plays a crucial role in anti-atherosclerosis, PPARγ-mediated anti-atherosclerosis depends on the basic expression level and activity level of PPARγ. At the same time, PPARγ transcription activity is no longer the only criterion, and the mode of action of the compound and PPARγ is the key to PPARγ activity. Both protein post-translational modification and selective modulators are different modes of PPARγ activity regulation. The mode of action between the compound and PPARγ determines the intensity and breadth of PPARγ-mediated transcriptional activation.

However, there are still many questions to be solved, such as the proteases involved in various post-translational modifications, and the protein interactions and downstream target genes regulated by these modifications are still unclear. In addition to the identified post-translational modifications, novel modification patterns or modification sites are still to be discovered. Different post-translational modifications may also interact and form closely related network, which provides a strong guarantee for the fine control of protein functions. The post-translational modifications of proteins are usually reversible, while the de-modification of PPARγ is relatively lagging behind. Transcriptional alteration of post-translational modifications is an innovative idea of new agonist, and only phosphorylation is partially applied to PPARγ agonist,

deacetylation and sumoylation has not been involved. How to selectively activate partial downstream targets of PPARγ to protect from atherosclerosis and relative metabolic diseases as well as reducing adverse effects deserve further investigation.

AUTHOR CONTRIBUTIONS

LY, LW, ZS, XJ, and LL contributed to the literature search. LY, LW, ZS, and LL wrote and revised the manuscript. LL designed the frame of this manuscript. All authors contributed to this manuscript and approved the submitted version.

FUNDING

This work was supported by the Shanghai Frontiers Science Research Base of Exercise and Metabolic Health, the research program of exercise and public health (0831) in Shanghai University of Sport.

REFERENCES

Akiyama, T. E., Sakai, S., Lambert, G., Nicol, C. J., Matsusue, K., Pimprale, S., et al. (2002). Conditional disruption of the peroxisome proliferator-activated receptor gamma gene in mice results in lowered expression of ABCA1, ABCG1, and apoE in macrophages and reduced cholesterol efflux. *Mol. Cell. Biol.* 22, 2607–2619. doi: 10.1128/MCB.22.8.2607-2619.2002

Asteian, A., Blayo, A. L., He, Y., Koenig, M., Shin, Y., Kuruvilla, D. S., et al. (2015). Design, Synthesis, and Biological Evaluation of Indole Biphenylcarboxylic Acids as PPARγ Antagonists. *ACS Med. Chem. Lett.* 6, 998–1003. doi: 10.1021/acsmedchemlett.5b00218

Babaev, V. R., Yancey, P. G., Ryzhov, S. V., Kon, V., Breyer, M. D., Magnuson, M. A., et al. (2005). Conditional knockout of macrophage PPARgamma increases atherosclerosis in C57BL/6 and low-density lipoprotein receptor-deficient mice. *Arterioscler. Thromb. Vasc. Biol.* 25, 1647–1653. doi: 10.1161/01.ATV.0000173413.31789.1a

Banks, A. S., McAllister, F. E., Camporez, J. P., Zushin, P. J., Jurczak, M. J., Laznik-Bogoslavski, D., et al. (2015). An ERK/Cdk5 axis controls the diabetogenic actions of PPARgamma. *Nature* 517, 391–395. doi: 10.1038/nature13887

Barros, C. D., Amato, A. A., de Oliveira, T. B., Iannini, K. B., Silva, A. L., Silva, T. G., et al. (2010). Synthesis and anti-inflammatory activity of new arylidene-thiazolidine-2,4-diones as PPARgamma ligands. *Bioorg. Med. Chem.* 18, 3805–3811. doi: 10.1016/j.bmc.2010.04.045

Beltowski, J., Rachanczyk, J., and Wlodarczyk, M. (2013). Thiazolidinedione-induced fluid retention: recent insights into the molecular mechanisms. *PPAR Res.* 2013:628628. doi: 10.1155/2013/628628

Bennett, M. R., Sinha, S., and Owens, G. K. (2016). Vascular Smooth Muscle Cells in Atherosclerosis. *Circ. Res.* 118, 692–702. doi: 10.1161/circresaha.115.306361

Bouhlel, M. A., Derudas, B., Rigamonti, E., Dièvart, R., Brozek, J., Haulon, S., et al. (2007). PPARgamma activation primes human monocytes into alternative M2 macrophages with anti-inflammatory properties. *Cell Metab.* 6, 137–143. doi: 10.1016/j.cmet.2007.06.010

Brunmeir, R., and Xu, F. (2018). Functional Regulation of PPARs through Post-Translational Modifications. *Int. J. Mol. Sci.* 19:1738. doi: 10.3390/ijms19061738

Brust, R., Shang, J., Fuhrmann, J., Mosure, S. A., Bass, J., Cano, A., et al. (2018). A structural mechanism for directing corepressor-selective inverse agonism of PPARgamma. *Nat. Commun.* 9:4687. doi: 10.1038/s41467-018-07133-w

Calabrò, P., Samudio, I., Safe, S. H., Willerson, J. T., and Yeh, E. T. (2005). Inhibition of tumor-necrosis-factor-alpha induced endothelial cell activation by a new class of PPAR-gamma agonists. An in vitro study showing receptor-independent effects. *J. Vasc. Res.* 42, 509–516. doi: 10.1159/000088260

Calkin, A. C., Allen, T. J., Lassila, M., Tikellis, C., Jandeleit-Dahm, K. A., and Thomas, M. C. (2007). Increased atherosclerosis following treatment with a dual PPAR agonist in the ApoE knockout mouse. *Atherosclerosis* 195, 17–22. doi: 10.1016/j.atherosclerosis.2006.11.021

Camejo, G. (2016). Selective PPAR modulators (SPPARs) may fill the need for treatment of the atherogenic dyslipidemia of insulin resistance and type 2 diabetes: can they reduce the associated cardiac risk? *Atherosclerosis* 249, 224–225. doi: 10.1016/j.atherosclerosis.2016.03.026

Cao, Q., Rong, S., Repa, J. J., St Clair, R., Parks, J. S., and Mishra, N. (2014). Histone deacetylase 9 represses cholesterol efflux and alternatively activated macrophages in atherosclerosis development. *Arterioscler. Thromb. Vasc. Biol.* 34, 1871–1879. doi: 10.1161/atvbaha.114.303393

Cariou, B., Charbonnel, B., and Staels, B. (2012). Thiazolidinediones and PPARgamma agonists: time for a reassessment. *Trends Endocrinol. Metab.* 23, 205–215. doi: 10.1016/j.tem.2012.03.001

Carmona, M. C., Louche, K., Lefebvre, B., Pilon, A., Hennuyer, N., and Audinot-Bouchez, V. (2007). S 26948: a new specific peroxisome proliferator activated receptor gamma modulator with potent antidiabetes and antiatherogenic effects. *Diabetes* 56, 2797–2808. doi: 10.2337/db06-1734

Chandra, V., Huang, P., Hamuro, Y., Raghuram, S., Wang, Y., Burris, T. P., et al. (2008). Structure of the intact PPAR-gamma-RXR- nuclear receptor complex on DNA. *Nature* 456, 350–356. doi: 10.1038/nature07413

Charo, I. F. (2007). Macrophage polarization and insulin resistance: PPARgamma in control. *Cell Metab.* 6, 96–98. doi: 10.1016/j.cmet.2007.07.006

Chen, F. L., Yang, Z. H., Liu, Y., Li, L. X., Liang, W. C., Wang, X. C., et al. (2008). Berberine inhibits the expression of TNFalpha, MCP-1, and IL-6 in AcLDL-stimulated macrophages through PPARgamma pathway. *Endocrine* 33, 331–337. doi: 10.1007/s12020-008-9089-3

Chen, F. L., Yang, Z. H., Wang, X. C., Liu, Y., Yang, Y. H., Li, L. X., et al. (2010). Adipophilin affects the expression of TNF-alpha, MCP-1, and IL-6 in THP-1 macrophages. *Mol. Cell. Biochem.* 337, 193–199. doi: 10.1007/s11010-009-0299-7

Chen, J., Zhang, X., Millican, R., Sherwood, J., Martin, S., Jo, H., et al. (2021). Recent advances in nanomaterials for therapy and diagnosis for atherosclerosis. *Adv. Drug Deliv. Rev.* 170, 142–199. doi: 10.1016/j.addr.2021.01.005

Chen, W., Zhou, X. B., Liu, H. Y., Xu, C., Wang, L. L., and Li, S. (2009). P633H, a novel dual agonist at peroxisome proliferator-activated receptors alpha and gamma, with different anti-diabetic effects in db/db and KK-Ay mice. *Br. J. Pharmacol.* 157, 724–735. doi: 10.1111/j.1476-5381.2009.00231.x

Chen, Z., Ishibashi, S., Perrey, S., Osuga, J., Gotoda, T., Kitamine, T., et al. (2001). Troglitazone inhibits atherosclerosis in apolipoprotein E-knockout mice: pleiotropic effects on CD36 expression and HDL. *Arterioscler. Thromb. Vasc. Biol.* 21, 372–377. doi: 10.1161/01.atv.21.3.372

Chira, E. C., McMillen, T. S., Wang, S., Haw, A. III, O'Brien, K. D., Wight, T. N., et al. (2007). Tesaglitazar, a dual peroxisome proliferator-activated receptor alpha/gamma agonist, reduces atherosclerosis in female low density lipoprotein receptor deficient mice. *Atherosclerosis* 195, 100–109. doi: 10.1016/j.atherosclerosis.2006.12.012

Chistiakov, D. A., Orekhov, A. N., and Bobryshev, Y. V. (2015). Vascular smooth muscle cell in atherosclerosis. *Acta Physiol.* 214, 33–50. doi: 10.1111/apha.12466

Choi, J. H., Banks, A. S., Estall, J. L., Kajimura, S., Bostrom, P., Laznik, D., et al. (2010). Anti-diabetic drugs inhibit obesity-linked phosphorylation of PPARgamma by Cdk5. *Nature* 466, 451–456. doi: 10.1038/nature09291

Choi, J. H., Banks, A. S., Kamenecka, T. M., Busby, S. A., Chalmers, M. J., Kumar, N., et al. (2011). Antidiabetic actions of a non-agonist PPARgamma ligand blocking Cdk5-mediated phosphorylation. *Nature* 477, 477–481. doi: 10.1038/nature10383

Choi, S., Jung, J. E., Yang, Y. R., Kim, E. S., Jang, H. J., Kim, E. K., et al. (2015). Novel phosphorylation of PPARgamma ameliorates obesity-induced adipose tissue inflammation and improves insulin sensitivity. *Cell Signal.* 27, 2488–2495. doi: 10.1016/j.cellsig.2015.09.009

Choi, S. S., Kim, E. S., Koh, M., Lee, S. J., Lim, D., Yang, Y. R., et al. (2014). A novel non-agonist peroxisome proliferator-activated receptor gamma (PPARgamma) ligand UHC1 blocks PPARgamma phosphorylation by cyclin-dependent kinase 5 (CDK5) and improves insulin sensitivity. *J. Biol. Chem.* 289, 26618–26629. doi: 10.1074/jbc.M114.566794

Colca, J. R., McDonald, W. G., and Adams, W. J. (2018). MSDC-0602K, a metabolic modulator directed at the core pathology of non-alcoholic steatohepatitis. *Expert Opin. Investig. Drugs* 27, 631–636. doi: 10.1080/13543784.2018.1494153

Crossno, J. T. Jr., Majka, S. M., Grazia, T., Gill, R. G., and Klemm, D. J. (2006). Rosiglitazone promotes development of a novel adipocyte population from bone marrow-derived circulating progenitor cells. *J. Clin. Invest.* 116, 3220–3228. doi: 10.1172/jci28510

DePaoli, A. M., Higgins, L. S., Henry, R. R., Mantzoros, C., and Dunn, F. L. (2014). Can a selective PPARγ modulator improve glycemic control in patients with type 2 diabetes with fewer side effects compared with pioglitazone? *Diabetes Care* 37, 1918–1923. doi: 10.2337/dc13-2480

Dias, M. M. G., Batista, F. A. H., Tittanegro, T. H., de Oliveira, A. G., Le Maire, A., Torres, F. R., et al. (2020). PPARgamma S273 Phosphorylation Modifies the Dynamics of Coregulator Proteins Recruitment. *Front. Endocrinol.* 11:561256. doi: 10.3389/fendo.2020.561256

Dunn, F. L., Higgins, L. S., Fredrickson, J., DePaoli, A. M., and INT131-004 study group (2011). Selective modulation of PPARgamma activity can lower plasma glucose without typical thiazolidinedione side-effects in patients with Type 2 diabetes. *J. Diabetes Complications* 25, 151–158. doi: 10.1016/j.jdiacomp.2010.06.006

Durham, A. L., Speer, M. Y., Scatena, M., Giachelli, C. M., and Shanahan, C. M. (2018). Role of smooth muscle cells in vascular calcification: implications in atherosclerosis and arterial stiffness. *Cardiovasc. Res.* 114, 590–600. doi: 10.1093/cvr/cvy010

Fajas, L., Auboeuf, D., Raspé, E., Schoonjans, K., Lefebvre, A. M., Saladin, R., et al. (1997). The organization, promoter analysis, and expression of the human PPARgamma gene. *J. Biol. Chem.* 272, 18779–18789. doi: 10.1074/jbc.272.30.18779

Falk, E. (2006). Pathogenesis of atherosclerosis. *J. Am. Coll. Cardiol.* 47, C7–C12. doi: 10.1016/j.jacc.2005.09.068

Finn, A. V., Saeed, O., and Virmani, R. (2012). Macrophage subsets in human atherosclerosis. *Circ. Res.* 110:e64. doi: 10.1161/circresaha.112.268714

Fu, M., Zhu, X., Wang, Q., Zhang, J., Song, Q., Zheng, H., et al. (2001). Platelet-derived growth factor promotes the expression of peroxisome proliferator-activated receptor gamma in vascular smooth muscle cells by a phosphatidylinositol 3-kinase/Akt signaling pathway. *Circ. Res.* 89, 1058–1064. doi: 10.1161/hh2301.099642

Garin-Shkolnik, T., Rudich, A., Hotamisligil, G. S., and Rubinstein, M. (2014). FABP4 attenuates PPARgamma and adipogenesis and is inversely correlated with PPARgamma in adipose tissues. *Diabetes* 63, 900–911. doi: 10.2337/db13-0436

Ge, C., Zhao, G., Li, B., Li, Y., Cawthorn, W. P., MacDougald, O. A., et al. (2018). Genetic inhibition of PPARgamma S112 phosphorylation reduces bone formation and stimulates marrow adipogenesis. *Bone* 107, 1–9. doi: 10.1016/j.bone.2017.10.023

Gilardi, F., Giudici, M., Mitro, N., Maschi, O., Guerrini, U., Rando, G., et al. (2014). LT175 is a novel PPARalpha/gamma ligand with potent insulin-sensitizing effects and reduced adipogenic properties. *J. Biol. Chem.* 289, 6908–6920. doi: 10.1074/jbc.M113.506394

Gu, H. F., Li, N., Xu, Z. Q., Hu, L., Li, H., Zhang, R. J., et al. (2019). Chronic Unpredictable Mild Stress Promotes Atherosclerosis via HMGB1/TLR4-Mediated Downregulation of PPARgamma/LXRalpha/ABCA1 in ApoE(-/-) Mice. *Front. Physiol.* 10:165. doi: 10.3389/fphys.2019.00165

Hall, J. A., Ramachandran, D., Roh, H. C., DiSpirito, J. R., Belchior, T., Zushin, P. H., et al. (2020). Obesity-Linked PPARgamma S273 Phosphorylation Promotes Insulin Resistance through Growth Differentiation Factor 3. *Cell Metab.* 32, 665–675.e6. doi: 10.1016/j.cmet.2020.08.016

Haschemi, A., Chin, B. Y., Jeitler, M., Esterbauer, H., Wagner, O., Bilban, M., et al. (2011). Carbon monoxide induced PPARγ SUMOylation and UCP2 block inflammatory gene expression in macrophages. *PLoS One* 6:e26376. doi: 10.1371/journal.pone.0026376

Hernandez-Quiles, M., Broekema, M. F., and Kalkhoven, E. (2021). PPARgamma in Metabolism, Immunity, and Cancer: unified and Diverse Mechanisms of Action. *Front. Endocrinol.* 12:624112. doi: 10.3389/fendo.2021.624112

Higgins, L. S., and Depaoli, A. M. (2010). Selective peroxisome proliferator-activated receptor gamma (PPARgamma) modulation as a strategy for safer therapeutic PPARgamma activation. *Am. J. Clin. Nutr.* 91, 267S–272S. doi: 10.3945/ajcn.2009.28449E

Hu, Y., Li, X., Zhi, X., Cong, W., Huang, B., Chen, H., et al. (2021). RANKL from bone marrow adipose lineage cells promotes osteoclast formation and bone loss. *EMBO Rep.* 22:e52481. doi: 10.15252/embr.202152481

Iankova, I., Petersen, R. K., Annicotte, J. S., Chavey, C., Hansen, J. B., Kratchmarova, I., et al. (2006). Peroxisome proliferator-activated receptor gamma recruits the positive transcription elongation factor b complex to activate transcription and promote adipogenesis. *Mol. Endocrinol.* 20, 1494–1505. doi: 10.1210/me.2005-0222

Janani, C., and Ranjitha Kumari, B. D. (2015). PPAR gamma gene–a review. *Diabetes Metab. Syndr.* 9, 46–50. doi: 10.1016/j.dsx.2014.09.015

Jang, J. Y., Bae, H., Lee, Y. J., Choi, Y. I., Kim, H. J., Park, S. B., et al. (2018). Structural Basis for the Enhanced Anti-Diabetic Efficacy of Lobeglitazone on PPARgamma. *Sci. Rep.* 8:31. doi: 10.1038/s41598-017-18274-1

Jennewein, C., Kuhn, A. M., Schmidt, M. V., Meilladec-Jullig, V., von Knethen, A., Gonzalez, F. J., et al. (2008). Sumoylation of peroxisome proliferator-activated receptor gamma by apoptotic cells prevents lipopolysaccharide-induced NCoR removal from kappaB binding sites mediating transrepression of proinflammatory cytokines. *J. Immunol.* 181, 5646–5652. doi: 10.4049/jimmunol.181.8.5646

Johnson, J. L. (2017). Metalloproteinases in atherosclerosis. *Eur. J. Pharmacol.* 816, 93–106. doi: 10.1016/j.ejphar.2017.09.007

Kalliora, C., Kyriazis, I. D., Oka, S. I., Lieu, M. J., Yue, Y., Area-Gomez, E., et al. (2019). Dual peroxisome-proliferator-activated-receptor-alpha/gamma activation inhibits SIRT1-PGC1alpha axis and causes cardiac dysfunction. *JCI Insight* 5:e129556. doi: 10.1172/jci.insight.129556

Katafuchi, T., Holland, W. L., Kollipara, R. K., Kittler, R., Mangelsdorf, D. J., and Kliewer, S. A. (2018). PPARgamma-K107 SUMOylation regulates insulin sensitivity but not adiposity in mice. *Proc. Natl. Acad. Sci. U. S. A.* 115, 12102–12111. doi: 10.1073/pnas.1814522115

Kaul, U., Parmar, D., Manjunath, K., Shah, M., Parmar, K., Patil, K. P., et al. (2019). New dual peroxisome proliferator activated receptor agonist-Saroglitazar in diabetic dyslipidemia and non-alcoholic fatty liver disease: integrated analysis of the real world evidence. *Cardiovasc. Diabetol.* 18:80. doi: 10.1186/s12933-019-0884-3

Kilroy, G., Kirk-Ballard, H., Carter, L. E., and Floyd, Z. E. (2012). The ubiquitin ligase Siah2 regulates PPARγ activity in adipocytes. *Endocrinology* 153, 1206–1218. doi: 10.1210/en.2011-1725

Kim, J. H., Park, K. W., Lee, E. W., Jang, W. S., Seo, J., Shin, S., et al. (2014). Suppression of PPARγ through MKRN1-mediated ubiquitination and degradation prevents adipocyte differentiation. *Cell Death Differ.* 21, 594–603. doi: 10.1038/cdd.2013.181

Kim, M. Y., Woo, E. M., Chong, Y. T., Homenko, D. R., and Kraus, W. L. (2006). Acetylation of estrogen receptor alpha by p300 at lysines 266 and 268 enhances the deoxyribonucleic acid binding and transactivation activities of the receptor. *Mol. Endocrinol.* 20, 1479–1493. doi: 10.1210/me.2005-0531

Kolli, V., Stechschulte, L. A., Dowling, A. R., Rahman, S., Czernik, P. J., and Lecka-Czernik, B. (2014). Partial agonist, telmisartan, maintains PPARγ serine 112 phosphorylation, and does not affect osteoblast differentiation and bone mass. *PLoS One* 9:e96323. doi: 10.1371/journal.pone.0096323

Kraakman, M. J., Liu, Q., Postigo-Fernandez, J., Ji, R., Kon, N., Larrea, D., et al. (2018). PPARgamma deacetylation dissociates thiazolidinedione's metabolic benefits from its adverse effects. *J. Clin. Invest.* 128, 2600–2612. doi: 10.1172/JCI98709

Kvandová, M., Majzúnová, M., and Dovinová, I. (2016). The role of PPARgamma in cardiovascular diseases. *Physiol. Res.* 65, S343–S363. doi: 10.33549/physiolres.933439

Laghezza, A., Piemontese, L., Cerchia, C., Montanari, R., Capelli, D., Giudici, M., et al. (2018). Identification of the First PPARalpha/gamma Dual Agonist Able To Bind to Canonical and Alternative Sites of PPARgamma and To Inhibit Its Cdk5-Mediated Phosphorylation. *J. Med. Chem.* 61, 8282–8298. doi: 10.1021/acs.jmedchem.8b00835

Law, R. E., Goetze, S., Xi, X. P., Jackson, S., Kawano, Y., Demer, L., et al. (2000). Expression and function of PPARgamma in rat and human vascular smooth muscle cells. *Circulation* 101, 1311–1318. doi: 10.1161/01.cir.101.11.1311

Lee, D. H., Huang, H., Choi, K., Mantzoros, C., and Kim, Y. B. (2012). Selective PPARγ modulator INT131 normalizes insulin signaling defects and improves bone mass in diet-induced obese mice. *Am. J. Physiol. Endocrinol. Metab.* 302, E552–E560. doi: 10.1152/ajpendo.00569.2011

Lehman, J. J., Barger, P. M., Kovacs, A., Saffitz, J. E., Medeiros, D. M., and Kelly, D. P. (2000). Peroxisome proliferator-activated receptor gamma coactivator-1 promotes cardiac mitochondrial biogenesis. *J. Clin. Invest.* 106, 847–856. doi: 10.1172/jci10268

Lehrke, M., and Lazar, M. A. (2005). The many faces of PPARgamma. *Cell* 123, 993–999. doi: 10.1016/j.cell.2005.11.026

Li, A. C., Binder, C. J., Gutierrez, A., Brown, K. K., Plotkin, C. R., Pattison, J. W., et al. (2004). Differential inhibition of macrophage foam-cell formation and atherosclerosis in mice by PPARα, β/δ, and γ. *J. Clin. Invest.* 114, 1564–1576. doi: 10.1172/jci200418730

Li, D., Zhang, L., Xu, L., Liu, L., He, Y., Zhang, Y., et al. (2017). WIP1 phosphatase is a critical regulator of adipogenesis through dephosphorylating PPARγ serine 112. *Cell. Mol. Life Sci.* 74, 2067–2079. doi: 10.1007/s00018-016-2450-4

Li, J. J., Wang, R., Lama, R., Wang, X., Floyd, Z. E., Park, E. A., et al. (2016). Ubiquitin Ligase NEDD4 Regulates PPARγ Stability and Adipocyte Differentiation in 3T3-L1 Cells. *Sci. Rep.* 6:38550. doi: 10.1038/srep38550

Li, P., Fan, W., Xu, J., Lu, M., Yamamoto, H., Auwerx, J., et al. (2011). Adipocyte NCoR knockout decreases PPARgamma phosphorylation and enhances PPARgamma activity and insulin sensitivity. *Cell* 147, 815–826. doi: 10.1016/j.cell.2011.09.050

Libby, P., Bornfeldt, K. E., and Tall, A. R. (2016). Atherosclerosis: successes, Surprises, and Future Challenges. *Circ. Res.* 118, 531–534. doi: 10.1161/CIRCRESAHA.116.308334

Lim, S., Ahn, B. Y., Chung, S. S., Park, H. S., Cho, B. J., Kim, M., et al. (2009). Effect of a peroxisome proliferator-activated receptor gamma sumoylation mutant on neointimal formation after balloon injury in rats. *Atherosclerosis* 206, 411–417. doi: 10.1016/j.atherosclerosis.2009.02.031

Lim, S., Lee, K. S., Lee, J. E., Park, H. S., Kim, K. M., Moon, J. H., et al. (2015). Effect of a new PPAR-gamma agonist, lobeglitazone, on neointimal formation after balloon injury in rats and the development of atherosclerosis. *Atherosclerosis* 243, 107–119. doi: 10.1016/j.atherosclerosis.2015.08.037

Liu, D., Wang, X., Zhang, M., Tian, J., Liu, M., Jin, T., et al. (2020). WISP1 alleviates lipid deposition in macrophages via the PPARgamma/CD36 pathway in the plaque formation of atherosclerosis. *J. Cell. Mol. Med.* 24, 11729–11741. doi: 10.1111/jcmm.15783

Liu, L., Fan, L., Chan, M., Kraakman, M. J., Yang, J., Fan, Y., et al. (2020). PPARgamma Deacetylation Confers the Antiatherogenic Effect and Improves Endothelial Function in Diabetes Treatment. *Diabetes* 69, 1793–1803. doi: 10.2337/db20-0217

Lu, Y., Zhou, Q., Shi, Y., Liu, J., Zhong, F., Hao, X., et al. (2013). SUMOylation of PPARγ by rosiglitazone prevents LPS-induced NCoR degradation mediating down regulation of chemokines expression in renal proximal tubular cells. *PLoS One* 8:e79815. doi: 10.1371/journal.pone.0079815

Luo, F., Wang, Z. H., Du, L. L., and Wang, J. (2007). [Effects of PPAR-gamma agonist and MMP-2 on formation of atherosclerosis plaque in rabbits]. *Zhonghua Bing Li Xue Za Zhi* 36, 556–557.

Machado-Oliveira, G., Ramos, C., Marques, A. R. A., and Vieira, O. V. (2020). Cell Senescence, Multiple Organelle Dysfunction and Atherosclerosis. *Cells* 9:2146. doi: 10.3390/cells9102146

Marfella, R., D'Amico, M., Esposito, K., Baldi, A., Di Filippo, C., Siniscalchi, M., et al. (2006). The ubiquitin-proteasome system and inflammatory activity in diabetic atherosclerotic plaques: effects of rosiglitazone treatment. *Diabetes* 55, 622–632. doi: 10.2337/diabetes.55.03.06.db05-0832

Martens, F. M., Visseren, F. L., Lemay, J., de Koning, E. J., and Rabelink, T. J. (2002). Metabolic and additional vascular effects of thiazolidinediones. *Drugs* 62, 1463–1480. doi: 10.2165/00003495-200262100-00004

Meredith, D., Panchatcharam, M., Miriyala, S., Tsai, Y. S., Morris, A. J., Maeda, N., et al. (2009). Dominant-negative loss of PPARgamma function enhances smooth muscle cell proliferation, migration, and vascular remodeling. *Arterioscler. Thromb. Vasc. Biol.* 29, 465–471. doi: 10.1161/ATVBAHA.109.184234

Montanari, R., Capelli, D., Yamamoto, K., Awaishima, H., Nishikata, K., Barendregt, A., et al. (2020). Insights into PPARgamma Phosphorylation and Its Inhibition Mechanism. *J. Med. Chem.* 63, 4811–4823. doi: 10.1021/acs.jmedchem.0c00048

Nakaya, H., Summers, B. D., Nicholson, A. C., Gotto, A. M. Jr., Hajjar, D. P., and Han, J. (2009). Atherosclerosis in LDLR-knockout mice is inhibited, but not reversed, by the PPARgamma ligand pioglitazone. *Am. J. Pathol.* 174, 2007–2014. doi: 10.2353/ajpath.2009.080611

Namgaladze, D., Kemmerer, M., von Knethen, A., and Brüne, B. (2013). AICAR inhibits PPARγ during monocyte differentiation to attenuate inflammatory responses to atherogenic lipids. *Cardiovasc. Res.* 98, 479–487. doi: 10.1093/cvr/cvt073

Oppi, S., Nusser-Stein, S., Blyszczuk, P., Wang, X., Jomard, A., Marzolla, V., et al. (2020). Macrophage NCOR1 protects from atherosclerosis by repressing a pro-atherogenic PPARgamma signature. *Eur. Heart J.* 41, 995–1005. doi: 10.1093/eurheartj/ehz667

Osman, I., and Segar, L. (2016). Pioglitazone, a PPARgamma agonist, attenuates PDGF-induced vascular smooth muscle cell proliferation through AMPK-dependent and AMPK-independent inhibition of mTOR/p70S6K and ERK signaling. *Biochem. Pharmacol.* 101, 54–70. doi: 10.1016/j.bcp.2015.11.026

Ozasa, H., Ayaori, M., Iizuka, M., Terao, Y., Uto-Kondo, H., Yakushiji, E., et al. (2011). Pioglitazone enhances cholesterol efflux from macrophages by increasing ABCA1/ABCG1 expressions via PPARγ/LXRα pathway: findings from in vitro and ex vivo studies. *Atherosclerosis* 219, 141–150. doi: 10.1016/j.atherosclerosis.2011.07.113

Pascual, G., Fong, A. L., Ogawa, S., Gamliel, A., Li, A. C., Perissi, V., et al. (2005). A SUMOylation-dependent pathway mediates transrepression of inflammatory response genes by PPAR-gamma. *Nature* 437, 759–763. doi: 10.1038/nature03988

Pourcet, B., Staels, B., and Glineur, C. (2013). PPAR SUMOylation: some useful experimental tips. *Methods Mol. Biol.* 952, 145–161. doi: 10.1007/978-1-62703-155-4_10

Qiang, L., Wang, L., Kon, N., Zhao, W., Lee, S., Zhang, Y., et al. (2012). Brown remodeling of white adipose tissue by SirT1-dependent deacetylation of Ppargamma. *Cell* 150, 620–632. doi: 10.1016/j.cell.2012.06.027

Reinhold, S., Blankesteijn, W. M., and Foulquier, S. (2020). The Interplay of WNT and PPARgamma Signaling in Vascular Calcification. *Cells* 9:2658. doi: 10.3390/cells9122658

Ribeiro Filho, H. V., Guerra, J. V., Cagliari, R., Batista, F. A. H., Le Maire, A., Oliveira, P. S. L., et al. (2019). Exploring the mechanism of PPARgamma phosphorylation mediated by CDK5. *J. Struct. Biol.* 207, 317–326. doi: 10.1016/j.jsb.2019.07.007

Silva, J. C. (2018). GQ-11: a new PPAR agonist improves obesity-induced metabolic alterations in LDLr(-/-) mice. *Int. J. Obes.* 42, 1062–1072.

Silva, J. C., Cesar, F. A., de Oliveira, E. M., Turato, W. M., Tripodi, G. L., Castilho, G., et al. (2016). New PPARgamma partial agonist improves obesity-induced metabolic alterations and atherosclerosis in LDLr(-/-) mice. *Pharmacol. Res.* 104, 49–60. doi: 10.1016/j.phrs.2015.12.010

Silva, J. C., de Oliveira, E. M., Turato, W. M., Trossini, G. H. G., Maltarollo, V. G., Pitta, M. G. R., et al. (2018). GQ-11: a new PPAR agonist improves obesity-induced metabolic alterations in LDLr(-/-) mice. *Int. J. Obes.* 42, 1062–1072. doi: 10.1038/s41366-018-0011-7

Sohn, J. H., Kim, J. I., Jeon, Y. G., Park, J., and Kim, J. B. (2018). Effects of Three Thiazolidinediones on Metabolic Regulation and Cold-Induced Thermogenesis. *Mol. Cells* 41, 900–908. doi: 10.14348/molcells.2018.0294

Sohn, K. A., Cruciani-Guglielmacci, C., Kassis, N., Clement, L., Ouali, F., and Cauzac, M. (2009). S26948, a new specific peroxisome proliferator activated receptor gamma modulator improved in vivo hepatic insulin sensitivity in 48 h lipid infused rats. *Eur. J. Pharmacol.* 608, 104–111. doi: 10.1016/j.ejphar.2009.02.033

Song, J. W., Nam, H. S., Ahn, J. W., Park, H. S., Kang, D. O., Kim, H. J., et al. (2021). Macrophage targeted theranostic strategy for accurate detection and rapid stabilization of the inflamed high-risk plaque. *Theranostics* 11, 8874–8893. doi: 10.7150/thno.59759

Srivastava, R. A. (2011). Evaluation of anti-atherosclerotic activities of PPAR-alpha, PPAR-gamma, and LXR agonists in hyperlipidemic atherosclerosis-susceptible F(1)B hamsters. *Atherosclerosis* 214, 86–93. doi: 10.1016/j.atherosclerosis.2010.10.033

Sueyoshi, S., Mitsumata, M., Kusumi, Y., Niihashi, M., Esumi, M., Yamada, T., et al. (2010). Increased expression of peroxisome proliferator-activated receptor (PPAR)-alpha and PPAR-gamma in human atherosclerosis. *Pathol. Res. Pract.* 206, 429–438. doi: 10.1016/j.prp.2010.01.010

Tabas, I. (2017). 2016 Russell Ross Memorial Lecture in Vascular Biology: molecular-Cellular Mechanisms in the Progression of Atherosclerosis. *Arterioscler. Thromb. Vasc. Biol.* 37, 183–189. doi: 10.1161/ATVBAHA.116.308036

Tian, L., Wang, C., Hagen, F. K., Gormley, M., Addya, S., Soccio, R., et al. (2014). Acetylation-defective mutant of Pparγ is associated with decreased lipid synthesis in breast cancer cells. *Oncotarget* 5, 7303–7315. doi: 10.18632/oncotarget.2371

Tsuboi, T., Lu, R., Yonezawa, T., Watanabe, A., Woo, J. T., Abe-Dohmae, S., et al. (2020). Molecular mechanism for nobiletin to enhance ABCA1/G1 expression in mouse macrophages. *Atherosclerosis* 297, 32–39. doi: 10.1016/j.atherosclerosis.2020.01.024

Vallee, A., Vallee, J. N., and Lecarpentier, Y. (2019). Metabolic reprogramming in atherosclerosis: opposed interplay between the canonical WNT/beta-catenin pathway and PPARgamma. *J. Mol. Cell. Cardiol.* 133, 36–46. doi: 10.1016/j.yjmcc.2019.05.024

van Beekum, O., Fleskens, V., and Kalkhoven, E. (2009). Posttranslational modifications of PPAR-gamma: fine-tuning the metabolic master regulator. *Obesity* 17, 213–219. doi: 10.1038/oby.2008.473

Verrier, E., Wang, L., Wadham, C., Albanese, N., Hahn, C., Gamble, J. R., et al. (2004). PPARgamma agonists ameliorate endothelial cell activation via inhibition of diacylglycerol-protein kinase C signaling pathway: role of diacylglycerol kinase. *Circ. Res.* 94, 1515–1522. doi: 10.1161/01.Res.0000130527.92537.06

Vigueira, P. A., McCommis, K. S., Hodges, W. T., Schweitzer, G. G., Cole, S. L., Oonthonpan, L., et al. (2017). The beneficial metabolic effects of insulin sensitizers are not attenuated by mitochondrial pyruvate carrier 2 hypomorphism. *Exp. Physiol.* 102, 985–999. doi: 10.1113/EP086380

Viles-Gonzalez, J. F., Choi, B. G., Fuster, V., and Badimon, J. J. (2004). Peroxisome proliferator-activated receptor ligands in atherosclerosis. *Expert Opin. Investig. Drugs* 13, 1393–1403. doi: 10.1517/13543784.13.11.1393

Wadosky, K. M., and Willis, M. S. (2012). The story so far: post-translational regulation of peroxisome proliferator-activated receptors by ubiquitination and SUMOylation. *Am. J. Physiol. Heart Circ. Physiol.* 302, H515–H526. doi: 10.1152/ajpheart.00703.2011

Wang, J., Uryga, A. K., Reinhold, J., Figg, N., Baker, L., Finigan, A., et al. (2015). Vascular Smooth Muscle Cell Senescence Promotes Atherosclerosis and Features of Plaque Vulnerability. *Circulation* 132, 1909–1919. doi: 10.1161/circulationaha.115.016457

Wang, M., and Tafuri, S. (2003). Modulation of PPARgamma activity with pharmaceutical agents: treatment of insulin resistance and atherosclerosis. *J. Cell. Biochem.* 89, 38–47. doi: 10.1002/jcb.10492

Watanabe, M., Takahashi, H., Saeki, Y., Ozaki, T., Itoh, S., Suzuki, M., et al. (2015). The E3 ubiquitin ligase TRIM23 regulates adipocyte differentiation via stabilization of the adipogenic activator PPARγ. *Elife* 4:e05615. doi: 10.7554/eLife.05615

Xie, X., Chen, W., Zhang, N., Yuan, M., Xu, C., Zheng, Z., et al. (2017). Selective Tissue Distribution Mediates Tissue-Dependent PPARγ Activation and Insulin Sensitization by INT131, a Selective PPARγ Modulator. *Front. Pharmacol.* 8:317. doi: 10.3389/fphar.2017.00317

Xu, C., Wang, L. L., Liu, H. Y., Zhou, X. B., Cao, Y. L., and Li, S. (2006). C333H, a novel PPARalpha/gamma dual agonist, has beneficial effects on insulin resistance and lipid metabolism. *Acta Pharmacol. Sin.* 27, 223–228. doi: 10.1111/j.1745-7254.2006.00263.x

Yamaguchi, K., Wakatsuki, T., Soeki, T., Niki, T., Taketani, Y., Oeduka, H., et al. (2014). Effects of telmisartan on inflammatory cytokines and coronary plaque component as assessed on integrated backscatter intravascular ultrasound in hypertensive patients. *Circ. J.* 78, 240–247. doi: 10.1253/circj.cj-13-0741

Yang, H., Cheng, J., Song, Z., Li, X., Zhang, Z., Mai, Y., et al. (2013). The anti-adipogenic effect of PGRN on porcine preadipocytes involves ERK1,2 mediated PPARgamma phosphorylation. *Mol. Biol. Rep.* 40, 6863–6872. doi: 10.1007/s11033-013-2804-z

Yang, X., Yao, H., Chen, Y., Sun, L., Li, Y., Ma, X., et al. (2015). Inhibition of Glutathione Production Induces Macrophage CD36 Expression and Enhances Cellular-oxidized Low Density Lipoprotein (oxLDL) Uptake. *J. Biol. Chem.* 290, 21788–21799. doi: 10.1074/jbc.M115.654582

Yin, R., Dong, Y. G., and Li, H. L. (2006). PPARgamma phosphorylation mediated by JNK MAPK: a potential role in macrophage-derived foam cell formation. *Acta Pharmacol. Sin.* 27, 1146–1152. doi: 10.1111/j.1745-7254.2006.00359.x

Yu, X. H., Fu, Y. C., Zhang, D. W., Yin, K., and Tang, C. K. (2013). Foam cells in atherosclerosis. *Clin. Chim. Acta* 424, 245–252. doi: 10.1016/j.cca.2013.06.006

Zadelaar, A. S., Boesten, L. S., Jukema, J. W., van Vlijmen, B. J., Kooistra, T., Emeis, J. J., et al. (2006). Dual PPARalpha/gamma agonist tesaglitazar reduces atherosclerosis in insulin-resistant and hypercholesterolemic ApoE*3Leiden mice. *Arterioscler. Thromb. Vasc. Biol.* 26, 2560–2566. doi: 10.1161/01.Atv.0000242904.34700.66

Zhang, L., and Chawla, A. (2004). Role of PPARgamma in macrophage biology and atherosclerosis. *Trends Endocrinol. Metab.* 15, 500–505. doi: 10.1016/j.tem.2004.10.006

Zhang, L. L., Gao, C. Y., Fang, C. Q., Wang, Y. J., Gao, D., Yao, G. E., et al. (2011). PPARgamma attenuates intimal hyperplasia by inhibiting TLR4-mediated inflammation in vascular smooth muscle cells. *Cardiovasc. Res.* 92, 484–493. doi: 10.1093/cvr/cvr238

Zhang, Y., Shi, X., Han, J., Peng, W., Fang, Z., Zhou, Y., et al. (2021). Convallatoxin Promotes M2 Macrophage Polarization to Attenuate Atherosclerosis Through PPARgamma-Integrin alphavbeta5 Signaling Pathway. *Drug Des. Devel. Ther.* 15, 803–812. doi: 10.2147/DDDT.S288728

Zhang, Y., Wang, Y., Li, X., Gu, K., Li, M., Zhang, Y., et al. (2020). WSF-7 Inhibits Obesity-Mediated PPARγ Phosphorylation and Improves Insulin Sensitivity in 3T3-L1 Adipocytes. *Biol. Pharm. Bull.* 43, 526–532. doi: 10.1248/bpb.b19-00986

Zhang, Y., Yang, X., Bian, F., Wu, P., Xing, S., Xu, G., et al. (2014). TNF-alpha promotes early atherosclerosis by increasing transcytosis of LDL across endothelial cells: crosstalk between NF-kappaB and PPAR-gamma. *J. Mol. Cell. Cardiol.* 72, 85–94. doi: 10.1016/j.yjmcc.2014.02.012

Zinn, A., Felson, S., Fisher, E., and Schwartzbard, A. (2008). Reassessing the cardiovascular risks and benefits of thiazolidinediones. *Clin. Cardiol.* 31, 397–403. doi: 10.1002/clc.20312

Conflict of Interest: The authors declare that the research was conducted in the absence of any commercial or financial relationships that could be construed as a potential conflict of interest.

Publisher's Note: All claims expressed in this article are solely those of the authors and do not necessarily represent those of their affiliated organizations, or those of the publisher, the editors and the reviewers. Any product that may be evaluated in this article, or claim that may be made by its manufacturer, is not guaranteed or endorsed by the publisher.

Copyright © 2022 Yin, Wang, Shi, Ji and Liu. This is an open-access article distributed under the terms of the Creative Commons Attribution License (CC BY). The use, distribution or reproduction in other forums is permitted, provided the original author(s) and the copyright owner(s) are credited and that the original publication in this journal is cited, in accordance with accepted academic practice. No use, distribution or reproduction is permitted which does not comply with these terms.

frontiers in Physiology

MINI REVIEW
published: 03 March 2022
doi: 10.3389/fphys.2022.837723

New Insights Into the Role of Inflammation in the Brain in Heart Failure

*Emilio Badoer**

School of Health and Biomedical Sciences, RMIT University, Melbourne, VIC, Australia

Heart failure is a growing medical problem. Although the underlying aetiology of heart failure differs according to the phenotype, there are some common characteristics observed in patients with heart failure. These include an increased sympathetic nerve activity, an activated renin–angiotensin system, and inflammation. The mechanisms mediating the increased sympathetic activity are not completely understood but the central nervous system plays a major role. Activation of the renin–angiotensin system plays an active role in the remodelling of the heart and in fluid and electrolyte imbalance. The presence of a central renin–angiotensin system means that locally produced angiotensin in the brain may also play a key role in autonomic dysfunction seen in heart failure. Markers of inflammation in the heart and in the circulation are observed in patients diagnosed with heart failure. Circulating pro-inflammatory cytokines can also influence cardiac function further afield than just locally in the heart including actions within the brain to activate the sympathetic nervous system. Preclinical evidence suggests that targeting the pro-inflammatory cytokines would be a useful therapy to treat heart failure. Most clinical studies have been disappointing. This mini-review suggests that pro-inflammatory cytokines in the brain play a key role and there is a problem associated with access of effective doses of the drugs to the site of action in the brain. The recent advances in nanotechnology delivery techniques may provide exciting future technology to investigate the role of specific pro-inflammatory mediators as novel targets within the brain in the treatment of heart failure.

Keywords: inflammation, central nervous system, heart failure, nanoparticles, TNF, interleukins

OPEN ACCESS

Edited by:
James Todd Pearson, National Cerebral and Cardiovascular Center, Japan

Reviewed by:
Baojian Xue, The University of Iowa, United States

***Correspondence:**
Emilio Badoer
emilio.badoer@rmit.edu.au

Specialty section:
This article was submitted to Integrative Physiology, a section of the journal Frontiers in Physiology

Received: *17 December 2021*
Accepted: *15 February 2022*
Published: *03 March 2022*

Citation:
Badoer E (2022) New Insights Into the Role of Inflammation in the Brain in Heart Failure. Front. Physiol. 13:837723. doi: 10.3389/fphys.2022.837723

INTRODUCTION

Heart Failure Is a Growing Problem

Heart failure is a growing medical problem. Although some studies had suggested that the growth in heart failure cases had plateaued, more recent evidence shows that the worldwide incidence of heart failure continues to grow, particularly in the elderly citizens of our community (Roth et al., 2015; Conrad et al., 2018; Cleland et al., 2019). The cost to the health system of caring for patients with heart failure is huge and in the United States alone, the total cost has been estimated to be over $30 billion annually, an extraordinary amount (Bozkurt et al., 2021b). By world standards, the fastest rate of rise in the prevalence of heart failure is occurring

in China and India (Bragazzi et al., 2021). Given the population of these two countries, the future global health burden of heart failure is starkly clear.

Phenotype of Heart Failure

Heart failure, as the name suggests, is a functionally abnormal heart that results from either structural and/or functional deficits. These induce an elevation in intracardiac pressures and/or reduced cardiac output. The level of ejection fraction has normally determined the phenotype of heart failure and the latest terminology that has been suggested defines three over-arching phenotypes; (i) heart failure with reduced ejection fraction (HFrEF) where ejection fraction is less than 40%, (ii) heart failure with mildly reduced ejection fraction (HRmEF) where ejection fraction is between 41 to 49%, (iii) heart failure with preserved ejection fraction (HFpEF) where ejection fraction is greater than 50% (Bozkurt et al., 2021a). The majority of patients diagnosed with heart failure have ejection fractions less than 50% (i.e., HFrEF or HFmEF). Generally, patients with HFrEF are believed to have worse prognosis but not all studies provide evidence for this view (Pocock et al., 2013). Accurate diagnosis of the phenotype of heart failure is important in guiding therapy. Pharmacological treatment of patients with HFrEF is more successful than in patients with HFpEF where convincing evidence of reduced mortality and morbidity is somewhat scarce. Some recent trials suggest there may be a benefit (Solomon et al., 2016, 2020).

Characteristics of Heart Failure: Increased Sympathetic Nerve Activity

Although the underlying aetiology of heart failure differs according to the phenotype, as suggested by the different responses to pharmacological treatment, there are some common characteristics observed in patients with heart failure. These include an increased sympathetic nerve activity, an activated renin–angiotensin system, and inflammation. Why, then, does pharmacological therapy improve HFrEF with relatively little impact on HFpEF?

Increased sympathetic nerve activity occurs in all phenotypes of heart failure (Parati and Esler, 2012). Initially, the increase in sympathetic nerve activity is compensatory but the sustained increase eventually is detrimental and worsens the prognosis (Kaye et al., 1995; **Figure 1**). The mechanisms mediating the increased sympathetic activity are not completely understood but the work in preclinical models of heart failure indicate that the central nervous system plays a major role, particularly nuclei such as the hypothalamic paraventricular nucleus (PVN), the nuclei of the lamina terminalis that lack a blood–brain barrier [e.g., the subfornical organ (SFO)] and medullary nuclei such as the rostral and caudal ventrolateral medulla (RVLM and CVLM, respectively; Xu et al., 2012).

The PVN projects to the intermediolateral cell column were sympathetic preganglionic motor neurons reside, and the PVN also sends collaterals to the RVLM neurons which send direct projections to the sympathetic preganglionic motor neurons as well (Shafton et al., 1998). Thus, the PVN has the anatomical connections that directly and indirectly influence sympathetic nerve activity. The PVN also receives inputs from the SFO and RVLM. An imbalance of excitatory and inhibitory inputs within the PVN has been suggested to contribute to the excessive sympathetic nerve activity in heart failure in rats (Zheng et al., 2011), suggesting these anatomical pathways play an important role. Peripheral afferent inputs that appear to contribute to the activation of the central pathways mediating the increased sympathetic outflow in heart failure include overactivity of the afferent renal nerves, overactivity of the carotid sinus afferents and angiotensin II (Schultz et al., 2015; Zheng et al., 2018).

Characteristics of Heart Failure: Activation of the Renin–Angiotensin System

In heart failure, there is activation of the renin–angiotensin system which plays an active role in the remodelling of the heart and in fluid and electrolyte imbalance which are compensatory initially but eventually leads to worsening of the condition (**Figure 1**). Given the wide distribution of the renin–angiotensin system in the cardiovascular system and in the heart, it is not surprising that angiotensin-converting enzyme inhibitors and angiotensin receptor blockers have become key first line therapeutic interventions in heart failure.

The renin–angiotensin system is complex and consists of different receptor subtypes and, upon activation, they may initiate similar or even antagonistic responses, as is seen with the activation of type 1 (AT1R) and type 2 (AT2R) angiotensin receptors in various tissues (Kurdi et al., 2005). In addition to the classical ten amino acid peptide, angiotensin II, there are several angiotensin peptides (e.g., Ang 1-7, Ang 2-8 and Ang 1-9) produced by metabolism of angiotensin II by different enzymes. These peptides may have their own actions through binding to the classical or their own specific receptors such as in the case with Ang 1-7 that can bind AT1R, AT2R and the *mas* receptor (Iusuf et al., 2008). The latter may be particularly important for cardiac hypertrophy and fibrosis (Wang et al., 2017).

Adding to the complexity is the fact that components of the renin–angiotensin system are widely distributed and can induce local production of angiotensin (for example in the heart) as well as systemic production of angiotensin. Further, the presence of a central renin–angiotensin system means that locally produced angiotensin in the brain can also play a key role in cardiovascular disease and autonomic dysfunction. Additionally, centrally mediated actions can be elicited by peripherally produced angiotensin II acting on nuclei that lack a blood brain barrier, like the SFO (Wright and Harding, 2013).

Angiotensin II can elicit an increase in sympathetic nerve activity and this involves both central as well as peripheral sites of action. Several nuclei within the central nervous system, like the PVN, SFO and RVLM, have dense concentrations of angiotensin receptors and contribute to the increase in sympathetic nerve activity induced by angiotensin II and observed in heart failure (Zheng et al., 2009; Wang et al., 2014; Sharma et al., 2021). Thus, there exists an inter-relationship between the renin–angiotensin system and sympathetic nerve

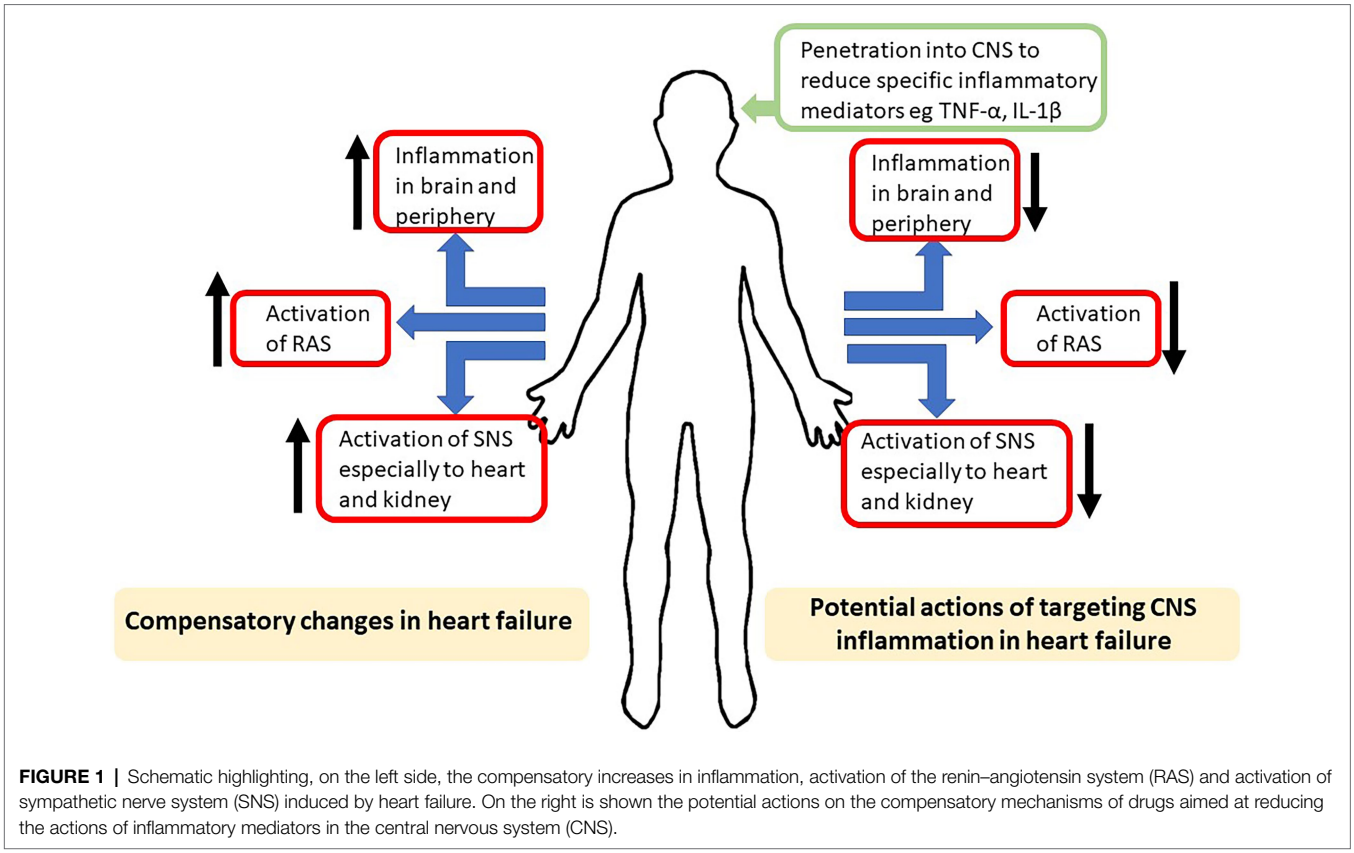

FIGURE 1 | Schematic highlighting, on the left side, the compensatory increases in inflammation, activation of the renin–angiotensin system (RAS) and activation of sympathetic nerve system (SNS) induced by heart failure. On the right is shown the potential actions on the compensatory mechanisms of drugs aimed at reducing the actions of inflammatory mediators in the central nervous system (CNS).

activation in heart failure. This inter-relationship may also exist with inflammation since angiotensin II can mediate inflammatory responses and could contribute to the increase in inflammation that is seen in heart failure.

Characteristics of Heart Failure: Increased Inflammation

Markers of inflammation in the heart and in the circulation are observed in patients diagnosed with heart failure (**Figure 1**). Indeed, the levels of circulating cytokines are correlated with the severity of heart failure and prognosis (Rauchhaus et al., 2000; Braunwald, 2008). It has been known for some time that pro-inflammatory cytokines, for example tumour necrosis factor alpha (TNF-α), interleukin-1β, interleukin-2 and interleukin-4, can induce pulmonary oedema, ventricular contractility abnormalities and dysfunctional cardiac metabolism which can result in reduced cardiac function (Hegewisch et al., 1990; Bradham et al., 2002).

Circulating pro-inflammatory cytokines can also influence cardiac function further afield than just locally in the heart. More recent work has suggested that circulating pro-inflammatory cytokines can activate the sympathetic nervous system *via* activation of cells within the SFO. The effects of circulating pro-inflammatory cytokines on sympathetic nerve activity can be reproduced by direct microinjection of those pro-inflammatory cytokines into the SFO (Wei et al., 2015). The mechanisms involved are not clear but activation of the local renin–angiotensin system in the SFO and subsequent increases in prostaglandins and reactive oxygen species in the PVN and further cytokine production in the PVN appear to be involved (Wei et al., 2015). A critical role of the pro-inflammatory cytokine, TNF-α, in the SFO is further reinforced by the finding that the knockdown of the TNF-α receptor 1 in the SFO reduced the increase in sympathetic nerve activity normally observed in the myocardial infarction-induced model of heart failure (Yu et al., 2017). Despite the improved cardiac haemodynamics in the treated rats, cardiac function did not improve over the short observation period.

Thus, although abundant preclinical evidence would suggest that targeting the pro-inflammatory cytokines would be a useful therapy to treat heart failure, functional improvement in heart failure still appears elusive. To date, it has been very disappointing to see the results of clinical trials that have attempted to inhibit the actions of pro-inflammatory cytokines. Clinical trials targeting TNF-α using etanercept or infliximab in heart failure (e.g., RENAISSANCE, RECOVER, RENEWAL and ATTACH) were prematurely terminated due to the lack of beneficial outcomes or, in some instances, worse outcomes for patients (Chung et al., 2003; Mann et al., 2004). Although such trials have not provided the outcomes expected based on preclinical studies, there may still be some positive and encouraging signs emerging from more recent studies targeting other pro-inflammatory cytokines (CANTOS trial). In particular, the finding using

Canakinumab to inhibit interleukin-1β function, showed a reduction in hospitalisations and mortality due to heart failure (Everett et al., 2018).

What Are the Key Challenges?

It would appear perplexing that studies in animals strongly suggest a role of pro-inflammatory cytokines in the aetiology of heart failure, yet the outcomes of clinical trials using anti-inflammatory therapeutics have been decidedly unimpressive and have not provided support for such a view. What could explain this paradox? There are several possibilities that could be considered, and I would like to focus on two in this mini-review; Firstly, the target needs to be more specifically identified. Second, the inflammatory mediators in the CNS play a greater role, thus targeting these more specifically may be required.

Targeting Specific Pro-Inflammatory Mediators and the Role of the CNS

The evidence to date indicates that pro-inflammatory mediators like TNF-α, interleukins, reactive oxygen species and angiotensin II are increased in heart failure. These increases occur locally within the myocardium, systemically (i.e., circulating in the blood) and within the central nervous system. Therapeutic agents like angiotensin-converting enzyme inhibitors and angiotensin II receptor blockers are front line therapy for heart failure, both in HFrEF and HFpEF. However, the evidence suggests they ameliorate the symptoms of HFrEF and have positive outcomes, but they have little or no positive influence on HFpEF. Anti-TNF-α treatments investigated in animal models of heart failure showed great promise; unfortunately, these hopes have not been fulfilled in clinical studies. But as noted earlier, there is a glimmer of hope from the recent findings in the CANTOS trial raising the possibility that specific targeting of interleukin-1β may be beneficial. This does raise the possibility that targeting specific pro-inflammatory mediators may be the way forward and clearly needs more work.

Another issue that needs to be addressed is the role of inflammatory mediators within the CNS, which may be playing a larger role than hitherto appreciated. Circumstantial evidence for this view arises from many studies. For example, TNF-α is increased in specific brain nuclei known to influence sympathetic nerve function (Kang et al., 2008). Direct microinjections of TNF-α into specific brain nuclei increases sympathetic nerve activity (Korim et al., 2019). and anti-TNF-α treatment reduces the abnormally elevated sympathetic nerve activity in an ischaemia-induced model of heart failure in rats (Guggilam et al., 2007). These studies suggest a key role for TNF-α within the brain in heart failure aetiology. This view is further supported by studies in which reducing the synthesis of TNF-α by decreasing the function of TNF-α-converting enzyme resulted in improved systemic haemodynamic variables while increased levels of the enzyme resulted in worse symptoms of heart failure in rats (Yu et al., 2019).

Interleukins in the brain are also important. The gene transfer of human interleukin-10 (a potent anti-inflammatory) using intraventricular administration in a rat model of heart failure resulted in amelioration of heart failure symptoms (Yu et al., 2007). Similarly, inhibition of pro-inflammatory cytokines in the brain using pentoxifylline reduced the neurohumoral excitation, that normally accompanies heart failure, in the coronary ligation model of heart failure in rats (Kang et al., 2008).

It should not be forgotten that there may exist a complex relationship between central and peripheral pro-inflammatory mediators. For example, elevated levels of circulating pro-inflammatory cytokines and angiotensin II can activate neurons in the SFO and result.

in an increased production of pro-inflammatory mediators within the brain. Pro-inflammatory processes in the brain may contribute to the sympathetic nerve dysregulation observed in heart failure; for example, increased levels of reactive oxygen species (Gao et al., 2004; Guggilam et al., 2007; Sharma and Patel, 2017). Inhibition of the production of reactive oxygen species in the brain ameliorated the autonomic dysfunction normally observed in ischaemia-induced heart failure in mice (Lindley et al., 2004). It is also noteworthy that increased production of reactive oxygen species can also be induced by angiotensin II (Gao et al., 2004). Thus, pro-inflammatory mediators could maintain the increased sympathetic nerve activity and contribute to the detrimental outcomes in heart failure. In this regard, it is interesting to note the findings of a recent Cochrane review on the impact of six different angiotensin-converting enzyme inhibitors on outcomes in patients with HFpEF. This review found little or no effect on all-cause and cardiovascular mortality and quality of life measures of angiotensin-converting enzyme inhibitors on this phenotype of heart failure (Martin et al., 2021). However, only one of the inhibitors used is known to cross the blood brain barrier leaving the question of whether targeting of pro-inflammatory mediators, like angiotensin within the CNS is beneficial in heart failure unanswered. Since attenuating the increase in pro-inflammatory cytokines in the CNS can ameliorate the increase in sympathetic nerve activity observed in heart failure, perhaps further studies which target specific peripheral and CNS pro-inflammatory mediators is needed (**Figure 1**).

New Developments in Targeting Pro-Inflammatory Mediators in the CNS

From the preceding arguments, targeting specific pro-inflammatory mediators in the CNS may be a novel therapeutic approach to deal with the detrimental outcomes in heart failure and needs to be addressed. However, there is perhaps, a more critical issue, and that is related to the access of effective doses of the drugs to the site of action in the CNS. It is not possible to answer this easily because targeting the CNS for therapeutic intervention presents unique challenges due to the presence of the blood brain barrier and the ability to get drugs effectively to their site of action. Recent advances in delivery technology, however, are exciting (Vashist et al., 2018; Moura et al., 2019; Saeedi et al., 2019; Shahjin et al., 2020). Among the possibilities are (i) transient disruption of the blood brain barrier, (ii) direct microinjections into the cerebrospinal fluid, a rather invasive methodology which is

unlikely to be welcomed by patients for regular ongoing treatment, (iii) extracellular vesicles and (iv) nanotechnology transporting techniques. The latter is particularly attractive and is advancing at a rapid rate (Saeedi et al., 2019).

Nanotechnology involving nanoparticles that contain two chemicals, one used as a diagnostic marker to allow for visualisation and tracking of the particle, and the second a therapeutic agent, have been described. An example is the recent targeting of microglia with such nanoparticles containing the anti-inflammatory drug, rolipram (Cahalane et al., 2020). In this *in vitro* study, microglia preferentially took up the nanoparticles compared to astrocytes. A promising result for future *in vivo* studies, given the role of microglia in inflammatory mediated processes within the brain.

Other studies have used specific cell/cell receptor targeting techniques to improve penetration into the CNS. For example, the use of liposomes containing anti-vesicular cell adhesion molecule-1, to target vascular endothelial cells *in vivo*, increased penetration into the CNS dramatically. This technique has been useful in reducing inflammation in the brain and restoring integrity of the blood brain barrier in a model of brain inflammation (Marcos-Contreras et al., 2020). A similar targeting technique has been used *in vivo* to alter the behaviour of mice in studies of depression. Using negatively charged liposomes containing trefoil factor 3, because of its anti-depressant functions, resulted in improved mobility and reduced immobility in behavioural tests in mice (Qin et al., 2014). A similar positive outcome has been observed using a more targeted approach in which the liposomes were modified so that their affinity for monocytes was markedly increased (Qin et al., 2015). Other strategies utilised include stimuli sensitive nanoparticles. These exciting methodologies utilise environmentally sensitive nanoparticles that can change their shape according to the micro-environment, for example pH. redox capability, presence of enzymes (Lee and Thompson, 2017; Mohamed et al., 2019). Together, these new innovative developments in nanotechnology increase the likelihood that penetration into the CNS will improve dramatically in the future and suggests that a more targeted approach to dealing with inflammatory processes in the brain is on the way.

In summary, heart failure is a growing medical problem which will place a continued heavy burden on health budgets. The level of ejection fraction has normally determined the phenotype of heart failure, but most patients diagnosed with heart failure have ejection fractions less than 50%. Although the underlying aetiology of heart failure differs according to the phenotype, as suggested by the different responses to pharmacological treatment, there are some common characteristics observed in patients with heart failure. These include an increased sympathetic nerve activity, an activated renin–angiotensin system, and inflammation. The mechanisms mediating the increased sympathetic activity are not completely understood but the central nervous system plays a major role. Activation of the renin–angiotensin system plays an active role in the remodelling of the heart and in fluid and electrolyte imbalance which are compensatory initially but eventually leads to worsening of heart failure. The presence of a central renin–angiotensin system means that locally produced angiotensin in the brain may also play a key role in autonomic dysfunction seen in heart failure. Markers of inflammation in the heart and in the circulation are observed in patients diagnosed with heart failure. Circulating pro-inflammatory cytokines can also influence cardiac function further afield than just locally in the heart. More recent work has suggested that circulating pro-inflammatory cytokines can also activate the sympathetic nervous system. Strong preclinical evidence would suggest that targeting the pro-inflammatory cytokines would be a useful therapy to treat heart failure. However, most clinical studies do not support such a view, though there may be a glimmer of hope in recent studies (CANTOS trial). If specific pro-inflammatory mediators in the CNS contribute to the detrimental outcomes in heart failure, I suggest that a key problem is associated with access of effective doses of the drugs to the site of action in the CNS. The recent advances in delivery technology, particularly nanotechnology transporting techniques, are evolving at a rapid rate and may provide exciting future technology to investigate the role of specific pro-inflammatory mediators as novel targets within the brain in the treatment of heart failure.

AUTHOR CONTRIBUTIONS

The author confirms being the sole contributor of this work and has approved it for publication.

REFERENCES

Bozkurt, B., Coats, A. J. S., Tsutsui, H., Abdelhamid, C. M., Adamopoulos, S., Albert, N., et al. (2021a). Universal definition and classification of heart failure: a report of the Heart Failure Society of America, heart failure Association of the European Society of cardiology, Japanese heart failure society and writing Committee of the Universal Definition of heart failure: endorsed by the Canadian heart failure society, heart failure Association of India, Cardiac Society of Australia and new Zealand, and Chinese heart failure association. *Eur. J. Heart Fail.* 23, 352–380. doi: 10.1002/ejhf.2115

Bozkurt, B., Hershberger, R. E., Butler, J., Grady, K. L., Heidenreich, P. A., Isler, M. L., et al. (2021b). 2021 ACC/AHA key data elements and definitions for heart failure: A report of the American College of Cardiology/American Heart Association task force on clinical data standards (writing committee to develop clinical data standards for heart failure). *Circ. Cardiovasc. Qual. Outcomes* 14:e000102. doi: 10.1161/HCQ.0000000000000102

Bradham, W. S., Bozkurt, B., Gunasinghe, H., Mann, D., and Spinale, F. G. (2002). Tumor necrosis factor-alpha and myocardial remodeling in progression of heart failure: a current perspective. *Cardiovasc. Res.* 53, 822–830. doi: 10.1016/S0008-6363(01)00503-X

Bragazzi, N. L., Zhong, W., Shu, J., Abu Much, A., Lotan, D., Grupper, A., et al. (2021). Burden of heart failure and underlying causes in 195 countries and territories from 1990 to 2017. *Eur. J. Prev. Cardiol.* 28, 1682–1690. doi: 10.1093/eurjpc/zwaa147

Braunwald, E. (2008). Biomarkers in heart failure. *N. Engl. J. Med.* 358, 2148–2159. doi: 10.1056/NEJMra0800239

Cahalane, C., Bonezzi, J., Shelestak, J., Clements, R., Boika, A., Yun, Y. H., et al. (2020). Targeted delivery of Anti-inflammatory and imaging agents

to microglial cells with polymeric nanoparticles. *Mol. Pharm.* 17, 1816–1826. doi: 10.1021/acs.molpharmaceut.9b00489

Chung, E. S., Packer, M., Lo, K. H., Fasanmade, A. A., and Willerson, J. T. Anti-TNF Therapy Against Congestive Heart Failure Investigators (2003). Randomized, double-blind, placebo-controlled, pilot trial of infliximab, a chimeric monoclonal antibody to tumor necrosis factor-α, in patients with moderate-to-severe heart failure: results of the anti-TNF therapy Against congestive heart failure (ATTACH) trial. *Circulation* 107, 3133–3140. doi: 10.1161/01.CIR.0000077913.60364.D2

Cleland, J. G. F., Van Veldhuisen, D. J., and Ponikowski, P. (2019). The year in cardiology 2018: heart failure. *Eur. Heart J.* 40, 651–661. doi: 10.1093/eurheartj/ehz010

Conrad, N., Judge, A., Tran, J., Mohseni, H., Hedgecott, D., Crespillo, A. P., et al. (2018). Temporal trends and patterns in heart failure incidence: a population-based study of 4 million individuals. *Lancet* 391, 572–580. doi: 10.1016/S0140-6736(17)32520-5

Everett, B. M., Donath, M. Y., Pradhan, A. D., Thuren, T., Pais, P., Nicolau, J. C., et al. (2018). Anti-inflammatory therapy with Canakinumab for the prevention and management of Diabetes. *J. Am. Coll. Cardiol.* 71, 2392–2401. doi: 10.1016/j.jacc.2018.03.002

Gao, L., Wang, W., Li, Y. L., Schultz, H. D., Liu, D., Cornish, K. G., et al. (2004). Superoxide mediates sympathoexcitation in heart failure: roles of angiotensin II and NAD(P)H oxidase. *Circ. Res.* 95, 937–944. doi: 10.1161/01.RES.0000146676.04359.64

Guggilam, A., Haque, M., Kerut, E. K., Mcilwain, E., Lucchesi, P., Seghal, I., et al. (2007). TNF-α blockade decreases oxidative stress in the paraventricular nucleus and attenuates sympathoexcitation in heart failure rats. *Am. J. Physiol. Heart Circ. Physiol.* 293, H599–H609. doi: 10.1152/ajpheart.00286.2007

Hegewisch, S., Weh, H. J., and Hossfeld, D. K. (1990). TNF-induced cardiomyopathy. *Lancet* 335, 294–295. doi: 10.1016/0140-6736(90)90115-L

Iusuf, D., Henning, R. H., Van Gilst, W. H., and Roks, A. J. (2008). Angiotensin-(1-7): pharmacological properties and pharmacotherapeutic perspectives. *Eur. J. Pharmacol.* 585, 303–312. doi: 10.1016/j.ejphar.2008.02.090

Kang, Y. M., Zhang, Z. H., Xue, B., Weiss, R. M., and Felder, R. B. (2008). Inhibition of brain proinflammatory cytokine synthesis reduces hypothalamic excitation in rats with ischemia-induced heart failure. *Am. J. Physiol. Heart Circ. Physiol.* 295, H227–H236. doi: 10.1152/ajpheart.01157.2007

Kaye, D. M., Lefkovits, J., Jennings, G. L., Bergin, P., Broughton, A., and Esler, M. D. (1995). Adverse consequences of high sympathetic nervous activity in the failing human heart. *J. Am. Coll. Cardiol.* 26, 1257–1263. doi: 10.1016/0735-1097(95)00332-0

Korim, W. S., Elsaafien, K., Basser, J. R., Setiadi, A., May, C. N., and Yao, S. T. (2019). In renovascular hypertension, TNF-α type-1 receptors in the area postrema mediate increases in cardiac and renal sympathetic nerve activity and blood pressure. *Cardiovasc. Res.* 115, 1092–1101. doi: 10.1093/cvr/cvy268

Kurdi, M., De Mello, W. C., and Booz, G. W. (2005). Working outside the system: an update on the unconventional behavior of the renin-angiotensin system components. *Int. J. Biochem. Cell Biol.* 37, 1357–1367. doi: 10.1016/j.biocel.2005.01.012

Lee, Y., and Thompson, D. H. (2017). Stimuli-responsive liposomes for drug delivery. *Wiley Interdiscip. Rev. Nanomed. Nanobiotechnol.* 9:1450. doi: 10.1002/wnan.1450

Lindley, T. E., Doobay, M. F., Sharma, R. V., and Davisson, R. L. (2004). Superoxide is involved in the central nervous system activation and sympathoexcitation of myocardial infarction-induced heart failure. *Circ. Res.* 94, 402–409. doi: 10.1161/01.RES.0000112964.40701.93

Mann, D. L., Mcmurray, J. J., Packer, M., Swedberg, K., Borer, J. S., Colucci, W. S., et al. (2004). Targeted anticytokine therapy in patients with chronic heart failure: results of the randomized Etanercept worldwide evaluation (RENEWAL). *Circulation* 109, 1594–1602. doi: 10.1161/01.CIR.0000124490.27666.B2

Marcos-Contreras, O. A., Greineder, C. F., Kiseleva, R. Y., Parhiz, H., Walsh, L. R., Zuluaga-Ramirez, V., et al. (2020). Selective targeting of nanomedicine to inflamed cerebral vasculature to enhance the blood-brain barrier. *Proc. Natl. Acad. Sci. U. S. A.* 117, 3405–3414. doi: 10.1073/pnas.1912012117

Martin, N., Manoharan, K., Davies, C., and Lumbers, R. T. (2021). Beta-blockers and inhibitors of the renin-angiotensin aldosterone system for chronic heart failure with preserved ejection fraction. *Cochrane Database Syst. Rev.* 5:CD012721. doi: 10.1002/14651858.CD012721.pub3

Mohamed, S. M., Veeranarayanan, S., Maekawa, T., and Kumar, D. S. (2019). External stimulus responsive inorganic nanomaterials for cancer theranostics. *Adv. Drug Deliv. Rev.* 138, 18–40. doi: 10.1016/j.addr.2018.10.007

Moura, R. P., Martins, C., Pinto, S., Sousa, F., and Sarmento, B. (2019). Blood-brain barrier receptors and transporters: an insight on their function and how to exploit them through nanotechnology. *Expert Opin. Drug Deliv.* 16, 271–285. doi: 10.1080/17425247.2019.1583205

Parati, G., and Esler, M. (2012). The human sympathetic nervous system: its relevance in hypertension and heart failure. *Eur. Heart J.* 33, 1058–1066. doi: 10.1093/eurheartj/ehs041

Pocock, S. J., Ariti, C. A., Mcmurray, J. J., Maggioni, A., Kober, L., Squire, I. B., et al. (2013). Predicting survival in heart failure: a risk score based on 39 372 patients from 30 studies. *Eur. Heart J.* 34, 1404–1413. doi: 10.1093/eurheartj/ehs337

Qin, J., Yang, X., Mi, J., Wang, J., Hou, J., Shen, T., et al. (2014). Enhanced antidepressant-like effects of the macromolecule trefoil factor 3 by loading into negatively charged liposomes. *Int. J. Nanomedicine* 9, 5247–5257. doi: 10.2147/OPTH.S69335

Qin, J., Yang, X., Zhang, R. X., Luo, Y. X., Li, J. L., Hou, J., et al. (2015). Monocyte mediated brain targeting delivery of macromolecular drug for the therapy of depression. *Nanomedicine* 11, 391–400. doi: 10.1016/j.nano.2014.09.012

Rauchhaus, M., Doehner, W., Francis, D. P., Davos, C., Kemp, M., Liebenthal, C., et al. (2000). Plasma cytokine parameters and mortality in patients with chronic heart failure. *Circulation* 102, 3060–3067. doi: 10.1161/01.CIR.102.25.3060

Roth, G. A., Forouzanfar, M. H., Moran, A. E., Barber, R., Nguyen, G., Feigin, V. L., et al. (2015). Demographic and epidemiologic drivers of global cardiovascular mortality. *N. Engl. J. Med.* 372, 1333–1341. doi: 10.1056/NEJMoa1406656

Saeedi, M., Eslamifar, M., Khezri, K., and Dizaj, S. M. (2019). Applications of nanotechnology in drug delivery to the central nervous system. *Biomed. Pharmacother.* 111, 666–675. doi: 10.1016/j.biopha.2018.12.133

Schultz, H. D., Marcus, N. J., and Del Rio, R. (2015). Mechanisms of carotid body chemoreflex dysfunction during heart failure. *Exp. Physiol.* 100, 124–129. doi: 10.1113/expphysiol.2014.079517

Shafton, A. D., Ryan, A., and Badoer, E. (1998). Neurons in the hypothalamic paraventricular nucleus send collaterals to the spinal cord and to the rostral ventrolateral medulla in the rat. *Brain Res.* 801, 239–243. doi: 10.1016/S0006-8993(98)00587-3

Shahjin, F., Chand, S., and Yelamanchili, S. V. (2020). Extracellular vesicles as drug delivery vehicles to the central nervous system. *J. Neuroimmune Pharmacol.* 15, 443–458. doi: 10.1007/s11481-019-09875-w

Sharma, N. M., Haibara, A. S., Katsurada, K., Nandi, S. S., Liu, X., Zheng, H., et al. (2021). Central Ang II (angiotensin II)-mediated Sympathoexcitation: role for HIF-1α (hypoxia-inducible factor-1α) facilitated Glutamatergic tone in the Paraventricular nucleus of the hypothalamus. *Hypertension* 77, 147–157. doi: 10.1161/HYPERTENSIONAHA.120.16002

Sharma, N. M., and Patel, K. P. (2017). Post-translational regulation of neuronal nitric oxide synthase: implications for sympathoexcitatory states. *Expert Opin. Ther. Targets* 21, 11–22. doi: 10.1080/14728222.2017.1265505

Solomon, S. D., Claggett, B., Lewis, E. F., Desai, A., Anand, I., Sweitzer, N. K., et al. (2016). Influence of ejection fraction on outcomes and efficacy of spironolactone in patients with heart failure with preserved ejection fraction. *Eur. Heart J.* 37, 455–462. doi: 10.1093/eurheartj/ehv464

Solomon, S. D., Vaduganathan, M., L. Claggett, B., Packer, M., Zile, M., Swedberg, K., et al. (2020). Sacubitril/valsartan Across the Spectrum of ejection fraction in heart failure. *Circulation* 141, 352–361. doi: 10.1161/CIRCULATIONAHA.119.044586

Vashist, A., Kaushik, A., Vashist, A., Bala, J., Nikkhah-Moshaie, R., Sagar, V., et al. (2018). Nanogels as potential drug nanocarriers for CNS drug delivery. *Drug Discov. Today* 23, 1436–1443. doi: 10.1016/j.drudis.2018.05.018

Wang, J., He, W., Guo, L., Zhang, Y., Li, H., Han, S., et al. (2017). The ACE2-Ang (1-7)-mas receptor axis attenuates cardiac remodeling and fibrosis in post-myocardial infarction. *Mol. Med. Rep.* 16, 1973–1981. doi: 10.3892/mmr.2017.6848

Wang, Y., Seto, S. W., and Golledge, J. (2014). Angiotensin II, sympathetic nerve activity and chronic heart failure. *Heart Fail. Rev.* 19, 187–198. doi: 10.1007/s10741-012-9368-1

Wei, S. G., Yu, Y., Zhang, Z. H., and Felder, R. B. (2015). Proinflammatory cytokines upregulate sympathoexcitatory mechanisms in the subfornical organ of the rat. *Hypertension* 65, 1126–1133. doi: 10.1161/HYPERTENSIONAHA.114.05112

Wright, J. W., and Harding, J. W. (2013). The brain renin-angiotensin system: a diversity of functions and implications for CNS diseases. *Pflugers Arch.* 465, 133–151. doi: 10.1007/s00424-012-1102-2

Xu, B., Zheng, H., and Patel, K. P. (2012). Enhanced activation of RVLM-projecting PVN neurons in rats with chronic heart failure. *Am. J. Physiol. Heart Circ. Physiol.* 302, H1700–H1711. doi: 10.1152/ajpheart.00722.2011

Yu, Y., Cao, Y., Bell, B., Chen, X., Weiss, R. M., Felder, R. B., et al. (2019). Brain TACE (tumor necrosis factor-α–converting enzyme) contributes to sympathetic excitation in heart failure rats. *Hypertension* 74, 63–72. doi: 10.1161/HYPERTENSIONAHA.119.12651

Yu, Y., Wei, S. G., Weiss, R. M., and Felder, R. B. (2017). TNF-α receptor 1 knockdown in the subfornical organ ameliorates sympathetic excitation and cardiac hemodynamics in heart failure rats. *Am. J. Physiol. Heart Circ. Physiol.* 313, H744–H756. doi: 10.1152/ajpheart.00280.2017

Yu, Y., Zhang, Z. H., Wei, S. G., Chu, Y., Weiss, R. M., Heistad, D. D., et al. (2007). Central gene transfer of interleukin-10 reduces hypothalamic inflammation and evidence of heart failure in rats after myocardial infarction. *Circ. Res.* 101, 304–312. doi: 10.1161/CIRCRESAHA.107.148940

Zheng, H., Katsurada, K., Liu, X., Knuepfer, M. M., and Patel, K. P. (2018). Specific afferent renal denervation prevents reduction in neuronal nitric oxide synthase Within the Paraventricular nucleus in rats With chronic heart failure. *Hypertension* 72, 667–675. doi: 10.1161/HYPERTENSIONAHA.118.11071

Zheng, H., Li, Y. F., Wang, W., and Patel, K. P. (2009). Enhanced angiotensin-mediated excitation of renal sympathetic nerve activity within the paraventricular nucleus of anesthetized rats with heart failure. *Am. J. Physiol. Regul. Integr. Comp. Physiol.* 297, R1364–R1374. doi: 10.1152/ajpregu.00149.2009

Zheng, H., Liu, X., Li, Y., Sharma, N. M., and Patel, K. P. (2011). Gene transfer of neuronal nitric oxide synthase to the paraventricular nucleus reduces the enhanced glutamatergic tone in rats with chronic heart failure. *Hypertension* 58, 966–973. doi: 10.1161/HYPERTENSIONAHA.111.176222

Conflict of Interest: The author declares that the research was conducted in the absence of any commercial or financial relationships that could be construed as a potential conflict of interest.

Publisher's Note: All claims expressed in this article are solely those of the authors and do not necessarily represent those of their affiliated organizations, or those of the publisher, the editors and the reviewers. Any product that may be evaluated in this article, or claim that may be made by its manufacturer, is not guaranteed or endorsed by the publisher.

Copyright © 2022 Badoer. This is an open-access article distributed under the terms of the Creative Commons Attribution License (CC BY). The use, distribution or reproduction in other forums is permitted, provided the original author(s) and the copyright owner(s) are credited and that the original publication in this journal is cited, in accordance with accepted academic practice. No use, distribution or reproduction is permitted which does not comply with these terms.

frontiers in Physiology

MINI REVIEW
published: 07 March 2022
doi: 10.3389/fphys.2022.840826

The Influence of Modifiable Factors on Breast and Prostate Cancer Risk and Disease Progression

*Keely Tan and Matthew J. Naylor**

Charles Perkins Centre, School of Medical Sciences, Faculty of Medicine and Health, University of Sydney, Sydney, NSW, Australia

Breast and prostate cancers are among the most commonly diagnosed cancers worldwide, and together represented almost 20% of all new cancer diagnoses in 2020. For both cancers, the primary treatment options are surgical resection and sex hormone deprivation therapy, highlighting the initial dependence of these malignancies on the activity of both endogenous and exogenous hormones. Cancer cell phenotype and patient prognosis is not only determined by the collection of specific gene mutations, but through the interaction and influence of a wide range of different local and systemic components. While genetic risk factors that contribute to the development of these cancers are well understood, increasing epidemiological evidence link modifiable lifestyle factors such as physical exercise, diet and weight management, to drivers of disease progression such as inflammation, transcriptional activity, and altered biochemical signaling pathways. As a result of this significant impact, it is estimated that up to 50% of cancer cases in developed countries could be prevented with changes to lifestyle and environmental factors. While epidemiological studies of modifiable risk factors and research of the biological mechanisms exist mostly independently, this review will discuss how advances in our understanding of the metabolic, protein and transcriptional pathways altered by modifiable lifestyle factors impact cancer cell physiology to influence breast and prostate cancer risk and prognosis.

Keywords: breast cancer, prostate cancer, modifiable risk factors, lifestyle, environmental, inflammation, reactive oxygen species

OPEN ACCESS

Edited by:
Geoffrey A. Head, Baker Heart and Diabetes Institute, Australia

Reviewed by:
Erik D. Hanson, University of North Carolina at Chapel Hill, United States

***Correspondence:**
Matthew J. Naylor
matthew.naylor@sydney.edu.au

Specialty section:
This article was submitted to Integrative Physiology, a section of the journal Frontiers in Physiology

Received: *21 December 2021*
Accepted: *11 February 2022*
Published: *07 March 2022*

Citation:
Tan K and Naylor MJ (2022) The Influence of Modifiable Factors on Breast and Prostate Cancer Risk and Disease Progression. Front. Physiol. 13:840826. doi: 10.3389/fphys.2022.840826

INTRODUCTION

Breast and prostate cancers are among the most commonly diagnosed cancers worldwide, representing 19% of all new cancer diagnoses and 10.7% of cancer-related deaths in 2020 alone (Sung et al., 2021). The pathophysiology of these cancers relies on the complex interplay and exploitation of various biological systems, with systems biology techniques, such as 'omic' approaches, now being employed to understand their pathogenesis (Du and Elemento, 2015). Past research in breast and prostate cancer predominantly focused on aberrations in the human genome driving disease development, but it is now increasingly apparent that this represents only one piece of the complex cancer puzzle (Wang et al., 2018; Wu et al., 2018). While genome and other non-modifiable factors such as age,

ethnicity and family history contribute to an individual's disease risk (Nindrea et al., 2017), factors associated with lifestyle choices and environmental influences are becoming increasingly recognized as additional pieces that complete this puzzle (Stein and Colditz, 2004) (**Figure 1**). Breast and prostate cancer risk of immigrants originally from low disease prevalence countries, increases to reflect that of the destination country (Shimizu et al., 1991; Kolonel et al., 2004), confirming the importance of external factors in the etiology of the diseases. A study of twins demonstrated that heritable factors contributed to 42 and 27% of an individual's risk for prostate and breast cancer, respectively, (Lichtenstein et al., 2000), further demonstrating the major contribution of external factors to disease risk. In addition to being significant risk factors, external factors also influence disease progression post-diagnosis (Davies et al., 2011; Cannioto et al., 2021). As a result, lifestyle changes are being encouraged by health professionals as strategies for cancer prevention, and are thought to have the potential to prevent up to 50% of all cancer cases in developed countries (Stein and Colditz, 2004). Despite current population data demonstrating the significant impact of these modifiable factors on disease progression, the mechanisms of how these external factors influence cell biology to impact cancer phenotype and disease progression is not well understood. This mini review will describe how these modifiable factors can affect cellular systems, including the epigenome, transcriptome, proteome and cellular metabolome, which ultimately determines cancer phenotype.

EPIDEMIOLOGICAL EVIDENCE

Modifiable risk factors encompasses both lifestyle choices and environmental exposures. These include physical exercise, diet, weight management, tobacco intake, exposure to environmental pollutants and infections (Stein and Colditz, 2004). These factors can contribute to an individual's disease risk, recovery rate and likelihood of disease recurrence, with physical exercise, diet, and weight management being most relevant to breast and prostate cancer (**Figure 1**). Current epidemiological evidence highlights the positive effects of increasing physical exercise, a healthy diet and maintaining a healthy weight in the prevention and overall disease outcomes for breast cancer patients (Cannioto et al., 2021; Lubian Lopez et al., 2021). Interestingly, the impact of lifestyle interventions on prostate cancer risk has been inconsistent, with some studies demonstrating no effect, while others show decreased disease risk (Shephard, 2017; Sorial et al., 2019). While the contribution to disease risk is controversial, the consensus is that these interventions are beneficial in decreasing an individual's risk of mortality and improving overall outcomes (Kenfield et al., 2011). As a result, it is important to understand the mechanisms of how these modifiable factors can influence patient risk and disease progression to effectively implement these strategies in the clinic. The physiology behind the lifestyle interventions resulting in these outcomes is complex, multi-factorial and often overlap with one another. Implementation of these lifestyle factors may modulate the impact of certain biological molecules, combat the chronic inflammatory state of tumors, decrease

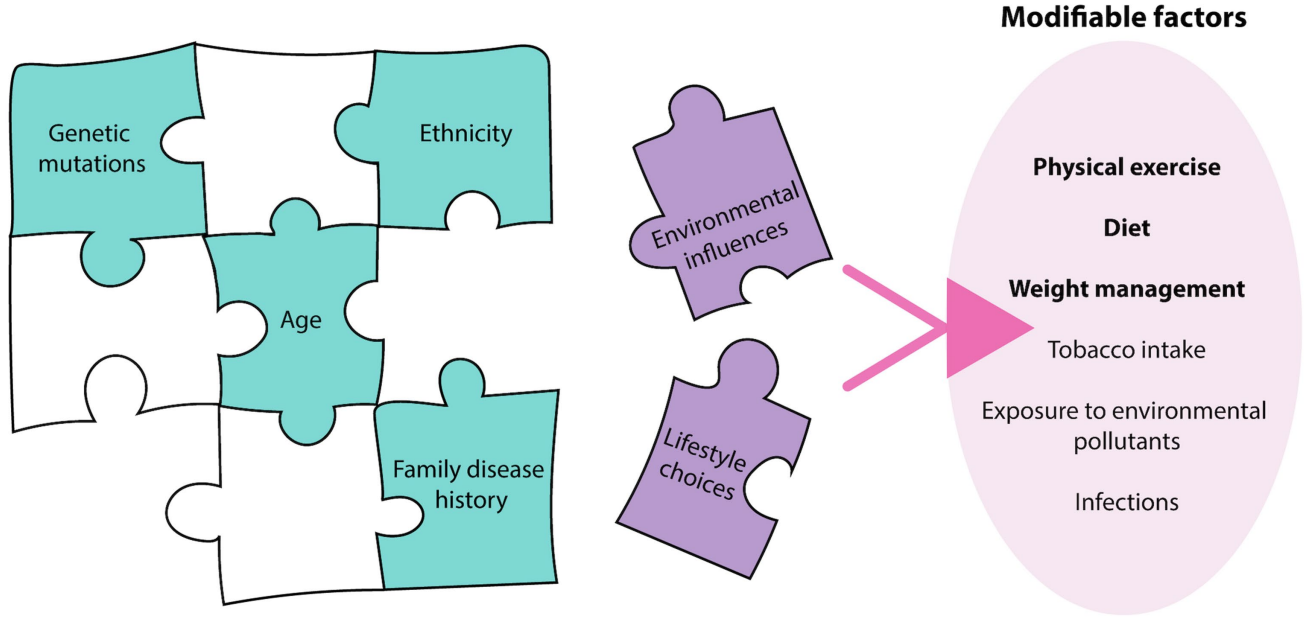

FIGURE 1 | Breast and prostate cancer etiology. The etiology of breast and prostate cancer relies on many pieces of a complex puzzle, where environmental influences and lifestyle choices, termed modifiable factors, may complete this puzzle. There are various modifiable factors that may contribute to cancer initiation, with physical exercise, diet, and weight management most relevant to breast and prostate cancer.

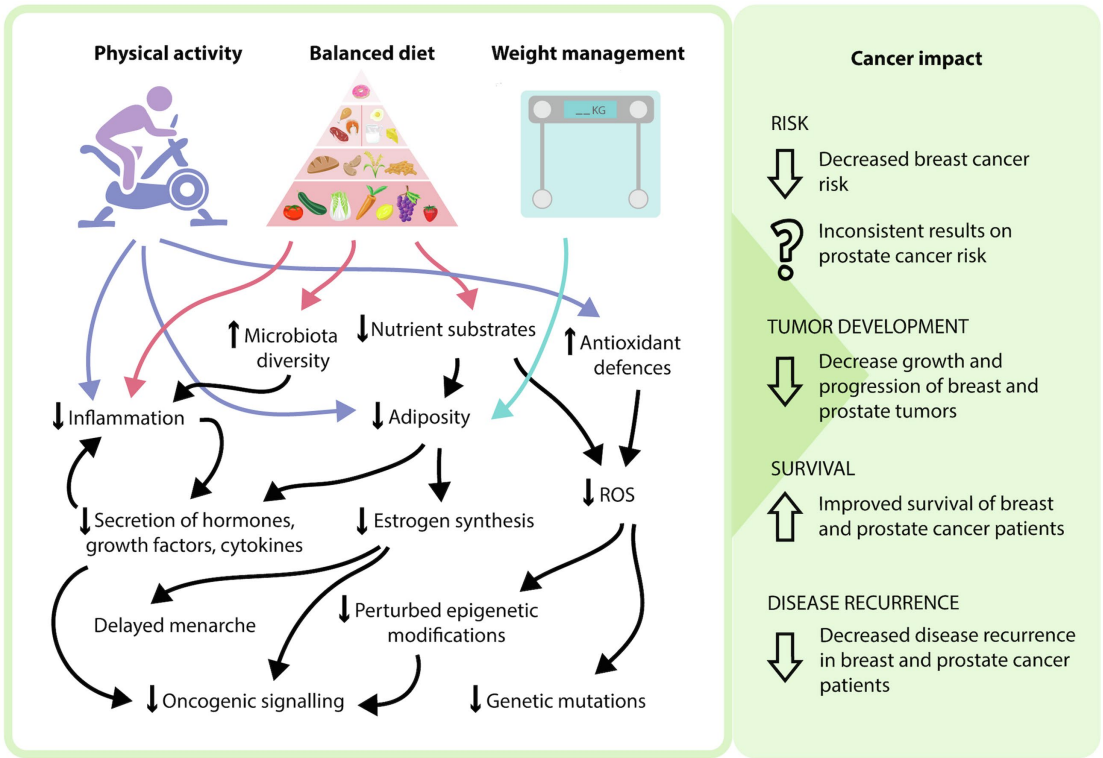

FIGURE 2 | Potential mechanisms of how modifying lifestyle factors can influence cancer phenotype. In general, a side effect of increased physical activity and a balanced diet is weight management and adipose tissue loss. The incorporation of these three modifiable lifestyle factors can result in various physiological effects, including a decrease in nutrient substrates, adipose tissue, proinflammatory processes, reactive oxygen species-mediated effects, and oncogenic signaling, as well as an increase in antioxidant defenses and microbiota diversity. At the patient level, this may explain the reduced risk of breast cancer, decreased progression of breast and prostate cancers, as well as increased survival and decreased disease recurrence that occurs with modifying these lifestyle factors.

the expression and activity of pro-oncogenic genes and signaling pathways through epigenetic mechanisms, and improve regulation of oxidative stress to minimize oxidative damage (**Figure 2**).

METABOLIC AND HORMONAL INFLUENCE

The response to lifestyle and environmental cues occurs initially at the metabolic and hormonal level, which can dynamically alter gene expression through epigenetic and transcriptional mechanisms (Wong et al., 2017). While food consumption stimulates the release of hormones and metabolites such as insulin and insulin-like growth factor (IGF)-1 (Clemmons, 2012; Vernieri et al., 2016), overnutrition is linked to the perturbed activity of these hormones. The increased activity of insulin and IGF-1 result in the activation of oncogenic signaling pathways and subsequently increase proliferation and disease progression (Pollak, 2012). In addition, metabolic substrates derived from lipids, protein and carbohydrates can provide a constant supply of ATP and metabolic precursors for biochemical processes crucial for tumor progression, such as lipid membrane synthesis (Hanahan and Weinberg, 2011; Vernieri et al., 2016). Furthermore, there is a plethora of evidence to support the link between nutritional choices and gut microbiota composition, with low microbiota diversity associated with cancer (Plaza-Diaz et al., 2019; Wastyk et al., 2021). Multi-omic approaches have been used to link gut microbial dysbiosis with the advancement of breast and prostate cancer (Komorowski and Pezo, 2020; Liu et al., 2021). Evidence indicates that this may be due to the contribution of dysbiosis-related metabolites in chronic inflammation, immune cell recruitment and cancer cell dissemination (Buchta Rosean et al., 2019; Lee et al., 2021). Using metagenomics, Liu and colleagues demonstrated that dysbiosis accelerated prostate cancer progression through upregulation of lysophosphatidylcholine acyltransferase 1 (LPCAT1), a key enzyme in the phospholipid remodeling pathway (Liu et al., 2021). In addition, the gut microbiome-associated metabolites may influence cancer progression indirectly by altering the breast microbiome through systemic effects (Costa et al., 2021). Extending upon this, nutritional metabolomics can provide detailed analyses of metabolites related to the consumption of certain foods, such as alcohol and animal fats, which can be predictive of breast and prostate cancer risk. For example, elevated lysophosphatidylcholines C17:0 and C18:0 levels have been associated with increased prostate cancer risk (Playdon et al.,

2017; Röhnisch et al., 2020). As nutrition has the potential to contribute to tumor growth through the discussed metabolic mechanisms, dietary interventions such as "short-term fasting" have been trailed and found to reduce blood glycemia, hyperinsulinemia and IGF-1 levels (Vernieri et al., 2016). Furthermore, participation in physical activity can influence hormone and metabolite levels, such as decreasing insulin and IGF-1 levels, thus reducing their oncogenic effects (Thomas et al., 2017).

In addition to metabolic disruptions, ongoing overnutrition results in adipose tissue accumulation. Adipose tissue is known to be a source of estrogen production, particularly in postmenopausal women whose ovaries are no longer the major estrogen source (Hetemaki et al., 2021). Postmenopausal women with increased BMI or weight have an increased risk of developing hormone receptor positive breast cancer (Brown et al., 2017). Aromatase, a key enzyme involved in estrogen biosynthesis, is expressed in adipose tissue with increased BMI correlating with increased aromatase expression (Zhao et al., 2016). Estrogen has a demonstrated role in breast cancer initiation, proliferation and progression (Han et al., 2018; Xue et al., 2019), subsequently estrogen exposure has been strongly linked to the development of breast cancer, even in premenopausal women. In fact, there is a 5% increased risk of breast cancer correlated with each year younger at menarche and a 3.5% increase related to each year older at menopause due to the prolonged period of estrogen exposure (Ramakrishnan et al., 2002; Collaborative Group on Hormonal Factors in Breast, 2012). There are various factors that can promote the onset of menarche, with diet, physical activity and BMI being recognized as contributing external factors (Ramezani Tehrani et al., 2014). Diet has been closely linked to menarcheal age, with overnutrition and obesity correlated with decreased age, and undernutrition associated with an increased age to onset of menarche (Merzenich et al., 1993). While this correlation between diet, obesity and spermarche may also be evident in boys, the relationship is harder to determine given that it is more difficult to determine spermarche onset (Wagner et al., 2012; Deng et al., 2018). Research indicates that testosterone levels may not explain the potential relationship between obesity and spermarche, given that obesity has been associated with lower testosterone levels (Glass et al., 1977), however elevated leptin associated with increased adiposity has been highlighted as a potential mediator of pubertal age (Wagner et al., 2012). This may suggest that dietary choices as early as childhood, could contribute to an individual's breast and prostate cancer risk later in life.

IMMUNE FUNCTION AND INFLAMMATION

Adipose tissue, a major consequence of an unhealthy diet and a sedentary lifestyle, is comprised of adipocytes, adipose stem cells, endothelial cells, immune cells and fibroblasts. Adipose tissue can secrete a range of hormones, growth factors and cytokines, termed adipokines (Gilbert and Slingerland, 2013; Lenz et al., 2020). The balance of these factors is dependent on the composition of the adipose tissue, with the onset of obesity identified as a driver of adipose remodeling. This alters the size and composition of adipose tissue, with an increase in preadipocytes and a decrease in mature adipocytes (Picon-Ruiz et al., 2017). The hypertrophy and proliferation of adipose tissue that occurs with progressive weight gain eventually results in adipose tissue hypoxia, triggering hypoxia-inducible factor-1 (HIF1) transcriptional activity (Lee et al., 2014). Recent multi-omic analysis has revealed that HIF1 transcriptional activity is dependent on its cofactor CDK8, which indirectly represses MYC target genes as an adaptive response to promote cell survival (Andrysik et al., 2021). In addition, HIF1 activity upregulates other genes, including vascular endothelial growth factor, which promotes angiogenesis and metastasis of breast and prostate cancer cells (Li et al., 2018; Melegh and Oltean, 2019). Increased HIF1 activity, and the predominantly preadipocyte phenotype, also increases leptin levels while decreasing adiponectin levels, propagating a proinflammatory environment (Gilbert and Slingerland, 2013). The imbalance of these hormones transforms the adipose tissue immune landscape, increasing the recruitment of various proinflammatory immune cells, such as macrophages, resulting in increased immune cell infiltration (Wu et al., 2019). These proinflammatory immune cells in conjunction with the preadipocytes, increase the secretion of inflammatory adipokines such as tumor necrosis factor alpha (TNF-α) and interleukin (IL)-1β, creating a chronic inflammatory condition associated with tumorigenesis (Gilbert and Slingerland, 2013; Picon-Ruiz et al., 2017). The preadipocyte phenotype discourages mature adipocyte differentiation, thus maintaining a proinflammatory state. However, this elevated immune cell mobilization and infiltration is not limited only to states of high adiposity and is typical of breast and prostate cancers (Wu et al., 2020; Xu et al., 2021). Thus, lifestyle interventions such as physical exercise, may improve the inflammatory state of all patients (Khosravi et al., 2019). While the exact mechanisms are not fully understood, one hypothesis is that exercise reduces monocyte cytokine production (Khosravi et al., 2021).

In addition to the impact of adipose tissue expansion through overnutrition, the uptake of certain nutrients, such as saturated fatty acids (SFAs), can also trigger inflammation. SFAs induce toll like receptor (TLR) activation, particularly TLR4 (Rogero and Calder, 2018), with activation of the TLR pathway resulting in increased activity of the transcription factor nuclear factor kappa-light-chain-enhancer of activated B cells (NF-kB), which is responsible for regulating over 100 proinflammatory genes (Pradere et al., 2014), further perpetuating a chronic inflammatory state. Therefore, nutrition choices and the accumulation of adipose tissue may influence the tumor microenvironment required for breast and prostate cancer growth and progression. By actively increasing levels of physical exercise and incorporating a heathier diet, this may decrease adipose-associated inflammation. In addition to the effects of decreased adipose tissue accumulation, partaking in physical exercise, particularly aerobic focused activity, has the capacity to improve immunity and reduce inflammation through the activation of β-adrenergic receptor (β-AR) signaling (Hong et al., 2014). Upon binding

of circulating catecholamines to the β-AR of immune cells, adenylyl cyclase is activated to produce cAMP and activate PKA. The functional consequences of activating this pathway are dependent on the immune cell subtype (Simpson et al., 2021), but a hypothesized mechanism is that exercise-induced activation of the β-AR signaling pathway diminishes the TNF proinflammatory signaling axis, although this relationship is not as strong in obese individuals (Hong et al., 2014). Furthermore, physical exercise has been linked to alterations of the lipid profile and cytokine levels, such that there is an increase in high-density-lipoprotein levels and IL10 levels, respectively. Modulation of these parameters is associated with decreased chronic inflammation (Koelwyn et al., 2015; Meneses-Echavez et al., 2016). A recent study has also used multi-omic and immune profiling to demonstrate striking benefits of a high-fermented-food diet. This diet increased gut microbiome diversity, as well as decreasing inflammatory markers, such as IL-6 and IL-10 (Wastyk et al., 2021). While this study was only performed in healthy adults, there have been some *in vitro* and *in vivo* studies highlighting the benefits of fermented foods in breast and prostate cancer, but these findings are yet to be confirmed in the clinic (Tasdemir and Sanlier, 2020).

REGULATION OF OXIDATIVE STRESS-INDUCED DNA DAMAGE

It is well established that the role of reactive oxygen species (ROS) is paradoxical, in that it has the potential to be beneficial and detrimental to the progression of tumors, depending on the balance of antioxidants (Aggarwal et al., 2019; Perillo et al., 2020). For simplicity, this review will only discuss the pro-tumorigenic impact of ROS. This notion of oxidative stress arises from inefficient clearance of excess free radicals, and is commonly associated with the initiation of cancers, as it can cause oxidative damage to lipids, proteins and DNA, contributing to genomic instability and mutation (Sharifi-Rad et al., 2020). This process can occur naturally with aging, from external environmental stressors, such ultraviolet radiation, and also from lifestyle factors, such as nutritional choices. During overnutrition, the uptake of carbohydrates, lipids and protein trigger the production of ROS, predominantly due to the excess supply of energy substrates for mitochondrial metabolism (McMurray et al., 2016; Saha et al., 2017). This continued state of overnutrition can result in mitochondrial dysfunction and further increase oxidative stress and oxidative stress-induced DNA damage. In addition to food consumption, there has also been a strong link between alcohol intake and breast and prostate cancer risk through the production of ROS species and acetaldehyde arising from alcohol metabolism (Dickerman et al., 2016; Wang et al., 2017).

In a pre-malignant context, increased ROS levels provide the opportunity for driver somatic mutations to occur, which during malignancy can drive phenotypes such as cell proliferation (Perillo et al., 2020) and epithelial-mesenchymal transition (EMT) (Radisky et al., 2005) important for metastatic progression. In addition, multi-omics approaches have identified different cancers exhibit varied levels of ROS metabolism, and are beginning to investigate the use of a ROS index to measure cancer outcomes (Shen et al., 2020). Thus, the implementation of diet changes and weight management could influence the amount of oxidative stress and subsequently minimize the effects on cellular damage prior to and following the initiation of carcinogenesis. In addition to dietary modifications, research has indicated that participation in regular, and moderate to high-intensity physical exercise may improve antioxidant defenses both in adult and elderly individuals by upregulating antioxidant enzymes, allowing the body to adopt mechanisms to effectively process large quantities of ROS (Powers et al., 2020). These adaptive mechanisms may be beneficial in managing the potential increase in oxidative stress to decrease the risk and rate of mutation accumulation, and subsequent disease initiation. Conversely, the pro-tumorigenic role of ROS is generally associated with a parallel increase in antioxidant capacity (Perillo et al., 2020) and thus, the contribution of exercise-induced antioxidant capacity in a malignant context may be controversial. Nevertheless, high levels of endogenous antioxidants from physical exercise may act to protect surrounding noncancer tissue against chemotherapy-induced toxicity (Smuder, 2019).

REVERSIBLE GENE REGULATION AND ONCOGENIC SIGNALING

While genomic material encodes the genotype of an organism, it is the regulation of DNA through epigenetic and transcriptional mechanisms that modulates gene and subsequent protein expression and activity that contribute to phenotype (Mikhed et al., 2015). These reversible modifications can be activated in response to environmental and lifestyle factors (Alegria-Torres et al., 2011) and occur through DNA methylation, histone modification or microRNA expression, with hypermethylation of CpG islands characteristic of both breast and prostate cancer (Garcia-Martinez et al., 2021; Macedo-Silva et al., 2021). More recently, epigenomic approaches have explored how obesity and menopause impact the DNA methylation profile of breast cancer patients, identifying a different epigenome signature in postmenopausal patients with a BMI > 25 compared to premenopausal patients with a BMI < 25 (Crujeiras et al., 2017), suggesting that obesity-induced alterations to the epigenome may contribute to aggressive disease. In addition, hypermethylation of CpG islands through DNA methyltransferase (DNMT) upregulation, inhibits the transcription of various tumor suppressor genes, such as *P21* and *BRCA1*, allowing the proliferation and growth of cancer cells (Banerjee et al., 2014; Pathania et al., 2015). The effects of DNA methylation can be functionally predicted through model-based algorithmic analysis of proteomic data, demonstrating the upregulation of various oncogenic signaling proteins, which then have the potential to further potentiate DNMT hypermethylation *via* a feedback loop system (Emran et al., 2019). While there are several factors that can alter epigenetic mechanisms, ROS have been implicated as a major regulator of transcriptional activity and the cellular proteome (Bhat et al., 2018), and as discussed

ROS levels can be regulated through various lifestyle interventions. While the effects of lifestyle choices begin with metabolic changes that influence the epigenome, the subsequently altered epigenome then has the potential to influence the tumor microenvironment. By modifying these lifestyle choices, an array of physiological effects may occur that can impact the risk, progression, and overall prognosis of breast and prostate cancer patients (**Figure 2**).

CONCLUDING REMARKS

With a global goal of decreasing cancer disease burden, this mini review outlines the physiology behind why lifestyle modifications may succeed as a tool to achieve this. Not only would these changes positively impact the number of cancer diagnoses and outcomes, but it would also concurrently decrease the burden of other worldwide epidemics such as obesity and type II diabetes. While the traditional approach to cancer therapy is dependent on pharmacological interventions, it is now being increasingly recognized that external influence may complement these therapies. These may include, but are not limited to, increasing physical exercise, improving dietary choices, and weight management. Future research should incorporate systems biology techniques to provide a more mechanistic and holistic view on the impact of these modifiable factors on the interactions between the various biological components that contribute to tumorigenesis.

AUTHOR CONTRIBUTIONS

KT designed the study, was responsible for writing the article and the creation of all Figures. MN designed the study and was responsible for writing and revising the manuscript. All authors contributed to the generation of the concepts and ideas provided.

FUNDING

This work was supported by Cancer Council NSW Research Project Grant (RG 20–08) and Priority-driven Collaborative Cancer Research Scheme (grant #1130499), funded by the National Breast Cancer Foundation Australia with the assistance of Cancer Australia awarded to MN.

REFERENCES

Aggarwal, V., Tuli, H. S., Varol, A., Thakral, F., Yerer, M. B., Sak, K., et al. (2019). Role of reactive oxygen species in cancer progression: molecular mechanisms and recent advancements. *Biomol. Ther.* 9:735. doi: 10.3390/biom9110735

Alegria-Torres, J. A., Baccarelli, A., and Bollati, V. (2011). Epigenetics and lifestyle. *Epigenomics* 3, 267–277. doi: 10.2217/epi.11.22

Andrysik, Z., Bender, H., Galbraith, M. D., and Espinosa, J. M. (2021). Multi-omics analysis reveals contextual tumor suppressive and oncogenic gene modules within the acute hypoxic response. *Nat. Commun.* 12:1375. doi: 10.1038/s41467-021-21687-2

Banerjee, J., Mishra, R., Li, X., Jackson, R. S. 2nd, Sharma, A., and Bhowmick, N. A. (2014). A reciprocal role of prostate cancer on stromal DNA damage. *Oncogene* 33, 4924–4931. doi: 10.1038/onc.2013.431

Bhat, A. V., Hora, S., Pal, A., Jha, S., and Taneja, R. (2018). Stressing the (Epi)genome: dealing with reactive oxygen species in cancer. *Antioxid. Redox Signal.* 29, 1273–1292. doi: 10.1089/ars.2017.7158

Brown, K. A., Iyengar, N. M., Zhou, X. K., Gucalp, A., Subbaramaiah, K., Wang, H., et al. (2017). Menopause is a determinant of breast aromatase expression and its associations With BMI, inflammation, and systemic markers. *J. Clin. Endocrinol. Metab.* 102, 1692–1701. doi: 10.1210/jc.2016-3606

Buchta Rosean, C., Bostic, R. R., Ferey, J. C. M., Feng, T.-Y., Azar, F. N., Tung, K. S., et al. (2019). Pre-existing commensal dysbiosis is a host-intrinsic regulator of tissue inflammation and tumor cell dissemination in hormone receptor-positive breast cancer. *Cancer Res.* 79, 3662–3675. doi: 10.1158/0008-5472.CAN-18-3464

Cannioto, R. A., Hutson, A., Dighe, S., McCann, W., McCann, S. E., Zirpoli, G. R., et al. (2021). Physical activity Before, During, and After chemotherapy for high-risk breast cancer: relationships With survival. *J. Natl. Cancer Inst.* 113, 54–63. doi: 10.1093/jnci/djaa046

Clemmons, D. R. (2012). Metabolic actions of IGF-I in Normal physiology and diabetes. *Endocrinol. Metab. Clin. N. Am.* 41, 425–443. doi: 10.1016/j.ecl.2012.04.017

Collaborative Group on Hormonal Factors in Breast, C. (2012). Menarche, menopause, and breast cancer risk: individual participant meta-analysis, including 118 964 women with breast cancer from 117 epidemiological studies. *Lancet Oncol.* 13, 1141–1151. doi:10.1016/S1470-2045(12)70425-4.

Costa, D. A., Guilherme Nobre, J., Vaz Batista, M., Ribeiro, C., Calle, C., Cortes, A., et al. (2021). Human microbiota and breast cancer—is there Any relevant link? – A literature review and new horizons Toward personalised medicine. *Front. Microbiol.* 12:584332. doi: 10.3389/fmicb.2021.584332

Crujeiras, A. B., Diaz-Lagares, A., Stefansson, O. A., Macias-Gonzalez, M., Sandoval, J., Cueva, J., et al. (2017). Obesity and menopause modify the epigenomic profile of breast cancer. *Endocr. Relat. Cancer* 24, 351–363. doi: 10.1530/ERC-16-0565

Davies, N. J., Batehup, L., and Thomas, R. (2011). The role of diet and physical activity in breast, colorectal, and prostate cancer survivorship: a review of the literature. *Br. J. Cancer* 105, S52–S73. doi: 10.1038/bjc.2011.423

Deng, Y., Liang, J., Zong, Y., Yu, P., Xie, R., Guo, Y., et al. (2018). Timing of spermarche and menarche among urban students in Guangzhou, China: trends from 2005 to 2012 and association with obesity. *Sci. Rep.* 8:263. doi: 10.1038/s41598-017-18423-6

Dickerman, B. A., Markt, S. C., Koskenvuo, M., Pukkala, E., Mucci, L. A., and Kaprio, J. (2016). Alcohol intake, drinking patterns, and prostate cancer risk and mortality: a 30-year prospective cohort study of Finnish twins. *Cancer Causes Control* 27, 1049–1058. doi: 10.1007/s10552-016-0778-6

Du, W., and Elemento, O. (2015). Cancer systems biology: embracing complexity to develop better anticancer therapeutic strategies. *Oncogene* 34, 3215–3225. doi: 10.1038/onc.2014.291

Emran, A. A., Chatterjee, A., Rodger, E. J., Tiffen, J. C., Gallagher, S. J., Eccles, M. R., et al. (2019). Targeting DNA methylation and EZH2 activity to overcome melanoma resistance to immunotherapy. *Trends Immunol.* 40, 328–344. doi: 10.1016/j.it.2019.02.004

Garcia-Martinez, L., Zhang, Y., Nakata, Y., Chan, H. L., and Morey, L. (2021). Epigenetic mechanisms in breast cancer therapy and resistance. *Nat. Commun.* 12:1786. doi: 10.1038/s41467-021-22024-3

Gilbert, C. A., and Slingerland, J. M. (2013). Cytokines, obesity, and cancer: new insights on mechanisms linking obesity to cancer risk and progression. *Annu. Rev. Med.* 64, 45–57. doi: 10.1146/annurev-med-121211-091527

Glass, A. R., Swerdloff, R. S., Bray, G. A., Dahms, W. T., and Atkinson, R. L. (1977). Low serum testosterone and sex-hormone-binding-globulin in massively obese men. *J. Clin. Endocrinol. Metab.* 45, 1211–1219. doi: 10.1210/jcem-45-6-1211

Han, R., Gu, S., Zhang, Y., Luo, A., Jing, X., Zhao, L., et al. (2018). Estrogen promotes progression of hormone-dependent breast cancer through CCL2-

CCR2 axis by upregulation of twist via PI3K/AKT/NF-κB signaling. *Sci. Rep.* 8:9575. doi: 10.1038/s41598-018-27810-6

Hanahan, D., and Weinberg, R. A. (2011). Hallmarks of cancer: the next generation. *Cell* 144, 646–674. doi: 10.1016/j.cell.2011.02.013

Hetemaki, N., Mikkola, T. S., Tikkanen, M. J., Wang, F., Hamalainen, E., Turpeinen, U., et al. (2021). Adipose tissue estrogen production and metabolism in premenopausal women. *J. Steroid Biochem. Mol. Biol.* 209:105849. doi: 10.1016/j.jsbmb.2021.105849

Hong, S., Dimitrov, S., Pruitt, C., Shaikh, F., and Beg, N. (2014). Benefit of physical fitness against inflammation in obesity: role of beta adrenergic receptors. *Brain Behav. Immun.* 39, 113–120. doi: 10.1016/j.bbi.2013.12.009

Kenfield, S. A., Stampfer, M. J., Giovannucci, E., and Chan, J. M. (2011). Physical activity and survival after prostate cancer diagnosis in the health professionals follow-up study. *J. Clin. Oncol.* 29, 726–732. doi: 10.1200/JCO.2010.31.5226

Khosravi, N., Hanson, E. D., Farajivafa, V., Evans, W. S., Lee, J. T., Danson, E., et al. (2021). Exercise-induced modulation of monocytes in breast cancer survivors. *Brain Behav. Immun. Health* 14:100216. doi: 10.1016/j.bbih.2021.100216

Khosravi, N., Stoner, L., Farajivafa, V., and Hanson, E. D. (2019). Exercise training, circulating cytokine levels and immune function in cancer survivors: a meta-analysis. *Brain Behav. Immun.* 81, 92–104. doi: 10.1016/j.bbi.2019.08.187

Koelwyn, G. J., Wennerberg, E., Demaria, S., and Jones, L. W. (2015). Exercise in regulation of inflammation-immune axis function in cancer initiation and progression. *Oncology* 29, 908–920.

Kolonel, L. N., Altshuler, D., and Henderson, B. E. (2004). The multiethnic cohort study: exploring genes, lifestyle and cancer risk. *Nat. Rev. Cancer* 4, 519–527. doi: 10.1038/nrc1389

Komorowski, A. S., and Pezo, R. C. (2020). Untapped "-omics": the microbial metagenome, estrobolome, and their influence on the development of breast cancer and response to treatment. *Breast Cancer Res. Treat.* 179, 287–300. doi: 10.1007/s10549-019-05472-w

Lee, K. A., Luong, M. K., Shaw, H., Nathan, P., Bataille, V., and Spector, T. D. (2021). The gut microbiome: what the oncologist ought to know. *Br. J. Cancer* 125, 1197–1209. doi: 10.1038/s41416-021-01467-x

Lee, Y. S., Kim, J. W., Osborne, O., Oh, D. Y., Sasik, R., Schenk, S., et al. (2014). Increased adipocyte O2 consumption triggers HIF-1alpha, causing inflammation and insulin resistance in obesity. *Cell* 157, 1339–1352. doi: 10.1016/j.cell.2014.05.012

Lenz, M., Arts, I. C. W., Peeters, R. L. M., de Kok, T. M., and Ertaylan, G. (2020). Adipose tissue in health and disease through the lens of its building blocks. *Sci. Rep.* 10:10433. doi: 10.1038/s41598-020-67177-1

Li, X., Gao, Y., Li, J., Zhang, K., Han, J., Li, W., et al. (2018). FOXP3 inhibits angiogenesis by downregulating VEGF in breast cancer. *Cell Death Dis.* 9:744. doi: 10.1038/s41419-018-0790-8

Lichtenstein, P., Holm, N. V., Verkasalo, P. K., Iliadou, A., Kaprio, J., Koskenvuo, M., et al. (2000). Environmental and heritable factors in the causation of cancer--analyses of cohorts of twins from Sweden, Denmark, and Finland. *N. Engl. J. Med.* 343, 78–85. doi: 10.1056/NEJM200007133430201

Liu, Y., Yang, C., Zhang, Z., and Jiang, H. (2021). Gut microbiota dysbiosis accelerates prostate cancer progression through increased LPCAT1 expression and enhanced DNA repair pathways. *Front. Oncol.* 11:679712. doi: 10.3389/fonc.2021.679712

Lubian Lopez, D. M., Butron Hinojo, C. A., Castillo Lara, M., Sanchez-Prieto, M., Sanchez-Borrego, R., Ladron, M., et al. (2021). Relationship of breast volume, obesity and central obesity with different prognostic factors of breast cancer. *Sci. Rep.* 11:1872. doi: 10.1038/s41598-021-81436-9

Macedo-Silva, C., Benedetti, R., Ciardiello, F., Cappabianca, S., Jeronimo, C., and Altucci, L. (2021). Epigenetic mechanisms underlying prostate cancer radioresistance. *Clin. Epigenetics* 13:125. doi: 10.1186/s13148-021-01111-8

McMurray, F., Patten, D. A., and Harper, M. E. (2016). Reactive oxygen species and oxidative stress in obesity-recent findings and empirical approaches. *Obesity (Silver Spring)* 24, 2301–2310. doi: 10.1002/oby.21654

Melegh, Z., and Oltean, S. (2019). Targeting angiogenesis in prostate cancer. *Int. J. Mol. Sci.* 20:2676. doi: 10.3390/ijms20112676

Meneses-Echavez, J. F., Correa-Bautista, J. E., Gonzalez-Jimenez, E., Schmidt Rio-Valle, J., Elkins, M. R., Lobelo, F., et al. (2016). The effect of exercise training on mediators of inflammation in breast cancer survivors: a systematic review with meta-analysis. *Cancer Epidemiol. Biomark. Prev.* 25, 1009–1017. doi: 10.1158/1055-9965.EPI-15-1061

Merzenich, H., Boeing, H., and Wahrendorf, J. (1993). Dietary fat and sports activity as determinants for age at menarche. *Am. J. Epidemiol.* 138, 217–224. doi: 10.1093/oxfordjournals.aje.a116850

Mikhed, Y., Gorlach, A., Knaus, U. G., and Daiber, A. (2015). Redox regulation of genome stability by effects on gene expression, epigenetic pathways and DNA damage/repair. *Redox Biol.* 5, 275–289. doi: 10.1016/j.redox.2015.05.008

Nindrea, R. D., Aryandono, T., and Lazuardi, L. (2017). Breast cancer risk From modifiable and non-modifiable risk factors among women in Southeast asia: a meta-analysis. *Asian Pac. J. Cancer Prev.* 18, 3201–3206. doi: 10.22034/APJCP.2017.18.12.3201

Pathania, R., Ramachandran, S., Elangovan, S., Padia, R., Yang, P., Cinghu, S., et al. (2015). DNMT1 is essential for mammary and cancer stem cell maintenance and tumorigenesis. *Nat. Commun.* 6:6910. doi: 10.1038/ncomms7910

Perillo, B., Di Donato, M., Pezone, A., Di Zazzo, E., Giovannelli, P., Galasso, G., et al. (2020). ROS in cancer therapy: the bright side of the moon. *Exp. Mol. Med.* 52, 192–203. doi: 10.1038/s12276-020-0384-2

Picon-Ruiz, M., Morata-Tarifa, C., Valle-Goffin, J. J., Friedman, E. R., and Slingerland, J. M. (2017). Obesity and adverse breast cancer risk and outcome: mechanistic insights and strategies for intervention. *CA Cancer J. Clin.* 67, 378–397. doi: 10.3322/caac.21405

Playdon, M. C., Ziegler, R. G., Sampson, J. N., Stolzenberg-Solomon, R., Thompson, H. J., Irwin, M. L., et al. (2017). Nutritional metabolomics and breast cancer risk in a prospective study. *Am. J. Clin. Nutr.* 106, 637–649. doi: 10.3945/ajcn.116.150912

Plaza-Diaz, J., Alvarez-Mercado, A. I., Ruiz-Marin, C. M., Reina-Perez, I., Perez-Alonso, A. J., Sanchez-Andujar, M. B., et al. (2019). Association of breast and gut microbiota dysbiosis and the risk of breast cancer: a case-control clinical study. *BMC Cancer* 19:495. doi: 10.1186/s12885-019-5660-y

Pollak, M. (2012). The insulin and insulin-like growth factor receptor family in neoplasia: an update. *Nat. Rev. Cancer* 12, 159–169. doi: 10.1038/nrc3215

Powers, S. K., Deminice, R., Ozdemir, M., Yoshihara, T., Bomkamp, M. P., and Hyatt, H. (2020). Exercise-induced oxidative stress: friend or foe? *J. Sport Health Sci.* 9, 415–425. doi: 10.1016/j.jshs.2020.04.001

Pradere, J. P., Dapito, D. H., and Schwabe, R. F. (2014). The yin and Yang of toll-like receptors in cancer. *Oncogene* 33, 3485–3495. doi: 10.1038/onc.2013.302

Radisky, D. C., Levy, D. D., Littlepage, L. E., Liu, H., Nelson, C. M., Fata, J. E., et al. (2005). Rac1b and reactive oxygen species mediate MMP-3-induced EMT and genomic instability. *Nature* 436, 123–127. doi: 10.1038/nature03688

Ramakrishnan, R., Khan, S. A., and Badve, S. (2002). Morphological changes in breast tissue with menstrual cycle. *Mod. Pathol.* 15, 1348–1356. doi: 10.1097/01.MP.0000039566.20817.46

Ramezani Tehrani, F., Mirmiran, P., Gholami, R., Moslehi, N., and Azizi, F. (2014). Factors influencing menarcheal age: results from the cohort of Tehran lipid and glucose study. *Int J Endocrinol Metab* 12:e16130. doi: 10.5812/ijem.16130

Rogero, M. M., and Calder, P. C. (2018). Obesity, inflammation, toll-Like receptor 4 and fatty acids. *Nutrients* 10:432. doi: 10.3390/nu10040432

Röhnisch, H. E., Kyro, C., Olsen, A., Thysell, E., Hallmans, G., and Moazzami, A. A. (2020). Identification of metabolites associated with prostate cancer risk: a nested case-control study with long follow-up in the northern Sweden health and disease study. *BMC Med.* 18:187. doi: 10.1186/s12916-020-01655-1

Saha, S. K., Lee, S. B., Won, J., Choi, H. Y., Kim, K., Yang, G.-M., et al. (2017). Correlation between oxidative stress, nutrition, and cancer initiation. *Int. J. Mol. Sci.* 18:1544. doi: 10.3390/ijms18071544

Sharifi-Rad, M., Anil Kumar, N. V., Zucca, P., Varoni, E. M., Dini, L., Panzarini, E., et al. (2020). Lifestyle, oxidative stress, and antioxidants: back and forth in the pathophysiology of chronic diseases. *Front. Physiol.* 11:694. doi: 10.3389/fphys.2020.00694

Shen, S., Yan, Z., Wu, J., Liu, X., Guan, G., Zou, C., et al. (2020). Characterization of ROS metabolic equilibrium reclassifies pan-cancer samples and guides pathway targeting therapy. *Front. Oncol.* 10:581197. doi: 10.3389/fonc.2020.581197

Shephard, R. J. (2017). Physical activity and prostate cancer: an updated review. *Sports Med.* 47, 1055–1073. doi: 10.1007/s40279-016-0648-0

Shimizu, H., Ross, R. K., Bernstein, L., Yatani, R., Henderson, B. E., and Mack, T. M. (1991). Cancers of the prostate and breast among Japanese

and white immigrants in Los Angeles County. *Br. J. Cancer* 63, 963–966. doi: 10.1038/bjc.1991.210

Simpson, R. J., Bosslau, T. K., Weyh, C., Niemiro, G. M., Batatinha, H., Smith, K. A., et al. (2021). Exercise and adrenergic regulation of immunity. *Brain Behav. Immun.* 97, 303–318. doi: 10.1016/j.bbi.2021.07.010

Smuder, A. J. (2019). Exercise stimulates beneficial adaptations to diminish doxorubicin-induced cellular toxicity. *Am. J. Phys. Regul. Integr. Comp. Phys.* 317, R662–R672. doi: 10.1152/ajpregu.00161.2019

Sorial, E., Si, S., Fritschi, L., Darcey, E., Leavy, J. E., Girschik, J., et al. (2019). Lifetime recreational physical activity and the risk of prostate cancer. *Cancer Causes Control* 30, 617–625. doi: 10.1007/s10552-019-01138-6

Stein, C. J., and Colditz, G. A. (2004). Modifiable risk factors for cancer. *Br. J. Cancer* 90, 299–303. doi: 10.1038/sj.bjc.6601509

Sung, H., Ferlay, J., Siegel, R. L., Laversanne, M., Soerjomataram, I., Jemal, A., et al. (2021). Global cancer statistics 2020: GLOBOCAN estimates of incidence and mortality worldwide for 36 cancers in 185 countries. *CA Cancer J. Clin.* 71, 209–249. doi: 10.3322/caac.21660

Tasdemir, S. S., and Sanlier, N. (2020). An insight into the anticancer effects of fermented foods: a review. *J. Funct. Foods* 75:104281. doi: 10.1016/j.jff.2020.104281

Thomas, R. J., Kenfield, S. A., and Jimenez, A. (2017). Exercise-induced biochemical changes and their potential influence on cancer: a scientific review. *Br. J. Sports Med.* 51, 640–644. doi: 10.1136/bjsports-2016-096343

Vernieri, C., Casola, S., Foiani, M., Pietrantonio, F., de Braud, F., and Longo, V. (2016). Targeting cancer metabolism: dietary and pharmacological interventions. *Cancer Discov.* 6, 1315–1333. doi: 10.1158/2159-8290.CD-16-0615

Wagner, I. V., Sabin, M. A., Pfaffle, R. W., Hiemisch, A., Sergeyev, E., Korner, A., et al. (2012). Effects of obesity on human sexual development. *Nat. Rev. Endocrinol.* 8, 246–254. doi: 10.1038/nrendo.2011.241

Wang, G., Zhao, D., Spring, D. J., and DePinho, R. A. (2018). Genetics and biology of prostate cancer. *Genes Dev.* 32, 1105–1140. doi: 10.1101/gad.315739.118

Wang, J., Heng, Y. J., Eliassen, A. H., Tamimi, R. M., Hazra, A., Carey, V. J., et al. (2017). Alcohol consumption and breast tumor gene expression. *Breast Cancer Res.* 19:108. doi: 10.1186/s13058-017-0901-y

Wastyk, H. C., Fragiadakis, G. K., Perelman, D., Dahan, D., Merrill, B. D., Yu, F. B., et al. (2021). Gut-microbiota-targeted diets modulate human immune status. *Cell* 184, 4137–4153.e14. doi: 10.1016/j.cell.2021.06.019

Wong, C. C., Qian, Y., and Yu, J. (2017). Interplay between epigenetics and metabolism in oncogenesis: mechanisms and therapeutic approaches. *Oncogene* 36, 3359–3374. doi: 10.1038/onc.2016.485

Wu, Q., Li, B., Li, Z., Li, J., Sun, S., and Sun, S. (2019). Cancer-associated adipocytes: key players in breast cancer progression. *J. Hematol. Oncol.* 12:95. doi: 10.1186/s13045-019-0778-6

Wu, S., Zhu, W., Thompson, P., and Hannun, Y. A. (2018). Evaluating intrinsic and non-intrinsic cancer risk factors. *Nat. Commun.* 9:3490. doi: 10.1038/s41467-018-05467-z

Wu, Z., Chen, H., Luo, W., Zhang, H., Li, G., Zeng, F., et al. (2020). The landscape of immune cells infiltrating in prostate cancer. *Front. Oncol.* 10:517637. doi: 10.3389/fonc.2020.517637

Xu, Q., Chen, S., Hu, Y., and Huang, W. (2021). Landscape of immune microenvironment Under immune cell infiltration pattern in breast cancer. *Front. Immunol.* 12:711433. doi: 10.3389/fimmu.2021.711433

Xue, M., Zhang, K., Mu, K., Xu, J., Yang, H., Liu, Y., et al. (2019). Regulation of estrogen signaling and breast cancer proliferation by an ubiquitin ligase TRIM56. *Oncogene* 8:30. doi: 10.1038/s41389-019-0139-x

Zhao, H., Zhou, L., Shangguan, A. J., and Bulun, S. E. (2016). Aromatase expression and regulation in breast and endometrial cancer. *J. Mol. Endocrinol.* 57, R19–R33. doi: 10.1530/JME-15-0310

Conflict of Interest: The authors declare that the research was conducted in the absence of any commercial or financial relationships that could be construed as a potential conflict of interest.

Publisher's Note: All claims expressed in this article are solely those of the authors and do not necessarily represent those of their affiliated organizations, or those of the publisher, the editors and the reviewers. Any product that may be evaluated in this article, or claim that may be made by its manufacturer, is not guaranteed or endorsed by the publisher.

Copyright © 2022 Tan and Naylor. This is an open-access article distributed under the terms of the Creative Commons Attribution License (CC BY). The use, distribution or reproduction in other forums is permitted, provided the original author(s) and the copyright owner(s) are credited and that the original publication in this journal is cited, in accordance with accepted academic practice. No use, distribution or reproduction is permitted which does not comply with these terms.

frontiers in Physiology

REVIEW
published: 16 March 2022
doi: 10.3389/fphys.2022.858941

The Paraventricular Nucleus of the Hypothalamus in Control of Blood Pressure and Blood Pressure Variability

*Bojana Savić[1], David Murphy[2] and Nina Japundžić-Žigon[1]**

[1]Laboratory for Cardiovascular Pharmacology and Toxicology, Faculty of Medicine, Institute of Pharmacology, Clinical Pharmacology and Toxicology, University of Belgrade, Belgrade, Serbia, [2]Molecular Neuroendocrinology Research Group, Bristol Medical School, Translational Health Sciences, University of Bristol, Bristol, United Kingdom

The paraventricular nucleus (PVN) is a highly organized structure of the hypothalamus that has a key role in regulating cardiovascular and osmotic homeostasis. Functionally, the PVN is divided into autonomic and neuroendocrine (neurosecretory) compartments, both equally important for maintaining blood pressure (BP) and body fluids in the physiological range. Neurosecretory magnocellular neurons (MCNs) of the PVN are the main source of the hormones vasopressin (VP), responsible for water conservation and hydromineral balance, and oxytocin (OT), involved in parturition and milk ejection during lactation. Further, neurosecretory parvocellular neurons (PCNs) take part in modulation of the hypothalamic–pituitary–adrenal axis and stress responses. Additionally, the PVN takes central place in autonomic adjustment of BP to environmental challenges and contributes to its variability (BPV), underpinning the PVN as an autonomic master controller of cardiovascular function. Autonomic PCNs of the PVN modulate sympathetic outflow toward heart, blood vessels and kidneys. These pre-autonomic neurons send projections to the vasomotor nucleus of rostral ventrolateral medulla and to intermediolateral column of the spinal cord, where postganglionic fibers toward target organs arise. Also, PVN PCNs synapse with NTS neurons which are the end-point of baroreceptor primary afferents, thus, enabling the PVN to modify the function of baroreflex. Neuroendocrine and autonomic parts of the PVN are segregated morphologically but they work in concert when the organism is exposed to environmental challenges *via* somatodendritically released VP and OT by MCNs. The purpose of this overview is to address both neuroendocrine and autonomic PVN roles in BP and BPV regulation.

Keywords: blood pressure, blood pressure variability, PVN, vasopressin, oxytocin, baroreflex

OPEN ACCESS

Edited by:
Geoffrey A. Head, Baker Heart and Diabetes Institute, Australia

Reviewed by:
Stephanie Tjen-A-Looi, University of California, Irvine, United States
Hreday Sapru, Rutgers New Jersey Medical School, United States

****Correspondence:***
Nina Japundžić-Žigon
nina.zigon@med.bg.ac.rs

Specialty section:
This article was submitted to Integrative Physiology, a section of the journal Frontiers in Physiology

Received: *20 January 2022*
Accepted: *15 February 2022*
Published: *16 March 2022*

Citation:
Savić B, Murphy D and Japundžić-Žigon N (2022) The Paraventricular Nucleus of the Hypothalamus in Control of Blood Pressure and Blood Pressure Variability. Front. Physiol. 13:858941. doi: 10.3389/fphys.2022.858941

INTRODUCTION

Occupying a small portion of the vertebrate brain (1%), the PVN is a highly organized effector structure (Swanson, 1995; Benarroch, 2005). This hypothalamic nucleus is located bilaterally around the third ventricle (Badoer, 2001). Morphological studies of the PVN reveal different cell populations within its borders, such that the PVN can be divided into at least three

magnocellular (anterior, posterior and medial subnuclei) and five parvocellular (dorsal, lateral, medial, periventricular and anterior subnucleus) compartments (Swanson and Kuypers, 1980; Sawchenko and Swanson, 1982a; Swanson and Sawchenko, 1983; Badoer, 2001; Pyner, 2009). Two functionally separate areas of the PVN, neuroendocrine and autonomic, subserve its potential to regulate BP, making the PVN a major integrative site of cardiovascular function (Swanson and Kuypers, 1980; Swanson and Sawchenko, 1983; Son et al., 2013; Sladek et al., 2015). Blood pressure, which is defined by peripheral vascular resistance and cardiac output (resultant of heart rate and stroke volume), is modified by both neuroendocrine and autonomic premotor PVN in at least three different effector pathways (**Figure 1**): neurosecretory magnocellular, neurosecretory parvocellular, and pre-autonomic parvocellular neural pathway (Badoer, 2001; Sladek et al., 2015).

MODULATION OF BLOOD PRESSURE BY THE NEUROENDOCRINE PVN

Over 30 distinct neurotransmitters and neuromodulators have been identified to be synthesized within the PVN (Swanson and Sawchenko, 1983). Most abundantly expressed are vasopressin (VP) and oxytocin (OT), which are produced by the magnocellular neurons (MCNs) of the PVN (Swanson and Sawchenko, 1980; Sladek et al., 2015). VP is best known for its role in maintaining cardiovascular and body fluid balance, whereas OT takes part in parturition, lactation and accompanying reproductive behaviors (Gimpl and Fahrenholz, 2001; Koshimizu et al., 2006; Stoop, 2014). Additionally, VP and corticotropin-releasing hormone (CRH) expressing parvocellular neurons (PCNs) of the PVN possess a secretory capacity and mediate the central response of the hypothalamic–pituitary–adrenal (HPA) axis to stress (Swanson and Sawchenko, 1980; Sawchenko et al., 1996; Benarroch, 2005; Sladek et al., 2015). Magnocellular and parvocellular neuroendocrine neurons of the PVN initiate a downstream chain of events that dictate changes in BP.

The Role of Neurosecretory MCNs in BP Regulation

Magnocellular neurons express VP and OT in large quantities (Dierickx, 1980). Located mostly in the medial and the lateral posterior subdivision of the PVN, MCNs send their axonal projections to neurohypophysis, from where VP and OT is released into the systemic circulation (Armstrong et al., 1980; Swanson and Sawchenko, 1983; Sladek et al., 2015). Once secreted into blood, these peptide hormones act upon distant targets (Dierickx, 1980; Gutkowska et al., 2000; Japundžić-Žigon, 2013). VP and OT exert their effects through activation of cognate receptors that are expressed both in the brain and periphery (Brinton et al., 1984; Ostrowski et al., 1992; Hirasawa et al., 1994; Adan et al., 1995; Kato et al., 1995). VP receptors (VR) and OT receptors (OTR) are a subfamily of G coupled receptors (G protein-coupled receptors—GPCRs) with high structural homology (85% homology found between V1aR and OTR; Barberis et al., 1998; Thibonnier et al., 2002; Koshimizu et al., 2012). In the periphery, VP mainly engages V1aR and V2R, while in the central nervous system VP action is mostly mediated by V1aR and far less by V1bRs (Ostrowski et al., 1992, 1994; Young et al., 2006; Roper et al., 2011; Russell and Brunton, 2017).

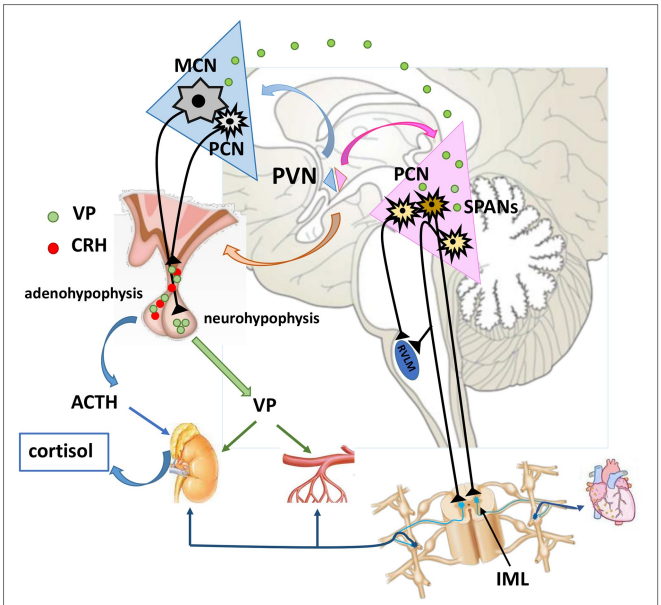

FIGURE 1 | Neuroendocrine and pre-autonomic paraventricular nucleus in cardiovascular regulation. MCNs synthetize VP which is transported *via* their axons to neurohypophysis for systemic release. Once in the circulation, VP reaches distant targets (kidneys, resistance vessels) to exert its effects. Some portion of VP is released intranuclearly, and modulates the activity of pre-autonomic PCNs. These pre-autonomic neurons have the potential to modulate the autonomic outflow toward heart, kidneys and arterioles. Additionally, VP is co-expressed with CRH alternating the reactivity of HPA axis. VP, vasopressin; CRH, corticotropin-releasing hormone; ACTH, adrenocorticotropic hormone; MCN, Magnocellular neuron; PCNs, parvocellular neuron; SPANs, spinally projecting pre-autonimic neurons; RVLM, rostral ventrolateral medulla; IML, intermediolateral nucleus.

Peripheral VP and OT in Blood Pressure Regulation

The strongest stimulus for the MCNs to secret VP into the bloodstream is hyperosmotic change (McKinley et al., 2004). Hyperosmolality of blood is sensed by circumventricular organs

Abbreviations: ACTH, Adrenocorticotropic hormone; ADH, Antidiuretic hormone; ANP, Atrial natriuretic peptide; AP, Area postrema; AQP-2, Aquaporin 2; AT1R, Angiotensin II receptor type 1; AV3V, Anteroventral third ventricle; BHR, Borderline hypertensive rats; BPV, BP variability; BP, Blood pressure; BRS, Baroreflex sensitivity; CRH, Corticotropin-releasing hormone; CRHR2, corticotropin-releasing hormone receptor; DMV, dorsal motor nucleus of vagus; GABA, γaminobutyric acid; GPCRs, G protein-coupled receptors; HF, High frequency; HPA, Hypothalamo–hypophyseal axis; HRV, Heart rate variability; IML, Intermediolateral nucleus; LF, Low frequency; MCNs, Magnocellular neurons; MnPO, Medial preoptic nucleus; NO, Nitrogen oxide; NTS, Nucleus tractus solitarius; OT, Oxytocin; OTR, Oxytocin receptor; OVLT, Organum vasculosum laminae terminalis; PCNs, Parvocelular neuron; PVN, Paraventricular nucleus; RVLM, Rostral ventrolateral medulla; SFO, Circumventricular subfornical organ; SHR, Spontaneously hypertensive rats; SND, Sympathetic nerve discharge; SPANs, Spinally projecting pre-utonimic neurons; VLF, Very low frequency; VLM, Ventrolateral medulla; VP, Vasopressin; VR, Vasopressin receptor.

in the periventricular region of the third ventricle (anteroventral third ventricle—AV3V), which is devoid of the blood brain barrier. The circumventricular subfornical organ (SFO) and *organum vasculosum laminae terminalis* (OVLT) are richly vascularised, and their neurons easily sense perturbations in blood osmolality (Leng et al., 1989; Cunningham and Sawchenko, 1991; McKinley et al., 2004). From these structures, direct or indirect (*via* medial preoptic nucleus—MnPO) excitatory axonal projections to MCNs, stimulate the secretion of VP into circulation (Leng et al., 2001; McKinley et al., 2004). Additionally, several other stimuli trigger VP secretion: decreased blood volume and pressure which induce reduction of stretch in low-pressure receptors of venous system and high-pressure baroreceptors respectively and ANG II (Japundžić-Žigon et al., 2020).

The best known roles of peripheral VP are water conservation in kidneys and vasoconstriction (Altura and Altura, 1984; Bankir, 2001; Sladek et al., 2015). Indeed, VP is often referred to as antidiuretic hormone (ADH), due to its role in water conservation by the activation of V2Rs in the kidneys (Ostrowski et al., 1993; Gordan et al., 2015). Even small changes in VP concentration in the serum will activate renal V2Rs, with highest affinity to VP, to preserve water (Japundžić-Žigon, 2013). V2Rs are located in the basolateral membrane of the epithelial cells of the collecting ducts of the kidney. Activation of V2R is responsible for a cascade of events that involve phosphorylation of aquaporin 2 (AQP-2) and its translocation into the luminal membrane of epithelial cells, leading to reabsorption of water by the kidneys. VP also affects AQP-2 transcription rates and increases AQP-2 protein abundance (Imbert et al., 1975; Knepper, 1997; Bankir, 2001; Wilson et al., 2013; Jung and Kwon, 2016).

The vasoconstrictor effect of VP is mediated by V1aRs located on blood vessels. Although *in vitro* studies confirm VP as a most potent vasoconstrictor agent, relatively high concentrations of VP are necessary to elevate BP *in vivo* under basal physiological conditions (Altura and Altura, 1984; Johnston, 1985; Koshimizu et al., 2006) in respect to much less potent vasoconstrictors at molar level such as angiotensin II and noradrenalin. Nevertheless, vascular V1aRs are crucial for BP maintenance during hypovolemia and hypotension (Koshimizu et al., 2012). Also, in some vascular beds, such as in lung, liver and kidneys VP activates V1aR and V2R to produce nitrogen monoxide (NO) dependent vasodilatation (Liard, 1984; Hirsch et al., 1989; Russ and Walker, 1992; Aki et al., 1994; Koshimizu et al., 2006).

Circulating VP can circumvent the blood brain barrier and reach centrally located receptors (Landgraf and Neumann, 2004). The most prominent impact of peripheral VP on blood pressure is exerted at the level of area postrema (AP), where it can modify the activity of the baroreflex (Brizzee and Walker, 1990; Hasser et al., 1997). Even though the VP effects on baroreflex are controversial, the majority of studies report enhancement of baroreflex sensitivity (BRS; Brizzee and Walker, 1990; Hasser and Bishop, 1990; Hasser et al., 1997; Koshimizu et al., 2006). Further support is provided by experiments which show that lesions of the AP region disable peripheral VP to modulate baroreflex (Hasser et al., 1997). Also, VP deficient Brattleboro rats exhibit decreased BRS (Imai et al., 1983b). Pharmacological studies suggest that this effect is conveyed by V1aR (Imai et al., 1983a; Hasser and Bishop, 1990; Sampey et al., 1999). The effect of VP on BRS is complex, and when VP is released centrally during stress and exercise, it will act oppositely and reduce BRS *via* medullary V1aRs (Unger et al., 1986).

Afferents that originate from stretch receptors and baroreceptors are tonically active under physiological conditions and inhibit VP secretion from MCNs, while decrease in blood volume and BP leads to disinhibition and consequent release of VP (Bisset and Chowdrey, 1988). Before it reaches the PVN, the information from the baroreceptors is conveyed *via* the *nucleus tractus solitarius* (NTS) and ventrolateral medulla (VLM). Afferents arising from the NTS (A2 type neurons) and VLM (A1 cell group) that project to MCNs are primarily noradrenergic (Sawchenko and Swanson, 1982b). Putative inhibitory mechanisms involve NTS residing GABAergic neurons which silence the noradrenergic excitatory pathways directed to the magnocellular subdivision of the PVN (Jhamandas and Renaud, 1987; Bisset and Chowdrey, 1988; Leng et al., 1999).

Altogether, it seems that the minor effect of VP on BP maintenance under basal physiological conditions is due to the BRS enhancement *via* AP and consequent decrease in heart rate which efficiently oppose its vasoconstrictor performance on the periphery (Abboud et al., 1990; Koshimizu et al., 2006).

Oxytocin is a nonapeptide hormone best known for inducing uterine contractions during labor and milk ejection during lactation (Dale, 1906; Ott and Scott, 1910; Du Vigneaud, 1954). Apart from these primary roles, OT is involved in a large number of physiological activities, including cardiovascular control (Maier et al., 1998). OT secretion in hypothalamus is not only sex dependent, and it can be modulated by hyperosmotic stimuli, hypovolemia and ANG II (Kadekaro et al., 1992; Gimpl and Fahrenholz, 2001). Mechanisms underlying OT involvement in BP regulation are not yet fully elucidated (Gutkowska et al., 2000). OT activity usually correlates with BP decrease in many species. Experiments with RNA interference report that blocking brain OT RNA leads to an increase in BP (Petersson et al., 1996, 1997; Maier et al., 1998). One of the putative mechanisms behind OT modulation of BP lies in its engagement with electrolyte excretion in the kidneys. It is suggested that OT induced natriuresis is mediated by atrial natriuretic peptide (ANP; Verbalis et al., 1991; Conrad et al., 1993; Gutkowska et al., 2000). However, this natriuretic effect is not confirmed in humans, and it appears that it is present only in certain species, such as rats (Rasmussen et al., 2004).

Since VP and OT share very similar primary structures (only differing by 2 amino acids at positions 3 and 8), as well as their receptors, OT can bind with high affinity to V1aRs as well as OTRs (Gimpl and Fahrenholz, 2001; De Bree et al., 2003). OT receptors have a wide distribution in the body (Adan et al., 1995). As well as the reproductive system, OTRs can be found within the brain and heart (Adan et al., 1995; Gutkowska et al., 1997). OT induced peripheral vasoconstriction can be mediated by V1aRs. *In vitro* studies reveal that the potency of OT to contract blood vessel smooth muscle cells is much less than VP, with the exception of the umbilical

artery at term (Altemus et al., 2001). When vascular tone is already increased, OT will produce NO dependent vasodilatation in some vascular beds, like in basilar arteries (Katusic et al., 1986; Russ et al., 1992; Thibonnier et al., 1999). It seems that OT is not responsible for modulating the peripheral resistance in pregnant rats, and does not play a significant role in setting the levels of BP under physiological conditions (Miller et al., 2002).

Even though experimental evidence does not support strong involvement of VP and OT in BP regulation under baseline physiological conditions, studies with VP and OT gene knock-out mice provide a contrasting insight. VP knock-out mice exhibit lower basal values of BP, while OT deficient mice demonstrate elevated BP and HR values in comparison to wild type controls (Bernatova et al., 2004; Koshimizu et al., 2006). Apart from being normotensive, VP deficient Brattleboro rats exhibit decreased BRS. However, it should be noted that the complex and unpredictable developmental compensations occurring in global knock-out mice makes the interpretation of adult phenotypes problematic (Valtin, 1982; Imai et al., 1983b; Bohus and de Wied, 1998).

Intranuclear OT and VP in Blood Pressure Regulation

Vasopressin and OT can be synthesized and released from dendrites and soma of MCNs and this can happen without cell depolarization (Scala-Guenot et al., 1987; Moos et al., 1989, 1998; Pow and Morris, 1989; Neumann et al., 1993b; Ludwig et al., 1995, 2002; Hurbin et al., 1998, 2002). VP in the extracellular space can exert both autocrine and paracrine effects (Ludwig and Stern, 2015). Intranuclear VP can activate V1aRs and V1bR expressed on MCNs, or it can spill over through the extracellular space into the cerebrospinal fluid (Landgraf and Neumann, 2004) and reach remote targets (Hurbin et al., 1998, 2002; Son et al., 2013). It has been proposed that intranuclear receptors optimize the firing rate of the entire population of MCNs to best respond to physiological demands (Son et al., 2013). Somatodendritic release depends on the quality and intensity of stimulus and it can be regulated independently from systemic release (Pow and Morris, 1989; Neumann et al., 1993a; Ota et al., 1994; Kendrick et al., 1997; Gouzènes et al., 1998; Landgraf and Neumann, 2004). It has been suggested that the autocontrol of MCN by intranuclear VP can be either inhibitory or excitatory (Inenaga and Yamashita, 1986; Gouzènes et al., 1998; Dayanithi et al., 2000; Landgraf and Neumann, 2004). Additionally, somatodendritically released VP (**Figure 1**) can activate surrounding silent MCNs (Moos et al., 1998), or depolarize neighboring interneurons and PCNs (Carette and Poulain, 1989; Son et al., 2013). Activation of autonomic PCNs through engagement of V1aRs, especially during hyperosmotic stimulus, is particularly important in terms of integration of neuroendocrine and autonomic regulation of blood pressure (Swanson and Sawchenko, 1980; Son et al., 2013). It has also been reported that intranuclear V1bRs participate in setting sympathetic outflow toward the kidneys (El-Werfali et al., 2015).

The Role of PVN Neurosecretory PCNs in BP Regulation

Stress is an attributed risk factor for cardiovascular diseases that can trigger bad clinical outcomes (Hjemdahl, 2002; Rosmond, 2005). PVN involvement in the stress response has been documented in spontaneously hypertensive rats (SHRs) and other experimental models (Benarroch, 2005). The PVN promotes several aspects of hemodynamic regulation during stress (Herman et al., 1996; Benarroch, 2005). Anterior and medial PCNs that synthesize CRH, are responsible for activating the HPA axis during exposure to stress (Rivier and Vale, 1983; Swanson et al., 1983; Sawchenko et al., 1996; Sladek et al., 2015). Apart from expressing CRH, PCNs produce VP as secretagogue. It appears that the CRH:VP ratio is dictated by the type of stressor, and is crucial for maintaining responsiveness of the HPA axis during chronic stress (Sawchenko and Swanson, 1982a; Swanson and Sawchenko, 1983; Whitnall et al., 1985; de Goeij et al., 1992; Aguilera, 1994; Sawchenko et al., 1996; Amaya et al., 2001). Both CRH and VP are axonally transported to eminentia mediana and released into the portal circulation. Borne by the portal bloodstream, they reach adenohypophysis, where they act on corticotropic cells. CRH stimulates the release of adrenocorticotropic hormone (ACTH), whereas VP potentiates its release by activating V1bRs (Benarroch, 2005). Once in the systemic circulations (**Figure 1**), ACTH acts on the cells of *zona fasciculata* in adrenal gland to release glucocorticoids (Myers et al., 2012; Sladek et al., 2015). Cortisol when in excess, has been shown to contribute to hypertension (Kelly et al., 1998). Additionally, elegant ontogenetic experiments suggest that CRH PCNs can increase BP and heart rate *via* axonal projections to the NTS (Wang et al., 2019), involving corticotropin-releasing hormone receptor type 2 (CRHR2), also associated with hypertension triggered by intermittent hypoxia (Wang et al., 2019).

It has been shown that forced swimming and social confrontation, stressors employed in experimental conditions, can induce somatodendritic release of VP and OT (Wotjak et al., 1996; Engelmann et al., 2001; Ebner et al., 2005), which in turn modifies the activity of the HPA axis. Intranuclear VP has an inhibitory effect on CRH PCNs and consequently reduces secretion of ACTH (Wotjak et al., 1996, 2002; Bosch et al., 2004; Ebner et al., 2005). Extracellular OT exhibits both inhibitory and excitatory influence on the activity of the HPA axis (Neumann et al., 2000; Heinrichs et al., 2002; Neumann, 2002; Landgraf and Neumann, 2004).

THE ROLE OF THE "PRE-AUTONOMIC" PVN IN BP REGULATION

Apart from being locally regulated, the cardiovascular system is subject to central control by numerous relevant brain areas (Dampney, 1994). It is well established that PVN takes an important central place in such control. Numerous studies show that the PVN is implicated in the heightened sympathetic tone observed in hypertension (Allen, 2002;

Dampney et al., 2018). The autonomic PVN consists of morphologically and functionally diverse cell populations with a specific topography (Stern, 2001; Dampney et al., 2018). It occupies ventromedial, lateral and dorsal (dorsal cap) subdivision of PVN (Nunn et al., 2011; Sladek et al., 2015). More precisely, these PCNs are pre-autonomic, since they control functionally different sympathetic and parasympathetic centers downstream in the medulla: NTS, dorsal motor nucleus of vagus (DMV) and rostral ventrolateral medulla (RVLM), and the spinal cord: intermediolateral nucleus (IML). Therefore, the "pre-autonomic" premotor PVN is responsible for altering the autonomic output toward the cardiovascular and renal systems (Strack et al., 1989a; Coote et al., 1998; Portillo et al., 1998; Coote, 2005; Dampney et al., 2018). Hence it is not surprising that PVN is commonly referred to as an "autonomic master controller," a term originally introduced by Loewy (1991). There are at least 3 pathways (**Figure 1**) through which PVN modulates sympathetic outflow (Pyner, 2009):

The first pathway includes PVN pre-sympathetic neurons that have axonal projections that terminate on somata of motor sympathetic preganglionic neurons (SPNs) in the thoraco-lumbal IML. These neurons are usually named as spinally projecting pre-autonomic neurons (SPANs; Dampney, 1994; Badoer, 2001; Nunn et al., 2011). The IML is the final spot of central integration and origin of preganglionic fibers which regulate the activity of blood vessels, heart, kidneys and adrenal gland. Therefore, this is a particularly important target of the PVN pre-autonomic neurons, displaying its enormous potential to directly alternate neurogenic output to the cardiorenal system (Strack et al., 1989a; Dampney, 1994; Badoer, 2001).

The second pathway involves pre-sympathetic PVN neurons that exert indirect influence on sympathetic activity. These neurons terminate at the level of the motor pressor nucleus of the RVLM, responsible for setting sympathetic tone. From there, second order neurons arise and project to SPNs in the thoracic and lumbar IML and change sympathetic outflow toward the cardiovascular system and the kidneys (Dampney, 1994; Badoer, 2001). In general, PVN neurons projecting to RVLM are in greater number than PVN neurons projecting monosinaptically to IML. Therfore, RVLM is a structure embedding most of the pre-sympathetic neurons, which are projecting to IML to exert major autonomic cardiovascular control (Badoer, 2001). Some of the sympatho-excitatory effects in the PVN-RVLM pathways are glutamate mediated (Yang and Coote, 1998). Additionally, evidence has emerged, that PVN can interfere with this PVN-RVLM pathway through its glutamatergic synapses within medial subnucleus of the NTS (mNTS; Kawabe et al., 2008). Using anterograde and retrograde tracing, Kawabe working group confirmed the presence of such bilateral glutamatergic projections spanning to mNTS. They showed that unilateral PVN stimulation with N-methyl-D-aspartic acid (NMDA) leads to increase in mean arterial pressure and greater splanchic nerve activity, and that this effect is emphasized by bilateral blockade of glutamate ionotropic receptors within the mNTS. The authors suggested that PVN glutamatergic pathways directed toward NTS, stimulate inhibition of RVLM-mediated cardiovascular overactivity. Therefore, PVN stimulation with NMDA evokes both RVLM and NTS neuronal routes, but the effects are opposing (Kawabe et al., 2008). Further, same authors showed that tachycardia induced by NMDA stimulation of the PVN is a result of conjoined inhibition of vagal (*via* ionotropic glutamate and GABA receptors in the mNTS) and activation of sympathetic outputs (*via* spinal ionotropic glutamate) toward heart, without involvement of spinal VRs and OTRs (Kawabe et al., 2009).

A third pathway is represented by PVN pre-autonomic neurons that can change sympathetic tone both directly and indirectly. Around 30 % of PVN neurons innervate SPNs in the IML, but send collaterals to the RVLM, thus having a dual regulatory role (Badoer, 2001).

The majority of PVN autonomic regulatory function is conveyed by SPANs (Coote, 2007). Since the relevant portion of SPANs is implicated in cardiovascular control (Badoer, 1996; Badoer, 2001; Pyner, 2009; Nunn et al., 2011), this makes them an attractive target for new drug development.

Although their exact functions have yet to be elucidated, SPANs have been suggested to regulate blood volume (Lovick et al., 1993; Pyner and Coote, 2000), circadian variations in BP (Cui et al., 2001), stress induced cardiovascular responses (Jansen et al., 1995a) and much more (Nunn et al., 2011). For these reasons SPANs are referred to as "central command neurons" (Jansen et al., 1995a). Discovering their primary physiological function is further complicated by the fact that SPANs express a lot of different neuroactive substances/neurotransmitters. Indeed, it appears that the majority of these neurons synthesize more than one neurotransmitter (Nunn et al., 2011). The largest portion of SPANs (up to 40 %) is positive for VP and OT (usually co-expressed), as well as dynorphin (Hallbeck and Blomqvist, 1999; Xi et al., 1999; Hallbeck, 2000; Hallbeck et al., 2001). Others possess met-endorphin (up to 20%) and dopamine, met-enkephalin (up to 10 %), leu-enkephalin, somatostatin, ANG II and ANP (Sawchenko and Swanson, 1982a; Cechetto and Saper, 1988; Strack et al., 1989b; Jansen et al., 1995b).

Functional *in vivo* studies show that spinal levels of VP and OT increase with PVN stimulation (Pittman et al., 1984; Malpas and Coote, 1994). The presence of V1aR and OTR has been confirmed in the gray matter of the spinal cord (Desaulles et al., 1995; Sermasi et al., 1998; Pyner, 2009). Intrathecal pretreatment with V1aR antagonist in the lower thoracic region prevents the increase in renal sympathetic nerve activity and mean arterial pressure normally triggered by the stimulation of the PVN (Malpas and Coote, 1994). It cannot be excluded that some of the OT effects are conveyed *via* spinal V1aRs as well (Sermasi and Coote, 1994). Similar effects are also observed with OTR selective antagonists which abolish the effects of increased heart rate following the PVN stimulation (Yang et al., 2009). These experimental data highlight VP and OT as PVN SPAN transmitters. VP and OT induce cardio-acceleratory and pressor effects in lower and upper thoracic spinal cord respectively (Pyner, 2009). The majority of

vasopressinergic projections implicated in cardiovascular control originate in the lateral and ventral medial subdivision of parvocellular PVN and some portion is found in dorsal parvocellular part (Riphagen and Pittman, 1989; Hallbeck and Blomqvist, 1999). Oxytocinergic SPANs are located in the lateral parvocellular region and dorsal cap (Sawchenko and Swanson, 1982a; Pyner, 2009).

The effects of dopamine as a putative SPAN neurotransmitter are controversial (Strack et al., 1989b; Nunn et al., 2011). Some studies on rats suggest its excitatory influence on SPNs, while others report an inhibitory activity (Gladwell et al., 1999; Gladwell and Coote, 1999a,b; Yang et al., 2002).

Pharmacological experiments with a glutamate antagonist, following chemical stimulation of PVN, imply glutamate as an additional excitatory neurotransmitter of SPANs (Yang et al., 2002).

Although SPANs are positive for enkephalins and ANG II, their influence on sympathetic outflow has not yet been recorded (Sawchenko and Swanson, 1982a; Cechetto and Saper, 1988; Jansen et al., 1995b; Hallbeck and Blomqvist, 1999; Hallbeck et al., 2001). Despite its abundant expression in the nervous system, the presence of inhibitory γ-aminobutyric acid (GABA) as a SPAN output neurotransmitter has not been confirmed (Macdonald and Olsen, 1994; Watkins et al., 2009).

Modulation of SPAN Activity

Spinally projecting pre-autonomic neuron activity can be modulated in various ways. A lot has been discovered about the neurotransmitter content of SPANs, but the data regarding receptors expressed on SPANs and molecules their receptors bind is lacking (Nunn et al., 2011). Learning about the neurotransmitters which can modulate the activity of SPANs will open venues to novel therapeutic agents.

It is well established that the PVN is involved in increased sympathetic activity driven by osmotic stimulation, but the mechanisms behind it are poorly understood. Some studies suggest involvement of intranuclear VP released from soma and dendrites of MCNs (Son et al., 2013; Ribeiro et al., 2015). Intranuclear VP stimulates V1aRs expressed on pre-sympathetic parvocellular subdivisions (including SPANs) of the PVN. This leads to increase in sympathetic outflow toward heart, blood vessels and kidneys, followed by BP increase, suggesting this pathway as potential pathophysiological mechanism in neurogenic hypertension (Son et al., 2013; Ribeiro et al., 2015).

Under basal physiological conditions, PVN neurons are tonically inhibited by surrounding GABA neurons, keeping the spontaneously generated nerve impulses at low rate, despite the excitatory influence of glutamate (Kannan et al., 1989; Martin et al., 1991; Badoer et al., 2002; Li et al., 2006). SPANs are confirmed to be silenced by GABA (Cui et al., 2001; Li et al., 2002). This inhibition could be dependent on extrasynaptic GABA ("volume" GABA transmission), but it can also be affected by the rate that glial cells take up GABA from the extracellular space (Brickley et al., 1996; Farrant and Nusser, 2005; Park et al., 2009). GABAA α2-subunit is abundantly expressed in the PVN (Fritschy and Mohler, 1995). Blockage of GABAA receptors by the selective antagonist bicuculline leads to an increase in BP and heart rate (Martin et al., 1991; Martin and Haywood, 1993). Interfering with GABA orchestrated SPAN activity is an appealing therapeutic opportunity, since increasing GABA inhibitory influence would lead to reduction of sympathetic tone and consequently BP decrease (Nunn et al., 2011).

Although injections of ATII in the PVN change blood pressure *via* angiotensin II receptor type 1 (AT1R; Bains et al., 1992), and this involves the activity of SPANs, it seems that this connection is indirect (Bains and Ferguson, 1995; Li et al., 2003). AT1Rs are expressed in parvocellular division of the PVN on neurons projecting to medulla, not IML (Oldfield et al., 2001; Cato and Toney, 2005).

Spinally projecting pre-autonomic neurons, as well as PCNs which project to RVLM are barosensitive. Under basal physiological conditions, these neurons exhibit spontaneous activity, but they are inhibited by rising pressure (Dampney et al., 2018). Axons arising from caudal NTS neurons terminate on PCNs in the dorsal cap of the PVN. Putative targets of these projections are pre-sympathetic PCNs or GABA interneurons (Pyner, 2009; Dampney, 2017). Other studies do not impose an important role of SPANs in the baroreflex response (Haselton et al., 1994). Volume load is another feedback mechanism that can modify the activity of SPANs, with PVN being a command center of low-pressure blood volume receptors located in the veno-atrial junction (Gupta et al., 1966; Lovick and Coote, 1988; Lovick et al., 1993; Deng and Kaufman, 1995). Additionally, SPANs can be modulated by some types of stressors, such as psychological stress. It has been shown that conditional fear engages around 10 % of SPANs (Carrive and Gorissen, 2008; Dampney et al., 2018). Also SPANs are affected by temperature, different humoral factors, and inputs from higher brain areas (Dampney et al., 2018).

PARAVENTRICULAR NUCLEUS AND BLOOD PRESSURE SHORT-TERM VARIABILITY

The peripheral sympathetic nervous system controlling the cardiovascular system has rhythmic activity that creates distinct patterns of sympathetic nerve discharge (SND) in response to physiological demands and pathophysiological conditions. Using frequency analysis of SND, components of SND were identified including fast cardiac and respiratory rhythms, and slow vasomotor rhythm. It is generally believed that the brain is the source of SND. Thus, which parts of the brain are involved, and how they generate peripheral SND rhythms is still unanswered. Two main theories have been postulated, both of which raised considerable criticism. A theory of a central oscillator/pacemaker suggests that the RVLM is the main structure responsible for generating peripheral sympathetic discharge patterns *via* axonal projections to preganglionic neurons in IML. Recordings of intracellular neuronal activity from medullary slices, uncovered ramp like depolarization following each action potential, leading to subsequent action potential suggestive of pacemaker activity

(Li and Guyenet, 1996). This observation was seriously challenged by the *in vivo* study in rats by Lipski et al. (1996) who observed that RVLM neurons fire irregularly, at much higher discharge rates than the ones in SND, with no evidence of gradual depolarization between individual action potentials (Lipski et al., 1996). They suggested that the regular pattern of firing of RVLM neurons seen in medullary slices, was produced by deafferentation. The work of Lipski and colleagues imposes the network hypothesis, where the activity of pre-sympathetic neurons depends on their antecedent excitatory inputs opposed by tonic inhibitory inputs (setting the level of their excitability). For detailed review refer to Malpas (1998). Geber and Barman postulated a theory of a network of brainstem neurons, whose combined action creates inherent rhythmicity entrained by the baroreflex. These include sympatho-excitatory and sympatho-inhibitory neurons distributed over a wide portion of the lower brainstem that do not have necessarily spontaneous activity (Barman and Gebber, 2000).

In addition to RVLM neurons, hypothalamic PVN SPANs provide monosynaptic inputs to preganglionic neurons in IML. Malpas and Coote (1994) were first to provide evidence in anesthetized rats that chemical stimulation of the PVN by microinjections of homocysteic acid increases the amplitude of renal SND, by recruiting more active fibers, and that this can be blocked by intrathecal injection of V1R antagonist. At the same time the frequency of renal SND, which is modulated by periodic baroreflex inputs (Ninomiya et al., 1990; Malpas and Ninomiya, 1992), remained unaffected. The first experimental evidence that PVN SPANs can incite BPV at the same stimulation frequency was demonstrated in rats by Stauss and associates (Stauss and Kregel, 1996; Stauss et al., 1997). PVN electrically stimulated at frequencies between 0.1 Hz - 0.5 Hz were found to create the same frequencies in the SND pattern and generate BPV in the low frequency (LF) band, which is abolished by α-adrenergic blockade (Japundzic et al., 1990). Stimulation frequencies above 0.5 Hz did not induce BP variations as the blood vessels behaved like cut off filters to high frequencies. Studies on isolated rat vascular smooth muscle cells showed that transmission of fast SND rhythms to BPV is limited by the sluggish, metabotropic α-adrenoceptor signaling, and not by an intrinsic inability of the cells to contract and relax at higher rates (Julien et al., 2001). Thus, SND frequencies higher than 0.5 Hz in rats induce vasoconstriction, increase peripheral resistance and the mean value of BP. It follows that the faster components of BPV, the cardiac component and the respiratory component, are non-neural, created by the perturbations of the circulation induced by the contracting heart and inspiratory movements (Japundzic et al., 1990; Japundzic-Zigon, 1998). The non-neural origin also stands for the slowest, and dominant component of BPV, the very low frequency (VLF) component, which was found to be created by inherent myogenic activity of mesenteric and renal vasculature (VanBavel et al., 1991; Janssen et al., 1995). Although non-neuronal in nature, all the components of BPV can be modulated by the activity of the nervous system and neurohormones (Japundžić-Žigon et al., 2020).

We have investigated the neurochemical contribution of the PVN to short-term BPV, and found that both VP and OT modulate short-term BPV. Using pharmacological and genetic tools in conscious rats we have shown that VP modulates BPV in a complex manner: peripherally as a hormone and centrally as neurotransmitter/modulator (Japundzic-Zigon, 2001, 2013; Japundzić-Zigon et al., 2004, 2018, 2020; Milutinović et al., 2006a,b; Stojicić et al., 2008; Milutinović-Smiljanić et al., 2013; Lozić et al., 2016; Savić et al., 2020). Using spectral analysis of BPV, we found that peripheral administration of non-peptide and selective V1aR or V2R antagonists to conscious normotensive rats under baseline physiological conditions increases BPV, suggesting a buffering role for VP in the VLF domain (Japundzic-Zigon, 2001). We postulated that the decrease of VLF-BPV by VP could be mediated either by the enhancement of the baroreflex sensitivity which normally opposes VLF-BPV, or by the modulation of vasomotion in mesenteric and renal vascular beds (Janssen et al., 1995). In SHR, the buffering capacity of VP on BPV under baseline condition is not preserved (Japundzić-Zigon et al., 2004). This could be due to pathological remodeling of the vasculature in SHR (Head, 1991; Vágnes et al., 2000) making it more sensitive to vasoconstrictors, including VP. Another possibility, even more likely is that impaired baroreflex in SHRs (Dampney, 2017) reduces its capacity to buffer VLF-BPV (Dampney, 2017). However, during hemorrhage, when VP is released in excess in blood, in support of circulation, it acts similarly in normotensive and hypertensive rat strains, and prevents the respiratory related high frequency (HF-BPV) increase, possibly as a consequence of V1aR-mediated vasoconstriction which prevents the unloading of thoracic vessels underlying HF-BPV increase.

Intracerebroventricular injection of selective V1aR, V1bR and V2R antagonists to conscious normotensive rats uncovered that VP acts also centrally to buffer VLF-BPV under baseline physiological conditions by the stimulation of V1aRs possibly in AP, accessible from both sides of the blood brain barrier. However, when VP release is stimulated by stress (Stojicić et al., 2006, 2008; Milutinović et al., 2006b), or by drugs (Milutinović et al., 2006a) and when VP is injected centrally (Milutinović et al., 2006b), an increase of the sympathetically mediated LF-BPV and of the respiration mediated HF-BPV was observed (Milutinović et al., 2006a,b). These effects of VP could involve central V1aR found in abundance in the RVLM where integration of the sympathetic outflow to vasculature occurs; and in the pre-Bötzinger area, where the breathing pattern is set. These central effects of VP could be beneficial and contribute to the lifesaving effect of VP in hemorrhagic, septic and cardiogenic shock as a results of increased tissue oxygenation and additional sympathetic activation, acting synergistically with powerful V1aR mediated peripheral vasoconstriction (Levy et al., 2018). VP can also modulate respiration indirectly (Stojicić et al., 2008) by an anxiogenic action characterized by hyperventilation that occurs possibly by the stimulation of V1bR in bed nucleus *stria terminalis* (Griebel et al., 2002).

Paraventricular nucleus is a recognized key integrative site of the behavioral, autonomic and endocrine response to stress, expressing V1aRs and V1bRs on somata and dendrites of MCNs

and surrounding glia. Stress has been shown to induce VP and OT release in the PVN too (Nishioka et al., 1998; Landgraf and Neumann, 2004), and we have shown that VP and OT act locally, in an autocrine and paracrine manner, to modulate the neuro-cardiogenic stress response. Using adenoviral gene transfer technology we have increased the gene expression and the number of V1aRs in the PVN of Wistar rats. The V1aR rat phenotype had decreased sensitivity of the baroreflex under baseline physiological conditions which was further decreased by stress along with a marked increase of the sympathetically mediated LF-BPV and LF heart rate variability (LF-HRV). These effects could be abolished by intranuclear application of V1aR antagonist. This suggests that V1aR in the PVN can increase the sympathetic outflow to the periphery and modulate BPV and HRV during stress (Lozić et al., 2014; Japundžić-Žigon et al., 2020). In clinical practice, the increase in LF-HRV has been found to predict the occurrence of life threatening arrhythmias in susceptible populations (Huikuri and Stein, 2013). In contrast to V1aR, OTR over-expression in the PVN of Wistar rats had no effect on BPV under baseline conditions but this rat phenotype exhibited reduced baroreflex desensitization by stress and reduced LF-BP increase suggesting that OTR over-expressing rat phenotype is resilient to stress (Lozić et al., 2014; Japundžić-Žigon et al., 2020). In this context, it is important to stress that the modulation of the baroreceptor desensitization during stress by VP seems to be complex and involves more than one central structure and type of VRs (Milutinović-Smiljanić et al., 2013).

A number of clinical studies in hypertensive patients unequivocally show that enhanced BPV increases the risk for developing cardiovascular complications (Mancia and Grassi, 2000). Thus, BPV, and especially sympathetically derived LF-BPV, emerged as an independent predictor of stroke, coronary artery disease, heart and renal failure, as well as all-cause mortality (Mancia et al., 1994; Mancia and Parati, 2003; Messerli et al., 2019; Parati et al., 2020). Our group investigated expression of PVN VP and VRs in the genesis of hypertension. Borderline hypertensive rats (BHR) have a genetic predisposition for hypertension and will develop it when exposed to environmental challenges. Under baseline physiological conditions BHRs have increased expression of VP and V1bR in the PVN and consequently increased plasma VP concentrations, as a constitutive trait (Savić et al., 2020). Spectral markers of sympathetic activity toward blood vessels, LF-BP, and the heart, LF/HF-HR, are comparable to normotensive rats under baseline physiological conditions, suggesting that increased expression of V1bR and VP in BHRs is confined to magnocellular (endocrine) portion of the PVN affecting plasma VP only. However, when exposed to repeated stress and prolonged isotonic saline load, BHRs exhibited LF-BPV increase depicting sympathetic overload, and overt hypertension. In these rats no changes in VP and VR gene transcription in the PVN was noted. Moreover, systemic VP release was decreased, refuting involvement of VP in stress-induced hypertension (Savić et al., 2020).

CONCLUSION

It is well established that PVN has a paramount role in cardiovascular regulation and contributes to the severity of cardiovascular diseases. Both neuroendocrine and autonomic PVN, have a dynamic part in adjusting the circulation to physiological demands and in the modulation of short-term BPV. Thus, elucidating the tightly intertwined mechanisms underlying complexity of the PVN network in health and disease may open up new therapeutic venues.

AUTHOR CONTRIBUTIONS

BS, DM, and NJ-Ž: outlining paper draft, writing and refining the manuscript, and critical reading of the manuscript. All of the authors have read and approved the manuscript.

FUNDING

This work was supported by Serbian Ministry of Education, Science and Technological Development (no. 200110, BS, NJ-Ž), British Heart Foundation (RG/11/28714, DM; FS/12/5/29339, DM), and BBSRC (BB/J005452/1, DM).

REFERENCES

Abboud, F. M., Floras, J. S., Aylward, P. E., Guo, G. B., Gupta, B. N., and Schmid, P. G. (1990). Role of vasopressin in cardiovascular and blood pressure regulation. *J. Vasc. Res.* 27, 106–115. doi: 10.1159/000158801

Adan, R. A., Van Leeuwen, F. W., Sonnemans, M. A., Brouns, M., Hoffman, G., Verbalis, J. G., et al. (1995). Rat oxytocin receptor in brain, pituitary, mammary gland, and uterus: partial sequence and immunocytochemical localization. *Endocrinology* 136, 4022–4028. doi: 10.1210/endo.136.9.7649111

Aguilera, G. (1994). Regulation of pituitary ACTH secretion during chronic stress. *Front. Neuroendocrinol.* 15, 321–350. doi: 10.1006/frne.1994.1013

Aki, Y., Tamaki, T., Kiyomoto, H., He, H., Yoshida, H., Iwao, H., et al. (1994). Nitric oxide may participate in V2 vasopressin-receptor-mediated renal vasodilation. *J. Cardiovasc. Pharmacol.* 23, 331–336. doi: 10.1097/00005344-199402000-00023

Allen, A. M. (2002). Inhibition of the hypothalamic paraventricular nucleus in spontaneously hypertensive rats dramatically reduces sympathetic vasomotor tone. *Hypertension* 39, 275–280. doi: 10.1161/hy0202.104272

Altemus, M., Redwine, L. S., Leong, Y. M., Frye, C. A., Porges, S. W., and Carter, C. S. (2001). Responses to laboratory psychosocial stress in postpartum women. *Psychosom. Med.* 63, 814–821. doi: 10.1097/00006842-200109000-00015

Altura, B. M., and Altura, B. T. (1984). Actions of vasopressin, oxytocin, and synthetic analogs on vascular smooth muscle. *Fed. Proc.* 43, 80–86.

Amaya, F., Tanaka, M., Hayashi, S., Tanaka, Y., and Ibata, Y. (2001). Hypothalamo–pituitary–adrenal axis sensitization after chronic salt loading. *Neuroendocrinology* 73, 185–193. doi: 10.1159/000054635

Armstrong, W. E., Warach, S., Hatton, G. I., and McNeill, T. H. (1980). Subnuclei in the rat hypothalamic paraventricular nucleus: a cytoarchitectural, horseradish peroxidase and immunocytochemical analysis. *Neuroscience* 5, 1931–1958. doi: 10.1016/0306-4522(80)90040-8

Badoer, E. (1996). Cardiovascular role of parvocellular neurons in the paraventricular nucleus of the hypothalamus. *Physiology* 11, 43–47. doi: 10.1152/physiologyonline.1996.11.1.43

Badoer, E. (2001). Proceedings of the Australian physiological and pharmacological society symposium: the hypothalamus, hypothalamic paraventricular nucleus

and cardiovascular regulation. *Clin. Exp. Pharmacol. Physiol.* 28, 95–99. doi: 10.1046/j.1440-1681.2001.03413.x

Badoer, E., Ng, C.-W., and De Matteo, R. (2002). Tonic sympathoinhibition arising from the hypothalamic PVN in the conscious rabbit. *Brain Res.* 947, 17–24. doi: 10.1016/S0006-8993(02)02901-3

Bains, J. S., and Ferguson, A. V. (1995). Paraventricular nucleus neurons projecting to the spinal cord receive excitatory input from the subfornical organ. *Am. J. Phys.* 268, R625–R633.

Bains, J. S., Potyok, A., and Ferguson, A. V. (1992). Angiotensin II actions in paraventricular nucleus: functional evidence for neurotransmitter role in efferents originating in subfornical organ. *Brain Res.* 599, 223–229. doi: 10.1016/0006-8993(92)90395-P

Bankir, L. (2001). Antidiuretic action of vasopressin: quantitative aspects and interaction between V1a and V2 receptor–mediated effects. *Cardiovasc. Res.* 51, 372–390. doi: 10.1016/S0008-6363(01)00328-5

Barberis, C., Mouillac, B., and Durroux, T. (1998). Structural bases of vasopressin/oxytocin receptor function. *J. Endocrinol.* 156, 223–229. doi: 10.1677/joe.0.1560223

Barman, S. M., and Gebber, G. L. (2000). "Rapid" rhythmic discharges of sympathetic nerves: sources, mechanisms of generation, and physiological relevance. *J. Biol. Rhythm.* 15, 365–379. doi: 10.1177/074873000129001468

Benarroch, E. E. (2005). Paraventricular nucleus, stress response, and cardiovascular disease. *Clin. Auton. Res.* 15, 254–263. doi: 10.1007/s10286-005-0290-7

Bernatova, I., Rigatto, K. V., Key, M. P., and Morris, M. (2004). Stress-induced pressor and corticosterone responses in oxytocin-deficient mice. *Exp. Physiol.* 89, 549–557. doi: 10.1113/expphysiol.2004.027714

Bisset, G. W., and Chowdrey, H. S. (1988). Control of release of vasopressin by neuroendocrine reflexes. *Q. J. Exp. Physiol.* 73, 811–872. doi: 10.1113/expphysiol.1988.sp003223

Bohus, B., and de Wied, D. (1998). The vasopressin deficient Brattleboro rats: a natural knockout model used in the search for CNS effects of vasopressin. *Prog. Brain Res.* 119, 555–573. doi: 10.1016/s0079-6123(08)61593-9

Bosch, O. J., Krömer, S. A., Brunton, P. J., and Neumann, I. D. (2004). Release of oxytocin in the hypothalamic paraventricular nucleus, but not central amygdala or lateral septum in lactating residents and virgin intruders during maternal defence. *Neuroscience* 124, 439–448. doi: 10.1016/j.neuroscience.2003.11.028

Brickley, S. G., Cull-Candy, S. G., and Farrant, M. (1996). Development of a tonic form of synaptic inhibition in rat cerebellar granule cells resulting from persistent activation of GABAA receptors. *J. Physiol.* 497, 753–759. doi: 10.1113/jphysiol.1996.sp021806

Brinton, R. E., Gee, K. W., Wamsley, J. K., Davis, T. P., and Yamamura, H. I. (1984). Regional distribution of putative vasopressin receptors in rat brain and pituitary by quantitative autoradiography. *Proc. Natl. Acad. Sci. U. S. A.* 81, 7248–7252.

Brizzee, B. L., and Walker, B. R. (1990). Vasopressinergic augmentation of cardiac baroreceptor reflex in conscious rats. *Am. J. Phys.* 258, R860–R868.

Carette, B., and Poulain, P. (1989). Vasopressin-sensitive neurons in the lateral paraventricular nucleus area in a guinea pig slice preparation. *Brain Res. Bull.* 22, 969–974. doi: 10.1016/0361-9230(89)90008-7

Carrive, P., and Gorissen, M. (2008). Premotor sympathetic neurons of conditioned fear in the rat. *Eur. J. Neurosci.* 28, 428–446. doi: 10.1111/j.1460-9568.2008.06351.x

Cato, M. J., and Toney, G. M. (2005). Angiotensin II excites paraventricular nucleus neurons that innervate the rostral ventrolateral medulla: an in vitro patch-clamp study in brain slices. *J. Neurophysiol.* 93, 403–413. doi: 10.1152/jn.01055.2003

Cechetto, D. F., and Saper, C. B. (1988). Neurochemical organization of the hypothalamic projection to the spinal cord in the rat. *J. Comp. Neurol.* 272, 579–604. doi: 10.1002/cne.902720410

Conrad, K. P., Gellai, M., North, W. G., and Valtin, H. (1993). Influence of oxytocin on renal hemodynamics and sodium excretion. *Ann. N. Y. Acad. Sci.* 689, 346–362. doi: 10.1111/j.1749-6632.1993.tb55559.x

Coote, J. H. (2005). A role for the paraventricular nucleus of the hypothalamus in the autonomic control of heart and kidney. *Exp. Physiol.* 90, 169–173. doi: 10.1113/expphysiol.2004.029041

Coote, J. H. (2007). Landmarks in understanding the central nervous control of the cardiovascular system. *Exp. Physiol.* 92, 3–18. doi: 10.1113/expphysiol.2006.035378

Coote, J. H., Yang, Z., Pyner, S., and Deering, J. (1998). Control of sympathetic outflows by the hypothalamic paraventricular nucleus. *Clin. Exp. Pharmacol. Physiol.* 25, 461–463. doi: 10.1111/j.1440-1681.1998.tb02235.x

Cui, L. N., Coderre, E., and Renaud, L. P. (2001). Glutamate and GABA mediate suprachiasmatic nucleus inputs to spinal-projecting paraventricular neurons. *Am. J. Phys. Regul. Integr. Comp. Phys.* 281, R1283–R1289. doi: 10.1152/ajpregu.2001.281.4.R1283

Cunningham, E. T., and Sawchenko, P. E. (1991). Reflex control of magnocellular vasopressin and oxytocin secretion. *Trends Neurosci.* 14, 406–411. doi: 10.1016/0166-2236(91)90032-P

Dale, H. H. (1906). On some physiological actions of ergot. *J. Physiol.* 34, 163–206. doi: 10.1113/jphysiol.1906.sp001148

Dampney, R. A. (1994). Functional organization of central pathways regulating the cardiovascular system. *Physiol. Rev.* 74, 323–364. doi: 10.1152/physrev.1994.74.2.323

Dampney, R. A. L. (2017). Resetting of the baroreflex control of sympathetic vasomotor activity during natural behaviors: description and conceptual model of central mechanisms. *Front. Neurosci.* 11:461.

Dampney, R. A., Michelini, L. C., Li, D.-P., and Pan, H.-L. (2018). Regulation of sympathetic vasomotor activity by the hypothalamic paraventricular nucleus in normotensive and hypertensive states. *Am. J. Physiol. Heart Circ. Physiol.* 315, H1200–H1214. doi: 10.1152/ajpheart.00216.2018

Dayanithi, G., Sabatier, N., and Widmer, H. (2000). Intracellular calcium signalling in magnocellular neurones of the rat supraoptic nucleus: understanding the autoregulatory mechanisms. *Exp. Physiol.* 85, 75S–84S.

De Bree, F. M., Van Der Kleij, A. A. M., Nijenhuis, M., Zalm, R., Murphy, D., and Burbach, J. P. H. (2003). The hormone domain of the vasopressin prohormone is required for the correct prohormone trafficking through the secretory pathway. *J. Neuroendocrinol.* 15, 1156–1163. doi: 10.1111/j.1365-2826.2003.01114.x

de Goeij, D. C. E., Jezova, D., and Tilders, F. J. H. (1992). Repeated stress enhances vasopressin synthesis in corticotropin releasing factor neurons in the paraventricular nucleus. *Brain Res.* 577, 165–168. doi: 10.1016/0006-8993(92)90552-K

Deng, Y., and Kaufman, S. (1995). Effect of pregnancy on activation of central pathways following atrial distension. *Am. J. Phys. Regul. Integr. Comp. Phys.* 269, R552–R556. doi: 10.1152/ajpregu.1995.269.3.R552

Desaulles, E., Reiter, M. K., and Feltz, P. (1995). Electrophysiological evidence for oxytocin receptors on sympathetic preganglionic neurones – an in vitro study on the neonatal rat. *Brain Res.* 699, 139–142. doi: 10.1016/0006-8993(95)01019-R

Dierickx, K. (1980). Immunocytochemical localization of the vertebrate cyclic nonapeptide neurohypophyseal hormones and neurophysins. *Int. Rev. Cytol.* 62, 119–185.

Du Vigneaud, V. (1954). Hormones of the posterior pituitary gland: oxytocin and vasopressin. *Harvey Lect.* 50, 1–26.

Ebner, K., Wotjak, C. T., Landgraf, R., and Engelmann, M. (2005). Neuroendocrine and behavioral response to social confrontation: residents versus intruders, active versus passive coping styles. *Horm. Behav.* 47, 14–21. doi: 10.1016/j.yhbeh.2004.08.002

El-Werfali, W., Toomasian, C., Maliszewska-Scislo, M., Li, C., and Rossi, N. F. (2015). Haemodynamic and renal sympathetic responses to V1b vasopressin receptor activation within the paraventricular nucleus. *Exp. Physiol.* 100, 553–565. doi: 10.1113/expphysiol.2014.084426

Engelmann, M., Ebner, K., Landgraf, R., Holsboer, F., and Wotjak, C. T. (2001). Emotional stress triggers intrahypothalamic but not peripheral release of oxytocin in male rats. *J. Neuroendocrinol.* 11, 867–872. doi: 10.1046/j.1365-2826.1999.00403.x

Farrant, M., and Nusser, Z. (2005). Variations on an inhibitory theme: phasic and tonic activation of GABAA receptors. *Nat. Rev. Neurosci.* 6, 215–229. doi: 10.1038/nrn1625

Fritschy, J.-M., and Mohler, H. (1995). GABAA-receptor heterogeneity in the adult rat brain: differential regional and cellular distribution of seven major subunits. *J. Comp. Neurol.* 359, 154–194. doi: 10.1002/cne.903590111

Gimpl, G., and Fahrenholz, F. (2001). The oxytocin receptor system: structure, function, and regulation. *Physiol. Rev.* 81, 629–683. doi: 10.1152/physrev.2001.81.2.629

Gladwell, S. J., and Coote, J. H. (1999a). Fast excitatory post synaptic potentials and their response to catecholaminergic antagonists in rat sympathetic preganglionic neurones in vitro. *Neurosci. Lett.* 268, 89–92.

Gladwell, S. J., and Coote, J. H. (1999b). Inhibitory and indirect excitatory effects of dopamine on sympathetic preganglionic neurones in the neonatal rat spinal cord in vitro. *Brain Res.* 818, 397–407.

Gladwell, S. J., Pyner, S., Barnes, N. M., and Coote, J. H. (1999). D(1)-like dopamine receptors on retrogradely labelled sympathoadrenal neurones in the thoracic spinal cord of the rat. *Exp. Brain Res.* 128, 377–382. doi: 10.1007/s002210050857

Gordan, R., Gwathmey, J. K., and Xie, L.-H. (2015). Autonomic and endocrine control of cardiovascular function. *World J. Cardiol.* 7, 204–214. doi: 10.4330/wjc.v7.i4.204

Gouzènes, L., Desarménien, M. G., Hussy, N., Richard, P., and Moos, F. C. (1998). Vasopressin regularizes the phasic firing pattern of rat hypothalamic magnocellular vasopressin neurons. *J. Neurosci.* 18, 1879–1885. doi: 10.1523/JNEUROSCI.18-05-01879.1998

Griebel, G., Simiand, J., Serradeil-Le Gal, C., Wagnon, J., Pascal, M., Scatton, B., et al. (2002). Anxiolytic- and antidepressant-like effects of the non-peptide vasopressin V_{1b} receptor antagonist, SSR149415, suggest an innovative approach for the treatment of stress-related disorders. *Proc. Natl. Acad. Sci. U. S. A.* 99, 6370–6375. doi: 10.1073/pnas.092012099

Gupta, P. D., Henry, J. P., Sinclair, R., and Von Baumgarten, R. (1966). Responses of atrial and aortic baroreceptors to nonhypotensive hemorrhage and to tranfusion. *Am. J. Phys.* 211, 1429–1437.

Gutkowska, J., Jankowski, M., Lambert, C., Mukaddam-Daher, S., Zingg, H. H., and McCann, S. M. (1997). Oxytocin releases atrial natriuretic peptide by combining with oxytocin receptors in the heart. *Proc. Natl. Acad. Sci. U.S.A.* 94, 11704–11709.

Gutkowska, J., Jankowski, M., Mukaddam-Daher, S., and McCann, S. M. (2000). Oxytocin is a cardiovascular hormone. *Braz. J. Med. Biol. Res.* 33, 625–633. doi: 10.1590/S0100-879X2000000600003

Hallbeck, M. (2000). Dynorphin mRNA-expressing neurons in the rat paraventricular hypothalamic nucleus project to the spinal cord. *Neurosci. Lett.* 285, 161–164. doi: 10.1016/S0304-3940(00)01093-4

Hallbeck, M., and Blomqvist, A. (1999). Spinal cord-projecting vasopressinergic neurons in the rat paraventricular hypothalamus. *J. Comp. Neurol.* 411, 201–211. doi: 10.1002/(SICI)1096-9861(19990823)411:2<201::AID-CNE3>3.0.CO;2-3

Hallbeck, M., Larhammar, D., and Blomqvist, A. (2001). Neuropeptide expression in rat paraventricular hypothalamic neurons that project to the spinal cord. *J. Comp. Neurol.* 433, 222–238. doi: 10.1002/cne.1137

Haselton, J. R., Goering, J., and Patel, K. P. (1994). Parvocellular neurons of the paraventricular nucleus are involved in the reduction in renal nerve discharge during isotonic volume expansion. *J. Auton. Nerv. Syst.* 50, 1–11. doi: 10.1016/0165-1838(94)9017-1

Hasser, E. M., and Bishop, V. S. (1990). Reflex effect of vasopressin after blockade of V1 receptors in the area postrema. *Circ. Res.* 67, 265–271. doi: 10.1161/01.RES.67.2.265

Hasser, E. M., Bishop, V. S., and Hay, M. (1997). Interactions between vasopressin and baroreflex control of the sympathetic nervous system. *Clin. Exp. Pharmacol. Physiol.* 24, 102–108. doi: 10.1111/j.1440-1681.1997.tb01791.x

Head, R. J. (1991). Hypernoradrenergic innervation and vascular smooth muscle hyperplastic change. *Blood Vessels* 28, 173–178. doi: 10.1159/000158858

Heinrichs, M., Neumann, I., and Ehlert, U. (2002). Lactation and stress: protective effects of breast-feeding in humans. *Stress* 5, 195–203. doi: 10.1080/1025389021000010530

Herman, J. P. -F., Prewitt, C. M., and Cullinan, W. E. (1996). Neuronal circuit regulation of the hypothalamo–pituitary–adrenocortical stress axis. *Crit. Rev. Neurobiol.* 10, 371–394. doi: 10.1615/CritRevNeurobiol.v10.i3-4.50

Hirasawa, A., Hashimoto, K., and Tsujimoto, G. (1994). Distribution and developmental change of vasopressin V1A and V2 receptor mRNA in rats. *Eur. J. Pharmacol. Mol. Pharmacol.* 267, 71–75. doi: 10.1016/0922-4106(94)90226-7

Hirsch, A. T., Dzau, V. J., Majzoub, J. A., and Creager, M. A. (1989). Vasopressin-mediated forearm vasodilation in normal humans. Evidence for a vascular vasopressin V2 receptor. *J. Clin. Invest.* 84, 418–426. doi: 10.1172/JCI114182

Hjemdahl, P. (2002). Stress and the metabolic syndrome: an interesting but enigmatic association. *Circulation* 106, 2634–2636. doi: 10.1161/01.CIR.0000041502.43564.79

Huikuri, H. V., and Stein, P. K. (2013). Heart rate variability in risk stratification of cardiac patients. *Prog. Cardiovasc. Dis.* 56, 153–159. doi: 10.1016/j.pcad.2013.07.003

Hurbin, A., Boissin-Agasse, L., Orcel, H., Rabié, A., Joux, N., Desarménien, M. G., et al. (1998). The V1a and V1b, but not V2, vasopressin receptor genes are expressed in the supraoptic nucleus of the rat hypothalamus, and the transcripts are essentially colocalized in the vasopressinergic magnocellular neurons. *Endocrinology* 139, 4701–4707. doi: 10.1210/endo.139.11.6320

Hurbin, A., Orcel, H., Alonso, G., Moos, F., and Rabié, A. (2002). The vasopressin receptors colocalize with vasopressin in the magnocellular neurons of the rat supraoptic nucleus and are modulated by water balance. *Endocrinology* 143, 456–466. doi: 10.1210/endo.143.2.8643

Imai, Y., Nolan, P. L., and Johnston, C. I. (1983a). Endogenous vasopressin modulates the baroreflex sensitivity in rats. *Clin. Exp. Pharmacol. Physiol.* 10, 289–292. doi: 10.1111/j.1440-1681.1983.tb00199.x

Imai, Y., Nolan, P. L., and Johnston, C. I. (1983b). Restoration of suppressed baroreflex sensitivity in rats with hereditary diabetes insipidus (Brattleboro rats) by arginine-vasopressin and DDAVP. *Circ. Res.* 53, 140–149.

Imbert, M., Chabardes, D., Montegut, M., Clique, A., and Morel, F. (1975). Vasopressin dependent adenylate cyclase in single segments of rabbit kidney tubule. *Pflugers Arch.* 357, 173–186. doi: 10.1007/BF00585973

Inenaga, K., and Yamashita, H. (1986). Excitation of neurones in the rat paraventricular nucleus in vitro by vasopressin and oxytocin. *J. Physiol.* 370, 165–180. doi: 10.1113/jphysiol.1986.sp015928

Jansen, A. S., Nguyen, X. V., Karpitskiy, V., Mettenleiter, T. C., and Loewy, A. D. (1995a). Central command neurons of the sympathetic nervous system: basis of the fight-or-flight response. *Science* 270, 644–646.

Jansen, A. S. P., Wessendorf, M. W., and Loewy, A. D. (1995b). Transneuronal labeling of CNS neuropeptide and monoamine neurons after pseudorabies virus injections into the stellate ganglion. *Brain Res.* 683, 1–24. doi: 10.1016/0006-8993(95)00276-v

Janssen, B. J., Oosting, J., Slaaf, D. W., Persson, P. B., and Struijker-Boudier, H. A. (1995). Hemodynamic basis of oscillations in systemic arterial pressure in conscious rats. *Am. J. Phys.* 269, H62–H71.

Japundzic, N., Grichois, M. L., Zitoun, P., Laude, D., and Elghozi, J. L. (1990). Spectral analysis of blood pressure and heart rate in conscious rats: effects of autonomic blockers. *J. Auton. Nerv. Syst.* 30, 91–100.

Japundzic-Zigon, N. (1998). Physiological mechanisms in regulation of blood pressure fast frequency variations. *Clin. Exp. Hypertens.* 20, 359–388.

Japundzic-Zigon, N. (2001). Effects of nonpeptide V1a and V2 antagonists on blood pressure fast oscillations in conscious rats. *Clin. Exp. Hypertens.* 23, 277–292. doi: 10.1081/CEH-100102667

Japundžić-Žigon, N. (2013). Vasopressin and oxytocin in control of the cardiovascular system. *Curr. Neuropharmacol.* 11, 218–230. doi: 10.2174/1570159X11311020008

Japundzic-Zigon, N. (2013). Vasopressin and oxytocin in control of the cardiovascular system. *Curr. Neuropharmacol.* 11, 218–230. doi: 10.2174/1570159X11311020008

Japundžić-Žigon, N., Lozić, M., Šarenac, O., and Murphy, D. (2020). Vasopressin & oxytocin in control of the cardiovascular system: an updated review. *Curr. Neuropharmacol.* 18, 14–33. doi: 10.2174/1570159X17666190717150501

Japundzić-Zigon, N., Milutinović, S., and Jovanović, A. (2004). Effects of nonpeptide and selective V1 and V2 antagonists on blood pressure short-term variability in spontaneously hypertensive rats. *J. Pharmacol. Sci.* 95, 47–55. doi: 10.1254/jphs.95.47

Japundžić-Žigon, N., Šarenac, O., Lozić, M., Vasić, M., Tasić, T., Bajić, D., et al. (2018). Sudden death: neurogenic causes, prediction and prevention. *Eur. J. Prev. Cardiol.* 25, 29–39. doi: 10.1177/2047487317736827

Jhamandas, J. H., and Renaud, L. P. (1987). Neurophysiology of a central baroreceptor pathway projecting to hypothalamic vasopressin neurons. *Can. J. Neurol. Sci.* 14, 17–24. doi: 10.1017/S0317167100026111

Johnston, C. I. (1985). Vasopressin in circulatory control and hypertension. *J. Hypertens.* 3, 557–569. doi: 10.1097/00004872-198512000-00001

Julien, C., Malpas, S. C., and Stauss, H. M. (2001). Sympathetic modulation of blood pressure variability. *J. Hypertens.* 19, 1707–1712. doi: 10.1097/00004872-200110000-00002

Jung, H. J., and Kwon, T.-H. (2016). Molecular mechanisms regulating aquaporin-2 in kidney collecting duct. *Am. J. Physiol. Ren. Physiol.* 311, F1318–F1328. doi: 10.1152/ajprenal.00485.2016

Kadekaro, M., Summy-Long, J. Y., Freeman, S., Harris, J. S., Terrell, M. L., and Eisenberg, H. M. (1992). Cerebral metabolic responses and vasopressin and oxytocin secretions during progressive water deprivation in rats. *Am. J. Phys.* 262, R310–R317. doi: 10.1152/ajpregu.1992.262.2.R310

Kannan, H., Hayashida, Y., and Yamashita, H. (1989). Increase in sympathetic outflow by paraventricular nucleus stimulation in awake rats. *Am. J. Phys.* 256, R1325–R1330. doi: 10.1152/ajpregu.1989.256.6.R1325

Kato, Y., Igarashi, N., Hirasawa, A., Tsujimoto, G., and Kobayashi, M. (1995). Distribution and developmental changes in vasopressin V2 receptor mRNA in rat brain. *Differentiation* 59, 163–169. doi: 10.1046/j.1432-0436.1995.5930163.x

Katusic, Z. S., Shepherd, J. T., and Vanhoutte, P. M. (1986). Oxytocin causes endothelium-dependent relaxations of canine basilar arteries by activating V1-vasopressinergic receptors. *J. Pharmacol. Exp. Ther.* 236, 166–170

Kawabe, T., Chitravanshi, V. C., Kawabe, K., and Sapru, H. N. (2008). Cardiovascular function of a glutamatergic projection from the hypothalamic paraventricular nucleus to the nucleus tractus solitarius in the rat. *Neuroscience* 153, 605–617. doi: 10.1016/j.neuroscience.2008.02.076

Kawabe, T., Chitravanshi, V. C., Nakamura, T., Kawabe, K., and Sapru, H. N. (2009). Mechanism of heart rate responses elicited by chemical stimulation of the hypothalamic paraventricular nucleus in the rat. *Brain Res.* 1248, 115–126. doi: 10.1016/j.brainres.2008.10.059

Kelly, J. J., Mangos, G., Williamson, P. M., and Whitworth, J. A. (1998). Cortisol and hypertension. *Clin. Exp. Pharmacol. Physiol.* 25, S51–S56. doi: 10.1111/j.1440-1681.1998.tb02301.x

Kendrick, K. M., Da Costa, A. P. C., Broad, K. D., Ohkura, S., Guevara, R., Lévy, F., et al. (1997). Neural control of maternal behaviour and olfactory recognition of offspring. *Brain Res. Bull.* 44, 383–395. doi: 10.1016/S0361-9230(97)00218-9

Knepper, M. A. (1997). Molecular physiology of urinary concentrating mechanism: regulation of aquaporin water channels by vasopressin. *Am. J. Physiol. Renal Physiol.* 272, F3–F12. doi: 10.1152/ajprenal.1997.272.1.F3

Koshimizu, T.-A., Nakamura, K., Egashira, N., Hiroyama, M., Nonoguchi, H., and Tanoue, A. (2012). Vasopressin V1a and V1b receptors: from molecules to physiological systems. *Physiol. Rev.* 92, 1813–1864. doi: 10.1152/physrev.00035.2011

Koshimizu, T.-A., Nasa, Y., Tanoue, A., Oikawa, R., Kawahara, Y., Kiyono, Y., et al. (2006). V1a vasopressin receptors maintain normal blood pressure by regulating circulating blood volume and baroreflex sensitivity. *Proc. Natl. Acad. Sci. U. S. A.* 103, 7807–7812. doi: 10.1073/pnas.0600875103

Landgraf, R., and Neumann, I. D. (2004). Vasopressin and oxytocin release within the brain: a dynamic concept of multiple and variable modes of neuropeptide communication. *Front. Neuroendocrinol.* 25, 150–176. doi: 10.1016/j.yfrne.2004.05.001

Leng, G., Blackburn, R. E., Dyball, R. E., and Russell, J. A. (1989). Role of anterior peri-third ventricular structures in the regulation of supraoptic neuronal activity and neurohypophysical hormone secretion in the rat. *J. Neuroendocrinol.* 1, 35–46. doi: 10.1111/j.1365-2826.1989.tb00074.x

Leng, G., Brown, C. H., Bull, P. M., Brown, D., Scullion, S., Currie, J., et al. (2001). Responses of magnocellular neurons to osmotic stimulation involves coactivation of excitatory and inhibitory input: an experimental and theoretical analysis. *J. Neurosci.* 21, 6967–6977. doi: 10.1523/JNEUROSCI.21-17-06967.2001

Leng, G., Brown, C. H., and Russell, J. A. (1999). Physiological pathways regulating the activity of magnocellular neurosecretory cells. *Prog. Neurobiol.* 57, 625–655. doi: 10.1016/S0301-0082(98)00072-0

Levy, B., Fritz, C., Tahon, E., Jacquot, A., Auchet, T., and Kimmoun, A. (2018). Vasoplegia treatments: the past, the present, and the future. *Crit. Care* 22:52. doi: 10.1186/s13054-018-1967-3

Li, D.-P., Chen, S.-R., and Pan, H.-L. (2002). Nitric oxide inhibits spinally projecting paraventricular neurons through potentiation of presynaptic GABA release. *J. Neurophysiol.* 88, 2664–2674. doi: 10.1152/jn.00540.2002

Li, D.-P., Chen, S.-R., and Pan, H.-L. (2003). Angiotensin II stimulates spinally projecting paraventricular neurons through presynaptic disinhibition. *J. Neurosci.* 23, 5041–5049. doi: 10.1523/JNEUROSCI.23-12-05041.2003

Li, Y. W., and Guyenet, P. G. (1996). Activation of GABAB receptors increases a potassium conductance in rat bulbospinal neurons of the C1 area. *Am. J. Phys. Regul. Integr. Comp. Phys.* 271, R1304–R1310. doi: 10.1152/ajpregu.1996.271.5.R1304

Li, Y.-F., Jackson, K. L., Stern, J. E., Rabeler, B., and Patel, K. P. (2006). Interaction between glutamate and GABA systems in the integration of sympathetic outflow by the paraventricular nucleus of the hypothalamus. *Am. J. Physiol. Heart Circ. Physiol.* 291, H2847–H2856. doi: 10.1152/ajpheart.00625.2005

Liard, J. F. (1984). Vasopressin in cardiovascular control: role of circulating vasopressin. *Clin. Sci.* 67, 473–481. doi: 10.1042/cs0670473

Lipski, J., Kanjhan, R., Kruszewska, B., and Rong, W. (1996). Properties of presympathetic neurones in the rostral ventrolateral medulla in the rat: an intracellular study "in vivo". *J. Physiol.* 490, 729–744. doi: 10.1113/jphysiol.1996.sp021181

Loewy, A. D. (1991). Forebrain nuclei involved in autonomic control. *Prog. Brain Res.* 87, 253–268.

Lovick, T. A., and Coote, J. H. (1988). Effects of volume loading on paraventriculo-spinal neurones in the rat. *J. Auton. Nerv. Syst.* 25, 135–140.

Lovick, T. A., Malpas, S., and Mahony, M. T. (1993). Renal vasodilatation in response to acute volume load is attenuated following lesions of parvocellular neurones in the paraventricular nucleus in rats. *J. Auton. Nerv. Syst.* 43, 247–255.

Lozić, M., Greenwood, M., Šarenac, O., Martin, A., Hindmarch, C., Tasić, T., et al. (2014). Overexpression of oxytocin receptors in the hypothalamic PVN increases baroreceptor reflex sensitivity and buffers BP variability in conscious rats. *Br. J. Pharmacol.* 171, 4385–4398. doi: 10.1111/bph.12776

Lozić, M., Tasić, T., Martin, A., Greenwood, M., Šarenac, O., Hindmarch, C., et al. (2016). Over-expression of V1A receptors in PVN modulates autonomic cardiovascular control. *Pharmacol. Res.* 114, 185–195. doi: 10.1016/j.phrs.2016.10.024

Ludwig, M., Callahan, M. F., and Morris, M. (1995). Effects of tetrodotoxin on osmotically stimulated central and peripheral vasopressin and oxytocin release. *Neuroendocrinology* 62, 619–627.

Ludwig, M., Sabatier, N., Bull, P. M., Landgraf, R., Dayanithi, G., and Leng, G. (2002). Intracellular calcium stores regulate activity-dependent neuropeptide release from dendrites. *Nature* 418, 85–89. doi: 10.1038/nature00822

Ludwig, M., and Stern, J. (2015). Multiple signalling modalities mediated by dendritic exocytosis of oxytocin and vasopressin. *Philos. Trans. R. Soc. Lond. Ser. B Biol. Sci.* 370. doi: 10.1098/rstb.2014.0182

Macdonald, R. L., and Olsen, R. W. (1994). GABAA receptor channels. *Annu. Rev. Neurosci.* 17, 569–602. doi: 10.1146/annurev.ne.17.030194.003033

Maier, T., Dai, W. J., Csikós, T., Jirikowski, G. F., Unger, T., and Culman, J. (1998). Oxytocin pathways mediate the cardiovascular and behavioral responses to substance P in the rat brain. *Hypertension* 31, 480–486. doi: 10.1161/01.HYP.31.1.480

Malpas, S. C. (1998). The rhythmicity of sympathetic nerve activity. *Prog. Neurobiol.* 56, 65–96. doi: 10.1016/S0301-0082(98)00030-6

Malpas, S. C., and Coote, J. H. (1994). Role of vasopressin in sympathetic response to paraventricular nucleus stimulation in anesthetized rats. *Am. J. Phys.* 266, R228–R236. doi: 10.1152/ajpregu.1994.266.1.R228

Malpas, S. C., and Ninomiya, I. (1992). Effect of asphyxia on the frequency and amplitude modulation of synchronized renal nerve activity in the cat. *J. Auton. Nerv. Syst.* 40, 199–205.

Mancia, G., Frattola, G., Parati, C., , Santuccin, C., and Ulian, L. (1994). Blood pressure variability and organ damage. *J. Cardiovasc. Pharmacol.* 24, S6–S11.

Mancia, G., and Grassi, G. (2000). Mechanisms and Clinical Implications of Blood Pressure Variability. *J. Cardiovasc. Pharmacol.* 21, S15–S19. doi: 10.1097/00005344-200000004-00003

Mancia, G., and Parati, G. (2003). The role of blood pressure variability in end-organ damage. *J. Hypertens.* 21, S17–S23. doi: 10.1097/00004872-200307006-00004

Martin, D. S., and Haywood, J. R. (1993). Hemodynamic responses to paraventricular nucleus disinhibition with bicuculline in conscious rats. *Am. J. Phys.* 265, H1727–H1733. doi: 10.1152/ajpheart.1993.265.5.H1727

Martin, D. S., Segura, T., and Haywood, J. R. (1991). Cardiovascular responses to bicuculline in the paraventricular nucleus of the rat. *Hypertension* 18, 48–55. doi: 10.1161/01.HYP.18.1.48

McKinley, M. J., Mathai, M. L., McAllen, R. M., McClear, R. C., Miselis, R. R., Pennington, G. L., et al. (2004). Vasopressin secretion: osmotic and hormonal regulation by the lamina terminalis. *J. Neuroendocrinol.* 16, 340–347. doi: 10.1111/j.0953-8194.2004.01184.x

Messerli, F. H., Hofstetter, L., Rimoldi, S. F., Rexhaj, E., Bangalore, S. (2019). Risk factor variability and cardiovascular outcome: JACC review topic of the week. *J. Am. Coll. Cardiol.* 73, 2596–2603. doi: 10.1016/j.jacc.2019.02.063

Miller, M. E., Davidge, S. T., and Mitchell, B. F. (2002). Oxytocin does not directly affect vascular tone in vessels from nonpregnant and pregnant rats. *Am. J. Phys. Heart Circ. Phys.* 282, H1223–H1228. doi: 10.1152/ajpheart.00774.2001

Milutinović, S., Murphy, D., and Japundžić-Žigon, N. (2006a). Central cholinergic modulation of blood pressure short-term variability. *Neuropharmacology* 50, 874–883. doi: 10.1016/j.neuropharm.2005.12.009

Milutinović, S., Murphy, D., and Japundžić-Žigon, N. (2006b). The role of central vasopressin receptors in the modulation of autonomic cardiovascular controls: a spectral analysis study. *Am. J. Phys. Regul. Integr. Comp. Phys.* 291, R1579–R1591. doi: 10.1152/ajpregu.00764.2005

Milutinović-Smiljanić, S., Šarenac, O., Lozić-Djurić, M., Murphy, D., and Japundžić-Žigon, N. (2013). Evidence for involvement of central vasopressin V1b and V2 receptors in stress-induced baroreflex desensitization. *Br. J. Pharmacol.* 169, 900–908. doi: 10.1111/bph.12161

Moos, F., Gouzènes, L., Brown, D., Dayanithi, G., Sabatier, N., Boissin, L., et al. (1998). New aspects of firing pattern autocontrol in oxytocin and vasopressin neurones. *Adv. Exp. Med. Biol.* 449, 153–162.

Moos, F., Poulain, D. A., Rodriguez, F., Guerne, Y., Vincent, J.-D., and Richard, P. (1989). Release of oxytocin within the supraoptic nucleus during the milk ejection reflex in rats. *Exp. Brain Res.* 76, 593–602. doi: 10.1007/BF00248916

Myers, B., McKlveen, J. M., and Herman, J. P. (2012). Neural regulation of the stress response: the many faces of feedback. *Cell. Mol. Neurobiol.* doi: 10.1007/s10571-012-9801-y

Neumann, I. D. (2002). Involvement of the brain oxytocin system in stress coping: interactions with the hypothalamo–pituitary–adrenal axis. *Prog. Brain Res.* 139, 147–162. doi: 10.1016/s0079-6123(02)39014-9

Neumann, I., Ludwig, M., Engelmann, M., Pittman, Q. J., and Landgraf, R. (1993a). Simultaneous microdialysis in blood and brain: oxytocin and vasopressin release in response to central and peripheral osmotic stimulation and suckling in the rat. *Neuroendocrinology* 58, 637–645.

Neumann, I., Russell, J. A., and Landgraf, R. (1993b). Oxytocin and vasopressin release within the supraoptic and paraventricular nuclei of pregnant, parturient and lactating rats: a microdialysis study. *Neuroscience* 53, 65–75.

Neumann, I. D., Torner, L., and Wigger, A. (2000). Brain oxytocin: differential inhibition of neuroendocrine stress responses and anxiety-related behaviour in virgin, pregnant and lactating rats. *Neuroscience* 95, 567–575. doi: 10.1016/s0306-4522(99)00433-9

Ninomiya, I., Akiyama, T., and Nishiura, N. (1990). Mechanism of cardiac-related synchronized cardiac sympathetic nerve activity in awake cats. *Am. J. Physiol.* 259, R499–R506.

Nishioka, T., Anselmo-Franci, J. A., Li, P., Callahan, M. F., and Morris, M. (1998). Stress increases oxytocin release within the hypothalamic paraventricular nucleus. *Brain Res.* 781, 57–61. doi: 10.1016/S0006-8993(97)01159-1

Nunn, N., Womack, M., Dart, C., and Barrett-Jolley, R. (2011). Function and pharmacology of spinally-projecting sympathetic pre-autonomic neurones in the paraventricular nucleus of the hypothalamus. *Curr. Neuropharmacol.* 9, 262–277. doi: 10.2174/157015911795596531

Oldfield, B. J., Davern, P. J., Giles, M. E., Allen, A. M., Badoer, E., and McKinley, M. J. (2001). Efferent neural projections of angiotensin receptor (AT1) expressing neurones in the hypothalamic paraventricular nucleus of the rat. *J. Neuroendocrinol.* 13, 139–146. doi: 10.1046/j.1365-2826.2001.00597.x

Ostrowski, N. L., Lolait, S. J., Bradley, D. J., O'Carroll, A. M., Brownstein, M. J., and Young, W. S. (1992). Distribution of V1a and V2 vasopressin receptor messenger ribonucleic acids in rat liver, kidney, pituitary and brain. *Endocrinology* 131, 533–535. doi: 10.1210/endo.131.1.1535312

Ostrowski, N. L., Lolait, S. J., and Young, W. S. (1994). Cellular localization of vasopressin V1a receptor messenger ribonucleic acid in adult male rat brain, pineal, and brain vasculature. *Endocrinology* 135, 1511–1528. doi: 10.1210/endo.135.4.7925112

Ostrowski, N. L., Young, W. S., Knepper, M. A., and Lolait, S. J. (1993). Expression of vasopressin V1a and V2 receptor messenger ribonucleic acid in the liver and kidney of embryonic, developing, and adult rats. *Endocrinology* 133, 1849–1859. doi: 10.1210/endo.133.4.8404628

Ota, M., Crofton, J. T., and Share, L. (1994). Hemorrhage-induced vasopressin release in the paraventricular nucleus measured by in vivo microdialysis. *Brain Res.* 658, 49–54. doi: 10.1016/S0006-8993(09)90009-9

Ott, I., and Scott, J. C. (1910). The action of infundibulin upon the mammary secretion. *Exp. Biol. Med.* 8, 48–49. doi: 10.3181/00379727-8-27

Parati, G., Torlasco, C., Pengo, M., Bilo, G., and Ochoa, J. E. (2020). Blood pressure variability: its relevance for cardiovascular homeostasis and cardiovascular diseases. *Hypertens. Res.* 43, 609–620. doi: 10.1038/s41440-020-0421-5

Park, J. B., Jo, J. Y., Zheng, H., Patel, K. P., and Stern, J. E. (2009). Regulation of tonic GABA inhibitory function, presympathetic neuronal activity and sympathetic outflow from the paraventricular nucleus by astroglial GABA transporters. *J. Physiol.* 587, 4645–4660. doi: 10.1113/jphysiol.2009.173435

Petersson, M., Alster, P., Lundeberg, T., and Uvnäs-Moberg, K. (1996). Oxytocin causes a long-term decrease of blood pressure in female and male rats. *Physiol. Behav.* 60, 1311–1315. doi: 10.1016/S0031-9384(96)00261-2

Petersson, M., Lundeberg, T., and Uvnäs-Moberg, K. (1997). Oxytocin decreases blood pressure in male but not in female spontaneously hypertensive rats. *J. Auton. Nerv. Syst.* 66, 15–18. doi: 10.1016/s0165-1838(97)00040-4

Pittman, Q. J., Riphagen, C. L., and Lederis, K. (1984). Release of immunoassayable neurohypophyseal peptides from rat spinal cord, in vivo. *Brain Res.* 300, 321–326. doi: 10.1016/0006-8993(84)90842-4

Portillo, F., Carrasco, M., and Vallo, J. J. (1998). Separate populations of neurons within the paraventricular hypothalamic nucleus of the rat project to vagal and thoracic autonomic preganglionic levels and express c-Fos protein induced by lithium chloride. *J. Chem. Neuroanat.* 14, 95–102. doi: 10.1016/S0891-0618(97)10022-9

Pow, D. V., and Morris, J. F. (1989). Dendrites of hypothalamic magnocellular neurons release neurohypophysial peptides by exocytosis. *Neuroscience* 32, 435–439. doi: 10.1016/0306-4522(89)90091-2

Pyner, S. (2009). Neurochemistry of the paraventricular nucleus of the hypothalamus: implications for cardiovascular regulation. *J. Chem. Neuroanat.* 38, 197–208. doi: 10.1016/j.jchemneu.2009.03.005

Pyner, S., and Coote, J. H. (2000). Identification of branching paraventricular neurons of the hypothalamus that project to the rostroventrolateral medulla and spinal cord. *Neuroscience* 100, 549–556. doi: 10.1016/S0306-4522(00)00283-9

Rasmussen, M. S., Simonsen, J. A., Sandgaard, N. C. F., Høilund-Carlsen, P. F., and Bie, P. (2004). Effects of oxytocin in normal man during low and high sodium diets. *Acta Physiol. Scand.* 181, 247–257. doi: 10.1111/j.1365-201X.2004.01286.x

Ribeiro, N., Panizza, H., do, N., Santos, K. M. D., Ferreira-Neto, H. C., and Antunes, V. R. (2015). Salt-induced sympathoexcitation involves vasopressin V1a receptor activation in the paraventricular nucleus of the hypothalamus. *Am. J. Phys. Regul. Integr. Comp. Phys.* 309, R1369–R1379. doi: 10.1152/ajpregu.00312.2015

Riphagen, C. L., and Pittman, Q. J. (1989). Mechanisms underlying the cardiovascular responses to intrathecal vasopressin administration in rats. *Can. J. Physiol. Pharmacol.* 67, 269–275. doi: 10.1139/y89-044

Rivier, C., and Vale, W. (1983). Interaction of corticotropin-releasing factor and arginine vasopressin on adrenocorticotropin secretionin vivo. *Endocrinology* 113, 939–942. doi: 10.1210/endo-113-3-939

Roper, J. A., O'Carroll, A.-M., Young, W. S., and Lolait, S. J. (2011). The vasopressin Avpr1b receptor: Molecular and pharmacological studies. *Stress* 14, 98–115. doi: 10.3109/10253890.2010.512376

Rosmond, R. (2005). Role of stress in the pathogenesis of the metabolic syndrome. *Psychoneuroendocrinology* 30, 1–10. doi: 10.1016/j.psyneuen.2004.05.007

Russ, R. D., Resta, T. C., and Walker, B. R. (1992). Pulmonary vasodilatory response to neurohypophyseal peptides in the rat. *J. Appl. Physiol.* 73, 473–478. doi: 10.1152/jappl.1992.73.2.473

Russ, R. D., and Walker, B. R. (1992). Role of nitric oxide in vasopressinergic pulmonary vasodilatation. *Am. J. Phys.* 262, H743–H747. doi: 10.1152/ajpheart.1992.262.3.H743

Russell, J. A., and Brunton, P. J. (2017). Oxytocin: control of secretion by the brain and central roles. *Ref. Mod. Neurosci. Biobehav. Psychol.* doi: 10.1016/b978-0-12-809324-5.02246-x

Sampey, D. B., Burrell, L. M., and Widdop, R. E. (1999). Vasopressin V2 receptor enhances gain of baroreflex in conscious spontaneously hypertensive rats. *Am. J. Phys. Regul. Integr. Comp. Phys.* 276, R872–R879. doi: 10.1152/ajpregu.1999.276.3.R872

Savić, B., Martin, A., Mecawi, A. S., Bukumirić, Z., Antunes-Rodrigues, J., Murphy, D., et al. (2020). Vasopressin and v1br gene expression is increased in the hypothalamic PVN of borderline hypertensive rats. *Hypertens. Res.* 43, 1165–1174. doi: 10.1038/s41440-020-0469-2

Sawchenko, P. E., Brown, E. R., Chan, R. K., Ericsson, A., Li, H. Y., Roland, B. L., et al. (1996). The paraventricular nucleus of the hypothalamus and the functional neuroanatomy of visceromotor responses to stress. *Prog. Brain Res.* 107, 201–222.

Sawchenko, P. E., and Swanson, L. W. (1982a). Immunohistochemical identification of neurons in the paraventricular nucleus of the hypothalamus that project

to the medulla or to the spinal cord in the rat. *J. Comp. Neurol.* 205, 260–272. doi: 10.1002/cne.902050306

Sawchenko, P. E., and Swanson, L. W. (1982b). The organization of noradrenergic pathways from the brainstem to the paraventricular and supraoptic nuclei in the rat. *Brain Res. Rev.* 4, 275–325. doi: 10.1016/0165-0173(82)90010-8

Scala-Guenot, D. D., Di Scala-Guenot, D., Strosser, M. T., and Richard, P. (1987). Electrical stimulations of perifused magnocellular nuclei in vitro elicit Ca2 -dependent, tetrodotoxin-insensitive release of oxytocin and vasopressin. *Neurosci. Lett.* 76, 209–214. doi: 10.1016/0304-3940(87)90717-8

Sermasi, E., and Coote, J. H. (1994). Oxytocin acts at V1 receptors to excite sympathetic preganglionic neurones in neonate rat spinal cord in vitro. *Brain Res.* 647, 323–332. doi: 10.1016/0006-8993(94)91331-5

Sermasi, E., Howl, J., Wheatley, M., and Coote, J. H. (1998). Localisation of arginine vasopressin V 1a receptors on sympatho-adrenal preganglionic neurones. *Exp. Brain Res.* 119, 85–91. doi: 10.1007/s002210050322

Sladek, C. D., Michelini, L. C., Stachenfeld, N. S., Stern, J. E., and Urban, J. H. (2015). Endocrine-autonomic linkages. *Compr. Physiol.* 5, 1281–1323. doi: 10.1002/cphy.c140028

Son, S. J., Filosa, J. A., Potapenko, E. S., Biancardi, V. C., Zheng, H., Patel, K. P., et al. (2013). Dendritic peptide release mediates interpopulation crosstalk between neurosecretory and preautonomic networks. *Neuron* 78, 1036–1049. doi: 10.1016/j.neuron.2013.04.025

Stauss, H. M., and Kregel, K. C. (1996). Frequency response characteristic of sympathetic-mediated vasomotor waves in conscious rats. *Am. J. Phys.* 271, H1416–H1422. doi: 10.1152/ajpheart.1996.271.4.H1416

Stauss, H. M., Persson, P. B., Johnson, A. K., and Kregel, K. C. (1997). Frequency-response characteristics of autonomic nervous system function in conscious rats. *Am. J. Phys.* 273, H786–H795.

Stern, J. E. (2001). Electrophysiological and morphological properties of pre-autonomic neurones in the rat hypothalamic paraventricular nucleus. *J. Physiol.* 537, 161–177. doi: 10.1111/j.1469-7793.2001.0161k.x

Stojicić, S., Milutinović, S., Sarenac, O., Zivković, S., and Japundzić-Zigon, N. (2006). Central vasopressin V^{1a} and V^{1b} receptors modulate the cardiovascular response to air-jet stress in conscious rats. *Biomed. Tech.* 51, 268–271. doi: 10.1515/BMT.2006.053

Stojicić, S., Milutinović-Smiljanić, S., Sarenac, O., Milosavljević, S., Paton, J. F. R., Murphy, D., et al. (2008). Blockade of central vasopressin receptors reduces the cardiovascular response to acute stress in freely moving rats. *Neuropharmacology* 54, 824–836. doi: 10.1016/j.neuropharm.2007.12.013

Stoop, R. (2014). Neuromodulation by oxytocin and vasopressin in the central nervous system as a basis for their rapid behavioral effects. *Curr. Opin. Neurobiol.* 29, 187–193. doi: 10.1016/j.conb.2014.09.012

Strack, A. M., Sawyer, W. B., Hughes, J. H., Platt, K. B., and Loewy, A. D. (1989a). A general pattern of CNS innervation of the sympathetic outflow demonstrated by transneuronal pseudorabies viral infections. *Brain Res.* 491, 156–162. doi: 10.1016/0006-8993(89)90098-x

Strack, A. M., Sawyer, W. B., Platt, K. B., and Loewy, A. D. (1989b). CNS cell groups regulating the sympathetic outflow to adrenal gland as revealed by transneuronal cell body labelling with pseudorabies virus. *Brain Res.* 491, 274–296. doi: 10.1016/0006-8993(89)90063-2

Swanson, L. W. (1995). Mapping the human brain: past, present, and future. *Trends Neurosci.* 18, 471–474. doi: 10.1016/0166-2236(95)92766-J

Swanson, L. W., and Kuypers, H. G. (1980). The paraventricular nucleus of the hypothalamus: cytoarchitectonic subdivisions and organization of projections to the pituitary, dorsal vagal complex, and spinal cord as demonstrated by retrograde fluorescence double-labeling methods. *J. Comp. Neurol.* 194, 555–570. doi: 10.1002/cne.901940306

Swanson, L. W., and Sawchenko, P. E. (1980). Paraventricular nucleus: a site for the integration of neuroendocrine and autonomic mechanisms. *Neuroendocrinology* 31, 410–417. doi: 10.1159/000123111

Swanson, L. W., and Sawchenko, P. E. (1983). Hypothalamic integration: organization of the paraventricular and supraoptic nuclei. *Annu. Rev. Neurosci.* 6, 269–324. doi: 10.1146/annurev.ne.06.030183.001413

Swanson, L. W., Sawchenko, P. E., Rivier, J., and Vale, W. W. (1983). Organization of ovine corticotropin-releasing factor immunoreactive cells and fibers in the rat brain: an immunohistochemical study. *Neuroendocrinology* 36, 165–186. doi: 10.1159/000123454

Thibonnier, M., Coles, P., Thibonnier, A., and Shoham, M. (2002). Molecular pharmacology and modeling of vasopressin receptors. *Prog. Brain Res.* 139, 179–196. doi: 10.1016/s0079-6123(02)39016-2

Thibonnier, M., Conarty, D. M., Preston, J. A., Plesnicher, C. L., Dweik, R. A., and Erzurum, S. C. (1999). Human vascular endothelial cells express oxytocin receptors. *Endocrinology* 140, 1301–1309. doi: 10.1210/endo.140.3.6546

Unger, T., Rohmeiss, P., Demmert, G., Ganten, D., Lang, R. E., and Luft, F. C. (1986). Differential modulation of the baroreceptor reflex by brain and plasma vasopressin Hypertension. 140, 1301–1309. doi: 10.1161/01.hyp.8.6_pt_2.ii157

Vågnes, O., Feng, J. J., Iversen, B. M., and Arendshorst, W. J. (2000). Upregulation of V(1) receptors in renal resistance vessels of rats developing genetic hypertension. *Am. J. Physiol. Ren. Physiol.* 278, F940–F948. doi: 10.1152/ajprenal.2000.278.6.F940

Valtin, H. (1982). The discovery of the Brattleboro rat, recommended nomenclature, and the question of proper controls. *Ann. N. Y. Acad. Sci.* 394, 1–9. doi: 10.1111/j.1749-6632.1982.tb37405.x

VanBavel, E., Giezeman, M. J., Mooij, T., and Spaan, J. A. (1991). Influence of pressure alterations on tone and vasomotion of isolated mesenteric small arteries of the rat. *J. Physiol.* 436, 371–383. doi: 10.1113/jphysiol.1991.sp018555

Verbalis, J. G., Mangione, M. P., and Stricker, E. M. (1991). Oxytocin produces natriuresis in rats at physiological plasma concentrations. *Endocrinology* 128, 1317–1322. doi: 10.1210/endo-128-3-1317

Wang, L. A., Nguyen, D. H., and Mifflin, S. W. (2019). Corticotropin-releasing hormone projections from the paraventricular nucleus of the hypothalamus to the nucleus of the solitary tract increase blood pressure. *J. Neurophysiol.* 121, 602–608. doi: 10.1152/jn.00623.2018

Watkins, N. D., Cork, S. C., and Pyner, S. (2009). An immunohistochemical investigation of the relationship between neuronal nitric oxide synthase, GABA and presympathetic paraventricular neurons in the hypothalamus. *Neuroscience* 159, 1079–1088. doi: 10.1016/j.neuroscience.2009.01.012

Whitnall, M. H., Mezey, Ë., and Gainer, H. (1985). Co-localization of corticotropin-releasing factor and vasopressin in median eminence neurosecretory vesicles. *Nature* 317, 248–250. doi: 10.1038/317248a0

Wilson, J. L. L., Miranda, C. A., and Knepper, M. A. (2013). Vasopressin and the regulation of aquaporin-2. *Clin. Exp. Nephrol.* 17, 751–764. doi: 10.1007/s10157-013-0789-5

Wotjak, C. T., Kubota, M., Liebsch, G., Montkowski, A., Holsboer, F., Neumann, I., et al. (1996). Release of vasopressin within the rat paraventricular nucleus in response to emotional stress: a novel mechanism of regulating adrenocorticotropic hormone secretion? *J. Neurosci.* 16, 7725–7732. doi: 10.1523/JNEUROSCI.16-23-07725.1996

Wotjak, C. T., Ludwig, M., Ebner, K., Russell, J. A., Singewald, N., Landgraf, R., et al. (2002). Vasopressin from hypothalamic magnocellular neurons has opposite actions at the adenohypophysis and in the supraoptic nucleus on ACTH secretion. *Eur. J. Neurosci.* 16, 477–485. doi: 10.1046/j.1460-9568.2002.02101.x

Xi, D., Kusano, K., and Gainer, H. (1999). Quantitative analysis of oxytocin and vasopressin messenger ribonucleic acids in single magnocellular neurons isolated from supraoptic nucleus of rat hypothalamus. *Endocrinology* 140, 4677–4682. doi: 10.1210/endo.140.10.7054

Yang, Z., and Coote, J. H. (1998). Influence of the hypothalamic paraventricular nucleus on cardiovascular neurones in the rostral ventrolateral medulla of the rat. *J. Physiol.* 513, 521–530.

Yang, Z., Han, D., and Coote, J. H. (2009). Cardiac sympatho-excitatory action of PVN-spinal oxytocin neurones. *Auton. Neurosci.* 147, 80–85. doi: 10.1016/j.autneu.2009.01.013

Yang, Z., Wheatley, M., and Coote, J. H. (2002). Neuropeptides, amines and amino acids as mediators of the sympathetic effects of paraventricular nucleus activation in the rat. *Exp. Physiol.* 87, 663–674. doi: 10.1113/eph8702439

Young, W. S., Li, J., Wersinger, S. R., and Palkovits, M. (2006). The vasopressin 1b receptor is prominent in the hippocampal area CA2 where it is unaffected by restraint stress or adrenalectomy. *Neuroscience* 143, 1031–1039. doi: 10.1016/j.neuroscience.2006.08.040

Conflict of Interest: The authors declare that the research was conducted in the absence of any commercial or financial relationships that could be construed as a potential conflict of interest.

Publisher's Note: All claims expressed in this article are solely those of the authors and do not necessarily represent those of their affiliated organizations, or those of the publisher, the editors and the reviewers. Any product that may

be evaluated in this article, or claim that may be made by its manufacturer, is not guaranteed or endorsed by the publisher.

Copyright © 2022 Savić, Murphy and Japundžić-Žigon. This is an open-access article distributed under the terms of the Creative Commons Attribution License (CC BY). The use, distribution or reproduction in other forums is permitted, provided the original author(s) and the copyright owner(s) are credited and that the original publication in this journal is cited, in accordance with accepted academic practice. No use, distribution or reproduction is permitted which does not comply with these terms.

frontiers in Physiology

ORIGINAL RESEARCH
published: 24 March 2022
doi: 10.3389/fphys.2022.841078

A Novel Organ-Specific Approach to Selectively Target Sensory Afferents Innervating the Aortic Arch

Khalid Elsaafien[1,2], Scott W. Harden[1,2], Dominique N. Johnson[3], Aecha K. Kimball[3], Wanhui Sheng[1,2], Justin A. Smith[1], Karen A. Scott[1,2], Charles J. Frazier[1,2], Annette D. de Kloet[2,3,4] and Eric G. Krause[1,2,4]**

[1] Department of Pharmacodynamics, College of Pharmacy, University of Florida, Gainesville, FL, United States, [2] Center for Integrative Cardiovascular and Metabolic Diseases, University of Florida, Gainesville, FL, United States, [3] Department of Physiology and Functional Genomics, College of Medicine, University of Florida, Gainesville, FL, United States, [4] Evelyn F. and William L. McKnight Brain Institute, University of Florida, Gainesville, FL, United States

The brain maintains cardiovascular homeostasis, in part, *via* the arterial baroreflex which senses changes in blood pressure (BP) at the level of the aortic arch. Sensory afferents innervating the aortic arch employ baroreceptors to convert stretch exerted on the arterial wall into action potentials carried by the vagus nerve to second order neurons residing within the nucleus of the solitary tract (NTS). Although the baroreflex was described more than 80 years ago, the specific molecular, structural, and functional phenotype of the baroreceptors remain uncharacterized. This is due to the lack of tools that provide the genetic and target organ specificity that is required to selectively characterize baroreceptor afferents. Here, we use a novel approach to selectively target baroreceptors. Male mice on a C57BL/6J background were anesthetized with isoflurane, intubated, and artificially ventilated. Following sternotomy, the aortic arch was exposed, and a retrograde adeno-associated virus was applied to the aortic arch to direct the expression of channelrhoropsin-2 (ChR2) and/or tdTomato (tdTom) to sensory afferents presumably functioning as baroreceptors. Consistent with the structural characteristics of arterial baroreceptors, robust tdTom expression was observed in nerve endings surrounding the aortic arch, within the fibers of the aortic depressor and vagus nerves, cell bodies of the nodose ganglia (NDG), and neural projections to the caudal NTS (cNTS). Additionally, the tdTom labeled cell bodies within the NDG also expressed mRNAs coding for the mechanically gated ion channels, PIEZO-1 and PIEZO-2. *In vitro* electrophysiology revealed that pulses of blue light evoked excitatory post-synaptic currents in a subset of neurons within the cNTS, suggesting a functional connection between the labeled aortic arch sensory afferents and second order neurons. Finally, the *in vivo* optogenetic stimulation of the cell bodies of the baroreceptor expressing afferents in the NDG produced robust depressor responses. Together, these results establish a novel approach for selectively targeting sensory neurons innervating the aortic arch. This approach may be used to investigate arterial baroreceptors structurally and functionally, and to assess their role in the etiology or reversal of cardiovascular disease.

Keywords: baroreceptors, sensory neurons, aortic arch, baroreflex, nodose ganglia, vagal afferents, blood pressure

OPEN ACCESS

Edited by:
Geoffrey A. Head, Baker Heart and Diabetes Institute, Australia

Reviewed by:
Dongze Zhang, University of Nebraska Medical Center, United States
Eduardo Colombari, Universidade Estadual Paulista, Brazil

****Correspondence:***
Eric G. Krause
ekrause@cop.ufl.edu
Annette D. de Kloet
adekloet@ufl.edu

Specialty section:
This article was submitted to Integrative Physiology, a section of the journal Frontiers in Physiology

Received: *21 December 2021*
Accepted: *16 February 2022*
Published: *24 March 2022*

Citation:
Elsaafien K, Harden SW, Johnson DN, Kimball AK, Sheng W, Smith JA, Scott KA, Frazier CJ, de Kloet AD and Krause EG (2022) A Novel Organ-Specific Approach to Selectively Target Sensory Afferents Innervating the Aortic Arch. Front. Physiol. 13:841078. doi: 10.3389/fphys.2022.841078

INTRODUCTION

The arterial baroreflex exerts moment-to-moment control and regulation over blood pressure (BP), keeping pressure within arterial walls at optimal levels for survival (Kirchheim, 1976; Brown, 1980; Kumada et al., 1990). Sensory neurons innervating the aortic arch employ baroreceptors that sense stretch in arterial walls and convey these signals to the nucleus of the solitary tract (NTS) in the hindbrain (Benarroch, 2008; Wehrwein and Joyner, 2013). These sensory afferents have their cell bodies in the nodose ganglion of the vagus nerve (NDG) and project to the NTS through the vagus nerve (cranial nerve X), providing moment-to-moment- feedback that controls heart rate (HR) and BP (Benarroch, 2008; Wehrwein and Joyner, 2013). An increase in BP results in mechanostimulation of the aortic arch wall, which activates baroreceptors (Kirchheim, 1976). This activation triggers afferent signals transmitted to the NTS. Subsequently, stimulating a neural reflex (known as the baroreflex) that reduces sympathetic, but increases parasympathetic, outflow to cardiovascular tissues restoring BP and HR to homeostatic levels (Spyer, 1989; Andresen and Kunze, 1994). While the baroreflex is well established, the molecular, structural, and functional phenotype of the sensory neurons that invoke its influence over cardiovascular function have not been completely discerned.

With the recent development of highly selective tools for probing neural circuits; viscero-sensory afferents, and neural reflexes became well characterized through targeted genetic manipulations (Saleeba et al., 2019). However, the vast majority of what's known about baroreceptor expressing afferents arises from studies that utilize pharmacological manipulation and peripheral nerve stimulation (Schmidt, 1968; Sapru et al., 1981; Fan et al., 1996). Only recently, studies began to unravel unique markers expressed by baroreceptor containing afferents that can be utilized to characterize the baroreflex (Zeng et al., 2018; Min et al., 2019). These studies found that sensory neurons innervating the vasculature express the mechanically activated ion channels PIEZO-1 and PIEZO-2. This allowed for the specific genetic manipulation of vagal afferents expressing PIEZOs. Leading to the detailed structural and functional mapping of vagal afferents that express PIEZOs and also receive input from the aortic arch (Zeng et al., 2018; Min et al., 2019). However, vagal afferents are comprised of sensory neurons that receive a variety of input from cardio-pulmonary and gastrointestinal organs (Berthoud and Neuhuber, 2000; Kubin et al., 2006; Bai et al., 2019; Kupari et al., 2019). Furthermore, PIEZOs are not only involved in aortic stretch sensation, but also in airway (Ranade et al., 2014; Woo et al., 2015; Nonomura et al., 2017), and stomach stretch sensation (Alcaino et al., 2017; Min et al., 2021; Oh et al., 2021). Thus, there is a need to develop approaches that target single modality sensory vagal afferents that innervate the aortic arch. Such tools would allow the specific/selective structural and functional characterization of baroreceptor expressing afferents.

In the current study, we sought to develop a novel organ-specific approach to selectively target sensory neurons innervating the aortic arch. Using a retrograde adeno-associated virus (AAVrg) we directed the expression of channelrhodopsin-2 (ChR2) and/or tdTomato (tdTom) within neurons that presumably function as baroreceptors innervating the aortic arch. Our anatomical analysis revealed the successful expression of tdTom selectively in these neurons. Consistent with the established neuroanatomical circuit of the baroreflex, we observed expression of tdTom in nerve endings innervating the aortic arch that projected through the aortic depressor nerve (ADN) to the NDG of vagus nerve. The cell bodies of these sensory afferents that reside in the NDG were found to express PIEZOs, and they send projections that terminate in the NTS. Our *in vitro* electrophysiology confirmed a functional glutamatergic connection between the baroreceptors, targeted by our approach, and neurons of the NTS. Furthermore, *in vivo* optogenetic stimulation of the cell bodies of neurons that express baroreceptors produced depressor responses. Altogether, our results demonstrate that our organ-specific approach to selectively target sensory neurons innervating the aortic arch is anatomically and functionally valid.

MATERIALS AND METHODS

Animals

Studies were conducted in 23 male C57BL/6J mice. Mice were 8–10 weeks old at the initiation of studies. All animals were maintained in temperature and humidity-controlled rooms on 12:12-h light-dark cycles. In all cases, food and water were available *ad libitum*. All procedures were approved by the Institutional Animal Care and Use Committees at the University of Florida and were conducted in accordance with the National Institutes of Health Guide for the Care and Use of Laboratory Animals.

Viral Constructs

Retrograde Adeno-Associated Viral vectors [AAVrg; i.e., AAV-CAG-hChR2-H134R-tdTomato (Cat#: 28017-AAVrg) and pAAV-CAG-tdTomato (codon diversified) (Cat#: 59462-AAVrg)] that allow the expression of tdTomato (tdTom) and/or the light sensitive cation channel, channelrhodopsin-2 (ChR2), were obtained from Addgene, and used at a titer of $\geq 7 \times 10\hat{}12$ vg/mL.

Cardiothoracic Surgery

Animals were anesthetized using isoflurane (3–5% in O_2) and administered analgesics (Bupernex; 0.1 mg kg^{-1} s.c.). Following the induction of anesthesia, animals were intubated and artificially ventilated (Tidal Vol; 0.2 ml, Min Vol; 26 ml min^{-1}, Pressure 21 cmH_2O). A longitudinal midline cervical incision was made from the sternal notch to the mid-chest. Following the retraction of the pre-tracheal muscles, smooth-tipped micro-surgical forceps were inserted behind the sternum and over the trachea to bluntly dissect the pleura away. A bone nipper was then used to perform a midline sternotomy (approximately 3–4 mm). This exposed the aortic arch in the pericardial cavity. Subsequently, a glass micropipette was then filled with the viral constructs. Approximately 1 μl was applied to the aortic arch by "painting" the virus on the vascular wall. Briefly, viral constructs were applied to the vascular wall of the aortic arch where the right

brachiocephalic trunk, left common carotid, and left subclavian artery branch off the aortic arch. Viral constructs were left *in situ* for 5 min to allow for the diffusion of AAVrg into the aortic arch. It is worth noting that the viral constructs were not injected into the aortic arch or systemic circulation, but rather, were discretely painted onto the vascular wall. Finally, the sternum and the skin were sutured with 5–0 absorbable and non-absorbable sutures, respectively. Mice were allowed to recover for 21 days before neuroanatomical, *in vitro* electrophysiological, or *in vivo* cardiovascular studies were performed.

Experimental Protocols

Neuroanatomical Studies

Mice that received an AAVrg to direct the expression of tdTom (n = 4) within the sensory neurons that innervate the aortic arch were anesthetized with pentobarbital (50 mg kg^{-1}, i.p.) and transcardially perfused with RNase-free-isotonic saline followed by 4% paraformaldehyde. The aortic arch and the carotid sinus were collected and stored in RNase-free saline at 4°C for further processing. The left and right nodose ganglia (LNG and RNG, respectively) were dissected and placed in 4% paraformaldehyde for 5 min before they were stored in 20% RNase-free sucrose at 4°C. Brains were extracted and post-fixed for approximately 4 h after which they were stored in 30% RNase-free sucrose at 4°C.

The intact aortic arch, carotid sinus, LNG, and RNG were mounted (whole-mount) onto Fisherbrand Superfrost Plus Gold Microscope Slides (Thermo Fisher Scientific, Waltham, MA, United States). A laser-scanning confocal microscope (Nikon Instruments Inc., Melville, NY, United States) was used to assess viral expression at the aortic arch and the NDG. Tissue from animals with successful expression of the viral constructs were further processed. The LNG and RNG were processed for RNAscope *in situ* hybridization, and the hindbrains were processed for immunohistochemistry.

In vitro Electrophysiology

Slice Preparation

Mice that received an AAVrg to direct the expression of ChR2 and tdTom (n = 7) within baroreceptor expressing neurons were anesthetized with ketamine HCl (0.1 mL of 100 mg mL^{-1}; i.p.). Following decapitation and rapid brain extraction, a Leica VT1000 vibratome was used to obtain 300 μm thick horizontal sections submerged in ice-cold sucrose-laden artificial cerebrospinal fluid (aCSF) containing (in mM): 205 sucrose, 10 dextrose, 1 $MgSO_4$, 2 KCl, 1.25 NaH_2PO_4, 1 $CaCl_2$, and 25 $NaHCO_3$, oxygenated with 95% O_2/5% CO_2. Slices were transferred to an incubation chamber containing low-calcium high-magnesium aCSF (designed to minimize excitotoxicity) containing (in mM): 124 NaCl, 10 dextrose, 3 $MgSO_4$, 2.5 KCl, 1.23 NaH_2PO_4, 1 $CaCl_2$, and 25 $NaHCO_3$, oxygenated with 95% O_2/5% CO_2 and maintained at 35°C. After 30 min the incubation chamber was removed from heat and permitted to passively equilibrate to room temperature for at least 30 min prior to recording. Recordings were performed in aCSF containing (in mM): 126 NaCl, 11 dextrose, 1.5 $MgSO_4$, 3 KCl, 1.2 NaH_2PO_4, 2.4 $CaCl_2$, and 25 $NaHCO_3$, oxygenated with 95% O_2/5% CO_2 and maintained at 28°C flowing through a perfusion chamber (JG-23W/HP, Warner Instruments, Holliston, MA, United States) at a rate of 2 mL min^{-1}. Patch pipettes were prepared from 1.5 mm OD/0.86 mm ID filamented fire-polished borosilicate glass (Sutter Instruments BF150-86-10, Novato, CA, United States) using a Flaming/Brown pipette puller (Sutter Instrument SU-P97, Novato, CA, United States) to achieve a 4–6 MΩ open-tip resistance when filled with a cesium-based internal solution containing (in mM): 115 Cs-gluconate, 10 di-tris phosphocreatine, 10 HEPES, 0.5 EGTA, 2 $MgCl_2$, 4 Na_2ATP, 0.4 Na_3GTP, 5 QX-314 chloride, adjusted to pH 7.25 and 295 mOsm. The liquid junction potential of this pipette solution against aCSF is calculated to be 15.95 mV, and data presented are uncorrected. Cells were visualized with an Olympus BX51WI upright stereomicroscope using IR-DIC optics and a 12-bit CCD camera (QImaging Rolera-XR) and μManager software (Edelstein et al., 2010). Fluorescence illumination (for imaging and optogenetic stimulation) was achieved using a TTL-controlled LED light source (X-Cite 110LED, Excelitas Technologies, Waltham, MA, United States) and standard filter cubes (XF404, XF414, from Omega Optical).

Patch-Clamp Electrophysiology

Electrophysiological recordings were performed using a CV-7B headstage with a MultiClamp 700B amplifier, a DigiData 1440A digital acquisition system, and pClamp 11 software (Axon Instruments/Molecular Devices). Recordings were acquired at 20 kHz and low-pass filtered using a 4-pole Bessel filter with a 2 kHz –3 dB cutoff. Passive membrane properties for each neuron were determined using a voltage-clamp protocol containing a 10 mV hyperpolarizing step (to measure membrane and access resistance) and a pair of 10 mV ramps (to measure whole-cell capacitance) (Golowasch et al., 2009). Optogenetic excitation was achieved using a 20 ms pulse of blue light delivered through the objective lens. Membrane tests (–10 mV hyperpolarizing steps) were repeated in voltage clamp every 10 s during time-course experiments and cells were omitted if access resistance changed by more than 10 MΩ over the course of an experiment. All experiments were performed in the continuous presence of the $GABA_A$ receptor antagonist picrotoxin (PTX, 100 μM). In experiments where light-evoked currents were challenged with glutamate receptor antagonists, the extracellular solution was switched to aCSF containing DNQX (20 μM) to block AMPA and kainate receptors. In cases where light-evoked currents were still visible NMDA receptor antagonist AP5 (40 μM) was also added to the aCSF. To quantify optogenetic excitation, data were low-pass filtered using a Gaussian filter (1 ms halfwidth), light-evoked currents were quantified relative to baseline as the negative peak observed in a 40 ms window following light exposure.

In vivo Cardiovascular Recordings

Mice that received an AAVrg to direct the expression of ChR2 and/or tdTom (n = 6 per group) within baroreceptor expressing afferents were anesthetized with isoflurane (3–5% in O_2). A Millar catheter (Model SPR1000, Millar, Inc., Houston, TX, United States) was implanted into the left common carotid artery as previously described (Elsaafien et al., 2021; Frazier et al., 2021; Mohammed et al., 2021). Fiberoptic posts where then

placed above the LNG. Following establishing baseline BP, blue light was illuminated in the LNG (473 nm, 10 mW output; 20 ms pulse width; 1, 5, 10 Hz for 1 min). Blood pressure (BP) and heart rate (HR) data were sampled/recorded at 1 kHz and analyzed using LabChart 8 software (AD Instruments, Colorado Springs, CO, United States). BP and HR were analyzed at 30 s bins for 2 and 5 min prior to and following optical stimulation, respectively.

RNAscope *in situ* Hybridization and Immunohistochemistry

Section Preparation

Each NDG was sectioned at 10 μm into 6 serial sections using a Leica CM3050 S cryostat (Leica, Buffalo Grove, IL, United States). Sections were immediately mounted onto Fisherbrand SuperFrost Plus Gold Microscope Slides (Thermo Fisher Scientific, Waltham, MA, United States). After air-drying at room temperature for 1 h, slides were rinsed with PBS, incubated in 4% PFA for 5 min, and then dehydrated for 5 min in 50, 75, and 100% EtOH. Following that, slides are incubated in H_2O_2 for 10 min, rinsed with PBS, and allowed to dry for 10–15 min before being stored at −80°C for further processing. The hindbrain was sectioned at 30 μm into 4 serial coronal sections using a Leica CM3050 S cryostat (Leica, Buffalo Grove, IL, United States). Sections were stored in cryoprotective solution at −20°C, until further processing.

In situ Hybridization

RNAscope *in situ* hybridization was performed using the RNAscope® V2 Multiplex Fluorescent Reagent Kit (Advanced Cell Diagnostics, Newark, CA, United States) as per the manufacturer's instructions with slight modification to the pretreatment procedure that allows for preservation of the tdTomato, while still providing optimal mRNA signal. The probes used for these studies were as follows: PIEZO-1 (Mm-Piezo1-O2; Cat. No. 529091), and PIEZO-2 (Mm-Piezo2-E39-E44; Cat. No. 433421). Upon completion of the hybridization for either PIEZO-1 or PIEZ0-2, sections immediately underwent IHC for m-Cherry to amplify the tdTom signal.

Immunohistochemistry

Following RNAscope *in situ* hybridization, standard IHC protocols were used to amplify the tdTom signal in sections through the NDG. Sections were incubated in rabbit anti-m-Cherry at 1:2000 (Cat#: ab167453, abcam). Secondary antibodies were purchased from Jackson ImmunoResearch (Cy3 donkey anti-rabbit, Cat#: 711-165-152) and used at a 1:500 dilution. Briefly, sections were rinsed then incubated in blocking solution (2% normal donkey serum and 0.2% Triton X in 50 mM KPBS) for 2 h at 25°C and then in the primary antibody (diluted in blocking solution) for 18 h at 4°C. Sections were again rinsed 5 × 5 min (50 mM KPBS) before incubation in the secondary antibody in blocking solution for 2 h at 25°C. After a final series of rinses, slides were allowed to air dry and then coverslipped using Prolong™ Gold Antifade Mountant.

Image Capture and Processing

Images were captured and processed using a laser-scanning confocal microscope (Nikon Instruments Inc., Melville, NY, United States). Large coronal scans captured at 10 x magnification throughout the aortic arch and carotid sinus (whole-mount), NDG (whole-mount LNG and RNG), and hindbrain (coronal sections) were acquired to assess the expression of tdTomato. Regions with high expression of tdTom were then imaged at 20x magnification and z-stacks through sections were acquired. For *in situ* hybridization in the NDG, z-stacks of the proteins and mRNAs of interest were captured at 40° magnification. An average of 20 optical sections were collected per z-stack (0.5 μm between z-steps). Sections hybridized with the probes of interest (PIEZO-1 or PIEZO-2) were used to determine the exposure time and image processing required to provide optimal visualization of RNA signal. As described in detail in de Kloet et al. (2016), these same parameters were then used to assess background fluorescence in sections hybridized with the negative control probe (DapB). Importantly, using these exposure times and image processing parameters there was minimal or no fluorescence in sections hybridized with the negative control probe. All representative photomicrographs were then prepared using Adobe Photoshop 2021 to adjust brightness and contrast to provide optimal visualization. Final figures and schematics were prepared in Adobe Illustrator 2021.

Statistics

All *in vitro* electrophysiology data were analyzed using a custom software written in OriginC by CJF (Originlab, Northampton, MA, United States). The effect of voltage or glutamate receptor antagonists on light-evoked currents across cells was evaluated using ratio *t*-tests (paired *t*-tests performed on log-transformed peak currents). Data in the text are reported as mean ± SEM.

All *in vivo* cardiovascular data were analyzed in Labchart 8 (AD Instruments, Colorado Springs, CO, United States). Two-way ANOVAs with Tukey's multiple comparison tests were performed using GraphPad Prism. Data are expressed as mean ± SEM.

RESULTS

Sensory Neurons Innervating the Aortic Arch Terminate in the Caudal Nucleus of the Solitary Tract

Neuroanatomical studies were performed to assess the specificity and selectivity of the current approach in targeting the sensory neurons that innervate the aortic arch. Mice received an AAVrg to direct the expression of tdTom (n = 4) within the nerve endings innervating the aortic arch (**Figure 1A**). After 3 weeks, the aortic arch, NDG and the hindbrain were collected. Imaging of whole-mount samples revealed the incoming ADN as it innervates the aortic arch. The ADN contacted the peak of the left common carotid and the left subclavian arteries and

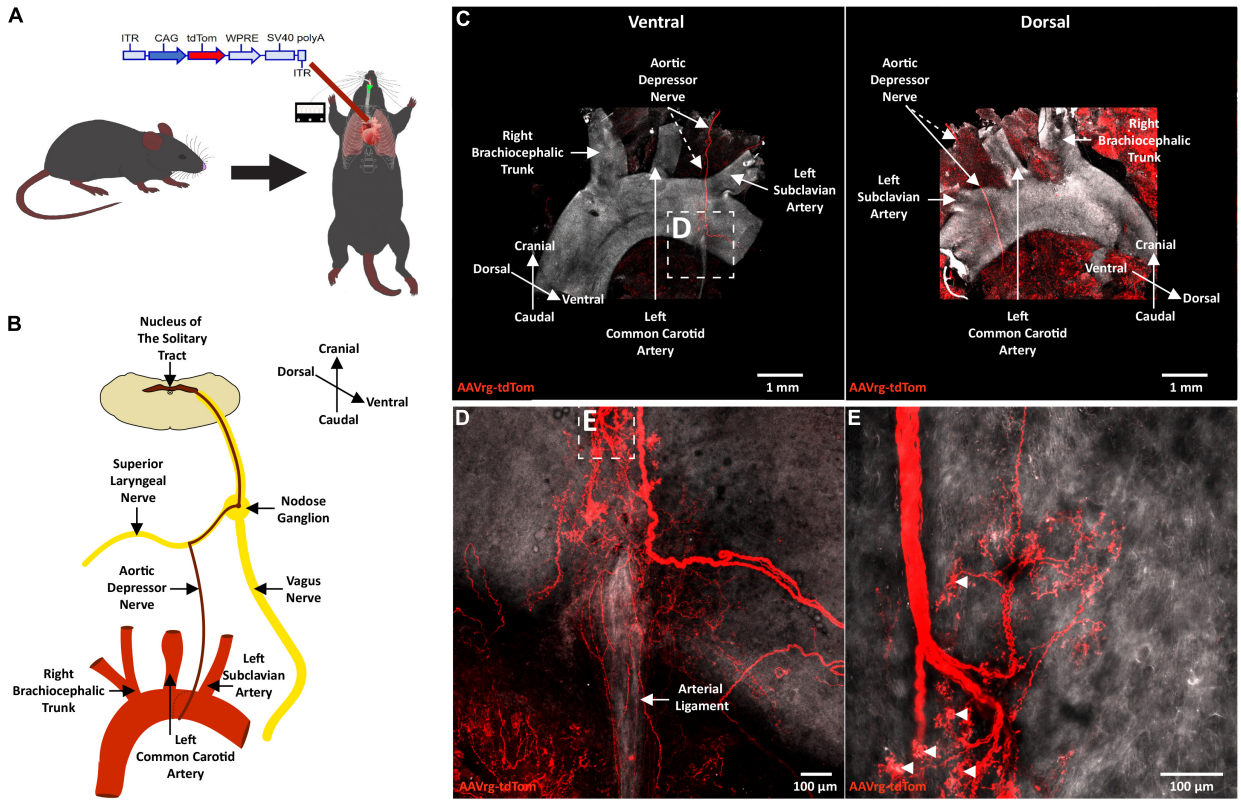

FIGURE 1 | Terminals of sensory neurons innervating the aortic arch are selectively labeled with a retrograde adeno-associated viral vector. **(A)** A schematic diagram depicting the cardiothoracic surgery performed to allow for the application of an AAVrg to the aortic arch to direct the expression of tdTom within the sensory neurons innervating the aortic arch (n = 4). **(B)** A schematic demonstrating the sensory innervation of the aortic arch. **(C)** A representative photomicrograph of a whole-mount aortic arch showing selective expression of tdTom in the sensory nerve terminals innervating the aortic arch ventrally (left) and dorsally (right). **(D,E)** Higher magnification scans revealing the morphology of the sensory nerve terminals innervating the aortic arch.

bifurcated caudally with each branch innervating the dorsal or ventral surface in a saddle-like pattern (**Figure 1B**). tdTom was observed within fibers surrounding the aortic arch and projecting through the ADN (**Figure 1C**). Higher magnification scans revealed the morphology of the nerve endings as abundant flower-spray endings (**Figures 1D,E**). This is consistent with previous description of the sensory innervation of the aortic arch (Aumonier, 1972; Krauhs, 1979; Min et al., 2019). These sensory afferents ascend through the ADN to join the vagus nerve through the superior laryngeal nerve (**Figure 1B**). To assess the specificity of our approach in targeting the aortic arch, the carotid sinus was imaged. No fibers or nerve endings were observed at the carotid bifurcation (**Supplementary Figure 1**). The NDG of the vagus nerve is where the cell bodies of these sensory neurons reside (Aumonier, 1972; Krauhs, 1979; Zeng et al., 2018; Min et al., 2019). We observed the expression of tdTom in fibers running through the vagus nerve and in cell bodies within LNG and RNG (87 ± 15 neurons; **Figure 2**). From the NDG of the vagus, these sensory neurons project to and terminate in the NTS (Mendelowitz et al., 1992). By scanning coronal sections of the whole extent of the hindbrain, we observed that terminals expressing tdTom were only localized to the cNTS (**Figure 3**). Our neuroanatomical results are consistent with previous reports describing the neuroanatomy of sensory neurons that innervate the aortic arch. Hence, our approach to retrogradely label nerve endings innervating the aortic arch is highly specific and selective in targeting single modality fibers.

Cell Bodies of the Sensory Neurons Innervating the Aortic Arch Express PIEZOs

Cell bodies of sensory neurons innervating cardio-pulmonary and gastrointestinal organs are found within the NDG (Kupari et al., 2019). Recently, mechanically activated ion channels PIEZO-1 and PIEZO-2 have been shown to be expressed in sensory neurons that innervate the aortic arch and sense stretch in the arterial wall (Zeng et al., 2018; Min et al., 2019). Thus, we performed RNAscope *in situ* hybridization to label the mRNAs coding for PIEZO-1 and PIEZO-2 in the NDG of mice that received AAVrg-tdTom into the aortic arch. As expected, we found the cell bodies of the NDG that expressed tdTom to also express both PIEZO-1 (**Figure 4A**) and PIEZO-2 (**Figure 4B**). These results demonstrate that our approach is selective in labeling sensory vagal afferents that sense stretch at the level of the aortic arch.

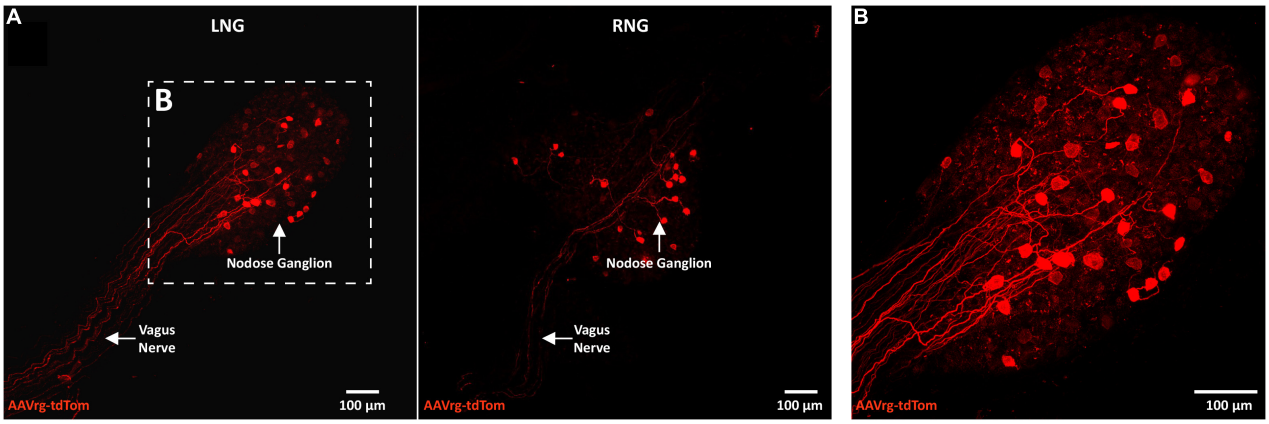

FIGURE 2 | The cell bodies of sensory neurons innervating the aortic arch are in the nodose ganglia of the vagus. **(A)** A representative photomicrograph of a whole-mount left nodose ganglion (LNG) and right nodose ganglion (RNG) depicting the expression of tdTom within fibers in the vagus nerve and cell bodies of the nodose ganglia (n = 4). **(B)** A higher magnification of cell bodies expressing tdTom in the LNG.

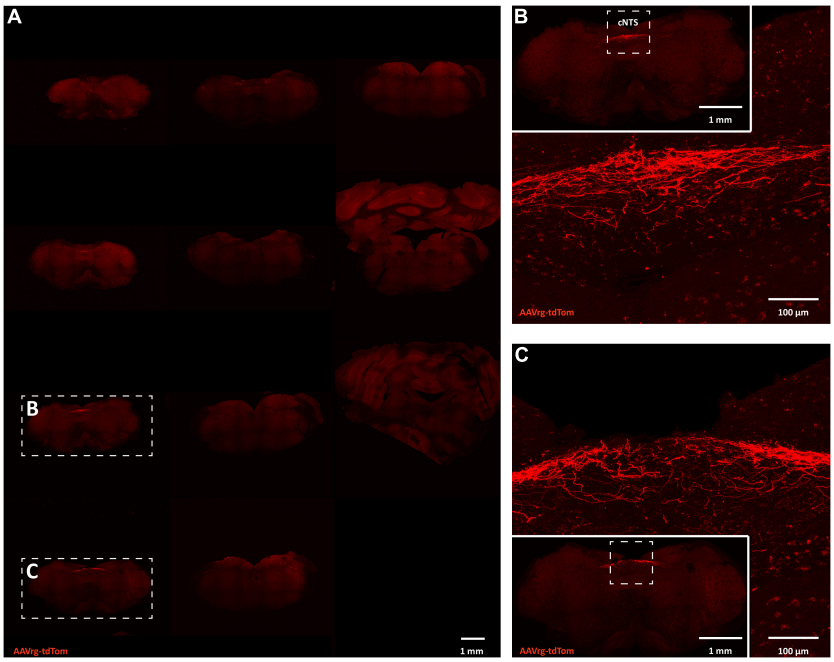

FIGURE 3 | Sensory neurons innervating the aortic arch terminate in the nucleus of the solitary tract. **(A)** Large scans of coronal sections of hindbrain revealing expression of tdTom within fibers in the caudal nucleus of the solitary tract (cNTS; n = 4). **(B,C)** Higher magnification representative image of the cNTS.

Fibers of the Sensory Neurons Innervating the Aortic Arch Form Functional Connections With Nucleus of the Solitary Tract Neurons

Next, we next sought to characterize the connectivity between sensory neurons innervating the aortic arch and the NTS. Mice received an AAVrg to direct the expression of ChR2 and tdTom (n = 7) within the sensory afferents of the aortic arch. Following recovery, horizontal sections of the NTS were prepared to perform *in vitro* electrophysiology (**Figure 5A**). NTS neurons in close proximity to fibers expressing ChR2/tdTomato were targeted for whole-cell patch-clamp recording (**Figures 5B–E**). Following establishment of a whole-cell patch-clamp recording, passive membrane properties were evaluated in voltage clamp at −70 mV using a cesium-based internal solution (see Section "Materials and Methods"). Under these conditions holding current was −13.77 ± 2.78 pA, membrane resistance was 1.23 ± 0.166 GΩ, and whole-cell capacitance was 31.83 ± 2.71 pF (n = 14 cells across 7 mice). To evaluate whether these NTS neurons received synaptic inputs from ChR2-expressing axons of baroreceptor expressing neurons, cells were voltage clamped

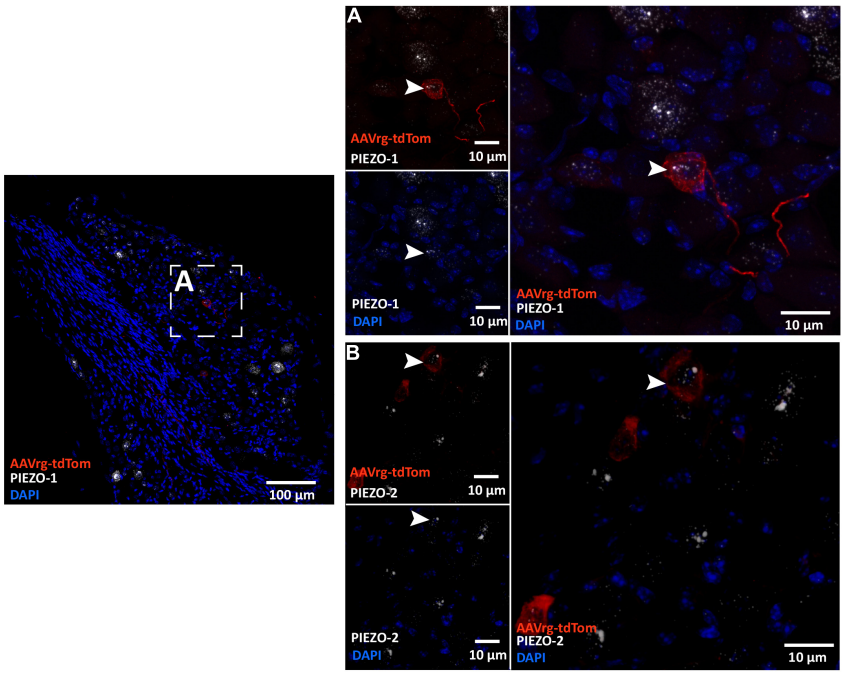

FIGURE 4 | Sensory neurons innervating the aortic arch express the mechanically activated ion channels PIEZO-1 and PIEZO-2. Representative photomicrographs demonstrating the colocalization of the nodose ganglia neurons that expressed tdTom with the mRNAs of **(A)** PIEZO-1 and **(B)** and PIEZO-2.

at −50 mV in the continuous presence of the $GABA_A$ receptor antagonist PTX (100 μM). Blue light pulses (20 ms) were then used to evoke neurotransmitter release from ChR2/tdTomato-expressing axon terminals arriving from the aortic arch. We found that blue light evoked an excitatory current in 14 of 109 NTS cells tested (−71.41 ± 17.68 pA at −50 mV, n = 14 cells across 7 mice, **Figures 5E,F**). In all cases, light-evoked responses were observed as an inward current at −50 mV, which was significantly reduced at 0 mV (−11.51 ± 3.13 pA, p = 4.58e-6, **Figures 5F,G**). These results indicate that baroreceptor expressing afferents that make synaptic connections with NTS neurons are likely glutamatergic. To further test this hypothesis, a subset of light-evoked responses was subsequently challenged with bath applied glutamate receptor antagonists. Bath-application of ionotropic glutamate receptor antagonists DNQX or DNQX + AP5 effectively eliminated light-evoked currents (amplitude reduced from −68.20 ± 39.97 pA to −4.18 ± 1.90 pA, **Figures 5H,I**, p = 9.31e-5, n = 7, 4), confirming they were mediated by activation of glutamatergic receptors. These results demonstrate that the labeled sensory neurons innervating the aortic arch form functional glutamatergic synaptic connections with NTS neurons.

In vivo Optogenetic Excitation of Sensory Neurons Innervating the Aortic Arch Produces Depressor Responses

Next, we assessed the effects of the *in vivo* optogenetic stimulation of the sensory neurons innervating the aortic arch on BP and HR. Mice received an injection of AAVrg to direct the expression of ChR2 and/or tdTom (n = 6 per group) within the baroreceptor expressing afferents. Following recovery, the left common carotid artery was catheterized to record BP, and a fiberoptic post was placed above the LNG to optogenetically stimulate the cell bodies of the baroreceptors (**Figure 6A**). Following baseline recording (**Table 1**), the optogenetic stimulation (473 nm, 10 mW output; 20 ms pulse width; 1, 5, 10 Hz for 1 min) of the cell bodies of baroreceptor expressing afferents elicited frequency-dependent depressor responses (**Figure 6B**). In comparison to control groups that only expressed tdTom, BP (tdTom vs. ChR2; 1 Hz: +0.5 ± 0.8 vs. +1.0 ± 0.8 mmHg, 5 Hz: +0.5 ± 0.4 vs. −1.8 ± 0.6 mmHg, 10 Hz: +0.05 ± 0.9 vs. −4.9 ± 1.3 mmHg at 1 min, n = 6 per group, **Figure 6C**) and HR (tdTom vs. ChR2; 1 Hz: +0.5 ± 2.1 vs. −2.4 ± 0.7 bpm, 5 Hz: +1.7 ± 2.2 vs. −4.1 ± 0.8 bpm, 10 Hz: −1.6 ± 0.7 vs. −4.6 ± 0.9 bpm at 1 min, n = 6 per group, **Figure 6C**) were significantly reduced in response to blue light illumination. Altogether, our anatomical and functional data suggest that the current approach targets neurons that express baroreceptors in the aortic arch with high specificity, and further demonstrates selective optogenetic activation of these neurons elicits a depressor response.

DISCUSSION

Sensory nerve endings located at the aortic arch employ baroreceptors that convert stretch exerted on the arterial wall into action potentials carried by the vagus nerve to second order neurons residing within the NTS. This provides moment-to-moment feedback control of HR and BP (Benarroch, 2008;

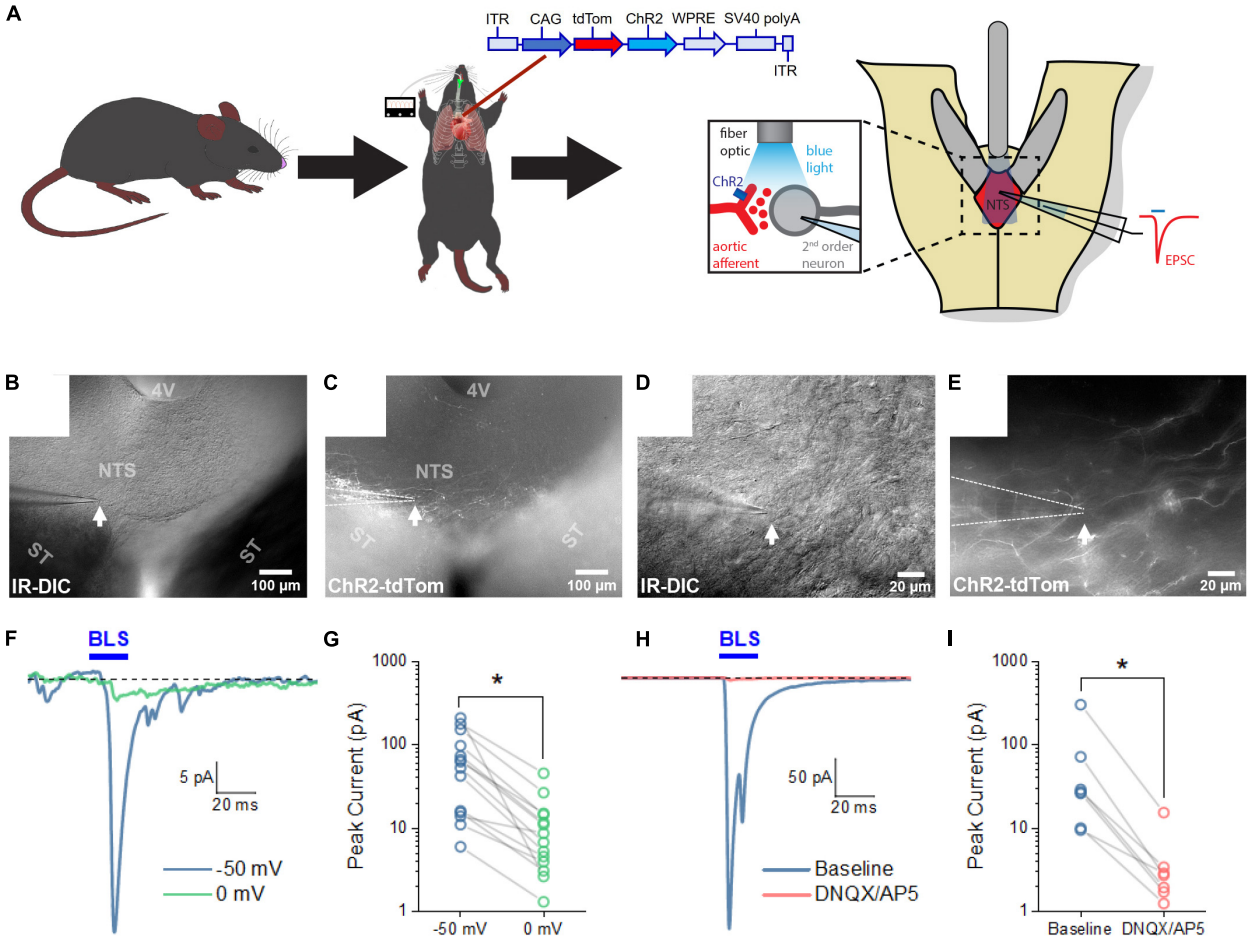

FIGURE 5 | Blue light stimulation of baroreceptors induces glutamate release onto NTS neurons. **(A)** AAVrg applied to the aortic arch to direct the expression of ChR2 and tdTom within sensory neurons innervating the aortic arch (n = 7). Light-sensitive synapses in the NTS were characterized using whole-cell patch-clamp in horizontal brain slices. **(B–E)** Neurons in close approximation with ChR2/tdTom axons were targeted for study using a combination of infrared differential interference contrast (IR-DIC) and epifluorescence microscopy. **(F)** Representative traces from an NTS neuron demonstrating an excitatory current produced by 20 ms blue light stimulation (BLS). Light-evoked currents were substantially reduced when neurons were voltage clamped at 0 mV. Traces shown are the mean of 10 consecutive sweeps. **(G)** Mean peak light-evoked inward current at -50 and 0 mV (n = 14 cells from seven animals). **(H)** Representative traces demonstrating light-evoked inward current is also strongly attenuated by bath application of glutamate receptor antagonists. Traces shown are the mean of 30 consecutive sweeps. **(I)** Light-evoked currents were significantly reduced by ionotropic glutamate receptor antagonist (n = 7).

Wehrwein and Joyner, 2013). Here, we used a novel organ-specific approach to selectively target baroreceptor expressing afferents with an AAVrg conjugated to tdTom and/or ChR2. Our anatomical results revealed robust tdTom expression in nerve endings surrounding the aortic arch, within the fibers of the ADN and vagus nerves, cell bodies of the NDG, and neural projections to the cNTS. Additionally, the tdTom labeled cell bodies within the NDG expressed mRNAs coding for the mechanically gated ion channels, PIEZO-1 and PIEZO-2. *In vitro* electrophysiology revealed that pulses of blue light evoked excitatory post-synaptic currents in a subset of neurons within the cNTS, suggesting a functional connection between the labeled aortic arch sensory afferents and second order neurons. Finally, *in vivo* optogenetic stimulation of the cell bodies of baroreceptor expressing afferents in NDG produced robust depressor responses. Altogether, our results demonstrate that the current approach selectively targets and labels baroreceptor expressing afferents in the aortic arch.

Viscero-sensory afferents convey the status of visceral organs to second order neurons in the NTS (Andresen and Paton, 2011). This includes physiological signals from cardio-pulmonary and gastrointestinal tract (GIT) organs that project to the NTS through the vagus nerve, where the cell bodies of these afferents reside in the NDG (Berthoud and Neuhuber, 2000; Kubin et al., 2006; Bai et al., 2019; Kupari et al., 2019). The recent development of advanced genetic tools allows for the anatomical and functional characterization of vagal sensory afferents with spatial and temporal resolution (Saleeba et al., 2019). Using the Cre-LoxP system and virally mediated gene transfer targeted to the GIT, it was possible to anatomically and functionally characterize vagal sensory neurons that innervate the GIT (Han et al., 2018). While these advanced genetic technologies allowed

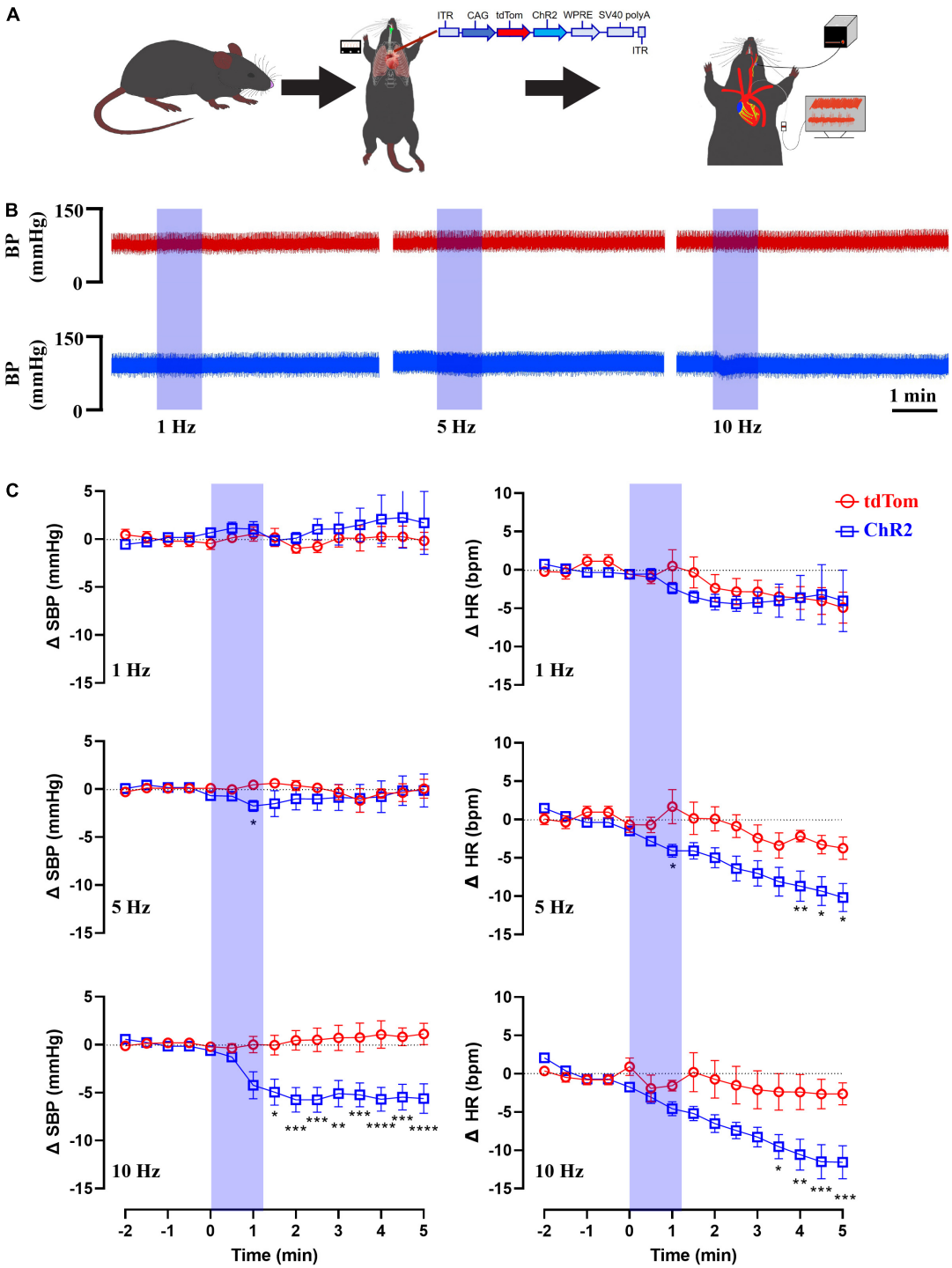

FIGURE 6 | Blue light stimulation of baroreceptors elicits depressor responses. **(A)** AAVrg applied to the aortic arch to direct the expression of ChR2 and/or tdTom within baroreceptors (n = 6 per group). **(B)** Representative traces of arterial pressure and heart rate following the optogenetic stimulation of baroreceptors cell bodies at 1, 5, and 10 Hz (473 nm, 10 mW output; 20 ms pulse width; for 1 min). **(C)** Time-course changes in systolic blood pressure (SBP) and heart rate (HR) in control (tdTom) and experimental (ChR2) groups. *$p < 0.05$, **$p < 0.01$, ***$p < 0.001$, ****$p < 0.0001$; Two-way ANOVA followed by Tukey's *post hoc* test. n = 6 per group.

for the selective characterization of sensory circuits, viscero-sensory afferents, and neural reflexes, baroreceptor expressing sensory afferents are yet to be fully characterized. This is due to the fact that selective targeting of such afferents is challenging. Unlike the GIT, where viral vectors can be injected into the gut wall, injection of viral vectors into the vasculature is problematic.

TABLE 1 | Body weights, baseline mean blood pressure (MBP), and heart rate (HR) prior to optogenetic stimulation.

	Body weight (g)	MBP (mmHg)	HR (bpm)
tdTom	29.1 ± 0.5	1 Hz: 75.2 ± 5.9	1 Hz: 487 ± 12
		5 Hz: 77.2 ± 4.4	5 Hz: 473 ± 11
		10 Hz: 77.5 ± 3.6	10 Hz: 472 ± 7
ChR2	29.8 ± 0.9	1 Hz: 80.6 ± 7.6	1 Hz: 449 ± 4
		5 Hz: 78.4 ± 6.1	5 Hz: 462 ± 11
		10 Hz: 78.7 ± 6.7	10 Hz: 465 ± 13

Data expressed as mean ± SEM, n = 6 per group.

Furthermore, the aortic arch is located in the thoracic cavity which is difficult to access in small rodents for recovery surgeries. To circumvent these challenges, we have developed a novel approach that selectively targets and labels sensory neurons innervating the aortic arch. This approach involves (1) a novel surgical approach that exposes the aortic arch in mice, and (2) the application of viral vectors to the aortic arch by "painting" the virus on the vascular wall.

Our anatomical studies demonstrate the selective targeting of fibers that convey a single modality to the NTS. Following the application of an AAVrg to the aortic arch, we directed the expression of tdTom within sensory afferents that contain baroreceptors. Consistent with previous studies describing the anatomy/morphology of baroreceptor containing afferents (Aumonier, 1972; Krauhs, 1979; Min et al., 2019), we found abundant tdTom expression within nerve endings surrounding the aortic arch. The morphology of these terminals resembled flower-spray endings, spanning the dorsal and ventral surface of the aortic arch in a claw-like pattern. Both dorsal and ventral fibers joined the ADN and terminated in the cNTS through the vagus nerve. This is consistent with previous studies that anatomically mapped the projections of vagal baroreceptors (Cottle, 1964; Lipski et al., 1975). For example, following the selective transection of the vagus nerve in cats, axonal and terminal degeneration were found in the NTS (Cottle, 1964). Furthermore, antidromic stimulation of baroreceptor expressing fibers, demonstrated that these fibers terminate in the NTS (Lipski et al., 1975). In addition, previous studies demonstrated that cardiovascular vagal afferents terminate in the cNTS (Mendelowitz et al., 1992), whereas afferents arising from the GIT terminate in the rostral NTS (Han et al., 2018). This suggests that our approach selectively targets aortic arch afferents that terminate in the caudal portion of the NTS.

Sensory neurons innervating the aortic arch convey chemosensory and mechanosensory signals to the NTS. It is widely accepted in the literature that fibers in the ADN contain baroreceptors. Electrical stimulation of the ADN produces robust depressor responses (Schmidt, 1968; Sapru et al., 1981; Fan et al., 1996). Furthermore, electrophysiological recordings from the ADN demonstrate a change in discharge to hemodynamic stimuli (Kobayashi et al., 1999). However, studies utilizing recordings from single ADN fibers demonstrate that some fibers change their firing in response to switching from normocapnic hyperoxia and hypercapnic hypoxia (Brophy et al., 1999). These results suggest that fibers in the ADN sense both chemosensory and mechanosensory stimuli. More recently, baroreceptors sensing stretch (mechanosensory) at the aortic arch were shown to express the mechanically gated ion channels, PIEZO-1 and PIEZO-2 (Zeng et al., 2018; Min et al., 2019). Therefore, to examine whether our approach specifically labels baroreceptors, we used RNAscope *in situ* hybridization to label the mRNAs coding for both PIEZOs in the NDG. We found the labeled NDG neurons that received input from the aortic arch express both PIEZO-1 and PIEZO-2. This suggests that the current approach labels sensory afferents that utilize mechanically gated ion channels to detect stretch at the aortic arch. However, it is possible that the current approach also labels chemosensory afferents. Previous studies demonstrate that the majority of chemoreceptor expressing afferents terminate in the most caudal portion of the NTS (Colombari and Talman, 1995; Colombari et al., 1996), whereas baroreceptor expressing afferents terminate in the caudal and intermediate portions of the NTS (Mendelowitz et al., 1992). Our confocal scans of the entire brainstem revealed that labeled fibers from the aortic arch were only found in the caudal and intermediate NTS. Moreover, nerve fibers terminating at the aortic arch exhibited distinct baroreceptor morphology, characterized by abundant flower-spray endings (Cheng et al., 1997; Min et al., 2019). These labeled fibers did not exhibit chemoreceptor morphology which is described as pericellular endings innervating small intensity fluorescent cell bodies. These chemosensory nerve endings are abundantly found at the carotid sinus (Cheng et al., 1997) and we obtained additional confocal scans of the carotid sinus to discern whether our approach also labeled chemosensory afferents. We did not observe any nerve endings or fibers at the carotid sinus (**Supplementary Figure 1**); however, the same animals exhibited robust and apparent tdTom labeled fibers at the aortic arch (**Figure 1**). This suggests that our approach is selective in labeling mechano-sensory afferents at the aortic arch that presumably contain baroreceptors. Thus, our current approach may be utilized to genetically manipulate baroreceptor expressing sensory afferents to examine their physiological function.

Baroreceptors sense stretch at the wall of the aortic arch and activate the baroreflex to modulate BP at homeostatic levels. An increase in BP also increases stretch on the wall of the aortic arch, stimulating baroreceptors (Kirchheim, 1976). This activates the baroreceptors to trigger afferent signals conveyed to the NTS (Benarroch, 2008; Wehrwein and Joyner, 2013). Subsequently, stimulating a neural reflex (known as the baroreflex) that reduces HR by reducing sympathetic outflow and increasing parasympathetic output (Zeng et al., 2018; Min et al., 2019). This reduces BP back to homeostatic levels (Spyer, 1989; Andresen and Kunze, 1994). Conversely, a drop in BP (such as in postural hypotension) triggers baroreceptor unloading leading to increases in BP (Thrasher, 2005). Thus, baroreceptors detect moment-to-moment fluctuations in BP to maintain vascular resistance and cardiovascular output at optimal levels, ensuring sufficient blood flow to the body. Here, we used an AAVrg to direct the expression of ChR2 within nerve endings surrounding the aortic arch to stimulate baroreceptors. Our

in vitro electrophysiological studies confirmed the functionality of the ChR2 molecule in baroreceptor expressing afferents, as pulsing blue light on ChR2 expressing fibers in the cNTS elicited glutamatergic-dependent excitatory post-synaptic currents in NTS neurons. Thus, we utilized an *in vivo* approach to record BP while the cell bodies of afferents containing baroreceptors in the NDG were optogenetically activated to simulate mechano-stimulation. Consistent with previous studies demonstrating that the electrical stimulation of the ADN results in hypotension (Schmidt, 1968; Sapru et al., 1981; Fan et al., 1996), we observed robust reductions in BP and HR upon blue light stimulation of baroreceptor containing neurons. This suggests that our current approach can be combined with advanced genetic technologies to selectively interrogate the physiological function of baroreceptor expressing vagal afferents.

The results of the current study demonstrate that our approach is highly selective in targeting baroreceptor expressing sensory afferents. This warrants future studies that interrogate pathophysiological function of these afferents. In hypertension, 19% of patients suffer from drug-resistant hypertension despite the plethora of anti-hypertensive treatments (Carey et al., 2019). This is often termed as "neurogenic hypertension" due to the neuronal impairments that lead to augmented sympathetic outflow (Smith et al., 2004, 2002; Oliveira-Sales et al., 2016; Korim et al., 2019). Some of the first evidence for the role of baroreceptor fibers in cardiovascular control and hypertension, originated from denervation studies (Krieger, 1964). In this study, 140 rats were subjected to denervation of aortic depressor fibers, and were observed for one year. Rats exhibited a hypertensive phenotype one week following denervation, where the hypertension was permanent in 75% of the rats observed up to one year (Krieger, 1964). This study demonstrates that integrity of baroreceptor expressing afferents is crucial for maintaining BP. In fact, baroreflex dysfunction is well documented in hypertension (Parmer et al., 1992; Oliveira-Sales et al., 2016). Baroreflex sensitivity is impaired in hypertension leading to failure in maintaining BP levels (Brook and Julius, 2000). Interestingly, it has been demonstrated that baroreflex dysfunction precedes sympathetic augmentation in rodent models of hypertension, which altogether occurs prior to BP elevations and the establishment of hypertension (Oliveira-Sales et al., 2016). Thus, exploiting the modulatory influence of the afferent baroreceptor signals may have potential therapeutic effects in hypertension.

While the current manuscript evaluates the specificity of a novel approach to express light sensitive molecules in baroreceptor expressing neurons, there are some limitations. The current study utilizes *in vitro* electrophysiology to assess the functionality of the ChR2 molecule. We demonstrate that pulsing light on terminals in the NTS originating from baroreceptor expressing neurons in the NDG reliably produces glutamatergic-dependent excitatory post-synaptic currents in NTS neurons. Further direct validation of the ChR2 molecule used in the current manuscript may require whole-cell recordings of somatic responses to optogenetic stimulation in baroreceptor expressing neurons in the NDG itself. Additionally, the current manuscript does not assess the long-term stability of the ChR2 molecule. This could be achieved by expressing ChR2 in baroreceptor containing neurons for a longer duration than in the current study. This would be followed by assessing the long-term expression of the ChR2 molecule by using *in vitro* electrophysiology and *in situ* hybridization for mRNAs for ChR2. Moreover, *in vivo* optogenetic studies are used to evaluate changes in BP following optogenetic stimulation. In these studies, we found the somatic stimulation of baroreceptor expressing neurons in the NDG to produce depressor responses; however, *in vivo* optogenetic stimulation combined with electrophysiological nerve recording of the ADN and stimulation of fibers in the NTS would more directly validate the functional connectivity between baroreceptor expressing neurons in the NDG and the NTS through the ADN. Finally, the current study uses stimulation frequencies of 1–10 Hz for *in vivo* optogenetic studies. While baroreceptor expressing fibers respond differentially to electrical stimulation (C-type: 1–10 Hz, A-type: >10 Hz) (Fan and Andresen, 1998), the optogenetic somatic stimulation of baroreceptor expressing neurons in the NDG that express ChR2 are expected to achieve suprathreshold depolarization when exposed to pulses of blue light at that location, regardless of whether the axons are unmyelinated or myelinated (Lin et al., 2009).

In conclusion, the present study establishes a novel approach to selectively target single modality vagal afferent fibers that convey stretch at the aortic arch to the NTS. Furthermore, we demonstrate that our approach can be combined with advanced genetic tools to interrogate the physiological function of baroreceptors. Using the current approach may lead to characterizing the molecular, anatomical, functional, and pathological phenotype of baroreceptors with high spatial and temporal resolution.

DATA AVAILABILITY STATEMENT

The original contributions presented in the study are included in the article/**Supplementary Material**, further inquiries can be directed to the corresponding authors.

ETHICS STATEMENT

All procedures were reviewed and approved by the Institutional Animal Care and Use Committees at the University of Florida and were conducted in accordance with the National Institutes of Health Guide for the Care and Use of Laboratory Animals.

AUTHOR CONTRIBUTIONS

KE, ADK, and EGK conceived, designed, supervised, and coordinated the study, and wrote the manuscript. KE performed the cardiothoracic surgeries. KE, SWH, DNJ, WS, JAS, and KAS conducted experiments and acquired data. KE, AKK, SWH, and CJF analyzed data. KE, CJF, ADK, and EGK contributed unpublished reagents and analytic tools. KE and SWH wrote the first draft of the

manuscript. KE, SWH, DNJ, WS, JAS, KAS, CJF, ADK, and EGK edited and revised the manuscript. All authors contributed to the article and approved the submitted version.

FUNDING

This work was supported by American Heart Association grant 17GRNT33660969 and National Institute of Health (National Heart Lung and Blood Institute) grants HL-125805 (ADK), HL-145028 (ADK), HL-136595 (EGK), HL-096830 (EGK), and HL-122494 (EGK).

ACKNOWLEDGMENTS

We would like to acknowledge Elaine M. Sumners and Mohan K. Raizada for generously donating the mouse ventilator used to artificially ventilate mice during cardiothoracic surgeries.

SUPPLEMENTARY MATERIAL

The Supplementary Material for this article can be found online at: https://www.frontiersin.org/articles/10.3389/fphys.2022.841078/full#supplementary-material

REFERENCES

Alcaino, C., Farrugia, G., and Beyder, A. (2017). Mechanosensitive piezo channels in the gastrointestinal tract. *Curr. Top Membr.* 79, 219–244. doi: 10.1016/bs.ctm.2016.11.003

Andresen, M. C., and Kunze, D. L. (1994). Nucleus tractus solitarius–gateway to neural circulatory control. *Annu. Rev. Physiol.* 56, 93–116. doi: 10.1146/annurev.ph.56.030194.000521

Andresen, M. C., and Paton, J. F. R. (2011). ""The Nucleus of the Solitary Tract: Processing Information from Viscerosensory Afferents,"," in *Central regulation of autonomic functions*, eds I. J. Llewellyn-Smith and A. J. M. Verberne (Oxford: Oxford University Press), 23–46. doi: 10.1093/acprof:oso/9780195306637.003.0002

Aumonier, F. J. (1972). Histological observations on the distribution of baroreceptors in the carotid and aortic regions of the rabbit, cat and dog. *Acta Anatomica.* 82, 1–16. doi: 10.1159/000143797

Bai, L., Mesgarzadeh, S., Ramesh, K. S., Huey, E. L., Liu, Y., Gray, L. A., et al. (2019). Genetic identification of vagal sensory neurons that control feeding. *Cell* 179, 1129.e–1143.e. doi: 10.1016/j.cell.2019.10.031

Benarroch, E. E. (2008). The arterial baroreflex: functional organization and involvement in neurologic disease. *Neurology* 71, 1733–1738. doi: 10.1212/01.wnl.0000335246.93495.92

Berthoud, H. R., and Neuhuber, W. L. (2000). Functional and chemical anatomy of the afferent vagal system. *Auton. Neurosci.* 85, 1–17. doi: 10.1016/S1566-0702(00)00215-0

Brook, R. D., and Julius, S. (2000). Autonomic imbalance, hypertension, and cardiovascular risk. *Am. J. Hypertens.* 13, 112S–122S. doi: 10.1016/s0895-7061(00)00228-4

Brophy, S., Ford, T. W., Carey, M., and Jones, J. F. (1999). Activity of aortic chemoreceptors in the anaesthetized rat. *J. Physiol.* 514(Pt 3), 821–828. doi: 10.1111/j.1469-7793.1999.821ad.x

Brown, A. M. (1980). Receptors under pressure. An update on baroreceptors. *Circ. Res.* 46, 1–10. doi: 10.1161/01.res.46.1.1

Carey, R. M., Sakhuja, S., Calhoun, D. A., Whelton, P. K., and Muntner, P. (2019). Prevalence of Apparent Treatment-Resistant Hypertension in the United States. *Hypertension* 73, 424–431. doi: 10.1161/HYPERTENSIONAHA.118.12191

Cheng, Z., Powley, T. L., Schwaber, J. S., and Doyle, F. J. (1997). A laser confocal microscopic study of vagal afferent innervation of rat aortic arch: chemoreceptors as well as baroreceptors. *J Auton. Nerv. Syst.* 67, 1–14. doi: 10.1016/s0165-1838(97)00085-4

Colombari, E., Menani, J. V., and Talman, W. T. (1996). Commissural NTS contributes to pressor responses to glutamate injected into the medial NTS of awake rats. *Am. J. Physiol.* 270, R1220–R1225. doi: 10.1152/ajpregu.1996.270.6.R1220

Colombari, E., and Talman, W. T. (1995). Denervation supersensitivity to glutamate in the nucleus tractus solitarii after removal of the nodose ganglion. *Brain Res.* 677, 110–116. doi: 10.1016/0006-8993(95)00131-9

Cottle, M. K. (1964). Degeneration studies of primary afferents of ixth and xth cranial nerves in the cat. *J. Comp. Neurol.* 122, 329–345. doi: 10.1002/cne.901220304

de Kloet, A. D., Wang, L., Ludin, J. A., Smith, J. A., Pioquinto, D. J., Hiller, H., et al. (2016). Reporter mouse strain provides a novel look at angiotensin type-2 receptor distribution in the central nervous system. *Brain Struct. Funct.* 221, 891–912. doi: 10.1007/s00429-014-0943-1

Edelstein, A., Amodaj, N., Hoover, K., Vale, R., and Stuurman, N. (2010). Computer control of microscopes using μManager. *Curr. Protoc. Mol. Biol.* 14, Unit14.20. doi: 10.1002/0471142727.mb1420s92

Elsaafien, K., Kirchner, M. K., Mohammed, M., Eikenberry, S. A., West, C., Scott, K. A., et al. (2021). Identification of Novel Cross-Talk between the Neuroendocrine and Autonomic Stress Axes Controlling Blood Pressure. *J. Neurosci.* 41, 4641–4657. doi: 10.1523/JNEUROSCI.0251-21.2021

Fan, W., and Andresen, M. C. (1998). Differential frequency-dependent reflex integration of' ' myelinated and nonmyelinated rat aortic baroreceptors. *Am. J. Physiol.-Heart Circul. Physiol.* 275, H632–H640. doi: 10.1152/ajpheart.1998.275.2.H632

Fan, W., Reynolds, P. J., and Andresen, M. C. (1996). Baroreflex frequency-response characteristics to aortic depressor and carotid sinus nerve stimulation in rats. *Am. J. Physiol.* 271, H2218–H2227. doi: 10.1152/ajpheart.1996.271.6.H2218

Frazier, C. J., Harden, S. W., Alleyne, A. R., Mohammed, M., Sheng, W., Smith, J. A., et al. (2021). An Angiotensin-Responsive Connection from the Lamina Terminalis to the Paraventricular Nucleus of the Hypothalamus Evokes Vasopressin Secretion to Increase Blood Pressure in Mice. *J. Neurosci.* 41, 1429–1442. doi: 10.1523/JNEUROSCI.1600-20.2020

Golowasch, J., Thomas, G., Taylor, A. L., Patel, A., Pineda, A., Khalil, C., et al. (2009). Membrane capacitance measurements revisited: dependence of capacitance value on measurement method in nonisopotential neurons. *J. Neurophysiol.* 102, 2161–2175. doi: 10.1152/jn.00160.2009

Han, W., Tellez, L. A., Perkins, M. H., Perez, I. O., Qu, T., Ferreira, J., et al. (2018). A Neural Circuit for Gut-Induced Reward. *Cell* 175, 665.e–678.e. doi: 10.1016/j.cell.2018.08.049

Kirchheim, H. R. (1976). Systemic arterial baroreceptor reflexes. *Physiol. Rev.* 56, 100–177. doi: 10.1152/physrev.1976.56.1.100

Kobayashi, M., Cheng, Z. B., Tanaka, K., and Nosaka, S. (1999). Is the aortic depressor nerve involved in arterial chemoreflexes in rats? *J. Auton. Nerv. Syst.* 78, 38–48. doi: 10.1016/s0165-1838(99)00054-5

Korim, W. S., Elsaafien, K., Basser, J. R., Setiadi, A., May, C. N., and Yao, S. T. (2019). In renovascular hypertension, TNF-α type-1 receptors in the area postrema mediate increases in cardiac and renal sympathetic nerve activity and blood pressure. *Cardiovasc. Res.* 115, 1092–1101. doi: 10.1093/cvr/cvy268

Krauhs, J. M. (1979). Structure of rat aortic baroreceptors and their relationship to connective tissue. *J. Neurocytol.* 8, 401–414. doi: 10.1007/BF01214800

Krieger, E. M. (1964). Neurogenic hypertension in the rat. *Circ. Res.* 15, 511–521. doi: 10.1161/01.res.15.6.511

Kubin, L., Alheid, G. F., Zuperku, E. J., and McCrimmon, D. R. (2006). Central pathways of pulmonary and lower airway vagal afferents. *J. Appl. Physiol.* 101, 618–627. doi: 10.1152/japplphysiol.00252.2006

Kumada, M., Terui, N., and Kuwaki, T. (1990). Arterial baroreceptor reflex: its central and peripheral neural mechanisms. *Prog. Neurobiol.* 35, 331–361. doi: 10.1016/0301-0082(90)90036-g

Kupari, J., Häring, M., Agirre, E., Castelo-Branco, G., and Ernfors, P. (2019). An atlas of vagal sensory neurons and their molecular specialization. *Cell Rep* 27, 2508.e–2523.e. doi: 10.1016/j.celrep.2019.04.096

Lin, J. Y., Lin, M. Z., Steinbach, P., and Tsien, R. Y. (2009). Characterization of engineered channelrhodopsin variants with improved properties and kinetics. *Biophys. J.* 96, 1803–1814. doi: 10.1016/j.bpj.2008.11.034

Lipski, J., McAllen, R. M., and Spyer, K. M. (1975). The sinus nerve and baroreceptor input to the medulla of the cat. *J. Physiol.* 251, 61–78. doi: 10.1113/jphysiol.1975.sp011081

Mendelowitz, D., Yang, M., Andresen, M. C., and Kunze, D. L. (1992). Localization and retention in vitro of fluorescently labeled aortic baroreceptor terminals on neurons from the nucleus tractus solitarius. *Brain Res.* 581, 339–343. doi: 10.1016/0006-8993(92)90729-s

Min, S., Chang, R. B., Prescott, S. L., Beeler, B., Joshi, N. R., Strochlic, D. E., et al. (2019). Arterial Baroreceptors Sense Blood Pressure through Decorated Aortic Claws. *Cell Rep.* 29, 2192.e–2201.e. doi: 10.1016/j.celrep.2019.10.040

Min, S., Oh, Y., Verma, P., Whitehead, S. C., Yapici, N., Van Vactor, D., et al. (2021). Control of feeding by Piezo-mediated gut mechanosensation in Drosophila. *Elife* 10:e63049. doi: 10.7554/eLife.63049

Mohammed, M., Johnson, D. N., Wang, L. A., Harden, S. W., Sheng, W., Spector, E. A., et al. (2021). Targeting angiotensin type 2 receptors located on pressor neurons in the nucleus of the solitary tract to relieve hypertension in mice. *Cardiovasc. Res.* doi: 10.1093/cvr/cvab085[Epub ahead of print].

Nonomura, K., Woo, S.-H., Chang, R. B., Gillich, A., Qiu, Z., Francisco, A. G., et al. (2017). Piezo2 senses airway stretch and mediates lung inflation-induced apnoea. *Nature* 541, 176–181. doi: 10.1038/nature20793

Oh, Y., Lai, J. S.-Y., Min, S., Huang, H.-W., Liberles, S. D., Ryoo, H. D., et al. (2021). Periphery signals generated by Piezo-mediated stomach stretch and Neuromedin-mediated glucose load regulate the Drosophila brain nutrient sensor. *Neuron* 109, 1979.e–1995.e. doi: 10.1016/j.neuron.2021.04.028

Oliveira-Sales, E. B., Colombari, E., Abdala, A. P., Campos, R. R., and Paton, J. F. R. (2016). Sympathetic overactivity occurs before hypertension in the two-kidney, one-clip model. *Exp. Physiol.* 101, 67–80. doi: 10.1113/EP085390

Parmer, R. J., Cervenka, J. H., and Stone, R. A. (1992). Baroreflex sensitivity and heredity in essential hypertension. *Circulation* 85, 497–503. doi: 10.1161/01.cir.85.2.497

Ranade, S. S., Woo, S.-H., Dubin, A. E., Moshourab, R. A., Wetzel, C., Petrus, M., et al. (2014). Piezo2 is the major transducer of mechanical forces for touch sensation in mice. *Nature* 516, 121–125. doi: 10.1038/nature13980

Saleeba, C., Dempsey, B., Le, S., Goodchild, A., and McMullan, S. (2019). A student's guide to neural circuit tracing. *Front. Neurosci.* 13:897. doi: 10.3389/fnins.2019.00897

Sapru, H. N., Gonzalez, E., and Krieger, A. J. (1981). Aortic nerve stimulation in the rat: cardiovascular and respiratory responses. *Brain Res. Bull.* 6, 393–398. doi: 10.1016/S0361-9230(81)80009-3

Schmidt, E. M. (1968). Blood pressure response to aortic nerve stimulation in swine. *Am. J. Physiol.* 215, 1488–1492. doi: 10.1152/ajplegacy.1968.215.6.1488

Smith, P. A., Graham, L. N., Mackintosh, A. F., Stoker, J. B., and Mary, D. A. S. G. (2002). Sympathetic neural mechanisms in white-coat hypertension. *J. Am. Coll. Cardiol.* 40, 126–132. doi: 10.1016/s0735-1097(02)01931-9

Smith, P. A., Graham, L. N., Mackintosh, A. F., Stoker, J. B., and Mary, D. A. S. G. (2004). Relationship between central sympathetic activity and stages of human hypertension. *Am. J. Hypertens.* 17, 217–222. doi: 10.1016/j.amjhyper.2003.10.010

Spyer, K. M. (1989). Neural mechanisms involved in cardiovascular control during affective behaviour. *Trends Neurosci.* 12, 506–513. doi: 10.1016/0166-2236(89)90111-2

Thrasher, T. N. (2005). Baroreceptors, baroreceptor unloading, and the long-term control of blood pressure. *Am. J. Physiol. Regul. Integr. Comp. Physiol.* 288, R819–R827. doi: 10.1152/ajpregu.00813.2004

Wehrwein, E. A., and Joyner, M. J. (2013). Regulation of blood pressure by the arterial baroreflex and autonomic nervous system. *Handb. Clin .Neurol.* 117, 89–102. doi: 10.1016/B978-0-444-53491-0.00008-0

Woo, S.-H., Lukacs, V., de Nooij, J. C., Zaytseva, D., Criddle, C. R., Francisco, A., et al. (2015). Piezo2 is the principal mechanotransduction channel for proprioception. *Nat. Neurosci.* 18, 1756–1762. doi: 10.1038/nn.4162

Zeng, W.-Z., Marshall, K. L., Min, S., Daou, I., Chapleau, M. W., Abboud, F. M., et al. (2018). PIEZOs mediate neuronal sensing of blood pressure and the baroreceptor reflex. *Science* 362, 464–467. doi: 10.1126/science.aau6324

Conflict of Interest: The authors declare that the research was conducted in the absence of any commercial or financial relationships that could be construed as a potential conflict of interest.

Publisher's Note: All claims expressed in this article are solely those of the authors and do not necessarily represent those of their affiliated organizations, or those of the publisher, the editors and the reviewers. Any product that may be evaluated in this article, or claim that may be made by its manufacturer, is not guaranteed or endorsed by the publisher.

Copyright © 2022 Elsaafien, Harden, Johnson, Kimball, Sheng, Smith, Scott, Frazier, de Kloet and Krause. This is an open-access article distributed under the terms of the Creative Commons Attribution License (CC BY). The use, distribution or reproduction in other forums is permitted, provided the original author(s) and the copyright owner(s) are credited and that the original publication in this journal is cited, in accordance with accepted academic practice. No use, distribution or reproduction is permitted which does not comply with these terms.

frontiers in Physiology

ORIGINAL RESEARCH
published: 25 March 2022
doi: 10.3389/fphys.2022.841076

Arterial Baroreflex Inhibits Muscle Metaboreflex Induced Increases in Effective Arterial Elastance: Implications for Ventricular-Vascular Coupling

*Joseph Mannozzi, Jong-Kyung Kim, Javier A. Sala-Mercado, Mohamed-Hussein Al-Hassan, Beruk Lessanework, Alberto Alvarez, Louis Massoud, Tauheed Bhatti, Kamel Aoun and Donal S. O'Leary**

Department of Physiology, Wayne State University School of Medicine, Detroit, MI, United States

OPEN ACCESS

Edited by:
James Todd Pearson, National Cerebral and Cardiovascular Center, Japan

Reviewed by:
Takuya Nishikawa, National Cerebral and Cardiovascular Center, Japan
Kazunori Uemura, National Cerebral and Cardiovascular Center, Japan

***Correspondence:**
Donal S. O'Leary
doleary@med.wayne.edu

Specialty section:
This article was submitted to Integrative Physiology, a section of the journal Frontiers in Physiology

Received: *21 December 2021*
Accepted: *18 February 2022*
Published: *25 March 2022*

Citation:
Mannozzi J, Kim J-K, Sala-Mercado JA, Al-Hassan M-H, Lessanework B, Alvarez A, Massoud L, Bhatti T, Aoun K and O'Leary DS (2022) Arterial Baroreflex Inhibits Muscle Metaboreflex Induced Increases in Effective Arterial Elastance: Implications for Ventricular-Vascular Coupling. Front. Physiol. 13:841076. doi: 10.3389/fphys.2022.841076

The ventricular-vascular relationship assesses the efficacy of energy transferred from the left ventricle to the systemic circulation and is quantified as the ratio of effective arterial elastance to maximal left ventricular elastance. This relationship is maintained during exercise via reflex increases in cardiovascular performance raising both arterial and ventricular elastance in parallel. These changes are, in part, due to reflexes engendered by activation of metabosensitive skeletal muscle afferents—termed the muscle metaboreflex. However, in heart failure, ventricular-vascular uncoupling is apparent and muscle metaboreflex activation worsens this relationship through enhanced systemic vasoconstriction markedly increasing effective arterial elastance which is unaccompanied by substantial increases in ventricular function. This enhanced arterial vasoconstriction is, in part, due to significant reductions in cardiac performance induced by heart failure causing over—stimulation of the metaboreflex due to under perfusion of active skeletal muscle, but also as a result of reduced baroreflex buffering of the muscle metaboreflex-induced peripheral sympatho-activation. To what extent the arterial baroreflex modifies the metaboreflex-induced changes in effective arterial elastance is unknown. We investigated in chronically instrumented conscious canines if removal of baroreflex input via sino-aortic baroreceptor denervation (SAD) would significantly enhance effective arterial elastance in normal animals and whether this would be amplified after induction of heart failure. We observed that effective arterial elastance (E_a), was significantly increased during muscle metaboreflex activation after SAD (0.4 ± 0.1 mmHg/mL to 1.4 ± 0.3 mmHg/mL). In heart failure, metaboreflex activation caused exaggerated increases in E_a and in this setting, SAD significantly increased the rise in E_a elicited by muscle metaboreflex activation (1.3 ± 0.3 mmHg/mL to 2.3 ± 0.3 mmHg/mL). Thus, we conclude that the arterial baroreflex does buffer muscle metaboreflex induced increases in E_a and this buffering likely has effects on the ventricular-vascular coupling.

Keywords: effective arterial elastance (Ea), arterial baroreflex, muscle metaboreflex activation, ventricular vascular coupling, neural control of cardiovascular system

INTRODUCTION

During prolonged exercise the metabolite balance in active skeletal muscle becomes skewed as a result of an inability to actively remove metabolic waste. These excess metabolites in turn activate metabosensitive skeletal muscle afferents that enhance sympathetic outflow to the heart and peripheral vasculature—termed the muscle metaboreflex (Kaufman et al., 1983, 1984; Sunagawa et al., 1983; Adreani et al., 1985; Stone et al., 1985; Hansen et al., 1994; Boushel et al., 1998; Sala-Mercado et al., 2007; Kaur et al., 2016). The increased sympathetic outflow to the heart induces profound increases in ventricular function and heart rate, which thereby increases cardiac output (Melcher and Donald, 1981; O'Leary et al., 1997, 1999; Augustyniak et al., 2000; Ansorge et al., 2002; Crisafulli et al., 2003, 2006; Sala-Mercado et al., 2014; Mannozzi et al., 2021b). Indeed, during submaximal dynamic exercise increases in cardiac output are the primary mechanism mediating metaboreflex induced increases in arterial pressure as little net peripheral vasoconstriction usually occurs (Hanna and Kaufman, 1985; Sheriff et al., 1990; Kelly et al., 1992; O'Leary et al., 1997, 1999; Crisafulli et al., 2003, 2011; Sala-Mercado et al., 2014; Mannozzi et al., 2021b). Muscle metaboreflex vascular control is restrained via reflex induced β_2 mediated vasodilation, as well as selective arterial baroreflex buffering of peripheral sympatho-activation which combined limits increases in systemic vasoconstriction (Kelly et al., 1992; Kim et al., 2005b; Ky et al., 2013). However, in heart failure the mechanisms mediating muscle metaboreflex pressor responses shifts as a result of an inability to improve ventricular function and cardiac output, not only due to the overarching pathology but also due to profound coronary vasoconstriction which actively restrains increases in cardiac function (Melcher and Donald, 1981; O'Leary et al., 1985; Ansorge et al., 2005; Sala-Mercado et al., 2006; Crisafulli et al., 2007; Coutsos et al., 2013; Mannozzi et al., 2021b). Muscle metaboreflex activation in heart failure now elicits substantial increases in peripheral sympathetic activity that evokes vasoconstriction of even the active skeletal muscle—the very tissue from which the reflex arises (Hanna and Kaufman, 1985; Rotto and Kaufman, 1985; Hammond et al., 2001; Kaur et al., 2017). The exaggerated vascular responses observed in heart failure are, in part, a result of attenuated arterial baroreflex buffering of the muscle metaboreflex (Kim et al., 2005b; Ky et al., 2013). In heart failure the strength of the arterial baroreflex is reduced thereby limiting the ability to buffer metaboreflex—induced sympatho-activation (Chen et al., 1991; Osterziel et al., 1995; Fisher et al., 2005; Kim et al., 2005a,b; Iellamo et al., 2006; Otsuki et al., 2008; Kaur et al., 2015a). These profound changes in arterial baroreflex—muscle metaboreflex interactions in heart failure could have marked effects on effective arterial elastance and thereby impact total systemic perfusion by impeding ventricular—arterial energy transfer.

Ventricular—vascular coupling is an assessment of cardiovascular efficiency wherein energy transfer to and propagation of that energy through the systemic circulation is quantified by assessing changes in arterial and ventricular elastance (Chantler et al., 1985; Burkhoff and Sagawa, 1986; Little and Cheng, 1991; Sved et al., 2000; Loimaala et al., 2003; Kim et al., 2011). These metrics were first developed in part as a mechanism to deduce stroke work (Sunagawa et al., 1985; Thames et al., 1993), and then latter uses and modifications of each metric were used to ascertain aspects of ventricular function (Wyss et al., 1983; Cote et al., 1985; O'Leary, 1985; Burkhoff and Sagawa, 1986; Little and Cheng, 1991; Robert et al., 2000; Sved et al., 2000; Loimaala et al., 2003; Sala-Mercado et al., 2006, 2014; Sheriff, 2006) and the arterial load imposed on the left ventricle—termed effective arterial elastance (E_a) (Chantler et al., 1985; Burkhoff and Sagawa, 1986; Kim et al., 2011; Reddy et al., 2017; Mannozzi et al., 2021b). The latter of these two metrics coupled with measurements of stroke work has been used to deduce the relative maintenance of ventricular-vascular coupling at rest and during exercise in animal models and humans (Kaufman et al., 1982; Chantler et al., 1985; O'Leary, 1985; Burkhoff and Sagawa, 1986; Kass, 2005; Redfield et al., 2005; Chantler and Lakatta, 2012; Reddy et al., 2017; Mannozzi et al., 2021b). Most notably in healthy active subjects alterations in E_a contribute to the maintenance of the ventricular-vascular coupling relationship and that even with additional sympathetic input during exercise, such as with muscle metaboreflex activation, the relative changes in E_a favor improvements in stroke work (Melcher and Donald, 1981; Sala-Mercado et al., 2014; Mannozzi et al., 2020, 2021b). However, in heart failure the ventricular-vascular relationship is significantly uncoupled at rest and this relationship unravels further with reflex sympathetic activation as increases in E_a remain unmatched due to an inability to improve ventricular function and thus the ability to improve stroke work is stifled (Melcher and Donald, 1981; Sala-Mercado et al., 2006; Mannozzi et al., 2021b).

The significant increases in E_a observed during sympathetic activation during exercise in normal and heart failure subjects are a result of large increases in heart rate but also though significant increases in peripheral vasoconstriction (Mannozzi et al., 2021b), both of which are not only affected by muscle metaboreflex activation but also likely modified by arterial baroreflex function during exercise (Augustyniak et al., 1985; Hanna and Kaufman, 1985; O'Leary and Augustyniak, 1998; Farquhar et al., 2000; Hammond et al., 2001; Ichinose et al., 2002; Kim et al., 2005a,b; Iellamo et al., 2006; Ky et al., 2013; Kaur et al., 2015a,b, 2018; Jozwiak et al., 2019; Mannozzi et al., 2021b). To date, no study has evaluated the relative contribution of arterial baroreflex buffering of muscle metaboreflex induced increases on E_a and stroke work. Furthermore, the relative assessment of these variables also pertains to the level of control the arterial baroreflex exerts that inhibits or engenders muscle metaboreflex maintenance of ventricular-vascular coupling during exercise. We hypothesize that the arterial baroreflex likely restrains muscle metaboreflex induced increases in E_a. In heart failure, arterial baroreflex function is significantly attenuated and thus the ability to restrain increases in E_a will be reduced and could thereby contribute to enhanced ventricular-vascular uncoupling observed during muscle metaboreflex activation in heart failure.

MATERIALS AND METHODS

Experimental Subjects

10 mongrel canines of either sex of 18–25 kg were selected based on their willingness to run on a motor driven treadmill at 3.2 km/h with 0% grade. We have previously shown that gender does not influence the strength or mechanisms of muscle metaboreflex activation (Limberg et al., 2015). Additionally, studies in young adults have shown that gender does not significantly impact baroreflex mediated responses (Furlan et al., 1998; Kim et al., 2004). All animals in this study underwent a 14-day acclimatization to laboratory spaces and personnel prior to any volitional exercise and surgical procedures. Five of the 11 animals were selected to undergo sino-aortic barodenervation via two separate anesthetic events after completion of control experiments. All surgical and experimental protocols outlined in this study were reviewed and approved by the Wayne State University Institute for the Care and Use Committee (IUCAC) and meet requirements set by the National Institutes of Health Guide to the Care and Use of Laboratory Animals.

Surgical Instrumentation

All animals utilized in this study underwent a series of two surgical procedures with a minimum of 14 days to recover between procedures. The anesthetic and analgesic regimen for all surgical procedures is as follows; animals were initially anesthetized using Thiopental sodium (25 mg/kg) and maintained using isoflurane gas (1.5–2.5%). Analgesia was maintained by application of a fentanyl patch (TD 125–150 μg/h) preoperatively and left for 3 days. To prevent infection prophylactic antibiotics Cephazolin (500 mg IV) was administered during the procedure and Cephalexin (30 mg/kg) was administered after twice daily by mouth. Additional analgesic management was provided during the recovery from each procedure by administration of buprenorphine (0.015 mg/kg IV) and acepromazine (0.1 mg/kg IM) on an as needed basis. All anesthetic, analgesic and surgical procedures performed in this study have been used previously (Hanna and Kaufman, 1985; Augustyniak et al., 2000; Hammond et al., 2001; Kim et al., 2005a,b; Sala-Mercado et al., 2006, 2014; Ky et al., 2013).

The first surgical procedure was a left thoracotomy in which a 20PAU flow probe (Transonic Systems, Ithaca NY) was placed on the ascending aorta for measures of cardiac output and 3 stainless steel pacing electrodes were sutured to the apex of the left ventricle for induction of heart failure via rapid ventricular pacing at 225–245 bpm for 25–30 days. In this procedure unrelated to the current study two sonomicrometry crystals (Ontario, Canada) were implanted into the myocardium, a 3PSB flow probe (Transonic Systems, Ithaca NY) was placed on the circumflex artery. The pericardium was reapproximated and the chest was closed in layers. All cables and leads were exteriorized dorsally between the scapulae. Animals were given a minimum of 14 days to recover prior to the next procedure.

The second surgical procedure utilized a left retroperitoneal approach for placement of a 10PAU blood flow probe (Transonic Systems, Ithaca, NY) on the terminal aorta to measure hindlimb blood flow. Caudally to the flow probe a vascular occluder (Invivo Metric, Healdsburg CA) was placed to induce progressive reductions in hindlimb blood flow to elicit the muscle metaboreflex during exercise. Cranially to the flow probe a 19-gauge polyvinyl catheter (Tygon, S54-HL, Norton) was placed for measures of mean arterial pressure. Unrelated to the current study a 4PSB flow probe (Transonic Systems, Ithaca, NY) was placed on the renal artery. Additionally, 7 animals in this study during this procedure were instrumented with a 19-gauge polyvinyl catheter (Tygon, S54-HL, Norton) in the jugular vein for measures unrelated to the current study. The surgical site was closed in layers and all cables, catheters and occluder lines were tunneled subcutaneously and exteriorized dorsally between the scapulae. Animals were given 14 days minimally to recover prior to any experimental protocols.

Sino-Aortic Baroreceptor Denervation (SAD) consisted of two additional anesthetic events in five animals after completion of control experimental protocols utilizing the same anesthetic and analgesic methods described above. Removal of sino-aortic baroreceptor input was achieved through bilateral transection of the aortic depressor and carotid sinus nerves as previously described by Sheriff et al. (1987), Kim et al. (2005b), and Ky et al. (2013). Animals were given a minimum of 7 days to recover prior to transection of the contralateral side of the previous procedure. All five animals received 7 days minimally after the second transection to recovery prior to any experimental procedures. Functional assessments of denervation were ascertained via lack of any significant change in heart rate in response to increases in arterial pressure ($>$ 30 mmHg) induced i.v., infusion of phenylephrine.

Placement of a Central Venous Catheter was performed during the second procedure in animals which did not undergo SAD by placing a catheter in the jugular vein and advancing it to the atrial caval junction. In subjects that underwent SAD the CVP catheter was placed during the SAD procedure in the same manner as the control animals. The central venous catheter was used to assess central venous pressure.

Experimental Procedures and Data Acquisition

All experiments were performed minimally 14 days after the second surgical procedure or minimally 7 days after the second SAD procedure. All animals served as their own control within their separate experimental groups. These groups were divided as follows: 5 animals performed control experiments prior to immediate induction of heart failure via rapid ventricular pacing ($Control_{group}$). The second group also contained 5 animals which after completion of control experiments underwent SAD and then repeated all the control experiments prior to induction of heart failure (SAD_{group}). For each experiment animals were brought to the laboratory space and acclimated to the environment and personnel for 15–30 min prior to the beginning of the experiment. Once the experiment began the animals flow probes were connected to bench top flow meters (Transonic Systems, Ithaca NY) and catheters were connected to pressure transducers (Transpac IV; Abbott Laboratories, Abbot

Park IL). The pressure transducers were connected to a Gould recording system model RS3800 (Dataq, Akron Ohio). All data was acquired in Windaq (Dataq, Akron Ohio) acquisition software. Heart rate was determined using a cardiotachometer that was triggered by the peak cardiac output signal. One-minute steady state values were taken during rest, exercise (3.2 km/h with 0% grade), and during exercise (3.2 km/h with 0% grade) with sequential reductions in hindlimb blood flow to elicit the muscle metaboreflex in a controlled repeatable fashion using the hindlimb vascular occluder. These experiments were repeated after induction of heart failure via rapid ventricular pacing at a rate of 225–245 bpm for 25–30 days in the $Control_{group}$ animals. In the SAD_{group} animals, experiments were repeated after SAD prior to heart failure induction and then repeated after.

Metaboreflex Activation

The muscle metaboreflex is a sympathetically mediated response elicited by buildup of metabolic waste in active skeletal muscle (Kaufman et al., 1983, 1984; Mittelstadt et al., 1985; Stone et al., 1985; Boushel et al., 1998; Hammond et al., 2001; Kaur et al., 2016). This reflex was first discovered as a result of circulatory occlusion of exercising voluntary muscles in humans (Alam, 1937) which continues to be used as a technique to investigate this reflex across a variety of models (White, 1981; Iellamo et al., 1997; Hammond et al., 2000; Ichinose et al., 2002, 2017; Crisafulli et al., 2003, 2006, 2007, 2011; Edwards et al., 2008; Fisher et al., 2010; Hart et al., 2010; Choi et al., 2012, 2013; Antunes-Correa et al., 2014; Boulton et al., 2018; Cristina-Oliveira et al., 2020). Studies in canines show that the muscle metaboreflex is not tonically active at low workloads inasmuch as hindlimb blood flow must be reduced below a critical threshold level before reflex responses are observed (Hanna and Kaufman, 1985; Rotto and Kaufman, 1985; Kelly et al., 1992; O'Leary et al., 1997; Augustyniak et al., 2000; Hammond et al., 2001; Kaur et al., 2015b, 2017; Mannozzi et al., 2020). As workload increases, this threshold becomes closer and closer to the normal prevailing level of blood flow such that at relatively moderate workloads no threshold is often observed indicating that this reflex is tonically active (Hanna and Kaufman, 1985; Hammond et al., 2001). After induction of heart failure, during moderate exercise hindlimb blood flow is well below the threshold as ascribed in control experiments. Thus, indicating that at least a portion of the excessive sympatho-activation seen during moderate exercise in heart failure is due to excessive activation of the muscle metaboreflex (Hanna and Kaufman, 1985; Kelly et al., 1992; Augustyniak et al., 2000; Hammond et al., 2001; Kaur et al., 2015b). Thus, the use of artificially induced metabolite accumulation in active skeletal muscle via partial reductions in blood flow affords a repeatable, reproducible manner in which to understand muscle metaboreflex characteristics with and without disease.

Data Analysis

One-minute steady state averages of cardiac output, heart rate, mean arterial pressure, hindlimb blood flow, and other data unrelated to this study was exported into excel and calculations of additional hemodynamic parameters were completed. Steady state averages were taken after a 3-min acclimatization period at each workload, rest, exercise, and exercise with each reduction in hindlimb blood flow.

Calculations

Stroke Volume = Cardiac output/heart rate

Non-Ischemic Vascular Resistance (NIVR)—an assessment of the resistance of the entire vascular system that subtracts the contribution of the ischemic hindlimb.

NIVR = mean arterial pressure/(cardiac output – hindlimb blood flow)

Effective Arterial Elastance (E_a) = NIVR × heart rate

Stroke Work = (Stroke Volume/1,000) × mean arterial pressure

Statistics

Systat Software (Systat 13.0) was used for statistical analyses. Data were analyzed using a Two-way ANOVA for repeated measures within each group ($Control_{group}$, SAD_{group}) where each animal in each group served as its own control. No direct assessments were performed across groups comparing $Control_{group}$ to SAD_{group} except for assessing the relative change between normal heart failure and heart failure with SAD. When a significant interaction was observed, individual means were compared using a C matrix test for simple effects and a modified Bonferroni was used as a *post-hoc* test. The relative change in one variable between two states within the same group was assessed using a Students Paired *t*-test after determining the variables normality using a Shapiro-Wilks test. For the assessment of relative change between normal heart failure and heart failure with SAD a Welches *t*-test was used after determining the variables normality using a Shapiro-Wilks test. All data are reported as means ± standard error of the mean. Statistical significance was determined by an α level of $P < 0.05$.

RESULTS

Figure 1 shows the average hemodynamic responses in the $Control_{group}$ at rest, exercise, and exercise with muscle metaboreflex activation (MMA) before and after induction of heart failure. In healthy subjects during the transition from rest to exercise significant increases in heart rate, stroke volume, cardiac output, and hindlimb blood flow occurred. No significant change in mean arterial pressure occurred during the transition from rest to exercise. Non-ischemic vascular resistance was significantly reduced with exercise. In response to muscle metaboreflex activation, heart rate, stroke volume, cardiac output, and mean arterial pressure all significantly increased whereas, no significant change in non-ischemic vascular resistance occurred. Hindlimb blood flow was significantly reduced with muscle metaboreflex activation as a result of inflation of the hindlimb vascular occluders. At rest after induction of heart failure, stroke volume, cardiac output, mean arterial pressure and hindlimb blood flow were all significantly lower than the control values. During steady state mild exercise after the induction of heart failure, heart rate, stroke volume, cardiac output, mean arterial pressure and hindlimb blood flow all increased vs. the values observed at rest. Non ischemic vascular resistance was

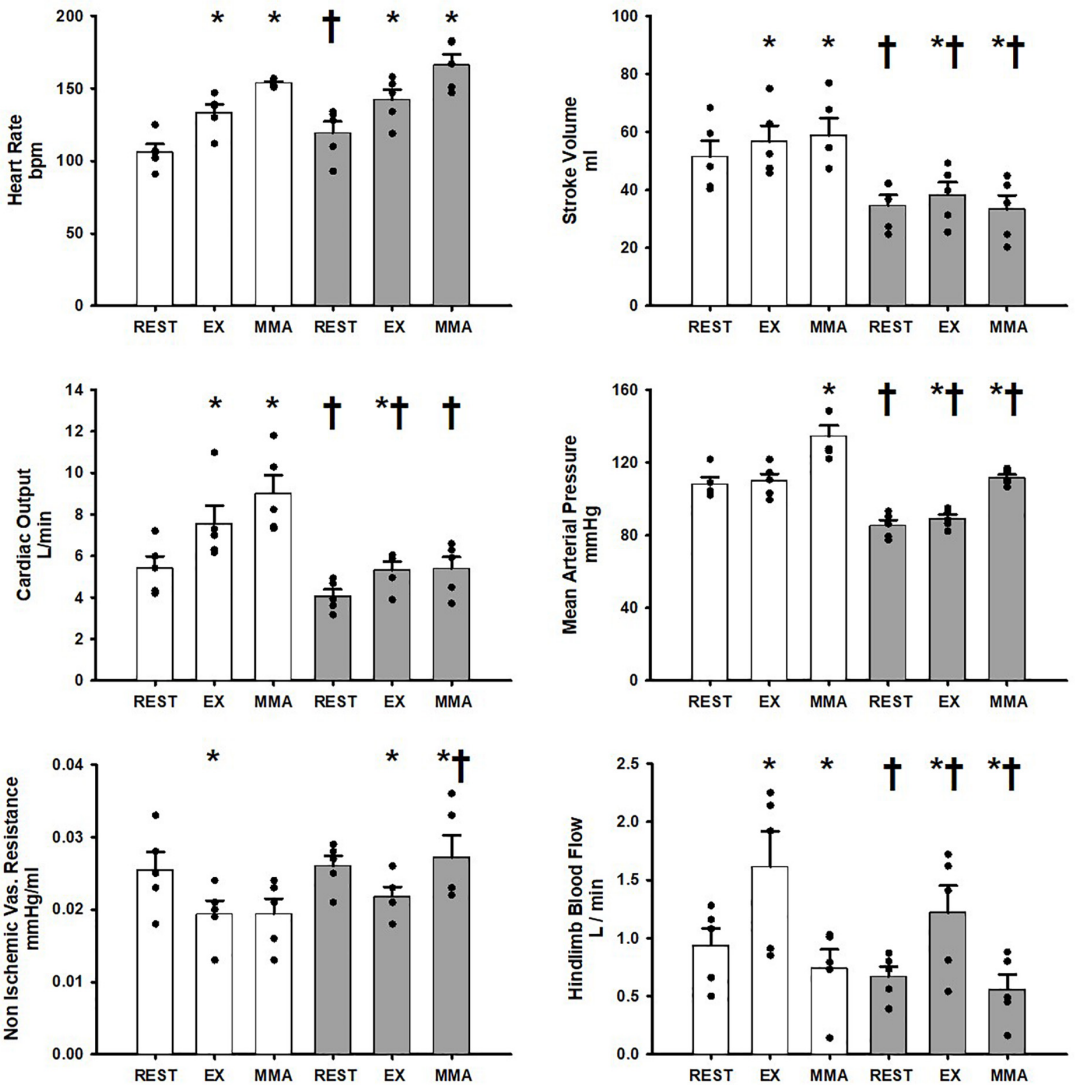

FIGURE 1 | Average 1-min steady state hemodynamics from the $Control_{group}$ at rest, exercise (EX), and exercise with muscle metaboreflex activation (MMA) before (white) and after induction of heart failure (gray). Data are reported as means with standard error. Observed data points are overlain on corresponding bar graphs. Statistical significance vs. previous workload is depicted as * and vs. previous condition as † where $P < 0.05$. ($N = 5$).

significantly reduced in the transition from rest to exercise. Although, significant increases in stroke volume, cardiac output, mean arterial pressure and hindlimb blood flow occurred with exercise in heart failure, all of these values were significantly reduced vs. control. No significant changes as a result of heart failure induction were observed in heart rate, and non-ischemic vascular resistance during exercise. Hindlimb blood flow was significantly reduced in heart failure during muscle metaboreflex activation when compared to control. Muscle metaboreflex activation after induction of heart failure caused significant increases in heart rate and mean arterial pressure whereas stroke volume was significantly reduced. Non-Ischemic vascular resistance increased significantly with Muscle metaboreflex activation in heart failure and was significantly greater when compared to control. After induction of heart failure, muscle metaboreflex activation failed to induce any significant increase in cardiac output which remained significantly lower than the corresponding value in control. Furthermore, during muscle metaboreflex activation in heart mean arterial pressure and stroke volume were reduced relative to control.

Figure 2 shows the hemodynamic responses in the SAD_{group} during rest, exercise, and muscle metaboreflex activation. All of the control hemodynamics of the SAD_{group} from rest to exercise and exercise to muscle metaboreflex activation show the same significant changes as from the $Control_{group}$ (Control data for both $Control_{group}$ and SAD_{group} shown in white in both **Figures 1**, **2**). After SAD (orange bars) all resting baseline values were the same except for a significant increase in heart rate and a significant reduction in stroke volume. After SAD significant increases in heart rate, stroke volume, cardiac output, and hindlimb blood flow occurred with exercise similarly as in the $Control_{group}$. A significant reduction in non-ischemic

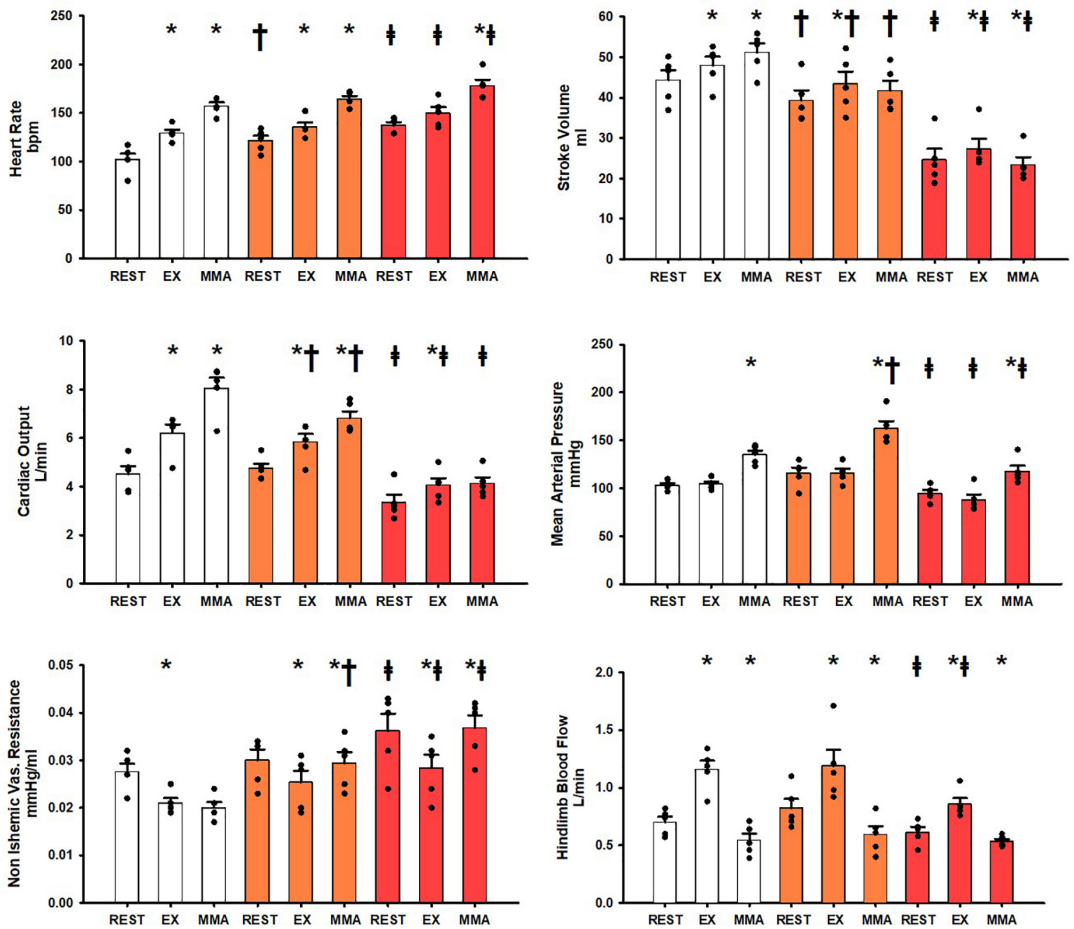

FIGURE 2 | Average 1-min steady state hemodynamics from the SAD_{group} at rest, exercise (EX), and exercise with muscle metaboreflex activation (MMA) before (white) an after SAD (orange) and after induction of heart failure post SAD (red). Data are reported as means with standard error. Observed data points are overlain on corresponding bar graphs. Statistical significance vs. previous workload depicted as * where $P < 0.05$. Comparisons of the condition of SAD vs. control depicted as † where $P < 0.05$. Comparisons of the condition of heart failure vs. SAD depicted as ‡ where $P < 0.05$. ($N = 5$).

vascular resistance was observed, while no significant change was observed in mean arterial pressure with exercise. SAD significantly reduced cardiac output and stroke volume during exercise relative to control. With muscle metaboreflex activation after SAD, significant increases in heart rate, cardiac output, mean arterial pressure, and non-ischemic vascular conductance were observed. No significant change was observed in stroke volume. SAD induced significant reductions in stroke volume and cardiac output during exercise and muscle metaboreflex activation relative to control. A significant increase in non-ischemic vascular resistance was observed during muscle metaboreflex activation as a result of SAD relative to control. Heart failure (red) induction induced significant reductions in stroke volume, cardiac output, mean arterial pressure, and hindlimb blood flow, in the SAD_{group} baseline resting values. Conversely significant increases in heart rate, and non-ischemic vascular resistance were observed at rest after induction of heart failure relative to SAD (orange). In response to exercise after induction of heart failure in the SAD_{group}, significant increases in stroke work, cardiac output, and hindlimb blood flow occurred. No significant change was observed in heart rate, and significant reductions in non-ischemic vascular resistance were observed. Heart failure induced significant reductions in stroke volume, cardiac output, mean arterial pressure, and hindlimb blood flow relative to control. Non-ischemic vascular resistance was significantly increased during exercise after induction of heart failure relative to control. In the transition from exercise to muscle metaboreflex activation in heart failure significant increases in heart rate, mean arterial pressure, and non-ischemic vascular resistance occurred. Conversely a significant reduction in stroke volume occurred while no significant increase in cardiac output occurred in response to muscle metaboreflex activation during heart failure. Heart failure induction after SAD induced significant reductions in stroke volume, mean arterial pressure, and cardiac output during muscle metaboreflex activation whereas heart failure induced significant increases in non-ischemic vascular resistance and heart rate. There was no significant difference between hindlimb blood flow during metaboreflex activation in SAD or SAD after induction of heart failure.

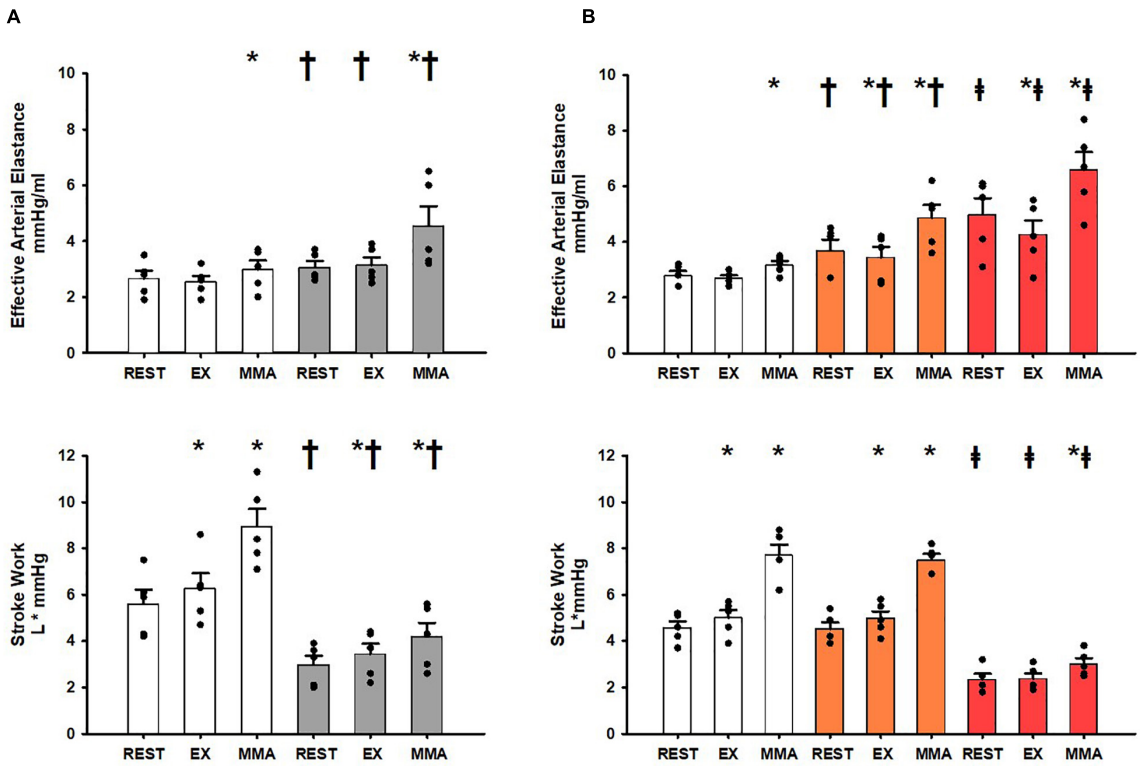

FIGURE 3 | (A) Average 1-min steady state values of Effective Arterial Elastance and Stroke Work in the $Control_{group}$ at rest, exercise (EX), and exercise with muscle metaboreflex activation (MMA) before (white) and after induction of heart failure (gray). Statistical significance vs. previous workload depicted * and vs. previous condition as † where $P < 0.05$. ($N = 5$). **(B)** Average 1-min steady state values of Effective Arterial Elastance and Stroke Work in the SAD_{group} at res, exercise (EX), and exercise with muscle metaboreflex activation (MMA) before (white) and after SAD (orange), and after heart failure induction post SAD (red). Statistical significance vs. previous workload depicted as * where $P < 0.05$. Comparisons of the condition of SAD vs. control depicted as † where $P < 0.05$. Comparisons of the condition of heart failure vs. SAD depicted as ‡ where $P < 0.05$. ($N = 5$) Data for **(A,B)** are reported as means with standard error. Observed data points are overlain on corresponding bar graphs.

Figure 3A shows the changes in a component (E_a) and an index (stroke work) of ventricular-vascular coupling at rest, exercise, and muscle metaboreflex activation in both the $Control_{group}$ before (white) and after induction of heart failure (gray). In response to mild exercise no significant changes occurred in E_a whereas stroke work was significantly increased. With muscle metaboreflex activation significant increases in stroke work and E_a occurred albeit the increase in E_a was small but this is likely a result of this conservative assessment of E_a as shown previously by Mannozzi et al. (2020, 2021b). After induction of heart failure significant increases in E_a were only in response to muscle metaboreflex activation. E_a during rest, exercise, and muscle metaboreflex activation was significantly increased relative to control. Stroke Work was significantly lower in rest, exercise, and muscle metaboreflex activation after induction of heart failure, however, significant increases in the responses from rest to exercise and exercise to muscle metaboreflex activation were observed. **Figure 3B** shows the changes in E_a and stroke work in the SAD_{group} before (white) and after SAD (orange) as well as with SAD after induction of heart failure (red). Responses in E_a and stroke work before SAD in normal animals were similar to the $Control_{group}$. After SAD (orange) Ea was significantly increased at all workloads relative to control whereas stroke work was not significantly different at rest or during exercise or muscle metaboreflex activation relative to SAD_{group} control. Significant increases were observed between exercise and muscle metaboreflex activation in both E_a and stroke work, furthermore the increase in E_a was significantly greater compared to SAD_{group} control. After induction of heart failure (red) E_a was significantly enhanced, and stroke work was significantly attenuated at all workloads relative to control. In response to exercise E_a was significantly reduced and no significant change was observed in stroke work. With muscle metaboreflex activation in heart failure, significant increases in E_a and stroke work occurred, however, the level of stroke work observed during muscle metaboreflex activation was significantly attenuated and the level of E_a was significantly increases relative to SAD (orange).

Figure 4 shows the relative change from exercise to muscle metaboreflex activation in the assessments of ventricular-vascular coupling; E_a and stroke work. **Figure 4A** shows the relative change in control and heart failure in the $Control_{group}$ where the change in E_a was significantly increased and the change in stroke work was significantly attenuated in heart failure. **Figure 4B** shows the relative change before and after SAD. SAD caused a significant increase in the relative change of E_a from exercise

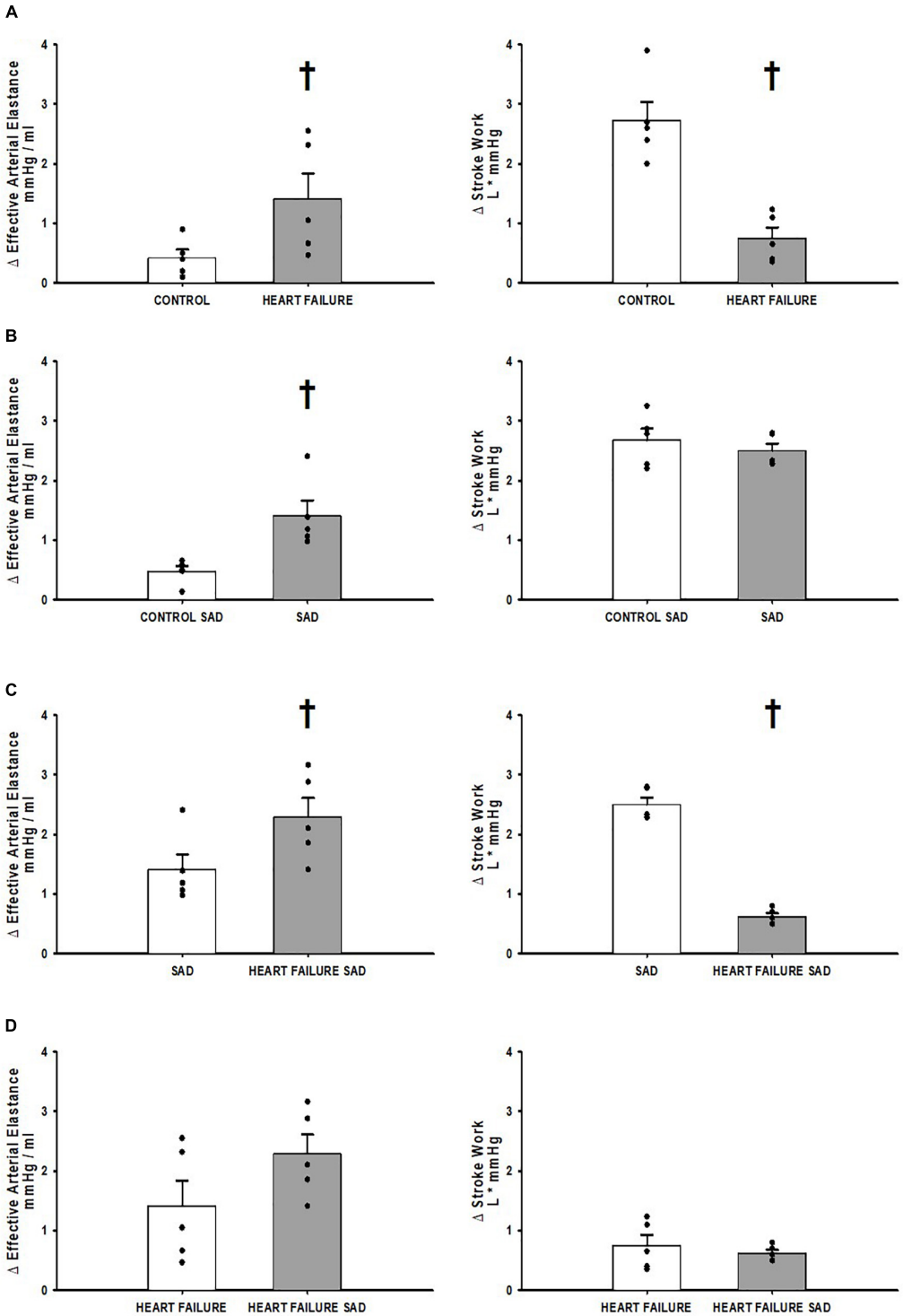

FIGURE 4 | (A) The relative change in Effective Arterial Elastance and Stroke Work in the transition from exercise to exercise with muscle metaboreflex activation before (white) and after induction of heart failure (gray) in the $Control_{group}$. **(B)** The relative change in Effective Arterial Elastance and Stroke Work in the transition from exercise to exercise with muscle metaboreflex activation before (white) and after SAD (gray) in the SAD_{group}. **(C)** The relative change in Effective Arterial Elastance and Stroke Work in the transition from exercise to exercise with muscle metaboreflex activation in normal animals with SAD (white) and after induction of heart failure post SAD (gray) in the SAD_{group}. **(D)** The relative change in Effective Arterial Elastance and Stroke Work in the transition from exercise to exercise with muscle metaboreflex activation in heart failure animals from the $Control_{group}$ (white) and heart failure animals post SAD from the SAD_{group} (gray). For all panels data are reported as means with standard error where data points are overlain on corresponding bar graphs. Statistical significance vs. the previous state as †where $P < 0.05$. An $N = 5$ was used for each bar graph in every panel.

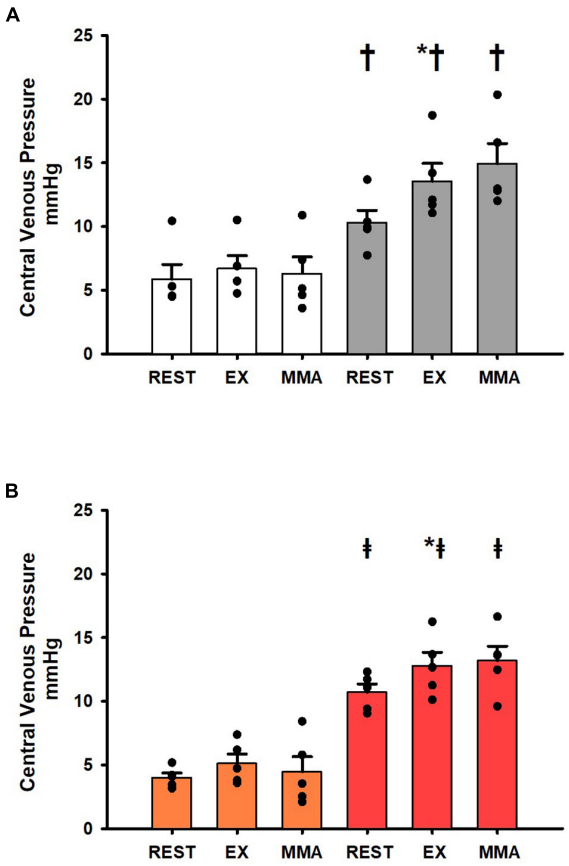

FIGURE 5 | (A) Average 1-min steady state values of central venous pressure from the $Control_{group}$ at rest, exercise (EX), and exercise with muscle metaboreflex activation (MMA) before (white) and after induction of heart failure (gray). Data are reported as means with standard error. Observed data points are overlain on corresponding bar graphs. Statistical significance vs. previous workload is depicted as * and vs. previous condition as † where $P < 0.05$. ($N = 5$). **(B)** Average 1-min steady state values of central venous pressure from the SAD_{group} at rest, exercise (EX), and exercise with muscle metaboreflex activation (MMA) after SAD (orange) and after induction of heart failure post SAD (red). Data are reported as means with standard error. Observed data points are overlain on corresponding bar graphs. Statistical significance vs. previous workload depicted as * where $P < 0.05$. Comparisons of the condition of SAD vs. Heart failure SAD depicted as ‡ where $P < 0.05$. ($N = 5$).

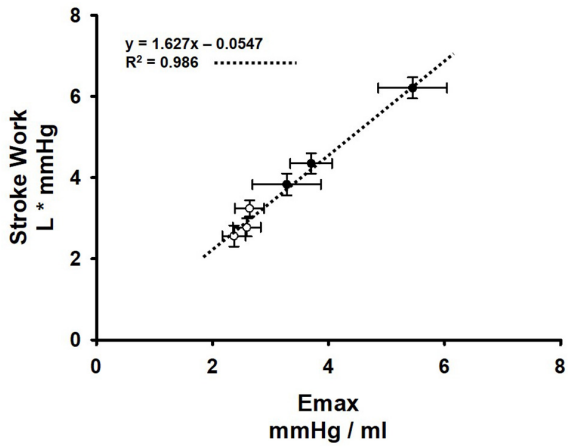

FIGURE 6 | Relationship between ventricular maximal elastance (Emax) and stroke work before (black circles) and after induction of heart failure (white circles) at rest, mild exercise, and muscle metaboreflex activation. A linear regression (dotted line) was performed on these points. and the R_2 value are shown on the plot. Error bars depict standard error of the mean in both directions (Data points were calculated from primary data collected in experiments which were reported in Coutsos et al. (2010, 2013) ($N = 6$).

to muscle metaboreflex activation with no significant change in stroke work. **Figure 4C** shows the relative change in the SAD_{group} between SAD prior to and after induction of heart failure. Significant increases in the relative change of E_a were observed in the heart failure group relative to control. The relative change in stroke work was significantly less in heart failure when compared to control. **Figure 4D** is a comparison of the relative change in heart failure from the $Control_{group}$ and the SAD_{group}. This assessment was done using a Welches *t*-test for assumed unequal variances due to the different treatment of SAD. The SAD heart failure E_a response was larger but not significantly different from control. Furthermore, no significant relative change from exercise to muscle metaboreflex activation in stroke work was observed.

Figure 5 shows the changes in central venous pressure at rest, exercise, and exercise with muscle metaboreflex activation in both the $Control_{group}$ and SAD_{group} before and after induction of heart failure. No significant changes were observed in central venous pressure across rest, exercise, and exercise with muscle metaboreflex activation before induction of heart failure (**Figure 5A**). After induction of heart failure central venous pressure was significantly increased across all settings. Furthermore, central venous pressure significantly increased from rest to exercise, however, there was no change in CVP with metaboreflex activation. These changes in CVP with exercise and metaboreflex activation before and after induction of heart failure were similar after SAD (**Figure 5B**).

DISCUSSION

This is the first study to quantify arterial baroreflex restraint of muscle metaboreflex-induced increases in effective arterial elastance and how this interaction changes after the induction of heart failure. We observed that the arterial baroreflex significantly buffers muscle metaboreflex—induced increases in E_a likely via restraint of peripheral vasoconstriction. This buffering could contribute importantly to the ability to raise cardiac output inasmuch as large increases in E_a act to inhibit effective energy transfer from the heart to the vasculature. Despite the large increases in E_a with metaboreflex activation in normal animals after SAD, stroke work was well maintained. This is likely due to large increases in ventricular contractility as we have previously shown that in baro-intact animals metaboreflex activation causes substantial increases in ventricular maximal elastance (O'Leary et al., 1985, 1999; Sala-Mercado et al., 2006, 2014). Furthermore, we observed that in heart failure, E_a is significantly enhanced as

previously described (Mannozzi et al., 2021b). The rise in E_a with metaboreflex activation after SAD in heart failure tended to be greater (p = 0.07, **Figure 4D**) suggesting that although arterial baroreflex buffering capacity in heart failure is attenuated, some degree of restraint may be maintained.

Arterial Baroreflex—Muscle Metaboreflex Interaction

The arterial baroreflex is the primary mechanism maintaining homeostatic blood pressure through postural changes and exercise (Mitchell et al., 1983; Ferguson et al., 1992; Farquhar et al., 2000; DiCarlo and Bishop, 2001; Ichinose et al., 2002, 2008; Iellamo et al., 2006, 2013; Joyner, 2006; Edwards et al., 2008; Greaney et al., 2014; Kaur et al., 2015a; Jozwiak et al., 2019). Moreover, the arterial baroreflex has been previously described as a buffer for muscle metaboreflex induced pressor responses during exercise (Sheriff et al., 1987; Ichinose et al., 2002, 2008, 2015; Kim et al., 2005a,b; Iellamo et al., 2006, 2013; Joyner, 2006; Edwards et al., 2008; Fisher et al., 2010; Ky et al., 2013; Kaur et al., 2015a, 2018; Fu and Ogoh, 2019). The arterial baroreflex modulates pressure through dynamic control of both the parasympathetic and sympathetic arms of the autonomic system. First and foremost, baroreflex function modulates parasympathetic activity to induce rapid changes in heart rate to modify cardiac output and therefore blood pressure (Vianna et al., 1985; Little and Cheng, 1993; Osterziel et al., 1995; Segers et al., 2002; Iellamo et al., 2006; Joyner, 2006; Harthmann et al., 2007; Edwards et al., 2008; Chen et al., 2010; Walley, 2016; Al-Khateeb et al., 2017). Secondarily, the arterial baroreflex modulates sympathetic activity to the heart and peripheral vasculature to maintain blood pressure (Mitchell et al., 1983; Ferguson et al., 1992; Sheriff et al., 1998; Farquhar et al., 2000; DiCarlo and Bishop, 2001; Zucker, 2006; Greaney et al., 2014; Walley, 2016; Jozwiak et al., 2019). The latter of these two mechanisms of blood pressure regulation is likely the primary mechanism by which the arterial baroreflex alters the muscle metaboreflex induced pressor responses during exercise (Kim et al., 2005b; Ky et al., 2013).

The muscle metaboreflex induces profound increases in blood pressure during exercise primarily through robust increases in ventricular maximal elastance and heart rate which thereby increases cardiac output and blood pressure (Melcher and Donald, 1981; Drew et al., 1985; Rotto and Kaufman, 1985; Olivier and Stephenson, 1993; O'Leary et al., 1999; Augustyniak et al., 2000; Crisafulli et al., 2003, 2006, 2011; Boushel, 2010; Mannozzi et al., 2021b). The metaboreflex also exerts control over the peripheral vasculature by both eliciting paradoxical β_2 mediated peripheral vasodilation via release of epinephrine from the adrenal glands and counteracting sympathetic vasoconstriction of inactive vascular beds as well as the coronary circulation and even the active skeletal muscle (Coutsos et al., 2010, 2013; Hanna and Kaufman, 1985; Augustyniak et al., 2000; Hammond et al., 2001; Najjar et al., 2004; Ansorge et al., 2005; Kaur et al., 2015b, 2017, 2018). The net results are a little marked change in total peripheral resistance which is reflected by only small increases in E_a. When left unchecked by the arterial baroreflex, the muscle metaboreflex is capable of marked peripheral vasoconstriction including within the active skeletal muscle itself which thereby amplifies the metaboreflex responses causing large increases in E_a (Kelly et al., 1992; Kim et al., 2005b; Ky et al., 2013; Kaur et al., 2015a,b, 2017). Therefore, baroreflex restraint of metaboreflex pressor responses occurs primarily via inhibition of peripheral vasoconstriction. Thus, the much greater metaboreflex pressor response after SAD stems from substantial systemic vasoconstriction now joining the large increases in cardiac output which then can produce profound increases in arterial blood pressure (Sheriff et al., 1987; Kim et al., 2005b; Ky et al., 2013).

In heart failure, the ability to raise ventricular function during metaboreflex activation is markedly impaired, both due to the inherent ventricular dysfunction as well as heightened reflex coronary vasoconstriction (Coutsos et al., 2010, 2013; Hanna and Kaufman, 1985; Hammond et al., 2001; Ansorge et al., 2002, 2005). In contrast to normal individuals, in heart failure substantial peripheral vasoconstriction now occurs with metaboreflex activation (Najjar et al., 2004; Kim et al., 2005b; Crisafulli et al., 2007; Ky et al., 2013). This is likely due to impaired baroreflex buffering of peripheral sympatho-activation (Kim et al., 2005b; Ky et al., 2013). During metaboreflex activation in heart failure this enhanced systemic vasoconstriction coupled with increased tachycardia causes significantly greater increases in E_a from the already elevated levels. This shift in metaboreflex mechanisms toward peripheral vasoconstriction in heart failure remains after SAD, with a modest increase in the vasoconstrictor response and thus increases in E_a. Thus, in contrast to the normal condition, SAD does not markedly alter the mechanisms of metaboreflex response, just allows some exaggeration of peripheral vasoconstriction which indicates a reduced role of the baroreflex in modifying the metaboreflex in heart failure. This is supported by the changes in E_a observed.

Implications for Ventricular-Vascular Coupling

Ventricular-vascular coupling is a dynamic interplay between ventricular and vascular components ensuring adequate transfer and systemic propagation of ventricular work. Maintenance of this relationship is paramount to the ability to adequately provide systemic perfusion while enduring orthostatic postural changes and maintaining workload performance during exercise. A significant shift in ether the ability to maintain ventricular function, i.e., ventricular maximal elastance (Emax) or maintain an appropriate effective arterial elastance will ultimately upend this relationship, such as occurs in aging populations, heart failure, and hypertension (Kaufman et al., 1982; Chantler et al., 1985; Cote et al., 1985; O'Leary, 1985; Eichhorn et al., 1992; Laprad et al., 1999; Fadel, 2015; Chantler, 2017; Faconti et al., 2017) and thus may compromise the ability to maintain cardiovascular control during normal activities of daily life. These intolerances may be caused by both aberrant arterial baroreflex and muscle metaboreflex function.

In normal animals during muscle metaboreflex activation, we observed that little increase in Ea occurs and in previous studies we showed that Emax increases substantially with metaboreflex activation (Coutsos et al., 2010, 2013). Thus, the ventricular-vascular coupling ratio (E_a/Emax) declines which favors the large increases in cardiac output and stroke work seen in the present and previous studies (Sala-Mercado et al., 2006, 2014; Mannozzi et al., 2021b). Stroke work can be affected by a number of factors including ventricular preload, afterload, and contractility. There were no effects of SAD or muscle metaboreflex activation on ventricular preload as reflected by the changes in CVP (**Figure 5**). **Figure 6** shows primary data which were obtained in a previous study (Coutsos et al., 2013) now replotted anew describing the relationship between Emax and stroke work ($n = 6$). Shown are the average values at rest, mild exercise, and muscle metaboreflex activation before (closed circles) and after (open circles) the induction of heart failure. In these settings there was a markedly linear relationship between Emax and stroke work: as Emax rose with exercise and metaboreflex activation, highly proportional increases in stroke work also occurred ($R^2 = 0.986$). In the present study or previous studies, we have not measured Emax after SAD, however we could calculate SW. In the normal animal after SAD, large increases in E_a occurred with similar increases in SW. Assuming the relationship shown in **Figure 6** holds after SAD, this would indicate a similar increase in Emax occurred after SAD as previously shown in normal animals at this workload (Sala-Mercado et al., 2006, 2014). Thus, with a larger increase in E_a and little change in Emax, the ventricular—vascular relationship would become slightly less efficient thereby limiting the increase in cardiac output, as was observed (**Figure 2**). In heart failure, E_a is substantially increased at rest (**Figure 1**) and Emax is markedly attenuated (Sala-Mercado et al., 2006, 2014), thus the ventricular – vascular relationship is uncoupled causing a lower cardiac output (Sala-Mercado et al., 2006, 2014; Mannozzi et al., 2021b; **Figure 2**). In response to muscle metaboreflex activation, E_a increases substantially (**Figure 1**) however Emax is little changed (Sala-Mercado et al., 2006, 2014) which thereby further uncouples an already unbalanced ventricular—vascular relationship. After SAD, with metaboreflex activation the rise in E_a tended to be even more exaggerated (**Figure 4**, panel D, ΔE_a $p = 0.07$ heart failure vs. heart failure + SAD) and given the same small increase in stroke work, any small rise in Emax is likely little changed (**Figure 6**) from that observed in baro-intact animals (Sala-Mercado et al., 2006, 2014) therefore the substantially uncoupled ventricular-vascular relationship persists, preventing any increase in cardiac output.

Limitations

We utilized imposed reductions in hindlimb blood flow to activate the muscle metaboreflex during mild exercise, a setting wherein little, if any, tonic activation of this reflex exists in normal subjects (Hanna and Kaufman, 1985; Augustyniak et al., 2001; O'Leary et al., 2004). However, in heart failure, hindlimb blood flow during exercise is low and often well below any threshold level necessary to activate the reflex. In this setting, metaboreflex responses are similar as those seen in normal subjects when hindlimb blood flow is reduced to similar levels (Hammond et al., 2001). So, whereas the methods we used artificially activate the metaboreflex, the responses observed likely reflect those seen with natural reflex stimulation. Recent studies in humans indicate that skeletal muscle afferents are activated at relatively low workloads and thus contribute to the normal cardiovascular responses to mild exercise and that this contribution is exaggerated in patients with heart failure (White, 1981; Amann et al., 1985, 2014; Barbosa et al., 2016).

In these studies, we measured CVP as an index of ventricular preload. However, CVP is not left ventricular end diastolic pressure. Thus, it is possible that changes in left ventricular preload did occur which could affect stroke work. However, **Figure 6** shows a highly linear relationship between stroke work and Emax. spanning rest to exercise and metaboreflex activation before after induction of heart failure, therefore if preload changes did occur, it appears that the major factor affecting stroke work in these studies would be Emax and the resultant changes in ventricular-vascular coupling.

CONCLUSION

We conclude that the arterial baroreflex actively restrains muscle metaboreflex induced increases in E_a. This likely contributes to the ability of the muscle metaboreflex to preserve and even optimize the ventricular-vascular relationship through robust increases in ventricular elastance that are not overshadowed by effective arterial elastance (Melcher and Donald, 1981; Sala-Mercado et al., 2006, 2014; Mannozzi et al., 2021b). In heart failure, arterial baroreflex buffering of metaboreflex-induced sympatho-activation is reduced and thus contributes to an enhanced E_a during exercise. However, complete removal of the arterial baroreflex in heart failure reveled that a degree of restraint is intact likely preserving what little ventricular-vascular coupling remains. To what degree this restraint could be improved to further maintain or even restore some amount of ventricular-vascular coupling is unknown. Previous studies focused on the benefits of exercise regimes on the restoration of cardiac and autonomic function have shown promise in improving baroreflex function (Adreani et al., 1985; Andrade et al., 1985; Iellamo et al., 2007; Besnier et al., 2017; Mannozzi et al., 2021a) and this may be a mechanism of improving the ventricular-vascular coupling relationship in various cardiovascular pathologies.

DATA AVAILABILITY STATEMENT

The raw data supporting the conclusions of this article will be made available by the authors, without undue reservation.

ETHICS STATEMENT

The animal study was reviewed and approved by the Wayne State University Institute for the Care and Use Committee (IUCAC).

AUTHOR CONTRIBUTIONS

DO'L and JM contributed to conception, design of research, performed the experiments, interpreted results of experiments, and drafted the manuscript. DO'L, JM, J-KK, M-HA-H, BL, AA, LM, TB, JS-M, and KA analyzed the data and performed the experiments. JM prepared the figures. DO'L, J-KK, M-HA-H, and JM edited and revised the manuscript. All authors approved final version of manuscript.

FUNDING

This work was supported by the National Heart, Lung, and Blood Institute grants HL-055473, HL-126706, and HL-120822.

ACKNOWLEDGMENTS

We thank Audrey Nelson, Jody Helm-Day, and Sue Harris for expert technical assistance and animal care.

REFERENCES

Adreani, C. M., Hill, J. M., and Kaufman, M. P. (1985). Responses of group III and IV muscle afferents to dynamic exercise. *J. Appl. Physiol.* 82, 1811–1817. doi: 10.1152/jappl.1997.82.6.1811

Al-Khateeb, A. A., Limberg, J. K., Barnes, J. N., Joyner, M. J., Charkoudian, N., and Curry, T. B. (2017). Acute cyclooxygenase inhibition and baroreflex sensitivity in lean and obese adults. *Clin. Auton. Res.* 27, 17–23. doi: 10.1007/s10286-016-0389-z

Alam, M. S. F. (1937). Observations in man upon a blood pressure raising reflex arising from the voluntary muscles. *J. Physiol.* 89, 372–383. doi: 10.1113/jphysiol.1937.sp003485

Amann, M., Blain, G. M., Proctor, L. T., Sebranek, J. J., Pegelow, D. F., and Dempsey, J. A. (1985). Group III and IV muscle afferents contribute to ventilatory and cardiovascular response to rhythmic exercise in humans. *J. Appl. Physiol.* 109, 966–976. doi: 10.1152/japplphysiol.00462.2010

Amann, M., Venturelli, M., Ives, S. J., Morgan, D. E., Gmelch, B., Witman, M. A., et al. (2014). Group III/IV muscle afferents impair limb blood in patients with chronic heart failure. *Int. J. Cardiol.* 174, 368–375. doi: 10.1016/j.ijcard.2014.04.157

Andrade, D. C., Arce-Alvarez, A., Toledo, C., Diaz, H. S., Lucero, C., Schultz, H. D., et al. (1985). Exercise training improves cardiac autonomic control, cardiac function, and arrhythmogenesis in rats with preserved-ejection fraction heart failure. *J. Appl. Physiol.* 123, 567–577. doi: 10.1152/japplphysiol.00189.2017

Ansorge, E. J., Augustyniak, R. A., Perinot, M. L., Hammond, R. L., Kim, J. K., Sala-Mercado, J. A., et al. (2005). Altered muscle metaboreflex control of coronary blood flow and ventricular function in heart failure. *Am. J. Physiol. Heart Circ. Physiol.* 288, H1381–H1388. doi: 10.1152/ajpheart.00985.2004

Ansorge, E. J., Shah, S. H., Augustyniak, R. A., Rossi, N. F., Collins, H. L., and O'Leary, D. S. (2002). Muscle metaboreflex control of coronary blood flow. *Am. J. Physiol. Heart Circ. Physiol.* 283, H526–H532.

Antunes-Correa, L. M., Nobre, T. S., Groehs, R. V., Alves, M. J., Fernandes, T., Couto, G. K., et al. (2014). Molecular basis for the improvement in muscle metaboreflex and mechanoreflex control in exercise-trained humans with chronic heart failure. *Am. J. Physiol. Heart Circ. Physiol.* 307, H1655–H1666. doi: 10.1152/ajpheart.00136.2014

Augustyniak, R. A., Ansorge, E. J., Kim, J. K., Sala-Mercado, J. A., Hammond, R. L., Rossi, N. F., et al. (1985). Cardiovascular responses to exercise and muscle metaboreflex activation during the recovery from pacing-induced heart failure. *J. Appl. Physiol.* 101, 14-22. doi: 10.1152/japplphysiol.00072.2006

Augustyniak, R. A., Ansorge, E. J., and O'Leary, D. S. (2000). Muscle metaboreflex control of cardiac output and peripheral vasoconstriction exhibit different latencies. *Am. J. Physiol. Heart Circ. Physiol.* 278, H530–H537. doi: 10.1152/ajpheart.2000.278.2.H530

Augustyniak, R. A., Collins, H. L., Ansorge, E. J., Rossi, N. F., and O'Leary, D. S. (2001). Severe exercise alters the strength and mechanisms of the muscle metaboreflex. *Am. J. Physiol. Heart Circ. Physiol.* 280, H1645–H1652. doi: 10.1152/ajpheart.2001.280.4.H1645

Barbosa, T. C., Vianna, L. C., Fernandes, I. A., Prodel, E., Rocha, H. N., Garcia, V. P., et al. (2016). Intrathecal fentanyl abolishes the exaggerated blood pressure response to cycling in hypertensive men. *J. Physiol.* 594, 715–725. doi: 10.1113/JP271335

Besnier, F., Labrunee, M., Pathak, A., Pavy-Le Traon, A., Gales, C., Senard, J. M., et al. (2017). Exercise training-induced modification in autonomic nervous system: an update for cardiac patients. *Ann. Phys. Rehabil. Med.* 60, 27–35. doi: 10.1016/j.rehab.2016.07.002

Boulton, D., Taylor, C. E., Green, S., and Macefield, V. G. (2018). The metaboreflex does not contribute to the increase in muscle sympathetic nerve activity to contracting muscle during static exercise in humans. *J. Physiol.* 596, 1091–1102. doi: 10.1113/JP275526

Boushel, R. (2010). Muscle metaboreflex control of the circulation during exercise. *Acta. Physiol. (Oxf)* 199, 367–383. doi: 10.1111/j.1748-1716.2010.02133.x

Boushel, R., Madsen, P., Nielsen, H. B., Quistorff, B., and Secher, N. H. (1998). Contribution of pH, diprotonated phosphate and potassium for the reflex increase in blood pressure during handgrip. *Acta. Physiol. Scand.* 164, 269–275. doi: 10.1046/j.1365-201X.1998.00429.x

Burkhoff, D., and Sagawa, K. (1986). Ventricular efficiency predicted by an analytical model. *Am. J. Physiol.* 250, R1021–R1027. doi: 10.1152/ajpregu.1986.250.6.R1021

Chantler, P. D. (2017). Arterial ventricular uncoupling with age and disease and recoupling with exercise. *Exerc. Sport Sci. Rev.* 45, 70–79. doi: 10.1249/JES.0000000000000100

Chantler, P. D., and Lakatta, E. G. (2012). Arterial-ventricular coupling with aging and disease. *Front. Physiol.* 3:90. doi: 10.3389/fphys.2012.00090

Chantler, P. D., Lakatta, E. G., and Najjar, S. S. (1985). Arterial-ventricular coupling: mechanistic insights into cardiovascular performance at rest and during exercise. *J. Appl. Physiol.* 105, 1342-1351. doi: 10.1152/japplphysiol.90600.2008

Chen, J. S., Wang, W., Bartholet, T., and Zucker, I. H. (1991). Analysis of baroreflex control of heart rate in conscious dogs with pacing-induced heart failure. *Circulation* 83, 260–267. doi: 10.1161/01.cir.83.1.260

Chen, X., Sala-Mercado, J. A., Hammond, R. L., Ichinose, M., Soltani, S., Mukkamala, R., et al. (2010). Dynamic control of maximal ventricular elastance via the baroreflex and force-frequency relation in awake dogs before and after pacing-induced heart failure. *Am. J. Physiol. Heart Circ. Physiol.* 299, H62–H69. doi: 10.1152/ajpheart.00922.2009

Choi, H. M., Stebbins, C. L., Lee, O. T., Nho, H., Lee, J. H., Chun, J. M., et al. (2013). Augmentation of the exercise pressor reflex in prehypertension: roles of the muscle metaboreflex and mechanoreflex. *Appl. Physiol. Nutr. Metab.* 38, 209–215. doi: 10.1139/apnm-2012-0143

Choi, H. M., Stebbins, C. L., Nho, H., Kim, K. A., Kim, C., and Kim, J. K. (2012). Skeletal muscle metaboreflex is enhanced in postmenopausal women. *Eur. J. Appl. Physiol.* 112, 2671–2678. doi: 10.1007/s00421-011-2245-0

Cote, A. T., Bredin, S. S., Phillips, A. A., Koehle, M. S., Glier, M. B., Devlin, A. M., et al. (1985). Left ventricular mechanics and arterial-ventricular coupling following high-intensity interval exercise. *J. Appl. Physiol.* 115, 1705-1713. doi: 10.1152/japplphysiol.00576.2013

Coutsos, M., Sala-Mercado, J. A., Ichinose, M., Li, Z., Dawe, E. J., and O'Leary, D. S. (2010). Muscle metaboreflex-induced coronary vasoconstriction functionally limits increases in ventricular contractility. *J. Appl. Physiol.* 109, 271-278. doi: 10.1152/japplphysiol.01243.2009

Coutsos, M., Sala-Mercado, J. A., Ichinose, M., Li, Z., Dawe, E. J., and O'Leary, D. S. (2013). Muscle metaboreflex-induced coronary vasoconstriction limits ventricular contractility during dynamic exercise in heart failure. *Am. J. Physiol. Heart Circ. Physiol.* 304, H1029–H1037. doi: 10.1152/ajpheart.00879.2012

Crisafulli, A., Piras, F., Filippi, M., Piredda, C., Chiappori, P., Melis, F., et al. (2011). Role of heart rate and stroke volume during muscle metaboreflex-induced cardiac output increase: differences between activation during and after exercise. *J. Physiol. Sci.* 61, 385–394. doi: 10.1007/s12576-011-0163-x

Crisafulli, A., Salis, E., Pittau, G., Lorrai, L., Tocco, F., Melis, F., et al. (2006). Modulation of cardiac contractility by muscle metaboreflex following efforts of different intensities in humans. *Am. J. Physiol. Heart Circ. Physiol.* 291, H3035–H3042. doi: 10.1152/ajpheart.00221.2006

Crisafulli, A., Salis, E., Tocco, F., Melis, F., Milia, R., Pittau, G., et al. (2007). Impaired central hemodynamic response and exaggerated vasoconstriction during muscle metaboreflex activation in heart failure patients. *Am. J. Physiol. Heart Circ. Physiol.* 292, H2988–H2996. doi: 10.1152/ajpheart.00008.2007

Crisafulli, A., Scott, A. C., Wensel, R., Davos, C. H., Francis, D. P., Pagliaro, P., et al. (2003). Muscle metaboreflex-induced increases in stroke volume. *Med. Sci. Sports Exerc.* 35, 221–228. doi: 10.1249/01.MSS.0000048639.02548.24

Cristina-Oliveira, M., Meireles, K., Spranger, M. D., O'Leary, D. S., Roschel, H., and Pecanha, T. (2020). Clinical safety of blood flow-restricted training? A comprehensive review of altered muscle metaboreflex in cardiovascular disease during ischemic exercise. *Am. J. Physiol. Heart Circ. Physiol.* 318, H90–H109. doi: 10.1152/ajpheart.00468.2019

DiCarlo, S. E., and Bishop, V. S. (2001). Central baroreflex resetting as a means of increasing and decreasing sympathetic outflow and arterial pressure. *Ann. N Y Acad. Sci.* 940, 324–337. doi: 10.1111/j.1749-6632.2001.tb03688.x

Drew, R. C., Bell, M. P., and White, M. J. (1985). Modulation of spontaneous baroreflex control of heart rate and indexes of vagal tone by passive calf muscle stretch during graded metaboreflex activation in humans. *J. Appl. Physiol.* 104, 716-723. doi: 10.1152/japplphysiol.00956.2007

Edwards, N. C., Ferro, C. J., Townend, J. N., and Steeds, R. P. (2008). Aortic distensibility and arterial-ventricular coupling in early chronic kidney disease: a pattern resembling heart failure with preserved ejection fraction. *Heart* 94, 1038–1043. doi: 10.1136/hrt.2007.137539

Eichhorn, E. J., Willard, J. E., Alvarez, L., Kim, A. S., Glamann, D. B., Risser, R. C., et al. (1992). Are contraction and relaxation coupled in patients with and without congestive heart failure? *Circulation* 85, 2132–2139. doi: 10.1161/01.cir.85.6.2132

Faconti, L., Bruno, R. M., Buralli, S., Barzacchi, M., Dal Canto, E., Ghiadoni, L., et al. (2017). Arterial-ventricular coupling and parameters of vascular stiffness in hypertensive patients: role of gender. *JRSM Cardiovasc. Dis.* 6:2048004017692277. doi: 10.1177/2048004017692277

Fadel, P. J. (2015). Reflex control of the circulation during exercise. *Scand. J. Med. Sci. Sports* 25, 74–82. doi: 10.1111/sms.12600

Farquhar, W. B., Taylor, J. A., Darling, S. E., Chase, K. P., and Freeman, R. (2000). Abnormal baroreflex responses in patients with idiopathic orthostatic intolerance. *Circulation* 102, 3086–3091. doi: 10.1161/01.cir.102.25.3086

Ferguson, D. W., Berg, W. J., Roach, P. J., Oren, R. M., and Mark, A. L. (1992). Effects of heart failure on baroreflex control of sympathetic neural activity. *Am. J. Cardiol.* 69, 523–531. doi: 10.1016/0002-9149(92)90998-e

Fisher, J. P., Bell, M. P., and White, M. J. (2005). Cardiovascular responses to human calf muscle stretch during varying levels of muscle metaboreflex activation. *Exp. Physiol.* 90, 773–781. doi: 10.1113/expphysiol.2005.030577

Fisher, J. P., Seifert, T., Hartwich, D., Young, C. N., Secher, N. H., and Fadel, P. J. (2010). Autonomic control of heart rate by metabolically sensitive skeletal muscle afferents in humans. *J. Physiol.* 588, 1117–1127. doi: 10.1113/jphysiol.2009.185470

Fu, Q., and Ogoh, S. (2019). Sex differences in baroreflex function in health and disease. *J. Physiol. Sci.* 69, 851–859. doi: 10.1007/s12576-019-00727-z

Furlan, R., Jacob, G., Snell, M., Robertson, D., Porta, A., Harris, P., et al. (1998). Chronic orthostatic intolerance: a disorder with discordant cardiac and vascular sympathetic control. *Circulation* 98, 2154–2159. doi: 10.1161/01.cir.98.20.2154

Greaney, J. L., Matthews, E. L., Boggs, M. E., Edwards, D. G., Duncan, R. L., and Farquhar, W. B. (2014). Exaggerated exercise pressor reflex in adults with moderately elevated systolic blood pressure: role of purinergic receptors. *Am. J. Physiol. Heart Circ. Physiol.* 306, H132–H141. doi: 10.1152/ajpheart.00575.2013

Hammond, R. L., Augustyniak, R. A., Rossi, N. F., Churchill, P. C., Lapanowski, K., and O'Leary, D. S. (2000). Heart failure alters the strength and mechanisms of the muscle metaboreflex. *Am. J. Physiol. Heart Circ. Physiol.* 278, H818–H828. doi: 10.1152/ajpheart.2000.278.3.H818

Hammond, R. L., Augustyniak, R. A., Rossi, N. F., Lapanowski, K., Dunbar, J. C., and O'Leary, D. S. (2001). Alteration of humoral and peripheral vascular responses during graded exercise in heart failure. *J. Appl. Physiol.* 90, 55–61. doi: 10.1152/jappl.2001.90.1.55

Hanna, R. L., and Kaufman, M. P. (1985). Role played by purinergic receptors on muscle afferents in evoking the exercise pressor reflex. *J. Appl. Physiol.* 94, 1437–1445. doi: 10.1152/japplphysiol.01011.2002

Hansen, J., Thomas, G. D., Jacobsen, T. N., and Victor, R. G. (1994). Muscle metaboreflex triggers parallel sympathetic activation in exercising and resting human skeletal muscle. *Am. J. Physiol.* 266, H2508–H2514. doi: 10.1152/ajpheart.1994.266.6.H2508

Hart, E. C., Joyner, M. J., Wallin, B. G., Karlsson, T., Curry, T. B., and Charkoudian, N. (2010). Baroreflex control of muscle sympathetic nerve activity: a nonpharmacological measure of baroreflex sensitivity. *Am. J. Physiol. Heart Circ. Physiol.* 298, H816–H822. doi: 10.1152/ajpheart.00924.2009

Harthmann, A. D., De Angelis, K., Costa, L. P., Senador, D., Schaan, B. D., Krieger, E. M., et al. (2007). Exercise training improves arterial baro- and chemoreflex in control and diabetic rats. *Auton. Neurosci.* 133, 115–120. doi: 10.1016/j.autneu.2006.10.004

Ichinose, M., Ichinose-Kuwahara, T., Kondo, N., and Nishiyasu, T. (2015). Increasing blood flow to exercising muscle attenuates systemic cardiovascular responses during dynamic exercise in humans. *Am. J. Physiol. Regul. Integr. Comp. Physiol.* 309, R1234–R1242. doi: 10.1152/ajpregu.00063.2015

Ichinose, M., Ichinose-Kuwahara, T. K., Watanabe, K., Kondo, N., and Nishiyasu, T. (2017). The carotid baroreflex modifies the pressor threshold of the muscle metaboreflex in humans. *Am. J. Physiol. Heart Circ. Physiol.* 313, H650H657. doi: 10.1152/ajpheart.00816.2016

Ichinose, M., Saito, M., Wada, H., Kitano, A., Kondo, N., and Nishiyasu, T. (2002). Modulation of arterial baroreflex dynamic response during muscle metaboreflex activation in humans. *J. Physiol.* 544, 939–948. doi: 10.1113/jphysiol.2002.024794

Ichinose, M., Sala-Mercado, J. A., O'Leary, D. S., Hammond, R. L., Coutsos, M., Ichinose, T., et al. (2008). Spontaneous baroreflex control of cardiac output during dynamic exercise, muscle metaboreflex activation, and heart failure. *Am. J. Physiol. Heart Circ. Physiol.* 294, H1310–H1316. doi: 10.1152/ajpheart.01187.2007

Iellamo, F., Di Rienzo, M., Lucini, D., Legramante, J. M., Pizzinelli, P., Castiglioni, P., et al. (2006). Muscle metaboreflex contribution to cardiovascular regulation during dynamic exercise in microgravity: insights from mission STS-107 of the space shuttle Columbia. *J. Physiol.* 572, 829–838. doi: 10.1113/jphysiol.2005.102426

Iellamo, F., Legramante, J. M., Raimondi, G., and Peruzzi, G. (1997). Baroreflex control of sinus node during dynamic exercise in humans: effects of central command and muscle reflexes. *Am. J. Physiol.* 272, H1157–H1164. doi: 10.1152/ajpheart.1997.272.3.H1157

Iellamo, F., Manzi, V., Caminiti, G., Sposato, B., Massaro, M., Cerrito, A., et al. (2013). Dose-response relationship of baroreflex sensitivity and heart rate variability to individually-tailored exercise training in patients with heart failure. *Int. J. Cardiol.* 166, 334–339. doi: 10.1016/j.ijcard.2011.10.082

Iellamo, F., Sala-Mercado, J. A., Ichinose, M., Hammond, R. L., Pallante, M., Ichinose, T., et al. (2007). Spontaneous baroreflex control of heart rate during exercise and muscle metaboreflex activation in heart failure. *Am. J. Physiol. Heart Circ. Physiol.* 293, H1929–H1936. doi: 10.1152/ajpheart.00564.2007

Joyner, M. J. (2006). Baroreceptor function during exercise: resetting the record. *Exp. Physiol.* 91, 27–36. doi: 10.1113/expphysiol.2005.032102

Jozwiak, M., Millasseau, S., Richard, C., Monnet, X., Mercado, P., Depret, F., et al. (2019). Validation and critical evaluation of the effective arterial elastance in critically Ill patients. *Crit. Care Med.* 47, e317–e324. doi: 10.1097/CCM.0000000000003645

Kass, D. A. (2005). Ventricular arterial stiffening: integrating the pathophysiology. *Hypertension* 46, 185–193. doi: 10.1161/01.HYP.0000168053.34306.d4

Kaufman, M. P., Iwamoto, G. A., Longhurst, J. C., and Mitchell, J. H. (1982). Effects of capsaicin and bradykinin on afferent fibers with ending in skeletal muscle. *Circ. Res.* 50, 133–139. doi: 10.1161/01.res.50.1.133

Kaufman, M. P., Longhurst, J. C., Rybicki, K. J., Wallach, J. H., and Mitchell, J. H. (1983). Effects of static muscular contraction on impulse activity of groups III and IV afferents in cats. *J. Appl. Physiol. Respir. Environ. Exerc. Physiol.* 55, 105–112. doi: 10.1152/jappl.1983.55.1.105

Kaufman, M. P., Rybicki, K. J., Waldrop, T. G., and Ordway, G. A. (1984). Effect of ischemia on responses of group III and IV afferents to contraction. *J. Appl. Physiol. Respir. Environ. Exerc. Physiol.* 57, 644–650. doi: 10.1152/jappl.1984.57.3.644

Kaur, J., Alvarez, A., Hanna, H. W., Krishnan, A. C., Senador, D., Machado, T. M., et al. (2016). Interaction between the muscle metaboreflex and the arterial baroreflex in control of arterial pressure and skeletal muscle blood flow. *Am. J. Physiol. Heart Circ. Physiol.* 311, H1268–H1276. doi: 10.1152/ajpheart.00501.2016

Kaur, J., Krishnan, A. C., Senador, D., Alvarez, A., Hanna, H. W., and O'Leary, D. S. (2018). Altered arterial baroreflex-muscle metaboreflex interaction in heart failure. *Am. J. Physiol. Heart Circ. Physiol.* 315, H1383–H1392. doi: 10.1152/ajpheart.00338.2018

Kaur, J., Machado, T. M., Alvarez, A., Krishnan, A. C., Hanna, H. W., Altamimi, Y. H., et al. (2015a). Muscle metaboreflex activation during dynamic exercise vasoconstricts ischemic active skeletal muscle. *Am. J. Physiol. Heart Circ. Physiol.* 309, H2145–H2151. doi: 10.1152/ajpheart.00679.2015

Kaur, J., Senador, D., Krishnan, A. C., Hanna, H. W., Alvarez, A., Machado, T. M., et al. (2017). Muscle metaboreflex-induced vasoconstriction in the ischemic active muscle is exaggerated in heart failure. *Am. J. Physiol. Heart Circ. Physiol.* 314, H11-H18. doi: 10.1152/ajpheart.00375.2017

Kaur, J., Spranger, M. D., Hammond, R. L., Krishnan, A. C., Alvarez, A., Augustyniak, R. A., et al. (2015b). Muscle metaboreflex activation during dynamic exercise evokes epinephrine release resulting in beta2-mediated vasodilation. *Am. J. Physiol. Heart Circ. Physiol.* 308, H524–H529. doi: 10.1152/ajpheart.00648.2014

Kelly, R. P., Ting, C. T., Yang, T. M., Liu, C. P., Maughan, W. L., Chang, M. S., et al. (1992). Effective arterial elastance as index of arterial vascular load in humans. *Circulation* 86, 513–521. doi: 10.1161/01.cir.86.2.513

Kim, A., Deo, S. H., Vianna, L. C., Balanos, G. M., Hartwich, D., Fisher, J. P., et al. (2011). Sex differences in carotid baroreflex control of arterial blood pressure in humans: relative contribution of cardiac output and total vascular conductance. *Am. J. Physiol. Heart Circ. Physiol.* 301, H2454–H2465. doi: 10.1152/ajpheart.00772.2011

Kim, J. K., Augustyniak, R. A., Sala-Mercado, J. A., Hammond, R. L., Ansorge, E. J., Rossi, N. F., et al. (2004). Heart failure alters the strength and mechanisms of arterial baroreflex pressor responses during dynamic exercise. *Am. J. Physiol. Heart Circ. Physiol.* 287, H1682–H1688. doi: 10.1152/ajpheart.00358.2004

Kim, J. K., Sala-Mercado, J. A., Rodriguez, J., Scislo, T. J., and O'Leary, D. S. (2005b). Arterial baroreflex alters strength and mechanisms of muscle metaboreflex during dynamic exercise. *Am. J. Physiol Heart Circ. Physiol.* 288, H1374–H1380. doi: 10.1152/ajpheart.01040.2004

Kim, J. K., Sala-Mercado, J. A., Hammond, R. L., Rodriguez, J., Scislo, T. J., and O'Leary, D. S. (2005a). Attenuated arterial baroreflex buffering of muscle metaboreflex in heart failure. *Am. J. Physiol. Heart Circ. Physiol.* 289, H2416–H2423. doi: 10.1152/ajpheart.00654.2005

Ky, B., French, B., May Khan, A., Plappert, T., Wang, A., Chirinos, J. A., et al. (2013). Ventricular-arterial coupling, remodeling, and prognosis in chronic heart failure. . *J. Am. Coll. Cardiol.* 62, 1165–1172. doi: 10.1016/j.jacc.2013.03.085

Laprad, S. L., Augustyniak, R. A., Hammond, R. L., and O'Leary, D. S. (1999). Does gender influence the strength and mechanisms of the muscle metaboreflex during dynamic exercise in dogs? *Am. J. Physiol.* 276, R1203–R1208. doi: 10.1152/ajpregu.1999.276.4.R1203

Limberg, J. K., Taylor, J. L., Mozer, M. T., Dube, S., Basu, A., Basu, R., et al. (2015). Effect of bilateral carotid body resection on cardiac baroreflex control of blood pressure during hypoglycemia. *Hypertension* 65, 1365–1371. doi: 10.1161/HYPERTENSIONAHA.115.05325

Little, W. C., and Cheng, C. P. (1993). Effect of exercise on left ventricular-arterial coupling assessed in the pressure-volume plane. *Am. J. Physiol.* 264, H1629–H1633. doi: 10.1152/ajpheart.1993.264.5.H1629

Little, W. C., and Cheng, C. P. (1991). Left ventricular-arterial coupling in conscious dogs. *Am. J. Physiol.* 261, H70–H76.

Loimaala, A., Huikuri, H. V., Koobi, T., Rinne, M., Nenonen, A., and Vuori, I. (2003). Exercise training improves baroreflex sensitivity in type 2 diabetes. *Diabetes* 52, 1837–1842. doi: 10.2337/diabetes.52.7.1837

Mannozzi, J., Massoud, L., Kaur, J., Coutsos, M., and O'Leary, D. S. (2021b). Ventricular contraction and relaxation rates during muscle metaboreflex activation in heart failure: are they coupled? *Exp. Physiol.* 106, 401–411. doi: 10.1113/EP089053

Mannozzi, J., Al-Hassan, M. H., Lessanework, B., Alvarez, A., Senador, D., and O'Leary, D. S. (2021a). Chronic ablation of trpv1 sensitive skeletal muscle afferents attenuates the muscle metaboreflex. *Am. J. Physiol. Regul. Integr. Comp. Physiol.* 321, R385–R395. doi: 10.1152/ajpregu.00129.2021

Mannozzi, J., Kaur, J., Spranger, M. D., Al-Hassan, M. H., Lessanework, B., Alvarez, A., et al. (2020). Muscle metaboreflex-induced increases in effective arterial elastance: effect of heart failure. *Am. J. Physiol. Regul. Integr. Comp. Physiol.* 319, R1–R10. doi: 10.1152/ajpregu.00040.2020

Melcher, A., and Donald, D. E. (1981). Maintained ability of carotid baroreflex to regulate arterial pressure during exercise. *Am. J. Physiol.* 241, H838–H849. doi: 10.1152/ajpheart.1981.241.6.H838

Mitchell, J. H., Kaufman, M. P., and Iwamoto, G. A. (1983). The exercise pressor reflex: its cardiovascular effects, afferent mechanisms, and central pathways. *Annu. Rev. Physiol.* 45, 229–242. doi: 10.1146/annurev.ph.45.030183.001305

Mittelstadt, S. W., Bell, L. B., O'Hagan, K. P., and Clifford, P. S. (1985). Muscle chemoreflex alters vascular conductance in nonischemic exercising skeletal muscle. *J. Appl. Physiol.* 77, 2761-2766. doi: 10.1152/jappl.1994.77.6.2761

Najjar, S. S., Schulman, S. P., Gerstenblith, G., Fleg, J. L., Kass, D. A., O'Connor, F., et al. (2004). Age and gender affect ventricular-vascular coupling during aerobic exercise. *J. Am. Coll. Cardiol.* 44, 611–617. doi: 10.1016/j.jacc.2004.04.041

O'Leary, D. S. (1985). Autonomic mechanisms of muscle metaboreflex control of heart rate. *J. Appl. Physiol.* 74, 1748–1754. doi: 10.1152/jappl.1993.74.4.1748

O'Leary, D. S., and Augustyniak, R. A. (1998). Muscle metaboreflex increases ventricular performance in conscious dogs. *Am. J. Physiol.* 275, H220–H224. doi: 10.1152/ajpheart.1998.275.1.H220

O'Leary, D. S., Augustyniak, R. A., Ansorge, E. J., and Collins, H. L. (1999). Muscle metaboreflex improves O2 delivery to ischemic active skeletal muscle. *Am. J. Physiol.* 276, H1399–H1403. doi: 10.1152/ajpheart.1999.276.4.H1399

O'Leary, D. S., Rossi, N. F., and Churchill, P. C. (1997). Substantial cardiac parasympathetic activity exists during heavy dynamic exercise in dogs. *Am. J. Physiol.* 273, H2135–H2140. doi: 10.1152/ajpheart.1997.273.5.H2135

O'Leary, D. S., Sala-Mercado, J. A., Augustyniak, R. A., Hammond, R. L., Rossi, N. F., and Ansorge, E. J. (2004). Impaired muscle metaboreflex-induced increases in ventricular function in heart failure. *Am. J. Physiol Heart Circ. Physiol.* 287, H2612–H2618. doi: 10.1152/ajpheart.00604.2004

O'Leary, D. S., Sala-Mercado, J. A., Hammond, R. L., Ansorge, E. J., Kim, J. K., Rodriguez, J., et al. (1985). Muscle metaboreflex-induced increases in cardiac sympathetic activity vasoconstrict the coronary vasculature. *J. Appl. Physiol.* 103, 190–194. doi: 10.1152/japplphysiol.00139.2007

Olivier, N. B., and Stephenson, R. B. (1993). Characterization of baroreflex impairment in conscious dogs with pacing-induced heart failure. *Am. J. Physiol.* 265, R1132–R1140. doi: 10.1152/ajpregu.1993.265.5.R1132

Osterziel, K. J., Hanlein, D., Willenbrock, R., Eichhorn, C., Luft, F., and Dietz, R. (1995). Baroreflex sensitivity and cardiovascular mortality in patients with mild to moderate heart failure. *Heart* 73, 517–522. doi: 10.1136/hrt.73.6.517

Otsuki, T., Maeda, S., Iemitsu, M., Saito, Y., Tanimura, Y., Ajisaka, R., et al. (2008). Systemic arterial compliance, systemic vascular resistance, and effective arterial elastance during exercise in endurance-trained men. *Am. J. Physiol. Regul. Integr. Comp. Physiol.* 295, R228–R235. doi: 10.1152/ajpregu.00009.2008

Reddy, Y. N. V., Andersen, M. J., Obokata, M., Koepp, K. E., Kane, G. C., Melenovsky, V., et al. (2017). Arterial stiffening with exercise in patients with heart failure and preserved ejection fraction. *J. Am. Coll. Cardiol.* 70, 136–148. doi: 10.1016/j.jacc.2017.05.029

Redfield, M. M., Jacobsen, S. J., Borlaug, B. A., Rodeheffer, R. J., and Kass, D. A. (2005). Age- and gender-related ventricular-vascular stiffening: a community-based study. *Circulation* 112, 2254–2262. doi: 10.1161/CIRCULATIONAHA.105.541078

Robert, A. Collins HL, Ansorge EJ, Rossi NF, and O'Leary DS. (2000). Severe exercise alters the strength and mechanisms of the muscle metaboreflex. *Am. J. Physiol. Heart Circ. Physiol.* 280, H1645–H1652.

Rotto, D. M., and Kaufman, M. P. (1985). Effect of metabolic products of muscular contraction on discharge of group III and IV afferents. *J. Appl. Physiol.* 64, 2306–2313. doi: 10.1152/jappl.1988.64.6.2306

Sala-Mercado, J. A., Hammond, R. L., Kim, J. K., McDonald, P. J., Stephenson, L. W., and O'Leary, D. S. (2007). Heart failure attenuates muscle metaboreflex

control of ventricular contractility during dynamic exercise. *Am. J. Physiol. Heart Circ. Physiol.* 292, H2159–H2166. doi: 10.1152/ajpheart.01240.2006

Sala-Mercado, J. A., Hammond, R. L., Kim, J. K., Rossi, N. F., Stephenson, L. W., and O'Leary, D. S. (2006). Muscle metaboreflex control of ventricular contractility during dynamic exercise. *Am. J. Physiol. Heart Circ. Physiol.* 290, H751–H757.

Sala-Mercado, J. A., Moslehpour, M., Hammond, R. L., Ichinose, M., Chen, X., Evan, S., et al. (2014). Stimulation of the cardiopulmonary baroreflex enhances ventricular contractility in awake dogs: a mathematical analysis study. *Am. J. Physiol. Regul. Integr. Comp. Physiol.* 307, R455–R464. doi: 10.1152/ajpregu.00510.2013

Segers, P., Stergiopulos, N., and Westerhof, N. (2002). Relation of effective arterial elastance to arterial system properties. *Am. J. Physiol. Heart Circ. Physiol.* 282, H1041–H1046. doi: 10.1152/ajpheart.00764.2001

Sheriff, D. D. (2006). Baroreflex resetting during exercise: mechanisms and meaning. *Am J Physiol. Heart Circ. Physiol.* 290, H1406–H1407. doi: 10.1152/ajpheart.01275.2005

Sheriff, D. D., Augustyniak, R. A., and O'Leary, D. S. (1998). Muscle chemoreflex-induced increases in right atrial pressure. *Am. J. Physiol.* 275, H767–H775. doi: 10.1152/ajpheart.1998.275.3.H767

Sheriff, D. D., O'Leary, D. S., Scher, A. M., and Rowell, L. B. (1990). Baroreflex attenuates pressor response to graded muscle ischemia in exercising dogs. *Am. J. Physiol.* 258, H305–H310. doi: 10.1152/ajpheart.1990.258.2.H305

Sheriff, D. D., Wyss, C. R., Rowell, L. B., and Scher, A. M. (1987). Does inadequate oxygen delivery trigger pressor response to muscle hypoperfusion during exercise? *Am. J. Physiol.* 253, H1199–H1207. doi: 10.1152/ajpheart.1987.253.5.H1199

Stone, A. J., Copp, S. W., Kim, J. S., and Kaufman, M. P. (1985). Combined, but not individual, blockade of ASIC3, P2X, and EP4 receptors attenuates the exercise pressor reflex in rats with freely perfused hindlimb muscles. *J. Appl. Physiol.* 119, 1330–1336. doi: 10.1152/japplphysiol.00630.2015

Sunagawa, K., Maughan, W. L., Burkhoff, D., and Sagawa, K. (1983). Left ventricular interaction with arterial load studied in isolated canine ventricle. *Am. J. Physiol.* 245, H773–H780. doi: 10.1152/ajpheart.1983.245.5.H773

Sunagawa, K., Maughan, W. L., and Sagawa, K. (1985). Optimal arterial resistance for the maximal stroke work studied in isolated canine left ventricle. *Circ. Res.* 56, 586–595. doi: 10.1161/01.res.56.4.586

Sved, A. F., Ito, S., and Madden, C. J. (2000). Baroreflex dependent and independent roles of the caudal ventrolateral medulla in cardiovascular regulation. *Brain Res. Bull.* 51, 129–133. doi: 10.1016/s0361-9230(99)00234-8

Thames, M. D., Kinugawa, T., Smith, M. L., and Dibner-Dunlap, M. E. (1993). Abnormalities of baroreflex control in heart failure. *J. A. Coll. Cardiol.* 22, A56–A60.

Vianna, L. C., Fernandes, I. A., Barbosa, T. C., Teixeira, A. L., and Nobrega, A. C. L. (1985). Capsaicin-based analgesic balm attenuates the skeletal muscle metaboreflex in healthy humans. *J. Appl. Physiol.* 125, 362-368. doi: 10.1152/japplphysiol.00038.2018

Walley, K. R. (2016). Left ventricular function: time-varying elastance and left ventricular aortic coupling. *Crit. Care* 20:270. doi: 10.1186/s13054-016-1439-6

White, C. W. (1981). Abnormalities in baroreflex control of heart rate in canine heart failure. *Am. J. Physiol.* 240, H793–H799. doi: 10.1152/ajpheart.1981.240.5.H793

Wyss, C. R., Ardell, J. L., Scher, A. M., and Rowell, L. B. (1983). Cardiovascular responses to graded reductions in hindlimb perfusion in exercising dogs. *Am. J. Physiol.* 245, H481–H486. doi: 10.1152/ajpheart.1983.245.3.H481

Zucker, I. H. (2006). Novel mechanisms of sympathetic regulation in chronic heart failure. *Hypertension* 48, 1005–1011. doi: 10.1161/01.HYP.0000246614.47231.25

Conflict of Interest: The authors declare that the research was conducted in the absence of any commercial or financial relationships that could be construed as a potential conflict of interest.

Publisher's Note: All claims expressed in this article are solely those of the authors and do not necessarily represent those of their affiliated organizations, or those of the publisher, the editors and the reviewers. Any product that may be evaluated in this article, or claim that may be made by its manufacturer, is not guaranteed or endorsed by the publisher.

Copyright © 2022 Mannozzi, Kim, Sala-Mercado, Al-Hassan, Lessanework, Alvarez, Massoud, Bhatti, Aoun and O'Leary. This is an open-access article distributed under the terms of the Creative Commons Attribution License (CC BY). The use, distribution or reproduction in other forums is permitted, provided the original author(s) and the copyright owner(s) are credited and that the original publication in this journal is cited, in accordance with accepted academic practice. No use, distribution or reproduction is permitted which does not comply with these terms.

frontiers in Physiology

REVIEW
published: 31 March 2022
doi: 10.3389/fphys.2022.803274

Human Face Perception Using Electroencephalography and Magnetoencephalography

Kensaku Miki[1,2,3], Yasuyuki Takeshima[3], Shoko Watanabe[4] and Ryusuke Kakigi[3]*

[1] Integrative Physiology, College of Nursing, Aichi Medical University, Nagakute, Japan, [2] School of Nursing, Japanese Red Cross Toyota College of Nursing, Toyota, Japan, [3] Department of Integrative Physiology, National Institute for Physiological Sciences, National Institutes of Natural Sciences, Okazaki, Japan, [4] Higashi Owari National Hospital, National Hospital Organization, Nagoya, Japan

OPEN ACCESS

Edited by:
Geoffrey A. Head, Baker Heart and Diabetes Institute, Australia

Reviewed by:
Satoshi Eifuku, Fukushima Medical University, Japan
Seppo P. Ahlfors, Massachusetts General Hospital and Harvard Medical School, United States

***Correspondence:**
Kensaku Miki
miki.kensaku.769@mail.aichi-med-u.ac.jp

Specialty section:
This article was submitted to Integrative Physiology, a section of the journal Frontiers in Physiology

Received: *27 October 2021*
Accepted: *16 February 2022*
Published: *31 March 2022*

Citation:
Miki K, Takeshima Y, Watanabe S and Kakigi R (2022) Human Face Perception Using Electroencephalography and Magnetoencephalography. Front. Physiol. 13:803274. doi: 10.3389/fphys.2022.803274

The face has a large amount of information that is useful for humans in social communication. Recently, non-invasive methods have been used to investigate human brain activity related to perception and cognition processes. Electroencephalography (EEG) and magnetoencephalography (MEG) have excellent temporal resolution and reasonably good spatial resolution. Therefore, they are useful to investigate time sequences of human brain activity related to the face perception process. In this review, we introduce our previous EEG and MEG studies of human face perception that demonstrated the following characteristics of face perception processing: (1) Event-related components in the temporal area related to the activity in the inferior temporal (IT) area, corresponding to the fusiform face area (FFA), are evoked approximately 180 msec after the presentation of a face. The activity in the IT area plays an important role in the detection processing of a face, and the contours of a face affect the activity in the IT areas. (2) Event-related components in the temporal area related to the superior temporal sulcus (STS) activity are larger when eyes are averted than when directly looking into the eyes. (3) The direction of features of a face affects the face perception processing in the right hemisphere. On the other hand, the matching of the direction between the contours and features of a face affects the processing in the left hemisphere. (4) Random dots blinking (RDB), which uses temporal changes in patterns of many small dots to present stimuli without a change in luminance during the presentation of a face, is a useful visual stimulus method to investigate the brain activity related to face perception processing in the IT area using EEG and MEG.

Keywords: electroencephalography (EEG), magnetoencephalography (MEG), face, N170, inferior temporal (IT), superior temporal sulcus (STS)

HIGHLIGHTS

In this review, we discuss the following characteristics of face perception processing based on our previous electroencephalography (EEG) and magnetoencephalography (MEG) studies:

- Event-related components related to the activity in the inferior temporal (IT) area are evoked after the presentation of a face. In addition, the activity in the IT area plays an important role in the detection processing of a face and the contours of a face affect the activity in the IT area.
- Event-related components related to the superior temporal sulcus (STS) activity are larger when eyes are averted than when looking straight.
- The direction of the features of a face affects the face perception processing in the right hemisphere. On the other hand, the matching of the direction between the contours and features of a face affects the processing in the left hemisphere.
- Random dots blinking, which presents stimuli without a change in luminance during the presentation of a face, is a useful visual stimulus method to investigate face perception processing.

INTRODUCTION

Facial information, such as sex, familiarity, and expression, plays an important part in our daily lives. By judging facial information, especially expressions, one can read and sympathize with others' emotions through social interaction. In psychology, human face perception is one of the main topics. Therefore, many studies have been performed and models of human face perception were suggested (e.g., Bruce and Young, 1986).

In addition, there are many studies of human face perception using non-invasive methods for human subjects. Functional magnetic resonance imaging (fMRI) has an excellent spatial resolution that is sufficient to detect activated areas due to an increase in blood flow in the brain areas. Previous fMRI studies on human face perception revealed a specific area related to face perception, termed the fusiform face area (FFA) (for example, Kanwisher et al., 1997).

On the other hand, electroencephalography (EEG) has an excellent temporal resolution. In addition, high-density recordings can provide reasonably good spatial resolution. Therefore, EEG detects time sequences of human face perception. A well-known component related to human face perception is a negative component that occurs at approximately 170 msec after the presentation of a face, which is termed N170 (for example, Bentin et al., 1996). N170 is the most well-known component related to face perception because it is larger for faces than other objects (chair and car). Magnetoencephalography (MEG) also has the excellent temporal and spatial resolution and is equally useful to investigate the face perception process.

In this review, we have introduced a series of previous EEG and MEG studies on human face perception and discussed the following characteristics of face perception processing: (1) the inferior temporal (IT) activity evoked by a face (Watanabe et al., 1999a,b), (2) the effects of face contours and features on processing for face perception (Miki et al., 2007), (3) the effects of eye aversion on event-related potentials (ERPs) (Watanabe et al., 2002), (4) face inversion effects and differences between the right and left hemispheres in face perception (Watanabe et al., 2003; Miki et al., 2011), and (5) a useful visual stimulus method for investigating face perception (Miki et al., 2009).

THE INFERIOR TEMPORAL ACTIVITY EVOKED BY A FACE

A previous study using MEG (Watanabe et al., 1999a) investigated the temporal and spatial characteristic processes in human face perception. Twelve normal adult subjects with normal and corrected visual acuity participated in this study.

During MEG recording, 1M and 2M components were identified for face with opened eyes and face with closed eyes in both hemispheres. The 1M component was identified approximately 132 msec after the presentation of each stimulus and the activity in the occipital area related to primary visual perception represented by a change in luminance was estimated from the 1M component. The 2M component was identified approximately 179 msec after face stimulation (face with opened eyes and face with closed eyes) in ten subjects for each stimulus in the right but in only five subjects in

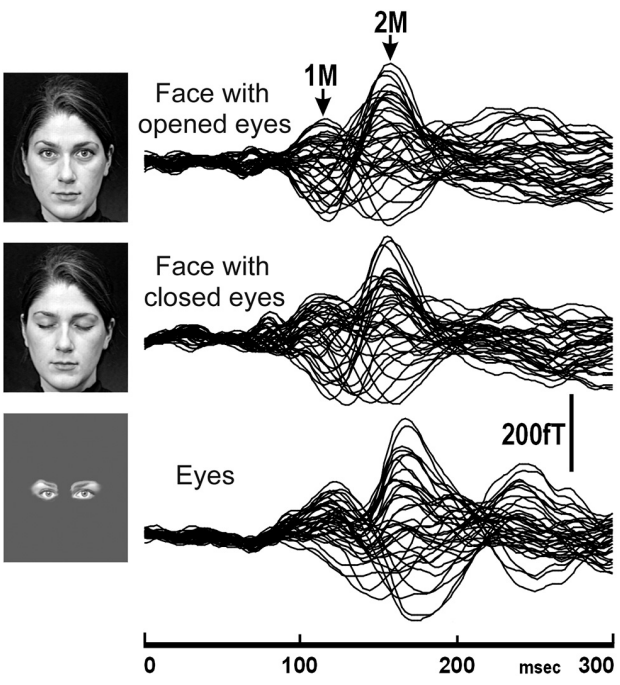

FIGURE 1 | The MEG waveforms of a representative subject in response to the presentation of stimuli, face with opened eyes, face with closed eyes, and eyes recorded from the right hemisphere. The MEG waveforms recorded from 37 channels are superimposed [adopted from Watanabe et al. (1999b)]. MEG, magnetoencephalography.

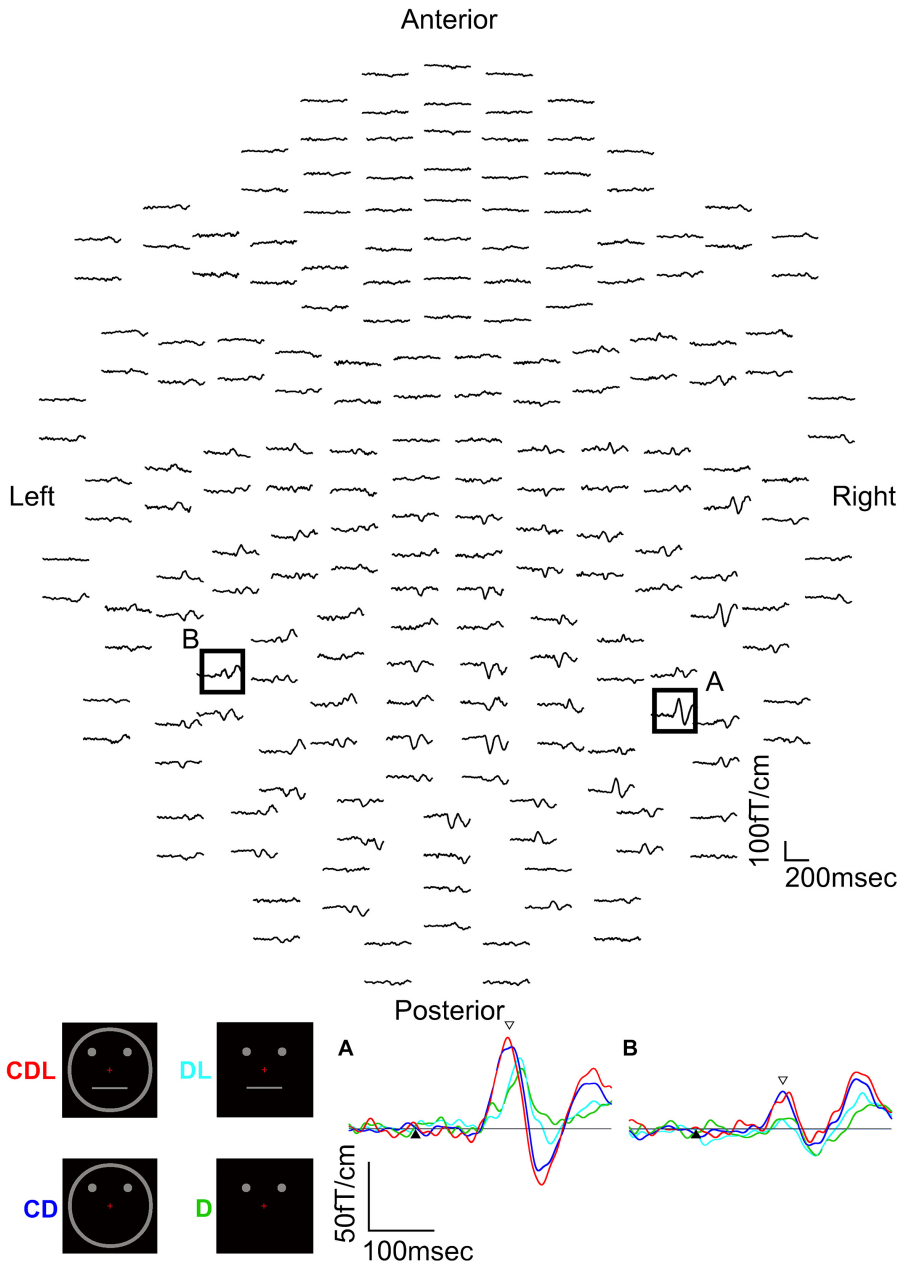

FIGURE 2 | MEG waveforms (upper) of a representative subject following the stimulus onset in the CDL condition. MEG waveforms (lower) at sensors A and B in the upper image show a clear component recorded for CDL, CD, DL, and D in the right and left hemispheres. **(A)** Representative waveforms at sensor A in the right hemisphere of the upper image. **(B)** Representative waveforms at sensor B in the left hemisphere of the upper image. Black arrows show the stimulus onset and white arrows show the response selected for further analysis [adopted from Miki et al. (2007)]. MEG, magnetoencephalography; CDL, contour, dots, and line; CD, contour and dots; DL, dots and line; D, dots only.

the left hemisphere. In addition, there was no significant difference in the 2M latency between face with opened eyes and face with closed eyes. The activity in the IT area around the FFA related to face perception was estimated from the 2M component.

Another previous MEG study (Watanabe et al., 1999b) investigated the difference in temporal and spatial characteristics of processes of perception of faces and eyes in humans. In this study, ten normal adult subjects with normal and corrected visual acuity had participated, and face with opened eyes, face with closed eyes, and eyes were presented (**Figure 1**).

In this study, 2M components were recorded for all subjects for each condition from the right hemisphere (**Figure 1**). On the other hand, a 2M component for eyes was recorded from the left hemisphere in all five subjects who had a clear 2M component for face with opened eyes and face with closed eyes. In both the right

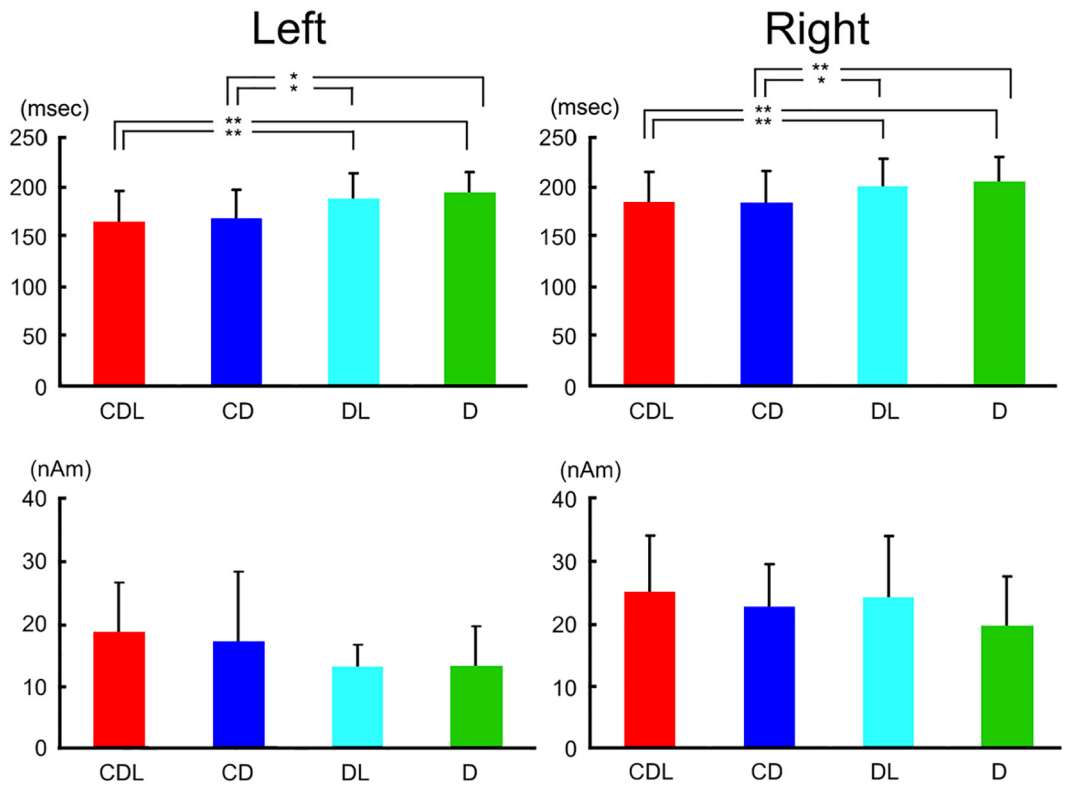

FIGURE 3 | Bar graphs of peak latency (upper) and the maximum amplitude of dipole moment (lower) for all conditions after stimulus onset in the right and left hemispheres. Error bar shows the SD [adopted from Miki et al. (2007)]. *$p < 0.05$ and **$p < 0.01$. SD, standard deviation.

and left hemispheres, the 2M latency for eyes was significantly longer than for face with opened eyes and face with closed eyes.

The above studies (Watanabe et al., 1999a,b) suggested that the MEG components related to IT activity reflect the process of detection of a face.

THE EFFECTS OF FACE CONTOURS AND FEATURES ON PROCESSING FOR FACE PERCEPTION

The above studies (Watanabe et al., 1999a,b) revealed that the IT area is involved in the detection of a face and that a face is detected faster than eyes. However, it is unknown why a face is detected faster than eyes and whether facial contours and features other than eyes are necessary for the rapid detection of a face. Therefore, we used a schematic face and recorded MEG responses evoked in the IT area to investigate the effects of face contours and features on the detection of the face (Miki et al., 2007). We examined thirteen normal adult subjects with normal or corrected visual acuity and presented four visual conditions as follows (**Figure 2**): (1) contour, two dots, and a horizontal line (CDL): a schematic face having contour (circle), eyes (two dots), and a mouth (horizontal line) was presented, (2) contour and two dots (CD): the horizontal line was removed from CDL, (3) two dots and a horizontal line (DL): the circle was removed from CDL, and (4) two dots (D): only two dots were presented (**Figure 2**).

The waveforms were recorded from 204 gradiometers by a 306-channel biomagnetometer in a representative subject following stimulus onset in CDL (**Figure 2**) and the waveforms in all conditions at representative sensors in each hemisphere of the same subject are shown in **Figure 2**. Using a single equivalent current dipole (ECD) model (Hämäläinen et al., 1993), ECDs were estimated in the IT area under all conditions for eleven of thirteen subjects in the right and left hemispheres. When the dipole moment of the estimated dipole was at a maximum after visual stimulus onset, the peak latency was significantly longer for DL and D than for CDL and CD in both hemispheres (**Figure 3**). On the other hand, regarding the maximum dipole moment of IT activity, it was larger for CDL than the others in both hemispheres, but there were no significant differences among conditions in either hemisphere due to the variability between individual subjects (**Figure 3**).

Previous ERP studies reported that it takes longer to recognize an image of the eyes only than the whole face (Bentin et al., 1996; Shibata et al., 2002; Itier et al., 2006). Moreover, Shibata et al. (2002) reported that the latency of N170 evoked by facial features (eye, nose, and mouth) was shorter with facial contours than without. Our study (Miki et al., 2007) is consistent with this study, suggesting that facial contour is one of the most important parts of face perception and shortens the perception process.

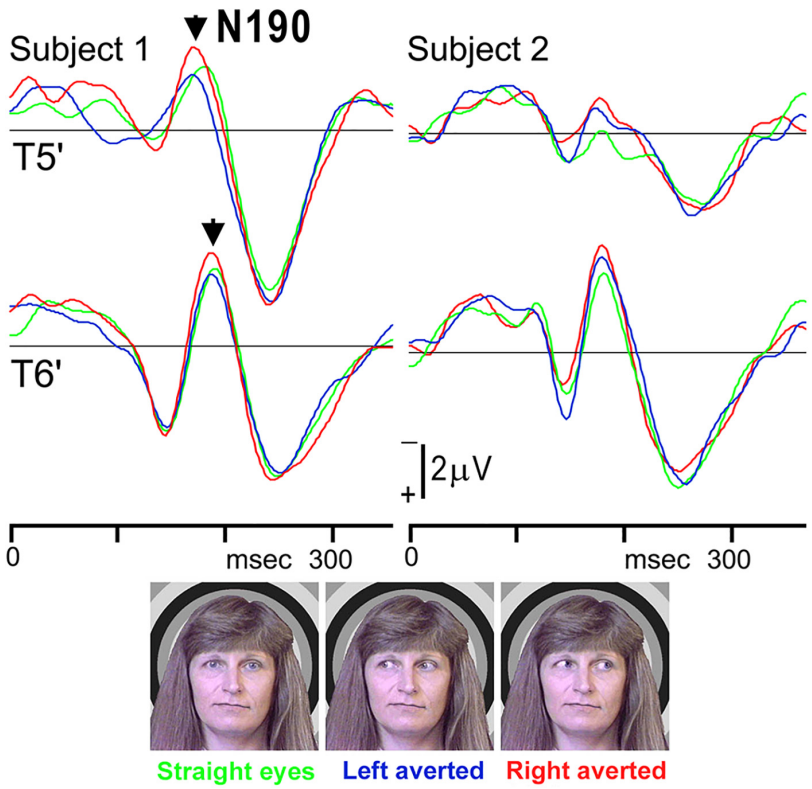

FIGURE 4 | ERP waveforms in two representative subjects for straight eyes, left averted, and right averted conditions at T5′ and T6′ electrodes in the left and right temporal areas, respectively. A negative component, N190, was clearly identified for all stimuli [adopted from Watanabe et al. (2002)]. ERP, event-related potentials.

TABLE 1 | Mean and SD of the maximum amplitude of the N190 component at T5′ and T6′ electrodes for straight eyes, left averted, right averted, and averted eyes (mean value of left averted and right averted).

	T5′	T6′
Straight eyes (μV)	−1.6 ± 0.8	−3.1 ± 2.4[a]
Left averted (μV)	−1.7 ± 0.9	−3.4 ± 2.7[a]
(%)	113.2 ± 52.4	113.4 ± 35.7
Right averted (μV)	−2.0 ± 0.9	−3.8 ± 2.8[a,b]
(%)	133.5 ± 61.2	126.4 ± 30.6[b]
Averted eyes (μV)	−1.8 ± 0.8	−3.6 ± 2.7[a,b]
(%)	119.3 ± 55.2	119.9 ± 24.6[b]

In addition, values for the three averted conditions are expressed as percentages after normalization with straight eyes to clarify the effects of aversion in each hemisphere more precisely [adopted from Watanabe et al. (2002)].
[a]*Inter-hemispheric difference: amplitude was significantly larger at the T6′ electrode than at the T5′ electrode ($p < 0.05$).*
[b]*Amplitude was significantly larger for right averted and averted eyes than straight eyes at the T6′ electrode ($p < 0.01$).*
SD, standard deviation.

THE EFFECTS OF EYE AVERSION ON EVENT-RELATED POTENTIALS

IT activity reflected the detection process of a face during face perception in our previous studies (Watanabe et al., 1999a,b), but we perceive facial information from facial parts (eyes and mouth). In particular, aversion of the eyes is highly important in social communication. The eye direction indicates attention to others or disgust, and we perceive others based on the direction of the eyes.

Therefore, we investigated whether eye direction indicates attention to others using faces with different eye directions in our previous study (Watanabe et al., 2002). Fourteen adult normal subjects with normal or corrected visual acuity had participated. Three visual stimuli were randomly presented (**Figure 4**): (1) straight eyes: a face with the eyes gazing at the viewer, (2) left averted: a face with the eyes averted to the left, and (3) right averted: a face with the eyes averted to the right. In ERPs for each condition, a large negative component (N190) at approximately 190–200 msec after stimulus onset was recorded at both the T5′ (left temporal area, 2 cm below T5 in the International 10–20 System) and T6′ (right temporal area, 2 cm below T6 in the International 10–20 System) electrodes (**Figure 4**). There were no significant differences among conditions in N190 latency, but N190 for right averted was significantly larger than that for straight eyes at the T6′ electrode (**Table 1**). N190 amplitudes were also larger for left averted at T6′ and for left and right averted at the T5′ electrode than for straight eyes, but the difference was not significant (**Table 1**). In addition, mean values for left averted and right averted were calculated as "averted eyes" and compared with those for straight eyes (**Table 1**). The peak latency did not significantly differ, but the amplitudes of N190 for averted eyes

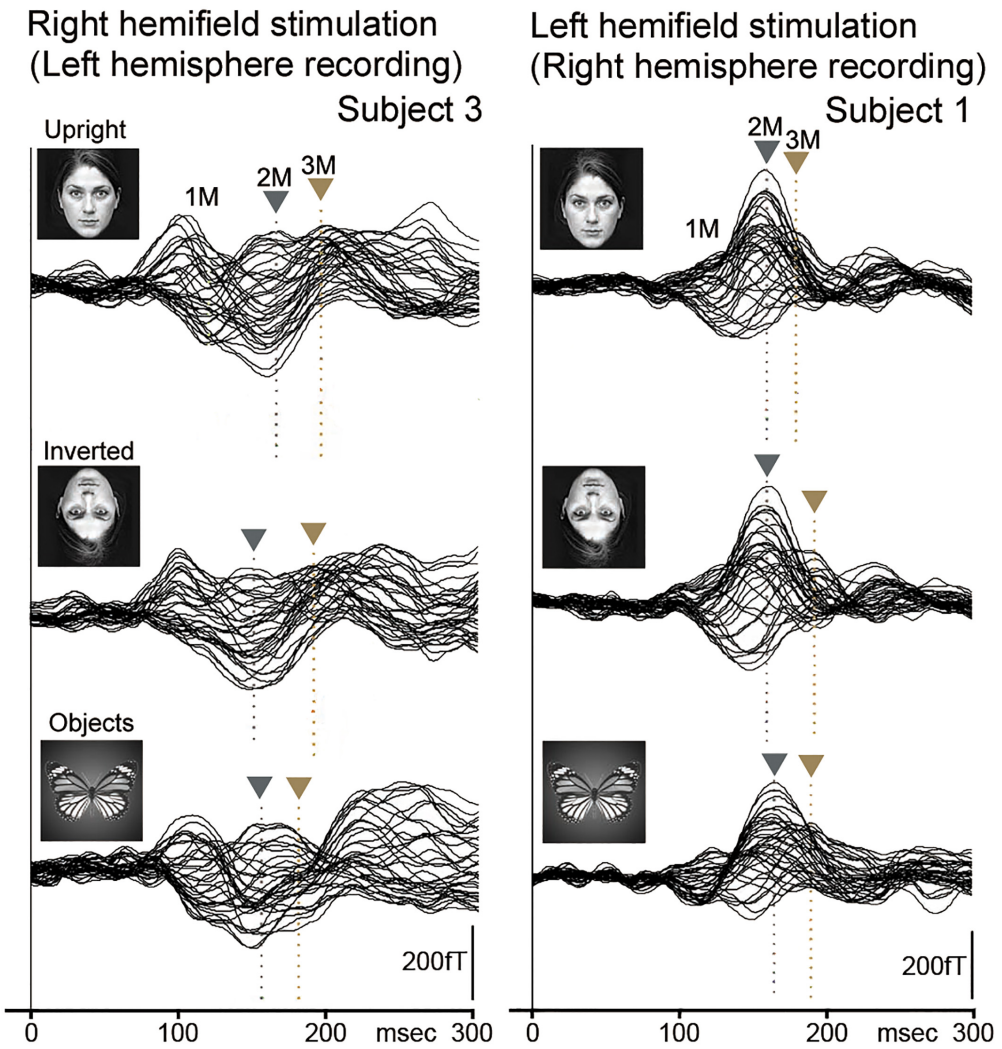

FIGURE 5 | The MEG waveforms for LHF and RHF stimulation in two representative subjects. MEG components (1M, 2M, and 3M) were clearly recorded in the right (LHF stimulation) and left hemispheres (RHF stimulation) in upright (upright face), inverted (inverted face), and objects (butterfly) conditions. The vertical gray and brown arrows indicate the peaks of 2M and 3M, respectively. In addition, the vertical gray and brown dotted lines indicate the peak latencies of 2M and 3M, respectively. 2M and 3M latencies for objects were not significantly different from those for faces (upright and inverted) [adopted from Watanabe et al. (2003)]. MEG, magnetoencephalography; LHF, left hemifield; RHF, right hemifield.

were larger than those for straight eyes at T5′ and significantly larger at T6′ electrodes (**Table 1**).

The superior temporal sulcus (STS) plays a role in the perception of gaze direction, eye and mouth movement, and body movement according to previous studies (e.g., De Souza et al., 2005). An fMRI study revealed that the perception of eye direction is mediated more by the STS (Hoffman and Haxby, 2000) and that the STS is important in the perception of the changeable aspects in face information. On the other hand, in our previous studies (Watanabe et al., 1999a; Miki et al., 2004), the IT activity was not affected by information of eyes or mouth form (opened or closed) within a face. Thus, the larger ERPs evoked by eye aversion in the present study (Watanabe et al., 2002) may be related to STS activity rather than IT activity. In addition, the activity when gazing to the right was greater than when gazing to the left. The following possibility was hypothesized: the eyes averted to the right may have more of an effect in right-handed persons because all subjects in this study were right-handed.

FACE INVERSION EFFECTS AND DIFFERENCES BETWEEN THE RIGHT AND LEFT HEMISPHERES IN FACE PERCEPTION

In previous psychophysical studies (e.g., Farah et al., 1995), people detected an inverted face slower and with more difficulty than an upright face. This phenomenon is termed the "face inversion effect" and it revealed that a process in face perception is specific to the upright direction.

Our MEG study (Watanabe et al., 2003) was performed to investigate evoked components by (1) upright faces (upright condition), (2) inverted faces (inverted condition), and (3) butterfly (objects condition) (**Figure 5**). Ten normal adult subjects with normal or corrected visual acuity had participated. For MEG recording, the sensor was placed covering temporo-occipital regions in the right and left hemispheres for left and right hemifield (LHF and RHF) stimulation, respectively, and right and left hemispheres were examined independently.

The evoked components (1M, 2M, and 3M) by each condition were identified, with the 2M component being the largest and most major among these components from the right and left hemispheres to LHF and RHF stimulations in representative subjects (**Figure 5**).

2M and 3M latencies were longer for the inverted condition than for the upright condition in the right hemisphere and shorter in the left hemisphere (**Figure 5** and **Table 2**), although 2M and 3M latencies were not significantly different between upright and inverted conditions (**Table 2**). In addition, 2M and 3M latencies for the objects condition were not significantly different from those for upright and inverted conditions, and the 3M amplitude in the left hemisphere was significantly smaller for the objects condition than for upright and inverted conditions (**Table 3**).

TABLE 2 | Mean and SD of peak latency (msec) of 2M and 3M components contralateral to the stimulated hemifield for upright (upright face), inverted (inverted face), and objects conditions [adopted from Watanabe et al. (2003)].

	Upright	Inverted	Objects
Left hemifield stimulation (Right hemisphere)			
2M	161.6 ± 11.8	164.3 ± 10.9	164.3 ± 11.3
3M	185.3 ± 15.4	187.3 ± 15.5	188.6 ± 13.7
Right hemifield stimulation (Left hemisphere)			
2M	155.1 ± 7.4	153.8 ± 5.8	157.0 ± 7.3
3M	183.5 ± 10.0	183.8 ± 9.0	183.9 ± 8.5

SD, standard deviation.

TABLE 3 | Mean and SD of the maximum amplitude of 2M and 3M components contralateral to the stimulated hemifield.

	Upright	Inverted	Objects
Left hemifield stimulation (Right hemisphere)			
2M	134.0 ± 49.1 fT	101.3 ± 11.8%	98.5 ± 22.4%
3M	90.0 ± 53.1 fT	111.7 ± 31.1%	122.8 ± 43.2%
Right hemifield stimulation (Left hemisphere)			
2M	96.6 ± 40.7 fT	99.1 ± 9.9%	102.9 ± 25.1%
3M	88.8 ± 31.2 fT	89.6 ± 23.1%	65.5 ± 17.3%[a]

For the upright (upright face) condition, MEG data are in fT. Values for inverted (inverted face) and objects conditions are expressed as percentages after normalization with maximum amplitudes for the upright condition [adopted from Watanabe et al. (2003)].

[a]The maximum amplitude for objects condition was significantly smaller than those for upright (upright face) ($p < 0.001$) and inverted (inverted face) ($p < 0.01$) conditions.

SD, standard deviation; MEG, magnetoencephalography.

In multiple source modeling, the 3-dipole model (early visual area, IT area, and lateral temporal area) was the most appropriate for upright and inverted conditions, but not for the objects condition.

A previous study (McCarthy et al., 1999) revealed that upright faces are more rapidly processed in the right hemisphere, whereas inverted faces are more rapidly processed in the left, i.e., the right hemisphere had better processing of information about upright faces and the left had better processing of information about inverted faces. Consistent with the previous study (McCarthy et al., 1999), our study (Watanabe et al., 2003) revealed the following: (1) there was a difference in the face perception process between right and left hemispheres, (2) there were differences in processing between upright and inverted faces due to temporal processing differences, and (3) there were differences in brain areas related to processing between faces and objects.

There was a difference in the face perception process between the right and left hemispheres; however, it is unknown why there is such a difference and how upright and inverted faces were processed. We investigated the effects of inverting facial contours (hair and chin) and features (eyes, nose, and mouth) on processing for face perception using MEG (Miki et al., 2011).

We examined ten normal adult subjects with normal or corrected visual acuity and presented three conditions as follows (**Figure 6**): (1) upright contours and upright features (U&U): contours (hair and chin) and features (eyes, nose, and mouth) upright, (2) upright contours and inverted features (U&I): contours remained upright, but the features were mirrored and inverted relative to the U&U condition, although the spatial relationship among the features was not changed, and (3) inverted contours and inverted features (I&I): A mirrored and inverted form of the image used in the U&U condition.

In both hemispheres, ECDs were located in the IT area, corresponding to FFA, for all conditions from all subjects. The waveforms were recorded from 204 gradiometers by a 306-channel biomagnetometer in a representative subject for the U&U condition and the waveforms in all conditions at representative sensors, where the largest component was

TABLE 4 | The peak latency and maximum amplitude of N-ERP250 at T5 and T6 (the temporal area).

	T5 (Left)		T6 (Right)	
	(μV)	(msec)	(μV)	(msec)
Upright	−1.30 ± 1.09	246.7 ± 15.5	−1.43 ± 0.79[c]	247.8 ± 14.5
Inverted	−1.37 ± 1.18	258.3 ± 18.1[a]	−1.55 ± 0.95[d]	258.5 ± 18.7[b]
Scrambled	−1.43 ± 1.39	261.0 ± 17.5[a]	−1.58 ± 0.81[d]	259.4 ± 18.1[b]
Star	−1.03 ± 0.86	252.9 ± 20.7	−0.95 ± 0.64	251.2 ± 17.0

Means and SD for upright, inverted, scrambled, and star [adopted from Miki et al. (2009)].

[a]$p < 0.01$ compared with upright.

[b]$p < 0.05$ compared with upright.

[c]$p < 0.05$ compared with star.

[d]$p < 0.01$ compared with star.

SD, standard deviation.

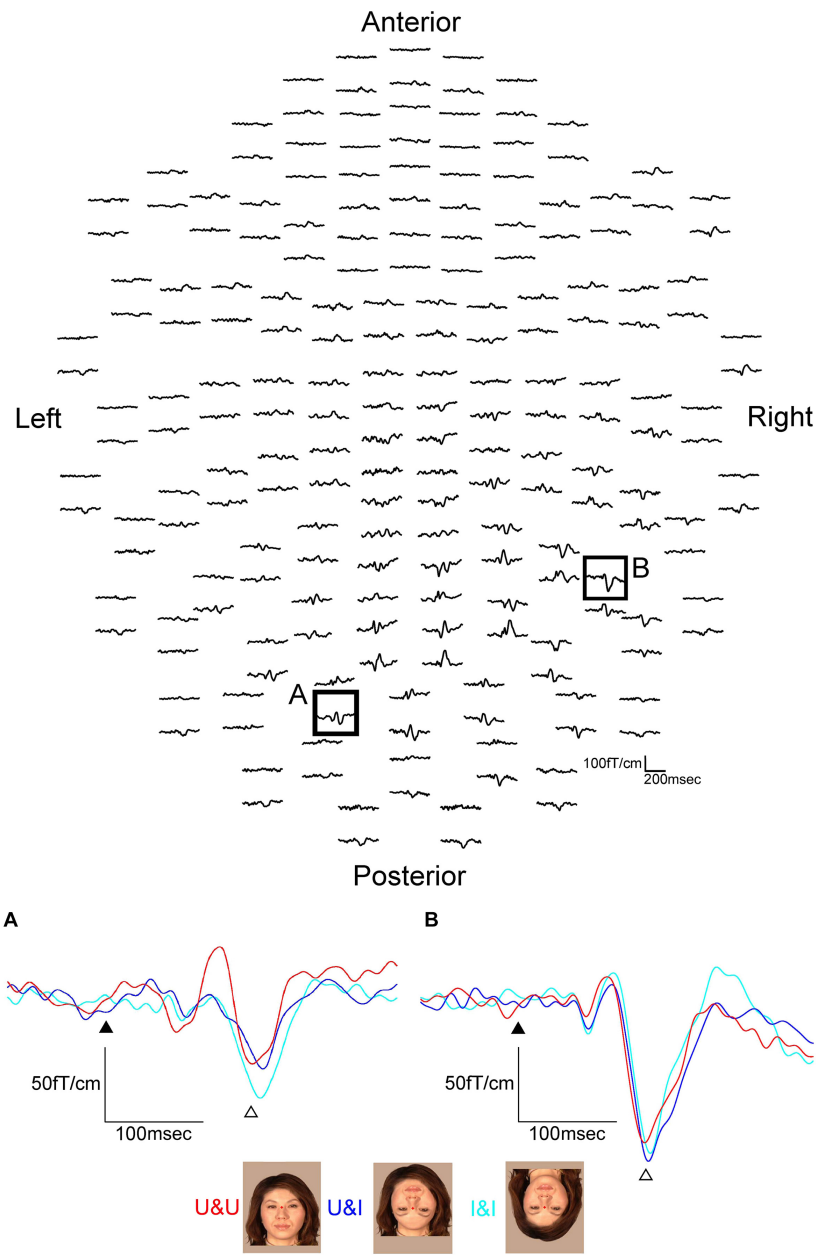

FIGURE 6 | MEG waveforms (upper) of a representative subject following stimulus onset in the U&U condition. MEG waveforms (lower) at sensors A and B in the upper image show a clear component recorded for U&U, U&I, and I&I conditions in the left and right hemispheres. **(A)** Representative waveforms at sensor A in the left hemisphere of the upper image. **(B)** Representative waveforms at sensor B in the right hemisphere of the upper image. Black arrows show the stimulus onset and white arrows show the response selected for further analysis. Responses after the stimulus onset were longer in latency for U&I and I&I than for U&U in the right hemisphere, but longer in latency for U&I than for U&U and I&I in the left hemisphere in this subject [adopted from Miki et al. (2011)]. MEG, magnetoencephalography; U&U, upright contours and upright features; U&I, upright contours and inverted features; I&I, inverted contours and inverted features.

identified for the U&U condition in each occipital or temporal area of the same subject, are shown in **Figure 6**.

Concerning the peak latency of the ECD, the latency was significantly longer for U&I and I&I than for U&U in the right hemisphere and significantly longer for U&I than for U&U and I&I in the left hemisphere (**Figure 7**). On the other hand, regarding the maximum moment (strength) of the ECD, it was smaller for U&U than for U&I and I&I conditions in the right hemisphere, although there were no significant differences among stimulus conditions in either hemisphere due to individual differences (**Figure 7**).

In the U&U condition, the spatial relationship among the facial features (eyes, nose, and mouth) was intact and the features were upright; however, in the U&I and I&I conditions, the

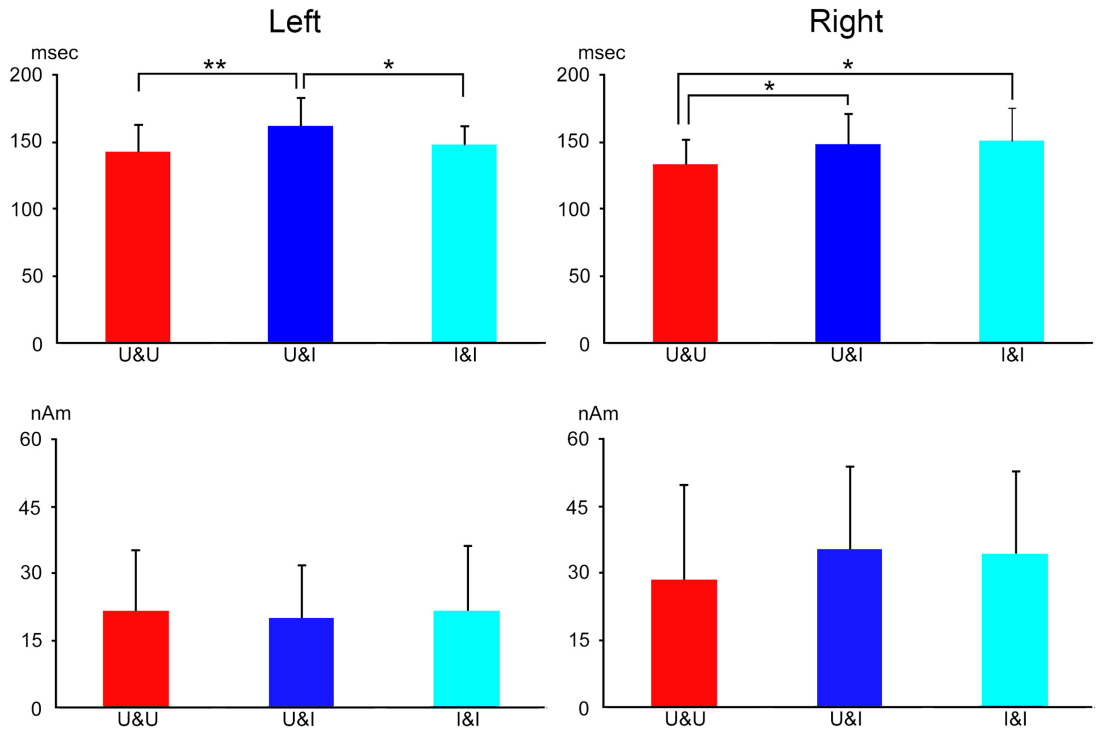

FIGURE 7 | Bar graph of peak latency (upper) and the maximum amplitude of dipole moment (lower) for all conditions after stimulus onset in the right and left hemispheres. Error bar shows the SD [adopted from Miki et al. (2011)]. *$p < 0.05$ and **$p < 0.01$. SD, standard deviation.

features were inverted but retained their spatial relationships even though the contours (hair and chin) of the face were upright or inverted. The U&U condition was considered "easier" to encode because it fits a normal template. In this study (Miki et al., 2011), the ECD was in both IT areas related to face perception, consistent with previous studies (e.g., Watanabe et al., 1999a,b). Based on previous studies (Watanabe et al., 1999a,b; Watanabe et al., 2003), we considered the right IT area related to face perception to be affected by the direction of features. On the other hand, in U&U and I&I conditions, the spatial relationships between the facial contours and features were intact whether the face was upright or inverted; however, in the U&I condition, they were disrupted. We considered the left IT area related to face perception to be affected by the disruption of the spatial relationships between the contours and features, different from the right hemisphere. This study (Miki et al., 2011) demonstrated the differences between the right and left hemispheres in face perception.

A USEFUL VISUAL STIMULUS METHOD FOR INVESTIGATING FACE PERCEPTION

In previous studies that investigated face perception, the luminance differed after visual stimuli were presented and the occipital area related to the primary visual perception was activated by this change in luminance. Therefore, the IT area related to face perception cannot be completely separated from strong- and long-lasting activities in the primary visual areas.

A useful visual stimulus method, random dots blinking (RDB), uses temporal changes in patterns of many small dots to present stimuli without a change in luminance during the presentation of an object (e.g., a circle, a letter, or a schematic face), which reduces activities in the occipital area related to the primary visual perception, and detects only activity in the IT area related to visual form perception, such as faces and letters (Okusa et al., 1998; Okusa et al., 2000). In the RDB method, white dots are presented on a black background. Each dot turns white or black according to a pseudorandom plan and subjects perceive the white dots to be moving randomly. While presenting the stimuli, the dots forming stimuli remain unchanged, whereas other dots are changed, and subjects perceive the shape of the stimuli without a change in luminance.

We investigated the face perception process using the RDB method in ten normal adult subjects with normal or corrected visual acuity (Miki et al., 2009). We presented visual stimuli using RDB. Four stimuli were presented as follows (**Figure 8**): (1) upright: a schematic face consisting of a large circle, two dots, and a straight line. (2) inverted: the upright stimulus was inverted, but the spatial relationship between the contours and features was preserved. (3) scrambled: the spatial relationship between the contours and features was distorted. The scrambled stimulus was vertically and horizontally symmetrical because subjects were unable to judge upright or inverted.

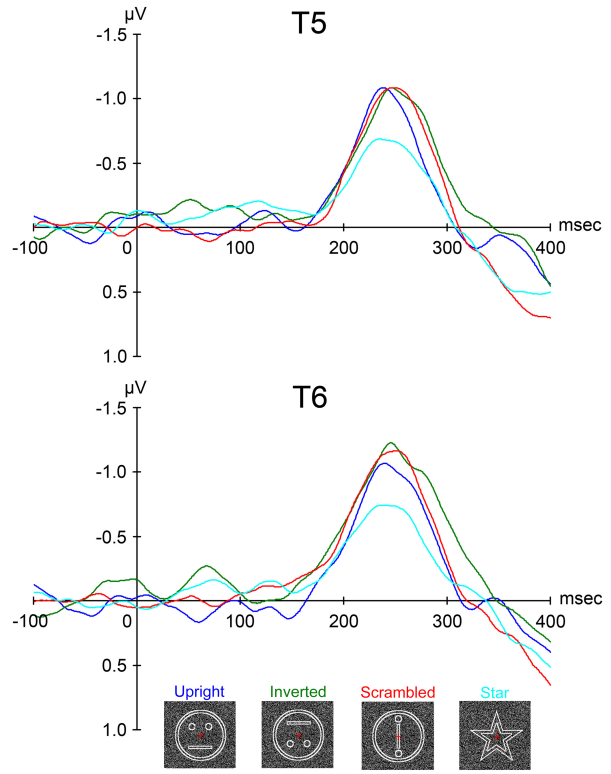

FIGURE 8 | The grand-averaged waveforms from all ten subjects of ERP for upright (schematic face), inverted (the upright stimulus inverted), scrambled (the same contours and features as in upright but with the spatial relation distorted), and star (a star shape whose occurrence was enumerated and then reported after sessions by the subjects) conditions at the T5 and T6 electrodes in the left and right temporal areas, respectively [adopted from Miki et al. (2009)]. ERP, event-related potential.

(4) star: subjects were asked to count the number of stars and to report it after the sessions in order to draw their attention to this stimulus and avoid paying attention to upright, inverted, and scrambled.

In a previous study using RDB (Okusa et al., 1998; Okusa et al., 2000), a clear evoked component peaking at around 200–300 msec was identified. In this study (Miki et al., 2009), we identified a component that had a peak deflection 200–300 msec after stimulus onset at T5 and T6 electrodes of the International 10–20 System in the left and right temporal areas, respectively. The peak latency when the amplitude of the component was maximal for each condition after the stimulus onset and the maximum amplitude of the component were individually measured within 300 msec.

The grand-averaged waveforms of evoked components after stimulus onset are shown in **Figure 8**. There was no component peaking at around 100 msec like P1 (or P100), which is considered to reflect the activities of the occipital areas related to the primary visual perception by luminance change in ERP studies. A clear negative component peaking at around 250 msec, termed N-ERP250, was identified at both the T5 (left) and T6 (right) electrodes in both temporal areas (**Figure 8**). At both electrodes, the latency of N-ERP250 was significantly shorter for upright than for inverted and scrambled and slightly shorter for upright than for star (**Figure 8** and **Table 4**). In addition, the amplitude of N-ERP250 was significantly larger for upright, inverted, and scrambled than for star at the T6 electrode in the right hemisphere and larger for upright, inverted, and scrambled than for star at the T5 electrode, although there were no significant differences among conditions at the T5 electrode (**Figure 8** and **Table 4**). We estimated the sources of N-ERP250 from the grand-averaged ERPs within 200–300 msec using brain electric source analysis as a multiple source model, and the estimated sources for each condition were located in the IT area, corresponding to FFA, related to face perception.

This study (Miki et al., 2009) revealed the following: (1) N-ERP250 is related to face perception, (2) the differences in N-ERP250 amplitude reflect differences between face perception and non-face perception processes, and (3) N-ERP250 is affected by not only the face direction but also the distortion in the spatial relation between the contours and features.

One previous study using intracranial ERP (Allison et al., 1999) reported that the first distinct response in visual ventral and lateral areas appears 200 msec after stimulus onset. In contrast, N-ERP250 in this study (Miki et al., 2009) was observed at a latency of 250 msec. Therefore, RDB stimuli activated a different subcortical pathway with slower conduction times before reaching the IT area.

DISCUSSION AND CONCLUSION

In this review, we discussed the following characteristics of face perception processing based on our previous EEG and MEG studies.

First, event-related components related to activity in the IT area, corresponding to FFA, were evoked after the presentation of a face, and the detection process for a face was shorter than that for eyes because the face is important for social communication. The facial contours affect and shorten this process; therefore, they are one of the most important parts of face perception.

Second, event-related components related to the STS activity were larger when eyes were averted than when straight. This suggested that the direction of gaze, especially eye aversion, is an important indicator of an individual's focus for automatic and unconscious attention.

Third, the face perception process was shortened by an upright face in the right hemisphere, whereas it was shortened by an inverted face in the left, revealing hemispheric differences in the face perception process. In addition, the direction of the features of a face affects the face perception processing in the right hemisphere, whereas matching of the direction between the contours and features of a face affects the processing in the left.

Lastly, using RDB without a change in luminance during the presentation of a face, the IT activity related to face perception was specifically detected without interference by activity in the occipital area related to the primary visual perception process. According to this method, the face perception process in the IT

area is shorter for an upright face rather than for an inverted face and non-face stimuli.

AUTHOR CONTRIBUTIONS

KM and SW designed and performed the experiments, and performed data recording and statistical analyses in our previous studies. YT made the program used for the stimulus presentation in our previous studies. KM wrote this review. RK made suggestions about this review. KM had the overall responsibility for this review. All authors contributed to the article and approved the submitted version.

FUNDING

This study was supported by JSPS KAKENHI Grant Number JP17K12101, a Grant-in-Aid from Japanese Red Cross Academy, a Grant-in-Aid from Daiko Foundation, and a Grant-in-Aid from Aichi Health Promotion Foundation to KM.

REFERENCES

Allison, T., Puce, A., Spencer, D. D., and McCarthy, G. (1999). Electrophysiological studies of human face perception. I: potentials generated in occipitotemporal cortex by face and non-face stimuli. *Cereb. Cortex.* 9, 415–430. doi: 10.1093/cercor/9.5.415

Bentin, S., Allison, T., Puce, A., Perez, E., and McCarthy, G. (1996). Electrophysiological Studies of face perception in humans. *J. Cogn. Neurosci.* 8, 551–565. doi: 10.1162/jocn.1996.8.6.551

Bruce, V., and Young, A. (1986). Understanding face recognition. *Br. J. Psycho.* 77, 305–327. doi: 10.1111/j.2044-8295.1986.tb02199.x

De Souza, W. C., Eifuku, S., Tamura, R., Nishijo, H., and Ono, T. (2005). Differential characteristics of face neuron responses within the anterior superior temporal sulcus of macaques. *J. Neurophysiol.* 94, 1252–1266. doi: 10.1152/jn.00949.2004

Farah, M. J., Wilson, K. D., Drain, H. M., and Tanaka, J. R. (1995). The inverted face inversion effect in prosopagnosia: evidence for mandatory, face-specific perceptual mechanisms. *Vision Research* 35, 2089–2093. doi: 10.1016/0042-6989(94)00273-O

Hämäläinen, M., Hari, R., Ilmoniemi, R. J., Knuutila, J., and Lounasmaa, O. V. (1993). Magnetoencephalography—Theory, instrumentation, and applications to non-invasive studies of the working brain. *Rev. Mod. Phys.* 65, 413–497. doi: 10.1103/RevModPhys.65.413

Hoffman, E. A., and Haxby, J. V. (2000). Distinct representations of eye gaze and identity in the distributed human neural system for face perception. *Nat. Neurosci.* 3, 80–84. doi: 10.1038/71152

Itier, R. J., Latinus, M., and Taylor, M. J. (2006). Face, eye and object early processing: what is the face specificity? *Neuroimage* 29, 667–676. doi: 10.1016/j.neuroimage.2005.07.041

Kanwisher, N., McDermott, J., and Chun, M. M. (1997). The fusiform face area: a module in human extrastriate cortex specialized for face perception. *J. Neurosci.* 17, 4302–4311. doi: 10.1523/JNEUROSCI.17-11-04302.1997

McCarthy, G., Puce, A., Belger, A., and Allison, T. (1999). Electrophysiological studies of human face perception. II: response properties of face specific potentials generated in occipitotemporal cortex. *Cereb. Cortex.* 9, 431–444. doi: 10.1093/cercor/9.5.431

Miki, K., Takeshima, Y., Watanabe, S., Honda, Y., and Kakigi, R. (2011). Effects of inverting contour and features on processing for static and dynamic face perception: an MEG study. *Brain Res.* 1383, 230–241. doi: 10.1016/j.brainres.2011.01.091

Miki, K., Watanabe, S., Honda, Y., Nakamura, M., and Kakigi, R. (2007). Effects of face contour and features on early occipitotemporal activity when viewing eye movement. *Neuroimage* 35, 1624–1635. doi: 10.1016/j.neuroimage.2007.01.040

Miki, K., Watanabe, S., Kakigi, R., and Puce, A. (2004). Magnetoencephalographic study of occipitotemporal activity elicited by viewing mouth movements. *Clin. Neurophysiol.* 115, 1559–1574. doi: 10.1016/j.clinph.2004.02.013

Miki, K., Watanabe, S., Takeshima, Y., Teruya, M., Honda, Y., and Kakigi, R. (2009). Effect of configural distortion on a face-related ERP evoked by random dots blinking. *Exp. Brain Res.* 193, 255–265. doi: 10.1007/s00221-008-1617-0

Okusa, T., Kakigi, R., and Osaka, N. (2000). Cortical activity related to cue-invariant shape perception in humans. *Neuroscience* 98, 615–624. doi: 10.1016/s0306-4522(00)00172-x

Okusa, T., Kaneoke, Y., Koyama, S., and Kakigi, R. (1998). Random dots blinking: a new approach to elucidate the activities of the extrastriate cortex in humans. *Neuroreport* 9, 3961–3965. doi: 10.1097/00001756-199812010-00035

Shibata, T., Nishijo, H., Tamura, R., Miyamoto, K., Eifuku, S., Endo, S., et al. (2002). Generators of visual evoked potentials for faces and eyes in the human brain as determined by dipole localization. *Brain Topogr.* 15, 51–63. doi: 10.1023/a:1019944607316

Watanabe, S., Kakigi, R., Koyama, S., and Kirino, E. (1999a). Human face perception traced by magneto- and electro-encephalography. *Brain Res. Cogn. Brain Res.* 8, 125–142. doi: 10.1016/s0926-6410(99)00013-0

Watanabe, S., Kakigi, R., Koyama, S., and Kirino, E. (1999b). It takes longer to recognize the eyes than the whole face in humans. *Neuroreport* 10, 2193–2198. doi: 10.1097/00001756-199907130-00035

Watanabe, S., Kakigi, R., and Puce, A. (2003). The spatiotemporal dynamics of the face inversion effect: a magneto- and electro-encephalographic study. *Neuroscience* 116, 879–895. doi: 10.1016/s0306-4522(02)00752-2

Watanabe, S., Miki, K., and Kakigi, R. (2002). Gaze direction affects face perception in humans. *Neurosci. Lett.* 325, 163–166. doi: 10.1016/S0304-3940(02)00257-4

Conflict of Interest: The authors declare that the research was conducted in the absence of any commercial or financial relationships that could be construed as a potential conflict of interest.

Publisher's Note: All claims expressed in this article are solely those of the authors and do not necessarily represent those of their affiliated organizations, or those of the publisher, the editors and the reviewers. Any product that may be evaluated in this article, or claim that may be made by its manufacturer, is not guaranteed or endorsed by the publisher.

Copyright © 2022 Miki, Takeshima, Watanabe and Kakigi. This is an open-access article distributed under the terms of the Creative Commons Attribution License (CC BY). The use, distribution or reproduction in other forums is permitted, provided the original author(s) and the copyright owner(s) are credited and that the original publication in this journal is cited, in accordance with accepted academic practice. No use, distribution or reproduction is permitted which does not comply with these terms.

frontiers | Frontiers in Physiology

REVIEW
published: 01 April 2022
doi: 10.3389/fphys.2022.848867

Benefits of Curcumin in the Vasculature: A Therapeutic Candidate for Vascular Remodeling in Arterial Hypertension and Pulmonary Arterial Hypertension?

Ke-Xue Li[1†], Zi-Chao Wang[2,3†], Jeremiah Ong'Achwa Machuki[1†], Meng-Zhen Li[2,3], Yu-Jie Wu[2,3], Ming-Kai Niu[2,3], Kang-Ying Yu[4], Qing-Bo Lu[5] and Hai-Jian Sun[2,3,6]**

[1]Department of Physiology, Xuzhou Medical University, Xuzhou, China, [2]State Key Laboratory of Natural Medicines, China Pharmaceutical University, Nanjing, China, [3]School of Traditional Chinese Pharmacy, China Pharmaceutical University, Nanjing, China, [4]Nursing School of Wuxi Taihu University, Wuxi, China, [5]School of Medicine, Southeast University, Nanjing, China, [6]Department of Pharmacology, Yong Loo Lin School of Medicine, National University of Singapore, Singapore, Singapore

OPEN ACCESS

Edited by:
Jacqueline Kathleen Phillips, Macquarie University, Australia

Reviewed by:
Eman Gohar, Vanderbilt University Medical Center, United States
Shruti Rawal Mahajan, Harvard Medical School, United States

***Correspondence:**
Qing-Bo Lu
230189857@seu.edu.cn
Hai-Jian Sun
sunhaijian927@163.com

†These authors have contributed equally to this work

Specialty section:
This article was submitted to Integrative Physiology, a section of the journal Frontiers in Physiology

Received: 05 January 2022
Accepted: 03 March 2022
Published: 01 April 2022

Citation:
Li K-X, Wang Z-C, Machuki JO, Li M-Z, Wu Y-J, Niu M-K, Yu K-Y, Lu Q-B and Sun H-J (2022) Benefits of Curcumin in the Vasculature: A Therapeutic Candidate for Vascular Remodeling in Arterial Hypertension and Pulmonary Arterial Hypertension? Front. Physiol. 13:848867. doi: 10.3389/fphys.2022.848867

Growing evidence suggests that hypertension is one of the leading causes of cardiovascular morbidity and mortality since uncontrolled high blood pressure increases the risk of myocardial infarction, aortic dissection, hemorrhagic stroke, and chronic kidney disease. Impaired vascular homeostasis plays a critical role in the development of hypertension-induced vascular remodeling. Abnormal behaviors of vascular cells are not only a pathological hallmark of hypertensive vascular remodeling, but also an important pathological basis for maintaining reduced vascular compliance in hypertension. Targeting vascular remodeling represents a novel therapeutic approach in hypertension and its cardiovascular complications. Phytochemicals are emerging as candidates with therapeutic effects on numerous pathologies, including hypertension. An increasing number of studies have found that curcumin, a polyphenolic compound derived from dietary spice turmeric, holds a broad spectrum of pharmacological actions, such as antiplatelet, anticancer, anti-inflammatory, antioxidant, and antiangiogenic effects. Curcumin has been shown to prevent or treat vascular remodeling in hypertensive rodents by modulating various signaling pathways. In the present review, we attempt to focus on the current findings and molecular mechanisms of curcumin in the treatment of hypertensive vascular remodeling. In particular, adverse and inconsistent effects of curcumin, as well as some favorable pharmacokinetics or pharmacodynamics profiles in arterial hypertension will be discussed. Moreover, the recent progress in the preparation of nano-curcumins and their therapeutic potential in hypertension will be briefly recapped. The future research directions and challenges of curcumin in hypertension-related vascular remodeling are also proposed. It is foreseeable that curcumin is likely to be a therapeutic agent for hypertension and vascular remodeling going forwards.

Keywords: hypertension, vascular remodeling, curcumin, vascular smooth muscle cells, endothelial cells

INTRODUCTION

Arterial hypertension, a multifactorial and chronic disease, is one of the leading causes of people disability and death around the world (Forouzanfar et al., 2017; Carey et al., 2018). As a common type of hypertension, pulmonary arterial hypertension (PAH) is a devastating disorder that is manifested by progressive pulmonary arteriole remodeling, vasoconstriction, pulmonary vascular stiffening, and increased right ventricular afterload (Thenappan et al., 2018). Studies have shown that hypertension originates from a combination of genetic, environmental, and social determinants (Carey et al., 2018). Uncontrolled high blood pressure results in a higher incidence of hypertension-related target organ damages, including myocardial infarction, heart failure, aortic dissection, renal damage, and stroke (Acelajado et al., 2019; Van Beusecum and Moreno, 2021). Large-scale epidemiological studies provide robust evidence that high blood pressure is closely associated with the risk of stroke, ischemic heart disease, heart failure, and non-cardiac vascular disease, without heterogeneity at all ages and in both sexes (Rapsomaniki et al., 2014). In 2019, the American College of Cardiology and American Heart Association classified hypertension as a systolic blood pressure >130 mmHg and a diastolic blood pressure of >80 mmHg (Arnett et al., 2019). These guidelines lead to the fact that nearly half of adults tend to be hypertensive (Arnett et al., 2019). Moreover, the prevalence of PAH ranges from 11 to 26 cases per million adults, and the mortality rate remains about 50% at 5 years of PAH despite the application of targeted drugs (Thenappan et al., 2018). Mechanistically, renal dysfunction, vascular dysfunction, and central nervous system disorder are critically involved in the pathogenesis of arterial hypertension (Ren et al., 2020; Zhang and Sun, 2020; Harrison et al., 2021). Mutations in the type II bone morphogenetic protein receptor (BMPR2), chronic inflammation, fibrosis, immune activation, and mitochondrial metabolic dysfunction are drivers for the pathogenesis of PAH (Thenappan et al., 2018). Overall, the pathophysiology of arterial hypertension and PAH is heterogeneous and multifactorial, thus, it is of great significance to comprehensively understand the pathogenesis of arterial hypertension and PAH. Despite current therapies, such as renin-angiotensin system blockers, calcium antagonists, steroidal mineralocorticoid receptor antagonists, and thiazide-type diuretic, almost half of hypertensive patients are not sufficiently controlled (Bakris et al., 2020). Optimizing the prevention, treatment, and recognition of hypertension requires a better understanding of the pathogenesis network of hypertension.

It is currently accepted that vascular remodeling is a characteristic during the development and progression of hypertension since hypertension is a driving force for endothelial cell activation, vascular smooth muscle cells (VSMCs) and adventitial fibroblasts dysfunction (Zhu et al., 2018; Zhang and Sun, 2021). Conversely, vascular remodeling/stiffening is an important pathological basis for maintaining high blood pressure, thus forming a vicious circle (Kostov, 2021). Specifically, the imbalanced vasoactive factors produced by the endothelium induce vasoconstriction, proinflammatory state, oxidative stress and deficiency of nitric oxide (NO), a critical event implicated in the pathophysiology of hypertension (Zhang and Sun, 2020). The anomalous apoptosis, phenotype conversion, proliferation, and migration of VSMCs are related to the progression of hypertension-induced vascular remodeling (Zhang and Sun, 2020). As important components of blood vessels, adventitial fibroblasts are essential for vascular homeostasis and their malfunction plays an important role in aortic maladaptation and hypertension-related vascular fibrosis (Ling et al., 2018; Tong et al., 2018). Animal and cellular experiments support the therapeutic potential of vascular remodeling reversal in hypertension and its related organ damage (Ouarné et al., 2021). Thus, a better understanding of the etiology of vascular remodeling might open new therapeutic approaches for hypertension.

Recently, nonpharmacological interventions are highly proposed for adults with elevated blood pressure or hypertension, and alternative therapies are therefore becoming an adjuvant treatment of hypertension (Arnett et al., 2019; Canale and Noce, 2021). In particular, phytochemicals are emerging as alternative therapies with therapeutic effects on a wide range of pathologies, including hypertension. Of those phytochemicals, curcumin is a highly pleiotropic molecule with anti-inflammatory, antioxidant, chemosensitizing, neuroprotective, renoprotective, hepatoprotective, lipid-modifying, glucose-lowering, anti-atherogenic effects (Hadi et al., 2019). Coincidentally, curcumin is found to exert anti-hypertensive actions through a broad spectrum of targets or signaling pathways (Hadi et al., 2019; Cox and Misiou, 2022). For example, supplementation of curcumin is able to improve PAH through reversing pulmonary vessel remodeling and fibrosis (Lin et al., 2006). Inhibition of nitric oxide synthesis (NOS) with N(ω)-nitro-L-arginine methyl ester (L-NAME) elevates arterial blood pressure and peripheral vascular resistance in male Sprague-Dawley rats, an effect that is largely mitigated by curcumin or hexahydrocurcumin treatment (Nakmareong et al., 2011; Nakmareong et al., 2012; Panthiya et al., 2022). Supplementation of curcumin reduces blood pressure and attenuates vascular oxidative stress and structural modifications in 2kidney-1clip (2K1C)-induced hypertensive rats (Boonla et al., 2014). Curcumin gavage attenuates 5/6 nephrectomy-induced systemic and glomerular hypertension, hyperfiltration, glomerular sclerosis, and interstitial fibrosis, which is associated with increased nuclear translocation of nuclear factor erythroid 2-related factor 2 (Nrf2) (Tapia et al., 2012). In a mouse model of cadmium-induced hypertension, curcumin is found to protect against vascular dysfunction through upregulation of endothelial nitric oxide synthase (eNOS) protein, restoration of glutathione redox ratio, and attenuation of oxidative stress (Kukongviriyapan et al., 2014). Similar to this finding, supplementation with curcumin significantly reduces blood pressure, alleviates oxidative stress, and increases plasma nitrate/nitrite and glutathione in the blood from rats with chronic exposure to lead and cadmium (Tubsakul et al., 2021). In addition, treatment with curcumin prevents cardiac dysfunction and heart failure in salt-sensitive Dahl rats, independently of hypertension (Morimoto et al., 2008;

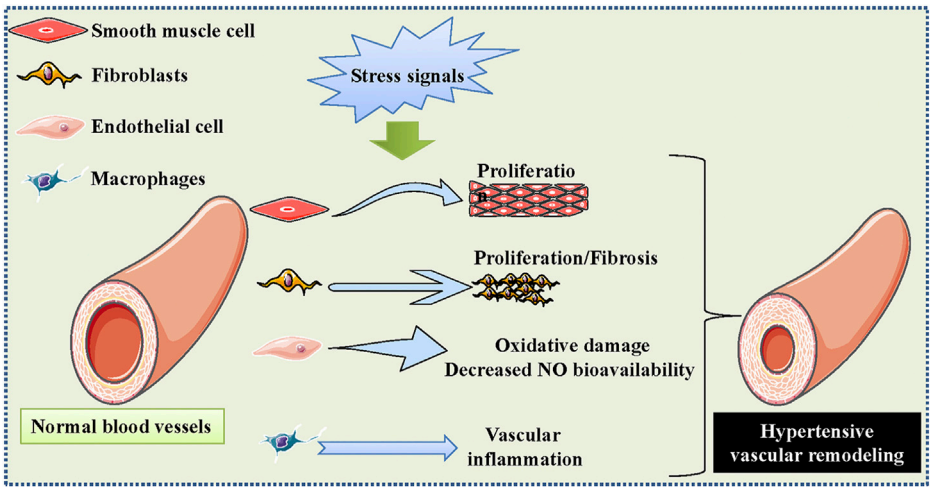

FIGURE 1 | Schematic presentation regarding the role of vascular dysfunction in hypertension. The blood vessels are constituted of VSMCs, endothelial cells, fibroblasts, extracellular matrix, and inflammatory cells, which are mandatory for vascular homeostasis. The excessive proliferation and migration of VSMCs, increased oxidative stress and impaired NO bioavailability in the endothelium, adventitial fibroblast activation, as well as macrophages-mediated vascular inflammation are important contributors to the development of hypertensive vascular remodeling. VSMCs, vascular smooth muscle cells; NO, nitric oxide.

Sunagawa et al., 2021). We have revealed that curcumin exhibits anti-hypertensive effects in spontaneously hypertensive rats (SHR) by suppressing vascular inflammation and remodeling (Sun H.-J. et al., 2017; Han et al., 2019). Very recently, a study by Kang's group has shown that curcumin reshapes the composition of the gut microbiota to grant antihypertensive effects (Li et al., 2021). These published papers provide ample evidence that curcumin is a promising protective agent against vascular dysfunction induced by PAH and arterial hypertension, such as primary hypertension, renovascular hypertension, salt sensitive hypertension, L-NAME-induced hypertension, angiotensin II (Ang II)-induced hypertension, 5/6 nephrectomy-induced systemic hypertension, and cadmium-induced hypertension. In the present review, we will recapitulate the cellular and molecular mechanisms that are responsible for curcumin-induced protection against hypertension and vascular remodeling. We further highlight the controversies and inconsistencies of curcumin in clinical settings. Eventually, we try to propose how addressing the bioavailability and pharmacokinetics of curcumin could help to prevent or treat hypertension-related vascular disorders.

ABERRANT VASCULAR CELL BEHAVIORS IN ARTERIAL HYPERTENSION AND PULMONARY ARTERIAL HYPERTENSION

The blood vessels are constituted of VSMCs, endothelial cells, adventitial fibroblasts, and extracellular matrix, and these components are mandatory for vascular homeostasis (Kim et al., 2019). It is well known that hypertension is intricately linked to large and small vascular remodeling impacting cardiovascular outcomes and prognosis (Briet and Schiffrin, 2013). Resistance small arteries are crucial players in the regulation of systemic blood pressure, and a functional reduction in small arteries is an early event in the initiation and progression of hypertension (De Ciuceis et al., 2007). The hypertrophic remodeling in resistance small arteries is detected in hypertension, which is characterized by an increase in the wall cross-sectional area, media-to-lumen ratio, and a decrease in internal diameter (Boari et al., 2010). These structural abnormalities are closely linked to enhanced vasoconstrictor response and progressive extracellular matrix deposition (Schiffrin et al., 1993; Rizzoni et al., 2000). The elastic properties of large arteries play a necessary role in the ventricular-aortic coupling, and such arteries are important determinants of systolic blood pressure (Briet and Schiffrin, 2013). The structural impairment of large arteries, such as collagen deposition and elastin fragmentation, leads to increased thickness and stiffness of the large arterial wall (Briet and Schiffrin, 2013). Elevated aortic stiffness is closely related to increased risk of cardiovascular events in hypertensive patients (Blacher et al., 1999; Aryal and Siddiqui, 2021). In the context of hypertension, vascular cells undergo cell proliferation, migration, and death, contributing to increased vascular thickness and stiffness, along with decreased compliance of blood vessels (**Figure 1**) (Brown et al., 2018). Specifically, VSMCs might exhibit phenotypic conversion from a differentiated to a dedifferentiated condition, which is a pathological hallmark of hypertension-triggered vascular remodeling (Laurent and Boutouyrie, 2015; Lu et al., 2018b). Endothelial cell inflammation and oxidative stress, increased endothelial cell permeability, impaired NO bioavailability, and destructed endothelial-dependent vasodilatation, are crucial initiating factors for blood pressure elevation (Sun et al., 2016; Sun HJ. et al., 2019). Activation of adventitial fibroblasts plays a critical role in the overproduction and deposition of collagens around the blood vessels, leading to vascular fibrosis and

remodeling in hypertension (Ling et al., 2018; Tong et al., 2018; Gumprecht et al., 2019; Ren et al., 2020; Wu et al., 2020; Tong et al., 2021). It is noteworthy to mention that communications between blood vessel cells are responsible for the development of hypertensive-related vascular remodeling (Sun HJ. et al., 2017; Zhang and Sun, 2020; Zhang and Sun, 2021). There is no doubt that impaired vascular cell function is one of the pathological characteristics for the development of arterial hypertension.

PAH-related vascular remodeling is associated with thickening of the tunica intima and tunica media (Humbert et al., 2008). The proliferation of pulmonary arterial endothelial cells and exuberant angiogenesis results in the formation of glomeruloid-like plexiform lesions, a common pathological feature of the pulmonary vessels of PAH patients (Tuder, 2017). Apart from this, changes in the production of various endothelial vasoactive molecules, including NO, prostacyclin, endothelin-1 (ET-1), serotonin, chemokines and thromboxane, play an important role in regulating the structural/functional alterations in the pulmonary vasculature (Tuder et al., 2013). It is convincing that excessive growth of pulmonary VSMCs could facilitate the development and progression of pulmonary vascular hypertrophy and structural remodeling in PAH (Jeffery and Morrell, 2002). Moreover, the structural changes in the intima, media and adventitia of pulmonary vessels contribute to a decrease in lumen diameter and reduced capacity for vasodilatation (Perros et al., 2005). In an autopsy series of 19 patients with PAH, an approximately 2- to 4-fold increase in adventitia thickness is observed in PAH lungs (Chazova et al., 1995). There is substantial evidence that the pulmonary arterial adventitia might function as an inflammatory cell signaling hub to boost pulmonary vascular remodeling (Pugliese et al., 2015; Stenmark et al., 2015). Apart from vascular cells, inflammatory cells and platelets may also play an essential role in the etiologies of arterial hypertension and PAH (Stumpf et al., 2016; Tuder, 2017), this deserves further studies. Collectively, in-depth elucidation of the intimate relationship between hypertension and vascular remodeling might permit novel therapeutic interventions of arterial hypertension and PAH.

Curcumin Provides Vascular Protection in Arterial Hypertension and Pulmonary Arterial Hypertension

As a yellow-colored hydrophobic polyphenol, curcumin is the main ingredient of spice turmeric with anti-inflammation, anti-carcinogenesis, anti-obesity, anti-angiogenesis, and anti-oxidant activities (Shishodia et al., 2005; Alappat and Awad, 2010; Meydani and Hasan, 2010). Accumulative evidence has demonstrated that curcumin is capable of preventing the development and progression of hypertension. For example, a study by Nakmareong et al. (2011) has revealed that administration of curcumin suppresses the elevation of blood pressure, decreases vascular resistance, and restores vascular responsiveness in L-NAME-infused rats. A later study by the same group has found that application of tetrahydrocurcumin, a major metabolite of curcumin, improves hypertension, along with reduced aortic wall thickness and stiffness in rats after L-NAME administration (Nakmareong et al., 2012). Oral gavage of curcumin prevents the elevation of blood pressure, diminishes the increased wall thickness and cross-sectional area of the aorta in experimental L-NAME-induced hypertensive rats (Hlavačková et al., 2011). Kukongviriyapan et al. (2014) have disclosed that both curcumin and tetrahydrocurcumin are effective in ameliorating cadmium-evoked hypertension and vascular dysfunction in mice (Kukongviriyapan et al., 2014; Sangartit et al., 2014). In agreement with these results, oral administration of hexahydrocurcumin, another major metabolite of curcumin, possesses antihypertensive actions by inhibiting vascular inflammation and oxidative stress, and activating the eNOS/NO pathway in aortic tissues, thus ameliorating vascular remodeling in hypertensive rats induced by L-NAME (Panthiya et al., 2022). As a result, it is clear that curcumin and its derivatives might provide a valuable way for the treatment of arterial hypertension or cadmium-induced hypertension.

It has been well established that curcumin treatment inhibits Ang II-induced hypertension and vasoconstriction, an effect that is mediated by downregulation of Ang II type 1 receptor (AT1R) expressions in the arteries (Yao et al., 2016). The elevated blood pressure and myocardial fibrosis are detected in male Sprague-Dawley rats subjected to Ang II infusion, whereas these abnormal changes are corrected by gastric gavage of curcumin (Pang et al., 2015). The myocardial protein level of AT1R is reduced, and the Ang II type 2 receptor (AT2R) expression is upregulated in curcumin-treated rats when compared to Ang II-infused rats (Pang et al., 2015). Furthermore, curcumin upregulates the protein level of angiotensin-converting enzyme 2 (ACE2) in the intermyocardium relative to the Ang II-treated rats (Pang et al., 2015). After 6 weeks of treatment, curcumin reduces blood pressure and vascular resistance in 2K1C-induced hypertensive rats, which is accompanied by attenuation of vascular structural modifications and oxidative stress (Boonla et al., 2014). A systematic review and meta-analysis has shown that long-term consumption of curcumin might improve systolic blood pressure, without affecting diastolic blood pressure (Hadi et al., 2019).

The clinical evolution of PAH results in a progressive debilitation, greatly reducing the quality of life in patient. Although the available drugs, such as prostanoids, phosphodiesterase inhibitors and antagonists of ET-1 for PAH therapy, the current therapeutic approaches are few and expensive. On the basis of the anti-inflammatory effects of curcumin, (Bronte et al., 2013) hypothesized a therapeutic role of curcumin or its derivatives for PAH (Bronte et al., 2013). Afterwards, curcumin and its analogues are reported to reverse the development of PAH and pulmonary vascular remodeling by preserving mitochondrial function in VSMCs (Chen et al., 2021), and retarding pulmonary fibrosis (Li et al., 2014). A series of curcumin analogues dilate rat pulmonary arteries via inhibiting phosphodiesterase-5 (PDE5) activities, suggesting that selective inhibition of PDE5 by curcumin may be a promising strategy for the prevention and treatment of PAH (Kruangtip et al., 2015). The Matrigel migration assay demonstrated that curcumin effectively prevented tumor necrosis factor-α (TNF-α)-induced

migration of human aortic smooth muscle cells by suppressing matrix metalloproteinase 9 (MMP-9) expression through downregulation of the nuclear translocation of NF-κB p50 and p65 (Yu and Lin, 2010). These above findings hint that curcumin may be a promising candidate for the prevention and treatment of hypertension. Despite the exciting results, the hypertension-lowering effects of curcumin should be treated with caution and more preclinical and clinical studies are warranted to ascertain these results.

The immune cell infiltrate is observed in blood vessels from arterial hypertension and PAH, including macrophages (Rabinovitch et al., 2014; Foley et al., 2021). Preclinical studies have provided that macrophage dysfunction underlies the development of vascular inflammation and remodeling in hypertension (Huo et al., 2021). Macrophages are phenotypically heterogeneous in which M1- and M2-type macrophages bear different features and functions (Stöger et al., 2012). A significant decrease of M2 macrophage markers and a marked increase of M1 macrophage markers play a pivotal role in hypertensive remodeling through numerous molecular mechanisms (Luo and Qiu, 2022), indicating that the pro-inflammatory status of macrophages drives the pathogenesis of hypertensive vascular remodeling. It is not surprising that curcumin could regulate macrophage functions in chronic inflammatory diseases (Mohammadi et al., 2019). It is reported that curcumin dose-dependently inhibits M1 macrophage polarization through downregulating toll-like receptor 4 (TLR4)-mediated activation of ERK, JNK, p38, and nuclear factor (NF)-κB (Zhou et al., 2015). In similarity with this finding, a curcumin derivative 2,6-bis(2,5-dimethoxybenzylidene)-cyclohexanone (BDMC33) is documented to suppress the secretion of pro-inflammatory mediators in stimulated macrophages via inhibition of NF-κB and MAPK signaling pathways, as well as suppression of prostaglandin E2 (PGE2) and cyclooxygenase (COX) expressions (Lee et al., 2011; Lee et al., 2012). Besides, administration of nano-emulsion curcumin blocks the phosphorylation of p65 NFκB and IκBα in macrophages induced by lipopolysaccharide (LPS), and reduces macrophage recruitment in a mouse model of peritonitis (Young et al., 2014). These findings suggest that curcumin could be used as a therapeutic agent in the management of hypertensive vascular remodeling by regulating macrophage polarization and activation, and curcumin may hold clinical promise for the prevention and treatment of hypertension due to its anti-inflammatory and immunomodulatory actions, especially considering that hypertension is also a chronic inflammatory disease (Sun H.-J. et al., 2017).

Curcumin Provides Vascular Protection in Hypertension Caused by Cadmium

Cadmium, a nonessential heavy metal, is documented to cause oxidative stress in various organs and tissues associated with hypertension (Pinheiro Júnior et al., 2020). A study by Greenwald's group showed that exposure of cadmium chloride results in hypertension, hypertrophic aortic wall, blunted vasodilation, increased aortic stiffness, collagen deposition, and accumulation of MMP-2 and MMP-9 levels in the aortic medial wall of male ICR mice, effects are largely ameliorated by tetrahydrocurcumin, a major metabolite of curcumin (Sangartit et al., 2014). The signaling mechanisms of tetrahydrocurcumin are shown to be associated with eNOS activation, enhanced antioxidant glutathione, decreased nitrate/nitrite level and oxidative stress in vascular tissues (Sangartit et al., 2014). Kukongviriyapan et al. found that intragastric administration of curcumin protected vascular dysfunction by increasing vascular responsiveness to acetylcholine, as well as normalizing the blood pressure elevation in cadmium chloride-challenged mice, a phenomenon that was eNOS-dependent (Kukongviriyapan et al., 2014). Exposure to lead and cadmium results in increases in blood pressure and peripheral vascular resistance, with a concomitant decrease in the blood pressure response to intravenous infusion to acetylcholine in male Sprague-Dawley rats (Tubsakul et al., 2021). By contrast, supplementation with curcumin effectively reduces blood pressure, alleviates oxidative stress, ameliorates vascular responsiveness through upregulation of eNOS and downregulation of the nicotinamide adenine dinucleotide phosphate (NADPH) oxidase expressions in the blood vessels of rats exposed to lead and cadmium (Tubsakul et al., 2021), an observation that supports the potential of curcumin as a candidate in the treatment of hypertension induced by the heavy metals. To this end, these findings consistently imply that curcumin might serve as a promising agent against hypertension and vascular remodeling induced by cadmium chloride due to its antioxidant, anti-nitrative, and chelating properties, which had also been meticulously introduced in a review (Kukongviriyapan et al., 2016). More experimental studies and clinical trials are required to replicate the benefit of curcumin and its active metabolites in hypertension and vascular remodeling upon cadmium chloride exposure.

Curcumin Nanomedicine in Hypertension

Although curcumin has been widely used for the treatment of various diseases, its unfavorable pharmacokinetics and pharmacodynamics profiles, including poor water solubility, poor bioavailability, and short biological half-life time, might hamper its biomedical and/or clinical applications (Pathak and Khandelwal, 2008). Indeed, approximately 60%–70% of oral administered curcumin is not absorbed due to their rapid hydrolyzation at physiological pH (Tønnesen et al., 2002; Anand et al., 2007). To resolve this obstacle, the microparticle-based systems are applied to enhance the bioavailability of curcumin (Shahani et al., 2010; Shome et al., 2016). Thus, the field of curcumin nanomedicine is flourishingly emerging (Pechanova and Dayar, 2020; Hesari and Mohammadi, 2021). To date, a number of nanomedicine-based drug delivery systems are used for curcumin delivery, such as mesoporous silica nanoparticles, exosomes, nanoemulsions, cyclodextrin inclusion complexes, nanogels, carbon nanotubes, liposomes, solid lipid nanoparticles, dendrosomes, dendrimers, polymeric nanoparticles, silver and gold nanoparticles, micelles, niosomes, nanocrystals, and nanosuspensions (Salehi and Del Prado-

Audelo, 2020). These promising approaches provide a solid platform to figure out the problems of curcumin delivery (Ahangari et al., 2019). Nanotechnology-mediated curcumin delivery formulation is used to treat a wide range of diseases, such as diabetes (Maradana et al., 2013), wound healing (Hussain et al., 2017), inflammatory diseases (Yallapu et al., 2015), neurodegenerative disorders (Rakotoarisoa and Angelova, 2018), and cancers (Yallapu et al., 2012). Nanocurcumin is also used to prevent and treat hypertension and its complications through improving its aqueous-phase solubility and bioavailability in the target tissues (Shome et al., 2016).

Compared to monocrotaline (MCT)-induced PAH rats, the right ventricular wall thickness and right ventricle weight/body weight ratio were largely reduced in PAH rats treated with curcumin nanoparticles (Rice et al., 2016). Besides, curcumin nanoparticles treatment attenuated MCT-induced expressions of TNF-α, interleukin 1β (IL-1β), nitrotyrosine, fibronectin, and myosin heavy chain-β in the right ventricle tissues (Rice et al., 2016). The delivery of curcumin to the vascular wall using hyaluronic acid-based nanocapsules caused a gradual inhibition of systolic blood pressure, diastolic blood pressure, and mean arterial pressure in hypertensive TGR(m-Ren2)27 rats (Czyzynska-Cichon and Janik-Hazuka, 2021). Surprisingly, administration of a curcumin solution (4.5 mg/kg) had no hypotensive effect in these animals (Czyzynska-Cichon and Janik-Hazuka, 2021), suggesting that hyaluronic acid-based nanocapsules might serve as a suitable approach to deliver hydrophobic and poorly bioavailable curcumin to the vascular wall (Czyzynska-Cichon and Janik-Hazuka, 2021). Curcumin nanoparticles encapsulated in poly(lactic-co-glycolic acid) (5 mg/kg/day) are found to normalize blood pressure and cardiovascular remodeling in male Wistar rats with diet-induced metabolic syndrome, an observation that is similar to the effects of unformulated curcumin (100 mg/kg/day) (Du Preez et al., 2019), implying that nanoparticle formulations might allow low-dose of curcumin to confer its benefits to health. Curcumin acetate nanocrystals significantly increase the pulmonary absorption time by 7.2-fold when compared to the sole curcumin, possibly because of the high lipophilicity of the former (Hu et al., 2017). This system achieves a better pharmacological efficacy in a MCT-induced rat model of PAH (Hu et al., 2017). A significant increase in physical properties, bioavailability, and stability is observed when curcumin is encapsulated in a nanoemulsion, and curcumin nanoemulsion shows significant anti-hypertensive and cholesterol-lowering activities, indicating the improved solubility of curcumin in the nanoemulsion system (Rachmawati et al., 2016). As aforementioned, curcumin nanoparticles provide feasible strategies for the sustained delivery of curcumin in a new discovery phase, thus improving its bioavailability and efficiency.

Despite having huge potential benefits of curcumin nanomedicine, the anti-hypertensive effects of curcumin nanomedicine are challenged by a study that encapsulation of curcumin in biodegradable poly(lactide-co-glycolic) acid nanoparticles failed to grant any protection against hypoxia-induced PAH in experimental animals (Devadasu et al., 2012). This study indicated that hypoxia conditions might affect the localization of particles in the lungs, which may be due to blood flow changes, increased barrier properties of the pulmonary vascular system, and decreased endocytosis (Devadasu et al., 2012). The tissue levels of curcumin under hypoxia circumstances are much lower than that of normoxic conditions because of the difference in particle dynamics, leading to failure of PAH treatment (Devadasu et al., 2012). Despite these contradictory results, more preclinical studies with rigorous experimental designs are warranted to verify the efficacy of nanomaterials-mediated curcumin transfer in hypertension. To sum up, nanomedicine bridges the gap between pharmaceutical limitations and the therapeutic potentials of curcumin via strengthening curcumin's pharmacokinetics, efficacy, and cellular uptake.

MOLECULAR MECHANISM OF CURCUMIN IMPROVING VASCULAR REMODELING IN HYPERTENSION

Next, the cellular and molecular mechanisms of actions of curcumin and its derivatives in hypertension and vascular remodeling will be critically described. In short, curcumin might benefit hypertension and vascular remodeling *via* multiple mechanisms, such as suppression of vascular contraction, inhibition of VSMC proliferation and migration, amelioration of endothelial cell dysfunction, and blockade of the renin angiotensin system (RAS), etc.

SUPPRESSION OF VASCULAR CONTRACTION

Elevated vascular resistance is one of the main pathological events in the development and maintenance of hypertension, paralleling by abnormal vasoconstriction, impaired vasodilation, and vascular remodeling (Jouen-Tachoire and Tucker, 2021; Mccoy and Lisenby, 2021; Prado et al., 2021). VSMC tone is mainly regulated by changes in both intracellular Ca^{2+} concentration and myofilament Ca^{2+} sensitivity, which is enhanced by L-type Ca^{2+} channels in the membrane of VSMCs and inositol 1,4,5-trisphosphate (IP3)-mediated Ca^{2+} release from sarcoplasmic reticulum via G protein-coupled receptor-induced phospholipase C activation (Karaki and Weiss, 1988; Karaki et al., 1997). Under physiological states, the L-type Ca^{2+} channels are slowly inactivated in the process of continuous depolarization, and the influx of Ca^{2+} is sufficient to mediate pressure-induced vasoconstriction of resistance vessels, thus contributing to the dynamic auto-regulation of systemic arteries (Nelson et al., 1990). However, the occurrence of abnormal arterial tension is closely linked with increased expressions of L-type Ca^{2+} channel α1C subunits, resulting in increasing blood pressure and flow (Wang et al., 1999). Therefore, L-type Ca^{2+} channel antagonists could be expected to act as adjuvants for anti-hypertensive agents as L-type Ca^{2+} channel overexpression is not limited to hypertension (Cox and Rusch, 2002). ET-1, a vasoactive peptide of 21-amino acids, is known as

one of the most potential vasoconstrictors, which plays a critical role in the development of hypertension by acting on endothelin receptor type A (ET_AR), type B1 ($ET_{B1}R$), and type B2 ($ET_{B2}R$) coupled with G proteins (Sakurai et al., 1990; Kedzierski et al., 2003). ET_AR and $ET_{B2}R$ mainly mediate vasoconstriction and cell proliferation, whereas $ET_{B1}R$ have vasodilatation, anti-inflammatory, and ET-1 peptides-clearing functions (Webb and Meek, 1997; Lüscher and Barton, 2000). Increased ET-1 expressions and altered expressions of ET-1 receptors are well characterized in hypertension (Wang B. et al., 2021). Accordingly, the antagonists of ET-1 or inhibitors of ET_A/ET_{B2} receptor are clinically important to prevent or treat cardiovascular illnesses including essential hypertension and PAH (Barton and Yanagisawa, 2019; Dhaun and Webb, 2019; Xiao et al., 2021). To this end, it is important to develop novel vasodilation drug candidates that affect both L-type Ca^{2+} channel- and ET-1-induced vascular constriction, thus advancing the development of antihypertensive drugs. Coincidentally, Park et al. (2015) have identified alkylsulfonyl and substituted benzenesulfonyl curcumin mimics as a dual antagonist of L-type Ca^{2+} channel and endothelin A/B2 receptor in VSMCs, representing them as potential drug candidates to treat hypertension and vascular remodeling. Also, circulating ET-1 plays a central role in regulating renal electrolyte and water handling (Tamás et al., 1994; Bomzon et al., 1997; Ota et al., 1998; Lynch et al., 2015), since intravenous infusion of ET-1 profoundly increases renal vascular resistance and decreases the excretion of sodium and water (Sørensen et al., 1995). Selective blockade of ET_AR and ET_BR differentially affects renal tubular water and salt handling in Wistar-Kyoto and Long-Evans rats (Girchev et al., 2006). On the contrary, centrally administered ET-1 had no effect on renal handling of water and electrolytes (Yamamoto et al., 1991). Given the role of ET-1 in renal electrolytes and water handling, and the opposed effects of curcumin on ET-1-mediated effects, it will be of importance to investigate whether curcumin lowers hypertension by affecting renal handling of water and electrolytes and renovascular contraction.

The exaggerated vasoconstrictor generation by cyclooxygenase-2 (COX-2) is a driving force for the development of hypertension-related vascular contraction (Virdis and Taddei, 2016). Thus, it is interesting to test whether curcumin conserves vascular function in hypertension by inhibiting COX-2 production. Accordingly, (Li and Tian, 2016) examined this hypothesis and found that demethoxycurcumin, a major component of *Curcuma longa* L, elevated endothelium-dependent contractions in renal arteries of SHR by normalization of COX-2 expression, indicating the benefits of demethoxycurcumin in endothelium-dependent contractions during the development of hypertension (Li and Tian, 2016).

Malfunction in vascular reactivity is an important component of diabetes-related hypertension (Farhangkhoee et al., 2003). Curcumin is reported to attenuate phenylephrine-induced increase in contraction during the early stage of streptozotocin-induced diabetic rats, suggesting a regulatory role of curcumin in cardiometabolic diseases-associated vascular dysfunction (Majithiya and Balaraman, 2005). Zakaria's group has uncovered that curcumin treatment reduces elevated systolic blood pressure and prevents aorta-exaggerated response to phenylephrine and potassium chloride (KCl) in diabetes-evoked hypertensive rats (Hassan et al., 2013; El-Bassossy et al., 2014). Further studies have suggested that curcumin functions as a heme oxygenase-1 (HO-1) inducer to protect against exaggerated vascular contractility by reducing TNF-α and aortic reactive oxygen species (ROS) levels (Hassan et al., 2013). In consistence with this finding, exogenous curcumin effectively abrogates high fructose-elicited contractile response of aortic rings to both phenylephrine and KCl through reduction of intracellular ROS and calcium (Mahmoud and El Bassossy, 2014). Overall, these published papers imply that curcumin acts as a promising candidate to suppress hypertension-induced vasoconstriction. In spite of this, more studies are necessary to affirm these observations, thus pointing towards that the vascular benefits of curcumin may be dependent on circumventing vasoconstriction in hypertension. Here, it should be mentioned that renal artery narrowing is a major driver for hypertensive development by producing renal vascular resistance from the glomerulus (Anderson et al., 2000). Increased renal arterial contraction and renovascular resistance are also closely associated with the pathologies of hypertension (Restini et al., 2018). Although the renoprotective roles of curcumin in hypertension (Boonla et al., 2014; Yaribeygi et al., 2021), it remains to be explored whether amelioration of renal function or inhibition of renovascular contraction contributed to the blood pressure lowering actions of curcumin.

INHIBITION OF VASCULAR SMOOTH MUSCLE CELL PROLIFERATION AND MIGRATION

Phenotypic switching, a prerequisite step for abnormal proliferation and migration of VSMCs, is characterized by a transition from a contractile phenotype (differentiated phenotype) to a synthetic phenotype (dedifferentiated phenotype) under various stimuli, including hypertension (Shi and Chen, 2014). Excessive proliferation and migration of VSMCs are important characteristics of hypertension, and reversing this process might be an important strategy to fight against hypertension and its associated vascular remodeling (Harrison et al., 2021). In light of the anti-hypertensive effects of curcumin, it is not unexpected to observe that curcumin might benefit hypertension by regulating the biological behaviors of VSMCs (**Figure 2**).

A previous report had shown that curcumin does-dependently inhibited the proliferation of rabbit VSMCs stimulated by fetal calf serum (Huang et al., 1992), indicating that curcumin is a promising remedy for the prevention of the pathologies of vascular remodeling-related diseases, such as atherosclerosis, restenosis, and hypertension. A later study further demonstrated that curcumin prevented cell proliferation, arrested the cell cycle progression, and facilitated cell apoptosis in VSMCs (Chen and Huang, 1998). Mechanistic studies have shown that the antiproliferative effects of

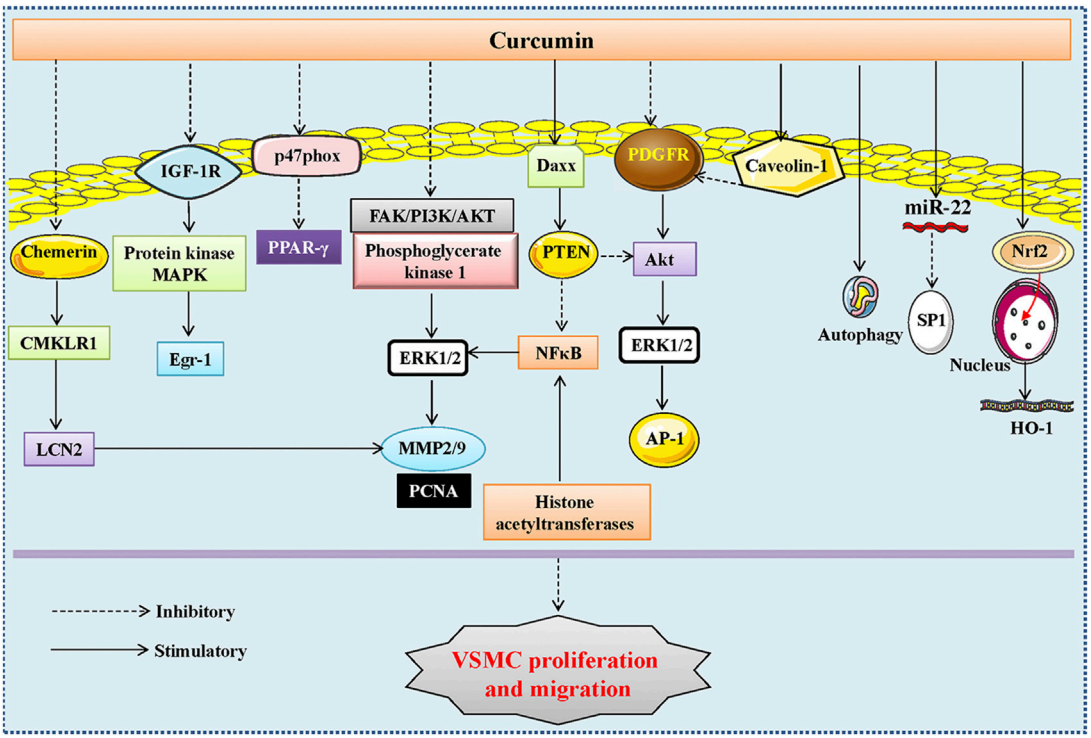

FIGURE 2 | The signaling pathways involved in the inhibitory action of curcumin in VSMC proliferation and migration. The inhibitory effects of curcumin and its analogue or derivatives in VSMC proliferation and migration were associated with inhibition of the FAK/PI3K/AKT and phosphoglycerate kinase 1/ERK1/2 signaling pathways, blockade of the protein kinase and mitogen-activated protein kinase (MAPK) and the p38 MAPK and Wnt/β-catenin signaling pathways, suppression of histone acetyltransferases and PDGF receptor-β phosphorylation, Akt and ERK1/2, inactivation of the IGF-1R/PKB/ERK1/2/Egr-1 axis, regulation of the PTEN/Akt pathway and the miR-22/SP1 axis, repression of the chemerin/CMKLR1/LCN2 signaling pathway, activation of caveolin-1, Nrf2/HO-1, PPAR-γ, autophagy, and Daxx. VSMCs, vascular smooth muscle cells; FAK, focal adhesion kinase; PI3K, phosphatidylinositol 3-kinase; AKT, protein kinase B; ERK1/2, extracellular signal regulated kinase 1/2; IGF-1R, insulin-like growth factor type 1 receptor; Egr-1, early growth response; PPAR-γ, peroxisome proliferator-activated receptor-γ; CMKLR1, chemokine-like receptor 1; LCN2, lipocalin-2; Nrf2, nuclear transcription factor E2-related factor-2; HO-1, heme oxygenase-1; PTEN, phosphatase and tensin homolog; PDGF, platelet-derived growth factor; SP1, specificity protein 1.

curcumin may be mediated by inhibition of protein tyrosine kinase activity and c-myc mRNA expression, while the apoptotic effects of curcumin might partly be modulated by suppression of protein tyrosine kinase activity, protein kinase C activity, c-myc mRNA expression and B-cell lymphoma-2 (Bcl-2) mRNA expression (Chen and Huang, 1998). Demethoxycurcumin, a major active curcuminoid from Curcuma longa, exhibits similar actions on fetal calf serum-stimulated VSMC proliferation and migration by downregulating the expression of MMP-2 and MMP-9 via dampening the focal adhesion kinase (FAK)/phosphatidylinositol 3-kinase (PI3K)/AKT (protein kinase B) and phosphoglycerate kinase 1/extracellular signal regulated kinase 1/2 signaling pathways (Sheu et al., 2013). Moreover, blockade of the protein kinase and mitogen-activated protein kinase (MAPK) pathways was also required for curcumin to restrain VSMC proliferation, inflammation, and oxidative stress (Nguyen et al., 2004). Collectively, these findings indicate that curcumin and its analogues can be developed to inhibit VSMC proliferation and migration through various signaling pathways.

A number of growth factors, such as platelet-derived growth factor (PDGF) and fibroblast growth factor, are responsible for the proliferation and migration of VSMCs, an event in the pathological changes of hypertension and vascular injury (Heldin and Westermark, 1999; Lu et al., 2018a). Consequently, blockade of PDGF signaling may represent an important avenue to restrain VSMC dedifferentiation, migration, proliferation, and extracellular matrix synthesis during the process of hypertension and restenosis after vascular injury. In this regard, Yang et al. examined the effects of curcumin on PDGF-stimulated VSMC proliferation and migration, and found that curcumin evoked a concentration-dependent inhibition of VSMC migration, proliferation, and collagen synthesis in PDGF-incubated VSMCs (Yang et al., 2006). Animal studies showed that carotid artery neointima formation was strikingly attenuated by perivascular administration of curcumin (Yang et al., 2006). Similar to this finding, dehydrozingerone, a structural analog of curcumin, induces a dose-dependent inhibition of PDGF-stimulated VSMC migration, proliferation, collagen synthesis *via* inhibiting the phosphorylation of PDGF-receptor (PDGFR) and AKT (Liu et al., 2008). Additionally, the anti-proliferative effects of curcumin on PDGF-induced VSMC proliferation are caveolin-1-dependent as disruption of caveolae with methyl-β-cyclodextrin eliminates curcumin-mediated effects, suggesting

that upregulation of caveolin-1 is implicated in curcumin-induced benefits in the vasculature (Zeng et al., 2013). Bisdemethoxycurcumin, a naturally occurring structural analog of curcumin, induces a concentration-dependent inhibition of PDGF-stimulated VSMC migration and proliferation *via* impeding the phosphorylation of PDGF receptor-β, AKT and ERK (Hua et al., 2013). Epidermal growth factor (EGF) acts on epidermal growth factor receptor (EGFR) to trigger numerous signaling cascades leading to the proliferation and migration of VSMCs. A host of transcription factors contribute to EGFR overexpression, including activator protein (AP-1). An interesting study showed that curcumin had the ability to halt VSMC proliferation by functioning as an AP-1 inhibitor (Hsieh et al., 2008a; Hsieh et al., 2008b). A better understanding of the underlying mechanisms involved in curcumin-regulated AP1 expression in VSMCs may offer potential targets in the treatment of hypertensive vascular remodeling. These findings provide evidence that the anti-proliferative effect of curcumin is largely linked to its ability to mitigate the PDGF and EGFR signaling pathways.

Phosphatase and tensin homolog (PTEN) is a well-recognized tumor suppressor gene that plays a fundamental role in the proliferation and migration of VSMCs, thus representing a potential target to treat vascular remodeling. HO-3867, a novel synthetic curcuminoid, is shown to inhibit the proliferation of serum-stimulated VSMC proliferation through activation of PTEN, followed by downregulation of MMP-2, MMP-9, and nuclear factor-kappaB (NF-κB) expressions in VSMCs (Selvendiran et al., 2009). Therefore, HO-3867, a potential derivative of curcumin, is capable of preventing vascular abnormalities by upregulating PTEN. ET-1 is known to participate in the etiologies of vascular pathologies, including hypertensive vascular remodeling, via hyperactivation of AKT and extracellular signal-regulated kinase 1/2 (ERK1/2) signaling. Curcumin treatment prevents ET-1-induced activation of AKT, ERK1/2, c-Raf, insulin-like growth factor type 1 receptor (IGF-1R), and early growth response (Egr)-1, which are well-known mitogenic and proliferative signaling molecules in VSMCs (Kapakos et al., 2012). Ang II is implicated in the proliferation and migration of VSMCs, contributing to the development and progression of vascular disorders, including atherosclerosis and hypertension. Mounting evidence indicates that activation of peroxisome proliferator-activated receptor-γ (PPAR-γ) circumvents Ang II-induced inflammation response and ROS production in VSMCs. This drives a possibility that curcumin might protect against Ang II-induced oxidative stress and inflammatory responses in VSMCs by upregulating PPAR-γ. Indeed, a study by Li et al. (2017) has shown that curcumin attenuates Ang II-induced expressions of inflammatory factors and oxidative stress through induction of PPAR-γ in VSMCs, which is accompanied by suppression of VSMC proliferation. In keeping with this, nicotinate-curcumin, an esterification derivative of niacin and curcumin, markedly prevents Ang II-induced VSMC phenotype switching, proliferation, and migration via regulating the PTEN/AKT pathway (Sun et al., 2021). As a group of short non-coding RNA, micro RNAs (miRNA) plays a critical role in the process of human diseases, including hypertension (Zhang and Sun, 2020; Zhang and Sun, 2021). Studies have illustrated that miR-22 plays an important role in vascular remodeling (Zheng and Xu, 2014), cardiac hypertrophy (Gurha et al., 2012; Huang et al., 2013), and spontaneous hypertension (Friese et al., 2013). It remains unknown as to whether curcumin regulates VSMC phenotype and proliferation by regulating miR-22. As expected, curcumin upregulated the expression of miR-22 to decrease the protein expression of specificity protein 1 (SP1), leading to an obvious inhibition of VSMC proliferation and migration, as well as vascular neointimal hyperplasia after vascular injury (Zhang et al., 2020). Chemerin, a novel adipokine, plays a crucial role in the process of atherosclerosis by acting on chemokine-like receptor 1 (CMKLR1) (Liu et al., 2019), and the chemerin/CMKLR1 signaling pathway is also involved in the regulation of intimal hyperplasia and hypertension (Kennedy et al., 2016; Artiach et al., 2018). A recent study has demonstrated that knockdown of CMKLR1 markedly inhibits VSMC proliferation and migration, and the lipocalin-2 (LCN2) acts as a key factor to mediate CMKLR1-induced VSMC functions through the p38 MAPK and Wnt/β-catenin signaling pathways (He et al., 2021). Importantly, curcumin targets this complex axis to inhibit VSMC proliferation and migration, thereby reducing atherosclerotic progression (He et al., 2021). Totally, curcumin and its analogues may be of potential use in the prevention or treatment of vascular diseases, including hypertensive vascular remodeling.

Induction of HO-1 is documented to obliterate the proliferation of VSMCs by upregulation of the cyclin-dependent kinase inhibitor p21, a negative dominator in cellular proliferation (Lee et al., 2004; Kim et al., 2009). A study by Shyy's group has illustrated that the phytochemical curcumin increments HO-1 expression through the nuclear translocation of Nrf2, a pivotal event involved in the suppression of VSMC proliferation (Pae et al., 2007). Additionally, curcumin inhibits the growth of TNF-α-induced human VSMCs in a HO-1-dependent manner since HO-1 inhibitor tin protoporphyrin abolishes the effects of curcumin in the context of TNF-α (Pae et al., 2007). Oxidized low-density lipoprotein (ox-LDL) is progressively increased in atherosclerosis, and it causes damages in blood vessels by inducing the conversion of a normal VSMC contraction phenotype to an abnormal synthetic phenotype, resulting in the migration of VSMCs into the intima (Allahverdian et al., 2014; Di and Maiseyeu, 2021). The protective effects of curcumin on ox-LDL-induced VSMC injury were examined by an *in vitro* experiment that VSMCs were treated with ox-LDL in the presence or absence of curcumin (Wang G. et al., 2021). The authors found that curcumin-mediated photodynamic therapy alleviated the phenotypic transformation, proliferation, and migration of VSMCs upon ox-LDL exposure, an effect that is associated with induction of autophagy (Wang G. et al., 2021). Furthermore, we have also disclosed that curcumin serves as an inhibitor of histone acetyltransferases (HAT) to suppress NF-κB upregulation and nod-like receptor family protein 3 (NLRP3) inflammasome activation in VSMCs, thus preventing VSMC phenotype switching, proliferation, migration, and vascular

remodeling in SHR (Sun H.-J. et al., 2017; Han et al., 2019). We further found that intragastric administration of curcumin attenuated hypertension, repressed NF-κB activation, NLRP3 and MMP-9 expressions in the aortas, reduced the media thickness and the ratio of media thickness to lumen diameter in the aortas of SHR (Han et al., 2019). Extracellular vesicles are becoming a research hotspot since they are recognized as potential therapeutic targets and drug delivery systems by transferring their loaded molecules such as miRNA, proteins, and cytokines between cells (Sun HJ. et al., 2017). Correspondingly, extracellular vesicles-mediated interactions between vascular endothelial cells and VSMCs are essential in the development of cardiovascular diseases, including hypertension (Zhang and Sun, 2022). Treatment with normal endothelial extracellular vesicles reduces the proliferation and migration of VSMCs, whereas treatment with LPS-induced endothelial extracellular vesicles promotes the proliferation of VSMCs by regulating several miRNAs, including miR-92a-3p, miR-126-5p, miR-125a-3p, miR-143-3p, to name a few (Xiang et al., 2021). Intriguingly, the same group further showed that treatment with curcumin and nicotinic-curcumin reduced endothelial extracellular vesicle secretion, possibly by inhibiting inflammation (Xiang et al., 2021), indicating that curcumin might regulate vascular functions through extracellular vesicles-mediated vascular cell communications in hypertension. This hypothesis still awaits further research.

The evidence for the favorable role of curcumin in PAH-related vascular remodeling is emerging. The thickness of pulmonary arterial media smooth cell layer and collagen fibers in adventitia tend to be normal in hypoxic hypercapnic rats treated with curcumin, thus leading to a decrease in pulmonary arterial pressure, in conjunction with a reversal of pulmonary vessel remodeling (Lin et al., 2006). Likewise, curcumin exposure promotes pulmonary VSMC apoptosis by regulating mitochondrial function, and prevents the expressions of pro-proliferative genes in pulmonary VSMCs by suppressing the PI3K/AKT pathway (Chen et al., 2021). Collectively, we and other groups provide direct evidence that curcumin plays a beneficial role in antagonizing vascular inflammation and remodeling in hypertension. However, whether curcumin could be used as an adjuvant or supplement for hypertension treatments in clinical applications still requires more verification and corroboration. Thoracic aortic aneurysm and abdominal aortic aneurysm are prevalent aortic disorders, which are characterized by VSMC phenotypic switching, VSMC apoptosis, extracellular matrix degradation, increased matrix metalloproteinase activity, secretion of inflammatory cytokines, and oxidative stress (Lu and Du, 2021). Preclinical studies have found that administration of curcumin is effective in suppressing the development of experimental aortic aneurysm by inhibiting VSMC phenotypic switching and apoptosis (Fan et al., 2012; Hosseini et al., 2021). However, these experiment results could not be reproduced in human studies. A parallel-group, randomized, placebo-controlled trial revealed that perioperative oral curcumin had no beneficial effects in elective abdominal aortic aneurysm repair, and induced a higher risk of acute kidney injury in 606 patients (Garg et al., 2018). In spite of this inconsistence, more preclinical and clinical studies are required to confirm the potential benefits of curcumin and its analogs in aortic aneurysm.

AMELIORATION OF ENDOTHELIAL CELL DYSFUNCTION

As a large paracrine organ, the vascular endothelium plays an important role in the regulation of cell growth, vascular tone, platelet and leukocyte interactions, as well as thrombogenicity (Sun et al., 2016; Gong et al., 2019). Disruption of endothelial function is a pivotal event in initiating various disorders, including arterial hypertension and PAH (Monteiro et al., 2019; Zhang and Sun, 2020). Endothelial dysfunction is hallmarked by increased ROS, overproduction of proinflammatory factors, deficiency of NO bioavailability, imbalanced productions in endothelium-released relaxing and contracting factors, enhanced leukocytes adhesion and permeability of endothelium (Monteiro et al., 2019). Furthermore, the proliferation, migration, and apoptosis of endothelial cells are intimately linked with endothelial dysfunction in hypertension and PAH (Zhang et al., 2018). Therapeutic strategies against vascular endothelial dysfunction are essential for preventing and treating vascular lesions, such as hypertension. A review has summarized that curcumin could improve endothelial dysfunction through its anti-inflammatory, anti-aging, antiangiogenic, and antioxidant properties (Zhang et al., 2018), suggesting that curcumin might ameliorate hypertension and its associated cardiovascular remodeling by reversing endothelial damage (Alidadi et al., 2021).

Endothelium-dependent vasorelaxation is impaired in aortic rings isolated from 2K1C hypertensive rats, which is compromised by curcumin treatment (Boonla et al., 2014). Additionally, administration of curcumin reverses hypertension-induced oxidative stress, vascular structural modifications, and eNOS inactivation (Boonla et al., 2014). Preservation of endothelial function is sufficient for curcumin to reduce blood pressure and decrease hindlimb vascular resistance (Boonla et al., 2014). As mentioned above, COX-2 is not only a driver for the exaggerated vasoconstrictor, but also a stimulator for vasodilation dysfunction in hypertension. Demethoxycurcumin rescued the attenuated endothelium-dependent relaxations, which was accompanied by the normalization of COX-2 expression in the renal arteries of SHR (Li and Tian, 2016). Tetrahydrocurcumin is established to prevent the elevation of blood pressure, peripheral vascular resistance, and aortic stiffness in rats after L-NAME administration (Nakmareong et al., 2012). These changes are associated with increased aortic eNOS expression, elevated plasma nitrate/nitrite, decreased oxidative stress, and enhanced blood glutathione (Nakmareong et al., 2012). Induction of HO-1 by curcumin alleviated metabolic syndrome-related hypertension and vascular complications by maintaining endothelial-dependent relaxation and NO generation in blood vessels (El-Bassossy et al., 2014). Curcumin is identified to be major constituents in turmeric and black seeds, whilst co-

administration of black seeds and turmeric lowers blood pressure and hypertriglyceridemia, hyperinsulinemia, and endothelial dysfunction in fructose-fed rat model of metabolic syndrome (Amin et al., 2015). In chronic cadmium exposure, curcumin and tetrahydrocurcumin protect vascular endothelium by increasing NO bioavailability and improving vascular function, thereby relieving vascular dysfunction and high blood pressure caused by cadmium toxicity (Kukongviriyapan et al., 2016; Almenara et al., 2020). In line with this, supplementation with curcumin significantly reduces blood pressure, alleviates oxidative stress, increases plasma nitrate/nitrite and glutathione in rats with chronic exposure to lead and cadmium (Tubsakul et al., 2021). These beneficial effects of curcumin are associated with the upregulation of the eNOS and subsequent improvement of vascular responsiveness (Tubsakul et al., 2021). Elevated blood pressure, increased oxidative stress, decreased plasma NO levels, and downregulation of eNOS expression in aortic tissues are found in L-NAME-induced hypertensive rats, whereas this phenomenon is largely eradicated by hexahydrocurcumin, a major metabolite of curcumin (Panthiya et al., 2022).

Injection of iron sucrose (10 mg/kg/day) for 8 weeks in male ICR mice induces iron overload, hypertension, impaired vascular function and blunted response of the autonomic nervous system (Sangartit et al., 2016). These abnormalities are corrected by tetrahydrocurcumin in combination with deferiprone (Sangartit et al., 2016). Electron microscope showed that the endothelial cells of pulmonary arterioles tend to be normal after curcumin treatment in PAH rats (Li et al., 2014). A clinical study has found that supplementation of curcumin improves resistance artery endothelial function in healthy middle-aged and older adults by increasing vascular NO bioavailability and reducing oxidative stress (Santos-Parker et al., 2017), further confirming the benefits of curcumin in vascular endothelial function. Overall, pharmacological intervention of endothelial dysfunction by curcumin could be utilized as an effective avenue for hypertension therapy. These above findings hint that curcumin grants protection against hypertension due to its benefits on the endothelium. It is anticipated that the continuous studies of curcumin in the vascular endothelium will provide great hope for therapeutic approaches for hypertension.

The endothelial to mesenchymal transition (EndMT) has recently emerged as one of the key phenomena driving endothelial dysfunction and vascular remodeling in several vascular diseases, such as arterial hypertension and PAH (Li et al., 2018; Botts et al., 2021). Consequently, inhibition of EndMT might provide novel therapeutic approaches for vascular inflammation-related diseases (Lu et al., 2019; Xu et al., 2021). Chen and coworkers found that curcumin inhibited transforming growth factor β1 (TGF-β1)-induced EndMT in endothelial cells Nrf2-upregulated dimethylarginine dimethylaminohydrolase-1 (DDAH1) expressions, leading to a reduction in endothelial cell fibrosis (Chen et al., 2020). However, there is no direct evidence showing that curcumin attenuated the development of hypertension by restraining the process of EndMT in endothelial cells. It is certain that the regulation of EndMT by curcumin could provide novel insights into hypertension-induced endothelial dysfunction, thus yielding novel therapeutic approaches.

BLOCKADE OF THE RENIN ANGIOTENSIN SYSTEM

It is well known that activation of the RAS plays a pathogenic role in the development and progression of hypertension. As a principal effector peptide within RAS, Ang II is a potential regulator of arterial blood pressure by binding to two distinct receptors: the AT1R and AT2R. Most actions of Ang II are primarily transmitted via AT1R, such as vasoconstriction, cardiac contractility, and reduced vascular compliance. Blockade of AT1R is an efficient approach to attenuate blood pressure in hypertensive patients and animals. Yang et al. have found that curcumin dose- and time-dependently downregulates AT1R expressions in VSMCs through reducing the binding of SP1 with the AT1R promoter, suggesting that the effect of curcumin on AT1R expression at the transcriptional level (Yao et al., 2016). In addition, these authors further demonstrate that curcumin treatment reduces Ang II-induced hypertension and vasoconstriction, concomitant with reduction of AT1R expression in the arteries, indicating that downregulation of AT1R is an important mechanism for curcumin to prevent the development of hypertension in an Ang II-induced hypertensive models (Yao et al., 2016).

Angiotensin-converting enzyme (ACE), a membrane-bound enzyme, is known to act on diverse peptide substrates in the extracellular space, and this peptidyl dipeptidase cleaves off His-Leu from angiotensin I to produce Ang II (identical to kininase II), which cleaves off Phe-Arg from bradykinin to yield inactive residue (Gouda et al., 2021). Thus, inhibition of ACE is capable of blocking the formation of Ang II and potentiating the effects of bradykinin (Marceau and Bachelard, 2020). A large body of studies are devoted to demonstrate the therapeutic potential of ACE inhibitors for hypertension (Prieto et al., 2021). A series of experiments have shown that the actions of bradykinin are mainly mediated by its receptors B1 and B2 (Cui et al., 2005). Incubation of Ang II stimulates gene expression of both B1 and B2 receptors in cardiomyocytes and VSMCs, an effect that is abolished by concurrent inhibition of the AT1 receptor with losartan (Kintsurashvili et al., 2001). Similarly, exogenous ACE strongly upregulates the genes of bradykinin receptors B1 and B2 in VSMCs, whereas this phenomenon is not altered by addition of specific Ang II antagonists for the AT1 and AT2 receptors, as well as the ACE inhibitor captopril (Kintsurashvili et al., 2001). It is reported that curcumin could suppress the formation and action of NF-κB and AP-1 through interacting with such transcriptional factors (Aggarwal et al., 2003; Kang et al., 2004). Interestingly, pretreatment with transcriptional inhibitor curcumin completely abolishes the effects of ACE on B1 and B2 receptors, suggesting that ACE challenge results in upregulations of the bradykinin B1 and B2 receptor genes through activating the NF-κB and AP-1 signaling pathways (Kintsurashvili et al., 2001). As a widely used compound, curcumin might be used to treat hypertension by

modulating the interaction of ACE with bradykinin system in VSMCs dependent on NF-κB and AP-1 signaling.

OTHER MECHANISMS

Oral gavage of curcumin partially prevents L-NAME-induced hypertension in rats, accompanied by decreased wall thickness and cross-sectional area of the aorta (Hlavačková et al., 2011), indicating that administration of curcumin is effective in preventing negative changes in blood vessel morphology under hypertensive conditions. Interestingly, it is reported that tetrahydrocurcumin, a major metabolite of curcumin, could inhibit the elevation of blood pressure, restore vascular responsiveness to vasoactive substance, and suppress vascular resistance of rats treated with L-NAME, an effect that is likely to be more effective than those of curcumin (Nakmareong et al., 2011). Mechanistically, the improvement of hypertensive vascular remodeling by tetrahydrocurcumin is mediated by suppression of oxidative stress and nitrative stress in the aortic tissues (Nakmareong et al., 2011). Moreover, Saowanee and coworkers also demonstrated that tetrahydrocurcumin treatment reversed the deleterious effects of L-NAME on blood pressure, peripheral vascular resistance, aortic stiffness, and oxidative stress in rats (Nakmareong et al., 2011). The favorable actions of tetrahydrocurcumin were related to increased aortic eNOS expression, elevated plasma nitrate/nitrite, decreased oxidative stress with reduced superoxide production and enhanced blood glutathione (Nakmareong et al., 2011). In parallel to this, L-NAME supplementation leads to upregulations of NF-κB, vascular cell adhesion molecule 1 (VCAM-1), intercellular adhesion molecule 1 (ICAM-1), TNF-α, p-ERK1/2, phosphorylated-c-Jun N-terminal kinases (p-JNK), phosphorylated-mitogen activated protein kinase p38 (p-p38), transforming growth factor-beta 1 (TGF-β1), MMP-9 and collagen type 1 in rat aortas, with a concomitant decrease in eNOS expression in aortic tissues (Panthiya et al., 2022). However, these abnormal alterations are obviously reversed by hexahydrocurcumin treatment (Panthiya et al., 2022). Growing evidence has highlighted the importance of gut dysbiosis and gut-brain communication dysregulation in the pathogenesis of hypertension (Li et al., 2020; Sharma et al., 2020). Transplantation of fecal bacteria from normotensive rats to hypertensive rats is found to alleviate the development of hypertension (Toral et al., 2019). Retrograde viral tracing in hypertensive rodents showed increased neural connections from the intestine to the hypothalamus paraventricular nucleus (PVN), an important cardioregulatory region in the central nervous system (Toral et al., 2019). This provides intuitive evidence to recognize the microbiota-gut-brain axis as a new mechanism involved in hypertension pathologies (Toral et al., 2019). As anticipated, the elevated blood pressure of SHR is markedly inhibited by curcumin treatment by altering the gut microbial composition and improving intestinal pathology and integrity (Li et al., 2021). The gut benefits of curcumin are related to reduced neuroinflammation and oxidative stress in the PVN (Li et al., 2021). This observation suggests that reconstruction of the gut microbiota and normalization of the gut-brain communications partially contribute to the anti-hypertensive effects of curcumin. Previously, the dietary compound curcumin has been documented to prevent heart failure-induced increases in both myocardial wall thickness and diameter by inhibiting p300-HAT activity (Morimoto et al., 2008). Very recently, the same research group has shown that oral supplementation of curcumin decreases hypertension-induced increase in posterior wall thickness and left ventricle mass index, even though without affecting blood pressure and systolic function in Dahl salt-sensitive rats (Sunagawa et al., 2021). Mechanistically, curcumin acts as an inhibitor of p300-HAT activity to attenuate the acetylation levels of GATA binding protein 4 (GATA4), a hypertrophy-responsive transcription factor in the hearts of hypertensive rats (Sunagawa et al., 2021).

These published results suggest that curcumin and its metabolites may be used as dietary supplements to antagonize hypertension and its associated vascular dysfunction through suppressing vascular inflammation, oxidative stress, restoring eNOS/NO signaling, reshaping gut microbial composition, and inhibiting p300-HAT activity (**Figure 3**). Despite this, further studies are required to determine whether tetrahydrocurcumin is superior to curcumin in the treatment of hypertension and vascular remodeling and to explore the underlying mechanisms. Although both women and men develop high blood pressure, the sex differences in hypertensive prevalence are well recognized for decades (Tipton and Sullivan, 2014; Muiesan et al., 2016; Ramirez and Sullivan, 2018; Zhang and Sun, 2020). In other words, men have a higher prevalence of hypertension than women before menopause, whereas a higher prevalence of hypertension is found in women after menopause relative to age-matched men (Muiesan et al., 2016), indicating a regulator role of estrogen in regulating blood pressure. Despite the sex differences in the prevalence of hypertension, the current treatment guidelines appear to be the same for different genders (James et al., 2014). To date, no studies have been carried out to compare the therapeutic effect of curcumin on hypertension in different genders. Considering the continuous advancement of individualized treatment in hypertension, it will be interesting to know whether the blood pressure lowering actions of curcumin are related to gender differences.

CLINICAL TRIALS OF CURCUMIN

The healthy benefits of curcumin in hypertension have gained tremendous attention because of the increasing epidemic of hypertension. However, these preclinical results await further clinical translation. Actually, the clinical trials of curcumin have been flourishing during the last decades. Acute coronary syndrome (ACS), a pathological condition whereby the blood supply to the cardiac tissues is cut off, is composed of ST-segment elevation myocardial infarction, non-ST-segment elevation myocardial infarction, and unstable angina (Paradiso-Hardy et al., 2003). Dyslipidemia and hyperglycemia are characteristic features in patients with ACS (Goyal et al., 2004). A randomized,

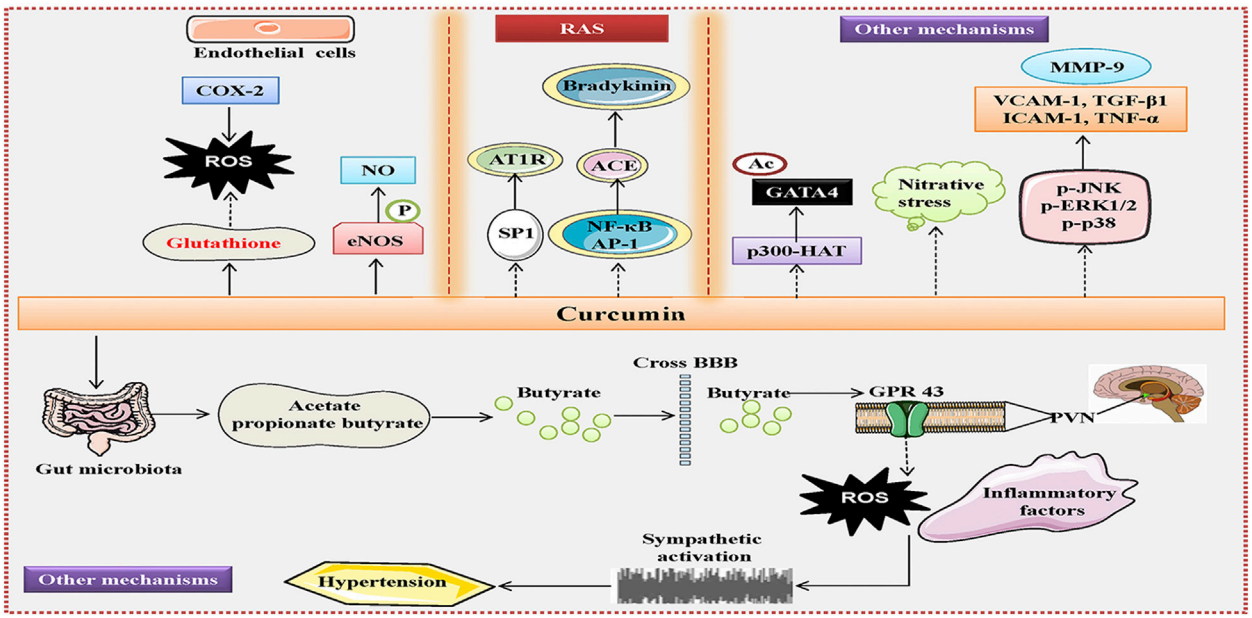

FIGURE 3 | Curcumin-mediated anti-hypertensive signaling pathways, associated with amelioration of endothelial dysfunction and inhibition of the RAS, as well as other mechanisms. Curcumin attenuates the development of hypertension and vascular remodeling through increasing NO bioavailability, decreasing oxidative stress, nitrative stress, and inflammation in the endothelium, blocking of the RAS, inhibiting the p300-HAT to reduce GATA4 acetylation, altering the gut microbial composition and improving intestinal pathology and integrity, inhibiting neuroinflammation and oxidative stress in the PVN. NO, nitric oxide; RAS, renin angiotensin system; HAT, histone acetyltransferase; GATA4, GATA binding protein 4; GPR 43, G protein-coupled receptor 43; PVN, paraventricular nucleus.

double-blind, controlled trial has shown that oral administration of curcumin for 2 months obviously reduces total cholesterol and low-density lipoprotein cholesterol in ACS patients (Alwi et al., 2008). This study suggests the lipid-lowering effects of curcumin in subjects suffering from ACS. In similarity with this study, administration of curcumin for 7 days effectively reduces serum total cholesterol levels by 11.63%, and increased serum HDL cholesterol by 29% in ten healthy human volunteers (Soni and Kuttan, 1992), indicating that curcumin might act as a chemopreventive agent against diseases related to lipid metabolism disturbance, such as atherosclerosis. However, improving the lipid profiles does not mean that curcumin is protective against ACS and/or atherosclerosis. Further research is warranted to examine whether curcumin could delay or reverse the development of ACS and/or atherosclerosis.

The blood glucose-lowering effects of curcumin were first reported in 1972 (Srinivasan, 1972), and Srinivasan found that ingestion of turmeric powder (5 g) over a period reduced the blood sugar level from 140 to 70 mg/dl in a male patient who had diabetes for 16 years (Srinivasan, 1972), suggesting curcumin's ability to decrease blood glucose levels. One study evaluated the effects of curcuminoids (NCB-02) in reducing oxidative stress and inflammatory markers in type 2 diabetic patients (Usharani et al., 2008). Intake of NCB-02 (300 mg of curcumin, twice a day) significantly improved endothelial function and reduced oxidative stress and inflammatory markers in these patients with type 2 diabetes (Usharani et al., 2008). (Wickenberg et al., 2010) assessed the actions of curcuma longa on postprandial plasma glucose, insulin levels and glycemic index in healthy subjects, and they found that ingestion of curcuma longa increased postprandial serum insulin levels, without affecting plasma glucose levels and glycemic index in healthy participants (Wickenberg et al., 2010). This study suggests the capability of curcuma longa to promote insulin secretion. Another group conducted a randomized, double-blinded, placebo-controlled trial to examine the effects of curcumin in delaying development of type 2 diabetes mellitus in the prediabetic population (Chuengsamarn et al., 2012). They found that after 9 months of treatment, curcumin-treated patients exhibited a better overall function of β-cells, higher pancreatic β cell function (HOMA-β) and adiponectin, lower C-peptide and Homeostatic Model Assessment for Insulin Resistance (HOMA-IR) when compared with the placebo group in prediabetic subjects (Chuengsamarn et al., 2012). This study demonstrated for the first time that curcumin intervention may be beneficial for a prediabetic population. However, a study by Hodaei et al. found that supplementation with curcumin caused a beneficial effect on the body weight, body mass index, waist circumference, and fasting blood glucose, but had no effect on the hemoglobin A1c (HbA1c), insulin, malondialdehyde (MDA), total antioxidant capacity (TAC), HOMA-IR, and HOMA-β in overweight patients with type 2 (Hodaei et al., 2019). Regarding these discrepancies, long-term trials with larger number of patients are needed to confirm whether curcumin's effects on diabetes are transient or long-lasting.

Diabetic kidney disease is believed to be a major cause of chronic kidney disease and end stage kidney disease (ESKD),

which is associated with high mortality and morbidity worldwide (Sun H. J. et al., 2019). A previous study was conducted to investigate the effects of curcumin on serum and urinary levels of TGF-β, IL-8, and TNF-α, as well as proteinuria, in patients with diabetic nephropathy (Khajehdehi et al., 2011). This study demonstrated for the first time that serum concentrations of TGF-β and IL-8, as well as urinary protein excretion were significantly decreased in these patients after turmeric supplementation (Khajehdehi et al., 2011). Most importantly, no adverse effects were detected during the supplementation of turmeric, indicating that turmeric could be recommended as a safe adjuvant therapy for patients with diabetic nephropathy. Despite this, larger, randomized clinical trials should further confirm the above observations, and determine the optimal concentration and duration of curcumin to achieve the therapeutic effects.

Likewise, curcumin supplementation may exert beneficial effects on the management of hypertension. A double-blinded, randomized, controlled trial was implemented to explore whether an enhanced bioavailable curcumin formulation, CurQfen®, could improve cardiovascular disease-related blood biomarkers and arterial function in young obese men (Campbell et al., 2019). They showed that intervention of curcumin for 12 weeks obviously lowers the levels of homocysteine, and enhances the levels of high-density lipoprotein levels in these young obese subjects when compared to the placebo group (Campbell et al., 2019). However, no changes in endothelial function, augmentation index, central blood pressure, the circulating levels of glucose, insulin, leptin, and adiponectin were observed in the curcumin group relative to the control group (Campbell et al., 2019). Morand's group examined the effects of an acute intake of curcumin on vascular functions in 18 healthy smokers, and their results showed that intake of curcumin for 2 h had no significant effect on vascular function assessed by flow-mediated dilation (Barber-Chamoux et al., 2018). A subgroup analysis on the basis of the gender or the cardiovascular-risk score revealed that curcumin exerted an obvious effect on vascular function in both women and subjects with lower cardiovascular risk (Barber-Chamoux et al., 2018). This clinical trial highlights a huge variability in the efficacy of curcumin across smokers, which may be mainly due to gender differences and cardiovascular risk levels (Barber-Chamoux et al., 2018). A clinical trial results showed that curcumin supplementation for 12 weeks improves resistance artery endothelial function by increasing vascular NO bioavailability and reducing oxidative stress in thirty-nine healthy middle-aged and older adults (Santos-Parker et al., 2017). A randomized and placebo-controlled study was carried out to determine the actions of curcumin on the clinical symptoms in patients suffering from relapsing or refractory lupus nephritis (Khajehdehi et al., 2012). This study showed that oral supplementation of turmeric was effective in ameliorating proteinuria, hematuria, and systolic blood pressure in such patients, representing turmeric as an adjuvant safe therapy for subjects with lupus nephritis (Khajehdehi et al., 2012). Although a wide range of clinical trials on curcumin's benefits in human ailments have been completed, the exact roles of curcumin in arterial hypertension and PAH are needed to evaluated by long-term clinical studies with large samples. A search on www.clinicaltrials.gov (accessed in December 2021) indicated that a total of 210 clinical trials were conducted to examine the role of curcumin in different human diseases, and further analysis revealed that 39 clinical trials with curcumin are ongoing. These currently progressing clinical studies provide robust evidence to confirm curcumin's therapeutic potential for human diseases. Interestingly, almost the majority of clinical trials are investigating curcumin's therapeutic effects on human diseases, rather than its metabolites or analogs, although the metabolites or analogs of curcumin might hold better benefits on human health. More clinical trials are still needed to verify the pros and cons of between curcumin and its metabolites/analogs in the treatment of human diseases, thus maximizing the clinical benefits of curcumin or its metabolites/analogs. Here, we also hope that there will be more clinical trials to explore and verify the antihypertensive effects of curcumin and its analogs.

CHALLENGES AND FUTURE DIRECTIONS

As a naturally occurring bioactive compound, curcumin plays a critical role in human nutrition because of its anti-oxidative and anti-inflammatory abilities. As such, curcumin is known as a promising candidate that can prevent and treat a wide spectrum of diseases. Indeed, the evidence for the potential of curcumin as a therapeutic agent and/or nutraceutical has greatly increased during the last several decades. The increased interest has spurred the growth of preclinical and clinical studies to assess the efficiency of curcumin and its formulations. Although the great therapeutic potential of curcumin in various diseases, including arterial hypertension and PAH, these findings should be treated carefully before clinical translation due to some crucial challenges.

Firstly, the poor bioavailability of curcumin leads to inconsistent and unstable results, and this restricts the therapeutic usages of curcumin in functional and nutritious foods. Secondly, the lower plasma and tissue levels of curcumin may be attributed to its poor absorption, rapid metabolism, and fast elimination, resulting in a low level of free curcumin even if a high concentration of curcumin is used (Kunati et al., 2018). This results in a great possibility that the metabolites of curcumin may be responsible for the biological and pharmacological actions rather than the free curcumin (Nelson et al., 2017). Once absorbed in the body, curcumin may undergo the modification of conjugations, such as sulfation and glucuronidation, and the major metabolites of curcumin are glucuronides of tetrahydrocurcumin and hexahydrocurcumin (Anand et al., 2007). In addition, dihydroferulic acid, ferulic acid, and sulfate conjugates are minorbiliary metabolites of curcumin (Anand et al., 2007). Intriguingly, tetrahydrocurcumin and hexahydrocurcumin, known as curcumin metabolites, are found to hold considerable promise in the treatment of various diseases, including hypertension. Thus, it is highly possible that the metabolites of curcumin might account for its antihypertensive effects,

TABLE 1 | Vascular benefits of curcumin in hypertension from *in vivo* studies.

Formulations	Dose	Disease model	Benefits	References
Curcumin	50 and 100 mg/kg/d	L-NAME-induced hypertensive rats	Suppressing the blood pressure elevation; decreasing vascular resistance; restoring vascular responsiveness; reinstating eNOS protein expression in the aortic tissues; reducing vascular oxidative stress	Nakmareong et al. (2011)
Tetrahydrocurcumin	50 and 100 mg/kg/d	L-NAME-induced hypertensive rats	Suppressing the blood pressure elevation; decreasing vascular resistance; restoring vascular responsiveness; reinstating eNOS protein expression in the aortic tissues; reducing vascular oxidative stress; the antihypertensive effects of tetrahydrocurcumin are apparently more potent than curcumin	Nakmareong et al. (2011)
Tetrahydrocurcumin	50 and 100 mg/kg/d	L-NAME-induced hypertensive rats	Decreasing blood pressure, peripheral vascular resistance, aortic stiffness and oxidative stress; elevating aortic eNOS expression and plasma nitrate/nitrite	Nakmareong et al. (2012)
Hexahydrocurcumin	20, 40 or 80 mg/kg/d	L-NAME-induced hypertensive rats	Inhibiting the development of hypertension, vascular dysfunction, and remodeling; exhibiting antioxidant and anti-inflammation potential	Panthiya et al. (2022)
Curcumin	100 mg/kg/d	L-NAME-induced hypertensive rats	Decreasing hypertension, wall thickness and cross-sectional area of the aorta, as well as vascular fibrosis	Hlavačková et al. (2011)
Curcumin	50 and 100 mg/kg/d	2K1C-induced hypertensive rats	Reducing plasma angiotensin converting enzyme levels; improving endothelial dysfunction and vascular remodeling; raising nitric oxide availability; reducing oxidative stress	Boonla et al. (2014)
Curcumin	60 mg/kg/d	5/6 nephrectomized rats	Attenuating systemic and glomerular hypertension; increasing plasma creatinine and blood urea nitrogen; enhancing nuclear translocation of Nrf2	Tapia et al. (2012)
Curcumin	50 mg/kg/d	Salt-sensitive Dahl rats	Preventing the deterioration of systolic function and heart failure-induced increases in myocardial wall thickness	Morimoto et al. (2008)
Curcumin	50 mg/kg/d	Salt-sensitive Dahl rats	Decreasing posterior wall thickness and left ventricle mass index; without affecting the blood pressure and systolic function	Sunagawa et al. (2021)
Curcumin	100 mg/kg/day	Spontaneously hypertensive rats	Attenuating hypertension; reducing NFκB activation, NLRP3 and matrix metalloproteinase-9 expressions and aortic media thickness	Han et al. (2019)
Curcumin	100 mg/kg/day	Spontaneously hypertensive rats	Attenuating hypertension and vascular remodeling	Sun et al. (2017a)
Curcumin	100 or 300 mg/kg/day	Spontaneously hypertensive rats	Decreasing blood pressure, altering the gut microbial composition and improved intestinal pathology and integrity	Li et al. (2021)
Curcumin	300 mg/kg/d	Ang II-induced hypertensive mice	Reducing hypertension in C57Bl/6J mice; lowering AT1R expression in the arteries and decreasing Ang II-mediated vasoconstriction in the mesenteric artery	Yao et al. (2016)
Curcumin	150 mg/kg/d	Ang II-infused hypertensive rats	Decreasing the mean arterial blood pressure; attenuating myocardial fibrosis; reducing AT1R expression; upregulating AT2R expression	Pang et al. (2015)
Curcumin in hyaluronic acid-based nanocapsules	4.5 mg/kg/d	Hypertensive TGR(m-Ren2) 27 rats	Resulting in a gradual inhibition of SBP, DBP and MAP	Czyzynska-Cichon and Janik-Hazuka, (2021)
Curcumin nanoparticles	5 mg/kg/d	Rats with diet-Induced metabolic syndrome	Normalizing blood pressure; reducing the left ventricular diastolic stiffness.	Du Preez et al. (2019)
Curcumin	100 mg/L	Cadmium-induced mice	Increasing vascular responsiveness; normalizing the blood pressure levels; upregulating eNOS protein; restoration of glutathione redox ratio and alleviation of oxidative stress	Kukongviriyapan et al. (2014)
Curcumin	100 mg/L	Lead acetate- and cadmium chloride-treated rats	Reducing blood pressure; alleviating oxidative stress; increasing plasma nitrate/nitrite and glutathione in the blood	Tubsakul et al. (2021)
Tetrahydrocurcumin	50 and 100 mg/kg/d	Cadmium-induced mice	Decreasing arterial blood pressure; restoring vascular responses to vasoactive agents; decreasing aortic stiffness and hypertrophic aortic wall remodeling as well as vascular fibrosis	Sangartit et al. (2014)
Tetrahydrocurcumin	50 mg/kg/d	Iron-overloaded mice	Attenuating hypertension, vascular dysfunction, baroreflex dysfunction, and oxidative stress	Sangartit et al. (2016)
Curcumin	50 mg/kg/d	Hypoxic hypercapnic rats		Lin et al. (2006)

(Continued on following page)

TABLE 1 | (*Continued*) Vascular benefits of curcumin in hypertension from *in vivo* studies.

Formulations	Dose	Disease model	Benefits	References
			Decreasing PAH; improving pulmonary vessel remodeling; inhibiting the deposition of collagen I in pulmonary arterioles	
Curcumin	30 mg/kg/d	MCT-induced PAH rats	Reversing pulmonary vascular remodeling	Chen et al. (2021)
Curcumin	150 mg/kg/d	Hypoxic hypercapnic rats	Inhibiting the remodeling of pulmonary vessel; blocking proliferation of pulmonary arterial media smooth cell layer and collagen fibers in adventitia	Li et al. (2014)
Curcuminoids	4–18 μM	Isolated segments of rat pulmonary artery and aorta	Possessing vasorelaxant activity on pulmonary arteries	Kruangtip et al. (2015)
Curcumin nanoparticles	50 mg/kg/d	MCT-induced PAH rats	Reducing right ventricular wall thickness and right ventricle weight/body weight ratio; inhibiting right ventricular inflammation and fibrosis	Rice et al. (2016)
Curcumin acetate nanocrystals	2 mg/kg/d	MCT-induced PAH rats	Inhibiting the development of PAH.	Hu et al. (2017)

which merits further studies. Thirdly, the concentrations of curcumin vary in different foods or plants, the optimal dosage levels of curcumin with therapeutic effects are difficult to determine. Fourthly, different experimental conditions might be responsible for a big gap between animal and human studies. Of note, the method of extraction of the bioactive ingredients in curcumin may be an important factor affecting its blood pressure lowering effects. Further research is required to determine which bio-extraction method would yield curcumin with the highest bioactivity and the lowest toxicity. It is quite difficult to directly use curcumin-derived treatment without enough clinical studies even though animal studies are available. Fifthly, animal studies are disputable since the different dose levels, research conditions, treatment time, and route of administration are used in distinct studies. Sixthly, in addition to the benefits of curcumin, we should also pay more attention to its side effects during its usages in preclinical and clinical studies. A study by Fu et al. examined the toxicity of liposomal curcumin in animal models, and results showed that dose-dependent hemolysis occurred when the therapeutic dose exceeded 20 mg/kg (Fu et al., 2021). A small number of diabetic patients experienced side effects, such as constipation and nausea, after oral administration of curcumin at a dose of 1.5 g/kg for 6 months (Patel et al., 2020). Lao et al. (2006) determined the maximum tolerable dose and safety of curcumin after a single oral dose (500–12,000 mg) in 34 healthy volunteers, and they found that 7 participants experienced diarrhea, headache, rash, and yellow stool. A phase I clinical trial explored the pharmacology of curcumin in fifteen patients with advanced colorectal cancer, and curcumin at doses ranging from 0.45 to 3.6 g/day for 1–4 months increased serum alkaline phosphatase and lactate dehydrogenase contents, along with nausea and diarrhea (Sharma et al., 2004). These studies might provide possible evidence that curcumin might cause several side effects at high concentrations which is a basis for some concern. More work is necessary to establish safe effective dose levels of curcumin. Similar to conventional drugs, curcumin is capable of drug-drug interactions with other medicines, which may result in lower effectiveness or increased toxicity (Bahramsoltani et al., 2017). For example, co-administration of curcumin with a number of conventional pharmacological drugs induced pharmacokinetic changes, including changes in maximal plasma concentration (Cmax) and area under the concentration time curve (AUC) (Bahramsoltani et al., 2017). Inhibition of cytochrome isoenzymes and P-glycoprotein may contribute to such drug interactions (Patel et al., 2020). Taking increased amounts of curcumin might also inhibit platelet aggregation and increase the activity of liver enzymes, induce gastrointestinal disorders, or contact dermatitis and hives (Fadus et al., 2017). However, the evidence for the curcumin-drug interactions is still lacking. Since then, more *in vitro* and *in vivo* studies are encouraged to judge the drug interactions of curcumin, thus avoiding unnecessary side effects when curcumin was used concomitantly with conventional pharmacological drugs. Dose-escalating results from clinical studies suggest that the safety of curcumin at doses up to 12 g/day over 3 months (Gupta et al., 2013). However, the clinical benefits of curcumin did not appear to be dose-related (Gupta et al., 2013). The dose-response effects of curcumin on mitigating vascular inflammation should be therefore carefully determined in order to establish the most effective dose of curcumin without toxic side effects. Overall, determining the most effective dose of curcumin without toxic side effects might help to recommend this fascinating polyphenol at the fore front of novel therapeutics. Seventhly, most of the animal experiments are conducted to determine whether curcumin could prevent hypertension since curcumin is mostly administered before or a few days before the hypertensive model starts, indicating a preventive aspect of curcumin in hypertension. Thus, more research is needed in the future to confirm whether curcumin is able to treat hypertension, i.e., curcumin is given at the middle and late stages of hypertensive models to confirm the curative effects of curcumin on hypertension, not just its preventive effects. Last but not least, it is still a challenge to recognize curcumin and its derivatives as prebiotics in the human gut although they possess the ability to reshape the composition of the gut

TABLE 2 | Vascular benefits of curcumin in hypertension from *in vitro* studies.

Formulations	Dose	Cell types	Benefits	Ref
Curcumin	20 μM	Primary VSMCs	Attenuating VSMC migration; inhibiting NLRP3 expression and IL-1β concentration in VSMCs	Han et al. (2019)
Curcumin	20 μM	Primary VSMCs	Preventing the NLRP3 inflammasome activation, VSMC phenotype switching and proliferation	Sun et al. (2017a)
Curcumin	10^{-6} M	A10 cells	Decreasing AT1R expression in a concentration- and time-dependent manner	Yao et al. (2016)
Curcumin	10 and 20 μM	Human aortic smooth muscle cells	Inhibiting TNF-α-induced migration of human aortic smooth muscle cells	Yu and Lin, (2010)
Curcumin	10^{-6}–10^{-4} M	Rabbit VSMCs	Exhibiting a greater inhibitory effect on platelet-derived growth factor- and serum-stimulated proliferation of rabbit VSMCs	Huang et al. (1992)
Curcumin	10^{-6}–10^{-5} M	A7R5 cells	Inhibiting the proliferation of A7R5 cells in a concentration-dependent manner	Chen and Huang, (1998)
Demethoxycurcumin	9, 18, 36, 72, or 144 μM	Primary rat VSMCs	Inhibit the migration of VSMCs by reducing the expression of MMP-2 and MMP-9	Sheu et al. (2013)
Curcumin-eluting PLLA films	0.1 mg	Human coronary artery smooth muscle cells	Preventing cell proliferation through the protein kinase (PK) and mitogen-activated protein kinase (MAPK) pathways	Nguyen et al. (2004)
Curcumin	1–25 μM	Primary rat VSMCs	Inhibiting platelet-derived growth factor-stimulated VSMC proliferation and migration	Yang et al. (2006)
Dehydrozingerone	1–50 μM	Primary rat VSMCs	Eliciting a concentration-dependent inhibition of PDGF-stimulated VSMC migration, proliferation, collagen synthesis	Liu et al. (2008)
Bisdemethoxycurcumin	5, 10, 25 μM	Primary rat VSMCs	Inhibiting PDGF-induced vascular smooth muscle cell motility and proliferation	Hua et al. (2013)
Curcumin	1, 10, and 100 μM	Rat VSMCs	Inhibiting the proliferation of VSMCs by serving as an AP-1 inhibitor	(Hsieh et al., 2008a; Hsieh et al., 2008b)
HO-3867	10 μM	Human aortic SMCs	Inhibiting the proliferation of serum-stimulated VSMCs by inducing cell cycle arrest	Selvendiran et al. (2009)
Curcumin	1–50 μM	A10 cells	Inhibiting ET-1-induced mitogenic and proliferative signaling events in VSMCs	Kapakos et al. (2012)
Curcumin	5, 10, 20 μM	Primary rat VSMCs	Inhibiting Ang II-induced inflammation and proliferation of rat VSMCs	Li et al. (2017)
Nicotinate-curcumin	1 μM	VSMCs	Inhibiting Ang II-induced vascular smooth muscle cell phenotype switching	Sun et al. (2021)
Curcumin	10, 20, 40 μM	Primary mouse VSMCs	Inhibiting the proliferation and migration of vascular smooth muscle cells by targeting the chemerin/CMKLR1/LCN2 axis	He et al. (2021)
Curcumin	25 μM	Airway smooth muscle cells	Inhibiting the proliferation of cells by upregulating the expression of caveolin-1 and blocking the activation of the ERK pathway	Zeng et al. (2013)
Curcumin	10 μM	A7R5 cells	Inhibiting the proliferation, migration and neointimal formation of VSMCs via activating miR-22	Zhang et al. (2020)
Curcumin	1, 5, 10, 20 μM	Primary rat VSMCs	Inducing growth inhibition in rat VSMCs by upregulation of HO-1	Pae et al. (2007)
Curcumin	Not Applicable	Primary pulmonary arterial smooth muscle cells	Promoting cell apoptosis; protecting mitochondrial function; suppressing the PI3K/AKT pathway	Chen et al. (2021)
Curcumin	20 μM	Mouse aortic smooth muscle cell line A7R5 cells	Inhibiting the phenotypic transformation, migration, and foaming of ox-LDL-treated VSMCs	Wang et al. (2021b)

microbiota. It is deserved to investigate which probiotics could be affected by curcumin, not only in hypertension, and it is also worth studying whether supplementation of probiotics into curcumin formulations could synergistically improve the efficiency of curcumin. It is hopeful that further research is needed to unravel these limitations and improve the efficacy of curcumin against hypertension.

In order to solve these above limitations, scientists have made great efforts. For instance, different modifications of curcumin and its delivery systems are developed to increase the stability, solubility, *in vivo* uptake, bioactivity, and safety of curcumin, such as nanoparticles, micellation, and conjugation with other materials (Adahoun et al., 2017; Akbar et al., 2018; Khayyal et al., 2018; Xu et al., 2018). It is certain that these modifications will greatly facilitate the development of curcumin-derived novel therapies with few side effects and high bioavailability, and improve the possibility of clinical transformation of curcumin. Given the capability of curcumin to reverse vascular remodeling in hypertension, curcumin may be postulated to be an attractive compound to prevent and treat hypertension and vascular remodeling through modulating a wide spectrum of signaling pathway. Nevertheless, the

complex regulatory mechanisms of curcumin in hypertension-associated vascular remodeling are incompletely understood. As a consequence, more studies are required to understand how curcumin and its metabolites benefit vascular dysfunction induced by hypertension.

CONCLUSION

Taken together, this review summarizes and discusses the therapeutic roles and molecular mechanisms of curcumin in hypertension and its related vascular remodeling (**Tables 1**, **2**). The novel insights into hypertensive vascular remodeling are highly acquired because of the increased incidence of hypertension. Continuous *in vitro*, *in vivo*, and clinical studies have identified the underlying molecules in curcumin-mediated benefits in hypertension-related vascular remodeling. As of yet, a growing body of impressive studies focusing on the effects of curcumin and its analogues on hypertensive vascular damage are growing in recent years. Importantly, nanotechnology is used to encapsulate curcumin, thereby enhancing its stability, bioavailability, bioactivity, and health benefits. Most importantly, more efforts are warranted to eliminate the debate between preclinical and human studies of curcumin. With our in-depth understandings towards the mechanistic network of curcumin in hypertensive vascular remodeling, we anticipate multiple novel curcumin therapeutics to evolve for hypertension and its associated vascular remodeling in the near future.

AUTHOR CONTRIBUTIONS

K-XL, Z-CW, Q-BL, and H-JS proposed the concept and wrote the manuscript. M-ZL, Y-JW, M-KN, and K-YY helped to draw schematic diagrams. JM, K-XL, Q-BL, and H-JS were responsible for reviewing and editing the original draft. All authors contributed significantly to this review.

FUNDING

This research was funded by the National Natural Science Foundation of China (8217021262 and 81700364), high-level introduction of talents and scientific research start-up funds of CPU (3150020068), Jiangsu Natural Science Foundation (BK20170179).

ACKNOWLEDGMENTS

We thank JM for his intelligent discussion in revision.

REFERENCES

Acelajado, M. C., Hughes, Z. H., Oparil, S., and Calhoun, D. A. (2019). Treatment of Resistant and Refractory Hypertension. *Circ. Res.* 124, 1061–1070. doi:10.1161/circresaha.118.312156

Adahoun, M. a. A., Al-Akhras, M.-A. H., Jaafar, M. S., and Bououdina, M. (2017). Enhanced Anti-cancer and Antimicrobial Activities of Curcumin Nanoparticles. *Artif. Cell Nanomedicine, Biotechnol.* 45, 98–107. doi:10.3109/21691401.2015.1129628

Aggarwal, B. B., Kumar, A., and Bharti, A. C. (2003). Anticancer Potential of Curcumin: Preclinical and Clinical Studies. *Anticancer Res.* 23, 363–398.

Ahangari, N., Kargozar, S., Ghayour-Mobarhan, M., Baino, F., Pasdar, A., Sahebkar, A., et al. (2019). Curcumin in Tissue Engineering: A Traditional Remedy for Modern Medicine. *Biofactors* 45, 135–151. doi:10.1002/biof.1474

Akbar, M. U., Zia, K. M., Nazir, A., Iqbal, J., Ejaz, S. A., and Akash, M. S. H. (2018). Pluronic-Based Mixed Polymeric Micelles Enhance the Therapeutic Potential of Curcumin. *AAPS PharmSciTech* 19, 2719–2739. doi:10.1208/s12249-018-1098-9

Alappat, L., and Awad, A. B. (2010). Curcumin and Obesity: Evidence and Mechanisms. *Nutr. Rev.* 68, 729–738. doi:10.1111/j.1753-4887.2010.00341.x

Alidadi, M., Liberale, L., Montecucco, F., Majeed, M., Al-Rasadi, K., Banach, M., et al. (2021). Protective Effects of Curcumin on Endothelium: An Updated Review. *Adv. Exp. Med. Biol.* 1291, 103–119. doi:10.1007/978-3-030-56153-6_6

Allahverdian, S., Chehroudi, A. C., Mcmanus, B. M., Abraham, T., and Francis, G. A. (2014). Contribution of Intimal Smooth Muscle Cells to Cholesterol Accumulation and Macrophage-like Cells in Human Atherosclerosis. *Circulation* 129, 1551–1559. doi:10.1161/circulationaha.113.005015

Almenara, C. C. P., Oliveira, T. F., and Padilha, A. S. (2020). The Role of Antioxidants in the Prevention of Cadmium-Induced Endothelial Dysfunction. *Cpd* 26, 3667–3675. doi:10.2174/1381612826666200415172338

Alwi, I., Santoso, T., Suyono, S., Sutrisna, B., Suyatna, F. D., Kresno, S. B., et al. (2008). The Effect of Curcumin on Lipid Level in Patients with Acute Coronary Syndrome. *Acta Med. Indones* 40, 201–210.

Amin, F., Gilani, A.-H., Mehmood, M. H., Siddiqui, B. S., and Khatoon, N. (2015). Coadministration of Black Seeds and Turmeric Shows Enhanced Efficacy in Preventing Metabolic Syndrome in Fructose-Fed Rats. *J. Cardiovasc. Pharmacol.* 65, 176–183. doi:10.1097/fjc.0000000000000179

Anand, P., Kunnumakkara, A. B., Newman, R. A., and Aggarwal, B. B. (2007). Bioavailability of Curcumin: Problems and Promises. *Mol. Pharmaceutics* 4, 807–818. doi:10.1021/mp700113r

Anderson, W. P., Kett, M. M., Stevenson, K. M., Edgley, A. J., Denton, K. M., and Fitzgerald, S. M. (2000). Renovascular Hypertension. *Hypertension* 36, 648–652. doi:10.1161/01.hyp.36.4.648

Arnett, D. K., Blumenthal, R. S., Albert, M. A., Buroker, A. B., Goldberger, Z. D., Hahn, E. J., et al. (20192019). 2019 ACC/AHA Guideline on the Primary Prevention of Cardiovascular Disease: A Report of the American College of Cardiology/American Heart Association Task Force on Clinical Practice Guidelines. *J. Am. Coll. Cardiol.* 74, e177–e646. doi:10.1016/j.jacc.2019.03.010

Artiach, G., Carracedo, M., Clària, J., Laguna-Fernandez, A., and Bäck, M. (2018). Opposing Effects on Vascular Smooth Muscle Cell Proliferation and Macrophage-Induced Inflammation Reveal a Protective Role for the Proresolving Lipid Mediator Receptor ChemR23 in Intimal Hyperplasia. *Front. Pharmacol.* 9, 1327. doi:10.3389/fphar.2018.01327

Aryal, S. R., Siddiqui, M., Sharifov, O. F., Coffin, M. D., Zhang, B., Gaddam, K. K., et al. (2021). Spironolactone Reduces Aortic Stiffness in Patients with Resistant Hypertension Independent of Blood Pressure Change. *J. Am. Heart Assoc.* 10, e019434. doi:10.1161/JAHA.120.019434

Bahramsoltani, R., Rahimi, R., and Farzaei, M. H. (2017). Pharmacokinetic Interactions of Curcuminoids with Conventional Drugs: A Review. *J. Ethnopharmacology* 209, 1–12. doi:10.1016/j.jep.2017.07.022

Bakris, G., Yang, Y. F., and Pitt, B. (2020). Mineralocorticoid Receptor Antagonists for Hypertension Management in Advanced Chronic Kidney Disease. *Hypertension* 76, 144–149. doi:10.1161/hypertensionaha.120.15199

Barber-Chamoux, N., Milenkovic, D., Verny, M. A., Habauzit, V., Pereira, B., Lambert, C., et al. (2018). Substantial Variability across Individuals in the Vascular and Nutrigenomic Response to an Acute Intake of Curcumin: A Randomized Controlled Trial. *Mol. Nutr. Food Res.* 62. doi:10.1002/mnfr.201700418

Barton, M., and Yanagisawa, M. (2019). Endothelin: 30 Years from Discovery to Therapy. *Hypertension* 74, 1232–1265. doi:10.1161/hypertensionaha.119.12105

Blacher, J., Guerin, A. P., Pannier, B., Marchais, S. J., Safar, M. E., and London, G. M. (1999). Impact of Aortic Stiffness on Survival in End-Stage Renal Disease. *Circulation* 99, 2434–2439. doi:10.1161/01.cir.99.18.2434

Boari, G. E., Rizzoni, D., De Ciuceis, C., Porteri, E., Avanzi, D., Platto, C., et al. (2010). Structural Alterations in Subcutaneous Small Resistance Arteries Predict Changes in the Renal Function of Hypertensive Patients. *J. Hypertens.* 28, 1951–1958. doi:10.1097/hjh.0b013e32833c2177

Bomzon, A., Holt, S., and Moore, K. (1997). Bile Acids, Oxidative Stress, and Renal Function in Biliary Obstruction. *Semin. Nephrol.* 17, 549–562.

Boonla, O., Kukongviriyapan, U., Pakdeechote, P., Kukongviriyapan, V., Pannangpetch, P., Prachaney, P., et al. (2014). Curcumin Improves Endothelial Dysfunction and Vascular Remodeling in 2K-1C Hypertensive Rats by Raising Nitric Oxide Availability and Reducing Oxidative Stress. *Nitric Oxide* 42, 44–53. doi:10.1016/j.niox.2014.09.001

Botts, S. R., Fish, J. E., and Howe, K. L. (2021). Dysfunctional Vascular Endothelium as a Driver of Atherosclerosis: Emerging Insights into Pathogenesis and Treatment. *Front. Pharmacol.* 12, 787541. doi:10.3389/fphar.2021.787541

Briet, M., and Schiffrin, E. L. (2013). Treatment of Arterial Remodeling in Essential Hypertension. *Curr. Hypertens. Rep.* 15, 3–9. doi:10.1007/s11906-012-0325-0

Bronte, E., Coppola, G., Di Miceli, R., Sucato, V., Russo, A., and Novo, S. (2013). Role of Curcumin in Idiopathic Pulmonary Arterial Hypertension Treatment: a New Therapeutic Possibility. *Med. Hypotheses* 81, 923–926. doi:10.1016/j.mehy.2013.08.016

Brown, I. A. M., Diederich, L., Good, M. E., Delalio, L. J., Murphy, S. A., Cortese-Krott, M. M., et al. (2018). Vascular Smooth Muscle Remodeling in Conductive and Resistance Arteries in Hypertension. *Atvb* 38, 1969–1985. doi:10.1161/atvbaha.118.311229

Campbell, M. S., Ouyang, A., I.M., K., Charnigo, R. J., Westgate, P. M., and Fleenor, B. S. (2019). Influence of Enhanced Bioavailable Curcumin on Obesity-Associated Cardiovascular Disease Risk Factors and Arterial Function: A Double-Blinded, Randomized, Controlled Trial. *Nutrition* 62, 135–139. doi:10.1016/j.nut.2019.01.002

Canale, M. P., Noce, A., Di Lauro, M., Marrone, G., Cantelmo, M., Cardillo, C., et al. (2021). Gut Dysbiosis and Western Diet in the Pathogenesis of Essential Arterial Hypertension: A Narrative Review. *Nutrients* 13, 1162. doi:10.3390/nu13041162

Carey, R. M., Muntner, P., Bosworth, H. B., and Whelton, P. K. (2018). Prevention and Control of Hypertension. *J. Am. Coll. Cardiol.* 72, 1278–1293. doi:10.1016/j.jacc.2018.07.008

Chazova, I., Loyd, J. E., Zhdanov, V. S., Newman, J. H., Belenkov, Y., and Meyrick, B. (1995). Pulmonary Artery Adventitial Changes and Venous Involvement in Primary Pulmonary Hypertension. *Am. J. Pathol.* 146, 389–397.

Chen, H.-W., and Huang, H.-C. (1998). Effect of Curcumin on Cell Cycle Progression and Apoptosis in Vascular Smooth Muscle Cells. *Br. J. Pharmacol.* 124, 1029–1040. doi:10.1038/sj.bjp.0701914

Chen, J., Jiang, W., Zhu, F., Wang, Q., Yang, H., and Wu, J. (2021). Curcumin Improves Pulmonary Hypertension Rats by Regulating Mitochondrial Function. *Biomed. Res. Int.* 2021, 1078019. doi:10.1155/2021/1078019

Chen, X., Chen, X., Shi, X., Gao, Z., and Guo, Z. (2020). Curcumin Attenuates Endothelial Cell Fibrosis through Inhibiting Endothelial-Interstitial Transformation. *Clin. Exp. Pharmacol. Physiol.* 47, 1182–1192. doi:10.1111/1440-1681.13271

Chuengsamarn, S., Rattanamongkolgul, S., Luechapudiporn, R., Phisalaphong, C., and Jirawatnotai, S. (2012). Curcumin Extract for Prevention of Type 2 Diabetes. *Diabetes Care* 35, 2121–2127. doi:10.2337/dc12-0116

Cox, F. F., Misiou, A., Vierkant, A., Ale-Agha, N., Grandoch, M., Haendeler, J., et al. (2022). Protective Effects of Curcumin in Cardiovascular Diseases-Impact on Oxidative Stress and Mitochondria. *Cells* 11, 342. doi:10.3390/cells11030342

Cox, R. H., and Rusch, N. J. (2002). New Expression Profiles of Voltage-Gated Ion Channels in Arteries Exposed to High Blood Pressure. *Microcirculation* 9, 243–257. doi:10.1080/mic.9.4.243.257

Cui, J., Melista, E., Chazaro, I., Zhang, Y., Zhou, X., Manolis, A. J., et al. (2005). Sequence Variation of Bradykinin Receptors B1 and B2 and Association with Hypertension. *J. Hypertens.* 23, 55–62. doi:10.1097/00004872-200501000-00013

Czyzynska-Cichon, I., Janik-Hazuka, M., Szafraniec-Szczęsny, J., Jasinski, K., Węglarz, W. P., Zapotoczny, S., et al. (2021). Low Dose Curcumin Administered in Hyaluronic Acid-Based Nanocapsules Induces Hypotensive Effect in Hypertensive Rats. *Ijn* 16, 1377–1390. doi:10.2147/ijn.s291945

Deciuceis, C., Porteri, E., Rizzoni, D., Rizzardi, N., Paiardi, S., Boari, G., et al. (2007). Structural Alterations of Subcutaneous Small-Resistance Arteries May Predict Major Cardiovascular Events in Patients with Hypertension. *Am. J. Hypertens.* 20, 846–852. doi:10.1016/j.amjhyper.2007.03.016

Devadasu, V. R., Wadsworth, R. M., and Ravi Kumar, M. N. V. (2012). Tissue Localization of Nanoparticles Is Altered Due to Hypoxia Resulting in Poor Efficacy of Curcumin Nanoparticles in Pulmonary Hypertension. *Eur. J. Pharmaceutics Biopharmaceutics* 80, 578–584. doi:10.1016/j.ejpb.2011.12.008

Dhaun, N., and Webb, D. J. (2019). Endothelins in Cardiovascular Biology and Therapeutics. *Nat. Rev. Cardiol.* 16, 491–502. doi:10.1038/s41569-019-0176-3

Di, L., and Maiseyeu, A. (2021). Low-density Lipoprotein Nanomedicines: Mechanisms of Targeting, Biology, and Theranostic Potential. *Drug Deliv.* 28, 408–421. doi:10.1080/10717544.2021.1886199

Du Preez, R., Pahl, J., Arora, M., Ravi Kumar, M. N. V., Brown, L., and Panchal, S. K. (2019). Low-Dose Curcumin Nanoparticles Normalise Blood Pressure in Male Wistar Rats with Diet-Induced Metabolic Syndrome. *Nutrients* 11, 1542. doi:10.3390/nu11071542

El-Bassossy, H. M., Hassan, N., and Zakaria, M. N. M. (2014). Heme Oxygenase-1 Alleviates Vascular Complications Associated with Metabolic Syndrome: Effect on Endothelial Dependent Relaxation and NO Production. *Chemico-Biological Interactions* 223, 109–115. doi:10.1016/j.cbi.2014.09.014

Fadus, M. C., Lau, C., Bikhchandani, J., and Lynch, H. T. (2017). Curcumin: An Age-Old Anti-inflammatory and Anti-neoplastic Agent. *J. Traditional Complement. Med.* 7, 339–346. doi:10.1016/j.jtcme.2016.08.002

Fan, J., Li, X., Yan, Y.-W., Tian, X.-H., Hou, W.-J., Tong, H., et al. (2012). Curcumin Attenuates Rat Thoracic Aortic Aneurysm Formation by Inhibition of the C-Jun N-Terminal Kinase Pathway and Apoptosis. *Nutrition* 28, 1068–1074. doi:10.1016/j.nut.2012.02.006

Farhangkhoee, H., Khan, Z. A., Mukherjee, S., Cukiernik, M., Barbin, Y. P., Karmazyn, M., et al. (2003). Heme Oxygenase in Diabetes-Induced Oxidative Stress in the Heart. *J. Mol. Cell Cardiol.* 35, 1439–1448. doi:10.1016/j.yjmcc.2003.09.007

Foley, A., Steinberg, B. E., and Goldenberg, N. M. (2021). Inflammasome Activation in Pulmonary Arterial Hypertension. *Front. Med. (Lausanne)* 8, 826557. doi:10.3389/fmed.2021.826557

Forouzanfar, M. H., Liu, P., Roth, G. A., Ng, M., Biryukov, S., Marczak, L., et al. (2017). Global Burden of Hypertension and Systolic Blood Pressure of at Least 110 to 115 Mm Hg, 1990-2015. *Jama* 317, 165–182. doi:10.1001/jama.2016.19043

Friese, R. S., Altshuler, A. E., Zhang, K., Miramontes-Gonzalez, J. P., Hightower, C. M., Jirout, M. L., et al. (2013). MicroRNA-22 and Promoter Motif Polymorphisms at the Chga Locus in Genetic Hypertension: Functional and Therapeutic Implications for Gene Expression and the Pathogenesis of Hypertension. *Hum. Mol. Genet.* 22, 3624–3640. doi:10.1093/hmg/ddt213

Fu, Y.-S., Chen, T.-H., Weng, L., Huang, L., Lai, D., and Weng, C.-F. (2021). Pharmacological Properties and Underlying Mechanisms of Curcumin and Prospects in Medicinal Potential. *Biomed. Pharmacother.* 141, 111888. doi:10.1016/j.biopha.2021.111888

Garg, A. X., Devereaux, P. J., Hill, A., Sood, M., Aggarwal, B., Dubois, L., et al. (2018). Oral Curcumin in Elective Abdominal Aortic Aneurysm Repair: a Multicentre Randomized Controlled Trial. *Cmaj* 190, E1273–e1280. doi:10.1503/cmaj.180510

Girchev, R., Backer, A., Markova, P., and Kramer, H. J. (2006). Renal Endothelin System and Excretory Function in Wistar-Kyoto and Long-Evans Rats. *Acta Physiol.* 186, 67–76. doi:10.1111/j.1748-1716.2005.01501.x

Gong, L., Lei, Y., Liu, Y., Tan, F., Li, S., Wang, X., et al. (2019). Vaccarin Prevents Ox-LDL-Induced HUVEC EndMT, Inflammation and Apoptosis by Suppressing ROS/p38 MAPK Signaling. *Am. J. Transl Res.* 11, 2140–2154.

Gouda, A. S., Adbelruhman, F. G., Elbendary, R. N., Alharbi, F. A., Alhamrani, S. Q., and Mégarbane, B. (2021). A Comprehensive Insight into the Role of Zinc Deficiency in the Renin-Angiotensin and Kinin-Kallikrein System Dysfunctions in COVID-19 Patients. *Saudi J. Biol. Sci.* 28, 3540–3547. doi:10.1016/j.sjbs.2021.03.027

Goyal, A., Petersen, J. L., and Mahaffey, K. W. (2004). The Evaluation and Management of Dyslipidemia and Impaired Glucose Metabolism during Acute Coronary Syndromes. *Curr. Cardiol. Rep.* 6, 300–307. doi:10.1007/s11886-004-0080-1

Gumprecht, J., Domek, M., Lip, G. Y. H., and Shantsila, A. (2019). Invited Review: Hypertension and Atrial Fibrillation: Epidemiology, Pathophysiology, and Implications for Management. *J. Hum. Hypertens.* 33, 824–836. doi:10.1038/s41371-019-0279-7

Gupta, S. C., Patchva, S., and Aggarwal, B. B. (2013). Therapeutic Roles of Curcumin: Lessons Learned from Clinical Trials. *Aaps j* 15, 195–218. doi:10.1208/s12248-012-9432-8

Gurha, P., Abreu-Goodger, C., Wang, T., Ramirez, M. O., Drumond, A. L., Van Dongen, S., et al. (2012). Targeted Deletion of microRNA-22 Promotes Stress-Induced Cardiac Dilation and Contractile Dysfunction. *Circulation* 125, 2751–2761. doi:10.1161/circulationaha.111.044354

Hadi, A., Pourmasoumi, M., Ghaedi, E., and Sahebkar, A. (2019). The Effect of Curcumin/Turmeric on Blood Pressure Modulation: A Systematic Review and Meta-Analysis. *Pharmacol. Res.* 150, 104505. doi:10.1016/j.phrs.2019.104505

Han, Y., Sun, H.-J., Tong, Y., Chen, Y.-Z., Ye, C., Qiu, Y., et al. (2019). Curcumin Attenuates Migration of Vascular Smooth Muscle Cells via Inhibiting NFκB-Mediated NLRP3 Expression in Spontaneously Hypertensive Rats. *J. Nutr. Biochem.* 72, 108212. doi:10.1016/j.jnutbio.2019.07.003

Harrison, D. G., Coffman, T. M., and Wilcox, C. S. (2021). Pathophysiology of Hypertension. *Circ. Res.* 128, 847–863. doi:10.1161/circresaha.121.318082

Hassan, N., El-Bassossy, H. M., and Zakaria, M. N. M. (2013). Heme Oxygenase-1 Induction Protects against Hypertension Associated with Diabetes: Effect on Exaggerated Vascular Contractility. *Naunyn-schmiedeberg's Arch. Pharmacol.* 386, 217–226. doi:10.1007/s00210-012-0822-3

He, Y., Wang, R., Zhang, P., Yan, J., Gong, N., Li, Y., et al. (2021). Curcumin Inhibits the Proliferation and Migration of Vascular Smooth Muscle Cells by Targeting the Chemerin/CMKLR1/LCN2 axis. *Aging* 13, 13859–13875. doi:10.18632/aging.202980

Heldin, C.-H., and Westermark, B. (1999). Mechanism of Action and *In Vivo* Role of Platelet-Derived Growth Factor. *Physiol. Rev.* 79, 1283–1316. doi:10.1152/physrev.1999.79.4.1283

Hesari, M., Mohammadi, P., Khademi, F., Shackebaei, D., Momtaz, S., Moasefi, N., et al. (2021). Current Advances in the Use of Nanophytomedicine Therapies for Human Cardiovascular Diseases. *Ijn* 16, 3293–3315. doi:10.2147/ijn.s295508

Hlavačková, L., Janegová, A., Uličná, O., Janega, P., Cerná, A., and Babál, P. (2011). Spice up the Hypertension Diet - Curcumin and Piperine Prevent Remodeling of Aorta in Experimental L-NAME Induced Hypertension. *Nutr. Metab. (Lond)* 8, 72.

Hodaei, H., Adibian, M., Nikpayam, O., Hedayati, M., and Sohrab, G. (2019). The Effect of Curcumin Supplementation on Anthropometric Indices, Insulin Resistance and Oxidative Stress in Patients with Type 2 Diabetes: a Randomized, Double-Blind Clinical Trial. *Diabetol. Metab. Syndr.* 11, 41. doi:10.1186/s13098-019-0437-7

Hosseini, A., Penson, P. E., Cicero, A. F. G., Golledge, J., Al-Rasadi, K., Jamialahmadi, T., et al. (2021). Potential Benefits of Phytochemicals for Abdominal Aortic Aneurysm. *Cmc* 28, 8595–8607. doi:10.2174/0929867328666210614113116

Hsieh, H.-L., Sun, C.-C., Wang, T.-S., and Yang, C.-M. (2008a). PKC-δ/c-Src-mediated EGF Receptor Transactivation Regulates Thrombin-Induced COX-2 Expression and PGE2 Production in Rat Vascular Smooth Muscle Cells. *Biochim. Biophys. Acta (Bba) - Mol. Cel Res.* 1783, 1563–1575. doi:10.1016/j.bbamcr.2008.03.016

Hsieh, H.-L., Sun, C.-C., Wu, C.-B., Wu, C.-Y., Tung, W.-H., Wang, H.-H., et al. (2008b). Sphingosine 1-phosphate Induces EGFR Expression via Akt/NF-Kb and ERK/AP-1 Pathways in Rat Vascular Smooth Muscle Cells. *J. Cel. Biochem.* 103, 1732–1746. doi:10.1002/jcb.21563

Hu, X., Yang, F.-F., Wei, X.-L., Yao, G.-Y., Liu, C.-Y., Zheng, Y., et al. (2017). Curcumin Acetate Nanocrystals for Sustained Pulmonary Delivery: Preparation, Characterization and *In Vivo* Evaluation. *J. Biomed. Nanotechnol* 13, 99–109. doi:10.1166/jbn.2017.2326

Hua, Y., Dolence, J., Ramanan, S., Ren, J., and Nair, S. (2013). Bisdemethoxycurcumin Inhibits PDGF-Induced Vascular Smooth Muscle Cell Motility and Proliferation. *Mol. Nutr. Food Res.* 57, 1611–1618. doi:10.1002/mnfr.201200852

Huang, H. C., Jan, T. R., and Yeh, S. F. (1992). Inhibitory Effect of Curcumin, an Anti-inflammatory Agent, on Vascular Smooth Muscle Cell Proliferation. *Eur. J. Pharmacol.* 221, 381–384. doi:10.1016/0014-2999(92)90727-l

Huang, Z.-P., Chen, J., Seok, H. Y., Zhang, Z., Kataoka, M., Hu, X., et al. (2013). MicroRNA-22 Regulates Cardiac Hypertrophy and Remodeling in Response to Stress. *Circ. Res.* 112, 1234–1243. doi:10.1161/circresaha.112.300682

Humbert, M., Montani, D., Perros, F., Dorfmüller, P., Adnot, S., and Eddahibi, S. (2008). Endothelial Cell Dysfunction and Cross Talk between Endothelium and Smooth Muscle Cells in Pulmonary Arterial Hypertension. *Vasc. Pharmacol.* 49, 113–118. doi:10.1016/j.vph.2008.06.003

Huo, M., Cao, X., Zhang, H., Lau, C. W., Hong, H., Chen, F. M., et al. (2021). Loss of Myeloid Bmal1 Exacerbates Hypertensive Vascular Remodelling through Interaction with STAT6 in Mice. *Cardiovasc. Res.* doi:10.1093/cvr/cvab336

Hussain, Z., Thu, H. E., Ng, S.-F., Khan, S., and Katas, H. (2017). Nanoencapsulation, an Efficient and Promising Approach to Maximize Wound Healing Efficacy of Curcumin: A Review of New Trends and State-Of-The-Art. *Colloids Surf. B: Biointerfaces* 150, 223–241. doi:10.1016/j.colsurfb.2016.11.036

James, P. A., Oparil, S., Carter, B. L., Cushman, W. C., Dennison-Himmelfarb, C., Handler, J., et al. (2014). 2014 Evidence-Based Guideline for the Management of High Blood Pressure in Adults. *Jama* 311, 507–520. doi:10.1001/jama.2013.284427

Jeffery, T. K., and Morrell, N. W. (2002). Molecular and Cellular Basis of Pulmonary Vascular Remodeling in Pulmonary Hypertension. *Prog. Cardiovasc. Dis.* 45, 173–202. doi:10.1053/pcad.2002.130041

Jouen-Tachoire, T. R. H., Tucker, S. J., and Tammaro, P. (2021). Ion Channels as Convergence Points in the Pathology of Pulmonary Arterial Hypertension. *Biochem. Soc. Trans.* 49, 1855–1865. doi:10.1042/bst20210538

Kang, G., Kong, P.-J., Yuh, Y.-J., Lim, S.-Y., Yim, S.-V., Chun, W., et al. (2004). Curcumin Suppresses Lipopolysaccharide-Induced Cyclooxygenase-2 Expression by Inhibiting Activator Protein 1 and Nuclear Factor κB Bindings in BV2 Microglial Cells. *J. Pharmacol. Sci.* 94, 325–328. doi:10.1254/jphs.94.325

Kapakos, G., Youreva, V., and Srivastava, A. K. (2012). Attenuation of Endothelin-1-Induced PKB and ERK1/2 Signaling, as Well as Egr-1 Expression, by Curcumin in A-10 Vascular Smooth Muscle Cells. *Can. J. Physiol. Pharmacol.* 90, 1277–1285. doi:10.1139/y2012-059

Karaki, H., Ozaki, H., Hori, M., Mitsui-Saito, M., Amano, K., Harada, K., et al. (1997). Calcium Movements, Distribution, and Functions in Smooth Muscle. *Pharmacol. Rev.* 49, 157–230.

Karaki, H., and Weiss, G. B. (1988). Calcium Release in Smooth Muscle. *Life Sci.* 42, 111–122. doi:10.1016/0024-3205(88)90674-1

Kedzierski, R. M., Grayburn, P. A., Kisanuki, Y. Y., Williams, C. S., Hammer, R. E., Richardson, J. A., et al. (2003). Cardiomyocyte-specific Endothelin A Receptor Knockout Mice Have normal Cardiac Function and an Unaltered Hypertrophic Response to Angiotensin II and Isoproterenol. *Mol. Cel Biol* 23, 8226–8232. doi:10.1128/mcb.23.22.8226-8232.2003

Kennedy, A. J., Yang, P., Read, C., Kuc, R. E., Yang, L., Taylor, E. J., et al. (2016). Chemerin Elicits Potent Constrictor Actions via Chemokine-like Receptor 1 (CMKLR1), Not G-Protein-Coupled Receptor 1 (GPR1), in Human and Rat Vasculature. *J. Am. Heart Assoc.* 5. doi:10.1161/JAHA.116.004421

Khajehdehi, P., Pakfetrat, M., Javidnia, K., Azad, F., Malekmakan, L., Nasab, M. H., et al. (2011). Oral Supplementation of Turmeric Attenuates Proteinuria, Transforming Growth Factor-β and Interleukin-8 Levels in Patients with Overt Type 2 Diabetic Nephropathy: A Randomized, Double-Blind and Placebo-Controlled Study. *Scand. J. Urol. Nephrol.* 45, 365–370. doi:10.3109/00365599.2011.585622

Khajehdehi, P., Zanjaninejad, B., Aflaki, E., Nazarinia, M., Azad, F., Malekmakan, L., et al. (2012). Oral Supplementation of Turmeric Decreases Proteinuria, Hematuria, and Systolic Blood Pressure in Patients Suffering from Relapsing or Refractory Lupus Nephritis: a Randomized and Placebo-Controlled Study. *J. Ren. Nutr.* 22, 50–57. doi:10.1053/j.jrn.2011.03.002

Khayyal, M. T., El-Hazek, R. M., El-Sabbagh, W. A., Frank, J., Behnam, D., and Abdel-Tawab, M. (2018). Micellar Solubilisation Enhances the Antiinflammatory Activities of Curcumin and Boswellic Acids in Rats with Adjuvant-Induced Arthritis. *Nutrition* 54, 189–196. doi:10.1016/j.nut.2018.03.055

Kim, H. W., Belin de Chantemèle, E. J., and Weintraub, N. L. (2019). Perivascular Adipocytes in Vascular Disease. *Atvb* 39, 2220–2227. doi:10.1161/atvbaha.119.312304

Kim, J.-Y., Cho, H.-J., Sir, J.-J., Kim, B.-K., Hur, J., Youn, S.-W., et al. (2009). Sulfasalazine Induces Haem Oxygenase-1 via ROS-dependent Nrf2 Signalling, Leading to Control of Neointimal Hyperplasia. *Cardiovasc. Res.* 82, 550–560. doi:10.1093/cvr/cvp072

Kintsurashvili, E., Duka, I., Gavras, I., Johns, C., Farmakiotis, D., and Gavras, H. (2001). Effects of ANG II on Bradykinin Receptor Gene Expression in Cardiomyocytes and Vascular Smooth Muscle Cells. *Am. J. Physiology-Heart Circulatory Physiol.* 281, H1778–H1783. doi:10.1152/ajpheart.2001.281.4.h1778

Kostov, K. (2021). The Causal Relationship between Endothelin-1 and Hypertension: Focusing on Endothelial Dysfunction, Arterial Stiffness, Vascular Remodeling, and Blood Pressure Regulation. *Life (Basel)* 11. doi:10.3390/life11090986

Kruangtip, O., Chootip, K., Temkitthawon, P., Changwichit, K., Chuprajob, T., Changtam, C., et al. (2015). Curcumin Analogues Inhibit Phosphodiesterase-5 and Dilate Rat Pulmonary Arteries. *J. Pharm. Pharmacol.* 67, 87–95. doi:10.1111/jphp.12302

Kukongviriyapan, U., Apaijit, K., and Kukongviriyapan, V. (2016). Oxidative Stress and Cardiovascular Dysfunction Associated with Cadmium Exposure: Beneficial Effects of Curcumin and Tetrahydrocurcumin. *Tohoku J. Exp. Med.* 239, 25–38. doi:10.1620/tjem.239.25

Kukongviriyapan, U., Pannangpetch, P., Kukongviriyapan, V., Donpunha, W., Sompamit, K., and Surawattanawan, P. (2014). Curcumin Protects against Cadmium-Induced Vascular Dysfunction, Hypertension and Tissue Cadmium Accumulation in Mice. *Nutrients* 6, 1194–1208. doi:10.3390/nu6031194

Kunati, S. R., Yang, S., William, B. M., and Xu, Y. (2018). An LC-MS/MS Method for Simultaneous Determination of Curcumin, Curcumin Glucuronide and Curcumin Sulfate in a Phase II Clinical Trial. *J. Pharm. Biomed. Anal.* 156, 189–198. doi:10.1016/j.jpba.2018.04.034

Lao, C. D., Ruffin, M. T., Normolle, D., Heath, D. D., Murray, S. I., Bailey, J. M., et al. (2006). Dose Escalation of a Curcuminoid Formulation. *BMC Complement. Altern. Med.* 6, 10. doi:10.1186/1472-6882-6-10

Laurent, S., and Boutouyrie, P. (2015). The Structural Factor of Hypertension. *Circ. Res.* 116, 1007–1021. doi:10.1161/circresaha.116.303596

Lee, K.-H., Abas, F., Alitheen, N. B. M., Shaari, K., Lajis, N. H., and Ahmad, S. (2011). A Curcumin Derivative, 2,6-Bis(2,5-Dimethoxybenzylidene)-Cyclohexanone (BDMC33) Attenuates Prostaglandin E2 Synthesis via Selective Suppression of Cyclooxygenase-2 in IFN-g/LPS-Stimulated Macrophages. *Molecules* 16, 9728–9738. doi:10.3390/molecules16119728

Lee, K.-H., Chow, Y.-L., Sharmili, V., Abas, F., Alitheen, N. B. M., Shaari, K., et al. (2012). BDMC33, A Curcumin Derivative Suppresses Inflammatory Responses in Macrophage-like Cellular System: Role of Inhibition in NF-Kb and MAPK Signaling Pathways. *Ijms* 13, 2985–3008. doi:10.3390/ijms13032985

Lee, T.-S., Chang, C.-C., Zhu, Y., and Shyy, J. Y.-J. (2004). Simvastatin Induces Heme Oxygenase-1. *Circulation* 110, 1296–1302. doi:10.1161/01.cir.0000140694.67251.9c

Li, H.-B., Xu, M.-L., Du, M.-M., Yu, X.-J., Bai, J., Xia, W.-J., et al. (2021). Curcumin Ameliorates Hypertension via Gut-Brain Communication in Spontaneously Hypertensive Rat. *Toxicol. Appl. Pharmacol.* 429, 115701. doi:10.1016/j.taap.2021.115701

Li, H.-B., Yang, T., Richards, E. M., Pepine, C. J., and Raizada, M. K. (2020). Maternal Treatment with Captopril Persistently Alters Gut-Brain Communication and Attenuates Hypertension of Male Offspring. *Hypertension* 75, 1315–1324. doi:10.1161/hypertensionaha.120.14736

Li, H.-Y., Yang, M., Li, Z., and Meng, Z. (2017). Curcumin Inhibits Angiotensin II-Induced Inflammation and Proliferation of Rat Vascular Smooth Muscle Cells by Elevating PPAR-γ Activity and Reducing Oxidative Stress. *Int. J. Mol. Med.* 39, 1307–1316. doi:10.3892/ijmm.2017.2924

Li, J. L., Fan, Y. Y., Ye, G. H., Dong, M. W., Lin, K. Z., Li, F., et al. (2014). Study on the Mechanism of How Curcumin Improves Pulmonary Vascular Remodeling Associated with Chronic Pulmonary Arterial Hypertension. *Zhongguo Ying Yong Sheng Li Xue Za Zhi* 30, 451–455.

Li, Y., Tian, D., Zhu, C., and Ren, L. (2016). Demethoxycurcumin Preserves Renovascular Function by Downregulating COX-2 Expression in Hypertension. *Oxid Med. Cel Longev* 2016, 9045736. doi:10.1155/2016/9045736

Li, Y., Lui, K. O., and Zhou, B. (2018). Reassessing Endothelial-To-Mesenchymal Transition in Cardiovascular Diseases. *Nat. Rev. Cardiol.* 15, 445–456. doi:10.1038/s41569-018-0023-y

Lin, Q., Wang, L. X., Chen, S. X., Zhou, X. F., Huang, X. Y., and Fan, X. F. (2006). Effect of Curcumin on Pulmonary Hypertension and wall Collagen of Pulmonary Arterioles of Chronic Hypoxic Hypercapnic Rats. *Zhongguo Ying Yong Sheng Li Xue Za Zhi* 22, 257–261.

Ling, L., Chen, D., Tong, Y., Zang, Y.-H., Ren, X.-S., Zhou, H., et al. (2018). Fibronectin Type III Domain Containing 5 Attenuates NLRP3 Inflammasome Activation and Phenotypic Transformation of Adventitial Fibroblasts in Spontaneously Hypertensive Rats. *J. Hypertens.* 36, 1104–1114. doi:10.1097/hjh.0000000000001654

Liu, H., Xiong, W., Luo, Y., Chen, H., He, Y., Cao, Y., et al. (2019). Adipokine Chemerin Stimulates Progression of Atherosclerosis in ApoE-/- Mice. *Biomed. Res. Int.* 2019, 7157865. doi:10.1155/2019/7157865

Liu, Y., Dolence, J., Ren, J., Rao, M., and Sreejayan, N. (2008). Inhibitory Effect of Dehydrozingerone on Vascular Smooth Muscle Cell Function. *J. Cardiovasc. Pharmacol.* 52, 422–429. doi:10.1097/fjc.0b013e31818aed93

Lu, H., Du, W., Ren, L., Hamblin, M. H., Becker, R. C., Chen, Y. E., et al. (2021). Vascular Smooth Muscle Cells in Aortic Aneurysm: From Genetics to Mechanisms. *J. Am. Heart Assoc.* 10, e023601. doi:10.1161/JAHA.121.023601

Lu, Q.-B., Wan, M.-Y., Wang, P.-Y., Zhang, C.-X., Xu, D.-Y., Liao, X., et al. (2018a). Chicoric Acid Prevents PDGF-BB-Induced VSMC Dedifferentiation, Proliferation and Migration by Suppressing ROS/NFκB/mTOR/P70S6K Signaling cascade. *Redox Biol.* 14, 656–668. doi:10.1016/j.redox.2017.11.012

Lu, Q.-B., Wang, H.-P., Tang, Z.-H., Cheng, H., Du, Q., Wang, Y.-B., et al. (2018b). Nesfatin-1 Functions as a Switch for Phenotype Transformation and Proliferation of VSMCs in Hypertensive Vascular Remodeling. *Biochim. Biophys. Acta (Bba) - Mol. Basis Dis.* 1864, 2154–2168. doi:10.1016/j.bbadis.2018.04.002

Lu, X., Gong, J., Dennery, P. A., and Yao, H. (2019). Endothelial-to-mesenchymal Transition: Pathogenesis and Therapeutic Targets for Chronic Pulmonary and Vascular Diseases. *Biochem. Pharmacol.* 168, 100–107. doi:10.1016/j.bcp.2019.06.021

Luo, P., and Qiu, B. (2022). The Role of Immune Cells in Pulmonary Hypertension: Focusing on Macrophages. *Hum. Immunol.* 83, 153–163. doi:10.1016/j.humimm.2021.11.006

Lüscher, T. F., and Barton, M. (2000). Endothelins and Endothelin Receptor Antagonists: Therapeutic Considerations for a Novel Class of Cardiovascular Drugs. *Circulation* 102, 2434–2440.

Lynch, I. J., Welch, A. K., Gumz, M. L., Kohan, D. E., Cain, B. D., and Wingo, C. S. (2015). Effect of Mineralocorticoid Treatment in Mice with Collecting Duct-specific Knockout of Endothelin-1. *Am. J. Physiology-Renal Physiol.* 309, F1026–F1034. doi:10.1152/ajprenal.00220.2015

Mahmoud, M. F., and El Bassossy, H. M. (2014). Curcumin Attenuates Fructose-Induced Vascular Dysfunction of Isolated Rat Thoracic Aorta Rings. *Pharm. Biol.* 52, 972–977. doi:10.3109/13880209.2013.874465

Majithiya, J. B., and Balaraman, R. (2005). Time-dependent Changes in Antioxidant Enzymes and Vascular Reactivity of Aorta in Streptozotocin-Induced Diabetic Rats Treated with Curcumin. *J. Cardiovasc. Pharmacol.* 46, 697–705. doi:10.1097/01.fjc.0000183720.85014.24

Maradana, M. R., Thomas, R., and O'sullivan, B. J. (2013). Targeted Delivery of Curcumin for Treating Type 2 Diabetes. *Mol. Nutr. Food Res.* 57, 1550–1556. doi:10.1002/mnfr.201200791

Marceau, F., Bachelard, H., Charest-Morin, X., Hébert, J., and Rivard, G. E. (2020). *In Vitro* Modeling of Bradykinin-Mediated Angioedema States. *Pharmaceuticals* 13, 201. doi:10.3390/ph13090201

Mccoy, E. K., and Lisenby, K. M. (2021). Aprocitentan (A Dual Endothelin-Receptor Antagonist) for Treatment-Resistant Hypertension. *J. Cardiovasc. Pharmacol.* 77, 699–706. doi:10.1097/fjc.0000000000001023

Meydani, M., and Hasan, S. T. (2010). Dietary Polyphenols and Obesity. *Nutrients* 2, 737–751. doi:10.3390/nu2070737

Mohammadi, A., Blesso, C. N., Barreto, G. E., Banach, M., Majeed, M., and Sahebkar, A. (2019). Macrophage Plasticity, Polarization and Function in Response to Curcumin, a Diet-Derived Polyphenol, as an Immunomodulatory Agent. *J. Nutr. Biochem.* 66, 1–16. doi:10.1016/j.jnutbio.2018.12.005

Monteiro, J. P., Bennett, M., Rodor, J., Caudrillier, A., Ulitsky, I., and Baker, A. H. (2019). Endothelial Function and Dysfunction in the Cardiovascular System: the Long Non-coding Road. *Cardiovasc. Res.* 115, 1692–1704. doi:10.1093/cvr/cvz154

Morimoto, T., Sunagawa, Y., Kawamura, T., Takaya, T., Wada, H., Nagasawa, A., et al. (2008). The Dietary Compound Curcumin Inhibits P300 Histone Acetyltransferase Activity and Prevents Heart Failure in Rats. *J. Clin. Invest.* 118, 868–878. doi:10.1172/JCI33160

Muiesan, M. L., Salvetti, M., Rosei, C. A., and Paini, A. (2016). Gender Differences in Antihypertensive Treatment: Myths or Legends? *High Blood Press. Cardiovasc. Prev.* 23, 105–113. doi:10.1007/s40292-016-0148-1

Nakmareong, S., Kukongviriyapan, U., Pakdeechote, P., Donpunha, W., Kukongviriyapan, V., Kongyingyoes, B., et al. (2011). Antioxidant and Vascular Protective Effects of Curcumin and Tetrahydrocurcumin in Rats with L-NAME-Induced Hypertension. *Naunyn-schmiedeberg's Arch. Pharmacol.* 383, 519–529. doi:10.1007/s00210-011-0624-z

Nakmareong, S., Kukongviriyapan, U., Pakdeechote, P., Kukongviriyapan, V., Kongyingyoes, B., Donpunha, W., et al. (2012). Tetrahydrocurcumin Alleviates Hypertension, Aortic Stiffening and Oxidative Stress in Rats with Nitric Oxide Deficiency. *Hypertens. Res.* 35, 418–425. doi:10.1038/hr.2011.180

Nelson, K. M., Dahlin, J. L., Bisson, J., Graham, J., Pauli, G. F., and Walters, M. A. (2017). The Essential Medicinal Chemistry of Curcumin. *J. Med. Chem.* 60, 1620–1637. doi:10.1021/acs.jmedchem.6b00975

Nelson, M. T., Patlak, J. B., Worley, J. F., and Standen, N. B. (1990). Calcium Channels, Potassium Channels, and Voltage Dependence of Arterial Smooth Muscle Tone. *Am. J. Physiology-Cell Physiol.* 259, C3–C18. doi:10.1152/ajpcell.1990.259.1.c3

Nguyen, K. T., Shaikh, N., Shukla, K. P., Su, S.-H., Eberhart, R. C., and Tang, L. (2004). Molecular Responses of Vascular Smooth Muscle Cells and Phagocytes to Curcumin-Eluting Bioresorbable Stent Materials. *Biomaterials* 25, 5333–5346. doi:10.1016/j.biomaterials.2003.12.033

Ota, K., Kimura, T., Shoji, M., Ota, M., Funyu, T., Mori, T., et al. (1998). Effects of Endothelin-Induced Nitric Oxide on Venous Circulation and Renal Water-Electrolyte Handling. *J. Cardiovasc. Pharmacol.* 31 (Suppl. 1), S128–S132. doi:10.1097/00005344-199800001-00039

Ouarné, M., Pena, A., and Franco, C. A. (2021). From Remodeling to Quiescence: The Transformation of the Vascular Network. *Cells Dev* 203735.

Pae, H.-O., Jeong, G.-S., Jeong, S.-O., Kim, H. S., Kim, S.-A., Kim, Y.-C., et al. (2007). Roles of Heme Oxygenase-1 in Curcumin-Induced Growth Inhibition in Rat Smooth Muscle Cells. *Exp. Mol. Med.* 39, 267–277. doi:10.1038/emm.2007.30

Pang, X. F., Zhang, L. H., Bai, F., Wang, N. P., Garner, R. E., Mckallip, R. J., et al. (2015). Attenuation of Myocardial Fibrosis with Curcumin Is Mediated by Modulating Expression of Angiotensin II AT1/AT2 Receptors and ACE2 in Rats. *Drug Des. Devel Ther.* 9, 6043–6054. doi:10.2147/DDDT.S95333

Panthiya, L., Tocharus, J., Onsa-Ard, A., Chaichompoo, W., Suksamrarn, A., and Tocharus, C. (2022). Hexahydrocurcumin Ameliorates Hypertensive and Vascular Remodeling in L-NAME-Induced Rats. *Biochim. Biophys. Acta (Bba) - Mol. Basis Dis.* 1868, 166317. doi:10.1016/j.bbadis.2021.166317

Paradiso-Hardy, F. L., Gordon, W. L., Jackevicius, C. A., Kertland, H. R., Pearson, G. J., Pickering, J. L., et al. (2003). The Importance of In-Hospital Statin Therapy for Patients with Acute Coronary Syndromes. *Pharmacotherapy* 23, 506–513. doi:10.1592/phco.23.4.506.32129

Park, C.-B., Ahn, C. M., Oh, S., Kwon, D., Cho, W.-C., Shin, W.-S., et al. (2015). Synthesis of Alkylsulfonyl and Substituted Benzenesulfonyl Curcumin Mimics as Dual Antagonist of L-type Ca2+ Channel and Endothelin A/B2 Receptor. *Bioorg. Med. Chem.* 23, 6673–6682. doi:10.1016/j.bmc.2015.09.004

Patel, S. S., Acharya, A., Ray, R. S., Agrawal, R., Raghuwanshi, R., and Jain, P. (2020). Cellular and Molecular Mechanisms of Curcumin in Prevention and Treatment of Disease. *Crit. Rev. Food Sci. Nutr.* 60, 887–939. doi:10.1080/10408398.2018.1552244

Pathak, N., and Khandelwal, S. (2008). Comparative Efficacy of Piperine, Curcumin and Picroliv against Cd Immunotoxicity in Mice. *Biometals* 21, 649–661. doi:10.1007/s10534-008-9150-y

Pechanova, O., Dayar, E., and Cebova, M. (2020). Therapeutic Potential of Polyphenols-Loaded Polymeric Nanoparticles in Cardiovascular System. *Molecules* 25, 3322. doi:10.3390/molecules25153322

Perros, F., Dorfmüller, P., and Humbert, M. (2005). Current Insights on the Pathogenesis of Pulmonary Arterial Hypertension. *Semin. Respir. Crit. Care Med.* 26, 355–364. doi:10.1055/s-2005-916149

Pinheiro Júnior, J. E. G., Moraes, P. Z., Rodriguez, M. D., Simões, M. R., Cibin, F., Pinton, S., et al. (2020). Cadmium Exposure Activates NADPH Oxidase, Renin-Angiotensin System and Cyclooxygenase 2 Pathways in Arteries, Inducing Hypertension and Vascular Damage. *Toxicol. Lett.* 333, 80–89.

Prado, A. F., Batista, R. I. M., Tanus-Santos, J. E., and Gerlach, R. F. (2021). Matrix Metalloproteinases and Arterial Hypertension: Role of Oxidative Stress and Nitric Oxide in Vascular Functional and Structural Alterations. *Biomolecules* 11, 585. doi:10.3390/biom11040585

Prieto, M. C., Gonzalez, A. A., Visniauskas, B., and Navar, L. G. (2021). The Evolving Complexity of the Collecting Duct Renin-Angiotensin System in Hypertension. *Nat. Rev. Nephrol.* 17, 481–492. doi:10.1038/s41581-021-00414-6

Pugliese, S. C., Poth, J. M., Fini, M. A., Olschewski, A., El Kasmi, K. C., and Stenmark, K. R. (2015). The Role of Inflammation in Hypoxic Pulmonary Hypertension: from Cellular Mechanisms to Clinical Phenotypes. *Am. J. Physiology-Lung Cell Mol. Physiol.* 308, L229–L252. doi:10.1152/ajplung.00238.2014

Rabinovitch, M., Guignabert, C., Humbert, M., and Nicolls, M. R. (2014). Inflammation and Immunity in the Pathogenesis of Pulmonary Arterial Hypertension. *Circ. Res.* 115, 165–175. doi:10.1161/circresaha.113.301141

Rachmawati, H., Soraya, I. S., Kurniati, N. F., and Rahma, A. (2016). *In Vitro* Study on Antihypertensive and Antihypercholesterolemic Effects of Curcumin Nanoemulsion. *Sci. Pharm.* 84, 131–140. doi:10.3797/scipharm.isp.2015.05

Rakotoarisoa, M., and Angelova, A. (2018). Amphiphilic Nanocarrier Systems for Curcumin Delivery in Neurodegenerative Disorders. *Medicines* 5, 126. doi:10.3390/medicines5040126

Ramirez, L. A., and Sullivan, J. C. (2018). Sex Differences in Hypertension: Where We Have Been and where We Are Going. *Am. J. Hypertens.* 31, 1247–1254. doi:10.1093/ajh/hpy148

Rapsomaniki, E., Timmis, A., George, J., Pujades-Rodriguez, M., Shah, A. D., Denaxas, S., et al. (2014). Blood Pressure and Incidence of Twelve Cardiovascular Diseases: Lifetime Risks, Healthy Life-Years Lost, and Age-specific Associations in 1·25 Million People. *The Lancet* 383, 1899–1911. doi:10.1016/s0140-6736(14)60685-1

Ren, X. S., Tong, Y., Qiu, Y., Ye, C., Wu, N., Xiong, X. Q., et al. (2020). MiR155-5p in Adventitial Fibroblasts-derived Extracellular Vesicles Inhibits Vascular Smooth Muscle Cell Proliferation via Suppressing Angiotensin-converting Enzyme Expression. *J. Extracellular Vesicles* 9, 1698795. doi:10.1080/20013078.2019.1698795

Restini, C. B. A., Ismail, A., Kumar, R. K., Burnett, R., Garver, H., Fink, G. D., et al. (2018). Renal Perivascular Adipose Tissue: Form and Function. *Vasc. Pharmacol.* 106, 37–45. doi:10.1016/j.vph.2018.02.004

Rice, K. M., Manne, N. D. P. K., Kolli, M. B., Wehner, P. S., Dornon, L., Arvapalli, R., et al. (2016). Curcumin Nanoparticles Attenuate Cardiac Remodeling Due to Pulmonary Arterial Hypertension. *Artif. Cell Nanomedicine, Biotechnol.* 44, 1909–1916. doi:10.3109/21691401.2015.1111235

Rizzoni, D., Porteri, E., Guefi, D., Piccoli, A., Castellano, M., Pasini, G., et al. (2000). Cellular Hypertrophy in Subcutaneous Small Arteries of Patients with Renovascular Hypertension. *Hypertension* 35, 931–935. doi:10.1161/01.hyp.35.4.931

Sakurai, T., Yanagisawa, M., Takuwat, Y., Miyazakit, H., Kimura, S., Goto, K., et al. (1990). Cloning of a cDNA Encoding a Non-isopeptide-selective Subtype of the Endothelin Receptor. *Nature* 348, 732–735. doi:10.1038/348732a0

Salehi, B., Del Prado-Audelo, M. L., Cortés, H., Leyva-Gómez, G., Stojanović-Radić, Z., Singh, Y. D., et al. (2020). Therapeutic Applications of Curcumin Nanomedicine Formulations in Cardiovascular Diseases. *Jcm* 9, 746. doi:10.3390/jcm9030746

Sangartit, W., Kukongviriyapan, U., Donpunha, W., Pakdeechote, P., Kukongviriyapan, V., Surawattanawan, P., et al. (2014). Tetrahydrocurcumin Protects against Cadmium-Induced Hypertension, Raised Arterial Stiffness and Vascular Remodeling in Mice. *PLoS One* 9, e114908. doi:10.1371/journal.pone.0114908

Sangartit, W., Pakdeechote, P., Kukongviriyapan, V., Donpunha, W., Shibahara, S., and Kukongviriyapan, U. (2016). Tetrahydrocurcumin in Combination with Deferiprone Attenuates Hypertension, Vascular Dysfunction, Baroreflex

Dysfunction, and Oxidative Stress in Iron-Overloaded Mice. *Vasc. Pharmacol.* 87, 199–208. doi:10.1016/j.vph.2016.10.001

Santos-Parker, J. R., Strahler, T. R., Bassett, C. J., Bispham, N. Z., Chonchol, M. B., and Seals, D. R. (2017). Curcumin Supplementation Improves Vascular Endothelial Function in Healthy Middle-Aged and Older Adults by Increasing Nitric Oxide Bioavailability and Reducing Oxidative Stress. *Aging* 9, 187–208. doi:10.18632/aging.101149

Schiffrin, E. L., Deng, L. Y., and Larochelle, P. (1993). Morphology of Resistance Arteries and Comparison of Effects of Vasoconstrictors in Mild Essential Hypertensive Patients. *Clin. Invest. Med.* 16, 177–186.

Selvendiran, K., Kuppusamy, M. L., Bratasz, A., Tong, L., Rivera, B. K., Rink, C., et al. (2009). Inhibition of Vascular Smooth-Muscle Cell Proliferation and Arterial Restenosis by HO-3867, a Novel Synthetic Curcuminoid, through Up-Regulation of PTEN Expression. *J. Pharmacol. Exp. Ther.* 329, 959–966. doi:10.1124/jpet.108.150367

Shahani, K., Swaminathan, S. K., Freeman, D., Blum, A., Ma, L., and Panyam, J. (2010). Injectable Sustained Release Microparticles of Curcumin: a New Concept for Cancer Chemoprevention. *Cancer Res.* 70, 4443–4452. doi:10.1158/0008-5472.can-09-4362

Sharma, R. A., Euden, S. A., Platton, S. L., Cooke, D. N., Shafayat, A., Hewitt, H. R., et al. (2004). Phase I Clinical Trial of Oral Curcumin. *Clin. Cancer Res.* 10, 6847–6854. doi:10.1158/1078-0432.ccr-04-0744

Sharma, R. K., Oliveira, A. C., Yang, T., Karas, M. M., Li, J., Lobaton, G. O., et al. (2020). Gut Pathology and its Rescue by ACE2 (Angiotensin-Converting Enzyme 2) in Hypoxia-Induced Pulmonary Hypertension. *Hypertension* 76, 206–216. doi:10.1161/hypertensionaha.120.14931

Sheu, M.-J., Lin, H.-Y., Yang, Y.-H., Chou, C.-J., Chien, Y.-C., Wu, T.-S., et al. (2013). Demethoxycurcumin, a Major Active Curcuminoid from Curcuma Longa , Suppresses Balloon Injury Induced Vascular Smooth Muscle Cell Migration and Neointima Formation: An *In Vitro* and *In Vivo* Study. *Mol. Nutr. Food Res.* 57, 1586–1597. doi:10.1002/mnfr.201200462

Shi, N., and Chen, S. Y. (2014). Mechanisms Simultaneously Regulate Smooth Muscle Proliferation and Differentiation. *J. Biomed. Res.* 28, 40–46. doi:10.7555/JBR.28.20130130

Shishodia, S., Sethi, G., and Aggarwal, B. B. (2005). Curcumin: Getting Back to the Roots. *Ann. New York Acad. Sci.* 1056, 206–217. doi:10.1196/annals.1352.010

Shome, S., Talukdar, A. D., Choudhury, M. D., Bhattacharya, M. K., and Upadhyaya, H. (2016). Curcumin as Potential Therapeutic Natural Product: a Nanobiotechnological Perspective. *J. Pharm. Pharmacol.* 68, 1481–1500. doi:10.1111/jphp.12611

Soni, K. B., and Kuttan, R. (1992). Effect of Oral Curcumin Administration on Serum Peroxides and Cholesterol Levels in Human Volunteers. *Indian J. Physiol. Pharmacol.* 36, 273–275.

Sørensen, S. S., Jensen, J. D., Madsen, J. K., and Pedersen, E. B. (1995). Effect of Isradipine on Renal Haemodynamics and Systemic Blood Pressure Changes Induced by Intravenous Infusion of Endothelin in Healthy Humans. *Nephrol. Dial. Transpl.* 10, 1324–1331.

Srinivasan, M. (1972). Effect of Curcumin on Blood Sugar as Seen in a Diabetic Subject. *Indian J. Med. Sci.* 26, 269–270.

Stenmark, K. R., Tuder, R. M., and El Kasmi, K. C. (20151985). Metabolic Reprogramming and Inflammation Act in Concert to Control Vascular Remodeling in Hypoxic Pulmonary Hypertension. *J. Appl. Physiol.* 119, 1164–1172. doi:10.1152/japplphysiol.00283.2015

Stöger, J. L., Gijbels, M. J., Van Der Velden, S., Manca, M., Van Der Loos, C. M., Biessen, E. A., et al. (2012). Distribution of Macrophage Polarization Markers in Human Atherosclerosis. *Atherosclerosis* 225, 461–468. doi:10.1016/j.atherosclerosis.2012.09.013

Stumpf, C., Raaz, D., Klinghammer, L., Schneider, M., Schmieder, R. E., Garlichs, C. D., et al. (2016). Platelet CD40 Contributes to Enhanced Monocyte Chemoattractant Protein 1 Levels in Patients with Resistant Hypertension. *Eur. J. Clin. Invest.* 46, 564–571. doi:10.1111/eci.12635

Sun, H.-J., Hou, B., Wang, X., Zhu, X.-X., Li, K.-X., and Qiu, L.-Y. (2016). Endothelial Dysfunction and Cardiometabolic Diseases: Role of Long Non-coding RNAs. *Life Sci.* 167, 6–11. doi:10.1016/j.lfs.2016.11.005

Sun, H.-J., Ren, X.-S., Xiong, X.-Q., Chen, Y.-Z., Zhao, M.-X., Wang, J.-J., et al. (2017a). NLRP3 Inflammasome Activation Contributes to VSMC Phenotypic Transformation and Proliferation in Hypertension. *Cell Death Dis* 8, e3074. doi:10.1038/cddis.2017.470

Sun, H. J., Wu, Z. Y., Nie, X. W., and Bian, J. S. (2019b). Role of Endothelial Dysfunction in Cardiovascular Diseases: The Link between Inflammation and Hydrogen Sulfide. *Front. Pharmacol.* 10, 1568. doi:10.3389/fphar.2019.01568

Sun, H. J., Zhu, X. X., Cai, W. W., and Qiu, L. Y. (2017b). Functional Roles of Exosomes in Cardiovascular Disorders: a Systematic Review. *Eur. Rev. Med. Pharmacol. Sci.* 21, 5197–5206. doi:10.26355/eurrev_201711_13840

Sun, H. J., Wu, Z. Y., Cao, L., Zhu, M. Y., Liu, T. T., Guo, L., et al. (2019a). Hydrogen Sulfide: Recent Progression and Perspectives for the Treatment of Diabetic Nephropathy. *Molecules* 24, 2857. doi:10.3390/molecules24152857

Sun, S.-y., Cao, Y.-m., Huo, Y.-j., Qiu, F., Quan, W.-j., He, C.-p., et al. (2021). Nicotinate-curcumin Inhibits AngII-Induced Vascular Smooth Muscle Cell Phenotype Switching by Upregulating Daxx Expression. *Cell Adhes. Migration* 15, 116–125. doi:10.1080/19336918.2021.1909899

Sunagawa, Y., Funamoto, M., Shimizu, K., Shimizu, S., Sari, N., Katanasaka, Y., et al. (2021). Curcumin, an Inhibitor of P300-HAT Activity, Suppresses the Development of Hypertension-Induced Left Ventricular Hypertrophy with Preserved Ejection Fraction in Dahl Rats. *Nutrients* 13, 2608. doi:10.3390/nu13082608

Tamás, P., Worgall, S., Sulyok, E., and Rascher, W. (1994). Renal Electrolyte and Water Handling in normal Pregnancy: Possible Role of Endothelin-1. *Eur. J. Obstet. Gynecol. Reprod. Biol.* 55, 89–95. doi:10.1016/0028-2243(94)90060-4

Tapia, E., Soto, V., Ortiz-Vega, K. M., Zarco-Márquez, G., Molina-Jijón, E., Cristóbal-García, M., et al. (2012). Curcumin Induces Nrf2 Nuclear Translocation and Prevents Glomerular Hypertension, Hyperfiltration, Oxidant Stress, and the Decrease in Antioxidant Enzymes in 5/6 Nephrectomized Rats. *Oxid Med. Cel Longev* 2012, 269039. doi:10.1155/2012/269039

Thenappan, T., Ormiston, M. L., Ryan, J. J., and Archer, S. L. (2018). Pulmonary Arterial Hypertension: Pathogenesis and Clinical Management. *Bmj* 360, j5492. doi:10.1136/bmj.j5492

Tipton, A. J., and Sullivan, J. C. (2014). Sex Differences in T Cells in Hypertension. *Clin. Ther.* 36, 1882–1900. doi:10.1016/j.clinthera.2014.07.011

Tong, Y., Ye, C., Ren, X.-S., Qiu, Y., Zang, Y.-H., Xiong, X.-Q., et al. (2018). Exosome-Mediated Transfer of ACE (Angiotensin-Converting Enzyme) from Adventitial Fibroblasts of Spontaneously Hypertensive Rats Promotes Vascular Smooth Muscle Cell Migration. *Hypertension* 72, 881–888. doi:10.1161/hypertensionaha.118.11375

Tong, Y., Ye, C., Zheng, F., Bo, J.-H., Wu, L.-L., Han, Y., et al. (2021). Extracellular Vesicle-Mediated miR135a-5p Transfer in Hypertensive Rat Contributes to Vascular Smooth Muscle Cell Proliferation via Targeting FNDC5. *Vasc. Pharmacol.* 140, 106864. doi:10.1016/j.vph.2021.106864

Tønnesen, H. H., Másson, M., and Loftsson, T. (2002). Studies of Curcumin and Curcuminoids. XXVII. Cyclodextrin Complexation: Solubility, Chemical and Photochemical Stability. *Int. J. Pharm.* 244, 127–135.

Toral, M., Robles-Vera, I., Visitación, N., Romero, M., Sánchez, M., Gómez-Guzmán, M., et al. (2019). Role of the Immune System in Vascular Function and Blood Pressure Control Induced by Faecal Microbiota Transplantation in Rats. *Acta Physiol.* 227, e13285. doi:10.1111/apha.13285

Tubsakul, A., Sangartit, W., Pakdeechote, P., Kukongviriyapan, V., Apaijit, K., and Kukongviriyapan, U. (2021). Curcumin Mitigates Hypertension, Endothelial Dysfunction and Oxidative Stress in Rats with Chronic Exposure to Lead and Cadmium. *Tohoku J. Exp. Med.* 253, 69–76. doi:10.1620/tjem.253.69

Tuder, R. M. (2017). Pulmonary Vascular Remodeling in Pulmonary Hypertension. *Cell Tissue Res* 367, 643–649. doi:10.1007/s00441-016-2539-y

Tuder, R. M., Stacher, E., Robinson, J., Kumar, R., and Graham, B. B. (2013). Pathology of Pulmonary Hypertension. *Clin. Chest Med.* 34, 639–650. doi:10.1016/j.ccm.2013.08.009

Usharani, P., Mateen, A. A., Naidu, M. U. R., Raju, Y. S. N., and Chandra, N. (2008). Effect of NCB-02, Atorvastatin and Placebo on Endothelial Function, Oxidative Stress and Inflammatory Markers in Patients with Type 2 Diabetes Mellitus. *Drugs R. D* 9, 243–250. doi:10.2165/00126839-200809040-00004

Van Beusecum, J. P., Moreno, H., and Harrison, D. G. (2021). Innate Immunity and Clinical Hypertension. *J. Hum. Hypertens.* doi:10.1038/s41371-021-00627-z

Virdis, A., and Taddei, S. (2016). Endothelial Dysfunction in Resistance Arteries of Hypertensive Humans. *J. Cardiovasc. Pharmacol.* 67, 451–457. doi:10.1097/fjc.0000000000000362

Wang, B., Sheng, Y., and Li, Y. (2021a). Lymphatic Microcirculation Profile in the Progression of Hypertension in Spontaneously Hypertensive Rats. *Microcirculation*, e12724. doi:10.1111/micc.12724

Wang, G., Zhu, Y., Li, K., Liao, B., Wang, F., Shao, L., et al. (2021b). Curcumin-mediated Photodynamic Therapy Inhibits the Phenotypic Transformation, Migration, and Foaming of Oxidized Low-Density Lipoprotein-Treated Vascular Smooth Muscle Cells by Promoting Autophagy. *J. Cardiovasc. Pharmacol.* 78, 308–318. doi:10.1097/fjc.0000000000001069

Wang, H. X., Davis, M. J., Rajanayagam, M. A. S., Potocnik, S. J., and Hill, M. A. (1999). Myogenic Reactivity of Rat Epineurial Arterioles: Potential Role in Local Vasoregulatory Events. *Am. J. Physiology-Heart Circulatory Physiol.* 277, H144–H151. doi:10.1152/ajpheart.1999.277.1.h144

Webb, M. L., and Meek, T. D. (1997). Inhibitors of Endothelin. *Med. Res. Rev.* 17, 17–67. doi:10.1002/(sici)1098-1128(199701)17:1<17::aid-med2>3.0.co;2-w

Wickenberg, J., Ingemansson, S. L., and Hlebowicz, J. (2010). Effects of Curcuma Longa (Turmeric) on Postprandial Plasma Glucose and Insulin in Healthy Subjects. *Nutr. J.* 9, 43. doi:10.1186/1475-2891-9-43

Wu, N., Ye, C., Zheng, F., Wan, G.-W., Wu, L.-L., Chen, Q., et al. (2020). MiR155-5p Inhibits Cell Migration and Oxidative Stress in Vascular Smooth Muscle Cells of Spontaneously Hypertensive Rats. *Antioxidants* 9, 204. doi:10.3390/antiox9030204

Xiang, D., Li, Y., Cao, Y., Huang, Y., Zhou, L., Lin, X., et al. (2021). Different Effects of Endothelial Extracellular Vesicles and LPS-Induced Endothelial Extracellular Vesicles on Vascular Smooth Muscle Cells: Role of Curcumin and its Derivatives. *Front. Cardiovasc. Med.* 8, 649352. doi:10.3389/fcvm.2021.649352

Xiao, Q., Li, X., Li, Y., Wu, Z., Xu, C., Chen, Z., et al. (2021). Biological Drug and Drug Delivery-Mediated Immunotherapy. *Acta Pharmaceutica Sinica B* 11, 941–960. doi:10.1016/j.apsb.2020.12.018

Xu, S., Ilyas, I., Little, P. J., Li, H., Kamato, D., Zheng, X., et al. (2021). Endothelial Dysfunction in Atherosclerotic Cardiovascular Diseases and beyond: From Mechanism to Pharmacotherapies. *Pharmacol. Rev.* 73, 924–967. doi:10.1124/pharmrev.120.000096

Xu, X.-Y., Meng, X., Li, S., Gan, R.-Y., Li, Y., and Li, H.-B. (2018). Bioactivity, Health Benefits, and Related Molecular Mechanisms of Curcumin: Current Progress, Challenges, and Perspectives. *Nutrients* 10, 1553. doi:10.3390/nu10101553

Yallapu, M. M., Jaggi, M., and Chauhan, S. C. (2012). Curcumin Nanoformulations: a Future Nanomedicine for Cancer. *Drug Discov. Today* 17, 71–80. doi:10.1016/j.drudis.2011.09.009

Yallapu, M. M., Nagesh, P. K. B., Jaggi, M., and Chauhan, S. C. (2015). Therapeutic Applications of Curcumin Nanoformulations. *Aaps j* 17, 1341–1356. doi:10.1208/s12248-015-9811-z

Yamamoto, T., Kimura, T., Ota, K., Shoji, M., Inoue, M., Sato, K., et al. (1991). Central Effects of Endothelin-1 on Vasopressin and Atrial Natriuretic Peptide Release and Cardiovascular and Renal Function in Conscious Rats. *J. Cardiovasc. Pharmacol.* 17 (Suppl. 7), S316–S318. doi:10.1097/00005344-199100177-00090

Yang, X., Thomas, D. P., Zhang, X., Culver, B. W., Alexander, B. M., Murdoch, W. J., et al. (2006). Curcumin Inhibits Platelet-Derived Growth Factor-Stimulated Vascular Smooth Muscle Cell Function and Injury-Induced Neointima Formation. *Atvb* 26, 85–90. doi:10.1161/01.atv.0000191635.00744.b6

Yao, Y., Wang, W., Li, M., Ren, H., Chen, C., Wang, J., et al. (2016). Curcumin Exerts its Anti-hypertensive Effect by Down-Regulating the AT1 Receptor in Vascular Smooth Muscle Cells. *Sci. Rep.* 6, 25579. doi:10.1038/srep25579

Yaribeygi, H., Maleki, M., Majeed, M., Jamialahmadi, T., and Sahebkar, A. (2021). Renoprotective Roles of Curcumin. *Adv. Exp. Med. Biol.* 1328, 531–544. doi:10.1007/978-3-030-73234-9_38

Young, N. A., Bruss, M. S., Gardner, M., Willis, W. L., Mo, X., Valiente, G. R., et al. (2014). Oral Administration of Nano-Emulsion Curcumin in Mice Suppresses Inflammatory-Induced NFκB Signaling and Macrophage Migration. *PLoS One* 9, e111559. doi:10.1371/journal.pone.0111559

Yu, Y.-M., and Lin, H.-C. (2010). Curcumin Prevents Human Aortic Smooth Muscle Cells Migration by Inhibiting of MMP-9 Expression. *Nutr. Metab. Cardiovasc. Dis.* 20, 125–132. doi:10.1016/j.numecd.2009.03.001

Zeng, X., Cheng, Y., Qu, Y., Xu, J., Han, Z., and Zhang, T. (2013). Curcumin Inhibits the Proliferation of Airway Smooth Muscle Cells *In Vitro* and *In Vivo*. *Int. J. Mol. Med.* 32, 629–636. doi:10.3892/ijmm.2013.1425

Zhang, H.-n., Xu, Q.-q., Thakur, A., Alfred, M. O., Chakraborty, M., Ghosh, A., et al. (2018). Endothelial Dysfunction in Diabetes and Hypertension: Role of microRNAs and Long Non-coding RNAs. *Life Sci.* 213, 258–268. doi:10.1016/j.lfs.2018.10.028

Zhang, J.-R., and Sun, H.-J. (2022). Extracellular Vesicle-Mediated Vascular Cell Communications in Hypertension: Mechanism Insights and Therapeutic Potential of ncRNAs. *Cardiovasc. Drugs Ther.* 36, 157–172. doi:10.1007/s10557-020-07080-z

Zhang, J.-R., and Sun, H.-J. (2020). LncRNAs and Circular RNAs as Endothelial Cell Messengers in Hypertension: Mechanism Insights and Therapeutic Potential. *Mol. Biol. Rep.* 47, 5535–5547. doi:10.1007/s11033-020-05601-5

Zhang, J.-R., and Sun, H.-J. (2021). MiRNAs, lncRNAs, and Circular RNAs as Mediators in Hypertension-Related Vascular Smooth Muscle Cell Dysfunction. *Hypertens. Res.* 44, 129–146. doi:10.1038/s41440-020-00553-6

Zhang, M., Li, Y., Xie, H., Chen, J., and Liu, S. (2020). Curcumin Inhibits Proliferation, Migration and Neointimal Formation of Vascular Smooth Muscle via Activating miR-22. *Pharm. Biol.* 58, 610–619. doi:10.1080/13880209.2020.1781904

Zheng, Y., and Xu, Z. (2014). MicroRNA-22 Induces Endothelial Progenitor Cell Senescence by Targeting AKT3. *Cell Physiol Biochem* 34, 1547–1555. doi:10.1159/000366358

Zhou, Y., Zhang, T., Wang, X., Wei, X., Chen, Y., Guo, L., et al. (2015). Curcumin Modulates Macrophage Polarization through the Inhibition of the Toll-like Receptor 4 Expression and its Signaling Pathways. *Cel Physiol Biochem* 36, 631–641. doi:10.1159/000430126

Zhu, X., Zhou, Z., Zhang, Q., Cai, W., Zhou, Y., Sun, H., et al. (2018). Vaccarin Administration Ameliorates Hypertension and Cardiovascular Remodeling in Renovascular Hypertensive Rats. *J. Cel. Biochem.* 119, 926–937. doi:10.1002/jcb.26258

Conflict of Interest: The authors declare that the research was conducted in the absence of any commercial or financial relationships that could be construed as a potential conflict of interest.

Publisher's Note: All claims expressed in this article are solely those of the authors and do not necessarily represent those of their affiliated organizations, or those of the publisher, the editors and the reviewers. Any product that may be evaluated in this article, or claim that may be made by its manufacturer, is not guaranteed or endorsed by the publisher.

Copyright © 2022 Li, Wang, Machuki, Li, Wu, Niu, Yu, Lu and Sun. This is an open-access article distributed under the terms of the Creative Commons Attribution License (CC BY). The use, distribution or reproduction in other forums is permitted, provided the original author(s) and the copyright owner(s) are credited and that the original publication in this journal is cited, in accordance with accepted academic practice. No use, distribution or reproduction is permitted which does not comply with these terms.

frontiers | Frontiers in Physiology

REVIEW
published: 04 April 2022
doi: 10.3389/fphys.2022.858654

Regional Differences in Sympathetic Nerve Activity Are Generated by Multiple Arterial Baroreflex Loops Arranged in Parallel

Kenju Miki, Shizuka Ikegame and Misa Yoshimoto*

Autonomic Physiology Laboratory, Faculty of Life Science and Human Technology, Nara Women's University, Kita-Uoya Nishimachi, Nara, Japan

OPEN ACCESS

Edited by:
Jacqueline Kathleen Phillips, Macquarie University, Australia

Reviewed by:
Patrick J Mueller, Wayne State University School of Medicine, United States
Fiona D McBryde, The University of Auckland, New Zealand

***Correspondence:**
Kenju Miki
k.miki@cc.nara-wu.ac.jp

Specialty section:
This article was submitted to Integrative Physiology, a section of the journal Frontiers in Physiology

Received: *20 January 2022*
Accepted: *15 March 2022*
Published: *04 April 2022*

Citation:
Miki K, Ikegame S and Yoshimoto M (2022) Regional Differences in Sympathetic Nerve Activity Are Generated by Multiple Arterial Baroreflex Loops Arranged in Parallel. Front. Physiol. 13:858654. doi: 10.3389/fphys.2022.858654

In this review, by evaluating the responses during freezing, rapid eye movement (REM) sleep, and treadmill exercise, we discuss how multiple baroreflex loops arranged in parallel act on different organs to modulate sympathetic nerve activity (SNA) in a region-specific and coordinated manner throughout the body. During freezing behaviors, arterial pressure (AP) remains unchanged, heart rate (HR) persistently decreases, renal SNA (RSNA) increases, and lumbar SNA (LSNA) remains unchanged. The baroreflex curve for RSNA shifts upward; that for LSNA remains unchanged; and that for HR shifts to the left. These region-specific changes in baroreflex curves are responsible for the region-specific changes in RSNA, LSNA, and HR during freezing. The decreased HR could allow the heart to conserve energy, which is offset by the increased RSNA caused by decreased vascular conductance, resulting in an unchanged AP. In contrast, the unchanged LSNA leaves the muscles in readiness for fight or flight. During REM sleep, AP increases, RSNA and HR decrease, while LSNA is elevated. The baroreflex curve for RSNA during REM sleep is vertically compressed in comparison with that during non-REM sleep. Cerebral blood flow is elevated while cardiac output is decreased during REM sleep. To address this situation, the brain activates the LSNA selectively, causing muscle vasoconstriction, which overcomes vasodilation of the kidneys as a result of the decreased RSNA and cardiac output. Accordingly, AP can be maintained during REM sleep. During treadmill exercise, AP, HR, and RSNA increase simultaneously. The baroreflex curve for RSNA shifts right-upward with the increased feedback gain, allowing maintenance of a stable AP with significant fluctuations in the vascular conductance of working muscles. Thus, the central nervous system may employ behavior-specific scenarios for modulating baroreflex loops for differential control of SNA, changing the SNA in a region-specific and coordinated manner, and then optimizing circulatory regulation corresponding to different behaviors.

Keywords: sympathetic nerve activity, baroreflex, freezing, REM sleep, exercise

INTRODUCTION

The body is a system of many organs, and each of these organs performs its independent function while coordinating with other organs to achieve an integrated function as a whole body. The parallel arrangement of each organ to the aorta has significant implications: this allows organs to regulate their blood flow independently without being affected by other organs. However, while each organ performs its metabolic activities with its specific organ blood flow, the organs cooperate to maintain an optimal perfusion pressure for organs, namely the arterial pressure (AP), under any change in the physiological states. Sympathetic nerve activity (SNA) plays a primary role in regulating organ blood flow. This review aims to discuss how SNA differently and cooperatively alters the blood flow to each organ and creates the optimal AP for the entire body. In this regard, recent studies have revealed the following three aspects of SNA regulation.

Multiple Arterial Baroreflex Loops Arranged in Parallel

Multiple arterial baroreflex loops are likely arranged in parallel for each organ. Sagawa proposed the theoretical framework for the parallel arrangement of arterial baroreflex loops and their involvement in AP regulation (Sagawa, 2011). However, there has been a lack of direct evidence supporting this hypothesis. Meanwhile, fragmentary evidence has been reported in anesthetized animals that the neuronal nuclei comprising the baroreceptor reflex pathway respond in a regionally different manner to drug administration. This suggests that the baroreflex pathway has discrete routes for distinct organs and that these pathways act on organs individually and in parallel. It is, therefore, reasonable to assume that the arterial baroreflex system has multiple individually discrete loops, which are arranged in parallel in an organ-specific manner. To experimentally examine this hypothesis, we have generated a full range of arterial baroreflex curves in conscious rats under various conditions (Miki et al., 2003; Nagura et al., 2004; Miki and Yoshimoto, 2018; Kondo et al., 2021).

Acute Shifts in Arterial Baroreflex Curves

The acute shifts in the input-output relationship of the baroreflex have been consistently induced by changes in daily behaviors such as sleep, exercise, mental stress (Miki and Yoshimoto, 2005), and pathological conditions such as heart failure (Xing et al., 2014). Input-out data of the arterial baroreflex has generally been fitted to a sigmoid curve to assess the shifts in the baroreflex loop. Kent's sigmoid curve has been widely used for this purpose (Kent et al., 1972). This model is used to quantify the feedback gain of the arterial baroreflex and changes in the maximum capacity of feedback regulation, AP threshold, etc. (Potts et al., 1993; Nagura et al., 2004); the changes in these variables have served as the basis for the discussion of the involvement of the central nervous system (CNS) above the medulla in the shift.

Regional Differences in Sympathetic Nerve Activity

Regional differences in SNA have been observed in many species, including rats, rabbits, sheep, and humans where experiments were carried out either in anesthetized or conscious states (Morrison, 2001; Park et al., 2008; Yoshimoto et al., 2011; Xing et al., 2014; Kondo et al., 2021). While there are many interesting issues to address regarding methods for measuring SNA (Malpas, 2010; Stocker and Muntzel, 2013; Hart et al., 2017), this review will focus primarily on the regional differences in SNA measured simultaneously at multiple sites in the same preparation. To assess regional differences in SNA, simultaneous measurement of the SNA in multiple regions in the same preparation is essential. Considering the difficulty in evaluating the absolute value of SNA, comparisons of changes in SNA by region should be made only when there is a clear difference between SNAs. However, comparing the degree of change in SNAs measured in different animals is challenging. Moreover, anesthesia has a profound effect on SNA (Stock et al., 1978; DeLalio and Stocker, 2021). Suppression of the higher CNS by anesthesia may affect the response of regional differences in SNA. Therefore, simultaneous measurement of SNA at multiple sites in conscious animals may have some advantages in studying the mechanism of regional differences in SNA.

In this review, we are discussing the functional diversity of the RSNA and LSNA, but what we are measuring is the extracellular potential of sympathetic fiber bundles, which also have even more diverse functions. For instance, RSNA is a recording of the extracellular potential of a mixture of the sympathetic fibers; it mediate vasoconstriction, Na^+ reabsorption, and renin release (DiBona and Kopp, 1997). The diverse functions of RNSA and LSNA itself need to be recognized, but this issue is out of the scope of the present review.

Central Scenarios Modulating Baroreflex Loops and Sympathetic Nerve Activity in a Region-specific and Coordinated Manner

To summarize the above three points, the arterial baroreflex has multiple pathways, and these are arranged in parallel to change the SNA in a regionally different manner, creating region-specific changes in the SNA of organs. We have been evaluating the arterial baroreflex by simultaneously and continuously measuring renal SNA (RSNA), lumbar SNA (LSNA), HR, and AP in conscious rats (Miki et al., 2003; Nagura et al., 2004; Kondo et al., 2021). We found that RSNA, LSNA, and HR changed in the same way in some cases, and in other cases, they changed in a region-specific manner. These data indicate that the CNS can modify SNA in an essentially region-specific manner and that these changes are coordinated and strategic in regulating AP. The following three examples, which pertain to freezing, rapid eye movement (REM) sleep, and treadmill exercise, illustrate how the arterial baroreflex loop can alter SNA in a region-specific, coordinated, and strategic manner. These examples highlight sophisticated control scenarios operated through arterial baroreflex loops to optimally regulate AP under different physiological situations.

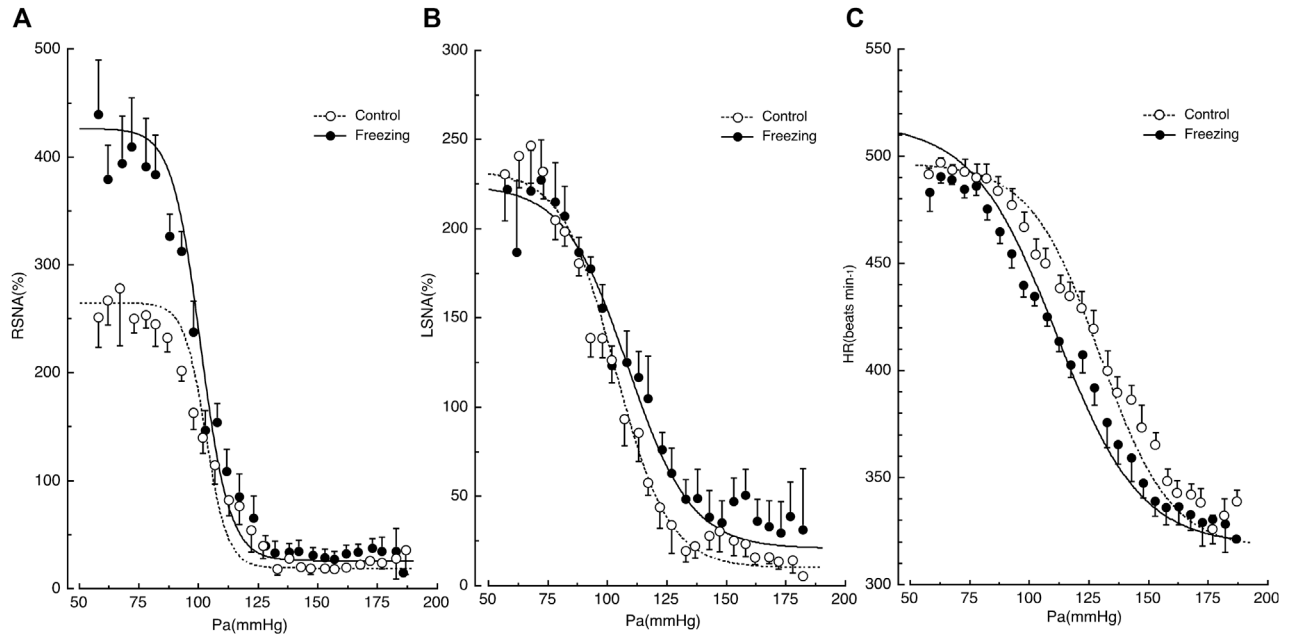

FIGURE 1 | Shifts in the baroreflex curves for renal sympathetic nerve activity (RSNA) in panel **(A)**, lumbar sympathetic nerve activity (LSNA) in panel **(B)**, and heart rate (HR) in panel **(C)** during the control and freezing periods. AP, arterial pressure. Symbols and bars indicate the mean and standard error of mean, respectively. The image was obtained with permission from the study by Kondo et al. (2021).

FREEZING: INNATE STRATEGIES FOR INCREASING THE CHANCE OF SURVIVAL AGAINST THREATS AND POTENTIAL DANGER

The freezing behavior is one of the innate responses of animals and can be classified as a preparatory reflex for threats and potential danger (Dampney, 2015; Kozlowska et al., 2015). When encountering unmanageable stresses, including predators, animals will freeze to conserve energy and create a state of readiness for fight or flight, thereby increasing the probability of survival. In humans, when exposed to unmanageable stresses such as natural disasters, individuals become apathetic and exhibit behaviors like freezing (Hagenaars et al., 2014). During freezing behavior, SNA plays a dominant role in modulating cardiovascular functions strategically to make the entire body ready for fight or flight.

When rats are exposed to loud noise, they exhibit freezing behavior in which the AP remains the same while HR decreases persistently, RSNA increases, and LSNA remains unchanged (Yoshimoto et al., 2010). The baroreflex curves for RSNA, LSNA, and HR are shifted in a region-specific manner during freezing behavior, as shown in **Figure 1** (Kondo et al., 2021). The rats remained still during freezing because they showed no change in muscle activity, which allows us to generate an entire range of baroreflex curves by administrating vasoactive drugs, because without any other disturbance, including spontaneous moving (Kondo et al., 2021). In conscious rats, artificial changes in AP sometimes produce spontaneous movements, which may alter SNA and HR. Therefore, it is not likely that muscle ergoreceptors would cause an increase in RSNA, as seen during exercise (Fisher et al., 2015). Consequently, it is highly possible that the region-specific changes in RSNA, LSNA, HR, and AP observed during freezing behavior are attributable to the survival strategy scenario in the CNS. The different shifts in the baroreflex curves for RSNA, LSNA, and HR are elicited by CNS, including the defense area (Coote et al., 1979; Hilton, 1982; Kozlowska et al., 2015) and the medullary baroreflex pathway (Dampney, 2015).

Region-specific Shifts in Baroreflex Curves

First, the baroreflex curve for RSNA shifted upward with a significant increase of 150% in the upper plateau and with no changes in the lower plateau (Kondo et al., 2021), while RSNA increased significantly during freezing. Thus, the CNS increases the maximal drive of RSNA to the kidney by 1.5-fold during freezing behavior, potentiating the baroreflex ability.

Second, the baroreflex curve for LSNA remained the same in comparison with the control state (Kondo et al., 2021), while LSNA did not change significantly during freezing. This suggests that the SNA drive to the muscle is not altered during freezing behavior over the entire range of AP changes. LSNA shows a negative correlation with muscle blood flow (Miki et al., 2004). Since freezing behavior is a state of readiness for fight or flight, the CNS may encounter a scenario where increased LSNA and suppressed muscle blood flow are not desirable in the same way that the increased RSNA suppressed renal blood flow.

Third, the baroreflex curve for HR shifted leftward during freezing behavior in a parallel manner, with significant reductions in the midpoint and threshold pressure (Kondo et al., 2021). This implies that the HR is set to lower levels across the entire range of AP changes. The reduction in HR offsets the reductions in renal vascular conductance due to the increase in RSNA, resulting in no change in AP during the freeze behavior. Furthermore, the decrease in HR allows myocardial energy to be conserved for the transition from freezing to the fight-or-flight state, when the heart's performance is rapidly activated.

These region-specific changes in baroreflex curves seem to represent a highly sophisticated strategy for survival. The heart conserves energy by decreasing cardiac function, and the resulting reduction in cardiac output is offset by a reduction in vascular conductance due to increased SNA in the kidneys and possibly the visceral system, leaving AP unchanged. Simultaneously, the LSNA remains unchanged, and muscles can be left in a state of readiness to be active at any time.

In summary, the CNS can modulate the baroreflex curves in a region-specific manner, resulting in regionally variable changes in SNA and causing changes in the function of each organ independently, while they are coordinately operated for survival during freezing behavior.

RAPID EYE MOVEMENT SLEEP: A PARADOX OF OPPOSITE DIRECTIONAL CHANGES IN SYMPATHETIC NERVE ACTIVITY

Sleep is classified primarily into non-rapid eye movement (NREM) sleep and REM sleep. During NREM sleep, the RSNA, LSNA, and HR are all decreased, and the AP is low and stable. REM sleep is also known as the autonomic storm period and paradoxical sleep. During REM sleep, AP rises and becomes unstable. RSNA decreases while LSNA increases during REM sleep, thus undergoing opposite changes. SNA and AP regulation during REM is unique and paradoxical compared to that in other physiological states, as shown in **Figure 3** (Nagura et al., 2004; Yoshimoto et al., 2011). The possible reasons why SNA and AP regulation during REM sleep are unique are discussed below.

Vertical Suppression of the Baroreflex Curve for Renal Sympathetic Nerve Activity During Rapid Eye Movement Sleep

We reported that AP increased by 5 mmHg, and RSNA decreased by 45% during REM sleep (Nagura et al., 2004). While this might imply that the reduction in RSNA was caused by simple baroreflex, the reduction is more likely attributable to the change in the baroreflex curve for RSNA, which is vertically suppressed during REM sleep in comparison with NREM sleep. Vertical compression is characterized by a significant decrease in the maximum level (upper plateau) and maximum gain (Nagura et al., 2004). This shift in the baroreflex curve causes a reduction in RSNA even though the AP does not change. A similar shift in the baroreflex curve for RSNA has been observed after treadmill exercise when the RSNA decreases by 25% even with no change in AP (Miki et al., 2003). Thus, the CNS actively reduces RSNA during REM sleep, thereby increasing the vascular conductance of the kidneys (Yoshimoto et al., 2004).

In contrast to the reduction in RSNA, LSNA increased significantly in a stepwise manner during REM sleep, as shown in **Figure 2**. Unfortunately, the changes in the baroreflex curve for LSNA have not been reported yet. Since LSNA increased in a sustained manner during REM sleep, we may speculate that the baroreflex curve for LSNA somehow likely shifted rightward. Muscle atonia occurs during REM sleep, thereby reducing the vascular conductance of muscles throughout the body. Moreover, the increased LSNA, which mainly innervates the muscles of the lower extremities, decreases the vascular conductance of the muscles of the lower extremities.

Physiological Contexts for the Reversed Sympathetic Nerve Activity Changes Occurring in Rapid Eye Movement Sleep

It is interesting to speculate why RSNA and LSNA change in opposite directions during REM sleep and why the vascular conductance of the organs they also innervate changes in different directions. REM sleep is a unique state in which brain activity increases to the level of awake states. The brain absorbs a large amount of the cardiac output; total cerebral blood flow at rest is 15–20% of total cardiac output in humans (Folino, 2006). To meet the increased metabolic demand of the brain during REM sleep, blood flow to the brain must increase. Besides the increase in brain blood flow, blood flow to the kidneys and splanchnic organs is also increased (Miki et al., 2004). Paradoxically, it is important to note that cardiac performance was the lowest during REM sleep (Miller and Horvath, 1976). The cardiac output changes with muscle activity but does not change in parallel with that of the brain. However, the brain can control SNA and the baroreflex curves. The brain activates muscle SNA selectively, causing vasoconstriction of the muscle, which is the largest organ in the body. This, in turn, overcomes the vasodilatation of the kidneys, splanchnic organs, and brain, as well as the reduction in cardiac output, such that AP can be maintained during REM sleep.

EXERCISE: SIMULTANEOUS INCREASES IN SYMPATHETIC NERVE ACTIVITY

Exercise involves muscle contraction, which causes muscle metabolism and requires increased muscle blood flow (Rowell, 1986). Meeting the muscle blood flow requirements to increase the metabolic rate is crucial for the performance of the exercise. SNA plays an essential role in adjusting muscle blood flow during exercise. The exercise-induced increase in SNA acts on the capacitance vessels, myocardial contractility, and cardiac pacemaker, increasing cardiac output to increase to nearly five times the resting level. In addition, increased SNA causes vasoconstriction of resistance vessels in inactive muscles and visceral organs, compensating for the increase in vascular

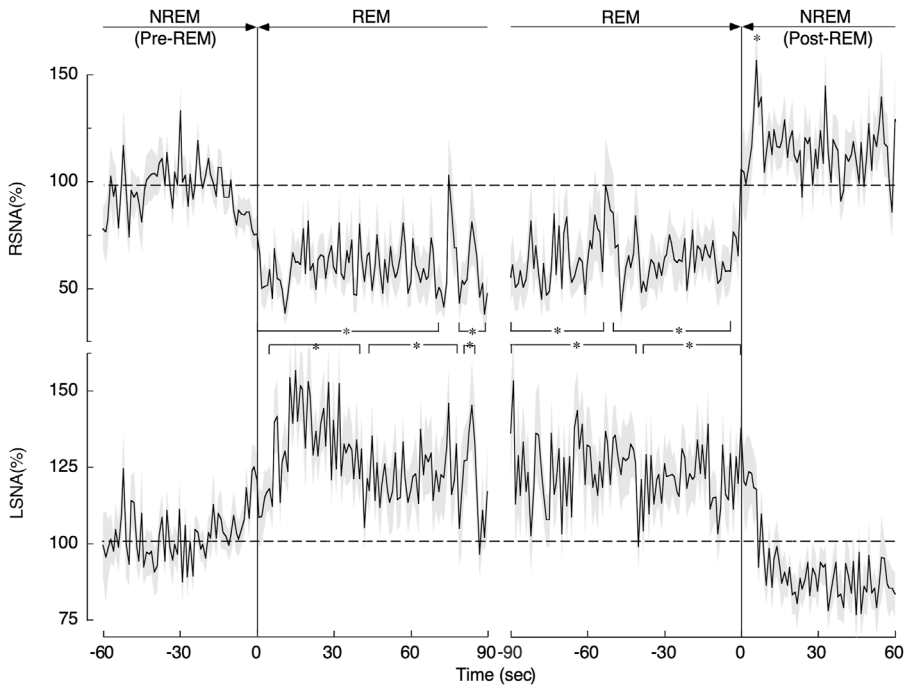

FIGURE 2 | Changes in renal sympathetic nerve activity (RSNA) and lumbar sympathetic nerve activity (LSNA) during the transition from non-rapid eye movement (NREM) sleep (pre-REM) to REM sleep and from the REM sleep to NREM (post-REM) sleep periods. Continuous drawn lines represent mean values and shaded areas above and below show the standard error of mean. *$p < 0.05$ indicates a significant difference from the average level obtained during the pre-REM period. The image was obtained with permission from the study by Yoshimoto et al. (2011).

conductance caused by muscle contraction. As a result, AP increases during exercise. Maintenance of high AP during exercise is vital to ensure stable muscle blood flow when large-volume muscles contract and vasodilation occurs. Furthermore, a striking variation in central venous pressure has been observed during dynamic exercise due to the mechanical effect of the muscle pump (Rowell, 1986). Since this leads to fluctuations in cardiac output, maintaining an adequately high AP is crucial to keep muscle blood flow during exercise.

SNA is believed to increase throughout the body during exercise. **Figure 3** shows the relationship between RSNA and LSNA with increasing exercise intensity in daily activity (Yoshimoto et al., 2011). The RSNA and LSNA increase linearly from NREM sleep to the grooming state, except during REM sleep. In humans, muscle SNA is slightly suppressed by light exercise but increases linearly with exercise intensity (Saito et al., 1993). There is substantial evidence for intensity and duration-dependent increases in muscle SNA to both the active and inactive limbs during isometric and dynamic exercise in humans (Fisher et al., 2015). SNA is likely to increase in most organs in proportion to the magnitude of the increase in muscle activity.

Exercise Shifts the Baroreflex Curve for Renal Sympathetic Nerve Activity Upward to the Right Compared to the Resting State

Figure 4 shows the shifts in the baroreflex curve for RSNA before, during, after the treadmill exercise (about 70% VO_2Max) in rats (Miki et al., 2003). Full-range baroreflex curves were generated by intravenously administering phenylephrine and nitroprusside. This right-upward shift in the baroreflex curve for RSNA allows AP and RSNA to increase simultaneously during exercise and increases the feedback gain to enhance the ability to suppress AP fluctuations. The shifts in the baroreflex curve for RSNA can be characterized into three parts: 1) an increase in central AP (rightward shift), 2) an increase in the minimum response level (upward shift), and 3) an increase in the feedback gain caused by the increase in response range of RSNA. For the mechanism underlying the shift in the baroreflex curve, please refer to the excellent review by Dampney (Dampney, 2017). Here, the significance of these three points in the regulation of circulation during exercise is addressed.

First, the rightward shift of the baroreflex curve for RSNA is indicated by an increase in the central blood pressure of the curve. The proximity of the prevailing AP during exercise to the central pressure is of significance. Thus, the AP during exercise is near the highest value of the feedback gain, providing the output of SNA at a high gain. In addition, it can respond to SNA in the same way even if it decreases or increases from the mean AP value.

Second, the upward shift of the baroreflex curve for RSNA is attributed to a significant increase in the minimum response level of SNA. At rest, when the AP rises, SNA is suppressed and reaches almost the zero level, and the contractile effect of SNA on peripheral blood vessels ceases. However, during exercise, even if the AP rises to a high level, SNA maintains a certain level of activity and can continuously maintain vasoconstriction of

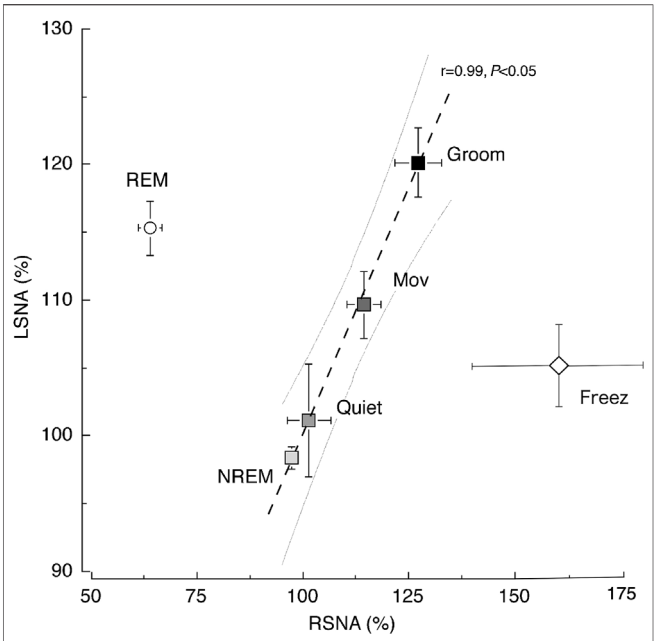

FIGURE 3 | Relationship between renal sympathetic nerve activity (RSNA) and lumbar sympathetic nerve activity (LSNA) across the behavioral states. A significant ($p < 0.05$) linear relationship was observed between RSNA and LSNA ($y = 0.72x + 27.76$) in the non-rapid eye movement (NREM) sleep, quiet awake (Quiet), moving (Mov), and grooming (Groom) states. The relationship between RSNA and LSNA during the REM sleep and freezing period (Freez) was dissociated from the line obtained during other behavioral states. Values are shown as the mean ± standard error of the mean. The gray curved lines are the 95% confidence bands for the regression line. The image was obtained with permission from the studies by Yoshimoto et al. (2010; 2011).

peripheral organs. This minimal level of SNA causes the resistance vessels of inactive muscles and internal organs throughout the body to constrict, thereby supporting increased blood flow to the active muscles.

Third, the feedback gain is the first derivative of the baroreflex curve and shows its maximum value at the central blood pressure value of the sigmoid curve. The gain curve of RSNA shifts to the right (hypertensive side) during treadmill exercise in rats, and the peak value increases by 2-fold (Miki et al., 2003). Thus, the degree of response of SNA is higher for the same AP variation, indicating that changes in SNA increase the ability to suppress AP fluctuations through feedback regulation, allowing for stable AP control during exercise.

By contrast, exercise shifts the baroreflex curve for HR as well (Ogoh et al., 2005; Raven et al., 2006), which is different from the shift of the baroreflex curve for SNA as described above. This difference may be due to regional differences in cardiac SNA, involvement of cardiac vagal nerve activity, and maximum heart rate. In particular, the changes in cardiac vagal activity during exercise have not been measured and are not known at present (Gourine and Ackland, 2019). Shifts in the baroreflex curve for HR and variability of HR are sometimes used for estimating changes in SNA (Monahan, 2007; Billman, 2013; Marmerstein et al., 2021). However, the baroreflex curves for HR and SNA are fundamentally different reflex loops, thus caution should be taken when making such extrapolations.

In summary, SNA increases uniformly throughout the body during exercise. The baroreflex curve for RSNA shifts right-upward, and a similar shift is thought to occur in the other SNA baroreflex curves. As a result, AP and SNA increase simultaneously during exercise. Besides, exercise increases the feedback gain, making it possible to maintain stable AP with a significant fluctuation in the vascular conductance of working muscles.

SUMMARY AND PERSPECTIVE

SNA shows regional differences in response to behavior and external stress, and these differences are accompanied by region-specific and behavior-specific shifts in the baroreflex curves for SNA. This review attempted to elucidate the reasons underlying the region-specific shifts in arterial baroreflex loops and their implications, focusing on three examples: freezing, REM sleep, and treadmill exercise. The shifts in the arterial baroreflex loop are highly plausible from the viewpoint of integrating AP regulation. Notably, the baroreflex loop acts independently and in parallel on each organ. These parallel arterial baroreflex loops account for regional differences in SNA. The CNS above the medulla can modulate each parallel baroreflex curve separately, producing context-specific changes in SNA: to prepare for battle against an inexorable enemy and increase the chances of survival

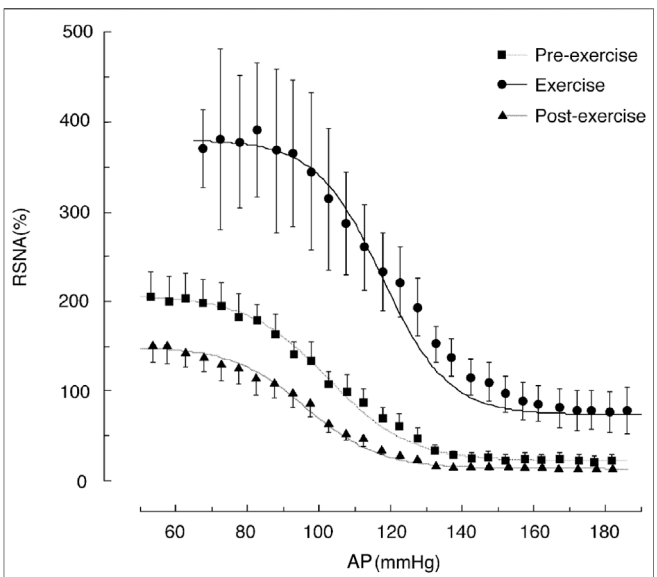

FIGURE 4 | Shifts in the baroreflex curves for renal sympathetic nerve activity (RSNA) during the pre-exercise, treadmill exercise, and post-exercise periods. The average oxygen consumption during treadmill exercise at a speed of 20 m/min with a 0% gradient performed in this study was 51 ml/min/kg, which was approximately 70% of the maximum oxygen consumption. The curves and bars indicate the mean and standard error of the mean, respectively, estimated over each 2.5-mmHg bin of arterial pressure (AP). The image was obtained with permission from the study by Miki et al. (2003).

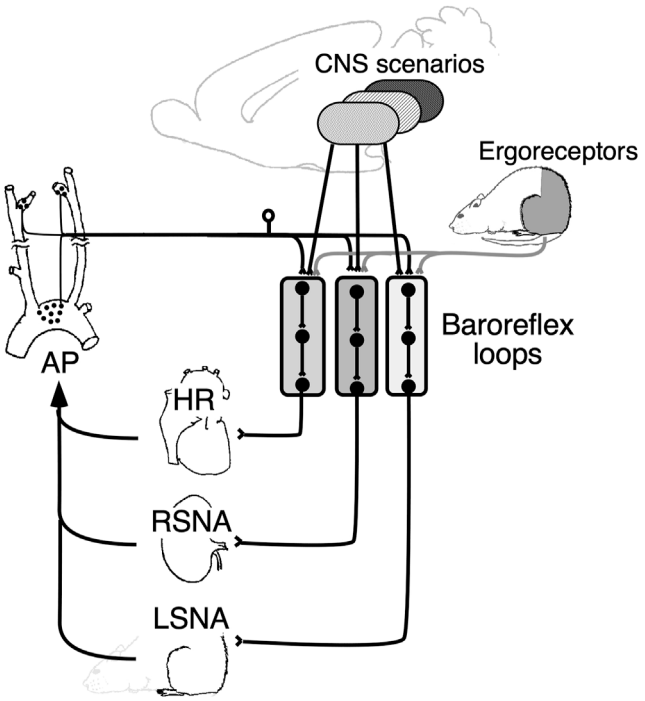

FIGURE 5 | Schematic diagram showing the role of parallel baroreflex loops in regulating sympathetic nerve activity and, thereby, arterial pressure (AP). Parallel baroreflex loops regulate heart rate (HR), renal sympathetic nerve activity (RSNA), and lumbar sympathetic nerve activity (LSNA) separately to generate region-specific changes in the SNA. Each arterial baroreflex loop receives similar stimulus information from the muscle ergoreceptors, but it receives separate and integrated information from the CNS above the medulla to optimize AP as a whole body.

during the freeze; to maintain cerebral blood flow during REM; and to maintain stable muscle blood flow during exercise. The CNS above the medulla is exposed to a number of scenarios that would change the baroreflex curve in a region-specific manner, and clarification of scenarios in contexts other than those discussed here is awaited.

Figure 5 shows a conceptual diagram of a multiple parallel arterial baroreflex loop. This view is consistent with previous studies conducted under anesthesia, showing discrete conduits within the central arterial baroreflex pathway, including the nucleus tractus solitarius (Polson et al., 2007; Scislo et al., 2008), caudal ventrolateral medulla (Miyawaki et al., 1997), and rostral ventrolateral medulla (McAllen and May 1994; Mueller et al., 2011; Farmer et al., 2019). Exactly how these nuclei relate to each other to cause region-specific changes in SNA, or whether they dynamically alter their networks, is of great interest and remains to be studied.

The blood supply of the individual organs is regulated by a balance between the local independent regulatory system, including autoregulation, and the central scenario that determines the optimal distribution of organ blood flow adapting to various physiological states. Multilayered redundancy of regulatory systems may work for keeping optimal organ blood flow adapting to various physiological states. The baroreflex is one of the control systems of central nervous system origin and is one of the components constituting a multilayered and redundant control system. In this review, we discussed shifts in the baroreflex curve in normal conditions, but the shifts may also occur in cardiovascular diseases and, in some cases, may not function properly. Further studies are needed to elucidate the details of the dysfunctional baroreflex curves for SNA and how it interacts with other regulatory systems, including the local autoregulation system in cardiovascular diseases.

AUTHOR CONTRIBUTIONS

KM, SI, and MY contributed to drafting, revising the manuscript, and approving the final version.

FUNDING

This work was supported in part by JST (Moonshot R&D) (Grant Number JPMJMS 2023).

ACKNOWLEDGMENTS

We would like to thank Editage (www.editage.com) for English language editing.

REFERENCES

Billman, G. E. (2013). The LF/HF Ratio Does Not Accurately Measure Cardiac Sympatho-Vagal Balance. *Front. Physio.* 4, 26. doi:10.3389/fphys.2013.00026

Coote, J. H., Hilton, S. M., and Perez-Gonzalez, J. F. (1979). Inhibition of the Baroreceptor Reflex on Stimulation in the Brain Stem Defence centre. *J. Physiol.* 288, 549–560.

Dampney, R. A. L. (2015). Central Mechanisms Regulating Coordinated Cardiovascular and Respiratory Function during Stress and Arousal. *Am. J. Physiology-Regulatory, Integr. Comp. Physiol.* 309, R429–R443. doi:10.1152/ajpregu.00051.2015

Dampney, R. A. L. (2017). Resetting of the Baroreflex Control of Sympathetic Vasomotor Activity during Natural Behaviors: Description and Conceptual Model of Central Mechanisms. *Front. Neurosci.* 11, 461. doi:10.3389/fnins.2017.00461

DeLalio, L. J., and Stocker, S. D. (2021). Impact of Anesthesia and Sex on Sympathetic Efferent and Hemodynamic Responses to Renal Chemo- and Mechanosensitive Stimuli. *J. Neurophysiol.* 126, 668–679. doi:10.1152/jn.00277.2021

DiBona, G. F., and Kopp, U. C. (1997). Neural Control of Renal Function. *Physiol. Rev.* 77, 75–197. doi:10.1152/physrev.1997.77.1.75

Farmer, D. G. S., Pracejus, N., Dempsey, B., Turner, A., Bokiniec, P., Paton, J. F. R., et al. (2019). On the Presence and Functional Significance of Sympathetic Premotor Neurons with Collateralized Spinal Axons in the Rat. *J. Physiol.* 597, 3407–3423. doi:10.1113/JP277661

Fisher, J. P., Young, C. N., and Fadel, P. J. (2015). Autonomic Adjustments to Exercise in Humans. *Compr. Physiol.* 5, 475–512. doi:10.1002/cphy.c140022

Folino, A. F. (2006). Cerebral Autoregulation in Neurally Mediated Syncope: Victim or Executioner? *Heart* 92, 724–726. doi:10.1136/hrt.2005.069179

Gourine, A. V., and Ackland, G. L. (2019). Cardiac Vagus and Exercise. *Physiology* 34, 71–80. doi:10.1152/physiol.00041.2018

Hagenaars, M. A., Roelofs, K., and Stins, J. F. (2014). Human Freezing in Response to Affective Films. *Anxiety, Stress, & Coping* 27, 27–37. doi:10.1080/10615806.2013.809420

Hart, E. C., Head, G. A., Carter, J. R., Wallin, B. G., May, C. N., Hamza, S. M., et al. (2017). Recording Sympathetic Nerve Activity in Conscious Humans and Other Mammals: Guidelines and the Road to Standardization. *Am. J. Physiol. Heart Circ. Physiol.* 312, H1031–H1051. doi:10.1152/ajpheart.00703.2016

Hilton, S. M. (1982). The Defence-Arousal System and its Relevance for Circulatory and Respiratory Control. *J. Exp. Biol.* 100, 159–174. doi:10.1242/jeb.100.1.159

Kent, B. B., Drane, J. W., Blumenstein, B., and Manning, J. W. (1972). A Mathematical Model to Assess Changes in the Baroreceptor Reflex. *Cardiology* 57, 295–310. doi:10.1159/000169528

Kondo, N., Yoshimoto, M., Ikegame, S., and Miki, K. (2021). Differential Shifts in Baroreflex Control of Renal and Lumbar Sympathetic Nerve Activity Induced by Freezing Behaviour in Rats. *Exp. Physiol.* 106, 2060–2069. doi:10.1113/EP089742

Kozlowska, K., Walker, P., McLean, L., and Carrive, P. (2015). Fear and the Defense Cascade: Clinical Implications and Management. *Harv. Rev. Psychiatry* 23, 263–287. doi:10.1097/HRP.0000000000000065

Malpas, S. C. (2010). Sympathetic Nervous System Overactivity and its Role in the Development of Cardiovascular Disease. *Physiol. Rev.* 90, 513–557. doi:10.1152/physrev.00007.2009

Marmerstein, J. T., McCallum, G. A., and Durand, D. M. (2021). Direct Measurement of Vagal Tone in Rats Does Not Show Correlation to HRV. *Sci. Rep.* 11, 1210. doi:10.1038/s41598-020-79808-8

McAllen, R. M., and May, C. N. (1994). Differential Drives from Rostral Ventrolateral Medullary Neurons to Three Identified Sympathetic Outflows. *Am. J. Physiol.* 267, R935–R944. doi:10.1152/ajpregu.1994.267.4.R935

Miki, K., Oda, M., Kamijyo, N., Kawahara, K., and Yoshimoto, M. (2004). Lumbar Sympathetic Nerve Activity and Hindquarter Blood Flow during REM Sleep in Rats. *J. Physiol.* 557, 261–271. doi:10.1113/jphysiol.2003.055525

Miki, K., and Yoshimoto, M. (2005). Differential Effects of Behaviour on Sympathetic Outflow during Sleep and Exercise. *Exp. Physiol.* 90, 155–158. doi:10.1113/expphysiol.2004.029033

Miki, K., and Yoshimoto, M. (2018). Exercise-Induced Modulation of Baroreflex Control of Sympathetic Nerve Activity. *Front. Neurosci.* 12, 493. doi:10.3389/fnins.2018.00493

Miki, K., Yoshimoto, M., and Tanimizu, M. (2003). Acute Shifts of Baroreflex Control of Renal Sympathetic Nerve Activity Induced by Treadmill Exercise in Rats. *J. Physiol.* 548, 313–322. doi:10.1113/jphysiol.2002.033050

Miller, J. C., and Horvath, S. M. (1976). Cardiac Output during Human Sleep. *Aviat Space Environ. Med.* 47, 1046–1051.

Miyawaki, T., Suzuki, S., Minson, J., Arnolda, L., Chalmers, J., Llewellyn-Smith, I., et al. (1997). Role of AMPA/kainate Receptors in Transmission of the Sympathetic Baroreflex in Rat CVLM. *Am. J. Physiol.* 272, R800–R812. doi:10.1152/ajpregu.1997.272.3.R800

Monahan, K. D. (2007). Effect of Aging on Baroreflex Function in Humans. *Am. J. Physiol. Regul. Integr. Comp. Physiol.* 293, R3–R12. doi:10.1152/ajpregu.00031.2007

Morrison, S. F. (2001). Differential Control of Sympathetic Outflow. *Am. J. Physiol. Regul. Integr. Comp. Physiol.* 281, R683–R698. doi:10.1152/ajpregu.2001.281.3.R683

Mueller, P. J., Mischel, N. A., and Scislo, T. J. (2011). Differential Activation of Adrenal, Renal, and Lumbar Sympathetic Nerves Following Stimulation of the Rostral Ventrolateral Medulla of the Rat. *Am. J. Physiol. Regul. Integr. Comp. Physiol.* 300, R1230–R1240. doi:10.1152/ajpregu.00713.2010

Nagura, S., Sakagami, T., Kakiichi, A., Yoshimoto, M., and Miki, K. (2004). Acute Shifts in Baroreflex Control of Renal Sympathetic Nerve Activity Induced by REM Sleep and Grooming in Rats. *J. Physiol.* 558, 975–983. doi:10.1113/jphysiol.2004.064527

Ogoh, S., Fisher, J. P., Dawson, E. A., White, M. J., Secher, N. H., and Raven, P. B. (2005). Autonomic Nervous System Influence on Arterial Baroreflex Control of Heart Rate during Exercise in Humans. *J. Physiol.* 566, 599–611. doi:10.1113/jphysiol.2005.084541

Park, J., Campese, V. M., Nobakht, N., and Middlekauff, H. R. (2008). Differential Distribution of Muscle and Skin Sympathetic Nerve Activity in Patients with End-Stage Renal Disease. *J. Appl. Physiol.* 105, 1873–1876. doi:10.1152/japplphysiol.90849.2008

Polson, J. W., Dampney, R. A., Boscan, P., Pickering, A. E., and Paton, J. F. (2007). Differential Baroreflex Control of Sympathetic Drive by Angiotensin II in the Nucleus Tractus Solitarii. *Am. J. Physiol. Regul. Integr. Comp. Physiol.* 293, R1954–R1960. doi:10.1152/ajpregu.00041.2007

Potts, J. T., Shi, X. R., and Raven, P. B. (1993). Carotid Baroreflex Responsiveness during Dynamic Exercise in Humans. *Am. J. Physiol.* 265, H1928–H1938. doi:10.1152/ajpheart.1993.265.6.H1928

Raven, P. B., Fadel, P. J., and Ogoh, S. (2006). Arterial Baroreflex Resetting during Exercise: a Current Perspective. *Exp. Physiol.* 91, 37–49. doi:10.1113/expphysiol.2005.032250

Rowell, L. B. (1986). *Human Circulation Regulation during Physical Stress*. New York: Oxford University Press.

Sagawa, K. (2011). Baroreflex Control of Systemic Arterial Pressure and Vascular Bed. *Compr. Physiol.* 1, 453–496. doi:10.1002/cphy.cp020314

Saito, M., Tsukanaka, A., Yanagihara, D., and Mano, T. (1993). Muscle Sympathetic Nerve Responses to Graded Leg Cycling. *J. Appl. Physiol.* 75, 663–667. doi:10.1152/jappl.1993.75.2.663

Scislo, T. J., Ichinose, T. K., and O'Leary, D. S. (2008). Stimulation of NTS A1 Adenosine Receptors Differentially Resets Baroreflex Control of Regional Sympathetic Outputs. *Am. J. Physiol. Heart Circ. Physiol.* 294, H172–H182. doi:10.1152/ajpheart.01099.2007

Stock, G., Schlor, K. H., Heidt, H., and Buss, J. (1978). Psychomotor Behaviour and Cardiovascular Patterns during Stimulation of the Amygdala. *Pflugers Arch.* 376, 177–184. doi:10.1007/bf00581581

Stocker, S. D., and Muntzel, M. S. (2013). Recording Sympathetic Nerve Activity Chronically in Rats: Surgery Techniques, Assessment of Nerve Activity, and Quantification. *Am. J. Physiol. Heart Circ. Physiol.* 305, H1407–H1416. doi:10.1152/ajpheart.00173.2013

Xing, D. T., May, C. N., Booth, L. C., and Ramchandra, R. (2014). Tonic Arterial Chemoreceptor Activity Contributes to Cardiac Sympathetic Activation in Mild Ovine Heart Failure. *Exp. Physiol.* 99, 1031–1041. doi:10.1113/expphysiol.2014.079491

Yoshimoto, M., Nagata, K., and Miki, K. (2010). Differential Control of Renal and Lumbar Sympathetic Nerve Activity during Freezing Behavior in Conscious Rats. *Am. J. Physiol. Regul. Integr. Comp. Physiol.* 299, R1114–R1120. doi:10.1152/ajpregu.00831.2009

Yoshimoto, M., Sakagami, T., Nagura, S., and Miki, K. (2004). Relationship between Renal Sympathetic Nerve Activity and Renal Blood Flow during Natural Behavior in Rats. *Am. J. Physiol. Regul. Integr. Comp. Physiol.* 286, R881–R887. doi:10.1152/ajpregu.00105.2002

Yoshimoto, M., Yoshida, I., and Miki, K. (2011). Functional Role of Diverse Changes in Sympathetic Nerve Activity in Regulating Arterial Pressure during REM Sleep. *Sleep* 34, 1093–1101. doi:10.5665/SLEEP.1168

Conflict of Interest: The authors declare that the research was conducted in the absence of any commercial or financial relationships that could be construed as a potential conflict of interest.

Publisher's Note: All claims expressed in this article are solely those of the authors and do not necessarily represent those of their affiliated organizations, or those of the publisher, the editors and the reviewers. Any product that may be evaluated in this article, or claim that may be made by its manufacturer, is not guaranteed or endorsed by the publisher.

Copyright © 2022 Miki, Ikegame and Yoshimoto. This is an open-access article distributed under the terms of the Creative Commons Attribution License (CC BY). The use, distribution or reproduction in other forums is permitted, provided the original author(s) and the copyright owner(s) are credited and that the original publication in this journal is cited, in accordance with accepted academic practice. No use, distribution or reproduction is permitted which does not comply with these terms.

frontiers | Frontiers in Physiology

SYSTEMATIC REVIEW
published: 11 April 2022
doi: 10.3389/fphys.2022.888324

Gut Microbial Community and Host Thermoregulation in Small Mammals

Xue-Ying Zhang[1] *and De-Hua Wang*[1,2,3]*

[1]State Key Laboratory of Integrated Management of Pest Insects and Rodents, Institute of Zoology, Chinese Academy of Sciences, Beijing, China, [2]School of Life Sciences, Shandong University, Qingdao, China, [3]CAS Center for Excellence in Biotic Interactions, University of Chinese Academy of Sciences, Beijing, China

The endotherms, particularly the small mammals living in the polar region and temperate zone, are faced with extreme challenges for maintaining stable core body temperatures in harsh cold winter. The non-hibernating small mammals increase metabolic rate including obligatory thermogenesis (basal/resting metabolic rate, BMR/RMR) and regulatory thermogenesis (mainly nonshivering thermogenesis, NST, in brown adipose tissue and skeletal muscle) to maintain thermal homeostasis in cold conditions. A substantial amount of evidence indicates that the symbiotic gut microbiota are sensitive to air temperature, and play an important function in cold-induced thermoregulation, via bacterial metabolites and byproducts such as short-chain fatty acids and secondary bile acids. Cold signal is sensed by specific thermosensitive transient receptor potential channels (thermo-TRPs), and then norepinephrine (NE) is released from sympathetic nervous system (SNS) and thyroid hormones also increase to induce NST. Meanwhile, these neurotransmitters and hormones can regulate the diversity and compositions of the gut microbiota. Therefore, cold-induced NST is controlled by both Thermo-TRPs—SNS—gut microbiota axis and thyroid—gut microbiota axis. Besides physiological thermoregulation, small mammals also rely on behavioral regulation, such as huddling and coprophagy, to maintain energy and thermal homeostasis, and the gut microbial community is involved in these processes. The present review summarized the recent progress in the gut microbiota and host physiological and behavioral thermoregulation in small mammals for better understanding the evolution and adaption of holobionts (host and symbiotic microorganism). The coevolution of host-microorganism symbionts promotes individual survival, population maintenance, and species coexistence in the ecosystems with complicated, variable environments.

Keywords: gut microbiota, norepinephrine (NE), small mammals, thermoregulation, thyroid hormones

OPEN ACCESS

Edited by:
Geoffrey A. Head, Baker Heart and Diabetes Institute, Australia

Reviewed by:
Naresh Chandra Bal, KIIT University, India
Christopher J. Madden, Oregon Health and Science University, United States

***Correspondence:**
De-Hua Wang
dehuawang@sdu.edu.cn

Specialty section:
This article was submitted to Integrative Physiology, a section of the journal Frontiers in Physiology

Received: *02 March 2022*
Accepted: *28 March 2022*
Published: *11 April 2022*

Citation:
Zhang X-Y and Wang D-H (2022) Gut Microbial Community and Host Thermoregulation in Small Mammals. Front. Physiol. 13:888324. doi: 10.3389/fphys.2022.888324

INTRODUCTION

The endotherms regulate thermogenesis and/or heat dissipation to maintain relatively high, stable core body temperatures (T_b, around 37°C in many species) in the fluctuating environments. Small mammals living in the polar region and temperate zone, due to with high ratios of body surface area to volume, are faced with extreme challenges in harsh winter with the characteristics of low temperatures and food shortage. During evolution, these mammals have developed multiple strategies, by adjusting morphological, physiological, and behavioral phenotypes, to adapt to variable environments, especially fluctuations of air temperatures (T_a). A crucial physiological

strategy for small mammals to cope with T_a fluctuations is changing metabolic rate for survival during seasonal acclimatization.

Some mammalian species are able to decrease metabolic rate and T_b, and enter torpor (such as *Phodopus sungorus* and *P. rovorovskii*) or hibernation (such as *Spermophilus dauricus*) to save energy and survive in winter (McNab, 2002; Chi et al., 2016; Ren et al., 2022). However, the non-hibernating small mammals (e.g., *Lasiopodomys brandtii* and *Meriones unguiculatus*) must increase metabolic rate including obligatory thermogenesis (basal/resting metabolic rate, BMR/RMR, with a difference of fasting for the former and no fasting for the latter before measurement) in the liver and other metabolic organs, and regulatory thermogenesis (mainly nonshivering thermogenesis, NST) in brown adipose tissue (BAT) and skeletal muscle to maintain thermal homeostasis in winter or during cold acclimation (Cannon and Nedergaard, 2004; Zhang and Wang, 2006; Nowack et al., 2017; Bal et al., 2018). Both the sympathetic nervous system (SNS) and thyroid hormones are required for regulating thermogenesis and T_b (Cannon and Nedergaard, 2004; Mullur et al., 2014). These non-hibernating mammals need consume more food to compensate for the high energy expenditure due to cold-induced thermogenesis (Zhang and Wang, 2006). In fact, food resource is not available all the time and is even of severe shortage in wild winter. Therefore, these small mammals have also evolved behavioral strategies, for example huddling and coprophagy, to decrease energy expenditure and increase energy harvest.

In addition to the physiological and behavioral strategies of the rodents themselves, a myriad of evidence indicates that the complex communities of symbiotic microorganisms residing in the gastrointestinal tract of animals can largely affect host phenotypes and fitness, such as energy metabolism, thermogenesis, immune function, endocrine activity and neuronal functions (Fetissov, 2017; Rastelli et al., 2019). This microbial community is specific to each host individual in spite of the existence of multiple bacterial taxa shared by the majority of hosts. The gut microbiota can degrade dietary fiber (nondigestible carbohydrates) into short-chain fatty acids (SCFAs, mainly acetate, propionate, and butyrate) and vitamins, and also contribute to metabolizing primary bile acids into secondary bile acids (SBAs) by enhancing deconjugation, dehydrogenation, and dehydroxylation via bacterial enzymes (Ridlon et al., 2006; Rastelli et al., 2019). It is verified that both SCFAs and SBAs are involved in stimulating gut hormone secretion and regulating appetite and thermogenesis. These metabolites and byproducts of microbiota can also directly interact with the enteric nervous system (ENS) and provide a link between the gut microbiota and host physiology and behavior (Worthmann et al., 2017). The experiments of gut microbiota transplant revealed that alteration in the gut microbiota induced variations in host phenotypes, further suggesting that the specific gut microbes are of importance for host fitness (Gould et al., 2018). Moreover, microbial communities codiversified with their host species, implying coevolution between the gut microbiota and their hosts (Ley et al., 2008; Groussin et al., 2017). Therefore, the evolution theory of host-microorganism symbioses assumes that microbial colonization in the mammalian intestinal tracts should be an evolution-driven process benefiting fitness of both sides. In this review, we summarize recent evidence about the physiological and behavioral strategies for maintaining T_b in response to changing T_a and the functions of the gut microbiota in host thermoregulation in small mammals for better understanding the evolution and adaption of holobionts.

Environmental Cues and Nonshivering Thermogenesis

Environmental cues play crucial roles in affecting animal's physiological and behavioral plasticity. Among these cues, T_a, due to its seasonal, daily and sometimes irregular fluctuations, is remarkable in affecting thermogenesis, energy balance and survival in small mammals living in the arctic and temperate regions. Small mammals change metabolic rate in response to T_a fluctuations. The metabolic rate, measured in the resting, awake, and postabsorptive state and named as the BMR, is kept at a constant, minimal level within a specific temperature range, which is defined as the thermoneutral zone (TNZ) (Gordon, 2012). The idea of a thermoneutral "zone" has been questioned and a thermoneutral point (TNP) was proposed, blow which metabolic rates increase and above which T_b increases based on studies in mice (Škop et al., 2020). In wide rodents such as Mongolian gerbils, there is a temperature range within which both RMR and T_b were kept relatively stable (Pan et al., 2014; Zhang et al., 2016; Ding et al., 2018). Energy expenditure (oxygen consumption) increases, due to cold-induced thermogenesis at T_a below the TNZ, and due to a Q10 effect (Mikane et al., 1999) or cooling mechanisms related with water balance and osmotic regulation at T_a above the TNZ (Kasza et al., 2019). Since thermal constraints across geographic gradients, each mammal species has formed species-specific TNZ, which may reflect the differences in the thermal biology among species (Bozinovic et al., 2014).

In eutherian mammals, BAT, has evolved as a specialized thermogenic organ and confers mammals an evolutionary consequence to survive the cold stress (Oelkrug et al., 2015). BAT depots are predominantly located in the intrascapular, dorso-cervical, subscapular and axillary regions, and sporadically in the pericardial and perirenal regions in rodents (Smith and Roberts, 1964; Symonds et al., 2015). The adipocytes in BAT contain dense mitochondria for high oxidative capacity and energy production, and dense vascularization helpful to transport nutrient and heat, as well as multilocular fat droplets to be mobilized into free fatty acids as fuel rapidly (Cannon and Nedergaard, 2004). Cold-induced BAT thermogenesis is mediated through stimulation of β3-adrenergic receptors (β3-AR)-dependent protein kinase A (PKA) signaling and activation of uncoupling protein 1 (UCP1). UCP1 is almost exclusively located in the inner mitochondrial membrane of brown adipocytes, and plays the function of uncoupling the proton motive force from ATP production and dissipating the electrochemical energy as heat (Cannon and Nedergaard, 2004). It was observed that BAT mass, mitochondrial protein content, cytochrome c oxidase (COX) activity and UCP1

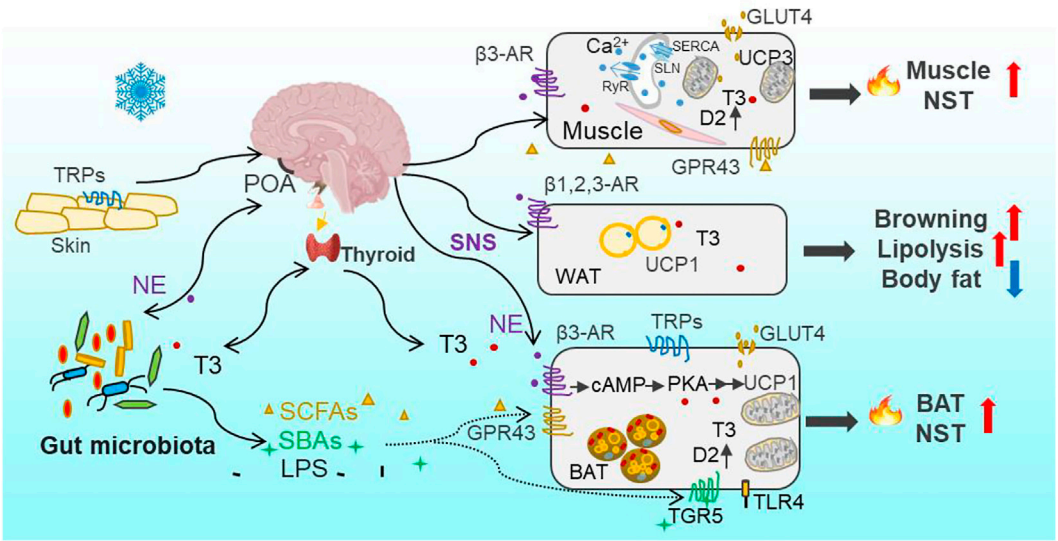

FIGURE 1 | Overview of cold-induced thermogenesis through Thermo-TRPs—SNS—gut microbiota—thermogenesis axis and thyroid—gut microbiota—thermogenesis axis. Cold is sensed by the thermosensitive transient receptor potential channels (Thermo-TRPs) on the skin and in the brain and other organs. Cold signal is transmitted through the sensory afferent nerve to the preoptic area (POA) in the hypothalamus and other thermoeffector efferent circuits, and leads to the activation of the sympathetic nervous system (SNS) to release norepinephrine (NE) and stimulate mitochondrial uncoupling protein 1 (UCP1) through β3 adrenergic receptors (*β*3-AR) and activation of PKA signaling pathway in brown adipose tissue (BAT). In parallel with the direct effect of NE on thermogenesis, the gut microbiota community is reconstructed through sensing cold signal or neuroactive signal of NE and, consequently, leads to increases in bacterial metabolites (short-chain fatty acids, SCFAs) and byproducts (secondary bile acids, SBAs). Both SCFAs and SBAs, via acting on their respective G protein-coupled receptors GPR43 and TGR5, can stimulate BAT nonshivering thermogenesis (NST). Moreover, the circulating bioactive tri-iodothyronine (T3) level increases after the brain receives cold signal, and promotes obligatory (basal metabolic rate, BMR) and regulatory thermogenesis. T3-induced thermogenesis is also mediated by bacterial metabolites (SCFAs) and byproducts (such as SBAs and lipopolysaccharides, LPS). The binding of SBAs-TGR5 or LPS-TLR4 (Toll-like receptor 4) can activate UCP1 expression in BAT, and stimulate local type 2 deiodinase (D2) to induce the conversion from the prohormone thyroxine (T4) to bioactive T3 as well. The binding of NE with *β*1,2,3-AR in white adipose tissue (WAT) activates lipolysis (catabolism of triglycerides) into free fatty acids as one source of fuel for BAT thermogenesis, leading to the decrease in body fat content. Cold-induced glucose uptake via glucose transporter (GLUT4) in adipocytes and muscle can also provide glucose as fuel for BAT and muscle thermogenesis. Muscle NST is mainly based on activities of sarcoplasmic reticulum ryanodine receptor (RyR)-mediated Ca^{2+}-leak, sarcolipin (SLN)-activated sarcoplasmatic reticulum Ca^{2+}-ATPase (SERCA), and mitochondrial UCP3 as well. SLN, via binding to SERCA, can uncouple ATP hydrolysis from Ca^{2+} transportation and as a result increase heat production.

expression increased, during cold exposure or cold acclimation in non-hibernating small mammals, such as in Brandt's voles (*Lasiopodomys brandtii*), Mongolian gerbils root voles (*Microtus oeconomus*) and plateau pikas (*Ochotona curzoniae*) (Wang et al., 2006; Zhang and Wang, 2006; Li and Wang, 2007). Cold-induced increases in sympathetic activation and UCP1 expression (browning) in white adipose tissue (WAT) can also help animals defense cold and maintain T_b (Bai et al., 2015; Shin et al., 2017). Our previous data confirmed that cold-induced phenotypic variations were initiated by increased release of norepinephrine (NE) and activation of cAMP-PKA-pCREB signaling pathway in BAT (Bo et al., 2019). Cold-induced lipolysis (catabolism of triglycerides) and glucose uptake via glucose transporter (GLUT4) in adipocytes provides the availability of free fatty acids and glucose as the sources of fuel for BAT thermogenesis (Townsend and Tseng, 2014; Garretson et al., 2016). Therefore, BAT plays its roles in regulating thermogenesis, and fatty acid and glucose metabolism.

Besides BAT-dependent thermogenesis in eutherian mammals, increasing evidence has shown that skeletal muscle also contributes importantly to cold-induced adaptive thermogenesis, independent of shivering or contraction (Nowack et al., 2017; Bal et al., 2018; Bal and Periasamy, 2020). The role of skeletal muscle NST is particually crucial in several specific endothms, such as birds, monotremes, marsupials, and wild boars, which lack BAT (Rowland et al., 2015). Lineage tracing studies have revealed that skeletal muscle and BAT arive from the same precursor cells in the dermomyotome expressing Pax3/7 (the transcription factor) and myogenic factor 5 (Myf5, the determination factor) (Lang et al., 2005; Sgaier et al., 2005), whereas the precursor for mature white adipocytes lacks Myf5 expression (Sanchez-Gurmaches et al., 2012). Moreover, recent evolutionary studies imply that NST in skeletal muscle originated much earlier than BAT-driven thermogenesis in vertebrates (Rowland et al., 2015; Grigg et al., 2022). The mechanism for muscle NST is based on activities of sarcoplasmic reticulum ryanodine receptor (RyR)-mediated Ca^{2+}-leak and sarcolipin (SLN)-activated sarcoplasmatic reticulum Ca^{2+}-ATPase (SERCA) (**Figure 1**) (Periasamy and Huke, 2001; Zima et al., 2010; Bal et al., 2012; Chambers et al., 2022). SLN, via binding to SERCA, uncouples ATP hydrolysis from Ca^{2+} transportation and as a result increases

heat production (Smith et al., 2002; Bal et al., 2012). In addition, the activation of mitochondrial UCP3 by intracellular levels of Ca^{2+} and fatty acids is also associated with muscle NST (Costford et al., 2007). Small mammals depend on increasing the adaptive thermogenesis deriving from BAT and skeletal muscle to maintain T_b relatively stable and survive in harsh winter.

Thermo-TRPs—SNS—Gut Microbiota—Thermogenesis Axis

Cold signal is sensed by a group of cold-sensitive thermoreceptors, the thermosensitive transient receptor potential channels (Thermo-TRPs), such as TRPA1 (<17°C) and TRPM8 (10–26°C), on the skin and in muscle, viscera, spine and brain, and transmitted through the sensory afferent nerve to the preoptic area (POA) in the hypothalamus and other thermoeffector efferent circuits (Morrison and Nakamura, 2019). There are also warm-sensitive thermoreceptors, such as TRPM2 (>42°C), TRPV1 (>42°C) and TRPV2 (>52°C) on the skin and body core (Hoffstaetter et al., 2018). These TRPs are activated by high T_a and transfer thermal signal to the central relevant thermoregulatory network and, consequently, lead to BAT atrophy and heat dissipation (Vandewauw et al., 2018). A rescent study identified the expression of TRPV1 as a specific characteristic of vascular smooth muscle (VSM)-derived adipocyte progenitor cells and the contribution of these cells to cold-induced BAT recruitment (Shamsi et al., 2021). TRPV1 is also involved in temperature preference behavior-associated thermoregulation in Mongolian gerbils (Wen et al., 2021). TRPs have been widely studied for cold or warm sensation in specific TRP knock-out laboratory models (Peier et al., 2002; Vandewauw et al., 2018), but the responses of TRPs to T_as are diversified in wild mammal species and in diverse tissues. For example, during cold acclimation, the expression of TRPM8 in small intestine increased in mice (Wen et al., 2020), and TRPA1 and TRPV2 in BAT increased in Brandt's voles, whereas TRPM2 decreased in Mongolian gerbils (unpublished data). TRPs can also be activated by ligands, such as capsaicin, menthol and bacterial endotoxins (lipopolysaccharides, LPS) (Peier et al., 2002; Baskaran et al., 2016; Boonen et al., 2018). Therefore, the functions of diverse TRPs should be widely investigated for better understanding how small mammals sense and tolerate extreme T_a particularly under the ecological contexts of heat waves and extremely cold weather.

Besides the central mechanism of thermoregulation, the peripheral gut microbial community is also involved in the regulation of host metabolic and thermal homeostasis. Several wild studies indicate that gut microbes vary with seasons, altitudes and geographies in small mammals (Maurice et al., 2015; Perofsky et al., 2019). The environmental factors such as diets, T_a and photoperiod influence the gut microbial community (Martinez-Mota et al., 2019; Suzuki et al., 2019; Khakisahneh et al., 2020). Our previous data identified that low T_a can directly drive gut microbial community assembly rather than cold-induced feeding effect, and intermittent fluctuations of low and high T_a altered the diversity and composition of gut microbiota (Bo et al., 2019; Khakisahneh et al., 2020). Cold-induced alteration in microbes induced increases in NE concentrations both in the intestine and BAT, and also increases in concentrations of bacterial metabolites and byproducts, such as SCFAs and SBAs in feces and blood (Worthmann et al., 2017; Bo et al., 2019). Consequently, these metabolites and byproducts, via their respective G protein-coupled receptors (such as GPR43/41, also named FFAR2/3) and the Takeda GPR (TGR5), promote host's adaptive thermogenesis both in BAT and skeletal muscle (**Figure 1**). Besides, the increase in NE production could conversely induce reshaping of the gut microbial community, which was verified by pharmacological NE manipulation (Bo et al., 2019). In addition, early evidence has shown that both the microbiota and their hosts produce the same neuroactive compounds (such as pheromones, hormones and neuropeptides) and the receptors, which enable bidirectional communications between the hosts and symbiotic microorganisms (Roth et al., 1982; Lyte, 2014). Therefore, the interaction between host neurotransmitters and gut microbes contributes to host thermoregulation and thermal homeostasis under the changing environments. Cumulatively, available experimental data suggest that the disturbance of gut microbial community may be a mechanism by which changing global temperatures are imposing impacts on fitness of animals in wild-living populations.

Thyroid—Gut Microbiota—Thermogenesis Axis

Thyroid hormones, particularly the bioactive tri-iodothyronine (T3), have important roles in regulating developmental and metabolic processes (Mullur et al., 2014; Ortiga-Carvalho et al., 2014). The intracellular T3 in tissues and serum T3 are generally derived from the prohormone thyroxine (T4) through the catalytic action of type 2 deiodinase (D2). D2 is highly expressed in the brain, pituitary, and peripheral tissues such as BAT and skeletal muscle (Brent, 2012; Mullur et al., 2014). When bound to the nuclear receptors (α and β) of thyroid hormones, T3 can regulate multiple transcriptional expressions such as adipose triglyceride lipase (Atg5), COX, UCP1 and GLUT4 responsible for fatty acid oxidation, heat production and glucose uptake in BAT (Mullur et al., 2014; Yau et al., 2019). In muscle, T3 can also modulate the expression of GLUT4, SERCA and UCP3 (Solanes et al., 2005; Salvatore et al., 2014). Thyroid hormones are tightly controlled and maintained within a narrow range of circulating levels by a negative feedback mechanism involving hypothalamic thyrotropin-releasing hormone (the hypothalamic-pituitary-thyroid axis, HPA axis) (Ortiga-Carvalho et al., 2014).

The external environment cues induce changes in internal hormones such as thyroid hormones, leptin (adipocytokine) and secretin (gut hormone), which can act as regulators for metabolism and thermogenesis (Zhang and Wang, 2006; Zhao and Wang, 2006; Li and Wang, 2007; Li et al., 2018; Khakisahneh et al., 2019). The circulating T3 and/or T3/T4 levels increased in winter and during low T_a or short-day acclimations in many mammal species such as in Brandt's voles, Mongolian gerbils, Daurian ground squirrels (*Spermophilus dauricus*), and plateau pikas (Li et al., 2001). Cold-induced increased levels of serum T3

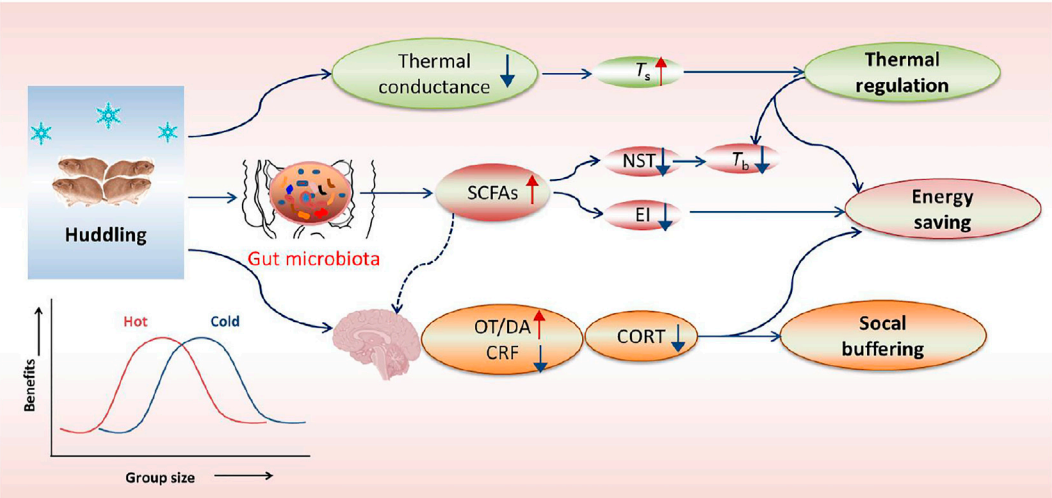

FIGURE 2 | Overview of huddling-related benefits in thermoregulation, energy saving and social buffering. In cold, the gregarious (social) rodents huddle together to reduce body surface area and thus decrease thermal conductance, but can keep a relatively high body surface temperature (T_s) and a low core body temperature (T_b). The social environment can facilitate gut microbial community with more beneficial bacteria and their metabolites such as short-chain fatty acids (SCFAs), thereby inducing decreases in nonshivering thermogenesis (NST) and energy intake (EI). Additionally, social environments particularly social bonding or attachment can also buffer stress responses, which is mediated by increased neurotransmitters such as dopamine (DA) and oxytocin (OT), but reduced corticotropin-releasing factor (CRF) in the limbic system and hypothalamus. The energetic benefit of huddling is dependent on group size and ambient temperatures (T_a), and it indicates a reversed U-shaped form, with an optimal group size for energy saving and other benefits.

promote obligatory (BMR) and regulatory thermogenesis (rNST) by stimulating mitochondrial biogenesis, generating and maintaining ion gradients, increasing ATP production, and increasing the expression of uncoupling proteins (UCPs) in liver, muscle and BAT (Mullur et al., 2014; Shu et al., 2017). Additionally, UCP1-independent thyroid thermogenesis was established in UCP1-ablated mice (Dittner et al., 2019), implying the compensatory role of skeletal muscle thermogenesis for cold defense in small mammals.

In addition to the direct effect of T3 on metabolism and thermogenesis, thyroid function is closely related to the homeostasis of intestinal microbial community. The pathologically, chemically or surgically induced thyroid dysfunction (such as hyperthyroidism or hypothyroidism) was associated with alterations in the diversity and composition of gut microbiota (Khakisahneh et al., 2022; Shin et al., 2020). For example, hyperthyroidism in human was followed by enrichments in gut pathogenic bacteria such as *Clostridium* and Enterobacteriaceae (Zhou et al., 2014). And the hyperthyroid gerbils exhibited increased abundances of pathogenic *Helicobacter* and *Rikenella*, and decreased abundances of beneficial *Butyricimonas* and *Parabacteroides* (Khakisahneh et al., 2022). Moreover, the previous data verified that microbiota transplant from normal donors to hyperthyroidism could buffer hyperthyroid-induced disorders in the microbial community and thermogenesis (Khakisahneh et al., 2022). Gut microbes through activation of D2 in the intestine and liver improve the conversion of bioactive T3 from inactive T4, thereby modulating local T3 levels and intestinal homeostasis (Kojima et al., 2019). The gut microbiota-derived SBAs can also activate D2 activity through TGR5 and increase cold-induced thermogenesis (**Figure 1**) (Watanabe et al., 2006; Worthmann et al., 2017). Moreover, bacterial LPS through binding Toll-like receptor 4 (TLR4) can stimulate T3 conversion by promoting D2 mRNA accumulation and enzyme activity in mouse mediobasal hypothalamus and rat astrocytes (Boelen et al., 2004; Lamirand et al., 2011). Collectively, the gut microbiota can sense hormones, and regulate thyroid hormone recycling and metabolism through bacterial metabolites and byproducts to modulate deiodinase activity (Virili and Centanni, 2015; Virili and Centanni, 2017; Lopes and Sourjik, 2018). Small mammals maintain metabolic and thermal homeostasis through the bidirectional communication between the thyroid and gut microbiota.

Huddling and Gut Microbiota

The group-living (gregarious or social) mammals have evolved cooperative (or social) behavior to optimize their fitness to survive in harsh environments. Huddling behavior is one type of highly-conserved cooperative behavioral strategies for social species to reduce thermoregulatory costs as well as predation risk (Ebensperger, 2001; Haig, 2008; Gilbert et al., 2010). In cold conditions, the gregarious rodents huddle together to reduce thermal conductance, and decrease NST and food intake, and as a consequence show an increased body surface temperature (T_s), but a reduced T_b (**Figure 2**), whereas the solitary species or non-huddling individuals increase thermogenesis to maintain T_b or entering hibernation to reduce temperature difference between the body and air (Nowack and Geiser, 2016; Sukhchuluun et al., 2018; Zhang et al., 2018). The energetic benefit of huddling depends on group sizes and T_a in a reversed U-shaped form (**Figure 2**), and the optimal group size for energy saving varies

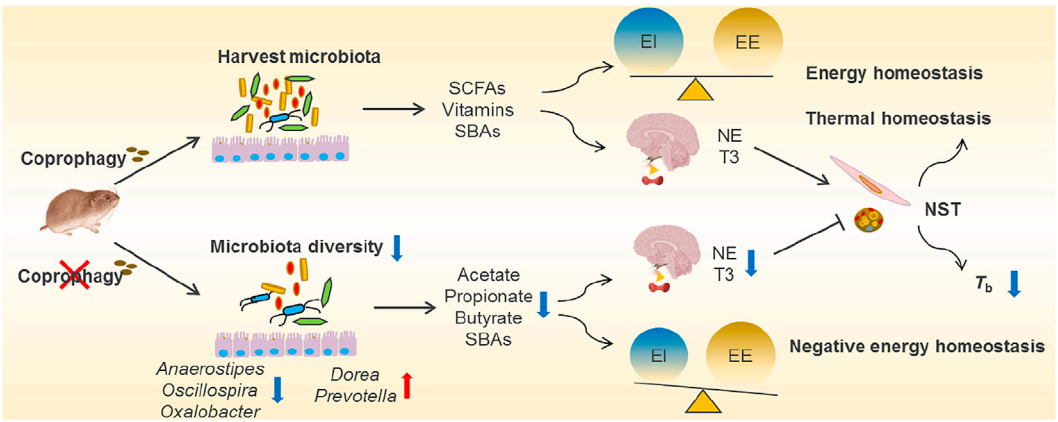

FIGURE 3 | Overview of coprophagy-associated benefits in harvesting intestinal microbiota and maintaining energy and thermal homeostasis. Coprophagy prevention (CP) leads to loss of beneficial bacteria such as *Anaerostipes, Oscillospira* and *Oxalobacter* for production of short-chain fatty acids (SCFAs, such as acetate, propionate and butyrate), vitamins and secondary bile acids (SBAs), and results in the negative energy homeostasis (imbalance between energy intake, EI, and energy expenditure, EE). The deficiency in energy supply to the brain impairs the neuroendocrinology and leads to decreases in norepinephrine (NE) and tri-iodothyronine (T3) in CP animals, consequently leading to decreases in nonshivering thermogenesis (NST) in BAT and muscle and a drop in core body temperatures (T_b).

with different temperatures (Gilbert et al., 2010). Increasing group size over the optimal size has little additional advantage to reduce energy metabolism, but indeed increases resource competition and disease risks among individuals (Gilbert et al., 2010; Škop et al., 2021). In addition, the benefit and intensity of huddling increase as T_a reduces, and decrease at high T_a and within TNZ (Gilbert et al., 2010). In conclusion, huddling is an active, complex social thermoregulation behavior, particularly beneficial for energy conservation for social species living in winter or exposing to low T_a.

Social environment (or sociability) can buffer stress responses and facilitate the gut microbial community. For example, social bonding or attachment in the prairie vole (*Microtus ochrogaster*) reduces stress hormone corticosterone (CORT) and confers social buffering benefit, which is mediated by increased neurotransmitters such as dopamine (DA) and oxytocin (OT), but reduced corticotropin-releasing factor (CRF) in the limbic system and hypothalamus (**Figure 2**) (Smith and Wang, 2014; Burkett et al., 2016). Our previous data in Brandt's voles showed that huddling animals had a healthier gut microbial community with more SCFAs-producing bacteria in comparison with non-huddling voles, indicating the energy-saving benefit of huddling is mediated by improving microbial homeostasis (**Figure 2**) (Zhang et al., 2018). Social status also shaped the diverse microbial community between dominants and subordinates in mice and *Tscherskia triton* (Zhao et al., 2020; Agranyoni et al., 2021). Whether gut microbial community mediates sociability-induced physiological and behavioral differences was validated by fecal/caecal microbiota transplant (FMT/CMT) using antibiotics-treated or germ-free mice or wild rodents. The mice with absence of gut microbiota elevated the level of corticosterone (the stress hormone) and displayed social behavioral deficits during the assessment of reciprocal social interactions (Buffington et al., 2016). In addition, normal microbiota colonization (co-housing or oral gavage) could effectively correct social impairments of the mice lacking the gut microbiota (Buffington et al., 2016; Chu et al., 2019). More importantly, a specific bacterial species, *Enterococcus faecalis*, has been identified to restrain stress responses and promote social activity in the mice following social stress (Wu et al., 2021). These substantial data support crucial functions of the gut microbiota in regulating sociability-related behavioral divergence and fitness benefits.

Coprophagy and Gut Microbiota

Coprophagy is the behavior of eating feces to help establish the intestinal microbiota, and to acquire protein and micronutrients, which is common in lagomorphs, rodents and other species (Soave and Brand, 1991). The term caecotrophy refers specially to soft faeces ingestion practiced by rabbits and small herbivores (small hindgut fermenters) (Hoernicke, 1981). The proximal colonic separation mechanism observed in many small herbivores can allow for retrograde fluid transport of digesta including bacteria from the proximal colon back into the caecum (Pei et al., 2001; Liu et al., 2007; Hagen et al., 2016). The accumulation of microorganisms in the caecum contributes to a high fermentation rate for bacterial synthesis of nutrients (Karasov et al., 2011). The high-fiber diets promote digesta retention time and production of more soft feces, and coprophagy increases in the periods with a higher energy demand, such as during pregnancy and lactation (Ebino et al., 1988; Hejcmanová et al., 2020). In many studies in rodents such as rats, mice, *L. brandtii* and *Microtus fortis*, prevention of coprophagy decreased body weight, and RMR and NST, suggesting that coprophagy contributes to energy balance and thermoregulation (Sukemori et al., 2003; Sassi et al., 2010; Kohl et al., 2014; Liu et al., 2016; Bo et al., 2020). The energetic and thermal benefits of interspecific coprophagy for survival were observed in plateau pikas that eat yak feces to supplement energy intake in winter (Speakman et al., 2021). Besides, coprophagy in the voles increases neurotransmitters in the hypothalamus and hippocampus, and

promotes cognitive performance (Bo et al., 2020). These data indicate that consumption of enough soft feces for herbivorous rodents is necessary to provide enough amounts of nutrients and energy for growth, thermoregulation, and neurodevelopment as well (**Figure 3**).

Supplement of nutrients and energy via coprophagy may be through harvesting the gut microbiota (self-inoculation). Prevention of coprophagy in Brand's voles reduced α diversity of gut microbial community and altered the composition of the gut microbiota, particularly decreased relative abundance of Firmicutes, including the families of Clostridiaceae, Lachnospiraceae and Ruminococcaceae, which all belong to highly cellulolytic bacteria (Bo et al., 2020). Accompanied by the reduced diversity of gut microbial community, coprophagy prevention also decreased the concentrations of bacterial metabolites, such as acetate, propionate and butyrate (**Figure 3**). Both the microbial community and the concentrations of SCFAs recovered after the voles were allowed coprophagy. Other evidence showed that the stomach of woodrats (*Neotoma* spp.) and mice harboured highly similar microbial community to large intestine, and the non-coprophagic mice altered the composition of microbiota and the profile of bile acid pool in the small intestine, but no changes were observed in the large intestine, indicating persistent self-reinoculation of microbiota via coprophagy (Kohl et al., 2014; Bogatyrev et al., 2020). In addition, supplementation of acetate reversed energetic, thermal and microbial homeostasis, and rescued neurological and cognitive deficits induced by coprophagy prevention in voles (Bo et al., 2020). However, it is worth mentioning that coprophagy may induce potential disease risk, since some pathogenic bacteria may be transmitted into the intestine from the feces or environments. All these findings reveal that coprophagy in herbivores promotes the stabilization of gut microbial community, and contributes to maintaining host energy balance, thermoregulation and neuronal function.

CONCLUSION AND PERSPECTIVES

Animals and plants are actually holobionts which consist of their own genes and those of symbiotic microorganisms as well. The developments of sequencing instruments, omics technology and bioinformatics advance our understanding of these microorganisms. Growing evidence indicates that bidirectional communication between the gut microbiota and animal organisms mediates host metabolic and thermal homeostasis in wild small mammals for environmental adaptations, which were summarized in this review. Besides, these microorganisms are involved in regulating host water and salt homeostasis (Nouri et al., 2022), immunity and disease defense (Rosshart et al., 2017), as well as population dynamics (Li et al., 2019; Li et al., 2020; Li et al., 2021) in wild-living populations. All in together, the coevolution of host-microorganism symbionts promotes individual survival, population maintenance, and species coexistence in the ecosystems with complicated, variable environments.

More studies should be performed to explore the contributions of BAT and muscle in cold- and diet-induced thermogenesis. Also, the mechanisms by which microbial metabolites and byproducts regulate thermal sensation, neural conductance, and BAT and muscle thermogenesis need to be uncovered for an integrative understanding of thermoregulation in endotherms. Future studies will still focus on much deeper investigations of the functions of specific microbes from the microbial community in wild mammals and try to screen out beneficial microbiota candidates for the therapeutic potentials. Moreover, we will benefit from the combined techniques of culturomics, gene engineering and editing to identify unknown microbes, and operate targeted genetic modifications of specific intestinal microbes for improving resistance to viral and bacterial infections. In addition, further research will be strengthened to investigate the interaction and coevolution between gut microbiomes and their hosts in ecological and evolutionary contexts. As human activity perturbations and climate changes aggravate in magnitude, frequency and duration, and as the uses of antibiotics, pesticides and food additives grow, understanding their profound impacts on the real-time adaptation and long-term evolution of host–microorganism interactions will be getting more and more beneficial and have broader implications on biodiversity protection and future disease therapy.

DATA AVAILABILITY STATEMENT

The raw data supporting the conclusion of this article will be made available by the authors, without undue reservation.

AUTHOR CONTRIBUTIONS

X-YZ wrote the manuscript; X-YZ and D-HW contributed to revision of the manuscript.

FUNDING

This study was supported by the National Natural Science Foundation of China (32090020 and 32070449), the Second Tibetan Plateau Scientific Expedition and Research program (2019QZKK05010212), and Strategic Priority Research Program of Chinese Academy of Sciences (Grant No. XDPB16).

REFERENCES

Agranyoni, O., Meninger-Mordechay, S., Uzan, A., Ziv, O., Salmon-Divon, M., Rodin, D., et al (2021). Gut Microbiota Determines the Social Behavior of Mice and Induces Metabolic and Inflammatory Changes in Their Adipose Tissue. *NPJ Biofilms Microbiomes* 7, 28. doi:10.1038/s41522-021-00193-9

Bai, Z., Wuren, T., Liu, S., Han, S., Chen, L., McClain, D., et al (2015). Intermittent Cold Exposure Results in Visceral Adipose Tissue "browning" in the Plateau

Pika (Ochotona Curzoniae). *Comp. Biochem. Physiol. A: Mol. Integr. Physiol.* 184, 171–178. doi:10.1016/j.cbpa.2015.01.019

Bal, N. C., Maurya, S. K., Sopariwala, D. H., Sahoo, S. K., Gupta, S. C., Shaikh, S. A., et al (2012). Sarcolipin Is a Newly Identified Regulator of Muscle-Based Thermogenesis in Mammals. *Nat. Med.* 18 (10), 1575–1579. doi:10.1038/nm.2897

Bal, N. C., and Periasamy, M. (2020). Uncoupling of Sarcoendoplasmic Reticulum Calcium ATPase Pump Activity by Sarcolipin as the Basis for Muscle Non-shivering Thermogenesis. *Phil. Trans. R. Soc. B* 375 (1793), 20190135. doi:10.1098/rstb.2019.0135

Bal, N. C., Sahoo, S. K., Maurya, S. K., and Periasamy, M. (2018). The Role of Sarcolipin in Muscle Non-shivering Thermogenesis. *Front. Physiol.* 9, 1217. doi:10.3389/fphys.2018.01217

Baskaran, P., Krishnan, V., Ren, J., and Thyagarajan, B. (2016). Capsaicin Induces browning of white Adipose Tissue and Counters Obesity by Activating TRPV1 Channel-dependent Mechanisms. *Br. J. Pharmacol.* 173, 2369–2389. doi:10.1111/bph.13514

Bo, T.-B., Zhang, X.-Y., Kohl, K. D., Wen, J., Tian, S.-J., and Wang, D.-H. (2020). Coprophagy Prevention Alters Microbiome, Metabolism, Neurochemistry, and Cognitive Behavior in a Small Mammal. *Isme J.* 14, 2625–2645. doi:10.1038/s41396-020-0711-6

Bo, T.-B., Zhang, X.-Y., Wen, J., Deng, K., Qin, X.-W., and Wang, D.-H. (2019). The Microbiota-Gut-Brain Interaction in Regulating Host Metabolic Adaptation to Cold in Male Brandt's Voles (*Lasiopodomys Brandtii*). *Isme J.* 13, 3037–3053. doi:10.1038/s41396-019-0492-y

Boelen, A., Kwakkel, J., Thijssen-Timmer, D., Alkemade, A., Fliers, E., and Wiersinga, W. (2004). Simultaneous Changes in central and Peripheral Components of the Hypothalamus-Pituitary-Thyroid axis in Lipopolysaccharide-Induced Acute Illness in Mice. *J. Endocrinol.* 182, 315–323. doi:10.1677/joe.0.1820315

Bogatyrev, S. R., Rolando, J. C., and Ismagilov, R. F. (2020). Self-reinoculation with Fecal flora Changes Microbiota Density and Composition Leading to an Altered Bile-Acid Profile in the Mouse Small Intestine. *Microbiome* 8, 19. doi:10.1186/s40168-020-0785-4

Boonen, B., Alpizar, Y., Meseguer, V., and Talavera, K. (2018). TRP Channels as Sensors of Bacterial Endotoxins. *Toxins* 10, 326. doi:10.3390/toxins10080326

Bozinovic, F., Ferri-Yáñez, F., Naya, H., Araújo, M., and Naya, D. E. (2014). Thermal Tolerances in Rodents: Species that Evolved in Cold Climates Exhibit a Wider Thermoneutral Zone. *Evol. Ecol. Res.* 16, 143–152.

Brent, G. A. (2012). Mechanisms of Thyroid Hormone Action. *J. Clin. Invest.* 122, 3035–3043. doi:10.1172/jci60047

Buffington, S. A., Di Prisco, G. V., Auchtung, T. A., Ajami, N. J., Petrosino, J. F., and Costa-Mattioli, M. (2016). Microbial Reconstitution Reverses Maternal Diet-Induced Social and Synaptic Deficits in Offspring. *Cell* 165, 1762–1775. doi:10.1016/j.cell.2016.06.001

Burkett, J. P., Andari, E., Johnson, Z. V., Curry, D. C., de Waal, F. B. M., and Young, L. J. (2016). Oxytocin-dependent Consolation Behavior in Rodents. *Science* 351, 375–378. doi:10.1126/science.aac4785

Cannon, B., and Nedergaard, J. (2004). Brown Adipose Tissue: Function and Physiological Significance. *Physiol. Rev.* 84, 277–359. doi:10.1152/physrev.00015.2003

Chambers, P. J., Juracic, E. S., Fajardo, V. A., and Tupling, A. R. (2022). Role of SERCA and Sarcolipin in Adaptive Muscle Remodeling. *Am. J. Physiology-Cell Physiol.* 322 (3), C382–C394. doi:10.1152/ajpcell.00198.2021

Chi, Q.-S., Wan, X.-R., Geiser, F., and Wang, D.-H. (2016). Fasting-induced Daily Torpor in Desert Hamsters *(Phodopus Roborovskii)*. *Comp. Biochem. Physiol. Part A: Mol. Integr. Physiol.* 199, 71–77. doi:10.1016/j.cbpa.2016.05.019

Chu, C., Murdock, M. H., Jing, D., Won, T. H., Chung, H., Kressel, A. M., et al (2019). The Microbiota Regulate Neuronal Function and Fear Extinction Learning. *Nature* 574, 543–548. doi:10.1038/s41586-019-1644-y

Costford, S. R., Seifert, E. L., Bézaire, V., F. Gerrits, M., Bevilacqua, L., Gowing, A., et al (2007). The Energetic Implications of Uncoupling Protein-3 in Skeletal Muscle. *Appl. Physiol. Nutr. Metab.* 32 (5), 884–894. doi:10.1139/h07-063

Ding, B.-Y., Chi, Q.-S., Liu, W., Shi, Y.-L., and Wang, D.-H. (2018). Thermal Biology of Two Sympatric Gerbil Species: The Physiological Basis of Temporal Partitioning. *J. Therm. Biol.* 74, 241–248. doi:10.1016/j.jtherbio.2018.03.025

Dittner, C., Lindsund, E., Cannon, B., and Nedergaard, J. (2019). At Thermoneutrality, Acute Thyroxine-Induced Thermogenesis and Pyrexia Are Independent of UCP1. *Mol. Metab.* 25, 20–34. doi:10.1016/j.molmet.2019.05.005

Ebensperger, L. A. (2001). A Review of the Evolutionary Causes of Rodent Group-Living. *Acta Theriol.* 46, 115–144. doi:10.4098/at.arch.01-16

Ebino, K. Y., Suwa, T., Kuwabara, Y., Saito, T. R., and Takahashi, K. W. (1988). Coprophagy in Female Mice during Pregnancy and Lactation. *Exp. Anim.* 37 (1), 101–104. doi:10.1538/expanim1978.37.1_101

Fetissov, S. O. (2017). Role of the Gut Microbiota in Host Appetite Control: Bacterial Growth to Animal Feeding Behaviour. *Nat. Rev. Endocrinol.* 13, 11–25. doi:10.1038/nrendo.2016.150

Garretson, J. T., Szymanski, L. A., Schwartz, G. J., Xue, B., Ryu, V., and Bartness, T. J. (2016). Lipolysis Sensation by white Fat Afferent Nerves Triggers Brown Fat Thermogenesis. *Mol. Metab.* 5, 626–634. doi:10.1016/j.molmet.2016.06.013

Gilbert, C., McCafferty, D., Le Maho, Y., Martrette, J. M., Giroud, S., Blanc, S., et al (2010). One for All and All for One: the Energetic Benefits of Huddling in Endotherms. *Biol. Rev. Camb Philos. Soc.* 85, 545–569. doi:10.1111/j.1469-185X.2009.00115.x

Gordon, C. J. (2012). Thermal Physiology of Laboratory Mice: Defining Thermoneutrality. *J. Therm. Biol.* 37, 654–685. doi:10.1016/j.jtherbio.2012.08.004

Gould, A. L., Zhang, V., Lamberti, L., Jones, E. W., Obadia, B., Korasidis, N., et al (2018). Microbiome Interactions Shape Host Fitness. *Proc. Natl. Acad. Sci. U S A.* 115, E11951–E11960. doi:10.1073/pnas.1809349115

Grigg, G., Nowack, J., Bicudo, J. E. P. W., Bal, N. C., Woodward, H. N., and Seymour, R. S. (2022). Whole-body Endothermy: Ancient, Homologous and Widespread Among the Ancestors of Mammals, Birds and Crocodylians. *Biol. Rev.* 97 (2), 766–801. doi:10.1111/brv.12822

Groussin, M., Mazel, F., Sanders, J. G., Smillie, C. S., Lavergne, S., Thuiller, W., et al (2017). Unraveling the Processes Shaping Mammalian Gut Microbiomes over Evolutionary Time. *Nat. Commun.* 8, 14319. doi:10.1038/ncomms14319

Hagen, K. B., Dittmann, M. T., Ortmann, S., Kreuzer, M., Hatt, J.-M., and Clauss, M. (2016). Retention of Solute and Particle Markers in the Digestive Tract of Chinchillas (*Chinchilla laniger*). *J. Anim. Physiol. Anim. Nutr.* 100, 801–806. doi:10.1111/jpn.12441

Haig, D. (2008). Huddling: Brown Fat, Genomic Imprinting and the Warm Inner Glow. *Curr. Biol.* 18, R172–R174. doi:10.1016/j.cub.2007.12.040

Hejcmanová, P., Ortmann, S., Stoklasová, L., and Clauss, M. (2020). Digesta Passage in Common Eland (*Taurotragus oryx*) on a Monocot or a Dicot Diet. *Comp. Biochem. Physiol. A. Mol. Integr. Physiol.* 246, 110720. doi:10.1016/j.cbpa.2020.110720

Hoernicke, H. (1981). Utilization of Caecal Digesta by Caecotrophy (Soft Faeces Ingestion) in the Rabbit. *Livestock Prod. Sci.* 8 (4), 361–366.

Hoffstaetter, L. J., Bagriantsev, S. N., and Gracheva, E. O. (2018). TRPs et al.: a molecular toolkit for thermosensory adaptations. *Pflugers Arch. - Eur. J. Physiol.* 470, 745–759. doi:10.1007/s00424-018-2120-5

Karasov, W. H., Martínez del Rio, C., and Caviedes-Vidal, E. (2011). Ecological Physiology of Diet and Digestive Systems. *Annu. Rev. Physiol.* 73, 69–93. doi:10.1146/annurev-physiol-012110-142152

Kasza, I., Adler, D., Nelson, D. W., Eric Yen, C.-L., Dumas, S., Ntambi, J. M., et al (2019). Evaporative Cooling Provides a Major Metabolic Energy Sink. *Mol. Metab.* 27, 47–61. doi:10.1016/j.molmet.2019.06.023

Khakisahneh, S., Zhang, X. Y., Nouri, Z., and Wang, D. H. (2020). Gut Microbiota and Host Thermoregulation in Response to Ambient Temperature Fluctuations. *mSystems* 5 (5), e00514. doi:10.1128/mSystems.00514-20

Khakisahneh, S., Zhang, X.-Y., Nouri, Z., Hao, S.-Y., Chi, Q.-S., and Wang, D.-H. (2019). Thyroid Hormones Mediate Metabolic Rate and Oxidative, Anti-oxidative Balance at Different Temperatures in Mongolian Gerbils (*Meriones unguiculatus*). *Comp. Biochem. Physiol. C: Toxicol. Pharmacol.* 216, 101–109. doi:10.1016/j.cbpc.2018.11.016

Khakisahneh, S., Zhang, X. Y., Nouri, Z., and Wang, D. H. (2022). Cecal Microbial Transplantation Attenuates Hyperthyroid-induced Thermogenesis in Mongolian Gerbils. *Microb. Biotechnol.* 15 (3), 817–831. doi:10.1111/1751-7915.13793

Kohl, K. D., Miller, A. W., Marvin, J. E., Mackie, R., and Dearing, M. D. (2014). Herbivorous Rodents (Neotoma spp.) Harbour Abundant and Active Foregut Microbiota. *Environ. Microbiol.* 16, 2869–2878. doi:10.1111/1462-2920.12376

Kojima, Y., Kondo, Y., Fujishita, T., Mishiro-Sato, E., Kajino-Sakamoto, R., Taketo, M. M., et al (2019). Stromal Iodothyronine Deiodinase 2 (DIO 2) Promotes the

Growth of Intestinal Tumors in Apc Δ716 Mutant Mice. *Cancer Sci.* 110, 2520–2528. doi:10.1111/cas.14100

Lamirand, A., Ramauge, M., Pierre, M., and Courtin, F. (2011). Bacterial Lipopolysaccharide Induces Type 2 Deiodinase in Cultured Rat Astrocytes. *J. Endocrinol.* 208, 183–192. doi:10.1677/joe-10-0218

Lang, D., Lu, M. M., Huang, L., Engleka, K. A., Zhang, M., Chu, E. Y., et al (2005). Pax3 Functions at a Nodal point in Melanocyte Stem Cell Differentiation. *Nature* 433, 884–887. doi:10.1038/nature03292

Ley, R. E., Hamady, M., Lozupone, C., Turnbaugh, P. J., Ramey, R. R., Bircher, J. S., et al (2008). Evolution of Mammals and Their Gut Microbes. *Science* 320, 1647–1651. doi:10.1126/science.1155725

Li, G., Wan, X., Yin, B., Wei, W., Hou, X., Zhang, X., et al (2021). Timing Outweighs Magnitude of Rainfall in Shaping Population Dynamics of a Small Mammal Species in Steppe Grassland. *Proc. Natl. Acad. Sci. U S A.* 118 (42), e2023691118. doi:10.1073/pnas.2023691118

Li, G., Li, J., Kohl, K. D., Yin, B., Wei, W., Wan, X., et al (2019). Dietary Shifts Influenced by Livestock Grazing Shape the Gut Microbiota Composition and Co-occurrence Networks in a Local Rodent Species. *J. Anim. Ecol.* 88 (2), 302–314. doi:10.1111/1365-2656.12920

Li, G., Yin, B., Li, J., Wang, J., Wei, W., Bolnick, D. I., et al (2020). Host-microbiota Interaction Helps to Explain the Bottom-Up Effects of Climate Change on a Small Rodent Species. *Isme J.* 14, 1795–1808. doi:10.1038/s41396-020-0646-y

Li, Q., Sun, R., Huang, C., Wang, Z., Liu, X., Hou, J., et al (2001). Cold Adaptive Thermogenesis in Small Mammals from Different Geographical Zones of China. *Comp. Biochem. Physiol. Part A: Mol. Integr. Physiol.* 129, 949–961. doi:10.1016/s1095-6433(01)00357-9

Li, X. S., and Wang, D. H. (2007). Photoperiod and Temperature Can Regulate Body Mass, Serum Leptin Concentration, and Uncoupling Protein 1 in Brandt's Voles (*Lasiopodomys Brandtii*) and Mongolian Gerbils (*Meriones unguiculatus*). *Physiol. Biochem. Zool.* 80, 326–334. doi:10.1086/513189

Li, Y., Schnabl, K., Gabler, S.-M., Willershäuser, M., Reber, J., Karlas, A., et al (2019). Secretin-Activated Brown Fat Mediates Prandial Thermogenesis to Induce Satiation. *Cell* 175 (6), 1561–1574. doi:10.1016/j.cell.2018.10.016

Liu, H. C., Yang, D. M., Long, C., Liao, P., Luo, L., Tao, S. L., et al (2016). Effects of Caecotrophy Prevention on Food Digestion and Growth in *Microtus Fortis*. *Acta Theriologica Sinica* 36, 64–71. doi:10.16829/j.slxb.201601007

Liu, Q.-S., Li, J.-Y., and Wang, D.-H. (2007). Ultradian Rhythms and the Nutritional Importance of Caecotrophy in Captive Brandt's Voles (*Lasiopodomys Brandtii*). *J. Comp. Physiol. B* 177, 423–432. doi:10.1007/s00360-006-0141-4

Lopes, J. G., and Sourjik, V. (2018). Chemotaxis of *Escherichia coli* to Major Hormones and Polyamines Present in Human Gut. *Isme J.* 12, 2736–2747. doi:10.1038/s41396-018-0227-5

Lyte, M. (2014). Microbial Endocrinology. *Gut microbes* 5, 381–389. doi:10.4161/gmic.28682

Martínez-Mota, R., Kohl, K. D., Orr, T. J., and Denise Dearing, M. (2019). Natural Diets Promote Retention of the Native Gut Microbiota in Captive Rodents. *Isme J.* 14, 67–78. doi:10.1038/s41396-019-0497-6

Maurice, C. F., Cl Knowles, S., Ladau, J., Pollard, K. S., Fenton, A., Pedersen, A. B., et al (2015). Marked Seasonal Variation in the Wild Mouse Gut Microbiota. *Isme J.* 9, 2423–2434. doi:10.1038/ismej.2015.53

McNab, B. K. (2002). *The Physiological Ecology of Vertebrates*. Ithaca: Cornell University Press.

Mikane, T., Araki, J., Suzuki, S., Mizuno, J., Shimizu, J., Mohri, S., et al (1999). O(2) cost of Contractility but Not of Mechanical Energy Increases with Temperature in Canine Left Ventricle. *Am. J. Physiology-Heart Circulatory Physiol.* 277, H65–H73. doi:10.1152/ajpheart.1999.277.1.h65

Morrison, S. F., and Nakamura, K. (2019). Central Mechanisms for Thermoregulation. *Annu. Rev. Physiol.* 81, 285–308. doi:10.1146/annurev-physiol-020518-114546

Mullur, R., Liu, Y.-Y., and Brent, G. A. (2014). Thyroid Hormone Regulation of Metabolism. *Physiol. Rev.* 94, 355–382. doi:10.1152/physrev.00030.2013

Nouri, Z., Zhang, X. Y., Khakisahneh, S., Degen, A. A., and Wang, D. H. (2022). The Microbiota-Gut-Kidney axis Mediates Host Osmoregulation in a Small Desert Mammal. *npj Biofilms and Microbiomes*. doi:10.1038/s41522-022-00280-5

Nowack, J., and Geiser, F. (2016). Friends with Benefits: the Role of Huddling in Mixed Groups of Torpid and Normothermic Animals. *J. Exp. Biol.* 219, 590–596. doi:10.1242/jeb.128926

Nowack, J., Giroud, S., Arnold, W., and Ruf, T. (2017). Muscle Non-shivering Thermogenesis and its Role in the Evolution of Endothermy. *Front. Physiol.* 8, 889. doi:10.3389/fphys.2017.00889

Oelkrug, R., Polymeropoulos, E. T., and Jastroch, M. (2015). Brown Adipose Tissue: Physiological Function and Evolutionary Significance. *J. Comp. Physiol. B* 185 (6), 587–606. doi:10.1007/s00360-015-0907-7

Ortiga-Carvalho, T. M., Sidhaye, A. R., and Wondisford, F. E. (2014). Thyroid Hormone Receptors and Resistance to Thyroid Hormone Disorders. *Nat. Rev. Endocrinol.* 10, 582–591. doi:10.1038/nrendo.2014.143

Pan, Q., Li, M., Shi, Y.-L., Liu, H., Speakman, J. R., and Wang, D.-H. (2014). Lipidomics Reveals Mitochondrial Membrane Remodeling Associated with Acute Thermoregulation in a Rodent with a Wide Thermoneutral Zone. *Lipids* 49, 715–730. doi:10.1007/s11745-014-3900-0

Pei, Y. X., Wang, D. H., and Hume, I. D. (2001). Selective Digesta Retention and Coprophagy in Brandt's Vole (*Microtus Brandti*). *J. Comp. Physiol. B* 171, 457–464. doi:10.1007/s003600100195

Peier, A. M., Moqrich, A., Hergarden, A. C., Reeve, A. J., Andersson, D. A., Story, G. M., et al (2002). A TRP Channel that Senses Cold Stimuli and Menthol. *Cell* 108, 705–715. doi:10.1016/s0092-8674(02)00652-9

Periasamy, M., and Huke, S. (2001). SERCA Pump Level Is a Critical Determinant of Ca2+Homeostasis and Cardiac Contractility. *J. Mol. Cell Cardiol.* 33, 1053–1063. doi:10.1006/jmcc.2001.1366

Perofsky, A. C., Lewis, R. J., and Meyers, L. A. (2019). Terrestriality and Bacterial Transfer: a Comparative Study of Gut Microbiomes in Sympatric Malagasy Mammals. *Isme J.* 13, 50–63. doi:10.1038/s41396-018-0251-5

Rastelli, M., Cani, P. D., and Knauf, C. (2019). The Gut Microbiome Influences Host Endocrine Functions. *Endocr. Rev.* 40, 1271–1284. doi:10.1210/er.2018-00280

Ren, Y., Song, S., Liu, X., and Yang, M. (2022). Phenotypic Changes in the Metabolic Profile and Adiponectin Activity during Seasonal Fattening and Hibernation in Female Daurian Ground Squirrels (Spermophilus Dauricus). *Integr. Zool.* 17 (2), 297–310. doi:10.1111/1749-4877.12504

Ridlon, J. M., Kang, D.-J., and Hylemon, P. B. (2006). Bile Salt Biotransformations by Human Intestinal Bacteria. *J. Lipid Res.* 47, 241–259. doi:10.1194/jlr.r500013-jlr200

Rosshart, S. P., Vassallo, B. G., Angeletti, D., Hutchinson, D. S., Morgan, A. P., Takeda, K., et al (2017). Wild Mouse Gut Microbiota Promotes Host Fitness and Improves Disease Resistance. *Cell* 171, 1015–1028. doi:10.1016/j.cell.2017.09.016

Roth, J., Leroith, D., Shiloach, J., Rosenzweig, J. L., Lesniak, M. A., and Havrankova, J. (1982). The Evolutionary Origins of Hormones, Neurotransmitters, and Other Extracellular Chemical Messengers: Implications for Mammalian Biology. *N. Engl. J. Med.* 306, 523–527. doi:10.1056/NEJM198203043060907

Rowland, L. A., Bal, N. C., and Periasamy, M. (2015). The Role of Skeletal-Muscle-Based Thermogenic Mechanisms in Vertebrate Endothermy. *Biol. Rev.* 90 (4), 1279–1297. doi:10.1111/brv.12157

Salvatore, D., Simonides, W. S., Dentice, M., Zavacki, A. M., and Larsen, P. R. (2014). Thyroid Hormones and Skeletal Muscle-New Insights and Potential Implications. *Nat. Rev. Endocrinol.* 10 (4), 206–214. doi:10.1038/nrendo.2013.238

Sanchez-Gurmaches, J., Hung, C.-M., Sparks, C. A., Tang, Y., Li, H., and Guertin, D. A. (2012). PTEN Loss in the Myf5 Lineage Redistributes Body Fat and Reveals Subsets of white Adipocytes that Arise from Myf5 Precursors. *Cel Metab.* 16, 348–362. doi:10.1016/j.cmet.2012.08.003

Sassi, P. L., Caviedes-Vidal, E., Anton, R., and Bozinovic, F. (2010). Plasticity in Food Assimilation, Retention Time and Coprophagy Allow Herbivorous Cavies (*Microcavia Australis*) to Cope with Low Food Quality in the Monte Desert. *Comp. Biochem. Physiol. Part A: Mol. Integr. Physiol.* 155, 378–382. doi:10.1016/j.cbpa.2009.12.007

Sgaier, S., Millet, S., Villanueva, M., Berenshteyn, F., Song, C., and Joyner, A. (2005). Morphogenetic and Cellular Movements that Shape the Mouse CerebellumInsights from Genetic Fate Mapping. *Neuron* 45, 27–40. doi:10.1016/s0896-6273(04)00802-5

Shamsi, F., Piper, M., Ho, L.-L., Huang, T. L., Gupta, A., Streets, A., et al (2021). Vascular Smooth Muscle-Derived Trpv1+ Progenitors Are a Source of Cold-Induced Thermogenic Adipocytes. *Nat. Metab.* 3 (4), 485–495. doi:10.1038/s42255-021-00373-z

Shin, H., Ma, Y., Chanturiya, T., Cao, Q., Wang, Y., Kadegowda, A. K. G., et al (2017). Lipolysis in Brown Adipocytes Is Not Essential for Cold-Induced Thermogenesis in Mice. *Cell Metab.* 26 (5), 764–777. doi:10.1016/j.cmet.2017.09.002

Shin, N. R., Bose, S., Wang, J. H., Nam, Y. D., Song, E. J., Lim, D. W., et al (2020). Chemically or Surgically Induced Thyroid Dysfunction Altered Gut Microbiota in Rat Models. *Faseb j.* 34, 8686–8701. doi:10.1096/fj.201903091rr

Shu, L., Hoo, R. L. C., Wu, X., Pan, Y., Lee, I. P. C., Cheong, L. Y., et al (2017). A-FABP Mediates Adaptive Thermogenesis by Promoting Intracellular Activation of Thyroid Hormones in Brown Adipocytes. *Nat. Commun.* 8, 14147. doi:10.1038/ncomms14147

Škop, V., Guo, J., Liu, N., Xiao, C., Hall, K. D., Gavrilova, O., et al (2020). Mouse Thermoregulation: Introducing the Concept of the Thermoneutral Point. *Cell Rep* 31, 107501. doi:10.1016/j.celrep.2020.03.065

Škop, V., Xiao, C., Liu, N., Gavrilova, O., and Reitman, M. L. (2021). The Effects of Housing Density on Mouse thermal Physiology Depend on Sex and Ambient Temperature. *Mol. Metab.* 53, 101332. doi:10.1016/j.molmet.2021.101332

Smith, A. S., and Wang, Z. (2014). Hypothalamic Oxytocin Mediates Social Buffering of the Stress Response. *Biol. Psychiatry* 76, 281–288. doi:10.1016/j.biopsych.2013.09.017

Smith, R. E., and Roberts, J. C. (1964). Thermogenesis of Brown Adipose Tissue in Cold-Acclimated Rats. *Am. J. Physiology-Legacy Content* 206, 143–148. doi:10.1152/ajplegacy.1964.206.1.143

Smith, W. S., Broadbridge, R., East, J. M., and Lee, A. G. (2002). Sarcolipin Uncouples Hydrolysis of ATP from Accumulation of Ca2+ by the Ca2+-ATPase of Skeletal-Muscle Sarcoplasmic Reticulum. *Biochem. J.* 361, 277–286. doi:10.1042/bj3610277

Soave, O., and Brand, C. D. (1991). Coprophagy in Animals: a Review. *Cornell Vet.* 81, 357–364.

Solanes, G., Pedraza, N., Calvo, V., Vidal-Puig, A., Lowell, B. B., and Villarroya, F. (2005). Thyroid Hormones Directly Activate the Expression of the Human and Mouse Uncoupling Protein-3 Genes through a Thyroid Response Element in the Proximal Promoter Region. *Biochem. J.* 386, 505–513. doi:10.1042/bj20041073

Speakman, J. R., Chi, Q., Ołdakowski, Ł., Fu, H., Fletcher, Q. E., Hambly, C., et al. (2021). Surviving winter on the Qinghai-Tibetan Plateau: Pikas Suppress Energy Demands and Exploit Yak Feces to Survive winter. *Proc. Natl. Acad. Sci. U S A.* 118 (30), e2100707118. doi:10.1073/pnas.2100707118

Sukemori, S., Ikeda, S., Kurihara, Y., and Ito, S. (2003). Amino Acid, mineral and Vitamin Levels in Hydrous Faeces Obtained from Coprophagy-Prevented Rats. *J. Anim. Physiol. Anim. Nutr.* 87, 213–220. doi:10.1046/j.1439-0396.2003.00415.x

Sukhchuluun, G., Zhang, X.-Y., Chi, Q.-S., and Wang, D.-H. (2018). Huddling Conserves Energy, Decreases Core Body Temperature, but Increases Activity in Brandt's Voles (*Lasiopodomys Brandtii*). *Front. Physiol.* 9, 563. doi:10.3389/fphys.2018.00563

Suzuki, T. A., Martins, F. M., and Nachman, M. W. (2019). Altitudinal Variation of the Gut Microbiota in Wild House Mice. *Mol. Ecol.* 28, 2378–2390. doi:10.1111/mec.14905

Symonds, M. E., Pope, M., and Budge, H. (2015). The Ontogeny of Brown Adipose Tissue. *Annu. Rev. Nutr.* 35 (1), 295–320. doi:10.1146/annurev-nutr-071813-105330

Townsend, K. L., and Tseng, Y.-H. (2014). Brown Fat Fuel Utilization and Thermogenesis. *Trends Endocrinol. Metab.* 25 (4), 168–177. doi:10.1016/j.tem.2013.12.004

Vandewauw, I., De Clercq, K., Mulier, M., Held, K., Pinto, S., Van Ranst, N., et al (2018). A TRP Channel Trio Mediates Acute Noxious Heat Sensing. *Nature* 555, 662–666. doi:10.1038/nature26137

Virili, C., and Centanni, M. (2017). "With a Little Help from My Friends" - the Role of Microbiota in Thyroid Hormone Metabolism and Enterohepatic Recycling. *Mol. Cell. Endocrinol.* 458, 39–43. doi:10.1016/j.mce.2017.01.053

Virili, C., and Centanni, M. (2015). Does Microbiota Composition Affect Thyroid Homeostasis? *Endocrine* 49, 583–587. doi:10.1007/s12020-014-0509-2

Wang, J.-M., Zhang, Y.-M., and Wang, D.-H. (2006). Seasonal Thermogenesis and Body Mass Regulation in Plateau Pikas (*Ochotona Curzoniae*). *Oecologia* 149, 373–382. doi:10.1007/s00442-006-0469-1

Watanabe, M., Houten, S. M., Mataki, C., Christoffolete, M. A., Kim, B. W., Sato, H., et al (2006). Bile Acids Induce Energy Expenditure by Promoting Intracellular Thyroid Hormone Activation. *Nature* 439, 484–489. doi:10.1038/nature04330

Wen, J., Bo, T., Zhang, X., Wang, Z., and Wang, D. (2020). Thermo-TRPs and Gut Microbiota Are Involved in Thermogenesis and Energy Metabolism during Low Temperature Exposure of Obese Mice. *J. Exp. Biol.* 223, jeb218974. doi:10.1242/jeb.218974

Wen, J., Bo, T., Zhao, Z., and Wang, D. (2021). Role of Transient Receptor Potential Vanilloid-1 in Behavioral Thermoregulation of the Mongolian Gerbil *Meriones unguiculatus*. *Integr. Zool.* doi:10.1111/1749-4877.12587

Worthmann, A., John, C., Rühlemann, M. C., Baguhl, M., Heinsen, F.-A., Schaltenberg, N., et al (2017). Cold-induced Conversion of Cholesterol to Bile Acids in Mice Shapes the Gut Microbiome and Promotes Adaptive Thermogenesis. *Nat. Med.* 23, 839–849. doi:10.1038/nm.4357

Wu, W.-L., Adame, M. D., Liou, C.-W., Barlow, J. T., Lai, T.-T., Sharon, G., et al (2021). Microbiota Regulate Social Behaviour via Stress Response Neurons in the Brain. *Nature* 595, 409–414. doi:10.1038/s41586-021-03669-y

Yau, W. W., Singh, B. K., Lesmana, R., Zhou, J., Sinha, R. A., Wong, K. A., et al (2019). Thyroid Hormone (T(3)) Stimulates Brown Adipose Tissue Activation via Mitochondrial Biogenesis and MTOR-Mediated Mitophagy. *Autophagy* 15 (1), 131–150. doi:10.1080/15548627.2018.1511263

Zhang, X.-Y., Sukhchuluun, G., Bo, T.-B., Chi, Q.-S., Yang, J.-J., Chen, B., et al (2018). Huddling Remodels Gut Microbiota to Reduce Energy Requirements in a Small Mammal Species during Cold Exposure. *Microbiome* 6, 103. doi:10.1186/s40168-018-0473-9

Zhang, X.-Y., and Wang, D.-H. (2006). Energy Metabolism, Thermogenesis and Body Mass Regulation in Brandt's Voles (*Lasiopodomys Brandtii*) during Cold Acclimation and Rewarming. *Horm. Behav.* 50, 61–69. doi:10.1016/j.yhbeh.2006.01.005

Zhang, X. Y., Chi, Q. S., Liu, W., and Wang, D. H. (2016). Studies of Behavioral and Physiological Ecology in Mongolian Gerbils (*Meriones unguiculatus*). *Sci. Sin Vitae* 46, 120–128. doi:10.1360/n052015-00351

Zhao, J., Li, G., Lu, W., Huang, S., and Zhang, Z. (2020). Dominant and Subordinate Relationship Formed by Repeated Social Encounters Alters Gut Microbiota in Greater Long-Tailed Hamsters. *Microb. Ecol.* 79, 998–1010. doi:10.1007/s00248-019-01462-z

Zhao, Z.-J., and Wang, D.-H. (2006). Short Photoperiod Influences Energy Intake and Serum Leptin Level in Brandt's Voles (*Microtus Brandtii*). *Horm. Behav.* 49, 463–469. doi:10.1016/j.yhbeh.2005.10.003

Zhou, L., Li, X., Ahmed, A., Wu, D., Liu, L., Qiu, J., et al (2014). Gut Microbe Analysis between Hyperthyroid and Healthy Individuals. *Curr. Microbiol.* 69, 675–680. doi:10.1007/s00284-014-0640-6

Zima, A. V., Bovo, E., Bers, D. M., and Blatter, L. A. (2010). Ca^2+ Spark-dependent and -independent Sarcoplasmic Reticulum Ca^2+ Leak in normal and Failing Rabbit Ventricular Myocytes. *J. Physiol.* 588 (Pt 23), 4743–4757. doi:10.1113/jphysiol.2010.197913

Conflict of Interest: The authors declare that the research was conducted in the absence of any commercial or financial relationships that could be construed as a potential conflict of interest.

Publisher's Note: All claims expressed in this article are solely those of the authors and do not necessarily represent those of their affiliated organizations, or those of the publisher, the editors and the reviewers. Any product that may be evaluated in this article, or claim that may be made by its manufacturer, is not guaranteed or endorsed by the publisher.

Copyright © 2022 Zhang and Wang. This is an open-access article distributed under the terms of the Creative Commons Attribution License (CC BY). The use, distribution or reproduction in other forums is permitted, provided the original author(s) and the copyright owner(s) are credited and that the original publication in this journal is cited, in accordance with accepted academic practice. No use, distribution or reproduction is permitted which does not comply with these terms.

frontiers | Frontiers in Physiology

ORIGINAL RESEARCH
published: 28 April 2022
doi: 10.3389/fphys.2022.840179

Protein Restriction in the Peri-Pubertal Period Induces Autonomic Dysfunction and Cardiac and Vascular Structural Changes in Adult Rats

Anna Rebeka Oliveira Ferreira[1], *Maiara Vanusa Guedes Ribeiro*[1], *Maria Natalia Chimirri Peres*[1], *Silvano Piovan*[1], *Géssica Dutra Gonçalves*[1], *Lucas Paulo Jacinto Saavedra*[1], *Juliana Nunes de Lima Martins*[2], *Marcos Divino Ferreira Junior*[3], *Keilah Valeria Naves Cavalcante*[3], *Gabriel kian Guimarães Lopes*[1], *Mariane Carneiro*[1], *Douglas Lopes Almeida*[1], *Rodrigo Mello Gomes*[3], *Jurandir Fernando Comar*[2], *James Andrew Armitage*[4], *Paulo Cezar de Freitas Mathias*[1†] *and Kesia Palma-Rigo*[1,5*†]

[1]*Laboratory of Secretion Cell Biology, Department of Biotechnology, Genetics and Cell Biology, State University of Maringa, Maringa, Brazil,* [2]*Laboratory of Liver Metabolism and Radioisotopes, Department of Biochemistry, State University of Maringa, Maringa, Brazil,* [3]*Laboratory of Endocrine Physiology and Metabolism, Department of Physiological Sciences, Federal University of Goias, Goiania, Brazil,* [4]*School of Medicine, Deakin University, Waurn Ponds, VIC, Australia,* [5]*Adventist College of Parana, Ivatuba, Brazil*

Perturbations to nutrition during critical periods are associated with changes in embryonic, fetal or postnatal developmental patterns that may render the offspring more likely to develop cardiovascular disease in later life. The aim of this study was to evaluate whether autonomic nervous system imbalance underpins in the long-term hypertension induced by dietary protein restriction during peri-pubertal period. Male Wistar rats were assigned to groups fed with a low protein (4% protein, LP) or control diet (20.5% protein; NP) during peri-puberty, from post-natal day (PN) 30 until PN60, and then all were returned to a normal protein diet until evaluation of cardiovascular and autonomic function at PN120. LP rats showed long-term increased mean arterial pressure (p = 0.002) and sympathetic arousal; increased power of the low frequency (LF) band of the arterial pressure spectral (p = 0.080) compared with NP animals. The depressor response to the ganglion blocker hexamethonium was increased in LP compared with control animals (p = 0.006). Pulse interval variability showed an increase in the LF band and LF/HF ratio (p = 0.062 and p = 0.048) in LP animals. The cardiac response to atenolol and/or methylatropine and the baroreflex sensitivity were similar between groups. LP animals showed ventricular hypertrophy (p = 0.044) and increased interstitial fibrosis (p = 0.028) compared with controls. Reduced protein carbonyls (PC) (p = 0.030) and catalase activity (p = 0.001) were observed in hearts from LP animals compared with control. In the brainstem, the levels of PC (p = 0.002) and the activity of superoxide dismutase and catalase (p = 0.044 and p = 0.012) were reduced in LP animals, while the levels of GSH and total glutathione were higher (p = 0.039 and p = 0.038) compared with NP animals. Protein restriction during peri-pubertal period leads to hypertension later in life accompanied by sustained sympathetic

OPEN ACCESS

Edited by:
James Todd Pearson, National Cerebral and Cardiovascular Center, Japan

Reviewed by:
Daniel Penteado Martins Dias, Barão de Mauá University Center, Brazil
Luciano Gonçalves Fernandes, Universidade Federal Rural do Rio de Janeiro, Brazil

***Correspondence:**
Kesia Palma-Rigo
kesiapalmarigo@hotmail.fr

[†]These authors have contributed equally to this work

Specialty section:
This article was submitted to Integrative Physiology, a section of the journal Frontiers in Physiology

Received: *20 December 2021*
Accepted: *22 March 2022*
Published: *28 April 2022*

Citation:
Ferreira ARO, Ribeiro MVG, Peres MNC, Piovan S, Gonçalves GD, Saavedra LPJ, Martins JNdL, Junior MDF, Cavalcante KVN, Lopes GkG, Carneiro M, Almeida DL, Gomes RM, Comar JF, Armitage JA, Mathias PCdF and Palma-Rigo K (2022) Protein Restriction in the Peri-Pubertal Period Induces Autonomic Dysfunction and Cardiac and Vascular Structural Changes in Adult Rats. Front. Physiol. 13:840179. doi: 10.3389/fphys.2022.840179

arousal, which may be associated with a disorganization of brain and cardiac redox state and structural cardiac alteration.

Keywords: low protein diet, hypertension, autonomic nervous system, developmental origins of health and disease, peri-puberty

1 INTRODUCTION

The World Health Organization (WHO) estimated that there are 1.28 billion hypertensive people in the world predisposing this population to stroke, myocardial infarction, heart failure and renal failure (WHO, 2021b). In 2019, 17.9 million people died from cardiovascular disease, with over three quarters of these individuals being based in low- and middle-income countries (WHO, 2021a). The projection for 2030 is that approximately 23.3 million people will die from cardiovascular disease across the globe, reinforcing the fact that hypertension is a public health problem associated with vast social and economic consequences (Mathers and Loncar, 2006).

There is now clear evidence that environmental insults, including dietary restriction or imbalance, during sensitive windows of development increases the susceptibility to noncommunicable chronic diseases in adulthood, including hypertension (Barker et al., 2002; Barker, 2004). This process, termed the Developmental Origins of Health and Disease, or developmental programming is not new, however the mechanisms underpinning the programming of hypertension are still being elucidated. Experimental programming models of malnutrition or nutritional imbalance during the perinatal period show that arterial hypertension may be associated with increase in vascular sympathetic tone (Mizuno et al., 2013; Prior et al., 2014; Barros et al., 2015; Paulino-Silva and Costa-Silva, 2016; Lim et al., 2021) as well as redox disorganization in the brainstem (Ferreira et al., 2016; Barrand et al., 2017; Ferreira et al., 2019), and heart (Nascimento et al., 2014). Furthermore, the hypertension may trigger a cardiac compensatory response, leading to cardiomyocyte hypertrophy, and greater collagen deposition (Rossini et al., 2017; De Jong et al., 2018; Assalin et al., 2019).

Post-weaning until the end of adolescence has also been established as a critical window of development. We have previously demonstrated metabolic disfunction in adult animals exposed to dietary protein restriction during puberty/adolescence (De Oliveira et al., 2013; De Oliveira et al., 2018). Furthermore, experimental studies in models of malnutrition in post-weaning/peri-puberty indicate that hypertension (Loss et al., 2007; Penitente et al., 2007; Murca et al., 2012; Penitente et al., 2014) and vascular sympathetic hyperactivity (Martins et al., 2011) occur immediately after the exposure period, and these may be associated with a central glutamate disorganization (Rodrigues et al., 2012). However, the long-term cardiovascular dysfunction in this model has not yet been evaluated, pointing to a hole in the literature concerning the programming of hypertension induced by insults during adolescence or the peri-pubertal period. The hypothesis of this study is that exposure to a low-protein diet during the peri-pubertal period induces hypertension in adulthood which is dependent on autonomic nervous system dysfunction.

2 METHODS

The experimental protocol was approved by the Research Ethics Committee for Animal Use and Experimentation at the State University of Maringa (protocol number 4833210519). Male Wistar rats were obtained from the Central Animal Facility of the State University of Maringa and kept in the Sectorial Vivarium of the Department of Biotechnology, Genetics and Cell Biology for adaptation for 5 days. Animals were housed three per cage (polypropylene cages with 40 × 34 × 17 cm) remaining under controlled temperature (22 ± 2°C) and photoperiod (07:00–19:00, light cycle) conditions, with *ad libtum* access to water and food.

At post-natal day (PN) 30 animals were assigned into two groups; those fed an isocaloric low-protein diet palletized (4% protein; LP) or a balanced commercial control diet (20.5% protein; Nuvital®, Curitiba/PR, Brazil; NP; **Table 1**) until PN60. After the dietary manipulation period, from PN60 until PN120, all animals were fed the same commercial control diet (20.5% protein; Nuvital®, Curitiba/PR, Brazil).

At PN120 both groups underwent evaluation of the cardiovascular and autonomic nervous systems; biochemical, food intake, body composition, histological evaluation; and biochemical assays of protein expression and oxidative stress.

2.1 Body Composition and Food Intake

Throughout the experimental period, food consumption was recorded three times a week. Weekly food intake was calculated according to the formula [absolute consumption of the week x 100/average weekly weight of the box]. Bodyweight was recorded on a weekly basis.

At PN 120 a cohort of animals was fasted overnight and then euthanized with a guillotine. Overnight fasting was performed in order to match metabolic conditions between the animals for subsequent biochemical analysis. Bodyweight was recorded, naso-anal length evaluated and fat depots (retroperitoneal, mesenteric) were dissected and weighed.

TABLE 1 | Composition of the isocaloric low- and normal-protein diets.

Diet components	Normal-protein (20.5%)	Low-protein (4.0%)
Sucrose	12.72	20.00
Cornstarch	52.75	64.25
Casein (88% protein)	23.33	4.55
Mix of mineral salts	3.20	3.20
Mix of vitamins	1.60	1.60
Soybean oil	4.80	4.80
Fish oil	1.60	1.60
Total (g)	100.0	100.0

2.2 Biochemical Parameters

Total blood was collected, and the serum separated for the biochemical dosages. Glycemia was quantified by the glucose oxidase method by spectrophotometry (semi-automatic biochemical analyzer, BIO 200FL, Bio Plus®, São Paulo/SP, Brazil), using a commercial kit (Gold Analisa®, Belo Horizonte/MG, Brazil). Total cholesterol was measured by the colorimetric method of cholesterol oxidase and triglycerides were measured using the colorimetric method of glycerol-3-phosphate oxidase using commercial kits (Gold Analisa®, BeloHorizonte/MG, Brazil). Both readings were performed on spectrophotometry equipment (Semi-automatic biochemical analyzer, BIO200FL, Bio Plus®, São Paulo/SP, Brazil).

HDL-cholesterol was determined after precipitation of chylomicrons and low-density lipoproteins with a commercial kit (Gold Analisa®, BeloHorizonte/MG, Brazil) and subsequent determination of HDL-cholesterol using the method described above for the measurement of total cholesterol.

2.3 Arterial and Venous Catheterization

After anesthesia (ketamine-xylazine; 75 mg + 15 mg/kg, i.p.) two cannulae (P10 -Micro-Renathane connected to P50 cannulae (ClearTygon)) were inserted; one into the femoral artery, for monitoring of arterial pressure, and one in the femoral vein, for drug administration. At the end of surgeries, animals received anti-inflammatory analgesic (Meloxican, 0.4 mg/kg, i.v.) and antibiotic (Enrofloxacin 5 mg/kg, i.v.) cover, the lines were heparinized (250 units/ml) after arterial catheter implantation and animals kept in individual boxes for recovery (Barros et al., 2015; Paulino-Silva and Costa-Silva, 2016; Simas et al., 2018). After 24 h of recovery, the protocol for assessment of cardiovascular function and its autonomic modulation was carried out over a period of 3 days.

2.4 Arterial Pressure Recording

After 1 hour of room adaptation, baseline arterial pressure records were performed for 30 min on each of the 3 days of the experimental protocol. Following baseline recording, intravenous injections were performed according to the protocol described below. Experiments were carried out between 10:00 and 14:00 in conscious free-moving animals in order to avoid the influence of circadian variations on cardiovascular autonomic modulation and to obtain recordings that were not subject to a high degree of locomotor activity.

The arterial cannula was connected to a pressure transducer (MLT0670, ADInstruments, Dunedin, and New Zealand) which was connected to a recording system (Insight, Ribeirão Preto, Brazil) that uses the DI 158 System for signal acquisition and analog-to-digital signal conversion (WinDaq lite, DataQinstruments, United States of America). Recordings were sampled at 1000 Hz.

Data were pre-analyzed using specific Advanced CODAS software (Data Q instruments, United States of America, https://www.dataq.com/products/windaq/, paid software) to objectively identify stable periods of recording and exclusion of erratic signals. The baseline values of Systolic Arterial Pressure (SAP), Diastolic (DAP), Mean (MAP) and pulse interval (PI) were transferred to a spreadsheet for analysis (Microsoft Excel, Redmond, WA, EUA) over 10 min of recording under stable conditions. Heart rate (HR) was calculated from the pulse interval (ms), considering formula (60000/PI in ms) and the pulse pressure was calculated through the difference between SAP and DAP.

2.5 Cardiovascular Variability and Baroreflex Sensitivity

The estimation of autonomic impact on baseline AP and PI was evaluated in the frequency domain through the analysis of MAP and PI variability, using CardioSeries 2.4 Software (USP - Ribeirão Preto, http://www.danielpenteado.com/, freely available). The power spectra were calculated using a fast Fourier transform (FFT) as previously describe (Santos et al., 2012; Silva et al., 2015; Speretta et al., 2016). Briefly, Beat-by-beat series obtained from pulsatile arterial pressure recordings were converted to data points every 100 ms using cubic spline interpolation (10 Hz). The interpolated series were divided into half-overlapping sequential sets of 512 data points (51.2 s). Before calculation of the spectral power density, segments were visually inspected, and nonstationary data were not taken into consideration. To confirm that the visual inspection of the time series was properly performed, a Hanning window was used to attenuate side effects and all segments had the spectrum computed using a direct FFT algorithm for discrete time series. All segments were visually inspected for abnormal spectra. The low frequency band of the MAP (LF-MAP: 0.2–0.75 Hz of the spectrum) was used as an estimate of vascular sympathetic activity whilst the low frequency band of PI (LF-PI: 0.2–0.75 Hz of the spectrum) estimates cardiac sympathetic activity. The high frequency band of the PI (HF-PI: 0,75–3 Hz of the spectrum) was used as an estimate of cardiac parasympathetic activity (Pagani et al., 1986; Kuwahara et al., 1994; De Andrade et al., 2014; Barros et al., 2015; Paulino-Silva and Costa-Silva, 2016). Sympathovagal balance was estimated by the LF/HF ratio in the PI spectrum (Barros et al., 2015; Paulino-Silva and Costa-Silva, 2016). Total variability of PI (Dobrek et al., 2013) was calculated from the sum of all the PI spectrum.

The spontaneous cardiac baroreflex sensitivity was evaluated through the sequence method using CardioSeries 2.4 Software (http://www.danielpenteado.com/, freely available), which calculates the spontaneous baroreflex through the angle of the linear regression between MAP and PI, with a delay of 3 heartbeats. Sequences with at least 3 intervals were considered only if the correlation of the coefficients was very high (>0.85). The spontaneous cardiac baroreflex sensitivity was estimated by the average of significant angles (Silva et al., 2015). The baroreflex effectiveness index (BEI) was calculated by the ratio between the total number of PI/MAP sequences and the total number of MAP ramps (Di Rienzo et al., 2001).

2.6 Sympathovagal Tone and Intrinsic Heart Rate

Baseline recordings of arterial pressure were performed on the first and second days of the experimental protocol. Then, methylatropine (3 mg/kg; i.v.; Sigma-Aldrich, San Luis, MO, EUA), a muscarinic antagonist, was used to estimate parasympathetic tone. After recovery, a selective β1 adrenergic antagonist, atenolol (4 mg/kg; i.v.; Sigma-Aldrich, San Luis, MO, EUA), was used for the assessment of cardiac sympathetic tone (Simas et al., 2018).

Heart rate was recorded for 15 min after injection of the first drug and, after stabilization, the second drug was infused to promote autonomic blockade. On the following day, the application sequence was performed in reversed order (Barros et al., 2015).

Analysis of the parasympathetic and sympathetic tone was achieved via the HR response to methylatropine and atenolol, respectively. Intrinsic HR was analyzed after each sequence of applications and averaged over the 2 days of the protocol (Barros et al., 2015; Simas et al., 2018).

2.7 Estimate of Induced Baroreflex Sensitivity

On the third day of the protocol, the induced baroreflex sensitivity was estimated by measuring responses to a vasopressor dose of the α1 adrenergic agonist phenylephrine (8 μg/kg; i. v.; Sigma-Aldrich, San Luis, MO, EUA). After a 20-minutes-recovery period a vasodepressor dose of intravenous sodium nitroprusside was delivered (50 μg/kg; i.v.; Sigma-Aldrich, San Luis, MO, EUA). The baroreflex sensitivity index was calculated from the HR variation as a function of MAP (ΔHR/ΔMAP) (Valenti et al., 2009; Valenti et al., 2011).

2.8 Vascular Sympathetic Tone

On the third day, 20 min after the evaluation of the induced baroreflex sensitivity and subsequent cardiovascular stabilization, an intravenous injection of a ganglion blocker, hexamethonium (30 mg/kg; i.v.; Sigma-Aldrich, San Luis, MO, EUA), was performed to assess the vascular sympathetic contribution to MAP (Radaelli et al., 2006). The vascular sympathetic tone was estimated by the MAP response to the ganglion blocker (Barros et al., 2015).

2.9 Oxidative Stress Parameters Assays

A separate cohort of animals was fasted for 12 hs then euthanized with guillotine (8:00–12:00) and the brain immediately removed. The brainstem was separated, snap-frozen and stored in liquid nitrogen. The thoracic cavity was opened, and the heart was removed, washed with 0.9% saline to remove blood, then snap frozen and stored in liquid nitrogen for storage at −80°C.

Frozen brainstem, and heart tissues were separately homogenized in van Potter-Elvehjem homogenizers with seven volumes of ice-cold 0.1 M potassium phosphate buffer (pH 7.4) and an aliquot was separated as total homogenate. The remaining homogenate was centrifuged (11,000 g/15 min) and the supernatant separated as soluble fractions of the homogenate.

2.9.1 Protein Carbonyl Groups

The levels of protein carbonyl groups were measured spectrophotometrically using 2,4-dinitrophenylhydrazine ($\varepsilon_{370} = 22 \times 10^3\ M^{-1}\ cm^{-1}$) and the results were expressed as nmol (mg protein)$^{-1}$ (Levine et al., 1990).

2.9.2 Glutathione Assay

Reduced glutathione (GSH) and oxidized glutathione (GSSG) were measured in the total homogenate. GSH and GSSG contents were measured spectrofluorimetrically (excitation at 350 nm and emission at 420 nm) by means of o-phthalaldehyde (OPT) assay as previously described (Hissin and Hilf, 1976). The fluorescence was estimated as GSH. For GSSG assay, samples were pre-incubated with 10 mM N-ethylmaleimide for 20 min and then with a mixture containing 1 M NaOH and 0.4 μM OPT to detect the fluorescence. Standard curves were prepared with GSH or GSSG and the contents were expressed as nmol (mg protein)$^{-1}$.

2.9.3 Enzyme Activities

The activity of catalase (CAT) was estimated by measuring the change in absorbance at 240 nm using H_2O_2 as substrate and expressed as μmol min^{-1} (mg protein)$^{-1}$ (Bergmeyer, 1974). Superoxide dismutase (SOD) activity was estimated by its capacity to inhibit pyrogallol autoxidation in an alkaline medium. The latter was measured at 420 nm (Marklund and Marklund, 1974). One SOD unit was considered the quantity of enzyme that was able to promote 50% inhibition and results are expressed as arbitrary units (mg protein)$^{-1}$.

Protein content: total protein was assayed in the total homogenate and supernatant using the Folin phenol reagent (Lowry et al., 1951).

2.10 Histological Analysis of the Heart

After euthanasia with guillotine (8:00–12:00) the heart was immediately removed and frozen for histological and molecular analyses. Heart samples were fixed in formalin, dehydrated in graded alcohols and embedded in histological paraffin (Histopar, Easypath, São Paulo, Brazil). Blocks were sectioned on a microtome (RM2245, Leica Microsystems, Wetzlar, Germany) as 6 μm thick non-serial sections and stained with Picrosirius Red, for measurement of total collagen. Analysis of cardiomyocyte diameter was performed on Hematoxylin and Eosin stained sections.

Photomicrographs were taken on light microscope coupled to a digital camera (DM500 plus ICC50 HD, Leica Microsystems, Wetzlar, Germany), at x1000 for the measurement of the cardiomyocytes (100 cardiomyocytes/group), x100 for the measurement of perivascular fibrosis (25 images/group) and x100 for the measurement of interstitial fibrosis (50 images/group). Photomicrographs of cross sections of the left ventricular cardiomyocytes were analyzed. The distance between the upper and lower parts of the plasma membrane of each cardiomyocyte in a set field was measured.

TABLE 2 | List of antibodies used for western immunoblotting.

Antibody	Manufacturer and Catalog	Source	Dilution
Anti-B1 AR	Thermo Fisher Scientific, MA United States (PA1-049)	Mouse monoclonal	1:1000
Anti α1 AR	Thermo Fisher Scientific, MA United States (PA1-047)	Mouse monoclonal	1:1000
Anti M1 R	Sigma Aldrich, MO United States (M9808)	Rabbit monoclonal	1:1000
Anti mTor	Thermo Fisher Scientific, MA United States	Mouse polyclonal	1:1000
Anti-SOD	Santa Cruz, CA, United States (SC-11407)	Rabbit polyclonal	1:1000
Anti-CAT	LifeSpan, WA, United States (LS-C21346)	Rabbit polyclonal	1:1000
Anti-GAPDH	Santa Cruz, CA, United States (SC-25778)	Rabbit polyclonal	1:1000

TABLE 3 | Effects of dietary protein restriction in peri-pubertal period on biometric and biochemical parameters.

Biometric and biochemical parameters	NP	LP	*p* value
Body weight (g)	398 ± 589	359 ± 8.04	0.0003***
Body length (cm)	23.96 ± 0.09	22.95 ± 0.19	0.0002***
Mesenteric fat pad (g/100 g bw)	0.70 ± 0.03	0.67 ± 0.02	0.580
Retroperitoneal fat pad (g/100 g bw)	1.29 ± 0.05	1.27 ± 0.05	0.765
Blood glucose (mmol L^{-1})	89 ± 2.61	101 ± 3.11	0.008**
Triglycerides (μmol L^{-1})	126 ± 9.48	128 ± 4.59	0.859
Total cholesterol (μmol L^{-1})	89 ± 3.38	82 ± 1.55	0.087
HDL - cholesterol (μmol L-)	53 ± 1.64	57 ± 2.57	0.195

NP: Normal protein diet; LP: Low protein diet; n = 8–27 animals per group. Values expressed as mean ± SEM ***p < *0.001*, **p < *0.01*, and *p < *0.05 indicate statistical significance (Student's T test).*

The mean cardiomyocyte diameter was calculated for each animal. Photomicrographs containing collagen labeling in the fields with sectioned arterioles were analyzed. The perivascular fibrosis index (PFI) was determined by dividing the total area of fibrosis and the area of the vessel lumen.

Interstitial fibrosis was analyzed by stereology, using a mesh composed of 594 test points. The percentage of interstitial fibrosis was calculated by the proportion between the number of points that reach the red, marked collagen, and the total test points. The mean of both PFI and Interstitial Fibrosis for each animal were calculated. Cardiomyocyte diameter and PFI analyzes were performed using ICY software (Institut Pasteur, Paris, France, https://icy.bioimageanalysis.org/, freely available). Interstitial fibrosis was assessed using Image Pro Plus v6 (Media Cybernetics, MD, United States, https://www.mediacy.com/imageproplus, paid software).

2.11 Western Blotting in Heart

Left ventricle samples, collected after euthanasia with guillotine (8:00–12:00) and frozen for histological and molecular analyses, were homogenized in RIPA lysis buffer with a protease inhibitor cocktail. The supernatant total protein content was quantified by Bradford assay. Samples were denatured in Laemmli buffer at 95°C for 5 min then aliquots of 20 μg of proteins from each sample were subjected to separation by SDS-PAGE. Protein separation was accompanied by a positive control with pre-determined staining (EZ-Run, Fisher BioReagents, Göteborg, SE). Separated proteins on the gel were transferred to nitrocellulose membranes (Amersham Protran, GE Healthcare, Little Chalfont, BUX, United Kingdom) in a wet transfer system, soaked in transfer buffer then the membranes were incubated with a blocking buffer, and subsequently incubated with primary antibodies (**Table 2**). Membranes were gently washed and incubated with HRP-conjugated secondary antibody, and covered with chemiluminescence detection solution (Amersham ECL, GE Healthcare, Little Chalfont, BUX, United Kingdom). Chemiluminescence was detected by an image documentation system (ImageQuant LAS 600 series, GE Healthcare, Chicago, IL, United States). The intensity of the resultant bands was quantified by relative optical density using FIJI software (ImageJ, NIH, Cambridge, MA, United States, https://imagej.net/software/fiji/downloads, freely available). GAPDH (Glyceraldehyde-3-Phosphate Dehydrogenase) was used as load control.

2.12 Statistical Analysis

The data are presented as mean ± standard error of the mean (SEM). The statistical analysis was performed after analysis of data distribution (Shapiro Wilk test). Results are considered significant when $p < 0.05$. GraphPad Prism 6 (GraphPad software, La Jolla, CA, United States, https://www.graphpad.com/scientific-software/prism/, paid software) was used for graphical representation and statistical analysis and the comparison between the groups was performed using the Student's T test or two-way ANOVA with time and diet as independent factors.

3 RESULTS

3.1 Food Intake, Body Weight, and Growth Parameters

Animals given a low protein diet during peri-puberty showed reduced food intake (LP: 608 ± 22.3 vs. NP: 699 ± 25 g/100 g BW; $p = 0.021$; **Figure 1B**.) over the peri-pubertal period, which also

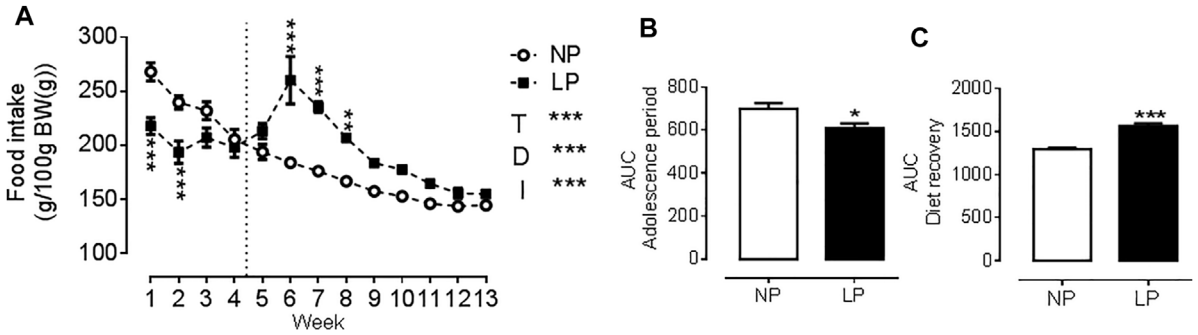

FIGURE 1 | Food consumption throughout the experimental protocol. Food consumption **(A)**, Area under the curve of food consumption during the peri-pubertal period **(B)**, Area under the curve of food consumption during the dietary recovery period **(C)**, $n = 18$ animals per group. NP, normal protein diet; LP, low protein diet; I, interaction between diet and time, AUC, area under the curve. Values presented as mean ± SD. ***$p < 0.001$, **$p < 0.01$, and *$p < 0.05$ indicate statistical significance (Two-way ANOVA or Student's T test).

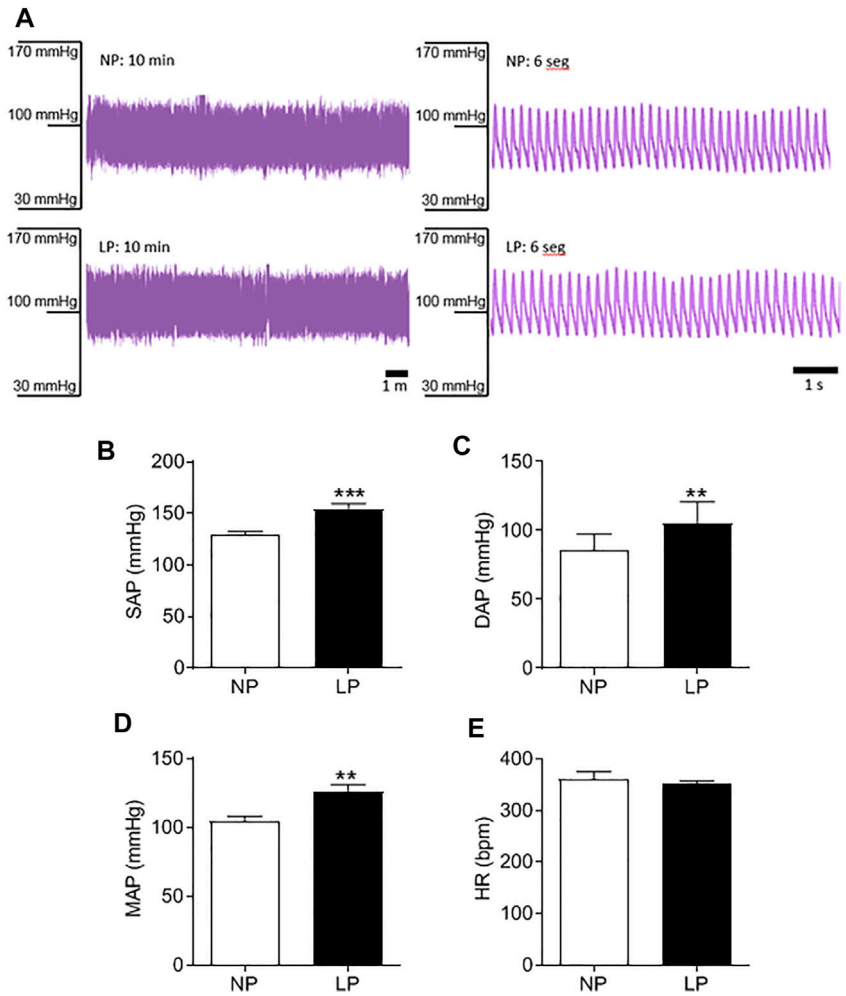

FIGURE 2 | Basal arterial pressure in 120 days old animal. Representative blood pressure traces of NP and LP animals in basal conditions **(A)**, Systolic arterial pressure **(B)**, diastolic arterial pressure **(C)**, mean arterial pressure **(D)** and heart rate **(E)**, $n = 9$–10 animals per group. NP, normal protein diet; LP, low protein diet. Values presented as mean ± SD ***$p < 0.001$, **$p < 0.01$, and *$p < 0.05$ indicate statistical significance (Student's T test).

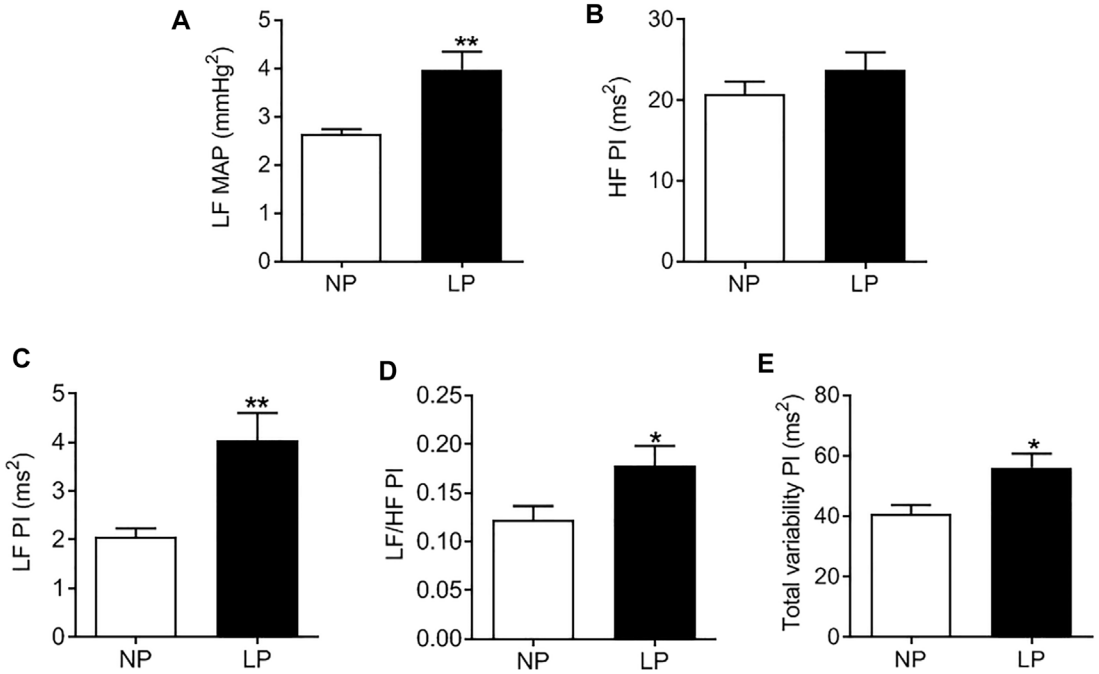

FIGURE 3 | Spectral analysis of arterial pressure and pulse interval in 120-day-old animals at baseline conditions. Low frequency zone of mean arterial pressure **(A)**, high frequency zone of pulse interval **(B)**, low frequency zone of pulse interval **(C)**, low frequency/high frequency pulse interval **(D)** ratio, total variability of the pulse interval (E), n = 7–9 animals per group. NP, normal protein diet; LP, low protein diet. Values presented as mean ± SD ***$p < 0.001$, **$p < 0.01$, and *$p < 0.05$ indicate statistical significance (Student's T test).

resulted in a reduction of total caloric intake of the same magnitude. In the period of dietary recovery, there was a rapid increase in food intake (LP: 1567 ± 28.7 vs. NP: 1295 ± 20.7 g/100 g BW; $p = 0.001$; **Figure 1C**.) but despite this catch-up growth LP animals had a lower body weight (LP: 359 ± 8.04 vs. NP: 398 ± 5.89 g; $p = 0.003$), with a reduction in naso-anal length (LP: 22.9 ± 0.19 vs. NP: 23.9 ± 0.09 cm; $p = 0.0002$) compared with controls at PN120 (**Table 3**).

LP animals showed an increase in fasting blood glucose (LP: 101.5 ± 3.11 vs. NP: 89.6 ± 2.61 mg/dl; $p = 0.0081$) compared with controls, but there was no change in the lipid profile. There was no significant difference in the mesenteric or retroperitoneal fat mass between groups (**Table 3**).

3.2 Arterial Pressure, Pulse Pressure, and Heart Rate

Good quality blood pressure traces were achieved for all animals (representative data shown in **Figure 2A**). LP animals showed an increase in SAP (LP: 154 ± 4.84 vs. NP: 129 ± 3.08 mmHg; $p = 0.0003$; **Figure 2B**), DAP (LP: 105 ± 4.93 vs. NP: 85 ± 3.69 mmHg; $p = 0.005$; **Figure 2C**) and MAP (LP: 126 ± 4.93 vs. NP: 104 ± 3.37 mmHg; $p = 0.002$; **Figure 2D**). There was no significant difference in heart rate between groups (**Figure 2E**).

3.3 Cardiovascular Variability

LP animals showed an increase in the LF-MAP band, indicating an increase in vascular sympathetic activity (LP: 3.9 ± 0.37 vs. NP: 2.8 ± 0.34 mmHg^2; $p = 0.080$; **Figure 3A**). There was no change in the HF-PI band (**Figure 3B**). The LP group showed an increase in the LF-PI band (LP: 4.04 ± 0.56 vs. NP: 2.3 ± 0.28 ms^2; $p = 0.062$; **Figure 3C**) and in the LF/HF ratio (LP: 0.17 ± 0.020 vs. NP: 0.12 ± 0.014; $p = 0.048$; **Figure 3D**) indicating an increase in sympathetic activity. The total PI variability (LP: 56 ± 4.49 vs. NP: 40 ± 3.03 ms^2; $p = 0.011$; **Figure 3E**) was also increased in LP animals.

3.4 Sympathovagal Tone and Intrinsic Heart Rate

Cardiac vagal tone, evaluated with methylatropine, and cardiac sympathetic tone, evaluated with atenolol, were similar between groups. The intrinsic heart rate, assessed after double autonomic blockade with methylatropine and atenolol, was also not altered in the LP group compared with control animals (**Table 4**).

3.5 Vascular Sympathetic Tone

Representative records of the depressor response to hexamethonium, a ganglionic blocker, are shown in **Figure 4A**. LP animals showed a greater decrease in MAP (LP: −46 ± 3.11 vs. NP: −34 ± 2.63 mmHg; $p = 0.006$; **Figure 4B**) and amplitude of the LF-MAP zone after injection of hexamethonium (LP: −2.93 ± 0.41 vs. NP: −1.86 ± 0.21 mmHg^2; $p = 0.032$; **Figure 4C**) compared with the control group. LP animals showed an increase in the pressure response to phenylephrine (LP: 76 ± 4.14 vs. NP: 60 ± 6.23 mmHg; $p = 0.049$), with no change in the pressure response to sodium nitroprusside (**Table 4**).

TABLE 4 | Cardiovascular autonomic evaluation after drug injection.

Parameters	NP	LP	*p* value
Control of autonomic tone			
Δ HR after methylatropine, bpm	86.20 ± 4.61	82 ± 8.11	0.735
Δ HR after atenolol, bpm	–57 ± 7.73	–46 ± 4.22	0.208
Intrinsic heart rate, bpm	347 ± 7.52	357 ± 5.37	0.281
Baroreflex sensitivity			
BEI	0.20 ± 0.014	0.22 ± 0.018	0.391
GAIN (spontaneous baroreflex)	7.13 ± 0.79	6.21 ± 0.37	0.311
Bradycardic response, bpm/mmHg	–2.21 ± 0.40	–2.13 ± 0.25	0.802
Tachycardic response, bpm/mmHg	–3.03 ± 0.60	–3.40 ± 0.37	0.689
Δ SAP after phenylephrine, mmHg	60 ± 6.23	76 ± 4.14	0.049*
Δ SAP after sodium nitroprusside, mmHg	–45.83 ± 3.615	–45.37 ± 3.11	0.926

NP: Normal protein diet; LP: Low protein diet; Parasympathetic and sympathetic activity induced by methylatropine and atenolol (ΔHR, after application stabilization - basal HR); Intrinsic heart rate after double blocking with methylatropine and atenolol; Baroreflex effectiveness index (BEI); Gain baroreflex (GAIN); Baroreflex induced by phenylephrine and calculated sodium nitroprusside (ΔHR/ΔMAP); Pressure response to phenylephrine and sodium nitroprusside; n = 9–18 animals per group. Values exposed in mean ± SEM ***p < *0.001*, **p < *0.01*, and *p < *0.05 indicating statistical significance (Student T test).*

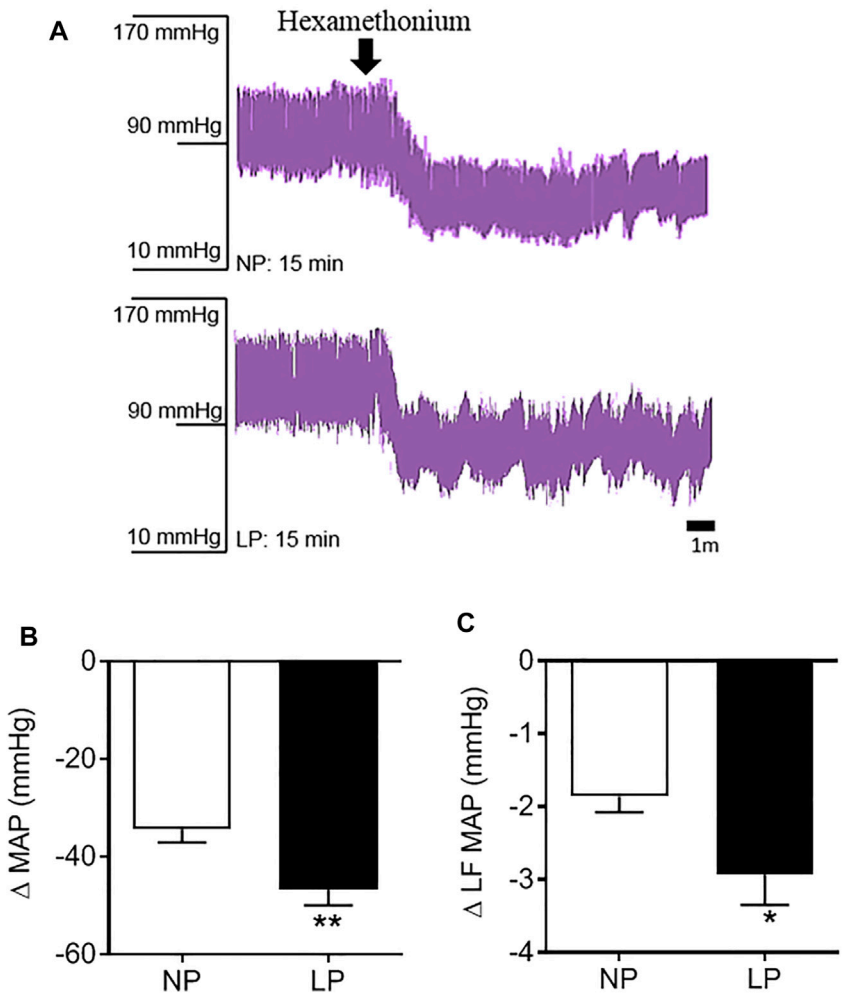

FIGURE 4 | Pressure response to hexamethonium. Representative records of the depressor response to hexamethonium **(A)**, Change in mean arterial pressure **(B)**, and the low frequency zone of mean arterial pressure in response to hexamethonium **(C)**, *n* = 10–13 animals per group. NP, normal protein diet; LP, low protein diet. Values presented as mean ± SD ***$p < 0.001$, **$p < 0.01$, and *$p < 0.05$ indicate statistical significance (Student's T test).

TABLE 5 | Oxidative stress in brainstem.

Parameters	NP	LP	*p* value
Carbonyl protein groups	10.06 ± 0.55	6.69 ± 0.52	0.002**
GSH (nmol mg^{-1})	10.11 ± 0.62	12.91 ± 0.85	0.039*
GSSG (nmol mg^{-1})	0.15 ± 0.01	0.16 ± 0.01	>0.999
GSH + 2xGSSG (nmol mg^{-1})	10.41 ± 0.62	13.23 ± 0.85	0.038*
GSH/GSSG	67.4 ± 4.1	80.6 ± 5.3	0.101
SOD (U mg^{-1})	1.25 ± 0.03	1.09 ± 0.06	0.044*
Catalase (μmol·min^{-1} mg^{-1})	30.5 ± 1.5	23.8 ± 1.5	0.012*

*NP: Normal protein diet; LP: Low protein diet; Carbonylated proteins, reduced glutathione (GSH), oxidized glutathione (GSSG) and activity of catalase (CAT) and superoxide dismutase enzymes (SOD); n = 4–7 animals per group. Values exposed in mean ± SEM ***p < 0.001, **p < 0.01, and *p < 0.05 indicating statistical significance (Student T test).*

3.6 Sensitivity of Cardiac Baroreflex

The LP group showed no change in reflex bradycardia induced by phenylephrine or reflex tachycardia after sodium nitroprusside injection. The spontaneous baroreflex assessed by the BEI and gain, was similar between the groups (**Table 4**).

3.7 Oxidative Stress in the Brainstem

The levels of protein carbonyl groups were lower in LP animals compared with control rats (LP: 6 ± 0.52 vs. NP: 10 ± 0.55 mg/protein; $p = 0.002$). The activities of SOD (NP: 1.25 ± 0.03 vs. LP: 1.09 ± 0.06 U mg^{-1}; $p = 0.044$) and CAT (LP: 23 ± 1.47 vs. NP: 30 ± 1.47 μmol min^{-1}·mg^{-1}; $p = 0.012$) were lower in the brainstem of rats fed a low protein diet (**Table 5**).

The levels of GSH (LP: 12 ± 0.85 vs. NP: 10 ± 0.62 nmol mg^{-1}; $p = 0.039$) and total glutathione (LP: 13 ± 0.85 vs. NP: 10 ± 0.62 nmol mg^{-1}; $p = 0.038$) were higher in the brainstem of LP rats. The levels of GSSG and the GSH/GSSG ratio were not different between the groups (**Table 5**).

3.8 Heart Histology

The LP group showed an increase in the cardiomyocyte diameter (LP: 11.50 ± 0.435 vs. NP: 10.44 ± 0.263 μm; $p = 0.044$; **Figure 5A**) and interstitial fibrosis (LP: 7.20 ± 0.59 vs. NP: 5.40 ± 0.43 μm; $p = 0.028$; **Figure 5B**), however, there was no change in perivascular fibrosis compared with the control group (**Figure 5C**).

3.9 Protein Abundance and Oxidative Stress in the Heart

The levels of protein carbonyl groups, a pro-oxidative marker, were lower in LP rats compared with NP animals (LP: 5 ± 0.56 vs. NP: 6 ± 0.33 mg/protein; $p = 0.030$). GSH and GSSG content in the heart were similar between the groups, however, CAT activity

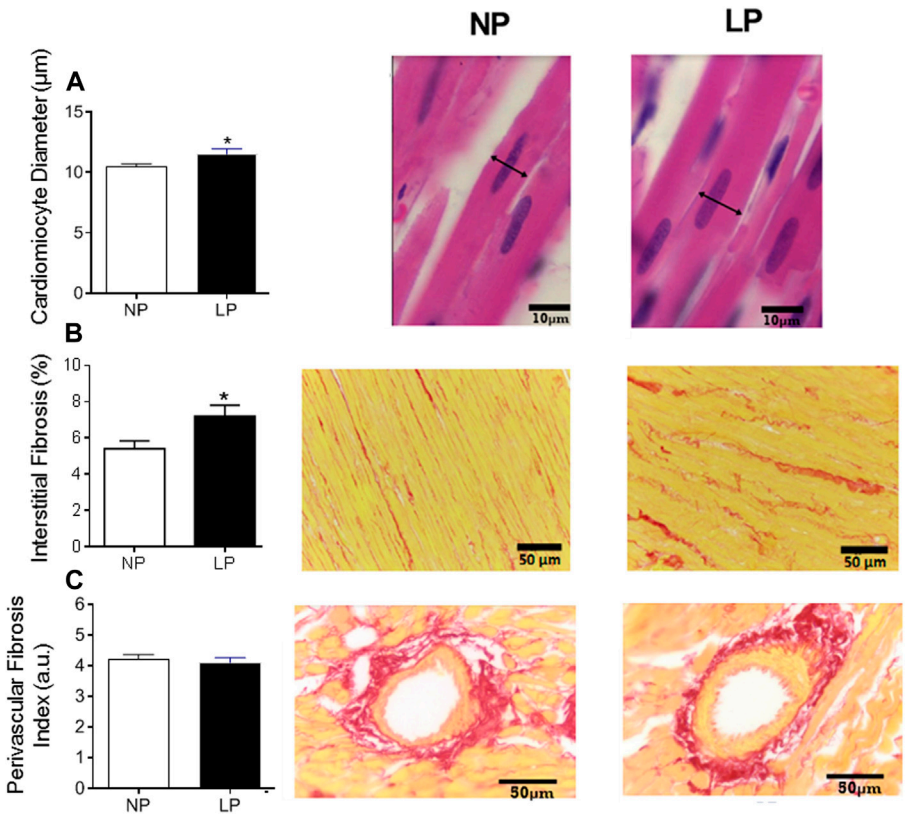

FIGURE 5 | Histological analysis of the heart. Mean value of cardiomyocytes in cross section (scale bar = 10 μm) and representative pictures from each group **(A)**, cardiac interstitial fibrosis (scale bar = 50 μm) and representative pictures from each group **(B)** and perivascular fibrosis index in the left ventricular vasculature (scale bar = 50 μm) and representative pictures from each group **(C)**, $n = 5–10$ animals per group. NP, normal protein diet; LP, low protein diet. Values presented as mean ± SD ***$p <$ 0.001, **$p < 0.01$, and *$p < 0.05$ indicate statistical significance (Student's T test).

TABLE 6 | Oxidative Stress and receptor protein abundance in Heart.

Parameters	NP	LP	*p* value
Oxidative stress			
Carbonyl protein groups	6.92 ± 0.33	5.01 ± 0.57	0.030*
GSH (nmol mg^{-1})	6.11 ± 0.33	5.11 ± 0.57	0.166
GSSG (nmol mg^{-1})	0.10 ± 0.01	0.10 ± 0.01	>0.999
GSH + 2xGSSG (nmol mg^{-1})	6.32 ± 0.33	5.31 ± 0.57	0.166
GSH/GSSG	60.9 ± 4.1	51.1 ± 5.7	0.200
Catalase (μmol·min^{-1} mg^{-1})	32.5 ± 1.7	19.9 ± 2.0	0.001**

NP, Normal protein diet; LP, Low protein diet; Carbonylated proteins, reduced glutathione (GSH), oxidized glutathione (GSSG), activity of catalase enzymes (CAT) and superoxide dismutase enzymes (SOD); n = *4–7 animals per group. Values exposed in mean ± SEM* ***p < 0.001, **p < 0.01, and *p < 0.05 *indicating statistical significance (Student T test).*

was lower in LP rats (LP: 19 ± 2.05 vs. NP: 32 ± 1.76 μmol min^{-1}·mg^{-1}; $p = 0.001$) (**Table 6**).

In the heart, the abundance of beta 1, alpha 1, muscarinic 1, and catalase receptors were similar between groups. However, the expression of superoxide dismutase decreased in the LP group (LP: 77.85 ± 6.04 vs. 100 ± 2.78 kDa; $p = 0.018$) (**Figure 6**).

4 DISCUSSION

This work demonstrates that dietary protein restriction in peri-pubertal period followed by 60 days of nutritional recovery results in hypertension in young adulthood which appears to be underpinned by sympathetic hyperactivity. This is the first demonstration of adult neurogenic hypertension programmed in the peri-pubertal period, while other studies have addressed the effect of low protein diet on blood pressure just after the exposure to the insult (Loss et al., 2007; Penitente et al., 2007; Del Carmen Miñana-Solis and Escobar, 2008; Martins et al., 2011; Murca et al., 2012; Gomide et al., 2013; Penitente et al., 2014; Cappelli et al., 2018). In the context of DOHaD concept the studies have explored an earlier susceptible window of development, the peri-natal period (Latorraca et al., 1998; De Oliveira et al., 2011; De Brito Alves et al., 2014; De Oliveira et al., 2014; Nascimento et al., 2014; Barros et al., 2015; De Oliveira et al., 2016; Ferreira et al., 2016; Paulino-Silva and Costa-Silva, 2016; Rossini et al., 2017; Barros et al., 2018; Martins et al., 2018; Assalin et al., 2019; Ferreira et al., 2019). The exact stimulus to the neurogenic hypertension is difficult to determine as the LP animals were hypophagic during the period of protein restriction, which also induced a caloric-restriction in peri-puberty, and a critical window of development (De Oliveira et al., 2013; De Oliveira et al., 2018). When reverted to the control diet, LP animals were hyperphagic, and therefore demonstrated a catch-up growth, albeit without evidence of elevated adipose tissue accumulation, which is also known in peri-natal programmed hypertension. In young adult life, at PN120, LP animals showed an increase in arterial pressure, cardiac (LF-PI) and vascular sympathetic tone (LF-MAP), an exacerbated depressor response to hexamethonium and greater reduction in the LF-MAP band in response to hexamethonium, indicating sympathetic arousal. In addition, LP animals demonstrated cardiac remodeling in the form of cardiomyocyte hypertrophy and increased interstitial fibrosis, without elevated perivascular collagen deposition. These alterations point to a precocious cardiac remodeling process, which may be a consequence of the hypertension or altered sympathovagal tone. These changes are associated with disorganization of the redox state in the heart and brainstem

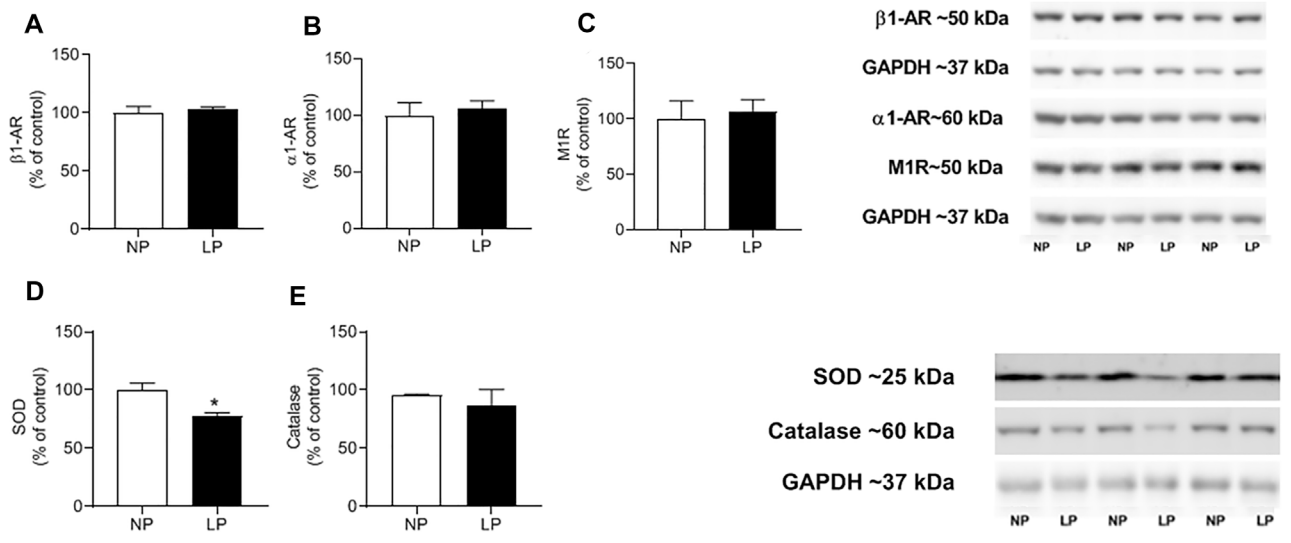

FIGURE 6 | Cardiac protein expression. Mean value of western blot in beta-1 receptor (Anti-B1) **(A)**, alpha-1 receptor (Anti- α1) **(B)**, muscarinic-1 receptor (Anti-M1) **(C)** and superoxide dismutase enzymes (SOD) **(D)**, activity of catalase enzymes (CAT) **(E)** and representative immunoblots are show on the up-right corner, $n = 4–7$ animals per group. NP, normal protein diet; LP, low protein diet. Values presented as mean ± SD ***$p < 0.001$, **$p < 0.01$, and *$p < 0.05$ indicate statistical significance (Student's T test).

stimulated by early exposure to malnutrition, which may be responsible for the altered autonomic balance.

Rat models of developmentally programmed hypertension following perinatal protein restriction (De Brito Alves et al., 2014; Barros et al., 2015; Paulino-Silva and Costa-Silva, 2016) suggest an increase in arterial pressure, cardiac sympathetic tonus and a vascular sympathetic hyperactivity, suggesting that protein restriction at critical stages of development contributes to increased sympathetic activity (Martins et al., 2011; Barros et al., 2015; Paulino-Silva and Costa-Silva, 2016). The present study shows that LP exposure in the peri-pubertal period (a later susceptible window of development) induces an increase in systolic, diastolic, and mean arterial pressure and cardiovascular sympathetic hyperactivity by young adulthood. These changes may be dependent on precocious changes to cardiac structure induced by the early insult. Previous studies point to an increase in blood pressure and sympathetic activity immediately after the caloric-protein insult during post-weaning/peri-pubertal period (Loss et al., 2007; Penitente et al., 2007; Murca et al., 2012; Penitente et al., 2014). We suggest that the autonomic dysfunction and hypertension observed in the present adult LP animals, exposed to protein restriction in peri-puberty, may be an indicative of hypertension developed in the peri-pubertal period that was maintained until adulthood.

During the exposure to the low protein diet, food intake was reduced, which leads to a caloric protein restriction, as observed previously (De Oliveira et al., 2013; De Oliveira et al., 2018). This pattern of ingestion may add confounding factors in the mechanism of blood pressure regulation as caloric restriction may also reduce blood pressure, secondary weight loss, and lowering of insulin resistance (Nicoll and Henein, 2018). Paradoxically, the benefit of a low protein diet on metabolism and blood pressure is controversial and may depend on the developmental window of the exposure and type of macronutrients that are substituted for protein (Laeger et al., 2018). Considering the previously described insulin resistance in this animal model of programming (De Oliveira et al., 2013) and the present increase in blood pressure we may suggest that here, the deleterious effect of low protein diet outweighs any putative beneficial effects of the caloric restriction. Furthermore, it is important to consider that in the present study animals are exposed to a dietary recovery of 60 days between the dietary insult and the timepoint of parameters' evaluation. Interestingly, the changes observed in response to protein restriction followed by catchup growth mirror those of other models where animals exposed to an obesogenic diet in early life or in adulthood also develop elevated blood pressure driven by sympathetic activation, cardiac remodeling and biochemical as well as molecular biological changes in the brain (Prior et al., 2014; Lim et al., 2016; Barrand et al., 2017; De Jong et al., 2018). It is yet to be determined whether the primary driver is adiposity or the protein restriction *per se*, however the similarity in phenotype between these disparate models may indicate that modification in adipocyte biology or activity may be a contributor to the overall mechanism.

The sympathetic hyperactivity observed in LP animals may be related to increased vasoconstrictor response dependent on the activity of the alpha-1 adrenergic receptor, given the increased pressure response to phenylephrine. However, there is also strong evidence for a neurogenic basis for the hypertension, as the LP animals showed exacerbated hypotension and a greater fall in the variability of the LF-AP band when exposed to hexamethonium, a ganglionic blocker. A similar profile was observed in offspring animals exposed to maternal low protein diet (Barros et al., 2015). Furthermore, other models of hypertension as the SHR animals, a model widely known for its neurogenic hypertension (Li et al., 2015) and in obesity related hypertension, which also has a neurogenic origin (Prior et al., 2010; Armitage et al., 2012; Burke et al., 2013) also exhibited a greater drop in blood pressure and low-frequency band of blood pressure in response hexamethonium infusion.

The sensitivity of spontaneous or induced baroreflex was not altered in the present study, corroborating with other programed hypertension models induced by perinatal LP diet exposure (Barros et al., 2015; Paulino-Silva and Costa-Silva, 2016). The absence of altered baroreflex sensitivity may be a consequence of baroreflex resetting (Loss et al., 2007; Penitente et al., 2007; Murca et al., 2012), due to chronic elevation of arterial pressure, however, this aspect was not explored in the present study.

Models of hypertension programmed by perinatal LP diet exposure are associated with evidence of increased sympathetic activity and oxidative stress and decrease in antioxidant defenses in the brainstem (Ferreira et al., 2016; Ferreira et al., 2019) and in the heart (Nascimento et al., 2014). The present study shows a disorganization of these antioxidant pathways rather than a wholesale shift towards oxidative stress. We observed a decrease in the product of protein oxidation in the heart and brainstem. A similar profile was observed by Ferreira et al. (2019), who showed that carbonylated proteins and SOD were decreased, while malonildialdehyde, a lipid peroxidation marker, and glutathione transferase enzyme were increased in the brainstem in PN150 rats exposed to perinatal protein restriction (Ferreira et al., 2019). Oxidative stress is a mechanism involved in the sympathetic arousal generated from the brainstem and resulting in cardiac remodeling (Rossini et al., 2017; Assalin et al., 2019). Therefore, the present disorganization of the redox state must be better explored to assess its role as a mediator of the observed dysfunctions.

The increase in the cardiomyocyte diameter and interstitial fibrosis in relatively young animals exposed to the peri-pubertal protein restriction, and in the absence of perivascular fibrosis observed, suggests that we are observing the beginning of a cardiac remodeling process following elevated blood pressure and ANS dysregulation. Programming studies with LP diet during pregnancy point to a more advanced cardiac morphological disorganization at PN60 or PN112, including collagen deposition in the heart (Rossini et al., 2017; Assalin et al., 2019), decreased number of cardiomyocytes (Silva et al., 2013; Rossini et al., 2017; Assalin et al., 2019), and changes in heart expression of miRNA related to cardiac structure and function (Assalin et al., 2019). The difference in the cardiac histological profile observed between perinatal insult versus the insult during peri-puberty may indicate that peri-pubertal period is a less vulnerable period in terms of disease acquisition, or it may simply represent a rightward shift in the curve. Future studies are required to better understand the natural history of this programmed cardiovascular disease, among them, we emphasize the importance of recording blood pressure from peri-pubertal period until adulthood using telemetric device, to

explore the time course of the blood pressure increase and the evolution of the autonomic dysfunction observed at PN120.

The present study showed that caloric protein restriction during peri-pubertal period induces a neurogenic form of hypertension in adulthood, underpinned by greater sympathetic activity and associated with a disorganization of the cerebral redox state, and structural cardiac alterations. These outcomes, if transferrable to humans, further highlights the relevance of a balanced diet in peri-pubertal period for the prevention and control of the hypertension pandemic. This study points to pathophysiological mechanisms of hypertension and its close relationship with populations in underdeveloped and developing countries exposed to protein and caloric restriction. Taken together, these results are relevant to reflections on public policies for the control of cardiovascular risk, especially in populations vulnerable to transient malnutrition.

DATA AVAILABILITY STATEMENT

The raw data supporting the conclusion of this article will be made available by the authors, without undue reservation.

ETHICS STATEMENT

The animal study was reviewed and approved by Ethic Committee on Animal Use of the State University of Maringa (CEUA/UEM).

AUTHOR CONTRIBUTIONS

AF, KP-R, PM, and JA contributed to the design of the study project, data analysis and writing of the manuscript. AF, MR, MP, GG, SP, LS, KC, MJ, GL, MC, and JM contributed to the performance of the experiments and data analysis. RG, DA, PM, and JC helped in the interpretation of the results. All authors approved the final version of the manuscript.

FUNDING

CAPES (Coordination for the Improvement of Higher Education Personnel), CNPq (National Council for Scientific and Technological Development) (grant number 500698/2013-9, 400762/2014-5) and grant JBS (José Batista Sobrinho).

REFERENCES

Armitage, J. A., Burke, S. L., Prior, L. J., Barzel, B., Eikelis, N., Lim, K., et al. (2012). Rapid Onset of Renal Sympathetic Nerve Activation in Rabbits Fed a High-Fat Diet. *Hypertension* 60, 163–171. doi:10.1161/hypertensionaha.111.190413

Assalin, H. B., Gontijo, J. A. R., and Boer, P. A. (2019). miRNAs, Target Genes Expression and Morphological Analysis on the Heart in Gestational Protein-Restricted Offspring. *PLoS One* 14, e0210454. doi:10.1371/journal.pone.0210454

Barker, D., Eriksson, J., Forsén, T., and Osmond, C. (2002). Fetal Origins of Adult Disease: Strength of Effects and Biological Basis. *Int. J. Epidemiol.* 31, 1235–1239. doi:10.1093/ije/31.6.1235

Barker, D. J. (2004). The Developmental Origins of Chronic Adult Disease. *Acta Paediatr. Suppl.* 93, 26–33. doi:10.1111/j.1651-2227.2004.tb00236.x

Barrand, S., Crowley, T. M., Wood-Bradley, R. J., De Jong, K. A., and Armitage, J. A. (2017). Impact of Maternal High Fat Diet on Hypothalamic Transcriptome in Neonatal Sprague Dawley Rats. *PLoS ONE* 12, e0189492. doi:10.1371/journal.pone.0189492

Barros, M. A. V., De Brito Alves, J. L., Nogueira, V. O., Wanderley, A. G., and Costa-Silva, J. H. (2015). Maternal Low-Protein Diet Induces Changes in the Cardiovascular Autonomic Modulation in Male Rat Offspring. *Nutr. Metab. Cardiovasc. Dis.* 25, 123–130. doi:10.1016/j.numecd.2014.07.011

Barros, M. A. V., Andrade, E. B., Barros, R. G. N., Costa, I. K. M., Costa, I. C. L., Vitorino, G. F. A., et al. (2018). Low-protein Diet Does Not Alter Reproductive, Biochemical, and Hematological Parameters in Pregnant Wistar Rats. *Braz. J. Med. Biol. Res.* 51, e6602. doi:10.1590/1414-431x20186602

Bergmeyer, H. U. (1974). *Methods of Enzymatic Analysis*. Weinheim: Chemie-Academic Press.

Burke, S. L., Prior, L. J., Lukoshkova, E. V., Lim, K., Barzel, B., Davern, P. J., et al. (2013). Reduced Preprandial Dipping Accounts for Rapid Elevation of Blood Pressure and Renal Sympathetic Nerve Activity in Rabbits Fed a High-Fat Diet. *Chronobiol. Int.* 30, 726–738. doi:10.3109/07420528.2013.784771

Cappelli, A. P. G., Zoppi, C. C., Silveira, L. R., Batista, T. M., Paula, F. M., da Silva, P. M. R., et al. (2018). Reduced Glucose-induced Insulin Secretion in Low-protein-fed Rats Is Associated with Altered Pancreatic Islets Redox Status. *J. Cel Physiol.* 233, 486–496. doi:10.1002/jcp.25908

De Andrade, O., Borghi, S. M., De Souza, H. C. D., Fontes, M. A. P., and Martins-Pinge, M. C. (2014). Paraventricular Nucleus of Hypothalamus Participates in the Sympathetic Modulation and Spontaneous Fluctuation of Baroreflex during Head up Tilt in Unanesthetized Rats. *Neurosci. Lett.* 558, 1–7. doi:10.1016/j.neulet.2013.09.039

De Brito Alves, J. L., Nogueira, V. O., De Oliveira, G. B., Da Silva, G. S. F., Wanderley, A. G., Leandro, C. G., et al. (2014). Short- and Long-Term Effects of a Maternal Low-Protein Diet on Ventilation, O2/CO2chemoreception and Arterial Blood Pressure in Male Rat Offspring. *Br. J. Nutr.* 111, 606–615. doi:10.1017/S0007114513002833

De Jong, K. A., Barrand, S., Wood-Bradley, R. J., De Almeida, D. L., Czeczor, J. K., Lopaschuk, G. D., et al. (2018). Maternal High Fat Diet Induces Early Cardiac Hypertrophy and Alters Cardiac Metabolism in Sprague Dawley Rat Offspring. *Nutr. Metab. Cardiovasc. Dis.* 28, 600–609. doi:10.1016/j.numecd.2018.02.019

De Oliveira, J. C., Scomparin, D. X., Andreazzi, A. E., Branco, R. C. S., Martins, A. G., Gravena, C., et al. (2011). Metabolic Imprinting by Maternal Protein Malnourishment Impairs Vagal Activity in Adult Rats. *J. Neuroendocrinol.* 23, 148–157. doi:10.1111/j.1365-2826.2010.02095.x

De Oliveira, J. C., Lisboa, P. C., De Moura, E. G., Barella, L. F., Miranda, R. A., Malta, A., et al. (2013). Poor Pubertal Protein Nutrition Disturbs Glucose-Induced Insulin Secretion Process in Pancreatic Islets and Programs Rats in Adulthood to Increase Fat Accumulation. *J. Endocrinol.* 216, 195–206. doi:10.1530/JOE-12-0408

De Oliveira, J. C., Miranda, R. A., Barella, L. F., Torrezan, R., Agostinho, A. R., Ribeiro, T. A. S., et al. (2014). Impaired β-cell Function in the Adult Offspring of Rats Fed a Protein-Restricted Diet during Lactation Is Associated with Changes in Muscarinic Acetylcholine Receptor Subtypes. *Br. J. Nutr.* 111, 227–235. doi:10.1017/s0007114513002213

De Oliveira, J. C., Gomes, R. M., Miranda, R. A., Barella, L. F., Malta, A., Martins, I. P., et al. (2016). Protein Restriction during the Last Third of Pregnancy Malprograms the Neuroendocrine Axes to Induce Metabolic Syndrome in Adult Male Rat Offspring. *Endocrinology* 157, 1799–1812. doi:10.1210/en.2015-1883

De Oliveira, J. C., De Moura, E. G., Miranda, R. A., De Moraes, A. M. P., Barella, L. F., da Conceição, E. P. S., et al. (2018). Low-protein Diet in Puberty Impairs Testosterone Output and Energy Metabolism in Male Rats. *J. Endocrinol.* 237, 243–254. doi:10.1530/JOE-17-0606

del Carmen Miñana-Solis, M., and Escobar, C. (2008). Post-weaning Protein Malnutrition in the Rat Produces Short and Long Term Metabolic Impairment, in Contrast to Earlier and Later Periods. *Int. J. Biol. Sci.* 4, 422–432. doi:10.7150/ijbs.4.422

Di Rienzo, M., Parati, G., Castiglioni, P., Tordi, R., Mancia, G., and Pedotti, A. (2001). Baroreflex Effectiveness index: an Additional Measure of Baroreflex Control of Heart Rate in Daily Life. *Am. J. Physiol. Regulatory Integr. Comp. Physiol.* 280, R744–R751. doi:10.1152/ajpregu.2001.280.3.r744

Dobrek, L., Skowron, B., Baranowska, A., and Thor, P. J. (2013). Spectral Heart Rate Variability Analysis in Experimental Obstructive and Chemical Overactive Bladder Models. *Adv. Clin. Exp. Med.* 22, 337–346.

Ferreira, D. S., Liu, Y., Fernandes, M. P., and Lagranha, C. J. (2016). Perinatal Low-Protein Diet Alters Brainstem Antioxidant Metabolism in Adult Offspring. *Nutr. Neurosci.* 19, 369–375. doi:10.1179/1476830515Y.0000000030

Ferreira, D. J. S., Pedroza, A. A., Braz, G. R. F., Fernandes, M. P., and Lagranha, C. J. (2019). Mitochondrial Dysfunction: Maternal Protein Restriction as a Trigger of Reactive Species Overproduction and Brainstem Energy Failure in Male Offspring Brainstem. *Nutr. Neurosci.* 22, 778–788. doi:10.1080/1028415x.2018.1444543

Gomide, J. M. C., De Menezes, R. C., Fernandes, L. G., Silva, F. C., Cardoso, L. M., Miranda, P. H., et al. (2013). Increased Activity of the Renin-Angiotensin and Sympathetic Nervous Systems Is Required for Regulation of the Blood Pressure in Rats Fed a Low-Protein Diet. *Exp. Physiol.* 98, 57–66. doi:10.1113/expphysiol.2012.066712

Hissin, P. J., and Hilf, R. (1976). A Fluorometric Method for Determination of Oxidized and Reduced Glutathione in Tissues. *Anal. Biochem.* 74, 214–226. doi:10.1016/0003-2697(76)90326-2

Kuwahara, M., Yayou, K.-i., Ishii, K., Hashimoto, S.-i., Tsubone, H., and Sugano, S. (1994). Power Spectral Analysis of Heart Rate Variability as a New Method for Assessing Autonomic Activity in the Rat. *J. Electrocardiol.* 27, 333–337. doi:10.1016/s0022-0736(05)80272-9

Laeger, T., Castaño-Martinez, T., Werno, M. W., Japtok, L., Baumeier, C., Jonas, W., et al. (2018). Dietary Carbohydrates Impair the Protective Effect of Protein Restriction against Diabetes in NZO Mice Used as a Model of Type 2 Diabetes. *Diabetologia* 61, 1459–1469. doi:10.1007/s00125-018-4595-1

Latorraca, M. Q., Reis, M. A. B., Carneiro, E. M., Mello, M. A. R., Velloso, L. A., Saad, M. J. A., et al. (1998). Protein Deficiency and Nutritional Recovery Modulate Insulin Secretion and the Early Steps of Insulin Action in Rats. *J. Nutr.* 128, 1643–1649. doi:10.1093/jn/128.10.1643

Levine, R. L., Garland, D., Oliver, C. N., Amici, A., Climent, I., Lenz, A.-G., et al. (1990). [49] Determination of Carbonyl Content in Oxidatively Modified Proteins. *Methods Enzymol.* 186, 464–478. doi:10.1016/0076-6879(90)86141-h

Li, P., Gong, J.-X., Sun, W., Zhou, B., and Kong, X.-Q. (2015). Hexamethonium Attenuates Sympathetic Activity and Blood Pressure in Spontaneously Hypertensive Rats. *Mol. Med. Rep.* 12, 7116–7122. doi:10.3892/mmr.2015.4315

Lim, K., Barzel, B., Burke, S. L., Armitage, J. A., and Head, G. A. (2016). Origin of Aberrant Blood Pressure and Sympathetic Regulation in Diet-Induced Obesity. *Hypertension* 68, 491–500. doi:10.1161/hypertensionaha.116.07461

Lim, K., Burke, S. L., Marques, F. Z., Jackson, K. L., Gueguen, C., Sata, Y., et al. (2021). Leptin and Melanocortin Signaling Mediates Hypertension in Offspring from Female Rabbits Fed a High-Fat Diet during Gestation and Lactation. *Front. Physiol.* 12, 890. doi:10.3389/fphys.2021.693157

Loss, I. d. O., Fernandes, L. G., Martins, C. D. D., Cardoso, L. M., Silva, M. E., Dias-da-Silva, V. J., et al. (2007). Baroreflex Dysfunction in Rats Submitted to Protein Restriction. *Life Sci.* 81, 944–950. doi:10.1016/j.lfs.2007.08.005

Lowry, O., Rosebrough, N., Farr, A. L., and Randall, R. (1951). Protein Measurement with the Folin Phenol Reagent. *J. Biol. Chem.* 193, 265–275. doi:10.1016/s0021-9258(19)52451-6

Marklund, S., and Marklund, G. (1974). Involvement of the Superoxide Anion Radical in the Autoxidation of Pyrogallol and a Convenient Assay for Superoxide Dismutase. *Eur. J. Biochem.* 47, 469–474. doi:10.1111/j.1432-1033.1974.tb03714.x

Martins, C. D., Chianca, D. A., Jr., and Fernandes, L. G. (2011). Cardiac Autonomic Balance in Rats Submitted to Protein Restriction after Weaning. *Clin. Exp. Pharmacol. Physiol.* 38, 89–93. doi:10.1111/j.1440-1681.2010.05468.x

Martins, I. P., De Oliveira, J. C., Pavanello, A., Matiusso, C. C. I., Previate, C., Tófolo, L. P., et al. (2018). Protein-restriction Diet during the Suckling Phase Programs Rat Metabolism against Obesity and Insulin Resistance Exacerbation Induced by a High-Fat Diet in Adulthood. *J. Nutr. Biochem.* 57, 153–161. doi:10.1016/j.jnutbio.2018.03.017

Mathers, C. D., and Loncar, D. (2006). Projections of Global Mortality and Burden of Disease from 2002 to 2030. *Plos Med.* 3, e442. doi:10.1371/journal.pmed.0030442

Mizuno, M., Siddique, K., Baum, M., and Smith, S. A. (2013). Prenatal Programming of Hypertension Induces Sympathetic Overactivity in Response to Physical Stress. *Hypertension* 61, 180–186. doi:10.1161/hypertensionaha.112.199356

Murca, T. M., Magno, T. S. d. R., De Maria, M. L. d. A., Capuruço, C. A. B., Chianca, D. A., and Ferreira, A. J. (2012). Cardiac Responses of Rats Submitted to Postnatal Protein Restriction. *Appl. Physiol. Nutr. Metab.* 37, 455–462. doi:10.1139/h2012-017

Nascimento, L., Freitas, C. M., Silva-Filho, R., Leite, A. C. R., Silva, A. B., da Silva, A. I., et al. (2014). The Effect of Maternal Low-Protein Diet on the Heart of Adult Offspring: Role of Mitochondria and Oxidative Stress. *Appl. Physiol. Nutr. Metab.* 39, 880–887. doi:10.1139/apnm-2013-0452

Nicoll, R., and Henein, M. (2018). Caloric Restriction and its Effect on Blood Pressure, Heart Rate Variability and Arterial Stiffness and Dilatation: a Review of the Evidence. *Int. J. Mol. Sci.* 19, 751. doi:10.3390/ijms19030751

Pagani, M., Lombardi, F., Guzzetti, S., Rimoldi, O., Furlan, R., Pizzinelli, P., et al. (1986). Power Spectral Analysis of Heart Rate and Arterial Pressure Variabilities as a Marker of Sympatho-Vagal Interaction in Man and Conscious Dog. *Circ. Res.* 59, 178–193. doi:10.1161/01.res.59.2.178

Paulino-Silva, K. M., and Costa-Silva, J. H. (2016). Hypertension in Rat Offspring Subjected to Perinatal Protein Malnutrition Is Not Related to the Baroreflex Dysfunction. *Clin. Exp. Pharmacol. Physiol.* 43, 1046–1053. doi:10.1111/1440-1681.12628

Penitente, A. R., Fernandes, L. G., Cardoso, L. M., Silva, M. E., Pedrosa, M. L., Silva, A. L., et al. (2007). Malnutrition Enhances Cardiovascular Responses to Chemoreflex Activation in Awake Rats. *Life Sci.* 81, 609–614. doi:10.1016/j.lfs.2007.07.006

Penitente, A. R., Novaes, R. D., Silva, M. E., Silva, M. F., Quintão-Júnior, J. F., Guatimosim, S., et al. (2014). Basal and β-Adrenergic Cardiomyocytes Contractility Dysfunction Induced by Dietary Protein Restriction Is Associated with Downregulation of SERCA2a Expression and Disturbance of Endoplasmic Reticulum Ca2+Regulation in Rats. *Cell Physiol. Biochem.* 34, 443–454. doi:10.1159/000363013

Prior, L. J., Eikelis, N., Armitage, J. A., Davern, P. J., Burke, S. L., Montani, J.-P., et al. (2010). Exposure to a High-Fat Diet Alters Leptin Sensitivity and Elevates Renal Sympathetic Nerve Activity and Arterial Pressure in Rabbits. *Hypertension* 55, 862–868. doi:10.1161/hypertensionaha.109.141119

Prior, L. J., Davern, P. J., Burke, S. L., Lim, K., Armitage, J. A., and Head, G. A. (2014). Exposure to a High-Fat Diet during Development Alters Leptin and Ghrelin Sensitivity and Elevates Renal Sympathetic Nerve Activity and Arterial Pressure in Rabbits. *Hypertension* 63, 338–345. doi:10.1161/hypertensionaha.113.02498

Radaelli, A., Castiglioni, P., Centola, M., Cesana, F., Balestri, G., Ferrari, A. U., et al. (2006). Adrenergic Origin of Very Low-Frequency Blood Pressure Oscillations in the Unanesthetized Rat. *Am. J. Physiol. Heart Circulatory Physiol.* 290, H357–H364. doi:10.1152/ajpheart.00773.2005

Rodrigues, F. A., Chianca-Jr, D. A., Jr., and Gonçalves Fernandes, L. (2012). Malnutrition Affects the Pressor Response to Microinjection of L-Glutamate into the RVLM of Awake Rats. *Biol. Res.* 45, 337–343. doi:10.4067/S0716-97602012000400002

Rossini, K. F., Oliveira, C. A. d., Rebelato, H. J., Esquisatto, M. A. M., and Catisti, R. (2017). Gestational Protein Restriction Increases Cardiac Connexin 43 mRNA Levels in Male Adult Rat Offspring. *Arq Bras Cardiol.* 109, 63–70. doi:10.5935/abc.20170081

Santos, S. O., Loureiro, S. M. A., Alves, I. G. N., Jesus, C. S. d., Santos, P. R. d., Santos, M. R. V. d., et al. (2012). Experimental Gestational Hypothyroidism Evokes Hypertension in Adult Offspring Rats. *Auton. Neurosci.* 170, 36–41. doi:10.1016/j.autneu.2012.07.004

Silva, R. B., Mesquita, F. F., Andreo, M., Assalin, H. B., Rocha Gontijo, J. A., and Boer, P. A. (2013). Effect of Gestational Protein Restriction on Left Ventricle Hypertrophy and Heart Angiotensin II Signaling Pathway in Adult Offspring Rats. *Health* 05, 78–84. doi:10.4236/health.2013.54a011

Silva, A. S., Ariza, D., Dias, D. P. M., Crestani, C. C., and Martins-Pinge, M. C. (2015). Cardiovascular and Autonomic Alterations in Rats with Parkinsonism

Induced by 6-OHDA and Treated with L-DOPA. *Life Sci.* 127, 82–89. doi:10.1016/j.lfs.2015.01.032

Simas, B. B., Nunes, E. A., Crestani, C. C., and Speretta, G. F. (2018). Cardiovascular and Metabolic Consequences of the Association between Chronic Stress and High-Fat Diet in Rats. *Stress* 21, 247–256. doi:10.1080/10253890.2018.1437413

Speretta, G. F., Silva, A. A., Vendramini, R. C., Zanesco, A., Delbin, M. A., Menani, J. V., et al. (2016). Resistance Training Prevents the Cardiovascular Changes Caused by High-Fat Diet. *Life Sci.* 146, 154–162. doi:10.1016/j.lfs.2016.01.011

Valenti, V. E., Ferreira, C., Meneghini, A., Ferreira, M., Murad, N., Ferreira Filho, C., et al. (2009). Evaluation of Baroreflex Function in Young Spontaneously Hypertensive Rats. *Arq Bras Cardiol.* 92, 205–215. doi:10.1590/s0066-782x2009000300009

Valenti, V. E., De Abreu, L. C., Colombari, E., Sato, M. A., and Ferreira, C. (2011). The Variability of Baroreflex Sensitivity in Juvenile, Spontaneously Hypertensive Rats. *CardioVascular J. Africa* 22, 14–17. doi:10.5830/cvja-2010-007

WHO (2021a). Cardiovascular Diseases (CVDs). Fact sheet, 11 June 2021. Available at: https://www.who.int/news-room/fact-sheets/detail/cardiovascular-diseases-(cvds) (Accessed February, , 2022).

WHO (2021b). Hypertension. Fact sheet, 25 August 2021. Available at: https://www.who.int/news-room/fact-sheets/detail/hypertension (Accessed February, 2022).

Conflict of Interest: The authors declare that the research was conducted in the absence of any commercial or financial relationships that could be construed as a potential conflict of interest.

Publisher's Note: All claims expressed in this article are solely those of the authors and do not necessarily represent those of their affiliated organizations, or those of the publisher, the editors and the reviewers. Any product that may be evaluated in this article, or claim that may be made by its manufacturer, is not guaranteed or endorsed by the publisher.

Copyright © 2022 Ferreira, Ribeiro, Peres, Piovan, Gonçalves, Saavedra, Martins, Junior, Cavalcante, Lopes, Carneiro, Almeida, Gomes, Comar, Armitage, Mathias and Palma-Rigo. This is an open-access article distributed under the terms of the Creative Commons Attribution License (CC BY). The use, distribution or reproduction in other forums is permitted, provided the original author(s) and the copyright owner(s) are credited and that the original publication in this journal is cited, in accordance with accepted academic practice. No use, distribution or reproduction is permitted which does not comply with these terms.

frontiers | Frontiers in Physiology

BRIEF RESEARCH REPORT
published: 09 May 2022
doi: 10.3389/fphys.2022.871962

Acute Cannabigerol Administration Lowers Blood Pressure in Mice

*Victoria L. Vernail[1], Sarah S. Bingaman[1], Yuval Silberman[1], Wesley M. Raup-Konsavage[2], Kent E. Vrana[2] and Amy C. Arnold[1]**

[1]Department of Neural and Behavioral Sciences, Penn State College of Medicine, Hershey, PA, United States, [2]Department of Pharmacology, Penn State College of Medicine, Hershey, PA, United States

Cannabigerol is a cannabinoid compound synthesized by *Cannabis sativa*, which in its acid form acts as the substrate for both Δ^9-tetraydrocannabinol and cannabidiol formation. Given its lack of psychoactive effects, emerging research has focused on cannabigerol as a potential therapeutic for health conditions including algesia, epilepsy, anxiety, and cancer. While cannabigerol can bind to classical cannabinoid receptors, it is also an agonist at α2-adrenoreceptors (α2AR) which, when activated, inhibit presynaptic norepinephrine release. This raises the possibility that cannabigerol could activate α2AR to reduce norepinephrine release to cardiovascular end organs to lower blood pressure. Despite this possibility, there are no reports examining cannabigerol cardiovascular effects. In this study, we tested the hypothesis that acute cannabigerol administration lowers blood pressure. Blood pressure was assessed *via* radiotelemetry at baseline and following intraperitoneal injection of cannabigerol (3.3 and 10 mg/kg) or vehicle administered in a randomized crossover design in male C57BL/6J mice. Acute cannabigerol significantly lowered mean blood pressure (–28 ± 2 mmHg with 10 mg/kg versus –12 ± 5 mmHg vehicle, respectively; $p = 0.018$), with no apparent dose responsiveness (–22 ± 2 mmHg with 3.3 mg/kg). The depressor effect of cannabigerol was lower in magnitude than the α2AR agonist guanfacine and was prevented by pretreatment with the α2AR antagonist atipamezole. These findings suggest that acute cannabigerol lowers blood pressure in phenotypically normal mice likely *via* an α2AR mechanism, which may be an important consideration for therapeutic cannabigerol administration.

Keywords: cardiovascular, mouse models, cannabinoids, adrenoreceptors, radiotelemetry

OPEN ACCESS

Edited by:
James Todd Pearson, National Cerebral and Cardiovascular Center, Japan

Reviewed by:
Christopher Schaich, Wake Forest School of Medicine, United States
Cecilia Hillard, Medical College of Wisconsin, United States

****Correspondence:***
Amy C. Arnold
aca17@psu.edu

Specialty section:
This article was submitted to Integrative Physiology, a section of the journal Frontiers in Physiology

Received: *08 February 2022*
Accepted: *22 April 2022*
Published: *09 May 2022*

Citation:
Vernail VL, Bingaman SS, Silberman Y, Raup-Konsavage WM, Vrana KE and Arnold AC (2022) Acute Cannabigerol Administration Lowers Blood Pressure in Mice. Front. Physiol. 13:871962. doi: 10.3389/fphys.2022.871962

INTRODUCTION

Cannabinoids from *Cannabis sativa* are of growing interest due to their potential therapeutic benefits (Kovalchuk and Kovalchuk, 2020), and may represent an appealing alternative to current medications whose effectiveness is confounded by adverse side effects. In this regard, cannabis has been studied for treatment of chronic pain, cancer, epilepsy, anxiety, metabolic conditions, and several other diseases (Committee on the Health Effects of Marijuana et al., 2017). Compounds of particular interest include Δ^9-tetraydrocannabinol (Δ^9-THC), cannabidiol (CBD), and more recently cannabigerol (CBG). CBG, in its acid form, is the parent compound to cannabinoids such as Δ^9-THC and CBD (Nachnani et al., 2021), and has similar properties to CBD including analgesia, neuroprotective, anticancer, anti-inflammatory, and antibacterial effects. In contrast to Δ^9-THC, the main psychoactive component of cannabis which induces euphoria, both CBD and CBG lack psychoactive properties. There are other notable differences between these cannabinoids, including

their binding at the classical cannabinoid receptors, cannabinoid receptor type 1 (CB1R) and type 2 (CB2R). While Δ^9-THC is an agonist at CB2R and partial agonist at CB1R, CBD is an inverse agonist/antagonist at these receptors. CBG binds as a weak/partial agonist to CB1R and CB2R, but with lower affinity than Δ^9-THC (Rosenthaler et al., 2014; Nachnani et al., 2021).

In addition to cannabinoid receptors, CBG appears to be a potent agonist with nanomolar affinity at α2-adrenoreceptors (α2AR) in peripheral tissues and the central nervous system (Cascio et al., 2010; Cathel et al., 2014). α2AR are presynaptic autoreceptors found both peripherally and centrally, which inhibit norepinephrine release to reduce sympathetic nervous system activity. Importantly, reduced norepinephrine release onto cardiovascular end organs, such as the heart and vasculature, can reduce vasoconstriction, heart rate, and cardiac contractility to lower blood pressure (Giovannitti et al., 2015). This raises the possibility that CBG may activate α2AR to lower blood pressure, which could have significant implications for potential therapeutic properties of this compound. Despite evidence for α2AR activation, the potential blood pressure effects of CBG remain unknown. Therefore, in this study, we tested the hypothesis that acute CBG administration can reduce blood pressure *via* an α2AR mechanism in conscious mice using a gold standard real-time radiotelemetry approach.

MATERIALS AND METHODS

Approvals

All procedures were approved by the Institutional Animal Care and Use Committee at the Penn State College of Medicine and conformed to the NIH Guide for the Care and Use of Laboratory Animals.

Animal Models

Male C57BL/6J mice (Jackson Laboratory, Bar Harbor, ME, United States) were used in these studies. Mice were fed a standard chow diet (Teklad 2018; Envigo, Indianapolis, IN, United States) and normal tap water *ad libitum* and housed on a 12-h light-dark schedule in a room with controlled humidity and temperature (~23 °C). At approximately 8 weeks of age, mice were implanted with radiotelemetry probes (HD-X10, Data Sciences International, St. Paul, MN, United States), with the tip of the probe advanced *via* the carotid artery into the aortic arch, which allows for continuous measurement of blood pressure, heart rate, and locomotor activity in conscious freely moving animals. Following surgery, mice were individually housed and allowed to recover for at least 10 days prior to experiments.

Acute CBG Administration

Baseline blood pressure, heart rate, and locomotor activity were recorded in conscious mice for 20 min prior to drug treatment. Mice then received a single intraperitoneal injection of CBG (3.3 and 10 mg/kg) or vehicle (1:1:18 DMSO: Tween80: Saline). Treatments were given in a randomized order, with at least one-week washout, in a crossover design. These doses and route of administration of CBG were chosen based on previous studies showing neuroprotective, anti-inflammatory, anti-nociceptive, and antiemetic effects in rodents (Rock et al., 2011; Borrelli et al., 2013; Valdeolivas et al., 2015; Zagzoog et al., 2020). Changes in blood pressure, heart rate, and locomotor activity from baseline were assessed for 3 hours post-injection, to capture the known time course for peak plasma concentrations of CBG following intraperitoneal injection in rodents (Deiana et al., 2012). Data were averaged into 5-min bins across the recording period to determine peak changes. Six mice were implanted with radiotelemetry probes for this experiment. The signal was lost in one probe mid-way through the study due to clots in the sensing catheter and, therefore, only five mice are included in the 3.3 mg/kg CBG dose. Animals were acclimated to intraperitoneal injections for 5 days prior to experiments to attempt to minimize confounding effects of handling stress.

Potential α2AR Mechanisms Involved in CBG Depressor Effects

To determine if α2AR mechanisms are involved in the depressor effects of CBG, a second experiment was conducted using the same crossover study design in which a separate cohort of mice (n = 5) received intraperitoneal injection of CBG (10 mg/kg), the α2AR agonist guanfacine (1 mg/kg), or the α2AR antagonist atipamezole (3 mg/kg) + CBG (10 mg/kg). Atipamezole was given 10 min prior to CBG administration. The doses and time course for guanfacine and atipamezole were selected based on prior literature showing cardiovascular effectiveness of these drugs in mice (Janssen et al., 2004; Ying et al., 2014). The dose of CBG was selected as it produced significant blood pressure lowering effects in the first experiment following acute administration. To ensure our findings reflect pharmacological antagonism of CBG rather than additive effects of the combined drugs, we performed a third experiment in which a separate cohort of mice (n = 3) received intraperitoneal injection of atipamezole (3 mg/kg) or atipamezole (3 mg/kg) plus CBG (10 mg/kg; given at 10 min after atipamezole administration). Given the time course for CBG depressor effects in the first experiment, data were recorded for 2 hours post-drug administration and averaged in 5-min bins for these second and third experiments.

Statistical Analysis

Data are presented as mean ± SEM and were analyzed by GraphPad Prism (Version 9.3.0). For experiments examining acute CBG versus vehicle administration, given the missing data within one dose, changes in blood pressure and heart rate were assessed *via* mixed effects models with post hoc Šídák's multiple comparisons to account for the repeated measures and to assess main effects of drug, timepoint (baseline vs. post-drug), and their interaction. Locomotor activity was analyzed as an area under the curve (AUC) to summarize changes across the entire treatment period, and analyzed across groups *via* a mixed effects model to examine treatment effect. The time for

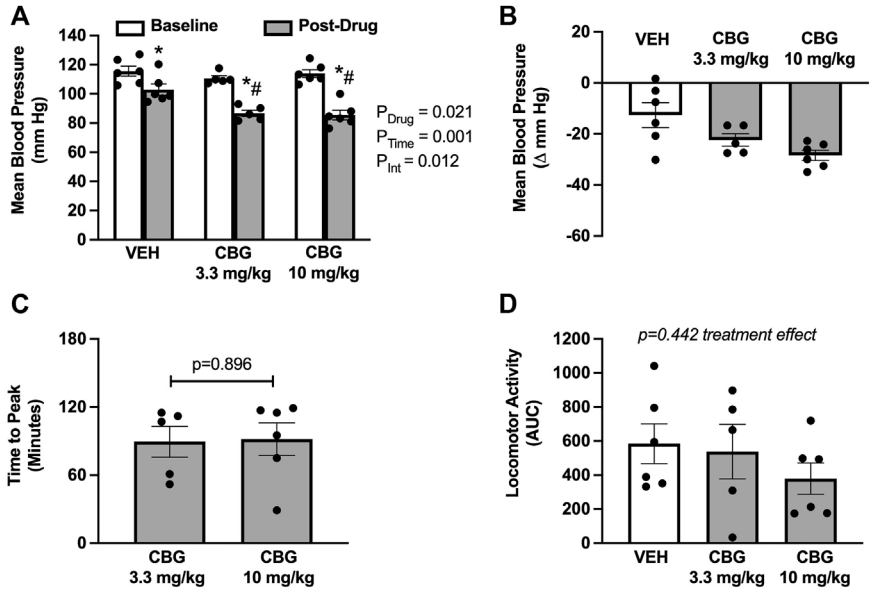

FIGURE 1 | Acute cannabigerol (CBG) administration decreases mean blood pressure. **(A)** CBG significantly lowered mean blood pressure when compared with vehicle (VEH) administration (P_{Drug} = 0.021, P_{Time}<0.001, P_{Int} = 0.019; mixed effects model; *p < 0.05 versus baseline and # p < 0.05 versus vehicle following post hoc Šídák's multiple comparisons test). **(B)** The magnitude of depressor effect of CBG was greater than VEH when shown as the peak change from baseline (–28 ± 2 at 10 mg/kg *vs*. –22 ± 2 at 3 mg/kg *vs*. –12 ± 5 mmHg vehicle). **(C)** The peak blood pressure lowering effect of CBG occurred on average at ~90 min for both 3.3 and 10 mg/kg doses (p = 0.896 paired t-test). **(D)** There were no differences in the area under the curve (AUC) for locomotor activity over the study period across treatments [f (2,9) = 0.895; p = 0.442 mixed effects model]. N = 5–6/group.

TABLE 1 | Blood pressure and heart rate following acute CBG administration.

Parameter, units	Vehicle	CBG 3.3 mg/kg	CBG 10 mg/kg	P_{Drug}	P_{Time}	P_{Int}
SBP, mmHg						
Baseline	132 ± 4	128 ± 2	131 ± 3	0.029	0.001	0.018
Post-Drug	120 ± 5*	103 ± 3*	99 ± 4*			
DBP, mmHg						
Baseline	106 ± 6	104 ± 3	106 ± 3	0.173	0.001	0.049
Post-Drug	89 ± 6*	71 ± 3*	73 ± 4*			
HR, bpm						
Baseline	583 ± 27	518 ± 14	481 ± 11	0.003	0.004	0.502
Post-Drug	527 ± 22	439 ± 23*	450 ± 25			

CBG, cannabigerol; SBP, systolic blood pressure; DBP, diastolic blood pressure; HR, heart rate.

Data are mean ± SEM and were analyzed by mixed effects models to assess for main effects of vehicle versus CBG treatment (P_{Drug}), baseline versus post-drug timepoint (P_{Time}), and their interaction (P_{Int}).

**p < 0.05 versus baseline following post hoc Šídák's multiple comparisons test.*

peak changes in blood pressure following CBG and dose responsiveness for peak change in mean blood pressure were analyzed *via* paired t-test. For experiments examining potential α2AR mechanisms involved in CBG depressor effects, changes in blood pressure and heart rate following either CBG versus guanfacine, CBG versus atipamezole + CBG, or atipamezole versus atipamezole + CBG were assessed *via* two-way repeated measures ANOVA to assess main effects of drug, time, and their interaction with post hoc Šídák's multiple comparisons. A p-value of <0.05 was considered statistically significant.

RESULTS

Acute CBG Lowers Blood Pressure, but Does Not Alter Heart Rate or Locomotor Activity

Acute CBG administration elicited a significant decrease in mean blood pressure compared with vehicle (**Figure 1A**). There was no apparent dose responsiveness for the CBG doses used in this study (**Figure 1B**; Δ from baseline: −22 ± 2 at 3.3 mg/kg versus −28 ± 2 mmHg at 10 mg/kg). On average, the peak decrease in

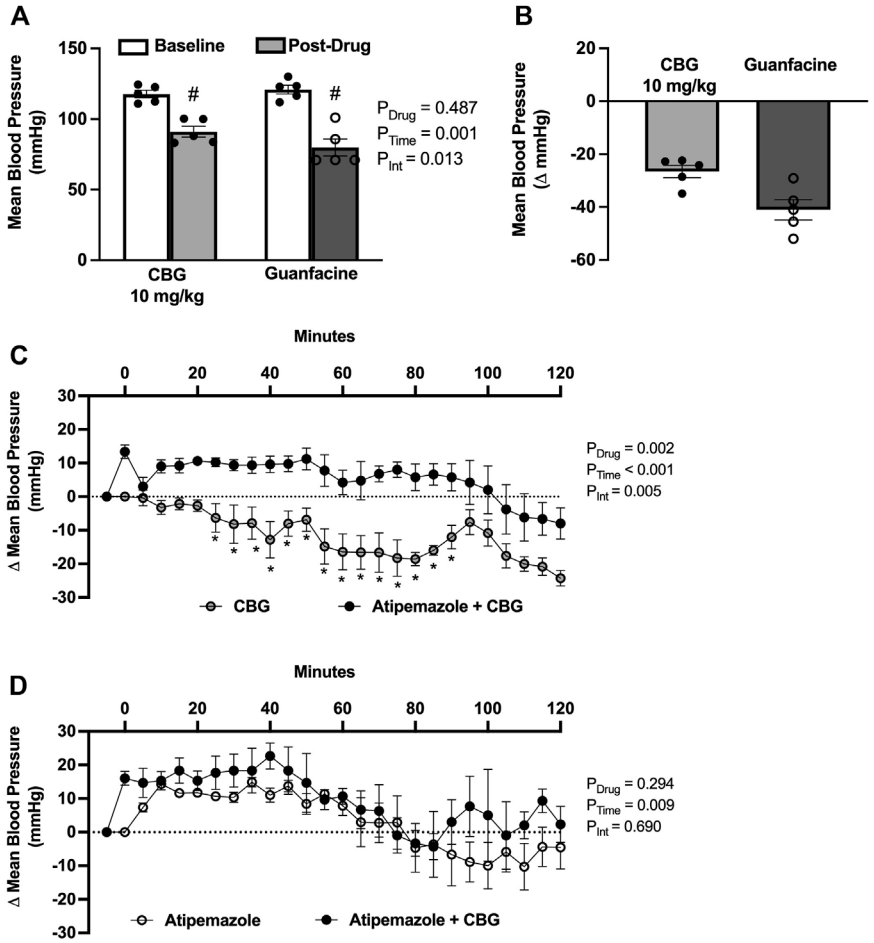

FIGURE 2 | Acute cannabigerol (CBG) lowers blood pressured *via* an alpha2-adrenoreceptor (α2AR) mechanism. **(A)** CBG (10 mg/kg, i.p.) lowered mean blood pressure to a lesser extent than guanfacine (1 mg/kg, i.p.) administration (P_{Drug} = 0.487, P_{Time} = 0.001, P_{Int} = 0.013; two-way repeated measures ANOVA; # $p < 0.01$ versus baseline following post hoc Šídák's multiple comparisons test; N = 5/group). **(B)** The magnitude of depressor effect of CBG was less than guanfacine when shown as the peak change from baseline (–27 ± 2 *vs*. –41 ± 4 mmHg, respectively). **(C)** Pretreatment with the α2AR antagonist atipamezole (3 mg/kg, i.p.) prevented CBG (10 mg/kg, i.p.) blood pressure lowering effects (P_{Drug} = 0.001, P_{Time}<0.001, P_{Int} = 0.001; two-way repeated measures ANOVA; *$p < 0.05$ versus atipamezole + CBG following post hoc Šídák's multiple comparisons tests; N = 5/group). **(D)** There were no significant differences in the blood pressure effects of atipamezole versus atipamezole plus CBG (P_{Drug} = 0.294, P_{Time}<0.001, P_{Int} = 0.690; two-way repeated measures ANOVA; N = 3/group).

mean blood pressure elicited by CBG was observed at 90-min post-administration, with no difference between doses (**Figure 1C**). CBG also significantly lowered systolic and diastolic blood pressure compared with vehicle (**Table 1**), again with no dose responsiveness. There were no differences in heart rate responses following CBG versus vehicle administration (**Table 1**). There were also no differences in locomotor activity over the study period across treatment groups (**Figure 1D**).

Acute CBG Lowers Blood Pressure *via* an α2AR Mechanism

To determine if the acute blood pressure lowering effects of CBG are mediated *via* an α2AR mechanism, we first compared the magnitude of depressor response to a known α2AR agonist, guanfacine. We found that both CBG and guanfacine lowered mean blood pressure from baseline, with the peak decrease being smaller for CBG (**Figures 2A,B**). We next determined if the blood pressure lowering effects of CBG could be prevented by pretreatment with atipamezole, an α2AR antagonist. Atipamezole alone caused an ~13 mmHg increase in mean blood pressure, reflecting disinhibition of norepinephrine release *via* α2AR. Importantly, atipamezole prevented the drop in mean blood pressure elicited by acute CBG administration (**Figure 2C**). Mean blood pressure responses to atipamezole versus atipamezole plus CBG were similar (**Figure 2D**).

DISCUSSION

The cannabinoid system is involved in several aspects of cardiovascular regulation including control of blood vessel tone, cardiac contractility, blood pressure, and vascular

inflammation (Pacher et al., 2005). CBG is a less studied phytocannabinoid with evidence emerging for many potential beneficial effects; however, its impact on the cardiovascular system is unknown. We found that acute CBG administration elicits a significant decrease in blood pressure in phenotypically normal male mice, without altering heart rate or locomotor activity. Additionally, our data suggest that the blood pressure lowering effects of CBG are mediated through an α2AR mechanism. Overall, the present study provides new mechanistic insight into the cardiovascular effects of CBG in the context of normal blood pressure.

Currently, little is known about the effects of CBG on the cardiovascular system, with no reports related to blood pressure. To our knowledge, only one study has examined cardiovascular-related effects of CBG and showed inhibition of platelet aggregation induced by adrenaline in human platelets suggesting anti-thrombotic activity (Formukong et al., 2011). We found that acute CBG lowered mean blood pressure in mice by ~28 mmHg (compared with ~12 mmHg for vehicle treatment), without effects on heart rate. The lack of a compensatory heart rate increase in response to the decrease in blood pressure with CBG may indicate impairment of the arterial baroreceptor reflex, which is a homeostatic mechanism to correct for changes in blood pressure. However, this impairment remains to be tested. We did not observe evidence of dose-responsiveness for CBG; however, only two doses were fully examined in this study and future studies may need to include additional doses of CBG. The 10 mg/kg dose of CBG has been widely shown as effective in rodents models of neurodegenerative diseases and inflammatory bowel disease (Rock et al., 2011; Borrelli et al., 2013). An intermediate dose of 5.6 mg/kg was tested in three mice in the present study, but again, showed no evidence for dose responsiveness in terms of ability to lower mean blood pressure (−28 ± 4 mmHg). Higher doses were not tested as 10 mg/kg of CBG decreased blood pressure substantially, and it is likely a floor effect would be observed. Our finding for lack of dose responsiveness is consistent with a recent report showing variability in effective concentrations for CBG in terms of analgesic and anti-inflammatory effects in mice (Kogan et al., 2021).

The peak effects of CBG occurred on average at 90 min post administration, which is within the time course previously reported for peak plasma concentrations of CBG in rodents (Deiana et al., 2012). This prolonged time course for effects on blood pressure may suggest activation of central neurocircuits, as direct vascular effects of vasoactive agents typically occur within a shorter time frame [e.g., seconds-minutes; (White et al., 1999)]. Additionally, cannabinoids such as Δ^9-THC, as well as synthetic cannabinoid receptor agonists, are known to decrease psychomotor activity resulting in sedation (Bosier et al., 2010; Boggs et al., 2018), which could limit their use for therapeutic treatment. Our results show that CBG did not acutely alter locomotor activity, which is consistent with a lack of psychomotor and sedative effects to confound blood pressure changes. As mice were studied during the light cycle, however, it is unclear if CBG would impact blood pressure and locomotor activity differently during the more active dark cycle.

We further provide evidence that depressor effects of CBG are mediated by an α2AR mechanism. Agonists of α2AR, such as guanfacine and clonidine, act centrally with peak plasma concentrations within 1–4 h (Dollery and Davies, 1980; van Zwieten et al., 1984). These drugs are of therapeutic interest due to their antihypertensive and analgesic properties, but are often limited by sedation. Previous studies have shown that CBG can activate α2AR, and that these receptors are involved in effects on hyperphagia and peripheral tissue contraction (Cascio et al., 2010; Brierley et al., 2016). In support of this, we show that CBG depressor effects are prevented by pretreatment with the α2AR antagonist atipamezole. We further show that blood pressure effects of atipamezole are similar to that of atipamezole plus CBG, supporting pharmacological α2AR antagonism rather than additive effects of the drug combination. Of interest, CBG lowered blood pressure to a lesser extent than the α2AR agonist guanfacine. It is known that guanfacine has high selectivity for the $\alpha2_a$ receptor subtype in brain and reduces blood pressure less than clonidine. Similar to our findings, CBG was found to have less potency and efficacy than the α2AR agonist dexmedetomidine at inhibiting electrically-evoked vas deferens contraction (Cascio et al., 2010). Thus, it is possible that CBG is a less potent α2AR agonist, engages a different α2AR subtype, or can act on peripheral versus central α2AR for cardiovascular effects. Unfortunately, pharmacological probes and animal models to dissect the importance of peripheral versus central α2AR to CBG effects are not currently available.

To date, research on the effects of cannabinoid compounds on cardiovascular function is conflicting, with some studies showing cardioprotection and others showing adverse cardiovascular outcomes (Mittleman et al., 2001; Mukamal et al., 2008; Wolff et al., 2011; Abuhasira et al., 2021). These disparate findings may reflect differences in cannabinoids and the models used, mode of administration, or effects on cannabinoid versus other receptors in the periphery and central nervous system. Our finding that CBG lowers blood pressure is consistent with reports that: synthetic cannabinoids including Δ^9-THC may decrease blood pressure (Jones, 2002); cannabis users have increased risk of orthostatic hypotension (Mathew et al., 1992); CBD causes vasorelaxation in human mesenteric arteries (Stanley et al., 2015) and lowers blood pressure in hypertensive rats (Baranowska-Kuczko et al., 2020); and the sympathetic nervous appears to play a role in the cardiovascular depression effects of endocannabinoids (Niederhoffer et al., 2003; Dean, 2011). Despite this literature for other cannabinoids, very little is known about adverse effects or medication interactions for CBG, including potential effects on the cardiovascular system. Our findings may suggest caution against use of CBG in healthy individuals due to the potential for hypotension but may provide a new therapeutic approach to lower blood pressure in the context of hypertension.

Overall, these findings add to the growing literature regarding the role of cannabinoids in blood pressure regulation. Additional research on CBG is needed to define the precise molecular mechanisms and sites of action, effects of more chronic administration, and potential for therapeutic use to lower blood pressure in models of hypertension. Further, this study only included male mice and thus sex differences were not explored. Females tend to have lower resting blood pressure

(Sandberg and Ji, 2012; Joyner et al., 2016) and are more sensitive to α2AR agonism (Mitrovic et al., 2003), and thus may exhibit greater depressor responses to CBG. Our findings suggest that acute CBG lowers blood pressure in phenotypically normal mice likely *via* an α2AR mechanism, which may be an important consideration for therapeutic CBG administration.

DATA AVAILABILITY STATEMENT

The original contributions presented in the study are included in the article/Supplementary Material, further inquiries can be directed to the corresponding author.

ETHICS STATEMENT

The animal study was reviewed and approved by Penn State College of Medicine Institutional Animal Care and Use Committee (IACUC).

AUTHOR CONTRIBUTIONS

Participated in research design: SB, WR-K, KV, YS, AA; Conducted experiments: VV, SB, ACA; Contributed new reagents or analytic tools: WR-K, KV; Performed data analysis: VV, AA; Wrote first draft of the manuscript: VV, AA; Provided critical revisions to the manuscript: SB, WR-K, KV, YS.

FUNDING

This study was funded by grants from the NIH (R01 HL156986) and the Pennsylvania Options for Wellness.

ACKNOWLEDGMENTS

The authors would like to acknowledge the members of the state-approved Medical Marijuana Academic Clinical Research Center at Penn State for support and discussions of the data.

REFERENCES

Abuhasira, R., Haviv, Y. S., Leiba, M., Leiba, A., Ryvo, L., and Novack, V. (2021). Cannabis Is Associated with Blood Pressure Reduction in Older Adults - A 24-hours Ambulatory Blood Pressure Monitoring Study. *Eur. J. Intern. Med.* 86, 79–85. doi:10.1016/j.ejim.2021.01.005

Baranowska-Kuczko, M., Kozłowska, H., Kloza, M., Sadowska, O., Kozłowski, M., Kusaczuk, M., et al. (2020). Vasodilatory Effects of Cannabidiol in Human Pulmonary and Rat Small Mesenteric Arteries: Modification by Hypertension and the Potential Pharmacological Opportunities. *J. Hypertens.* 38, 896–911. doi:10.1097/HJH.0000000000002333

Boggs, D. L., Cortes-Briones, J. A., Surti, T., Luddy, C., Ranganathan, M., Cahill, J. D., et al. (2018). The Dose-dependent Psychomotor Effects of Intravenous Delta-9-Tetrahydrocannabinol (Δ9-THC) in Humans. *J. Psychopharmacol.* 32, 1308–1318. doi:10.1177/0269881118799953

Borrelli, F., Fasolino, I., Romano, B., Capasso, R., Maiello, F., Coppola, D., et al. (2013). Beneficial Effect of the Non-psychotropic Plant Cannabinoid Cannabigerol on Experimental Inflammatory Bowel Disease. *Biochem. Pharmacol.* 85, 1306–1316. doi:10.1016/j.bcp.2013.01.017

Bosier, B., Sarre, S., Smolders, I., Michotte, Y., Hermans, E., and Lambert, D. M. (2010). Revisiting the Complex Influences of Cannabinoids on Motor Functions Unravels Pharmacodynamic Differences between Cannabinoid Agonists. *Neuropharmacology* 59, 503–510. doi:10.1016/j.neuropharm.2010.07.005

Brierley, D. I., Samuels, J., Duncan, M., Whalley, B. J., and Williams, C. M. (2016). Cannabigerol Is a Novel, Well-Tolerated Appetite Stimulant in Pre-satiated Rats. *Psychopharmacology* 233, 3603–3613. doi:10.1007/s00213-016-4397-4

Cascio, M., Gauson, L., Stevenson, L., Ross, R., and Pertwee, R. (2010). Evidence that the Plant Cannabinoid Cannabigerol Is a Highly Potent α2-adrenoceptor Agonist and Moderately Potent 5HT1A Receptor Antagonist. *Br. J. Pharmacol.* 159, 129–141. doi:10.1111/j.1476-5381.2009.00515.x

Cathel, A. M., Reyes, B. A. S., Wang, Q., Palma, J., Mackie, K., Van Bockstaele, E. J., et al. (2014). Cannabinoid Modulation of Alpha2adrenergic Receptor Function in Rodent Medial Prefrontal Cortex. *Eur. J. Neurosci.* 40, 3202–3214. doi:10.1111/ejn.12690

Committee on the Health Effects of MarijuanaAn Evidence Review and Research AgendaBoard on Population Health and Public Health PracticeHealth and Medicine DivisionNational Academies of Sciences, Engineering, and Medicine (2017). *The Health Effects of Cannabis and Cannabinoids: The Current State of Evidence and Recommendations for Research*. Washington, D.C.: National Academies Press. doi:10.17226/24625

Dean, C. (2011). Cannabinoid and GABA Modulation of Sympathetic Nerve Activity and Blood Pressure in the Dorsal Periaqueductal Gray of the Rat. *Am. J. Physiology-Regulatory, Integr. Comp. Physiology* 301, R1765–R1772. doi:10.1152/ajpregu.00398.2011

Deiana, S., Watanabe, A., Yamasaki, Y., Amada, N., Arthur, M., Fleming, S., et al. (2012). Plasma and Brain Pharmacokinetic Profile of Cannabidiol (CBD), Cannabidivarine (CBDV), Δ9-tetrahydrocannabivarin (THCV) and Cannabigerol (CBG) in Rats and Mice Following Oral and Intraperitoneal Administration and CBD Action on Obsessive-Compulsive Behaviour. *Psychopharmacology* 219, 859–873. doi:10.1007/s00213-011-2415-0

Dollery, C., and Davies, D. (1980). Centrally Acting Drugs in Antihypertensive Therapy. *Br. J. Clin. Pharmacol.* 10, 5S–12S. doi:10.1111/j.1365-2125.1980.tb04898.x

Formukong, E. A., Evans, A. T., and Evans, F. J. (2011). The Inhibitory Effects of Cannabinoids, the Active Constituents of Cannabis Sativa L. On Human and Rabbit Platelet Aggregation. *J. Pharm. Pharmacol.* 41, 705–709. doi:10.1111/j.2042-7158.1989.tb06345.x

Giovannitti, J. A., Thoms, S. M., and Crawford, J. J. (2015). Alpha-2 Adrenergic Receptor Agonists: A Review of Current Clinical Applications. *Anesth. Prog.* 62, 31–38. doi:10.2344/0003-3006-62.1.31

Janssen, B. J. A., De Celle, T., Debets, J. J. M., Brouns, A. E., Callahan, M. F., and Smith, T. L. (2004). Effects of Anesthetics on Systemic Hemodynamics in Mice. *Am. J. Physiology-Heart Circulatory Physiology* 287, H1618–H1624. doi:10.1152/ajpheart.01192.2003

Jones, R. T. (2002). Cardiovascular System Effects of Marijuana. *J. Clin. Pharmacol.* 42, 58S–63S. doi:10.1002/j.1552-4604.2002.tb06004.x

Joyner, M. J., Wallin, B. G., and Charkoudian, N. (2016). Sex Differences and Blood Pressure Regulation in Humans. *Exp. Physiol.* 101, 349–355. doi:10.1113/EP085146

Kogan, N. M., Lavi, Y., Topping, L. M., Williams, R. O., McCann, F. E., Yekhtin, Z., et al. (2021). Novel CBG Derivatives Can Reduce Inflammation, Pain and Obesity. *Molecules* 26, 5601. doi:10.3390/molecules26185601

Kovalchuk, O., and Kovalchuk, I. (2020). Cannabinoids as Anticancer Therapeutic Agents. *Cell. Cycle* 19, 961–989. doi:10.1080/15384101.2020.1742952

Mathew, R. J., Wilson, W. H., Humphreys, D., Lowe, J. V., and Wiethe, K. E. (1992). Middle Cerebral Artery Velocity during Upright Posture after Marijuana Smoking. *Acta Psychiatr. Scand.* 86, 173–178. doi:10.1111/j.1600-0447.1992.tb03247.x

Mitrovic, I., Margeta-Mitrovic, M., Bader, S., Stoffel, M., Jan, L. Y., and Basbaum, A. I. (2003). Contribution of GIRK2-Mediated Postsynaptic Signaling to Opiate and α 2 -adrenergic Analgesia and Analgesic Sex Differences. *Proc. Natl. Acad. Sci. U.S.A.* 100, 271–276. doi:10.1073/pnas.0136822100

Mittleman, M. A., Lewis, R. A., Maclure, M., Sherwood, J. B., and Muller, J. E. (2001). Triggering Myocardial Infarction by Marijuana. *Circulation* 103, 2805–2809. doi:10.1161/01.CIR.103.23.2805

Mukamal, K. J., Maclure, M., Muller, J. E., and Mittleman, M. A. (2008). An Exploratory Prospective Study of Marijuana Use and Mortality Following Acute Myocardial Infarction. *Am. Heart J.* 155, 465–470. doi:10.1016/j.ahj.2007.10.049

Nachnani, R., Raup-Konsavage, W. M., and Vrana, K. E. (2021). The Pharmacological Case for Cannabigerol. *J. Pharmacol. Exp. Ther.* 376, 204–212. doi:10.1124/jpet.120.000340

Niederhoffer, N., Schmid, K., and Szabo, B. (2003). The Peripheral Sympathetic Nervous System Is the Major Target of Cannabinoids in Eliciting Cardiovascular Depression. *Schmiedeb. Arch. Pharmacol.* 367, 434–443. doi:10.1007/s00210-003-0755-y

Pacher, P., Bátkai, S., and Kunos, G. (2005). Blood Pressure Regulation by Endocannabinoids and Their Receptors. *Neuropharmacology* 48, 1130–1138. doi:10.1016/j.neuropharm.2004.12.005

Rock, E. M., Goodwin, J. M., Limebeer, C. L., Breuer, A., Pertwee, R. G., Mechoulam, R., et al. (2011). Interaction between Non-psychotropic Cannabinoids in Marihuana: Effect of Cannabigerol (CBG) on the Anti-nausea or Anti-emetic Effects of Cannabidiol (CBD) in Rats and Shrews. *Psychopharmacology* 215, 505–512. doi:10.1007/s00213-010-2157-4

Rosenthaler, S., Pöhn, B., Kolmanz, C., Nguyen Huu, C., Krewenka, C., Huber, A., et al. (2014). Differences in Receptor Binding Affinity of Several Phytocannabinoids Do Not Explain Their Effects on Neural Cell Cultures. *Neurotoxicology Teratol.* 46, 49–56. doi:10.1016/j.ntt.2014.09.003

Sandberg, K., and Ji, H. (2012). Sex differences in primary hypertension. *Biol sex dif* 3, 7. doi:10.1186/2042-6410-3-7

Stanley, C. P., Hind, W. H., Tufarelli, C., and O'Sullivan, S. E. (2015). Cannabidiol causes endothelium-dependent vasorelaxation of human mesenteric arteries *via* CB1activation. *Cardiovasc. Res.* 107, 568–578. doi:10.1093/cvr/cvv179

Valdeolivas, S., Navarrete, C., Cantarero, I., Bellido, M. L., Muñoz, E., and Sagredo, O. (2015). Neuroprotective Properties of Cannabigerol in Huntington's Disease: Studies in R6/2 Mice and 3-Nitropropionate-Lesioned Mice. *Neurotherapeutics* 12, 185–199. doi:10.1007/s13311-014-0304-z

van Zwieten, P. A., Thoolen, M. J., and Timmermans, P. B. (1984). The Hypotensive Activity and Side Effects of Methyldopa, Clonidine, and Guanfacine. *Hypertension* 6, 1128. doi:10.1161/01.HYP.6.5_Pt_2.II28

White, M., Fourney, A., Mikes, E., and Leenen, F. H. (1999). Effects of Age and Hypertension on Cardiac Responses to the Alpha1-Agonist Phenylephrine in Humans. *Am. J. Hypertens.* 12, 151–158. doi:10.1016/s0895-7061(98)00220-9

Wolff, V., Lauer, V., Rouyer, O., Sellal, F., Meyer, N., Raul, J. S., et al. (2011). Cannabis Use, Ischemic Stroke, and Multifocal Intracranial Vasoconstriction. *Stroke* 42, 1778–1780. doi:10.1161/STROKEAHA.110.610915

Ying, Z., Xu, X., Bai, Y., Zhong, J., Chen, M., Liang, Y., et al. (2014). Long-Term Exposure to Concentrated Ambient PM 2.5 Increases Mouse Blood Pressure through Abnormal Activation of the Sympathetic Nervous System: A Role for Hypothalamic Inflammation. *Environ. Health Perspect.* 122, 79–86. doi:10.1289/ehp.1307151

Zagzoog, A., Mohamed, K. A., Kim, H. J. J., Kim, E. D., Frank, C. S., Black, T., et al. (2020). *In Vitro* and *In Vivo* Pharmacological Activity of Minor Cannabinoids Isolated from Cannabis Sativa. *Sci. Rep.* 10, 20405. doi:10.1038/s41598-020-77175-y

Conflict of Interest: The authors declare that the research was conducted in the absence of any commercial or financial relationships that could be construed as a potential conflict of interest.

Publisher's Note: All claims expressed in this article are solely those of the authors and do not necessarily represent those of their affiliated organizations, or those of the publisher, the editors and the reviewers. Any product that may be evaluated in this article, or claim that may be made by its manufacturer, is not guaranteed or endorsed by the publisher.

Copyright © 2022 Vernail, Bingaman, Silberman, Raup-Konsavage, Vrana and Arnold. This is an open-access article distributed under the terms of the Creative Commons Attribution License (CC BY). The use, distribution or reproduction in other forums is permitted, provided the original author(s) and the copyright owner(s) are credited and that the original publication in this journal is cited, in accordance with accepted academic practice. No use, distribution or reproduction is permitted which does not comply with these terms.

frontiers | Frontiers in Physiology

MINI REVIEW
published: 10 May 2022
doi: 10.3389/fphys.2022.829920

Cardiometabolic Effects of Postnatal High-Fat Diet Consumption in Offspring Exposed to Maternal Protein Restriction *In Utero*

Aiany Cibelle Simões-Alves[1], *Ana Paula Fonseca Cabral Arcoverde-Mello*[1], *Jéssica de Oliveira Campos*[1], *Almir Gonçalves Wanderley*[2], *Carol Virginia Gois Leandro*[1], *João Henrique da Costa-Silva*[1] *and Viviane de Oliveira Nogueira Souza*[1]*

[1]*Laboratory of Nutrition, Physical Activity and Phenotypic Plasticity, Department of Physical Education and Sport Sciences, Universidade Federal de Pernambuco UFPE, Vitória de Santo Antão, Brazil,* [2]*Department of Physiology and Pharmacology, Universidade Federal de Pernambuco UFPE, Recife, Brazil*

In recent decades, the high incidence of infectious and parasitic diseases has been replaced by a high prevalence of chronic and degenerative diseases. Concomitantly, there have been profound changes in the behavior and eating habits of families around the world, characterizing a "nutritional transition" phenomenon, which refers to a shift in diet in response to modernization, urbanization, or economic development from undernutrition to the excessive consumption of hypercaloric and ultra-processed foods. Protein malnutrition that was a health problem in the first half of the 20th century has now been replaced by high-fat diets, especially diets high in saturated fat, predisposing consumers to overweight and obesity. This panorama points us to the alarming coexistence of both malnutrition and obesity in the same population. In this way, individuals whose mothers were undernourished early in pregnancy and then exposed to postnatal hyperlipidic nutrition have increased risk factors for developing metabolic dysfunction and cardiovascular diseases in adulthood. Thus, our major aim was to review the cardiometabolic effects resulting from postnatal hyperlipidic diets in protein-restricted subjects, as well as to examine the epigenetic repercussions occasioned by the nutritional transition.

Keywords: hypertension, obesity, nutrition transition, saturated fatty acids, dyslipidemia

OPEN ACCESS

Edited by:
Jacqueline Kathleen Phillips, Macquarie University, Australia

Reviewed by:
Keshari Thakali, University of Arkansas for Medical Sciences, United States

***Correspondence:**
Viviane de Oliveira Nogueira Souza
viviane.nogueira@ufpe.br

Specialty section:
This article was submitted to Integrative Physiology, a section of the journal Frontiers in Physiology

Received: *06 December 2021*
Accepted: *29 March 2022*
Published: *10 May 2022*

Citation:
Simões-Alves AC, Arcoverde-Mello APFC, Campos JdO, Wanderley AG, Leandro CVG, da Costa-Silva JH and de Oliveira Nogueira Souza V (2022) Cardiometabolic Effects of Postnatal High-Fat Diet Consumption in Offspring Exposed to Maternal Protein Restriction In Utero. Front. Physiol. 13:829920. doi: 10.3389/fphys.2022.829920

INTRODUCTION

In the second half of the 20th century, a change in the dietary habits of the population, mainly in the western part of the world, was observed, called a phenomenon of "nutrition transition" (Hasan et al., 2016; Herran et al., 2016). The nutritional transition was characterized by a reduction in the prevalence of malnutrition in its various dimensions (energy and macro- or micronutrients), accompanied by excessive consumption of hypercaloric and ultra-processed foods, with a consequent increase in body weight (Abdullah, 2015), a high incidence of chronic diseases, and a high prevalence of obesity (Batista Filho and Rissin, 2003a; Batista Filho and Batista, 2010; Ribeiro et al., 2015). Concomitantly, it was possible to observe profound changes in the behavior and eating habits of families around the world (Popkin, 2015). Higher levels of undernutrition have been replaced by higher rates of overweight and obesity related to hyperlipidic and hypercaloric food consumption (Di Pietro et al., 2015). Epidemiological evidence has shown that nutritional deficiency

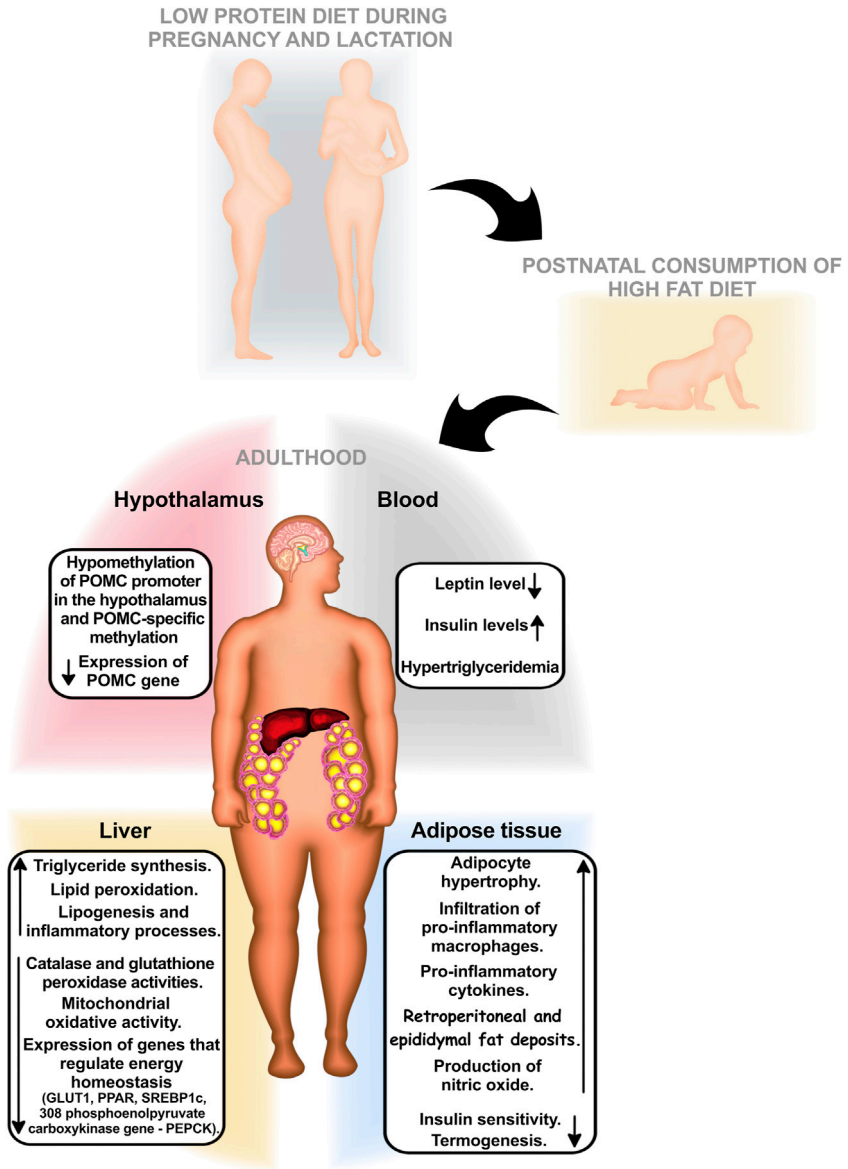

FIGURE 1 | Diets low in protein in the first years of life, followed by high consumption of high-fat diets, can increase the risk of cardiometabolic diseases in adulthood, such as hypertension, dyslipidemia, and type 2 diabetes.

in the first years of life accompanied by overnutrition, a *posteriori*, may increase the risk of dyslipidemia and other cardiometabolic diseases in adulthood, such as hypertension and type 2 diabetes (**Figure 1**) (Barker, 2007). In this context, individuals subjected to maternal protein undernutrition *in utero* have been considered those with a high risk of developing cardiometabolic dysfunctions in adulthood (Ashton, 2000; Hemachandra et al., 2006; Antony and Laxmaiah, 2008; Conde and Monteiro, 2014; Costa-Silva et al., 2015; Parra et al., 2015). Furthermore, studies have suggested that when these individuals are additionally subjected to inappropriate postnatal nutrition, especially hyperlipidic diets, they may significantly suffer heightened energy balance dysfunctions in adulthood (Desai et al., 2007). Thus, the eating habits and nutritional conditions in early phases of life play a key role in the etiology of these diseases by inducing physiological dysfunctions (Lucas, 1998; Victora et al., 2008; Wells, 2012). Many studies have suggested that external environmental inputs, such as nutrition, may modify the phenotype, leading to physiological adaptations without genetic changes. This phenomenon can be understood in the context of phenotypic plasticity. (West-Eberhard, 2003).

Phenotypic plasticity is molecularly based on epigenetic changes, such as DNA methylation, post-translational histone modifications, and microRNA expression (Wells, 2011). The epigenetic landscape was first described by Conrad Waddington in 1940 who studied the relationship between the

cause and effect in genes to produce a phenotype (Jablonka and Lamb, 2002). Currently, this concept is used for the process of gene expression and its link to modifications in the chromatin structure without altering the DNA sequence (Chong and Whitelaw, 2004; Egger et al., 2004). Changes in the chromatin structure are related to the increase or decrease in the electrostatic affinity of the DNA structure. DNA methylation, post-translational modifications of histones, and expression of microRNAs are capable of altering a chromatin structure (Sadakierska-Chudy and Filip, 2015). DNA methylation is related to the addition of methyl groups to DNA cytosine residues, usually cytosine, followed by the guanine residue (CpG dinucleotides), which can produce inhibition of gene expression by impairing transcription factor binding (Waterland and Michels, 2007; Mansego et al., 2013; Chango and Pogribny, 2015; Mitchell et al., 2016). As post-translational histone modifications (acetylation, methylation, ubiquitination, and phosphorylation) correspond to the addition of methyl, acetyl, or other groups to the histone tails, they increase or decrease the electrostatic affinity between histone proteins and DNA, thus promoting a structure of chromatin that is more or less permissive to gene transcription (Bowman and Poirier, 2015). The addition of acetyl groups to histones is regulated by the action of histone acetyltransferases (HATs), while the removal of acetyl groups is catalyzed by histone deacetylases (HDACs) (Graff and Tsai, 2013). MicroRNAs are small endogenous non-coding RNA molecules involved in gene regulation and function in protein-coding introns, non-coding gene introns, or non-coding gene exons; they have been implicated in many cellular processes, including proliferation, apoptosis, differentiation, senescence, and responses to stress and immunological stimuli (D'Ippolito and Iorio, 2013).

This provides the basis for an investigation on how the nutritional aspect can induce these epigenetic changes. The hypothesis is that epigenetic modifications are an extended mechanism that links maternal nutrition to the modulation of phenotypes in the offspring (Mazzio E. A. and Soliman K. F. A., 2014; Szarc vel Szic et al., 2015). Thus, this review will address the main cardiometabolic effects elicited by postnatal hyperlipidic diets in protein-restricted subjects during pregnancy and lactation.

MATERNAL PROTEIN UNDERNUTRITION AND DEVELOPMENT OF CARDIOMETABOLIC DISEASES

Developmental origins of health and diseases as proposed by Barker and colleagues in 1986 have been extensively studied as physiological consequences of perinatal nutritional factors (Barker and Osmond, 1986; Barker et al., 1989; Barker et al., 1993; Barker, 2007). This field of research proposes that cardiometabolic diseases can be "programmed" by the "adaptive" effects of both under- and overnutrition during early phases of growth and development, changing the cell physiology in the phenotype but without altering the genotype (Barker et al., 2005; West-Eberhard, 2005; Labayen et al., 2006; Andersen et al., 2009; Biosca et al., 2011). In this context, phenotypic plasticity has molecular basis, epigenetic alterations such as DNA methylation, histone acetylation, and microRNA expression (Wells, 2011). These epigenetic marks are established early in development and can persist for a lengthy period of time (John and Rougeulle, 2018).

Epigenetic modifications are widely hypothesized to be an overarching mechanism linking maternal nutrition to metabolic health phenotypes in the offspring (Mazzio EA. and Soliman KF., 2014; Szarc vel Szic et al., 2015). In this context, a low-protein diet (8% protein) during gestation and lactation has been associated with growth restriction, asymmetric reduction in organ growth, elevated systolic blood pressure, dyslipidemia, and increased fasting plasma insulin concentrations in most studies on rat offspring (Ozanne and Hales, 2004; Costa-Silva et al., 2009; Falcao-Tebas et al., 2012; Leandro et al., 2012; Fidalgo et al., 2013; de Brito Alves et al., 2014; Ferreira et al., 2015; de Brito Alves et al., 2016; Paulino-Silva and Costa-Silva, 2016; Barbosa et al., 2020). However, it is known that the magnitude of the cardiovascular and metabolic outcomes is dependent on both time exposure to a protein restricted-diet (Zohdi et al., 2012; Zohdi et al., 2014) and the growth trajectory throughout the postnatal period (Wells, 2007; Wells, 2011).

A relationship between maternal protein restriction, sympathetic overactivity, and hypertension has been suggested (Johansson et al., 2007; Franco et al., 2008; Barros et al., 2015). Currently, it is well accepted that perinatal protein malnutrition (6–9% protein) raises the risks of hypertension by mechanisms that have been shown to include abnormal vascular function in the adult rat male (Brawley et al., 2003; Franco et al., 2008), altered nephron morphology and function, and stimulation of the renin-angiotensin system in the adult rat male (Nuyt and Alexander, 2009; Siddique et al., 2014) as well as disruption in respiratory control in the rat male at 30 and 90 days of life (Chen et al., 2010; de Brito Alves et al., 2014; Barros et al., 2015; Costa-Silva et al., 2015; Paulino-Silva and Costa-Silva, 2016; de Brito Alves and Costa-Silva, 2018). Offspring from dams subjected to perinatal protein restriction had relevant short-term effects on the carotid body (CB) and sensitivity and respiratory functions as well as enhanced baseline sympathetic activity and amplified ventilatory and sympathetic responses to peripheral chemoreflex activation, prior to the establishment of hypertension (de Brito Alves et al., 2014; de Brito Alves et al., 2015). The mechanism involved in these effects seems to be linked with upregulation of the hypoxic inducible factor (HIF-1α) in the CB peripheral chemoreceptors (Ito et al., 2011; Ito et al., 2012; de Brito Alves et al., 2015; Nogueira et al., 2018). Studies showed that CB peripheral chemoreceptors in malnourished offspring were responsible for the enhanced respiratory frequency and CO_2 chemosensitivity in early life and the production of autonomic imbalance and the development of hypertension in adulthood (Nogueira et al., 2018). In addition, it was demonstrated that these cardiorespiratory disruptions observed in offspring were attenuated from mothers who performed physical activity during the perinatal period (Nogueira et al., 2019). Regarding epigenetics mechanisms involved in cardiometabolic effects elicited by protein

malnutrition, it was described as a decrease in the methylation at various positions of the ACE-1 promoter region in rat brain and an increase in transcription of this gene involved in the renin-angiotensin system and the maintenance of arterial blood pressure (Goyal et al., 2010). Similarly, in humans, the DNA methylation in the ACE gene promoter of peripheral blood leukocytes seems to be significantly lower in children of age ranging from 6 to 12 years born with low birth weight, resulting in greater ACE activity (Ajala et al., 2012; Rangel et al., 2014).

Maternal protein restriction affects insulin sensitivity in the offspring. Previous studies found that in rats, maternal protein restriction throughout pregnancy and lactation induced insulin resistance in the male offspring (Zambrano et al., 2006; Berends et al., 2018). This central insulin resistance is related to reduced protein levels of the p110β subunit of phosphoinositide 3-kinase (PI3K) and increased serine phosphorylation of IRS-1 in the arcuate nucleus (ARC) of the hypothalamus. The expression of the gene encoding protein tyrosine phosphatase 1B (PTP1B; Ptpn1) was also increased in the region of the hypothalamus (Berends et al., 2018); the mechanism appeared to increase insulin receptor signaling mediated by protein kinase C (PKC)-ζ in skeletal muscle of the offspring of rats fed with a low-protein diet during pregnancy and lactation (Chen et al., 2009). The ability of skeletal muscle to respond to maternal protein restriction is an adaptation to optimize the use of nutrients available during the life-span, and an important response in this process is the activation of genes that ameliorate or compensate for protein deficit by stimulating the expression of glucose transporters and glycolytic and lipolytic enzymes that attenuate the altered function of the mitochondria (da Silva Aragao et al., 2014; Claycombe et al., 2015). At 30 days, the transcriptional key enzymes of the glycolytic pathway were downregulated in extensor digitorum longus muscle in offspring. However, these effects were only observed at 90 days in soleus muscle of rats subjected to protein maternal undernutrition. PDK4 was the enzyme that was more affected. One important finding was that the observed acute (30 days) transcriptional changes did not remain in adult LP rats (90 days), except for PDK4. The robust PDK4 mRNA downregulation, observed in both soleus and EDL, at both ages, and the consequent downregulation of the PDK4 protein expression can be responsible for a state of reduced metabolic flexibility of skeletal muscle in response to maternal low-protein diet (de Brito Alves et al., 2017).

Studies in rodents subjected to perinatal protein malnutrition have observed an impact on liver function with the suppression of gluconeogenesis by a mechanism mediated mainly by the decrease in the level of hepatic phosphoenolpyruvate carboxykinase mRNA (Toyoshima et al., 2010), increase in blood cholesterol and triglycerides in the offspring at 110 days of life, and reduced gene expression for the glucokinase (GCK) enzyme, the glucose sensor in the liver, impairing the detection of glucose levels (Sosa-Larios et al., 2017); these effects have been accompanied by DNA hypomethylation and increased expression of genes involved in lipid metabolism (Radford et al., 2014) and hypomethylation of glucocorticoid receptors and PPAR-α promoters, which conditioned changes in the expression of their target genes (Sandovici et al., 2011); at 21 days, the mice showed a reduction in the microRNAs, namely, mmu-miR-615, mmu-miR-124, mmu-miR-376b, and mmu-let-7e, while mmu-miR-708 and mmu-miR-879 were increased after microarray analysis; bioinformatics analysis showed that target genes were mapped to inflammatory pathways, accompanied by elevation of serum levels of tumor necrosis factor-α (TNF-α) (Zheng et al., 2017).

POSTNATAL OVERNUTRITION AND DEVELOPMENT OF CARDIOMETABOLIC DISEASES IN MATERNAL PROTEIN-RESTRICTED SUBJECTS

Nutritional transition is a phenomenon well documented in developing countries in the 20th and 21st centuries and has induced a high incidence of the chronic diseases and a high prevalence of obesity (Batista Filho and Rissin, 2003b; Batista Filho and Batista, 2010; Ribeiro et al., 2015; Leocádio et al., 2021). It is evident that protein malnutrition was a health problem in the first half of the 20th century. Now, this has been replaced by a diet enriched in saturated fat or other high-fat diets, predisposing the population to overweight and obesity (Batista et al., 2013). Nowadays, it is suggested that two billion people in the world are overweight and obese individuals, with a major prevalence related to diet-induced obesity, which has been associated with cardiovascular and endocrine dysfunctions (Hotamisligil, 2006; Aubin et al., 2008; Zhang et al., 2012; Ng et al., 2014; Wensveen et al., 2015).

In the late 1980s–1990s, Barker et al. provided epidemiologic evidence of the programming of offspring metabolic syndrome, demonstrating that low birth weight was a significant predictor of adult obesity, diabetes, and cardiovascular disease, for promoting changes in the fetal environment, which can trigger genetic alterations and reflect on the maturation of fetal organs and systems (Barker, 1999; Barker, 2007). In a recent global survey conducted in 30 low-income countries, Abdullah (2015) related that the pattern of body weight gain of the population of developing countries is almost identical to that found in those countries and calculated the estimate of overweight over time, being higher in groups with less and less education. The coexistence of malnourished children and obese mothers in the same residence is a reality in Mexico (Kroker-Lobos et al., 2014), Colombia (Sarmiento et al., 2014), China (Feng et al., 2015), sub-Saharan Africa (Steyn and McHiza, 2014), and also in Brazil (Sousa et al., 2016). Short stature and obesity may reflect malnutrition and a poor quality diet in the first 2 years of life, followed by excess energy intake later in childhood (Abdullah, 2015).

Some studies have tried to mimic the nutritional transition, with peri- and postnatal nutritional mismatch, producing animal models that are based on maternal protein restriction during pregnancy and/or lactation, followed by the consumption of high-fat diets by the offspring, after weaning. Epidemiological studies have demonstrated that low birth weight makes

individuals more susceptible to hypercholesterolemia only when combined with postnatal consumption of a high-fat diet (Robinson et al., 2006). These results suggest that the postnatal nutritional environment may affect cholesterol metabolism differently in low birth weight individuals compared to their normal weight peers. One mechanism that may explain the link between prenatal growth and adult disease is a permanent change in gene expression in response to the early environment (Gluckman and Hanson, 2004).

Animal studies have shown that a high-fat diet significantly increased weights and body fat of malnourished rats in gestation and/or lactation, reduced lean body mass, and accentuated plasma leptin, an increase in glucose levels with increased insulin levels and hypertriglyceridemia in male rats (Desai et al., 2015). Assessing the effects of a nutritional transition model with incompatibility between peri- and postnatal diets in mice, Sellayah et al. (2014) offered a control diet (18% protein) or protein-restricted diet (9% protein) during pregnancy and lactation to mothers. After weaning, the male pups began to receive a standard diet (7% fat) or a high-fat diet (45% fat) until 30 weeks of age. The authors observed that offspring maternal protein restriction to those who consumed high-fat diet resulted in an increase in body adiposity, even without changing the total weight or increasing the lipid content in muscle tissue. While the consumption of a high-fat diet by animals that had not suffered previous malnutrition promoted an increase in energy expenditure and expression of proteins related to thermogenesis (uncoupling protein 1 - UCP1; adrenergic receptor beta 3 - β-3AR) in brown adipose tissue, the maternal protein restriction did not show the same response. These results suggested that a mismatch can attenuate diet-induced thermogenesis and contribute to the development of obesity. Animals with maternal protein restriction (5% protein) fed for 4 weeks with a high-fat diet showed a relatively dangerous increase in the white adipose tissue and a decrease in gross gastrocnemius muscle weight in males even without causing changes in bodyweight; in addition, males and females exhibited anxiety-like behaviors (de Almeida Silva et al., 2020).

The increase in white adipose tissue may be one of the factors that contribute to the development of cardiometabolic diseases in maternal protein-restricted individuals. A continuous intake of an HF diet can promote adipocyte hypertrophy and dysfunction and induce the infiltration of pro-inflammatory macrophages in adipose tissue, increasing the production of pro-inflammatory cytokines in this tissue (Ouchi et al., 2011). An increased immune activity is associated with a high consumption of high-fat diets and favors the maintenance of chronic systemic inflammatory processes, originating in adipose tissue (Wensveen et al., 2015; Ertunc and Hotamisligil, 2016; Lyons et al., 2016). Using a mouse model of a prenatal low-protein diet (LP, 8% protein) followed by a normal or postnatal diet high-energy in fat (HE, 45% fat) for 12 weeks, maternal protein restriction added to a high-fat diet interacts to affect growth recovery and leads to an increase of the offspring's adipocyte tissue, which correlates with the phenotype of inflammation in adipose tissue (Xie et al., 2017). In this study, adipose tissue macrophage infiltration was not affected by the LP diet, as evidenced by the lack of difference in the number of CD68 cells in the adipose tissue. However, after postnatal treatment of HE, there were fewer cells of adipose tissue macrophages M1b subtypes (CD11c + CD206+) in f1 offspring from maternal LP dam than those on the normal protein maternal diet. The maternal LP diet interacts with the postnatal high-fat diet to impact the macrophage phenotypes of the existing adipose tissue, although the prenatal LP diet may not influence the ability of monocyte/macrophage migration from adipose tissue in F1 mouse offspring. At 60 days of age, the interaction between low maternal protein during pregnancy and lactation (9% casein) and offspring's high-fat diet, after weaning (45% lipids), increased retroperitoneal and epididymal fat deposits and increased the production of nitric oxide by adipocyte macrophages (Alheiros-Lira et al., 2017). Adipose tissue with dysfunctional signaling has been considered to trigger reduced insulin sensitivity (Caricilli et al., 2008; Calder, 2012) and change the plasma and tissue lipid profile (Ralston et al., 2017) in addition to promoting cardiovascular disorders (Wang and Hu, 2017). A high production of nitric oxide has been implicated in the apoptosis of macrophages (Sarih et al., 1993) and pathogenesis of inflammatory diseases (Borges et al., 2013), suggesting high immunoreactivity induced by dietary fatty acids after metabolic programming with maternal protein restriction. Maternal prenatal malnutrition appears to modify the programs of the gene expression profile of offspring adipose tissue over the long term; this, combined with obesogenic nutrition, predisposes prenatal malnourished individuals to an altered lipid metabolism and fat accumulation in adulthood (Lukaszewski et al., 2011).

Maternal protein restriction (8% casein) during pregnancy and lactation followed by a post-weaning HF diet (41% fat) induced an increase in the percentage of visceral fat, reduced insulin sensitivity, and increased food intake in rat males at 90 days of age (Gosby et al., 2010). In an experimental design with Sprague–Dawley rats, Iwasa et al. (2017) demonstrated that the consumption of a post-weaning high-fat diet (62.2% of calories from fat) induced an increase in the serum leptin level and a trend toward a reduction in the hypothalamic POMC mRNA level in the offspring of undernourished dams, whereas it had no effect on the levels of orexigenic factors or other anorexigenic factors. Male mice at 220 days of life malnourished during pregnancy and lactation and fed with a high-fat postnatal diet showed increased gene expression of POMC and MC4R in the hypothalamus and hypomethylation of the POMC promoter in the hypothalamus (Zheng et al., 2021). Vickers et al. (2000) studied the interaction between restricted maternal diet and amplification by a post-weaning high-fat diet and demonstrated that deep adult hyperphagia is a consequence of fetal programming and an essential contributing factor to adult pathophysiology.

At the serum level, the activity of adipokines, such as leptin, in malnourished organisms, presents divergent behavior and suggests action and selective sensitivity, both with endocrine regulation function (do Prado et al., 2009), in both immune (Arroyo Hornero et al., 2020) and physiological systems. A

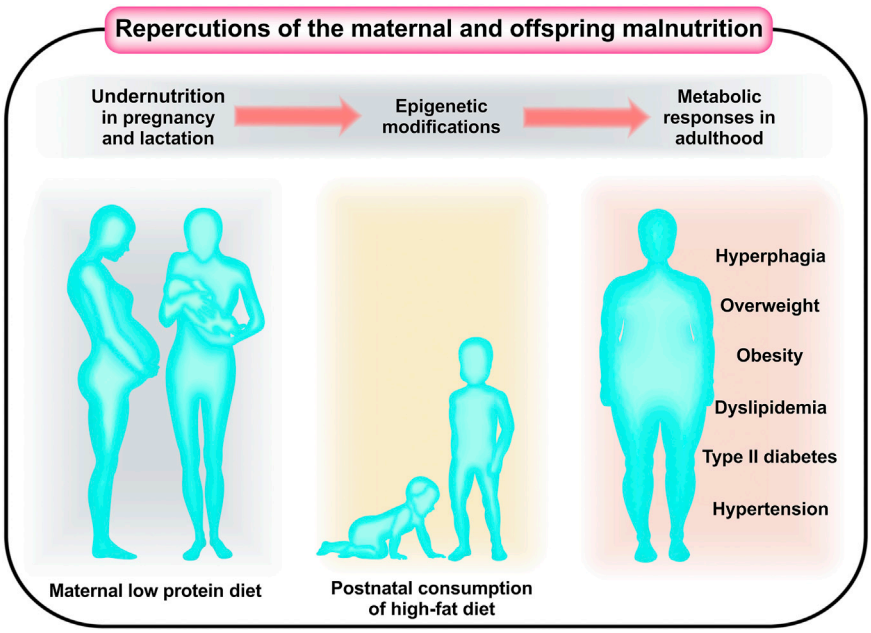

FIGURE 2 | Graphic summary of the repercussions of the postnatal consumption of high-fat diets in individuals subjected to protein restriction during pregnancy and lactation.

study by Sellayah et al. (2014) sought to evaluate the effects of incompatibility between the fetal nutritional environment poor in proteins and a lipid-rich environment in the post-weaning period; Wistar rats received a control diet (18% casein) or with protein restriction (9%) during pregnancy and standard diet during lactation. Pups, including males and females, started to receive a control diet (7% lipids and 15% casein) or a high-fat diet (45% lipids and 26% casein), from weaning to 16 weeks of age, when they were evaluated. The study demonstrated that the nutritional mismatch exacerbates the increase in blood pressure promoted by maternal malnutrition, regardless of increased body adiposity, glucose, or leptin levels, modulated upward only by the high-fat diet and not by the maternal diet during pregnancy. Post-weaning hyperlipidic diets have numerous impacts on glycolipid metabolism in offspring with maternal protein restriction, insulin intolerance, decreased insulin sensitivity, higher triglyceride/high-density lipoprotein ratio and high levels of leptin and interleukin-6 in adipose tissue and low adiponectin (Wu et al., 2020).

Another organ that appears to be particularly affected by the nutritional transition and which is at the central core of the development of a range of metabolic diseases is the liver. The liver is sensitive to dietary modulations. A shortage of amino acids, for example, has been related to liver diseases (Nishi et al., 2018). In an experimental model of protein malnutrition, hepatocytes isolated from rats fed with 5% casein protein for 14 days showed increased triglyceride synthesis (Taguchi et al., 2017). Transcription factors, such as the carbohydrate-sensitive response element-binding protein (ChREBp), peroxisome proliferator-activated receptors (PPAR), and the sterol regulating element-binding protein, (SREBp) respond to excessive lipid consumption, and they control energetic homeostasis and can activate pathways related to lipogenesis and inflammatory processes in liver tissue (Mello et al., 2016; Shimano and Sato, 2017; Li et al., 2019). Chmurzynska et al. (2012) showed that the altered response to a high-fat diet programmed by maternal nutrition during pregnancy was detected as an altered gene expression in 10-week-old rats and central adiposity in 16-week-old rats. Hepatic transcription of PPARγ in response to the high-fat diet was dependent on maternal nutrition. Male rats subjected to maternal protein restriction and fed with a high-fat diet showed an increase in PPAR levels, while rats with a normoprotein maternal diet and a postnatal diet rich in fatty acids showed a reduction in PPAR levels. Likewise, activation of the *PPARα* gene by a high-fat diet was dependent on prenatal nutrition (Chmurzynska et al., 2012).

Assessing the structure of liver tissue, a study by Souza-Mello et al. (2007) demonstrated that nutritional mismatch with a low protein maternal diet (9% during pregnancy and lactation) and a postnatal diet rich in lipids (50% of the total caloric component) induces an increase in blood pressure and gonadal adiposity, in addition to worsening liver steatosis in male rats. However, the mechanisms are still unclear, but they may be related to an increased activity of lipid synthesis and oxidation as a strategy to save proteins in conditions of scarcity and in the regulation of transcription factors and gene expression related to glycolipid metabolism. In an experimental study with sheep, a 50% reduction in dietary proteins during pregnancy and lactation, followed by post-weaning consumption of a high-fat diet (38% fat), increased the hepatic triglyceride content in lambs, with

permanent reduction induction in the expression of genes that regulate energy homeostasis (*GLUT1*, *PPAR*, *SREBP1c*, and phosphoenolpyruvate carboxykinase gene—*PEPCK*) (Souza-Mello et al., 2007).

During fasting states, the use of fatty acids as an energy substrate occurs through β-oxidation, mainly in a mitochondrial environment (Reddy and Rao, 2006), with the action of key enzymes such as acyl-CoA dehydrogenase, enoyl-CoA hydrolase, and β-hydroxycil CoA-dehydrogenase (Jones, 2016). Elevated insulin and glucose levels regulate the synthesis of triacylglycerols, stimulating the activity of transcription factors such as ChREBp and the sterol regulatory element-binding protein SREBp and activated by peroxisome proliferator receptors PPAR. These factors increase the expression of lipogenic enzymes such as acetyl-coenzyme A carboxylase (Zhao et al., 2012) and fatty acid synthase FAS (Canbay et al., 2007). Imbalances in transport mechanisms or in the activation of transcription factors can then induce excessive accumulation of triglycerides within hepatocytes and trigger liver diseases (Titchenell et al., 2017).

The increase in energy levels induces a reduction in mitochondrial oxidative activity, while the increase in lipid peroxidation induces damage to mitochondria. In the liver, a maternal protein restriction of Wistar rats (casein 8%) during pregnancy and lactation, followed by a diet with post-weaning HF until 90 days of life (32% of the caloric percentage originated in lipids and 59% at more than saturated fatty acids), induced a reduction in all respiratory states of liver mitochondria, (Vickers et al., 2000) greater mitochondrial edema compared to controls enhanced after the addition of $Ca2^{+}$ and prevented in the presence of EGTA (calcium chelator) and cyclosporine A (transition pore inhibitor of mitochondrial permeability), and greater oxidation of liver proteins and lipid peroxidation, with a reduction in catalase and glutathione peroxidase activities. These data suggest that adult rats subjected to maternal protein restriction were more susceptible to liver mitochondrial damage caused by a diet rich in saturated fatty acids after weaning (Simoes-Alves et al., 2019). **Figure 2** summarizes the repercussions of the consumption of high-fat diets postnatally in individuals subjected to protein restriction during pregnancy and lactation.

CONCLUSION

A shift in the nutritional status of the perinatal and postnatal environment induces accelerated recovery growth and adjustments in autonomic modulation and insulin sensitivity as well as mitochondrial dysfunction. A post-weaning high-caloric/high-fat diet potentiates these adjustments, exacerbating deleterious changes in important metabolic organs, namely, hepatic, adipose, and muscular tissue. The epigenetic repercussions of postnatal metabolic overload may be etiological sources of cardiometabolic diseases, which affect the subjects suffering nutritional transition.

AUTHOR CONTRIBUTIONS

AS-A, AA-M, JC, AW, CL, JC-S, and VO drafted the manuscript, critically revised the intellectual content and performed final review of the manuscript.

FUNDING

This study was supported financially by Fundação de Amparo the Ciência e Tecnologia de Pernambuco-PE-Brazil (PRONEM 0797-4.05/14), the Conselho Nacional de Desenvolvimento Científico e Tecnológico—Brazil (CNPq n° 311386/2019-9), and the CAPES/COFECUB Program (number: 797-14 and 923-20). ACSA, APFCAM, and JOC are graduate students supported by fellowship grants from the Coordination for the Improvement of Higher Education Personnel (Scholarship—CAPES).

ACKNOWLEDGMENTS

The authors thank Marcela Lima, for graphical support with the figures in this study. The English text of this study has been revised by Sidney Pratt, Canadian, MAT (The Johns Hopkins University) and RSAdip—TESL (Cambridge University).

REFERENCES

Abdullah, A. (2015). The Double Burden of Undernutrition and Overnutrition in Developing Countries: an Update. *Curr. Obes. Rep.* 4 (3), 337–349. doi:10.1007/s13679-015-0170-y

Ajala, A. R., Almeida, S. S., Rangel, M., Palomino, Z., Strufaldi, M. W. L., Puccini, R. F., et al. (2012). Association of ACE Gene Insertion/deletion Polymorphism with Birth Weight, Blood Pressure Levels, and ACE Activity in Healthy Children. *Am. J. Hypertens.* 25 (7), 827–832. doi:10.1038/ajh.2012.50

Alheiros-Lira, M. C., Jurema-Santos, G. C., da-Silva, H. T., da-Silva, A. C., Moreno Senna, S., Ferreira e Silva, W. T., et al. (2017). Effects of High-Fat Diet on Somatic Growth, Metabolic Parameters and Function of Peritoneal Macrophages of Young Rats Submitted to a Maternal Low-Protein Diet. *Br. J. Nutr.* 117 (6), 796–803. doi:10.1017/S0007114517000708

Almeida Silva, L. C., Oliveira, A. C., Cavalcante-Silva, V., Franco, M. d. C., and D'Almeida, V. (2020). Hyperlipidic Diet Affects Body Composition and Induces Anxiety-like Behaviour in Intrauterine Growth-restricted Adult Mice. *Exp. Physiol.* 105 (12), 2061–2072. doi:10.1113/EP088859

Andersen, L. G., Ängquist, L., Gamborg, M., Byberg, L., Bengtsson, C., Canoy, D., et al. (2009). Birth Weight in Relation to Leisure Time Physical Activity in Adolescence and Adulthood: Meta-Analysis of Results from 13 Nordic Cohorts. *PloS one* 4 (12), e8192. doi:10.1371/journal.pone.0008192

Antony, G. M., and Laxmaiah, A. (2008). Human Development, Poverty, Health & Nutrition Situation in India. *Indian J. Med. Res.* 128, 198–205.

Arroyo Hornero, R., Hamad, I., Côrte-Real, B., and Kleinewietfeld, M. (2020). The Impact of Dietary Components on Regulatory T Cells and Disease. *Front. Immunol.* 11, 253. doi:10.3389/fimmu.2020.00253

Ashton, N. (2000). Perinatal Development and Adult Blood Pressure. *Braz. J. Med. Biol. Res.* 33, 731–740. doi:10.1590/s0100-879x2000000700002

Aubin, M. C., Lajoie, C., Clément, R., Gosselin, H., Calderone, A., and Perrault, L. P. (2008). Female Rats Fed a High-Fat Diet Were Associated with Vascular Dysfunction and Cardiac Fibrosis in the Absence of Overt Obesity and Hyperlipidemia: Therapeutic Potential of Resveratrol. *J. Pharmacol. Exp.*

Therjournal Pharmacol. Exp. Ther. 325 (3), 961–968. doi:10.1124/jpet.107.135061

Barbosa, S. d. S., Mello, A. P. d. F. A. C., Nogueira, V. d. O., da Silva, I. F., de Melo, P. E. D., Dos Santos, C. R., et al. (2020). Consumption of a High-fat Diet Does Not Potentiate the Deleterious Effects on Lipid and Protein Levels and Body Development in Rats Subjected to Maternal Protein Restriction. *Clin. Exp. Pharmacol. Physiol.* 47 (3), 412–421. doi:10.1111/1440-1681.13210

Barker, D. J. P. (1999). Fetal Origins of Cardiovascular Disease. *Ann. Med.* 31 (Suppl. 1), 3–6. doi:10.1080/07853890.1999.11904392

Barker, D. J. P., Godfrey, K. M., Gluckman, P. D., Harding, J. E., Owens, J. A., and Robinson, J. S. (1993). Fetal Nutrition and Cardiovascular Disease in Adult Life. *The Lancet* 341 (8850), 938–941. doi:10.1016/0140-6736(93)91224-a

Barker, D. J. P., Osmond, C., Forsén, T. J., Kajantie, E., and Eriksson, J. G. (2005). Trajectories of Growth Among Children Who Have Coronary Events as Adults. *N. Engl. J. Med.* 353 (17), 1802–1809. doi:10.1056/NEJMoa044160

Barker, D. J. P., Osmond, C., Winter, P. D., Margetts, B., and Simmonds, S. J. (1989). WEIGHT IN INFANCY AND DEATH FROM ISCHAEMIC HEART DISEASE. *The Lancet* 334 (8663), 577–580. doi:10.1016/S0140-6736(89)90710-1

Barker, D. J. P. (2007). The Origins of the Developmental Origins Theory. *J. Intern. Med.* 261 (5), 412–417. doi:10.1111/j.1365-2796.2007.01809.x

Barker, D., and Osmond, C. (1986). Infant Mortality, Childhood Nutrition, and Ischaemic Heart Disease in England and Wales. *The Lancet* 327 (8489), 1077–1081. doi:10.1016/s0140-6736(86)91340-1

Barros, M. A. V., De Brito Alves, J. L., Nogueira, V. O., Wanderley, A. G., and Costa-Silva, J. H. (2015). Maternal Low-Protein Diet Induces Changes in the Cardiovascular Autonomic Modulation in Male Rat Offspring. *Nutr. Metab. Cardiovasc. Dis.* 25 (1), 123–130. doi:10.1016/j.numecd.2014.07.011

Batista Filho, M., and Batista, L. V. (2010). Transição Alimentar/Nutricional Ou Mutação Antropológica? *J. Ciência e Cultura* 62, 26–30.

Batista Filho, M., and Rissin, A. (2003a). A transição nutricional no Brasil: tendências regionais e temporais. *Cad. Saúde Pública* 19, S181–S191. doi:10.1590/s0102-311x2003000700019

Batista Filho, M., and Rissin, A. (2003b). A transição nutricional no Brasil: tendências regionais e temporais. *J. Cadernos de Saúde Pública* 19, S181–S191.

Batista, T. M., Ribeiro, R. A., da Silva, P. M. R., Camargo, R. L., Lollo, P. C. B., Boschero, A. C., et al. (2013). Taurine Supplementation Improves Liver Glucose Control in normal Protein and Malnourished Mice Fed a High-Fat Diet. *Mol. Nutr. Food Res.* 57 (3), 423–434. doi:10.1002/mnfr.201200345

Berends, L. M., Dearden, L., Tung, Y. C. L., Voshol, P., Fernandez-Twinn, D. S., and Ozanne, S. E. (2018). Programming of central and Peripheral Insulin Resistance by Low Birthweight and Postnatal Catch-Up Growth in Male Mice. *Diabetologia* 61 (10), 2225–2234. doi:10.1007/s00125-018-4694-z

Biosca, M., Rodríguez, G., Ventura, P., Samper, M. P., Labayen, I., Collado, M. P., et al. (2011). Central Adiposity in Children Born Small and Large for Gestational Age. *Nutr. Hosp.* 26 (5), 971–976. doi:10.1590/s0212-16112011000500008

Borges, M. C., Vinolo, M. A. R., Crisma, A. R., Fock, R. A., Borelli, P., Tirapegui, J., et al. (2013). High-fat Diet Blunts Activation of the Nuclear Factor-Kb Signaling Pathway in Lipopolysaccharide-Stimulated Peritoneal Macrophages of Wistar Rats. *Nutrition* 29 (2), 443–449. doi:10.1016/j.nut.2012.06.008

Bowman, G. D., and Poirier, M. G. (2015). Post-translational Modifications of Histones that Influence Nucleosome Dynamics. *Chem. Rev.* 115 (6), 2274–2295. doi:10.1021/cr500350x

Brawley, L., Itoh, S., Torrens, C., Barker, A., Bertram, C., Poston, L., et al. (2003). Dietary Protein Restriction in Pregnancy Induces Hypertension and Vascular Defects in Rat Male Offspring. *Pediatr. Res.* 54 (1), 83–90. doi:10.1203/01.PDR.0000065731.00639.02

Calder, P. C. (2012). The Role of marine omega-3 (N -3) Fatty Acids in Inflammatory Processes, Atherosclerosis and Plaque Stability. *Mol. Nutr. Food Res.* 56 (7), 1073–1080. doi:10.1002/mnfr.201100710

Canbay, A., Bechmann, L., and Gerken, G. (2007). Lipid Metabolism in the Liver. *Z. Gastroenterol.* 45 (1), 35–41. doi:10.1055/s-2006-927368

Caricilli, A. M., Nascimento, P. H., Pauli, J. R., Tsukumo, D. M. L., Velloso, L. A., Carvalheira, J. B., et al. (2008). Inhibition of Toll-like Receptor 2 Expression Improves Insulin Sensitivity and Signaling in Muscle and white Adipose Tissue of Mice Fed a High-Fat Diet. *J. Endocrinol.* 199, 399–406. doi:10.1677/JOE-08-0354

Chango, A., and Pogribny, I. (2015). Considering Maternal Dietary Modulators for Epigenetic Regulation and Programming of the Fetal Epigenome. *Nutrients* 7 (4), 2748–2770. doi:10.3390/nu7042748

Chen, J.-H., Martin-Gronert, M. S., Tarry-Adkins, J., and Ozanne, S. E. (2009). Maternal Protein Restriction Affects Postnatal Growth and the Expression of Key Proteins Involved in Lifespan Regulation in Mice. *PLoS One* 4 (3), e4950. doi:10.1371/journal.pone.0004950

Chen, J.-H., Tarry-Adkins, J. L., Matharu, K., Yeo, G. S. H., and Ozanne, S. E. (2010). Maternal Protein Restriction Affects Gene Expression Profiles in the Kidney at Weaning with Implications for the Regulation of Renal Function and Lifespan. *Clin. Sci. (Lond)* 119, 373–387. doi:10.1042/CS20100230

Chmurzynska, A., Stachowiak, M., Gawecki, J., Pruszynska-Oszmalek, E., and Tubacka, M. (2012). Protein and Folic Acid Content in the Maternal Diet Determine Lipid Metabolism and Response to High-Fat Feeding in Rat Progeny in an Age-dependent Manner. *Genes Nutr.* 7 (2), 223–234. doi:10.1007/s12263-011-0253-7

Chong, S., and Whitelaw, E. (2004). Epigenetic Germline Inheritance. *Curr. Opin. Genet. Development* 14 (6), 692–696. doi:10.1016/j.gde.2004.09.001

Claycombe, K. J., Roemmich, J. N., Johnson, L., Vomhof-DeKrey, E. E., and Johnson, W. T. (2015). Skeletal Muscle Sirt3 Expression and Mitochondrial Respiration Are Regulated by a Prenatal Low-Protein Diet. *J. Nutr. Biochem.* 26 (2), 184–189. doi:10.1016/j.jnutbio.2014.10.003

Conde, W. L., and Monteiro, C. A. (2014). Nutrition Transition and Double burden of Undernutrition and Excess of Weight in Brazil. *Am. J. Clin. Nutr.* 100 (6), 1617S–22S. doi:10.3945/ajcn.114.084764

Costa-Silva, J. H., de Brito-Alves, J. L., Barros, M. A. d. V., Nogueira, V. O., Paulino-Silva, K. M., de Oliveira-Lira, A., et al. (2015). New Insights on the Maternal Diet Induced-Hypertension: Potential Role of the Phenotypic Plasticity and Sympathetic-Respiratory Overactivity. *Front. Physiol.* 6 (345). doi:10.3389/fphys.2015.00345

Costa-Silva, J. H., Silva, P. A., Pedi, N., Luzardo, R., Einicker-Lamas, M., Lara, L. S., et al. (2009). Chronic Undernutrition Alters Renal Active Na+ Transport in Young Rats: Potential Hidden Basis for Pathophysiological Alterations in Adulthood? *Eur. J. Nutr.* 48, 437–445. doi:10.1007/s00394-009-0032-z

D'Ippolito, E., and Iorio, M. (2013). MicroRNAs and Triple Negative Breast Cancer. *Ijms* 14 (11), 22202–22220. doi:10.3390/ijms141122202

da Silva Aragão, R., Guzmán-Quevedo, O., Pérez-García, G., Manhães-de-Castro, R., and Bolaños-Jiménez, F. (2014). Maternal Protein Restriction Impairs the Transcriptional Metabolic Flexibility of Skeletal Muscle in Adult Rat Offspring. *Br. J. Nutr.* 112 (3), 328–337. doi:10.1017/S0007114514000865

de Brito Alves, J. L., and Costa-Silva, J. H. (2018). Maternal Protein Malnutrition Induced-Hypertension: New Evidence about the Autonomic and Respiratory Dysfunctions and Epigenetic Mechanisms. *Clin. Exp. Pharmacol. Physiol.* 45 (5), 422–429. doi:10.1111/1440-1681.12892

de Brito Alves, J. L., de Oliveira, J. M. D., Ferreira, D. J. S., Barros, M. A. d. V., Nogueira, V. O., Alves, D. S., et al. (2016). Maternal Protein Restriction Induced-Hypertension Is Associated to Oxidative Disruption at Transcriptional and Functional Levels in the Medulla Oblongata. *Clin. Exp. Pharmacol. Physiol.* 43 (12), 1177–1184. doi:10.1111/1440-1681.12667

de Brito Alves, J. L., Nogueira, V. O., Cavalcanti Neto, M. P., Leopoldino, A. M., Curti, C., Colombari, D. S., et al. (2015). Maternal Protein Restriction Increases Respiratory and Sympathetic Activities and Sensitizes Peripheral Chemoreflex in Male Rat Offspring. *J. Nutr.* 145 (5), 907–914. doi:10.3945/jn.114.202804

de Brito Alves, J. L., Nogueira, V. O., de Oliveira, G. B., da Silva, G. S. F., Wanderley, A. G., Leandro, C. G., et al. (2014). Short- and Long-Term Effects of a Maternal Low-Protein Diet on Ventilation, O2/CO2chemoreception and Arterial Blood Pressure in Male Rat Offspring. *Br. J. Nutr.* 111 (4), 606–615. doi:10.1017/S0007114513002833

de Brito Alves, J. L., Toscano, A. E., da Costa-Silva, J. H., Vidal, H., Leandro, C. G., and Pirola, L. (2017). Transcriptional Response of Skeletal Muscle to a Low Protein Perinatal Diet in Rat Offspring at Different Ages: The Role of Key Enzymes of Glucose-Fatty Acid Oxidation. *J. Nutr. Biochem.* 41, 117–123. doi:10.1016/j.jnutbio.2016.12.002

Desai, M., Babu, J., and Ross, M. G. (2007). Programmed Metabolic Syndrome: Prenatal Undernutrition and Postweaning Overnutrition. *Am. J. Physiology-Regulatory, Integr. Comp. Physiol.* 293 (6), R2306–R2314. doi:10.1152/ajpregu.00783.2006

Desai, M., Jellyman, J. K., and Ross, M. G. (2015). Epigenomics, Gestational Programming and Risk of Metabolic Syndrome. *Int. J. Obes.* 39 (4), 633–641. doi:10.1038/ijo.2015.13

Di Pietro, G., Cardoso, D. S., da Silva, H. M. B. S., Santos, J. C., Dos Santos, J. R., and Simões, R. A. (2015). Profile Development of Noncommunicable Chronic Diseases in a Brazilian Rural Town. *J. Am. Coll. Nutr.* 34 (3), 191–198. doi:10.1080/07315724.2014.926162

do Prado, W. L., de Piano, A., Lazaretti-Castro, M., de Mello, M. T., Stella, S. G., Tufik, S., et al. (2009). Relationship between Bone mineral Density, Leptin and Insulin Concentration in Brazilian Obese Adolescents. *J. Bone Miner Metab.* 27 (5), 613–619. doi:10.1007/s00774-009-0082-6

Egger, G., Liang, G., Aparicio, A., and Jones, P. A. (2004). Epigenetics in Human Disease and Prospects for Epigenetic Therapy. *Nature* 429 (6990), 457–463. doi:10.1038/nature02625

Ertunc, M. E., and Hotamisligil, G. S. (2016). Lipid Signaling and Lipotoxicity in Metaflammation: Indications for Metabolic Disease Pathogenesis and Treatment. *J. lipid Res.* 57, 2099–2114. doi:10.1194/jlr.R066514

Falcão-Tebas, F., Bento-Santos, A., Antônio Fidalgo, M., de Almeida, M. B., Antônio dos Santos, J., Lopes de Souza, S., et al. (2012). Maternal Low-Protein Diet-Induced Delayed Reflex Ontogeny Is Attenuated by Moderate Physical Training during Gestation in Rats. *Br. J. Nutr.* 107 (3), 372–377. doi:10.1017/s0007114511002947

Feng, A., Wang, L., Chen, X., Liu, X., Li, L., Wang, B., et al. (2015). Developmental Origins of Health and Disease (DOHaD): Implications for Health and Nutritional Issues Among Rural Children in China. *Bst* 9, 82–87. doi:10.5582/bst.2015.01008

Ferreira, D. S., Liu, Y., Fernandes, M. P., and Lagranha, C. J. (2015). Perinatal Low-Protein Diet Alters Brainstem Antioxidant Metabolism in Adult Offspring. *Nutr. Neurosci.* 19, 369–375. doi:10.1179/1476830515Y.0000000030

Fidalgo, M., Falcão-Tebas, F., Bento-Santos, A., de Oliveira, E., Nogueira-Neto, J. F., de Moura, E. G., et al. (2013). Programmed Changes in the Adult Rat Offspring Caused by Maternal Protein Restriction during Gestation and Lactation Are Attenuated by Maternal Moderate-Low Physical Training. *Br. J. Nutr.* 109 (3), 449–456. doi:10.1017/s0007114512001316

Franco, M. C. P., Casarini, D. E., Carneiro-Ramos, M. S., Sawaya, A. L., Barreto-Chaves, M. L. M., and Sesso, R. (2008). Circulating Renin-Angiotensin System and Catecholamines in Childhood: Is There a Role for Birthweight? *Clin. Sci.* 114, 375–380. doi:10.1042/CS20070284

Gluckman, P. D., and Hanson, M. A. (2004). Living with the Past: Evolution, Development, and Patterns of Disease. *Science* 305 (5691), 1733–1736. doi:10.1126/science.1095292

Gosby, A. K., Maloney, C. A., and Caterson, I. D. (2010). Elevated Insulin Sensitivity in Low-Protein Offspring Rats Is Prevented by a High-Fat Diet and Is Associated with Visceral Fat. *Obesity (Silver Spring)* 18 (8), 1593–1600. doi:10.1038/oby.2009.449

Goyal, R., Goyal, D., Leitzke, A., Gheorghe, C. P., and Longo, L. D. (2010). Brain Renin-Angiotensin System: Fetal Epigenetic Programming by Maternal Protein Restriction during Pregnancy. *Reprod. Sci.* 17 (3), 227–238. doi:10.1177/1933719109351935

Gräff, J., and Tsai, L.-H. (2013). Histone Acetylation: Molecular Mnemonics on the Chromatin. *Nat. Rev. Neurosci.* 14 (2), 97–111. doi:10.1038/nrn3427

Hasan, M. T., Soares Magalhães, R. J., Williams, G. M., and Mamun, A. A. (2016). Long-term Changes in Childhood Malnutrition Are Associated with Long-Term Changes in Maternal BMI: Evidence from Bangladesh, 1996-2011. *Am. J. Clin. Nutr.* 104 (4), 1121–1127. doi:10.3945/ajcn.115.111773

Hemachandra, A. H., Klebanoff, M. A., Duggan, A. K., Hardy, J. B., and Furth, S. L. (2006). The Association between Intrauterine Growth Restriction in the Full-Term Infant and High Blood Pressure at Age 7 years: Results from the Collaborative Perinatal Project. *Int. J. Epidemiol.* 35 (4), 871–877. doi:10.1093/ije/dyl080

Herrán, O. F., Patiño, G. A., and Del Castillo, S. E. (20162010). Transición alimentaria y exceso de peso en adultos. Encuesta de la Situación Nutricional en Colombia, 2010. *Biomedica* 36 (1), 109–120. doi:10.7705/biomedica.v36i1.2579

Hotamisligil, G. S. (2006). Inflammation and Metabolic Disorders. *Nature* 444 (7121), 860–867. doi:10.1038/nature05485

Ito, T., Funamoto, K., Sato, N., Nakamura, A., Tanabe, K., and Hoshiai, T. (2012). Maternal Undernutrition Induces the Expression of Hypoxia-Related Genes in the Fetal Brain. *Tohoku J. Exp. Med.* 226 (1), 37–44. doi:10.1620/tjem.226.37

Ito, T., Tanabe, K., Nakamura, A., Funamoto, K., Aoyagi, A., Sato, K., et al. (2011). Aberrant Expression of Hypoxia-Inducible Factor 1.ALPHA. In the Fetal Heart Is Associated with Maternal Undernutrition. *Tohoku J. Exp. Med.* 224 (3), 163–171. doi:10.1620/tjem.224.163

Iwasa, T., Matsuzaki, T., Yano, K., Tungalagsuvd, A., Munkhzaya, M., Mayila, Y., et al. (2017). The Effects of Prenatal Undernutrition and a High-Fat Postnatal Diet on central and Peripheral Orexigenic and Anorexigenic Factors in Female Rats. *Endocr. J.* 64 (6), 597–604. doi:10.1507/endocrj.EJ16-0593

Jablonka, E., and Lamb, M. J. (2002). The Changing Concept of Epigenetics. *Ann. N. Y Acad. Sci.* 981, 82–96. doi:10.1111/j.1749-6632.2002.tb04913.x

Johansson, S., Norman, M., Legnevall, L., Dalmaz, Y., Lagercrantz, H., and Vanpée, M. (2007). Increased Catecholamines and Heart Rate in Children with Low Birth Weight: Perinatal Contributions to Sympathoadrenal Overactivity. *J. Intern. Med.* 261 (5), 480–487. doi:10.1111/j.1365-2796.2007.01776.x

John, R. M., and Rougeulle, C. (2018). Developmental Epigenetics: Phenotype and the Flexible Epigenome. *Front. Cel Dev. Biol.* 6, 130. doi:10.3389/fcell.2018.00130

Jones, J. G. (2016). Hepatic Glucose and Lipid Metabolism. *Diabetologia* 59 (6), 1098–1103. doi:10.1007/s00125-016-3940-5

Kroker-Lobos, M. F., Pedroza-Tobías, A., Pedraza, L. S., and Rivera, J. A. (2014). The Double burden of Undernutrition and Excess Body Weight in Mexico. *Am. J. Clin. Nutr.* 100 (6), 1652s–1658s. doi:10.3945/ajcn.114.083832

Labayen, I., Moreno, L. A., Blay, M. G., Blay, V. A., Mesana, M. I., González-Gross, M., et al. (2006). Early Programming of Body Composition and Fat Distribution in Adolescents. *J. Nutr.* 136 (1), 147–152. doi:10.1093/jn/136.1.147

Leandro, C. G., da Silva Ribeiro, W., Dos Santos, J. A., Bento-Santos, A., Lima-Coelho, C. H., Falcão-Tebas, F., et al. (2012). Moderate Physical Training Attenuates Muscle-specific Effects on Fibre Type Composition in Adult Rats Submitted to a Perinatal Maternal Low-Protein Diet. *Eur. J. Nutr.* 51 (7), 807–815. doi:10.1007/s00394-011-0259-3

Leocádio, P. C. L., Lopes, S. C., Dias, R. P., Alvarez-Leite, J. I., Guerrant, R. L., Malva, J. O., et al. (2021). The Transition from Undernutrition to Overnutrition under Adverse Environments and Poverty: The Risk for Chronic Diseases. *Front. Nutr.* 8, 676044. doi:10.3389/fnut.2021.676044

Li, G., Jiang, Q., and Xu, K. (2019). CREB Family: A Significant Role in Liver Fibrosis. *Biochimie* 163, 94–100. doi:10.1016/j.biochi.2019.05.014

Lucas, A. (1998). Programming by Early Nutrition: An Experimental Approach. *J. Nutr.* 128 (2), 401S–406S. doi:10.1093/jn/128.2.401S

Lukaszewski, M.-A., Mayeur, S., Fajardy, I., Delahaye, F., Dutriez-Casteloot, I., Montel, V., et al. (2011). Maternal Prenatal Undernutrition Programs Adipose Tissue Gene Expression in Adult Male Rat Offspring under High-Fat Diet. *Am. J. Physiology-Endocrinology Metab.* 301, E548–E559. doi:10.1152/ajpendo.00011.2011

Lyons, C., Kennedy, E., and Roche, H. (2016). Metabolic Inflammation-Differential Modulation by Dietary Constituents. *Nutrients* 8 (5), 247. doi:10.3390/nu8050247

Mansego, M. L., Milagro, F. I., Campión, J., and Martínez, J. A. (2013). Techniques of DNA Methylation Analysis with Nutritional Applications. *J. Nutrigenet Nutrigenomics* 6 (2), 83–96. doi:10.1159/000350749

Mazzio, E. A., and Soliman, K. F. (2014b). Epigenetics and Nutritional Environmental Signals. *Integr. Comp. Biol.* 54 (1), 21–30. doi:10.1093/icb/icu049

Mazzio, E. A., and Soliman, K. F. A. (2014a). Epigenetics and Nutritional Environmental Signals. *Integr. Comp. Biol.* 54 (1), 21–30. doi:10.1093/icb/icu049

Mello, T., Materozzi, M., and Galli, A. (2016). PPARs and Mitochondrial Metabolism: From NAFLD to HCC. *PPAR Res.* 2016, 1–18. doi:10.1155/2016/7403230

Mitchell, C., Schneper, L. M., and Notterman, D. A. (2016). DNA Methylation, Early Life Environment, and Health Outcomes. *Pediatr. Res.* 79 (1-2), 212–219. doi:10.1038/pr.2015.193

Ng, M., Fleming, T., Robinson, M., Thomson, B., Graetz, N., Margono, C., et al. (2014). Global, Regional, and National Prevalence of Overweight and Obesity in Children and Adults during 1980-2013: a Systematic Analysis for the Global

Burden of Disease Study 2013. *Lancet* 384 (9945), 766–781. doi:10.1016/S0140-6736(14)60460-8

Nishi, H., Yamanaka, D., Kamei, H., Goda, Y., Kumano, M., Toyoshima, Y., et al. (2018). Importance of Serum Amino Acid Profile for Induction of Hepatic Steatosis under Protein Malnutrition. *Sci. Rep.* 8 (1), 5461. doi:10.1038/s41598-018-23640-8

Nogueira, V., Brito-Alves, J., Fontes, D., Oliveira, L., Lucca, W., Tourneur, Y., et al. (2018). Carotid Body Removal Normalizes Arterial Blood Pressure and Respiratory Frequency in Offspring of Protein-Restricted Mothers. *Hypertens. Res.* 41 (12), 1000–1012. doi:10.1038/s41440-018-0104-7

Nogueira, V. O., Andrade, L. D. S., Rocha-Júnior, R. L., Melo, P. E. D., Helvécio, E., Fontes, D. A. F., et al. (2019). Maternal Physical Activity Prevents the Overexpression of Hypoxia-Inducible Factor 1-α and Cardiorespiratory Dysfunction in Protein Malnourished Rats. *Sci. Rep.* 9 (1), 14406. doi:10.1038/s41598-019-50967-7

Nuyt, A. M., and Alexander, B. T. (2009). Developmental Programming and Hypertension. *Curr. Opin. Nephrol. Hypertens.* 18 (2), 144–152. doi:10.1097/MNH.0b013e328326092c

Ouchi, N., Parker, J. L., Lugus, J. J., and Walsh, K. (2011). Adipokines in Inflammation and Metabolic Disease. *Nat. Rev. Immunol.* 11 (2), 85–97. doi:10.1038/nri2921

Ozanne, S. E., and Hales, C. N. (2004). Catch-up Growth and Obesity in Male Mice. *Nature* 427, 411–412. doi:10.1038/427411b

Parra, D. C., Iannotti, L., Gomez, L. F., Pachón, H., Haire-Joshu, D., Sarmiento, O. L., et al. (2015). The Nutrition Transition in Colombia over a Decade: a Novel Household Classification System of Anthropometric Measures. *Arch. Public Health* 73 (1), 12. doi:10.1186/s13690-014-0057-5

Paulino-Silva, K. M., and Costa-Silva, J. H. (2016). Hypertension in Rat Offspring Subjected to Perinatal Protein Malnutrition Is Not Related to the Baroreflex Dysfunction. *Clin. Exp. Pharmacol. Physiol.* 43 (11), 1046–1053. doi:10.1111/1440-1681.12628

Popkin, B. M. (2015). Nutrition Transition and the Global Diabetes Epidemic. *Curr. Diab Rep.* 15 (9), 64. doi:10.1007/s11892-015-0631-4

Radford, E. J., Ito, M., Shi, H., Corish, J. A., Yamazawa, K., Isganaitis, E., et al. (2014). In Utero undernourishment Perturbs the Adult Sperm Methylome and Intergenerational Metabolism. *Science* 345 (6198), 1255903. doi:10.1126/science.1255903

Ralston, J. C., Lyons, C. L., Kennedy, E. B., Kirwan, A. M., and Roche, H. M. (2017). Fatty Acids and NLRP3 Inflammasome-Mediated Inflammation in Metabolic Tissues. *Annu. Rev. Nutr.* 37, 77–102. doi:10.1146/annurev-nutr-071816-064836

Rangel, M., dos Santos, J. C., Ortiz, P. H. L., Hirata, M., Jasiulionis, M. G., Araujo, R. C., et al. (2014). Modification of Epigenetic Patterns in Low Birth Weight Children: Importance of Hypomethylation of the ACE Gene Promoter. *PLoS One* 9 (8), e106138. doi:10.1371/journal.pone.0106138

Reddy, J. K., and Sambasiva Rao, M. (2006). Lipid Metabolism and Liver Inflammation. II. Fatty Liver Disease and Fatty Acid Oxidation. *Am. J. Physiology-Gastrointestinal Liver Physiol.* 290 (5), G852–G858. doi:10.1152/ajpgi.00521.2005

Ribeiro, A. M., Lima, M. d. C., Lira, P. I. C. d., and Silva, G. A. P. d. (2015). Baixo peso ao nascer e obesidade: associação causal ou casual? *Revista Paulista de Pediatria* 33 (3), 340–348. doi:10.1016/j.rpped.2014.09.007

Robinson, S. M., Robinson, S. M., Batelaan, S. F., Syddall, H. E., Sayer, A. A., Dennison, E. M., et al. (2006). Combined Effects of Dietary Fat and Birth Weight on Serum Cholesterol Concentrations: the Hertfordshire Cohort Study. *Am. J. Clin. Nutr.* 84 (1), 237–244. doi:10.1093/ajcn/84.1.237

Sadakierska-Chudy, A., and Filip, M. (2015). A Comprehensive View of the Epigenetic Landscape. Part II: Histone post-translational Modification, Nucleosome Level, and Chromatin Regulation by ncRNAs. *Neurotox Res.* 27 (2), 172–197. doi:10.1007/s12640-014-9508-6

Sandovici, I., Smith, N. H., Nitert, M. D., Ackers-Johnson, M., Uribe-Lewis, S., Ito, Y., et al. (2011). Maternal Diet and Aging Alter the Epigenetic Control of a Promoter-Enhancer Interaction at the Hnf4a Gene in Rat Pancreatic Islets. *Proc. Natl. Acad. Sci. U.S.A.* 108 (13), 5449–5454. doi:10.1073/pnas.1019007108

Sarih, M., Souvannavong, V., and Adam, A. (1993). Nitric Oxide Synthase Induces Macrophage Death by Apoptosis. *Biochem. Biophysical Res. Commun.* 191 (2), 503–508. doi:10.1006/bbrc.1993.1246

Sarmiento, O. L., Parra, D. C., González, S. A., González-Casanova, I., Forero, A. Y., and Garcia, J. (2014). The Dual burden of Malnutrition in Colombia. *Am. J. Clin. Nutr.* 100 (6), 1628s–1635s. doi:10.3945/ajcn.114.083816

Sellayah, D., Dib, L., Anthony, F. W., Watkins, A. J., Fleming, T. P., Hanson, M. A., et al. (2014). Effect of Maternal Protein Restriction during Pregnancy and Postweaning High-Fat Feeding on Diet-Induced Thermogenesis in Adult Mouse Offspring. *Eur. J. Nutr.* 53 (7), 1523–1531. doi:10.1007/s00394-014-0657-4

Shimano, H., and Sato, R. (2017). SREBP-regulated Lipid Metabolism: Convergent Physiology - Divergent Pathophysiology. *Nat. Rev. Endocrinol.* 13 (12), 710–730. doi:10.1038/nrendo.2017.91

Siddique, K., Guzman, G. L., Gattineni, J., and Baum, M. (2014). Effect of Postnatal Maternal Protein Intake on Prenatal Programming of Hypertension. *Reprod. Sci.* 21 (12), 1499–1507. doi:10.1177/1933719114530186

Simões-Alves, A. C., Costa-Silva, J. H., Barros-Junior, I. B., da Silva Filho, R. C., Vasconcelos, D. A. A., Vidal, H., et al. (2019). Saturated Fatty Acid-Enriched Diet-Impaired Mitochondrial Bioenergetics in Liver from Undernourished Rats during Critical Periods of Development. *Cells* 8 (4), 335. doi:10.3390/cells8040335

Sosa-Larios, T. C., Miliar-Garcia, A. A., Morimoto, S., and Jaramillo-Flores, M. E. (2017). Retracted Article: Alterations in Lipid Metabolism Due to a Protein-Restricted Diet in Rats during Gestation And/or Lactation. *Food Funct.* 9, 1274. doi:10.1039/c7fo01513e

Sousa, C. P., Olinda, R. A., and Pedraza, D. F. (2016). Prevalence of Stunting and Overweight/obesity Among Brazilian Children According to Different Epidemiological Scenarios: Systematic Review and Meta-Analysis. *Sao Paulo Med. J.* 134, 251–262. doi:10.1590/1516-3180.2015.0227121

Souza-Mello, V., Mandarim-de-Lacerda, C. A., and Aguila, M. B. (2007). Hepatic Structural Alteration in Adult Programmed Offspring (Severe Maternal Protein Restriction) Is Aggravated by post-weaning High-Fat Diet. *Br. J. Nutr.* 98 (6), 1159–1169. doi:10.1017/s0007114507771878

Steyn, N. P., and McHiza, Z. J. (2014). Obesity and the Nutrition Transition in Sub-Saharan Africa. *Ann. N.Y. Acad. Sci.* 1311, 88–101. doi:10.1111/nyas.12433

Szarc vel Szic, K. S., Declerck, K., Vidaković, M., and Vanden Berghe, W. (2015). From Inflammaging to Healthy Aging by Dietary Lifestyle Choices: Is Epigenetics the Key to Personalized Nutrition? *Clin. Epigenet* 7, 33. doi:10.1186/s13148-015-0068-2

Taguchi, Y., Toyoshima, Y., Tokita, R., Kato, H., Takahashi, S.-I., and Minami, S. (2017). Triglyceride Synthesis in Hepatocytes Isolated from Rats Fed a Low-Protein Diet Is Enhanced Independently of Upregulation of Insulin Signaling. *Biochem. Biophysical Res. Commun.* 490 (3), 800–805. doi:10.1016/j.bbrc.2017.06.120

Titchenell, P. M., Lazar, M. A., and Birnbaum, M. J. (2017). Unraveling the Regulation of Hepatic Metabolism by Insulin. *Trends Endocrinol. Metab.* 28 (7), 497–505. doi:10.1016/j.tem.2017.03.003

Toyoshima, Y., Tokita, R., Ohne, Y., Hakuno, F., Noguchi, T., Minami, S., et al. (2010). Dietary Protein Deprivation Upregulates Insulin Signaling and Inhibits Gluconeogenesis in Rat Liver. *J. Mol. Endocrinol.* 45 (5), 329–340. doi:10.1677/JME-10-0102

Vickers, M. H., Breier, B. H., Cutfield, W. S., Hofman, P. L., and Gluckman, P. D. (2000). Fetal Origins of Hyperphagia, Obesity, and Hypertension and Postnatal Amplification by Hypercaloric Nutrition. *Am. J. Physiology-Endocrinology Metab.* 279 (1), E83–E87. doi:10.1152/ajpendo.2000.279.1.E83

Victora, C. G., Adair, L., Fall, C., Hallal, P. C., Martorell, R., Richter, L., et al. (2008). Maternal and Child Undernutrition: Consequences for Adult Health and Human Capital. *The Lancet* 371 (9609), 340–357. doi:10.1016/S0140-6736(07)61692-4

Wang, D. D., and Hu, F. B. (2017). Dietary Fat and Risk of Cardiovascular Disease: Recent Controversies and Advances. *Annu. Rev. Nutr.* 37 (1), 423–446. doi:10.1146/annurev-nutr-071816-064614

Waterland, R. A., and Michels, K. B. (2007). Epigenetic Epidemiology of the Developmental Origins Hypothesis. *Annu. Rev. Nutr.* 27, 363–388. doi:10.1146/annurev.nutr.27.061406.093705

Wells, J. C. K. (2012). Obesity as Malnutrition: the Role of Capitalism in the Obesity Global Epidemic. *Am. J. Hum. Biol.* 24 (3), 261–276. doi:10.1002/ajhb.22253

Wells, J. C. K. (2007). The Programming Effects of Early Growth. *Early Hum. Development* 83 (12), 743–748. doi:10.1016/j.earlhumdev.2007.09.002

Wells, J. C. K. (2011). The Thrifty Phenotype: An Adaptation in Growth or Metabolism? *Am. J. Hum. Biol.* 23 (1), 65–75. doi:10.1002/ajhb.21100

Wensveen, F. M., Jelenčić, V., Valentić, S., Šestan, M., Wensveen, T. T., Theurich, S., et al. (2015). NK Cells Link Obesity-Induced Adipose Stress to Inflammation and Insulin Resistance. *Nat. Immunol.* 16 (4), 376–385. doi:10.1038/ni.3120

West-Eberhard, M. J. (2003). *Developmental Plasticity and Evolution*. Oxford University Press.

West-Eberhard, M. J. (2005). Phenotypic Accommodation: Adaptive Innovation Due to Developmental Plasticity. *J. Exp. Zool.* 304B (6), 610–618. doi:10.1002/jez.b.21071

Wu, Y., Yin, G., Wang, P., Huang, Z., and Lin, S. (2020). Effects of Different Diet Induced Postnatal Catch up Growth on Glycolipid Metabolism in Intrauterine Growth Retardation Male Rats. *Exp. Ther. Med.* 20 (6), 1. doi:10.3892/etm.2020.9263

Xie, L., Zhang, K., Rasmussen, D., Wang, J., Wu, D., Roemmich, J. N., et al. (2017). Effects of Prenatal Low Protein and Postnatal High Fat Diets on Visceral Adipose Tissue Macrophage Phenotypes and IL-6 Expression in Sprague Dawley Rat Offspring. *PLoS One* 12 (1), e0169581. doi:10.1371/journal.pone.0169581

Zambrano, E., Bautista, C. J., Deás, M., Martínez-Samayoa, P. M., González-Zamorano, M., Ledesma, H., et al. (2006). A Low Maternal Protein Diet during Pregnancy and Lactation Has Sex- and Window of Exposure-specific Effects on Offspring Growth and Food Intake, Glucose Metabolism and Serum Leptin in the Rat. *J. Physiol.* 571 (Pt 1), 221–230. doi:10.1113/jphysiol.2005.100313

Zhang, Y., Yuan, M., Bradley, K. M., Dong, F., Anversa, P., and Ren, J. (2012). Insulin-Like Growth Factor 1 Alleviates High-Fat Diet-Induced Myocardial Contractile Dysfunction. *Hypertension* 59 (3), 680–693. doi:10.1161/HYPERTENSIONAHA.111.181867

Zhao, J., Goldberg, J., Bremner, J. D., and Vaccarino, V. (2012). Global DNA Methylation Is Associated with Insulin Resistance. *Diabetes* 61 (2), 542–546. doi:10.2337/db11-1048

Zheng, J., Xiao, X., Zhang, Q., Wang, T., Yu, M., and Xu, J. (2017). Maternal Low-Protein Diet Modulates Glucose Metabolism and Hepatic MicroRNAs Expression in the Early Life of Offspring †. *Nutrients* 9 (3), 205. doi:10.3390/nu9030205

Zheng, J., Zhang, L., Liu, J., Li, Y., and Zhang, J. (2021). Long-Term Effects of Maternal Low-Protein Diet and Post-weaning High-Fat Feeding on Glucose Metabolism and Hypothalamic POMC Promoter Methylation in Offspring Mice. *Front. Nutr.* 8, 657848. doi:10.3389/fnut.2021.657848

Zohdi, V., Lim, K., Pearson, J., and Black, M. (2014). Developmental Programming of Cardiovascular Disease Following Intrauterine Growth Restriction: Findings Utilising a Rat Model of Maternal Protein Restriction. *Nutrients* 7 (1), 119–152. doi:10.3390/nu7010119

Zohdi, V., Sutherland, M. R., Lim, K., Gubhaju, L., Zimanyi, M. A., and Black, M. J. (2012). Low Birth Weight Due to Intrauterine Growth Restriction And/or Preterm Birth: Effects on Nephron Number and Long-Term Renal Health. *Int. J. Nephrol.* 2012, 1–13. doi:10.1155/2012/136942

Conflict of Interest: The authors declare that the research was conducted in the absence of any commercial or financial relationships that could be construed as a potential conflict of interest.

Publisher's Note: All claims expressed in this article are solely those of the authors and do not necessarily represent those of their affiliated organizations, or those of the publisher, the editors and the reviewers. Any product that may be evaluated in this article, or claim that may be made by its manufacturer, is not guaranteed or endorsed by the publisher.

Copyright © 2022 Simões-Alves, Arcoverde-Mello, Campos, Wanderley, Leandro, da Costa-Silva and de Oliveira Nogueira Souza. This is an open-access article distributed under the terms of the Creative Commons Attribution License (CC BY). The use, distribution or reproduction in other forums is permitted, provided the original author(s) and the copyright owner(s) are credited and that the original publication in this journal is cited, in accordance with accepted academic practice. No use, distribution or reproduction is permitted which does not comply with these terms.

frontiers | Frontiers in Physiology

REVIEW
published: 24 May 2022
doi: 10.3389/fphys.2022.887779

Osmoregulation and the Hypothalamic Supraoptic Nucleus: From Genes to Functions

André Souza Mecawi[1]*, *Wamberto Antonio Varanda*[2‡] and *Melina Pires da Silva*[3]*

[1]Laboratory of Molecular Neuroendocrinology, Department of Biophysics, Paulista School of Medicine, Federal University of São Paulo, São Paulo, Brazil, [2]Department of Physiology, Faculty of Medicine of Ribeirão Preto, University of São Paulo, Ribeirão Preto, Brazil, [3]Laboratory of Cellular Neuroendocrinology, Department of Biophysics, Paulista School of Medicine, Federal University of São Paulo, São Paulo, Brazil

Due to the relatively high permeability to water of the plasma membrane, water tends to equilibrate its chemical potential gradient between the intra and extracellular compartments. Because of this, changes in osmolality of the extracellular fluid are accompanied by changes in the cell volume. Therefore, osmoregulatory mechanisms have evolved to keep the tonicity of the extracellular compartment within strict limits. This review focuses on the following aspects of osmoregulation: 1) the general problems in adjusting the "milieu interieur" to challenges imposed by water imbalance, with emphasis on conceptual aspects of osmosis and cell volume regulation; 2) osmosensation and the hypothalamic supraoptic nucleus (SON), starting with analysis of the electrophysiological responses of the magnocellular neurosecretory cells (MNCs) involved in the osmoreception phenomenon; 3) transcriptomic plasticity of SON during sustained hyperosmolality, to pinpoint the genes coding membrane channels and transporters already shown to participate in the osmosensation and new candidates that may have their role further investigated in this process, with emphasis on those expressed in the MNCs, discussing the relationships of hydration state, gene expression, and MNCs electrical activity; and 4) somatodendritic release of neuropeptides in relation to osmoregulation. Finally, we expect that by stressing the relationship between gene expression and the electrical activity of MNCs, studies about the newly discovered plastic-regulated genes that code channels and transporters in the SON may emerge.

Keywords: magnocellular neurosecretory cells, osmoregulation, gene plasticity, ions channels, transporters, supraoptic nucleus

OPEN ACCESS

Edited by:
Geoffrey A. Head,
Baker Heart and Diabetes Institute, Australia

Reviewed by:
Mike Ludwig,
University of Edinburgh, United Kingdom
Thomas Fisher,
University of Saskatchewan, Canada

***Correspondence:**
André Souza Mecawi
mecawi@unifesp.br
Melina Pires da Silva
melynamoraes@gmail.com

‡*Retired*

Specialty section:
This article was submitted to Integrative Physiology, a section of the journal Frontiers in Physiology

Received: *02 March 2022*
Accepted: *18 April 2022*
Published: *24 May 2022*

Citation:
Mecawi AS, Varanda WA and da Silva MP (2022) Osmoregulation and the Hypothalamic Supraoptic Nucleus: From Genes to Functions. Front. Physiol. 13:887779. doi: 10.3389/fphys.2022.887779

INTRODUCTION

The water molecule has very particular physicochemical properties, mainly due to an asymmetrical distribution of charges. Even though the molecule is neutral, it behaves like a structural dipole, allowing interaction through hydrogen bonding and giving rise to a property known as cohesion. Also, by being a dipole, it can interact with ions of both polarities, entering the crystal structure and dissolving the salt. This property makes water a universal solvent, at least in terms of biological relevance in maintaining the process of life. Therefore, variations in the water activity inside and/or outside a cell will be accompanied by changes in the activity of electrolytes, in general, and in the structure of macromolecules in particular, two fundamental properties necessary for biochemical reactions to occur appropriately.

In higher organisms, the total body water accounts for 60–70% of weight and is distributed among several defined compartments. In the 19th century, Claude Bernard (Gross, 1998) recognized that cells live in the so-called "milieu interieur", which is aqueous in nature, whose composition and volume must be within strict limits for life to be maintained. The existence of water was a prerequisite for the establishment of life on earth, serving not only as a polar medium for dissolving hydrophilic substances but also acting in the organization of apolar and amphipathic molecules such as the structuring of cell membranes (Tanford, 1978; Krimm, 1980). Since life probably began in a pristine ocean with high Na^+ concentration, mammals inherited from primitive multicellular ancestors an aqueous extracellular compartment having ionic concentrations corresponding to approximately 1/3 of those observed in the ocean, with Na^+ as the primary ion in the extracellular medium.

The long-timescale required by the evolutionary processes that resulted in today's highly complex organisms is very intricate and essentially dependent on the emergence of specialized tissues to control and maintain the "milieu interieur" in a steady-state condition. That is especially true concerning the maintenance of body water content and osmolality. The conquest of dry environments by vertebrates was especially challenging from the standpoint of keeping an osmotic equilibrium between the intra- and extracellular compartments. Undoubtedly, physiological systems' emergence and efficiency gain specialized in 1) sensing osmotic changes; 2) coordinating adequate multimodal defense responses; and 3) effective management of electrolytes and water fluxes across the plasma membrane. These were essential for attaining the great evolutionary success of terrestrial vertebrates.

In mammals, the hypothalamic-neurohypophysial system (HNS) is the crucial neuroendocrine apparatus responsible for controlling extracellular osmolality. The HNS fulfills the three central aspects involved in osmoregulation mentioned above: 1) it is composed of specialized osmosensing magnocellular neurosecretory cells (MNCs), located in the hypothalamic supraoptic and paraventricular nuclei (SON and PVN); 2) it coordinates the multimodal responses by secreting the neuropeptides arginine-vasopressin (AVP) and oxytocin (OXT) into the circulation; and 3) it finely adjusts kidney function, the primary organ involved in the control of extracellular volume and composition. The present review focuses on the basic concepts related to water and electrolyte movement across the plasma membrane and discusses the molecular and cellular mechanisms involved in osmosensing by the MNCs in mammals. We give special attention to the processes at the plasma membrane involving channels and transporters, which regulate cellular excitability and the osmosensory processes in MNCs. Based on the recently described changes in the supraoptic nucleus transcriptome in response to prolonged dehydration, we also discuss the molecular plasticity of the NHS and its consequences for osmoreception. Finally, we pay attention to somatodendritic release of neuropeptides in relation to osmoregulation.

Water Movement Across the Plasma Membrane

Despite the high intensity of water exchange between the extra- and intracellular compartments, the process is essentially passive: water always moves according to its chemical gradient. In other words, all one needs to induce a net water flux across cell membranes is an osmotic ($\Delta\pi$) and/or a hydrostatic pressure gradient (ΔP). This fact has an interesting experimental implication: similar results should be obtained by applying either an osmotic or a hydrostatic pressure gradient.

Another point of interest is that cell membranes, in general, show considerable osmotic water permeability. Small values are found in cells of the thick ascending limb of Henle's loop in mammalian kidneys and the highest are found in the plasma membrane of red blood cells (Reuss, 2008). This property is a function of both the proteins present in the membrane and those in the phospholipid bilayer itself. Bilayers containing sphingolipids and/or cholesterol have lower water permeability compared to bilayers formed exclusively of phospholipids (Finkelstein and Cass, 1967; Finkelstein, 1976). The asymmetrical distribution of lipids between the bilayer leaflets and the sequestration of specific lipids in rafts also influence the permeability to water (Hill and Zeidel, 2000; Rawicz et al., 2008; Delpire and Gagnon, 2018). The water permeability is also dependent on the presence of water channels of the aquaporin family (Zeidel et al., 1992; Su et al., 2020). These channels have a ubiquitous distribution. While AQP2 (among others) is present in the collecting ducts of the kidney and their expression is mainly controlled by AVP (Fushimi et al., 1993), AQP1 and AQP4 have been described in astrocytes and ependymocytes in the brain (Verkman et al., 2011, 2017). In any case, water has an equilibrium distribution across the plasma membrane. An imbalance in the osmotic and/or a hydrostatic pressure gradient will result in a net influx or outflux of water, impacting the cell volume.

Interestingly, there is no single molecule responsible for sensing osmotic changes in the cell. Instead, changes in osmolality result in changes in the water activity. Therefore, the ionic strength of the intracellular solution can vary with the cell volume, leading to dysfunctional biochemical processes, impairment of electrical excitability, protein phase separation, changes in membrane tension, etc. (Model et al., 2021).

Cell Volume

When exposed to challenges in osmolality, cells first respond as osmometers, and then the influx or efflux of solutes is modified to counterbalance volume changes due to the concomitant water flow. This biphasic response involves the activation of a repertoire of membrane channels and transporters to circumvent the volume changes.

In response to a decrease in extracellular osmolality, the volume of the cell first increases in proportion to the imposed reduction of osmolality. Then an outflow of volume primarily induced by a net flux of osmotically active solutes directed from the intra-to the extracellular space is observed. This response is known as regulatory volume decrease (RVD) and has a time course dependent on the cell type (Grinstein et al., 1982; Hazama and Okada, 1988; Sato et al., 2011; Okada et al., 2019). For more details about cell volume regulation, see Strange, 1992, Strange, 2004). Therefore, several mechanisms have evolved to maintain the cell volume under isotonic conditions and restore it when

changes in osmolality are imposed on the system. The ubiquitous Na^+/K^+ ATPase was one of the first mechanisms to be recognized in this respect. The active movement of Na^+ out of the intracellular compartment linked to the generally low membrane permeability to Na^+ place this ion preferentially in the extracellular compartment, acting as an osmotically effective solute, as recognized long ago (Leaf, 1959; Tosteson and Hoffman, 1960; Ussing, 1960). To counterbalance volume changes, cells can lose K^+ when a reduction of volume is necessary or gain Na^+ to increase their volume. Because a movement of anions is coupled to the fluxes of Na^+ and K^+, a repertoire of membrane channels and transporters is used to cope with the osmotic challenges. HCO_3^- and Cl^- are the main counterions participating in the process. In this way, the coupled exchange of Na^+/H^+ and Cl^-/HCO_3^- contributes to controlling the intracellular pH and cell volume recovery in response to a hyperosmotic challenge. The concerted action of these two types of transporters ultimately results in a net gain of NaCl and the associated volume of water by the cell (Grinstein and Rothstein, 1986; Humphreys et al., 1995; Hughes et al., 2010; Romero et al., 2013; Li et al., 2021).

Another important class of transporters is the CCC family (cation-chloride cotransporters), which couples the movement of Cl^-, Na^+, and K^+ across the cell membrane to that of water, to counterbalance the effects of changes in tonicity. Among these cotransporters are NKCC1 and NKCC2, which import chloride, sodium, and potassium to the cell, and KCC2, which in turn exports K^+ and Cl^- from the cytoplasm. Besides their role in setting the electrical excitability of cells, via control of the intracellular chloride concentration (Russell, 2000; Blaesse et al., 2009), they also participate in the response to hypotonicity: while KCC is activated by dephosphorylation of serine-threonine residues, NKCC1 is inhibited by this process (Bize et al., 1999), resulting in a net loss of KCl by the cell and reduction of its volume (Chew et al., 2019)

Those transporters act in synchrony with several ion channels, particularly chloride channels. Numerous putative anion channels are linked to volume regulation and are activated by hypotonicity, i.e., the net entrance of water to the cytoplasm. Cell swelling has been shown to activate large-conductance chloride channels in several vertebrate cell types (Grinstein et al., 1982; Doroshenko and Neher, 1992; Nilius et al., 1994; Jentsch, 2002; Wang et al., 2005; Poletto Chaves and Varanda, 2008; Okada et al., 2019). We should note that the activity of a volume regulated anion channel (VRAC) has been recently associated with a protein of the LRRC8 family, coded by several homologous genes of the mammalian genome (Bize et al., 1999; Qiu et al., 2014; Voss et al., 2014; Pedersen et al., 2016; König and Stauber, 2019).

Magnocellular Neurosecretory Cells and Brain Osmoreception

Since the maintenance of cell volume is highly dependent on the osmolality of the extracellular fluid, systems have been selected for sensing and correcting changes in both volume and osmolality of the "milieu interieur". Although most cells face constant osmotic challenges and may change their activity in response to such perturbations, only a small number of them participate in specific mechanisms aimed to restore body fluid homeostasis. In a series of pioneering experiments, Verney and collaborators "...postulated that the neurohypophysis was functionally linked with sensory elements sensitive to changes in the osmotic pressure of their vascular environment. Such elements were termed osmoreceptors..." (see Jewell and Verney, 1957). Based on the latest advances in the field, it is clear that the osmoreceptors are not formed by a single molecular entity. Instead, each osmoreceptor unit must be associated with a cellular entity able to couple changes in osmolality, resultant from changes in the activity of water, to changes in its plasma membrane electrical activity. So far, the commonly accepted evidence indicates that the brain osmoreceptors are comprised by a very small number of specialized neurons able to transduce changes in their cell volume into electrophysiological responses (Prager-Khoutorsky et al., 2014). Several pioneer studies have identified two types of osmoreceptor neurons: 1) a subset of neurons located in the *lamina terminalis*, at the *organum vasculosum lamina terminalis* (OVLT) and the subfornical organ (SFO), two circumventricular structures outside the blood-brain-barrier; and 2) the neurosecretory MNCs, located in the PVN and SON (for a review, see Bourque, 2008). These two subsets of neurons (circumventricular and neurosecretory) are functionally connected, i.e., OVLT and SFO neurons send afferents to the SON and PVN to control their electrical activity, and consequently the neurosecretory response (Johnson and Gross, 1993; Bourque and Oliet, 2003). While cells in the OVLT and SFO are mainly involved in conveying thirst and/or sodium appetite information to the cortex (Egan et al., 2003; Bourque, 2008; Allen et al., 2017; Matsuda et al., 2017). The MNCs of both SON and PVN produce and secrete AVP and OXT through the neurohypophysis to the circulation. Those osmosensitive neurons respond to changes as low as 1% in osmolality in an independent manner by modifying the frequency and/or the discharge pattern of action potentials (Poulain and Wakerley, 1982).

In this context, the MNCs play unique roles in the osmoregulatory process because they have the following basic properties: 1) intrinsic osmosensitivity; 2) integration of osmoreceptive information from the circumventricular organs; and 3) synthesis and secretion of two of the main hormones controlling renal water and sodium excretion. While the SON has a very homogenous neuronal population (the vast majority are MNCs), send axonal projections mainly to the neurohypophysis, and produces mainly AVP and OXT, the PVN is more complex. Besides the AVP and OXT MNCs projecting to the neurohypophysis, the PVN also has several subsets of parvocellular neurons which produce other neuropeptides (such as CRH, TRH, SST, etc.) and project to the median eminence to control the adenohypophysis function; to the brainstem to control autonomic outflow; and to limbic structures to control behavioral responses (de Souza Mecawi et al., 2015; Dos-Santos et al., 2019). Thus, here we focus on the osmosensory processes, electrophysiological responses, and the molecular plasticity of the MNCs of the SON and their related glial cells.

The SON is located bilaterally to the optic chiasm and integrates afferent information from other areas involved in the maintenance of the osmolality of the extracellular fluid (Yang et al., 1994; Richard and Bourque, 1995). As previously described, MNCs not only secrete AVP and OXT under the control of other osmosensory areas, but also respond intrinsically to direct osmotic stimulation. This fact has been demonstrated by results from experiments performed in intact anesthetized animals (Brimble and Dyball, 1977; Poulain et al., 1977; Wakerley et al., 1978; Poulain and Wakerley, 1982), in slices where the synaptic inputs have been pharmacologically blocked (da Silva et al., 2013, 2015), and in isolated MNCs from both SON and PVN (Oliet and Bourque, 1992, 1993; Zhang et al., 2007). It has been demonstrated that changing cell volume by osmotic stimulation or direct pressure application with a patch pipette activates mechanosensitive ion channels in these cells (Oliet and Bourque, 1993; Zhang and Bourque, 2003). The question that arises here is: Which ultrastructural cellular component could be responsible for coupling changes in volume to electric plasma membrane responses? Super-resolution images obtained by structured illumination microscopy have revealed that MNCs contain many actin filaments and microtubules in their somata, with exclusive organization compared with cells in other brain regions, such as the cortex, as well as with hippocampal and other hypothalamic neurons (Prager-Khoutorsky et al., 2014). Additionally, the density/array of actin filaments and microtubules are substantially changed in response to salt-loading (Barad et al., 2020; Hicks et al., 2020), reinforcing the hypothesis that these elements participate in the mechanotransduction process. Based on the assumption that cytoskeleton components can redistribute forces across the lipid bilayer (Ingber, 1997), Zhang et al. (2007) proposed that osmosensory transduction depends on the amount and structure of F-actin filaments present in MNCs. In their study, the pretreatment of acutely isolated MNCs with cytochalasin-D, a compound that promotes actin depolymerization, reduced the mechanosensitivity index, and the opposite was observed with jasplakinolide, a cell-permeable actin polymerization agent. The authors concluded that osmosensory transduction relies on changes in the cell volume and also speculated about possible physical interaction of actin filament with stretch-inactivated cation channels (Zhang et al., 2007). In another respect, a study performed in the same year by Tobin and Ludwig (2007), revealed that induction of actin polymerization by jasplakinolide did not alter peptide release in the neuronal lobe during high-K^+-stimulation, demonstrating that the axonal peptide release is not dependent on actin filaments remodeling. The gating model proposed assumes that during hypertonicity, the cell shrinkage would lead to a reorganization of the microtubules in a direct way, causing a compression force sufficient to change the channel conformation and induce its activation (Prager-Khoutorsky et al., 2014). This phenomenon was further linked to the modulation of TRPV channels in the MNCs (Ciura, 2006; Ciura et al., 2011; Moriya et al., 2015; Zaelzer et al., 2015). Therefore, those findings reinforce the idea that the ultrastructure of cytoskeleton elements has important functional roles in associating volume changes with plasma membrane events in the MNCs. Nevertheless, implicit in the mechanosensitive argument is the assumption that MNCs respond to steady changes in osmolality with a steady change in cell volume, i.e., these cells should present neither RVD nor regulatory volume increase (RVI). Therefore, it seems that the response of MNCs to osmotic challenges is more complex than those predicted by a simple osmometer.

Based on the assumption that water fluxes across the plasma membrane lead to changes in cell volume, elegant studies were performed combining voltage-clamp recording and soma volume measurements during variations imposed on the extracellular fluid osmolality (Oliet and Bourque, 1993; Zhang et al., 2007). Changes in osmotic pressure, induced by either hypertonic stimulus or hydrostatic pressure (applied through a patch pipette), resulted in decreased cell volume and activation of an inward current with a linear *IxV* relationship and reversal potential around −10 mV. These data suggest the involvement of voltage-independent and non-selective cation channels in the osmotransduction mechanism (Bourque, 1989; Oliet and Bourque, 1993, 1994). These responses occurred in the absence of changes in the extracellular Na^+ concentration and were due to the cell volume-dependent regulation (Oliet and Bourque, 1993). In both cases, the conductance activated by both osmotic stress and hydrostatic pressure was entirely blocked by Gd^{3+} (Oliet and Bourque, 1996; Zhang et al., 2007), a potent but not exclusive blocker of stretch-inactivated channels (Elinder and Arhem, 1994; Hongo et al., 1997). In neurons of the cortex and hippocampus (Oliet and Bourque, 1993), the hypertonicity/hypotonicity and the negative/positive pressure also provoke volume changes, but these are not accompanied by variations in membrane conductance (Oliet and Bourque, 1993). These results support the hypothesis that intrinsic osmosensory transduction is a property of the MNCs themselves and that the mechanism involved seems to be basically a mechanical process.

Mechanical transduction by ion channels may occur in any cell, including red blood cells (for a review, see Sachs, 2015). Both stretch-activated channels (SACs) and stretch-inactivated channels (SICs) (Sachs, 2010) have been described in MNCs. Single-channel analysis revealed that hypertonicity-induced cell shrinkage increases the probability of SIC opening, consistent with the resting potential depolarization observed in whole-cell recordings (Bourque and and Oliet, 1997; Bourque, 1998; Zhang et al., 2007). At first glance, this evidence implies that RVI may be absent in these cells and that they lack a volume regulatory mechanism. Although the short-term (a few minutes) response of MNCs to hypertonicity is a decrease in cell volume, other processes seem to occur in the long run (tens of minutes to hours), including somatic hypertrophy of MNCs after hyperosmotic challenge (Hatton and Walters, 1973; Shah et al., 2014). Shah et al. (2014) reported a significant increase in the cross-sectional area of the cell after a considerable delay upon exposure of isolated MNCs to a *in vivo* hyperosmotic condition. This phenomenon is dependent on the exocytotic fusion of secretory vesicles and therefore is dependent on calcium entry in the cell and activation of phospholipase C. In line with the above results, Sato-Numata et al. (Sato-Numata

et al., 2021) reported that AVP MNCs responded to a hyperosmotic challenge with both a membrane shrinkage and a massive release of the hormone, leading to a decrease in secretory volume. This latter phenomenon was impaired by tetanus toxin and blockers of T-type calcium channels, suggesting that it originates from vesicle fusion to the plasma membrane. They also found that the addition of flufenamic acid, which blocks voltage-gated Ca^{2+} channels (T and N types), prevents both the firing rate increase and the associated neuropeptide secretion. Under this experimental condition, the RVI mechanism became evident. According to the authors, RVI is hidden behind a substantial exocytosis, which occurs in a hyperosmotic stimulation and is dependent on the functioning of the Na^+/H^+ exchanger and of the Cl^-/HCO_3^- anion exchanger. As pointed out by Zhang and Bourque (2003), MNCs possess a significant membrane reserve, which allows them to blunt the membrane tension induced by osmotic perturbation. Would this be sufficient to ensure the maintenance of the stimulus-secretion coupling when the MNCs are exposed to a long period (hours to days) of hyperosmotic challenge, such as during prolonged water deprivation or salt-loading? As we discuss in the coming sections, under chronic dehydration, the MNCs experience dramatic transcriptomic remodeling, which includes changes in the expression of several genes encoding plasma membrane channels and transporters (Hindmarch et al., 2006; Greenwood M. P. et al., 2015; Johnson et al., 2015; Pauža et al., 2021). Another important adaptation is the increased complexity of the cytoskeleton array observed during sustained hyperosmolality (Barad et al., 2020; Hicks et al., 2020), whose crucial role for osmosensitivity was previously demonstrated by Prager-Khoutorsky et al. (2014), also discussed later in this review. Thus, the new molecular phenotype of the MNCs under chronic osmotic challenge might also help understanding how they are able to ensure the continuous AVP and OXT secretion, essential for survival during dehydration, despite the incessant plasma membrane insertion due to the vesicle fusion. Therefore, the fusion of membrane secretory vesicles added to the bilayer blunts the development of tension and masks the volume regulatory mechanism. These results may explain, at least in part, the absence of membrane tension for gating mechanosensitive channels and suggest another gating mechanism involving the cytoskeleton components, besides the classical bilayer-tension phenomenon. In this context, it is known that MNCs readily express a plethora of ion channels and transporters that may contribute to the complexity of the osmosensing mechanism.

Genes, Channels, Transporters and Osmoregulation in the SON

Pauža and collaborators recently classified and catalogued all membrane transporters coded by mRNAs expressed in the SON of control rats. About 400 mRNAs coding membrane transporters and 220 mRNAs coding channels (or channel subunits) have been identified in the SON under isotonic conditions (see **Figure 3** and Supplementary Figures 6 and 8 in Pauža et al., 2021). Therefore, in this section we focus on the discussion of key mRNAs that code channels and transporters (classified according to the International Union of Basic and Clinical Pharmacology, IUPHAR) in the SON, the functional relevance as well as the plastic response after dehydration.

As a brain nucleus with high metabolic demand and implicated in the synthesis and release of large amounts of peptides in the periphery and the CNS (Roy et al., 2021), it is not surprising that the genes mostly expressed in the SON encode proteins directly related to mitochondrial ATP synthesis and use by active transport processes, such as Na^+/K^+ ATPase and H^+ ATPase. The most expressed mRNA of a cotransporter was *Slc22a17*, coding the protein BOCT1. This transporter has been described as highly expressed in the brain, mainly in neurons (Bennett et al., 2011). It was recently demonstrated that BOCT1 works as a membrane receptor for circulating lipocalin 2, a biomarker of acute and chronic renal injury (Jaberi et al., 2021). Hyperosmolality upregulates BOCT1 expression in collecting duct cell lines via CREB signaling, suggesting that this protein contributes to osmotolerance at the renal level (Jaberi et al., 2021). It was previously demonstrated that peripheral lipocalin 2 can cross the blood-brain barrier and act on the PVN neurons to modulate food intake (Mosialou et al., 2017). Thus, we can speculate that this transporter may also mediate some of the lipocalin 2 effects on the MNCs and/or participate in their osmosensory process. The second most expressed mRNA was *Slc1a3*, also known as GLAST1 (sodium-dependent glutamate/aspartate transporter), present in glial cells and shown to increase in the SON in conditions of heart failure (Potapenko et al., 2012) and salt loading (Choe et al., 2016). It also plays an important role in modulating the extracellular levels of glutamate in the SON to control the MNCs activity (Souza et al., 2020). In the control state SON, *Aqp4* is the highest expressed among mRNAs coding channels. As previously mentioned, astrocytes are rich in AQP4. Recently, it was demonstrated that AQP4 is required for the osmotically induced increase in neuronal activity of AVP-producing MNCs by mediating the retraction of astrocyte GFAP filaments (Wang et al., 2021). Next comes *Gja1*, which encodes connexin 43, important for intercellular communication among glial cells, mainly astrocytes (Duan et al., 2004). Furthermore, a heterotypic connexin 43/32 gap junction has been described between astrocytes and neurons in the SON. When this heterotypic gap junction was blocked by carbenoxolone, the FOS activation in the MNCs in response to salt overload was significantly reduced, indicating a key role played by connexin 43 in the astrocyte-MNC communication during hypertonicity-induced AVP secretion (Duan et al., 2004). The ion channel-related mRNA *Gabra1* coding for the gamma-aminobutyric acid type A receptor subunit alpha-1 is also highly expressed in the control SON (Pauža et al., 2021). MNCs isolated from adult rat brains respond to GABA, functionally demonstrating that those neurons express GABA receptors (Oliet and Bourque, 1992). It was shown that the gamma-aminobutyric acid type A receptor subunit alpha-1 and -2 are co-expressed with the gamma 2 subunit in MNCs, suggesting they may express GABAA receptors with benzodiazepine type 1 and 2 pharmacological

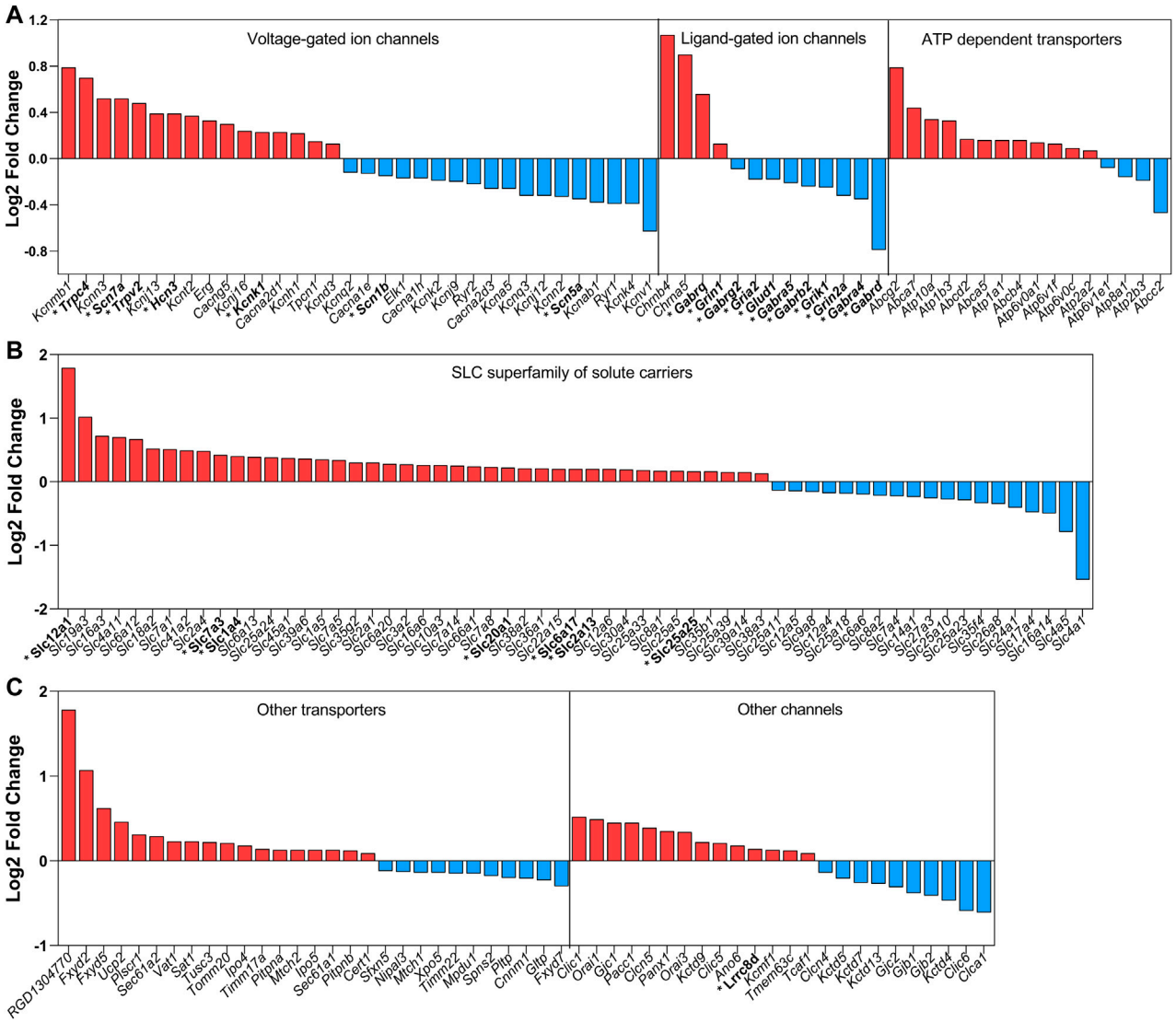

FIGURE 1 | Summary of the mRNA coding channels and transporters found to be changed by water deprivation for 3 days. Data obtained with the RNAseq approach by Pauža et al. (2021). In red are the upregulated mRNAs and in blue are the downregulated mRNAs. In this global analysis, we found coding mRNAs significantly and differentially regulated for 34 voltage-gated channels (16 up and 18 down), 13 ligand-gated ion channels (4 up and 9 down), 24 other ion channels (14 up and 10 down), 61 SLC superfamily of solute carriers (42 up and 19 down) and 29 of other transporters (18 up and 11 down). The mRNAs coding channels and transporters that we discuss in the present review are highlighted with an asterisk and in bold.

properties (Fenelon and Herbison, 1995). Despite having inhibitory effects in most neurons in the adult brain, there is strong evidence indicating that GABA acting via GABAA receptors is excitatory in the adult AVP-producing MNCs under basal condition (Haam et al., 2012). In sequence are mRNAs coding the glutamate-activated NMDA and AMPA channel subunits, *Grin1* and *Gria2* respectively, highly expressed in the SON (Pauža et al., 2021). The stimulatory effect of L-glutamate on MNCs' electrical activity and hormonal secretion was demonstrated both *in vitro* (Richard and Bourque, 1995; Sladek et al., 1995) and *in vivo* (Xu and Herbert, 1998; Onaka and Yagi, 2001). It was further shown that the activity of AVP- and OXT-producing neurons is differentially modulated by NMDA and AMPA L-glutamate receptors. These results suggest that the AVP neurons are influenced by both NMDA and AMPA receptors, while the OXT neurons seem to be mainly regulated by AMPA receptors (Nissen et al., 1995; Richardson and Wakerley, 1997). By using intra-SON microinjection, Busnardo et al. (2012) demonstrated that AVP and OXT secretion is mediated by AMPA receptors. In this context, it has recently been shown in *in vivo* experiments that hyperosmolality and hemorrhage affect AVP secretion through activation of NMDA and AMPA receptors (Vilhena-Franco et al., 2018; Busnardo et al., 2021; Dos-Santos et al., 2022). Those findings indicate that the MNCs are subject to the influence of both L-glutamate and GABA activated channels and that their

close interaction with astrocytes is essential to integrate the osmoreception process in the SON.

Additionally, Pauža et al. (2021) have also demonstrated that the mRNA expression of each channel and transporter was changed in the SON of rats exposed to 72 h of water deprivation. Since it is practically impossible to discuss every gene upregulated/downregulated in the SON after osmotic stress, a global view can be seen in **Figure 1**. This figure summarizes the data regarding all mRNA coding channels and transporters found to be changed by 3 days of water deprivation, using the RNAseq approach (Pauža et al., 2021). The great majority of those channels and transporters have not yet been characterized with respect to their protein expression and/or function in the MNCs and/or their associated glial cells in the SON.

When animals are subjected to a prolonged dehydration time, the whole transcriptome of the SON is remodeled to guarantee adequate response of the MNCs to the imposed condition. Murphy's group has used the transcriptome approach in the recent years to describe the remodeling of the SON global gene expression in dehydrated animals and to discover new players regulating the MNCs activity-synthesis-secretion response, such as CREB3L1 (Greenwood M. et al., 2015), CAPRIN2, (Konopacka et al., 2015a), RASD1 (Greenwood et al., 2016) and NKCC2 (Konopacka et al., 2015b). However, except for *Slc12a1*, coding NKCC2, and a few other new genes discovered to be regulated by hyperosmolality in the SON, most of the membrane transporters and channels described have not yet been investigated regarding their role in osmosensitive processes. To summarize the data related to the expression of membrane transporters and channels in the SON in response to prolonged hyperosmolality in rats, we have integrated data from four publications revealing new possible players in the regulation of MNCs' electrophysiological response. While Hindmarch et al. (2006) and Greenwood M. P. et al. (2015) used the microarray technology to analyze the SON transcriptomic response, Johnson et al. (2015) and Pauža et al. (2021) took advantage of the next generation RNAseq technique. Furthermore, Hindmarch et al. (2006) and Pauža et al. (2021) used 3 days of water deprivation to stimulate the SON, while Johnson et al. (2015) used 5 days of salt loading (hypertonic saline as the only fluid available), and Greenwood et al. (Greenwood M. P. et al., 2015) compared the SON transcriptomic response to 3 days of water deprivation or 7 days of salt loading. Water deprivation and salt loading can both increase *Avp* and *Oxt* mRNA expression and peptide secretion. However, while water deprivation is associated with a decrease in the extracellular volume and activation of the peripheral renin-angiotensin system, prolonged salt loading has no significant effects on extracellular volume and inhibits the activity of the peripheral renin-angiotensin system (Greenwood M. P. et al., 2015). Thus, despite the methodological caveats among these works and the important physiological differences between water deprivation and salt loading models, the prolonged hyperosmotic response of the MNCs is conserved. Those data show that the expression of seven core genes coding channels and transporters was increased: *Trpv2, Kcnk1, Slc1a4, Slc7a3, Slc20a1, Slc25a25,* and *Slc41a2* (**Figure 2**).

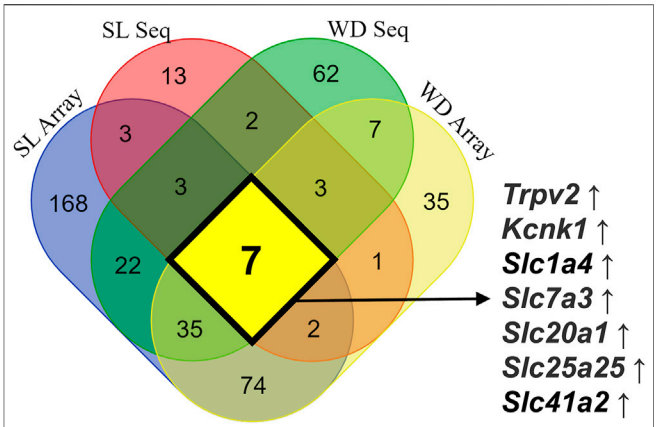

FIGURE 2 | Integrated data on the expression of mRNA coding ion channels and membrane transporters in the SON in response to long-term exposure to hyperosmolality in rats. Microarray data obtained from water-deprived (WD) rats are from Hindmarch et al. (2006), microarray information from WD and salt loading (SL) rats is from Greenwood M. P. et al. (2015), RNAseq data obtained from SL rats are from Johnson et al. (2015), and finally data on RNAseq obtained from WD rats are from Pauža et al. (2021). This integrated analysis revealed seven core genes coding channels and transporters consistently upregulated by sustained hyperosmotic stimulation: *Trpv2, Kcnk1, Slc1a4, Slc7a3, Slc20a1, Slc25a25,* and *Slc41a2*.

Over the last few years, the development of the RNAseq technique has also allowed a deeper examination of specific genes enriched in specific cell populations. In this way, single-cell transcriptome data have revealed a set of genes positively enriched in AVP- and OXT-producing neurons along with hypothalamic development in mice (Romanov et al., 2020). The results regarding positively enriched genes that encode channels and transporters in both *Avp* and *Oxt* neurons are summarized in **Figure 3**.

Based on these results, in the following paragraphs we emphasize the current literature, indicating the possible roles played by some membrane ion channels and transporters on the osmosensitivity and electrophysiological activity of MNCs.

TRPV Channels

In 1997, a gene encoding OSM-9, which is related to aversive behavior of *Caenorhabditis elegans* to strong hypertonic environments, was shown to be required for mechanosensation. This gene encodes a predicted protein with structural similarities to the mammalian transient receptor potential vanilloid (TRPV) (Caterina et al., 1997; Colbert et al., 1997; Lee et al., 2016). Their molecular structure encompasses six transmembrane domains and a three to five multiple ankyrin-binding sequence repeats in the N-terminal and a large C-terminal intracellular domain (Liedtke and Kim, 2005). It has been demonstrated that TRPV1 participates in the mechanoelectrical transduction of MNCs in response to short-term hyperosmolality. In mice MNCs, the cationic conductance induced by hypertonicity is blocked by ruthenium red, a non-selective antagonist of TRPV channels (Sharif-Naeini et al., 2006). The same pattern of response was also observed in neurons from

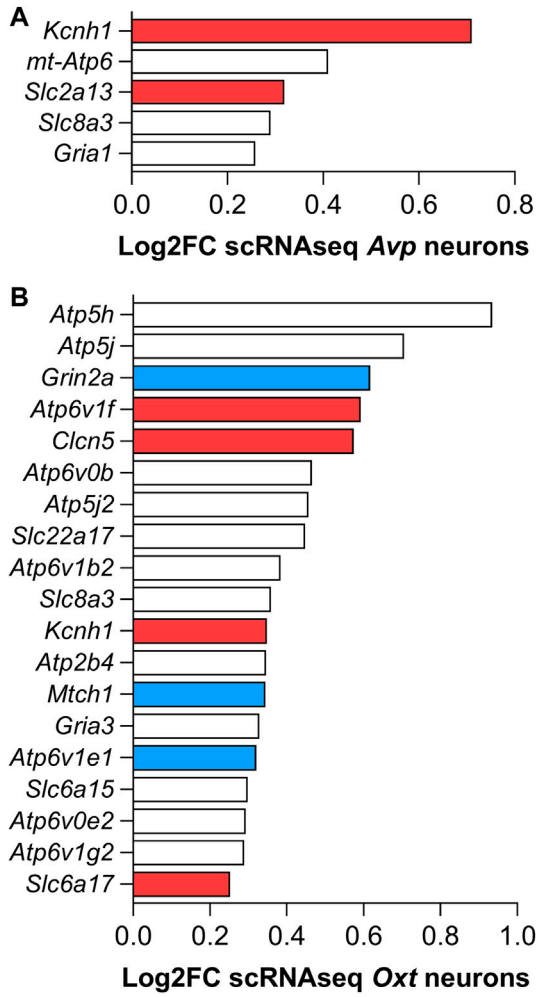

FIGURE 3 | Set of mRNAs coding channels and membrane transporters positively enriched in **(A)** AVP- and **(B)** OXT-producing hypothalamic mouse neurons found with the single-cell RNAseq transcriptome analysis by Romanov et al. (2020). Red colored bars refer to the genes that, besides being positively enriched on AVP- and/or OXT-producing neurons in mice, are also up-regulated by 3 days water deprivation in the SON of rats. Blue colored bars refer to down-regulated genes (Pauža et al., 2021). White bars refer to genes also regulated in the SON but not discussed in this review.

the OVLT (Ciura, 2006; Ciura et al., 2011). Intriguingly, HEK 293 cells heterologously expressing the classical TRPV1 channel did not respond to hypertonic stimulation (Liedtke et al., 2000). Although *Trpv1* was detected in MNCs by reverse transcription-polymerase chain reaction (RT-PCR), no signals for the N terminus of Trpv1 (exons 2–6) were detected in the SON (Sharif-Naeini et al., 2006). Immunohistochemistry experiments confirmed this result, showing immunoreactivity to TRPV1 when MNCs were probed with an antibody against the C-terminal but not against the N-terminal (Sharif-Naeini et al., 2006). The N-terminal region absent in MNCs represents a portion containing capsaicin-binding sites (Caterina et al., 1997), and explains why these cells' activity did not change when exposed to capsaicin (Sharif-Naeini et al., 2006), a selective agonist of TRPV1. Additionally, neurons isolated from mice lacking *Trpv1* lost their ability to respond to increases in osmolality, indicating that *Trpv1* encodes a potential osmosensory channel in the SON (Sharif-Naeini et al., 2006). Taken together, these results lead to the conclusion that TRPV1 channels in MNCs have a particular molecular structure and that one or more *Trpv1* splice variants seem to be necessary to encode a capsaicin-insensitive channel (Sharif-Naeini et al., 2006; Moriya et al., 2015).

Alternative splicing is considered to be one of the major sources of the functional diversity of proteins (Johnson et al., 2003). To date, four TRPV1 splice variants containing modifications in the N-terminal intracellular domains have been described: 1) vanilloid receptor 5′ splice variant (VR.5′sv), which was the first variant reported and characterized regarding the lack of exons one to four and 7 (Schumacher et al., 2000); 2) TRPV1 beta (TRPV1b), which contains a modification in the N-terminal encoded by exon seven resulting in the loss of 30 nucleotides (Wang et al., 2004); 3) TRPV1var, which lacks exon 1, part of exon 16 and presents a failure in the splice out of intron 5 (Tian et al., 2006); 4) stretch-inhibitable nonselective cation channels (SICs) have identical trans-membrane-spanning domains as VR.5`sv. The C-terminal of SIC diverges from TRPV1 and VR.5'sv. It was demonstrated that the C terminal of SIC is derived from two related but independent genes (Schumacher et al., 2000; Xue et al., 2001; Tian et al., 2006). Xue et al. (2001) found that human and mouse TRPV genes share an extensive sequence homology, but only through exon 15. The remaining sequences encoding the proposed C-terminal domain of SIC matched the gene encoding vanilloid receptor-related–osmotically activated channel (VROAC, now called TRPV4).

Three out of four variants were identified in the SON by Moriya et al. (2015): full-length *Trpv1*, *Trpv1b* and SIC. Although MNCs express *Trpv1* mRNA, able to encode the full-length TRPV1, including the 36 amino acids essential to capsaicin action, the isolated MNCs did not respond to capsaicin (Sharif-Naeini et al., 2006; Moriya et al., 2015). Unlike Moriya and collaborators (2015), Zaelzer et al. (2015), using PCR cloning, isolated *Trpvdn*, a cDNA containing an open reading frame encoding all of 5–15 exons of *Trpv1*. Transfection of *Trpv1dn* into HEK293 cells induced the expression of a 58 Kd protein (truncated ΔN-TRPV1). This protein is significantly smaller than the full-length TRPV1, but sufficient to make the cell sensitive to hypertonicity. Most important, the expression of *Trpv1dn* in isolated MNCs from *Trpv1* knockout mice rescued the neurons' ability to respond to osmotic stimuli.

An *in vitro* study demonstrated that the C-terminus of ΔN-TRPV1 physically interacts with microtubules (Goswami et al., 2004, 2007), suggesting that cytoskeleton elements may be part of the mechanism of channel activation. As described by Prager-Khoutorsky et al. (2014), microtubules have a unique array in the MNCs. Therefore, a proposed gating model assumes that during acute hypertonicity, cell shrinkage leads directly to reorganization of the microtubules, causing a compression force sufficient to change the channel conformation and induce its activation (Prager-Khoutorsky et al., 2014). At the molecular level, an

elegant study conducted by Fisher´s group, showed that activation of ΔN-TRPV1 also involves phospholipase C (PLC) (Bansal and Fisher, 2017). Additionally, PLCδ1 knockout mice display an impaired electrophysiological response to increases in extracellular osmolality (Park et al., 2021). The idea is that PLCδ1 activated by Ca^{2+} influx during osmotically evoked MNCs action potential drives a positive feedback loop leading to a stronger activation of ΔN- TRPV1 (Park et al., 2021).

In spite of this compelling molecular and functional evidence about the role of ΔN-TRPV1 in MNCs' osmosensitivity, we should note that *Trpv2* showed the highest level of expression among the mRNAs encoding TRPV channels in the SON of rats in the control condition (Pauža et al., 2021). Furthermore, *Trpv2* mRNA is consistently increased in response to chronic hyperosmolality in this nucleus (**Figure 2**). Besides this, TRPV2 protein is preferentially expressed in the MNCs of both the SON and PVN (Wainwright et al., 2004; Nedungadi et al., 2012b). The TRPV2 was also demonstrated to have its expression increased at both mRNA and protein levels in parallel with the increased levels of AVP heteronuclear RNA and protein levels in both SON and PVN of rats submitted to chronic bile duct ligation (Nedungadi et al., 2012a). This animal model is widely used to activate MNCs' AVP hypersecretion, culminating in a secondary plasma hypoosmolality (Balapattabi et al., 2020). Studies of peripheral osmosensitive cells, such as vascular aortic smooth muscle cells, treated with *Trpv2* antisense oligonucleotides demonstrated reduced TRPV2 expression, suppression of the nonselective cationic current and elevation of the intracellular Ca^{2+} concentration in response to hypotonic stimulation (Muraki et al., 2003). Later, it was also demonstrated that TRPV2 is critical for the osmotic response in skeletal muscle fibers. The TRPV2 dominant-negative showed lower membrane depolarization, a reduced intracellular Ca^{2+} concentration and RVI response. The authors further demonstrated that the response of TRPV2 depends on the sequential activation of STE20/SPS1-related proline/alanine-rich kinase (SPAK) and NKCC1 cotransporter (Zanou et al., 2015).

Similarly to TRPV1 (Prager-Khoutorsky et al., 2014), TRPV2 also interacts with cytoskeleton structures, mainly with actin filaments, and its activation depends on rearrangements of the actin filaments in response to mechanical stimulation (Sugio et al., 2017; Yadav and Goswami, 2020). The cortical actin filaments of the MNCs are uniquely organized, and their increased array complexity after salt-loading treatment seems to be involved in the elevated osmo-responsiveness following sustained intracellular dehydration (Barad et al., 2020). Hence, TRPV2 might have an actin filament interaction-dependent role in the MNCs' volume-electrical activity coupling efficiency, maintenance and/or potentiation during prolonged dehydrated state.

Due to the lack of functional evidence about the role of TRPV2 in the MNCs' osmosensitivity and the fact that smooth and skeletal muscle cells are not osmosensitive in the same way as MNCs, we can only speculate about a possible role of this channel in the control of the intrinsic osmosensitivity and electrophysiological properties. Future studies need to be carried out to clarify if TRPV2 participates in the osmosensitivity process of MNCs, especially under chronic hyperosmotic stimulation. A point that still needs to be elucidated for both TRPV1 and TRPV2, or even other mechano-gated channels, is whether the traction force induced by cytoskeleton elements occurs only in the C-terminal end, or it is somehow transferred to the lipid bilayer, resulting in a membrane-tension-complex for activation.

Other potential osmoreceptors are the canonical transient receptor potential (TRPC) 5 and 6. Although not investigated in MNCs, TRPC5 (Jemal et al., 2014) and TRPC6 (Wilson and Dryer, 2014) channels were also shown to be sensitive to mechanical and osmotic stress in heterologous expression systems, but different from TRPVs expressed in the MNCs, TRPC5 and 6 are sensitive to hypotonic stress. These canonical members, especially TRPC4, were recently linked to neuronal exocytosis by mediating additional Ca^{2+} influx followed by mGluRs activation (Jeon et al., 2021). In MNCs, Nedungadi and Cunningham (2014) and Pauža et al. (2021) identified the presence and increased gene expression of *Trpc4* after 48 h of water deprivation, suggesting the participation of this channel in osmoregulation.

In summary, although the results described above convincingly point to ΔN-TRPV1 as the main molecular mechanism coupling hyperosmolality to electrical responses in the MNCs, a significant number of studies have shown that modulation of MNCs' activity during osmotic challenges relies on several additional factors, including a variety of other ion channels and transporters (Stern and Ludwig, 2001; Pires da Silva et al., 2016; Bansal and Fisher, 2017; Ferreira-Neto et al., 2021). The list of genes up and downregulated in the SON in response to water deprivation reinforces this argument (**Figure 1**). Therefore, depending on the time window of the osmotic challenge, MNCs might recruit distinct channels and transporters to collectively coordinate their electrophysiological response to extracellular osmolality.

Potassium Channels

Among the mRNAs coding for ion channels is *Kcnk1, which* is consistently upregulated by hyperosmolality. This gene is responsible for coding the potassium two pore domain channel subfamily K member 1, also known as TWIK1. Each subunit of the genes coding the channels of this family is responsible for the expression of the two-pore loop domains that form one ion pathway selective to K^+ (Kwon et al., 2021). It has been demonstrated that these channels can also be modulated by temperature and osmolality (Talley et al., 2003). The TWIK1 is expressed at the brain level in both neurons and astrocytes (Kwon et al., 2021). Single-channel recordings from isolated MNCs have also identified some background (leak) K^+ channels (TREK-1, TREK-2, and a novel TREK), which are sensitive to membrane stretching (Han et al., 2003). Additionally, voltage-gated K^+ channels also seem to play a role in the osmotically evoked MNCs' activity by shaping their firing pattern (Zhang et al., 2009). Electrophysiological recording in acutely isolated MNCs showed that hypertonicity (325 mOsm/KgH_2O) induces an outward current whose equilibrium potential is near to that

expected for K^+ (Zhang et al., 2009). The authors hypothesized that it is mediated by KV7/M-type channels, since the outward hypertonic sensitive-current was blocked by XE991 and enhanced by retigabin, a selective inhibitor and activator of M-type K^+ currents, respectively. The contribution of this current to osmosensitivity of MNCs is unusual, but could contribute to the transition from continuous to burst activity (Zhang et al., 2009).

Single-cell RNAseq revealed that mRNA coding *Kcnh1* is positively enriched in both *Avp*- and *Oxt*-producing MNCs (**Figure 3**) (Romanov et al., 2020). Furthermore, our SON RNAseq data also demonstrate increased expression of this gene after 3 days of water deprivation (Pauža et al., 2021). Kcnh1 codes the K^+ channel KCNH1, also known as Ether-à-go-go1 (Eag1), a voltage-gated K^+ channel family member, with four alternative transcripts identified in the human brain (Ramos Gomes et al., 2015). Recently, this channel was identified in the presynaptic terminals of parallel fiber–Purkinje cells, acting as a modulator of presynaptic action potentials and regulating the Ca^{2+} influx and neurotransmitter release during high-frequency burst firing. Furthermore, the authors found no changes in the excitability or action potential shape at the cell somata (Mortensen et al., 2015). Thus, despite no characterization of the KCNH1 functional protein expression in the MNCs or at the neurohypophysial terminal so far, this channel is another candidate for participation in the control of MNCs' electric activity and/or in the neuropeptide secretion as a response to hyperosmotic stimulus. However, future functional studies need to be carried out to clarify its possible role on MNCs' physiological responses.

Sodium Channels

Even in the absence of osmotic disturbances, changes in Na^+ concentration also activate inward currents in MNCs, which are a consequence of changes in the Na^+ driving force and the relative membrane permeability to this ion (Bourque, 1989). Physiologically, this phenomenon becomes significant when considering that *in vivo*, systemic osmotic pressure disturbances are accompanied by parallel changes in the Na^+ concentration in the extracellular fluid. Therefore, it is reasonable to assume that non-voltage and/or voltage-dependent Na^+ channels may act as sensors to detect increments in Na^+ concentration in the SON, contributing to the modulation of MNCs' electrical properties during osmotic stress.

Non-voltage dependent channels, particularly the epithelial Na^+ channel (ENaC), were identified in the SON by immunocytochemistry (Amin et al., 2005) and their functionality was ascertained by Teruyama et al. (2012), by associating pharmacology and electrophysiological recordings in brain slice preparations. They demonstrated that ENaC has a significant influence on the resting membrane potential of MNCs, since its blockage, by amiloride or benzamil, resulted in hyperpolarization of the membrane potential and cessation of action potential firing (Teruyama et al., 2012). Additionally, the expression and activity of ENaC are influenced by a high sodium diet (Garty and Palmer, 1997). A diet based on high NaCl intake for 7 days increased the expression of the channel (Sharma et al., 2017) and caused a depolarization of the membrane potential of MNCs, which was restored to basal levels by benzamil (Teruyama et al., 2012). Therefore, the steady-state Na^+ leak current mediated by ENaC also seems crucial for controlling MNCs' excitability and firing pattern, which ultimately controls hormone secretion during osmotic imbalance induced by changes in extracellular Na^+ concentration.

Besides this, several voltage-dependent sodium channels also seem to control MNCs' activity during osmotic challenge. Transcriptome analysis of the SON of water-deprived rats demonstrated an increase in the expression of *Scn7a* and a decrease in *Scn1b* and *Scn5a* mRNAs (**Figure 1**) (Pauža et al., 2021). Additionally, after 10 days of salt-loading, two Na^+ channel α subunits and the corresponding β1 and β2 subunits were shown to be upregulated, both at the mRNAs and protein levels, suggesting a physiological role of these channels (Black et al., 2013, 2014). These molecular findings point to the distinct regulatory effects of water deprivation and salt-loading on sodium voltage-gated ion channels.

The presence and functionality of these sodium channels in the membrane, whose genes were upregulated, were confirmed by electrophysiological detection of a transient Na^+ current (Tanaka et al., 1999). A significant difference was found for isolated cells from salt-loaded compared with those from euhydrated animals. A salt-loading diet induced a large transient Na^+ current, and this response became more evident by applying slow-ramp depolarization voltage protocols. It was possible to observe an even more significant increase in amplitude and density of the persistent Na^+ current evoked at subthreshold potentials (Tanaka et al., 1999). As far as we know, the functional impact of sodium voltage-gated ion channels' plasticity in MNCs following water deprivation is still unknown.

Assuming that non-voltage and voltage-dependent sodium channels are also part of the mechanisms controlling the excitability of MNCs when the extracellular fluid homeostasis is disturbed by increases in extracellular Na^+, an intriguing question arises: Are MNCs subject to a dual control system, i.e., how are sodium mechanisms integrated with those derived from changes in osmotic pressure only?

It was previously demonstrated *in vivo* that changes in plasma osmolality and extracellular sodium concentration could individually modulate the release of AVP in cells of goats, sheep and dogs (Olsson and Kolmodin, 1974; McKinley et al., 1978; Thrasher et al., 1980). Assuming that the release of neuropeptides is directly correlated with the firing rate of MNCs (Poulain and Wakerley, 1982), these cells are expected to present different electrical behavior for each kind of stimulus. In fact, in isolated MNCs obtained from coronal hypothalamic slices of rats, Voisin et al. (1999) observed that hypertonic stimulation with excess NaCl is significantly more potent to depolarize the membrane potential than an equivalent osmotic stimulus induced by mannitol. Additionally, in the absence of osmotic perturbation, MNCs are still efficient in changing their intrinsic activity during manipulation of extracellular sodium concentration. The inward current induced by isoosmotic increases in the extracellular sodium concentration (osmolality constant at 290 $mOsm/kgH_2O$) or applications of hypertonic mannitol (+30 $mOsm/kgH_2O$, with extracellular sodium constant

at 125 mM) were present in both situations. However, only osmotically evoked currents induced by mannitol were able to change the membrane conductance of MNCs. Thus, associated with the fact that sodium currents were successfully inhibited by Gd^{3+}, a blocker of SIC/ΔN-TRPV1 channels, the authors suggested that the Na^+ sensitive current in MNCs flows through mechanosensitive cation channels in a coincident manner.

Despite all these facts, it was demonstrated that TRPV1 knockout rats show normal AVP secretion and thirst behavior in response to hypernatremia (Tucker and Stocker, 2016), suggesting that other channels are involved in the osmosensation process. Several sodium channel genes are expressed in the SON, some of which are significantly regulated during osmotic challenge (Hindmarch et al., 2006; Konopacka et al., 2015a; Johnson et al., 2015; Pauža et al., 2021). Therefore, since the electrical activity itself may modulate the expression of sodium channels, as previously suggested (Offord and Catterall, 1989), the remodeling of the electrogenic machinery may also be a crucial phenomenon for MNCs to maintain efficient neuropeptide secretion during a chronic osmotic disturbance.

Glial cells also substantially contribute to the control of MNCs' activity during osmotic challenge. It has been shown that taurine is an essential gliotransmitter released to inhibit the firing rate of MNCs during hypotonic disturbances (Decavel and Hatton, 1995; Choe et al., 2012). Additionally, there is experimental evidence showing that the expression of the protein c-FOS (a marker of cell activity) in SON astrocytes, induced by a hyperosmotic stimulation, precedes the increased expression of the same protein in MNCs (Ludwig et al., 1996; Yuan et al., 2009). Interestingly, c-FOS protein in MNCs was inhibited by fluorocitrate, a glial metabolic inhibitor (Yuan et al., 2009).

Mice astrocytes express the sodium channel sensor (Na_x) and are the primary site of sodium-level sensing in SFO (Iadecola, 2007; Hiyama and Noda, 2016), suggesting a homeostatic control mechanism of the SON by these cells (Watanabe et al., 2006). However, an important point to be considered is that mice and rats show differences in the Na_x expression, implying that the mechanism involved in Na^+ detection in this nucleus may be specific to each rodent species. According to Nehmé et al. (2012), Na_x is more strongly expressed in rats than in mice. This evidence may explain, at least in part, why Na_x deficient mice present normal AVP secretion after dehydration (Nagakura et al., 2010). Therefore, neighboring cells, like astrocytes, may constitute active elements involved in response to hypertonic stimulation. However, little is known about how these cells drive these responses and whether they are necessary to trigger osmoregulation-related cell behavior.

HCN Channels and Its Interaction With Nitric Oxide

An important family of channels related to the electrophysiological properties of MNCs is the hyperpolarization-activated cyclic nucleotide-gated potassium channel (HCN) (Ghamari-Langroudi and Bourque, 2000; Pires da Silva et al., 2016). Four subtypes of HCN channels (HCN1-HCN4) have been identified, and all of them are expressed in MNCs, with HCN-3 and HCN-4 mRNAs having the highest expression levels (Monteggia et al., 2000; Notomi and Shigemoto, 2004; Pires da Silva et al., 2016). These channels are involved in basic neuronal properties in the SON, including regulation of the resting membrane potential and spontaneous firing rate (Pires da Silva et al., 2016), besides promoting excitatory drive, contributing to the phasic and tonic firing in these cells (Ghamari-Langroudi and Bourque, 2000). HCN channels are endogenously inhibited by NO, since the blockage of nNOS by L-NAME results in a significant increase in the macroscopic current (I_h) carried by these ion channels (Pires da Silva et al., 2016). In the same study, voltage-clamp experiments, performed in brain slices and *in situ* preparations, revealed that hypertonicity significantly increases the I_h current, which is directly correlated with increased release of neuropeptides. The effect of hypertonicity on HCN channels is also enhanced by L-NAME, indicating the existence of nitrergic inhibition even during hyperosmotic stress. Besides this, hypotonicity changed neither the instantaneous nor the steady-state I_h current, ruling out this pathway during this type of stimulation (Pires da Silva et al., 2016). Despite being upregulated at the mRNA level, indicating a possible increase in protein expression, in hypoglossal motoneurons, for example, the HCN channels are also functionally highly regulated by post-translational modification, such as S-nitrosylation (Wenker et al., 2012). The nitric oxide produced by the action of the enzyme nitric oxide synthase (NOS) was reported to be the main factor for S-nitrosylation in proteins (Jaffrey et al., 2001).

Interestingly, the transcriptome data show that the mRNA for the neuronal isoform of NOS (nNOS, coded by the gene *Nos1*) is the most upregulated enzyme in the SON after water deprivation (Pauža et al., 2021). This neuronal isoform is the most expressed type in the SON (Bhat et al., 1996), and it has been directly correlated with changes in plasma osmolality (Vincent and Kimura, 1992; Kadowaki et al., 1994; Ueta et al., 1995; Srisawat et al., 2004; Yamova et al., 2007). Following nNOS activation, L-arginine is oxidized, producing equimolar concentrations of NO and L-citrulline (Bush et al., 1992). This reaction occurs in the MNCs themselves (da Silva et al., 2013), and NO seems to act through autocrine, paracrine, and/or endocrine pathways (Calabrese et al., 2007; Bahadoran et al., 2020). Accumulated data show that the endogenously produced NO has an inhibitory role on MNCs (Liu et al., 1997; Ozaki et al., 2001; Stern and Ludwig, 2001; Ventura et al., 2008; da Silva et al., 2013; Reis et al., 2016). This inhibition can happen by two distinct routes: 1) by influencing synaptic plasticity, and 2) by directly modifying the function of a wide range of proteins, including those operating via ion channels.

Regarding synaptic plasticity, it was demonstrated that sodium nitroprusside (SNP, a donor of NO) increased the frequency of spontaneous inhibitory postsynaptic currents but did not affect the excitatory ones mediated by non-NMDA glutamate receptors (Ozaki et al., 2001). The same pattern of response was also demonstrated in measurements of $GABA_A$ miniature inhibitory postsynaptic currents, which reflect the activity of a

single synaptic site (Stern and Ludwig, 2001). Therefore, according to the authors, NO has an indirect paracrine effect on the activity of MNCs by potentiating GABAergic inputs. Although there is no doubt that NO potentiates GABAergic synaptic input, there are also findings of direct action of NO on the MNCs, independent of synaptic inputs. In this case, the HCNs, working as intrinsic peacemakers in various cell types, seem to be the NO target.

NO has considerable ability to interact with cysteine residues, forming nitrosothiol adducts. These interactions influence several cellular processes by altering the function of proteins via reversibly binding to thiol groups of cysteine residues (Hess et al., 2005). This association results in a more stable complex, S-nitrosothiol, which prolongs the biological activity of NO (Ahern, 2002). Pretreatment of brain slices of the SON with N-ethylmaleimide, a cysteine oxidant, prevents L-arginine's nitrergic inhibition of I_h currents. Additionally, denitrosylation induced by ascorbate resulted in a significant increase in I_h currents, revealing an endogenous nitrosylation of HCN channels and a cGMP independent signaling pathway of NO in MNCs in basal condition and during a hypertonic challenge (Pires da Silva et al., 2016). Thus, the inhibitory effects of NO on GABAergic inputs and HCN channels occur synergistically to control the MNCs' excitability, and consequently the release of neuropeptides. During short-term osmotic pressure perturbation, nitrergic inhibition is still present, indicating that NO works by self-regulating the neuroendocrine system to avoid neuronal hyperexcitability and neuronal cell death.

Based on the results described above, we can say that because nNOS activation depends on intracellular calcium, ΔN-TRPV1 (and potentially other channels of the TRPV family, such as TRPV2) would represent an important pathway for Ca^{2+} entry and NO synthesis during hyperosmotic perturbation. Additionally, since the activation of classical TRPV1 by NO-cysteine S-nitrosylation was also confirmed to occur in cysteine 553 and 558 (Yoshida et al., 2006), and ΔN-TRPV1 conserved these residues (Zaelzer et al., 2015), it is reasonable to assume that NO can also promote S-nitrosylation of ΔN-TRPV1 and other membrane channels and transporters controlling MNCs' excitability and hormone secretion. However, whether it acts only through HCN channels or involves other ion channels or intracellular signaling in MNCs is still unknown. For other aspects related to NO's effect on MNC activity, please see Ruginsk et al. (2015).

Transporters

Evidence about the participation of transporters in osmoregulation has also emerged from four publications (Hindmarch et al., 2006; Greenwood M. P. et al., 2015; Johnson et al., 2015; Pauža et al., 2021). After prolonged hypertonicity, five of the genes were identified that consistently increased mRNA for membrane transporters in the SON. 1) *Slc1a4*, coding the alanine/serine/cysteine/threonine transporter 1 (ASCT1); 2) *Slc7a3*, coding the cationic amino acid transporter 3 (CAT3), involved in the uptake of the amino acids ornithine, lysine and arginine in a sodium-independent manner; 3) *Slc20a1*, coding a sodium-dependent phosphate transporter 1 (PiT1); 4) *Slc25a25*, coding the mitochondrial phosphate carrier 3 (APC3); and 5) Slc41a2, coding a plasma membrane magnesium transporter (**Figure 2**). CAT3 is specifically present in neuronal cells (Hosokawa et al., 1999), while PiT1 is widely expressed in neurons, astrocytes and vascular endothelial cells (Inden et al., 2016). Finally, the mitochondrial phosphate carrier 3 is expressed in the inner mitochondrial membrane and works as a Ca^{2+}-regulated shuttle for Pi and ATP-Mg^{2+}, helping to control the mitochondrial metabolism (Anunciado-Koza et al., 2011).

The NKCC2, long known to be expressed in the apical membrane of the thick ascending limb of Henle's loop, was found to be the most intensively upregulated gene coding for transporters of the SLC superfamily after water deprivation in the SON (Pauža et al., 2021). This transporter belongs to the subfamily of cation-chloride electroneutral cotransporters that couple the movement of sodium, potassium and chloride across the plasma membrane. Under physiological conditions, they have small or no impact. However, when cells are subjected to hyperosmotic shrinkage, their participation seems fundamental to restoring homeostasis. In the case of MNCs, it was demonstrated that the gene *Slc12a1* encoding NKCC2 transporters is upregulated during an acute hypertonic stimulus (hours) as well as after prolonged water deprivation or salt loading (Konopacka et al., 2015b). The idea is that NKCC2, associated with NKCC1 (Haam et al., 2012), impairs $GABA_A$ receptor-mediated hyperpolarization by shifting the E_{GABA} in AVP neurons to a more positive value. Therefore, during AVP-$GABA_A$ receptor activation, robust membrane depolarization occurs, so an increase in the secretion of neuropeptides is expected. An integrative view assumes that AVP enhances the activity of NKCC2 expressed in the kidneys through V2-type receptors (Caceres et al., 2009). Therefore, during chronic osmotic challenges, AVP might contribute to increased NaCl reuptake, and in the last instance, aggravate the development of pathologies such as hypertension, edema, and others. However, this is only speculation based on limited evidence.

Another interesting gene enriched in AVP neurons and having increased expression in the SON following water deprivation is *Slc2a13,* coding the H (+)-myo-inositol symporter, which is fundamental for osmotic balance in the brain (Schneider, 2015). This gene was previously demonstrated to increase its expression after hypertonic stimulation in *C. elegans*. Additionally, mutant animals for this gene were hypersensitive to osmotic stress, indicating that this transporter is crucial for the osmoprotective response in *C. elegans* (Kage-Nakadai et al., 2011).

Except for NKCC1, NKCC2 and a few other membrane transporters, there is not much data available about the expression of these other transporters mentioned above or their possible role on MNCs' response to changes in osmolality. Further studies are necessary to discover their possible regulatory function on the MNC stimulus-synthesis-secretion response.

Somatodendritic Peptide Release and Osmoregulation

Osmotic challenges also trigger other vital functions in the SON, including the somatodendritic release of AVP and OXT.

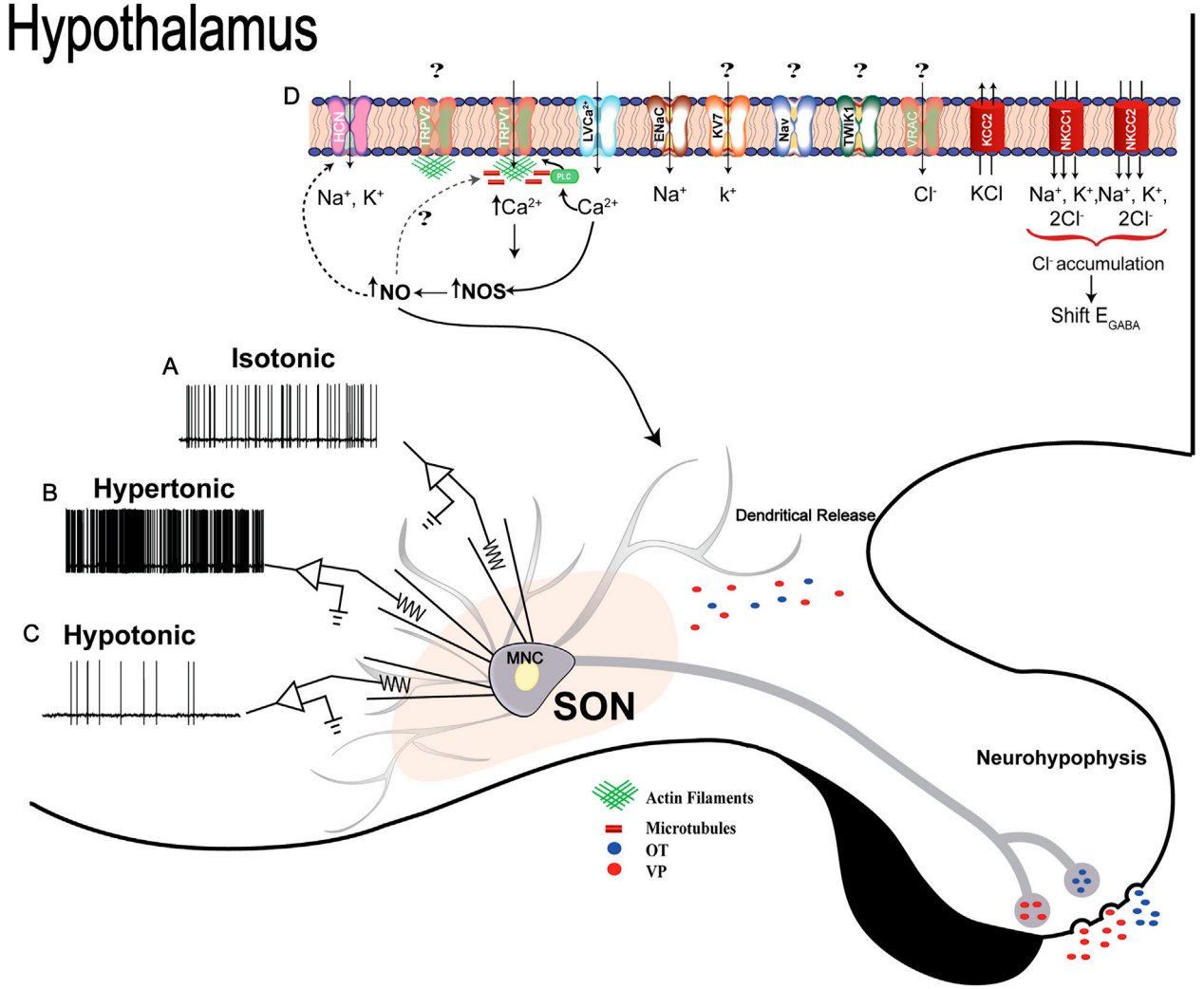

FIGURE 4 | Osmosensitivity of MNCs: **(A, B**, and **C)**, representative traces of intrinsic electrical responses of one MNC in isotonic, hypertonic or hypotonic conditions, respectively, measured using the whole-cell patch-clamp technique. The MNC increases its firing frequency in hypertonic challenges, while the opposite effect is observed during a hypotonic stimulation. The electrical activity of MNCs is directly correlated with neuropeptide secretion, so an increase in AVP and OTX secretion during hypertonicity and a decrease in hypotonicity are expected. Osmotic challenge also triggers AVP and OTX release as a self-regulatory mechanism (details described in the text). **(D)** Schematic representation of ion channels, transporters, and intracellular events recruited after osmotic challenges in MNCs. Although ΔN-TRPV1 has been described as the main molecular mechanism coupling hyperosmolality to electrical responses in the MNCs, Trpv2 was described as the main ion channel gene upregulated in the SON. However, there is no available evidence about the participation of TRPV2 in the MNCs' osmosensitivity. While microtubules and actin filaments are essential for ΔN-TRPV1 channel activation, TRPV2 seems to interact only with actin filaments. HCN channels, mainly type 3, are also involved in controlling MNCs' electrical properties in hypertonic conditions, and their conductance is modulated by nitric oxide in an S-nitrosylated-dependent mechanism. Sodium non-voltage dependent channels are also part of the mechanisms controlling the excitability of MNCs when the extracellular fluid homeostasis is disturbed by increases in extracellular Na^+. Potassium voltage-dependent channels (KV7/M-type), in turn, are activated to shape the firing pattern of the neurons during an osmotically evoked activity. Evidence about transporters' participation in osmoregulation has also emerged. NKCC1, NKCC2 and KCC2 are the principal elements involved. These transporters act in synchrony with several ion channels, particularly chloride (VRAC), to couple changes in osmolality and cell volume of MNCs to the electrical phenomena. Numerous ion channels and transporters also seem to be involved, but further studies are necessary to discover their possible regulatory function in the MNCs stimulus-synthesis-secretion response.

Although it has been known for 3 decades that neuropeptides are released within the SON (Mason et al., 1986), the variety of roles played by them is not entirely understood.

Initially, the intranuclear release of neuropeptides was described as a crucial self-regulatory mechanism of MNCs because the peptide released would act on their receptors to modulate the neuronal activity (Kombian et al., 1997; Gouzènes et al., 1998; Ludwig, 1998). Hypertonic challenge is a well-known condition that stimulates AVP and OXT secretion as a consequence of changes in the electrical activity of MNCs. However, what worked well for peripheral release did not apply to events occurring within the SON. The dynamics of the somatodendritic release of peptides are different from those of peripheral secretion. In this case, the release is delayed relative to

peripheral peptide secretion, and it occurs over a much longer time (Ludwig, 1998). This observation indicates that different regulatory mechanisms are recruited for each compartment. Under physiological conditions, the somatodendritic AVP secretion was shown to be dependent on the firing pattern, i.e., it was rarely observed in response to the continuous firing of action potentials but was intensified by clustered firing activity, a response significantly enhanced by the activation of NMDA receptors (Pitra et al., 2019). Additionally, Gillard et al. (2007) reported consistent evidence that during osmotic challenge, NO is also involved in the local AVP release. According to the authors, the NO produced during hyperosmotic stress indirectly sustains AVP release through a paracrine action, facilitating glutamate/aspartate release. The AVP released also acts back through V2 receptors, increasing the intracellular calcium concentration and potentiating the intranuclear AVP release during strong physiological demand.

The neuropeptides within the SON also mediate communication between neurons and vessels to control the blood flow. It is already known that, unlike in other cells, neurons do not have much reserve of energy, so they use the local vasculature to meet their metabolic demand (Attwell and Laughlin, 2001). Consequently, there is a strong relationship between neuronal activity and blood flow in the brain, a phenomenon called neurovascular coupling (Raichle and Mintun, 2006). In cortical areas, for instance, this phenomenon is well understood, and when cortical neurons increase their activity, the cerebral blood flow also does, to supply this region with the proper amounts of oxygen and glucose (Li et al., 2009). Although the SON is extensively vascularized, it was shown that the metabolic supply of MNCs is independent of its local vasculature, suggesting another function of the coupling in this region (Badaut et al., 2001). A contemporary study demonstrated that acute systemic salt-loading induces intranuclear VP release, which acts through a V1a type receptor to modulate the activity of parenchymal SON arterioles. This interaction results in vasoconstriction and reduced oxygen levels, creating a hypoxic microenvironment, which will promote increased excitability of vasopressin neurons. According to the authors, this works as a positive feedback signaling mechanism during osmotic challenge and characterizes it as an inverse neurovascular coupling in this nucleus (Roy et al., 2021).

Concerning the release of the somatodendritic peptide, the studies presented above shed new light on the possible mechanisms that promote the efficient but not exhaustive secretion of peptides during a challenging situation. So far, the take home message is that somatodendritic release of peptides is essential for the self-control mechanism. However, since the amount of neuropeptides released by dendrites is a hundred to thousand-fold greater than the basal concentration in plasma and cerebral spinal fluid, and their half-life is much longer in the brain (up to 20 min) than in the blood (Ludwig and Leng, 2006), an exciting point to consider is non-canonical roles are played by peptides released in the SON, but this is a subject for another review. Somatodendritic AVP and OXT released act pre- and post-synaptically for self-control of MNCs' excitability. But this is not their only purpose! They are also involved in the morphological plasticity of glial cells, synaptogenesis, and behavioral regulation, including memory, learning, and social recognition (Mens et al., 1983; Theodosis et al., 1986; Argiolas and Gessa, 1991; Engelmann et al., 1994, 1996; Ludwig and Leng, 2006).

CONCLUSION

Taken together, the information discussed in this review indicates that several players and mechanisms act in concert to determine the MNCs' biophysical properties necessary to couple changes in osmolality and cell volume to the electrical phenomena occurring in the plasma membrane (**Figure 4**). Depending on the timespan of the disturbance, a high degree of morphological and physiological plasticity is needed to sustain the stimulus-activity-secretion response. In other words, unlike short-term stimuli, chronic challenges are multi-dimensional, ranging from gene expression modulation to membrane electrophysiological responses. All changes occur to reconfigure the MNCs' activity necessary to sustain the release of neuropeptides in response to changing physiological demand. As discussed here, it seems that many questions still require further investigation, by combining state of art techniques ranging from molecules to whole organisms. New functional discoveries related to genes coding membrane channels and transporters that emerged from transcriptome studies in the SON might help in that respect.

AUTHOR CONTRIBUTIONS

All authors revised the literature, wrote the manuscript, organized the figures and revised the final version equally.

FUNDING

This work was supported by grants from Fundação de Amparo à Pesquisa do Estado de São Paulo to MPS (2018/07027-5, 2019/26034-5), ASM (2019/27581-0); Conselho Nacional de Desenvolvimento Científico e Tecnológico to ASM (309882/2020-6), and Coordenação de Aperfeiçoamento de Pessoal de Nível Superior- Brazil (CAPES, Finance code 001) to MPS and ASM.

REFERENCES

Ahern, G. (2002). cGMP and S-Nitrosylation: Two Routes for Modulation of Neuronal Excitability by NO. *Trends Neurosci.* 25, 510–517. doi:10.1016/S0166-2236(02)02254-3

Allen, W. E., DeNardo, L. A., Chen, M. Z., Liu, C. D., Loh, K. M., Fenno, L. E., et al. (2017). Thirst-associated Preoptic Neurons Encode an Aversive Motivational Drive. *Science* 80357, 1149–1155. doi:10.1126/science.aan6747

Amin, M. S., Wang, H.-W., Reza, E., Whitman, S. C., Tuana, B. S., and Leenen, F. H. H. (2005). Distribution of Epithelial Sodium Channels and Mineralocorticoid Receptors in Cardiovascular Regulatory Centers in Rat Brain. *Am. J. Physiology-*

Regulatory, Integr. Comp. Physiology 289, R1787–R1797. doi:10.1152/ajpregu.00063.2005

Anunciado-Koza, R. P., Zhang, J., Ukropec, J., Bajpeyi, S., Koza, R. A., Rogers, R. C., et al. (2011). Inactivation of the Mitochondrial Carrier SLC25A25 (ATP-Mg2+/Pi Transporter) Reduces Physical Endurance and Metabolic Efficiency in Mice. *J. Biol. Chem.* 286, 11659–11671. doi:10.1074/jbc.M110.203000

Argiolas, A., and Gessa, G. L. (1991). Central Functions of Oxytocin. *Neurosci. Biobehav. Rev.* 15, 217–231. doi:10.1016/S0149-7634(05)80002-8

Attwell, D., and Laughlin, S. B. (2001). An Energy Budget for Signaling in the Grey Matter of the Brain. *J. Cereb. Blood Flow. Metab.* 21, 1133–1145. doi:10.1097/00004647-200110000-00001

Badaut, J., Nehlig, A., Verbavatz, J.-M., Stoeckel, M.-E., Freund-Mercier, M.-J., and Lasbennes, F. (2001). Hypervascularization in the Magnocellular Nuclei of the Rat Hypothalamus: Relationship with the Distribution of Aquaporin-4 and Markers of Energy Metabolism. *J. Neuroendocrinol.* 12, 960–969. doi:10.1046/j.1365-2826.2000.00539.x

Bahadoran, Z., Carlström, M., Mirmiran, P., and Ghasemi, A. (2020). Nitric Oxide: To Be or Not to Be an Endocrine Hormone? *Acta Physiol.* 229. doi:10.1111/apha.13443

Balapattabi, K., Little, J. T., Bachelor, M. E., Cunningham, R. L., and Cunningham, J. T. (2020). Sex Differences in the Regulation of Vasopressin and Oxytocin Secretion in Bile Duct Ligated Rats. *Neuroendocrinology*. 111, 237–248. doi:10.1159/000508104

Bansal, V., and Fisher, T. E. (2017). Osmotic Activation of a Ca2+ -dependent Phospholipase C Pathway that Regulates ΔN TRPV1-Mediated Currents in Rat Supraoptic Neurons. *Physiol. Rep.* 5, e13259. doi:10.14814/phy2.13259

Barad, Z., Jacob-Tomas, S., Sobrero, A., Lean, G., Hicks, A.-I., Yang, J., et al. (2020). Unique Organization of Actin Cytoskeleton in Magnocellular Vasopressin Neurons in Normal Conditions and in Response to Salt-Loading. *eneuro* 7, 0351–19. doi:10.1523/ENEURO.0351-19.2020

Bennett, K. M., Liu, J., Hoelting, C., and Stoll, J. (2011). Expression and Analysis of Two Novel Rat Organic Cation Transporter Homologs, SLC22A17 and SLC22A23. *Mol. Cell. Biochem.* 352, 143–154. doi:10.1007/s11010-011-0748-y

Bhat, G., Mahesh, V. B., Aguan, K., and Brann, D. W. (1996). Evidence that Brain Nitric Oxide Synthase Is the Major Nitric Oxide Synthase Isoform in the Hypothalamus of the Adult Female Rat and that Nitric Oxide Potently Regulates Hypothalamic cGMP Levels. *Neuroendocrinology* 64, 93–102. doi:10.1159/000127104

Bize, I., Güvenç, B., Robb, A., Buchbinder, G., and Brugnara, C. (1999). Serine/threonine Protein Phosphatases and Regulation of K-Cl Cotransport in Human Erythrocytes. *Am. J. Physiology-Cell Physiology* 277, C926–C936. doi:10.1152/ajpcell.1999.277.5.C926

Black, J. A., Hoeijmakers, J. G., Faber, C. G., Merkies, I. S., and Waxman, S. G. (2013). Nav1.7: Stress-Induced Changes in Immunoreactivity within Magnocellular Neurosecretory Neurons of the Supraoptic Nucleus. *Mol. Pain* 9, 1744–8069. doi:10.1186/1744-8069-9-39

Black, J. A., Vasylyev, D., Dib-Hajj, S. D., and Waxman, S. G. (2014). Nav1.9 Expression in Magnocellular Neurosecretory Cells of Supraoptic Nucleus. *Exp. Neurol.* 253, 174–179. doi:10.1016/j.expneurol.2014.01.004

Blaesse, P., Airaksinen, M. S., Rivera, C., and Kaila, K. (2009). Cation-Chloride Cotransporters and Neuronal Function. *Neuron* 61, 820–838. doi:10.1016/j.neuron.2009.03.003

Bourque and, C. W., and Oliet, S. H. R. (1997). Osmoreceptors in the Central Nervous System. *Annu. Rev. Physiol.* 59, 601–619. doi:10.1146/annurev.physiol.59.1.601

Bourque, C. W. (1998). Osmoregulation of Vasopressin Neurons: a Synergy of Intrinsic and Synaptic Processes. *Prog. Brain Res.* 119, 59–76. doi:10.1016/s0079-6123(08)61562-9

Bourque, C. W. (2008). Central Mechanisms of Osmosensation and Systemic Osmoregulation. *Nat. Rev. Neurosci.* 9, 519–531. doi:10.1038/nrn2400

Bourque, C. W. (1989). Ionic Basis for the Intrinsic Activation of Rat Supraoptic Neurones by Hyperosmotic Stimuli. *J. Physiol.* 417, 263–277. doi:10.1113/jphysiol.1989.sp017800

Bourque, C. W., and Oliet, S. H. R. (2003). Osmoreceptors in the Central Nervous System. *Annu. Rev. Physiol.* 59, 601–619. doi:10.1146/ANNUREV.PHYSIOL.59.1.601

Brimble, M. J., and Dyball, R. E. J. (1977). Characterization of the Responses of Oxytocin- and Vasopressin-Secreting Neurones in the Supraoptic Nucleus to Osmotic Stimulation. *J. Physiol.* 271, 253–271. doi:10.1113/jphysiol.1977.sp011999

Bush, P. A., Gonzalez, N. E., Griscavage, J. M., and Ignarro, L. J. (1992). Nitric Oxide Synthase from Cerebellum Catalyzes the Formation of Equimolar Quantities of Nitric Oxide and Citrulline from L-Arginine. *Biochem. Biophysical Res. Commun.* 185, 960–966. doi:10.1016/0006-291X(92)91720-B

Busnardo, C., Crestani, C. C., Resstel, L. B. M., Tavares, R. F., Antunes-Rodrigues, J., and Corrêa, F. M. A. (2012). Ionotropic Glutamate Receptors in Hypothalamic Paraventricular and Supraoptic Nuclei Mediate Vasopressin and Oxytocin Release in Unanesthetized Rats. *Endocrinology* 153, 2323–2331. doi:10.1210/en.2011-2079

Busnardo, C., Fassini, A., Rodrigues, B., Antunes-Rodrigues, J., Crestani, C. C., and Corrêa, F. M. A. (2021). N-Methyl-D-aspartate Glutamate Receptor Modulates Cardiovascular and Neuroendocrine Responses Evoked by Hemorrhagic Shock in Rats. *BioMed Res. Int.* 2021, 1–11. doi:10.1155/2021/1156031

Caceres, P. S., Ares, G. R., and Ortiz, P. A. (2009). cAMP Stimulates Apical Exocytosis of the Renal Na+-K+-2Cl− Cotransporter NKCC2 in the Thick Ascending Limb. *J. Biol. Chem.* 284, 24965–24971. doi:10.1074/jbc.M109.037135

Calabrese, V., Mancuso, C., Calvani, M., Rizzarelli, E., Butterfield, D. A., and Giuffrida Stella, A. M. (2007). Nitric Oxide in the Central Nervous System: Neuroprotection versus Neurotoxicity. *Nat. Rev. Neurosci.* 8, 766–775. doi:10.1038/nrn2214

Caterina, M. J., Schumacher, M. A., Tominaga, M., Rosen, T. A., Levine, J. D., and Julius, D. (1997). The Capsaicin Receptor: a Heat-Activated Ion Channel in the Pain Pathway. *Nature* 389, 816–824. doi:10.1038/39807

Chew, T. A., Orlando, B. J., Zhang, J., Latorraca, N. R., Wang, A., Hollingsworth, S. A., et al. (2019). Structure and Mechanism of the Cation-Chloride Cotransporter NKCC1. *Nature* 572, 488–492. doi:10.1038/s41586-019-1438-2

Choe, K. Y., Olson, J. E., and Bourque, C. W. (2012). Taurine Release by Astrocytes Modulates Osmosensitive Glycine Receptor Tone and Excitability in the Adult Supraoptic Nucleus. *J. Neurosci.* 32, 12518–12527. doi:10.1523/JNEUROSCI.1380-12.2012

Choe, K. Y., Prager-Khoutorsky, M., Farmer, W. T., Murai, K. K., and Bourque, C. W. (2016). Effects of Salt Loading on the Morphology of Astrocytes in the Ventral Glia Limitans of the Rat Supraoptic Nucleus. *J. Neuroendocrinol.* 28. doi:10.1111/jne.12370

Ciura, S., Liedtke, W., and Bourque, C. W. (2011). Hypertonicity Sensing in Organum Vasculosum Lamina Terminalis Neurons: A Mechanical Process Involving TRPV1 but Not TRPV4. *J. Neurosci.* 31, 14669–14676. doi:10.1523/JNEUROSCI.1420-11.2011

Ciura, S. (2006). Transient Receptor Potential Vanilloid 1 Is Required for Intrinsic Osmoreception in Organum Vasculosum Lamina Terminalis Neurons and for Normal Thirst Responses to Systemic Hyperosmolality. *J. Neurosci.* 26, 9069–9075. doi:10.1523/JNEUROSCI.0877-06.2006

Colbert, H. A., Smith, T. L., and Bargmann, C. I. (1997). OSM-9, A Novel Protein with Structural Similarity to Channels, Is Required for Olfaction, Mechanosensation, and Olfactory Adaptation inCaenorhabditis Elegans. *J. Neurosci.* 17, 8259–8269. doi:10.1523/JNEUROSCI.17-21-08259.1997

da Silva, M. P., Merino, R. M., Mecawi, A. S., Moraes, D. J., and Varanda, W. A. (2015). *In Vitro* differentiation between Oxytocin- and Vasopressin-Secreting Magnocellular Neurons Requires More Than One Experimental Criterion. *Mol. Cell. Endocrinol.* 400, 102–111. doi:10.1016/j.mce.2014.11.004

da Silva, M. P., Ventura, R. R., and Varanda, W. A. (2013). Hypertonicity Increases NO Production to Modulate the Firing Rate of Magnocellular Neurons of the Supraoptic Nucleus of Rats. *Neuroscience* 250, 70–79. doi:10.1016/j.neuroscience.2013.06.067

de Souza Mecawi, A., Ruginsk, S. G., Elias, L. L. K., Varanda, W. A., and Antunes-Rodrigues, J. (2015). "Neuroendocrine Regulation of Hydromineral Homeostasis," in *Comprehensive Physiology* (Wiley), 1465–1516. doi:10.1002/cphy.c140031

Decavel, C., and Hatton, G. I. (1995). Taurine Immunoreactivity in the Rat Supraoptic Nucleus: Prominent Localization in Glial Cells. *J. Comp. Neurol.* 354, 13–26. doi:10.1002/cne.903540103

Delpire, E., and Gagnon, K. B. (2018). Water Homeostasis and Cell Volume Maintenance and Regulation. *Curr. Top. Membr.* 81, 3–52. doi:10.1016/bs.ctm.2018.08.001

Doroshenko, P., and Neher, E. (1992). Volume-sensitive Chloride Conductance in Bovine Chromaffin Cell Membrane. *J. Physiol.* 449, 197–218. doi:10.1113/JPHYSIOL.1992.SP019082

Dos-Santos, R. C., Reis, L. C., Perello, M., Ferguson, A. V., and Mecawi, A. S. (2019). The Actions of Ghrelin in the Paraventricular Nucleus: Energy Balance and Neuroendocrine Implications. *Ann. N.Y. Acad. Sci.* 1455, 81–97. doi:10.1111/nyas.14087

Dos-Santos, R. C., Vilhena-Franco, T., Reis, L. C., Elias, L. L. K., Antunes-Rodrigues, J., and Mecawi, A. S. (2022). AMPA and Angiotensin Type 1 Receptors Are Necessary for Hemorrhage-Induced Vasopressin Secretion. *Braz J. Med. Biol. Res.* 55. doi:10.1590/1414-431x2021e11635

Duan, L., Yuan, H., Su, C.-J., Liu, Y.-Y., and Rao, Z.-R. (2004). Ultrastructure of Junction Areas between Neurons and Astrocytes in Rat Supraoptic Nuclei. *Wjg* 10, 117. doi:10.3748/wjg.v10.i1.117

Egan, G., Silk, T., Zamarripa, F., Williams, J., Federico, P., Cunnington, R., et al. (2003). Neural Correlates of the Emergence of Consciousness of Thirst. *Proc. Natl. Acad. Sci. U.S.A.* 100, 15241–15246. doi:10.1073/pnas.2136650100

Elinder, F., and Arhem, P. (1994). Effects of Gadolinium on Ion Channels in the Myelinated Axon of *Xenopus laevis*: Four Sites of Action. *Biophysical J.* 67, 71–83. doi:10.1016/S0006-3495(94)80456-4

Engelmann, M., Ludwig, M., and Landgraf, R. (1994). Simultaneous Monitoring of Intracerebral Release and Behavior: Endogenous Vasopressin Improves Social Recognition. *J. Neuroendocrinol.* 6, 391–395. doi:10.1111/j.1365-2826.1994.tb00598.x

Engelmann, M., Wotjak, C. T., Neumann, I., Ludwig, M., and Landgraf, R. (1996). Behavioral Consequences of Intracerebral Vasopressin and Oxytocin: Focus on Learning and Memory **This Paper Is Dedicated to Our Friend and Scientific Teacher Prof. Dr Armin Ermisch (1935-1995). *Neurosci. Biobehav. Rev.* 20, 341–358. doi:10.1016/0149-7634(95)00059-3

Fenelon, V. S., and Herbison, A. E. (1995). Characterisation of GABAA Receptor Gamma Subunit Expression by Magnocellular Neurones in Rat Hypothalamus. *Mol. Brain Res.* 34, 45–56. doi:10.1016/0169-328X(95)00130-K

Ferreira-Neto, H. C., Antunes, V. R., and Stern, J. E. (2021). Purinergic P2 and Glutamate NMDA Receptor Coupling Contributes to Osmotically Driven Excitability in Hypothalamic Magnocellular Neurosecretory Neurons. *J. Physiol.* 599, 3531–3547. doi:10.1113/JP281411

Finkelstein, A., and Cass, A. (1967). Effect of Cholesterol on the Water Permeability of Thin Lipid Membranes. *Nature* 216, 717–718. doi:10.1038/216717a0

Finkelstein, A. (1976). Water and Nonelectrolyte Permeability of Lipid Bilayer Membranes. *J. Gen. Physiol.* 68, 127–135. doi:10.1085/jgp.68.2.127

Fushimi, K., Uchida, S., Harat, Y., Hirata, Y., Marumo, F., and Sasaki, S. (1993). Cloning and Expression of Apical Membrane Water Channel of Rat Kidney Collecting Tubule. *Nature* 361, 549–552. doi:10.1038/361549a0

Garty, H., and Palmer, L. G. (1997). Epithelial Sodium Channels: Function, Structure, and Regulation. *Physiol. Rev.* 77, 359–396. doi:10.1152/physrev.1997.77.2.359

Ghamari-Langroudi, M., and Bourque, C. W. (2000). Excitatory Role of the Hyperpolarization-Activated Inward Current in Phasic and Tonic Firing of Rat Supraoptic Neurons. *J. Neurosci.* 20, 4855–4863. doi:10.1523/jneurosci.20-13-04855.2000

Gillard, E. R., Coburn, C. G., de Leon, A., Snissarenko, E. P., Bauce, L. G., Pittman, Q. J., et al. (2007). Vasopressin Autoreceptors and Nitric Oxide-dependent Glutamate Release Are Required for Somatodendritic Vasopressin Release from Rat Magnocellular Neuroendocrine Cells Responding to Osmotic Stimuli. *Endocrinology* 148, 479–489. doi:10.1210/en.2006-0995

Goswami, C., Dreger, M., Jahnel, R., Bogen, O., Gillen, C., and Hucho, F. (2004). Identification and Characterization of a Ca2+-Sensitive Interaction of the Vanilloid Receptor TRPV1 with Tubulin. *J. Neurochem.* 91, 1092–1103. doi:10.1111/j.1471-4159.2004.02795.x

Goswami, C., Hucho, T. B., and Hucho, F. (2007). Identification and Characterisation of Novel Tubulin-Binding Motifs Located within the C-Terminus of TRPV1. *J. Neurochem.* 101, 250–262. doi:10.1111/j.1471-4159.2006.04338.x

Gouzènes, L., Desarménien, M. G., Hussy, N., Richard, P., and Moos, F. C. (1998). Vasopressin Regularizes the Phasic Firing Pattern of Rat Hypothalamic Magnocellular Vasopressin Neurons. *J. Neurosci.* 18, 1879–1885. doi:10.1523/JNEUROSCI.18-05-01879.1998

Greenwood, M., Greenwood, M. P., Mecawi, A. S., Loh, S. Y., Rodrigues, J. A., Paton, J. F. R., et al. (2015). Transcription Factor CREB3L1 Mediates cAMP and Glucocorticoid Regulation of Arginine Vasopressin Gene Transcription in the Rat Hypothalamus. *Mol. Brain* 8, 68. doi:10.1186/s13041-015-0159-1

Greenwood, M. P., Greenwood, M., Mecawi, A. S., Antunes-Rodrigues, J., Paton, J. F. R., and Murphy, D. (2016). Rasd1, a Small G Protein with a Big Role in the Hypothalamic Response to Neuronal Activation. *Mol. Brain* 9, 1. doi:10.1186/s13041-015-0182-2

Greenwood, M. P., Mecawi, A. S., Hoe, S. Z., Mustafa, M. R., Johnson, K. R., Al-Mahmoud, G. A., et al. (2015). A Comparison of Physiological and Transcriptome Responses to Water Deprivation and Salt Loading in the Rat Supraoptic Nucleus. *Am. J. Physiology-Regulatory, Integr. Comp. Physiology* 308, R559–R568. doi:10.1152/ajpregu.00444.2014

Grinstein, S., Clarke, C. A., Dupre, A., and Rothstein, A. (1982). Volume-induced Increase of Anion Permeability in Human Lymphocytes. *J. Gen. Physiol.* 80, 801–823. doi:10.1085/jgp.80.6.801

Grinstein, S., and Rothstein, A. (1986). Mechanisms of Regulation of the Na+/H+ Exchanger. *J. Membrain Biol.* 90, 1–12. doi:10.1007/BF01869680

Gross, C. G. (1998). Claude Bernard and the Constancy of the Internal Environment. *Neuroscientist* 4, 380–385. doi:10.1177/107385849800400520

Haam, J., Popescu, I. R., Morton, L. A., Halmos, K. C., Teruyama, R., Ueta, Y., et al. (2012). GABA Is Excitatory in Adult Vasopressinergic Neuroendocrine Cells. *J. Neurosci.* 32, 572–582. doi:10.1523/JNEUROSCI.3826-11.2012

Han, J., Gnatenco, C., Sladek, C. D., and Kim, D. (2003). Background and Tandem-pore Potassium Channels in Magnocellular Neurosecretory Cells of the Rat Supraoptic Nucleus. *J. Physiology* 546, 625–639. doi:10.1113/jphysiol.2002.032094

Hatton, G. I., and Walters, J. K. (1973). Induced Multiple Nucleoli, Nucleolar Margination, and Cell Size Changes in Supraoptic Neurons during Dehydration and Rehydration in the Rat. *Brain Res.* 59, 137–154. doi:10.1016/0006-8993(73)90256-4

Hazama, A., and Okada, Y. (1988). Ca2+ Sensitivity of Volume-Regulatory K+ and Cl- Channels in Cultured Human Epithelial Cells. *J. Physiol.* 402, 687–702. doi:10.1113/JPHYSIOL.1988.SP017229

Hess, D. T., Matsumoto, A., Kim, S.-O., Marshall, H. E., and Stamler, J. S. (2005). Protein S-Nitrosylation: Purview and Parameters. *Nat. Rev. Mol. Cell Biol.* 6, 150–166. doi:10.1038/nrm1569

Hicks, A. I., Barad, Z., Sobrero, A., Lean, G., Jacob-Tomas, S., Yang, J., et al. (2020). Effects of Salt Loading on the Organisation of Microtubules in Rat Magnocellular Vasopressin Neurones. *J. Neuroendocrinol.* 32. doi:10.1111/jne.12817

Hill, W. G., and Zeidel, M. L. (2000). Reconstituting the Barrier Properties of a Water-Tight Epithelial Membrane by Design of Leaflet-specific Liposomes. *J. Biol. Chem.* 275, 30176–30185. doi:10.1074/jbc.M003494200

Hindmarch, C., Yao, S., Beighton, G., Paton, J., and Murphy, D. (2006). A Comprehensive Description of the Transcriptome of the Hypothalamoneurohypophyseal System in Euhydrated and Dehydrated Rats. *Proc. Natl. Acad. Sci. U.S.A.* 103, 1609–1614. doi:10.1073/pnas.0507450103

Hiyama, T. Y., and Noda, M. (2016). Sodium Sensing in the Subfornical Organ and Body-Fluid Homeostasis. *Neurosci. Res.* 113, 1–11. doi:10.1016/j.neures.2016.07.007

Hongo, K., Pascarel, C., Cazorla, O., Gannier, F., Le Guennec, J., and White, E. (1997). Gadolinium Blocks the Delayed Rectifier Potassium Current in Isolated guinea-pig Ventricular Myocytes. *Exp. Physiol.* 82, 647–656. doi:10.1113/expphysiol.1997.sp004053

Hosokawa, H., Ninomiya, H., Sawamura, T., Sugimoto, Y., Ichikawa, A., Fujiwara, K., et al. (1999). Neuron-specific Expression of Cationic Amino Acid Transporter 3 in the Adult Rat Brain. *Brain Res.* 838, 158–165. doi:10.1016/S0006-8993(99)01686-8

Hughes, A. L. H., Pakhomova, A., and Brown, P. D. (2010). Regulatory Volume Increase in Epithelial Cells Isolated from the Mouse Fourth Ventricle Choroid Plexus Involves Na+-H+ Exchange but Not Na+-K+-2Cl− Cotransport. *Brain Res.* 1323, 1–10. doi:10.1016/j.brainres.2009.12.094

Humphreys, B. D., Jiang, L., Chernova, M. N., and Alper, S. L. (1995). Hypertonic Activation of AE2 Anion Exchanger in Xenopus Oocytes via NHE-Mediated Intracellular Alkalinization. *Am. J. Physiology-Cell Physiology* 268, C201–C209. doi:10.1152/ajpcell.1995.268.1.C201

Iadecola, C. (2007). Astrocytes Take Center Stage in Salt Sensing. *Neuron* 54, 3–5. doi:10.1016/j.neuron.2007.03.013

Inden, M., Iriyama, M., Zennami, M., Sekine, S.-i., Hara, A., Yamada, M., et al. (2016). The Type III Transporters (PiT-1 and PiT-2) Are the Major Sodium-dependent Phosphate Transporters in the Mice and Human Brains. *Brain Res.* 1637, 128–136. doi:10.1016/j.brainres.2016.02.032

Ingber, D. E. (1997). Tensegrity: the Architectural Basis of Cellular Mechanotransduction. *Annu. Rev. Physiol.* 59, 575–599. doi:10.1146/annurev.physiol.59.1.575

Jaberi, S. A., Cohen, A., D'Souza, C., Abdulrazzaq, Y. M., Ojha, S., Bastaki, S., et al. (2021). Lipocalin-2: Structure, Function, Distribution and Role in Metabolic Disorders. *Biomed. Pharmacother.* 142, 112002. doi:10.1016/j.biopha.2021.112002

Jaffrey, S. R., Erdjument-Bromage, H., Ferris, C. D., Tempst, P., and Snyder, S. H. (2001). Protein S-Nitrosylation: a Physiological Signal for Neuronal Nitric Oxide. *Nat. Cell Biol.* 3, 193–197. doi:10.1038/35055104

Jemal, I., Soriano, S., Conte, A. L., Morenilla, C., and Gomis, A. (2014). G Protein-Coupled Receptor Signalling Potentiates the Osmo-Mechanical Activation of TRPC5 Channels. *Pflugers Arch. - Eur. J. Physiol.* 466, 1635–1646. doi:10.1007/s00424-013-1392-z

Jentsch, T. J. (2002). Chloride Channels Are Different. *Nature* 415, 276–277. doi:10.1038/415276a

Jeon, J., Bu, F., Sun, G., Tian, J.-B., Ting, S.-M., Li, J., et al. (2021). Contribution of TRPC Channels in Neuronal Excitotoxicity Associated with Neurodegenerative Disease and Ischemic Stroke. *Front. Cell Dev. Biol.* 8. doi:10.3389/fcell.2020.618663

Jewell, P. A., and Verney, E. B. (1957). An Experimental Attempt to Determine the Site of the Neurohypophysial and Osmoreceptors in the Dog. *Phil. Trans. R. Soc. Lond. B* 240, 197–324. doi:10.1098/rstb.1957.0002

Johnson, A. K., and Gross, P. M. (1993). Sensory Circumventricular Organs and Brain Homeostatic Pathways. *FASEB J.* 7, 678–686. doi:10.1096/FASEBJ.7.8.8500693

Johnson, J. M., Castle, J., Garrett-Engele, P., Kan, Z., Loerch, P. M., Armour, C. D., et al. (2003). Genome-Wide Survey of Human Alternative Pre-mRNA Splicing with Exon Junction Microarrays. *Science* 302, 2141–2144. doi:10.1126/science.1090100

Johnson, K. R., Hindmarch, C. C. T., Salinas, Y. D., Shi, Y., Greenwood, M., Hoe, S. Z., et al. (2015). Correction: A RNA-Seq Analysis of the Rat Supraoptic Nucleus Transcriptome: Effects of Salt Loading on Gene Expression. *PLoS One* 10, e0131892. doi:10.1371/journal.pone.0131892

Kadowaki, K., Kishimoto, J., Leng, G., and Emson, P. C. (1994). Up-regulation of Nitric Oxide Synthase (NOS) Gene Expression Together with NOS Activity in the Rat Hypothalamo-Hypophysial System after Chronic Salt Loading: Evidence of a Neuromodulatory Role of Nitric Oxide in Arginine Vasopressin and Oxytocin Secretion. *Endocrinology* 134, 1011–1017. doi:10.1210/endo.134.3.7509733

Kage-Nakadai, E., Uehara, T., and Mitani, S. (2011). H+/myo-inositol Transporter Genes, hmit-1.1 and hmit-1.2, Have Roles in the Osmoprotective Response in *Caenorhabditis elegans*. *Biochem. Biophysical Res. Commun.* 410, 471–477. doi:10.1016/j.bbrc.2011.06.001

Kombian, S. B., Mouginot, D., and Pittman, Q. J. (1997). Dendritically Released Peptides Act as Retrograde Modulators of Afferent Excitation in the Supraoptic Nucleus *In Vitro*. *Neuron* 19, 903–912. doi:10.1016/S0896-6273(00)80971-X

König, B., and Stauber, T. (2019). Biophysics and Structure-Function Relationships of LRRC8-Formed Volume-Regulated Anion Channels. *Biophysical J.* 116, 1185–1193. doi:10.1016/J.BPJ.2019.02.014

Konopacka, A., Greenwood, M., Loh, S.-Y., Paton, J., and Murphy, D. (2015a). RNA Binding Protein Caprin-2 Is a Pivotal Regulator of the Central Osmotic Defense Response. *Elife* 4. doi:10.7554/eLife.09656

Konopacka, A., Qiu, J., Yao, S. T., Greenwood, M. P., Greenwood, M., Lancaster, T., et al. (2015b). Osmoregulation Requires Brain Expression of the Renal Na-K-2Cl Cotransporter NKCC2. *J. Neurosci.* 35, 5144–5155. doi:10.1523/JNEUROSCI.4121-14.2015

Krimm, S. (1980). The Hydrophobic Effect: Formation of Micelles and Biological Membranes, Charles Tanford, Wiley-Interscience, New York, 1980, 233 Pp. Price: $18.50. *J. Polym. Sci. B Polym. Lett. Ed.* 18, 687. doi:10.1002/pol.1980.130181008

Kwon, O., Yang, H., Kim, S.-C., Kim, J., Sim, J., Lee, J., et al. (2021). TWIK-1 BAC-GFP Transgenic Mice, an Animal Model for TWIK-1 Expression. *Cells* 10, 2751. doi:10.3390/cells10102751

Leaf, A. (1959). Maintenance of Concentration Gradients and Regulation of Cell Volume. *Ann. N. Y. Acad. Sci.* 72, 396–404. doi:10.1111/j.1749-6632.1959.tb44168.x

Lee, E. C., Kim, H., Ditano, J., Manion, D., King, B. L., and Strange, K. (2016). Abnormal Osmotic Avoidance Behavior in *C. elegans* Is Associated with Increased Hypertonic Stress Resistance and Improved Proteostasis. *PLoS One* 11, e0154156. doi:10.1371/journal.pone.0154156

Li, N., Jia, X., Murari, K., Parlapalli, R., Rege, A., and Thakor, N. V. (2009). High Spatiotemporal Resolution Imaging of the Neurovascular Response to Electrical Stimulation of Rat Peripheral Trigeminal Nerve as Revealed by *In Vivo* Temporal Laser Speckle Contrast. *J. Neurosci. Methods* 176, 230–236. doi:10.1016/j.jneumeth.2008.07.013

Li, Y., Zhou, X., and Sun, S. X. (2021). Hydrogen, Bicarbonate, and Their Associated Exchangers in Cell Volume Regulation. *Front. Cell Dev. Biol.* 9. doi:10.3389/fcell.2021.683686

Liedtke, W., Choe, Y., Martí-Renom, M. A., Bell, A. M., Denis, C. S., Sali, A., et al. (2005). Vanilloid Receptor-Related Osmotically Activated Channel (VR-OAC), A Candidate Vertebrate Osmoreceptor. *Cell* 103, 525–35. doi:10.1016/s0092-8674(00)00143-4

Liedtke, W., and Kim, C. (2005). Functionality of the TRPV Subfamily of TRP Ion Channels: Add Mechano-TRP and Osmo-TRP to the Lexicon!. *Cell. Mol. Life Sci.* 62, 2985–3001. doi:10.1007/s00018-005-5181-5

Liu, Q.-S., Jia, Y.-S., and Ju, G. (1997). Nitric Oxide Inhibits Neuronal Activity in the Supraoptic Nucleus of the Rat Hypothalamic Slices. *Brain Res. Bull.* 43, 121–125. doi:10.1016/s0361-9230(96)00209-2

Ludwig, M. (1998). Dendritic Release of Vasopressin and Oxytocin. *J. Neuroendocrinol.* 10, 881–895. doi:10.1046/j.1365-2826.1998.00279.x

Ludwig, M., Johnstone, L. E., Neumann, I., Landgraf, R., and Russell, J. A. (1996). Direct Hypertonic Stimulation of the Rat Supraoptic Nucleus Increases C-Fos Expressionin Glial Cells rather Than Magnocellular Neurones. *Cell Tissue Res.* 287, 79–90. doi:10.1007/s004410050733

Ludwig, M., and Leng, G. (2006). Dendritic Peptide Release and Peptide-dependent Behaviours. *Nat. Rev. Neurosci.* 7, 126–136. doi:10.1038/nrn1845

Mason, W. T., Hatton, G. I., Ho, Y. W., Chapman, C., and Robinson, I. C. F. (1986). Central Release of Oxytocin, Vasopressin and Neurophysin by Magnocellular Neurone Depolarization: Evidence in Slices of Guinea Pig and Rat Hypothalamus. *Neuroendocrinology* 42, 311–322. doi:10.1159/000124457

Matsuda, T., Hiyama, T. Y., Niimura, F., Matsusaka, T., Fukamizu, A., Kobayashi, K., et al. (2017). Distinct Neural Mechanisms for the Control of Thirst and Salt Appetite in the Subfornical Organ. *Nat. Neurosci.* 20, 230–241. doi:10.1038/nn.4463

McKinley, M. J., Denton, D. A., and Weisinger, R. S. (1978). Sensors for Antidiuresis and Thirst-Osmoreceptors or CSF Sodium Detectors? *Brain Res.* 141, 89–103. doi:10.1016/0006-8993(78)90619-4

Mens, W. B. J., Witter, A., and Van Wimersma Greidanus, T. B. (1983). Penetration of Neurohypophyseal Hormones from Plasma into Cerebrospinal Fluid (CSF): Half-Times of Disappearance of These Neuropeptides from CSF. *Brain Res.* 262, 143–149. doi:10.1016/0006-8993(83)90478-X

Model, M. A., Hollembeak, J. E., and Kurokawa, M. (2021). Macromolecular Crowding: a Hidden Link between Cell Volume and Everything Else. *Cell Physiol. Biochem.* 55, 25–40. doi:10.33594/000000319

Monteggia, L. M., Eisch, A. J., Tang, M. D., Kaczmarek, L. K., and Nestler, E. J. (2000). Cloning and Localization of the Hyperpolarization-Activated Cyclic Nucleotide-Gated Channel Family in Rat Brain. *Mol. Brain Res.* 81, 129–139. doi:10.1016/S0169-328X(00)00155-8

Moriya, T., Shibasaki, R., Kayano, T., Takebuchi, N., Ichimura, M., Kitamura, N., et al. (2015). Full-length Transient Receptor Potential Vanilloid 1 Channels Mediate Calcium Signals and Possibly Contribute to Osmoreception in Vasopressin Neurones in the Rat Supraoptic Nucleus. *Cell Calcium* 57, 25–37. doi:10.1016/j.ceca.2014.11.003

Mortensen, L. S., Schmidt, H., Farsi, Z., Barrantes-Freer, A., Rubio, M. E., Ufartes, R., et al. (2015). K V 10.1 Opposes Activity-dependent Increase in Ca 2+ Influx into the Presynaptic Terminal of the Parallel Fibre-Purkinje Cell Synapse. *J. Physiol.* 593, 181–196. doi:10.1113/jphysiol.2014.281600

Mosialou, I., Shikhel, S., Liu, J.-M., Maurizi, A., Luo, N., He, Z., et al. (2017). MC4R-dependent Suppression of Appetite by Bone-Derived Lipocalin 2. *Nature* 543, 385–390. doi:10.1038/nature21697

Muraki, K., Iwata, Y., Katanosaka, Y., Ito, T., Ohya, S., Shigekawa, M., et al. (2003). TRPV2 Is a Component of Osmotically Sensitive Cation Channels in Murine Aortic Myocytes. *Circulation Res.* 93, 829–838. doi:10.1161/01.RES.0000097263.10220.0C

Naeini, R. S., Witty, M.-F., Séguéla, P., Bourque, C. W., Naeini, R. S., Witty, M.-F., et al. (2006). An N-Terminal Variant of Trpv1 Channel Is Required for Osmosensory Transduction. *Nat. Neurosci.* 9, 93–98. doi:10.1038/nn1614

Nagakura, A., Hiyama, T. Y., and Noda, M. (2010). Nax-deficient Mice Show Normal Vasopressin Response to Dehydration. *Neurosci. Lett.* 472, 161–165. doi:10.1016/j.neulet.2010.01.077

Nedungadi, T. P., Carreño, F. R., Walch, J. D., Bathina, C. S., and Cunningham, J. T. (2012a). Region-Specific Changes in Transient Receptor Potential Vanilloid Channel Expression in the Vasopressin Magnocellular System in Hepatic Cirrhosis-Induced Hyponatraemia. *J. Neuroendocrinol.* 24, 642–652. doi:10.1111/j.1365-2826.2011.02273.x

Nedungadi, T. P., and Cunningham, J. T. (2014). Differential Regulation of TRPC4 in the Vasopressin Magnocellular System by Water Deprivation and Hepatic Cirrhosis in the Rat. *Am. J. Physiology-Regulatory, Integr. Comp. Physiology* 306, R304–R314. doi:10.1152/ajpregu.00388.2013

Nedungadi, T. P., Dutta, M., Bathina, C. S., Caterina, M. J., and Cunningham, J. T. (2012b). Expression and Distribution of TRPV2 in Rat Brain. *Exp. Neurol.* 237, 223–237. doi:10.1016/j.expneurol.2012.06.017

Nilius, B., Oike, M., Zahradnik, I., and Droogmans, G. (1994). Activation of a Cl-Current by Hypotonic Volume Increase in Human Endothelial Cells. *J. Gen. Physiol.* 103, 787–805. doi:10.1085/jgp.103.5.787

Nissen, R., Hu, B., and Renaud, L. P. (1995). Regulation of Spontaneous Phasic Firing of Rat Supraoptic Vasopressin Neurones *In Vivo* by Glutamate Receptors. *J. Physiol.* 484, 415–424. doi:10.1113/jphysiol.1995.sp020674

Nehmé, B., Henry, M., Mouginot, O., and Drolet, G. (2012). The Expression Pattern of the Na+ Sensor, NaX in the Hydromineral Homeostatic Network: A Comparative Study between the Rat and Mouse. *Front. Neuroanat.* 6. doi:10.3389/fnana.2012.00026

Notomi, T., and Shigemoto, R. (2004). Immunohistochemical Localization of Ih Channel Subunits, HCN1-4, in the Rat Brain. *J. Comp. Neurol.* 471, 241–276. doi:10.1002/cne.11039

Offord, J., and Catterall, W. A. (1989). Electrical Activity, cAMP, and Cytosolic Calcium Regulate mRNA Encoding Sodium Channel α Subunits in Rat Muscle Cells. *Neuron* 2, 1447–1452. doi:10.1016/0896-6273(89)90190-6

Okada, Y., Numata, T., Sato-Numata, K., Sabirov, R. Z., Liu, H., Mori, S.-i., et al. (2019). Roles of Volume-Regulatory Anion Channels, VSOR and Maxi-Cl, in Apoptosis, Cisplatin Resistance, Necrosis, Ischemic Cell Death, Stroke and Myocardial Infarction. *Curr. Top. Membr.* 83, 205–283. doi:10.1016/BS.CTM.2019.03.001

Oliet, S. H., and Bourque, C. W. (1992). Properties of Supraoptic Magnocellular Neurones Isolated from the Adult Rat. *J. Physiol.* 455, 291–306. doi:10.1113/jphysiol.1992.sp019302

Oliet, S. H. R., and Bourque, C. (1993). Mechanosensitive Channels Transduce Osmosensitivity in Supraoptic Neurons. *Nature* 364, 341–343. doi:10.1038/364341a0

Oliet, S. H. R., and Bourque, C. W. (1996). Gadolinium Uncouples Mechanical Detection and Osmoreceptor Potential in Supraoptic Neurons. *Neuron* 16, 175–181. doi:10.1016/S0896-6273(00)80034-3

Oliet, S. H. R., and Bourque, C. W. (1994). Osmoreception in Magnocellular Neurosecretory Cells: from Single Channels to Secretion. *Trends Neurosci.* 17, 340–344. doi:10.1016/0166-2236(94)90177-5

Olsson, K., and Kolmodin, R. (1974). Dependence of Basic Secretion of Antidiuretic Hormone on Cerebrospinal Fluid [Na+]. *Acta Physiol. Scand.* 91, 286–288. doi:10.1111/j.1748-1716.1974.tb05684.x

Onaka, T., and Yagi, K. (2001). Involvement of N-Methyl-D-Aspartic Acid Receptor Activation in Oxytocin and Vasopressin Release after Osmotic Stimuli in Rats. *J. Neuroendocrinol.* 13, 166–174. doi:10.1046/j.1365-2826.2001.00607.x

Ozaki, S., Shibuya, I., Kabashima, U., Isse, F., Noguchi, M., Ueta, N., et al. (2001). Preferential Potentiation by Nitric Oxide of Spontaneous Inhibitory Postsynaptic Currents in Rat Supraoptic Neurones. *J. Neuroendocrinol.* 12, 273–281. doi:10.1046/j.1365-2826.2000.00448.x

Park, S. J., Haan, K. D., Nakamura, Y., Fukami, K., and Fisher, T. E. (2021). PLCδ1 Plays Central Roles in the Osmotic Activation of ΔN-TRPV1 Channels in Mouse Supraoptic Neurons and in Murine Osmoregulation. *J. Neurosci.* 41, 3579–3587. doi:10.1523/JNEUROSCI.2892-20.2021

Pauža, A. G., Mecawi, A. S., Paterson, A., Hindmarch, C. C. T., Greenwood, M., Murphy, D., et al. (2021). Osmoregulation of the Transcriptome of the Hypothalamic Supraoptic Nucleus: A Resource for the Community. *J. Neuroendocrinol.* 33. doi:10.1111/jne.13007

Pedersen, S. F., Okada, Y., and Nilius, B. (2016). Biophysics and Physiology of the Volume-Regulated Anion Channel (VRAC)/Volume-Sensitive Outwardly Rectifying Anion Channel (VSOR). *Pflugers Arch. - Eur. J. Physiol.* 468, 371–383. doi:10.1007/S00424-015-1781-6

Pires da Silva, M., de Almeida Moraes, D. J., Mecawi, A. d. S., Rodrigues, J. A., and Varanda, W. A. (2016). Nitric Oxide Modulates HCN Channels in Magnocellular Neurons of the Supraoptic Nucleus of Rats by an S-nitrosylation-dependent Mechanism. *J. Neurosci.* 36, 11320–11330. doi:10.1523/JNEUROSCI.1588-16.2016

Pitra, S., Zhang, M., Cauley, E., and Stern, J. E. (2019). NMDA Receptors Potentiate Activity-dependent Dendritic Release of Neuropeptides from Hypothalamic Neurons. *J. Physiol.* 597, 1735–1756. doi:10.1113/JP277167

Poletto Chaves, L. A., and Varanda, W. A. (2008). Volume-activated Chloride Channels in Mice Leydig Cells. *Pflugers Arch. - Eur. J. Physiol.* 457, 493–504. doi:10.1007/s00424-008-0525-2

Potapenko, E. S., Biancardi, V. C., Zhou, Y., and Stern, J. E. (2012). Altered Astrocyte Glutamate Transporter Regulation of Hypothalamic Neurosecretory Neurons in Heart Failure Rats. *Am. J. Physiology-Regulatory, Integr. Comp. Physiology* 303, R291–R300. doi:10.1152/ajpregu.00056.2012

Poulain, D. A., Wakerley, J. B., and Dyball, R. E. J. (1977). Electrophysiological Differentiation of Oxytocin-And Vasopressin-Secreting Neurones. *Proc. R. Soc. Lond. B* 196, 367–384. doi:10.1098/rspb.1977.0046

Poulain, D. A., and Wakerley, J. B. (1982). Electrophysiology of Hypothalamic Magnocellular Neurones Secreting Oxytocin and Vasopressin. *Neuroscience* 7, 773–808. doi:10.1016/0306-4522(82)90044-6

Prager-Khoutorsky, M., Khoutorsky, A., and Bourque, C. W. (2014). Unique Interweaved Microtubule Scaffold Mediates Osmosensory Transduction via Physical Interaction with TRPV1. *Neuron* 83, 866–878. doi:10.1016/j.neuron.2014.07.023

Qiu, Z., Dubin, A. E., Mathur, J., Tu, B., Reddy, K., Miraglia, L. J., et al. (2014). SWELL1, a Plasma Membrane Protein, Is an Essential Component of Volume-Regulated Anion Channel. *Cell* 157, 447–458. doi:10.1016/j.cell.2014.03.024

Raichle, M. E., and Mintun, M. A. (2006). BRAIN WORK AND BRAIN IMAGING. *Annu. Rev. Neurosci.* 29, 449–476. doi:10.1146/annurev.neuro.29.051605.112819

Ramos Gomes, F., Romaniello, V., Sánchez, A., Weber, C., Narayanan, P., Psol, M., et al. (2015). Alternatively Spliced Isoforms of KV10.1 Potassium Channels Modulate Channel Properties and Can Activate Cyclin-dependent Kinase in Xenopus Oocytes. *J. Biol. Chem.* 290, 30351–30365. doi:10.1074/jbc.M115.668749

Rawicz, W., Smith, B. A., McIntosh, T. J., Simon, S. A., and Evans, E. (2008). Elasticity, Strength, and Water Permeability of Bilayers that Contain Raft Microdomain-Forming Lipids. *Biophysical J.* 94, 4725–4736. doi:10.1529/biophysj.107.121731

Reis, W. L., Biancardi, V. C., Zhou, Y., and Stern, J. E. (2016). A Functional Coupling between Carbon Monoxide and Nitric Oxide Contributes to Increased Vasopressin Neuronal Activity in Heart Failure Rats. *Endocrinology* 157, 2052–2066. doi:10.1210/en.2015-1958

Reuss, L. (2008). "Water Transport across Cell Membranes," in *eLS* (Wiley). doi:10.1002/9780470015902.a0020621

Richard, D., and Bourque, C. W. (1995). Synaptic Control of Rat Supraoptic Neurones during Osmotic Stimulation of the Organum Vasculosum Lamina Terminalis *In Vitro*. *J. Physiol.* 489, 567–577. doi:10.1113/jphysiol.1995.sp021073

Richardson, C. M., and Wakerley, J. B. (1997). Glutamate Excitation of Oxytocin Neurones *In Vitro* Involves Predominantly Non-NMDA Receptors. *Brain Res.* 767, 158–161. doi:10.1016/S0006-8993(97)00728-2

Romanov, R. A., Tretiakov, E. O., Kastriti, M. E., Zupancic, M., Häring, M., Korchynska, S., et al. (2020). Molecular Design of Hypothalamus Development. *Nature* 582, 246–252. doi:10.1038/s41586-020-2266-0

Romero, M. F., Chen, A.-P., Parker, M. D., and Boron, W. F. (2013). The SLC4 Family of Bicarbonate Transporters. *Mol. Aspects Med.* 34, 159–182. doi:10.1016/j.mam.2012.10.008

Roy, R. K., Althammer, F., Seymour, A. J., Du, W., Biancardi, V. C., Hamm, J. P., et al. (2021). Inverse Neurovascular Coupling Contributes to Positive Feedback Excitation of Vasopressin Neurons during a Systemic Homeostatic Challenge. *Cell Rep.* 37, 109925. doi:10.1016/j.celrep.2021.109925

Ruginsk, S. G., Mecawi, A. d. S., da Silva, M. P., Reis, W. L., Coletti, R., Lima, J. B. M. d., et al. (2015). Gaseous Modulators in the Control of the Hypothalamic Neurohypophyseal System. *Physiology* 30, 127–138. doi:10.1152/physiol.00040.2014

Russell, J. M. (2000). Sodium-Potassium-Chloride Cotransport. *Physiol. Rev.* 80, 211–276. doi:10.1152/physrev.2000.80.1.211

Sachs, F. (2015). Mechanical Transduction by Ion Channels: A Cautionary Tale. *Wjn* 5, 74. doi:10.5316/wjn.v5.i3.74

Sachs, F. (2010). Stretch-Activated Ion Channels: What Are They? *Physiology* 25, 50–56. doi:10.1152/physiol.00042.2009

Sato, K., Numata, T., Saito, T., Ueta, Y., and Okada, Y. (2011). V 2 Receptor-Mediated Autocrine Role of Somatodendritic Release of AVP in Rat Vasopressin Neurons under Hypo-Osmotic Conditions. *Sci. Signal.* 4. doi:10.1126/scisignal.2001279

Sato-Numata, K., Numata, T., and Ueta, Y. (2021). Vasopressin Neurons Respond to Hyperosmotic Stimulation with Regulatory Volume Increase and Secretory Volume Decrease by Activating Ion Transporters and Ca2+ Channels. *Cell. Physiol. biochem.* 55, 119–134. doi:10.33594/000000342

Schneider, S. (2015). Inositol Transport Proteins. *FEBS Lett.* 589, 1049–1058. doi:10.1016/j.febslet.2015.03.012

Schumacher, M. A., Moff, I., Sudanagunta, S. P., and Levine, J. D. (2000). Molecular Cloning of an N-Terminal Splice Variant of the Capsaicin Receptor. *J. Biol. Chem.* 275, 2756–2762. doi:10.1074/jbc.275.4.2756

Shah, L., Bansal, V., Rye, P. L., Mumtaz, N., Taherian, A., and Fisher, T. E. (2014). Osmotic Activation of Phospholipase C Triggers Structural Adaptation in Osmosensitive Rat Supraoptic Neurons. *J. Physiol.* 592, 4165–4175. doi:10.1113/jphysiol.2014.273813

Sharma, K., Haque, M., Guidry, R., Ueta, Y., and Teruyama, R. (2017). Effect of Dietary Salt Intake on Epithelial Na+channels (ENaC) in Vasopressin Magnocellular Neurosecretory Neurons in the Rat Supraoptic Nucleus. *J. Physiol.* 595, 5857–5874. doi:10.1113/JP274856

Sladek, C. D., Fisher, K. Y., Sidorowicz, H. E., and Mathiasen, J. R. (1995). Osmotic Stimulation of Vasopressin mRNA Content in the Supraoptic Nucleus Requires Synaptic Activation. *Am. J. Physiology-Regulatory, Integr. Comp. Physiology* 268, R1034–R1039. doi:10.1152/ajpregu.1995.268.4.R1034

Souza, M. M., Vechiato, F. M. V., Debarba, L. K., Leao, R. M., Dias, M. V. S., Pereira, A. A., et al. (2020). Effects of Hyperosmolality on Hypothalamic Astrocytic Area, mRNA Expression and Glutamate Balance *In Vitro*. *Neuroscience* 442, 286–295. doi:10.1016/j.neuroscience.2020.06.029

Srisawat, R., Bishop, V. R., Bull, P. M., Douglas, A. J., Russell, J. A., Ludwig, M., et al. (2004). Regulation of Neuronal Nitric Oxide Synthase mRNA Expression in the Rat Magnocellular Neurosecretory System. *Neurosci. Lett.* 369, 191–196. doi:10.1016/j.neulet.2004.07.045

Stern, J. E., and Ludwig, M. (2001). NO Inhibits Supraoptic Oxytocin and Vasopressin Neurons via Activation of GABAergic Synaptic Inputs. *Am. J. Physiology-Regulatory, Integr. Comp. Physiology* 280, R1815–R1822. doi:10.1152/ajpregu.2001.280.6.R1815

Strange, K. (2004). Cellular Volume Homeostasis. *Adv. Physiology Educ.* 28, 155–159. doi:10.1152/advan.00034.2004

Strange, K. (1992). Regulation of Solute and Water Balance and Cell Volume in the Central Nervous System. *J Am Soc Nephrol* 3, 12–27. doi:10.1681/ASN.V3112

Su, W., Cao, R., Zhang, X.-y., and Guan, Y. (2020). Aquaporins in the Kidney: Physiology and Pathophysiology. *Am. J. Physiology-Renal Physiology* 318, F193–F203. doi:10.1152/ajprenal.00304.2019

Sugio, S., Nagasawa, M., Kojima, I., Ishizaki, Y., and Shibasaki, K. (2017). Transient Receptor Potential Vanilloid 2 Activation by Focal Mechanical Stimulation Requires Interaction with the Actin Cytoskeleton and Enhances Growth Cone Motility. *FASEB J.* 31, 1368–1381. doi:10.1096/fj.201600686RR

Talley, E. M., Sirois, J. E., Lei, Q., and Bayliss, D. A. (2003). Two-Pore-Domain (Kcnk) Potassium Channels: Dynamic Roles in Neuronal Function. *Neuroscientist* 9, 46–56. doi:10.1177/1073858402239590

Tanaka, M., Cummins, T. R., Ishikawa, K., Black, J. A., Ibata, Y., and Waxman, S. G. (1999). Molecular and Functional Remodeling of Electrogenic Membrane of Hypothalamic Neurons in Response to Changes in Their Input. *Proc. Natl. Acad. Sci. U.S.A.* 96, 1088–1093. doi:10.1073/pnas.96.3.1088

Tanford, C. (1978). The Hydrophobic Effect and the Organization of Living Matter. *Science* 200, 1012–1018. doi:10.1126/science.653353

Teruyama, R., Sakuraba, M., Wilson, L. L., Wandrey, N. E. J., and Armstrong, W. E. (2012). Epithelial Na+ Sodium Channels in Magnocellular Cells of the Rat Supraoptic and Paraventricular Nuclei. *Am. J. Physiology-Endocrinology Metabolism* 302, E273–E285. doi:10.1152/ajpendo.00407.2011

Theodosis, D. T., Montagnese, C., Rodriguez, F., Vincent, J.-D., and Poulain, D. A. (1986). Oxytocin Induces Morphological Plasticity in the Adult Hypothalamo-Neurohypophysial System. *Nature* 322, 738–740. doi:10.1038/322738a0

Thrasher, T. N., Brown, C. J., Keil, L. C., and Ramsay, D. J. (1980). Thirst and Vasopressin Release in the Dog: an Osmoreceptor or Sodium Receptor Mechanism? *Am. J. Physiology-Regulatory, Integr. Comp. Physiology* 238, R333–R339. doi:10.1152/ajpregu.1980.238.5.R333

Tian, W., Fu, Y., Wang, D. H., and Cohen, D. M. (2006). Regulation of TRPV1 by a Novel Renally Expressed Rat TRPV1 Splice Variant. *Am. J. Physiology-Renal Physiology* 290, F117–F126. doi:10.1152/ajprenal.00143.2005

Tobin, V. A., and Ludwig, M. (2007). The Role of the Actin Cytoskeleton in Oxytocin and Vasopressin Release from Rat Supraoptic Nucleus Neurons. *J. Physiol.* 582, 1337–1348. doi:10.1113/jphysiol.2007.132639

Tosteson, D. C., and Hoffman, J. F. (1960). Regulation of Cell Volume by Active Cation Transport in High and Low Potassium Sheep Red Cells. *J. Gen. Physiol.* 44, 169–194. doi:10.1085/jgp.44.1.169

Tucker, A. B., and Stocker, S. D. (2016). Hypernatremia-induced Vasopressin Secretion Is Not Altered in TRPV1−/− Rats. *Am. J. Physiology-Regulatory, Integr. Comp. Physiology* 311, R451–R456. doi:10.1152/ajpregu.00483.2015

Ueta, Y., Levy, A., Chowdrey, H. S., and Lightman, S. L. (1995). Water Deprivation in the Rat Induces Nitric Oxide Synthase (NOS) Gene Expression in the Hypothalamic Paraventricular and Supraoptic Nuclei. *Neurosci. Res.* 23, 317–319. doi:10.1016/0168-0102(95)00956-6

Ussing, H. H. (1960). The Frog Skin Potential. *J. Gen. Physiol.* 43, 135–147. doi:10.1085/jgp.43.5.135

Ventura, R. R., Aguiar, J. F., Antunes-Rodrigues, J., and Varanda, W. A. (2008). Nitric Oxide Modulates the Firing Rate of the Rat Supraoptic Magnocellular Neurons. *Neuroscience* 155, 359–365. doi:10.1016/j.neuroscience.2008.06.005

Verkman, A. S., Ratelade, J., Rossi, A., Zhang, H., and Tradtrantip, L. (2011). Aquaporin-4: Orthogonal Array Assembly, CNS Functions, and Role in Neuromyelitis Optica. *Acta Pharmacol. Sin.* 32, 702–710. doi:10.1038/aps.2011.27

Verkman, A. S., Smith, A. J., Phuan, P.-w., Tradtrantip, L., and Anderson, M. O. (2017). The Aquaporin-4 Water Channel as a Potential Drug Target in Neurological Disorders. *Expert Opin. Ther. Targets* 21, 1161–1170. doi:10.1080/14728222.2017.1398236

Vilhena-Franco, T., Valentim-Lima, E., Reis, L. C., Elias, L. L. K., Antunes-Rodrigues, J., and Mecawi, A. S. (2018). Role of AMPA and NMDA Receptors on Vasopressin and Oxytocin Secretion Induced by Hypertonic Extracellular Volume Expansion. *J. Neuroendocrinol.* 30, e12633. doi:10.1111/jne.12633

Vincent, S. R., and Kimura, H. (1992). Histochemical Mapping of Nitric Oxide Synthase in the Rat Brain. *Neuroscience* 46, 755–784. doi:10.1016/0306-4522(92)90184-4

Voisin, D. L., Chakfe, Y., and Bourque, C. W. (1999). Coincident Detection of CSF Na+ and Osmotic Pressure in Osmoregulatory Neurons of the Supraoptic Nucleus. *Neuron* 24, 453–460. doi:10.1016/S0896-6273(00)80858-2

Voss, F. K., Ullrich, F., Münch, J., Lazarow, K., Lutter, D., Mah, N., et al. (2014). Identification of LRRC8 Heteromers as an Essential Component of the Volume-Regulated Anion Channel VRAC. *Science* 344, 634–638. doi:10.1126/SCIENCE.1252826

Wainwright, A., Rutter, A. R., Seabrook, G. R., Reilly, K., and Oliver, K. R. (2004). Discrete Expression of TRPV2 within the Hypothalamo-Neurohypophysial System: Implications for Regulatory Activity within the Hypothalamic-Pituitary-Adrenal axis. *J. Comp. Neurol.* 474, 24–42. doi:10.1002/cne.20100

Wakerley, J. B., Poulain, D. A., and Brown, D. (1978). Comparison of Firing Patterns in Oxytocin- and Vasopressin-Releasing Neurones during Progressive Dehydration. *Brain Res.* 148, 425–440. doi:10.1016/0006-8993(78)90730-8

Wang, C., Hu, H.-Z., Colton, C. K., Wood, J. D., and Zhu, M. X. (2004). An Alternative Splicing Product of the Murine Trpv1 Gene Dominant Negatively Modulates the Activity of TRPV1 Channels. *J. Biol. Chem.* 279, 37423–37430. doi:10.1074/jbc.M407205200

Wang, J., Xu, H., Morishima, S., Tanabe, S., Jishage, K., Uchida, S., et al. (2005). Single-Channel Properties of Volume-Sensitive Cl− Channel in ClC-3-Deficient Cardiomyocytes. *Jjp* 55, 379–383. doi:10.2170/JJPHYSIOL.S655

Wang, X., Li, T., Liu, Y., Jia, S., Liu, X., Jiang, Y., et al. (2021). Aquaporin 4 Differentially Modulates Osmotic Effects on Vasopressin Neurons in Rat Supraoptic Nucleus. *Acta Physiol.* 232. doi:10.1111/apha.13672

Watanabe, E., Hiyama, T. Y., Shimizu, H., Kodama, R., Hayashi, N., Miyata, S., et al. (2006). Sodium-level-sensitive Sodium Channel Nax Is Expressed in Glial Laminate Processes in the Sensory Circumventricular Organs. *Am. J. Physiology-Regulatory, Integr. Comp. Physiology* 290, R568–R576. doi:10.1152/ajpregu.00618.2005

Wenker, I. C., Benoit, J. P., Chen, X., Liu, H., Horner, R. L., and Mulkey, D. K. (2012). Nitric Oxide Activates Hypoglossal Motoneurons by cGMP-dependent Inhibition of TASK Channels and cGMP-independent Activation of HCN Channels. *J. Neurophysiology* 107, 1489–1499. doi:10.1152/jn.00827.2011

Wilson, C., and Dryer, S. E. (2014). A Mutation in TRPC6 Channels Abolishes Their Activation by Hypoosmotic Stretch but Does Not Affect Activation by Diacylglycerol or G Protein Signaling Cascades. *Am. J. Physiology-Renal Physiology* 306, F1018–F1025. doi:10.1152/ajprenal.00662.2013

Xu, Z., and Herbert, J. (1998). Effects of Intracerebroventricular Dizocilpine (MK801) on Dehydration-Induced Dipsogenic Responses, Plasma Vasopressin and C-Fos Expression in the Rat Forebrain. *Brain Res.* 784, 91–99. doi:10.1016/S0006-8993(97)01186-4

Xue, Q., Yu, Y., Trilk, S. L., Jong, B. E., and Schumacher, M. A. (2001). The Genomic Organization of the Gene Encoding the Vanilloid Receptor: Evidence for Multiple Splice Variants. *Genomics* 76, 14–20. doi:10.1006/geno.2001.6582

Yadav, M., and Goswami, C. (2020). TRPV2 Interacts with Actin and Reorganizes Submembranous Actin Cytoskeleton. *Biosci. Rep.* 40. doi:10.1042/BSR20200118

Yamova, L., Dmitriy, A., Glazova, M., Chernigovskaya, E., and Huang, P. (2007). Role of Neuronal Nitric Oxide in the Regulation of Vasopressin Expression and Release in Response to Inhibition of Catecholamine Synthesis and Dehydration. *Neurosci. Lett.* 426, 160–165. doi:10.1016/j.neulet.2007.08.066

Yang, C. R., Senatorov, V. V., and Renaud, L. P. (1994). Organum Vasculosum Lamina Terminalis-Evoked Postsynaptic Responses in Rat Supraoptic Neurones *In Vitro*. *J. Physiol.* 477, 59–74. doi:10.1113/jphysiol.1994.sp020171

Yoshida, T., Inoue, R., Morii, T., Takahashi, N., Yamamoto, S., Hara, Y., et al. (2006). Nitric Oxide Activates TRP Channels by Cysteine S-Nitrosylation. *Nat. Chem. Biol.* 2, 596–607. doi:10.1038/nchembio821

Yuan, H., Gao, B., Duan, L., Jiang, S., Cao, R., Xiong, Y.-F., et al. (2009). Acute Hyperosmotic Stimulus-Induced Fos Expression in Neurons Depends on Activation of Astrocytes in the Supraoptic Nucleus of Rats. *J. Neurosci. Res.*, NA. doi:10.1002/jnr.22297

Zaelzer, C., Hua, P., Prager-Khoutorsky, M., Ciura, S., Voisin, D. L., Liedtke, W., et al. (2015). ΔN-TRPV1: A Molecular Co-detector of Body Temperature and Osmotic Stress. *Cell Rep.* 13, 23–30. doi:10.1016/j.celrep.2015.08.061

Zanou, N., Mondin, L., Fuster, C., Seghers, F., Dufour, I., de Clippele, M., et al. (2015). Osmosensation in TRPV2 Dominant Negative Expressing Skeletal Muscle Fibres. *J. Physiol.* 593, 3849–3863. doi:10.1113/JP270522

Zeidel, M. L., Ambudkar, S. V., Smith, B. L., and Agre, P. (1992). Reconstitution of Functional Water Channels in Liposomes Containing Purified Red Cell CHIP28 Protein. *Biochemistry* 31, 7436–7440. doi:10.1021/bi00148a002

Zhang, W., Wang, D., Liu, X.-H., Kosala, W. R. A., Rajapaksha, J. S., and Fisher, T. E. (2009). An Osmosensitive Voltage-Gated K+current in Rat Supraoptic Neurons. *Eur. J. Neurosci.* 29, 2335–2346. doi:10.1111/j.1460-9568.2009.06772.x

Zhang, Z., and Bourque, C. W. (2003). Osmometry in Osmosensory Neurons. *Nat. Neurosci.* 6, 1021–1022. doi:10.1038/nn1124

Zhang, Z., Kindrat, A. N., Sharif-Naeini, R., and Bourque, C. W. (2007). Actin Filaments Mediate Mechanical Gating during Osmosensory Transduction in Rat Supraoptic Nucleus Neurons. *J. Neurosci.* 27, 4008–4013. doi:10.1523/JNEUROSCI.3278-06.2007

Conflict of Interest: The authors declare that the research was conducted in the absence of any commercial or financial relationships that could be construed as a conflict of interest.

Publisher's Note: All claims expressed in this article are solely those of the authors and do not necessarily represent those of their affiliated organizations, or those of the publisher, the editors and the reviewers. Any product that may be evaluated in this article, or claim that may be made by its manufacturer, is not guaranteed or endorsed by the publisher.

Copyright © 2022 Mecawi, Varanda and da Silva. This is an open-access article distributed under the terms of the Creative Commons Attribution License (CC BY). The use, distribution or reproduction in other forums is permitted, provided the original author(s) and the copyright owner(s) are credited and that the original publication in this journal is cited, in accordance with accepted academic practice. No use, distribution or reproduction is permitted which does not comply with these terms.

frontiers | Frontiers in Physiology

ORIGINAL RESEARCH
published: 01 June 2022
doi: 10.3389/fphys.2022.820112

Conditional Regulation of Blood Pressure in Response to Emotional Stimuli by the Central Nucleus of the Amygdala in Rats

Ko Yamanaka[1]* *and Hidefumi Waki*[1,2]

[1]Department of Physiology, Graduate School of Health and Sports Science, Juntendo University, Inzai, Japan, [2]Institute of Health and Sports Science and Medicine, Juntendo University, Inzai, Japan

Humans and animals can determine whether a situation is favorable to them and act accordingly. For this, the autonomic tuning of the cardiovascular system to supply energy to active skeletal muscles through the circulatory system is as important as motor control. However, how the autonomic cardiovascular responses are regulated in dynamically changing environments and the neuronal mechanisms underlying these responses remain unclear. To resolve these issues, we recorded the blood pressure and heart rate of head-restrained rats during dynamically changing appetitive and aversive classical conditioning tasks. The rats displayed various associations between conditioned stimuli and unconditioned stimuli in appetitive (sucrose water), neutral (no outcome), and aversive (air puff) blocks. The blood pressure and heart rate in the appetitive block gradually increased in response to the reward-predicting cue and the response to the actual reward vigorously increased. The reward-predictive response was significantly higher than the responses obtained in the neutral and aversive condition blocks. To investigate whether the reward-predictive pressor response was caused by orofacial movements such as anticipatory licking behavior, we separately analyzed high- and low-licking trials. The conditioned pressor response was observed even in trials with low-licking behaviors. Blood pressure and heart rate responses to the air puff-predicting cue in the aversive block were not significantly different from the responses in the neutral block. The conditioned blood pressure response rapidly changed with condition block switching. Furthermore, to examine the contribution of the amygdala as an emotion center to these conditioned responses, we bilaterally microinjected a $GABA_A$ receptor agonist, muscimol, into the central nucleus of the amygdala. Pharmacological inactivation of the central nucleus of the amygdala significantly decreased the reward-predictive pressor responses. These results suggest that the blood pressure is adaptively and rapidly regulated by emotional conditioned stimuli and that the central nucleus of the amygdala participates in regulating the pressor response in dynamically changing situations.

Keywords: blood pressure, heart rate, licking behavior, classical conditioning, amygdala, rat, brain

OPEN ACCESS

Edited by:
Geoffrey A. Head,
Baker Heart and Diabetes Institute, Australia

Reviewed by:
Alan Sved,
University of Pittsburgh, United States
Mazher Mohammed,
University of Florida, United States

***Correspondence:**
Ko Yamanaka
k-yamana@juntendo.ac.jp

Specialty section:
This article was submitted to Integrative Physiology, a section of the journal Frontiers in Physiology

Received: *22 November 2021*
Accepted: *12 April 2022*
Published: *01 June 2022*

Citation:
Yamanaka K and Waki H (2022) Conditional Regulation of Blood Pressure in Response to Emotional Stimuli by the Central Nucleus of the Amygdala in Rats. Front. Physiol. 13:820112. doi: 10.3389/fphys.2022.820112

INTRODUCTION

In a dynamically changing environment, the ability to predict outcomes of future events allows getting rewards ahead of competitors and escaping from danger. The amygdala is classically believed to play a central role in negative emotions (Hilton and Zbrozyna, 1963; Pascoe and Kapp, 1985); however, its involvement in the emotional, attentional, and learning processes of external stimuli with positive consequences has also been reported in rodents (Holland and Gallagher, 1999; Everitt et al., 2003; Calu et al., 2010; Roesch et al., 2012; Kim et al., 2016), macaques (Baxter and Murray, 2002; Paton et al., 2006), and humans (Phelps and LeDoux, 2005). Shabel and Janak showed that the amygdala neuronal activities triggered by appetitive and aversive conditioned stimuli are similar and correlate with autonomic arousal such as changes in the blood pressure, suggesting that emotional arousal is coded in this brain region (Shabel and Janak, 2009; Shabel et al., 2011). Our previous study showed that electrical and chemical stimulations of the central nucleus of the amygdala (CeA) in anesthetized rats induce bidirectional (facilitatory or inhibitory) cardiovascular responses in a region-specific manner, indicating that the amygdala contributes to the neuronal circuitry modulating autonomic responses (Yamanaka et al., 2018). Conditioned cardiovascular responses are classically recorded during the anticipation of either appetitive or aversive outcomes (Harris and Brady, 1974; Cohen and Obrist, 1975). Because many of these studies have been conducted on free-moving animals, it is difficult to control animal behaviors such as freezing and fleeing. Furthermore, the autonomic cardiovascular response is dynamically regulated in subjects facing an environment where the emotional context dynamically changes. However, the amygdala's involvement has not been demonstrated.

Here, we hypothesized that the amygdala plays a role in the autonomic cardiovascular regulation involved in emotional arousal in response to salient external stimuli. Therefore, we recorded the blood pressure and heart rate of head-restrained rats during dynamically changing appetitive and aversive classical conditioning tasks and examined the effects of amygdala manipulation.

MATERIALS AND METHODS

Animals

A total of 10 male Wistar–Kyoto rats (age: 7 weeks and weight: 238 ± 39 g at the time of the first surgery) were used (Japan SLC, Inc., Japan). The animals were housed in a temperature-controlled room under a fixed 12/12 h dark/light cycle (6: 00–18:00/18:00–6:00). Food was available in the home cage *ad libitum*. Water access was restricted during behavioral learning of the task (up to 24 h) to increase the motivation for sucrose rewards. Rat body weights were measured every day to control that they were not less than 85% of the original weight. A few agar blocks (containing 15 ml water) were regularly given in the home cages. The animals had access to water *ad libitum* after surgery recovery and on the weekends. All experiments were approved by the Ethics Committee for Animal Experiments at Juntendo University and complied with the guidelines set by the Japan Physiological Society.

Surgeries

Two distinct surgeries were performed to implant first a radio transmitter for blood pressure recording and then head plates to fix the animal body during experiments. The recovery time after each surgery was more than a week. During surgery, the rectal temperature was monitored and maintained at 37°C using a heating pad (BWT-100, Bio Research Center, Japan). After surgery, antibiotics (benzylpenicillin, 1000 U, intramuscular, Meiji Seika Pharma, Japan) and analgesics (meloxicam, 1 mg/kg, subcutaneous, Boehringer Ingelheim, Germany) were administered.

Implantation of a Transmitter for Telemetry

A telemetric radio transmitter (HD-S10; Data Sciences International, USA) for chronic blood pressure recording from the abdominal aorta was implanted, as described in previous studies (Waki et al., 2003; Yamanaka et al., 2018). Rats were anesthetized with pentobarbital sodium (50 mg/kg) by intraperitoneal (i.p.) administration and isoflurane (2.0%–2.5% for maintenance) using an inhalation anesthesia apparatus (Univentor 400 anesthesia unit, Univentor, Sweden). The level of anesthesia was checked by assessing limb withdrawal to noxious pinching. After an abdominal midline incision was made in rats in a supine position, the intestines were moved aside to allow visualization and isolation of the abdominal aorta. The aorta was temporary aortic occluded using a sterilized string to prevent severe blood loss, and the tip of the transmitter catheter was inserted into the abdominal aorta with a 21G needle guide. The transmitter catheter was then fixed using tissue adhesive (Vetbond, 3M, United States) and the transmitter was sutured to the ventral wall of the abdominal cavity.

Implantation of a Head Plate

All procedures for the head plate implantation (CFR-1, Narishige, Japan) were previously established (Kimura et al., 2012). Rats were anesthetized with isoflurane (Pfizer, USA), 4.5%–5.0% for induction and 2.0%–2.5% for maintenance. Then, they were placed on a stereotaxic frame (SR-10R-HT, Narishige, Japan). A stainless-steel head plate was attached to the skull using tiny stainless-steel screw bolts (M1, 2 mm long; Yahata Neji Corporation, Japan) as anchors and dental resin cement (Super-Bond C&B, Sun Medical; Unifast II, GC Corporation, Japan).

Dynamically Changing Classical Conditioning Tasks

After at least a week of post-surgery recovery, the behavioral investigation was initiated. The rats were trained using a behavioral testing system for a classical conditioning task (Task Forcer, O'Hara and Co., Ltd., Japan). This task was used as a behavioral model to evaluate autonomic responses during

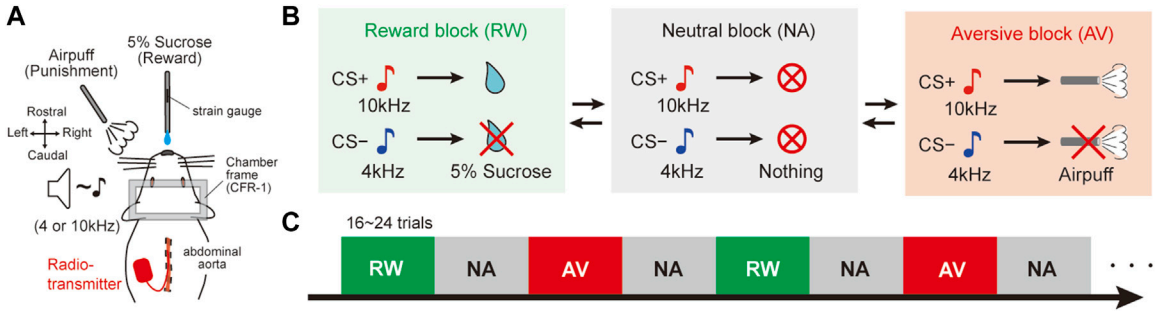

FIGURE 1 | Dynamically changing classical conditioning task with emotional valence. **(A)** Schematic diagram of the behavioral task. Stainless tubes for reward and air-puff delivery were placed in front of the face of head-fixed rats. A radio transmitter was implanted into the abdominal aorta to record the blood pressure by telemetry. A strain gauge was attached to the reward tube to monitor the amplitude of licking movements. **(B)** Pavlovian procedure with three distinct context blocks. In the reward (RW) block, a tone cue (CS+, 10 kHz) preceded the reward (US+, 5% sucrose), and another tone (CS−, 4 kHz) was not followed by a reward (US−). In the aversive (AV) blocks, CS + preceded an air puff (US+) and no air puff (US−) followed CS−. Both CS tones preceded nothing in the neutral (NA) blocks. CS, conditioned stimulus; US, unconditioned stimulus. **(C)** Trial sequence of the behavioral task. NA blocks were alternately deployed between RW and AV blocks. There were 16–24 trials per block. The order of the blocks was fixed, but they randomly started with RW or AV every experimental day. There was no cue indicating the block switch.

dynamic changing cue-outcome associations. Animals were fixed on a stereotaxic frame (SR-10R-HT, Narishige, Japan) in a sound-attenuated box (SAC-4201W, O'Hara and Co., Ltd., Japan). The beginning of the first session was dedicated to acclimatizing the rats to head fixation and teaching them that a reward was delivered from a spout tube located in front of their mouth. To achieve this aim, the rats were immobilized for 1 hour and given the reward several times until they licked the spout tube. Then, the task session started. Animals learned various associations between conditioned stimuli (CS) and unconditioned stimuli (US) in three experimental blocks (**Figures 1A,B**): 1) appetitive reward (RW) block: one tone cue (reward CS+, 10 kHz, 1 s, 60–70 dB) associated with sucrose delivery (reward US+; 5% sucrose, 0.08 ml) and another tone cue (reward CS−, 4 kHz, 1 s, 60–70 dB) associated with no reward (reward US−), 2) aversive (AV) block: the CS+ was associated with an air puff (aversive US+; 30–40 psi, 1 s) and the CS− was associated with no air puff (aversive US−), and 3) neutral (NA) block: both CS tones predicted nothing (neutral CS+ and CS−). The air puff was delivered through a stainless-steel tube (AG45-2–100, Φ2×100 mm, Kurita Seisakusho, Japan) placed 8–10 cm away from the rat's face, below its left eye. The time interval between CS offset to US onset (CS–US interval) was 15 s. The inter-trial interval was 60 ± 15 s. Each block consisted of 16–24 trials, and the order of the trials (CS + or CS− trial) was pseudo-randomly assigned. The animals could not predict the timing of the block switch because of the lack of cue at block changing. The order of the block presentation was fixed as RW and AV blocks were alternatively presented and the NA block was intercalated between them (**Figure 1C**; RW → NA → AV → NA → RW →. . .). The daily trials randomly started with RW or AV. For the learning process, the rats were initially trained only in the RW block. The AV context was then added, and the NA context training was included last. Orofacial licking movements indicating reward anticipation and consumption were monitored by measuring the strain on the reward spout tube (**Figure 1A**; KFG-2N-120-C1-23 amplified by DPM-911B, Kyowa, Japan).

Muscimol Injections

The link between context-based blood pressure responses and CeA activity was assessed using pharmacological inactivation experiments. Seven of the 10 animals were used in this experiment. The day before the injection experiment, two holes were drilled in the skull, approximately above the CeA, under anesthesia with isoflurane (2.0%–2.5% for maintenance) and covered with silicone (Dent Silicone-V, Shofu, Japan). Micropipettes were connected to a Hamilton microsyringe mounted on a syringe pump (LEGATO110, KD Scientific, United States) to control the injection rate (500 nL/min). The silicone lid was removed immediately before the classical conditioning task and a $GABA_A$ receptor agonist (muscimol, 80 pmol, 100 nL, M1523-10 MG, Sigma-Aldrich, United States) was microinjected (Stotz-Potter et al., 1996) into the bilateral CeA (1.8 mm caudal, 3.0 mm lateral from the bregma, and 7.0 mm ventral from the dura) using a glass micropipette (an outside diameter of 20–30 μm; GC200F-10, Harvard Apparatus, United States) under local anesthesia with lidocaine (Xylocaine Polyamp 1%, AstraZeneca). In the control experiment, saline (100 nL, Otsuka, Japan) was injected to measure cardiovascular responses induced by the volume of liquid injected. The order of administration of muscimol and saline was alternated between the animals. After bilateral injections, the micropipette was pulled out and the behavioral task was started. After completing the final experiments, the chemical inactivation site was identified and controlled by injecting fluorescent microspheres (FluoSpheres, 100 nL, Thermo Fisher Scientific, United States) with a separate pipette at the same stereotaxic coordinates as those used for muscimol injections.

Histology

After the last behavioral experiment, the rats were deeply anesthetized with sodium pentobarbital and isoflurane and

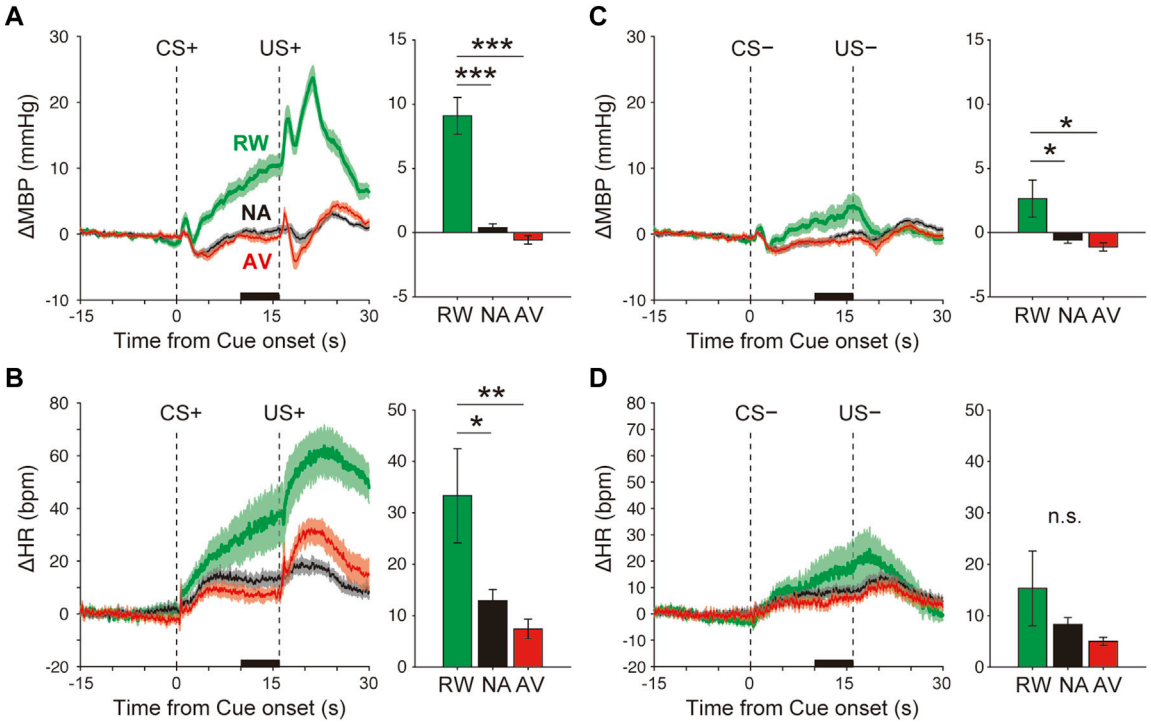

FIGURE 2 | Blood pressure and heart rate responses during the Pavlovian conditioning task. **(A–B)** Average responses of ΔMBP **(A)** and ΔHR **(B)** to CS+ and US+ during the reward (RW; green line and bar), neutral (NA; black line and bar), and aversive (AV; red line and bar) condition blocks. Lines and shadows indicate the mean ± standard error. The thick black line on the *X*-axis indicates the time window for a quantitative analysis. **(C–D)** Same as **A**–**B**, but during CS− and US−. $^{*}p < 0.05$, $^{***}p < 0.001$, one-way analysis of variance with a Tukey–Kramer post hoc test, and n = 10 rats.

intracardially perfused with saline and then 4% paraformaldehyde (163-20145, FUJIFILM Wako Pure Chemical Corporation, Japan). The brains were removed, post-fixed for at least 48 h in 4% paraformaldehyde, and then immersed in 30% sucrose. Once settled at the bottom of the sucrose solution, the brains were sliced into 50-μm-thick serial sections using a freezing microtome (REM-710; Yamato Kohki Industrial, Japan). The sections were then mounted on slides and imaged using a fluorescence microscope (EVOS FL Auto 2 imaging system, Thermo Fisher, United States) to map the drug injection sites in the amygdala.

Data Analysis and Statistics

The blood pressure and heart rate were recorded simultaneously during the classical conditioning tasks using the telemetry blood pressure recording system (PhysioTel, Data Sciences International, United States) with the PowerLab system (PowerLab/8s, ADInstruments, New Zealand). The mean blood pressure and heart rate were derived from pulsatile pressure signals using LabChart software (Version 8.0, AD Instruments). The data were subsequently analyzed in MATLAB (The MathWorks, United States). Artificial changes in the blood pressure (<50 mmHg) and heart rate (<200 bpm or >600 bpm) signals were removed and treated as missing values in the dataset. We mainly analyzed the blood pressure and heart rate between the CS onset and the US onset (CS–US interval). Changes in the mean blood pressure (ΔMean blood pressure; ΔMBP) and heart rate (ΔHeart rate; ΔHR) were calculated by subtracting mean values during the baseline period 5–15 s before the CS onset. One-way analysis of variance (ANOVA) with the Tukey–Kramer post hoc test was used to compare the magnitudes of the blood pressure and heart rate measured 6 s immediately before the US onset among RW, NA, and AV blocks (**Figure 2**). Considering that the autonomic cardiovascular response is influenced by movement and emotion, we attempted to distinguish whether the observed cardiovascular responses were caused by orofacial movements due to the anticipatory licking behavior and/or by emotions induced by the outcome prediction. We divided the trials into two groups based on whether the licking amplitude was lower or higher than the threshold level (three standard deviations [SD] from the baseline) during the CS–US interval. The licking amplitude was converted into absolute values and the change from the baseline value was calculated for each trial (ΔLicking). Averaged blood pressure, heart rate, and licking movements were plotted and compared for low- and high-licking groups using one-way ANOVA with the Tukey–Kramer post hoc test (**Figure 3**). Statistical comparisons of the blood pressure were performed using the averaged data for each CS in four trials before and after the block switch (one-way ANOVA with the Tukey–Kramer post hoc test, **Figure 4**). Finally, we quantified and compared the CS–US intervals between sessions with muscimol and saline

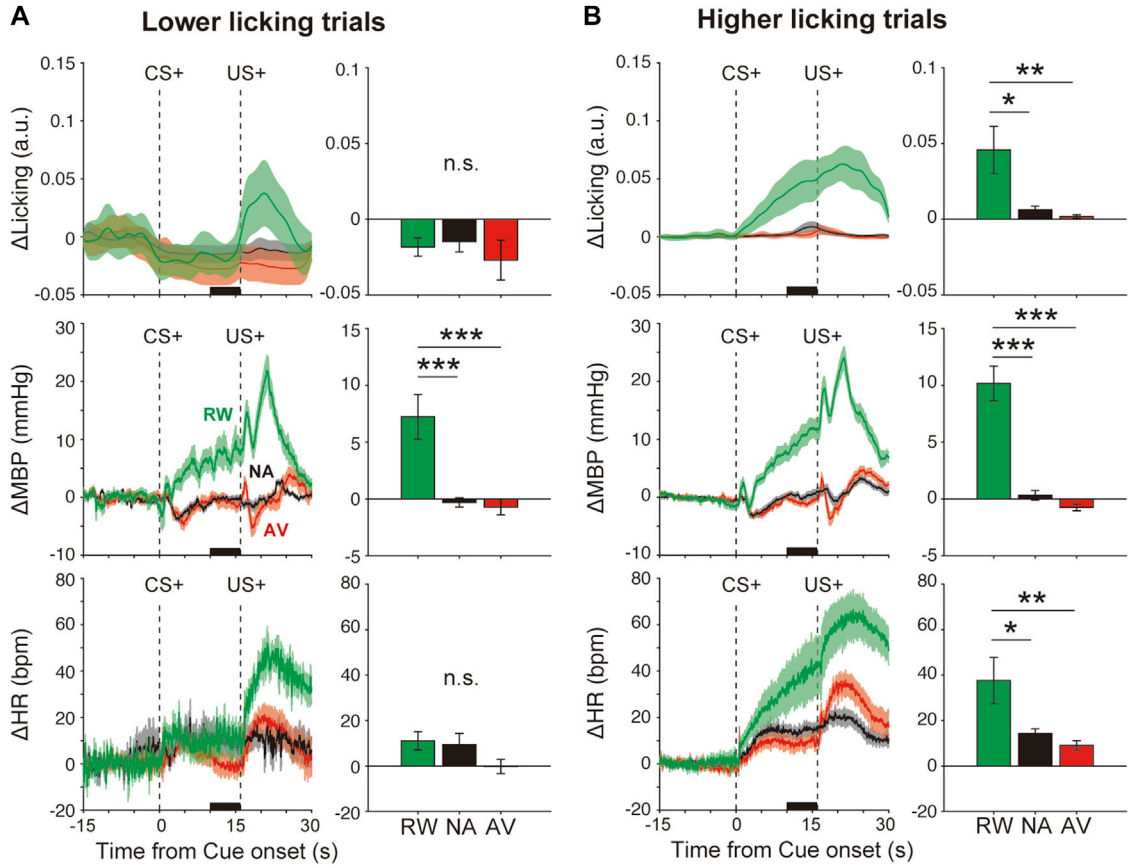

FIGURE 3 | Effects of orofacial licking movements on cardiovascular responses. Average responses and quantitative bar graphs (inset of each figure) of licking (ΔLicking; top panels), mean blood pressure (ΔMBP; middle panels), heart rate (ΔHR; bottom panels), and responses to CS+ (left panels) and CS– (right panels) during the reward (RW; green line and bar), neutral (NA; black line and bar), and aversive (AV; red line and bar) condition blocks in trials with a **(A)** lower-licking group or **(B)** higher-licking group than the threshold (two standard deviations from the baseline) during the CS–US interval. *$p < 0.05$, **$p < 0.01$, ***$p < 0.001$, one-way analysis of variance with a Tukey–Kramer post hoc test, and n = 10 rats.

injections to examine the effects of CeA inactivation. The average data of ΔMBP in response to CS+ with or without bilateral inactivation of the CeA before and after four trials at the condition block switch during the classical conditioning task were assessed. We then analyzed the data using two-way ANOVA and the post hoc Tukey–Kramer test with trials from the condition block change, and with drugs (muscimol vs. saline) as factors (**Figure 5**). Statistical analyses were conducted using the MATLAB Statistics and Machine Learning Toolbox (The MathWorks). The mean blood pressure was averaged and statistically tested across rats (**Figures 2–4**, n = 10; **Figure 5**, n = 6). The criterion for statistical significance was $p \leq 0.05$.

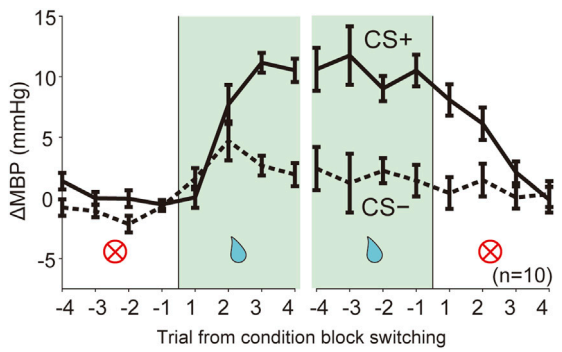

FIGURE 4 | Dynamic changes of blood pressure responses triggered by context block switching. Line plots showing averaged ΔMBP during four trials in each trial type CS (solid line, CS+; dashed line: CS–) before and after switching of the reward condition block (NA→RW, RW→NA). RW, reward block; NA, neutral block. n = 10 rats.

RESULTS

Blood Pressure and Heart Rate Responses During Classical Conditioning Tasks

Although the animal body weights tended to be higher at the beginning of the week (Monday: mean ± SD = 104 ± 7%, % body weight to that immediately before water restriction) than those at the end of the week (Friday: mean ± SD = 97 ± 5%), overall, the weights remained constant throughout the week. To examine the

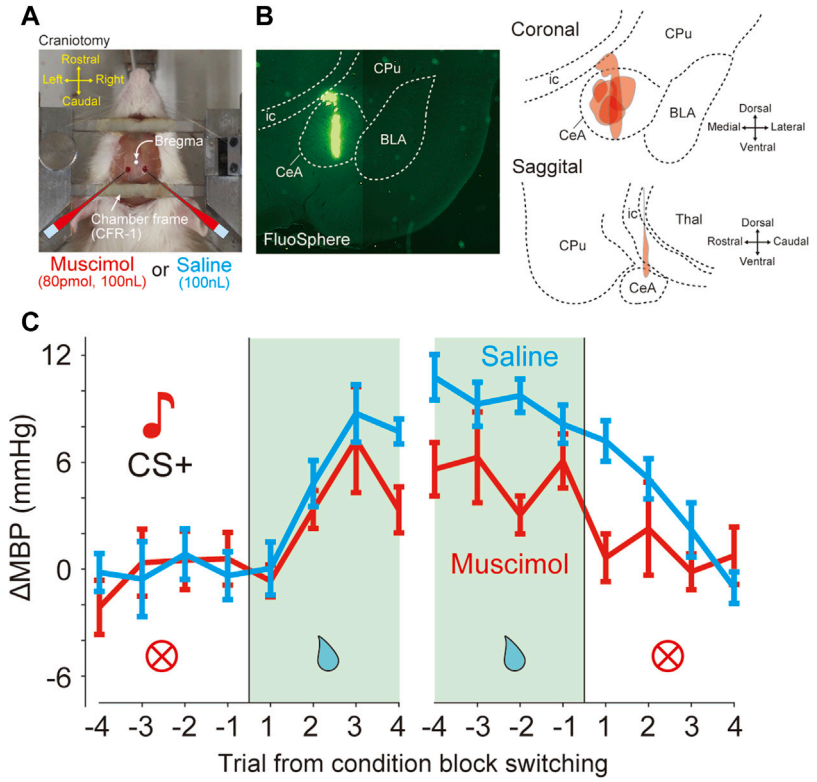

FIGURE 5 | Bilateral inactivation of CeA attenuated the pressor response induced by reward prediction **(A)** Photograph shows a view of a head-restraint rat from above during drug injection. Craniotomy just above the amygdala (1.8 mm caudal, 3.0 mm lateral from bregma) is performed for drug injection **(B)** Injection site of six rats in the bilateral CeA. Fluorospheres (100 nL) were injected at identical stereotaxic positions using glass micropipettes (left panel). Reconstruction of the injection site in the coronal and sagittal planes (right panels). BLA, basolateral amygdala; CeA, central nucleus of the amygdala; CPu, caudate putamen; ic, internal capsule; Thal, thalamus. **(C)** Effects of bilateral inactivation in the data averaged from the mean blood pressure (ΔMBP) in response to CS + before and after four trials at condition block switching during the dynamically changing classical conditioning tasks. Red and cyan lines indicate the data obtained with muscimol and saline injections (six rats).

effects of the head fixation to the stereotaxic frame, baseline blood pressure and heart rates during the first minute (immediately after immobilization) and the last minute (several hours after immobilization) of the task were plotted for each session (**Supplementary Figure S1A,B**). The blood pressure (130–140 mmHg) and heart rate (450–500 bpm) were high at the beginning of the training but decreased gradually as the training progressed to reach blood pressure (120–130 mmHg) and heart rate (350–400 bpm) values consistent with those from previous studies on classical conditioning tasks using reward and punishment in free-moving rodents (Shabel and Janak, 2009). In addition, absolute values of blood pressure and heart rate at the baseline (5–15 s before CS onset) for each trial after learning were approximately constant between 100 and 120 mmHg and between 300 and 350 bpm, respectively (**Supplementary Figure S1C,D**), during several hours of the experiment within a session. These results suggest that the immobilization did not overly stress the animals after habituation. Therefore, we subsequently analyzed data obtained after sufficient training. The data of the results of cardiovascular responses during the dynamically changing classical conditioning tasks (**Supplementary Figure S2, 3, 4**, **Supplementary Tables S1, S2**) were acquired from the session (day) 12 of the learning AV block, while the data of the results of inactivation experiments (**Supplementary Figure S5, 3, 4, 5, 6**, **Supplementary Tables S3**) were obtained afterward.

The averaged ΔMBP measured in response to the reward CS+ (+9.1 ± 1.4 mmHg) was significantly higher than that measured with the neutral CS+ (+0.4 ± 0.3 mmHg), $F_{(2,27)} = 37.7$, $p < 0.001$, and one-way ANOVA with the Tukey–Kramer post hoc test (**Figure 2A** and **Supplementary Figure S2**). The averaged ΔMBP triggered by aversive CS+ (−0.6 ± 0.3 mmHg) showed a tendency to decrease compared with that measured with neutral CS+, but was not significant ($p > 0.05$). Similarly, ΔHR in response to reward CS+ (33.3 ± 9.4 bpm) was significantly higher than that obtained in the NA block (12.9 ± 2.2 bpm), $F_{(2,27)} = 6.1$, $p = 0.007$, and one-way ANOVA with the Tukey–Kramer post hoc test (**Figure 2B** and **Supplementary Figure S2**). ΔHR induced by aversive CS+ (7.4 ± 1.9 bpm) showed a tendency to decrease compared with that of the neutral CS+ ($p > 0.05$). Although CS– (4 kHz tone) had no outcome in any trial throughout the classical conditioning tasks, ΔMBP, but not ΔHR (**Figure 2D** and

Supplementary Figure S2, $F_{(2,27)}$ = 1.5, p = 0.24), was significantly affected by reward CS− (ΔMBP, **Figure 2C** and **Supplementary Figure S2**, $F_{(2,27)}$ = 5.5, p = 0.01).

We evidenced cardiovascular responses associated with reward prediction. These might reflect the emotional responses induced by positive outcome-associated cues. However, these responses might be caused by other events such as anticipatory licking movements as we observed that some animals displayed high anticipatory licking, whereas others did fewer anticipatory licking movements (**Supplementary Figure S2**). To examine this possibility, we divided the data into two groups, lower and higher licking groups, compared with the threshold value (2 SD from the baseline), according to the licking movement amplitudes during the CS–US interval (**Supplementary Table S1**). Even in the low-licking group (**Figure 3A**, top panel, $F_{(2,26)}$ = 2.2, p > 0.05), ΔMBP induced by reward CS+ (+7.2 ± 2.0 mmHg) was significantly higher than that observed after neutral CS+ (−0.3 ± 0.4 mmHg) (**Figure 3A**, middle-left panel), $F_{(2,26)}$ = 14.5, p < 0.001, and one-way ANOVA with a Tukey–Kramer post hoc test). However, conditioned heart rate responses disappeared in the lower licking trials (**Figure 3A** bottom panel), RW versus NA, p = 0.13; $F_{(2,26)}$ = 2.2; and one-way ANOVA with Tukey–Kramer post hoc test. Conversely, in the higher licking trials (**Figure 3B** top panel, $F_{(2,27)}$ = 7.0, p = 0.003), ΔMBP ($F_{(2,27)}$ = 42.4, p < 0.001) and ΔHR ($F_{(2,27)}$ = 6.2, p = 0.006) were increased proportionally to the licking amplitude (**Figure 3B** middle and bottom panels), suggesting that licking movements strongly affected the cardiovascular responses, especially the heart rate. Therefore, at least for the blood pressure, it is possible that the condition-dependent responses were caused by the licking movements and by the emotional cue–outcome association.

Dynamic Changes in Cardiovascular Responses Triggered by the Context Block Switch

We assessed the predictive cardiovascular responses during condition block switching using dynamically changing appetitive and aversive classical conditioning tasks. The line plots of the averaged ΔMBP in response to CS+ and CS− in four trials before and after the block switch (**Figure 4**; NA→RW→NA, NA→AV→NA) indicate that the unanticipated switch from neutral to reward condition blocks (**Figure 4** and **Supplementary Table S2**, NA→RW) in the first trial resulted in ΔMBP triggered by reward CS+ (0.05 ± 0.87 mmHg, p = 1.000; one-way ANOVA with a Tukey–Kramer post hoc test, compared with ΔMBP induced by CS+ in the NA block) similar to those obtained in the previous NA condition block. However, responses to reward CS+ in the second (7.71 ± 1.61 mmHg, p = 0.075) and third (11.15 ± 0.82 mmHg, p < 0.001) trials were dramatically increased after the rats had been exposed to reward US+. Pressor responses to reward CS+ were maintained for a few trials after switching back to the neutral block (RW→NA): 8.08 ± 1.30 mmHg in the first trial (p = 0.047), 6.13 ± 1.34 mmHg in the second trial (p = 0.355), and 2.11 ± 0.91 mmHg in the third trial (p = 0.999) after block switching. Therefore, cardiovascular responses to reward-predictive cues rapidly changed, guided by reward expectations.

Bilateral Inactivation of the CeA Attenuated Reward Prediction-Induced Pressor Response

The $GABA_A$ receptor agonist muscimol or saline was microinjected immediately before the conditioning task (**Figure 5A**). In total, we performed microinjection experiments on seven rats. All animals were injected with both muscimol and saline in different sessions. The injection site was verified by histology using fluorescent microspheres (**Figure 5B**). Because it was possible that one of the seven rats might not have been injected with CeA, the following analysis was performed on the data of six animals excluding it. The effects of injections on each animal were averaged and analyzed statistically (muscimol injections, n = 6 and saline injections, n = 6). In the dynamically changing classical conditioning task, compared with saline, muscimol microinjection of CeA caused significant decreases in ΔMBP before and after switching from the RW blocks (**Figure 5C** and **Supplementary Table S3A**), the main effect for drug factor, $F_{(1,160)}$ = 7.47, p = 0.007; the main effect for trial factor, $F_{(15,160)}$ = 4.47, p < 0.001; no interaction between drug and trial factors $F_{(15,160)}$ = 0.62, p = 0.86, and two-way ANOVA. On the other hand, there was no significant difference in ΔHR (**Supplementary Figure S3A**; main effect for drug factor, $F_{(1,160)}$ = 2.54, p = 0.11) and the licking behavior (**Supplementary Figure S3B**; main effect for drug factor, $F_{(1,160)}$ = 1.02, p = 0.31) between muscimol and saline-injected animals as measured by the behavioral task.

In addition, we examined the effect on the baseline blood pressure after muscimol injection of CeA. However, there were no significant effects (**Supplementary Figure S4**; ΔMBP, time of injection, p = 0.80; drug (saline and muscimol), p = 0.10; ΔHR, time from injection, p = 0.39; drug (saline and muscimol), p = 0.53) or interactions (ΔMBP, time x drug, p = 0.89; ΔHR, time x drug, p = 0.68; two-way ANOVA).

A previous study reported that the effect of muscimol lasts for up to 3 h (Scheel-Kruger et al., 1977). In the muscimol injection experiments, the average time between the muscimol injection and the end of the task for each session in a day was 198 ± 43 min, which roughly corresponded to the duration of muscimol action. Moreover, we analyzed datasets obtained within 3 h after injection and observed similar effects, namely, a significant attenuation of the pressor response in the reward block (**Supplementary Figure S5A** and **Supplementary Table S3B**, main effect for drug factor, $F_{(1,160)}$ = 7.19, p = 0.008, main effect for trial factor, $F_{(15,160)}$ = 4.43, p < 0.001, no interaction between drug and trial factors $F_{(15,160)}$ = 0.77, p = 0.71, two-way ANOVA). When the analysis was limited and datasets were obtained within 2 h after injection, similar results were observed (**Supplementary Figure S5B** and **Supplementary Table S3C**, main effect for drug factor, $F_{(1,160)}$ = 10.06, p = 0.0018, main effect for trial factor, $F_{(15,160)}$ = 3.36, p < 0.0001, no interaction between drug and trial factors, $F_{(15,160)}$ = 0.53, p = 0.92, two-way ANOVA). In addition, to examine the sequential effects of muscimol and saline injections, we analyzed the effects of

drugs on blood pressure responses before and after the reward block switching in separate datasets in all six rats: 1) a dataset including a muscimol injection session followed by a saline injection session ("muscimol→saline" dataset), and 2) another dataset including a saline injection session followed by a muscimol injection session ("saline→muscimol" dataset). Consistent with our results as shown previously, a significant main effect of the drug was observed in both injection datasets (**Supplementary Figure S5C**, "muscimol→saline," $F_{(1,160)} = 5.08$, $p = 0.025$; **Supplementary Figure S5D**, "saline→muscimol," $F_{(1,160)} = 13.94$, $p = 0.0003$).

Furthermore, we examined the effects of CeA inactivation on blood pressure responses to the actual outcome, US+. CeA inactivation by the muscimol injection showed a decreasing trend in US+ response (0–5 s after US+ onset), but the effect was not significant on the main effects for drug factors (**Supplementary Figure S6**, $F_{(1,160)} = 2.98$, $p = 0.086$, two-way ANOVA).

DISCUSSION

The present study showed that reward prediction increased blood pressure. Switching condition blocks provoked a rapid regulation of the blood pressure. Furthermore, blocking the activity of CeA impaired the pressor responses induced by reward condition block. We demonstrated that cardiovascular responses were adaptively and rapidly regulated by positive emotional stimuli and CeA might have contributed to the adaptive regulation of the blood pressure.

A phasic and gradual increase of the blood pressure was observed in response to reward-predictive cues. The blood pressure responses were maintained in lower-licking trials. Both the blood pressure and heart rate increased with the licking movement amplitude, suggesting that they were affected by orofacial licking movements including changes in muscle activity and breathing. However, at least the blood pressure might be regulated by additional factors such as emotion.

Previous studies have reported cardiovascular responses during classical conditioning tasks using free-moving and restrained animals from several species, such as pigeons (Cohen and Durkovic, 1966), rabbits (Pascoe and Kapp, 1985; Powell et al., 1997), dogs (Dykman and Gantt, 1956; Obrist and Webb, 1967; Anderson and Brady, 1972), rodents (Holdstock and Schwartzbaum, 1965; Iwata and LeDoux, 1988; Shabel and Janak, 2009; Shabel et al., 2011), marmosets (Braesicke et al., 2005; Mikheenko et al., 2010), macaques (Randall et al., 1975), and humans (Hastings and Obrist, 1967; Wexler and De Leon, 1979). Appetitive conditioning using food or water as a reward US, induces pressor response and tachycardia during the CS–US interval, whereas, in aversive conditioning, using electrical shocks as punishment US often causes pressor response or tachycardia, although some bradycardia responses have been reported (Harris and Brady, 1974; Cohen and Obrist, 1975; Randall et al., 1975). Here, a small decrease in the blood pressure was induced by air-puff predicting CS+. Based on the remarkable cardiovascular responses, air puffs acted as the US (**Figure 2** and **Supplementary Figure S2**). Air-puff predicting CS + might have caused a slight suppression, and not a facilitation, of the cardiovascular responses because of the overtraining of animals, which could not avoid the punishment (e.g., learned helplessness), in the classical conditioning procedures. The lower response levels of aversive CS+ is that the air puff has been caused by the mildness of the stimulus compared with electrical shock and/or by a floor effect. In the present study, we used a neutral block in which CS+ was associated with no outcome as a different measure from the reward block. Because the activity of midbrain dopaminergic neurons encoding reward-prediction error signals decreases in no-reward-prediction cues (Matsumoto and Hikosaka, 2009), no outcome conditions might function as an aversive, rather than a neutral measure.

The roles of the amygdala in classical conditioning have already been examined, particularly in fear conditioning of free-moving animals. CeA has anatomical connections with various regions, such as the lateral hypothalamus, midbrain periaqueductal gray, locus coeruleus, and brainstem, to regulate autonomic and endocrine functions to promote defensive behaviors (such as attack, escape, and freeze) (Davis, 1992). Bilateral lesions to the amygdala attenuate responses associated with sympathetic excitation (pressor, tachycardia, and sympathetic cutaneous vasomotor alerting responses) induced by appetitive (Braesicke et al., 2005) and aversive (Iwata et al., 1986; LeDoux et al., 1990; Mikheenko et al., 2010) conditioning and unconditioning salient stimuli (Mohammed et al., 2013) in free-moving animals. These findings suggest that the amygdala is involved in autonomic arousal in emotional processing. Several studies have examined either appetitive or aversive condition blocks; however, little is known concerning autonomic tuning during dynamical alternations between appetitive and aversive conditions. Furthermore, it has been shown that disinhibition of CeA using bicuculline induced pressor and tachycardiac responses under anesthesia (Yamanaka et al., 2018), and the blockage of the amygdala by muscimol induced acute cutaneous vasodilatations and impaired sympathetic cutaneous vasoconstrictor alerting-responses under natural unconditioning situations (Mohammed et al., 2013). Our results are consistent with the previous findings that show that the amygdala (CeA) plays an important role in accelerating the blood pressure in response to salient stimuli (Iwata et al., 1986; LeDoux et al., 1990; Braesicke et al., 2005; Mikheenko et al., 2010; Mohammed et al., 2013).

The lack of significant changes in the cardiovascular responses to aversive-predicting cues activated by the amygdala is a limitation in the present study. This result might be caused by the imbalanced impact of the outcomes between the reward and relatively mild air puff, even though air puffs (air jets) are used as aversive stimuli (Knapp and Pohorecky, 1995; Belova et al., 2007; Cohen et al., 2012; Furlong et al., 2014). In addition, repeated air-puff stimulation has also been reported to cause habituation (Knapp and Pohorecky, 1995). To solve these problems, it is necessary to focus on earlier periods before habituation occurs, or

by using different types of aversive stimuli such as electrical shock. There were several problems with the pharmacological method in this study that were required to manipulate the neuronal activity, which might have resulted in a non-specific manipulation of neuronal circuits, variations in the injection site accuracy by diffusion of the drugs, and low temporal resolution of neuronal manipulation. Whether the attenuation of the predictive-pressor response elicited by CeA inactivation is caused by forgetting of the associative memory or by the inhibition of the autonomic drive based on memory although memory remains, is not clear in this study. To solve these problems, future studies are necessary to examine CeA-specific genetic manipulation using optogenetics and/or chemogenetics.

Our findings showed cardiovascular regulation and the involvement of CeA in dynamically changing CS–US associations. However, CeA is not the only contributor to the formation of predictive circulatory responses. The characteristic blood pressure responses rapidly (after a few trials) adapt immediately after condition block switching. Such a rapid switch is reminiscent of the activity of neurons of the amygdala (Belova et al., 2007), striatum (Lauwereyns et al., 2002), and of midbrain dopaminergic neurons (Roesch et al., 2007). Blockade of the dopamine D1 receptor in the striatum impairs context-dependent behavioral responses (Nakamura and Hikosaka, 2006; Ueda et al., 2017). The artificial inhibition of midbrain dopaminergic neurons during the fear-to-safety context switch induced a delay in the extinction of fear-conditioning behavior (Luo et al., 2018). In addition, dopaminergic neuron activity has also been reported to contribute to the prediction of reward and aversion stimuli (Matsumoto and Hikosaka, 2009; Moriya et al., 2018). Anatomically, the amygdala receives dopaminergic inputs (Garris and Wightman, 1995). There is a direct projection from the amygdala (basolateral region) to the striatum, whereas the projection from the striatum to the amygdala is believed to be polysynaptic. The activities of striatal neurons increase in response to reward-predicting cues, whereas they are attenuated by the blockade of the amygdala (Ambroggi et al., 2008). Therefore, the condition-dependent cardiovascular responses observed in the present study might reflect the differences in the outcome expectation, which are dependent on the functional interactions between the amygdala and striatum via dopaminergic inputs (Averbeck and Costa, 2017). Future studies should examine the functions of neuronal circuits potentially supporting and regulating the emotional expression suitable to a dynamically changing environment.

DATA AVAILABILITY STATEMENT

The raw data supporting the conclusion of this article will be made available by the authors, without undue reservation.

ETHICS STATEMENT

The animal study was reviewed and approved by the Ethics Committee for Animal Experiments at Juntendo University.

AUTHOR CONTRIBUTIONS

KY and HW designed the research; KY conducted the experiments; KY analyzed the data; and KY and HW wrote and reviewed the manuscript.

FUNDING

This work was supported by Grant-in-Aid for Scientific Research (C) 20K11396, (B) 19K22582, Young Scientists (B) 16K16485, Exploratory Research 19K22582 (to KY), the Joint Research Program of Juntendo University, Faculty of Health and Sports Science (to KY), MEXT-Supported Program for the Strategic Research Foundation at Private Universities, 2014-2018 (to HW), and the Private University Research Branding Project (to HW).

ACKNOWLEDGMENTS

We thank Drs. K. Nakamura, K. Enomoto and S. Nonomura for helpful comments and M. Koizumi and Y. Ueda for helping with the experimental setup. We are grateful to W. Kurosaka, G. Saito, A. Nakagawa, K. Tsukioka, and J. Kim for valuable discussion. The previous version of manuscript has been released in Research Square (DOI: 10.21203/rs.3.rs-109253/v2) as a preprint (Yamanaka and Waki, 2021).

SUPPLEMENTARY MATERIAL

The Supplementary Material for this article can be found online at: https://www.frontiersin.org/articles/10.3389/fphys.2022.820112/full#supplementary-material

REFERENCES

Ambroggi, F., Ishikawa, A., Fields, H. L., and Nicola, S. M. (2008). Basolateral Amygdala Neurons Facilitate Reward-Seeking Behavior by Exciting Nucleus Accumbens Neurons. *Neuron* 59, 648–661. doi:10.1016/j.neuron.2008.07.004

Anderson, D. E., and Brady, J. V. (1972). Differential Preparatory Cardiovascular Responses to Aversive and Appetitive Behavioral Conditioning. *Cond. Reflex* 7, 82–96. doi:10.1007/bf03000478

Averbeck, B. B., and Costa, V. D. (2017). Motivational Neural Circuits Underlying Reinforcement Learning. *Nat. Neurosci.* 20, 505–512. doi:10.1038/nn.4506

Baxter, M. G., and Murray, E. A. (2002). The Amygdala and Reward. *Nat. Rev. Neurosci.* 3, 563–573. doi:10.1038/nrn875

Belova, M. A., Paton, J. J., Morrison, S. E., and Salzman, C. D. (2007). Expectation Modulates Neural Responses to Pleasant and Aversive Stimuli in Primate Amygdala. *Neuron* 55, 970–984. doi:10.1016/j.neuron.2007.08.004

Braesicke, K., Parkinson, J. A., Reekie, Y., Man, M.-S., Hopewell, L., Pears, A., et al. (2005). Autonomic Arousal in an Appetitive Context in Primates: a Behavioural

and Neural Analysis. *Eur. J. Neurosci.* 21, 1733–1740. doi:10.1111/j.1460-9568.2005.03987.x

Calu, D. J., Roesch, M. R., Haney, R. Z., Holland, P. C., and Schoenbaum, G. (2010). Neural Correlates of Variations in Event Processing during Learning in Central Nucleus of Amygdala. *Neuron* 68, 991–1001. doi:10.1016/j.neuron.2010.11.019

Cohen, D. H., and Durkovic, R. G. (1966). Cardiac and Respiratory Conditioning, Differenatiation, and Extinction in the pigeon. *J. Exp. Anal. Behav.* 9, 681–688. doi:10.1901/jeab.1966.9-681

Cohen, D. H., and Obrist, P. A. (1975). Interactions between Behavior and the Cardiovascular System. *Circ. Res.* 37, 693–706. doi:10.1161/01.res.37.6.693

Cohen, J. Y., Haesler, S., Vong, L., Lowell, B. B., and Uchida, N. (2012). Neuron-Type-Specific Signals for Reward and Punishment in the Ventral Tegmental Area. *Nature* 482, 85–88. doi:10.1038/nature10754

Davis, M. (1992). The Role of the Amygdala in Fear-Potentiated Startle: Implications for Animal Models of Anxiety. *Trends Pharmacol. Sci.* 13, 35–41. doi:10.1016/0165-6147(92)90014-w

Dykman, R. A., and Gantt, W. H. (1956). Relation of Experimental Tachycardia to Amplitude of Motor Activity and Intensity of the Motivating Stimulus. *Am. J. Physiol.-Legacy Content* 185, 495–498. doi:10.1152/ajplegacy.1956.185.3.495

Everitt, B. J., Cardinal, R. N., Parkinson, J. A., and Robbins, T. W. (2003). Appetitive Behavior: Impact of Amygdala-Dependent Mechanisms of Emotional Learning. *Ann. N. Y Acad. Sci.* 985, 233–250. doi:10.1111/j.1749-6632.2003.tb07085.x

Furlong, T. M., Mcdowall, L. M., Horiuchi, J., Polson, J. W., and Dampney, R. A. L. (2014). The Effect of Air Puff Stress on C-Fos Expression in Rat Hypothalamus and Brainstem: central Circuitry Mediating Sympathoexcitation and Baroreflex Resetting. *Eur. J. Neurosci.* 39, 1429–1438. doi:10.1111/ejn.12521

Garris, P. A., and Wightman, R. M. (1995). Distinct Pharmacological Regulation of Evoked Dopamine Efflux in the Amygdala and Striatum of the Rat *In Vivo*. *Synapse* 20, 269–279. doi:10.1002/syn.890200311

Harris, A. H., and Brady, J. V. (1974). Animal Learning-Visceral and Autonomic Conditioning. *Annu. Rev. Psychol.* 25, 107–133. doi:10.1146/annurev.ps.25.020174.000543

Hastings, S. E., and Obrist, P. A. (1967). Heart Rate during Conditioning in Humans: Effect of Varying the Interstimulus (CS-UCS) Interval. *J. Exp. Psychol.* 74, 431–442. doi:10.1037/h0024710

Hilton, S. M., and Zbrożyna, A. W. (1963). Amygdaloid Region for Defence Reactions and its Efferent Pathway to the Brain Stem. *J. Physiol.* 165, 160–173. doi:10.1113/jphysiol.1963.sp007049

Holdstock, T. L., and Schwartzbaum, J. S. (1965). Classical Conditioning of Heart Rate and Galvanic Skin Response in the Rat. *Psychophysiology* 2, 25–38. doi:10.1111/j.1469-8986.1965.tb02631.x

Holland, P. C., and Gallagher, M. (1999). Amygdala Circuitry in Attentional and Representational Processes. *Trends Cogn. Sci.* 3, 65–73. doi:10.1016/s1364-6613(98)01271-6

Iwata, J., and LeDoux, J. E. (1988). Dissociation of Associative and Nonassociative Concomitants of Classical Fear Conditioning in the Freely Behaving Rat. *Behav. Neurosci.* 102, 66–76. doi:10.1037/0735-7044.102.1.66

Iwata, J., Ledoux, J. E., Meeley, M. P., Arneric, S., and Reis, D. J. (1986). Intrinsic Neurons in the Amygdaloid Field Projected to by the Medial Geniculate Body Mediate Emotional Responses Conditioned to Acoustic Stimuli. *Brain Res.* 383, 195–214. doi:10.1016/0006-8993(86)90020-x

Kim, J., Pignatelli, M., Xu, S., Itohara, S., and Tonegawa, S. (2016). Antagonistic Negative and Positive Neurons of the Basolateral Amygdala. *Nat. Neurosci.* 19, 1636–1646. doi:10.1038/nn.4414

Kimura, R., Saiki, A., Fujiwara-Tsukamoto, Y., Ohkubo, F., Kitamura, K., Matsuzaki, M., et al. (2012). Reinforcing Operandum: Rapid and Reliable Learning of Skilled Forelimb Movements by Head-Fixed Rodents. *J. Neurophysiol.* 108, 1781–1792. doi:10.1152/jn.00356.2012

Knapp, D. J., and Pohorecky, L. A. (1995). An Air-Puff Stimulus Method for Elicitation of Ultrasonic Vocalizations in Rats. *J. Neurosci. Methods* 62, 1–5. doi:10.1016/0165-0270(95)00044-5

Lauwereyns, J., Watanabe, K., Coe, B., and Hikosaka, O. (2002). A Neural Correlate of Response Bias in Monkey Caudate Nucleus. *Nature* 418, 413–417. doi:10.1038/nature00892

LeDoux, J., Cicchetti, P., Xagoraris, A., and Romanski, L. (1990). The Lateral Amygdaloid Nucleus: Sensory Interface of the Amygdala in Fear Conditioning. *J. Neurosci.* 10, 1062–1069. doi:10.1523/jneurosci.10-04-01062.1990

Luo, R., Uematsu, A., Weitemier, A., Aquili, L., Koivumaa, J., Mchugh, T. J., et al. (2018). A Dopaminergic Switch for Fear to Safety Transitions. *Nat. Commun.* 9, 2483. doi:10.1038/s41467-018-04784-7

Matsumoto, M., and Hikosaka, O. (2009). Two Types of Dopamine Neuron Distinctly Convey Positive and Negative Motivational Signals. *Nature* 459, 837–841. doi:10.1038/nature08028

Mikheenko, Y., Man, M.-S., Braesicke, K., Johns, M. E., Hill, G., Agustín-Pavón, C., et al. (2010). Autonomic, Behavioral, and Neural Analyses of Mild Conditioned Negative Affect in Marmosets. *Behav. Neurosci.* 124, 192–203. doi:10.1037/a0018868

Mohammed, M., Kulasekara, K., De Menezes, R. C., Ootsuka, Y., and Blessing, W. W. (2013). Inactivation of Neuronal Function in the Amygdaloid Region Reduces Tail Artery Blood Flow Alerting Responses in Conscious Rats. *Neuroscience* 228, 13–22. doi:10.1016/j.neuroscience.2012.10.008

Moriya, S., Yamashita, A., Kawashima, S., Nishi, R., Yamanaka, A., and Kuwaki, T. (2018). Acute Aversive Stimuli Rapidly Increase the Activity of Ventral Tegmental Area Dopamine Neurons in Awake Mice. *Neuroscience* 386, 16–23. doi:10.1016/j.neuroscience.2018.06.027

Nakamura, K., and Hikosaka, O. (2006). Role of Dopamine in the Primate Caudate Nucleus in Reward Modulation of Saccades. *J. Neurosci.* 26, 5360–5369. doi:10.1523/jneurosci.4853-05.2006

Obrist, P. A., and Webb, R. A. (1967). Heart Rate during Conditioning in Dogs: Relationship to Somatic-Motor Activity. *Psychophysiology* 4, 7–34. doi:10.1111/j.1469-8986.1967.tb02733.x

Pascoe, J. P., and Kapp, B. S. (1985). Electrophysiological Characteristics of Amygdaloid central Nucleus Neurons during Pavlovian Fear Conditioning in the Rabbit. *Behav. Brain Res.* 16, 117–133. doi:10.1016/0166-4328(85)90087-7

Paton, J. J., Belova, M. A., Morrison, S. E., and Salzman, C. D. (2006). The Primate Amygdala Represents the Positive and Negative Value of Visual Stimuli during Learning. *Nature* 439, 865–870. doi:10.1038/nature04490

Phelps, E. A., and LeDoux, J. E. (2005). Contributions of the Amygdala to Emotion Processing: from Animal Models to Human Behavior. *Neuron* 48, 175–187. doi:10.1016/j.neuron.2005.09.025

Powell, D. A., Chachich, M., Murphy, V., Mclaughlin, J., Tebbutt, D., and Buchanan, S. L. (1997). Amygdala-prefrontal Interactions and Conditioned Bradycardia in the Rabbit. *Behav. Neurosci.* 111, 1056–1074. doi:10.1037/0735-7044.111.5.1056

Randall, D. C., Brady, J. V., and Martin, K. H. (1975). Cardiovascular Dynamics during Classical Appetitive and Aversive Conditioning in Laboratory Primates. *Pav. J. Biol. Sci.* 10, 66–75. doi:10.1007/bf03001150

Roesch, M. R., Calu, D. J., and Schoenbaum, G. (2007). Dopamine Neurons Encode the Better Option in Rats Deciding between Differently Delayed or Sized Rewards. *Nat. Neurosci.* 10, 1615–1624. doi:10.1038/nn2013

Roesch, M. R., Esber, G. R., Li, J., Daw, N. D., and Schoenbaum, G. (2012). Surprise! Neural Correlates of Pearce-Hall and Rescorla-Wagner Coexist within the Brain. *Eur. J. Neurosci.* 35, 1190–1200. doi:10.1111/j.1460-9568.2011.07986.x

Scheel-Kruger, J., Cools, A. R., and Honig, W. (1977). Muscimol Antagonizes the Ergometrine-Induced Locomotor Activity in Nucleus Accumbens: Evidence for a GABA-Dopaminergic Interaction. *Eur. J. Pharmacol.* 42, 311–313. doi:10.1016/0014-2999(77)90300-4

Shabel, S. J., and Janak, P. H. (2009). Substantial Similarity in Amygdala Neuronal Activity during Conditioned Appetitive and Aversive Emotional Arousal. *Proc. Natl. Acad. Sci. U.S.A.* 106, 15031–15036. doi:10.1073/pnas.0905580106

Shabel, S. J., Schairer, W., Donahue, R. J., Powell, V., and Janak, P. H. (2011). Similar Neural Activity during Fear and Disgust in the Rat Basolateral Amygdala. *PLoS One* 6, e27797. doi:10.1371/journal.pone.0027797

Stotz-Potter, E., Willis, L., and Dimicco, J. (1996). Muscimol Acts in Dorsomedial but Not Paraventricular Hypothalamic Nucleus to Suppress Cardiovascular Effects of Stress. *J. Neurosci.* 16, 1173–1179. doi:10.1523/jneurosci.16-03-01173.1996

Ueda, Y., Yamanaka, K., Noritake, A., Enomoto, K., Matsumoto, N., Yamada, H., et al. (2017). Distinct Functions of the Primate Putamen Direct and Indirect

Pathways in Adaptive Outcome-Based Action Selection. *Front. Neuroanat.* 11, 66. doi:10.3389/fnana.2017.00066

Waki, H., Kasparov, S., Wong, L. F., Murphy, D., Shimizu, T., and Paton, J. F. R. (2003). Chronic Inhibition of Endothelial Nitric Oxide Synthase Activity in Nucleus Tractus Solitarii Enhances Baroreceptor Reflex in Conscious Rats. *J. Physiol.* 546, 233–242. doi:10.1113/jphysiol.2002.030270

Wexler, H. K., and De Leon, G. (1979). Classical Conditioning of Human Systolic Pressure: Replication and Extension Using Three Stimulus Durations. *Pav. J. Biol. Sci.* 14, 20–30. doi:10.1007/bf03001813

Yamanaka, K., and Waki, H. (2021). Regulation of Blood Pressure by the central Nucleus of the Amygdala in Dynamically Changing Appetitive and Aversive Classical Conditioning Tasks in Rats. Research Square [Preprint]. doi:10.21203/rs.3.rs-109253/v2 Available at: https://www.researchsquare.com/article/rs-109253/v2

Yamanaka, K., Takagishi, M., Kim, J., Gouraud, S. S., and Waki, H. (2018). Bidirectional Cardiovascular Responses Evoked by Microstimulation of the Amygdala in Rats. *J. Physiol. Sci.* 68, 233–242. doi:10.1007/s12576-017-0523-2

Conflict of Interest: The authors declare that the research was conducted in the absence of any commercial or financial relationships that could be construed as a potential conflict of interest.

Publisher's Note: All claims expressed in this article are solely those of the authors and do not necessarily represent those of their affiliated organizations, or those of the publisher, the editors, and the reviewers. Any product that may be evaluated in this article, or claim that may be made by its manufacturer, is not guaranteed or endorsed by the publisher.

Copyright © 2022 Yamanaka and Waki. This is an open-access article distributed under the terms of the Creative Commons Attribution License (CC BY). The use, distribution or reproduction in other forums is permitted, provided the original author(s) and the copyright owner(s) are credited and that the original publication in this journal is cited, in accordance with accepted academic practice. No use, distribution or reproduction is permitted which does not comply with these terms.

frontiers | Frontiers in Physiology

MINI REVIEW
published: 29 June 2022
doi: 10.3389/fphys.2022.896425

New Perspectives on Sex Steroid and Mineralocorticoid Receptor Signaling in Cardiac Ischemic Injury

Laura A. Bienvenu[1,2†], *James R. Bell*[3*†], *Kate L. Weeks*[2,4], *Lea M. D. Delbridge*[4‡] *and Morag J. Young*[2,5‡]

[1]Molecular Imaging and Theranostics Laboratory, Baker Heart and Diabetes Institute, Melbourne, VIC, Australia, [2]Baker Department of Cardiometabolic Health, University of Melbourne VIC, Melbourne, VIC, Australia, [3]Department of Microbiology, Anatomy, Physiology and Pharmacology, La Trobe University, Bundoora, VIC, Australia, [4]Department of Anatomy and Physiology, University of Melbourne, Parkville, VIC, Australia, [5]Cardiovascular Endocrinology Laboratory, Baker Heart and Diabetes Institute, Melbourne, VIC, Australia

OPEN ACCESS

Edited by:
James Todd Pearson,
National Cerebral and Cardiovascular Center, Japan

Reviewed by:
Rosemeire Kanashiro-Takeuchi,
University of Miami, United States

***Correspondence:**
James R. Bell
j.bell@latrobe.edu.au

†These authors have contributed equally to this work and share first authorship

‡These authors have contributed equally to this work and share senior authorship

Specialty section:
This article was submitted to Integrative Physiology, a section of the journal Frontiers in Physiology

Received: 15 March 2022
Accepted: 27 May 2022
Published: 29 June 2022

Citation:
Bienvenu LA, Bell JR, Weeks KL, Delbridge LMD and Young MJ (2022) New Perspectives on Sex Steroid and Mineralocorticoid Receptor Signaling in Cardiac Ischemic Injury. Front. Physiol. 13:896425. doi: 10.3389/fphys.2022.896425

The global burden of ischemic heart disease is burgeoning for both men and women. Although advances have been made, the need for new sex-specific therapies targeting key differences in cardiovascular disease outcomes in men and women remains. Mineralocorticoid receptor directed treatments have been successfully used for blood pressure control and heart failure management and represent a potentially valuable therapeutic option for ischemic cardiac events. Clinical and experimental data indicate that mineralocorticoid excess or inappropriate mineralocorticoid receptor (MR) activation exacerbates ischemic damage, and many of the intracellular response pathways activated in ischemia and subsequent reperfusion are regulated by MR. In experimental contexts, where MR are abrogated genetically or mineralocorticoid signaling is suppressed pharmacologically, ischemic injury is alleviated, and reperfusion recovery is enhanced. In the chronic setting, mineralocorticoid signaling induces fibrosis, oxidative stress, and inflammation, which can predispose to ischemic events and exacerbate post-myocardial infarct pathologies. Whilst a range of cardiac cell types are involved in mineralocorticoid-mediated regulation of cardiac function, cardiomyocyte-specific MR signaling pathways are key. Selective inhibition of cardiomyocyte MR signaling improves electromechanical resilience during ischemia and enhances contractile recovery in reperfusion. Emerging evidence suggests that the MR also contribute to sex-specific aspects of ischemic vulnerability. Indeed, MR interactions with sex steroid receptors may differentially regulate myocardial nitric oxide bioavailability in males and females, potentially determining sex-specific post-ischemic outcomes. There is hence considerable impetus for exploration of MR directed, cell specific therapies for both women and men in order to improve ischemic heart disease outcomes.

Keywords: cardiomyocyte, ischemia-reperfusion, mineralocorticoid, sex differences, nitric oxide

INTRODUCTION

Ischemic heart disease is a leading cause of mortality and morbidity for both men and women (Murray et al., 2012; Wong, 2014). Although the burden of ischemic heart disease has steadily decreased in higher-income countries over the past 25 years, the combination of population growth and aging has led to a 35% increase in deaths from ischemic heart disease globally since 1990 (Moran et al., 2014). Ischemic heart disease is most commonly associated with major coronary vessel atherosclerotic occlusion eventuating in myocardial infarction (MI), though impaired microvascular function is increasingly implicated as an underlying mechanism, especially in women (Maric-Bilkan et al., 2016; Mehta et al., 2016). While survival following a sudden cardiac event has improved, the impact of chronic cardiovascular disease post-MI is increasing. Despite new therapeutic interventions significantly improving acute MI survival, the probability of mortality within 5 years after a first MI remains at approximately 50% (Mozaffarian et al., 2015). Women are especially vulnerable to premature death within 1 and 5 years post-MI regardless of age (Mehta et al., 2016), and are more likely to develop heart failure (Leening et al., 2014). A new generation of novel molecular candidate targets for optimal therapeutic interventions in men and women with ischemic heart disease is urgently required. Mineralocorticoid receptor (MR) directed treatments have emerged as a valuable therapeutic approach in this setting (Buonafine et al., 2018). This review focuses on the clinical/pre-clinical evidence relating to MR influence in the myocardium, and the therapeutic potential for MR antagonists in treating or preventing cardiac ischemia and reperfusion injury in both men and women.

MINERALOCORTICOID RECEPTOR ACTIVATION AND CARDIAC ISCHEMIC INJURY

The MR is a steroid hormone receptor present in many cell types within the myocardium (Young and Clyne, 2021). MR activation by endogenous ligands aldosterone and cortisol (corticosterone in rodents) is conveyed by a combination of rapid (within minutes) "non-genomic" MR signaling pathways and "genomic" gene transcription and protein synthesis over hours-days (Alzamora et al., 2000; Hayashi et al., 2008; Nolly et al., 2014; Hermidorff et al., 2017; Ong and Young, 2017). The MR was initially recognized for its role in sodium and water homeostasis which occurs *via* direct regulation of sodium, potassium, and other electrolyte handling proteins in the distal nephron. Extensive experimental and clinical studies have highlighted the direct detrimental impact inappropriate MR activation has on the cardiovascular system (Young and Rickard, 2015).

Increased activation of MR *via* inappropriately elevated mineralocorticoid levels or tissue injury are associated with cardiovascular comorbidity and structural remodeling, including fibrosis and myocardial hypertrophy, thereby predisposing the ischemic heart to poor outcomes (Young and Clyne, 2021). MR antagonists have proven benefit for patients with all cause heart failure, with heart failure post-MI and in patients with moderate heart failure, and show potential for patients with heart failure with preserved ejection fraction (HFpEF) (Pitt et al., 1999; Pitt et al., 2003; Markowitz et al., 2012; Miller and Howlett, 2015). Clinical studies (**Table 1**) indicate that MR antagonists are underutilized and can provide specific benefit for patients with acute MI and high aldosterone levels (Beygui et al., 2009; Rao et al., 2013; Wong et al., 2021). Serum biomarkers for collagen turnover within the RALES and EPHESUS trials indicated MR suppression limits structural remodeling of the extracellular matrix in all cause heart failure and post-MI. However, clinical trials of MR antagonists also suggest that MI classification, heart failure status and timing of MR antagonist administration remain important factors in determining post-MI cardiovascular outcomes (Bulluck et al., 2019; Chen et al., 2021; Mares et al., 2022). The ALBATROSS trial concluded that early MR antagonist administration initiated within 72 h post-MI and prior to the onset of heart failure did not improve patient outcomes and survival six months post-MI (Beygui et al., 2016). In contrast, data from larger cohort populations in combination with results of the REMINDER trial indicated that MR antagonist use reduces the rate of cardiovascular related death irrespective of heart failure status (Beygui et al., 2018). Similarly, the MINIMISE trial reported mixed outcomes in acute ST-segment elevation myocardial infarction (STEMI) patients when MR antagonist was administered immediately prior to reperfusion (Bulluck et al., 2019). In this study infarct size at 3 months was unaffected, while left ventricular remodeling was reduced by MR antagonist therapy. This relative protection from structural remodeling prior to the onset of heart failure post-MI may be key to the benefits observed with MR antagonist administration. With the ongoing development of non-steroidal MR antagonists, additional trials will be required to determine their efficacy in different patient cohorts over an extended period post-MI to improve outcomes.

ISCHEMIA, REPERFUSION, AND THE MINERALOCORTICOID RECEPTOR

The mechanisms that underlie the tissue response to injury during ischemia/reperfusion and the progression to cardiac dysfunction have been studied extensively (Davidson et al., 2019). Interruption of coronary flow to the myocardium impairs cardiomyocyte steady-state metabolism, ultimately leading to dysfunction, arrhythmias, and cell death. The cellular response involves a complex series of events during ischemia can lead to cross-sarcolemmal ion imbalance, activation of stress-responsive intracellular signaling pathways and disruption of critical metabolic processes that contribute to the cardiac pathology. Reperfusion of the myocardium is hence essential to salvage viable myocardium, though this in itself can exacerbate the demise of "at risk" cardiomyocytes (Heusch, 2020). The loss of myocardium culminates in fibrosis and scarring, disrupting normal conduction pathways, which can promote vulnerability to arrhythmia and increase myocardial stiffness. Compensatory hypertrophic growth of the surviving myocardium post-MI maintains functional capacity in the short term, but ultimately the myocardium is unable to compensate for increased wall pressures leading to failure of myocardial pump function and death.

Preclinical and clinical studies further indicate aldosterone excess is a damage provocateur in the ischemic context (**Tables 1** and **2**).

TABLE 1 | Summary of clinical trials assessing MR antagonist intervention outcomes.

Disease	Intervention	Outcomes	References
Heart failure	Spironolactone	↓ deaths, ↓ heart failure hospitalization, improved heart failure symptoms	Pitt et al. (1999)
Heart failure post-MI	Eplerenone	↓ deaths/cardiovascular deaths, ↓ cardiovascular deaths and hospitalization	Pitt et al. (2003)
Post-MI	Spironolactone (at reperfusion)	no benefits (vs. standard therapy)	Beygui et al. (2016)
Post-STEMI	MR antagonist (meta-analysis)	↓ all-cause deaths	Beygui et al. (2018)
Post-STEMI	Spironolactone (at reperfusion)	no effect on MI size, improved LV EDV and ESV	Bullock et al. (2019)
Post-MI	MR antagonist (meta-analysis)	↓ all-cause deaths, ↓ cardiovascular event incidence	Chen et al. (2021)
Post-STEMI	MR antagonist (meta-analysis)	↓ all-cause deaths, ↑ LV ejection fraction	

MI, myocardial infarction; STEMI, ST-elevation myocardial infarction; LV, left ventricle; EDV, end-diastolic volume; ESV, end-systolic volume; ↑, increase; ↓, decrease

TABLE 2 | Summary of MR and sex-specific modulation of cardiac structure and function.

Model	Treatment	Intervention	Animal	Sex	Major findings			References
					Fibrosis	Inflammation	Function	
ER modulation								
WT	Aldo/salt	+ERα +ERβ	Rat	F only	↓ perivascular	↓ OPN		Vasan et al. (2004)
Cardiomyocyte-specific ERα overexpression		MI	Mouse	M vs. F	↓ LV (F only)	↑ p-JNK (F only)		Westerman et al. (2016)
Cardiomyocyte-specific ERβ overexpression		Coronary artery ligation	Mouse	M vs. F	↓remote LV (M only)		↑ ejection fraction ↑ diastolic function (F = M)	Kanashiro-Takeuchi et al. (2009)
ERβ deficient	DOC/salt		Mouse	M vs. F	↑ LV (F vs. M)			Gurgen et al. (2011)
MR modulation								
WT	Eplerenone	MI	Rat	M vs. F	↓ LV (F only)		↑ ejection fraction (F only)	Usher et al. (2010)
ERβ knockout	DOC/salt		Mouse	M vs. F	↑ LV (F only)			Lombès et al. (1995)
WT	DOC/salt +/- mTOR-I		Mouse	M vs. F	↑ LV (F only)	↓ (F only)	↑ ejection fraction (M only)	Grohe et al. (1997)
WT	Chronic NO deficiency (*in vivo*)	Acute I/R (*ex vivo*)	Mouse	M vs. F	↑ LV (M = F)	↑ (M = F)	↓ systolic function (F only)	Usher et al. (2010)
Cardiomyocyte-specific MR knockout	Chronic NO deficiency (*in vivo*)	Acute I/R (*ex vivo*)	Mouse	WT vs. KO	↓ LV (KO only)	↓ (KO only)	↑ systolic function (KO only)	Usher et al. (2010)

WT, wild type; Aldo/salt, aldosterone/salt treatment; ERα, estrogen receptor alpha; ERβ, estrogen receptor beta; F, female; M, male; OPN, osteopontin; MI, myocardial infarction; LV, left ventricle; p-JKN, phosphorylated c-Jun N-terminal kinase; DOC/salt, deoxycorticosterone/salt; mTOR-I, mammalian target of rapamycin inhibition; MR, mineralocorticoid receptor; NO, nitric oxide; I/R, ischemia/reperfusion; KO, knockout; ↑, increase; ↓, decrease; = , equal; +, activation; -, inhibition

Stimulation of MR by cortisol or aldosterone increase infarct size in *ex vivo* rat hearts even at low doses (Mihailidou et al., 2009), *via* mechanisms that are at least partly attributable to greater cardiomyocyte apoptotic vulnerability. Cardiomyocytes demonstrate aldosterone-induced apoptosis *via* rapid activation of calcineurin and NADPH oxidase/apoptosis signal-regulating kinase one signaling complexes (ASK1) (Mano et al., 2004; Hayashi et al., 2008). The activated MR also mediates upregulation of Ca^{2+} influx that augments cardiomyocyte apoptosis (Ferron et al., 2011). These detrimental actions are exacerbated by MR potentiation of reactive fibrotic remodeling (Brilla and Weber, 1992; Brilla, 2000; Rickard et al., 2009). Exposure of rodents to exogenous mineralocorticoids upregulates transcription of genes underlying extracellular matrix turnover and cardiac remodeling signaling cascades (Rude et al., 2005; Tsai et al., 2013). Together, these findings highlight the potential for MR inhibition to minimize myocardial remodeling following ischemia/reperfusion injury *via* both genomic and potentially non-genomic pathways.

Pre-Ischemic Regulation of Mineralocorticoid Receptor Activity

Many studies have assessed the conditioning capacity of pharmacological agents to minimize injury when administered

prior to the ischemic insult. Both long-term and acute inhibition of MR prior to an ischemic event has been shown to be beneficial. Spironolactone administered to rats for 1 month minimized ischemic contracture in isolated hearts subjected to 25 min low-flow ischemia (Rochetaing et al., 2003), indicating a Ca^{2+}-dependent mechanism underlying greater myocardial tolerance to the ischemic challenge. During reperfusion, hearts from rats receiving spironolactone exhibited greater functional recovery and less ventricular arrhythmias. Similarly, hearts perfused with 1 μM eplerenone immediately prior ischemia exhibited improved functional recovery in reperfusion and reduced infarct size (Chai et al., 2005). Paradoxically, aldosterone administered prior to ischemia has also been shown to significantly improve contractile function in reperfusion (Yoshino et al., 2014). This observation appears to be mediated by an MR-independent mechanism, for example *via* rapid activation of p38-MAPK which is an important mediator of ischemic preconditioning (Bassi et al., 2008; Bell et al., 2008).

Targeting Reperfusion Injury—A Role for Pharmacological Regulation of the Mineralocorticoid Receptor

Studies administering pharmacological agents prior to an ischemic insult have both provided considerable insight into the mechanisms of ischemia/reperfusion and identified numerous conditioning agents that could benefit patients undergoing cardiac surgery (Venugopal et al., 2009). However, the practical application of such agents in the clinical setting of a sudden, major ischemic event is very limited and the development of cardioprotective agents that can be administered at the time of reperfusion is a top priority.

Early studies showed that treatment with MR antagonists post-MI had little or no effect on the progression of infarct-healing but can prevent development of reactive fibrosis in the viable rodent myocardium (Delyani et al., 2001; Mill et al., 2003). However, in subsequent studies MR antagonists were found to be functionally beneficial following *in vivo*-MI in rodents for reducing fibrosis of viable myocardium, abrogating increases in left ventricular end diastolic pressure and left ventricular end diastolic volume, and maintaining left ventricular function (Cittadini et al., 2003; Fraccarollo et al., 2003; Fraccarollo et al., 2005). Eplerenone administered post-MI also reduces the onset and progress of cardiac tissue fibrosis (myocardial and aortic), enhances left ventricle ejection fraction and cardiac output, and limits left ventricle systolic area and weight independently of blood pressure (Masson et al., 2004; Wang et al., 2004). Thus, the timing of MR antagonist therapy is key to the functional and gene expression outcome *in vivo*. In addition to fibrotic and functional outcomes, MR blockers improve neovascular formation and reduce thinning and dilation of infarcted myocardial walls at early (3 days) and late (7 weeks) time points in experimental rodents. This action underpins the improvement in ventricular wall function and is associated with transient up-regulation of monocyte chemoattractant protein 1 (MCP-1), early monocyte and macrophage infiltration and expression of tumour necrosis factor alpha (TNFα) (Fraccarollo et al., 2008). These beneficial outcomes are mirrored in transgenic mice lacking the MR in cardiomyocytes, underscoring the central role of the receptor for the cardiomyocyte response to ischemia/reperfusion and are discussed further below (Fraccarollo et al., 2011).

Investigation of the effects of MR suppression on global remodeling of the left ventricular chamber have reported variable findings. In a rat model of MI, spironolactone showed no benefit for reducing left ventricle cardiac chamber mass index and wall thickness despite reduced cardiomyocyte cross sectional area and less fibrosis (Enomoto et al., 2005). Whereas other studies show reversal of left ventricle dilation and dysfunction with MR blockade post-MI *via* mechanisms that include suppression of NADPH oxidase and mitochondrial superoxide production (Matsumoto et al., 2004).

Genetic Manipulation of Mineralocorticoid Receptor Signaling Reveals Ischemic Vulnerability

To more precisely understand the specific myocardial cell types involved in mediating MR-dependent adverse and beneficial outcomes, targeted genetic manipulation studies have proved to be particularly informative (**Table 2**). Initial MR deletion mouse models were homologous MR knockout, which displayed neonatal lethality due to sodium wasting (Berger et al., 1998). Subsequent studies focused on genetic manipulation of MR in specific cell types, including macrophages, vascular smooth muscle, endothelial and cardiomyocytes (Young and Rickard, 2015). The cardiomyocyte MR knockout mouse (myo-MRKO) has demonstrated a range of novel and important actions of the MR in the regulation of the tissue response to cardiac ischemia including promoting an appropriate wound healing response in the infarct zone, enhanced neovascularization of the scar and maintenance of the microvascular capillary network, which together support cardiac functional recovery and long term viability (Fraccarollo et al., 2011).

Our studies subjecting *ex vivo* myo-MRKO hearts to an acute IR challenge demonstrated improved contractile functional recovery and lower vulnerability to arrhythmias compared with wild-type controls (Bienvenu et al., 2015). This was associated with reduced expression of the sodium-hydrogen exchanger (NHE-1) and reduced CaMKII autophosphorylation, both of which are predicted to minimize cardiomyocyte Na^+ and Ca^{2+} loading and suppress cardiac dysfunction in IR (Bell et al., 2014; Mattiazzi et al., 2015; Shattock et al., 2015). Genetic inhibition of CaMKII combined with MR antagonist treatment improved functional recovery and reduced diffuse fibrosis, suggesting that targeting both pathways can potentially improve contractile performance and reduce arrhythmic activity (Driessen et al., 2020). In a chronic model of MI, suppressing cardiomyocyte MR signaling was also beneficial. Targeted ablation of cardiomyocyte MR did not affect infarct size *in vivo*, yet morphological changes were minimized, and ventricular function better maintained in the subsequent 8 weeks post-MI (Fraccarollo et al., 2011). Expression of genes associated with hypertrophy, stiffness and fibrosis was

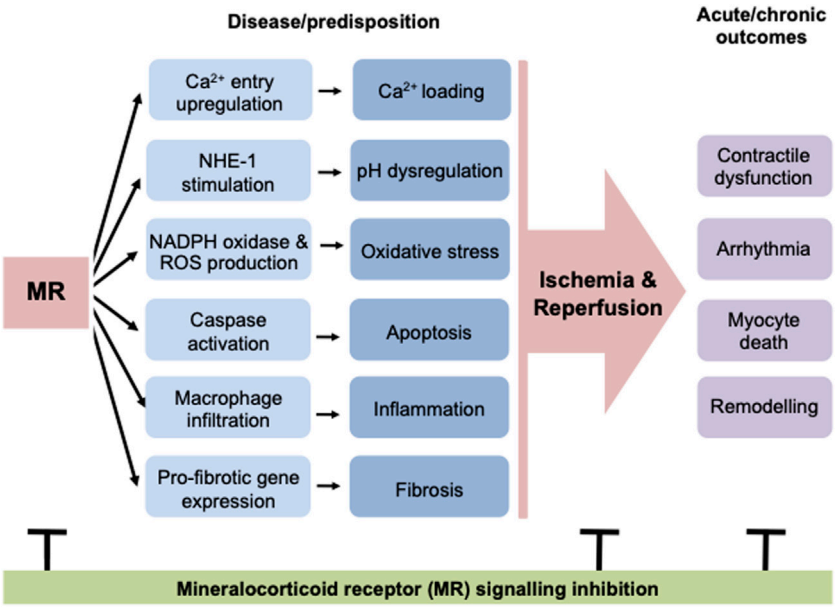

FIGURE 1 | MR activation leads to many detrimental changes in the heart, including cardiomyocyte cell death, inflammation and fibrosis. In addition to these structural changes, MR signaling leads to stimulation of calcium and sodium flux in cardiomyocytes, predisposing these cells to calcium loading and pH dysregulation. Overall these modulations of basal cardiac structure and function predispose the heart to ischemic events and result in worse outcomes after ischemia/reperfusion, increasing the incidence of contractile dysfunction and arrhythmia and also increasing cell death and consequently reactive fibrosis. The negative impacts of MR activation at a structural and functional level can be abrogated at early and late timepoints, both before and after an ischemic event. MR, mineralocorticoid receptor; NHE-1, sodium hydrogen exchanger-1; ROS, reactive oxygen species.

lower in surviving myocardium from myo-MRKO mice and myocardial/mitochondrial superoxide production was diminished (Fraccarollo et al., 2011). The authors concluded that a suppressed NFκB-mediated inflammatory response was key to minimizing apoptosis and enhancing healing in these mice.

Deletion of MR in other specific cell types of the myocardium (vascular smooth muscle, endothelial, macrophage cells) demonstrate cell-specific regulation of myocardial injury and repair pathways in a manner that would be predicted to confer protection in the ischemic setting (Bienvenu et al., 2012; Gueret et al., 2016; Fraccarollo et al., 2019). This demonstrates the importance of MR signaling across numerous cardiac cell types in the ischemic context. This may be critical to determining how targeting MR signaling may be optimized post-MI. Further studies are hence required to explore in greater detail how MR-mediated regulation of different cell populations within the heart interact to determine the functional and morphological responses to IR (**Figure 1**).

MINERALOCORTICOID RECEPTOR SIGNALING, SEX SPECIFICITY AND CARDIOPROTECTION

The incidence of cardiovascular disease (and more specifically ischemic heart disease) differs between the sexes, with earlier onset in men and increasing incidence in women post-menopause (Leening et al., 2014). Men and women exhibit differences in symptom presentation, efficacy of diagnosis and response to interventions (McSweeney et al., 2016). More specifically, in relation to myocardial infarction, sex-specific differences in pathophysiological mechanisms and outcomes is now being emphasized (Mehta et al., 2016). Women are more likely to develop heart failure after an acute MI, underscoring the need for new strategies and therapies to adequately address long term MI recovery in both sexes (Westerman and Wenger, 2016).

Most clinical studies assessing suppression of MR signaling have involved predominantly male cohorts, and even though data are adjusted to consider sex as a covariate, differences in clinical outcomes between men and women may not be observed (Pitt et al., 2003; Kanashiro-Takeuchi et al., 2009; Nicolaou, 2021). Moreover, serum aldosterone levels have been strongly correlated with left ventricular mass in females, but not males even when serum aldosterone levels are not elevated and the MR inhibitory effect of progesterone is taken into consideration (Vasan et al., 2004). Given the importance of cardiac hypertrophy and serum aldosterone levels as independent cardiovascular disease risk factors, this observation indicates that some of the differences observed for males and females in the clinical setting may also have an MR-dependent mechanism. Endothelial MR expression has been shown to be higher in female vessel wall, when compared with males (Faulkner et al., 2019). This observation reflects the fact that females have higher circulating levels of progesterone which is a natural antagonist of the MR and estrogen acting *via* the ERα inhibits MR activation. Higher

aldosterone levels and potentially tissue expression of MR in females is likely to be compensatory in premenopausal women.

Steroid hormone ligands for both receptors derive from the same cholesterol-derived progestogen pre-cursors. Relative levels of corticosteroids and sex steroids are hence closely linked. It is well established that estrogen receptors (ER) and MR are co-expressed in cardiomyocytes, fibroblasts and vascular cells (Lombès et al., 1995; Grohe et al., 1997), and that these can modulate cardiac structure and function in settings of IR. Transgenic animal models have shown that female hearts overexpressing ERα receptor subtype are relatively protected from MI-induced fibrosis and exhibit improved neovascularization (Mahmoodzadeh et al., 2014). Overexpression of the ERβ receptor subtype improves survival and cardiac function post-MI in both sexes, due in part to reduced disturbance of cardiomyocyte intracellular Ca^{2+} store management (Bell et al., 2013). In male hearts specifically, functional improvement was related to a lower level of cardiac fibrosis highlighting the role of ERβ in post-infarct remodeling (Schuster et al., 2016). In rodent models activation of both ERα and ERβ protects against the detrimental blood pressure, fibrotic and hypertrophic effects of mineralocorticoid excess (Arias-Loza et al., 2007). For example, deoxycorticosterone/salt-induced cardiovascular damage is reduced in females with intact ER signaling. Whereas genetic ablation of ERβ signaling produces a differential response to mineralocorticoid excess-induced cardiac fibrosis associated with mTOR (mammalian target of rapamycin) activation in both male and female mice (Gurgen et al., 2011; Gurgen et al., 2013). Moreover, the transcriptional activity of vascular MR can be inhibited by ERα, suggesting that MR/ER interactions contribute to the mechanisms of sex differences in cardiac MR activity (Barrett Mueller et al., 2014; Biwer et al., 2021). Rapid aldosterone effects may also be medicated by the G-protein coupled ER, though evidence of direct aldosterone binding remains contentious (Rossol-Haseroth et al., 2004; Michea et al., 2005; Gros et al., 2011; Gros et al., 2013). An important consideration moving forward will be developing a more detailed understanding of the nature of the interaction of MR with all ER subtypes in influencing genomic and rapid activation signaling pathways (Funder, 2011).

Experimental studies that specifically address sex-difference in MR involvement in cardiac ischemia are limited but some important leads have been reported. Suppression of MR signaling in rodents by eplerenone administered after MI has been shown to achieve more effective attenuation of left ventricular end diastolic volume enlargement in female compared to male hearts (Kanashiro-Takeuchi et al., 2009). Additionally, LV ejection fraction was increased in female hearts. Transcriptome analysis revealed that for female hearts, eplerenone reversed transcriptional responses for 19% of down regulated genes and for 44% of up-regulated genes, whereas only 4% of genes up-regulated in male hearts responded to eplerenone. These data indicate that MR blockade may preferentially reduce structural and functional changes in female hearts through initiation of specific transcriptional responses (Kanashiro-Takeuchi et al., 2009).

Nitric oxide (NO) signaling is known to be important in mediating cardioprotection (Griffiths et al., 2021)—and there is clear evidence of MR involvement in NO modulation in endothelial and other cell types. Heart failure is associated with low levels of bioavailable NO, and clinical evidence indicates sex differences in NO mediated responses (Zamani et al., 2015). In addition, an imbalance of NO levels has been shown to be a key component in the development of heart failure with preserved ejection fraction in males, but not necessarily females (Schiattarella et al., 2019; Tong et al., 2019). There is extensive experimental evidence to indicate that in female cardiac disease states, NO production and involvement in ROS modulation is important (Murphy et al., 2011; Casin et al., 2018). Targeting NO bioavailability is therefore considered an attractive target for sex-specific therapies in heart failure, but less is known about possible benefits in ischemic disease states. Given that there is evidence for an MR-NO signaling link in endothelial cells, regulating the MR has the potential to optimize NO conditions and support cardiomyocyte protection during cardiac ischemia/reperfusion (Jia et al., 2016; Victorio et al., 2016). Our experimental findings have shown that after chronic *in vivo* treatment with an NO-synthase inhibitor, male and female cardiomyocyte specific MR-KO mice exhibit different cardiac *ex vivo* responses. While female hearts showed MR-dependent abrogation of NO-deficiency induced ischemic injury (reperfusion arrhythmia, diastolic dysfunction and impaired contractile recovery), male animals did not exhibit a similar MR-NO deficiency response interaction (Bienvenu et al., 2017). More recently, it has been shown that ERα mediated NO production can abrogate the detrimental impact of MR activation in the microvasculature of obese female rodents, highlighting the interplay between MR and ER in the endothelium (Biwer et al., 2021). Further work is required to define the nature of the signaling relationship between MR, ER, and NO in order to effectively exploit this signaling axis for therapeutic outcomes in tissue injury due to ischemia and reperfusion.

CONCLUSION

In this review, the accumulating clinical and preclinical data indicating important involvement of MR signaling in mediating both acute and longer term cardiac ischemic damage have been considered. Whilst a range of cardiac cell types are involved (macrophages, endothelial, and vascular smooth muscle), the cardiomyocyte-specific mineralocorticoid signaling pathways appear to be key. Evidence supports a role for increased aldosterone levels and MR activation in mediating sex-specific aspects of ischemic vulnerability through MR-ER receptor interactions providing important insights into ischemic heart disease in women. While early clinical trials of MRA showed equal protection for heart failure in females as well as males, discrepancies remain between translation of experimental outcomes and observed clinical sex-differences in the etiology and diagnosis of heart failure. Thus, there is considerable impetus for exploration of mineralocorticoid-directed, cell-specific therapies for both women and men in order to improve ischemic heart disease

outcomes. Specific, ongoing challenges involve dissecting the integrative nature of the MR-ER-NO signaling axis so that sex-specific therapies can be identified to address both acute and chronic phases of ischemic injury. In this setting, preclinical mechanistic investigations of cell specific MR interactions with pathways regulating ischemia injury have considerable capacity to inform ongoing clinical studies.

AUTHOR CONTRIBUTIONS

LB and JB contributed equally to this manuscript and share first authorship. LD and MY contributed equally to this manuscript and share senior authorship. All authors (LB, JB, KW, LD, MY) contributed to the drafting of the manuscript and approved the submitted version.

REFERENCES

Alzamora, R., Michea, L., and Marusic, E. T. (2000). Role of 11β-Hydroxysteroid Dehydrogenase in Nongenomic Aldosterone Effects in Human Arteries. *Hypertension* 35 (5), 1099–1104. doi:10.1161/01.hyp.35.5.1099

Arias-Loza, P.-A., Hu, K., Dienesch, C., Mehlich, A. M., König, S., Jazbutyte, V., et al. (2007). Both Estrogen Receptor Subtypes, α and β, Attenuate Cardiovascular Remodeling in Aldosterone Salt-Treated Rats. *Hypertension* 50 (2), 432–438. doi:10.1161/HYPERTENSIONAHA.106.084798

Barrett Mueller, K., Lu, Q., Mohammad, N. N., Luu, V., McCurley, A., Williams, G. H., et al. (2014). Estrogen Receptor Inhibits Mineralocorticoid Receptor Transcriptional Regulatory Function. *Endocrinology* 155 (11), 4461–4472. doi:10.1210/en.2014-1270

Bassi, R., Heads, R., Marber, M., and Clark, J. (2008). Targeting P38-MAPK in the Ischaemic Heart: Kill or Cure? *Curr. Opin. Pharmacol.* 8 (2), 141–146. doi:10.1016/j.coph.2008.01.002

Bell, J. R., Bernasochi, G. B., Varma, U., Raaijmakers, A. J. A., and Delbridge, L. M. D. (2013). Sex and Sex Hormones in Cardiac Stress-Mechanistic Insights. *J. Steroid Biochem. Mol. Biol.* 137, 124–135. doi:10.1016/j.jsbmb.2013.05.015

Bell, J. R., Eaton, P., and Shattock, M. J. (2008). Role of P38-Mitogen-Activated Protein Kinase in Ischaemic Preconditioning in Rat Heart. *Clin. Exp. Pharmacol. Physiol.* 35 (2), 126–134. doi:10.1111/j.1440-1681.2007.04794

Bell, J. R., Vila-Petroff, M., and Delbridge, L. M. D. (2014). CaMKII-dependent Responses to Ischemia and Reperfusion Challenges in the Heart. *Front. Pharmacol.* 5, 96. doi:10.3389/fphar.2014.00096

Berger, S., Bleich, M., Schmid, W., Cole, T. J., Peters, J., Watanabe, H., et al. (1998). Mineralocorticoid Receptor Knockout Mice: Pathophysiology of Na + Metabolism. *Proc. Natl. Acad. Sci. U.S.A.* 95 (16), 9424–9429. doi:10.1073/pnas.95.16.9424

Beygui, F., Cayla, G., Roule, V., Roubille, F., Delarche, N., Silvain, J., et al. (2016). Early Aldosterone Blockade in Acute Myocardial Infarction. *J. Am. Coll. Cardiol.* 67 (16), 1917–1927. doi:10.1016/j.jacc.2016.02.033

Beygui, F., Montalescot, G., Vicaut, E., Rouanet, S., Van Belle, E., Baulac, C., et al. (2009). Aldosterone and long-term outcome after myocardial infarction: A substudy of the French nationwide Observatoire sur la Prise en charge hospitalière, l'Evolution à un an et les caRactéristiques de patients présentant un infArctus du myocarde avec ou sans onde Q (OPERA) study. *Am. Heart J.* 157 (4), 680–687. doi:10.1016/j.ahj.2008.12.013

Beygui, F., Van Belle, E., Ecollan, P., Machecourt, J., Hamm, C. W., Lopez De Sa, E., et al. (2018). Individual Participant Data Analysis of Two Trials on Aldosterone Blockade in Myocardial Infarction. *Heart* 104 (22), 1843–1849. doi:10.1136/heartjnl-2018-312950

Bienvenu, L. A., Morgan, J., Reichelt, M. E., Delbridge, L. M. D., and Young, M. J. (2017). Chronic *In Vivo* Nitric Oxide Deficiency Impairs Cardiac Functional Recovery after Ischemia in Female (But Not Male) Mice. *J. Mol. Cell. Cardiol.* 112, 8–15. doi:10.1016/j.yjmcc.2017.08.012

Bienvenu, L. A., Morgan, J., Rickard, A. J., Tesch, G. H., Cranston, G. A., Fletcher, E. K., et al. (2012). Macrophage Mineralocorticoid Receptor Signaling Plays a Key Role in Aldosterone-independent Cardiac Fibrosis. *Endocrinology* 153 (7), 3416–3425. doi:10.1210/en.2011-2098

Bienvenu, L. A., Reichelt, M. E., Morgan, J., Fletcher, E. K., Bell, J. R., Rickard, A. J., et al. (2015). Cardiomyocyte Mineralocorticoid Receptor Activation Impairs Acute Cardiac Functional Recovery after Ischemic Insult. *Hypertension* 66 (5), 970–977. doi:10.1161/HYPERTENSIONAHA.115.05981

Biwer, L. A., Carvajal, B. V., Lu, Q., Man, J. J., and Jaffe, I. Z. (2021). Mineralocorticoid and Estrogen Receptors in Endothelial Cells Coordinately Regulate Microvascular Function in Obese Female Mice. *Hypertension* 77 (6), 2117–2126. doi:10.1161/hypertensionaha.120.16911

Brilla, C. G., and Weber, K. T. (1992). Mineralocorticoid Excess, Dietary Sodium, and Myocardial Fibrosis. *J. Lab. Clin. Med.* 120 (6), 893–901.

Brilla, C. G. (2000). Aldosterone and Myocardial Fibrosis in Heart Failure. *Herz* 25 (3), 299–306. doi:10.1007/s000590050024

Bulluck, H., Fröhlich, G. M., Nicholas, J. M., Mohdnazri, S., Gamma, R., Davies, J., et al. (2019). Mineralocorticoid Receptor Antagonist Pre-treatment and Early Post-treatment to Minimize Reperfusion Injury after ST-Elevation Myocardial Infarction: The MINIMIZE STEMI Trial. *Am. Heart J.* 211, 60–67. doi:10.1016/j.ahj.2019.02.005

Buonafine, M., Bonnard, B., and Jaisser, F. (2018). Mineralocorticoid Receptor and Cardiovascular Disease. *Am. J. Hypertens.* 31 (11), 1165–1174. doi:10.1093/ajh/hpy120

Casin, K. M., Fallica, J., Mackowski, N., Veenema, R. J., Chan, A., St. Paul, A., et al. (2018). S -Nitrosoglutathione Reductase Is Essential for Protecting the Female Heart from Ischemia-Reperfusion Injury. *Circ. Res.* 123 (11), 1232–1243. doi:10.1161/circresaha.118.313956

Chai, W., Garrelds, I. M., Arulmani, U., Schoemaker, R. G., Lamers, J. M. J., and Danser, A. H. J. (2005). Genomic and Nongenomic Effects of Aldosterone in the Rat Heart: Why Is Spironolactone Cardioprotective? *Br. J. Pharmacol.* 145 (5), 664–671. doi:10.1038/sj.bjp.0706220

Chen, Q., Zhao, D., Sun, J., and Lu, C. (2021). Aldosterone Blockade in Acute Myocardial Infarction: A Systematic Review and Meta-Analysis. *Cardiovasc. Ther.* 2021, 1–18. doi:10.1155/2021/1710731

Cittadini, A., Monti, M. G., Isgaard, J., Casaburi, C., Stromer, H., Di Gianni, A., et al. (2003). Aldosterone Receptor Blockade Improves Left Ventricular Remodeling and Increases Ventricular Fibrillation Threshold in Experimental Heart Failure. *Cardiovasc. Res.* 58 (3), 555–564. doi:10.1016/s0008-6363(03)00251-7

Davidson, S. M., Ferdinandy, P., Andreadou, I., Bøtker, H. E., Heusch, G., Ibáñez, B., et al. (2019). Multitarget Strategies to Reduce Myocardial Ischemia/Reperfusion Injury. *J. Am. Coll. Cardiol.* 73 (1), 89–99. doi:10.1016/j.jacc.2018.09.086

Delyani, J. A., Robinson, E. L., and Rudolph, A. E. (2001). Effect of a Selective Aldosterone Receptor Antagonist in Myocardial Infarction. *Am. J. Physiology-Heart Circulatory Physiology* 281 (2), H647–H654. doi:10.1152/ajpheart.2001.281.2.h647

Driessen, H. E., Fontes, M. S., Stuijvenberg, L., Brans, M. A., Goumans, M. J., Vos, M. A., et al. (2020). A Combined CaMKII Inhibition and Mineralocorticoid Receptor Antagonism via Eplerenone Inhibits Functional Deterioration in Chronic Pressure Overloaded Mice. *J. Cell. Mol. Med.* 24 (15), 8417–8429. doi:10.1111/jcmm.15355

Enomoto, S., Yoshiyama, M., Omura, T., Matsumoto, R., Kusuyama, T., Kim, S., et al. (2005). Effects of Eplerenone on Transcriptional Factors and mRNA Expression Related to Cardiac Remodelling after Myocardial Infarction. *Heart* 91 (12), 1595–1600. doi:10.1136/hrt.2004.046540

Faulkner, J. L., Kennard, S., Huby, A.-C., Antonova, G., Lu, Q., Jaffe, I. Z., et al. (2019). Progesterone Predisposes Females to Obesity-Associated Leptin-Mediated Endothelial Dysfunction via Upregulating Endothelial MR (Mineralocorticoid Receptor) Expression. *Hypertension* 74 (3), 678–686. doi:10.1161/hypertensionaha.119.12802

Ferron, L., Ruchon, Y., Renaud, J.-F., and Capuano, V. (2011). T-type Ca2+ Signalling Regulates Aldosterone-Induced CREB Activation and Cell Death through PP2A Activation in Neonatal Cardiomyocytes. *Cardiovasc Res.* 90 (1), 105–112. doi:10.1093/cvr/cvq379

Fraccarollo, D., Berger, S., Galuppo, P., Kneitz, S., Hein, L., Schütz, G., et al. (2011). Deletion of Cardiomyocyte Mineralocorticoid Receptor Ameliorates Adverse

Remodeling after Myocardial Infarction. *Circulation* 123 (4), 400–408. doi:10.1161/CIRCULATIONAHA.110.983023

Fraccarollo, D., Galuppo, P., Hildemann, S., Christ, M., Ertl, G., and Bauersachs, J. (2003). Additive Improvement of Left Ventricular Remodeling and Neurohormonal Activation by Aldosterone Receptor Blockade with Eplerenone and ACE Inhibition in Rats with Myocardial Infarction. *J. Am. Coll. Cardiol.* 42 (9), 1666–1673. doi:10.1016/j.jacc.2003.05.003

Fraccarollo, D., Galuppo, P., Schmidt, I., Ertl, G., and Bauersachs, J. (2005). Additive Amelioration of Left Ventricular Remodeling and Molecular Alterations by Combined Aldosterone and Angiotensin Receptor Blockade after Myocardial Infarction. *Cardiovasc. Res.* 67 (1), 97–105. doi:10.1016/j.cardiores.2005.03.001

Fraccarollo, D., Galuppo, P., Schraut, S., Kneitz, S., van Rooijen, N., Ertl, G., et al. (2008). Immediate Mineralocorticoid Receptor Blockade Improves Myocardial Infarct Healing by Modulation of the Inflammatory Response. *Hypertension* 51 (4), 905–914. doi:10.1161/HYPERTENSIONAHA.107.100941

Fraccarollo, D., Thomas, S., Scholz, C.-J., Hilfiker-Kleiner, D., Galuppo, P., and Bauersachs, J. (2019). Macrophage Mineralocorticoid Receptor Is a Pleiotropic Modulator of Myocardial Infarct Healing. *Hypertension* 73 (1), 102–111. doi:10.1161/HYPERTENSIONAHA.118.12162

Funder, J. W. (2011). GPR30, Mineralocorticoid Receptors, and the Rapid Vascular Effects of Aldosterone. *Hypertension* 57 (3), 370–372. doi:10.1161/HYPERTENSIONAHA.110.165076

Griffiths, K., Lee, J. J., Frenneaux, M. P., Feelisch, M., and Madhani, M. (2021). Nitrite and Myocardial Ischaemia Reperfusion Injury. Where Are We Now? *Pharmacol. Ther.* 223, 107819. doi:10.1016/j.pharmthera.2021.107819

Grohé, C., Kahlert, S., Löbbert, K., Stimpel, M., Karas, R. H., Vetter, H., et al. (1997). Cardiac Myocytes and Fibroblasts Contain Functional Estrogen Receptors 1. *FEBS Lett.* 416 (1), 107–112. doi:10.1016/s0014-5793(97)01179-4

Gros, R., Ding, Q., Liu, B., Chorazyczewski, J., and Feldman, R. D. (2013). Aldosterone Mediates its Rapid Effects in Vascular Endothelial Cells through GPER Activation. *Am. J. Physiology-Cell Physiology* 304 (6), C532–C540. doi:10.1152/ajpcell.00203.2012

Gros, R., Ding, Q., Sklar, L. A., Prossnitz, E. E., Arterburn, J. B., Chorazyczewski, J., et al. (2011). GPR30 Expression Is Required for the Mineralocorticoid Receptor-independent Rapid Vascular Effects of Aldosterone. *Hypertension* 57 (3), 442–451. doi:10.1161/HYPERTENSIONAHA.110.161653

Gueret, A., Harouki, N., Favre, J., Galmiche, G., Nicol, L., Henry, J.-P., et al. (2016). Vascular Smooth Muscle Mineralocorticoid Receptor Contributes to Coronary and Left Ventricular Dysfunction after Myocardial Infarction. *Hypertension* 67 (4), 717–723. doi:10.1161/HYPERTENSIONAHA.115.06709

Gürgen, D., Hegner, B., Kusch, A., Catar, R., Chaykovska, L., Hoff, U., et al. (2011). Estrogen Receptor-β Signals Left Ventricular Hypertrophy Sex Differences in Normotensive Deoxycorticosterone Acetate-Salt Mice. *Hypertension* 57 (3), 648–654. doi:10.1161/HYPERTENSIONAHA.110.166157

Gürgen, D., Kusch, A., Klewitz, R., Hoff, U., Catar, R., Hegner, B., et al. (2013). Sex-specific mTOR Signaling Determines Sexual Dimorphism in Myocardial Adaptation in Normotensive DOCA-Salt Model. *Hypertension* 61 (3), 730–736. doi:10.1161/HYPERTENSIONAHA.111.00276

Hayashi, H., Kobara, M., Abe, M., Tanaka, N., Gouda, E., Toba, H., et al. (2008). Aldosterone Nongenomically Produces NADPH Oxidase–Dependent Reactive Oxygen Species and Induces Myocyte Apoptosis. *Hypertens. Res.* 31 (2), 363–375. doi:10.1291/hypres.31.363

Hermidorff, M. M., de Assis, L. V. M., and Isoldi, M. C. (2017). Genomic and Rapid Effects of Aldosterone: what We Know and Do Not Know Thus Far. *Heart Fail Rev.* 22 (1), 65–89. doi:10.1007/s10741-016-9591-2

Heusch, G. (2020). Myocardial Ischaemia-Reperfusion Injury and Cardioprotection in Perspective. *Nat. Rev. Cardiol.* 17 (12), 773–789. doi:10.1038/s41569-020-0403-y

Jia, G., Habibi, J., Aroor, A. R., Martinez-Lemus, L. A., DeMarco, V. G., Ramirez-Perez, F. I., et al. (2016). Endothelial Mineralocorticoid Receptor Mediates Diet-Induced Aortic Stiffness in Females. *Circ. Res.* 118 (6), 935–943. doi:10.1161/CIRCRESAHA.115.308269

Kanashiro-Takeuchi, R. M., Heidecker, B., Lamirault, G., Dharamsi, J. W., and Hare, J. M. (2009). Sex-specific Impact of Aldosterone Receptor Antagonism on Ventricular Remodeling and Gene Expression after Myocardial Infarction. *Clin. Transl. Sci.* 2 (2), 134–142. doi:10.1111/j.1752-8062.2009.00094.x

Leening, M. J. G., Ferket, B. S., Steyerberg, E. W., Kavousi, M., Deckers, J. W., Nieboer, D., et al. (2014). Sex Differences in Lifetime Risk and First Manifestation of Cardiovascular Disease: Prospective Population Based Cohort Study. *BMJ* 349, g5992. doi:10.1136/bmj.g5992

Lombès, M., Alfaidy, N., Eugene, E., Lessana, A., Farman, N., and Bonvalet, J. P. (1995). Prerequisite for Cardiac Aldosterone Action. Mineralocorticoid Receptor and 11 Beta-Hydroxysteroid Dehydrogenase in the Human Heart. *Circulation* 92 (2), 175–182. doi:10.1161/01.cir.92.2.175

Mahmoodzadeh, S., Leber, J., Zhang, X., Jaisser, F., Messaoudi, S., Morano, I., et al. (2014). Cardiomyocyte-specific Estrogen Receptor Alpha Increases Angiogenesis,Lymphangiogenesis and Reduces Fibrosis in the Female Mouse Heart Post-Myocardial Infarction. *J. Cell. Sci. Ther.* 05 (1), 153. doi:10.4172/2157-7013.1000153

Mano, A., Tatsumi, T., Shiraishi, J., Keira, N., Nomura, T., Takeda, M., et al. (2004). Aldosterone Directly Induces Myocyte Apoptosis through Calcineurin-dependent Pathways. *Circulation* 110 (3), 317–323. doi:10.1161/01.CIR.0000135599.33787.CA

Mares, A., Rodriguez, T., Deoker, A., Lehker, A., and Mukherjee, D. (2022). Effect of Mineralocorticoid Receptor Antagonists in Heart Failure with Preserved Ejection Fraction and with Reduced Ejection Fraction - A Narrative Review. *Cvp* 20 (1), 46–51. doi:10.2174/1570161119666210720120439

Maric-Bilkan, C., Arnold, A. P., Taylor, D. A., Dwinell, M., Howlett, S. E., Wenger, N., et al. (2016). Report of the National Heart, Lung, and Blood Institute Working Group on Sex Differences Research in Cardiovascular Disease. *Hypertension* 67 (5), 802–807. doi:10.1161/hypertensionaha.115.06967

Markowitz, M., Messineo, F., and Coplan, N. L. (2012). Aldosterone Receptor Antagonists in Cardiovascular Disease: a Review of the Recent Literature and Insight into Potential Future Indications. *Clin. Cardiol.* 35 (10), 605–609. doi:10.1002/clc.22025

Masson, S., Staszewsky, L., Annoni, G., Carlo, E., Arosio, B., Bai, A., et al. (2004). Eplerenone, a Selective Aldosterone Blocker, Improves Diastolic Function in Aged Rats with Small-To-Moderate Myocardial Infarction. *J. Cardiac Fail.* 10 (5), 433–441. doi:10.1016/j.cardfail.2004.02.010

Matsumoto, R., Yoshiyama, M., Omura, T., Kim, S., Nakamura, Y., Izumi, Y., et al. (2004). Effects of Aldosterone Receptor Antagonist and Angiotensin II Type I Receptor Blocker on Cardiac Transcriptional Factors and mRNA Expression in Rats with Myocardial Infarction. *Circ. J.* 68 (4), 376–382. doi:10.1253/circj.68.376

Mattiazzi, A., Bassani, R. A., Escobar, A. L., Palomeque, J., Valverde, C. A., Vila Petroff, M., et al. (2015). Chasing Cardiac Physiology and Pathology Down the CaMKII Cascade. *Am. J. Physiology-Heart Circulatory Physiology* 308 (10), H1177–H1191. doi:10.1152/ajpheart.00007.2015

McSweeney, J. C., Rosenfeld, A. G., Abel, W. M., Braun, L. T., Burke, L. E., Daugherty, S. L., et al. (2016). Preventing and Experiencing Ischemic Heart Disease as a Woman: State of the Science. *Circulation* 133 (13), 1302–1331. doi:10.1161/CIR.0000000000000381

Mehta, L. S., Beckie, T. M., DeVon, H. A., Grines, C. L., Krumholz, H. M., Johnson, M. N., et al. (2016). Acute Myocardial Infarction in Women. *Circulation* 133 (9), 916–947. doi:10.1161/CIR.0000000000000351

Michea, L., Delpiano, A. M., Hitschfeld, C., Lobos, L., Lavandero, S., and Marusic, E. T. (2005). Eplerenone Blocks Nongenomic Effects of Aldosterone on the Na+/H+ Exchanger, Intracellular Ca2+ Levels, and Vasoconstriction in Mesenteric Resistance Vessels. *Endocrinology* 146 (3), 973–980. doi:10.1210/en.2004-1130

Mihailidou, A. S., Loan Le, T. Y., Mardini, M., and Funder, J. W. (2009). Glucocorticoids Activate Cardiac Mineralocorticoid Receptors during Experimental Myocardial Infarction. *Hypertension* 54 (6), 1306–1312. doi:10.1161/HYPERTENSIONAHA.109.136242

Mill, J. G., Milanez, M. d. C., Resende, M. M. d., Gomes, M. d. G. S., and Leite, C. M. (2003). Spironolactone Prevents Cardiac Collagen Proliferation after Myocardial Infarction in Rats. *Clin. Exp. Pharmacol. Physiol.* 30 (10), 739–744. doi:10.1046/j.1440-1681.2003.03906.x

Miller, R. J. H., and Howlett, J. G. (2015). Evolving Role for Mineralocorticoid Receptor Antagonists in Heart Failure with Preserved Ejection Fraction. *Curr. Opin. Cardiol.* 30 (2), 168–172. doi:10.1097/HCO.0000000000000147

Moran, A. E., Forouzanfar, M. H., Roth, G. A., Mensah, G. A., Ezzati, M., Flaxman, A., et al. (2014). The Global Burden of Ischemic Heart Disease in 1990 and

2010. *Circulation* 129 (14), 1493–1501. doi:10.1161/CIRCULATIONAHA.113.004046

Mozaffarian, D., Benjamin, E. J., Go, A. S., Arnett, D. K., Blaha, M. J., Cushman, M., et al. (2015). Heart Disease and Stroke Statistics-2015 Update. *Circulation* 131 (4), e29–322. doi:10.1161/CIR.0000000000000152

Murphy, E., Lagranha, C., Deschamps, A., Kohr, M., Nguyen, T., Wong, R., et al. (2011). Mechanism of Cardioprotection: what Can We Learn from Females? *Pediatr. Cardiol.* 32 (3), 354–359. doi:10.1007/s00246-010-9877-4

Murray, C. J., Vos, T., Lozano, R., Naghavi, M., Flaxman, A. D., Michaud, C., et al. (2012). Disability-adjusted Life Years (DALYs) for 291 Diseases and Injuries in 21 Regions, 1990-2010: a Systematic Analysis for the Global Burden of Disease Study 2010. *Lancet* 380 (9859), 2197–2223. doi:10.1016/S0140-6736(12)61689-4

Nicolaou, P. A. (2021). Sex Differences in Heart Failure Medications Targeting the Renin-Angiotensin-Aldosterone System. *Eur. J. Pharmacol.* 897, 173961. doi:10.1016/j.ejphar.2021.173961

Nolly, M. B., Caldiz, C. I., Yeves, A. M., Villa-Abrille, M. C., Morgan, P. E., Amado Mondaca, N., et al. (2014). The Signaling Pathway for Aldosterone-Induced Mitochondrial Production of Superoxide Anion in the Myocardium. *J. Mol. Cell. Cardiol.* 67, 60–68. doi:10.1016/j.yjmcc.2013.12.004

Ong, G. S. Y., and Young, M. J. (2017). Mineralocorticoid Regulation of Cell Function: the Role of Rapid Signalling and Gene Transcription Pathways. *J. Mol. Endocrinol.* 58 (1), R33–r57. doi:10.1530/jme-15-0318

Pitt, B., Remme, W., Zannad, F., Neaton, J., Martinez, F., Roniker, B., et al. (2003). Eplerenone, a Selective Aldosterone Blocker, in Patients with Left Ventricular Dysfunction after Myocardial Infarction. *N. Engl. J. Med.* 348 (14), 1309–1321. doi:10.1056/NEJMoa030207

Pitt, B., Zannad, F., Remme, W. J., Cody, R., Castaigne, A., Perez, A., et al. (1999). The Effect of Spironolactone on Morbidity and Mortality in Patients with Severe Heart Failure. *N. Engl. J. Med.* 341 (10), 709–717. doi:10.1056/NEJM199909023411001

Rao, K. K., Enriquez, J. R., de Lemos, J. A., Alexander, K. P., Chen, A. Y., McGuire, D. K., et al. (2013). Use of Aldosterone Antagonists at Discharge after Myocardial Infarction: Results from the National Cardiovascular Data Registry Acute Coronary Treatment and Intervention Outcomes Network (ACTION) Registry-Get with the Guidelines (GWTG). *Am. Heart J.* 166 (4), 709–715. doi:10.1016/j.ahj.2013.06.020

Rickard, A. J., Morgan, J., Tesch, G., Funder, J. W., Fuller, P. J., and Young, M. J. (2009). Deletion of Mineralocorticoid Receptors from Macrophages Protects against Deoxycorticosterone/salt-Induced Cardiac Fibrosis and Increased Blood Pressure. *Hypertension* 54 (3), 537–543.doi:10.1161/hypertensionaha.109.131110

Rochetaing, A., Chapon, C., Marescaux, L., Bouil, A. L., Furber, A., and Kreher, P. (2003). Potential Beneficial as Well as Detrimental Effects of Chronic Treatment with Lisinopril and (Or) Spironolactone on Isolated Hearts Following Low-Flow Ischemia in Normal and Infarcted Rats. *Can. J. Physiol. Pharmacol.* 81 (9), 864–872. doi:10.1139/y03-081

Rossol-Haseroth, K., Zhou, Q., Braun, S., Boldyreff, B., Falkenstein, E., Wehling, M., et al. (2004). Mineralocorticoid Receptor Antagonists Do Not Block Rapid ERK Activation by Aldosterone. *Biochem. Biophysical Res. Commun.* 318 (1), 281–288. doi:10.1016/j.bbrc.2004.04.026

Rude, M. K., Duhaney, T.-A. S., Kuster, G. M., Judge, S., Heo, J., Colucci, W. S., et al. (2005). Aldosterone Stimulates Matrix Metalloproteinases and Reactive Oxygen Species in Adult Rat Ventricular Cardiomyocytes. *Hypertension* 46 (3), 555–561. doi:10.1161/01.HYP.0000176236.55322.18

Schiattarella, G. G., Altamirano, F., Tong, D., French, K. M., Villalobos, E., Kim, S. Y., et al. (2019). Nitrosative Stress Drives Heart Failure with Preserved Ejection Fraction. *Nature* 568 (7752), 351–356. doi:10.1038/s41586-019-1100-z

Schuster, I., Mahmoodzadeh, S., Dworatzek, E., Jaisser, F., Messaoudi, S., Morano, I., et al. (2016). Cardiomyocyte-specific Overexpression of Oestrogen Receptor β Improves Survival and Cardiac Function after Myocardial Infarction in Female and Male Mice. *Clin. Sci. (Lond)* 130 (5), 365–376. doi:10.1042/CS20150609

Shattock, M. J., Ottolia, M., Bers, D. M., Blaustein, M. P., Boguslavskyi, A., Bossuyt, J., et al. (2015). Na+/Ca2+exchange and Na+/K+-ATPase in the Heart. *J. Physiol.* 593 (6), 1361–1382. doi:10.1113/jphysiol.2014.282319

Tong, D., Schiattarella, G. G., Jiang, N., May, H. I., Lavandero, S., Gillette, T. G., et al. (2019). Female Sex Is Protective in a Preclinical Model of Heart Failure with Preserved Ejection Fraction. *Circulation* 140 (21), 1769–1771. doi:10.1161/circulationaha.119.042267

Tsai, C.-F., Yang, S.-F., Chu, H.-J., and Ueng, K.-C. (2013). Cross-talk between Mineralocorticoid Receptor/angiotensin II Type 1 Receptor and Mitogen-Activated Protein Kinase Pathways Underlies Aldosterone-Induced Atrial Fibrotic Responses in HL-1 Cardiomyocytes. *Int. J. Cardiol.* 169 (1), 17–28. doi:10.1016/j.ijcard.2013.06.046

Vasan, R. S., Evans, J. C., Benjamin, E. J., Levy, D., Larson, M. G., Sundstrom, J., et al. (2004). Relations of Serum Aldosterone to Cardiac Structure. *Hypertension* 43 (5), 957–962. doi:10.1161/01.HYP.0000124251.06056.8e

Venugopal, V., Ludman, A., Yellon, D. M., and Hausenloy, D. J. (2009). 'Conditioning' the Heart during Surgery. *Eur. J. Cardio-Thoracic Surg.* 35 (6), 977–987. doi:10.1016/j.ejcts.2009.02.014

Victorio, J. A., Clerici, S. P., Palacios, R., Alonso, M. J., Vassallo, D. V., Jaffe, I. Z., et al. (2016). Spironolactone Prevents Endothelial Nitric Oxide Synthase Uncoupling and Vascular Dysfunction Induced by β-Adrenergic Overstimulation. *Hypertension* 68 (3), 726–735. doi:10.1161/HYPERTENSIONAHA.116.07911

Wang, D., Liu, Y.-H., Yang, X.-P., Rhaleb, N.-E., Xu, J., Peterson, E., et al. (2004). Role of a Selective Aldosterone Blocker in Mice with Chronic Heart Failure. *J. Cardiac Fail.* 10 (1), 67–73. doi:10.1016/s1071-9164(03)00578-5

Westerman, S., and Wenger, N. K. (2016). Women and Heart Disease, the Underrecognized Burden: Sex Differences, Biases, and Unmet Clinical and Research Challenges. *Clin. Sci. (Lond)* 130 (8), 551–563. doi:10.1042/CS20150586

Wong, E. C., Fordyce, C. B., Wong, G., Lee, T., Perry-Arnesen, M., Mackay, M., et al. (2021). Predictors of the Use of Mineralocorticoid Receptor Antagonists in Patients with Left Ventricular Dysfunction Post-ST-Segment-Elevation Myocardial Infarction. *Jaha* 10 (14), e019167. doi:10.1161/jaha.120.019167

Wong, N. D. (2014). Epidemiological Studies of CHD and the Evolution of Preventive Cardiology. *Nat. Rev. Cardiol.* 11 (5), 276–289. doi:10.1038/nrcardio.2014.26

Yoshino, T., Nagoshi, T., Anzawa, R., Kashiwagi, Y., Ito, K., Katoh, D., et al. (2014). Preconditioning Actions of Aldosterone through P38 Signaling Modulation in Isolated Rat Hearts. *J. Endocrinol.* 222 (2), 289–299. doi:10.1530/JOE-14-0067

Young, M. J., and Clyne, C. D. (2021). Mineralocorticoid Receptor Actions in Cardiovascular Development and Disease. *Essays Biochem.* 65 (6), 901–911. doi:10.1042/ebc20210006

Young, M. J., and Rickard, A. J. (2015). Mineralocorticoid Receptors in the Heart: Lessons from Cell-Selective Transgenic Animals. *J. Endocrinol.* 224 (1), R1–R13. doi:10.1530/JOE-14-0471

Zamani, P., Rawat, D., Shiva-Kumar, P., Geraci, S., Bhuva, R., Konda, P., et al. (2015). Effect of Inorganic Nitrate on Exercise Capacity in Heart Failure with Preserved Ejection Fraction. *Circulation* 131 (4), 371–380. discussion 380. doi:10.1161/CIRCULATIONAHA.114.012957

Conflict of Interest: The authors declare that the research was conducted in the absence of any commercial or financial relationships that could be construed as a potential conflict of interest.

Publisher's Note: All claims expressed in this article are solely those of the authors and do not necessarily represent those of their affiliated organizations, or those of the publisher, the editors and the reviewers. Any product that may be evaluated in this article, or claim that may be made by its manufacturer, is not guaranteed or endorsed by the publisher.

Copyright © 2022 Bienvenu, Bell, Weeks, Delbridge and Young. This is an open-access article distributed under the terms of the Creative Commons Attribution License (CC BY). The use, distribution or reproduction in other forums is permitted, provided the original author(s) and the copyright owner(s) are credited and that the original publication in this journal is cited, in accordance with accepted academic practice. No use, distribution or reproduction is permitted which does not comply with these terms.

frontiers | Frontiers in Physiology

TYPE Original Research
PUBLISHED 19 August 2022
DOI 10.3389/fphys.2022.920196

Check for updates

OPEN ACCESS

EDITED BY
Jacqueline Kathleen Phillips,
Macquarie University, Australia

REVIEWED BY
Dan Li,
University of Oxford, United Kingdom
Julia Shanks,
The University of Auckland,
New Zealand

*CORRESPONDENCE
Hugo C. D. Souza,
hugocds@fmrp.usp.br

SPECIALTY SECTION
This article was submitted to Integrative Physiology,
a section of the journal
Frontiers in Physiology

RECEIVED 14 April 2022
ACCEPTED 25 July 2022
PUBLISHED 19 August 2022

CITATION
Vieira S, Aguilar BA, Veiga AC, Philbois SV, Freitas ACS, Rodrigues KP, Tank J and Souza HCD (2022), Integrative physiological study of adaptations induced by aerobic physical training in hypertensive hearts.
Front. Physiol. 13:920196.
doi: 10.3389/fphys.2022.920196

COPYRIGHT
© 2022 Vieira, Aguilar, Veiga, Philbois, Freitas, Rodrigues, Tank and Souza. This is an open-access article distributed under the terms of the Creative Commons Attribution License (CC BY). The use, distribution or reproduction in other forums is permitted, provided the original author(s) and the copyright owner(s) are credited and that the original publication in this journal is cited, in accordance with accepted academic practice. No use, distribution or reproduction is permitted which does not comply with these terms.

Integrative physiological study of adaptations induced by aerobic physical training in hypertensive hearts

Suenimeire Vieira[1], Bruno A. Aguilar[1], Ana Catarine Veiga[1], Stella V. Philbois[1], Ana Caroline S. Freitas[1], Karine P. Rodrigues[1], Jens Tank[2] and Hugo C. D. Souza[1]*

[1]Department of Physiology, Ribeirão Preto Medical School, University of São Paulo, São Paulo, Brazil, [2]Institute of Aerospace Medicine, German Aerospace Center, Cologne, Germany

Aerobic physical training reduces arterial pressure in patients with hypertension owing to integrative systemic adaptations. One of the key factors is the decrease in cardiac sympathetic influence. Thus, we hypothesized that among other causes, cardiac sympathetic influence reduction might be associated with intrinsic cardiac adaptations that provide greater efficiency. Therefore, 14 spontaneously hypertensive rats (SHR group) and 14 normotensive Wistar Kyoto rats (WKY group) were used in this study. Half of the rats in each group were trained to swim for 12 weeks. All animals underwent the following experimental protocols: double blockade of cardiac autonomic receptors with atropine and propranolol; echocardiography; and analysis of coronary bed reactivity and left ventricle contractility using the Langendorff technique. The untrained SHR group had a higher sympathetic tone, cardiac hypertrophy, and reduced ejection fraction compared with the untrained WKY group. In addition, reduced coronary bed reactivity due to increased flow, and less ventricular contractile response to dobutamine and salbutamol administration were observed. The trained SHR group showed fewer differences in echocardiographic parameters as the untrained SHR group. However, the trained SHR group showed a reduction in the cardiac sympathetic influence, greater coronary bed reactivity, and increased left intraventricular pressure. In conclusion, aerobic physical training seems to reduce cardiac sympathetic influence and increase contractile strength in SHR rats, besides the minimal effects on cardiac morphology. This reduction suggests intrinsic cardiac adaptations resulting in beneficial adjustments of coronary bed reactivity associated with greater left ventricular contraction.

KEYWORDS

hypertension, autonomic nervous system, cardiac adaptations, physical training, experimental study

1 Introduction

Systemic arterial hypertension is accompanied by a progressive increase in cardiac sympathetic autonomic drive, which contributes to the early development of heart failure (Borovac et al., 2020; Seravalle and Grassi, 2022). This sympathetic hyperactivity aims to maintain adequate cardiac output regardless of the individual's metabolic demand; although, other causes may be involved (Saxena et al., 2018). However, if the increase in arterial pressure persists, cardiac adaptations will become progressively relevant because of the significant augmentation of the sympathetic drive to the heart, resulting in adverse cardiac remodeling associated with reduced functional capacity (Floras, 2009; Oparil et al., 2018). Usually, this progression is silent, and in many patients, it is only noticed when damage to the heart is already at an advanced stage.

Conservative treatment is provided by administering different classes of drugs to reduce the preload and afterload (Diaconu et al., 2018). Nonetheless, new guidelines for managing hypertension recommend initiating treatment through regular aerobic physical exercises, especially in patients with grade I and II hypertension (Williams et al., 2018). However, the effects and mechanisms through which physical exercise influences hypertensive hearts remain unclear. More precisely, little is known about the relationship between cardiac sympathetic autonomic influence, coronary bed reactivity, and left ventricular contractility in hypertensive hearts, as well as the effects of aerobic physical training on these parameters. The literature suggests that long-term aerobic physical training can improve coronary flow regulation. However, little is known about this and the relationship between this improvement and cardiac functionality, especially left ventricular contractility (Laughlin et al., 1998; Jakovljevic et al., 2019). Therefore, we aimed to investigate the different aspects of cardiac adaptations promoted by aerobic physical training in spontaneously hypertensive rats (SHR) in an integrated way, focusing on autonomic control, coronary bed reactivity, and effects on left ventricular contractility, cardiac morphology, and function.

2 Materials and methods

2.1 Animals

Research trials were conducted on 18-week-old male Wistar Kyoto rats (WKY) and SHR. They were assigned to the following four groups: WKY untrained (N = 07), WKY trained (N = 07), SHR untrained (N = 07), and SHR-trained (N = 07). The rats were supplied by the Animal Facility of the Ribeirao Preto Medical School, University of São Paulo, Ribeirão Preto. They were housed in a room with strictly controlled temperature (21 ± 1°C) and a 12-h light/dark cycle, with unrestricted access to tap water and standard rat food (Nuvilab CR-1; Nuvital, Curitiba, Brazil). All experimental protocols performed in the current study were approved by the Committee on Animal Research and Ethics of Ribeirão Preto Medical School, University of São Paulo (Protocol 044/2020). This study was conducted in compliance with the ARRIVE guidelines.

2.2 Physical training

Aerobic physical training was carried out as previously described (Gardim et al., 2021). The rats in the training groups underwent aerobic physical training consisting of swimming sessions. The training program was conducted in two different stages over a total of 14 weeks. The first stage consisted of a 2-weeks adaptation period, during which the session length was gradually increased from 5 to 40 min/day, 5 times/week (in increments of 5 min/day). The second stage consisted of 12 weeks, with 40 min of physical training sessions conducted 5 times/week.

2.3 Experimental protocol

2.3.1 Echocardiography

Echocardiography was performed as previously described (Felix et al., 2018). At 32 weeks of age, the rats were evaluated by echocardiography using a Vevo 2,100® High-Resolution Imaging System (Visual Sonics, Toronto, ON, Canada) with a high-resolution transducer at 21 MHz. All animals were anesthetized with 1.5% isoflurane supplemented with 1% O_2 and placed on a heated platform (37°C). Electrocardiogram and platform temperature were monitored. All measurements were performed according to the American Society of Echocardiography standards by a single individual, blinded to the characteristics of each group (Sahn et al., 1978).

2.3.2 Recording of arterial pressure and heart rate

Forty-eight hours after the echocardiographic examination, the animals were anesthetized with ketamine and xylazine (80 mg/kg and 10 mg/kg, respectively). A polyethylene catheter (PE-50 soldered to PE-10; Intramedic, Clay Adams, Parsippany, NJ, United States) was implanted into the left femoral artery to record the hemodynamic parameters, systolic arterial pressure (SAP), diastolic arterial pressure (DAP), and mean arterial pressure (MAP). The catheters were tunneled subcutaneously, exteriorized at the nape, and filled with a heparinized saline solution (500 IU/ml) to prevent blood clotting.

Arterial pressure (AP) pressure was recorded in conscious rats kept in a quiet environment, using a pressure transducer (MLT0380, ADInstruments, Bella Vista, Australia), and the amplified signal (ML110, ADInstruments) was fed to a computer acquisition system (LabChart 7 Pro, ADInstruments). MAP and heart rate (HR) were calculated from arterial pulse pressure.

TABLE 1 Hemodynamic parameters and values of heart rate (HR) obtained before and after the double pharmacological blockade of cardiac autonomic receptors with atropine and propranolol, in Wistar Kyoto (WKY, *N* = 14) and Spontaneously Hypertensive Rats (SHR, *N* = 14) groups, both untrained (*N* = 07) and trained (*N* = 07).

	WKY		SHR		Hypertension factor		Physical training factor		Interaction	
	Untrained	Trained	Untrained	Trained	$F_{(d.f)}$	P	$F_{(d.f)}$	P	$F_{(d.f)}$	P
Hemodynamic Parameters										
SBP, mmHg	119 ± 3	118 ± 8	214 ± 3 [a,b]	173 ± 6 [a,b,c]	$F_{(1.27)}$: 196.758	<0.001	$F_{(1.27)}$: 15.909	<0.001	$F_{(1.27)}$: 13.844	<0.001
DBP, mmHg	77 ± 8	76 ± 12	174 ± 4 [a,b]	127 ± 20 [a,b,c]	$F_{(1.27)}$: 36.104	<0.001	$F_{(1.27)}$: 3.681	0.067	$F_{(1.27)}$: 3.422	0.077
MBP, mmHg	94 ± 6	93 ± 11	190 ± 3 [a,b]	142 ± 18 [a,b,c]	$F_{(1.27)}$: 41.985	<0.001	$F_{(1.27)}$: 4.776	0.039	$F_{(1.27)}$: 4.446	0.046
Double autonomic blockade										
Basal HR, bpm	349 ± 6	326 ± 5 [a]	391 ± 7 [a,b]	335 ± 8 [a,b,c]	$F_{(1.27)}$: 15.568	<0.001	$F_{(1.27)}$: 38.680	<0.001	$F_{(1.27)}$: 6.572	0.017
Atropine, bpm	411 ± 6	395 ± 5	415 ± 7	390 ± 5 [c]	$F_{(1.27)}$: 0.007	0.934	$F_{(1.27)}$: 11,750	0.002	$F_{(1.27)}$: 0.438	0.515
Propranolol, bpm	326 ± 7	305 ± 6 [a]	301 ± 5 [a]	290 ± 7 [a]	$F_{(1.27)}$: 10.822	0.003	$F_{(1.27)}$: 6.732	0.016	$F_{(1.27)}$: 0.735	0.400
Intrinsic HR, bpm	359 ± 5	336 ± 4 [a]	316 ± 4 [a,b]	304 ± 3 [a,b,c]	$F_{(1.27)}$: 91.740	<0.001	$F_{(1.27)}$: 23.100	<0.001	$F_{(1.27)}$: 0.425	0.520

All values are presented as the mean ± SEM., SAP, systolic arterial pressure; mmHg, millimeter of mercury; DAP, diastolic arterial pressure; MAP, mean arterial pressure; HR, heart rate; bpm, beats per minute; F, factor; d.f, degrees of freedom. [a] $p < 0.05$ vs. WKY, untrained; [b] $p < 0.05$ vs. WKY, trained; [c] $p < 0.05$ vs. SHR, untrained.

2.3.4 Cardiac sympathovagal balance after double blockade of autonomic receptors

Cardiac sympathovagal balance was assessed as previously described (Gardim et al., 2021). Twenty-4 hours after the surgical procedure, the femoral artery catheter was attached to a pressure transducer and pulsatile AP was sampled continuously (2 kHz). MAP and HR were calculated from pulsatile AP using a software program (PowerLab, LabChart8; ADInstruments).

Cardiac autonomic receptor blockade (both sympathetic and vagal) of HR was assessed by administering atropine (4 mg/kg) and propranolol (5 mg/kg). After the basal HR was recorded for 30 min, atropine was injected into half of the animals in each group. The HR was recorded for the next 15 min to assess the effect of muscarinic receptor blockade on the HR (sympathetic effect). Propranolol was subsequently injected into the same animals, and the HR was recorded for the next 15 min to determine intrinsic HR (iHR). In half of the animals, the atropine-propranolol sequence was reversed to a propranolol-atropine sequence, following the same recording procedure (15 min) for each drug used in the previous sequence to determine iHR. After 24 h the same procedure was performed, however the sequence of drugs was inverted in each animal.

2.3.5 Preparation of isolated hearts for perfusion—langendorff technique

Isolation of hearts for perfusion was performed as previously described (Felix et al., 2018). The hearts were perfused (8 ml/g) with Krebs–Henseleit solution and gassed with a combination of 95% O_2 and 5% CO_2 at 37°C. Coronary perfusion and left intraventricular pressure were measured using a latex balloon inserted into the left ventricle (LV). After 10 min of baseline stabilization, coronary bed reactivity was evaluated by gradually increasing the basal flow rate by 20% every 2 min until it reached 200%. The following parameters were recorded for each flow rate: coronary perfusion pressure, maximum left intraventricular pressure, maximum systolic contraction velocity (dP/dT_{max}), and maximum diastolic relaxation velocity (dP/dT_{min}). β-Adrenergic receptor sensitivity was evaluated using the cardiac dose-response curve, and the maximum intraventricular pressure response was obtained by the *bolus* administration of dobutamine (β1-adrenergic agonist, 0.5–50 nmol) and salbutamol (β2-adrenergic agonist, 5–100 nmol).

2.4 Statistical analysis

The results are presented as mean ± standard error. The effects of hypertension and physical training were assessed using a two-way analysis of variance. When appropriate, post-hoc comparisons were performed using the Student–Newman–Keuls test. The reactivity of the coronary vascular bed and dose-response curves of cardiac contractility after dobutamine and salbutamol administration were analyzed using a multivariate repeated-measures model, and post-hoc comparisons were performed when appropriate. Differences were considered statistically significant at $p < 0.05$. All statistical tests were performed using the SigmaPlot 11.0 software (Systat Software Inc., San Jose, CA, United States).

10.3389/fphys.2022.920196

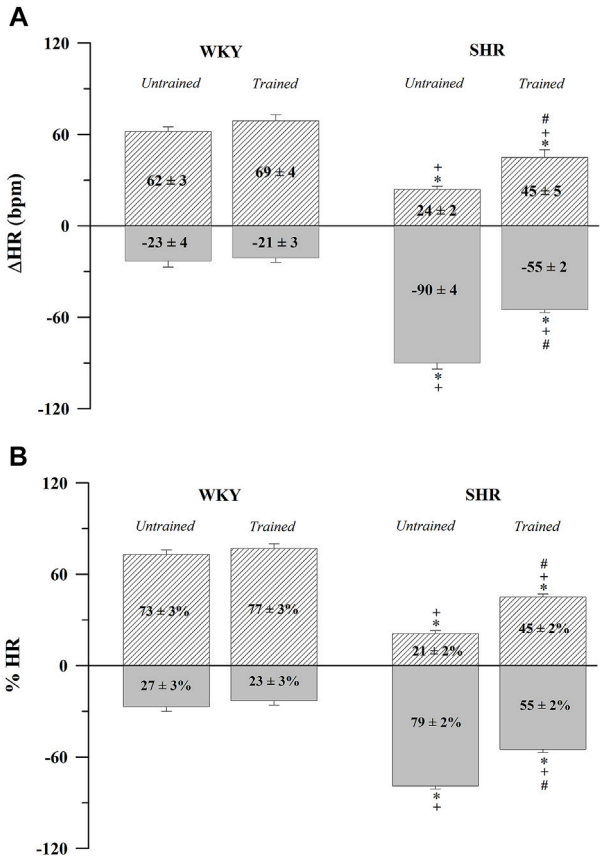

FIGURE 1
Absolute **(A)** and normalized **(B)** tonic autonomic cardiac responses to atropine (positive values) or propranolol (negative values) in trained (N = 07) and untrained (N = 07) normotensive Wistar Kyoto (WKY) and spontaneously hypertensive rats (SHR). Values are expressed as means ± standard error of the mean. *p < 0.05 vs. WKY untrained group; $^{+}$ p < 0.05 vs. WKY trained group; $^{\#}p$ < 0.05 vs. SHR untrained group.

3 Results

Table 1 shows the values of hemodynamic parameters for all groups and the HR values before and after the double blockade of cardiac autonomic receptors with atropine and propranolol. The SHR group had higher BP than the normotensive group. The trained SHR group had lower AP than the untrained SHR group, while both WKY groups (untrained and trained) did not differ in their AP.

The untrained SHR group had baseline tachycardia compared to the WKY group (391 ± 7 vs. 349 ± 6 bpm, p < 0.001). In contrast, both trained SHR (335 ± 8, p < 0.001) and WKY (326 ± 5 bpm, p < 0.021) groups showed bradycardia after aerobic exercise training. Administration of atropine promoted tachycardic responses in both untrained groups: WKY (411 ± 6 bpm) and SHR (415 ± 7 bpm). In a comparison of the untrained groups with their respective trained groups, the trained SHR group showed a lower tachycardic response (390 ± 5 vs. 415 ± 7 bpm, p < 0.005). Administration of propranolol promoted greater bradycardic responses in the untrained SHR group in compared to untrained WKY group (301 ± 5 vs. 326 ± 7 bpm, p < 0.003). Within the SHR groups, propranolol administration promoted similar bradycardic responses (301 ± 5 vs. 290 ± 7 bpm, p < 0.207, untrained and trained, respectively). Within the WKY groups, the WKY-trained group exhibited more prominent bradycardic responses (305 ± 6 vs. 326 ± 7 bpm, p < 0.021). Table 1 also shows the pacemaker iHR obtained after the double blockade of cardiac autonomic receptors. The untrained SHR group had a lower iHR than the untrained WKY group (316 ± 4 vs. 359 ± 5 bpm, p < 0.001). However, both trained groups, SHR (304 ± 3 bpm, p < 0.041) and WKY (336 ± 4 bpm, p < 0.001), showed a reduction in iHR.

In contrast, Figure 1 shows the absolute values (Figure 1A) and percentages (Figure 1B) of the HR variations after the administration of atropine (positive values) and propranolol (negative values). The untrained SHR group had lower absolute (24 ± 2 bpm, p < 0.001) and percentage (21 ± 2%, p < 0.001) positive values and higher absolute (−90 ± 4 bpm, p < 0.001) and percentage (79 ± 2%, p < 0.001) negative values after the administration of atropine and propranolol, respectively, compared with the WKY and trained SHR groups. In summary, Figure 1 shows that the WKY group had a predominant vagal autonomic influence in determining the baseline HR, whereas the SHR group had a predominant sympathetic autonomic influence. The trained SHR group showed a reduction in sympathetic influence; however, sympathetic predominance persisted.

The body weight and cardiac morphological parameters of all groups are shown in Table 2. The untrained SHR group had lower body weight (302 ± 3 vs. 374 ± 9 g, p < 0.001) and higher absolute (1.8 ± 0.07 vs. 1.2 ± 0.07 g, p < 0.001) and relative heart weight (6.0 ± 0.06 vs. 3.2 ± 0.07 mg/g, p < 0.001), relative PWT (7.5 ± 0.35 vs. 4.1 ± 0.45 mm/kg, p < 0.001), IVST (6.6 ± 0.31 vs. 3.4 ± 0.47 mm/kg, p < 0.001), RWT (0.52 ± 0.02 vs. 0.43 ± 0.02 mm/kg, p < 0.008) LVEDD (28.4 ± 0.9 vs. 21.2 ± 2.2 mm/kg, p < 0.010), LVESD (18.6 ± 0.86 vs. 13.2 ± 1.7 mm/kg, p < 0.015), and LV mass (4.2 ± 0.2 vs. 2.3 ± 0.1 mg/g, p < 0.001) than the untrained WKY group. However, the trained WKY and SHR groups did not differ from their respective untrained groups.

Table 3 presents the results of the functional parameters. The results showed that the untrained SHR group had lower EF (75 ± 1 vs. 78 ± 2%, p < 0.032) and SF (35 ± 1 vs. 39 ± 2%, p < 0.014) values than the untrained WKY group. The trained WKY and SHR groups did not differ from their respective untrained groups.

Figure 2 shows the coronary perfusion pressure results (Figure 2A), left ventricular systolic pressure (Figure 2B), maximum dP/dT (Figure 2C), and minimum dP/dT (Figure 2D) in response to a progressive increase in flow. The untrained SHR group had higher values of coronary perfusion

TABLE 2 General characteristics and cardiac morphology parameters for the Wistar Kyoto (WKY, *N* = 14) and spontaneously hypertensive rats (SHR, *N* = 14) groups, both untrained (*N* = 07) and trained (*N* = 07).

	WKY		SHR		Hypertension factor		Physical training factor		Interaction	
	Untrained	Trained	Untrained	Trained	$F_{(d.f)}$	P	$F_{(d.f)}$	P	$F_{(d.f)}$	P
Parameters										
Body weight, g	374 ± 9	357 ± 6	302 ± 3 [a,b]	314 ± 7 [a,b]	$F_{(1.27)}$: 72.032	<0.001	$F_{(1.27)}$: 0.115	0.737	$F_{(1.27)}$: 4.592	0.042
Heart weight, g	1.2 ± 0.07	1.3 ± 0.14	1.8 ± 0.07 [a,b]	1.8 ± 0.07 [a,b]	$F_{(1.27)}$: 36.181	<0.001	$F_{(1.27)}$: 0.122	0.730	$F_{(1.27)}$: 0.499	0.487
RHW, mg/g	3.2 ± 0.07	3.6 ± 0.08 [a]	6.0 ± 0.06 [a,b]	5.6 ± 0.07 [a,b,c]	$F_{(1.27)}$: 193.101	<0.001	$F_{(1.27)}$: 0.042	0.984	$F_{(1.27)}$: 32.397	<0.001
Cardiac Morphology										
PWT, mm/kg	4.1 ± 0.45	3.6 ± 0.38	7.5 ± 0.35 [a,b]	7.0 ± 0.49 [a,b]	$F_{(1.27)}$: 366.79	<0.001	$F_{(1.27)}$: 7.19	0.222	$F_{(1.27)}$: 0.005	0.942
IVST, mm/kg	3.4 ± 0.47	3.5 ± 0.37	6.6 ± 0.31 [a,b]	5.8 ± 1.1 [a,b]	$F_{(1.27)}$: 127.03	<0.001	$F_{(1.27)}$: 2.069	0.163	$F_{(1.27)}$: 2.593	0.120
RWT, mm/g	0.43 ± 0.02	0.42 ± 0.05	0.52 ± 0.02 [a,b]	0.63 ± 0.05 [a,b]	$F_{(1.27)}$: 14.898	<0.001	$F_{(1.27)}$: 1.594	0.219	$F_{(1.27)}$: 2.295	0.143
LVEDD, mm/kg	21.2 ± 2.16	23.7 ± 2.7	28.4 ± 0.9 [a,b]	28.1 ± 2.84 [a,b]	$F_{(1.27)}$: 45.41	<0.001	$F_{(1.27)}$: 1.502	0.232	$F_{(1.27)}$: 2.585	0.121
LVESD, mm/kg	13.2 ± 1.7	13.4 ± 1.5	18.6 ± 0.86 [a,b]	17.5 ± 1.9 [a,b]	$F_{(1.27)}$: 69.494	<0.001	$F_{(1.27)}$: 0.533	0.472	$F_{(1.27)}$: 1.189	0.286
LV mass, mg/g	2.3 ± 0.1	2.2 ± 0.1	4.2 ± 0.2 [a,b]	4.0 ± 0.1 [a,b]	$F_{(1.27)}$: 187.377	<0.001	$F_{(1.27)}$: 0.807	0.378	$F_{(1.27)}$: 0.137	0.715

All values are presented as the mean ± SD. g, grams; mg, milligrams; kg, kilograms; mm, millimeters; PWT, posterior wall thickness; IVST, interventricular septum thickness; RWT, relative wall thickness; LVEDD, left ventricular end-diastolic diameter; LVESD, left ventricular end-systolic diameter; LV, left ventricular; F, factor; d.f, degrees of freedom. [a] $p < 0.05$ vs. WKY, untrained; [b] $p < 0.05$ vs. WKY, trained.

TABLE 3 Cardiac function values obtained in the Wistar Kyoto (WKY, *N* = 14) and Spontaneously Hypertensive Rats (SHR, *N* = 14) groups, both untrained (*N* = 07) and trained (*N* = 07).

	WKY		SHR		Hypertension factor		Physical training factor		Interaction	
	Untrained	Trained	Untrained	Trained	$F_{(d.f)}$	P	$F_{(d.f)}$	P	$F_{(d.f)}$	P
Cardiac Function										
HR, bpm	335 ± 8	315 ± 6 [a]	360 ± 7 [a,b]	339 ± 7 [b,c]	$F_{(1.27)}$: 17.287	<0.001	$F_{(1.27)}$: 2.644	0.037	$F_{(1.27)}$: 0.165	0.688
LVEDV, µl/g	1.40 ± 0.11	1.59 ± 0.12	1.39 ± 0.13	1.44 ± 0.26	$F_{(1.27)}$: 0.181	0.674	$F_{(1.27)}$: 0.535	0.471	$F_{(1.27)}$: 0.219	0.644
LVESV, µl/g	0.30 ± 0.03	0.31 ± 0.04	0.35 ± 0.04	0.36 ± 0.05	$F_{(1.27)}$: 1.532	0.228	$F_{(1.27)}$: 0.389	0.845	$F_{(1.27)}$: 0.290	0.958
Stroke volume, µl/g	1.08 ± 0.07	1.30 ± 0.15	1.04 ± 0.10	1.11 ± 0.16	$F_{(1.27)}$: 0.876	0.359	$F_{(1.27)}$: 1.356	0.256	$F_{(1.27)}$: 0.339	0.566
Ejection fraction, %	78 ± 2	82 ± 2	75 ± 1 [a,b]	77 ± 2	$F_{(1.27)}$: 5.177	0.032	$F_{(1.27)}$: 2.5	0.127	$F_{(1.27)}$: 0.335	0.568
Shortening fraction, %	39 ± 2	43 ± 1	35 ± 1 [a,b]	37 ± 2 [b]	$F_{(1.27)}$: 7.108	0.014	$F_{(1.27)}$: 3.07	0.093	$F_{(1.27)}$: 0.284	0.599
Cardiac output, mL/min	131 ± 9	143 ± 18	111 ± 6	119 ± 16	$F_{(1.27)}$: 2.874	0.103	$F_{(1.27)}$: 0.579	0.454	$F_{(1.27)}$: 0.0302	0.863
Cardiac index, ml/g	0.35 ± 0.02	0.40 ± 0.02	0.37 ± 0.04	0.38 ± 0.02	$F_{(1.27)}$: 0.306	0.956	$F_{(1.27)}$: 1.225	0.279	$F_{(1.27)}$: 0.689	0.415

All values are presented as the mean ± SEM., bpm, beats per minute; µL, microliters; %, percentage; mL, milliliters; min, minute; g, grams; HR, heart rate; LVEDV, left ventricular end-diastolic volume; LVESV, left ventricular end-systolic volume; F, factor; d.f, degrees of freedom. [a] $p < 0.05$ vs. WKY, untrained; [b] $p < 0.05$ vs. WKY, trained; [c] $p < 0.05$ vs. SHR, untrained.

pressure and lower values of left ventricular systolic pressure and maximum and minimum dP/dT than the untrained WKY group. In contrast, the trained SHR group had higher values for all parameters than the untrained group. A comparison between both trained groups showed that the trained SHR group had the highest responses for all the parameters.

Figure 3 shows the variation in the Δ values of the left ventricular systolic pressure obtained after the administration of dobutamine (Figure 3A) and salbutamol (Figure 3B) and their respective maximal responses (Figures 3C,D, respectively). The untrained SHR group had lower left ventricular systolic pressure values for both dobutamine and salbutamol than untrained WKY group, including maximal response (dobutamine, 15 ± 3 vs. 78 ± 11 mmHg, $p < 0.001$); salbutamol, 18 ± 3 vs. 56 ± 8 mmHg, $p < 0.001$). Within the WKY groups, dobutamine or salbutamol promoted similar responses. In contrast, within the SHR groups, the trained SHR group had a significant increase, including in maximal responses to dobutamine (62 ± 12 vs.

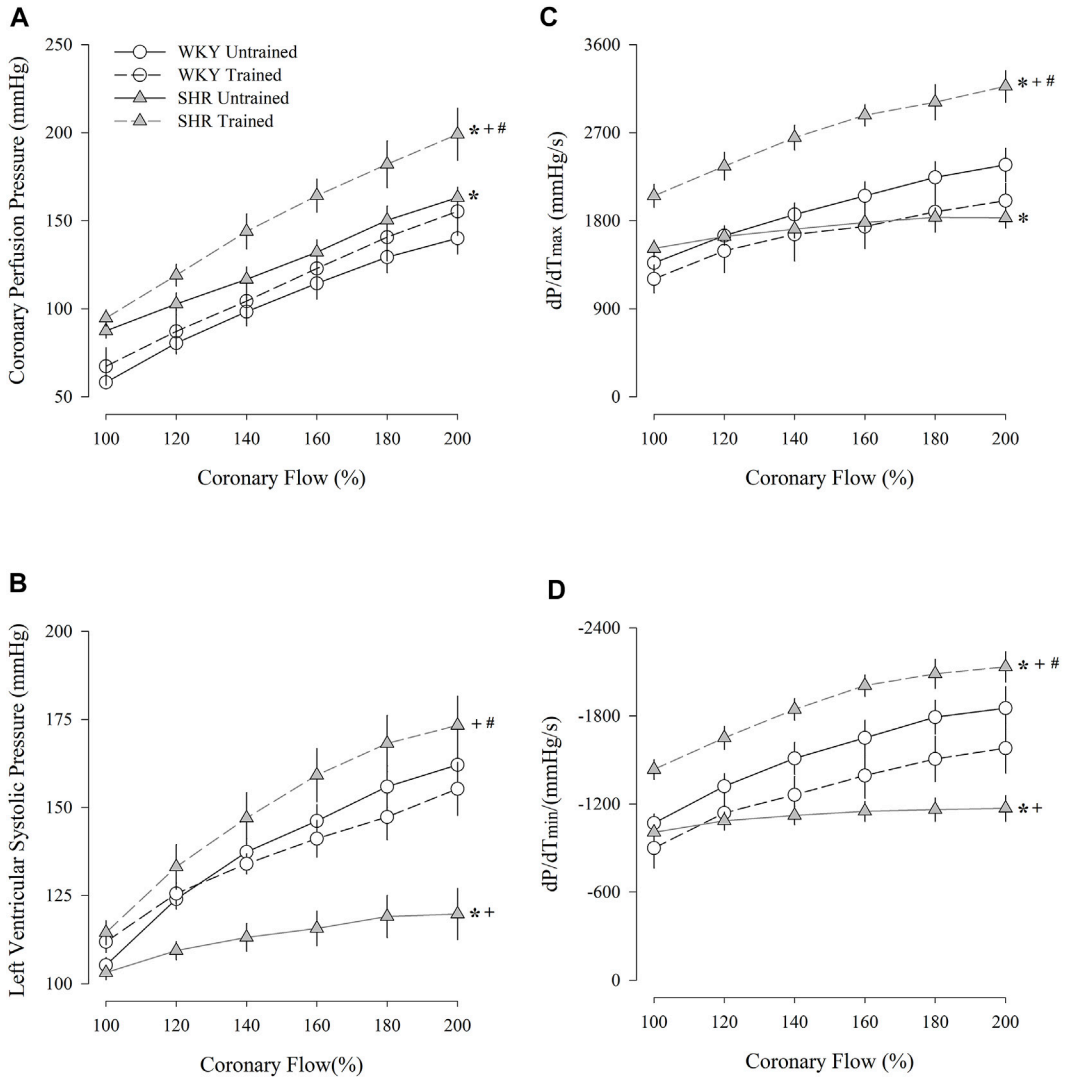

FIGURE 2
Coronary perfusion pressure **(A)**, left ventricular systolic pressure **(B)**, $dP/dT_{(max)}$ **(C)**, and $dP/dT_{(min)}$ **(D)** flow-induced in untrained (N = 07) and trained (N = 07) normotensive Wistar Kyoto (WKY) and hypertensive spontaneously rats (SHR). mmHg, millimeters of mercury; s, second; max, maximum; min; minimum. Values are expressed as means ± standard error of the mean. *$p < 0.05$ vs. WKY untrained group; $^{+}p < 0.05$ vs. WKY trained group; $^{\#}p < 0.05$ vs. SHR untrained group.

15 ± 3 mmHg, $p < 0.001$) and salbutamol (54 ± 9 vs. 18 ± 3 mmHg, $p < 0.001$).

Figure 4 shows the iHR responses of pacemakers in the isolated heart in relation to increased coronary flow (Figure 4A), administration of dobutamine (Figure 4B), and salbutamol (Figure 4C). Figure 4A shows that during the increase in flow percentage, the untrained WKY group had the highest iHR values, whereas the untrained SHR group had the lowest values. The trained groups showed similar values; however, compared to their respective untrained groups, the trained WKY group showed a reduction in iHR, while the trained SHR group showed an increase. Similar responses were observed in iHR after the administration of dobutamine (Figure 4B) and salbutamol (Figure 4C).

4 Discussion

The effects of aerobic physical training on cardiac autonomic control, morphology, and functionality were investigated in hypertensive rats. Our results suggested that untrained SHR had a greater sympathetic participation in determining the basal HR, which was associated with increased morphological parameters compared with untrained WKY rats. Our findings

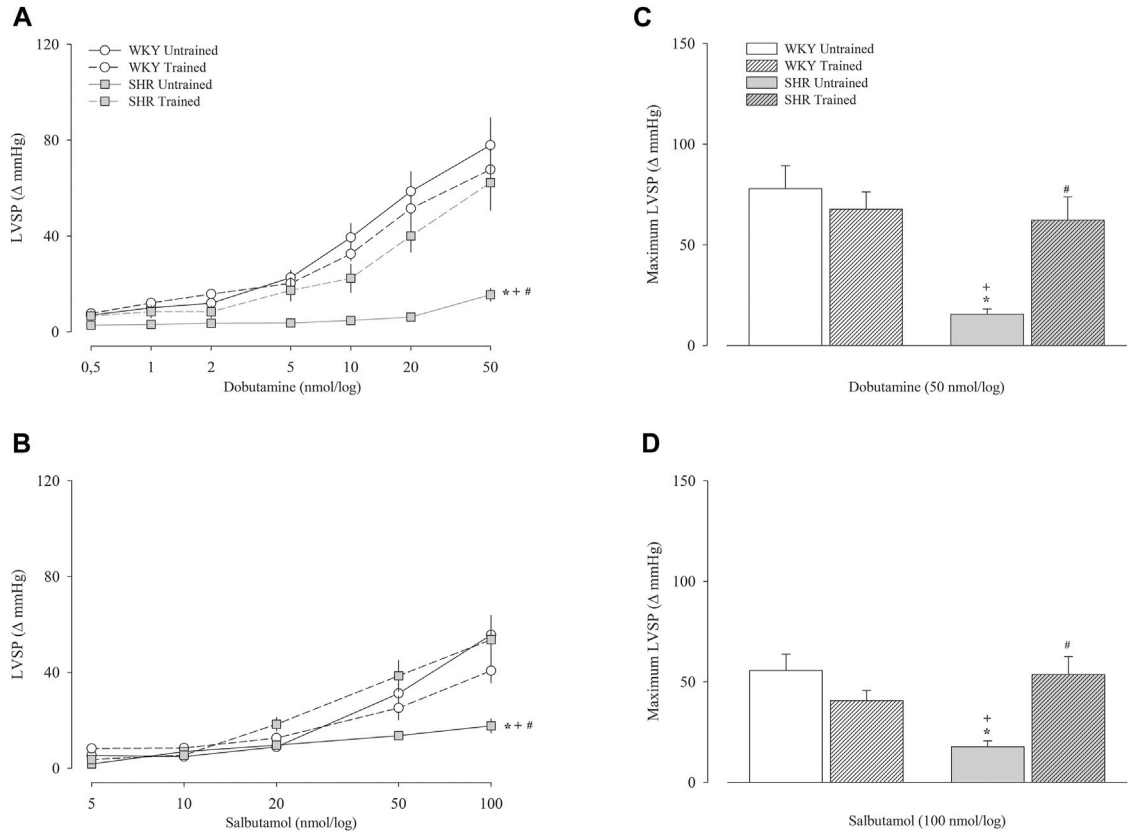

FIGURE 3
Left ventricular systolic pressure (LVSP) after administration of dobutamine **(A)** and salbutamol **(B)** in untrained (*N* = 07) and trained (*N* = 07) normotensive Wistar Kyoto (WKY) and hypertensive spontaneously rats (SHR). The graphs on the right represent the maximum response obtained for dobutamine (50 nmol) **(C)** and salbutamol (100 nmol) **(D)**. Values are expressed in delta (Δ). mmHg, millimeters of mercury. All values are presented as the mean ± standard error of the mean. $^{*}p < 0.05$ vs. WKY untrained group; $^{+}p < 0.05$ vs. WKY trained group; $^{\#}p < 0.05$ vs. SHR untrained group.

also showed lower coronary bed reactivity and reduced left ventricular contractility in response to increased flow or β-adrenergic agonist administration. Compared with untrained SHR, trained SHR showed a reduction in sympathetic participation on basal HR determination, and in the isolated heart had a greater coronary bed reactivity, and LV contractility in response to increased flow and dobutamine and salbutamol administration. However, we did not observe any significant modifications in the morphological parameters.

Double blockade of autonomic receptors with atropine and propranolol showed that untrained SHR had increased sympathetic participation in the determination of basal HR, despite reduced iHR. Therefore, together with cardiac hypertrophy, this may suggest important cardiac impairments (Tucker and Domino, 1988; Maskali et al., 2014). A reduction in iHR was also observed in the isolated hearts during the Langendorff protocol. However, while the iHR obtained in the double blockade of autonomic receptors was even more reduced in the trained SHR, the iHR obtained through the isolated heart was significantly increased compared to the untrained SHR; this is a paradox. The cause of this reduction in intrinsic pacemaker HR is unknown. A recent study on atrial preparations of SHR showed that the sympathetic and parasympathetic nerve terminals of the right atrium isolated from the SHR show a release of noradrenaline and acetylcholine in the absence of electric field and pharmacological stimulation. Nonetheless, this release of neurotransmitters does not regulate basal chronotropism. In this case, the reduced chronotropism in atrial preparations and in isolated heart from SHR should not involve neurogenic changes and is probably mediated by intrinsic changes in the atrial tissue. (Rodrigues et al., 2019). In contrast, our findings suggest that aerobic physical training contributes to adjustments in pacemaker intrinsic heart rate regulation.

Regarding cardiac hypertrophy, the effects of hypertension and chronic elevation of sympathetic activity on the heart are supported by our results. The SHR group had lower body mass and significantly higher heart mass than the WKY group, even in absolute values. Furthermore, despite normalizing by body mass,

10.3389/fphys.2022.920196

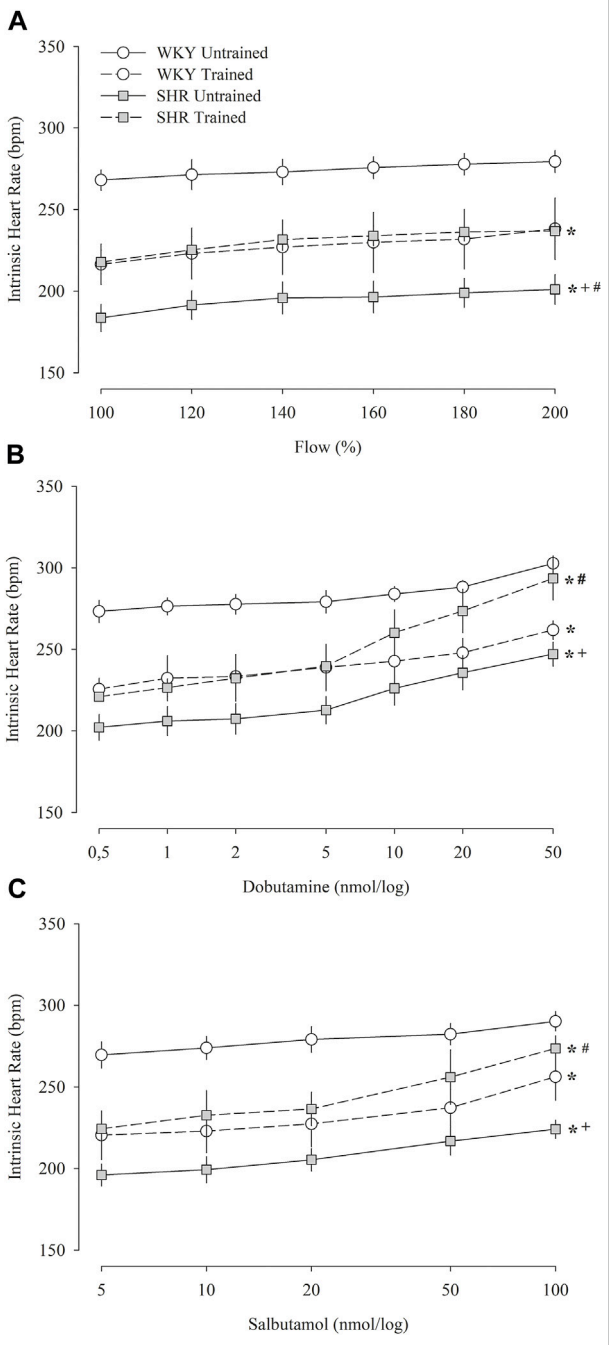

FIGURE 4
Intrinsic heart rate obtained in isolated hearts (Langendorff technique) during the percent increase in flow **(A)** and after multiple and sequential doses of dobutamine **(B)** and salbutamol **(C)** in untrained (N = 07) and trained (N = 07) normotensive Wistar Kyoto (WKY) and hypertensive spontaneously rats (SHR). bpm, beats per minute. All values are presented as the mean ± standard error of the mean. *$p < 0.05$ vs. WKY untrained group; $^{+}$ $p < 0.05$ vs. WKY trained group; $^{\#}p < 0.05$ vs. SHR untrained group.

the heart mass values of the SHR group were twice those of the WKY group. This result was consistent with the morphological values obtained through echocardiography, which were significantly higher in the hypertensive group than the normotensive group for all parameters. On the other hand, although the heart of hypertensive animals presented significantly higher dimensions than normotensive animals, such differences were not observed in functionality, except for a slight reduction in the ejection fraction. Therefore, the SHR group presented values of cardiac functionality similar to those of normotensive animals.

The cardiac morphological changes observed in hypertensive animals occur in response to the high peripheral resistance of the cardiac muscle, which reacts to such an overload by addition of sarcomeres in parallel (Yildiz et al., 2020). In the first weeks of life, the animal's heart manages through a hypertrophic response and other adaptations to preserve the parameters of cardiac functionality. However, after a longer period of pressure overload, the cardiac functionality parameters of hypertensive animals are impaired, which is due to a progressive inflammatory state that is sustained by adaptations promoted by the pathology itself (Conrad et al., 1991; Conrad et al., 1995; Xu et al., 2020). However, in our case, the animals were only 32 weeks old.

The study of isolated hearts allowed us to evaluate the cardiac parameters without directly influencing the autonomic nervous system. The high values of coronary perfusion pressure observed in the trained SHR group coincided with an increase in LV contraction strength and suggested a greater self-regulatory capacity of the coronary arteries. Increased LV contraction strength promotes greater pressure in the cardiac vascular beds, which hampers the flow from passing (Duncker and Bache, 2008). In contrast, normotensive animals did not show significant differences in LV systolic pressure, which supports the lack of any observed change in coronary perfusion pressure in the trained group.

Furthermore, coronary perfusion pressure was higher in hypertension-trained animals than in sedentary animals. The increase in perfusion pressure is due to an increase in flow, which is associated with an autoregulatory response to the constriction of the arterioles (Cowley, 1980; Goodwill et al., 2017). In this sense, the results indicate that aerobic physical training promotes an improvement in the self-regulatory mechanism of the coronary bed in hypertensive animals. The fact that physical training led to a similar improvement in both untrained and trained WKY rats can be attributed to the already adequate functioning of the coronary bed in these animals. Additionally, other studies that compared cardiovascular adaptations observed in SHR and WKY rats under different physical training protocols demonstrated that SHR rats are more susceptible to physical training owing to their impaired vascular condition. (Pagan et al., 2015).

Left ventricular systolic pressure refers to the maximum force of contraction produced by the myocardium, whereas dP/dT_{max} represents the maximum increase in intraventricular pressure and is associated with cardiac contractility (Frank and Levinson,

1968; Hamlin and del Rio, 2012). The reduction of such parameters, mainly at higher flow percentages, indicates losses in the physiological reserve for increases in strength and contraction speed and is often attributed to the proteins responsible for regulating calcium in cardiomyocytes (Carneiro-Júnior et al., 2013; Carneiro-Júnior et al., 2014). However, when subjected to the aerobic physical training protocol, the values of systolic pressure of the LV, dP/dT_{max}, and HR approached the values obtained in the normotensive groups, indicating important adaptations in the cardiac tissue. These results are supported by findings from other studies which indicate that among other adaptations, aerobic physical training in SHR promotes an improvement in the regulation of proteins involved in the processes of formation/degradation of collagen fibers, contractile function, and autonomic dysfunction (Masson et al., 2015; Locatelli et al., 2017; Pagan et al., 2019). The left ventricular relaxation rate was assessed using dP/dT_{min}. The results showed that hypertensive animals had a reduced dP/dT_{min} compared to normotensive animals, suggesting that the relaxation velocity of the left ventricular muscles was lower. These animals also presented with a high baseline HR indicating that the time available for myocardial relaxation is too short, which may in turn contribute to a lower end-diastolic volume. In addition, when we analyzed the delta variation of dP/dT_{min} in response to flow, we noticed no changes in response to the increase in flow, indicating that the maximum velocity of ventricular relaxation is within the physiological limits of the basal flow. These results are consistent with the published findings on left ventricular diastolic dysfunction in the respective lineage of animals, which is supported by the observed changes in intracellular calcium reuptake after cardiomyocyte excitation (Dupont et al., 2012). The physical training protocol in hypertensive animals promoted an increase in dP/dT_{min} and the response to flow variation, which may be associated with an improvement in intracellular calcium reuptake as demonstrated in other studies (Rolim et al., 2007; Yoshizaki et al., 2018).

In conclusion, our results showed that the reduction in the cardiac sympathetic autonomic effect induced by aerobic physical training was accompanied by an increase in left intraventricular pressure, suggesting recovery of intrinsic cardiac properties, such as contractility when analyzed by Langendorff technique. In contrast, the echocardiography did not show differences.

4.1 Study limitations

The echocardiographic recordings were performed with anesthetized animals, and these may have interfered with our results. We did not measure plasma catecholamines or cardiac norepinephrine spillover as more direct parameters to characterize central sympathetic drive and cardiac tone. Swimming training model is a less frequent training than motorized treadmill. However, satisfactory levels of aerobic physical training have been achieved according to the observed results. Another limitation was the choice to investigate only male rats. Although systemic arterial hypertension indiscriminately affects both the sexes, we are convinced that female SHR need to be exclusively studied to address hormonal issues, since ovarian hormones seem to participate directly and indirectly in cardiovascular autonomic regulation and influence cardiac morphology and functionality.

Data availability statement

The raw data supporting the conclusion of this article will be made available by the authors, without undue reservation.

Ethics statement

The animal study was reviewed and approved by Committee on Animal Research and Ethics of the Ribeirão Preto Medical School, University of São Paulo (Protocol 044/2020).

Author contributions

Authors' contribution: SV and HS participated in the study design and conceptualization, data collection, data analysis and manuscript preparation for the original draft, and review and editing. BA, AV, and AF participated in data analysis, and manuscript preparation for the original draft. SP participated in the study design and conceptualization, and manuscript preparation for review and editing. KR participated in the study design, data collection and data analysis. JT collaborated in the analysis of results, revision and editing of the manuscript.

Funding

This study was funded by the FAPESP (Process: 2014/01,937-9; 2021/14,938-7) and CNPq (Process: 141,693/2014-2).

Acknowledgments

We appreciate the technical support provided by Dr. Cybele Maria Prado for obtaining echocardiographic images.

Conflict of interest

The authors declare that the research was conducted in the absence of any commercial or financial relationships that could be construed as a potential conflict of interest.

Publisher's note

All claims expressed in this article are solely those of the authors and do not necessarily represent those of their affiliated organizations, or those of the publisher, the editors and the reviewers. Any product that may be evaluated in this article, or claim that may be made by its manufacturer, is not guaranteed or endorsed by the publisher.

References

Borovac, J. A., D'Amario, D., Bozic, J., and Glavas, D. (2020). Sympathetic nervous system activation and heart failure: current state of evidence and the pathophysiology in the light of novel biomarkers. *World J. Cardiol.* 12, 373–408. doi:10.4330/wjc.v12.i8.373

Carneiro-Júnior, M. A., Quintão-Júnior, J. F., Drummond, L. R., Lavorato, V. N., Drummond, F. R., Da Cunha, D. N. Q., et al. (2013). The benefits of endurance training in cardiomyocyte function in hypertensive rats are reversed within four weeks of detraining. *J. Mol. Cell. Cardiol.* 57, 119–128. doi:10.1016/j.yjmcc.2013.01.013

Carneiro-Júnior, M. A., Quintão-Júnior, J. F., Drummond, L. R., Lavorato, V. N., Drummond, F. R., Amadeu, M. A., et al. (2014). Effect of exercise training on Ca2+ release units of left ventricular myocytes of spontaneously hypertensive rats. *Braz. J. Med. Biol. Res.* 47, 960–965. doi:10.1590/1414-431X20144063

Conrad, C. H., Brooks, W. W., Robinson, K. G., and Bing, O. H. L. (1991). Impaired myocardial function in spontaneously hypertensive rats with heart failure. *Am. J. Physiol.* 260, H136–H145. doi:10.1152/ajpheart.1991.260.1.h136

Conrad, C. H., Brooks, W. W., Hayes, J. A., Sen, S., Robinson, K. G., and Bing, O. H. L. (1995). Myocardial fibrosis and stiffness with hypertrophy and heart failure in the spontaneously hypertensive rat. *Circulation* 91, 161–170. doi:10.1161/01.CIR.91.1.161

Cowley, A. W. (1980). The concept of autoregulation of total blood flow and its role in hypertension. *Am. J. Med.* 68, 906–916. doi:10.1016/0002-9343(80)90225-9

Diaconu, C. C., Drăgoi, C. M., Bratu, O. G., Neagu, T. P., Stoian, A. P., Cobelschi, P. C., et al. (2018). New approaches and perspectives for the pharmacological treatment of arterial hypertension. *Farmacia* 66, 408–415. doi:10.31925/farmacia.2018.3.4

Duncker, D. J., and Bache, R. J. (2008). Regulation of coronary blood flow during exercise. *Physiol. Rev.* 88, 1009–1086. doi:10.1152/physrev.00045.2006

Dupont, S., Maizel, J., Mentaverri, R., Chillon, J. M., Six, I., Giummelly, P., et al. (2012). The onset of left ventricular diastolic dysfunction in SHR rats is not related to hypertrophy or hypertension. *Am. J. Physiol. Heart Circ. Physiol.* 302, 1524–1532. doi:10.1152/ajpheart.00955.2010

Felix, A. C. S., Dutra, S. G. V., Gastaldi, A. C., Bonfim, P. C., Vieira, S., and de Souza, H. C. D. (2018). Physical training promotes similar effects to the blockade of angiotensin-converting enzyme on the cardiac morphology and function in old female rats subjected to premature ovarian failure. *Exp. Gerontol.* 109, 90–98. doi:10.1016/j.exger.2017.04.003

Floras, J. S. (2009). Sympathetic nervous system Activation in human heart failure. Clinical implications of an updated model. *J. Am. Coll. Cardiol.* 54, 375–385. doi:10.1016/j.jacc.2009.03.061

Frank, M. J., and Levinson, G. E. (1968). An index of the contractile state of the myocardium in man. *J. Clin. Invest.* 47, 1615–1626. doi:10.1172/JCI105853

Gardim, C. B., Veiga, A. C., Aguilar, B. A., Philbois, S. V., and Souza, H. C. D. (2021). Effects of chronic cholinergic stimulation associated with aerobic physical training on cardiac morphofunctional and autonomic parameters in spontaneously hypertensive rats. *Sci. Rep.* 11 (1), 17141. doi:10.1038/s41598-021-96505-2

Goodwill, A. G., Dick, G. M., Kiel, A. M., and Tune, J. D. (2017). Regulation of coronary blood flow. *Compr. Physiol.* 7, 321–382. doi:10.1002/cphy.c160016

Hamlin, R. L., and del Rio, C. (2012). dP/dtmax - a measure of "baroinometry. *J. Pharmacol. Toxicol. Methods* 66, 63–65. doi:10.1016/j.vascn.2012.01.001

Jakovljevic, B., Nikolic Turnic, T., Jeremic, N., Savic, M., Jeremic, J., Srejovic, I., et al. (2019). The impact of high-intensity interval training and moderate-intensity continuous training regimes on cardiodynamic parameters in isolated heart of normotensive and hypertensive rats. *Can. J. Physiol. Pharmacol* 97 (7), 631–637. doi:10.1139/cjpp-2018-0610

Laughlin, M. H., Oltman, C. L., and Bowles, D. K. (1998). Exercise training-induced adaptations in the coronary circulation. *Med. Sci. Sports Exerc.* 30, 352–360. doi:10.1097/00005768-199803000-00004

Locatelli, J., Paiva, N. C. N., Carvalho, S. H. R., Lavorato, V. N., Gomes, L. H. L. S., Castro, Q. J. T., et al. (2017). Swim training attenuates the adverse remodeling of LV structural and mechanical properties in the early compensated phase of hypertension. *Life Sci.* 187, 42–49. doi:10.1016/j.lfs.2017.08.014

Maskali, F., Poussier, S., Louis, H., Boutley, H., Lhuillier, M., Thornton, S. N., et al. (2014). Assessment of the early stage of cardiac remodeling of spontaneously hypertensive heart failure rats using the quantitative 3-dimensional analysis provided by acipimox-enhanced FDG-PET. *Int. J. Cardiovasc. Imaging* 30, 449–456. doi:10.1007/s10554-013-0350-3

Masson, G. S., Nair, A. R., Soares, P. P. S., Michelini, L. C., and Francis, J. (2015). Aerobic training normalizes autonomic dysfunction, HMGB1 content, microglia activation and inflammation in hypothalamic paraventricular nucleus of SHR. *Am. J. Physiol. Heart Circ. Physiol.* 309, H1115–H1122. doi:10.1152/ajpheart.00349.2015

Oparil, S., Acelajado, M. C., Bakris, G. L., Berlowitz, D. R., Cífková, R., Dominiczak, A. F., et al. (2018). Hypertension. *Nat. Rev. Dis. Prim.* 4, 18014. doi:10.1038/nrdp.2018.14

Pagan, L. U., Damatto, R. L., Cezar, M. D. M., Lima, A. R. R., Bonomo, C., Campos, D. H. S., et al. (2015). Long-term low intensity physical exercise attenuates heart failure development in aging spontaneously hypertensive rats. *Cell. Physiol. Biochem.* 36, 61–74. doi:10.1159/000374053

Pagan, L. U., Damatto, R. L., Gomes, M. J., Lima, A. R. R., Cezar, M. D. M., Damatto, F. C., et al. (2019). Low-intensity aerobic exercise improves cardiac remodelling of adult spontaneously hypertensive rats. *J. Cell. Mol. Med.* 23, 6504–6507. doi:10.1111/jcmm.14530

Rodrigues, J. Q. D., Camara, H., da Silva Junior, E. D., Godinho, R. O., and Jurkiewicz, A. (2019). Intrinsic adaptation of SHR right atrium reduces heart rate. *J. Cardiovasc. Pharmacol.* 74 (6), 542–548. doi:10.1097/FJC.0000000000000746

Rolim, N. P. L., Medeiros, A., Rosa, K. T., Mattos, K. C., Irigoyen, M. C., Krieger, E. M., et al. (2007). Exercise training improves the net balance of cardiac Ca2+ handling protein expression in heart failure. *Physiol. Genomics* 29, 246–252. doi:10.1152/physiolgenomics.00188.2006

Sahn, D. J., DeMaria, A., Kisslo, J., and Weyman, A. (1978). Recommendations regarding quantitation in M-mode echocardiography: results of a survey of echocardiographic measurements. *Circulation* 58, 1072–1083. doi:10.1161/01.CIR.58.6.1072

Saxena, T., Ali, A. O., and Saxena, M. (2018). Pathophysiology of essential hypertension: an update. *Expert Rev. Cardiovasc. Ther.* 16 (12), 879–887. doi:10.1080/14779072.2018.1540301

Seravalle, G., and Grassi, G. (2022). Sympathetic nervous system and hypertension: new evidences. *Auton. Neurosci.* 238, 102954. doi:10.1016/j.autneu.2022.102954

Tucker, D. C., and Domino, J. V. (1988). Balance among autonomic controls of heart rate in neonatal spontaneously hypertensive and borderline hypertensive rats. *J. Auton. Nerv. Syst.* 22, 11–21. doi:10.1016/0165-1838(88)90149-X

Williams, B., Mancia, G., Spiering, W., Rosei, E. A., Azizi, M., Burnier, M., et al. (2018). 2007 guidelines for the management of arterial hypertension: the task force for the management of arterial hypertension of the European society of hypertension (ESH) and of the European society of cardiology (ESC). *G. Ital Cardiol (Rome)* 19 (11 Suppl 1), 3S–73S. doi:10.1093/eurheartj/ehy339

Xu, M. L., Yu, X. J., Zhao, J. Q., Du, Y., Xia, W. J., Su, Q., et al. (2020). Calcitriol ameliorated autonomic dysfunction and hypertension by down-regulating inflammation and oxidative stress in the paraventricular nucleus of SHR. *Toxicol. Appl. Pharmacol.* 394, 114950. doi:10.1016/j.taap.2020.114950

Yildiz, M., Oktay, A. A., Stewart, M. H., Milani, R. V., Ventura, H. O., and Lavie, C. J. (2020). Left ventricular hypertrophy and hypertension. *Prog. Cardiovasc. Dis.* 63, 10–21. doi:10.1016/j.pcad.2019.11.009

Yoshizaki, A., Antonio, E. L., Silva Junior, J. A., Crajoinas, R. O., Silva, F. A., Girardi, A. C. C., et al. (2018). Swimming training improves myocardial mechanics, prevents fibrosis, and alters expression of Ca 2+ handling proteins in older rats. *J. Gerontol. A Biol. Sci. Med. Sci.* 73, 468–474. doi:10.1093/gerona/glx244

Frontiers in Physiology

Understanding how an organism's components work together to maintain a healthy state

The second most-cited physiology journal, promoting a multidisciplinary approach to the physiology of living systems - from the subcellular and molecular domains to the intact organism and its interaction with the environment.

Discover the latest Research Topics

See more →

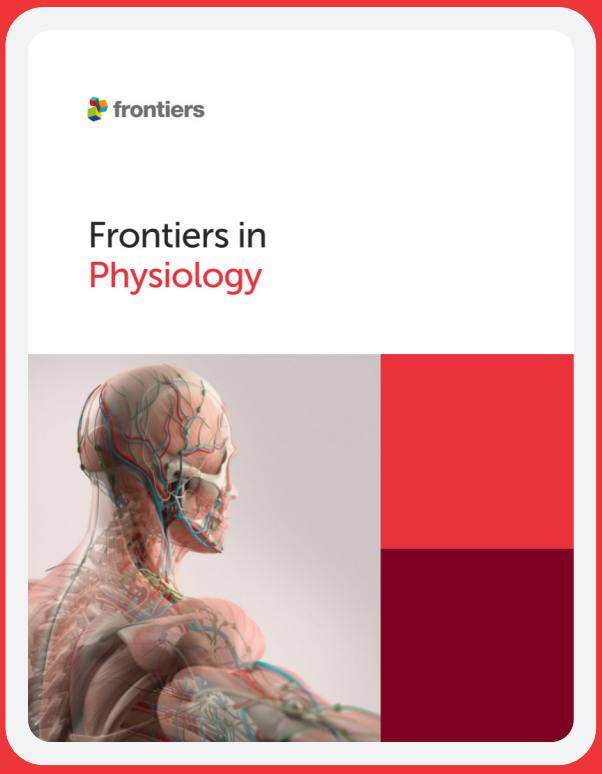

Frontiers

Avenue du Tribunal-Fédéral 34
1005 Lausanne, Switzerland
frontiersin.org

Contact us

+41 (0)21 510 17 00
frontiersin.org/about/contact